Allen, Pam, NMENV

ENTE

From: Maestas, Ricardo, NMENV
Sent: Thursday, November 14, 2013 2:49 PM
To: Kliphuis, Trais, NMENV; Allen, Pam, NMENV
Cc: Holmes, Steve, NMENV; Smith, Coleman, NMENV; Maestas, Ricardo, NMENV
Subject: Docs from EPA Website on Panel Closure and Repository Reconfiguration

Trais, Pam,

The following is the list of docs from EPA Website on *Panel Closure* and *Repository Reconfiguration* that I have printed and will give to Pam to include in the WIPP record so we can also have them for the Class 3 PMR Admin Record..

Thanks!

EPA Radiation Protection

http://www.epa.gov/rpdweb00/news/wipp-news.html#reconfig

Repository Reconfiguration

On August 30, 2011, the U.S. Department of Energy (DOE) provided a proposed planned change request that will relocate Panels 9 and 10 from the main north-south access drifts to south of the existing Panels 4 and 5 in the WIPP repository. DOE states that relocating these panels will enhance worker safety and reduce maintenance requirements by providing a more stable geotechnical environment.

The Department submitted a performance assessment (PA) for the proposed repository reconfiguration as part of their documentation package. The results of the PA show that WIPP will remain in compliance with all containment requirements found in 40 CFR 191 and have only a minor effect on total normalized releases from the repository.

Complete details of the repository reconfiguration planned change request (including an overview presentation provided at an August 2011 technical meeting) can be found below:

- DOE -- Letter to EPA transmitting Repository Reconfiguration planned change request (8/30/11) (PDF) (2 pp, 254K)
- DOE -- Enclosure #1: Waste Isolation Pilot Plant Repository Reconfiguration (PDF) (14 pp, 824K)
- DOE -- Enclosure #2: Performance Assessment for Repository Reconfiguration (PDF) (59 pp, 1,610K)
- DOE -- WIPP Repository Reconfiguration: Overview (8/23/11) (PDF) (12 pp, 713K)

**xxxx

- Meeting Minutes - Panel Closure Redesign Informal Public Meetings (December 2012) (PDF) (2 pp, 311K)

Panel Closure Redesign

On September 28, 2011, the U.S. Department of Energy (DOE) provided a planned change request for panel closure redesign, which would modify Condition 1 of the Final WIPP Certification Decision for 40 CFR Part 194.

After 12 years of operating experience, DOE has acquired considerable experience and knowledge regarding the behavior of the WIPP repository, along with the nature and behavior of disposed transuranic (TRU) waste. In EPA's 1998 WIPP Certification Decision, the Agency listed a number of conditions - one of which was that the panel closure system (PCS) to be used in WIPP be "Option D," as specified in DOE's Compliance Certification Application (CCA). This option specified that certain components be constructed using Salado Mass Concrete (SMC).

After numerous large scale tests, DOE states that SMC cannot meet the design and performance requirements for the panel closures as specified in the CCA. Since results from monitoring for explosive gases in the closed panels has established that the measured concentrations of methane and hydrogen will remain below the lower limits through the operational period, the Department has submitted a new panel closure design - the Run-of Mine Panel Closure (ROMPC).

The Department submitted a performance assessment (PA) for the proposed panel closure redesign as part of their documentation package. The results of the PA show that WIPP will remain in compliance with all disposal requirements 40 CFR Part 191, Subparts B and C, and essentially have the same performance as the original Option D design.

Complete details of the panel closure redesign planned change request (including an overview presentation provided at an August 2011 technical meeting) can be found below:

- DOE -- Letter to EPA transmitting Panel Closure Redesign planned change request (9/28/11) (PDF) (2 pp, 263K)
- DOE -- Enclosure: Panel Closure System Design (PDF) (108 pp, 3,210K)
- DOE -- WIPP Panel Closure Redesign: Overview (8/23/11) (PDF) (11 pp, 284K)

UPDATED: EPA has sent DOE a series of comments related to the initial proposal, and DOE has responded with supplemental information on the panel closure redesign and associated performance assessment (PCS-2012 PA). All of this information can be found below in Adobe .pdf format:

- EPA -- Letter to DOE transmitting comments on Panel Closure Redesign planned change request (12/22/11) (PDF) (5 pp, 208K)
- DOE -- Response to 12/22/11 EPA Comments (4/17/12) (PDF) (1 p, 175K)
  Enclosure 1 (PDF) (38 pp, 2,984K)

- DOE -- (Memorandum) Recommendations and Justifications of Parameter Values for the Run-of-Mine Salt Panel Closure System Design Modeled in the PCS-2012 PA (5/4/12) (PDF) (28 pp, 740K)
- DOE -- (Memorandum) An overview of the BRAGFLO two-phase flow parameters used to model the run-of-mine salt panel closures implemented in the PCS-2012 PA (6/7/12) (PDF) (2 pp, 263K)
- DOE -- Reponses to EPA Comments (6/14/12) (PDF) (4 pp, 237K)

- DOE -- Summary of Capillary Pressure Models (6/15/12) (PDF) (1 p, 38K)
- EPA -- (E-mail) Concurrence with proposed data ranges and values for PCS-2012 PA (6/19/12) (PDF) (1 p, 38K)

- DOE -- (Report) Analysis Plan for the 2012 WIPP Panel Closure System Performance Assessment (7/2/12) (PDF) (18 pp, 186K)
- DOE -- (Report) Generation of the LHS Samples for the AP-161 (PCS-2012) Revision 0 PA Calculations (9/6/12) (PDF) (172 pp, 2,111K)
- DOE -- (Report) Analysis Package for the Salado Flow Modeling Done in the AP-161 (PCS-2012) Performance Assessment (9/17/12) (PDF) (71 pp, 5,789K)
- DOE -- (Report) Analysis Package for Direct Brine Releases: 2012 Panel Closure System Performance Assessment (PCS-2012 PA) (10/1/12) (PDF) (32 pp, 1,311K)
- DOE -- (Report) CCDFGF Analysis Package for the AP-161 (PCS-2012) Performance Assessment (10/15/12) (PDF) (30 p, 6,686K)
- DOE -- (Report) Sensitivity of the AP-161 (PCS-2012) PA Releases to Parameters (10/15/12) (PDF) (34 pp, 858K)
- DOE -- (Report) Summary Report and Run Control for the 2012 WIPP Panel Closure System Performance Assessment (11/5/12) (PDF) (84 pp, 4,163K)

December 2012 Informal Public Meeting Materials (Carlsbad & Santa Fe, NM)

- DOE -- Fact Sheet: Proposed Panel Closure Redesign Planned Change Request (11/2012) (PDF) (2 pp, 213K)
- DOE -- Presentation: Panel Closure Redesign Planned Change Request (12/2012) (PDF) (9 pp, 487K)
- DOE -- Presentation: Performance Assessment of the WIPP Run-of-Mine Salt Panel Closure System (12/2012) (PDF) (22 pp, 1090K)
- EPA -- Presentation: WIPP Panel Closure Redesign Rulemaking (12/2012) (PDF) (7 pp, 140K)

EPA Radiation Protection

http://www.epa.gov/rpdweb00/news/wipp-news.html#pubmeetingspanelclosure

Informal Public Meetings -- Panel Closure Redesign

EPA will be holding two public meeting sessions in New Mexico related to DOE's panel closure redesign planned change request. The purpose of these meetings is to provide a forum to discuss the specifics of the panel closure redesign and EPA's upcoming proposed rulemaking, which is scheduled for publication in early 2013. The meetings will serve as an informal vehicle to get preliminary comments and input from members of the public in advance of the rulemaking and its associated formal public hearings. Staff from the US Department of Energy (DOE) and the New Mexico Environment Department (NMED) will also be on hand to answer any stakeholder questions/concerns. The logistics for both meetings in Carlsbad and Santa Fe are as follows:

Wednesday, December 5, 2012
Carlsbad, New Mexico
U.S. Department of Energy
Carlsbad Field Offic t
Skeen-Whitlock Building
Main Auditorium
4021 National Parks Highway
9:30 AM – 1:00 PM

Thursday, December 6, 2012
Santa Fe, New Mexico
New Mexico Environment Department
Harold L. Runnels Building
Auditorium
1190 St. Francis Drive
9:30 AM - 1:00 PM

UPDATED: Meeting minutes/notes have been compiled and can be viewed/downloaded in Adobe PDF format below.

- Meeting Minutes - Panel Closure Redesign Informal Public Meetings (December 2012) (PDF) (2 pp, 311K)

- DOE -- (Memorandum) Recommendations and Justifications of Parameter Values for the Run-of-Mine Salt Panel Closure System Design Modeled in the PCS-2012 PA (5/4/12) (PDF) (28 pp, 740K)
- DOE -- (Memorandum) An overview of the BRAGFLO two-phase flow parameters used to model the run-of-mine salt panel closures implemented in the PCS-2012 PA (6/7/12) (PDF) (2 pp, 263K)
- DOE -- Reponses to EPA Comments (6/14/12) (PDF) (4 pp, 237K)
- DOE -- Summary of Capillary Pressure Models (6/15/12) (PDF) (1 p, 38K)
- EPA -- (E-mail) Concurrence with proposed data ranges and values for PCS-2012 PA (6/19/12) (PDF) (1 p, 38K)

- DOE -- (Report) Analysis Plan for the 2012 WIPP Panel Closure System Performance Assessment (7/2/12) (PDF) (18 pp, 186K)
- DOE -- (Report) Generation of the LHS Samples for the AP-161 (PCS-2012) Revision 0 PA Calculations (9/6/12) (PDF) (172 pp, 2,111K)
- DOE -- (Report) Analysis Package for the Salado Flow Modeling Done in the AP-161 (PCS-2012) Performance Assessment (9/17/12) (PDF) (71 pp, 5,789K)
- DOE -- (Report) Analysis Package for Direct Brine Releases: 2012 Panel Closure System Performance Assessment (PCS-2012 PA) (10/1/12) (PDF) (32 pp, 1,311K)
- DOE -- (Report) CCDFGF Analysis Package for the AP-161 (PCS-2012) Performance Assessment (10/15/12) (PDF) (30 p, 6,686K)
- DOE -- (Report) Sensitivity of the AP-161 (PCS-2012) PA Releases to Parameters (10/15/12) (PDF) (34 pp, 858K)
- DOE -- (Report) Summary Report and Run Control for the 2012 WIPP Panel Closure System Performance Assessment (11/5/12) (PDF) (84 pp, 4,163K)

December 2012 Informal Public Meeting Materials (Carlsbad & Santa Fe, NM)

- DOE -- Fact Sheet: Proposed Panel Closure Redesign Planned Change Request (11/2012) (PDF) (2 pp, 213K)
- DOE -- Presentation: Panel Closure Redesign Planned Change Request (12/2012) (PDF) (9 pp, 487K)
- DOE -- Presentation: Performance Assessment of the WIPP Run-of-Mine Salt Panel Closure System (12/2012) (PDF) (22 pp, 1090K)
- EPA -- Presentation: WIPP Panel Closure Redesign Rulemaking (12/2012) (PDF) (7 pp, 140K)

EPA Meeting Minutes - Panel Closure Redesign
Informal Public meetings
December 2012

Carlsbad, 12/5/12

Mayor Janway:

- Carlsbad community values their involvement in all WIPP-related issues and view themselves as the primary and most important stakeholders.
- Stakeholders include all those that live in Carlsbad and the surrounding communities, and obviously those that work and are associated with the WIPP facility.
    - Are the interests of the true stakeholders being voiced and heard?
    - Are those opponents of WIPP-related issues simply trying to throw a wrench in the wheel, so to speak?
    - Are those in opposition to WIPP voicing legitimate concerns?
    - Incorporate lessons learned from oversight experience.
- Absolutely in-favor of panel closure planned change request, based on scientific and economic merit.

Jon Edwards/EPA:

- Show of interest is very impressive and appreciative.
- Three things to keep in mind:
    - These informal meetings are not required by our regulatory process, but we feel in our extensive experience that the early, informal feedback is the most beneficial to EPA.
    - In forming your comments, please really try and consider the technical/scientific/regulatory merits (positive and negative) of the rule and planned change, as we need to make sure we are doing a robust review of the change in case of a legal suit.
    - Want to think about better ways to engage the stakeholders, especially in light of days of budget cuts and limited resources.

Farok Sharif, NWP:

- Level of interest from the senatorial and congressional staff is very informed and supportive of the WIPP project.
- Especially Lynn Ditto from Sen. Bingaman's office, who is retiring

Santa Fe, 12/6/12

Mayor David Coss:

- In favor any EPA activity that supports open and transparent government.
- WIPP issues are very important to Santa Fe, either via LANL or waste transportation.
- Equality in terms of stakeholder pool; in support of Carlsbad Mayor Janway as the city and its inhabitants are the most impacted by the site change.
- In support of DOE's panel closure redesign, when looking at scientific, technical, and economic merits.

Jon Edwards/EPA:

- *See Carlsbad remarks*

D. Hancock/SRIC:

- Believes having no cost analysis is a deficiency.
- Why the ROMPCS given the other options, some of which were brought up by DOE in the past?
  - R. Patterson/DOE:
    - We looked at all the options again, and in our review DOE felt this was the best option to put forward at this time.
- Is there a summary of some of the other previous options submitted?
  - R. Patterson/DOE:
    - There is information on Options A – E in the CCA.

S. Kovac/NW:

- What are the specifications that DOE cannot adhere to with the Option D design?
  - R. Patterson/DOE:
    - This information is outlined in more detail in DOE's panel closure redesign planned change request.

J. Greenwald/CARD:

- Earlier consulting reports focused on sludges in relation to explosions. Were these incorporated into the newest PA, including those projected wastes (including RH)? Does this take into account the shielded containers. I would think that the use of shielded containers would lead to more RH in the waste panels, which would lead to more gas generation.
  - B. McInroy/DOE:
    - Yes, the parameters have remained the same. The annual report was published in October and is on our website. Section 3 of the report (and Appendix A & B) have the information you are looking for.
  - C. Camphouse/DOE:
    - This PA comparison was only from the PABC-2009. It does not take into account other planned change requests since that time.
  - R. Patterson/DOE:
    - DOE takes no credit for containers in PA modeling.
  - S. Kouba/DOE:
    - We measured gases in those panels that were closed, including those panels that had more percentage of sludges. However, the methane and hydrogen gas generation did not significantly increase.

- K. Economy/EPA:
    - Anything that will be changed in the future, especially related to waste inventory, we will obviously consider those, particularly in the next recertification. However, the panel closure design, this new PCS-2012 only changed the parameters for panel closure. This was to create a simple, quantifiable comparison.

J. Heaton/Carlsbad:

- We have been looking at this issue for quite a long time, and the foremost issue in Carlsbad's perspective is worker safety. Gas (hydrogen & methane) generations are not at the level of a combustible level, which was the intent of the original explosion walls in the Option D design. The cost difference between the two options is over a magnitude of ten, not including other safety factors and interruptions in waste disposal operations.
    - J. Greenwald/CARD:
        - I don't believe that DOE has gone up to speed on RH waste projections, and I am concerned about how this potential waste (e.g., shielded containers) will affect the PA.
    - T. Peake/EPA:
        - All of the regulatory limits for RH (and CH) are already being modeled in the PA.

J. Arends/CCNS:

- Wants to thank WIPP site for sending a copy of the permit mod.
- The most recent NMED permit mod (class 3) says that the costs associated with Option D would only be about $1.4 million, as opposed to tens of millions of dollars.

D. Sepic/Carlsbad:

- Extensive experience in mining, including the properties of salt and its healing/creep closure properties. I have friends and family that work and live in WIPP. I trust them more than any scientist. This new panel closure system is better than the Option D design (which had some flaws). The ROMPCS is a much better design and is definitely more cost effective. The pricing of concrete has more that doubled, and there is a shortage of concrete, all of which are issues. The total cost of implementation not only includes the concrete, but also all of the labor, mechanics, safety, and disposal operations are what creates a number into the millions of dollars. From a worker standpoint, the new panel closure design is a great change.
    - K. Economy/EPA:
        - I want to clarify that EPA is primarily concerned about the long-term performance. Is DOE modeling all of the factors

in a realistic manner as they relate to long-term performance. Cost issues are of no significance to us.

- CARD: Can you define long-term performance?
  - T. Peake/EPA:
    - Long-term performance is from facility closure to 10,000 years.
- CARD: Has the PA been peer reviewed? What about FEPs (e.g., earthquakes, etc.) in the models?
  - C. Camphouse/DOE:
    - PA calculations have been scrutinized heavily over the years. FEPs are included as part of the PA calculations.

D. Hancock/SRIC:

- Clarification on the 60-day comment period and on the public meetings?
  - J. Walsh/EPA:
    - We will get more input from OGC on the exact specifications, but there will be at least a 30-day comment period and informal meetings.
- I prefer the previous roundtable formats as opposed to the type of meeting we are having here today.

J. Heaton/Carlsbad:

- What about the timing of the recertification and panel closure rule?
  - T. Peake/EPA:
    - We are hoping to have this rule finalized before submittal of the next recertification in March 2014.

S. Kovac/NW:

- Gas generation levels are below explosion levels?
  - J. Walsh/EPA:
    - That is correct. There is a paper on EPA's website submitted by R. Nelson that deals with some of that data.
  - D. Hancock/SRIC:
    - You should ask that question at the pre-submittal permit mod meeting in two weeks.

D. Hancock/SRIC:

- Where is DOE in terms of producing additional information required as part of EPA's shielded container approval (e.g., procedure for showing that shipping dosnt' increase surface dose rate)? What is the time frame on DOE's submittal?
  - T. Peake/EPA:
    - We have not seen anything, so we have not inspected anything. EPA will go on a site-by-site basis initially and

then after the initial inspection it will be rolled into the waste characterization CCP inspections process.

- S. Kouba/DOE:
  - We have drafted some procedures and are planning to move forward, possibly sometime in the spring 2013 time frame.

- We are hopeful that as things proceed all documents will be made available (website), as they have been in the past.

J. Greenwald/CARD:

- Is EPA's radiation model still "reference man?" Makhijani states in his report that women and children (and especially fetuses) are more susceptible to radiation. Trucks that transport the waste can stop anywhere, and we believe that the shielded containers will have more and multiple exposures. I don't see an analysis of this on any DOE document. Also, I'm concerned about the women that work underground at WIPP, including pregnant women. I understand that EPA is behind in some of the updates of regulations related to radiation exposure and that is of a big concern to me. DOE waste shipment drivers should only be allowed to park in designated overnight areas as well.
  - T. Peake/EPA:
    - "Reference man" is how EPA looks at radiological effects on members of the public. When it was first developed, it looked at the average male. We have had questions (most notably from A. Makhijani) about updating it to incorporate females, children, etc., since they would have different rates and effects. EPA is trying to look at more age-specific data and incorporate it into our newest models. DOE and NRC are also involved in trying to take the latest information on dosimetry/dose conversion factors and update our regulations.
  - R. Patterson/EPA:
    - There are some issues dealing with the permit lawsuit that I don't want to get into, but the idea of the shielded container is that the container will be handled just like CH waste. There will be no additional exposure. There is a written policy at WIPP for women and pregnant women (DOE has provided this to J. Greenwald).
- The limits of surface dose of CH waste is under 200 mrem/hour, correct? What would you say is an average number for a CH container?
  - S. Kouba/DOE:
    - All drums are measured at the site before they go underground for disposal.
  - T. Peake/EPA:

        - They have dose limiting factors at the WIPP site. If there is something higher than their action limit, then they mark it off.
    - CARD:
        - A lot of the public view EPA's regulations as the highest end of information, which influences a lot of other decisions in other fields.

D. Hancock/SRIC:

- Do you have any responses to the waste inventory questions I submitted to DOE? I would like a written response.
    - B. McInroy/DOE:
        - Yes, we have prepared a response and will be sent to you shortly. If there is an issue with how we do the calculations, there is not much I can do as that is how I was directed by management.
        - We are always looking to improve the report and improve clarity and readability. Can we put the information normally shown in Appendix C in the body of the report? That's why we created the comparison table where we combined this information. This report is to show what is out at the sites; the emplacement data is in the WDS.
- This is an EPA issue, because it is incomprehensible that EPA would continue to allow DOE to submit erroneous information (i.e., double-counting) in its WDS and other waste inventory information without explaining discrepancies to the public.
    - T. Peake/EPA:
        - EPA will look into the issue further and provide comments in the future.

J. Heaton/Carlsbad:

- I think the issue here is that NMED's permit gets their information differently, and there are no limits.
    - D. Hancock/SRIC:
        - It is stated in the LWA that the waste limits are by container.
- Where in the LWA does it say container?
    - D. Hancock/SRIC:
        - There are numerous DOE documents that say so.
    - B. McInroy/DOE: WDS has always counted internal container volume.

J. Greenwald/CARD:

- This is my perception of RH waste inventory and shielded containers. DOE has not been able to put RH waste in the repository to meet its goals by site closure. The shielded container will solve the problem because more RH waste will be able to be emplaced in each room. If DOE came

out and recognized this assertion it would change NMED's permit from a 2 to a 3. It looks like a ploy by DOE to just solve the RH waste inventory problem at WIPP. It feels like a game between the regulators and it is maddening as a member of the public.

D. Hancock/EPA:

- Action items have not been followed up on; please resolve them in an appropriate manner. Defense determinations have not been made available. There is atomic defense activity waste that cannot by definition come to WIPP. This defense determination documentation needs to be made public.
    - T. Peake/EPA:
        - Further resolution needed DOE's lawyers and EPA needs to look at it as well.

J. Arends/CCNS:

- Would like to reiterate that RH inventory is huge and needs to be resolved.

J. Greenwald/CARD:

- During the last recert, the culebra wellheads were rising and falling. What is the current status? Also, R. Boeheim stated this rising and falling was due to drilling, which EPA agreed with. Have there been any changes to this? In addition, Dr. Richard Phillips stated that this rising and falling was due to rainwater infiltration into the culebra and magenta. Is the fluctuation between the wellhead levels are still within the expected ranges since the last recertification?
    - K. Economy/EPA:
        - DOE's information was reviewed during the last recertification and EPA found it to be technically sound. There have been no changes or anomalies in the well head data found in the ASER reports, and as far as EPA is concerned we do not question any information they have provided. We consider the issue closed unless there is additional new information submitted.
    - R. Lee/J. Walsh/EPA:
        - Yes, the levels in the wellheads are still within the expected ranges.
    - T. Peake/EPA:
        - We do not believe karst is an issue, as we have concluded during the certification and subsequent recertifications.
    - J. Walsh/EPA:
        - The data reviewed by R. Boeheim and Dr. Phillips during the last recertification were from a higher resolution calibration and sensitivity of equipment.

K. Brown/Carlsbad:

- I would like to ask that any future meetings be held in Carlsbad related to the WIPP site, as that is where the most vested stakeholders live and work. I am concerned about costs regarding the site as I represent over 29,000 people. The panel closure proposal I believe is a better idea than Option D and I agree with D. Sepic's previous sentiments.

J. Heaton/Carlsbad:

- Every two weeks we have over 45 citizens meet to discuss WIPP issues, and it is a very engaged community, on a daily basis. We have a hard time understanding why EPA has meetings over 300 miles away regularly, when they should be primarily held in Carlsbad with the primary stakeholders. We don't understand these constant attacks on the WIPP site.

Department of Energy
Carlsbad Field Office
P. O. Box 3090
Carlsbad, New Mexico 88221

SEP 28 2011

Mr. Jonathan Edwards
U.S. Environmental Protection Agency
Office of Air and Radiation
401 M Street S.W.
Washington D.C. 20460

Subject: Transmittal of Planned Change Request for Panel Closure Redesign

Dear Mr. Edwards:

This letter and its enclosure provide the U.S. Department of Energy (DOE) Waste Isolation Pilot Plant (WIPP) panel closure redesign change request to the U.S. Environmental Protection Agency (EPA). The proposed panel closure redesign will modify Condition 1 of the Final Certification Decision for 40 CFR Part 194.

In the 12 years since the WIPP facility commenced waste disposal operations the DOE has acquired considerable experience and knowledge regarding the behavior of the repository, and the nature and behavior of disposed transuranic (TRU) waste, including the potential for generation of explosive gases. Condition 1 of the Final Certification Decision for 40 CFR Part 194 specifies that the panel closure system (PCS) to be used in the WIPP repository be "Option D" as specified in the Compliance Certification Application (CCA). The Option D specified that certain components be constructed using Salado Mass Concrete (SMC).

Large scale testing has demonstrated that using SMC cannot meet the design and performance requirements for the panel closures as specified in the CCA. The results from monitoring for explosive gases in the closed panels has established that the measured concentrations of methane and hydrogen will remain below the lower explosive limits for these gases through the operational period. Based on these results, a new panel closure design identified as Run-of Mine Panel Closure (ROMPC) has been developed.

A performance assessment (PA) has been performed to evaluate the impacts of the ROMPC on the current compliance baseline. The results of the PA show that this change has essentially the same performance as the Option D design and that the WIPP will remain in compliance with the disposal requirements in 40 CFR Part 191, Subparts B and C.

In summary DOE is requesting that EPA modify Condition 1 of the Final Certification Decision for 40 CFR Part 194 by replacing the current panel closure design with the proposed design.

SEP 2 8 2011

If you have any questions regarding this request, please contact Russell Patterson at (575) 234-7457.

Sincerely,

Edward Ziemianski
Interim Manager

Enclosure

cc: w/enclosures

R. Lee, EPA	*ED
K. Economy, EPA	ED
S. Ghose, EPA	ED
J. Walsh, EPA	ED
N. Elkins, LANL	ED
T. Peake, EPA	ED
P. Shoemaker, SNL	ED
F. Sharif, WTS	ED
R. Chavez, RES	ED
S. Kouba, RES	ED
CBFO M&RC	

*ED denotes electronic distribution

DOE/CBFO-11-3479

Panel Closure System Design

Planned Change Request to the

EPA 40 CFR Part 194 Certification of

the Waste Isolation Pilot Plant

September 26, 2011

Table of Contents

Acronyms ii
Glossary of Terms iii
Executive Summary iv
1.0 Introduction 1
1.1 PCS Background 2
2.0 Nature and Scope of This Request 3
2.1 Scope of the Proposed Design Change 3
2.2 Rationale for the Proposed Request 4
3.0 Long-Term Performance of the ROMPC 7
3.1 Earlier Panel Closure Investigations 7
3.2 Recent PA Analysis 8
3.3 Results from the PC3R PA 11
4.0 Conclusions 13
References 14

Attachment A: *Radiolytic Hydrogen Generation and Methanogenesis in WIPP: An Empirical Point of View*
Attachment B: *Effective Permeability of the Redesigned Panel Closure System*
Attachment C: *Summary Report for the AP-151 (PC3R) Performance Assessment, Revision 1*

Acronyms

CBFO	Carlsbad Field Office
CCA	*Title 40 CFR Part 191 Compliance Certification Application for the Waste Isolation Pilot Plant* (DOE, 1996)
CCDF	Complementary Cumulative Distribution Function
CFR	*Code of Federal Regulations*
DOE	U.S. Department of Energy
DRZ	Disturbed Rock Zone
EPA	U.S. Environmental Protection Agency
NMED	New Mexico Environment Department
OPC	Ordinary Portland Cement
PA	Performance Assessment
PABC	Performance Assessment Baseline Calculations
PAVT	Performance Assessment Verification Test
PCS	Panel Closure System
PCR	Planned Change Request
PC3R	Panel Closure Redesign and Repository Reconfiguration Performance Assessment
RCRA	Resource Conservation and Recovery Act
ROM	Run-of-Mine
ROMPC	Run-of-Mine Panel Closure
SMC	Salado Mass Concrete
TRU	Transuranic
VOC	Volatile Organic Compound
WIPP	Waste Isolation Pilot Plant

Glossary of Terms

40 CFR Part 191	Environmental Radiation Protection Standards for the Management and Disposal of Spent Nuclear Fuel, High-Level and Transuranic Radioactive Wastes; Final Rule (EPA, 1993).
40 CFR Part 194	Criteria for the Certification and Re-Certification of the Waste Isolation Pilot Plant's Compliance with the 40 CFR Part 191 Disposal Regulations: Certification Decision; Final Rule (EPA, 1998a).
Certification	Any action taken by the Administrator of the U.S. Environmental Protection Agency under Section 8(d) of the Waste Isolation Pilot Plant Land Withdrawal Act.
Run-of-mine (ROM) salt	Salt produced from mining operations in the WIPP facility underground without undergoing any additional treatment.

Executive Summary

The U.S. Department of Energy (DOE) Carlsbad Field Office (CBFO) requests that the U.S. Environmental Protection Agency (EPA) modify Condition 1 of the Final Certification Rulemaking for 40 CFR Part 194 (EPA, 1998a). This condition specifies that the Panel Closure System (PCS) to be used in the Waste Isolation Pilot Plant (WIPP) repository should be the one designated as "Option D" in the Compliance Certification Application (CCA) (DOE, 1996), and that the concrete components of that closure should be constructed using Salado Mass Concrete (SMC). In the 12 years since the WIPP facility commenced waste handling operations the DOE has acquired considerable experience in the behavior of the underground, and in the nature and behavior of disposed transuranic (TRU) waste, including the potential for generation of explosive gases. In addition large scale testing has demonstrated that SMC cannot meet the design requirements for the closure as specified in the original certification application (WTS, 2003). The DOE has established a revised design which is much simpler and easier to construct. Accordingly the DOE is requesting that Condition 1 be changed, and that the new closure design be approved for use in all panels.

The DOE is making this proposal based on the following rationale:

The primary purpose of the PCS is to meet the Resource Conservation and Recovery Act (RCRA) requirements for closure of a disposal unit as defined in the WIPP Hazardous Waste Facility Permit (Permit). As noted in the CCA (Section 3.3.2), "Panel closures have been included for the purpose of Resource Conservation and Recovery Act (RCRA) disposal unit closure and to prevent potentially unacceptable levels of volatile organic compound release during waste management operations."

The panel closure system was not designed or intended to support long-term repository performance. However it is important to be able to represent the long-term behavior of the closure system in performance assessment (PA) calculations, in so far as it affects the flow of brine between waste panels under the various PA scenarios.

Attempts to develop SMC have shown that the material as specified did not meet the performance requirements laid out in the design specifications (WTS, 2003).

The simpler design will meet the same operational performance requirements of the Option D closure and will be simpler construction, will have less adverse impact on waste disposal operations and will be less expensive to construct.

The analyses provided with this planned change request (PCR) demonstrate that long-term releases are insensitive to a broad range of panel closure permeabilities, and that the impact of the proposed new closure design on long-term performance is negligible.

The revised design, known as the Run-of-Mine Panel Closure (ROMPC) comprises 100 ft of run-of-mine (ROM) salt backfill placed between two typical underground bulkheads. The construction methods and materials to be used to implement the design have been proven in previous mining and construction projects. The fabrication, installation, and maintenance of bulkheads are standard mining practices. The ROM salt backfill will be pushed up tight to all salt

surfaces of the drifts, including the back or roof. Over time creep closure of the drifts will cause the salt backfill to consolidate to a condition approaching intact salt with a low permeability.

Performance Assessment (PA) results demonstrate that the long-term performance of the revised design will be essentially the same as that to be expected from the Option D closure. Based on an analysis of creep and salt consolidation data, the permeability of the ROMPC is expected to fall within the range analyzed in earlier PAs. That is the short-term permeability might be high, but after 100 years, as the salt backfill consolidates further under the influence of creep closure of the entries, the permeability will approach that assumed for the Option D closure. A recent PA termed the Panel Closure Redesign and Repository Reconfiguration Performance Assessment (PC3R) has been run which combines a proposed reconfiguration of the repository as well as the modified panel closure system. Comparison of the PC3R results with that included in the most recent recertification (PABC-2009; DOE, 2009) indicated that the overall mean complimentary cumulative distribution functions (CCDF) obtained in the two analyses are virtually identical. The panel closure design and repository configuration changes investigated in the PC3R PA therefore have only a very minor impact on performance. It is also noted that the results of an earlier impact analysis in which a panel closure system consisting of 100 ft of ROM salt and a 30 ft explosion wall give a similar result (Vugrin and Dunagan, 2006). In this PA it was assumed that the explosion wall had no influence on long-term permeability which was given the same values as in PC3R. These results indicated that without the reconfiguration included in the PC3R PA the change in panel closure design had only a minor effect on long-term performance.

Based on these analyses and results, the DOE is requesting that the EPA remove Condition 1 as presented in the Final Rule (EPA, 1998a), and accept the revised design for panel closures as described herein.

1.0 Introduction

The U.S. Department of Energy (DOE) Carlsbad Field Office (CBFO) is submitting this Planned Change Request (PCR) to the U.S. Environmental Protection Agency (EPA) to request modification of Condition 1 of the Final Certification Rulemaking for 40 CFR Part 194.

Specifically, the Final Certification Rulemaking, Appendix A (EPA, 1998a), states:

In accordance with the Agency's authority under 194.4(a), the certification of compliance is subject to the following conditions:

Condition 1: 194.14(b), Disposal system design, panel closure system. The Department shall implement the panel seal design designated as Option D in Docket A-93-02, Item II-G-1 (October 29, 1996, Compliance Certification Application submitted to the Agency). The Option D design shall be implemented as described in Appendix PCS of Docket A-93-02, Item II-G-1, with the exception that the Department shall use Salado mass concrete (consistent with that proposed for the shaft seal system, and as described in Appendix SEAL of Docket A-93-02, Item II-G-1) instead of fresh water concrete.

The Option D closure consists of the installation of a concrete block explosion isolation wall, removal of the majority of the disturbed rock zone (DRZ) in the area of the closure, and emplacement of a large Salado Mass Concrete (SMC) monolith. This closure would be installed in each panel of the repository after waste emplacement in that panel is completed.

In addition to specifying the use of the "Option D" Panel Closure System (PCS) design in Condition 1, the EPA allowed the DOE to revisit the design of the PCS. Specifically, in the preamble to the Final Certification Rulemaking (EPA, 1998a), the EPA stated:

Nothing in this condition precludes DOE from reassessing the engineering of the panel seals at any time. Should DOE determine at any time that improvements in materials or construction techniques warrant changes to the panel seal design, DOE must inform EPA. If EPA concurs, and determines that such changes constitute a significant departure from the design on which certification is based, the Agency is authorized under 194.65 to initiate a rulemaking to appropriately modify the certification.

Based upon 12 years of experience in the disposal of waste in the underground, including observation and monitoring of the behavior of active and closed panels, together with engineering issues associated with Option D closure construction with SMC, the DOE has reassessed the engineering of the panel closure. As a result, the DOE has developed an alternate design which will not have an effect on the long-term performance of the repository, and will meet the requirements of the New Mexico Environment Department (NMED) in regard to operational period performance. Additionally, this new design will be simpler and can be installed at a significantly lower cost than the currently approved design. Accordingly, the DOE is requesting that this revised design be approved and Condition 1 of the 1998 Certification Decision be modified as appropriate.

The revised panel closure design, known as the Run-of-Mine Panel Closure System (ROMPC), was developed as part of CBFO's ongoing review of engineering aspects of the repository. The

design involves the use of bulkheads at either end of a 100 foot backfill comprised of run-of-mine (ROM) salt. The ROM salt backfill will be pushed up tight to all salt surfaces of the drifts, including the back or roof.

Section 2.0 of this request provides a description of the nature and scope of the proposed change to the design of the closure system. Section 3.0 provides an analysis of the long-term performance of the repository using this design, and discusses the results of recent performance assessment (PA) calculations which evaluate this performance. The analyses provided with this request demonstrate that long-term repository releases are unchanged over a broad range of panel closure permeabilities, and that the impact of the proposed new closure design on long-term performance is negligible relative to the performance of the Option D design.

In addition, three attachments are included with this request. Attachment A, *Radiolytic Hydrogen Generation and Methanogenesis in WIPP: An Empirical Point of View* summarizes monitoring data from closed panels, and Attachment B, *Effective Permeability of the Redesigned Panel Closure*, describes the expected behavior of the ROMPC in the context of the modeling results. Attachment C, *Summary Report for the AP-151 (PC3R) Performance Assessment Revision 1*, provides the results of the recent PA calculations conducted to demonstrate the performance of this closure.

1.1 PCS Background

The Compliance Certification Application (CCA: DOE, 1996) in Chapter 3 and Appendix PCS established the purpose of installing panel closures. The introduction to the facility description in Chapter 3 states,

> *The DOE will close each panel of waste with a panel closure system to provide for operational protection of workers, the public, and the environment from emplaced waste.*

In addition, Section 3.3.2 states:

> *Panel closures have been included for the purpose of Resource Conservation and Recovery Act (RCRA) disposal unit closure and to prevent potentially unacceptable levels of volatile organic compound release during waste management operations. The panel closure system was not designed or intended to support long-term repository performance.*

In the design report included in the CCA as Appendix PCS several designs were presented (Options A – D). These designs were to be used depending on the age and condition of the panel entries. The design report specified the use of Ordinary Portland Cement (OPC) for the concrete elements, but allowed the use of Salado Mass Concrete (SMC) as an option. SMC is a salt saturated concrete developed for use in the Shaft Seals and described in Appendix SEAL of the CCA. As noted above, in its Final Rule (EPA, 1998a) the EPA specified the use of Option D for all closures, and also the use of SMC rather than OPC.

During a series of test pours, it was determined that SMC as formulated would not be able to meet the specification requirements in the design report (WTS, 2003). As a result the DOE has, with the approval of EPA and NMED, emplaced temporary closures in various filled panels while gathering

information for a revised final closure. Panels 1 and 2 have used the explosion wall component from Option D, combined with periodic monitoring and assessment of the closure performance. Panels 3 – 4 use a simpler temporary closure comprising a ventilation bulkhead and a substantial barrier. These simpler closures have been used, again with the approval of EPA and NMED, to allow monitoring of potential explosive gas generation in the closed panels. This monitoring has established that the measured concentrations of methane and hydrogen are far below the minimum explosive concentrations for these gases, thereby allowing simplification of the design which is presented here (Attachment A). Panel 5 is currently undergoing closure, beginning with the explosion wall component. Option D continues to be the WIPP baseline panel closure design while the EPA considers this PCR.

2.0 Nature and Scope of This Request

2.1 Scope of the Proposed Design Change

The proposed design change presented here affects only the design of the panel closure system, as detailed in Condition 1 of the Final Certification (EPA, 1998a) and in the Permit (NMED, 2010) issued by the NMED. Condition 1 currently prescribes the installation of Option D with SMC. This design consists of emplacing a 12-foot concrete block explosion wall, removing most of the DRZ in the area of the closure, and emplacing a large concrete monolith (26 feet long). The concrete monolith would be keyed into the surrounding salt and the upper concrete/salt interface would be grouted. Figure 1 is a schematic representation of Option D provided in the CCA, Attachment PCS (DOE, 1996).

During the time since the initial certification of the WIPP facility, the DOE has reviewed various aspects of the required design and as a result has developed a new design which will be, easier to install, and less expensive while still achieving the performance objectives of protecting workers, the public and the environment. Information developed during this period include the testing of the SMC formulation specified in the CCA, Appendix SEAL and the development of a monitoring program to establish whether explosive concentrations of gas could develop in closed panels. The SMC testing (WTS, 2003) showed that the material as specified could not meet the performance requirements outlined in Appendix PCS, while the gas monitoring has shown that neither methane nor hydrogen concentrations approach anywhere near the lower explosive limits of these gases (Attachment A). Specifics of the rationale for the design change are given in the next section.

As a result of these activities, as well as the monitoring of the repository performance during its 12 years of operation, it has been determined that a simpler design is appropriate, and will be equally effective in meeting the performance requirements of the closure system. The ROMPC, shown in Figure 2, has two components: two bulkheads and a ROM salt backfill. The construction methods and materials to be used to implement the design have been proven in previous mining and construction projects. The ROM salt backfill will be pushed up to be in contact with the salt surfaces of the drifts, including the back or roof. A variety of techniques are available for placing the ROM salt. The bulk of the salt can be placed using load-haul-dump units and final placement against the back could use flingers or blowers. The ROM salt will be placed until the entire drift is filled over a minimum distance of 100 feet. Over time, creep closure of the drifts will ensure that the salt backfill consolidates to a condition approaching intact salt with a low permeability (Attachment B). The fabrication, installation, and maintenance

of ventilation bulkheads, such as those proposed for the closure, are standard practices at the WIPP facility.

2.2 Rationale for the Proposed Request

The CBFO is making this proposal based on the following rationale:

The primary purpose of the PCS is to control volatile organic compound (VOC) emissions during the operational life of the facility. The panel closure system was not designed or intended to support long-term repository performance. However it is important to be able to represent the long-term behavior of the closure system in performance assessment (PA) calculations, in so far as it affects the flow of brine between waste panels under the various PA scenarios.

Attempts to develop SMC have shown that the material as specified did not meet the performance requirements in Appendix PCS if prepared according to the specifications in Appendix SEAL (WTS, 2003).

An evaluation of the construction means and methods required to emplace Option D have determined that it will be hazardous to those involved in its construction, while the proposed simpler design will meet the same operational performance requirements of this closure (NMED Attachment G, see G-1e(1)).

The design of the ROMPC reduces complexity, enhances constructability, reduces the impacts on on-going repository operations, and reduces construction cost.

The analyses provided with this request, discussed in Section 3, and Attachment C, demonstrate that long-term releases are insensitive to a broad range of panel closure permeabilities, and that the impact of the proposed new closure design on long-term performance is negligible relative to the performance of the Option D design.

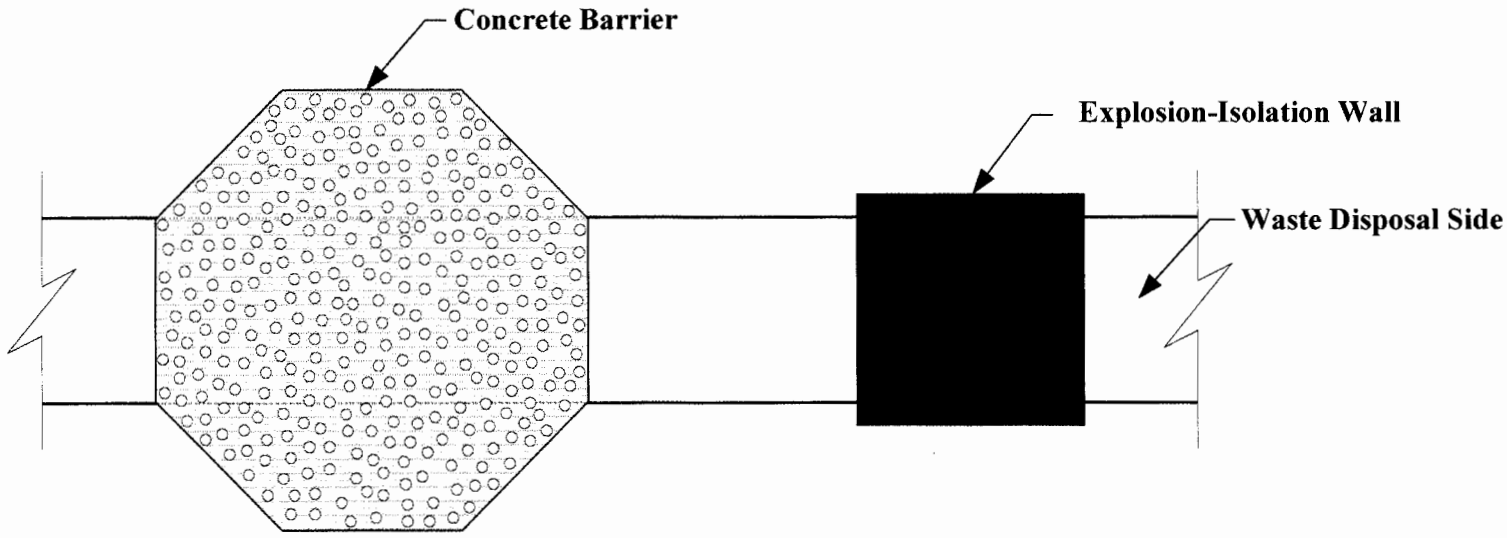

Figure 1. Option D Panel Closure System

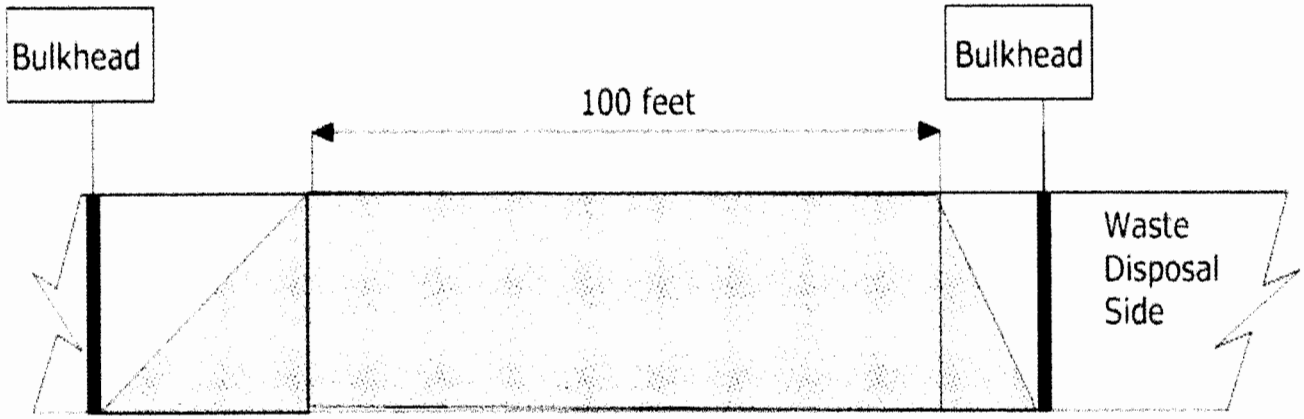

Figure 2: Proposed Run of Mine Panel Closure

3.0 Long-Term Performance of the ROMPC

3.1 Earlier Panel Closure Investigations

During the certification process in 1996 for the CCA, the CBFO used a model for the PA calculations with equal panel closure and DRZ permeability of 10^{-15} m^2 to demonstrate compliance with 40 CFR Part 191, Subparts B and C. As part of the EPA certification decision, a second EPA-mandated PA was run, the Performance Assessment Verification Test (PAVT) (McKinnon and Freeze, 1997a and 1997b) in which the panel closure retained a permeability of 10^{-15} m^2, but the DRZ was represented by a permeability which could vary between $10^{-12.5}$ and $10^{-19.4}$ m^2. The Option D panel closure design, mandated by EPA in Condition 1 of its certification of the WIPP in 1998, was not explicitly represented in the PA for the CCA or for the PAVT.

The Option D panel closure was introduced explicitly in an impact assessment in 2002 (Hansen, 2002). This assessment analyzed the panel closure's effects on repository performance. In this analysis, two panel closure cases were considered: one case represented the mandated Option D panel closure design, and a second case is based on the generic panel closure included in the PAs conducted for the CCA and the PAVT. The primary distinction between these two panel closure cases is the permeability of the panel closure material, which is quite low in the case of the Option D panel closure to fairly permeable in the CCA and PAVT panel closure case.

This impact assessment used the PAVT grid and developed an effective permeability for the panel closure. This effective permeability is a combination of the permeability for the concrete monolith and the open drift/explosion wall permeabilities surrounding the monolith. The concrete permeability was assigned a constant value equal to the mode of the distribution for SMC, 1.78×10^{-19} m^2. The effective permeabilities, the porosity, and the initial brine saturation of the two closures are shown in Table 1. It was found that releases for the Option D panel closure case and for the CCA/PAVT panel closures were nearly identical. This analysis concluded that releases from the repository were not sensitive to the permeability of the panel closures (Hansen 2002, Executive Summary).

Table 1. Effective Panel Closure Properties for the Panel Closure Impact Assessment.

Parameter	CCA/PAVT Closure	Option D Closure
Permeability (along the drift)	10^{-15} m^2	9.01×10^{-19} m^2
Permeability (perpendicular to the drift)	10^{-15} m^2	1.93×10^{-13} m^2
Porosity	0.075	0.15
Initial Brine Saturation	0.99	0.21

The results of this modeling established the long-term performance of the repository within a broad range of permeabilities for different panel closure configurations. Modeling completed with the Option D design represents a low-permeability closure, and the original PA results for the CCA and PAVT represented a high-permeability closure.

Based on an analysis of creep closure and salt consolidation data (Attachment B), the long-term permeability of the ROMPC is expected to fall near a value analyzed in the impact assessment. Within the first 100 years after closure installation, the effective permeability would be relatively high, but after 100 years, as the salt backfill consolidates further under the influence of creep

closure of the entries, the permeability will fall near the value assumed for the Option D closure in the 2002 PA. For this reason the influence of the ROMPC design on long-term repository performance is expected to be negligible, similar to the results for other closure designs assumed in earlier PAs. This result is again confirmed by the most recent PA calculations, as discussed below.

3.2 Recent PA Analysis

The DOE is in the process of submitting two PCRs to the EPA that propose changes to the repository. The first PCR is that discussed here, centered on the new design of the WIPP panel closure system. The second PCR (DOE, 2011) proposes the relocation of future waste panels 9 and 10 to the south end of the repository (i.e. south of panels 4 and 5) where they will be denoted as panels 9A and 10A. With panels 9 and 10 relocated, the current repository configuration will be modified to one with an open central drift area with panel closures installed only at the end of filled waste panels. In order to evaluate the effects of these changes on long-term performance, the DOE has conducted a single PA, called the PC3R PA, to determine the overall impact of the repository changes proposed in the two PCRs. Impacts of these changes are determined by way of a comparison of normalized releases and probabilities to those calculated in the current PA baseline from the second recertification application (DOE, 2009), called the Performance Assessment Baseline Calculation-2009 (PABC-2009) (Clayton et. al., 2009). The results from the PC3R PA and a comparison with the PABC-2009 are discussed in Camphouse et al., 2011 "*Summary Report for the AP-151 (PC3R) Performance Assessment, Revision 1*" which is included as Attachment C, and the results are briefly summarized here.

In the PC3R PA Panels 9 and 10 are relocated south of panels 4 and 5 and are denoted as panels 9A and 10A. This new configuration is shown in Figure 3. In addition to this reconfiguration, the PC3R PA changes the representation of the panel closures for panels 1through 8, 9A, and 10A. Panel closures are proposed to be modified from the current "Option D" design to that of a new design consisting of 100 feet of ROM salt emplaced in front of a bulkhead on the waste disposal side. The majority of PC3R PA parameter changes are due to the changes in the panel closure design, as discussed below.

The PC3R PA representation of the panel closure system has initial and short-term permeabilities and porosities that are significantly different from the permeabilities and porosities expected to be present for the vast majority of the 10,000 year regulatory timeframe. The short-term permeability of the panel closures is assumed to be controlled by the bulkheads at either end of the ROM salt backfill, and will have a high value, assumed to be 10^{-11} m^2. It is assumed that this permeability value will remain in effect for an initial time period of 100 years after closure. This initial time period is selected to be consistent with the length of time required for the porosity of the ROM salt used in the panel closures to consolidate to less than 5 percent, and is based on numerical simulations which have demonstrated this period of time to be less than 100 years (Callahan and DeVries, 1991). This time duration is also consistent with that proposed during the impact assessment for the 2002 panel closure redesign (Hansen and Thompson, 2002: Attachment B).

The permeability of the panel closure after 100 years is assumed to have decreased significantly due to the consolidation of the ROM salt driven by the creep closure of the entries. The values used for this permeability have been based on a panel closure redesign impact assessment performed in 2006 (Vugrin and Dunagan, 2006). In that analysis, the panel closure design consisted of 100 feet of ROM salt emplaced against a 30-foot mortared, solid concrete block wall on the waste disposal side. The parameter distributions for the long-term permeability of the ROM salt component developed during the impact assessment in 2006 (Vugrin, Hansen, and Thompson, 2006) are used to describe the long-term permeability of the panel closure implemented in the PC3R PA. The resulting probability distribution is shown in Table 2.

The value for permeability of the portion of the DRZ directly above and below the panel closure system is based on the analysis of Stein (2002). In the PC3R analysis the properties of this portion of the DRZ were prescribed so as to reflect the changing material properties of the redesigned closure system as a function of time. During the first 100 years while the ROM salt panel closures are reconsolidating, it is assumed that the DRZ directly above and below the panel closure is unaffected by the changing panel closure properties. Values used in this time frame are given in Table 2. After the first 100 years, permeability values of the DRZ above and below the panel closure are prescribed so as to be consistent with the permeabilities of the reconsolidated panel closures; that is, it is assumed that the creep closure which consolidates the ROM salt also leads to backpressure that facilitates the healing of the DRZ. As a result, the DRZ permeabilities around the closure are assigned the permeability distributions given to material PCS_T2 as shown in Table 3.

Table 2: Log of Intrinsic Permeability Values used for the DRZ-PCS around the PCS in the PC3R PA for the first 100 years.

Parameter (units)	Description	Distribution	Statistic	Value
DRZ_PCS:PRMX_LOG ($\log(m^2)$) DRZ_PCS:PRMY_LOG ($\log(m^2)$) DRZ_PCS:PRMZ_LOG ($\log(m^2)$)	Log of intrinsic permeability, x,y,z directions	Triangular	Mean	-16.0
			Median	-16.0
			Stan. Deviation	2.0
			Minimum	-19.4
			Maximum	-12.5

Table 3: Log of Intrinsic Permeability Values used for the long-term PCS in the PC3R PA

Parameter (units)	Description	Distribution	Statistic	Value
PCS_T2:PRMX_LOG ($\log(m^2)$) PCS_T2:PRMY_LOG ($\log(m^2)$) PCS_T2:PRMZ_LOG ($\log(m^2)$)	Log of intrinsic permeability, x,y,z directions	Triangular	Mean	-20.2
			Mode	-20.2
			Stan. Deviation	1.06
			Minimum	-22.8
			Maximum	-17.6

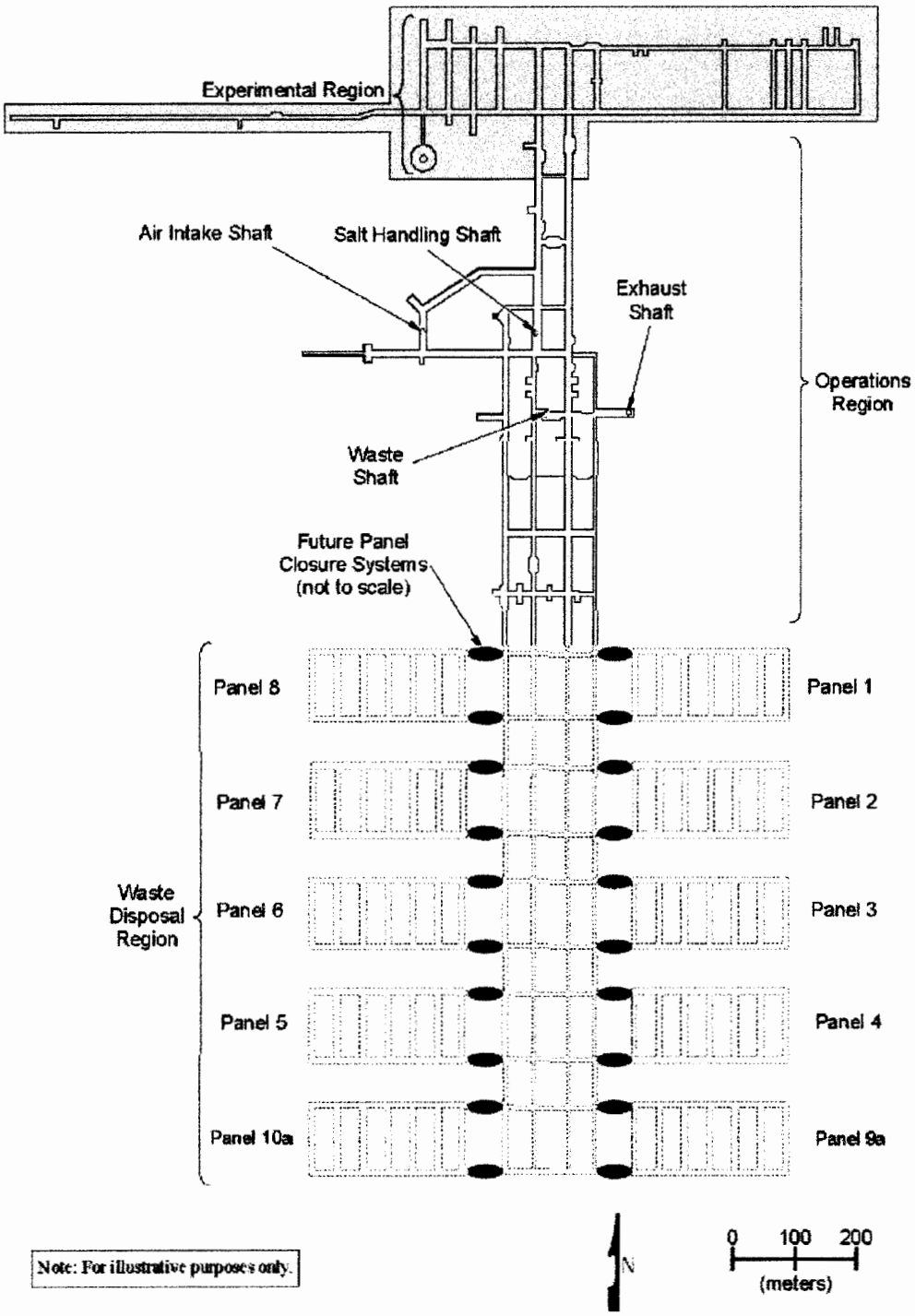

Figure 3: WIPP Layout Modeled in PC3R PA

3.3 Results from the PC3R PA

The total normalized releases for the PC3R PA, which combines the proposed reconfiguration of the repository and the modified panel closure system, are represented in Figure 4 as a mean CCDF. This figure also presents the results of the most recent recertification PA (PABC-2009, Clayton et al., 2009) which used the Option D panel closure design. As seen in that figure, the total mean normalized releases obtained in the two analyses are virtually identical for normalized release values less than approximately 0.1 EPA units. For normalized releases between 0.1 and 1.0 EPA units, the overall total release mean CCDF curve obtained in the PC3R PA is slightly above that calculated in the PABC-2009. For releases greater than 1 EPA unit, the CCDF curve obtained in the PABC-2009 is higher than that found in the PC3R PA. The results from the PC3R PA demonstrate that the cumulative changes for the new panel closure design and for the revised repository configuration produce only slight changes in total mean normalized releases relative to the current PA baseline, the PABC-2009. The small differences between the PABC-2009 and the PC3R PA are due to changes in direct brine releases, as discussed in Camphouse et al., 2011 (Attachment C).

A comparison of the statistics on the overall mean for total normalized releases obtained in the PC3R PA and the PABC-2009 can be seen in Table 4. At a probability of 0.1, values obtained for mean total releases are identical in both analyses. At a probability of 0.001, the decrease in direct brine releases (DBRs) in the PC3R PA results in a decrease in the mean total release by approximately 0.21 EPA units. Reductions are also seen in the upper and lower 95% confidence limits at a probability of 0.001 when compared to the PABC-2009 results.

Table 4: PC3R PA and PABC-2009 Statistics on the Overall Mean for Total Normalized Releases in EPA Units at Probabilities of 0.1 and 0.001

Probability	Analysis	Mean Total Release	90th Percentile	Lower 95% CL	Upper 95% CL	Release Limit
0.1	PC3R PA	0.09	0.16	0.09	0.10	1
	PABC-2009	0.09	0.16	0.09	0.10	1
0.001	PC3R PA	0.89	1.00	0.34	1.41	10
	PABC-2009	1.10	1.00	0.37	1.77	10

Finally it is noted that the results of the earlier impact analysis in which a PCS consisting of 100 ft of ROM salt and a 30 ft explosion wall also found that normalized releases were insensitive to the panel closure design (Vugrin and Dunagan, 2006). In this 2006 impact analysis, it was assumed that the explosion wall had no influence on long-term permeability of the panel closure system, and the ROM salt backfill had the same permeability values as in the PC3R PA. These results indicated that, without the reconfiguration included in the PC3R PA, the change in panel closure design had only a minor effect on long-term performance.

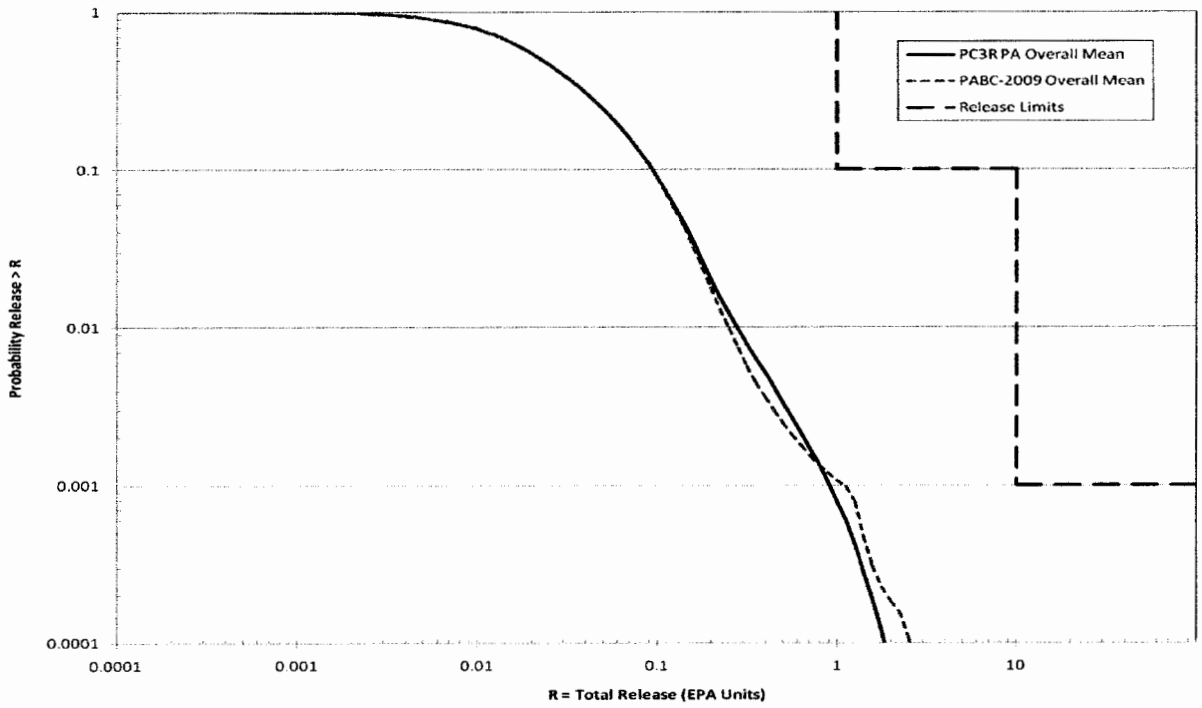

Figure 4: PC3R PA and PABC-2009 Overall Mean CCDFs for Total Normalized Releases

4.0 Conclusions

As a result of increased understanding of the repository and the stored waste obtained over 12 years of operation, the DOE has determined that a revision of the approved panel closure design can be made. The revised design described in this PCR will enhance constructability, reduce the impacts on on-going repository operations, and reduce construction cost. A change in the design specified in Condition 1 of the Final Rule (EPA, 1998a) is also required because of the problems in manufacturing SMC to the specifications in the CCA while meeting the design requirements of the Option D design.

An analysis of the results of earlier PAs suggests that this revised design will have essentially the same impact on long-term performance as the option D design. This is supported by new PA results in which the performance of the revised design is explicitly modeled, together with a proposed reconfiguration of Panels 9 and 10.

Based on these analyses and results, the DOE is requesting that the EPA remove Condition 1 as presented in the Final Rule (EPA, 1998a), and accept the revised design for panel closures as described herein.

References

Callahan, G.D. and K.L. DeVries. 1991. *Analysis of Backfilled Transuranic Waste Disposal Rooms*. SAND91-7052. Sandia National Laboratories, Carlsbad, New Mexico.

Camphouse, R. C., D. J. Clayton, D.J. Kicker, and J. J. Pasch. 2011. *Summary Report for the AP-151 (PC3R) Performance Assessment,* Revision 1, Sandia National Laboratories, Carlsbad, New Mexico, ERMS 555489.

Clayton, D.C., R. C. Camphouse, J. W. Garner, A. E. Ismail, T. B. Kirchner, K. L. Kuhlman, and M. B. Nemer. 2010. *Summary Report of the CRA-2009 Performance Assessment Baseline Calculation,* Revision 1, Sandia National Laboratories, Carlsbad, New Mexico, ERMS 553039.

DOE (U.S. Department of Energy). 1996. *Title 40 CFR Part 191 Compliance Certification Application for the Waste Isolation Pilot Plant*, DOE/CAO-1996-2184, U.S. Department of Energy, Carlsbad Area Office, Carlsbad, New Mexico.

DOE (U.S. Department of Energy), 2009. *Title 40 CFR Part 191 Compliance Re-Certification Application for the Waste Isolation Pilot Plant*, DOE/CBFO, U.S. Department of Energy, Carlsbad Field Office, Carlsbad, New Mexico.

DOE (U.S. Department of Energy), 2011. *Planned Change Request, Waste Isolation Pilot Plant Repository Reconfiguration*, U.S. Department of Energy, Carlsbad Field Office, Carlsbad, New Mexico.

EPA (U.S. Environmental Protection Agency). 1993. Environmental Radiation Protection Standards for the Management and Disposal of Spent Nuclear Fuel, High-Level and Transuranic Radioactive Wastes; Final Rule, *Federal Register*, Vol. 58, No. 242, pp. 66398-66416, December 20, 1993, U.S. Environmental Protection Agency, Office of Radiation and Indoor Air, Washington, D.C.

EPA (U.S. Environmental Protection Agency). 1998a. Criteria for the Certification and Re-Certification of the Waste Isolation Pilot Plants Compliance with the 40 CFR Part 191 Disposal Regulations: Certification Decision; Final Rule, *Federal Register*, Vol. 63, No. 95, pp. 27353-27406, May 18, 1998, U.S. Environmental Protection Agency, Office of Air and Radiation, Washington, D.C.

Hansen, C.. 2002. *Analysis Report for the Panel Closure Impact Assessment,* Revision 1, Sandia National Laboratories, Carlsbad, New Mexico, ERMS 523935.

MacKinnon, R. and G. Freeze. 1997a. *Summary of EPA-Mandated Performance Assessment Verification Test (Replicate 1) and Comparison with the Compliance Certification Application Calculations,* Revision 1, Sandia National Laboratories, Albuquerque, New Mexico, ERMS 422595.

MacKinnon, R. and G. Freeze. 1997b. *Supplemental Summary of EPA-Mandated Performance Assessment Verification Test (All Replicates) and Comparison with the Compliance Certification Application Calculations,* Revision 1, Sandia National Laboratories, Albuquerque, New Mexico, ERMS 414880.

NMED (State of New Mexico Environment department). 2010. *Hazardous Waste Facility Permit,* New Mexico Environment Department, Water and Waste Management Division.

Stein, J.S. 2002. Analysis Plan for Calculations of Salado Flow: Technical Baseline Migration (TBM) AP-086. Sandia National Laboratories, Carlsbad, New Mexico, ERMS 520612.
Vugrin, E.D. and S.C. Dunagan. 2006. *Analysis Package for the Impact Assessment of the Redesigned WIPP Panel Closure*. Sandia National Laboratories, Carlsbad, New Mexico, ERMS 543865.

Vugrin, E., F., Hansen, and B. Thompson.. 2006. Recommendation and Justification of Parameter Values Required for Representation of the Redesigned Panel Closure System, Memo to David Kessel dated March 23, 2006, Sandia National Laboratories, Carlsbad, New Mexico, ERMS 542894.

WTS (Washington TRU Solutions). 2003. *Salado Mass Concrete Test Program Final Report. Mine Engineering Repository Development Project*, Revision 1. July 17, 2003, Waste Isolation Pilot Plant, Carlsbad, New Mexico.

ATTACHMENT A

Radiolytic Hydrogen Generation and Methanogenesis in WIPP: An Empirical Point of View

ATTACHMENT A

Radiolytic Hydrogen Generation and Methanogenesis in WIPP: An Empirical Point of View

Radiolytic Hydrogen Generation and Methanogenesis in WIPP: An Empirical Point of View – 11040

R. A. Nelson
U.S. Department of Energy
PO Box 3090, Carlsbad, NM 88220

ABSTRACT

Geologic disposal of radioactive waste is internationally recognized as the most prudent management approach to the back end of the nuclear fuel cycle. Alpha-emitting isotopes in waste matrices containing hydrogenous materials generate radiolytic hydrogen, which must be managed to ensure concentrations never exceed flammability limits. In addition, past concerns have been raised that methanogenesis could also present explosion hazards during a geologic repository's operational lifetime.

Early (pre-operational) planning for the Waste Isolation Pilot Plant (WIPP) lead its original design to include explosion walls as part of the closure design in the event of a build-up of hydrogen or methane. This conservative approach simply assumed explosive gases could be present without detailed prediction of their concentration and extent. As the Department of Energy (DOE) emplaced waste after opening, the first two disposal panels were isolated from the ventilation circuit with the previously planned 4-meter thick explosion walls of robust concrete blocks. A separate requirement for an additional massive panel closure structure, which would make the closure system even more robust is also required, however a regulatory decision on their need is proposed for the near future.

When the third disposal panel was filled (WIPP plans a total of 10), DOE petitioned its primary repository regulators (The New Mexico Environment Department – NMED, and the Environmental Protection Agency – EPA) to allow monitoring of gases interior to the disposal panel in lieu of installing explosion walls. DOE argued that by routine monitoring, it could determine if flammable gases were building to potentially explosive levels or not. If concentrations approached action levels or if the monitoring system failed, DOE proposed to construct the explosion walls as originally conceived. This approach allowed DOE to conduct monitoring to potentially demonstrate that explosion walls, and eventually even more robust panel closures, might not be necessary for safe operation of the repository.

This paper describes the results of the first 3 years of hydrogen and methane monitoring in Panels 3 and 4 at WIPP. Flammable volatile organic compounds are also present in many of the waste streams emplaced at WIPP, but liquids are prohibited. Measurements of these flammable organic compounds are also made, but they play a minor role in the argument to eliminate explosion walls as part of the closure design at WIPP. Over 1000 air samples from all interior reaches of Panels 3 and 4 have been collected to date. Every single methane sample has been determined as "Non Detectable" at detection levels of about 30 parts per million. Radiolytically generated hydrogen in these same samples was typically found at levels in the few hundred parts per million, well below the action levels specified in the permit (~4 parts per thousand). The monitoring results indicate that the initial WIPP planning was overly conservative and that explosion walls and robust panel closures may not be needed during the operational lifetime of WIPP.

INTRODUTION

WIPP was constructed and its first disposal panel mined by the end of 1988. Although DOE considered WIPP ready for waste receipt, an 11-year period of regulatory licensing and permitting passed before the first shipment arrived for emplacement (1999). During this delay, several iterations of planning for final disposal panel closure resulted in a design for the panel closures that was based on very conservative assumptions [1].

With limited data on the expected concentrations of volatile organic compounds (VOCs) in the diverse array of transuranic (TRU) waste streams, and limited understanding of the potential for gas generation within the waste, conservative calculations resulted in a proposed design that included a massive concrete structure to be placed in the inlet and outlet drifts of each disposal panel. An assumed potential for a build-up of explosive gases within each panel also led to the proposal to install a massive explosion wall that would itself protect the panel closure from the blast effects so that the closure would continue to serve as a barrier to the VOCs.

In retrospect, these very conservative assumptions and calculations now appear unnecessary. It is prudent to re-examine the need for such robust structures to avoid cost and industrial accident vulnerability. Based on all the monitoring (both within the waste drums before ever shipping to WIPP, and monitoring of conditions in the filled disposal rooms of the repository), it is likely that a much lower cost closure can protectively serve the purpose.

GAS GENERATION MECHANISMS

This section describes the 3 primary sources of flammable gases that might pose a risk to WIPP workers and, to a much lesser extent, potentially exposed members of the public.

Potential Sources of Hydrogen

Hydrogen can be generated by two widely different radiological and chemical processes:

1) Radiolysis (ionizing radiation breaks bonds as it slows in hydrogenous materials), and
2) Corrosion of iron based materials under inundated conditions (no oxygen present).

Of the three primary types of ionizing radiation, radiolytic production of hydrogen is dominated by alpha radiation because of its high energy deposition rate as the alpha particles slow down in a solid matrix. This high energy deposition rate also comes with a short stopping range. The reader may recall their high school physics lesson when shown that a piece of paper is adequate to shield from alpha radiation. All the hydrogen bonds that the alpha particle can break are in the first few microns of the sheet of paper because the alpha radiation does not penetrate further into the solid. This short range also leads to another attribute of radiolysis in a solid matrix that is typically ignored. Because there is no physical movement of the matrix to expose new hydrogen atoms within the solid, radiolytic hydrogen generation rates monotonically decrease over time in all solids. This effect, known as "matrix depletion" occurs because the alpha radiation is coming from a solid source. In the case of transuranic (TRU) waste destined for disposal in WIPP, the dominant source of radiation is plutonium. Plutonium in intimate contact with organic matter (e.g., paper or plastic) will generate hydrogen at a rate that continually declines over time as more and more available hydrogen is released from the matrix. Because the source doesn't move with respect to the available hydrogen atoms, the probability of breaking a hydrogen bond and releasing that proton declines over time (and in direct proportion to cumulative dose deposited.

Note this decline in hydrogen generation rate is not associated with the radioactive lifetime of the source. The matrix depletion effect is more a measure of the homogeneity of mixing the radioactive source material within the hydrogenous matrix than of the specific radioactivity of the source [2].

In addition to radiolysis, hydrogen can be generated by anoxic (without oxygen) corrosion of various metal components of the waste and packaging (primarily iron and aluminum based materials). Anoxic conditions can only be expected under inundated conditions, where brine has somehow accumulated and completely surrounds the waste [3]. It should be noted that aluminum and aluminum alloy corrosion rates are much slower than those for iron based materials. Estimates of the rates of hydrogen production under anoxic and fully brine inundated conditions may be made, however these rates are quite uncertain in the short-term during disposal operations, and the likelihood of inundating brine accumulation in this time frame is highly unlikely in light of its observed absence since the first disposal rooms was mined over 20 years ago.

Other arguments against significant hydrogen generation by corrosion include the obvious fact that waste containers (typically drums) are painted. Initially corrosion will be inhibited until painted drum surfaces become exposed and internal steel components become accessible. In addition, after initial closure of a panel, oxygen-rich conditions will prevail, and the iron will oxidize (rust) with no hydrogen generation possible until all of the oxygen has been consumed. The oxidation rate is highly dependent on humidity as well [4]. The low humidity in deep reaches of the WIPP (away from fresh air intakes) minimizes oxidation, even of unpainted steel surfaces. This is evidenced from observation of un-rusted surfaces on many pieces of equipment or structures installed when the first openings were mined at WIPP in the early 1980's. In the routinely low humidity levels found in WIPP, steel surfaces become passivated and oxidation slows. Therefore, oxygen depletion in closed disposal panels is not expected quickly. But only after oxygen is depleted and in the presence of brine, could anoxic corrosion be expected to generate significant hydrogen.

In 2007, a calculation was made to bound the upper limit of hydrogen generation in panel 3 [5]. This radiolysis estimate was based on the actual waste types that had been emplaced at the time, and used the actual hydrogen measurements of head-space gas in individual payload containers made to demonstrate compliance with the license requirements of the shipping containers. That conservative estimate of the production rate of hydrogen by radiolysis was about 4.5E-05 moles per second for the entire inventory of waste in panel 3 (about 1 ml/s). Generation at this rate would lead to an average concentration of 4% by volume in an air-tight sealed panel in about 20 years (neglecting any loss of hydrogen by diffusion). This should be considered a lower bound on the time required to reach a lower flammability limit since the accumulation of hydrogen is mitigated by its ease of diffusion through even highly impermeable materials. The reader is also reminded of the many fractures and openings in the disturbed rock zone of a salt mine, which will not completely heal for many decades after disposal operations cease.

Potential Source of Methane

Methanogenesis or biomethanation is the formation of methane by microbes known as methanogens. Methanogenesis in microbes is a form of anaerobic respiration [6]. Methanogens do not use oxygen to breathe; in fact, oxygen inhibits the growth of methanogens. Organisms capable of producing methane have been identified only from the domain Archaea, a group

phylogenetically distinct from both eukaryotes and bacteria, although many live in close association with anaerobic bacteria. The production of methane is an important and widespread form of microbial metabolism. In most environments in the biosphere, it is the final step in the decomposition of biomass.

In addition, methanogenesis also requires the presence of liquid water, within which the methanogens metabolize. If there is oxygen present, methanogenesis is not. Conversely, if liquid water is not present, neither is methanogenesis. Therefore, just like hydrogen generation via anoxic iron corrosion, no methane can be expected as long as oxygen is present and inundating brine is not.

Flammable Volatile Organic Compounds

There are flammable VOCs in the waste. However these represent a fixed source which will deplete over time, and a source which is limited to levels well below flammability by the transportation requirements. Thus, flammable VOC components in filled panels are expected to remain quite small and further diminish over time. Hence they are not considered a significant issue related to the development of an explosive atmosphere in a full panel.

GAS MONITORING PROGRAM DESCRIPTION

In 2001, the National Academy of Sciences recommended DOE conduct pre-closure monitoring of gases in WIPP [7]:

> *The committee recommends pre-closure monitoring of gas generation rates, as well as the volume of hydrogen, carbon dioxide, and methane produced. Such monitoring could enhance confidence in the performance of the repository, especially if no gas generation is observed. Observation should continue at least until the repository shafts are sealed and longer if possible. The results of the gas generation monitoring program should be used to improve the performance assessment for recertification purposes.*

Then in 2003 [8] and again in 2004 [9], Congress directed the DOE to change the process used to characterize waste for WIPP (these statutes are referred to as Section 311 in this paper). Using nearly identical language in both years, Congress stated:

> *(a) The Secretary of Energy is directed to file a permit modification to the Waste Analysis Plan (WAP) and associated provisions contained in the Hazardous Waste Facility Permit for the Waste Isolation Pilot Plant (WIPP) .... (b) Compliance with the disposal room performance standards of the WAP hereafter shall be demonstrated exclusively by monitoring airborne volatile organic compounds in underground disposal rooms in which waste has been emplaced until panel closure.*

Section (b) essentially directed DOE to monitor VOC concentrations in the WIPP underground in lieu of the intrusive sampling and analysis required under the permit from the NMED. This gave DOE a way to conduct the hydrogen and methane monitoring recommended by the National Academy of Science by using the same sampling lines that were mandated by Section 311 for monitoring VOC concentrations in closed disposal rooms. While unrelated, the Section 311 permit modification was linked to approval to dispose of remote-handled waste at WIPP,

which was strongly rejected by WIPP critics. This delayed implementation of the sampling program until the modification became effective in October 2006, and sampling for VOCs began shortly thereafter in Panel 3, the active disposal unit at that time. It took several more months to obtain a permit modification to delay construction of explosion walls in panel 3 and begin making hydrogen and methane measurements in lieu of installing explosion walls. Sampling for hydrogen and methane began in August 2007.

The sampling is performed using long stainless steel tubing with a passivated inner surface and ~7mm in diameter. Sampling tubes were installed along the outer walls of each disposal room after panel excavation, and before waste emplacement operations began. There are two sampling tubes per disposal room; one that terminates at the inlet side of each room and another that terminates at the outlet side. Each sampling line terminates at a 3-way splitter that allows air to be simultaneously drawn from locations about 50 cm above the floor, 50 cm below the roof, and approximately at the mid-height of each room. Figure 1 schematically shows the sampling line network in a typical disposal panel (blue diamonds represent sample intake locations).

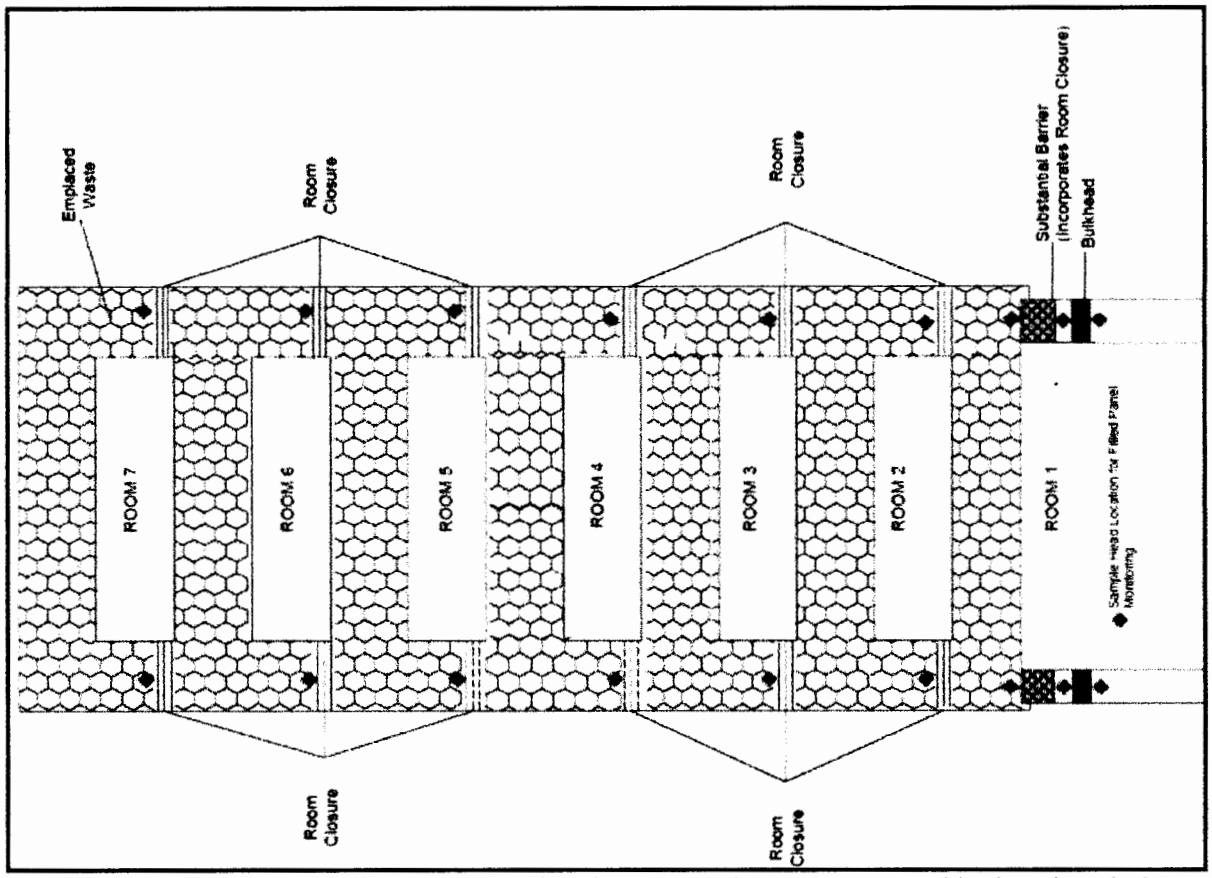

Fig. 1 Plan view of typical disposal panel showing disposal rooms separated by brattice cloth ventilation barriers (room closures) and gas sampling locations in the inlet and outlet sides of each of the seven disposal rooms.

In addition to the VOC monitoring lines, five more sampling locations are used to monitor for hydrogen and methane. These additional locations use a single inlet sampling point placed near the roof and include:

- the inlet of room 1,
- the waste side of the exhaust bulkhead,
- the accessible side of the exhaust bulkhead,
- the waste side of the intake bulkhead,
- the accessible side of the intake bulkhead.

Samples for analysis of hydrogen and methane concentrations are collected using the sub-atmospheric pressure grab sampling technique described in EPA Method TO-15 [10]. This method, which is the same for VOC sampling, uses an evacuated canister under vacuum (~0.05 mmHg) to draw an air sample through sample lines into a ~6 liter stainless steel canister with passivated interior surfaces. The passivation of tubing and canisters effectively seals the inner walls and prevents compounds from being retained on the surfaces of the sampling equipment. Sample lines are purged prior to collection as recommended by the method (about 3 times the sample line volume). At the end of each sampling period (about 6 minute grab sample at ~1 lpm), the canisters reach near atmospheric pressure.

There are no EPA-specific analytical methods which address hydrogen or methane. However, non-EPA methods are available. For the hydrogen and methane sampling, DOE uses a specially developed analytical test method for determination of hydrogen and methane using Gas Chromatography/Thermal Conductivity Detection.

The permit provisions include Action Levels based on the lower flammability limits for hydrogen and methane, referred to in the permit as lower explosive limits (LELs). In air, the lower flammability limit for hydrogen is generally considered to be 4 percent while that for methane is 5 percent. Both limits assume atmospheric oxygen levels are present.

The permit Action Level 1 for hydrogen and methane in a panel is 10 percent of the LEL which, for hydrogen, is 0.4 percent or 4000 ppm and for methane is 0.5 percent or 5000 ppm. If this Action Level is reached or exceeded, the monitoring will be increased to weekly. If the concentrations measured in subsequent sampling fall back below Action Level 1, the sampling frequency relaxes back from weekly to monthly.

Action Level 2 for hydrogen and methane in a panel is 20 percent of the LEL which, for hydrogen is 0.8 percent or 8000 ppm and for methane is 1 percent or 10,000 ppm. If Action Level 2 is achieved or exceeded for two successive weekly samples, the permit requires that monitoring cease and DOE is required to install the explosion isolation walls within 180 days.

When two flammable gases are mixed, the mixture may exhibit a different LEL than the individual gases. This is referred to as the composite LEL for the mixture. DOE evaluated whether or not the composite LEL should be used in determining the Action Levels and concluded that using the 10 percent and 20 percent thresholds was sufficiently conservative to assure action would be taken before potentially explosive levels of hydrogen or methane built up in filled panels. The additional conservatism added by using the composite LEL was not justified considering the additional complexity for demonstrating compliance (i.e., compliance using the composite value is based upon application of a mathematical formula and not on fixed, tabulated values in the permit).

As waste emplacement operations progress and each disposal room is filled within a panel, the filled room is cut off from ventilation by a barrier called a brattice curtain (or cloth), which is a simple canvas-like cloth suspended from the roof and attached to the sides and floor of the drift to effectively cut off the filled room from air ventilation underground. While some attention is given to sealing air flow from going around the barrier, the brattice cloth is by no means an air-tight seal. Small (millimeter scale) gaps remain. After panels 3 and 4 were filled, a metal bulkhead was constructed in both the inlet and outlet drifts (see Figure 1). This final ventilation barrier in each panel was augmented by a rubber (conveyor belt material) gasket bolted to the salt and bulkhead to form a seal. Again, small gaps remained. The reader is reminded that the salt creep process results in fractures and partings within the rock salt walls themselves that make the concept of a perfect gas seal impossible during the operational phase of the repository. Figure 2 shows photos of typical brattice cloth and metal bulkhead construction in WIPP.

Fig. 2 Photos of a typical ventilation barrier called a brattice curtain (top) separating each disposal room, and of a typical metal bulkhead (bottom) "sealing" the inlet and outlet drifts of each disposal panel from ventilation air in the rest of the mine.

DOE believes the use of the bulkhead, the accompanying monitoring, and related Action Levels will maintain safe and protective operations by ensuring that:

- physical access to the full panel is prevented,
- the panel is removed from active ventilation, and
- conditions inside the panel are regularly monitored so that preventive actions can be taken well in advance of the existence of a hazardous condition.

MONITORING RESULTS

Panel 3 was filled and closed in August 2007, while panel 4 was filled and closed in May 2009. Monthly hydrogen and methane sampling began in both panels the same month they were closed. Two results from over 1,000 samples collected since then stand out:

- All samples assayed less than the minimum detectable level for methane (<~20-30 ppm).
- Hydrogen results typically assay at several hundred ppm, when detected at all.

The monthly monitoring results for hydrogen in panels 3 and 4 are presented in Figures 3 and 4, respectively.

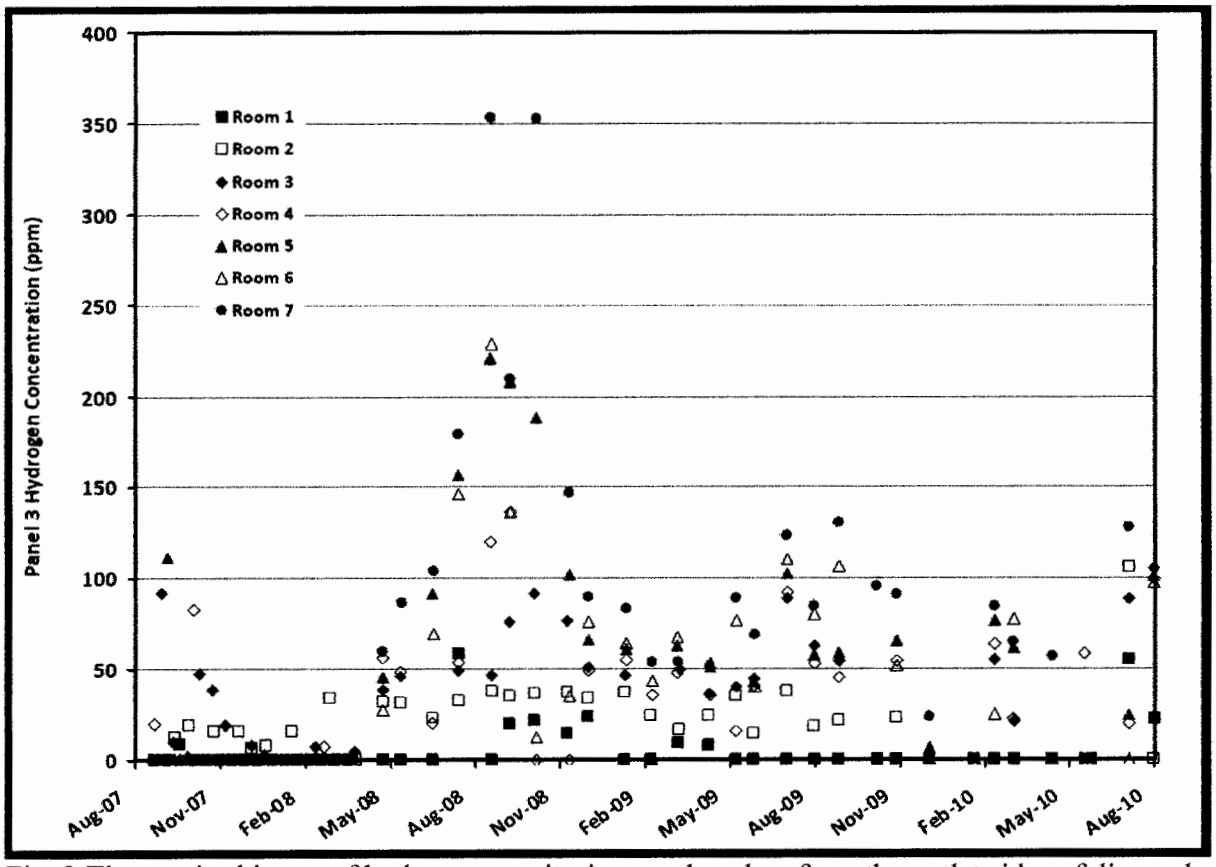

Fig. 3 Time series history of hydrogen monitoring results taken from the outlet sides of disposal rooms in closed panel 3 over a 3-year period.

In these time series plots, only the results from sampling the outlet sides of each disposal room are plotted. Only a handful (out of over 500) of samples taken from the inlet side assayed above the minimum detectable limit for hydrogen (~20-30 ppm), and therefore are not plotted. When outlet sample results assayed below the minimum detectable limit, the value was plotted at a concentration of zero in Figures 3 and 4.

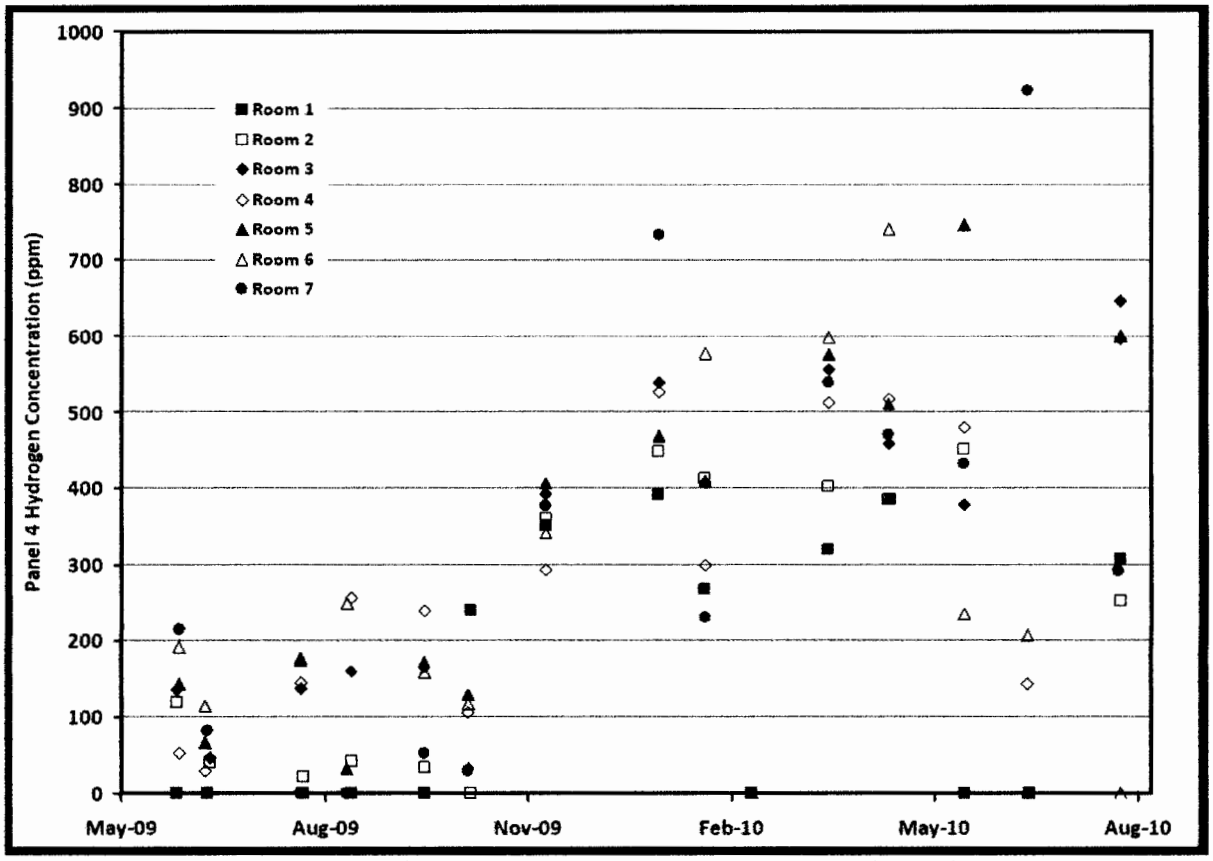

Fig. 4 Time series history of hydrogen monitoring results taken from the outlet side of disposal rooms in closed panel 4 over an 18-month period.

Interpreting these results is easy. There is no detectable methanogenesis occurring in either panels 3 or 4, and thereby by inference, no methanogenesis in panels 1 or 2 either. In contrast hydrogen generation by radiolysis is occurring and at levels easily detected by the analytic method used for assay. No steadily rising concentrations imply that the hydrogen is removed from the disposal rooms on a continuous basis. The removal process appears to be two-fold. The fact that the results from samples collected on the inlet side almost always assay below minimum detectable limits and those from the outlet side typically range in the few hundred ppm levels implies that there is a leakage flow due to differential pressure between the inlet and outlet sides of each disposal panel. The high sample-to-sample variability from each location implies that the release of hydrogen from the waste containers themselves varies over periods of weeks to months. This can be explained by normal barometric breathing.

The highest value of hydrogen measured to date was 923 ppm at the outlet side of room 7 (furthest into the disposal panel) in panel 4 in June 2010. This value is 25% of the Action Level 1 for hydrogen established in the permit (which in turn is 10% of the concentration considered

flammable - if oxygen were present at atmospheric levels). It should be noted that actions to minimize leakage ventilation through panel 4 began in earnest in November 2009, when running annual average carbon tetrachloride levels in the exhaust flow from the entire underground began climbing. A companion paper in session 063 (11039) at this symposium describes this effort in more detail [11].

Active disposal operations with high carbon tetrachloride content were ongoing in panel 5 at that time, but it was prudent to assume that some of the carbon tetrachloride originated from leakage flow through closed panel 4 since it held some of the high carbon tetrachloride waste as well. Therefore, DOE built an additional bulkhead at the inlet and outlet drifts of panel 4 and made extra efforts to seal panel 4 from leakage ventilation. These efforts were coincident with the slight step increase in the peak hydrogen concentration results as seen in Figure 4 in November 2009. The apparent increase may be attributed to the enhanced sealing efforts to minimize carbon tetrachloride leakage out of panel 4. However, the fact that hydrogen concentrations vary so much from one sample to the next indicates that it easily escapes the systems designed to block the carbon tetrachloride.

ELIMINATING EXPLOSION WALLS AND OPTIMIZING PANEL CLOSURES

Based on the monitoring results from 2007 to date, it would seem that massive panel closures and explosion walls to protect those closures might not be necessary and yet still be protective of workers and the environment. A companion paper in session 063 at this symposium discusses DOE's plans to seek regulatory approval to modify the massive closure design and replace it with a simple 30 meter long wall of run of mine salt [12]. Such a panel closure would likely be a better barrier in preventing panel-to-panel hydrologic communication in an assumed future human intrusion scenario, and would be a lot less costly. Upon filling a disposal panel with waste, the run of mine salt closure would simply be placed in the inlet and outlet drifts. A blower may be used to bring the pile up to the full height of the drifts. While this closure would not be air-tight, it would behave at least as well as the metal bulkheads in panels 3 and 4 described herein (the same leaky pathways around the closure through the disturbed rock zone would exist). Over time (a few decades), the salt creep closure would compact and begin reconsolidating the run of mine salt. Within a few hundred years, this panel closure would resemble the properties of intact salt. In contrast a massive monolith of concrete (the current panel closure stipulated for WIPP by its regulators) would not exhibit the immeasurably low permeability of healed intact salt, but would be considered more permeable.

CONCLUSIONS

Although basic knowledge and laboratory measurements made during the licensing and permitting phase showed that little or no gas generation would occur during the operational life of WIPP, in an abundance of caution, DOE and its regulators still proposed massive panel closures and large explosion walls to protect them. Based on monitoring results (at least for panel 3 and 4), these do not appear to be necessary, since levels of flammable gases and VOCs are present in only trace levels. The only VOC present in significant amounts in the TRU waste stream inventory (and then only in a small fraction of drums) is carbon tetrachloride, which ironically is not flammable.

Over 1000 gas samples collected in all areas of panels 3 and 4 show undetectable levels of methane, thereby confirming the expectation that methanogenesis is not occurring (oxygen is

present, and brine inundation is not). Hydrogen levels in those same samples are in the few hundred ppm range and vary significantly from sample to sample, thereby implying a continuous source, but an intermittent pathway out. This is consistent with barometric pumping of waste containers, superimposed on a steady leakage air flow, even through the further back disposal rooms in a panel.

DOE will continue to monitor for flammable gases in filled disposal panels and take steps to protect workers and the environment if levels rise and explosions walls become necessary. In the meantime, DOE will continue to make the case that there are more prudent and cost effective panel closure designs that should be considered.

REFERENCES

1. Conceptual Design for Operational Phase Panel Closure Systems, DOE-WIPP-95-2057, US Department of Energy, 1995.
2. Idaho National Engineering and Environmental Laboratory, 1990, "TRUPACT-II Matrix Depletion Program Final Report," INEL/EXT-98-00987, Rev. 1, prepared for the U.S. Department of Energy, Idaho Operations Office, Idaho Falls, Idaho.
3. Francis, A.J., Gillow, J.B., and M.R. Giles, 1997. Microbial Gas Generation Under Expected Waste Isolation Pilot Plant Repository Conditions. SAND96-2582, Sandia National Laboratories, Albuquerque, New Mexico.
4. Gillow, J.B. and A.J. Francis, 2002, Re-Evaluation of Microbial Gas Generation Under Expected Waste Isolation Pilot Plant Conditions, Data Summary and Progress Report (February 1 – July 15, 2002). Section 3.1 of Sandia Technical Baseline Report, July 31, 2002. Sandia National Laboratories, Albuquerque, New Mexico.
5. Devarakonda, M., Estimation of Hydrogen Generation Rates From Radiolysis in WIPP Panels, Letter from Washington TRU Solutions to D. Mercer, TS:06:02012, July 20, 2006
6. Thauer, R. K., Biochemistry of Methanogenesis, Microbiology, 1998, volume 144, pages 2377-2406.
7. National Academy of Sciences, 2001, Improving Operations and Long-Term Safety of the Waste Isolation Pilot Plant, Board on Radioactive Waste Management.
8. Section 311 of the Energy and Water Development Appropriations Act, 2004, Public Law 108-137 (December 1, 2003)
9. Section 310 of the Consolidated Appropriations Act for 2005, Public Law 108-447 (December 8, 2004)
10. Compendium of Methods for the Determination of Toxic Organic Compounds in Ambient Air: Methods TO-15, Second Edition, US Environmental Protection Agency, Research Triangle Park, NC, January 1999; EPA 600/625/R-96/010b.
11. Nelson, R.A., WIPP Status and Plans – 2010, Waste Management 2011 Conference, Phoenix, AZ, March, 2011.
12. Patterson, R.L., S. Kouba, and T. Klein, Panel Closure: A Change in WIPP's Future Operations through Regulatory Compliance, Waste Management 2011 Conference, Phoenix, AZ, March 2011.

ATTACHMENT B

Effective Permeability of the Redesigned Panel Closure System

ATTACHMENT B

Effective Permeability of the Redesigned Panel Closure System

Sandia National Laboratories

Operated for the U.S. Department of Energy by
Sandia Corporation

Carlsbad Programs Group
4100 National Parks Highway
Carlsbad, NM 88220

date: August 29, 2002

to: Paul E. Shoemaker, MS-1395 (6820)

from: F.D. Hansen, MS-1395 (6822)
T.W. Thompson, Golder Associates

subject: Effective Permeability of the Redesigned Panel Closure System

Introduction

This memorandum estimates permeabilities for the redesigned panel closure system described in the *Design Report for a Revised Panel Closure System at the Waste Isolation Pilot Plant* (Design Report) (Saeb and Case, 2002). This redesigned panel closure system consists of a mortared, solid concrete block wall placed in the panel entries over a length of 30 ft, and run-of-mine salt backfill placed on the outer side of this wall for a length of 100 ft. This backfill is not placed to any particular specifications, but it will be placed up to the back in the entry, and up to the ribs. The design report estimates the mortared block wall would exhibit a permeability of the order of 10^{-15} m^2 as emplaced. This wall is designed to continue to function throughout the operational period of 35 years, and it's permeability may be expected to remain relatively constant over this period. Beyond the 35 years the concrete wall may be expected to undergo progressive material failure and the permeability will gradually increase as the concrete block wall fractures and fails. However, the permeability of the salt backfill will reduce over time from the estimated as-emplaced value of 10^{-11} m^2 (Saeb and Case, 2002) as the loose salt consolidates. In the absence of pore pressure development, which could slow or impede consolidation, the mine-run salt may be expected to compress to very low permeability in less than 100 years. As discussed later it is not anticipated that significant pore pressures will be generated in the backfill until permeabilities of less than 10^{-15} m^2 are achieved.

The intent of this memorandum is to establish the order of magnitude of permeability of this redesigned closure as a function of time. Specifically, it demonstrates that in a fairly short time, of the order of 100 years or less, the closure system will achieve a permeability of lower than 10^{-15} m^2, and that the closure system permeability will be in the range of 10^{-15} to 10^{-19} m^2 beyond that time. The redesigned closure therefore will have a permeability in the range examined in the accompanying impact analysis (Hansen, 2002), so that the conclusions in that analysis regarding system performance can be applied to the redesigned closure. It should be noted, however, that while this memorandum demonstrates an expected range for the panel closure permeability, it is not intended to be used to define a permeability parameter for use in future Performance Assessment (PA) calculations.

Panel closure design

As noted in the introduction, and described in detail in the design report (Saeb and Case, 2002), the closure comprises a mortared, solid concrete block wall 30 ft. long, and run-of-mine salt backfill 100 ft long placed to leave no gaps against the roof and ribs (Figure 1).

The resistance to fluid flow of this closure system will be a composite of the resistance to flow of the different elements, including the wall, the crushed salt and the surrounding disturbed rock zone (DRZ). Each of these components will vary in its flow resistance over time, and each will dominate over a particular time period. Since the intent of this memorandum is to review the flow resistance of the closure itself for comparison to the range examined in the impact analysis, the effect of the DRZ is not considered here, although it will be relevant to overall performance.

During the operational period the conductivity of this closure will be dominated by the mortared cement block wall, which is estimated in the design report to have a permeability of $2x10^{-15}$ m^2. Over time the concrete wall will gradually fracture and fail under the loads applied by the creep of the surrounding salt, and its permeability will gradually increase. However, the same creep closure which causes the concrete block wall to fail will also gradually compact the salt backfill, thus slowly decreasing its permeability and this element will come to dominate the flow performance of the closure system.

It should be noted that the relevant parameter for flow performance is in fact the flow conductance, which is a function of permeability, area, and length. However the length of the closure considered in the Compliance Certification Application (CCA) and Performance Assessment Verification Test (PAVT) calculations, and in the accompanying impact analysis, is 40 m or 131 ft, which is essentially the same as the redesigned closure, while the area is the same in the CCA, PAVT and for the redesigned closure, so the comparison may be made on the basis of permeability alone.

Salt Consolidation

Closure of the entry due to creep around the crushed salt backfill will cause the backfill to consolidate leading to loss of porosity, increase in density and reduction in permeability. The backfill void volume will be approximately 33% when placed, this being a typical value for loosely emplaced disaggregated materials and being in the range anticipated by Saeb and Case (2002). When the salt is compressed and the porosity is reduced, its permeability decreases appreciably. It has been shown that when crushed salt re-consolidates to a density approaching 95% of intact salt, its permeability is approximately 10^{-19} m^2 (Hurtado et al., 1997). It has been postulated and confirmed that consolidation of granular rock salt occurs by two primary mechanisms: grain boundary pressure solution and dislocation creep (Spiers and Brzesowsky, 1993). As crushed salt is loaded, the principal densification mechanism of fluid-phase grain boundary solution/redeposition is rampant. As consolidation proceeds, the material attains sufficient density so that its response assumes the constitutive response of intact salt, and dislocation creep becomes important. Estimates of the rate of closure and the resulting loss of permeability can be made using measured closure rates from the Panel 1 entries and laboratory data on salt consolidation.

Data on the relationship between porosity and permeability of crushed salt have been obtained in a number of laboratory experiments evaluating the behavior of backfill material in rooms and of shaft seal components. A comprehensive data set is reported by Hurtado et al., (1997) and is included as Figure A7 in Appendix SEAL of the CCA (DOE, 1996). These data are presented in Figure 2, and show that for fractional densities above about 0.9 (equivalent to a porosity of 10%) permeabilities may be expected to be 10^{-15} m^2 or lower. If, as noted above, the run-of-mine salt is expected to have a porosity of the order of 33%, then to reach a porosity of 10% will require a volume strain of the order of 23%.

Unimpeded closure of entry drifts has been modeled and shows closure of the order of 10% in 10 years (Hansen et al., 1993). Actual measurements of roof-to-floor and rib-to-rib closure in the entries

corroborate these closure rates. Figures 3 and 4 show closure data for S1600 (the Panel 1 exhaust drift) and S1950 (the Panel 1 intake drift) respectively. These data are from the E407 monitoring point which is located approximately midway between the E300 main entry and Panel 1, or in the center of the proposed panel closure locations (DOE, 2001). These data indicate that closure rates, which are summarized in the following table, are reasonably stable, and uniform, and are similar for the mid and third points of each entry. If it is assumed that the rates measured over the last ten years will continue, then the volume closure expected of the two entries is as shown in Figure 5, with closure by 25% in between 20 or 30 years.

Closure Measurement Location	Exhaust Drift (S1600) (in/day)	Air Intake Drift (S1950) (in/day)
Vertical (Center)	0.00203	0.00364
Vertical (S. third point)	0.00185	0.00300
Vertical (N. third point)	0.00196	0.00365
Mean Vertical	0.00195	0.00333
Horizontal (Upper third point)	0.00230	0.00250
Horizontal (Center)	0.00216	0.00266
Horizontal (Lower third point)	0.00200	0.00261
Mean Horizontal	0.00215	0.00259

Closure to this extent in the presence of crushed salt may be expected to be slower for three reasons. First, it is likely that a long-term slow down of closure rates may be expected, although closure by 25% in say twice the calculated time, or 40 – 60 years, is not unreasonable. Second, as the backfill consolidates it may be expected that it will stiffen and apply some back stress that will slow the closure. Case (1994) used data from Holcomb and Hannum (1982) to estimate consolidation pressure-strain curves for loosely placed backfill (Figure 6), indicating that at strains of the order of 25% imposed under rapid loading quasi-static conditions back stress of the order of 2500 psi may be expected. However creep tests carried out on similar materials by Holcomb and Hannum show that under constant stress of this magnitude the crushed salt will consolidate over time (Figure 7). This creep will result in relaxation of any potential stress build up over the tens of years being considered here, so the potential for large back stresses being induced is small. Note that this behavior is confirmed by numerical calculations of the closure of backfilled rooms (Figure 8) (Callahan and DeVries, 1991) which show closure to very low porosities in a matter of a few tens of years, and by calculations of the consolidation of dynamically emplaced crushed salt in the shaft at a depth of 600m (Figure 9).

Third, back pressure could also be applied as a result of pore pressure build-up due to gas generation in the waste. Any microbial gas generation will occur fairly rapidly, at least within the time frame discussed here, and this gas may be expected to flow through the concrete wall and into the salt backfill. However through the early parts of its consolidation, where the permeability was greater than or equal to 10^{-15} m^2, any gas generated will flow out of the backfill into any remaining void space adjacent to the closure. As the permeability reduces still further the crushed salt may resist further consolidation, but the permeability will still be in the range estimated here.

Conclusion

When the redesigned closure is emplaced the flow resistance will be controlled by the mortared concrete block wall, and is expected to be of the order of 10^{-15} m^2. This permeability will be maintained at least

through the operational period of 35 years. After this time the permeability of this element may be expected to increase somewhat as the wall degrades on an unknown time frame under creep load. At the same time the run-of-mine salt backfill will be consolidating under the creep closure of the salt surrounding the entry. Extrapolation of existing closure data suggest volume closure of the order of 25% would occur in as little as 20 to 40 years; however it is likely that this will take longer as creep closure rates will probably reduce somewhat over time. Back stress due to the consolidation is expected to be minimal over the time scales of interest (tens of years) since any tendency for stress build up will be relaxed by creep consolidation of the backfill. Once a fractional density of about 0.9 (representing a porosity of about 10%, or about 25% closure from an original porosity of 35%) is reached permeabilities of the order of 10^{-15} m^2 may be expected, and it is reasonable to expect these conditions to be reached in a maximum of 100 years. Beyond that time, permeability may be expected to decrease further with additional consolidation and values of the order of 10^{-19} m^2 may be achieved. If gas generation occurs and the gas penetrates the backfill, then as the permeability decreases, pore pressures may build up leading to a slowing or stopping of consolidation. However this will not occur until the backfill permeability reaches at least 10^{-15} m^2: at higher permeabilities the pore pressures will be relieved by flow of gas. The permeability of the closures will therefore be expected to fall in the range covered in the accompanying impact assessment, i.e. 10^{-19} to 10^{-15} m^2.

References

Callahan, G. D. and K. L. DeVries. 1991. Analyses of Backfilled Transuranic Wastes Disposal Rooms. SAND91-7052. Sandia National Laboratories, Albuquerque, NM.

Case, J.B., 1994, "Backfill Evaluation Analysis Report," Westinghouse Waste Isolation Division, Carlsbad, NM, 1994.

Hansen, C., "Analysis Report for the Panel Closure Impact Assessment," Sandia National Laboratories, Carlsbad NM, August, 2002.

Hansen, F.D., M.S. Lin, L.L. VanSambeck, 1993. "Concept for Operational Period Seal Design at the Waste Isolation Pilot Plant," SAND93-0729, July 1993.

Holcomb, D.J. and D.W. Hannum, 1982, "Consolidation of Crushed Salt Backfill Under Conditions Appropriate to WIPP," SAND82-0630, November 1982.

Hurtado, L.D., M.K. Knowles, V.A. Kelley, T.L. Jones, J.B. Ognitz, T.W. Pfeifle, 1997. "WIPP Shaft Seal System Parameters Recommended to Support Compliance Calculations," SAND97-1287, December 1997.

Saeb, S and J. Case, 2002, "Design Report For A Revised Panel Closure System At The Waste Isolation Pilot Plant," Report to Westinghouse TRU Solutions, LLC., Rocksol Inc., Boulder CO.

Spiers, C.J., and R.H. Brzesowsky. 1993. "Densification Behavior of Wet Granular Salt: Theory Versus Experiment," *Seventh Symposium on Salt,* Kyoto, Japan, April 6-9, 1992. Eds. H. Kakihana, H.R. Hardy, Jr., T. Hoshi, and K. Toyokura. Amsterdam; New York, New York: Elsevier Science Publishers B.V. Vol. I, 83-92.

U.S. Department of Energy, 1996, "Title 40 CFR 191 Compliance Certification Application for the WIPP: Appendix SEAL," Carlsbad NM, 1996.

U.S. Department of Energy, 2001, "Geotechnical Analysis Report for July 1999-June 2000," DOE/WIPP 01-3177, Waste Isolation Pilot Plant, Carlsbad, New Mexico.

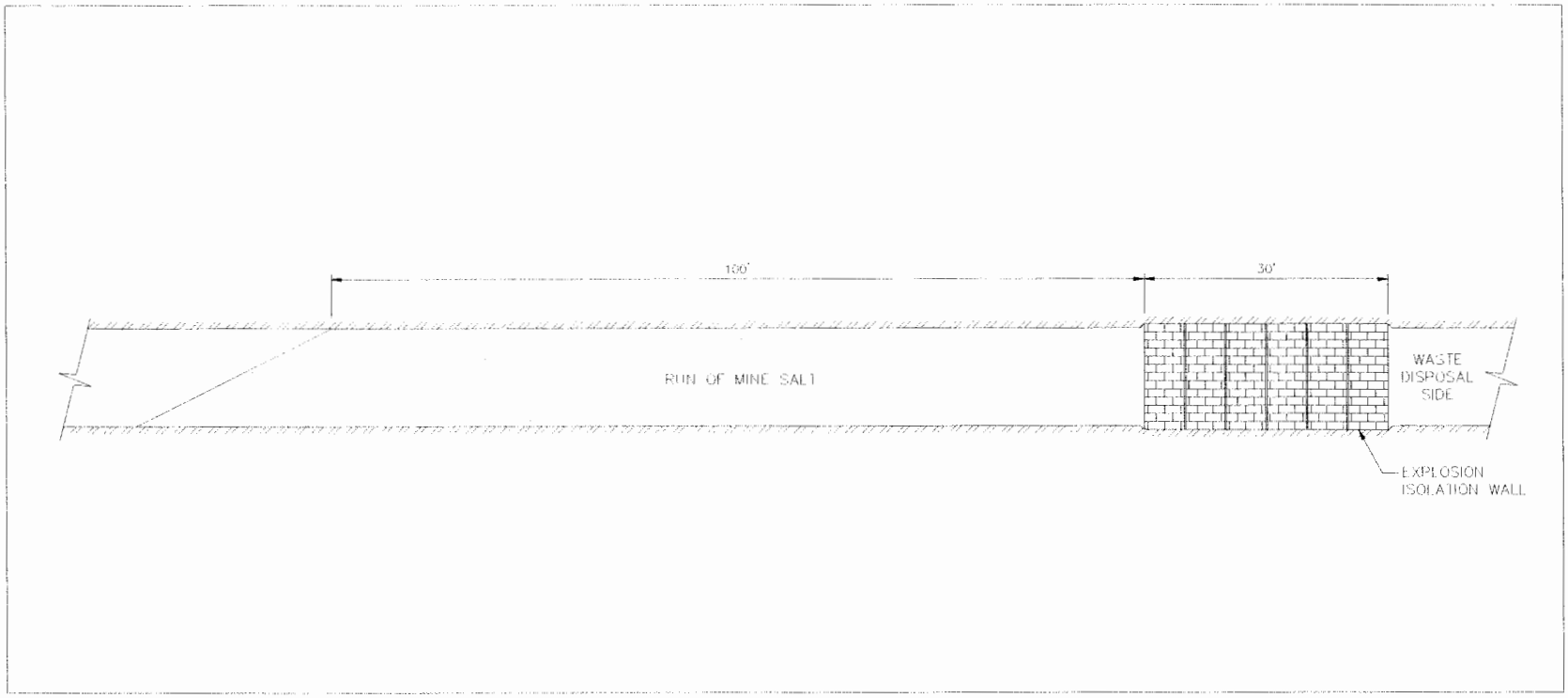

Figure 1. Explosion Isolation Wall in Combination with the Run-of-Mine Salt Backfill (Saeb and Case, 2002)

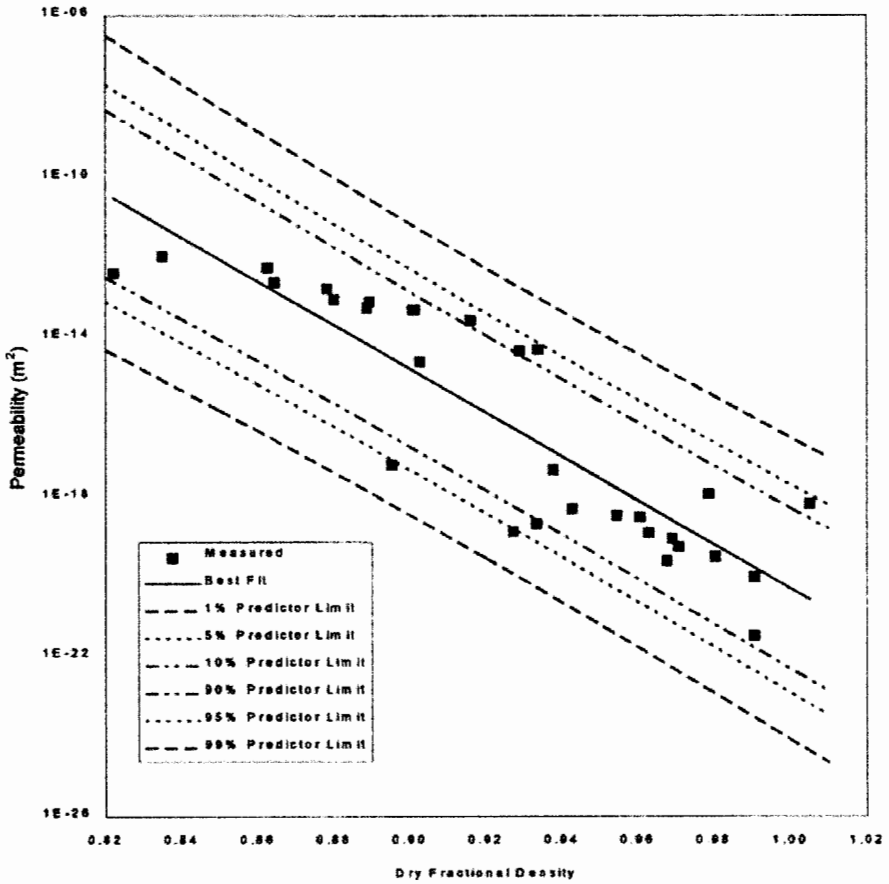

Figure 2. Permeability of Consolidated Crushed Salt as a Function of Fractional Density (DOE, 1996)

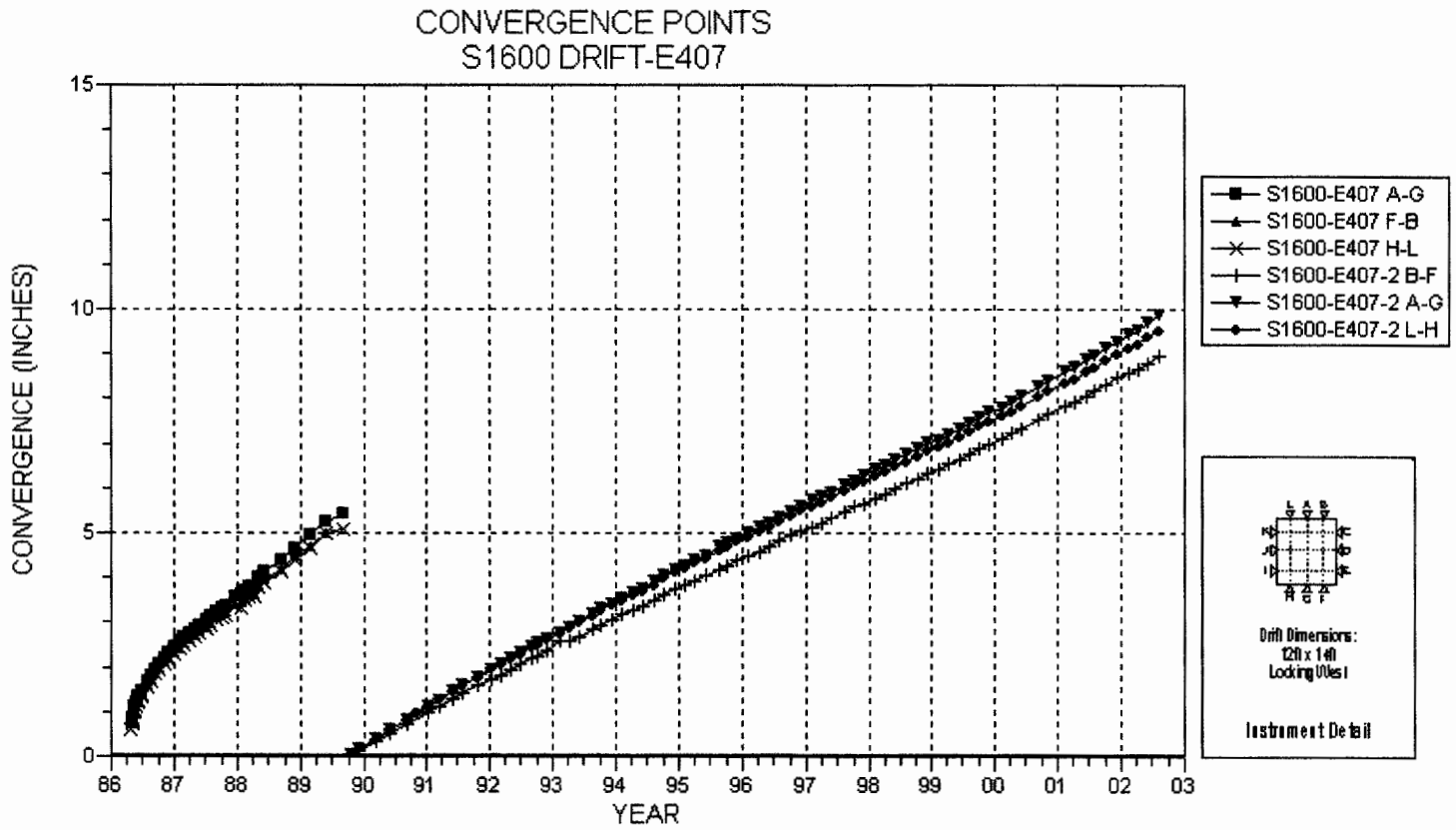

NOTES:
1. Excavation date: April 1986.

Figure 3: Closure Data for the Exhaust Drift (S1600) (DOE, 2001)

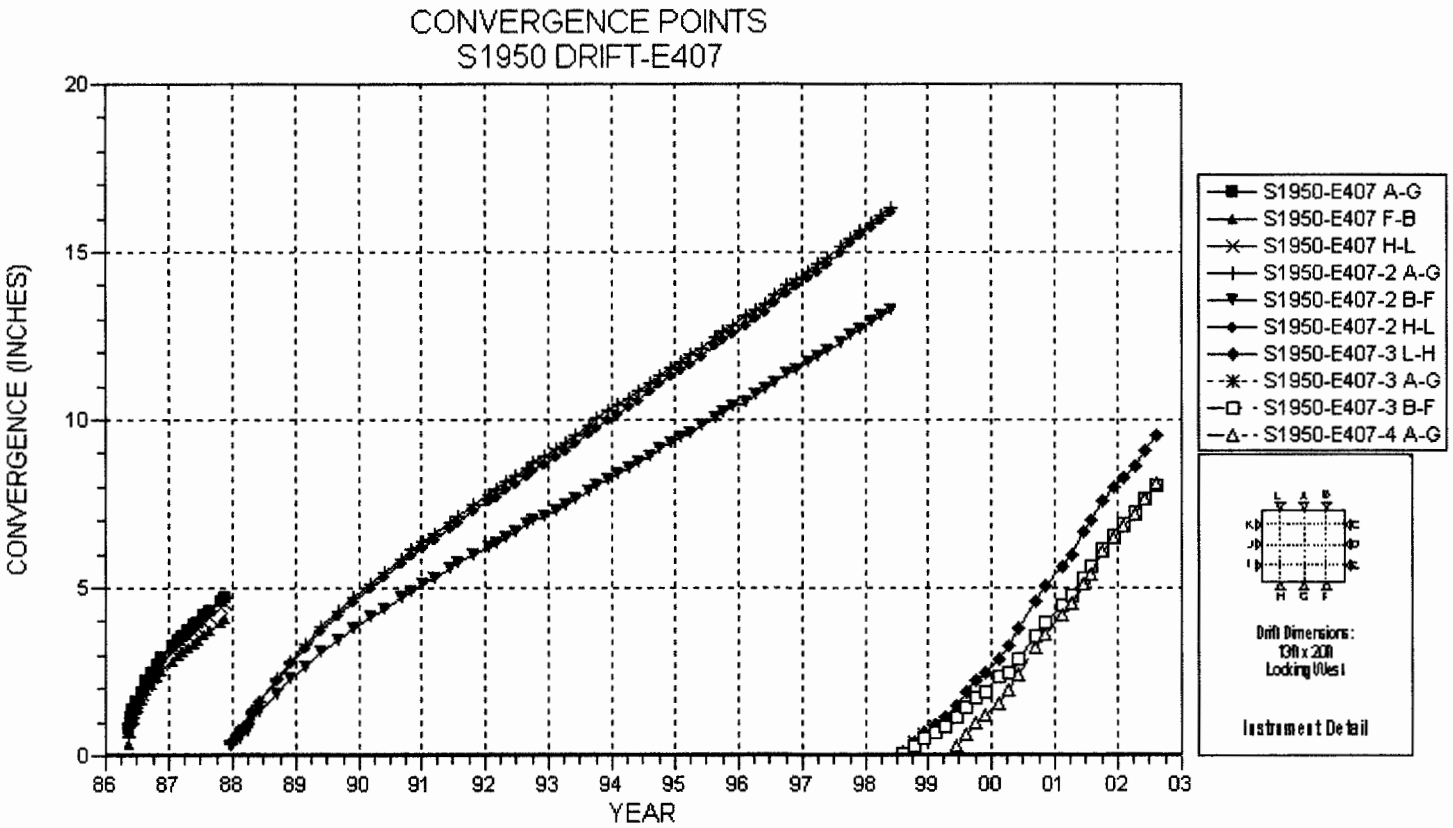

NOTES:
1. Excavation date: May 1986.

Figure 4: Closure Data for the Air Intake Drift (S1950) (DOE, 2001)

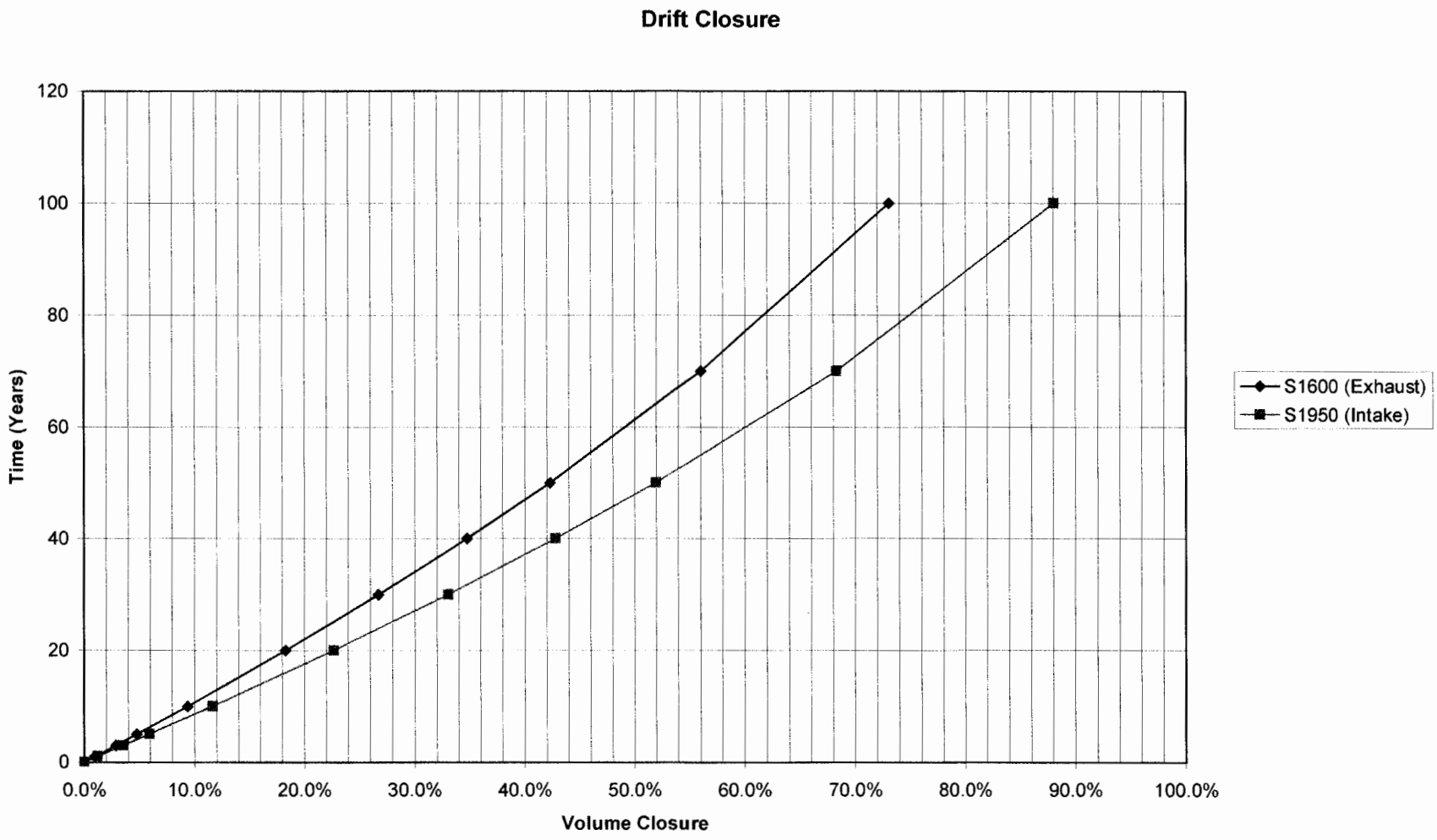

Figure 5. Calculated Drift Closure Assuming Constant Closure Rates and no Backstress

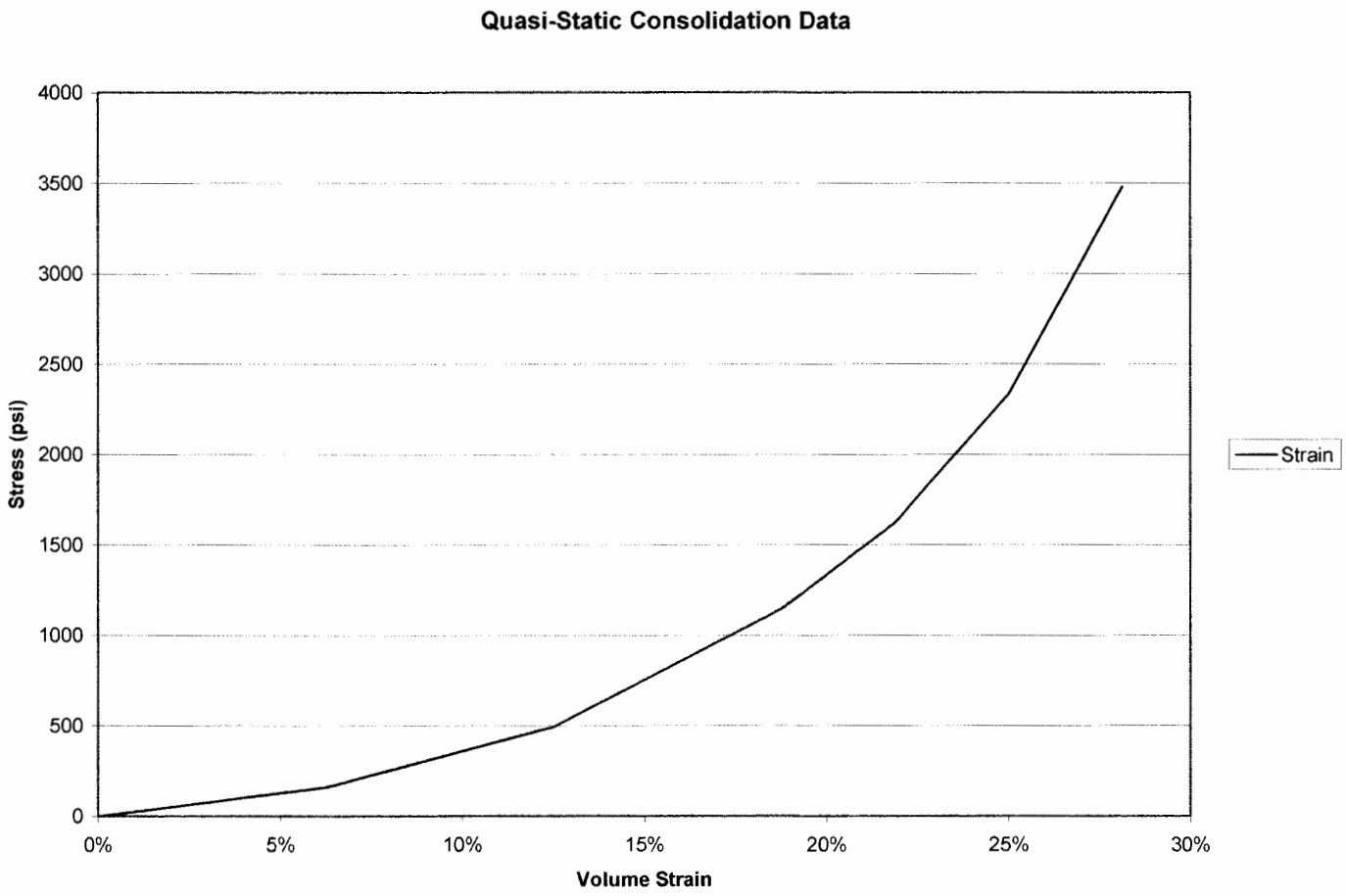

Figure 6: Quasi-Static Consolidation Data for Dry Crushed Salt (after Holcomb and Hannum, 1982 and Case, 1994)

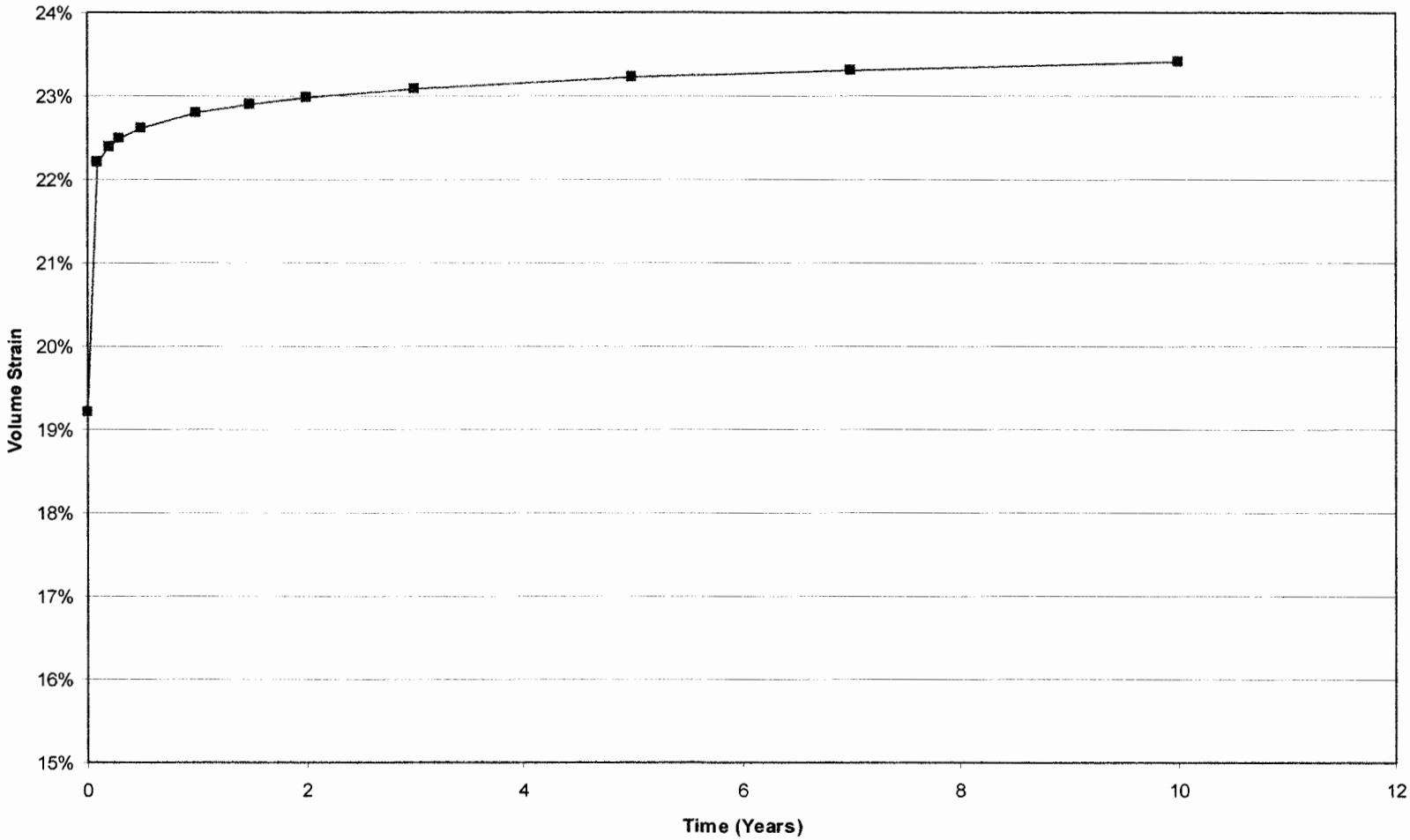

Figure 7: Creep Consolidation Data for Dry Crushed Salt (after Holcomb and Hannum, 1982)

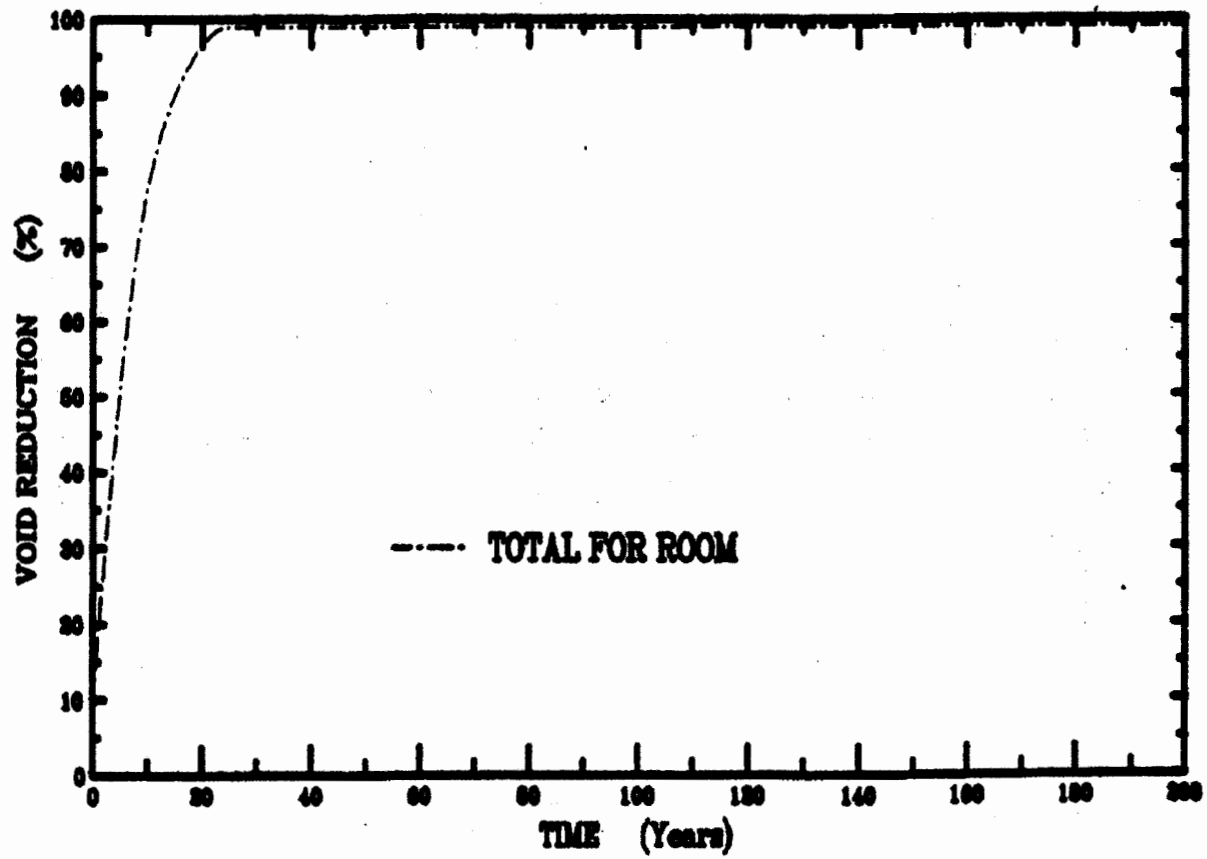

Figure 8. Void Reduction in a Disposal Room filled with Crushed Salt as a Function of Time (Callahan and DeVries, 1991).

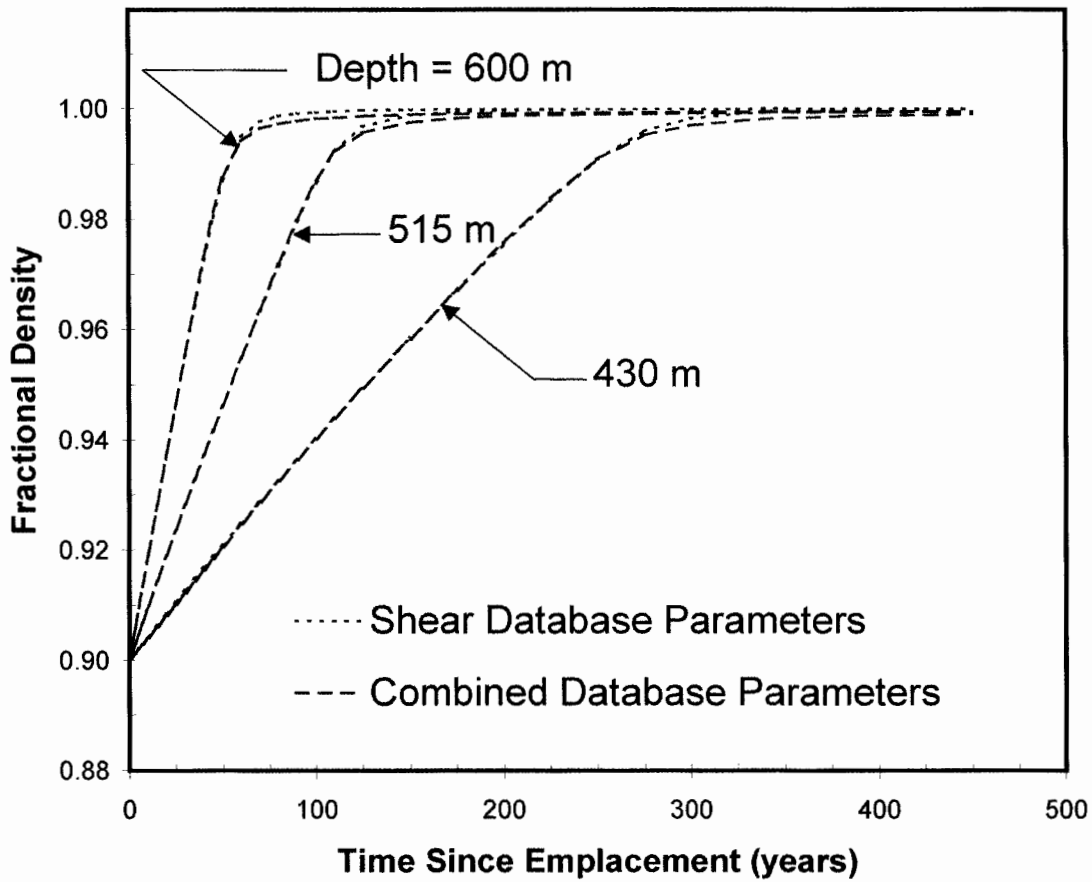

Figure 9. Calculated Fractional Density Versus Time for Crushed Salt Compacted in the Shaft.

ATTACHMENT C

Summary Report for the AP-151 (PC3R) Performance Assessment, Revision 1

555489

Sandia National Laboratories
Waste Isolation Pilot Plant

Summary Report for the AP-151 (PC3R) Performance Assessment

Revision 1

Author:	R. Chris Camphouse		5/17/11
	Print	Signature	Date
Author:	Daniel J. Clayton	(For)	5/17/11
	Print	Signature	Date
Author:	Dwayne C. Kicker		5/10/2011
	Print	Signature	Date
Author:	James J. Pasch	James J Pasch	5/10/2011
	Print	Signature	Date
Technical Review:	Sean C. Dunagan		5/10/11
	Print	Signature	Date
QA Review	Mario J. Chavez	Mario Chavez	5/16/11
	Print	Signature	Date
Management Review:	Moo Lee		5/17/11
	Print	Signature	Date

WIPP:1.4.1.2:PA:QA-L:554612

Information Only

Table of Contents

Executive Summary 5
1 Introduction 6
2 Repository Configuration Changes 7
2.1 Repository Reconfiguration 7
2.2 Parameters..... 11
Panel Closure Parameters 11
Panel Reconfiguration Parameters 14
2.3 Computational Grid Changes 15
2.4 FEPS Re-assessment 20
3 Methodology 20
4 Run Control 22
5 Results 22
5.1 Salado Flow Results 22
Undisturbed Scenario S1-BF 23
Disturbed Scenario S2-BF 28
Disturbed Scenario S4-BF 31
5.2 Brine Isolation after Intrusion 35
5.3 Actinide Mobilization and Transport 40
5.4 Cuttings and Cavings 43
5.5 Spallings..... 46
5.6 Direct Brine Releases 48
5.7 Total Normalized Releases 50
6 Summary 55
7 References 56

Acknowledgement

A portion of this summary report was written by James W. Garner. James became unavailable during the review and comment phase of report preparation, and was not available to sign the title page of the final document.

List of Figures

Figure 2-1: Historical WIPP Repository Layout 9
Figure 2-2: WIPP Layout Modeled in PC3R PA 10
Figure 2-3: PABC-2009 BRAGFLO grid (Δx, Δy, and Δz dimensions in meters) 16
Figure 2-4: PC3R PA BRAGFLO grid (Δx, Δy, and Δz dimensions in meters) 17
Figure 2-5: PABC-2009 DBR material map (logical grid) 18
Figure 2-6: PC3R PA DBR material map (logical grid) 19
Figure 5-1: Overall Means of Volume Averaged Porosity for the Waste Panel, Scenario S1-BF 25
Figure 5-2: Overall Means of Volume Averaged Pressure for the Waste Panel, Scenario S1-BF 25
Figure 5-3: Overall Means of Volume Averaged Pressure for the Waste Panel During the First 150 Years After Closure, Scenario S1-BF 26
Figure 5-4: Overall Means of Brine Saturation in the Waste Panel, Scenario S1-BF 26
Figure 5-5: Overall Means of Total Brine Flow Out of the Waste Panel, Scenario S1-BF 27
Figure 5-6: Overall Means of Total Brine Flow Up the Shaft, Scenario S1-BF. 27
Figure 5-7: Overall Means of Volume Averaged Porosity for the Waste Panel, Scenario S2-BF 29
Figure 5-8: Overall Means of Volume Averaged Pressure for the Waste Panel, Scenario S2-BF 29
Figure 5-9: Overall Means of Brine Saturation in the Waste Panel, Scenario S2-BF 30
Figure 5-10: Overall Means of Total Brine Flow Out of the Waste Panel, Scenario S2-BF 30
Figure 5-11: Overall Means of Total Brine Flow Up the Borehole, Scenario S2-BF 31
Figure 5-12: Overall Means of Volume Averaged Porosity for the Waste Panel, Scenario S4-BF 32
Figure 5-13: Overall Means of Volume Averaged Pressure for the Waste Panel, Scenario S4-BF 33
Figure 5-14: Overall Means of Volume Averaged Pressure for the Waste Panel During the First 700 Years After Closure, Scenario S4-BF 33
Figure 5-15: Overall Means of Brine Saturation in the Waste Panel, Scenario S4-BF 34
Figure 5-16: Overall Means of Total Brine Flow Out of the Waste Panel, Scenario S4-BF 34
Figure 5-17: Overall Means of Total Brine Flow Up the Borehole, Scenario S4-BF 35
Figure 5-18: PC3R PA Overall Waste Panel Pressure Means, Scenarios S1-BF, S2-BF, S4-BF, S6-BF 37
Figure 5-19: PC3R PA Overall Waste Panel Brine Volume Means, Scenarios S1-BF, S2-BF, S4-BF, S6-BF 38
Figure 5-20: PC3R PA Overall Waste Panel Brine Saturation Means, Scenarios S1-BF, S2-BF, S4-BF, S6-BF 38
Figure 5-21: PC3R PA Overall Central Region Brine Saturation Means, Scenarios S1-BF, S2-BF, S4-BF, S6-BF . 39
Figure 5-22: PC3R PA Overall Central Region Brine Volume Means, Scenarios S1-BF, S2-BF, S4-BF, S6-BF 39
Figure 5-23: PC3R PA Overall Central Region Pressure Means, Scenarios S1-BF, S2-BF, S4-BF, S6-BF 40
Figure 5-24: PC3R PA and PABC-2009 Replicate Means of Cumulative Flow up the Borehole 41
Figure 5-25: PC3R PA and PABC-2009 Overall Means of Cumulative Flow up the Borehole 42
Figure 5-26: PC3R PA and PABC-2009 Replicate Mean CCDFs for Normalized Transport Releases to the Culebra 42
Figure 5-27: PC3R PA and PABC-2009 Overall Mean CCDFs for Transport Releases to the Culebra 43
Figure 5-28: PC3R PA and PABC-2009 Overall Mean CCDFs for Normalized Cuttings and Cavings Releases 45
Figure 5-29: Cuttings and Cavings Area as a Function of Waste Shear Strength 45
Figure 5-30: PC3R PA and PABC-2009 Overall Mean CCDFs for Normalized Spallings Releases 47
Figure 5-31: DBR Volume vs. Pressure, Scenario S2-DBR, Replicate 1, Lower Intrusion, PC3R PA 49
Figure 5-32: PC3R PA and PABC-2009 Overall Mean CCDFs for Normalized Direct Brine Releases 50
Figure 5-33: PC3R PA Replicate 1 Total Normalized Releases 52
Figure 5-34: PC3R PA Replicate 2 Total Normalized Releases 52
Figure 5-35: PC3R PA Replicate 3 Total Normalized Releases 53
Figure 5-36: PC3R PA Mean and Quantile CCDFs for Total Normalized Releases, Replicates 1-3 53
Figure 5-37: PC3R PA Confidence Limits on Overall Mean for Total Normalized Releases 54

Figure 5-38: PC3R PA and PABC-2009 Overall Mean CCDFs for Total Normalized Releases *54*
Figure 5-39: PC3R PA Primary Components Contributing to Total Releases *55*

List of Tables

Table 1: Constant Parameters Used for Material PCS_T1 ..... *13*
Table 2: Sampled Parameters Used for Material PCS_T1 ..... *13*
Table 3: Log of Intrinsic Permeability Values used for Material PCS_T2 in the PC3R PA *14*
Table 4: Log of Intrinsic Permeability Values used for Material DRZ-PCS in the PC3R PA for the first 100 years. *14*
Table 5: PC3R PA Parameters Updated/Created Due to the Repository Reconfiguration *14*
Table 6: BRAGFLO Modeling Scenarios *23*
Table 7: PA Intrusion Scenarios Used in Calculating Direct Solids Releases *44*
Table 8: Cavings Area Statistics for the PABC-2009 and PC3R PA *44*
Table 9: Summary of Spallings Releases by Scenario *46*
Table 10: PABC-2009 and PC3R PA DBR Volume Statistics *48*
Table 11: PC3R PA and PABC-2009 Statistics on the Overall Mean for Total Normalized Releases in EPA Units at Probabilities of 0.1 and 0.001 ..... *51*

EXECUTIVE SUMMARY

Following the recertification of the WIPP in November of 2010 (U.S. EPA 2010), the DOE will submit two PCRs to the EPA that propose changes to the repository. The first PCR is centered on a new design of the WIPP panel closure system. The panel closure "Option D" design considered in the PABC-2009 (Clayton et al. 2010) is modified to a configuration consisting of 100 feet run of mine salt emplaced against a "significant barrier" on the waste disposal side. The second PCR proposes the relocation of future waste panels 9 and 10 to the south end of the repository where they are denoted as panels 9a and 10a. With panels 9 and 10 relocated, the current repository configuration is modified to one with an open central drift area with installed panel closures located only at the end of filled waste panels. The DOE has requested that SNL conduct a single PA to determine the overall impact of the repository changes proposed in the two PCRs. Impacts of these changes are determined by way of a comparison of results obtained with the reconfigured repository and panel closure redesign to those calculated in the PABC-2009. This report summarizes the results of the panel closure redesign and repository reconfiguration performance assessment, henceforth referred to as the PC3R PA.

Total normalized releases calculated in the PC3R PA remain below their regulatory limits. As a result, the panel closure design and repository configuration changes investigated in the PC3R PA would not result in WIPP non-compliance with the containment requirements of 40 CFR Part 191. Cuttings and cavings releases and direct brine releases are the two primary release components contributing to total releases in the PC3R PA. Cuttings and cavings releases are indistinguishable from those calculated in the PABC-2009. Changes in total releases are attributed to changes calculated in direct brine releases from the PABC-2009 to the PC3R PA. Differences are observed in PC3R PA spallings releases as compared to the PABC-2009, but these differences are relatively minor and do not have a significant impact on the overall total normalized releases found in the PC3R PA.

Information Only

1 INTRODUCTION

The Waste Isolation Pilot Plant (WIPP), located in southeastern New Mexico, has been developed by the U.S. Department of Energy (DOE) for the geologic (deep underground) disposal of transuranic (TRU) waste. Containment of TRU waste at the WIPP is regulated by the U.S. Environmental Protection Agency (EPA) according to the regulations set forth in Title 40 of the Code of Federal Regulations (CFR), Part 191. The DOE demonstrates compliance with the containment requirements according to the Certification Criteria in Title 40 CFR Part 194 by means of performance assessment (PA) calculations performed by Sandia National Laboratories (SNL). WIPP PA calculations estimate the probability and consequence of potential radionuclide releases from the repository to the accessible environment for a regulatory period of 10,000 years after facility closure. The models are maintained and updated with new information as part of a recertification process that occurs at five-year intervals following the receipt of the first waste shipment at the site in 1999.

In addition to its role in certification decisions for the repository, PA is used to determine the impacts of repository modifications proposed by the DOE as part of planned change requests (PCRs). Previous analyses have been performed to assess the impacts of modifications to the panel closure system implemented in the repository (Hansen 2002, Vugrin and Dunagan 2006). The 1998 rulemaking that certified WIPP to receive TRU waste had several conditions, one of which involved the design of the panel closure system. The EPA based its certification decision on the condition that the DOE implement the most robust panel closure design, referred to as the "Option D" design in the CCA (U.S. EPA 1998). With the recertification of the WIPP in November of 2010 (U.S. EPA 2010), a new PA baseline was established by the 2009 Performance Assessment Baseline Calculation (PABC-2009).

Following recertification of the facility, the DOE plans to submit two PCRs to the EPA that propose changes to the repository. The first PCR is centered on a new design of the WIPP panel closure system (PCS). The panel closure "Option D" design considered in the PABC-2009 (Clayton et al. 2010) is to be modified to a configuration consisting of 100 feet run of mine salt emplaced against a "significant barrier" on the waste disposal side. The second PCR proposes the relocation of future waste panels 9 and 10 to the south end of the repository, i.e. south of panels 4 and 5, where they will be denoted as panels 9a and 10a. With panels 9 and 10 relocated, the current repository configuration will be modified to one with an open central drift area with installed panel closures located only at the end of filled waste panels. The DOE has requested that SNL conduct a single PA to determine the overall impact of the repository changes proposed in the two PCRs. Impacts of these changes are determined by way of a comparison of release probabilities to those calculated in the PABC-2009. This report provides a summary of

calculations and analyses performed in the panel closure redesign and repository reconfiguration performance assessment, henceforth referred to as the PC3R PA.

The work undertaken in the PC3R PA is prescribed in AP-151, *Analysis Plan for the WIPP Panel Closure Redesign and Repository Reconfiguration Performance Assessment* (Camphouse 2010a), which was specifically written to determine the impact of changes proposed in the two PCRs on long-term repository performance. In order to isolate the impacts of the repository configuration and panel closure design changes, the PC3R PA was designed to deviate as little as possible from the PABC-2009 implementation. In particular, the PC3R PA utilizes the same waste inventory information, drilling rate and plugging pattern parameters, and radionuclide solubility parameters as were used in the PABC-2009. The PC3R PA examines all aspects of repository performance that are potentially impacted by the proposed changes to the repository.

2 REPOSITORY CONFIGURATION CHANGES

The following sections detail the changes to the repository configuration and panel closure design investigated in the PC3R PA. Following the discussion of the repository changes, the impacts of these changes on the parameters and computational grids used in the PC3R PA are presented.

2.1 Repository Reconfiguration

A schematic that depicts the WIPP spatial layout as it has been modeled in PA is shown in Figure 2-1. As seen in that figure, the waste disposal region consists of 10 waste panels. Panels 1-4 are located east of the central area with panels 5-8 located to the west. Panels 9 and 10 are located in the center area between panels 1-4 and panels 5-8. Additionally, panel closures are located at the innermost ends of panels 1-8. A set of panel closures is located between waste panels 9 and 10. Another set of closures is located between panels 1-10 and the southern end of the operations region. A final set of closures is located in the operations region south of the repository shafts. These locations of waste panels and panel closures have been implemented in the models used in performance assessments since the original CCA, including the PABC-2009.

The changes to the repository configuration that are modeled in the PC3R PA include the relocation of panels 9 and 10, the removal of panel closures in the central drift area, and a redesign of panel closures that remain. Panels 9 and 10 are relocated south of panels 4 and 5 in the PC3R PA and denoted as panels 9a and 10a. In effect, the waste area is lengthened with duplicate copies of panels 4 and 5, and their corresponding panel closures, located at the southernmost end of the repository. The resulting waste panel configuration consists of panels 1-4, 9a east of the central area and panels 10a, 5-8 west of the center. Panels 1-8, 9a, and 10a are modeled as having identical panel closures located at their innermost ends.

Informational Copy

With the relocation of panels 9 and 10 to the southernmost end of the repository, panel closures located in the central drift area are removed. Consequently, the set of panel closures located between current panels 9 and 10, between the waste disposal region and the operations area, and between the southern portion of the operations area and the repository shafts are not present in the PC3R PA representation of the repository.

Finally, the representation of panel closures that remain for panels 1-8, 9a, and 10a is changed in the PC3R PA. "Option D" panel closures were modeled in the PABC-2009, and are represented in Figure 2-1 by black segments at the ends of waste panels and at appropriate locations in the central drift area. Panel closures are proposed to be modified from the current "Option D" design to that of a new design consisting of 100 feet of run of mine salt emplaced against a significant barrier on the waste disposal side. As the characterization of the significant barrier is still underway, the redesigned panel closures are modeled in the PC3R PA as consisting solely of 100 feet of run of mine salt. The reconfigured repository modeled in the PC3R PA is shown in Figure 2-2, where redesigned closures are depicted by oval segments at the innermost ends of waste panels.

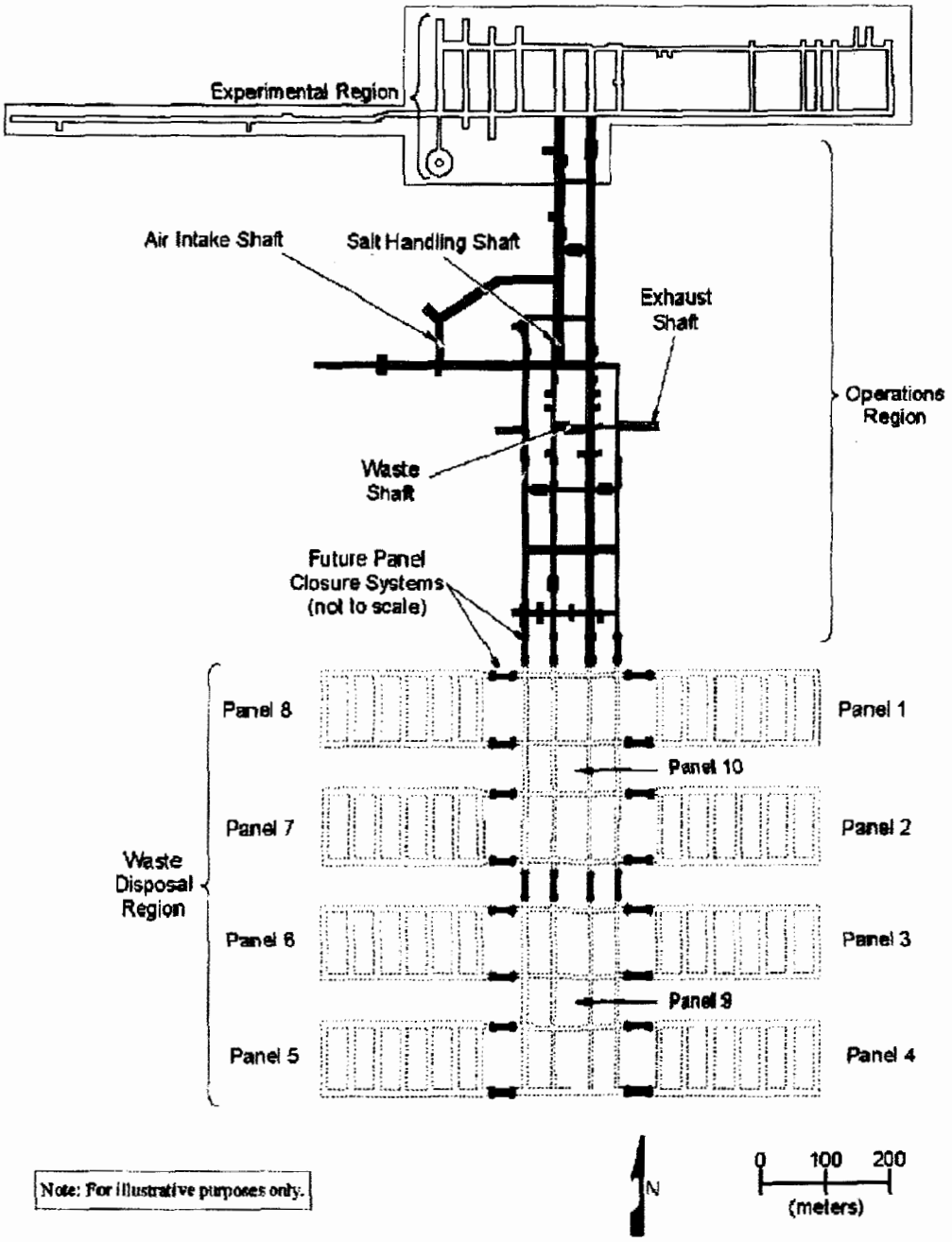

Figure 2-1: Historical WIPP Repository Layout

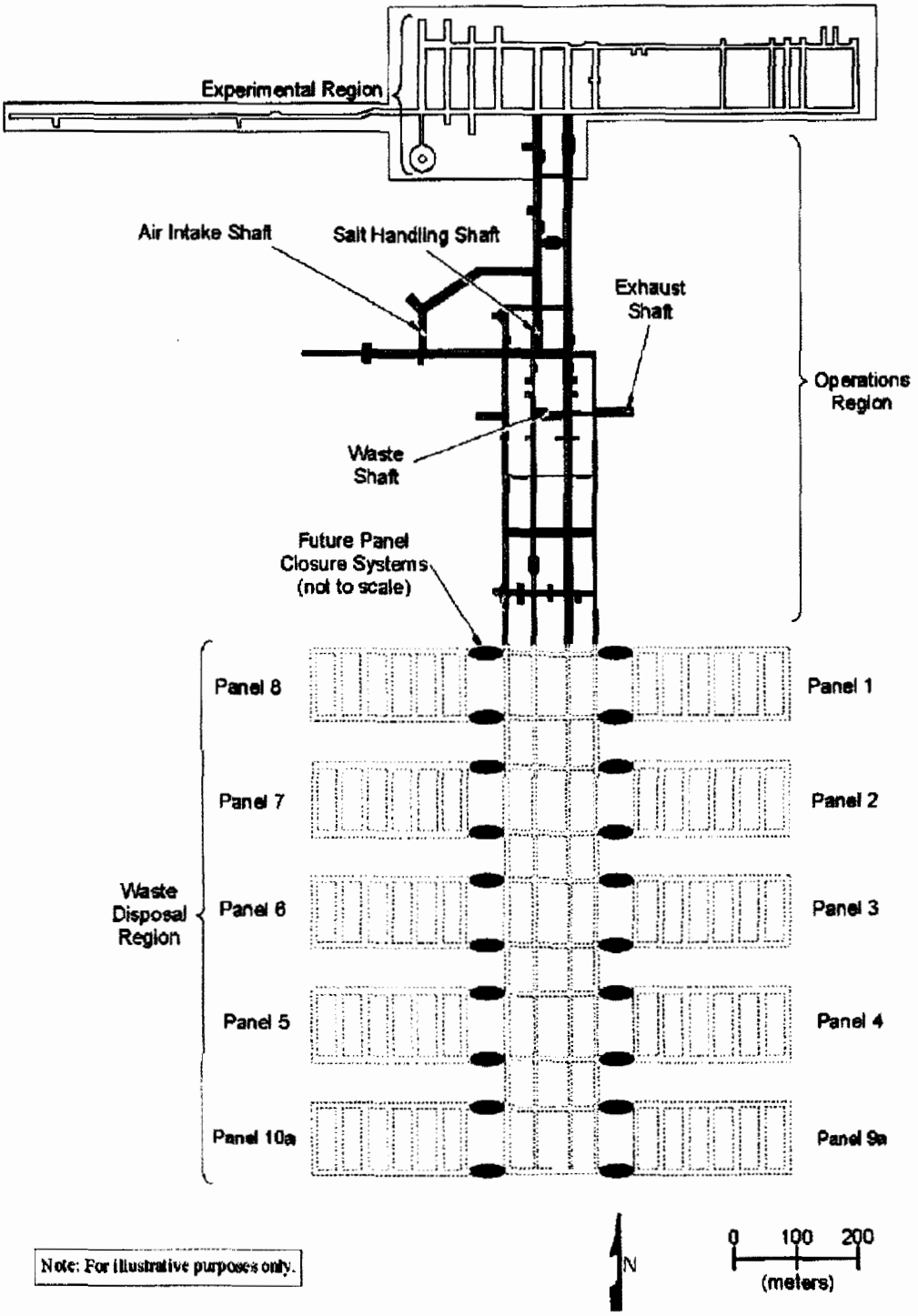

Figure 2-2: WIPP Layout Modeled in PC3R PA

2.2 Parameters

In order to isolate the impacts of the repository changes discussed above, the PC3R PA was designed to deviate as little as possible from the PABC-2009 implementation. However, changes due to the reconfigured waste panel and closure arrangement, as well as the implementation of panel closures consisting of 100 feet of run of mine salt, impact a subset of the parameters prescribed in the PABC-2009. Justifications of new and modified parameters used in the PC3R PA are provided in Camphouse (2010b, 2010c, 2011a). The same material property values and ranges used in the PABC-2009 were also used in the PC3R PA, with the exception of the material and property changes discussed below.

Panel Closure Parameters

The majority of PC3R PA parameter changes are due to the incorporation of run of mine salt panel closures, and these changes are now discussed. The PC3R PA panel closure system has initial permeabilities and porosities that are significantly different than the permeabilities and porosities expected to be present for the vast majority of the 10,000 year regulatory timeframe. In other words, PC3R panel closures have "short-term" initial characteristics and "long-term" characteristics. As a result, two materials are used to describe PC3R panel closures. Material PCS_T1 is the material used to represent panel closures for an initial time period of 100 years. Material PCS_T2 is the material used to represent closures for the remaining 9,900 years. Initial and long-term time periods are selected to be consistent with the lengths of time required for the porosity of the run of mine salt used in the panel closures to fall below 5 percent. Numerical simulations demonstrate this period of time to be less than 100 years (Callahan and DeVries 1991). This time duration is also consistent with that proposed during the 2002 panel closure redesign impact assessment (Hansen and Thompson 2002).

Constant values and probability distributions used for parameter sampling were established for properties associated with materials PCS_T1 and PCS_T2. Constant values and probability distributions corresponding to material PCS_T1 are shown in Table 1 and Table 2, respectively. Constant values and probability distributions established for material PCS_T2 properties COMP_RCK, SAT_RBRN, SAT_RGAS, RELP_MOD, CAP_MOD, KPT, PC_MAX, PO_MIN, PCT_A, PCT_EXP, and PORE_DIS are identical to those established for material PCS_T1. The value specified for the porosity of material PCS_T2, i.e. parameter PCS_T2:POROSITY, is 0.05 (dimensionless).

The panel closure redesign impact assessment performed in 2006 (Vugrin and Dunagan 2006) also used materials PCS_T1 and PCS_T2 to model the changing material properties of the panel closure as a function of time. In that analysis, the panel closure design consisted of 100 feet of run of mine salt emplaced against a 30 foot mortared, solid concrete block wall on the waste disposal side. Parameter distributions for the long-term permeability of the run of mine salt

component were developed during the 2006 impact assessment (Vugrin, Hansen, and Thompson 2006). The permeability distribution developed in that analysis is used to describe the long-term permeability of the panel closure implemented in the PC3R PA. The resulting probability distribution used to specify the log of intrinsic permeability of material PCS_T2 is shown in Table 3.

Stein (2002a) introduced material DRZ_PCS as the portion of the disturbed rock zone directly above and below the panel closure system. This material is used in PA to describe temporal characteristics of the DRZ about a panel closure. For the 100 foot run of mine salt panel closures implemented in the PC3R PA, the properties prescribed to material DRZ_PCS were done so as to reflect the changing material properties of the redesigned closure system as a function of time. During the first 100 years while the run of mine salt panel closures are reconsolidating to their steady-state properties, material DRZ_PCS is specified to have identical properties to the remaining DRZ. In other words, it is assumed that the DRZ directly above and below the panel closure is unaffected by the changing panel closure properties during the first 100 years. The permeabilities prescribed for material DRZ_PCS during the first 100 years are identical to those prescribed to the DRZ overall, i.e. those specified for PA material DRZ_1. These permeability distributions are given in Table 4. After the first 100 years, permeability values of material DRZ_PCS are prescribed so as to be consistent with the permeabilities of the reconsolidated panel closures. As a result, they are assigned the permeability distributions given to material PCS_T2 as shown in Table 3.

Table 1: Constant Parameters Used for Material PCS_T1

Parameter (units)	Description	Value
PCS_T1: COMP_RCK (Pa^{-1})	Bulk compressibility	$8x10^{-11}$
PCS_T1:POROSITY (n/a)	Effective porosity	0.33
PCS_T1:PRMX_LOG ($log(m^2)$)	Log of intrinsic permeability, x,y,z directions	-11.0
PCS_T1:PRMY_LOG ($log(m^2)$)		
PCS_T1:PRMZ_LOG ($log(m^2)$)		
PCS_T1:SAT_IBRN (n/a)	Initial brine saturation	0.054
PCS_T1:RELP_MOD (n/a)	Model number, relative permeability model	4.0
PCS_T1:CAP_MOD (n/a)	Model number, capillary pressure model	1.0
PCS_T1:KPT (n/a)	Flag for permeability determined threshold	0.0
PCS_T1:PC_MAX (Pa)	Maximum allowable capillary pressure	$1x10^8$
PCS_T1:PO_MIN (Pa)	Minimum brine pressure for capillary model KPC=3	$1.01325x10^5$
PCS_T1:PCT_A (Pa)	Threshold pressure linear parameter	0.0
PCS_T1:PCT_EXP (n/a)	Threshold pressure exponential parameter	0.0

Table 2: Sampled Parameters Used for Material PCS_T1

Parameter (units)	Description	Distribution	Statistic	Value
PCS_T1: SAT_RBRN (n/a)	Residual Brine Saturation	Cumulative with (Prob.,Value) Pairs (0,0) (0.5,0.2) (1.0,0.6)	Mean	0.25
			Median	0.2
			Stan. Deviation	0.176
			Minimum	0.0
			Maximum	0.6
PCS_T1: SAT_RGAS (n/a)	Residual Gas Saturation	Uniform	Mean	0.2
			Median	0.2
			Stan. Deviation	0.1155
			Minimum	0.0
			Maximum	0.4
PCS_T1: PORE_DIS (n/a)	Brooks-Corey pore distribution parameter	Cumulative with (Prob.,Value) Pairs (0,0.11) (0.5,0.94) (1.0,8.1)	Mean	2.52
			Median	0.94
			Stan. Deviation	2.48
			Minimum	0.11
			Maximum	8.1

Table 3: Log of Intrinsic Permeability Values used for Material PCS_T2 in the PC3R PA

Parameter (units)	Description	Distribution	Statistic	Value
PCS_T2:PRMX_LOG ($\log(m^2)$) PCS_T2:PRMY_LOG ($\log(m^2)$) PCS_T2:PRMZ_LOG ($\log(m^2)$)	Log of intrinsic permeability, x,y,z directions	Triangular	Mean	-20.2
			Mode	-20.2
			Stan. Deviation	1.06
			Minimum	-22.8
			Maximum	-17.6

Table 4: Log of Intrinsic Permeability Values used for Material DRZ-PCS in the PC3R PA for the first 100 years.

Parameter (units)	Description	Distribution	Statistic	Value
DRZ_PCS:PRMX_LOG ($\log(m^2)$) DRZ_PCS:PRMY_LOG ($\log(m^2)$) DRZ_PCS:PRMZ_LOG ($\log(m^2)$)	Log of intrinsic permeability, x,y,z directions	Triangular	Mean	-16.0
			Median	-16.0
			Stan. Deviation	2.0
			Minimum	-19.4
			Maximum	-12.5

Panel Reconfiguration Parameters

The relocation and re-sizing of current panels 9 and 10 to their 9a and 10a counterparts invoked modifications to some of the reference constants (material REFCON) used in the PABC-2009 as well as an updated value for parameter DRZ_1:EHEIGHT. Moreover, in the PC3R PA, the central drift area was assigned properties corresponding to material OPS_AREA in the PABC-2009. As the central drift area in the reconfigured repository has a much larger extent than did OPS_AREA in the PABC-2009, and is located between west and east waste panels, a new parameter OPS_AREA:EHEIGHT was established for use in the PC3R PA. The values specified for these remaining parameters in the PC3R PA are shown in Table 5.

Table 5: PC3R PA Parameters Updated/Created Due to the Repository Reconfiguration

Parameter (units)	Description	Value
REFCON:VREPOS (m^3)	Excavated storage volume of repository	4.609765×10^5
REFCON:FVW (n/a)	Fraction of repository volume occupied by waste in CCDFGF	0.367
REFCON:AREA_CH (m^2)	Area for CH Waste Disposal in CCDFGF	1.164×10^5
REFCON:ABERM (m^2)	Berm Area	7.85625×10^5
DRZ_1:EHEIGHT (m)	Effective height of the disturbed rock zone for DBR calculations	41.3

OPS_AREA:EHEIGHT (m)	Effective height of the operations area for DBR calculations	10.7

2.3 Computational Grid Changes

PA code BRAGFLO is used in two ways in WIPP PA calculations. First, it is used to calculate the flow of brine and gas in and around the repository for undisturbed and disturbed conditions. Second, it is used for the calculation of direct brine releases (DBRs). These two uses of BRAGFLO require different computational grids. The grid used to calculate brine and gas flow in and around the repository is different than that used to calculate DBRs. However, results obtained from the brine and gas flow calculation are used to initialize conditions in the DBR calculation. The changes proposed to the WIPP repository configuration impact the computational grids used in both applications of BRAGFLO. For the sake of completeness in this summary report, these changes are now briefly discussed. More detailed discussions of the PC3R PA BRAGFLO computational grids, and their differences in regard to the grids used in the PABC-2009, can be found in Camphouse and Clayton (2011) & Pasch and Camphouse (2011).

The historical WIPP configuration shown in Figure 2-1 has been the underlying motivation for the repository representation in prior BRAGFLO numerical grids, including the PABC-2009. Using that configuration, panel closures located in the central drift area were used to decompose the repository waste area into three regions in the PABC-2009. The southwest panel, panel 5 in Figure 2-1, was the panel in which inadvertent human intrusion was modeled in BRAGFLO. As a result, the southwest panel was modeled separately from the rest of the waste area. The remaining waste panels comprised two additional waste regions in the PABC-2009 BRAGFLO grid, namely the south rest of repository (SROR) (panels 3, 4, 6, and 9), and the north rest of repository (NROR) (panels 1, 2, 7, 8, and 10), with each region being separated by a panel closure. The location of a panel closure slightly south of the waste shaft resulted in the operations (Ops) and experimental (Exp) regions being separated by a material combining panel closure and waste shaft properties. The PABC-2009 BRAGFLO grid is shown in Figure 2-3. In that figure, regions labeled DRF_PCS and CONC_PCS represent components of "Option D" panel closures.

Information Only

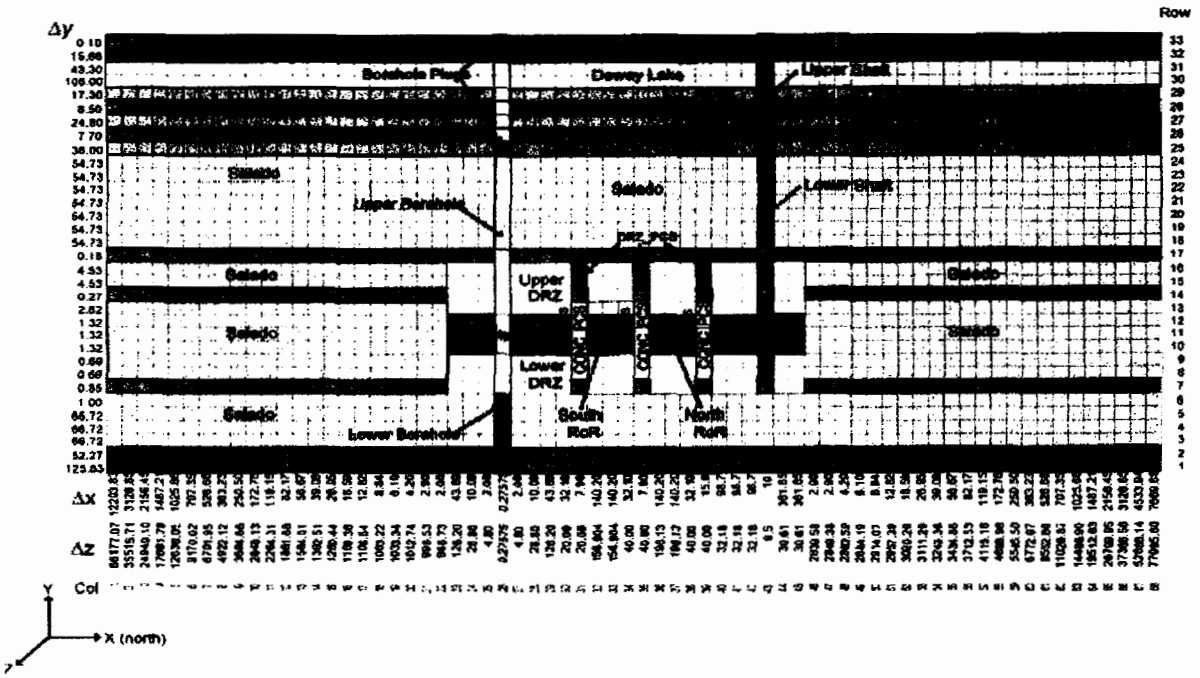

Figure 2-3: PABC-2009 BRAGFLO grid (Δx, Δy, and Δz dimensions in meters).

Following a similar strategy as for the historical WIPP layout shown in Figure 2-1, the reconfigured repository shown in Figure 2-2 guides the BRAGFLO computational grid implementation in the PC3R PA. In the PABC-2009, panel closures in the central area provided a natural way to demarcate the repository into northern and southern regions. In the reconfigured repository layout, the open central drift region between west and east waste panels results in a BRAGFLO grid with a west-to-east orientation. Panel 10a is used to model inadvertent human intrusion. This waste panel is separated from the remaining panels by the open central drift area. As a result, remaining panels are lumped together in a rest of repository (ROR) region in the PC3R PA BRAGFLO grid. The waste panel, center area, and ROR are separated by panel closures comprised of 100 feet run of mine salt. The PC3R PA BRAGFLO computational grid is shown in Figure 2-4.

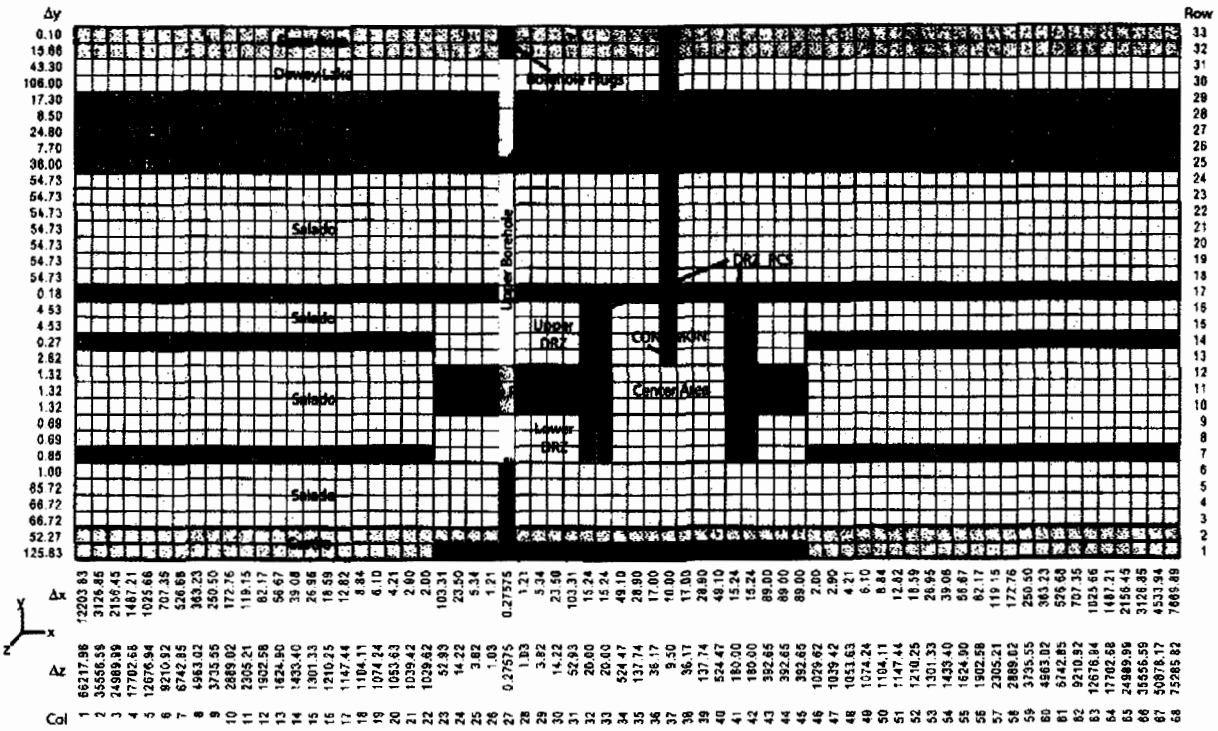

Figure 2-4: PC3R PA BRAGFLO grid (Δx, Δy, and Δz dimensions in meters).

Results from the PABC-2009 BRAGFLO calculation were used to initialize conditions in the PABC-2009 DBR calculation. The representation of the waste area by three waste regions in the PABC-2009 BRAGFLO grid yielded initial conditions to waste regions comprising the waste panel, the SROR, and the NROR in the PABC-2009 BRAGFLO DBR calculations (Clayton 2010). The initialization of these three regions in the DBR calculation resulted in the consideration of drilling intrusions into these regions in the PABC-2009 DBR analysis. These locations can be seen in the PABC-2009 DBR computational grid of Figure 2-5.

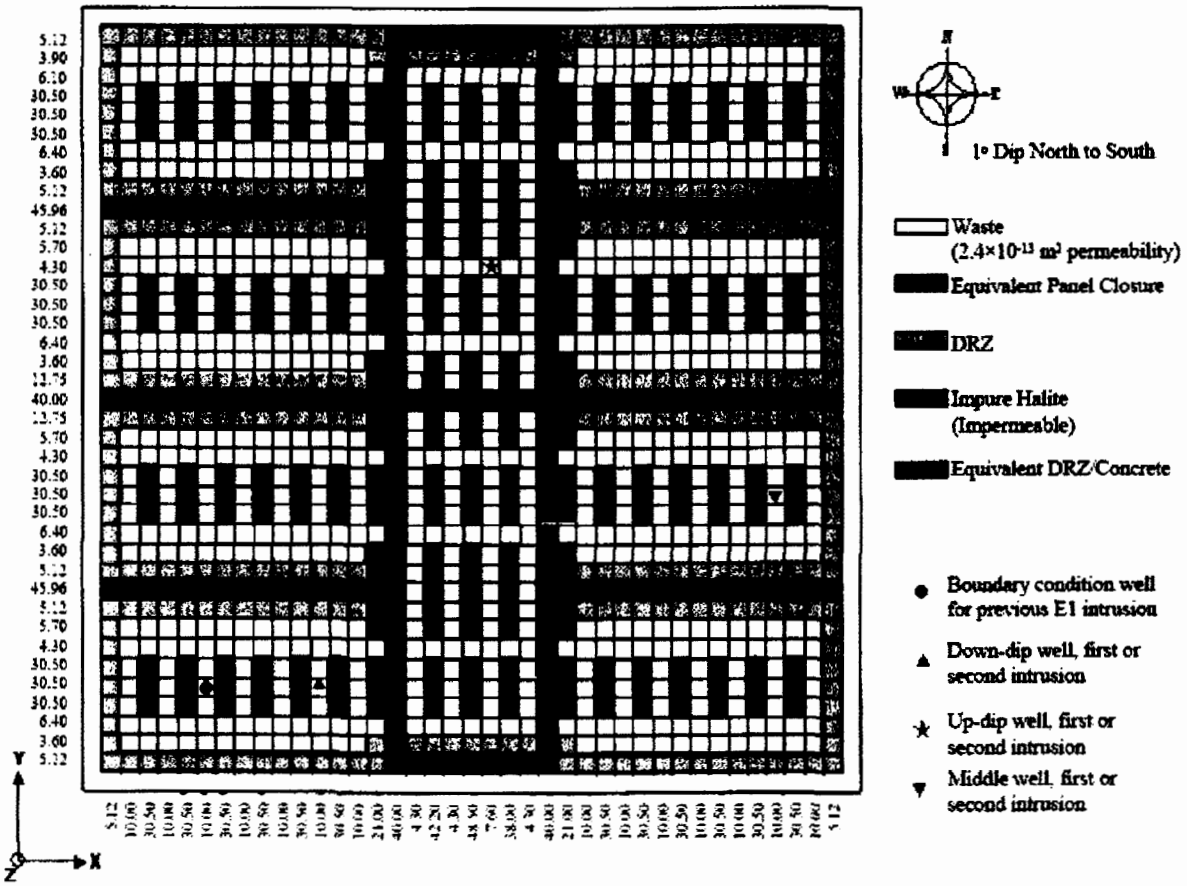

Note: Model cells are not to scale. The actual dimensions of the grid blocks are indicated along the edge of the diagram.

Figure 2-5: PABC-2009 DBR material map (logical grid).

The reconfigured repository seen in Figure 2-2 resulted in several changes to the numerical grid used to analyze direct brine releases in the PC3R PA. First, waste panels 9 and 10 were removed from the central drift area, relocated to the southernmost end of the repository, and denoted as panels 9a and 10a. As panels 9 and 10 have slightly less area than waste panels 1-8, panels 9a and 10a were resized to have areas equal to those of panels 1-8. Second, "Option D" panel closures in the PABC-2009 were replaced by panel closures consisting of 100 feet run of mine salt with properties corresponding to materials PCS_T1 and PCS_T2. Third, panel closures located in the central drift area in the PABC-2009 DBR grid were removed in the PC3R PA DBR grid. Fourth, the representation of the waste area by two regions in the PC3R PA BRAGFLO grid resulted in two drilling locations, an upper and a lower location, in the direct brine release analysis undertaken in the PC3R PA. These locations can be seen in the PC3R PA DBR computational grid of Figure 2-6.

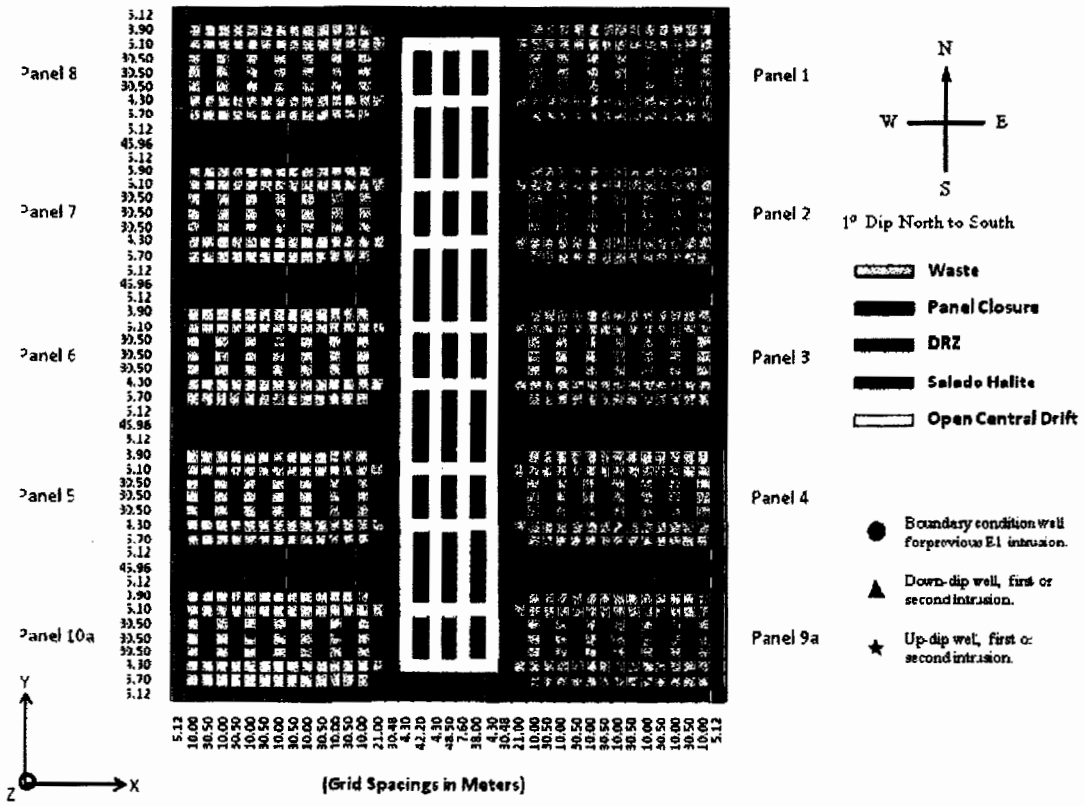

Figure 2-6: PC3R PA DBR material map (logical grid).

Material properties for the open central drift area in the PC3R PA are assigned values corresponding to the operations area (material OPS_AREA) in the PABC-2009. Parameter OPS_AREA:EHEIGHT was established for use in the PC3R PA DBR calculations in order to achieve agreement between the three-dimensional representation of the central region in BRAGFLO and the two-dimensional representation of this region in the DBR numerical grid. This property provides a means of matching porosity and pore compressibility in the central drift region across the BRAGFLO and DBR calculations. Its value is given in Table 5.

In both the PABC-2009 and the PC3R PA, consideration of drilling events was restricted to those repository regions with emplaced waste. Waste is not emplaced in the operations and experimental areas of the historical WIPP repository configuration, nor in the central drift area of the PC3R PA configuration. As a result, potential drilling intrusions into these areas will not result in cuttings, cavings, or spallings releases. Potential releases following an intrusion into these areas require that they contain a sufficient volume of waste-contaminated brine under sufficient pressure. For this to occur, brine must interact with waste in a panel and migrate to a non-waste containing region to be available for release at the time of intrusion. In all cases investigated in the Salado flow modeling of the PC3R PA (see Section 5.1 of this summary report), the total flow of brine out of the waste panel was reduced (on average) when compared

to results obtained in the PABC-2009. The panel closure redesign and repository configuration implemented in the PC3R PA does not result in an increase in contaminated brine leaving a waste panel. Furthermore, as discussed and demonstrated in Section 5.2, an intrusion into a waste panel will not result in a consequential increase in brine volume in the central drift area to later be released to the surface by a subsequent intrusion in that area. The brine available for release to the surface following a drilling event into the central drift region is brine present under undisturbed conditions, regardless of previous intrusions into a waste panel. In addition, drilling intrusions into the central drift region can only *reduce* releases following an intrusion into a waste panel. For quantification of releases, the consideration of drilling intrusions into waste-containing regions is sufficient, and is conservative.

2.4 FEPS Re-assessment

An assessment of the FEPs baseline was conducted to determine if the current FEPs basis remains valid in consideration of changes introduced by the PC3R PA, and was performed according to SP 9-4, *Performing FEPs Impact Assessment for Planned or Unplanned Changes.* The FEPs analysis concludes that no additional FEPs are needed to accurately represent the changes that represent the repository layout (including the location of the PCS) and the PCS design and construction. Additionally, no FEPs screening arguments and associated screening decisions require modification to account for the changes represented in the PC3R PA (Kirkes 2011).

3 METHODOLOGY

The performance assessment methodology accommodates both aleatory (i.e. stochastic) and epistemic (i.e. subjective) uncertainty in its constituent models. Aleatory uncertainty pertains to unknowable future events such as intrusion times and locations that may affect repository performance. It is accounted for by the generation of random sequences of future events. Epistemic uncertainty concerns parameter values that are assumed to be constants and the constants' true values are uncertain due to a lack of knowledge about the system. An example of a parameter with epistemic uncertainty is the permeability of a material. Epistemic uncertainty is accounted for by sampling of parameter values from assigned distributions. One set of sampled values required to run a WIPP PA calculation is termed a vector. In the PC3R PA, models were executed for three replicates of 100 vectors, each vector providing model realizations resulting from a particular set of parameter values. Parameter sampling performed in the PC3R PA is documented in Camphouse (2011b), and the sensitivities of variable output to sampled parameters are documented in Hansen (2011). A sample size of 10,000 possible sequences of future events is used in PA calculations to address aleatory uncertainty. The releases for each of 10,000 possible sequences of future events are tabulated for each of the 300 vectors, totaling 3,000,000 possible sequences.

For a random variable, the complementary cumulative distribution function (CCDF) provides the probability of the variable being greater than a particular value. By regulation, performance assessment results are presented as a distribution of CCDFs of releases (U.S. EPA 1996). Each individual CCDF summarizes the likelihood of releases across all futures for one vector of parameter values. The uncertainty in parameter values results in a distribution of CCDFs.

Releases are quantified in terms of "EPA units". Releases in EPA units result from a normalization by radionuclide and the total inventory. For each radionuclide, the ratio of its 10,000 year cumulative release (in curies) to its release limit is calculated. The sum of these ratios is calculated across the set of radionuclides and normalized by the transuranic inventory (in curies) of α-emitters with half-lives greater than 20 years. Mathematically, the formula used to calculate releases in terms of EPA units is of the form

$$R = \frac{1 \times 10^6\, curies}{C} \sum_i \frac{Q_i}{L_i}$$

where R is the normalized release in EPA units. Quantity Q_i is the 10,000 year cumulative release (in curies) of radionuclide i. Quantity L_i is the release limit for radionuclide i, and C is the total transuranic inventory (in curies) of α-emitters with half-lives greater than 20 years.

The PC3R PA was developed so that the structure of calculations performed therein was as similar as possible to that used in the PABC-2009. PABC-2009 calculated results potentially impacted by the repository reconfiguration and panel closure redesign discussed above were updated, while the results from previous PAs were used for individual numerical codes not affected by these changes. The PC3R PA utilized the same waste inventory information, drilling rate and plugging pattern parameters, and radionuclide solubility parameters as were used in the PABC-2009. In addition, transport releases through the Culebra calculated in the PABC-2009 were also used in the PC3R PA. Separate documentation was prepared describing calculations performed and results obtained for each code executed in the PC3R PA. Citations for this additional documentation are included in the references section of this summary report, and are indicated in the list below.

- Parameter Sampling (Camphouse 2011b)
- Sensitivity Analysis (Hansen 2011)
- Salado Flow (Camphouse and Clayton 2011)
- Cuttings, Cavings, and Spallings (Kicker 2011)
- Actinide Mobilization and Transport (Camphouse and Garner 2011)
- Direct Brine Releases (Pasch and Camphouse 2011)
- CCDF Normalized Releases (Camphouse 2011c)

Unconstrained Data

4 RUN CONTROL

Execution of Performance Assessment Codes for the WIPP Panel Closure Redesign and Repository Reconfiguration (Long 2011) provides documentation of run control and code execution for the PC3R PA. This document contains:

1. A description of the hardware platform and operating system used to perform the calculations.
2. A listing of the codes and versions used to perform the calculations.
3. A listing of the scripts used to run each calculation.
4. A listing of the input and output files for each calculation.
5. A listing of the library and class where each file is stored.
6. File naming conventions.

5 RESULTS

Summary results obtained from PC3R PA calculations are broken out in subsections below, and are compared to PABC-2009 results. Salado flow modeling results are presented in Subsection 5.1. The effectiveness of the redesigned panel closures in regard to the isolation of drilling intrusion effects is discussed in Subsection 5.2. Impacts of the repository reconfiguration and panel closure redesign on actinide mobilization and transport are shown in Subsection 5.3. Results obtained for cuttings and cavings are presented in Subsection 5.4. Spallings results are presented in Subsection 5.5. Direct brine releases are presented in Subsection 5.6. The impact of the changes investigated in the PC3R PA on regulatory compliance is discussed in terms of total normalized releases in Subsection 5.7. As the CCDF is the regulatory metric used to demonstrate compliance, comparisons of CCDFs obtained in the PC3R PA and the PABC-2009 are compared for each component of release in the appropriate subsection.

5.1 Salado Flow Results

The BRAGFLO software calculates the flow of brine and gas in the vicinity of the WIPP repository over the 10,000-year regulatory compliance period. During BRAGFLO calculations, stochastic uncertainty is addressed by defining a set of six scenarios for which brine and gas flow is calculated for each of the vectors generated via parameter sampling. The total number of BRAGFLO simulations executed in the PC3R PA is 1,800 (300 vectors times 6 scenarios).

The six scenarios used in the PC3R PA are unchanged from those used for the PABC-2009. The scenarios include one undisturbed scenario (S1-BF), four scenarios that include a single inadvertent future drilling intrusion into the repository during the 10,000 year regulatory period (S2-BF to S5-BF), and one scenario investigating the effect of two intrusions into a single waste panel (S6-BF). Two types of intrusions, denoted as E1 and E2, are considered. An E1 intrusion assumes the borehole passes through a waste-filled panel and into a pressurized brine pocket that

may exist under the repository in the Castile formation. An E2 intrusion assumes that the borehole passes through the repository but does not encounter a brine pocket. Scenarios S2-BF and S3-BF model the effect of an E1 intrusion occurring at 350 years and 1000 years, respectively, after the repository is closed. Scenarios S4-BF and S5-BF model the effect of an E2 intrusion at 350 and 1000 years. Scenario S6-BF models an E2 intrusion occurring at 1000 years, followed by an E1 intrusion into the same panel at 2000 years. Transport releases to the Culebra are captured in Scenario S6-BF. Scenario S6-BF is used for determining the radionuclide source term to the Culebra in the PA code PANEL, and results of this scenario are discussed in Subsection 5.3. Table 6 summarizes the six scenarios used in this analysis.

Table 6: BRAGFLO Modeling Scenarios

Scenario	Description
S1-BF	Undisturbed Repository
S2-BF	E1 intrusion at 350 years
S3-BF	E1 intrusion at 1,000 years
S4-BF	E2 intrusion at 350 years
S5-BF	E2 intrusion at 1,000 years
S6-BF	E2 intrusion at 1,000 years; E1 intrusion at 2,000 years.

Computed results are presented for the PC3R PA and compared with those obtained in the PABC-2009. Results are discussed in terms of overall means. Overall means are obtained by forming the average of the 300 realizations calculated for a given quantity and scenario. Results are presented for undisturbed scenario S1-BF. Intruded results are presented for scenarios S2-BF and S4-BF, as these are representative of the intrusion types considered in scenarios S2-BF to S5-BF with the only differences being the timing of drilling intrusions. The computational grids used to generate Salado flow results in the PABC-2009 and the PC3R PA are shown in Figure 2-3 and Figure 2-4, respectively.

Undisturbed Scenario S1-BF

Scenario S1-BF overall means of porosity in the waste panel, quantity WAS_POR, for the PC3R PA and the PABC-2009 are shown together in Figure 5-1. As is clear from that figure, there is very little difference in the time-histories of waste panel porosities for both analyses. Porosities in both analyses reduce rapidly, with the average porosity nearing its steady-state value within hundreds of years following facility closure.

Overall means of volume-averaged pressure in the waste panel, quantity WAS_PRES, for the PC3R PA and the PABC-2009 are shown together in Figure 5-2. As seen in that figure, the volume averaged pressure for the PC3R PA is slightly lower than that seen in the PABC-2009. The reason for this reduction is seen in Figure 5-3. In Figure 5-3, the overall mean of quantity WAS_PRES is plotted on a time scale of 0 to 150 years for both the PC3R PA and the PABC-2009. As the porosity of the waste panel rapidly decreases in the time period immediately after

facility closure, the higher permeability and porosity of the run of mine salt panel closure for the first 100 years allows the increasing pressure to be released into the open central area between the waste panel and the rest of the repository. At t = 100 years, the porosity and permeabilities of the panel closures are reduced to their steady-state values. At t = 100 years in Figure 5-3, there is a distinct increase in the rate of pressure rise in the waste panel. By this time, however, the porosity in the waste panel is nearing its steady-state value, and so much of the increasing pressure in the waste panel responsible for the decreasing porosity has been vented into the open central area. The net effect is a slightly reduced volume-averaged pressure in the waste panel for the PC3R PA.

The overall mean of brine saturation in the waste panel, quantity WAS_SATB, is shown in Figure 5-4. As seen in that figure, waste panel brine saturation results obtained in the PC3R PA for the undisturbed repository condition are nearly identical to those found in the PABC-2009.

The overall means of total brine flow out of the waste panel, quantity BRNWASOC, is shown in Figure 5-5. As seen in that figure, the brine flow out of the waste panel decreased for Scenario S1-BF in the PC3R PA. This reduction is due to the lower waste panel pressure as compared to the PABC-2009. The slightly lower long-term permeabilites of the PC3R PA panel closures also contributed to the reduction of brine flow out of the waste regions. While the larger initial porosity and permeabilities of the panel closures investigated in the PC3R PA allow pressure release from the waste panel into the center area for the first 100 years, their use does not result in an increase in brine flow out of the waste panel.

Overall means of total brine flow up the shaft, quantity BNSHUDRZ, are shown in Figure 5-6. In the PC3R PA, the shaft is directly above the open central region in the BRAGFLO grid. The open central region contains the open volume of the operations and experimental area as well as the open volume associated with panels 9 and 10 in the PABC-2009 grid. The increase in volume translates to a reduction in pressure in the center area. The total brine flow up the shaft decreased for Scenario S1-BF in the PC3R PA due to the lower pressure in the open central region.

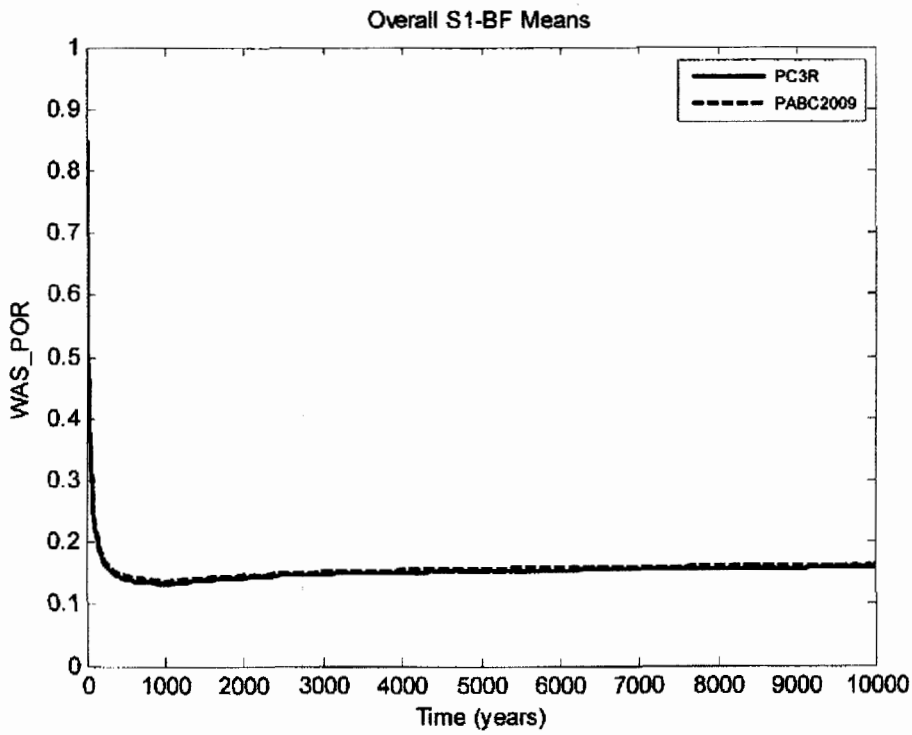

Figure 5-1: Overall Means of Volume Averaged Porosity for the Waste Panel, Scenario S1-BF

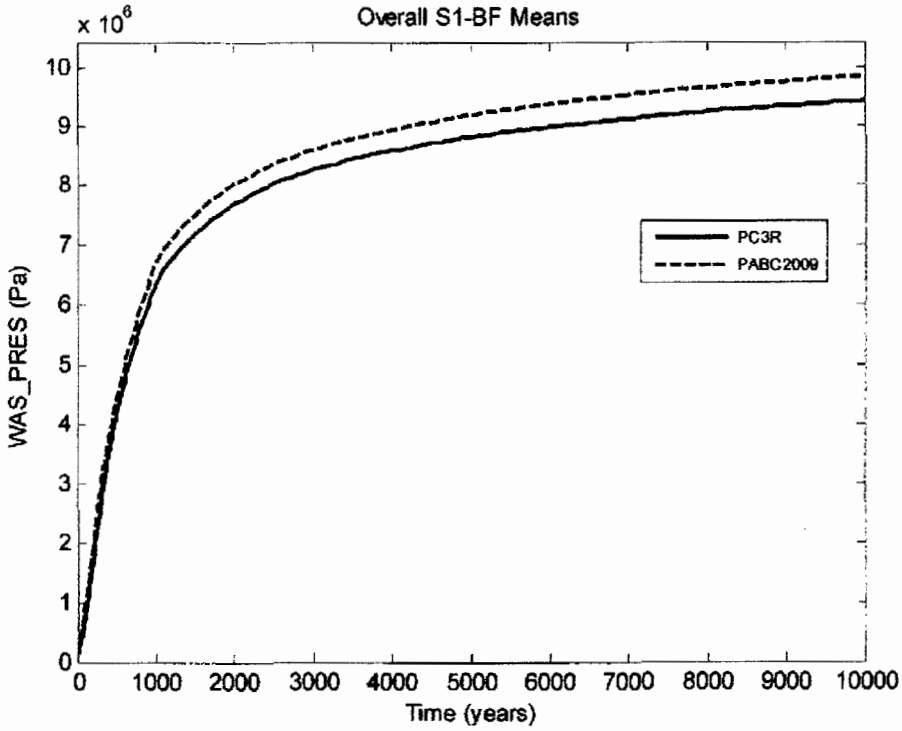

Figure 5-2: Overall Means of Volume Averaged Pressure for the Waste Panel, Scenario S1-BF

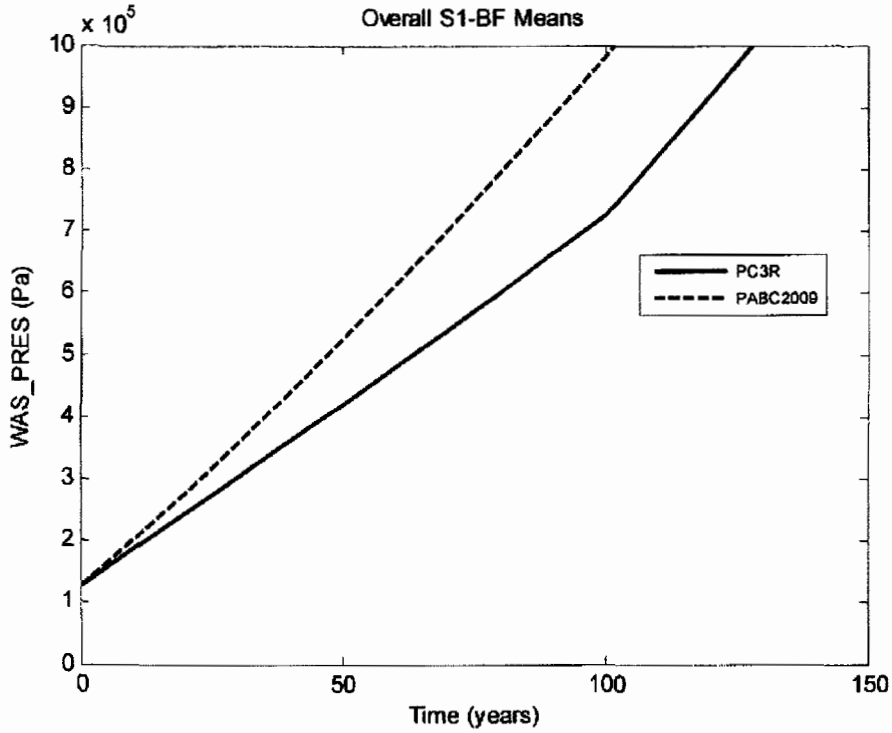

Figure 5-3: Overall Means of Volume Averaged Pressure for the Waste Panel During the First 150 Years After Closure, Scenario S1-BF

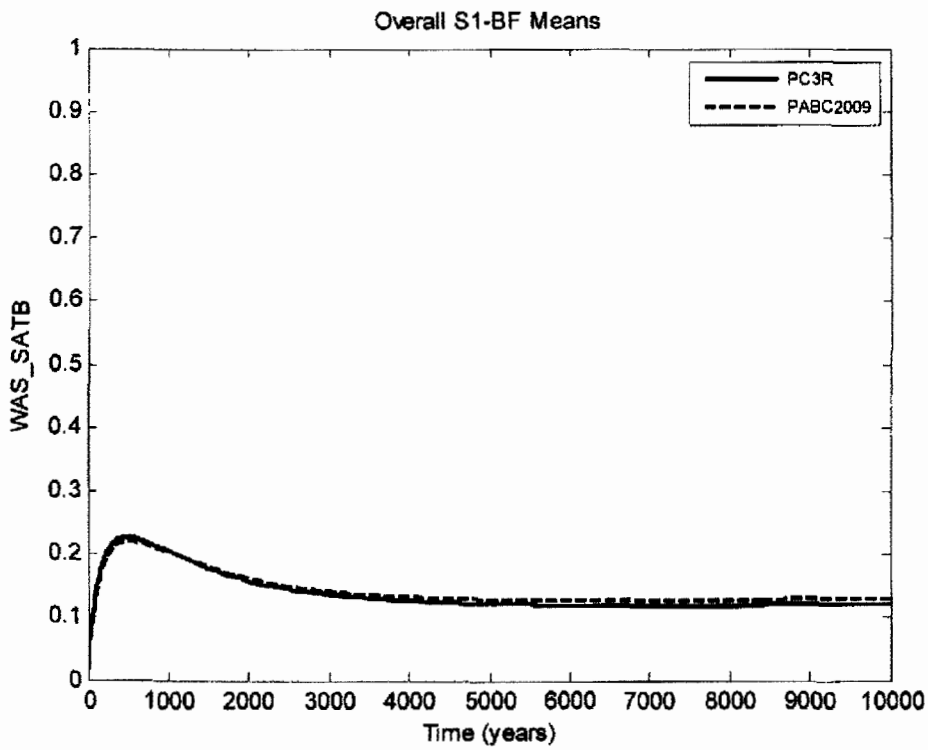

Figure 5-4: Overall Means of Brine Saturation in the Waste Panel, Scenario S1-BF

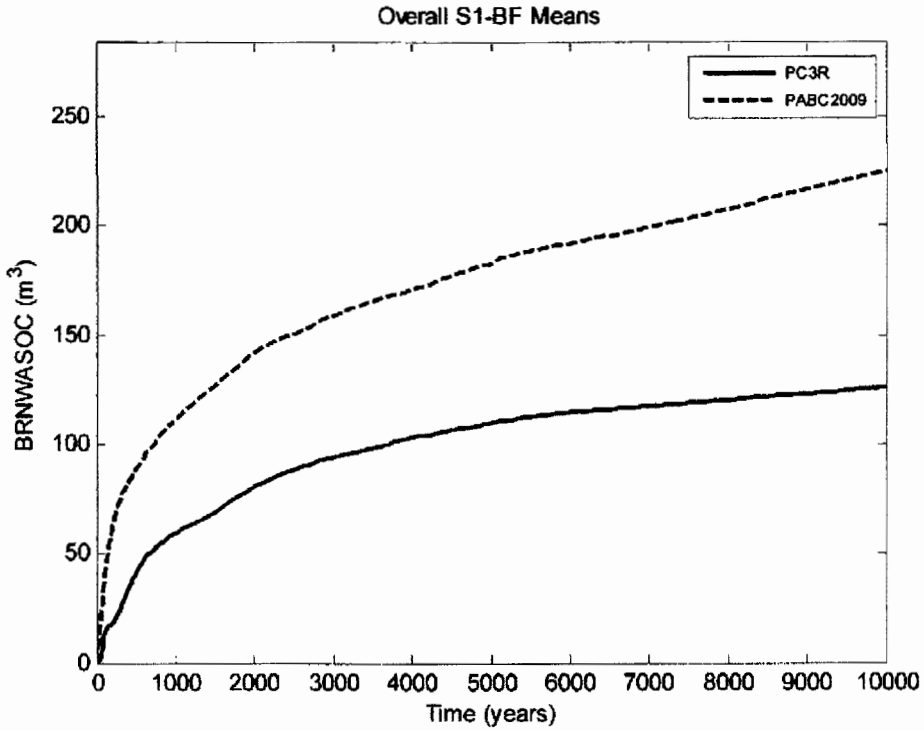

Figure 5-5: Overall Means of Total Brine Flow Out of the Waste Panel, Scenario S1-BF

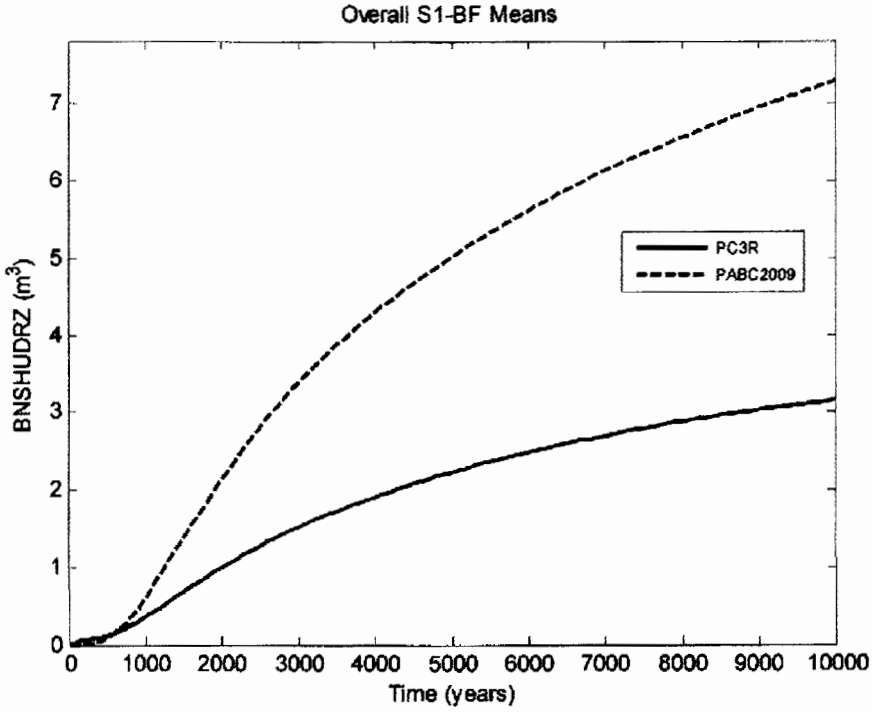

Figure 5-6: Overall Means of Total Brine Flow Up the Shaft, Scenario S1-BF.

Disturbed Scenario S2-BF

PC3R PA results for intrusion scenario S2-BF are now presented and compared with results obtained in the PABC-2009. As before, comparisons are made by use of overall means obtained in both analyses. A comparison of the PC3R PA and the PABC-2009 overall means of volume average porosity in the waste panel is provided in Figure 5-7. As can be seen in that figure, there is very close agreement between the porosities obtained in both analyses.

The overall means of volume averaged pressure obtained in the PC3R PA and the PABC-2009 are shown together in Figure 5-8. As seen in that figure, there is an increase in pressurization of the waste panel for a period of time following the drilling intrusion. This increase is due to the lower long-term permeability ranges of the PC3R panel closures. The result of this increased pressure, in combination with the "tighter" panel closures, is a reduction (on average) in the volume of brine in the waste panel. The reduction in waste panel brine volume as compared to the PABC-2009 yields a corresponding reduction in brine saturation, as seen in Figure 5-9. Gas generation processes in the waste panel require the availability of brine to proceed. The reduction in brine saturation seen in the PC3R PA for intrusion Scenario S2-BF results in an overall decrease in gas generation in the waste panel. The result is a gradual decrease over time in the volume-averaged pressure seen in the waste panel in the PC3R PA as compared to the PABC-2009, with the pressure seen in the PC3R PA eventually falling below that of the PABC-2009.

The overall means of total brine flow out of the waste panel for intrusion Scenario S2-BF are shown in Figure 5-10 for both the PC3R PA and the PABC-2009. As seen in that figure, there is very good agreement between the PC3R PA and PABC-2009 results, with a slight reduction evident in the average total flow out of the intruded waste panel for the PC3R PA. The repository configuration and panel closure design implemented in the PC3R PA does not result in an increase in brine flow out of the waste panel for E1 intrusion scenarios.

The overall means of total brine flow up the borehole, quantity BNBHUDRZ, are shown together for both analyses in Figure 5-11. As is clear in that figure, very good agreement is apparent between the PC3R PA and PABC-2009 results.

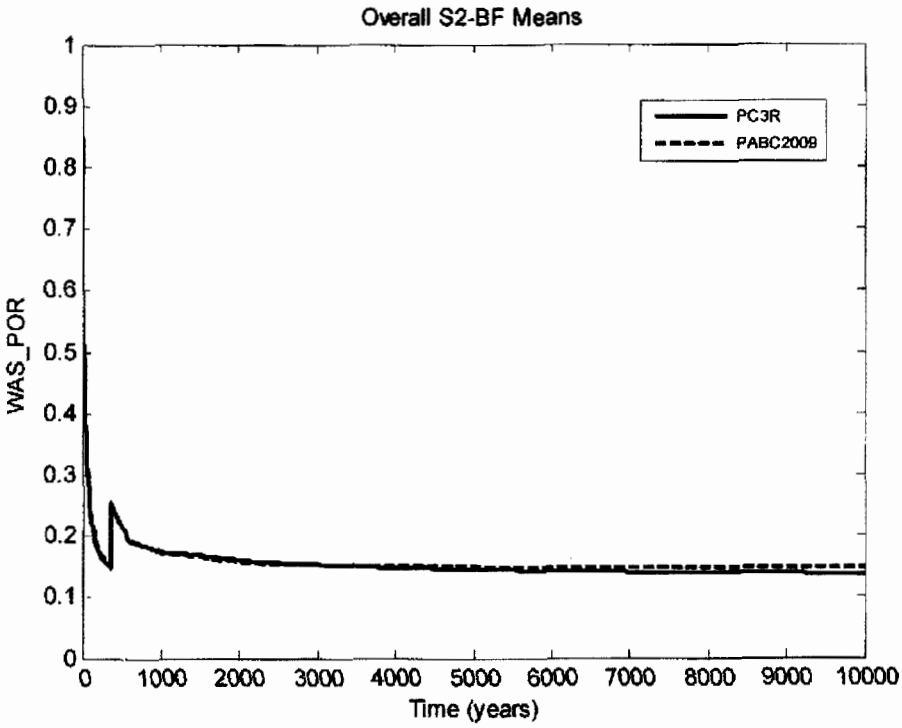

Figure 5-7: Overall Means of Volume Averaged Porosity for the Waste Panel, Scenario S2-BF

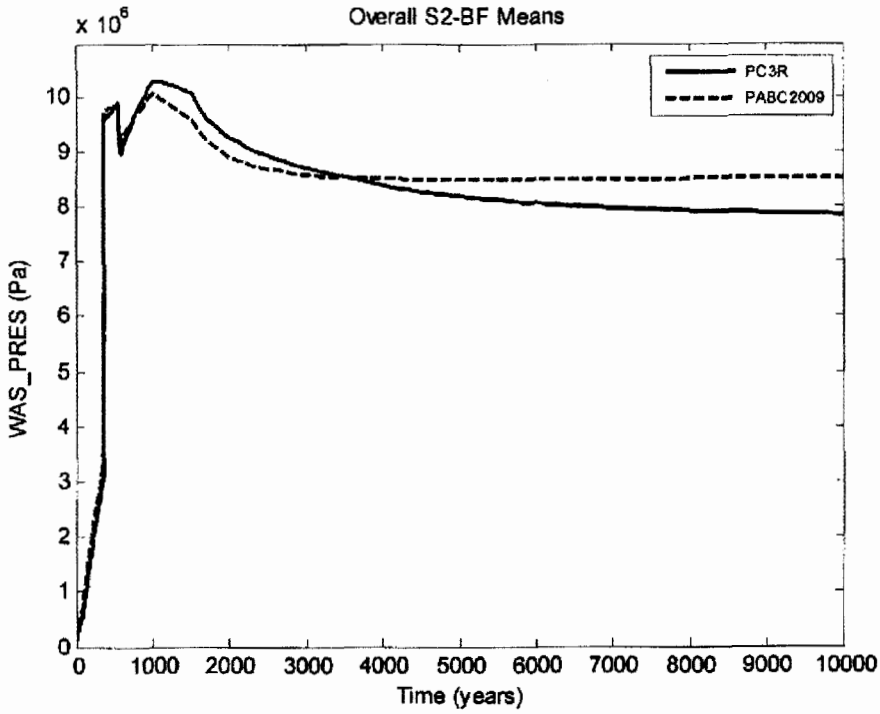

Figure 5-8: Overall Means of Volume Averaged Pressure for the Waste Panel, Scenario S2-BF

Internal Use Only

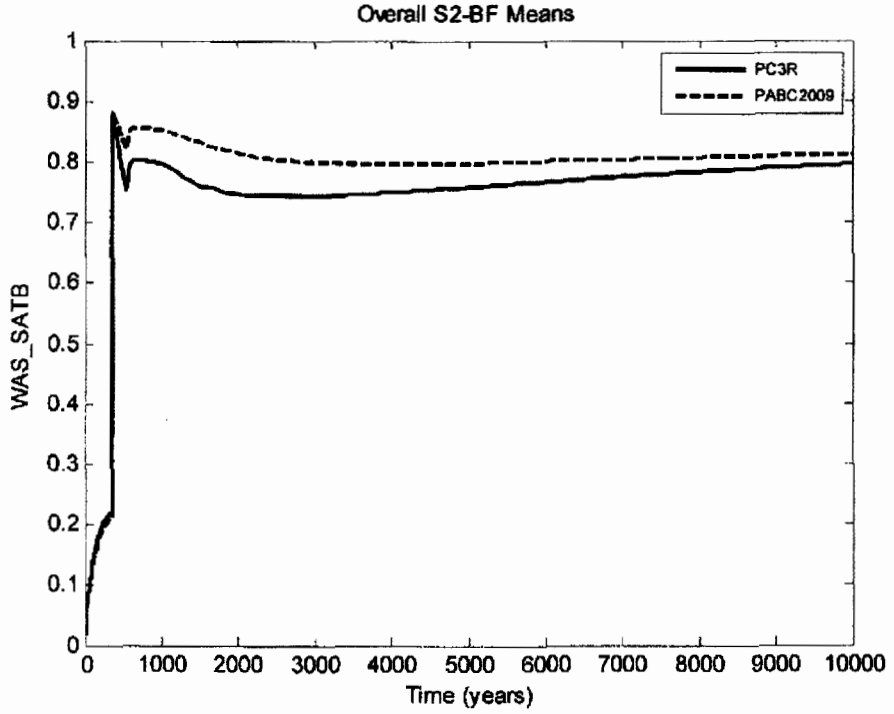

Figure 5-9: Overall Means of Brine Saturation in the Waste Panel, Scenario S2-BF

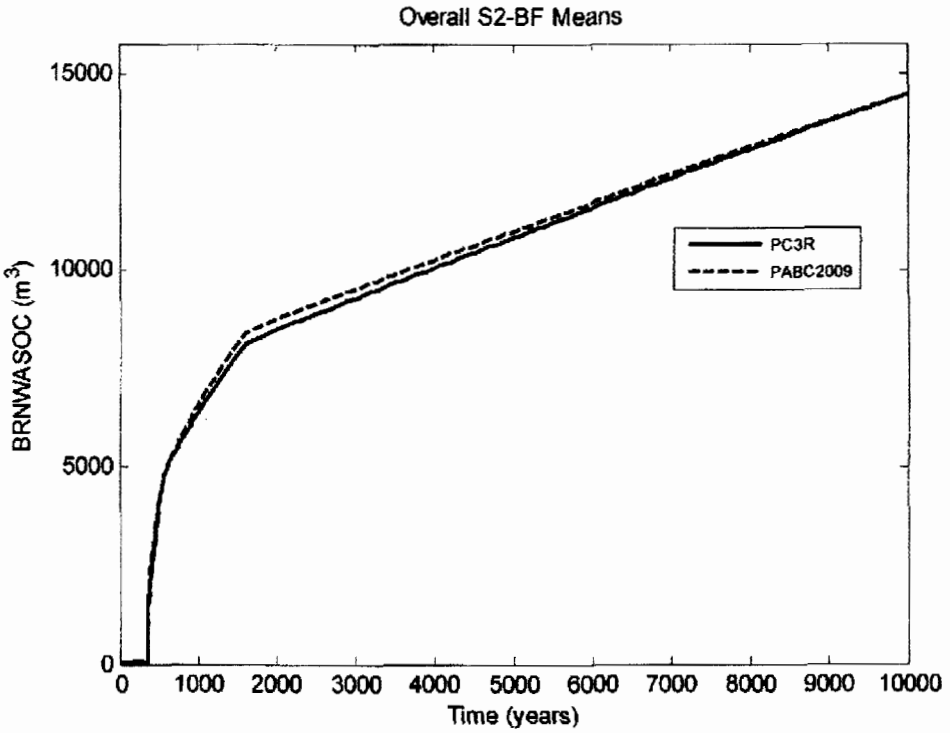

Figure 5-10: Overall Means of Total Brine Flow Out of the Waste Panel, Scenario S2-BF

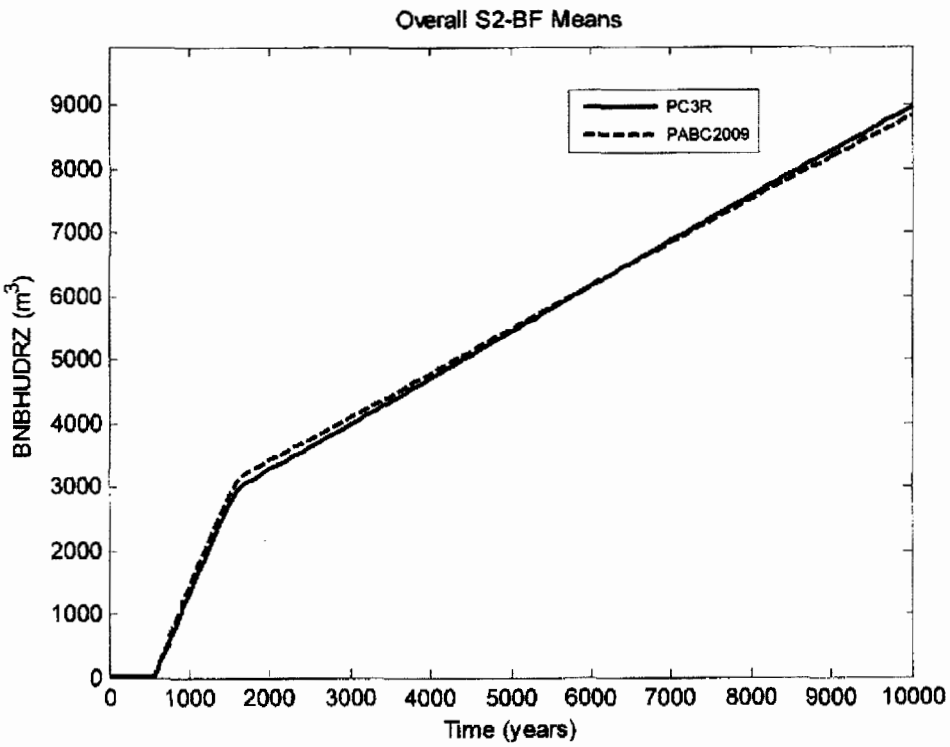

Figure 5-11: Overall Means of Total Brine Flow Up the Borehole, Scenario S2-BF

Disturbed Scenario S4-BF

PC3R PA results for intrusion scenario S4-BF are now presented and compared with results obtained in the PABC-2009. As before, comparisons are made by use of overall means obtained in both analyses. The overall means of volume averaged porosity for the waste panel in Scenario S4-BF are shown together in Figure 5-12 for both the PC3R PA and the PABC-2009. As seen in that figure, there is very close agreement in this quantity across both analyses, with the mean obtained in the PC3R PA attaining a slightly lower value by the end of the 10,000 year regulatory period.

The overall means of volume averaged pressure for the waste panel found in Scenario S4-BF for the PC3R PA and the PABC-2009 are shown in Figure 5-13. As seen in that figure, the waste panel mean average pressure found in the PC3R PA is lower than that seen in the PABC-2009. As discussed for Scenario S1-BF, the higher permeability values of the PC3R PA panel closures during the first 100 years allows some pressure release from the waste panel to the center region. The effect of this in Scenario S4-BF is clearly seen in Figure 5-14. In that figure, the rate of pressure increase in the waste panel found in the PC3R PA is lower during the first 100 years than that seen in the PABC-2009. The net result is a reduction in the overall mean pressure in the waste panel by the time the panel closures attain their long-term permeabilities. This reduced

pressure is maintained after the Scenario S4-BF drilling intrusion at 350 years, resulting in lower average pressure in the waste panel for the remaining duration of the 10,000 year regulatory period.

The waste panel pressure reduction seen in the PC3R PA calculations results in a corresponding slight increase in brine volume in the waste panel. The slight increase in brine volume translates to a slight increase in the mean brine saturation as seen in Figure 5-15. The lower mean pressure seen in the PC3R PA combined with the lower long-term permeabilities of the panel closures implemented therein results in an overall reduction in the overall mean of total brine flow out of the waste panel, as is illustrated in Figure 5-16. The repository configuration and panel closure design implemented in the PC3R PA did not yield an increase in brine flow out of the waste panel for E2 intrusion scenarios.

A slight increase was seen in the overall mean of total brine flow up the borehole in the PC3R PA as compared to the PABC-2009, as is shown in Figure 5-17, most likely due to the slight increase in the waste panel brine volume seen in the PC3R PA. This increase is slight, however, amounting to less that 50 m^3 by the end of the 10,000 year regulatory period.

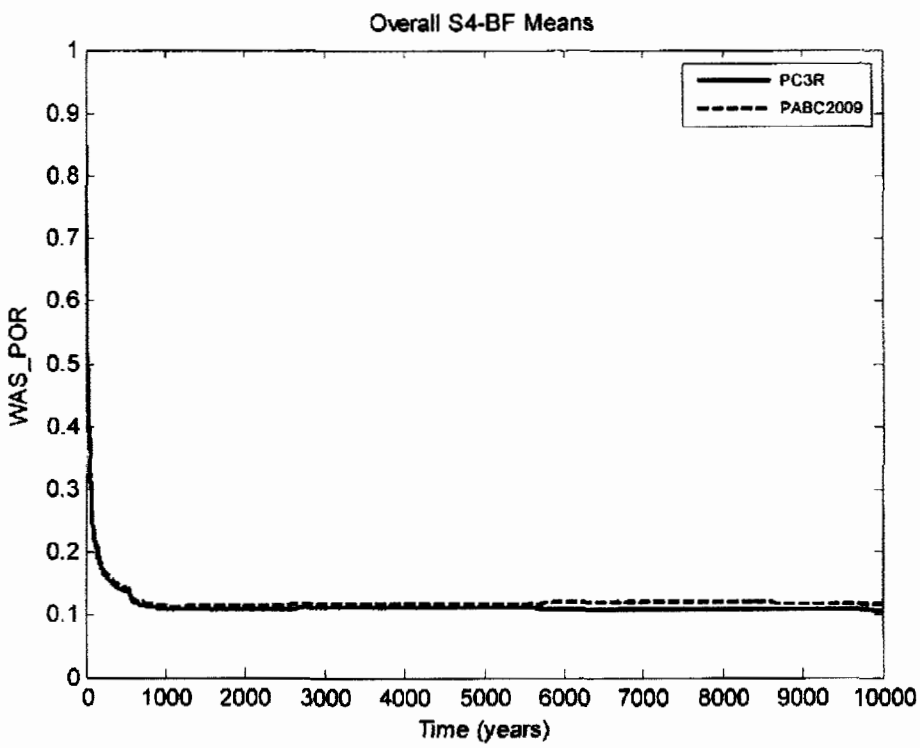

Figure 5-12: Overall Means of Volume Averaged Porosity for the Waste Panel, Scenario S4-BF

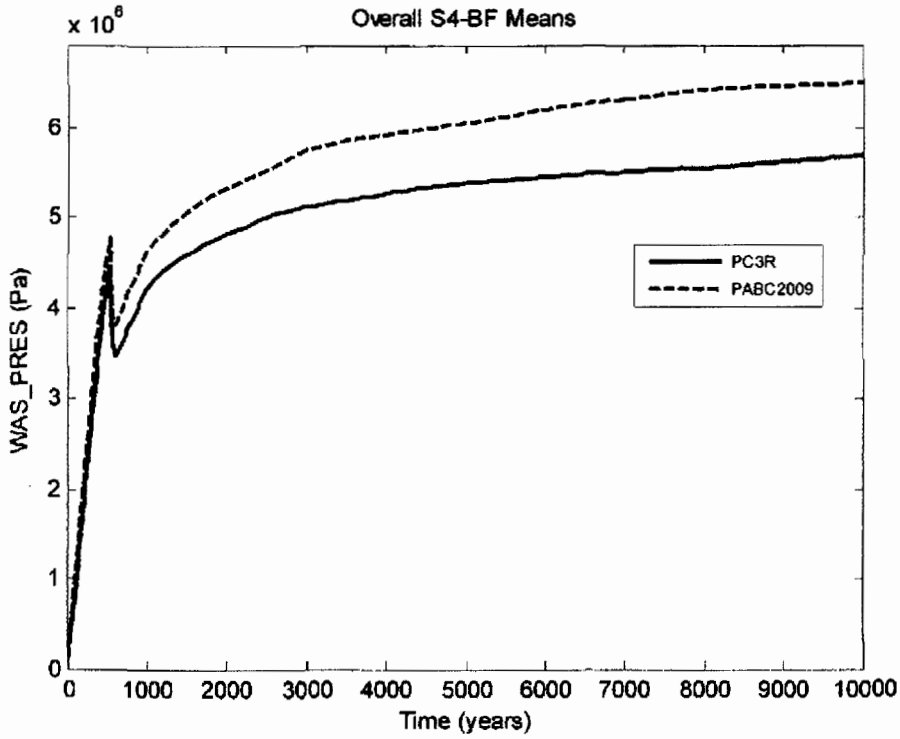

Figure 5-13: Overall Means of Volume Averaged Pressure for the Waste Panel, Scenario S4-BF

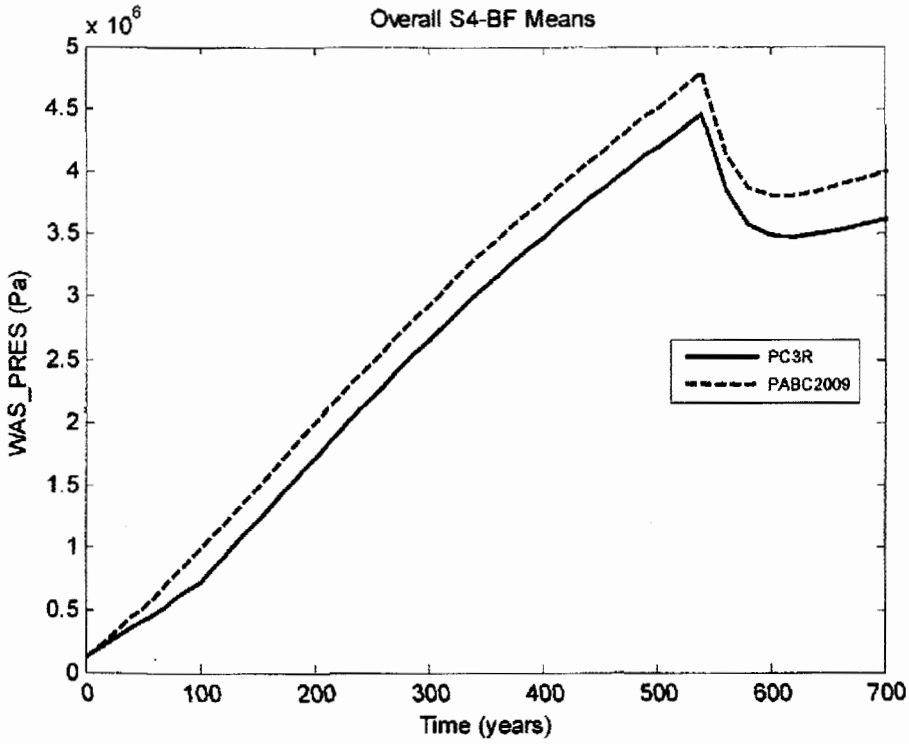

Figure 5-14: Overall Means of Volume Averaged Pressure for the Waste Panel During the First 700 Years After Closure, Scenario S4-BF

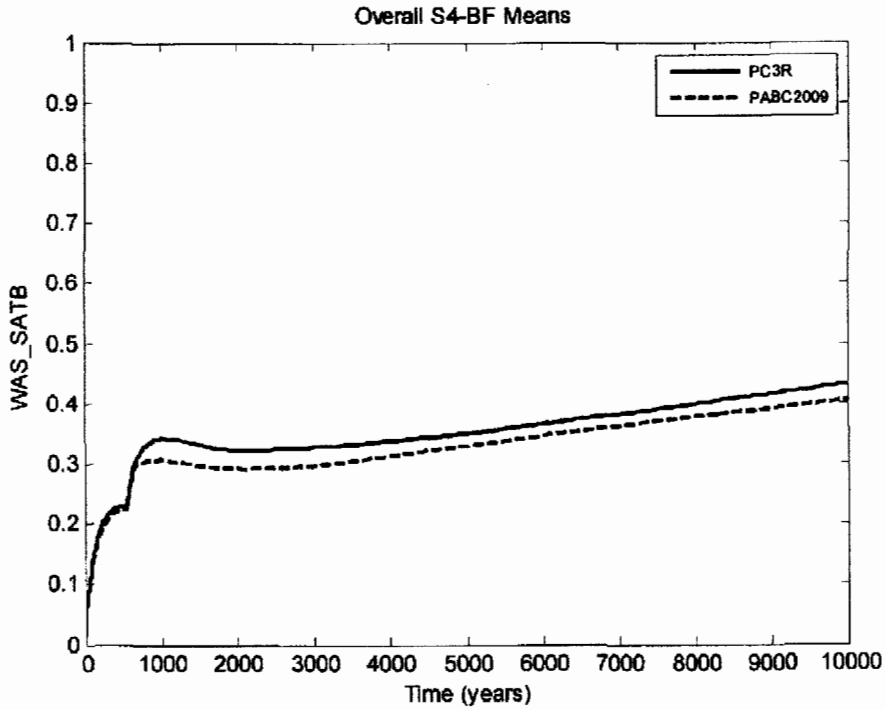

Figure 5-15: Overall Means of Brine Saturation in the Waste Panel, Scenario S4-BF

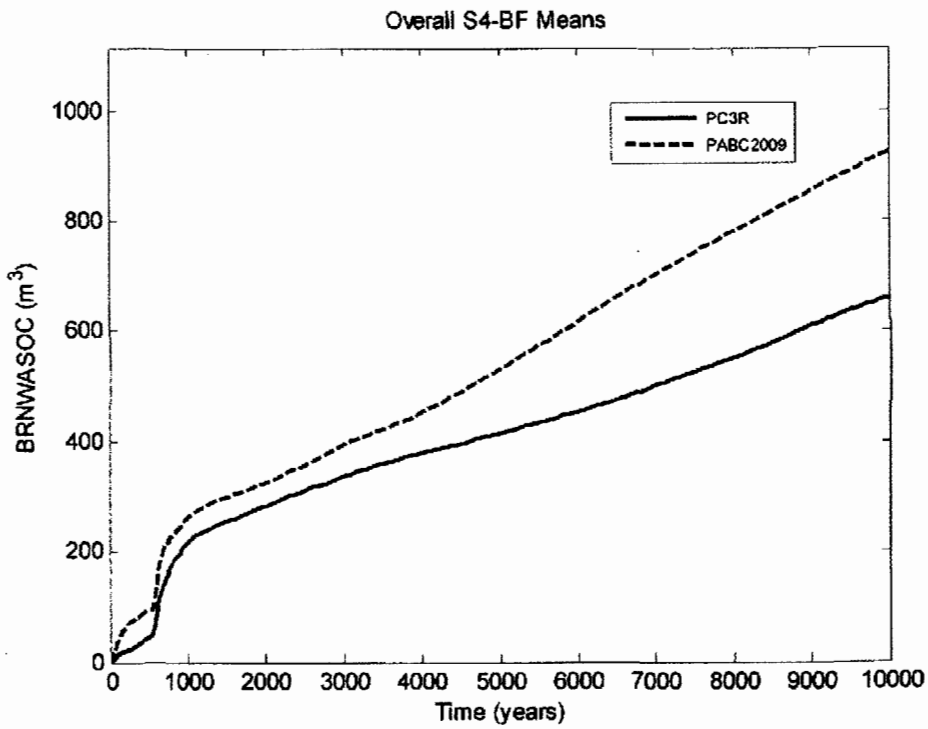

Figure 5-16: Overall Means of Total Brine Flow Out of the Waste Panel, Scenario S4-BF

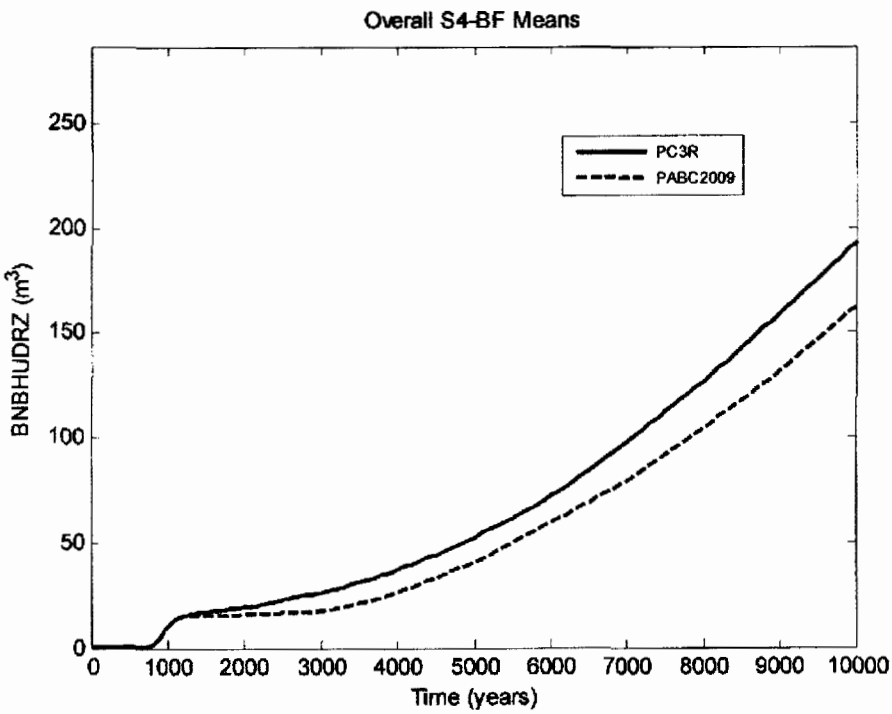

Figure 5-17: Overall Means of Total Brine Flow Up the Borehole, Scenario S4-BF

5.2 Brine Isolation after Intrusion

As discussed and demonstrated in the PC3R PA BRAGFLO results above, the cumulative brine flow out of an intruded waste panel was reduced on average as compared to the PABC-2009 results. One may also ask how the presence of relatively high pressures and brine volumes on one side of a redesigned panel closure impact brine volumes and saturations on the opposite side. In particular, is additional brine in the waste panel following an intrusion relocated to the central drift area where it can be released to the surface by a subsequent drilling intrusion in that region?

To answer this question, the PC3R PA overall pressure means in the waste panel for the undisturbed scenario and intrusion scenarios S2-BF, S4-BF, and S6-BF are shown together in Figure 5-18. As seen in that figure, there is significant variance in the average waste panel pressure in the scenarios considered. During the time duration of 0 to 2,000 years, for example, the average waste panel pressure varies from 0 Pa to over 10 MPa. Similar variance is seen in the average brine volume in the waste panel, as shown in Figure 5-19. Over the same time period of 2,000 years, the average brine volume in the waste panel varies from 0 m^3 to over 10,000 m^3 for intrusion scenario S2-BF. These substantial pressure and brine volume changes result in similar changes in the average waste panel brine saturation. As seen in Figure 5-20, the average brine saturation in the waste panel varies in the first 2,000 years from a value of 0 to a

value of nearly 0.9, representing nearly saturated conditions. Obviously, the influx of additional brine in the waste panel following an intrusion has a corresponding impact on the brine saturation therein. Moreover, there is a direct correspondence in the shape of the average brine volume curves of Figure 5-19 and the brine saturation curves of Figure 5-20. Time values at which brine volumes substantially increase correspond to time values at which brine saturations also increase. From these results, it is reasonable to conclude that an influx of brine into the center area following an intrusion in the waste panel would result in a corresponding change in the brine saturation of the central area.

The brine saturation for the central drift area is denoted by quantity OPS_SATB in the PC3R PA as that region is assigned material properties corresponding to the operations region of the PABC-2009 repository configuration. The overall PC3R PA brine saturation curves obtained for the central drift area for undisturbed scenario S1-BF and disturbance scenarios S2-BF, S4-BF, and S6-BF are shown together in Figure 5-21. As is clear in that figure, there is no discernable difference in the average brine saturation obtained in the central drift region for all scenarios considered, regardless of pressure and brine volume/saturation changes in the intruded waste panel. Brine saturation curves obtained for the central drift area in all intrusion scenarios are virtually unchanged from the brine saturation curve obtained for undisturbed conditions. Furthermore, as seen in Figure 5-22 there is very close agreement in the overall average brine volume in the central drift area, denoted as BRNVOL_O, for the undisturbed and all intrusion scenarios considered. All curves obtained for the average brine volume in the central drift area for all conditions considered are nearly identical to the curve obtained for undisturbed conditions. The reasonable conclusion to make is that changing repository conditions following an intrusion on one side of a redesigned panel closure do not result in consequential brine saturation and volume changes on the opposite side of the closure. More specifically, an E1 or E2 drilling intrusion into the waste panel will not result in a consequential increase in brine volume inside the central drift region to later be released to the surface by a subsequent intrusion in that area. The brine available for release to the surface following a drilling event into the central drift region is brine present under undisturbed conditions, regardless of previous intrusions into a waste panel.

While a drilling intrusion into a waste panel has an inconsequential impact on brine volumes and saturations in the central drift region, a waste panel intrusion does have an impact on pressure in the central region. The overall PC3R PA average pressures obtained for the central drift region, denoted as quantity OPS_PRES, for undisturbed scenario S1-BF and disturbance scenarios S2-BF, S4-BF, and S6-BF are shown together in Figure 5-23. As seen in that figure, there is actually a *reduction* in the average pressure of the central drift region for all intrusion scenarios considered as compared to undisturbed scenario S1-BF. This is due to eventual reductions in waste panel pressures following an intrusion as compared to undisturbed conditions. Given sufficient time, the tendency is for pressure on opposite sides of a panel closure to equilibrate. A

pressure reduction on one side of a panel closure corresponds to an eventual pressure reduction on the opposite side.

From the discussion above, a drilling intrusion on one side of a panel closure results in a reduction in pressure on the opposite side, but no consequential change to brine volume or brine saturation. As a result, it can be concluded that drilling intrusions in the central drift region will not impact brine volumes and saturations in a waste panel, but will cause reductions in pressure. Pressure reductions translate directly to reductions in spallings releases. Likewise, pressure reductions without an accompanying increase in brine saturation can only result in a reduction in direct brine releases. Therefore, drilling intrusions in the central drift region can only *reduce* releases due to a waste panel intrusion. For the quantification of releases in the PC3R PA, the consideration of drilling intrusions into waste-containing regions is sufficient, and is conservative.

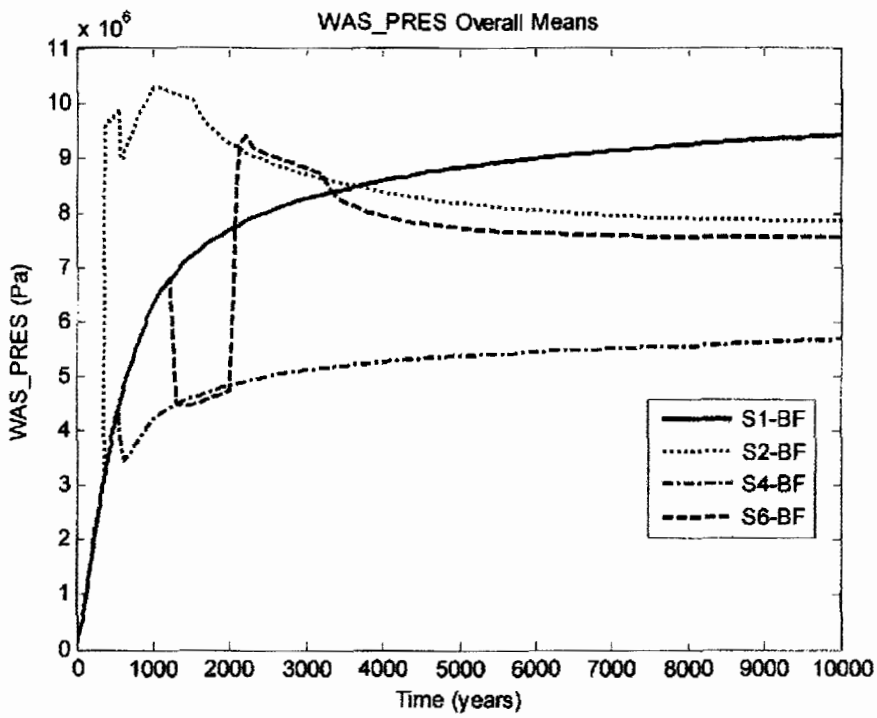

Figure 5-18: PC3R PA Overall Waste Panel Pressure Means, Scenarios S1-BF, S2-BF, S4-BF, S6-BF

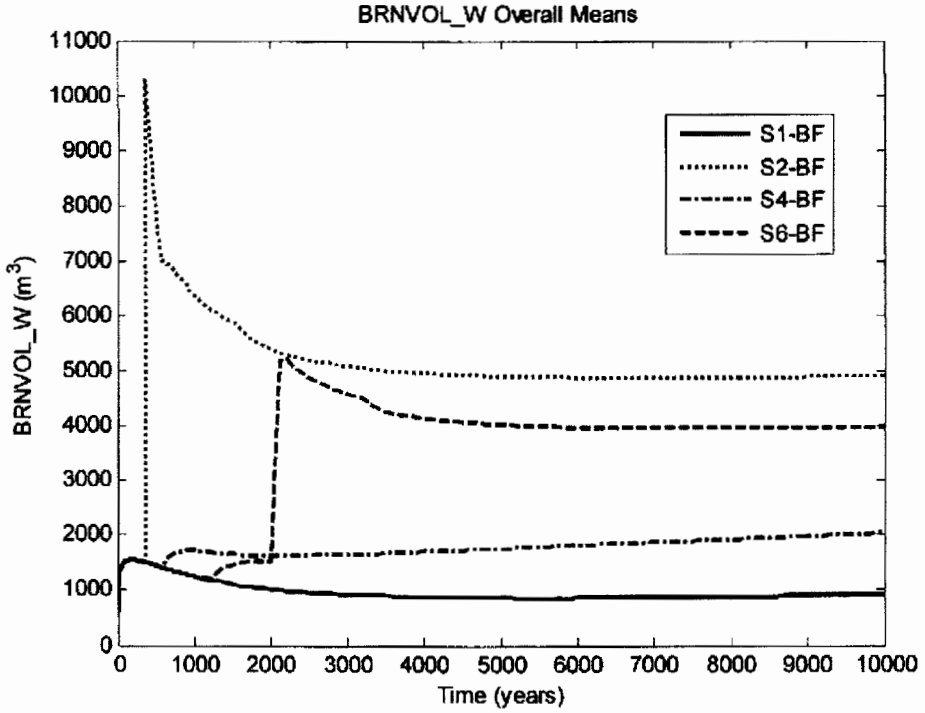

Figure 5-19: PC3R PA Overall Waste Panel Brine Volume Means, Scenarios S1-BF, S2-BF, S4-BF, S6-BF

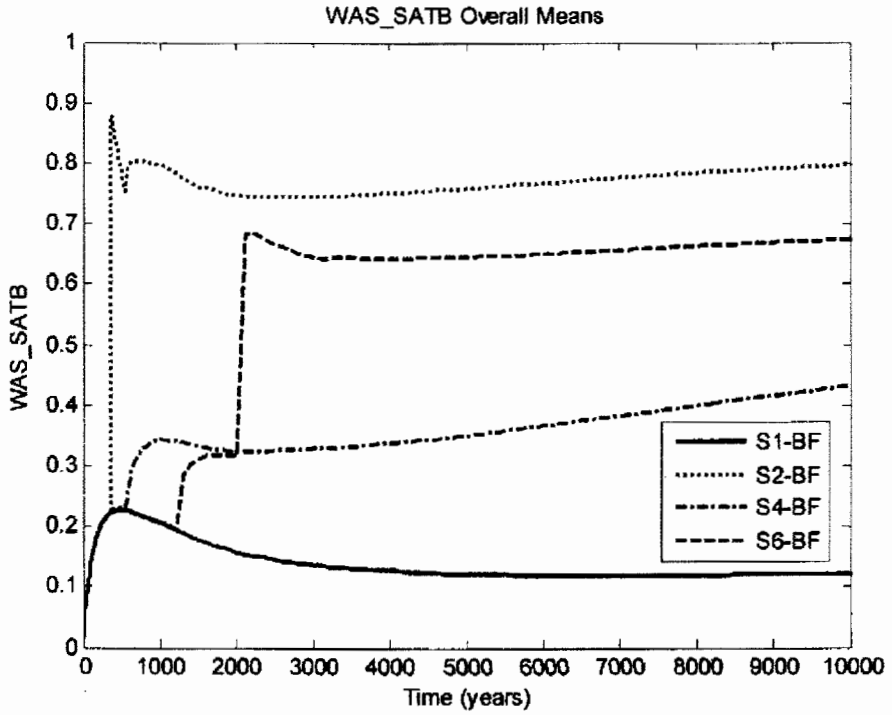

Figure 5-20: PC3R PA Overall Waste Panel Brine Saturation Means, Scenarios S1-BF, S2-BF, S4-BF, S6-BF

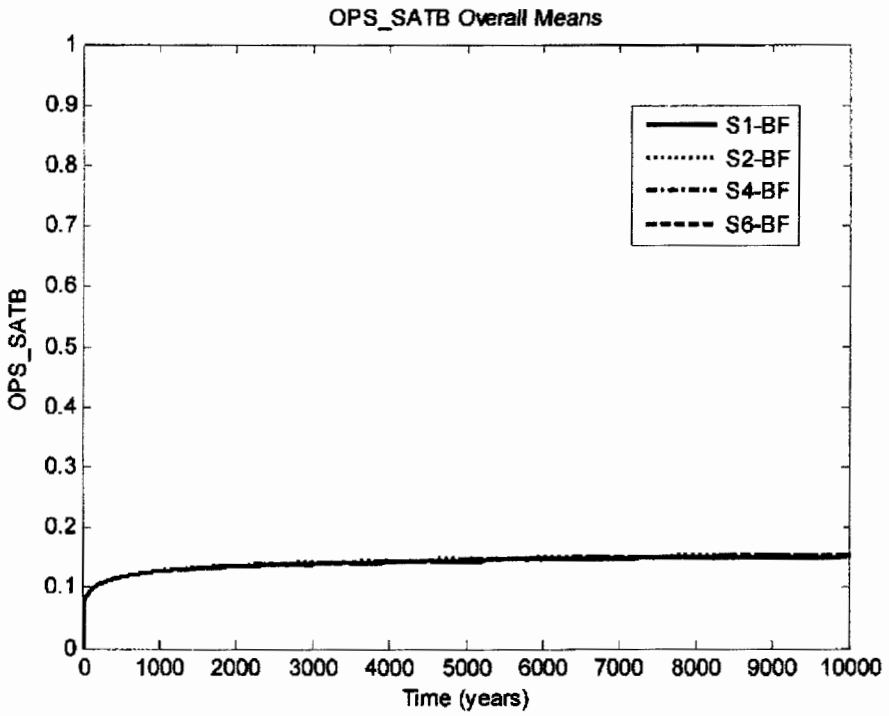

Figure 5-21: PC3R PA Overall Central Region Brine Saturation Means, Scenarios S1-BF, S2-BF, S4-BF, S6-BF

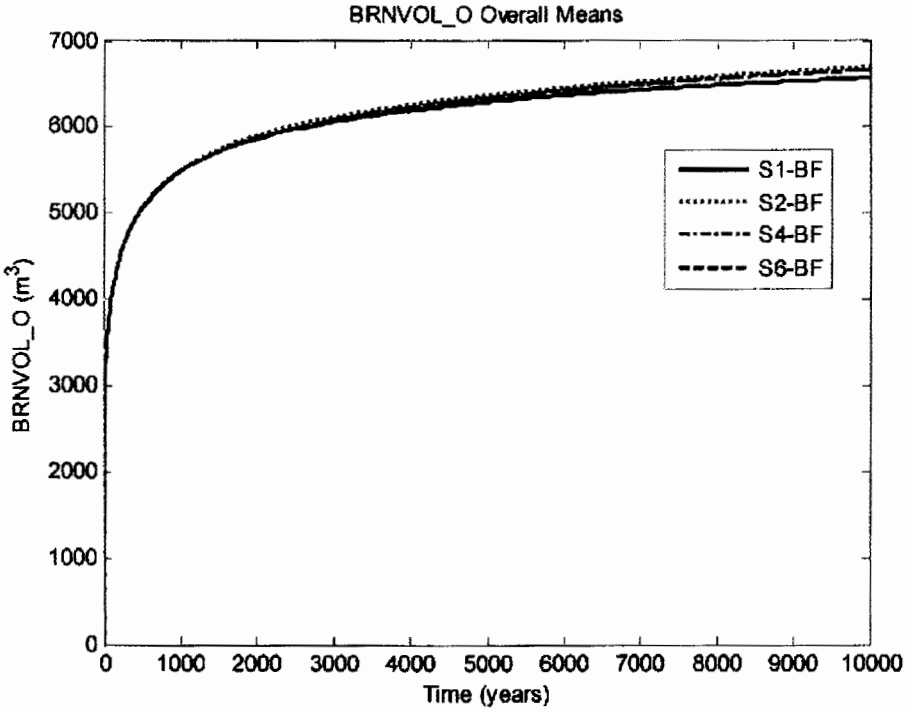

Figure 5-22: PC3R PA Overall Central Region Brine Volume Means, Scenarios S1-BF, S2-BF, S4-BF, S6-BF

Information Only

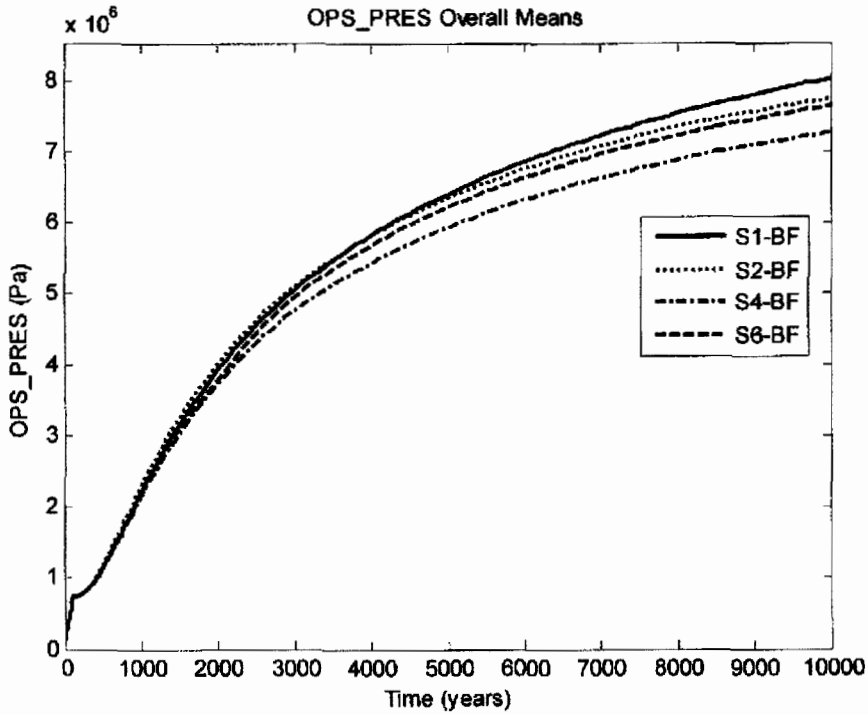

Figure 5-23: PC3R PA Overall Central Region Pressure Means, Scenarios S1-BF, S2-BF, S4-BF, S6-BF

5.3 Actinide Mobilization and Transport

Waste panels 9a and 10a in the reconfigured repository are slightly larger than their 9 and 10 counterparts in the historical WIPP configuration, and are of identical volume to panels 1-8. As a result, the waste inventory of a standard panel in the PC3R PA is exactly 10% of the overall inventory, a slight decrease from the value of 10.53% implemented in the PABC-2009. As the repository waste inventory, and corresponding actinide solubilities, used in the PABC-2009 were also prescribed in the PC3R PA calculations, the slight decrease in waste panel inventory has practically no impact on actinide concentration curves obtained in the two analyses. For all practical purposes, the concentration curves obtained in the two analyses are the same. As a result, changes in the amount of brine volume flowing up a borehole following an intrusion is the primary indicator of changes in transport releases between the PC3R PA and the PABC-2009. Consequently, Salado modeling results obtained for quantity BNBHUDRZ in intrusion scenario S6-BF are now presented and compared with their PABC-2009 counterparts.

The scenario S6-BF means of BNBHUDRZ for replicates 1 – 3 are shown in Figure 5-24 and compared to their PABC-2009 counterparts. In that figure, solid curves represent replicate means obtained in the PC3R PA. Dashed curves denote replicate means obtained in the PABC-2009. As is evident, there is very close agreement between the replicate means obtained in the two analyses. The PC3R PA and PABC-2009 overall means of brine volume up the borehole, calculated over all 300 vector realizations, are shown together in Figure 5-25 for intrusion

scenario S6-BF. Again, there is very close agreement between PC3R PA and PABC-2009 results.

As the volumes of brine flow up the intrusion borehole obtained in the PC3R PA and the PABC-2009 are very similar for intrusion scenarios S2-BF to S6-BF, it is concluded that transport releases obtained in these two analyses are also very similar as the waste inventory and corresponding actinide solubilities were unchanged from the PABC-2009 to the PC3R PA. This conclusion is further supported by the CCDF curves of normalized releases to the Culebra shown in Figure 5-26 and Figure 5-27. As seen in Figure 5-26, the replicate means of normalized transport releases to the Culebra obtained in the PC3R PA and the PABC-2009 are nearly identical. The same is true of the overall mean CCDF curves for transport releases to the Culebra, as evident in Figure 5-27.

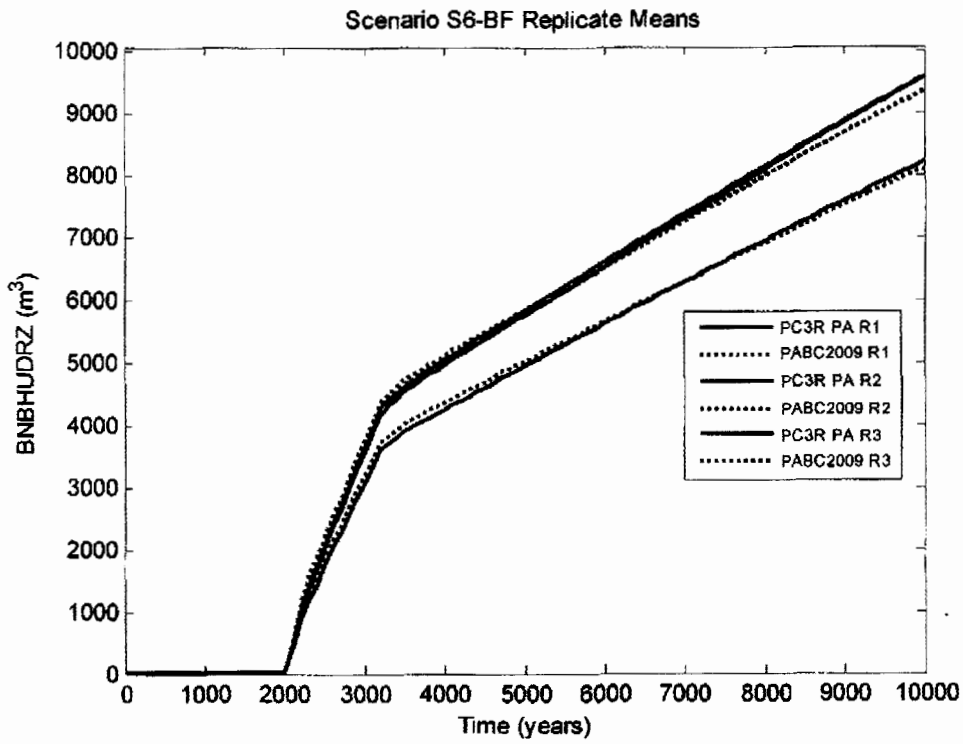

Figure 5-24: PC3R PA and PABC-2009 Replicate Means of Cumulative Flow up the Borehole

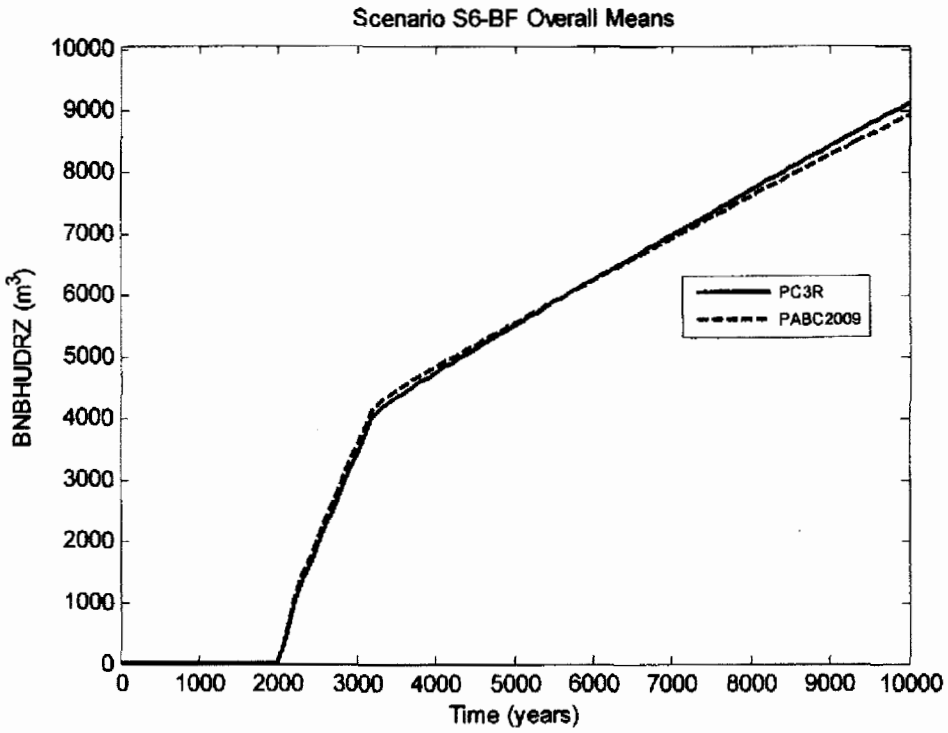

Figure 5-25: PC3R PA and PABC-2009 Overall Means of Cumulative Flow up the Borehole

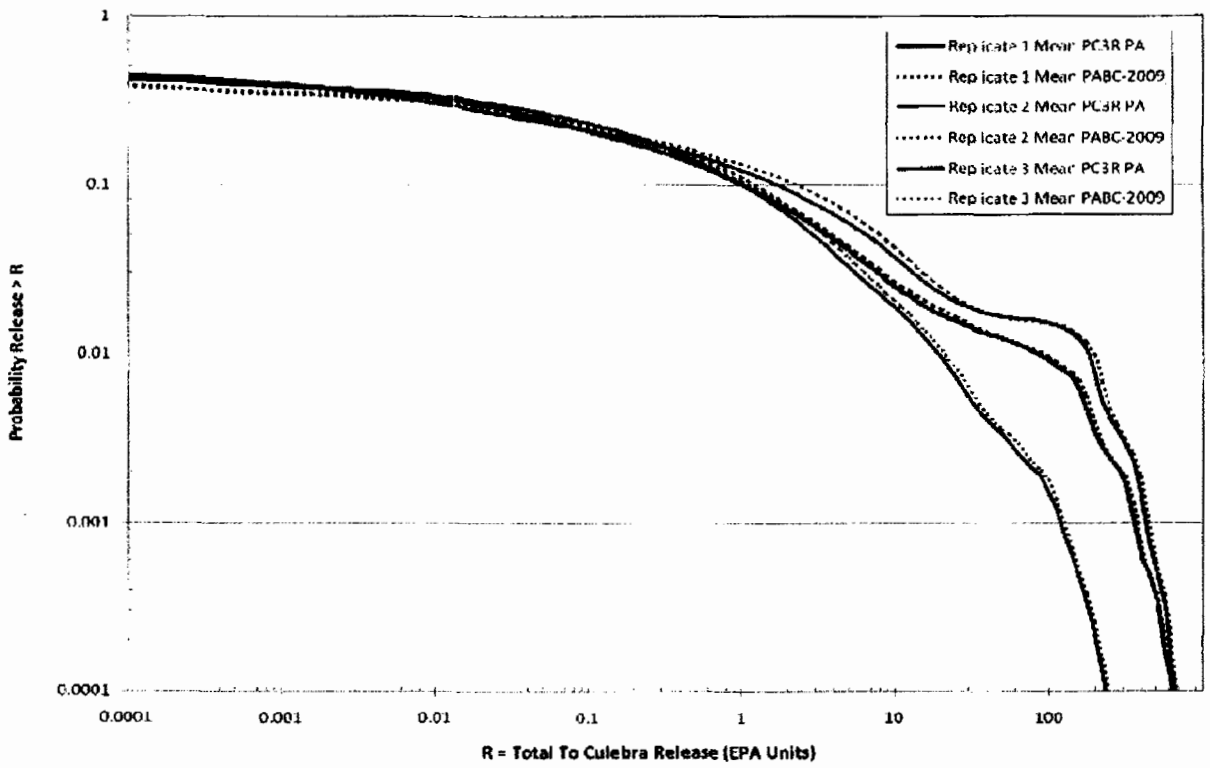

Figure 5-26: PC3R PA and PABC-2009 Replicate Mean CCDFs for Normalized Transport Releases to the Culebra

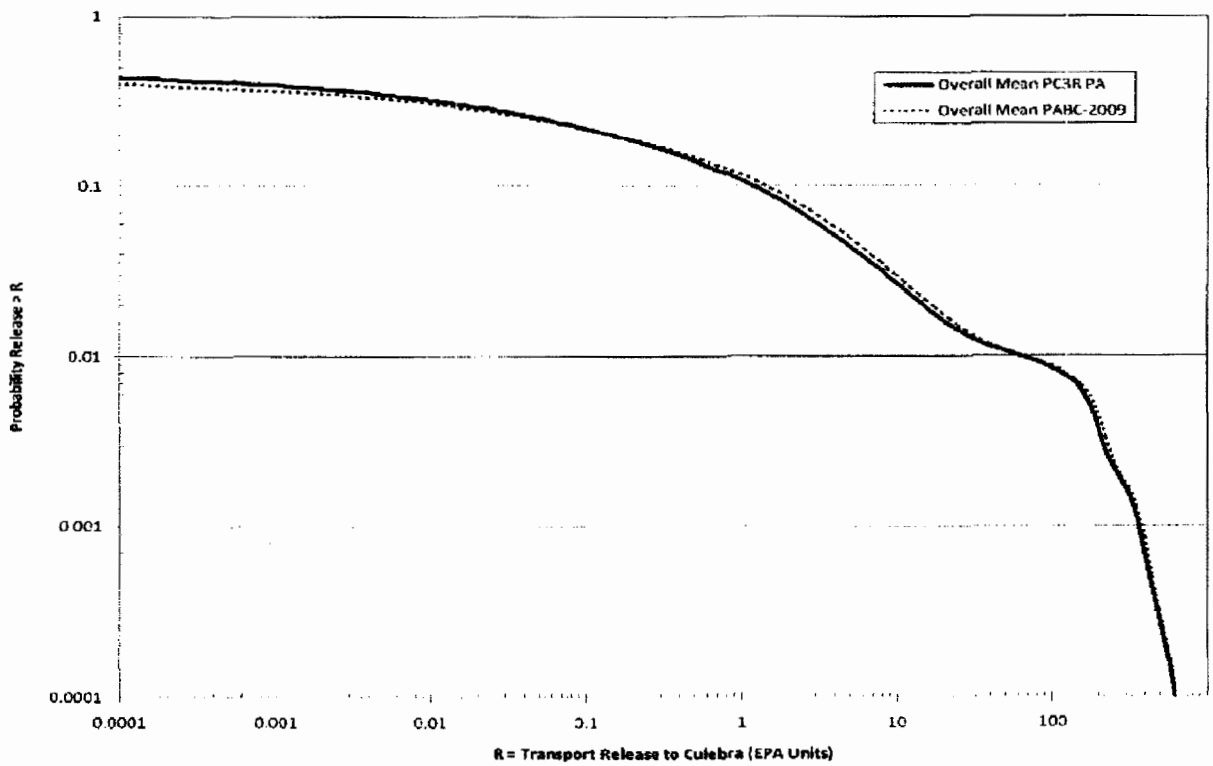

Figure 5-27: PC3R PA and PABC-2009 Overall Mean CCDFs for Transport Releases to the Culebra

5.4 Cuttings and Cavings

Cuttings and cavings are the solid waste material removed from the repository and carried to the surface by the drilling fluid during the process of drilling a borehole. Cuttings are the materials removed directly by the drill bit, and cavings are the material eroded from the walls of the borehole by shear stresses from the circulating drill fluid. The volume of cuttings and cavings material removed from a single drilling intrusion into the repository is assumed to be in the shape of a cylinder.

The PA code CUTTINGS_S calculates the cuttings and cavings areas removed for a set of vectors, scenarios, times, and locations. Results obtained by BRAGFLO in scenarios S1-BF to S5-BF are used to initialize the flow field properties necessary for the calculation of DBRs. This requires that results obtained on the BRAGFLO grid be mapped appropriately to the DBR grid. Code CUTTINGS_S is used to transfer the appropriate scenario results obtained with BRAGFLO to the DBR grid. These transferred flow results are used as initial conditions in the calculation of DBRs. As a result, intrusion scenarios used in the calculation of cuttings and cavings correspond to those used in the calculation of DBRs. Five intrusion scenarios are considered in the DBR calculations, and are listed in Table 7.

Table 7: PA Intrusion Scenarios Used in Calculating Direct Solids Releases

Scenario	Conditioning (or 1st) Intrusion Time (year) and Type	Intrusion Times – Subsequent (year)
S1-DBR	None	100, 350, 1000, 3000, 5000, 10000
S2-DBR	350, E1	550, 750, 2000, 4000, 10000
S3-DBR	1000, E1	1200, 1400, 3000, 5000, 10000
S4-DBR	350, E2	550, 750, 2000, 4000, 10000
S5-DBR	1000, E2	1200, 1400, 3000, 5000, 10000

While CUTTINGS_S uses these standard DBR scenarios as a basis for its calculations, it does so to provide flow field results (generated with BRAGFLO) as initial conditions to the DBR calculation at each subsequent intrusion time. CUTTINGS_S does not model the intrusion scenario itself. Scenario S1-DBR corresponds to an initial intrusion into the repository, with repository flow conditions at the time of intrusion transferred from BRAGFLO scenario S1-BF results. Scenarios S2-DBR through S5-DBR are used to model an intrusion into a repository that has already been penetrated. The times at which intrusions are assumed to occur for each scenario are outlined in the last column of Table 7; six intrusion times are modeled for scenario S1-DBR, while five times are modeled for each of scenarios S2-DBR through S5-DBR.

Cuttings and cavings results obtained for the PC3R PA are the same as for the PABC-2009, as is evident in the results of Table 8 and the CCDF curves of normalized cuttings and cavings releases shown in Figure 5-28.

Table 8: Cavings Area Statistics for the PABC-2009 and PC3R PA

Replicate	Cavings Area (m^2)		Vectors with no Cavings
	Maximum	Mean	
R1	0.748	0.177	9
R2	0.785	0.175	10
R3	0.753	0.178	11

Two uncertain sampled parameters affect the cavings calculations. The uncertainty in cavings areas arises primarily from the uncertainty in the shear strength of the waste (Kicker 2011). Lower shear strengths tend to result in larger cavings as is evident in Figure 5-29. The uncertainty in the drill string angular velocity has a smaller impact on the cavings results, but the combination of a low angular velocity and high shear strength can prohibit cavings from occurring. In fact, cavings did not occur in ten percent of all vectors (Table 8).

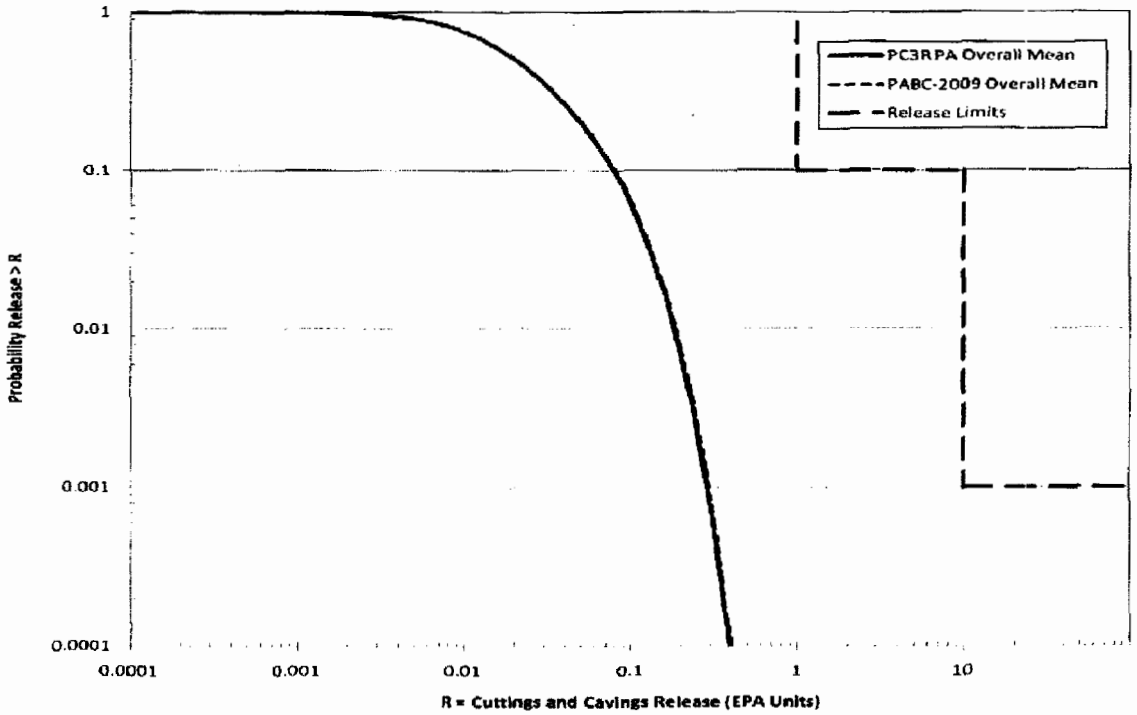

Figure 5-28: PC3R PA and PABC-2009 Overall Mean CCDFs for Normalized Cuttings and Cavings Releases

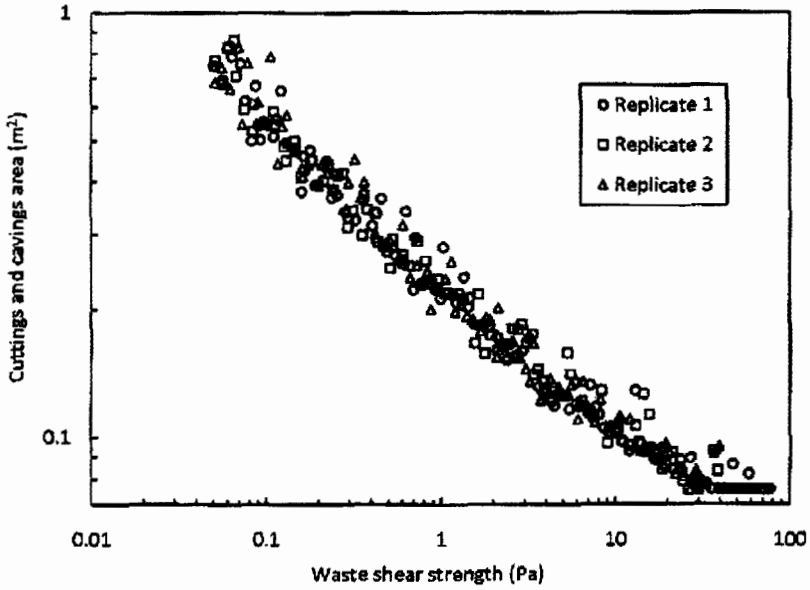

Figure 5-29: Cuttings and Cavings Area as a Function of Waste Shear Strength

5.5 Spallings

Calculation of the volume of solid waste material released to the surface from a single drilling intrusion into the repository due to spallings is a two-part procedure. The code DRSPALL calculates the spallings volumes from a single drilling intrusion at four values of repository pressure (10, 12, 14, and 14.8 MPa). The second step in calculating spallings volumes from a single intrusion consists of using the code CUTTINGS_S to interpolate the DRSPALL volumes. The spallings volume for a vector is then determined in CUTTINGS_S by linearly interpolating the volume calculated by DRSPALL based on the pressure calculated by BRAGFLO.

Table 9: Summary of Spallings Releases by Scenario

		Scenarios					Total
		S1-DBR	S2-DBR	S3-DBR	S4-DBR	S5-DBR	
PC3R PA							
R1	Maximum [m^3]	1.67	13.56	12.70	1.67	1.67	13.56
	Average nonzero volume [m^3]	0.31	0.74	0.78	0.27	0.30	0.53
	Number of nonzero volumes	84	102	86	40	53	365
	Percent of nonzero volumes	7.0%	10.2%	8.6%	4.0%	5.3%	7.0%
R2	Maximum [m^3]	1.43	8.48	6.64	0.60	0.60	8.48
	Average nonzero volume [m^3]	0.22	0.40	0.34	0.23	0.22	0.30
	Number of nonzero volumes	89	114	96	36	53	388
	Percent of nonzero volumes	7.4%	11.4%	9.6%	3.6%	5.3%	7.5%
R3	Maximum [m^3]	5.00	6.80	4.52	3.93	4.52	6.80
	Average nonzero volume [m^3]	0.42	0.59	0.39	0.37	0.32	0.44
	Number of nonzero volumes	79	98	83	33	51	344
	Percent of nonzero volumes	6.6%	9.8%	8.3%	3.3%	5.1%	6.6%
PABC-2009							
R1	Maximum [m^3]	2.24	8.29	7.97	1.67	1.67	8.29
	Average nonzero volume [m^3]	0.37	0.54	0.50	0.30	0.37	0.43
	Number of nonzero volumes	142	117	111	59	77	506
	Percent of nonzero volumes	7.9%	7.8%	7.4%	3.9%	5.1%	6.5%
R2	Maximum [m^3]	2.36	2.76	1.86	2.26	1.93	2.76
	Average nonzero volume [m^3]	0.32	0.39	0.37	0.50	0.47	0.39
	Number of nonzero volumes	168	122	122	57	84	553
	Percent of nonzero volumes	9.3%	8.1%	8.1%	3.8%	5.6%	7.1%
R3	Maximum [m^3]	4.91	6.23	2.62	1.47	1.49	6.23
	Average nonzero volume [m^3]	0.53	0.39	0.28	0.30	0.28	0.38
	Number of nonzero volumes	156	113	118	45	72	504
	Percent of nonzero volumes	8.7%	7.5%	7.9%	3.0%	4.8%	6.5%

DRSPALL volumes used in the PABC-2009 were also used in the PC3R PA. Utilizing these volumes and the PC3R PA repository pressures calculated by BRAGFLO, the impact of the repository reconfiguration and panel closure design on spallings volumes can be determined. Average and maximum statistics of spallings volumes for the intrusion scenarios considered by

CUTTINGS_S are shown in Table 9 for both the PC3R PA and the PABC-2009. While the results for the PABC-2009 and the PC3R PA calculations are similar for some scenarios, some significant differences in the spallings volumes are noted. For scenarios S2-DBR and S3-DBR, in which the borehole intrusion encounters a pressurized brine pocket, a sharp increase in spallings volume occurs across all three replicates. The results for scenarios S1-DBR, S4-DBR, and S5-DBR are mixed compared to the PABC-2009, showing both increases and decreases in spallings volume. Overall, the general trend shows a slightly higher average nonzero spallings volume, a larger maximum volume, and a larger percentage of vectors with spallings considering the total from all scenarios across all three replicates.

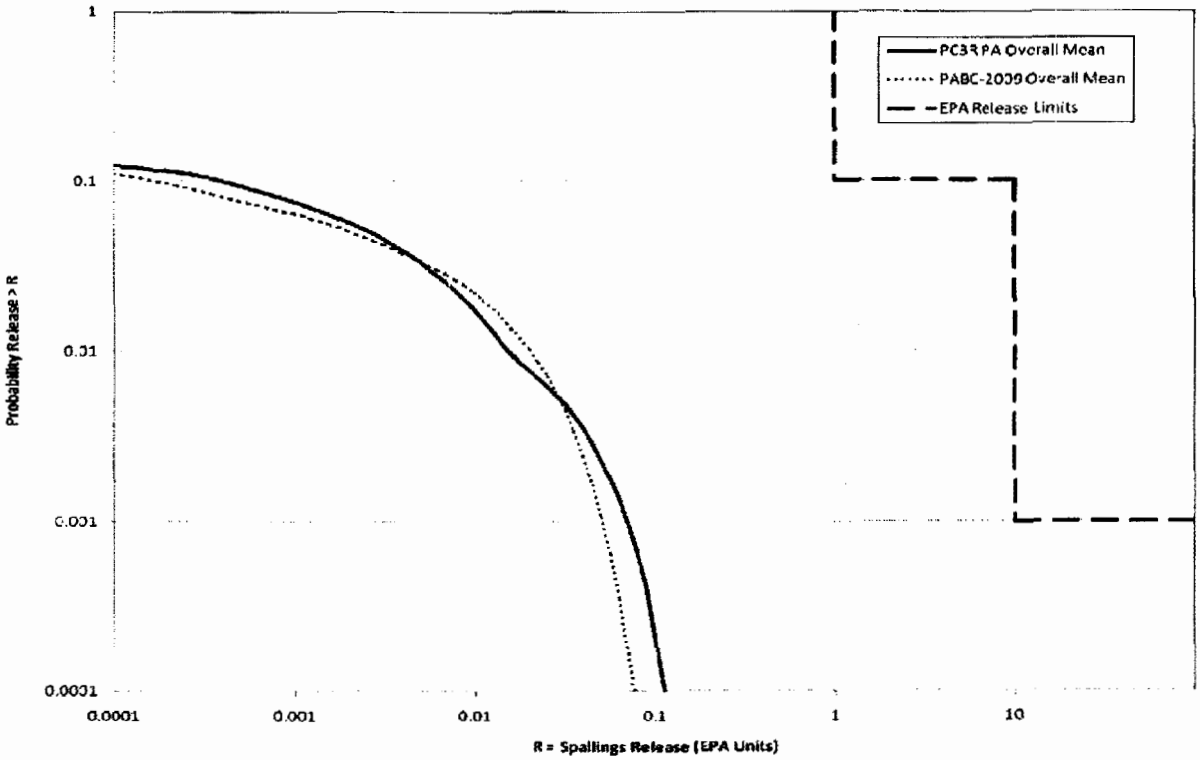

Figure 5-30: PC3R PA and PABC-2009 Overall Mean CCDFs for Normalized Spallings Releases

Spallings volumes are a function of repository pressure. The change in spallings volumes between the PC3R PA and the PABC-2009 is the result of changing repository pressures observed in BRAGFLO calculations for the PC3R PA. For intrusion scenarios that involve an encounter with a pressurized brine region below the repository, the slight reduction in the long-term PC3R PA panel closure permeabilities resulted in a slight increase in pressurization of the waste panel for a period of time following the intrusion. Since there is a minimum threshold pressure required to create spallings, an increase in repository pressure also increases the percentage of vectors with spallings. Repository pressures are also impacted by the slight increase in repository volume resulting from the slightly larger volumes of panels 9a 10a.

The impacts of the changes in spallings volumes on the overall mean CCDF for normalized spallings releases obtained in the PC3R PA can be seen in Figure 5-30. As seen in that figure, the CCDFs of spallings releases obtained in the PABC-2009 and the PC3R PA are similar. However, the PC3R PA CCDF curve shown in Figure 5-30 exhibits both increases and decreases in spallings releases when compared to PABC-2009 results. These changes are due to the spallings volume changes seen in the PC3R PA.

5.6 Direct Brine Releases

In this subsection, DBR results from the PC3R PA and the PABC-2009 are compared. Summary statistics of the calculated DBR volumes for replicates 1-3 and scenarios S1-DBR to S5-DBR are provided in Table 10. In that table, maximums shown are the maximum DBR volumes over all replicates, times, vectors and drilling locations. As seen by the statistics for the maximum DBR volumes in Table 10, the panel closure redesign and repository configuration implemented in the PC3R PA resulted in an increase in the maximum DBR volume as compared to the PABC-2009. The maximum DBR volume realized in the PABC-2009 was 48.2 m^3 while that seen in the PC3R PA is 52.0 m^3. However, the average DBR volume remained equal or decreased in the PC3R PA for all scenarios considered except for scenario S5-DBR. When calculated over all intrusion scenarios, the average volume reduced from a value of 1.34 m^3 in the PABC-2009 to a value of 1.14 m^3 in the PC3R PA. This reduction in the average DBR volume seen in the PC3R PA is a result of the lower number of vectors producing nonzero DBR volumes in that analysis. In the PABC-2009, a total of 2,474 vectors resulted in a nonzero DBR volume realization. The number of vectors resulting in nonzero DBR volumes in the PC3R PA is 2,273, a reduction by 201 vectors when compared to the PABC-2009 results.

Table 10: PABC-2009 and PC3R PA DBR Volume Statistics

	Maximum Volume (m^3)		Average Volume (m^3)		Number of Vectors	
Scenario	PABC-2009	PC3R PA	PABC-2009	PC3R PA	PABC-2009	PC3R PA
S1-DBR	21.9	29.7	0.1	0.1	258	257
S2-DBR	48.2	52.0	4.2	3.7	1071	962
S3-DBR	40.6	49.7	2.2	1.6	791	682
S4-DBR	20.4	28.1	0.1	0.1	145	148
S5-DBR	21.1	24.0	0.1	0.2	209	224
S1-DBR to S5-DBR	48.2	52.0	1.34	1.14	2474	2273

DBR releases are less likely to occur during upper drilling intrusions when compared with the lower drilling location. Of all the intrusions that had a non-zero DBR volume for the PC3R PA, 74.8% occurred during a lower drilling intrusion. Furthermore, of all the intrusions that had a non-zero DBR volume and occur during a lower drilling intrusion, 82.8% are found in scenarios S2-DBR and S3-DBR. Therefore, the majority of the non-zero DBR volumes occur when there is a previous E1 intrusion within the same panel. Not only are DBRs less likely to occur during

upper drilling intrusions, but also the DBR volumes from such intrusions tend to be much smaller than DBR volumes from lower drilling intrusions. For all three replicates of the PC3R PA, the maximum DBR volume for the upper drilling location is 22.0 m^3 compared to 52.0 m^3 for the lower drilling location (Pasch and Camphouse 2011). These observations support the conclusion that lower drilling intrusions are the primary source for significant DBRs.

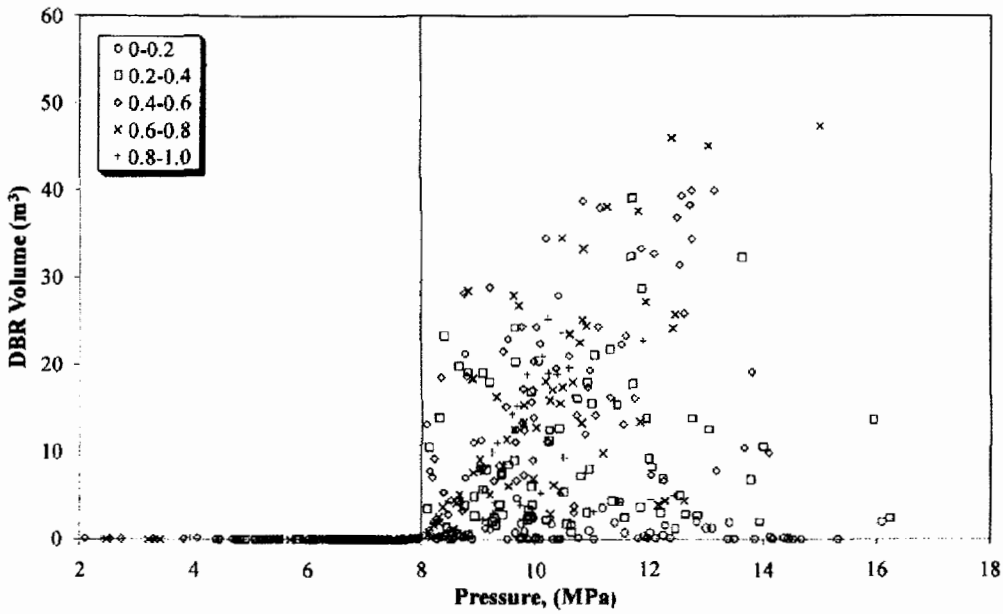

Figure 5-31: DBR Volume vs. Pressure, Scenario S2-DBR, Replicate 1, Lower Intrusion, PC3R PA

The combination of relatively high pressure and brine saturation in the intruded panel is required for direct brine release to the surface. Figure 5-31 shows a scatter plot of DBR volume versus pressure in the intruded panel at different intrusion times for the S2-DBR scenario, replicate 1, lower drilling intrusion for the PC3R PA. In that figure, symbols indicate the value of the mobile brine saturation, defined as brine saturation minus residual brine saturation in the waste. As prescribed by the conceptual model, there are no DBRs until pressures exceed 8 MPa as indicated by the vertical line in that figure. Above 8 MPa, a significant number of vectors have zero volumes; these vectors have mobile brine saturations less than zero and thus no brine is available in a mobile form to be released. Figure 5-31 shows a high concentration of results that are near a line extending from (8 MPa, 0 m^3) to (12 MPa, 30 m^3). As mobile saturation increases, the correlation between pressure and DBR volumes also increases.

To further facilitate comparisons of DBRs calculated in the PC3R PA to those obtained in the PABC-2009, the overall mean CCDFs obtained in these two analyses are plotted simultaneously in Figure 5-32. As seen in that figure, the CCDF curves obtained for direct brine releases in the

PABC-2009 and the PC3R PA are very similar. For releases up to roughly 0.1 EPA units, the CCDF curves obtained in both analyses are virtually identical. For releases between 0.1 and 1 EPA unit, the CCDF curve obtained in the PC3R PA is slightly above that calculated in the PABC-2009. For releases greater than 1 EPA unit, the CCDF curve obtained in the PABC-2009 is higher than that obtained in the PC3R PA. The decrease in the number of realizations with a nonzero DBR volume in the PC3R PA combined with the slight increase in the maximum DBR volume is most likely the cause for the differences observed in the DBR CCDF curves obtained in the PABC-2009 and the PC3R PA.

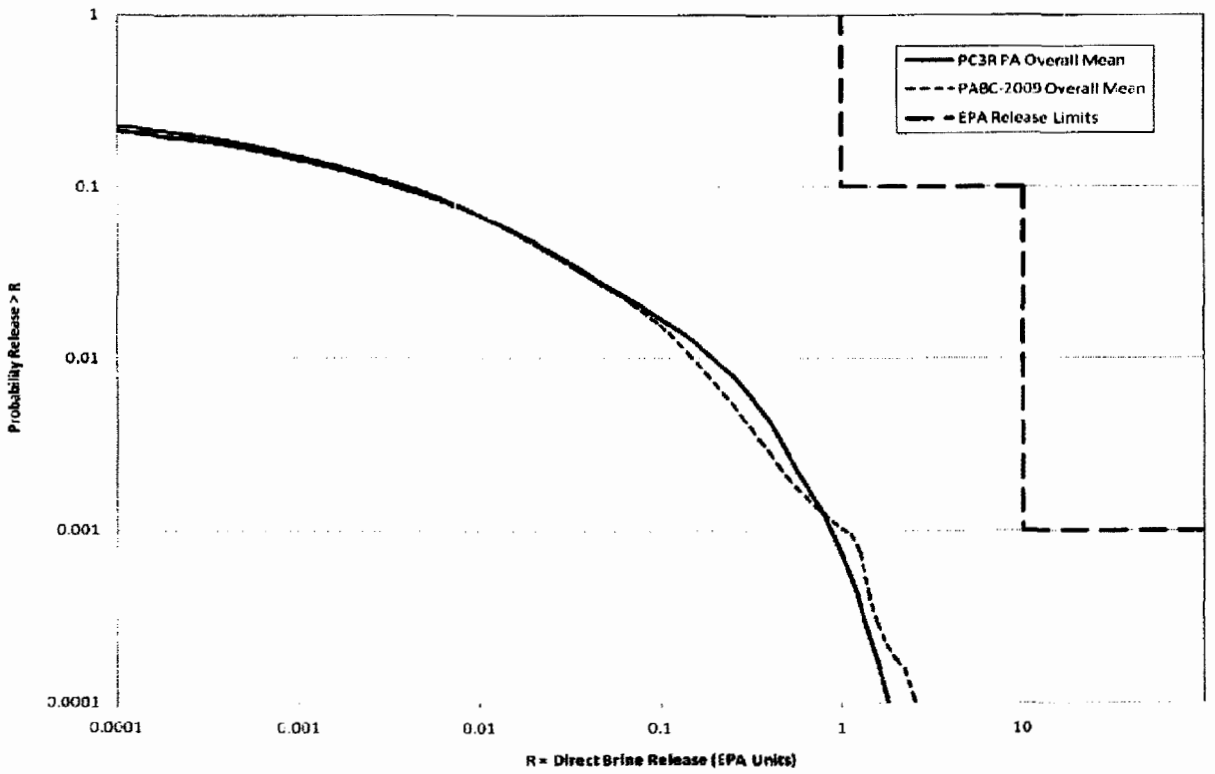

Figure 5-32: PC3R PA and PABC-2009 Overall Mean CCDFs for Normalized Direct Brine Releases

5.7 Total Normalized Releases

Total normalized releases for PC3R PA are presented in this section and subsequently compared to results obtained in the PABC-2009. Total releases are calculated by forming the summation of releases across each potential release pathway, namely cuttings and cavings releases, spallings releases, direct brine releases, and transport releases. As prescribed in AP-151 (Camphouse 2010a), transport results obtained in the PABC-2009 were used in the PC3R PA. PC3R PA CCDFs for total releases are presented in Figure 5-33, Figure 5-34, and Figure 5-35 for replicates 1, 2, and 3, respectively. Mean and quantile CCDF distributions for the three replicates are

shown together in Figure 5-36. Figure 5-37 contains the 95 percent confidence limits about the overall mean of total releases. As seen in Figure 5-37, the overall mean for normalized total releases and its lower/upper 95% confidence limits are well below acceptable release limits. As a result, the panel closure design and repository configuration changes investigated in the PC3R PA do no result in WIPP non-compliance with the containment requirements of 40 CFR Part 191.

PC3R PA and PABC-2009 overall mean CCDFs for total releases are shown together in Figure 5-38. As seen in that figure, the overall mean CCDFs obtained in the two analyses are virtually identical for release values less than approximately 0.1 EPA units. For releases between 0.1 and 1.0 EPA units, the overall total release mean CCDF curve obtained in the PC3R PA is slightly above that calculated in the PABC-2009. For releases greater than 1 EPA unit, the CCDF curve obtained in the PABC-2009 is higher than that found in the PC3R PA. These trends correspond exactly to the differences found for direct brine releases between the two analyses as discussed in Section 5.6 and illustrated in Figure 5-32. Indeed, as seen in Figure 5-39, cuttings and cavings releases and direct brine releases are the two primary release components contributing to total releases found in the PC3R PA. PC3R PA cuttings and cavings results are unchanged from those found in the PABC-2009. The panel closure design and repository configuration changes investigated in the PC3R PA have a slight impact on direct brine releases. The changes in the overall mean of total releases from the PABC-2009 to the PC3R PA are due to the changes in direct brine releases calculated in those analyses.

A comparison of the statistics on the overall mean for total normalized releases obtained in the PC3R PA and the PABC-2009 can be seen in Table 11. At a probability of 0.1, values obtained for mean total releases are identical in both analyses. At a probability of 0.001, the decrease in DBRs seen at that probability in the PC3R PA result in a decrease in the mean total release by approximately 0.21 EPA units. Reductions are also seen in the 90th percentile and the 95% confidence limits when compared to the PABC-2009 results.

Table 11: PC3R PA and PABC-2009 Statistics on the Overall Mean for Total Normalized Releases in EPA Units at Probabilities of 0.1 and 0.001

Probability	Analysis	Mean Total Release	90th Percentile	Lower 95% CL	Upper 95% CL	Release Limit
0.1	PC3R PA	0.09	0.16	0.09	0.10	1
	PABC-2009	0.09	0.16	0.09	0.10	1
0.001	PC3R PA	0.89	1.00	0.34	1.41	10
	PABC-2009	1.10	1.00	0.37	1.77	10

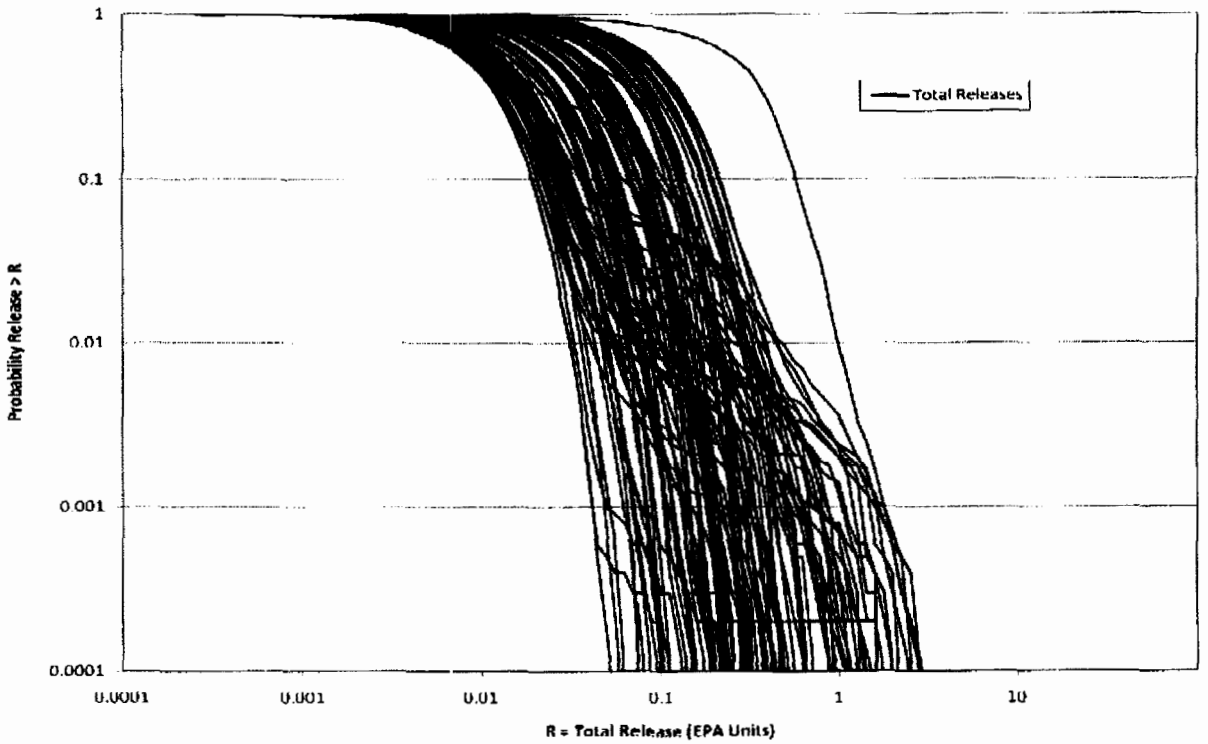

Figure 5-33: PC3R PA Replicate 1 Total Normalized Releases

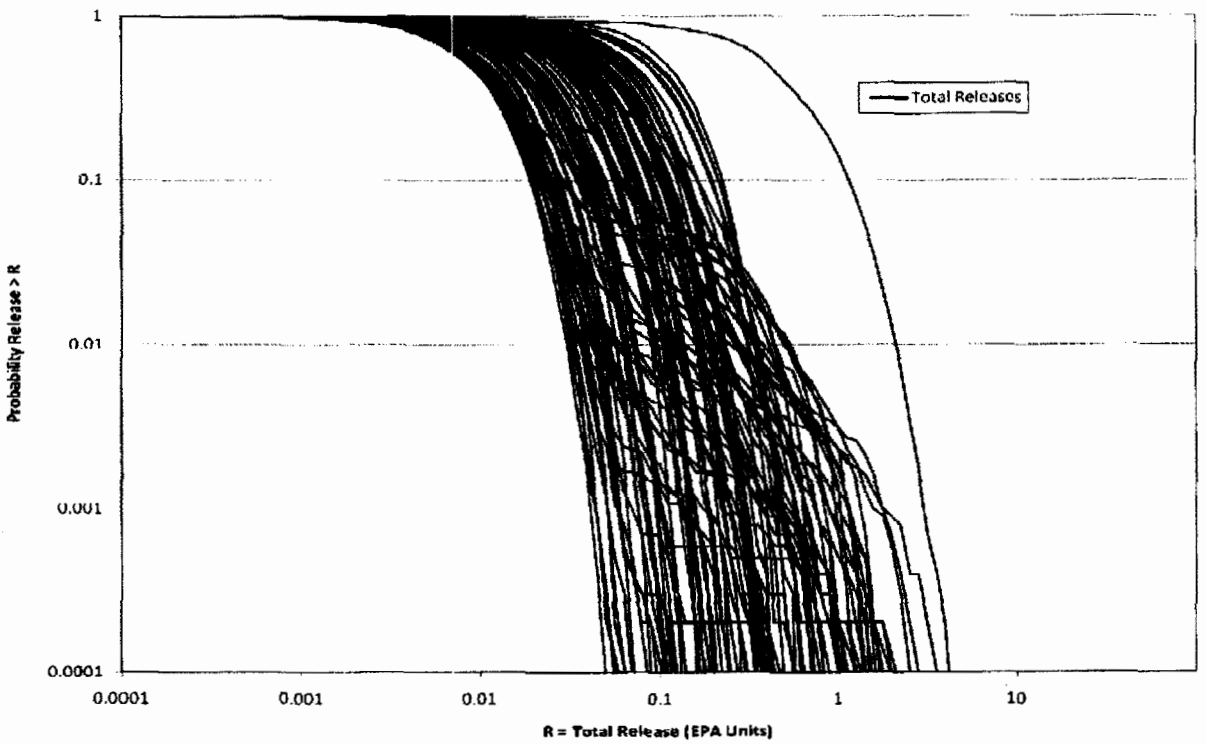

Figure 5-34: PC3R PA Replicate 2 Total Normalized Releases

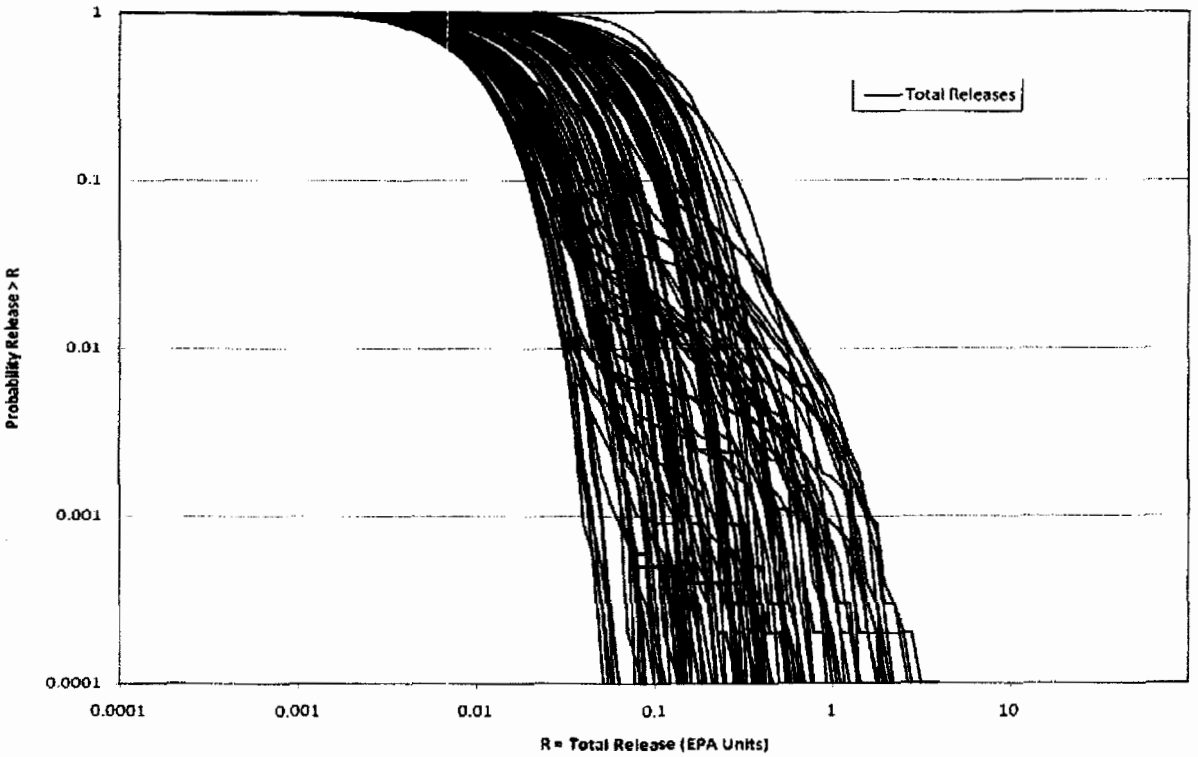

Figure 5-35: PC3R PA Replicate 3 Total Normalized Releases

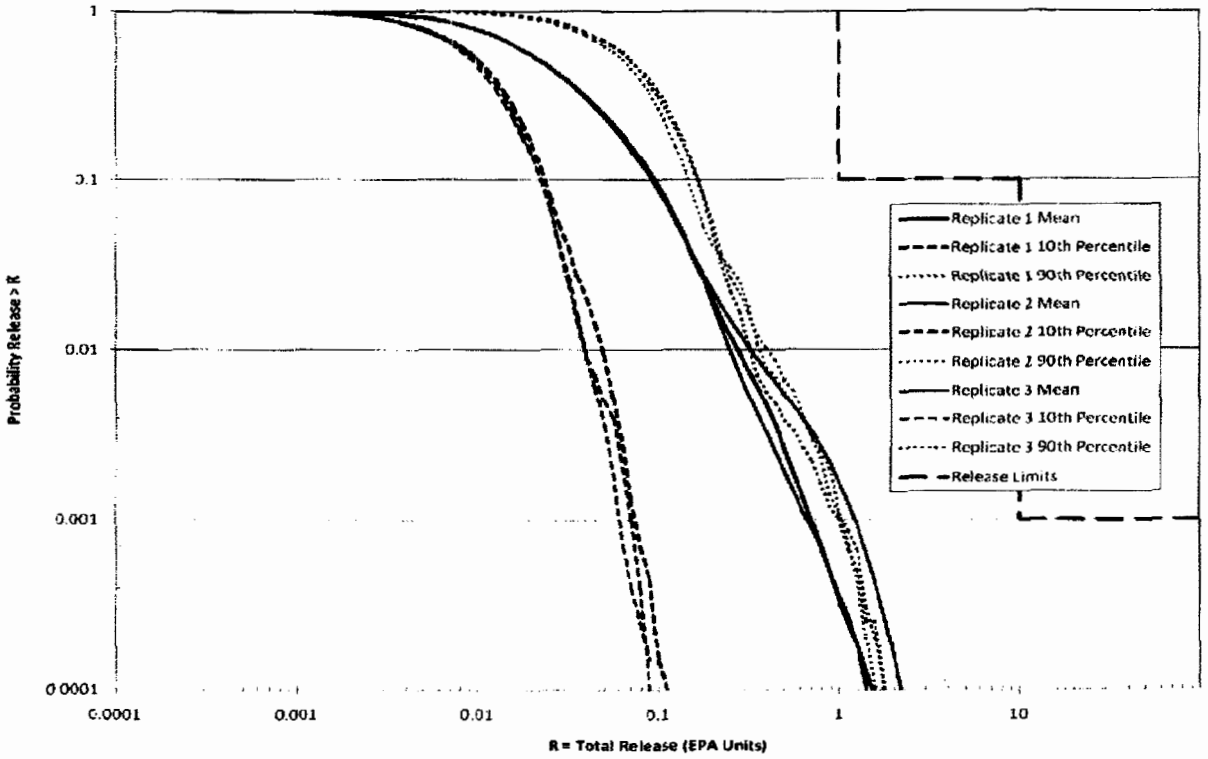

Figure 5-36: PC3R PA Mean and Quantile CCDFs for Total Normalized Releases, Replicates 1-3

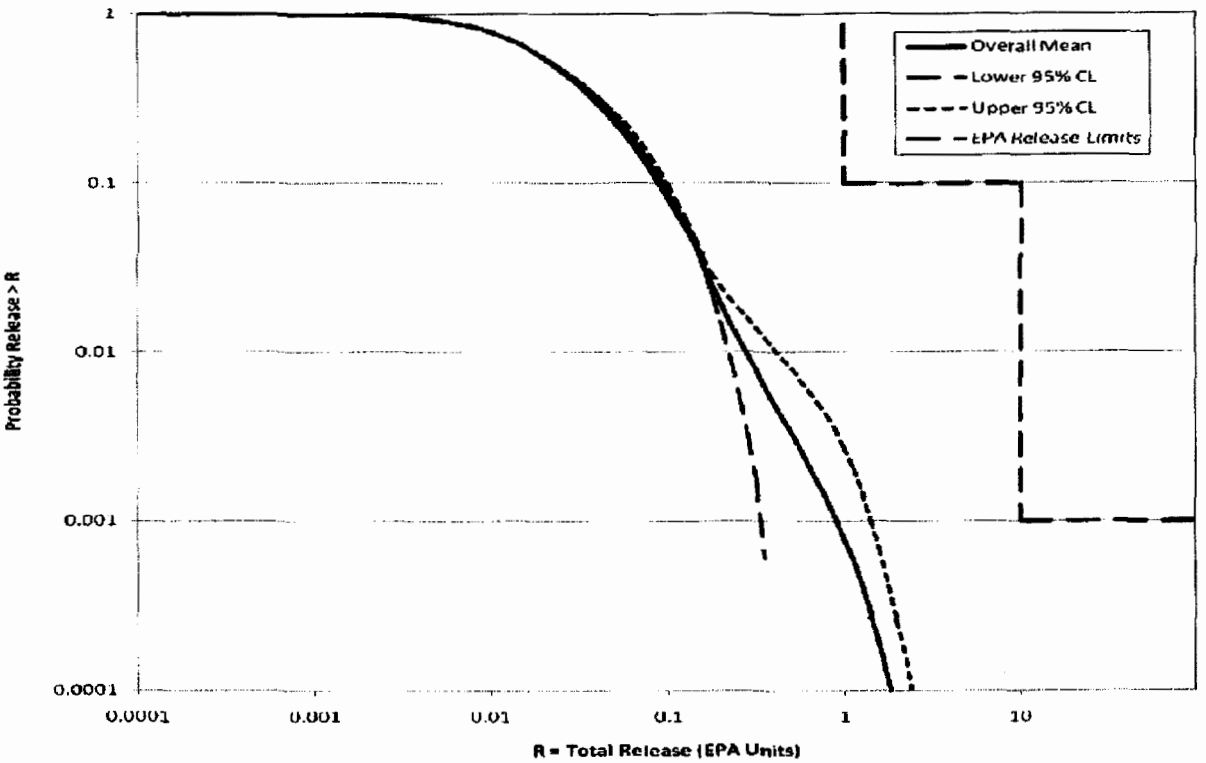

Figure 5-37: PC3R PA Confidence Limits on Overall Mean for Total Normalized Releases

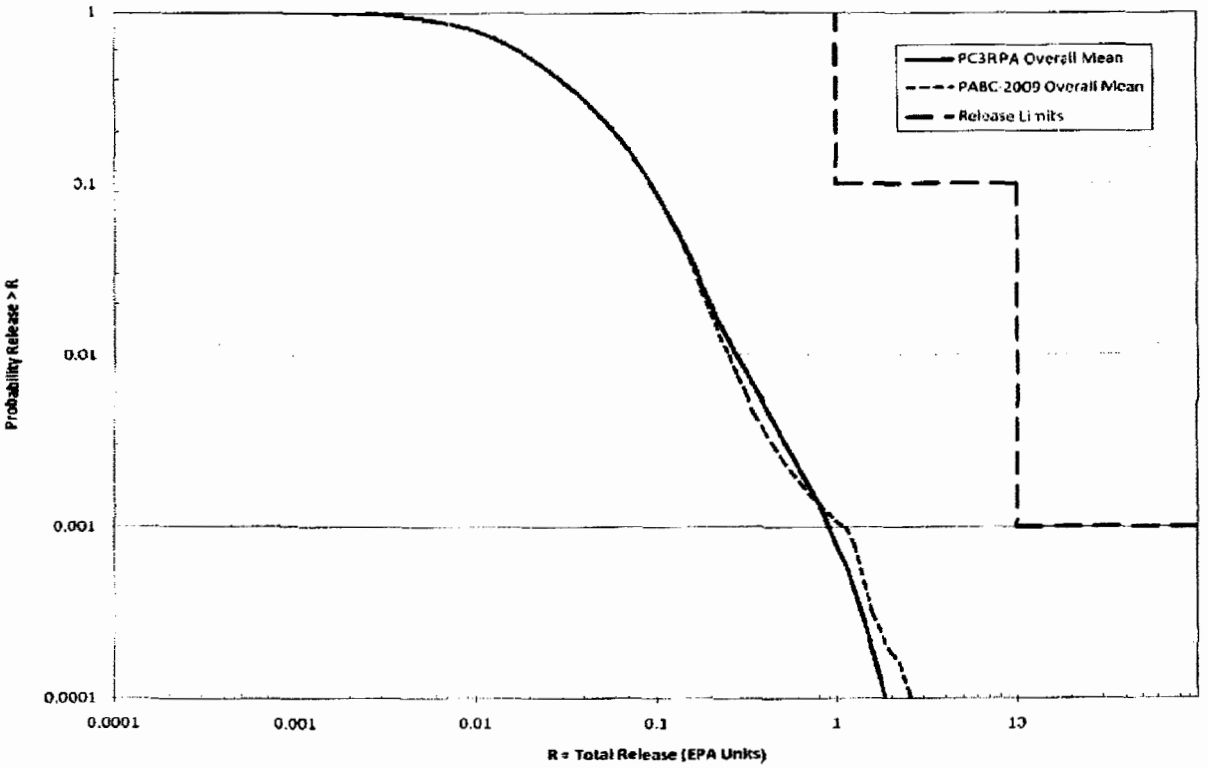

Figure 5-38: PC3R PA and PABC-2009 Overall Mean CCDFs for Total Normalized Releases

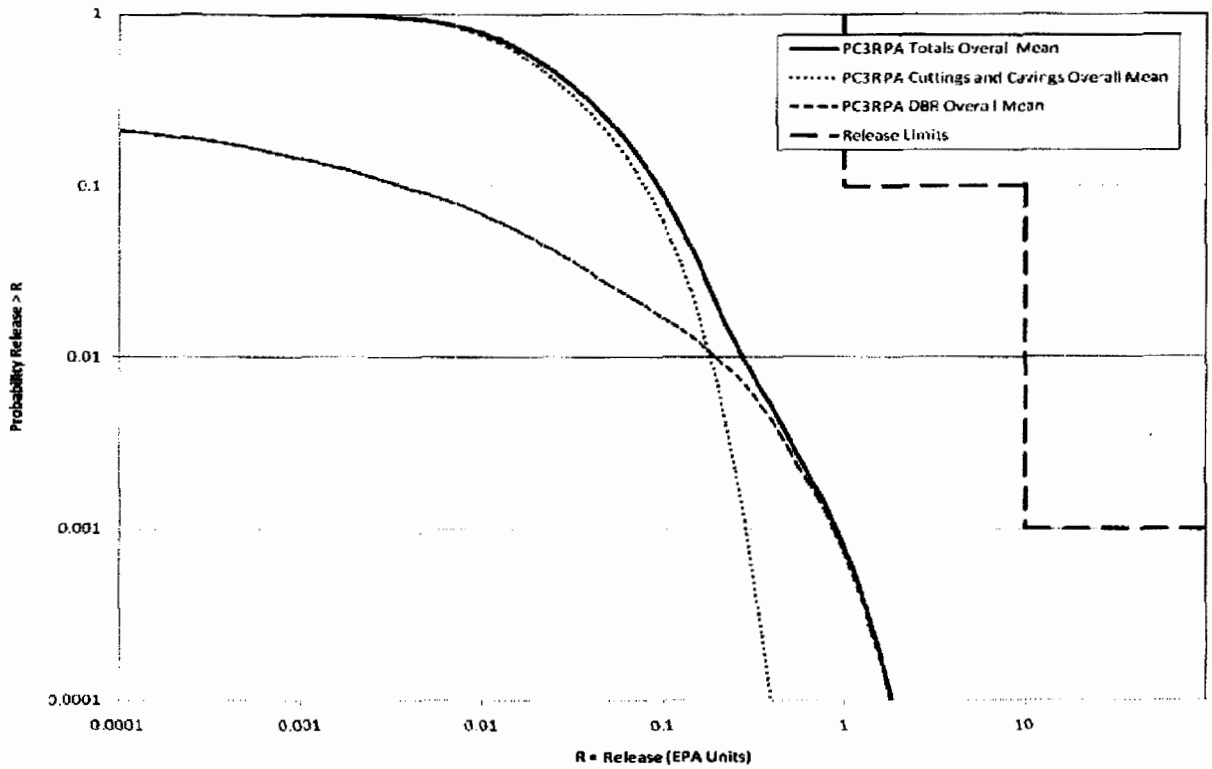

Figure 5-39: PC3R PA Primary Components Contributing to Total Releases

6 SUMMARY

Total normalized releases calculated in the PC3R PA remain below their regulatory limits. As a result, the panel closure design and repository configuration changes investigated in the PC3R PA would not result in WIPP non-compliance with the containment requirements of 40 CFR Part 191. Cuttings and cavings releases and direct brine releases are the two primary release components contributing to total releases in the PC3R PA. Cuttings and cavings releases are unchanged from those calculated in the PABC-2009. Changes in total releases are attributed to changes calculated in direct brine releases from the PABC-2009 to the PC3R PA. Differences are observed in PC3R PA spallings releases as compared to the PABC-2009, but these differences are relatively minor and do not have a significant impact on the overall total normalized releases found in the PC3R PA.

Several conclusions can be made regarding the impact of the panel closure redesign, the open central drift region, and the placement of panel closures in the reconfigured repository. Most significant among these are the following:

- The combination of initially high panel closure permeability and comparatively low pressure in the central drift region allows for pressure release from the waste regions into

the central drift area until the panel closures attain their steady-state permeability values at 100 years.

- The reconfigured repository and the redesigned panel closures implemented therein do not result in an increase in brine flow out of the waste regions when compared to the PABC-2009.
- The redesigned panel closures in combination with their placement in the repository reconfiguration effectively limit the impacts of drilling intrusion to the region being intruded. In particular, the brine available for release to the surface during a drilling event into the central drift region is equal to that present under undisturbed conditions, even if there have been prior intrusions into a waste panel.

7 REFERENCES

Callahan, G.D. and K.L. DeVries. 1991. Analysis of Backfilled Transuranic Waste Disposal Rooms. SAND91-7052. Sandia National Laboratories, Carlsbad, NM.

Camphouse, R.C. 2010a. Analysis Plan for the WIPP Panel Closure Redesign and Repository Reconfiguration. Sandia National Laboratories, Carlsbad, NM. ERMS 554595.

Camphouse, R.C. 2010b. Recommendation and Justification of Parameter Values Required for the WIPP Panel Closure Redesign and Repository Reconfiguration Performance Assessment, Memo to Records dated December 13, 2010. Sandia National Laboratories, Carlsbad, NM. ERMS 554614.

Camphouse, R.C. 2010c. Value Recommendation and Justification for Properties CAP_MOD, PCT_A and PCT_EXP for Materials PCS_T1 and PCS_T2 used in the WIPP Panel Closure Redesign and Repository Reconfiguration Performance Assessment, Memo to Records dated December 20, 2010. Sandia National Laboratories, Carlsbad, NM. ERMS 554623.

Camphouse, R.C. 2011a. Value Recommendation and Justification for Parameters DRZ_1:EHEIGHT and OPS_AREA:EHEIGHT needed during calculation of direct brine releases in the PC3R PA. Memo to Records Center, January 5, 2011. Sandia National Laboratories, Carlsbad, NM. ERMS 554694.

Camphouse, R.C. 2011b. Generation of the LHS Samples for the AP-151 (PC3R) PA Calculations. Sandia National Laboratories, Carlsbad, NM. ERMS 555232.

Camphouse, R.C. 2011c. CCDFGF Analysis Package for the AP-151 (PC3R) Performance Assessment. Sandia National Laboratories, Carlsbad, NM. ERMS 555244.

Camphouse, R.C. and Clayton, D.J. 2011. Analysis Package for Salado Flow Modeling Done in the AP-151 (PC3R) Performance Assessment. Sandia National Laboratories, Carlsbad, NM. ERMS 555204.

Camphouse, R.C. and Garner J.W. 2011. Impacts of PC3R PA Repository Configuration Changes on Calculated Transport Releases, Memo to Records dated March 29, 2011. Sandia National Laboratories, Carlsbad, NM. ERMS 555241.

Clayton, D.J. 2010. Analysis Package for Direct Brine Releases: CRA-2009 Performance Assessment Baseline Calculation, Revision 0. Sandia National Laboratories. Carlsbad, NM. ERMS 552829.

Clayton, D.J., R.C. Camphouse, J.W. Garner, A.E. Ismail, T.B. Kirchner, K.L. Kuhlman, M.B. Nemer. 2010. Summary Report of the CRA-2009 Performance Assessment Baseline Calculation. Sandia National Laboratories, Carlsbad, NM. ERMS 553039.

Hansen, C. W. 2002. Analysis Report for the Panel Closure Impact Assessment. Sandia National Laboratories, Carlsbad, NM. ERMS 523935.

Hansen, C.W. 2011. Sensitivity of the AP-151 (PC3R) PA Calculation Releases to Parameters. Sandia National Laboratories, Carlsbad, NM. ERMS 555288.

Hansen, F.D. and Thompson, T.W. 2002. Effective Permeability of the Redesigned Panel Closure System, Memo to Paul E. Shoemaker dated August 29, 2002. Sandia National Laboratories, Carlsbad, NM. ERMS 523476.

Kicker, D.C. 2011. Analysis Package for Cuttings, Cavings, and Spallings: Panel Closure Redesign and Repository Reconfiguration Performance Assessment (PC3R PA). Sandia National Laboratories, Carlsbad, NM. ERMS 555209.

Kirkes, G.R. 2011. Features, Events and Processes Assessment for Changes Described in Analysis Plan – 151, Revision 0. Sandia National Laboratories, Carlsbad, NM. ERMS 555237.

Long, J.J. 2011. Execution of Performance Assessment Codes for the WIPP Panel Closure Redesign and Repository Reconfiguration. Sandia National Laboratories, Carlsbad, NM. ERMS 555266.

Pasch, J.J. and Camphouse, R.C. 2011. Analysis Package for Direct Brine Releases: Panel Closure Redesign and Repository Reconfiguration Performance Assessment (PC3R PA). Sandia National Laboratories, Carlsbad, NM. ERMS 555249.

Stein, J.S. 2002a. Analysis Plan for Calculations of Salado Flow: Technical Baseline Migration (TBM) AP-086. Sandia National Laboratories, Carlsbad, NM. ERMS 520612.

U.S. Environmental Protection Agency (EPA). 1996. 40 CFR Part 194: Criteria for the Certification and Recertification of the Waste Isolation Pilot Plant's Compliance with the 40 CFR Part 191 Disposal Regulations; Final Rule. Federal Register, Vol. 61, 5223-5245.

U.S. Environmental Protection Agency (EPA). 1998. 40 CFR 194, Criteria for the Certification and Recertification of the Waste Isolation Pilot Plant's Compliance with the Disposal Regulations: Certification Decision: Final Rule, Federal Register. Vol. 63, 27354-27406. ERMS 251924.

U.S. Environmental Protection Agency (EPA). 2010. 40 CFR Part 194 Criteria for the Certification and Recertification of the Waste Isolation Pilot Plant's Compliance With the Disposal Regulations: Recertification Decision, Federal Register No. 222, Vol. 75, pp. 70584-70595, November 18, 2010.

Vugrin, E.D., S.C. Dunagan. 2006. Analysis Package for the Impact Assessment of the Redesigned WIPP Panel Closure. Sandia National Laboratories, Carlsbad, NM. ERMS 543865.

Vugrin, E., Hansen, F., and Thompson, B. Recommendation and Justification of Parameter Values Required for Representation of the Redesigned Panel Closure System, Memo to David Kessel dated March 23, 2006. Sandia National Laboratories, Carlsbad, NM. ERMS 542894.

Camphouse, Russell Chris

From: Clayton, Daniel James
Sent: Tuesday, April 05, 2011 1:37 PM
To: Camphouse, Russell Chris
Subject: RE: sig authority

I give R. Chris Camphouse signature authority for the PC3R PA summary report

---

From: Camphouse, Russell Chris
Sent: Tuesday, April 05, 2011 1:36 PM
To: Clayton, Daniel James
Subject: sig authority

Hi Dan,

Can you send someone signature authority for the title page of the summary report?

Thanks,

Chris

----------rccamph@sandia.gov----------
R. Chris Camphouse
Sandia National Laboratories
Carlsbad Programs Group
Performance Assessment and Decision Analysis Department

4100 National Parks Highway MS 1395
Carlsbad, NM 88220
Phone: (575) 234-0130
Fax: (575) 234-0061

Panel Closure Redesign:

Update

August 2011

Thomas Klein-URS, Regulatory and Environmental Services,
Carlsbad, NM 88220

Introduction

This presentation will cover operational and long-term design aspects:

- Major Design Criteria
- Research Activities
- Interim Closure
- Gas Monitoring
- Current Research Activities
- Planned Change Request
- Regulatory Schedule

Major Design Criteria

EPA Certification (long-term)

- Option D design represented in Performance Assessment
- Salado Mass Concrete

NMED Hazardous Waste Facility Permit (operational period)

- Limit migration of volatile organics at the point of compliance for 35 years.
- Maintain functionality under loads generated by salt creep.
- Maintain functionality under loads generated by internal pressures.
- Maintain functionality under loads generated by a postulated methane-based explosion.
- Limit migration of Volatile Organic Compounds (VOCs).

Research Activities

- 2001- DOE identified several changes needed to the panel closure design after initial investigations. These changes were:

  1. Replace Salado Mass Concrete with generic salt-based concrete. (EPA/NMED)
  2. Replace isolation wall with construction wall. (NMED)
  3. Replace freshwater grouting with salt-based grouting. (EPA/NMED)
  4. Allow option of implementation of panel closure completion within a year instead of 180 days. (NMED)

Interim Closure

- 2003- To comply with the requirements of the Hazardous Waste Facility Permit, the DOE constructed the block wall portion of the Panel Closure Option D design for Panels 1 and 2. This allowed DOE to study the effects of salt creep on the block wall and verify previously identified changes.

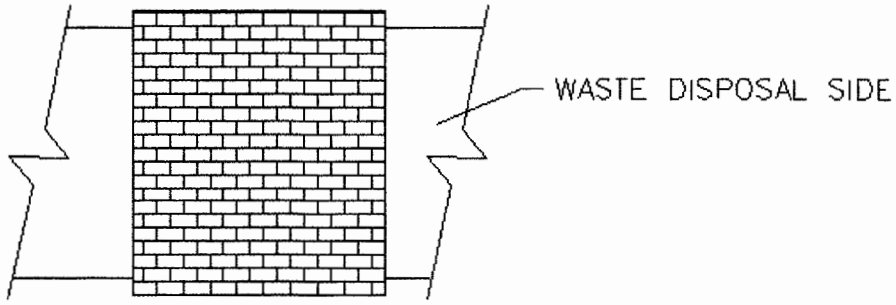

Gas Monitoring

•2007- DOE -Hydrogen and Methane monitoring is being performed in waste filled panels and the results have shown that methane and hydrogen levels are below regulatory limits (NMED).

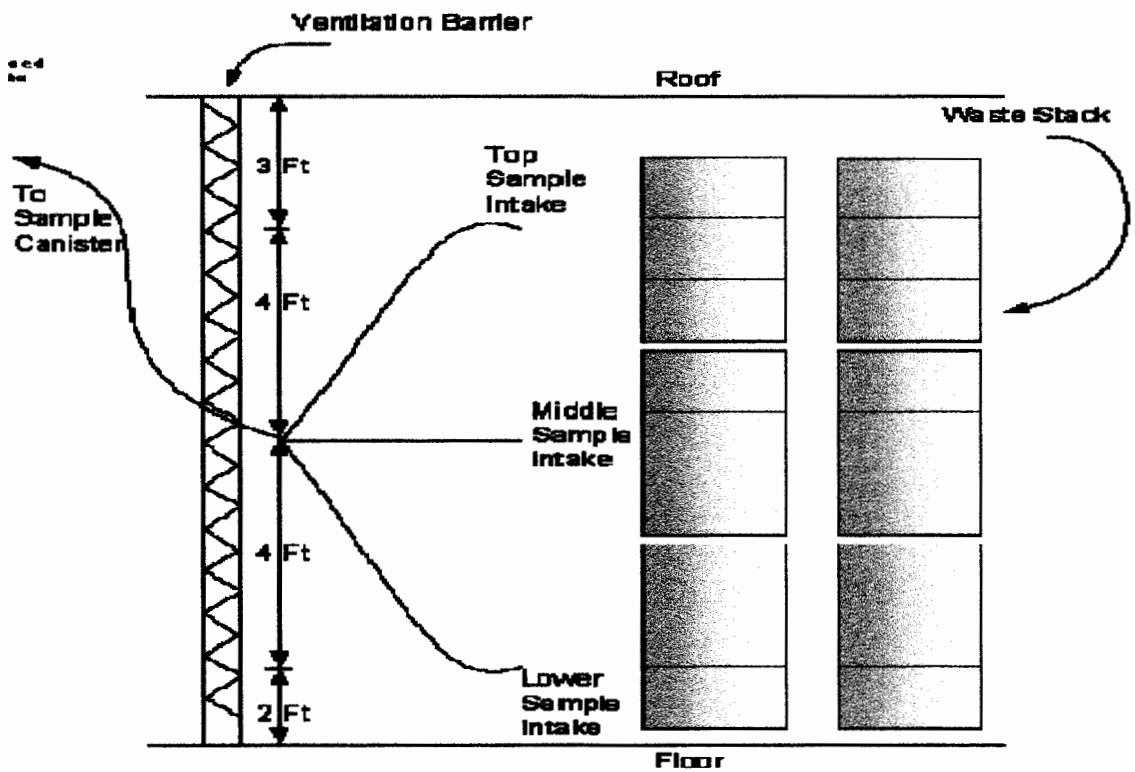

Combining Research Activities and the Planned Change Request

- Continue to collect Hydrogen, Methane and VOC data. (NMED)
- Review and evaluate Hydrogen, Methane and VOC data. (NMED)
- Run Performance Assessment with the new panel closure design represented in the models. (EPA)
- Integrate with new Hazardous Waste Facility Permit requirements. (NMED)

Planned Change Request

- Evaluates monitoring data from panels with emplaced waste and evaluates potential for explosive gas (NMED).

- Performance assessment that incorporates updated design (PC3R) (EPA).

- Ensure long-term porosities and permeability of the new design are comparable to the Option D design (EPA).

Planned Change Request Cont.

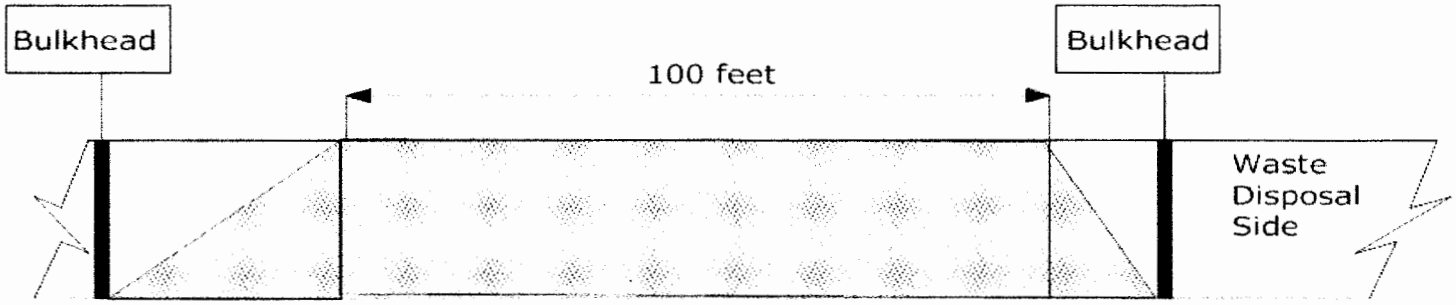

Figure 2: Proposed Run of Mine Panel Closure

Regulatory Schedule

EPA-Planned submittal September 2011.

-18 to 24 month review (Rulemaking)

-Projected approval 2013

NMED-Planned submittal January 2012.

-12 to 18 month review and comment period.

-Projected approval 2013.

Conclusion

- As a result of increased understanding of the repository and the stored waste obtained over 12 years of operation, the DOE has determined that a revision of the approved Option D panel closure design should be made.
- The revised design described in this PCR will reduce the risk of injury to construction workers, enhance constructability, reduce construction cost, and reduce the impacts on on-going repository operations.
- A change to the design specified in Condition 1 of the Certification Decision is required because of the problems in manufacturing SMC to the specifications in the CCA.

* An analysis of the results of earlier PAs suggests that this revised design will have a long-term performance essentially the same as with Option D.

UNITED STATES ENVIRONMENTAL PROTECTION AGENCY
WASHINGTON, D.C. 20460

DEC 22 2011

OFFICE OF
AIR AND RADIATION

Mr. Ed Ziemianski
Carlsbad Field Office
U.S. Department of Energy
P.O. Box 3090
Carlsbad, New Mexico 88221-3090

Dear Mr. Ziemianski:

On August 30 and September 28, 2011 the U.S. Department of Energy (DOE) submitted two Planned Change Requests (PCRs) to the U.S. Environmental Protection Agency for review. The first PCR (DOE/CBFO-11-3478) proposes relocating Waste Panels 9 and 10 to the south of existing Waste Panels 4 and 5, the second PCR (DOE/CBFO-11-3479) proposes replacing the current 'Option D' Panel Closure System (PCS) with an alternative design. Both PCR packages use the Panel Closure Redesign and Repository Reconfiguration (PC3R) Performance Assessment (PA) modeling results and analyses.

As you know, 40 CFR Part 194 specifies in Appendix A, Condition 1 that the Option D Panel Closure be implemented at WIPP. Thus, any change in the panel closure design requires modification to the rule. EPA is reviewing the PC3R PA package to determine if it is sufficient for us to move ahead with a rulemaking and to identify areas that need additional supporting information or modification. The first set of review questions and comments is included in this package, it focuses on changes to the panel closures. Within the next few weeks, EPA will be providing additional questions and comments to DOE related to both the PCS and the repository reconfiguration.

Your timely and considered response to the attached questions and comments, as well as those you will receive over the next few weeks, will allow us to determine whether a rulemaking is feasible prior to DOE's next submission for recertification.

Sincerely,

Alan D. Perrin, Acting Director
Radiation Protection Division

cc: (Electronic Distribution)
George Basabilvazo, DOE/CBFO
Russ Patterson, DOE/CBFO
Steve Kouba, RES
Mike Gross, RES
Paul Shoemaker, SNL
Christi Leigh, SNL
Moo Lee, SNL
Chris Camphouse, SNL
Trais Kliphuis, NMED
Thomas Kesterson, NMED
Nick Stone, EPA Region 6

Internet Address (URL) • http://www.epa.gov
Recycled/Recyclable • Printed with Vegetable Oil Based Inks on 100% Postconsumer, Process Chlorine Free Recycled Paper

Enclosure: First Set of EPA Questions to DOE
December 22, 2011

1 Parameters Related to Run of Mine (ROM) Panel Closure (PC)

This attachment provides initial questions and comments in EPA's ongoing review of the Panel Closure Redesign and Repository Reconfiguration Performance Assessment (PC3R PA). The focus of these comments are justifications for the parameters and parameter values that are new or have been changed from those in the 2009 Performance Assessment Baseline Calculation (PABC 2009 PA).

The starting points for reviewing each parameter are the descriptions and references provided in the *Summary Report for the AP-151 (PC3R) Performance Assessment, Rev. 1* (Camphouse et al. 2011, ERMS 555489) and in *Recommendation and Justification of Parameter Values Required for the WIPP Panel Closure Redesign and Repository Reconfiguration Performance Assessment* (Camphouse 2010b, ERMS 554614). The first of these is the principal document describing the PC3R PA and its results, and the second is the principal document describing and justifying the parameters and values that were used.

1.1 Duration of Time Period T1

Parameter Name	PABC 2009 Value	Used in PC3R PA ERMS 555489	Units
Duration of Time Period T1	Not Applicable	100	years

Technical Question 1.1a: Please clarify the justification of the 100 year duration for T1. Different documents have estimated different time periods for run of mine salt to reach steady state porosity. Specifically, the PC3R cites Callahan and DeVries (1991, SAND91-7052), who predict consolidation of ROM salt to a porosity of 0.05 in about 13 years, and Hansen and Thompson (2002, ERMS 523476), who predict consolidation of ROM salt to a higher porosity of 0.10 within 100 years.

Technical Question 1.1b: Please justify the assumption that loosely placed, ROM salt will consolidate to a porosity of 0.05 in 100 years when the cited source Hansen and Thompson (2002) concludes that the salt will consolidate to a porosity of only 0.10 within 100 years.

Technical Question 1.1c: Please justify the use of two time periods to represent consolidation of the ROM salt panel closure material, when additional time periods could provide a more refined representation of salt consolidation over time.

Completeness Question 1.1d: Please identify the effect of the rock bolts installed at WIPP for ground control on the consolidation rate for the ROM salt panel closure material.

EPA Concerns

DOE's justification for adopting 100 years as the time frame for the T1 time period is not clear, especially given the range of values given by different sources.

Hansen and Thompson (2002, p.4) estimated that a reduction of ROM salt porosity from 0.33 to 0.10 would occur within a maximum of 100 years, and indicate that it would take more than 100 years for ROM salt porosity to drop to the target value of 0.05.

Numerical simulations conducted by Callahan and DeVries (1991, Figure 4-2 SAND91-7052) predicted the essentially total reduction in the void volume of a room filled with crushed salt within about 25 years. These predictions do not seem to be supported by the measured closure rates of Panel 1 access drifts used in Hansen and Thompson (2002).

In DOE's proposed 2006 panel closure redesign (which also used 100 feet of loosely placed ROM salt for the panel closure material), a value of 200 years was used for creep closure to reduce the porosity from an initial value of 0.33 (averaged to 0.27 when combined with the porosity of the concrete block explosion wall) to a final value of 0.05 (Vugrin and Dunagan 2006, Table 3 and p. 15 ERMS 543865). No reason is given for reducing the time required to reach a .05 porosity value from 200 years to 100 years in the PC3R PA.

1.2 Panel Closure Porosity

Parameter Name	PABC 2009 Value	Used in PC3R PA ERMS 555489	Units
PCS_T2: POROSITY	0.05 for CONC_PCS	0.05	--

Technical Question 1.2a: Please provide justification that the T2 porosity is an appropriate target value that correlates to the permeability and compressibility values used in the PC3R PA.

Technical Question 1.2b: How sensitive a parameter is the final porosity of the panel closure? That is, how much would changing the value of PCS_T2: POROSITY (e.g. to 0.01 or 0.075) change calculated results, such as waste area saturation and pressure, that are known to impact performance?

EPA Concerns

DOE's reasoning in selecting the final T2 porosity value of 0.05 is not explicit. Because the assigned porosity of the panel closure at T2 is the value from which the long-term permeability and compressibility of the panel closure are defined, EPA is asking for more information on the parameter's justification and the importance of the specific value used.

1.3 Long-Term Panel Closure Permeability

Parameter Name	PABC 2009 Value	Used in PC3R PA ERMS 555489	Units
PCS_T2:PRMX_LOG PCS_T2:PRMY_LOG PCS_T2:PRMZ_LOG	-17, -20.8, -18.8 for CONC_PCS	-17.6,-22.8,-20.2 Triangular Distribution	$\log(m^2)$

Technical Question 1.3a: Please provide a source for the permeability values assigned to the ROM salt panel seal during time period T2 that provides traceability to original sources.

Technical Question 1.3b: Please justify the assignment of permeabilities to the ROM salt panel seal during time period T2 that represent fully consolidated salt rather than ROM salt consolidated to a porosity of 0.05.

Completeness Question 1.3c: Please provide design and performance information that justifies the stated assumption that the "substantial barrier" will have no impact on panel seal performance during time period T2.

Completeness Question 1.3d: Please justify the unstated assumption that repository gas pressure buildup during time period T2 will not inhibit or reverse consolidation of the ROM salt panel seal, potentially resulting in higher porosities and therefore higher permeabilities than the recommended values.

Completeness Question 1.3e: Please justify the unstated assumption that backpressure reduction through lateral halite movement at the unconstrained ends of the 100-ft panel closure backfill can be ignored during the consolidation process.

EPA Concerns

EPA is looking for clarification on the justification of the long-term panel closure permeability.

A compilation of laboratory-measured permeability values for WIPP crushed salt at various fractional densities was prepared by Hurtado et al. (1997, Table 2-1 SAND97-1287). The most relevant results were taken from Brodsky (1994, SAND93-7058), who measured the permeability of compacted ROM salt at fractional densities near 0.95 (equivalent to a porosity of 0.05) using brine as the fluid rather than gas.

Kelley et al. (1996, p. 1 ERMS 230995) provide a summary of permeability values at various densities. The T2 permeability values recommended by Camphouse (2010b, p. 4)) are most similar to those reported by Kelley et al. (1996, Table 6) for 200-years, which represented full reconsolidation. The values recommended by Camphouse are not identical to any of those presented in the 1996 Kelley report.

The PC3R T2 permeability values are similar to the values for fully reconsolidated crushed salt reported by Kelley et al. (1996) and Hurtado et al. (1997), but not representative of porosities equivalent to 0.05. The T2 permeabilities used to represent ROM salt at a porosity of 0.05 are generally 1.5 to 2 orders of magnitude lower than those reported by Butcher et al. (1991, reported in Hansen and Callahan, 1993), Brodsky (1994), Hurtado et al. (1997, SAND97-1287), and Hansen and Thompson (2002) for compacted salt equivalent to a porosity of 0.05.

1.4 Panel Closure DRZ Permeability

Parameter Name	PABC 2009 Value	Used in PC3R PA ERMS 555489	Units
Long Term T2 Values for the PCS DRZ			
PCS_T2:PRMX_LOG PCS_T2:PRMY_LOG PCS_T2:PRMZ_LOG	-20.7, -18.8, -17.0 for material CONC_PCS	-22.8, -20.2, -17.6 Triangular Distribution	$\log(m^2)$

Technical Question 1.4a: Please justify the assignment of permeability values to the PCS DRZ during time period T2 that appear to represent a fully reconsolidated material, when the ROM salt panel closure itself has not yet fully reconsolidated and stress equilibrium has not yet been achieved.

Completeness Question 1.4b: Please explain why the anhydrite marker beds surrounding the ROM salt panel seal are not treated in the same manner as those within the waste panel DRZ.

EPA Concerns

EPA cannot trace the justification for assigned permeabilities provided by Camphouse (2010, p. 5 ERMS 554614) to supporting documentation. Both the panel closure and the surrounding rock consist of essentially similar material, disturbed Salado halite. The porosity and permeability of the disturbed halite around an ROM salt panel closure will begin to decrease when back pressure from the compacting ROM salt begins to significantly increase.

As noted by Hansen and Callahan (1993, p. 7), laboratory results indicate that little resistance is created by crushed salt during consolidation until fractional densities on the order of 0.90 are achieved. According to Hansen and Thompson (2002, p. 2), a fractional density of 0.90 is equivalent to a porosity of 0.10 and a permeability on the order of 10^{-15} m^2. Full reconsolidation of the PCS DRZ halite would be unlikely to occur until the ROM salt panel closure is itself fully reconsolidated and stress equilibrium is achieved. The T2 permeabilities assigned to the ROM PC, and therefore, also to the T2 PCS DRZ halite, are more closely representative of fully reconsolidated salt at a porosity of about 0.01 than of a partially reconsolidated salt at a porosity of 0.05.

Department of Energy
Carlsbad Field Office
P. O. Box 3090
Carlsbad, New Mexico 88221
APR 17 2012

Mr. Jonathan Edwards, Director
Office of Radiation and Indoor Air
Radiation Protection Division
U. S. Environmental Protection Agency
Washington, D.C. 20460

Subject: Response to EPA Letter Dated December 22, 2011

Dear Mr. Edwards:

This letter is in reply to the Environmental Protection Agency's (EPA) December 22, 2011 letter regarding the first set of review questions and comments related to the Planned Change Request (PCR) for replacing the current "Option D" Panel Closure System (PCS) with an alternative design. In Enclosure 1 to this letter, the U.S. Department of Energy (DOE) Carlsbad Field Office (CBFO) is providing responses to EPA's questions. In addition, the DOE/CBFO is providing the references on compact disc, used in the responses (Enclosure 2).

If you have any questions, please contact Mr. Russ Patterson at (575) 234-7457.

Sincerely,

Jose R. Franco, Manager
Carlsbad Field Office

Enclosures (2)

cc: w/o enclosures

R. Lee, EPA	*ED
K. Economy, EPA	ED
S. Ghose, EPA	ED
J. Walsh, EPA	ED
T. Peake, EPA	ED
N. Elkins, LANL-CO	ED
P. Shoemaker, SNL-CPG	ED
G. Basabilvazo, CBFO	ED
R. Patterson, CBFO	ED
F. Sharif, WTS	ED
R. Chavez, RES	ED
S. Kouba, RES	ED
CBFO M&RC	

*ED denotes electronic distribution

CBFO:OESH:RLP:ANC:12-0728:UFC 5486.00

Enclosure 1

Responses to U.S. EPA Letter dated Dec 22, 2011

Responses to the review questions and comments contained in the U.S. Environmental Protection Agency (EPA) letter dated 22 December 2011 on panel closure properties in the Panel Closure Redesign and Repository Reconfiguration (PC3R) Performance Assessment (PA) are documented in this memorandum. These concerns and questions are identified here in italics to clearly distinguish them from the responses generated by the U.S. Department of Energy (DOE).

1.1 Duration of Time Period T1

Parameter Name	PABC 2009 Value	Used in PC3R PA ERMS 555489	Units
Duration of Time Period T1	Not Applicable	100	years

EPA Concerns

DOE's justification for adopting 100 years as the time frame for the T1 time period is not clear, especially given the range of values given by different sources.

Hansen and Thompson (2002, p. 4) estimated that a reduction of ROM salt porosity from 0.33 to 0.10 would occur within a maximum of 100 years, and indicate that it would take more than 100 years for ROM salt porosity to drop to the target value of 0.05.

Numerical simulations conducted by Callahan and DeVries (1991, Figure 4-2 SAND91-7052) predicted the essentially total reduction in the void volume of a room filled with crushed salt within about 25 years. These predictions do not seem to be supported by the measured closure rates of Panel 1 access drifts used in Hansen and Thompson (2002).

In DOE's proposed 2006 panel closure redesign (which also used 100 feet of loosely placed ROM salt for the panel closure material), a value of 200 years was used for creep closure to reduce the porosity from an initial value of 0.33 (averaged to 0.27 when combined with the porosity of the concrete block explosion wall) to a final value of 0.05 (Vugrin and Dunagan 2006, Table 3 and p. 15 ERMS 543865). No reason is given for reducing the time required to reach a .05 porosity value from 200 years to 100 years in the PC3R PA.

Technical Question 1.1a: *Please clarify the justification of the 100 year duration for T1. Different documents have estimated different time periods for run of mine salt to reach steady state porosity. Specifically, the PC3R cites Callahan and DeVries (1991, SAND91-7052), who predict consolidation of ROM salt to a porosity of 0.05 in about 13 years, and Hansen and Thompson (2002, ERMS 523476), who predict consolidation of ROM salt to a higher porosity of 0.10 within 100 years.*

Technical Question 1.1b: *Please justify the assumption that loosely placed, ROM salt will consolidate to a porosity of 0.05 in 100 years when the cited source Hansen and Thompson (2002) concludes that the salt will consolidate to a porosity of only 0.10 within 100 years.*

DOE Response to Technical Questions 1.1a and 1.1b:

The revised panel closure design will consist of 100 feet of run-of-mine (ROM) salt that is planned to be compacted to varying degrees (referred to herein as "crushed salt") emplaced so as to fill the entries, with additional barriers at each end of the crushed salt (Figure 1a). These barriers will consist of ventilation bulkheads similar to those currently used in the panels as room closures (Figure 2). The ventilation bulkheads are designed to restrict air flows and prevent personnel access into waste-filled areas during the operational phase. In Panels 1, 2, and 5, where explosion walls have already been emplaced in the panel entries, the explosion wall will be the inbye barrier and the ventilation bulkhead will be the outbye barrier (Figure 1b).

Final details of the emplacement of the crushed salt component of the revised panel closure are being developed, but it is expected that the final emplacement scheme will involve some degree of in-place compaction, with or without added moisture (moisture may be added because it accelerates the reconsolidation of the crushed salt). Given this uncertainty, a range of possible emplacement strategies are being assumed in order to cover the possible range of behaviors. At one end of the range is emplacement of dry ROM crushed salt with no initial compaction. The uncompacted ROM salt is assumed to have an as-emplaced porosity of 33%, equivalent to a fractional density of 67%. At the other extreme, the closure may be constructed in three layers that will be wetted and compacted to fractional densities of 85%, 80% and 70%, representing an average fractional density of 80%, or average porosity of 20%.

The salt rock surrounding the entries is creeping closed at a known rate. An example of this is shown in Figure 3. The measurements in Figure 3 are in the East-300 (exhaust) drift at location South-2833, which is between the entries to Panel 3. As the panel entries close, they cause consolidation of the crushed salt component. As discussed by several authors (e.g., Hansen et al., 1998; Spiers et al., 1988), consolidation of the crushed salt will take place through a combination of dislocation creep of the individual grains and various diffusional transfer mechanisms (pressure solution). The latter mechanisms, especially Fluid-Assisted Diffusional Transfer, will dominate in the presence of added brine and lead to much faster consolidation (Hansen et al., 1998). Eventually, the crushed salt will approach a condition equivalent to intact salt. During the consolidation process, as the salt reaches higher fractional densities, a back stress will be imposed on the surrounding rock mass, leading to healing of the disturbed rock zone (DRZ) and reduction in DRZ permeability.

Sources of data on the consolidation of crushed salt abound, although most of the data relate to the loading characteristics (e.g., Pfeifle et al., 1987; Kappei and Gessler, 1984; IT Corporation, 1987) or short-term creep compaction (e.g., Spiers et al., 1988). Much of the creep data are at stress levels higher than those expected in the early stages of consolidation of the closure. For example, as will be discussed later, the back stress imposed by the entry closure does not increase substantially until consolidation has reached fractional densities of the order of 98% or greater. Early stresses in the salt are of the order of 4 MPa (580 psi), while many of the creep tests have been performed at stresses of the order of 17 MPa (2500 psi). Estimates of the consolidation process must therefore rely upon numerical calculations using mechanical properties, both elastic and creep-related, obtained from laboratory testing.

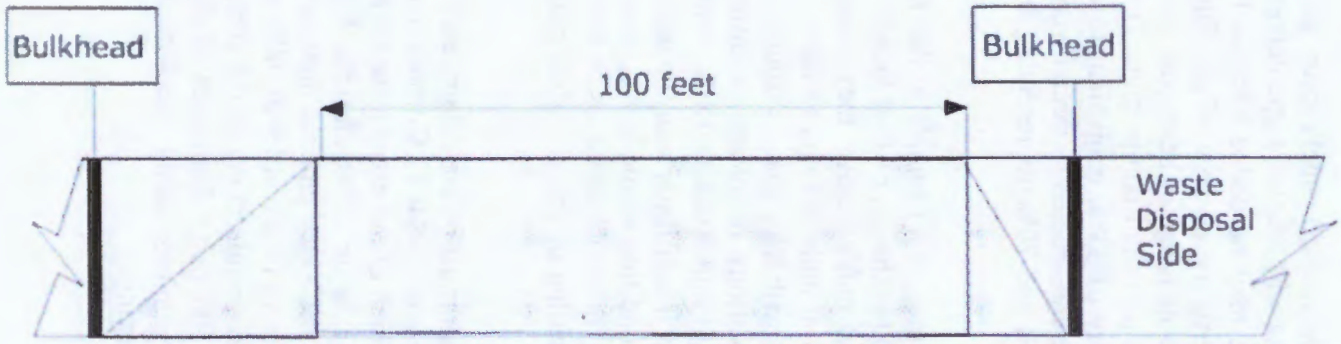

(a) Panel closure with 100 feet of run-of-mine salt between two ventilation bulkheads

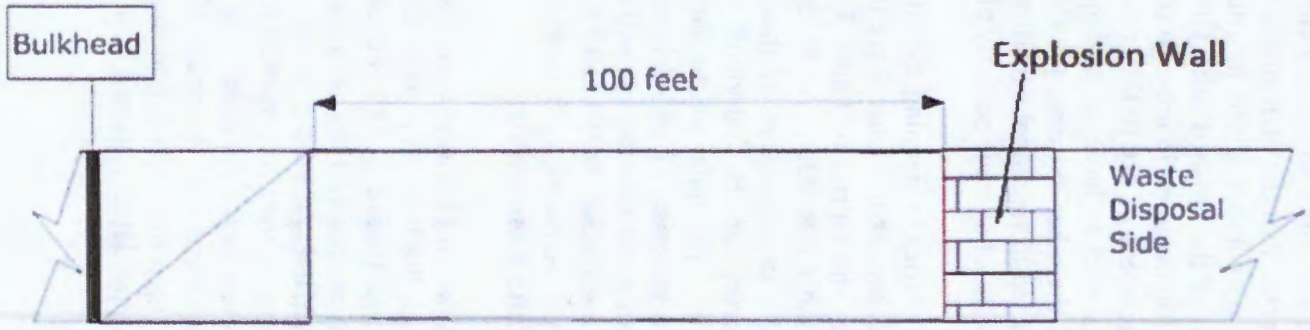

(b) Panel closure with 100 feet of run-of-mine salt between a ventilation bulkhead and an explosion wall

Figure 1. Schematic diagrams of the revised panel closure design (developed from descriptions obtained in "Design Report for a Panel Closure System at the Waste Isolation Pilot Plant," November 2011)

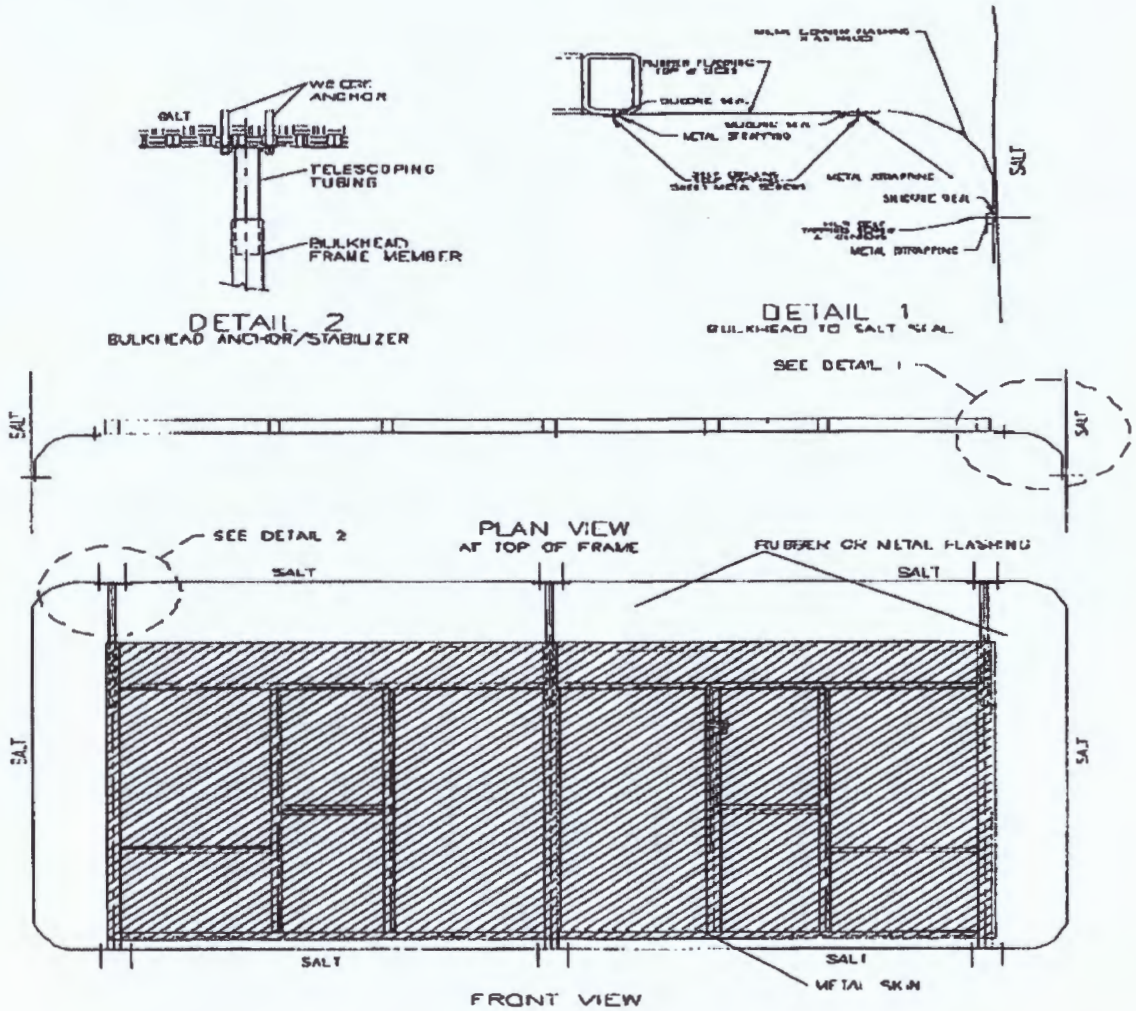

Figure 2. Typical design of a ventilation bulkhead that blocks the panel entry (U.S. DOE, 2009)

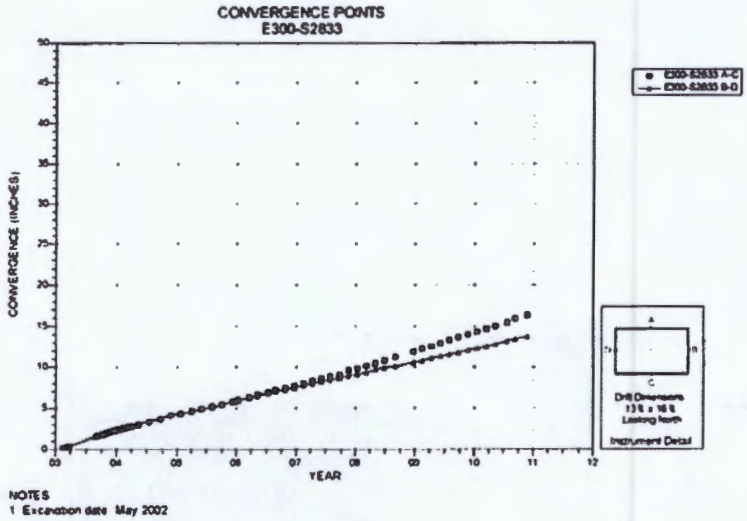

Figure 3. Convergence in the East-300 drift at South-2833 (U.S. DOE, 2011a)

A number of creep models for crushed salt have been developed by various authors (Hansen et al., 1998); however, the creep models most applicable to Waste Isolation Pilot Plant (WIPP) salt are those developed by Sjaardma and Krieg (1987), with further developments by Callahan (1999) and Hansen et al. (1998). These models have been used to estimate the time-dependent consolidation process.

Estimates of the consolidation process have been made in a series of calculations (Herrick, 2012) carried out using JAS3D (Blanford et al., 2001) with the Sjaardema and Krieg (1987) model for crushed salt, modified with a deviatoric creep compaction response (Stone, 1997). Simulations started with the crushed salt in the drift. The results are summarized in Figures 4 through 7 for initial emplacement porosities of 15%, 20%, 25%, and 33% (fractional densities of 85%, 80%, 75%, and 67%, respectively). These calculations show consolidation to a porosity of 5% in 40 years from an initial porosity of 15% (Figure 4) and in 140 years from an initial porosity of 33% (Figure 7). Based on these results and the current uncertainty over the emplacement of crushed salt, DOE is proposing to assume that 100 years is an appropriate value for the first time period during consolidation (i.e., T1 = 100 years), and that the porosity at 100 years, called the T1 porosity, has an expected value of 5%. Support for this approach comes from a number of sources, as described in the next few paragraphs.

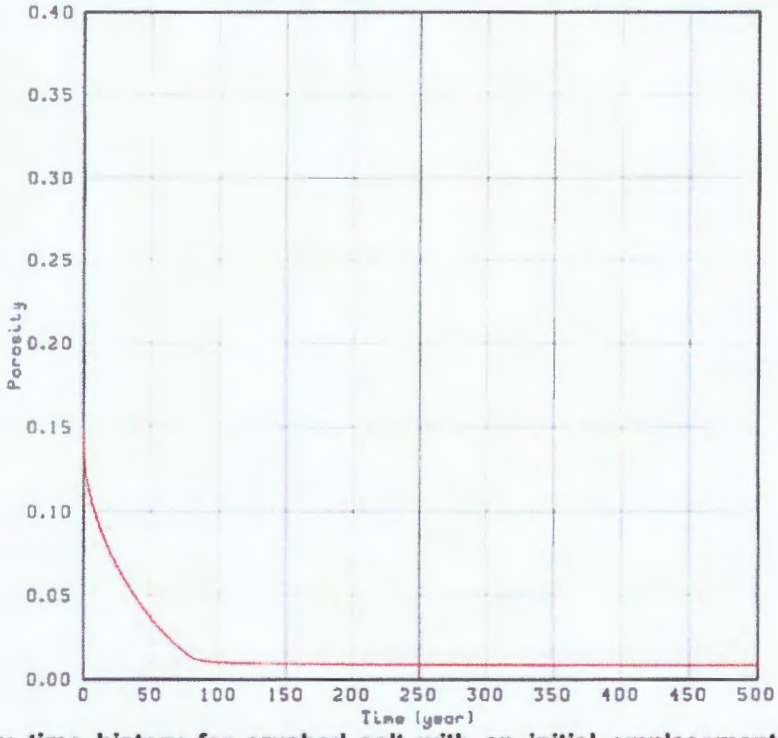

Figure 4. Porosity time history for crushed salt with an initial emplacement porosity of 15% (fractional density of 85%)

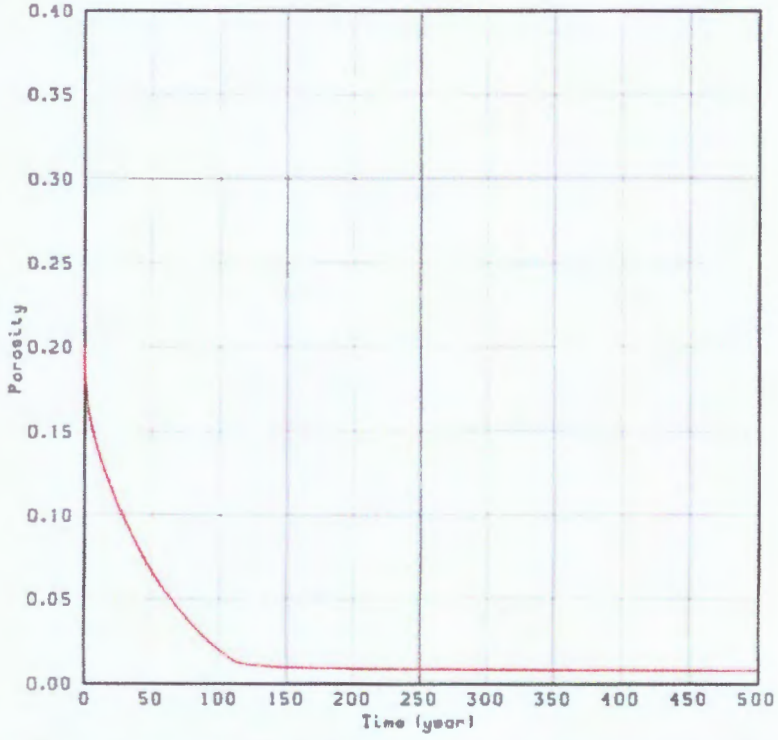

Figure 5. Porosity time history for crushed salt with an initial emplacement porosity of 20% (fractional density of 80%)

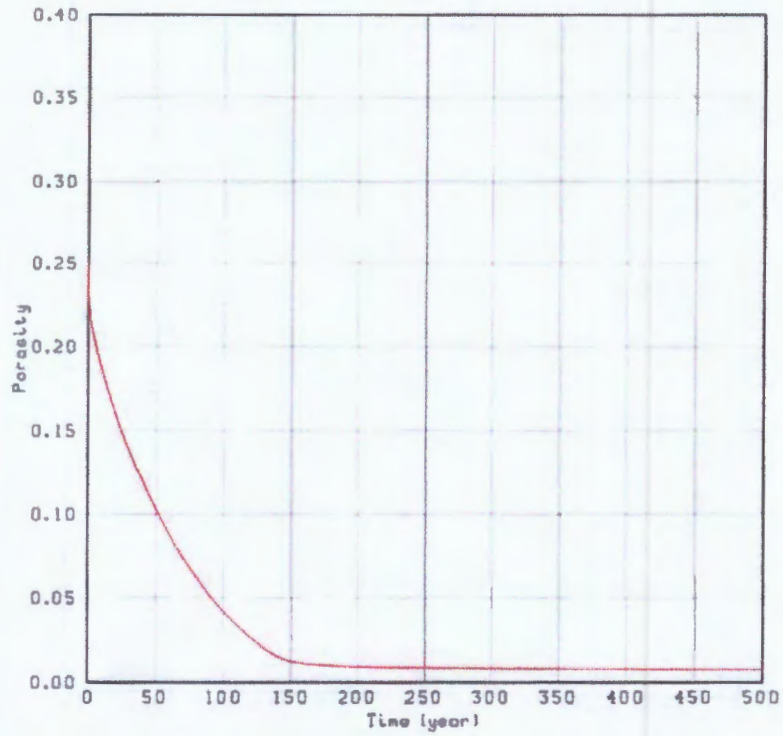

Figure 6. Porosity time history for crushed salt with an initial emplacement porosity of 25% (fractional density of 75%)

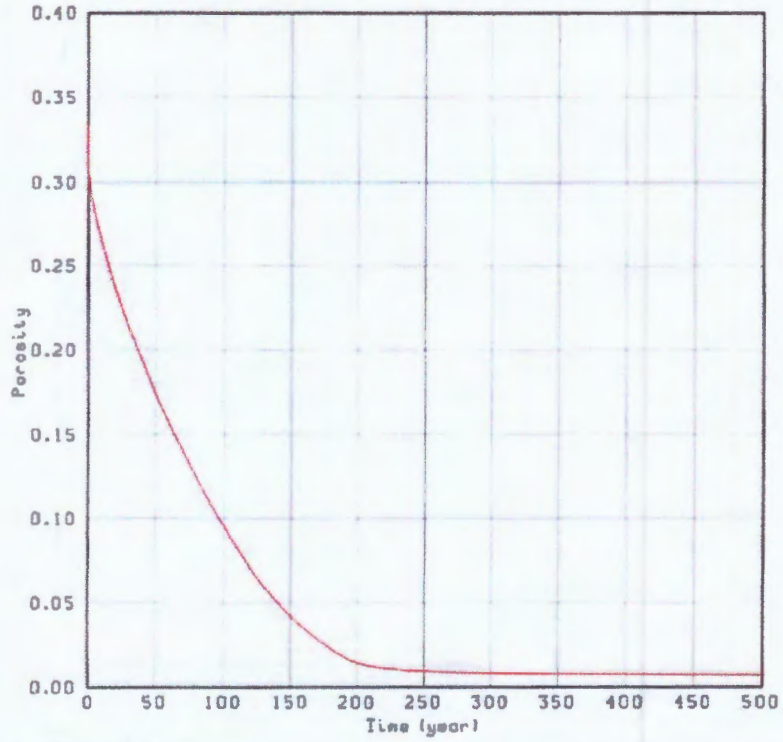

Figure 7. Porosity time history for crushed salt with an initial emplacement porosity of 33% (initial fractional density of 67%)

Hurtado et al. (1997) carried out a number of consolidation estimates for the proposed crushed salt component of the shaft seal. The crushed salt component of the proposed shaft seal will consist of mined WIPP crushed salt, dynamically precompacted with added moisture to a porosity of 10%. Calculations of the consolidation of this component due to creep closure of the shaft indicate that the crushed salt will be at an essentially intact condition (a fractional density approaching 1) within 100 years at a depth of 515 m and within 60 years at a depth of 600 m (Hurtado et al., 1997, Figure 2-3). Longer times are required at shallower depths due to the strong stress-dependence of shaft creep closure and consolidation. It should be noted that the closure rates of the approximately rectangular entries in which panel closures will be placed will be greater than for the circular shaft, and the panel closure entries are at a greater depth, about 655 m. Consolidation within the entries is therefore expected to proceed more quickly.

Additional calculations by Callahan (1999) show consolidation results for different crushed salt models at depths of 430 m, 515 m, and 600 m, indicating similar results (see Figure 8). Callahan and DeVries (1991) conducted calculations on the closure of disposal rooms backfilled with crushed salt that show closure to essentially intact densities in about 25 years (see Figure 9). These calculations used the Sjaardma and Krieg model, and while the closure of the disposal rooms would be expected to be faster than the entries because of the greater span of the rooms, the results confirm that the assumption of 100 years for T1 is reasonable for the panel entries.

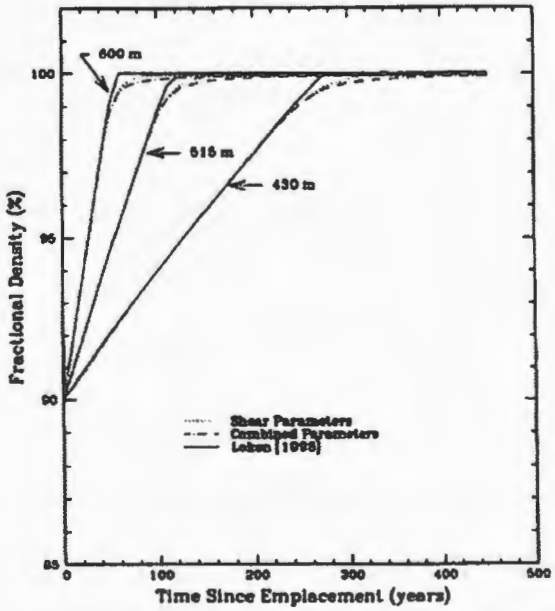

Figure 8. Fractional density versus time for a crushed salt shaft seal (Callahan, 1999, Figure 6-3)

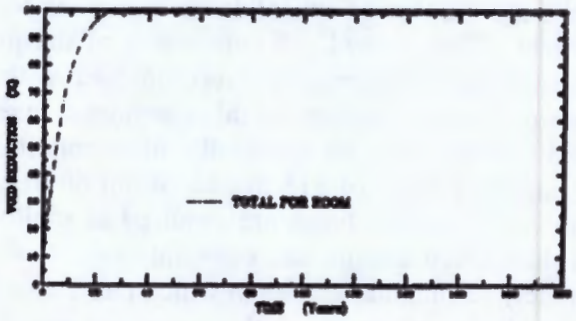

Figure 9. Void reduction versus time for a disposal room filled with crushed salt (Callahan and Devries, 1991, Figure 4-2)

Further support for T1 equal to 100 years comes from non-WIPP sources. For example, Shor et al. (1981) give results for compaction of wet salt at stresses of 20 bars (2 MPa, 290 psi), showing compaction from a void fraction of slightly more than 0.4 (porosity of 29%) to less than 0.2 (porosity 17%) in 10^4 minutes (about 7 days) (Shor et al., 1981, Figure 3). Spiers et al. (1988) show results for wet salt showing volume strains between 15% and 22% (porosities between 10% and 20%) in about 22 weeks of testing at 2 MPa (290 psi) (see Figures 10 and 11). Holcomb and Shields (1987) estimate times to 95% fractional density of 1.2×10^8 seconds (3.8 years) for salt under pressure of 0.69 MPa (100 psi) (Holcomb and Shields, 1987, Table 2).

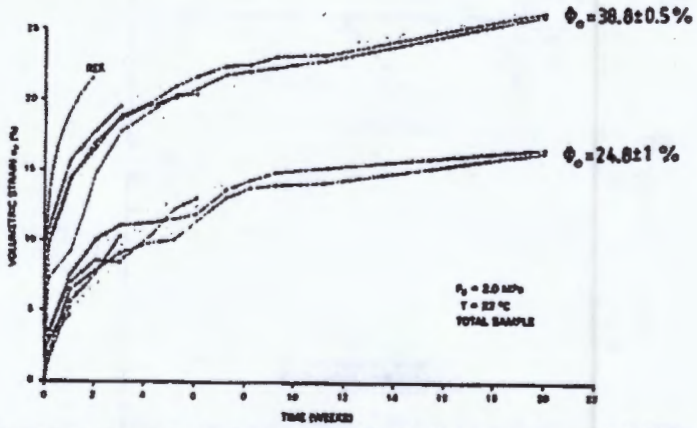

Figure 10. Volumetric strain versus time for wet salt under pressure of 2 MPa (Spiers et al., 1988, Figure 6.5)

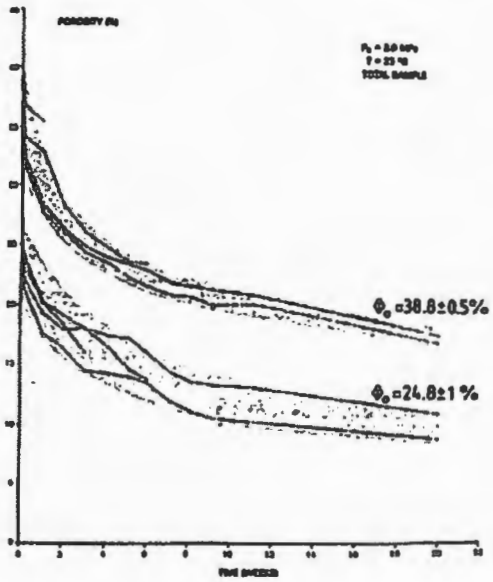

Figure 11. Total porosity versus time for wet salt under pressure of 2 MPa (Spiers et al., 1988, Figure 6.6)

As noted in Hansen and Thompson (2002), an estimate of the time to compaction can be made using the closure data for the entries. Unimpeded closure of entry drifts has been modeled and shows closure of the order of 10% in 10 years (Hansen et al., 1993). Actual measurements of roof-to-floor and rib-to-rib closure in the entries corroborate these closure rates (see Figure 3). These data also indicate that closure rates are reasonably stable and uniform. If it is assumed that the rates measured over the last 10 years continue, then the volume closure expected of the two entries is as shown in Figure 12, with volume closure of more than 30% by about 35 years. A volume closure of 30% increases the fractional density from 67% to 96% and decreases the porosity from 33% to 4%. It was noted in Hansen and Thompson (2002) that somewhat slower consolidation might be expected due to back pressure developed as the consolidation proceeds. However, recent JAS3D results show that a significant back stress does not develop before a fractional density of the order of 99%, suggesting that this effect may be rather small.

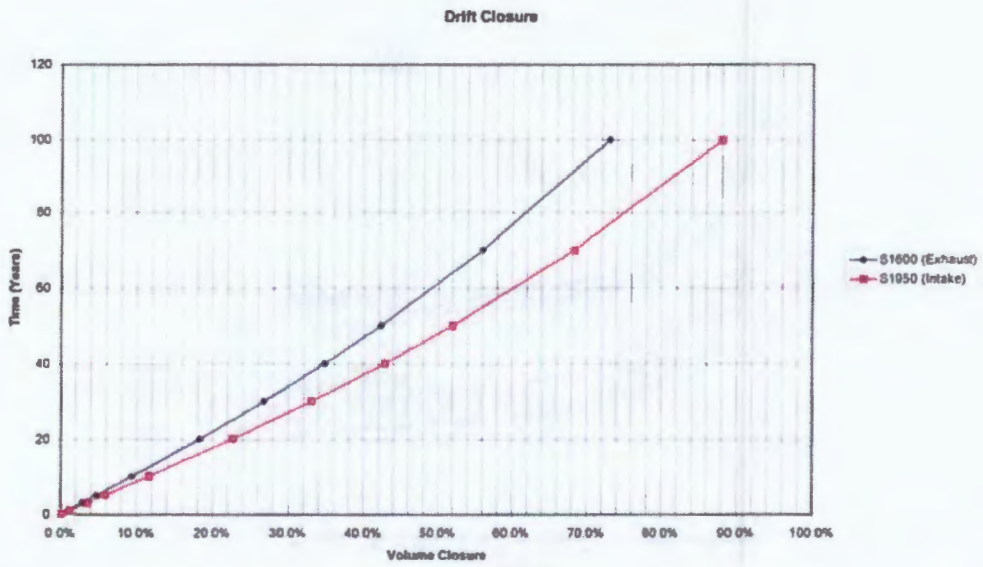

Figure 12. Calculated drift closure assuming constant closure rates and no backstress (from Hansen and Thompson, 2002)

As noted above, JAS3D results demonstrate that porosity will reach a value of 5% in less than 100 years when some compaction takes place during emplacement, and will reach this value in about 140 years when the salt is emplaced without compaction. The JAS3D results also demonstrate that compaction continues beyond these times, achieving porosity of the same order as for intact salt in 200 years after emplacement. It is therefore reasonable to assume that porosity will reach a value between 2.5% and 7.5% in the first 100 years (the range purposefully covers those cases which consolidate faster and those which consolidate slower), and that by 200 years the closure will have a porosity similar to the intact salt. The additional consolidation of crushed salt between 100 and 200 years will be accounted for by using three time periods: 0 to 100 years for the initial reconsolidation, 100 to 200 years for the intermediate state around 5% porosity, and 200 to 10,000 years to represent the long-term behavior of the fully reconsolidated crushed salt. Table 1 summarizes the proposed approach for porosity that is defined by three time periods.

Table 1. Definition of porosity using three time periods

Time Period	Assumed Porosity	Notes
0 to T1 (0 to 100 years)	33%	Assumes crushed salt is initially emplaced with minimal compaction.
T1 to T2 (100 to 200 years)	2.5% to 7.5%	Assumes that the expected T1 porosity is 5% at 100 years, consistent with the JAS3D results and supporting information from many sources. The range is designed to encompass the variability in initial emplacement (moistened versus dry; compacted versus uncompacted) for crushed salt.
T2 to 10,000 years (200 to 10,000 years	0.1% to 5.19%	Assumes that the porosity of crushed salt after 200 years is equal to the porosity for intact halite. Range is based on the S_HALITE:POROSITY parameter in performance assessment.

Technical Question 1.1c: *Please justify the use of two time periods to represent consolidation of the ROM salt panel closure material, when additional time periods could provide a more refined representation of salt consolidation over time.*

DOE Response to Technical Question 1.1c:
As discussed in the response to Questions 1.1a and 1.1b, the DOE intends to use three time periods, 0 to 100 years, 100 years to 200 years, and 200 years to 10,000 years, to provide a more refined representation of time-dependent consolidation of crushed salt in a panel closure. The rationale for the three time periods is discussed in the previous response.

Completeness Question 1.1d: *Please identify the effect of the rock bolts installed at WIPP for ground control on the consolidation rate for the ROM salt panel closure material.*

DOE Response to Technical Question 1.1d:
Rock bolts are used to control the skin around an opening by binding laminated strata or suspending weak or fractured material from more competent overlying rocks. Rock bolts are installed in all panel access/egress locations; the closure rates in Figure 3 are from entries with rock bolt support. Initially, 4-foot or 5-foot roof bolts are installed in new rooms and entries. If ground conditions deteriorate, 12-foot rock bolts are installed to further stabilize the rock around the opening.

Creep closure of an opening in salt is driven by the response of the rock mass surrounding the opening, and the rock bolts have no discernible impact on long-term creep closure of rooms and entries. As noted in the most recent Ground Control Annual Plan for the WIPP (U.S. DOE 2011b, section 6.2):

> "Geotechnical data indicate that roof bolt systems have little or no measurable effect on creep closure. The mechanism of creep and the ability of the salt to flow are driven by differential stresses initiated by excavation. The lithostatic stress at the disposal horizons is approximately 2,000 pounds per square inch. When dealing with stresses of this magnitude, it is nearly impossible from an engineering standpoint, and impractical from an economics standpoint, to design and install a mine-wide ground control system that would arrest these forces. Such a system would also reduce the waste isolation performance of the facility (the ability of salt to creep and encapsulate the waste), which is its primary function."

References for Responses to Questions 1.1

Blanford, M.L., M.W. Heinstein, and S.W. Key. 2001. JAS3D: A Multi-Strategy Iterative Code for Solid Mechanics Analysis User's Instructions, Release 2.0. Sandia National Laboratories, ERMS 552358.

Callahan G.D. and K.L DeVries. 1991. Analyses of Backfilled Transuranic Wastes Disposal Rooms. Sandia National Laboratories, SAND91-7052.

Callahan, G.D. 1999. Crushed Salt Constitutive Model. Sandia National Laboratories, SAND98-2680.

Hansen, F.D., M.S. Lin and L.L. VanSambeek. 1993. Concept for Operational Seal Design at the Waste Isolation Pilot Plant. Sandia National Laboratories, SAND93-0729.

Hansen, F.D., G.D. Callahan, M.C. Loken and K.D. Mellegard. 1998. Crushed-Salt Constitutive Model Update. Sandia National Laboratories, SAND97-2601.

Hansen F.D., and T.W. Thompson. 2002. Effective Permeability of the Redesigned Panel Closure System. Memorandum to Paul E. Shoemaker dated August 29, 2002. Sandia National Laboratories, ERMS 523476.

Herrick, C. 2012. Calculations Performed in Support of Reconsolidation of Crushed Salt in Panel Closures. Memorandum to WIPP Records Center dated March 29, 2012. Sandia National Laboratories, ERMS 557150.

Holcomb, D.J. and M. Shields. 1987. Hydrostatic Creep Consolidation of Crushed Salt with Added Water. Sandia National Laboratories, SAND87-1990.

Hurtado, L.D., M.K. Knowles, V.A. Kelley, T.L. Jones, J.B. Ogintz, and T.W. Pfeiffle. 1997. WIPP Shaft Seal System Parameters Recommended to Support Compliance Calculations. Sandia National Laboratories, SAND97-1287.

Kappei, G. and K. Gessler. 1984. In-situ Tests of the Behaviour of Backfill Materials and Accompanying Rock-Mechanical Laboratory Investigations. Second Conference on the Mechanical Behavior of Salt.

IT Corporation. 1987. Laboratory Investigation of Crushed Salt Consolidation and Fracture Healing. Prepared for the Office of Nuclear Waste Isolation, BMI/ONWI-631.

Nelson, J.W., P.C. Kelsall, J.B. Case and J.G. Franzone. 1983. Assessment of Crushed Salt Consolidation and Fracture Healing Processes in Nuclear Waste Repository in Salt. NM79-137, Office of Nuclear Waste Isolation, Battelle Memorial Institute.

Pfeiffle, T.W., P.E. Senseny and K.D. Mellengard. 1987. Influence of Variables on the Consolidation and Unconfined Compressive Strength of Crushed Salt. Office of Nuclear Waste Isolation, BMI/ONWI-627.

Shor, A.J., C.F. Baes, Jr., and C.M. Canonico. 1981. Consolidation and Permeability of Salt in Brine. Oak Ridge National Laboratory, ORNL-5774.

Sjaardma, G.D. and R.D. Krieg. 1987. Constitutive Model for the Consolidation of WIPP Crushed Salt and its Use in Analysis of Backfilled Shaft and Drift Configurations. Sandia National Laboratories, SAND87-1977.

Spiers, C.J., C.J. Peach, R.H. Brzesowsky, P.M.T.M. Schutjens, J.L. Liezenberg and H.J. Zwart. 1988. Long-term Rheological and Transport Properties of Dry and Wet Salt Rocks. Commission of the European Communities, Directorate-General Science, Research and Development, EUR 11848 EN, ISBN 92-825-9191-3.

Stone, C.M. 1997. SANTOS – A Two-Dimensional Finite Element Program for the Quasistatic, Large Deformation, Inelastic Response of Solids. Sandia National Laboratories, SAND90-0543.

U.S. Department of Energy (DOE). 2009. Drawing number 74-B-467. Bulkhead Detail Drawings. U.S. Department of Energy Carlsbad Field Office.

U.S. Department of Energy (DOE). 2011a. Geotechnical Analysis Report. March, 2011. DOE/WIPP 11-3177. U.S. Department of Energy Carlsbad Field Office.

U.S. Department of Energy (DOE). 2011b. Ground Control Annual Plan for the Waste Isolation Pilot Plant. U.S. DOE/WIPP-02-3212, Revision 9. U.S. Department of Energy Carlsbad Field Office.

1.2 Panel Closure Porosity

Parameter Name	PABC 2009 Value	Used in PC3R PA ERMS 555489	Units
PCS_T2: POROSITY	0.05 for CONC_PCS	0.05	--

EPA Concerns

DOE's reasoning in selecting the final T2 porosity value of 0.05 is not explicit. Because the assigned porosity of the panel closure at T2 is the value from which the long-term permeability and compressibility of the panel closure are defined, EPA is asking for more information on the parameter's justification and the importance of the specific value used.

Technical Question 1.2a: *Please provide justification that the T2 porosity is an appropriate target value that correlates to the permeability and compressibility values used in the PC3R PA.*

DOE Response to Technical Question 1.2a:

As discussed in the response to Question 1.1, room closure resulting from creep deformation of intact halite is expected to reconsolidate the crushed salt in a panel entry. The closure process is predicted to increase the fractional density of the crushed salt from its as-emplaced condition to a fractional density near 1.0, so that the consolidated salt becomes indistinguishable from the intact halite over long periods of time, estimated in the response to Question 1.1 to be 200 years. Drift closure calculations predict that the crushed salt in a panel entry will reconsolidate within 100 years to an expected porosity of about 0.05 (i.e., a fractional density greater than 0.95) at repository depth. Laboratory experiments on consolidated cores of crushed salt confirm that the intrinsic permeability of crushed salt decreases as the fraction density of the cores increases (Hurtado et al., 1997, Figure 2-1). Other observations of the behavior of crushed salt in similar situations support these results; it should be noted that although these examples are for different salt materials, the overall behavior of the crushed material may be expected to be similar in general. Observations from the BAMBUS II project at the Sigmundshall mine in Germany indicate consolidation of a crushed salt slurry to essentially an intact condition within tens of years (Bechthold et al., 2004, Figure 2.57). Consolidation to an essentially intact condition is also confirmed by observations at the Rocanville mine, where a consolidated salt plug was emplaced after a water inflow, and has been effective in sealing off a hydrostatic groundwater pressure of about 1200 psi (8.3 MPa) (Van Sambeek et al., 1995).

The state of the intact halite therefore provides an analog for the long-term state of the crushed salt in a panel entry. Intact halite may not always be an exact analog for the long-term state of the consolidated salt because the interconnected porosity of the *in situ* halite may be different than the interconnected porosity of the consolidated crushed salt; however, it is expected to be a good analogy in terms of porosity. The measured effective porosity used in performance assessment (PA) for intact halite varies from 0.001 to 0.0519 (parameter S_HALITE:POROSITY) (U.S. DOE, 2009, Appendix PA, Parameter 17; Ismail, 2007). This range is consistent with the predictions outlined in the answer to question 1.1a, which show a porosity for consolidated salt of less than 0.05 after 100 years in the case of moistened salt, and after 140 years for dry salt.

Based on this discussion, a target or expected value of 0.05 for the porosity at 100 years is quite reasonable, in part because it lies at the upper limit of the effective porosity for intact halite. Significant uncertainties exist in the consolidation process because of the uncertainties in the initial fractional density of the crushed salt and in wet versus dry emplacement. These uncertainties are represented by defining a range of values for the porosity at 100 years from 0.025 to 0.075. The proposed lower limit for the porosity range, 0.025, accounts for the fact that, under certain conditions of emplaced compaction and moisture, a porosity of 0.05 is achieved in less than 100 years. The upper limit of 0.075 acknowledges that more than 100 years may be required to achieve very low *in situ* porosities and permeabilities. The consolidation process will continue after 100 years, particularly for salt that is emplaced dry with minimal compaction. This is accounted for by assigning a second time period (100 to 200 years) during which consolidation of the crushed salt will continue and achieve essentially intact salt conditions regardless of the emplacement strategy.

As noted above, although the state of the intact halite provides an analog for the long-term state of the crushed salt in a panel entry, this analogy may not always be exact in the case of the permeability because the interconnected porosity of the *in situ* halite may be different than the interconnected porosity of the consolidated crushed salt. In this condition, the permeability of intact halite would be different than the permeability of the reconsolidated ROM salt at equal porosity. A similar effect has been observed in laboratory testing of consolidated crushed salt cores. At equivalent fractional densities, dry consolidated salt cores are more permeable than wet consolidated salt cores because of the difference in the mechanism causing consolidation. Under dry conditions, the effective consolidation mechanism is crystal plasticity, while under wet conditions the effective consolidation mechanism is pressure solution/redeposition (Hurtado et al., 1997, page 2-7). Pressure solution/redeposition under wet conditions generally produces higher consolidation rates and more deformation than crystal plasticity under dry conditions, leading to lower measured permeabilities for wet consolidated salt than for dry consolidated salt (Hurtado et al., 1997, Figure 2-1). For these reasons, the permeability assigned to the closure at a particular porosity will be determined in PA using actual data on consolidated salt, as discussed in the answer to Q1.3.

The pore-volume compressibility of consolidated salt has been determined as a function of porosity and bulk modulus (Hurtado et al., 1997, section 2.1.4). The bulk modulus of crushed salt has been measured experimentally by Holcomb and Hannum (1982). In this study, hydrostatic compaction tests were conducted with unload/reload cycles performed at prescribed levels of density. The data were later used by Sjaardema and Krieg (1987) to define an empirical model relating bulk to fractional density. For a porosity of 0.05, which is the mean porosity value at 100 years, the pore-volume compressibility is calculated as 1.6×10^{-9} 1/Pa (Hurtado et al., 1997, page 2-21). This value is the recommended value for the crushed salt during all time periods because the pore-volume compressibility is not expected to be a sensitive parameter in PA.

Technical Question 1.2b: *How sensitive a parameter is the final porosity of the panel closure? That is, how much would changing the value of PCS_T2: POROSITY (e.g. to 0.01 or 0.075) change calculated results, such as waste area saturation and pressure, that are known to impact performance?*

DOE Response to Technical Question 1.2b:

In the PC3R PA, material PCS_T2 is used to represent the crushed salt panel closure after it has undergone consolidation (Camphouse and Clayton, 2011). The porosity of material PCS_T2 is a constant value, 0.05, in the PC3R PA. In order to test the sensitivity of PA results to the final porosity of material PCS_T2, two additional BRAGFLO replicates were executed: one with a PCS_T2:POROSITY of 0.01 and the second with a PCS_T2:POROSITY of 0.075. These two values provide reasonable lower and upper limits for the porosity of material PCS_T2, as discussed in the response to Question 1.2a. The two additional BRAGFLO replicates used the same BRAGFLO grid as for the PC3R PA, providing a consistent comparison. Input files and simulation results corresponding to these BRAGFLO calculations can be found in CMS library LIBPC3R_BF in class COMMENT_CALCS.

The impact of changing the final porosity to 0.01 or 0.075 on the mean waste panel pressure for an E1 intrusion that hits a brine pocket at 350 years is presented in Figure 13. The mean waste panel pressure for PCS_T2:POROSITY values of 0.01, 0.05, and 0.075 are virtually identical for an E1 intrusion occurring at 350 years. Figure 14 shows that the same conclusion is true for an E2 intrusion into the waste panel at 350 years. Consequently, mean waste panel pressure is highly insensitive to changes in the long-term porosity of the panel closure.

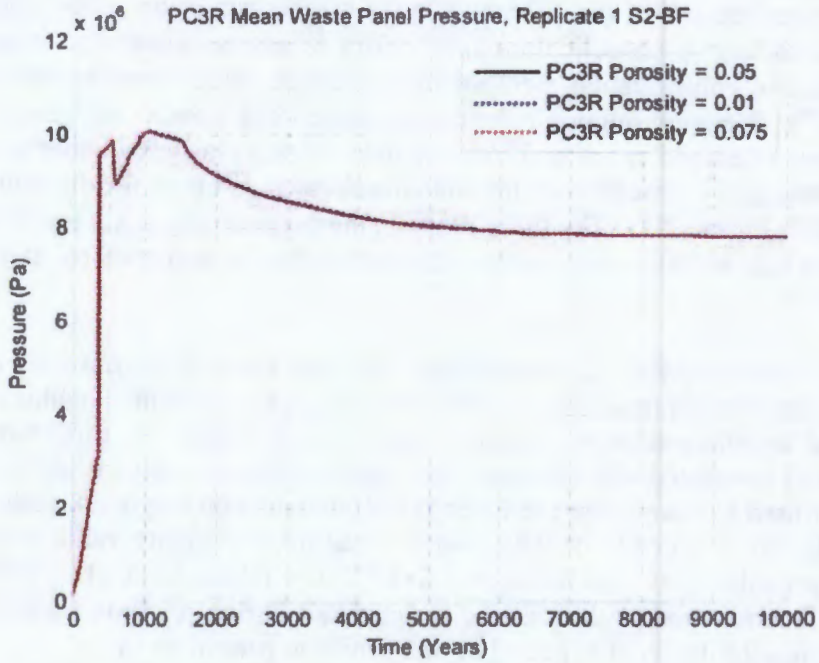

Figure 13. Mean waste panel pressure for long-term panel closure porosity values of 0.01, 0.05, and 0.075. E1 Intrusion at 350 years, Replicate 1.

A similar conclusion is true for mean brine saturation in the waste panel. Figures 15 and 16 show that the mean waste panel brine saturation for PCS_T2:POROSITY values of 0.01, 0.05, and 0.075 are indistinguishable for the case of an E1 intrusion into a waste panel at 350 years (Figure

15) or for an E2 intrusion into a waste panel at 350 years (Figure 16). Mean brine saturation in the waste panel is highly insensitive to changes in the long-term porosity of the panel closure.

From these results, it can be inferred that direct releases due to drilling intrusions into the repository are also insensitive to changes in long-term porosity of the panel closure. Cuttings and cavings releases are not a function of repository conditions, and are therefore completely independent of long-term closure porosity. Spallings release volumes are a function of waste panel pressure at the time of intrusion. Waste panel pressure is insensitive to changes in long-term closure porosity and consequently, spallings releases are also insensitive to long-term closure porosity. Direct brine release (DBR) volumes are dependent on waste panel pressure and brine saturation at the time of intrusion. DBRs will also be insensitive to changes in long-term closure porosity because waste panel pressure and waste panel brine saturation are insensitive to changes in long-term closure porosity.

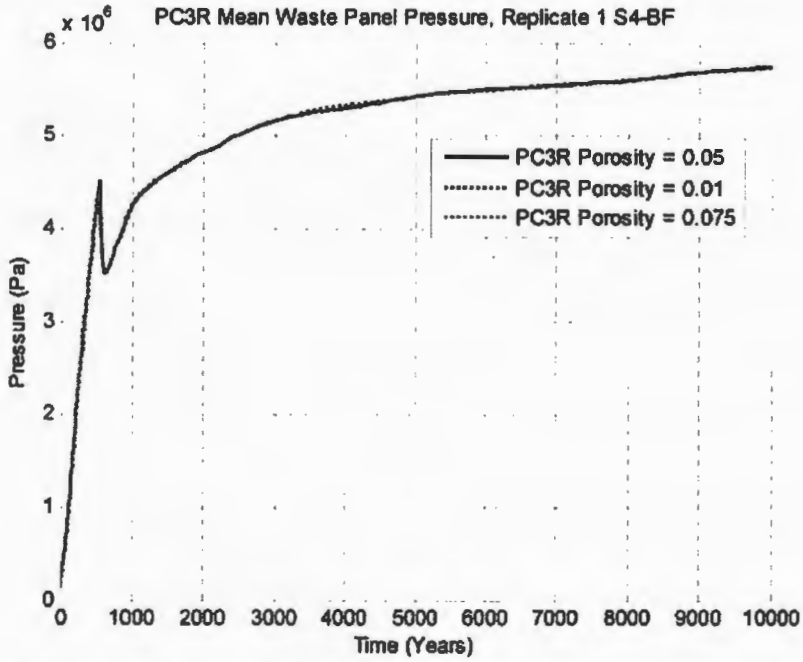

Figure 14. Mean waste panel pressure for long-term panel closure porosity values of 0.01, 0.05, and 0.075. E2 Intrusion at 350 years, Replicate 1.

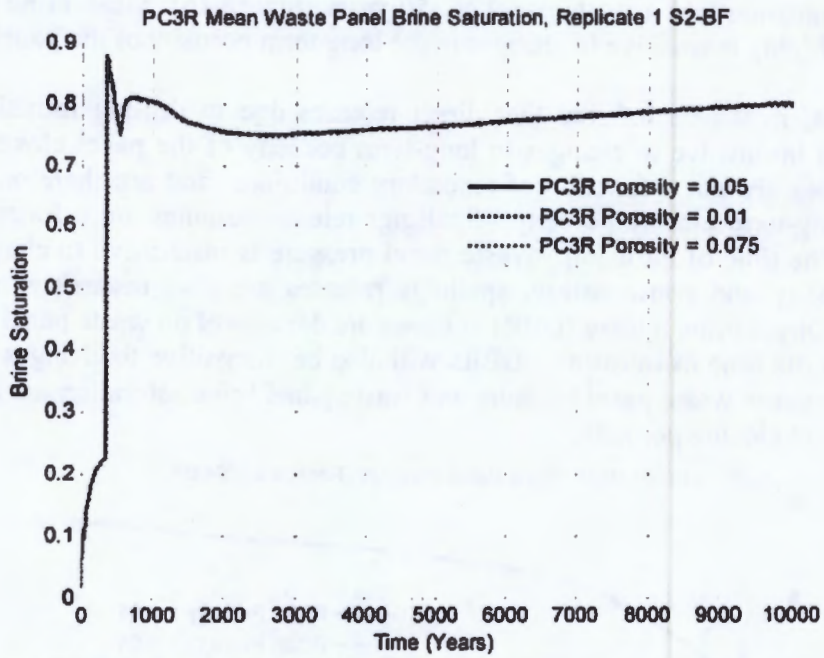

Figure 15: Mean waste panel brine saturation for long-term panel closure porosity of 0.01, 0.05, and 0.075. E1 Intrusion at 350 years, Replicate 1.

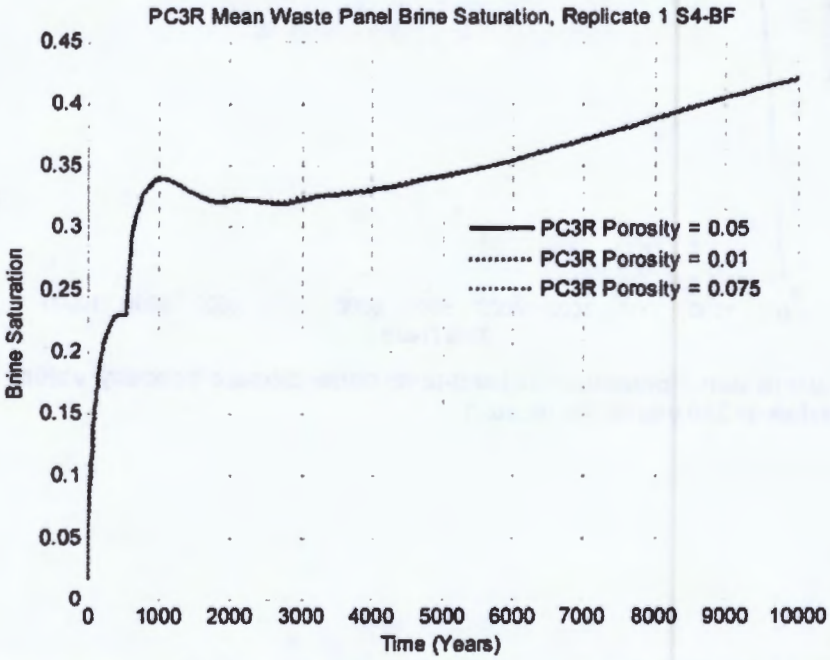

Figure 16. Mean waste panel brine saturation for long-term panel closure porosity of 0.01, 0.05, and 0.075. E2 Intrusion at 350 years, Replicate 1.

References for Questions 1.2

Bechthold, W., E. Smailos, S. Heusermann ,T. Bollingerfehr, B. Bazargan Sabet, T. Rothfuchs, P. Kamlot, J Grupa, S. Olivella, and F. D. Hansen. 2004. *Backfilling and Sealing of Underground Repositories for Radioactive Waste in Salt (BAMBUS II Project)*: Final Report. European Commission. Directorate General for Research. Office for Official Publications of the European Communities. Call No: EUR 20621 EN. Showcased in Research for Europe: Successful EU-funded projects by the Directorate General for Research.

Camphouse, R.C. and D.J. Clayton 2011. Analysis Package for Salado Flow Modeling Done in the AP-151 (PC3R) Performance Assessment. Sandia National Laboratories, ERMS 555204.

Holcomb, D.J., and D.W. Hannum, 1982. Consolidation of Crushed Salt Backfill Under Conditions Appropriate to the WIPP Facility. Sandia National Laboratories, SAND82-0630.

Hurtado, L.D., M.K. Knowles, V.A. Kelley, T.L. Jones, J. B. Ogintz, and T.W. Pfeiffle. 1997. WIPP Shaft Seal System Parameters Recommended to Support Compliance Calculations, Sandia National Laboratories, SAND97-1287.

Ismail, A.E. 2007. Revised Porosity Estimates for the DRZ. Sandia National Laboratories, ERMS 545755.

Sjaardema, G.D., and R.D. Krieg. 1987. A Constitutive Model for the Consolidation of WIPP Crushed Salt and Its Use in Analyses of Backfilled Shaft and Drift Configurations. Sandia National Laboratories, SAND87-1977.

U.S. Department of Energy (DOE). 2009. Title 40 CFR 191 Parts B and C Compliance Recertification Application. DOE/WIPP-09-3424. U.S. Department of Energy Carlsbad Field Office.

Van Sambeek, L.L., T. J. Eyerman, and F. D. Hansen. 1995. Case Studies of Sealing Methods and Materials Used in the Salt and Potash Mining Industries. Sandia National Laboratories, SAND95-1120.

1.3 Long-Term Panel Closure Permeability

Parameter Name	PABC 2009 Value	Used in PC3R PA ERMS 555489	Units
PCS_T2:PRMX_LOG PCS_T2:PRMY_LOG PCS_T2:PRMZ_LOG	-17, -20.8, -18.8 for CONC_PCS	-17.6, -22.8, -20.2 Triangular Distribution	$\log(m^2)$

EPA Concerns

EPA is looking for clarification on the justification of the long-term panel closure permeability.

A compilation of laboratory-measured permeability values for WIPP crushed salt at various fractional densities was prepared by Hurtado et al. (1997, Table 2-1 SAND97-1287). The most relevant results were taken from Brodsky (1994, SAND93-7058), who measured the permeability of compacted ROM salt at fractional densities near 0.95 (equivalent to a porosity of 0.05) using brine as the fluid rather than gas.

Kelley et al. (1996, p. 1 ERMS 230995) provide a summary of permeability values at various densities. The T2 permeability values recommended by Camphouse (2010b, p. 4) are most similar to those reported by Kelley et al. (1996, Table 6) for 200-years, which represented full reconsolidation. The values recommended by Camphouse are not identical to any of those presented in the 1996 Kelley report.

The PC3R T2 permeability values are similar to the values for fully reconsolidated crushed salt reported by Kelley et al. (1996) and Hurtado et al. (1997), but not representative of porosities equivalent to 0.05. The T2 permeabilities used to represent ROM salt at a porosity of 0.05 are generally 1.5 to 2 orders of magnitude lower than those reported by Butcher et al. (1991, reported in Hansen and Callahan, 1993), Brodsky (1994), Hurtado et al. (1997, SAND97-1287), and Hansen and Thompson (2002) for compacted salt equivalent to a porosity of 0.05.

Technical Question 1.3a: *Please provide a source for the permeability values assigned to the ROM salt panel seal during time period T2 that provides traceability to original sources.*

Technical Question 1.3b: *Please justify the assignment of permeabilities to the ROM salt panel seal during time period T2 that represent fully consolidated salt rather than ROM salt consolidated to a porosity of 0.05.*

<u>DOE Response to Technical Questions 1.3a and 1.3b:</u>

This response identifies the sources for the permeability values and an improved method for the assignment of permeabilities during the time periods from 100 to 200 years and from 200 years to 10,000 years. The proposal to use multiple time periods differs from the approach for the PC3R PA, which used a single time period from 100 years to 10,000 years.

The permeability values for consolidated crushed salt are based on experimental measurements of consolidated WIPP salt cores (Hurtado et al., 1997). The experimental program is summarized

in Hurtado et al., 1997 and further documented in additional Sandia documents (Brodsky, 1994; Brodsky et al., 1996; Ahrens and Hansen, 1995). These experimental data provided the basis for defining the permeability of the crushed salt component of the shaft seal system (U.S. DOE, 1996, Appendix SEALS, Figure A-7), and are an appropriate starting point for defining permeability ranges for the consolidated crushed salt in a panel closure. The experimental data have fractional densities[1] from 0.822 to 1.005[2] (porosities 0.178 to -0.005) (Hurtado et al., 1997, Table 2-1), a range that encompasses the recommended porosity range of 0.025 to 0.075 during 100 to 200 years and 0.001 to 0.0519 during 200 to 10,000 years (see response to Question 1.2a).

In assigning permeability values from porosities for PA, the data in Hurtado et al., 1997, Table 2-1, are represented as a function of porosity through a two-step relationship: (1) a least squares fit to the permeability data as a function of fractional density, and (2) a distribution that represents the residuals of the data about the least squares fit. This approach captures the mean variability of permeability with porosity and represents the uncertainty in the data set.

The values presented in Table 2-1 of Hurtado et al., 1997, include various sets of data. This analysis uses the brine permeability data from Brodsky, 1994, because the fractional densities of the samples for the brine data, 0.8953 to 1.0051, are equivalent to porosity from ~ 0 to 0.1047, which spans the porosity ranges of interest. The cores for gas permeability measurements (Brodsky et al., 1996; Ahrens and Hansen, 1995) have fractional densities from 0.8220 to 0.9339 (porosities 0.178 to 0.0661), which are generally beyond the range of interest here. Figure 17 presents the least squares fit to the logarithm (base 10) of the brine permeability data in the Table 2-1 of Hurtado et al., 1997.

Figure 18 is a plot, called a quantile-quantile plot, which shows the relationship between the quantiles of the residuals of the logarithm (base 10) of the permeability data relative to the least squares fit and the predicted residuals at the corresponding quantiles on a normal distribution. The residuals of the data completely define the parameters for the normal distribution: the mean is 0.0 and the standard deviation is 0.86. No subjective judgment is needed or used to define the parameters for the normal distribution. If the agreement with a normal distribution were exact, all points in Figure 18 would lie on the line with a slope of 1. Most points are quite close to the line in Figure 18, indicating that a normal distribution provides a very good representation of the residuals.

Figure 19 presents the range of permeability with uncertainty characterized by the normal distribution with $\mu = 0$ and $\sigma = 0.86$. The lines for ±2 standard deviations in Figure 19 are used to provide the effective upper and lower bounds for permeability. All the experimental data lie within ±2 standard deviations with the exception of the data point with a $\log_{10}$ permeability of -21.5.

[1] The relationship between porosity, ϕ, and fractional density, *fd*, is $\phi = 1 - fd$.

[2] Note that a recorded fractional density greater than 1 probably implies an uncertainty in the assumed intact salt density.

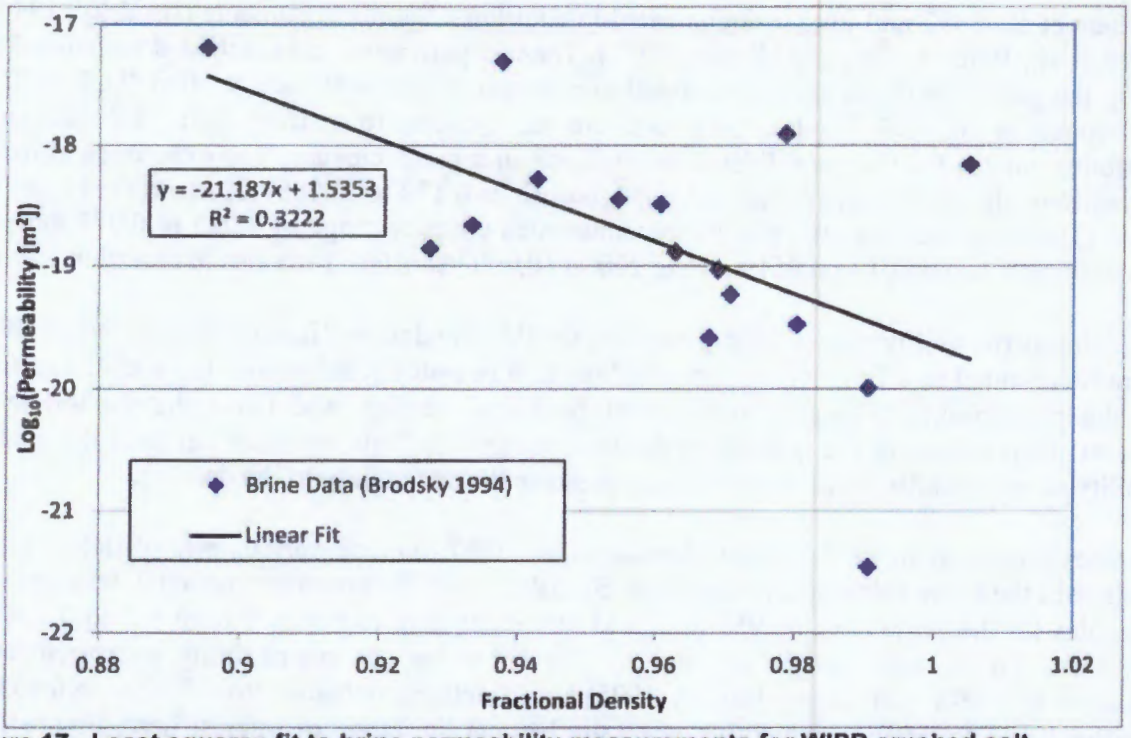

Figure 17. Least squares fit to brine permeability measurements for WIPP crushed salt

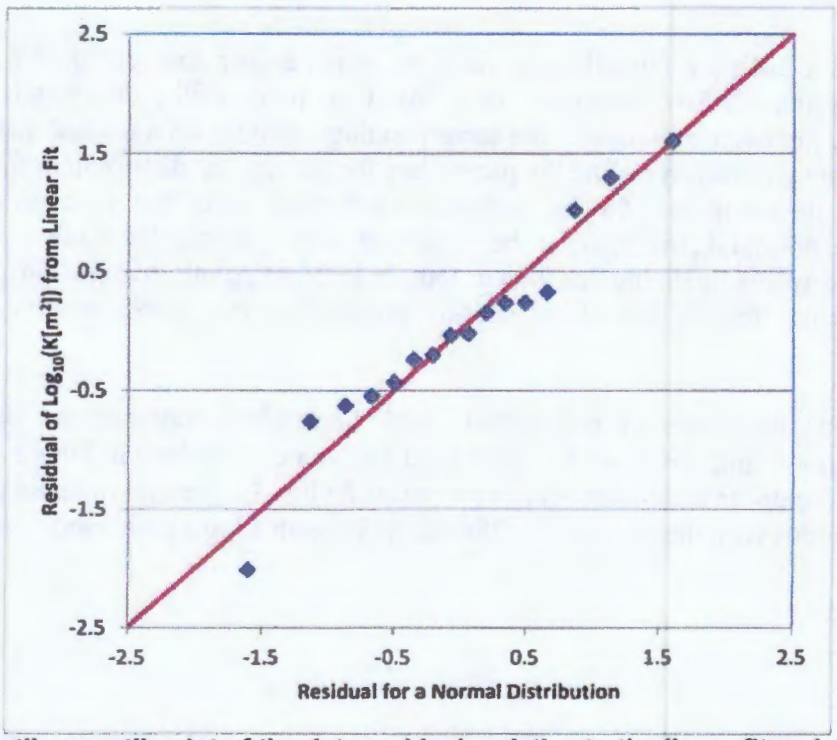

Figure 18. Quantile-quantile plot of the data residuals relative to the linear fit and of the predicted residuals for a normal distribution, $\mu = 0$ and $\sigma = 0.86$

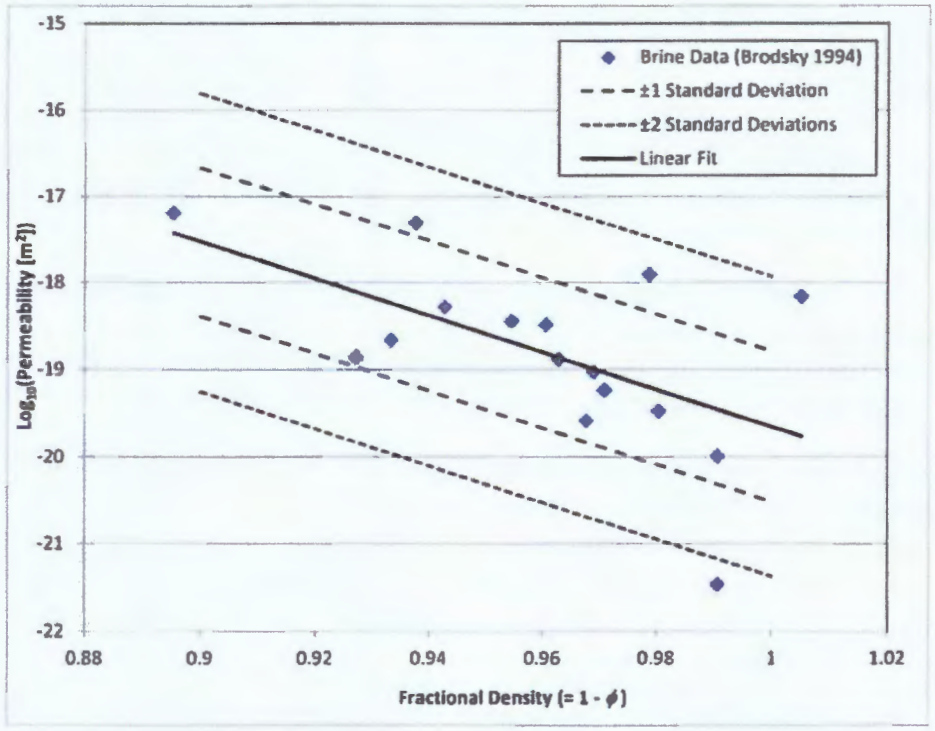

Figure 19. Variation of permeability with fractional density, based on the least squares fit with uncertainty defined by a normal distribution with $\mu = 0$ and $\sigma = 0.86$

Table 2 presents the expected permeabilities from 0 to 100 years, from 100 to 200 years, and from 200 to 10,000 years based on the analysis presented above. For the latter two time periods, the permeabilities are determined from the range of porosities established in the answer to question 1.1 (0.025 to 0.075 for 100 to 200 years, 0.001 to 0.0519 for 200 to 10,000 years), with the mean permeability for each porosity defined by the least squares fit (see Figure 17) and the minimum and maximum permeability values defined at ±2 standard deviations on the normal distribution (see Figure 19).

The permeability values in Table 2 are reasonable from several viewpoints:

- From 0 to 100 years, the crushed salt is assigned a permeability value of 10^{-11} m^2, representative of a very loose granular material.

- From 100 to 200 years, the permeability range in Table 2 encompasses a wide range of possible outcomes, from a very low permeability of 1.44×10^{-21} m^2 to a maximum permeability of 4.55×10^{-17} m^2, which is more than 4 orders of magnitude greater than the minimum value. This range will produce a range of hydrologic responses for the panel closure, from "tight" to much "looser" in terms of brine and gas flows across the closure, because of the uncertainties in emplacement of the crushed salt.

- From 200 to 10,000 years, the permeability range in Table 2 represents the response of almost fully compacted salt, with a minimum value of 4.46×10^{-22} m^2 and a maximum value

of 1.47×10^{-17} m^2. This range of values is purposefully greater than the range for intact halite in PA, which is 10^{-24} m^2 to 10^{-21} m^2. As noted previously, the consolidation mechanisms for moistened versus dry crushed salt are different and can lead to different levels of interconnected porosity and permeability for a given effective porosity (see response to Question 1.2a). Stated differently, the very low permeability of intact salt may not be attained for thousands of years, and the recommended permeability will produce a range of hydrologic responses for the panel closure.

- After 100 years, the range of permeabilities in Table 2 is similar to the permeability range for material DRZ_PCS in the PABC-2009, which is 2×10^{-21} m^2 to 1×10^{-17} m^2 at all times (Clayton et al., 2010). The permeability after 100 years is therefore consistent with the expected response for a healed DRZ above a panel closure, as represented in PABC-2009.

Table 2. Expected, Minimum, and Maximum Permeability Values Corresponding to the Least Squares Fit with Uncertainty Defined by a Normal Distribution

Porosity	Fractional Density	Expected Permeability (m^2)	Minimum[a] Permeability (m^2)	Maximum[a] Permeability (m^2)
0 to T1 (0 to 100 Years):				
0.33	0.67	1×10^{-11}	N/A	N/A
T1 to T2 (100 Years to 200 Years):				
0.025	0.975	7.55×10^{-20}	1.44×10^{-21}	3.96×10^{-18}
0.075	0.925	8.66×10^{-19}	1.65×10^{-20}	4.55×10^{-17}
T2 to 10,000 Years (200 Years to 10,000 Years):				
0.001	0.999	2.34×10^{-20}	4.46×10^{-22}	1.23×10^{-18}
0.0519	0.9481	2.80×10^{-19}	5.34×10^{-21}	1.47×10^{-17}

[a]Minimum corresponds to -2 standard deviations below the least squares fit; maximum corresponds to +2 standard deviations above the least squares fit.

Within performance assessment, the permeability-porosity relationship in Figures 17 through 19 can be represented with the following algorithm:

1. For each realization, sample the T1 porosity from a uniform distribution with a minimum of 0.025 and a maximum of 0.075, and sample the T2 porosity from a uniform distribution with a minimum of 0.001 and a maximum of 0.0519.

2. Calculate the expected values of the $\log_{10}$ (permeability) using the equation for the least squares fit in Figure 17.

3. Sample a normal distribution (mean of zero, standard deviation of 0.86) that is truncated at ±2 standard deviations for the residual of the final value of the $\log_{10}$ (permeability) relative to the least squares fit. This sampling is performed once per realization.

This algorithm can be expressed mathematically as:

$$\log(k_e) = -21.187(1-\phi_{T2}) + 1.5353,$$

$$k_{T2} = 10^{\log(k_e)+\alpha} = k_e 10^{\alpha},$$

where k_e is the expected value of permeability from the least squares fit (Figure 17),
ϕ_{T2} is the sampled value of porosity,
k_{T2} is the final value of permeability, and
α is the sampled value of a normal distribution with a mean of 0 and standard deviation of 0.86.

Completeness Question 1.3c: *Please provide design and performance information that justifies the stated assumption that the "substantial barrier" will have no impact on panel seal performance during time period T2.*

DOE Response to Technical Question 1.3c:
The design configuration for the panel closure consists of 100 feet of crushed ROM salt between two barriers. The barriers consist of two standard ventilation bulkheads placed at the ends of the salt or alternately, one standard ventilation bulkhead and a concrete block wall (see Figure 1). The ventilation bulkhead, shown in Figure 2, is a thin steel structure that is designed to restrict ventilation air flow and control personnel access during the operational period. The concrete block wall is 12 feet thick and was installed in Panels 1, 2, and 5 as an explosion barrier during the operational period. Some degradation of the block walls from creep closure of the panel entries is observable in the underground facility.

The steel bulkheads are designed to perform only during the operational period. These barriers are not expected to remain intact 100 years after repository closure because of creep closure of the panel entries. The block wall is also designed for the operational period. This wall is inspected on a regular basis, and in addition, the expected condition of the wall is assessed through numerical modeling (e.g., Rocksol, 2006). Inspection of the condition of the walls in Panels 1 and 2 several years after installation show surface spalling of the concrete on the outbye free face as a result of loading caused by inward creep of the salt. Numerical stress analysis implies that the free faces and the rib contacts will be in a condition of plastic yield with an unyielded core. No long-term stress analyses have been carried out; however, it is expected that the spalling and yield will be progressive, and that the walls will not be significant structures after the initial 100-year time period. These barriers will therefore have no significant impact on the long-term performance of the panel closures.

Completeness Question 1.3d: *Please justify the unstated assumption that repository gas pressure buildup during time period T2 will not inhibit or reverse consolidation of the ROM salt panel seal, potentially resulting in higher porosities and therefore higher permeabilities than the recommended values.*

DOE Response to Technical Question 1.3d:
Gas pressure could build up during consolidation of crushed salt, either because of trapped air in the pores or because of pressure buildup due to gas generation from corrosion or microbial degradation of waste in a disposal room. The gas pressure in a room may continue to increase after consolidation of the crushed salt, particularly because of long-term corrosion of iron-based materials in the waste and waste containers.

During early time periods (0 to 100 and 100 to 200 years) gas pressure will remain low. First, compressibility of gas trapped in the pore space of the closure does not produce a large change in pressure. The magnitude of this change can be estimated by assuming a slow, isentropic compression of the gas, under which condition:

pV^{γ} = constant,

or

$$p = p_i\left(\frac{V_i}{V}\right)^{\gamma},$$

where p_i and V_i are the initial pressure and initial volume, resp., V is the final volume, p is the final pressure, and γ is the isentropic exponent of the gas. For a tenfold decrease in pore volume, the pressure increases by a factor of 25 for an isentropic exponent of 1.4, which is typical of air. An initial pressure of 0.10 MPa (14.7 psi) would increase to 2.54 MPa (368 psi). During the initial time period (0 to 100 years), permeabilities of the crushed salt will remain reasonably high so that any pressure buildup of this nature will leak out through the half-length of 50 ft in the times available (tens of years). During the second time period (100 to 200 years), volume reduction due to consolidation will be much less, leading to lower pressure buildup. IT Corporation (1987) carried out calculations of consolidation of crushed salt for a generic salt repository in the Permian Basin at an assumed depth of 2384 ft, and included the possible effects of pressure of trapped air. While the conditions for these calculations were not exactly equivalent to those at the WIPP, it is of note that they showed only a minor effect, of the order of 5% delay in consolidation times, from air pressure buildup.

Similarly, the pressure buildup due to gas generation from waste degradation remains low during time periods T1 and T2. The mean pressure in waste panel (see red curve in Figure 20) is less than 2 MPa (290 psi) at 200 years and less than 3 MPa (435 psi) at 300 years. These pressures are quite small compared to the lithostatic stress at the disposal horizon. It follows that pressure changes from compressibility of gas in the pore space or due to gas generation from waste degradation will not significantly retard consolidation of the crushed salt during time periods T1 and T2.

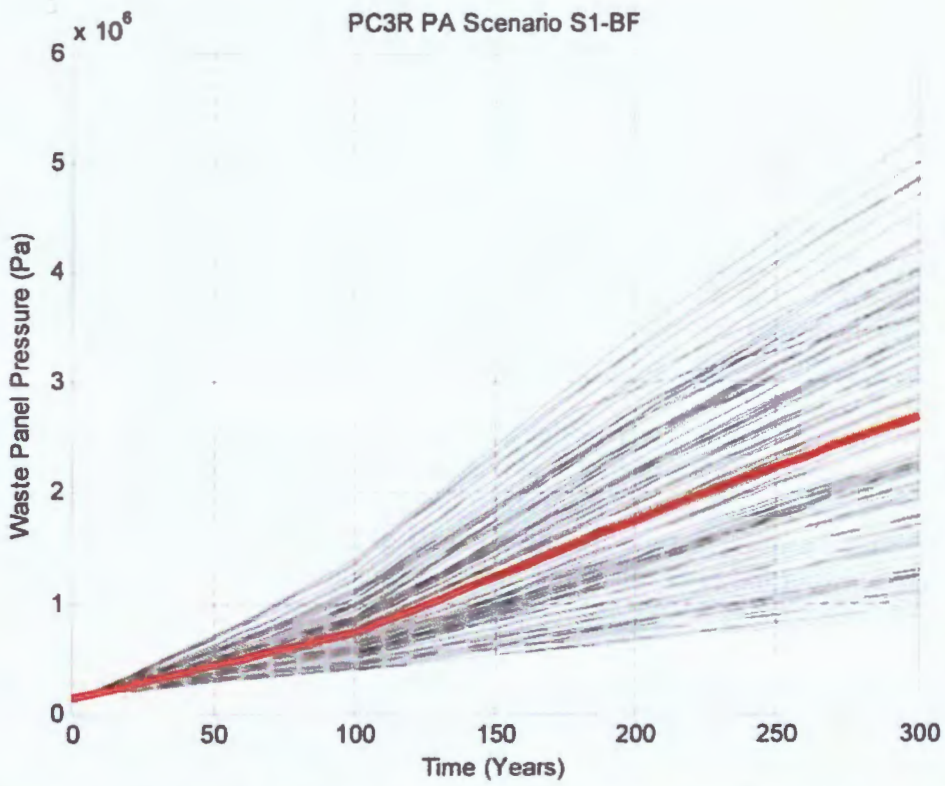

Figure 20. Waste panel pressure from the PC3R PA for Replicate 1, undisturbed scenario

After time T2, the gas pressure in the pores will not have a significant influence on the porosity or permeability of the crushed salt panel closures. Most of the consolidation has already taken place during T1 and T2, so the closure will have reached a condition largely indistinguishable from the intact halite, and the back stress from the surrounding rocks on the crushed salt will be increasing rapidly with time. If high gas pressure occurs in the disposal panels, the likely path for any fracture will be through the anhydrite marker beds, as currently assumed in performance assessment, rather than through the mass of the panel closure.

Completeness Question 1.3e: *Please justify the unstated assumption that backpressure reduction through lateral halite movement at the unconstrained ends of the 100-ft panel closure backfill can be ignored during the consolidation process.*

<u>DOE Response to Technical Question 1.3e:</u>
Three-dimensional (3D) calculations were performed to evaluate the magnitude of the lateral displacements throughout the 100-foot-long crushed salt component of the panel closure (Herrick, 2012). The 3D representation discretizes the central portion of the crushed salt component with grid blocks that are approximately 1 m on a side (see Figure 21). The crushed salt has an initial porosity of 33% and its dynamic response was simulated with the volumetric creep model in JAS3D (Blanford et al., 2001).

The boundary condition on the sides and bottom of the entry is one of zero normal displacement to represent the constraint from the walls. There is zero displacement in the x-direction (horizontal) at the mid-plane of the crushed salt because of symmetry. This symmetry plane passes through Node 1103, shown in the top portion of Figure 21. A vertical stress is applied on the upper surface of the model that increases from 0 to 15 MPa, the lithostatic stress at WIPP, over 500 years. No horizontal deformation is allowed on the sides in the z-direction since the goal of the calculations is to investigate horizontal behavior in the x-direction and to test for plane strain in that direction. Due to a lack of information on the coefficient of friction between the crushed salt and intact salt, an equivalent friction boundary condition was imposed that no displacements of the nodes on the top and bottom of the model were allowed in the horizontal directions. The JAS3D analyses for 1.3e do not include the underground stratigraphy.

Deformations, stresses, and strains were calculated at all nodes and elements of the mesh; however, emphasis is given to the material making up the inner rectangular block of material constituting the panel closure (shown as magenta-colored elements in the lower part of Figure 21). Due to symmetry, only the results for the left half of the salt are given. The nodes and elements considered within the left half of the inner rectangular block are shown in the lower drawing.

Figure 22 shows the deformed mesh at 0, 100, 200, 300, 400, and 500 years. Since it is a simplified model using an applied vertical stress on the upper surface only, the displacement of the top is not uniform. At the end of the simulation, it is obvious that the triangular end pieces are providing some lateral structural support as the deformation builds up. Note that there is no roof in this simulation to constrain the vertical deformation. There is visible horizontal bulging of the outer layers of the triangular ends as the deformation of the upper surface increases. Even though the triangular ends undergo apparent deformation, the interior elements that make up the panel closure do not show significant deviation from a plane strain condition. This is to be expected, and follows the well-established use of a plane strain assumption to represent the response of a cross-section in an entryway that is much longer than its characteristic lengths in the cross-section perpendicular to its longitudinal axis (see for example, Timoshenko and Goodier, 1951, Chapter 2, section 8).

The horizontal displacements in the x-direction (DISPLX) at the interior nodes are shown in Figure 23. The displacements (DISPLX) are in general small, the largest being about 15 cm (6 inches) at the ends. The temporary compaction as the material is stressed is a result of the uncoupling of deviatoric and volumetric inelastic behaviors in the model. The displacement decreases rapidly toward the center of the closure. By 5 m from the end, at Node 613, the displacement is approximately 15 mm; by 7 m from the end; at Node 627, the displacement is about 5 mm. The horizontal strains in the areas of these nodes are one to two hundredths of the vertical strain. These results suggest that the interior 70-75 feet can unequivocally be considered to be in a condition of plane strain. In addition, the small values of axial deformation away from the ends of the closure, and the rapid decrease of deformations away from those ends, indicate that the lateral movement of the ends will not have an effect on the rate of consolidation.

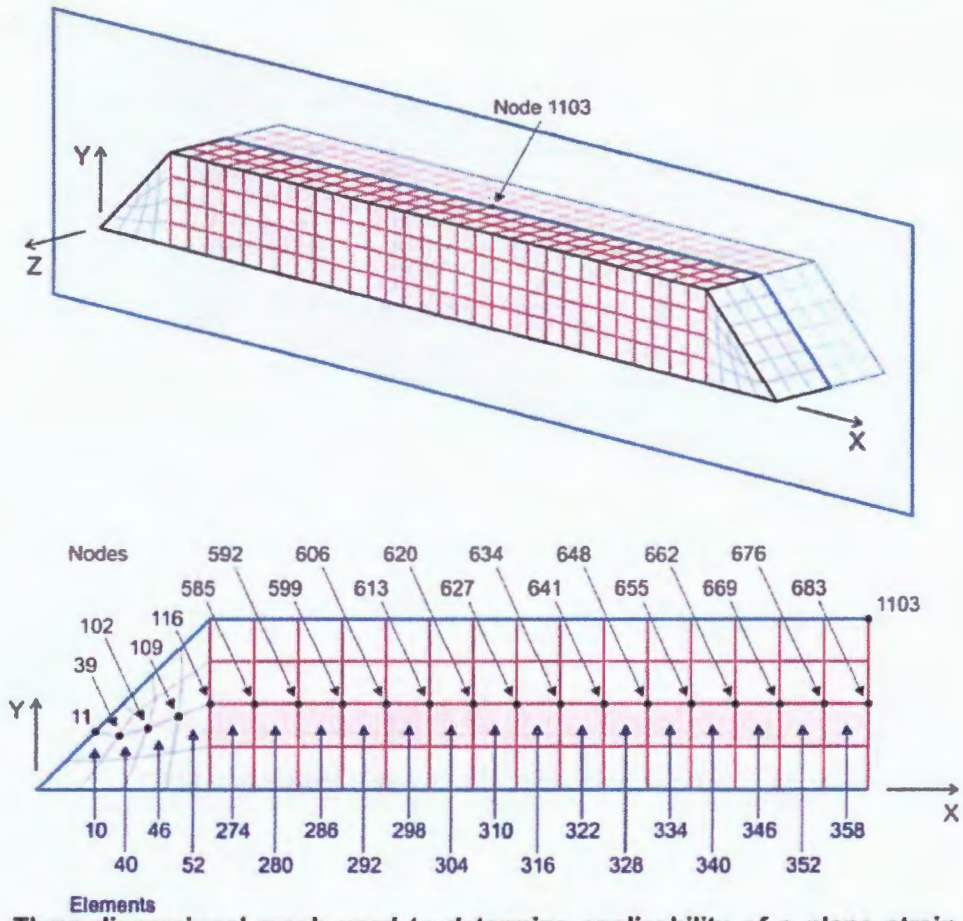

Figure 21. Three-dimensional mesh used to determine applicability of a plane strain condition. Lower figure shows the nodes and elements in the inner rectangular block (in cyan) that are used to define lateral displacements within the crushed salt.

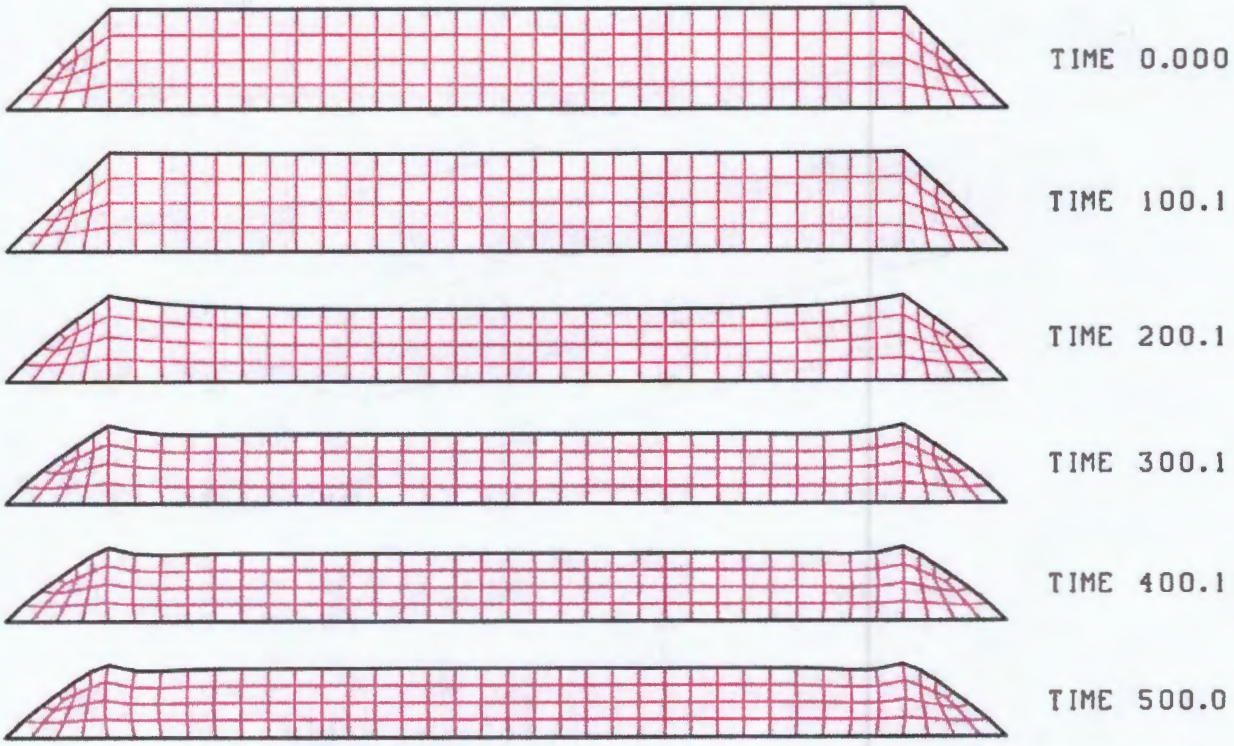

Figure 22. Deformed meshes at various times over the 500-year simulation period

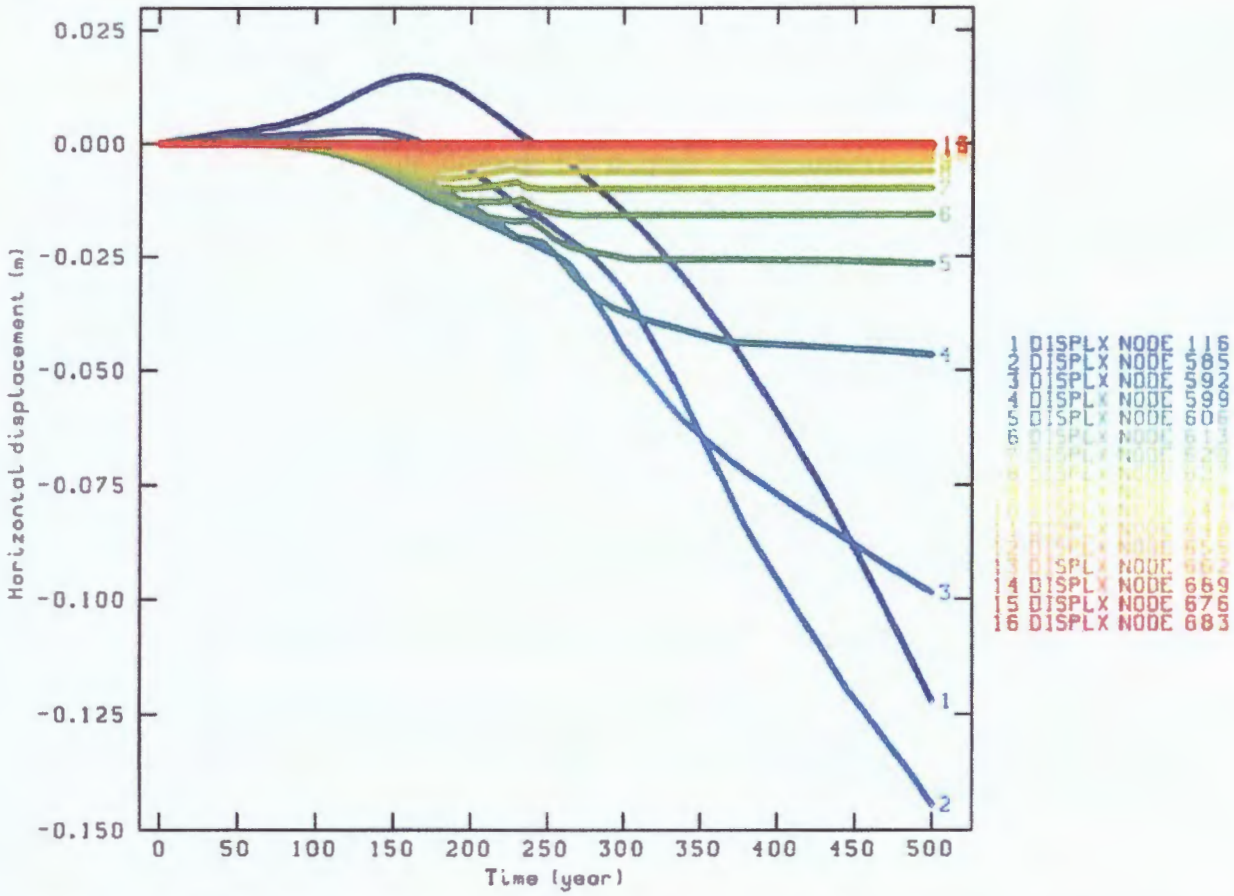

Figure 23. Plots of the horizontal displacements in the x-direction of the nodes shown in Figure 21~~Figure 21~~~~Figure 21~~

References for Questions 1.3

Ahrens, E.H., and F.D. Hansen. 1995. Large-Scale Dynamic Compaction Demonstration Using WIPP Salt: Fielding and Preliminary Results. Sandia National Laboratories, SAND95-1941.

Blanford, M.L., M.W. Heinstein, and S.W. Key. 2001. JAS3D: A Multi-Strategy Iterative Code for Solid Mechanics Analysis User's Instructions, Release 2.0. Sandia National Laboratories, ERMS 552358.

Brodsky, N.S. 1994. Hydrostatic and Shear Consolidation Tests with Permeability Measurements on Waste Isolation Pilot Plant Crushed Salt. Sandia National Laboratories, SAND93-7058.

Brodsky, N.S., F.D. Hansen, and T. Pfeifle. 1996. Properties of Dynamically Compacted WIPP Salt. *Proceedings of the 4th International Conference on the Mechanical Behavior of Salt, Montreal, Quebec, Canada, June 17-18, 1996.* Sandia National Laboratories, SAND96-0838C.

Clayton, D.J., R.C. Camphouse, J.W. Garner, A.E. Ismail, T.B. Kirchner, K.L. Kuhlman, and M.B. Nemer, 2010. Summary Report of the CRA-2009 Performance Assessment Baseline Calculation. Sandia National Laboratories, ERMS 553039.

Herrick, C. 2012. Calculations Performed in Support of Reconsolidation of Crushed Salt in Panel Closures. Memorandum to WIPP Records Center dated March 29, 2012. Sandia National Laboratories, ERMS 557150.

Hurtado, L.D., M.K. Knowles,V.A. Kelly, T.L. Jones, J.B. Ogintz, and T.W. Pfeifle. 1997. WIPP Shaft Seal System Parameters Recommended to Support Compliance Calculations. Sandia National Laboratories, SAND97-1287.

IT Corporation. 1987. Laboratory Investigation of Crushed Salt Consolidation and Fracture Healing. Prepared for the Office of Nuclear Waste Isolation, BMI/ONWI-631.

Rocksol Consulting Group, Inc. 2006. Further Assessment of the Short-term Stability of the 12 Foot Explosion Isolation Wall. Report prepared for Washington TRU Solutions, LLC.

Timoshenko, S and J.N. Goodier. 1951. Theory of Elasticity. McGraw-Hill, New York.

U.S. Department of Energy (DOE). 1996. Title 40 CFR Part 191 Compliance Certification Application for the Waste Isolation Pilot Plant. DOE/CAO-1996-2184, U.S. Department of Energy Carlsbad Area Office, Waste Isolation Pilot Plant.

1.4 Panel Closure DRZ Permeability

Parameter Name	PABC 2009 Value	Used in PC3R PA ERMS 555489	Units
Long-Term T2 Values for the PCS DRZ			
PCS_T2:PRMX_LOG PCS_T2:PRMY_LOG PCS_T2:PRMZ_LOG	-20.7, -18.8, -17.0 for material CONC_PCS	-22.8, -20.2, -17.6 Triangular Distribution	$\log(m^2)$

Technical Question 1.4a: *Please justify the assignment of permeability values to the PCS DRZ during time period T2 that appear to represent a fully reconsolidated material, when the ROM salt panel closure itself has not yet fully reconsolidated and stress equilibrium has not yet been achieved.*

DOE Response to Technical Question 1.4a:
This response identifies the values to be used for the DRZ permeability. As discussed in the answers to questions 1.1 and 1.3, it is our intent to use multiple time periods to represent the behavior of the PCS and the surrounding strata. This differs from the approach for the PC3R PA, which used a single time period from 100 years to 10,000 years.

Initially, it is expected that the DRZ around the closure will be no different from that around the disposal rooms, since there will be only very small back stress from the consolidating salt. Calculations of the back stress during consolidation (Figures 25 and 26) show that these stresses do not become appreciable until over 100 years after emplacement (Herrick, 2012). It is appropriate to maintain the same range of DRZ permeability around the closure as that around the disposal rooms for the first 200 years. The values assumed for the first two time periods will therefore range from $10^{-19.4}$ m^2 to $10^{-12.5}$ m^2.

After 200 years, back pressures will have built up to reasonable values of the order of 6 to 10 MPa (Figures 25 and 26). It has been shown by several authors that fractures in salt will heal rapidly under these levels of stress (e.g., IT Corporation, 1987, and Costin and Wawersik, 1980). For example, Costin and Wawersik state:

- Tensile fractures in salt will heal when subjected to nominal overburden pressures (10-35 MPa), to the extent that the resistance to crack propagation along the pre-existing fracture plane is approximately 70-80% of that through virgin material.
- The healing process takes place rapidly compared to the time scale over which mining or storage in salt occurs.
- The principal mechanism in healing appears to be creep of contact asperities along the fracture surface.

Given the values of back stress calculated for closures with some degree of emplaced compaction, and the rapid increase of stress even for the most extreme case of uncompacted dry salt, it is appropriate to assume a DRZ permeability after 200 years equivalent to that used for the

Option D case. The proposed values for DRZ permeability after 200 years are therefore 2×10^{-21} m^2 to 1×10^{-17} m^2 at all times (Clayton et al., 2010).

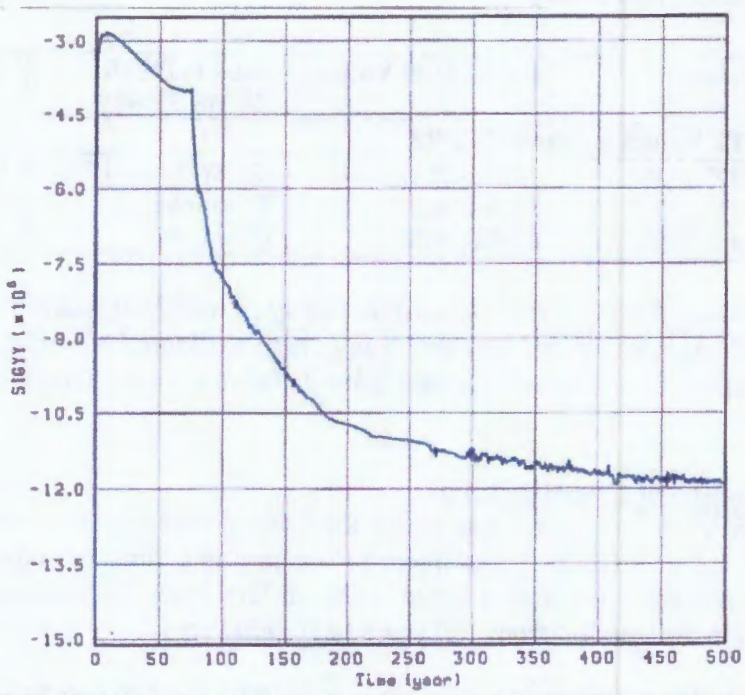

Figure 24. Vertical back stress on the roof of the panel entry for crushed salt with an initial emplacement porosity of 15% (fractional density of 85%)

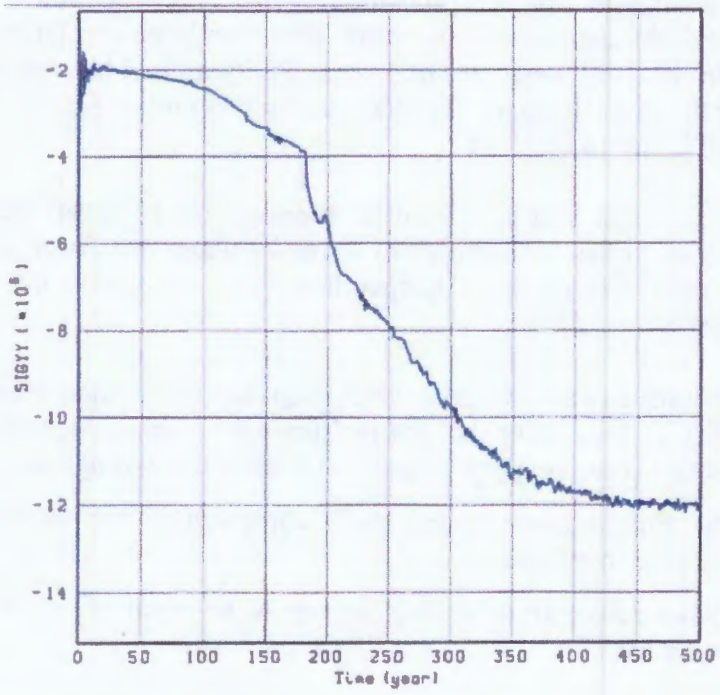

Figure 25. Vertical back stress on the roof of the panel entry for crushed salt with an initial emplacement porosity of 33% (fractional density of 67%)

EPA Technical Question 1.4b:
Please explain why the anhydrite marker beds surrounding the ROM salt panel seal are not treated in the same manner as those within the waste panel DRZ.

DOE Response to Technical Question 1.4b:
The anhydrite marker beds around the panel closure entries and the disposal room will have similar form prior to emplacing the crushed salt component of the panel closure. After emplacement and consolidation of the crushed salt, the vertical back stress on the roof of the panel increases to between 6 MPa and 10 MPA after 200 years (see Figures 25 and 26). This level of back stress will be sufficient to heal any fractures in the DRZ and to close fractures in the anhydrite, as discussed in the answer to Question 1.4a. The presence of high levels of back stress above the crushed salt component of the panel closure explains part of the reason why the anhydrite marker beds above the crushed salt component are not treated in the same manner as the marker beds above the waste panel.

A second reason relates to the representation of the marker beds in the BRAGFLO grid. The BRAGFLO simulations used in WIPP PA utilize an essentially two-dimensional representation of the repository to calculate brine and gas flow in a three-dimensional facility. The reasoning to include the anhydrite marker beds as elements separate from the "healed" DRZ above panel closures in BRAGFLO was based on BRAGFLO grid studies performed in 2003 (Stein and Zelinski, 2003).

Keeping the anhydrite marker bed material as a separate element above each panel closure in the BRAGFLO grid is done to capture a possible three-dimensional flow path in the two-dimensional BRAGFLO grid. More specifically, it is expected that fracturing may occur in the anhydrite marker beds for pressures above the fracture initiation pressure. When this fracturing occurs, it is expected that brine and gas under high pressure could go "around" panel closures by way of a flow path through the fractured anhydrite. In reference to the two-dimensional BRAGFLO repository representation, this flow path would be in the lateral direction, perpendicular to the 2-D plane considered in the model grid. The inclusion of separate anhydrite elements above panel closures in the BRAGFLO repository representation is intended to capture the effects of this out-of-plane flow path, around the panel closure through fractured anhydrite, in the two-dimensional BRAGFLO grid.

References for Questions 1.4:

Clayton, D.J., R.C. Camphouse, J.W. Garner, A.E. Ismail, T.B. Kirchner, K.L. Kuhlman, and M.B. Nemer. 2010. Summary Report of the CRA-2009 Performance Assessment Baseline Calculation. Sandia National Laboratories, ERMS 553039.

Costin, L.S. and W. R. Wawersik. 1980. Creep Healing of Fractures in Rock Salt. Sandia National Laboratories, SAND80-0392.

Herrick, C. 2012. Calculations Performed in Support of Reconsolidation of Crushed Salt in Panel Closures. Memorandum to WIPP Records Center dated March 29, 2012. Sandia National Laboratories, ERMS 557150.

IT Corporation. 1987. Laboratory Investigation of Crushed Salt Consolidation and Fracture Healing. Prepared for the Office of Nuclear Waste Isolation, BMI/ONWI-631.

Stein, J. and W. Zelinski. 2003. Analysis Package for: Testing of a Proposed BRAGFLO Grid to be used for the Compliance Recertification Application Performance Assessment Calculations. Sandia National Laboratories, ERMS 526868.

Date: May 3, 2012

Sandia National Laboratories

Operated for the U.S. Department of Energy by the
Sandia Corporation
Defense Waste Management Programs
4100 National Parks Highway
Carlsbad, New Mexico 88220

To: WIPP Records Center

From: R. Chris Camphouse (6211)
Michael Gross, WTS Subcontractor
Courtney G. Herrick, Sandia National Labs (6211)
Dwayne C. Kicker, The S.M. Stoller Corporation
Bill Thompson, Golder Associates

Technical Review: Ross Kirkes

QA Review: Shelly Nielsen

Management Review: Janis Trone

Subject: Recommendations and Justifications of Parameter Values for the Run-of-Mine Salt Panel Closure System Design Modeled in the PCS-2012 PA

1.0 Introduction

The Waste Isolation Pilot Plant (WIPP), located in southeastern New Mexico, has been developed by the U.S. Department of Energy (DOE) for the geologic (deep underground) disposal of transuranic (TRU) waste. Containment of TRU waste at the WIPP is regulated by the U.S. Environmental Protection Agency (EPA) according to the regulations set forth in Title 40 of the Code of Federal Regulations (CFR), Part 191. The DOE demonstrates compliance with the containment requirements according to the Certification Criteria in Title 40 CFR Part 194 by means of performance assessment (PA) calculations performed by Sandia National Laboratories (SNL). WIPP PA calculations estimate the probability and consequence of potential radionuclide releases from the repository to the accessible environment for a regulatory period of 10,000 years after facility closure. The models used in PA are maintained and updated with new information as part of an ongoing process. Improved information regarding important WIPP features, events, and processes typically results in refinements and modifications to PA models and the parameters used in them. Planned changes to the repository and/or the components therein also result in updates to WIPP PA models. WIPP PA models are used to support the repository recertification process that occurs at five-year intervals following the receipt of the first waste shipment at the site in 1999.

WIPP waste panel closures comprise a feature of the repository that has been represented in WIPP PA regulatory compliance demonstration since the Compliance Certification Application (CCA) of 1996. Panel closures are included in the repository as a safety measure during the

operational period. In particular, their presence in the repository is a means to protect workers from exposure to two potential hazards: 1) volatile organic compounds that may be present in emplaced waste materials and 2) an explosion which has been hypothesized to occur from gas generation causing methane concentration in the waste panels to reach a sufficiently high level. Panel closures were not developed to isolate radionuclides in the repository after closure. The DOE stated in the CCA (DOE 1996) that *"The panel closure system was not designed or intended to support long-term repository performance."* Panel closures are included in WIPP PA models principally because they are part of the disposal system, not because they play a substantive role in inhibiting the release of radionuclides to the outside environment.

The WIPP was certified to receive TRU waste in 1998. The 1998 rulemaking had several conditions, one of which involved the design of the panel closure system (PCS) implemented in the repository. The DOE presented four design options in the CCA, and

> "The EPA based its certification decision on the condition that DOE implement the most robust design [referred to in the CCA as "Option D"]. The Agency found the Option D design to be adequate, but also determined that the use of a Salado Mass Concrete- using brine rather than fresh water- would produce concrete seal permeabilities in the repository more consistent with the values used in DOE's performance assessment. Therefore, Condition 1 of the EPA's certification requires DOE to implement the Option D PCS at the WIPP, with Salado Mass Concrete" (EPA 1998).

The Option D panel closure system consists of three primary components: 1) a concrete block wall (the explosion wall), 2) open drift, and 3) a concrete monolith. The arrangement and dimensions of these components are illustrated in Figure 1.

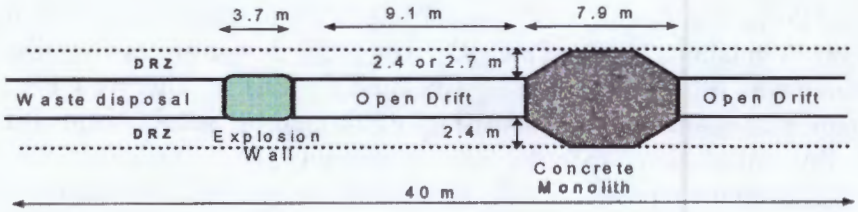

Figure 1: A Schematic of the "Option D" Panel Closure

Extensive refinement to WIPP panel closure modeling in PA has occurred since the implementation used in the CCA (Vugrin and Wagner 2006). In the CCA and the PAVT (MacKinnon and Freeze 1997) that followed, regulatory compliance was demonstrated with a generic panel closure that was not Option D. Following certification of the WIPP in 1998, and the mandate that Option D be implemented as the panel closure in WIPP, a PA was conducted in 2002 (Hansen 2002) with the aim of implementing an Option D panel closure into the repository

models used in WIPP PA, and to assess the impacts of panel closure design on long-term repository performance. Two panel closure cases were considered. The first was modeled upon the mandated Option D panel closure design. The second was the generic panel closure design implemented in the CCA and PAVT. Upon completion of the analysis, it was found that total normalized releases resulting from the two panel closure cases were nearly identical. Moreover, nearly identical distributions for each release component were calculated in the two panel closure cases. A more granular representation of the Option D panel closure was developed during the 2002 – 2003 Technical Baseline Migration (TBM) PA. Upon completion of the TBM PA, it was found that the TBM and PAVT produced releases that are nearly identical, indicating that repository performance is not significantly affected by changes in the panel closure properties (Dunagan 2003). The Option D panel closure representation developed during the TBM was used for the panel closure representation in the 2004 and 2009 Compliance Recertification Applications (CRA-2004 and CRA-2009, respectively).

Panel closures are represented in PA by way of their material properties and spatial extent. Due to the regulatory time scale of 10,000 years for which regulatory compliance must be demonstrated, there are uncertainties associated with panel closure material properties. These uncertainties in material properties are incorporated in PA. A material property with an associated uncertainty is assigned a distribution, and this distribution is randomly sampled. This sampling process allows for repository performance to be quantified over a range of material conditions, as well as an analysis of performance sensitivity to changes in material properties. As briefly described above, numerous studies have been conducted to date, often by way of full PA analyses, to quantify the impact of changes in panel closure material properties on regulatory compliance. In addition, several PA analyses have been performed (Hansen 2002, Vugrin & Dunagan 2006, Camphouse et al 2011) with the aim of determining the impact of panel closure redesigns on repository performance. Regulatory compliance has been met in all PA analyses performed to date, including those that incorporated changes to panel closure modeling. Regulatory compliance has been repeatedly shown to be primarily insensitive to panel closure material properties. A future PA is planned that incorporates a new panel closure design into the current PA baseline established by the 2009 Performance Assessment Baseline Calculation (PABC-2009) (Clayton et al., 2010). The name given to this planned panel closure PA is PCS-2012.

The PCS-2012 will quantify impacts of a run-of-mine (ROM) salt panel closure design by comparing total normalized releases to those found in the PABC-2009 where Option D was implemented as the panel closure. Calculations and analyses have been performed to develop material properties to be used in the PCS-2012, and are documented in DOE (2012) and Herrick (2012). This memorandum provides hydrologic and pore compressibility parameter values for the revised PCS in the PCS-2012 PA. Parameters are created as discussed in NP 9-2, *Parameters*. PCS-2012 parameters not listed in the memorandum will be equal to the values prescribed to them in the PABC-2009. In the discussion that follows, material parameters and timings are developed to account for the following physical processes and accepted rock mechanics principles:

1. Creep closure of the salt rock surrounding panel entries will cause consolidation of ROM salt emplaced in panel entries.

2. Eventually, the ROM salt comprising the closures will approach a condition similar to intact salt.
3. As ROM salt reaches higher fractional densities during consolidation, back stress will be imposed on the surrounding rock mass leading to eventual healing of the disturbed rock zone (DRZ).
4. DRZ healing above and below the ROM salt panel closures will reduce DRZ porosity and permeability in those areas.

A brief discussion of creep and reconsolidation of run-of-mine salt, and the DRZ healing that results, is the topic of the next section.

2.0 Creep and Reconsolidation of Run-of-Mine Salt

2.1 Creep Closure in Salt

The ability of salt to deform with time, eliminate voids, and create an impermeable salt barrier around the waste was one of the principal reasons for locating the WIPP repository in a bedded salt formation. The creep closure process is a complex and interdependent series of events starting after a region within the repository is excavated, which creates a disturbance in the stress field. Stress relief results in some degree of brittle fracturing and the formation of a DRZ surrounding excavations in all deep mines. For the WIPP, the DRZ is characterized by an increase in permeability, and may ultimately extend a few meters from the excavated region. Stress relief generates deviatoric stresses in the host rock, causing salt to deform by creep processes and to move inward to fill the excavated void. This process of salt creep will continue until deviatoric stress is dissipated and the system is once again at stress equilibrium (DOE 1996, Section 6.0.2.2 and Appendix PORSURF). Eventually, at equilibrium, deformation ceases, and the panel entry and any backfill (such as ROM salt) have undergone as much compaction as is possible by the weight of the rock above the repository horizon.

2.2 Mechanical Behavior of Run-of-Mine Salt

The mechanical behavior of ROM salt, which is also referred to as crushed salt, has been extensively studied and can be divided into three basic categories: elastic deformation, inelastic deformation, and failure (Callahan et al. 1995, Section 2.4.1). The inelastic behavior can further be divided into time-independent (instantaneous compaction) and time-dependent (creep consolidation) deformation. A number of parameters or characteristics are expected to affect the mechanical behavior of crushed salt. These parameters include (but are not limited to) density (or porosity), grain size and grain size distribution, moisture content, impurity content (such as clay, anhydrite, etc.), temperature, stress state (i.e., confining pressure and stress difference), and time.

Crushed salt is proposed as the main component of the redesigned panel closure, and over time this crushed salt will be consolidated by the creep closure of the entry. Crushed salt is also proposed as one component of the shaft seal, and an assessment of the mechanical behavior of crushed salt is provided as part of the WIPP shaft sealing system design (DOE 1996, Appendix SEAL). If salt reconsolidation is unimpeded by fluid pore pressures, the material will eventually achieve extremely low permeabilities approaching those of the native Salado Formation. Developments in support of the WIPP shaft seal system have produced confirming experimental results, constitutive material models, and construction methods that substantiate use of a salt

column to create a low permeability seal component. Other advantages of the use of crushed salt for sealing systems is that as a replacement of the natural material in its original setting it ensures physical, chemical, and mechanical compatibility with the host formation.

2.3 Response of the Disturbed Rock Zone

An underground excavation creates a disturbed zone in the surrounding rock. Microfracturing will occur in the rock adjacent to the drift wall, where confining stresses are low or nonexistent. The extent of the zone depends on the rock strength and the prevailing stress state, which is depth dependent.

In terms of WIPP repository applications, one of the most important features of salt as an isolation medium is its ability to heal previously damaged areas (Hansen 2003, Section 4.1). Damage recovery, or healing, arises when the magnitude of the deviatoric stress decreases relative to the applied mean stress. A decrease in deviatoric stress occurs as stresses approach lithostatic conditions, as would be the circumstance adjacent to the crushed salt barrier when it reaches a consolidated state. The healing mechanisms include microfracture closure and bonding of fracture surfaces. Microfracture closure is a mechanical response to increased compressive stress applied normal to the fractures, while bonding of fracture surfaces occurs either through crystal plasticity, a relatively slow process, or pressure solution and redeposition, a relatively rapid process (Spiers et al., 1988). Evidence for healing has been obtained in laboratory experiments, small-scale tests at WIPP and through observations of field analogs (Hansen 2003, Sections 4.5, 4.6, and 4.9).

2.4 Impact of ROM Salt Reconsolidation on Porosity and Permeability

Numerical modeling conducted as part of shaft sealing analyses provides density of the compacted salt column as a function of depth and time. Many calculations comparing models for consolidation of crushed salt were performed to quantify performance of the crushed salt column in the shaft seal (DOE 1996, Appendix SEAL; Callahan et al. 1995; Brodsky et al. 1996). From the density-permeability relationship of reconsolidating crushed salt, permeability of the compacted salt seal component is calculated. In general, results show that the bottom of the salt column consolidates rapidly, achieving permeability of 1×10^{-19} m^2 in about 50 years. By 100 years, the middle of the salt column reaches similar permeability.

Structural analysis calculations were developed to determine the fractional density of the crushed salt seal as a function of time and depth and, using these results, to determine permeability of the crushed salt as a function of time and depth (DOE 1996, Appendix SEAL, Section 7.4.2.1). The results of these calculations indicate that compacted salt will increase from its emplaced fractional density of 90% to a density of 95% approximately 40, 80, and 120 years after emplacement at the bottom, middle, and top of the shaft seal, respectively. Using the modified Sjaardema-Krieg creep consolidation model, the times required to fully reconsolidate the crushed salt to 100% fractional density are 70 years, 140 years, and 325 years at the bottom, middle, and top of the salt column, respectively. Based on these results, the desired fractional densities (hence, permeability) can be achieved over a substantial length of the compacted salt seal in the range of 50 to 100 years.

Additional details on the porosity and permeability of ROM salt are provided in Sections 5.1.1 and 5.1.2. Based on the calculations cited above and on in situ observations as described in Section 5.1.1, it is expected that a completely consolidated ROM salt-filled drift will achieve flow properties indistinguishable from natural Salado salt. The ability of salt to recover from damage and heal is a time-dependent process; eventually, the permeability of the consolidated ROM salt and the surrounding DRZ will return to that of intact salt.

3.0 Revised Design of the PCS

The DOE has submitted a planned change request (PCR) to the EPA requesting that EPA modify Condition 1 of the Final Certification Rulemaking for 40 CFR Part 194 (EPA, 1998) for the WIPP. Following the selection of the Option D panel closure design in 1998, the DOE has reassessed the engineering of the panel closure and established a revised design which is simpler, easier to construct and equally effective at performing its operational-period isolating function. Accordingly, the PCR submitted to EPA requested that Condition 1 be changed, and that a revised design for the panel closures be approved for use in all panels (DOE, 2011). The revised design of the PCS, known as the Run-of-Mine Panel Closure System (ROMPCS), comprises 100 feet of run-of-mine (ROM) salt with barriers at each end (Figure 2). The ROM salt is generated from ongoing mining operations at the WIPP and may be compacted and/or moistened as it is emplaced in a panel entry. The ROM salt will be emplaced to all salt surfaces (back, walls, etc.) as completely as practicable. After emplacement, creep closure of the panel entries will cause the ROM salt to consolidate to a condition approaching intact salt, with low porosity and low permeability.

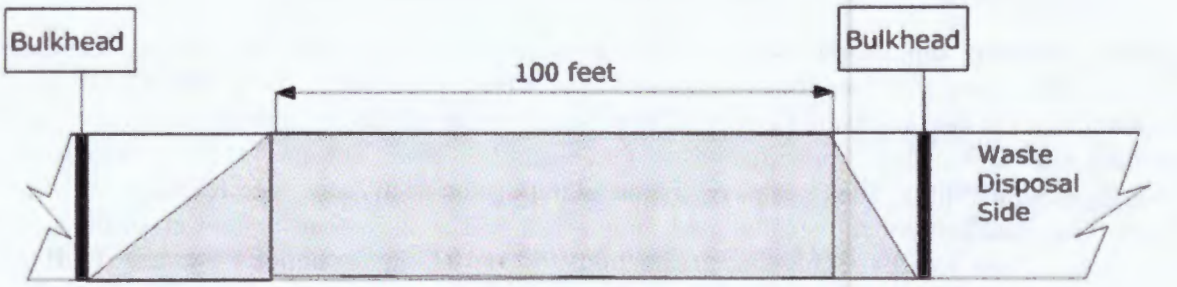

(a) Panel closure with 100 feet of ROM salt between two ventilation bulkheads

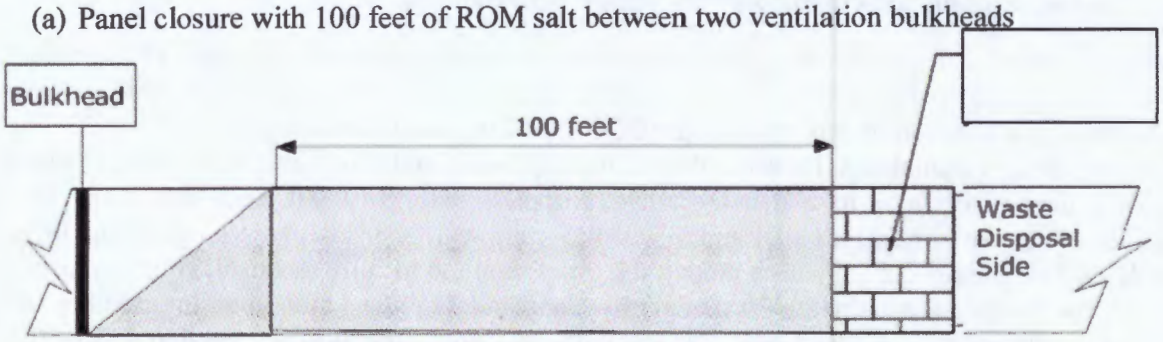

(b) Panel closure with 100 feet of ROM salt between a ventilation bulkhead & explosion wall

Figure 2. Schematic diagram of the revised panel closure design

The barriers will consist of ventilation bulkheads, similar to those currently used in the panels as room closures (Figure 3). The ventilation bulkheads are designed to restrict air flows and prevent personnel access into waste-filled areas during the operational phase. In Panels 1, 2, and 5, where explosion walls fabricated from concrete blocks have already been emplaced in the panel entries, an explosion wall is the inbye barrier and a ventilation bulkhead will be the outbye barrier, as shown in Figure 2b.

The emplacement scheme for the ROM salt will be finalized once *in situ* testing has been completed. It is expected that the final emplacement scheme will involve some degree of in-place compaction, with or without added moisture (moisture may be added because it accelerates the consolidation of the crushed salt). The emplacement technique and/or strategy *is not* important to long-term repository performance. In particular, the uncertainty in the final panel closure emplacement strategy is not a result of consideration of long-term panel closure characteristics. Panel closures are emplaced in the repository to protect workers during the operational phase of the facility. Emplacement uncertainty is due to current lack of operational experience in constructing/emplacing this type of closure system. The method used will be based on consideration of various operational variables. Cost, efficiency, short-term effectiveness, dust control, and other factors will all play into the final emplacement scheme. A range of possible emplacement strategies are being assumed in the PCS-2012 to develop panel closure materials, properties, and timings representative of all potential emplacement strategies.

At one end of the range is emplacement of dry ROM salt without any initial compaction. The uncompacted porosity of ROM salt is assumed to be 35%, based on several sources. Callahan and Devries (1991, Section 4.1 and Table 2-2) define the initial density of crushed salt as about 65% of intact density, based on data from (Sjaardema and Krieg, 1987) and (Weatherby, 1989). This initial density corresponds to an initial porosity of approximately 35% for the crushed salt. Recent work on backfill compaction in the German repository program also assumes an initial backfill porosity of 35% (Rothfuchs and Wieczorek, 2010). The uncompacted ROM salt is therefore assumed to have an initial porosity of 35%, equivalent to a fractional density of 65%. At the other extreme, the ROM salt may be emplaced in compacted layers that are wetted with a small amount of moisture to enhance the initial emplacement density and short-term consolidation. The average porosity of the compacted layers is estimated to be greater than 20%, based on engineering judgment. The values of the hydrologic and mechanical parameters for the PCS-2012 PA are intended to encompass both of these extremes.

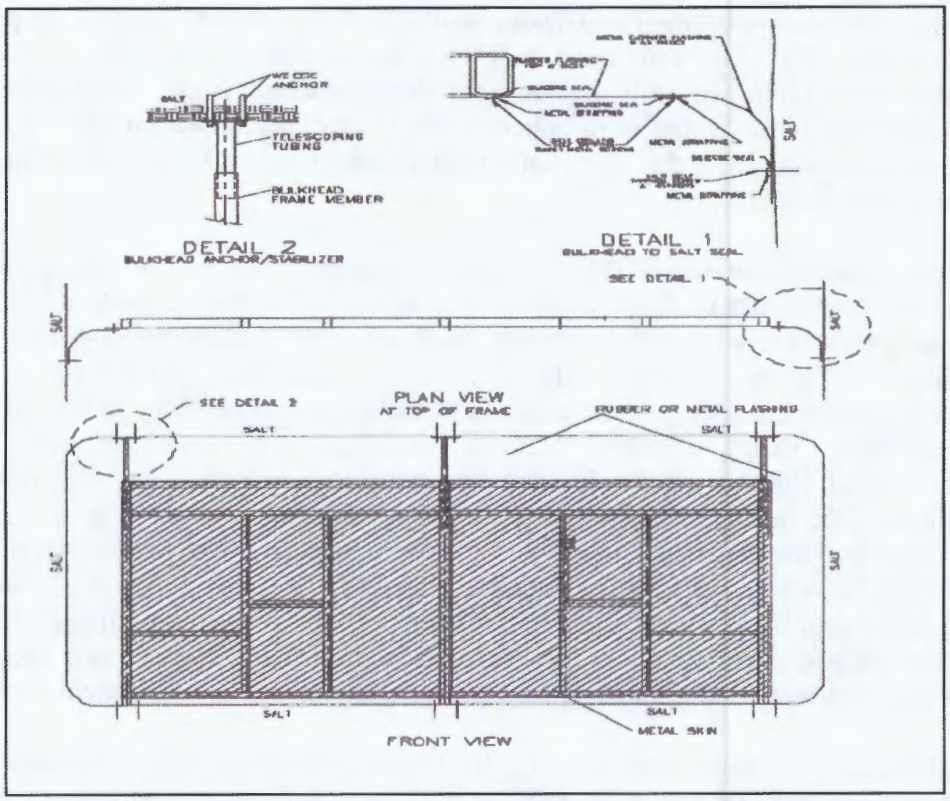

Figure 3. Typical design of a ventilation bulkhead that blocks the panel entry

The ROM salt is chemically compatible with the host rock because it is mined from the host rock at the repository horizon and because it has no additives, except for the possible addition of a small amount of moisture. The sheet metal in the ventilation bulkhead has small mass and is chemically similar to the iron-based metals in the waste and waste containers that are already in the repository. The materials in the redesigned PCS will therefore be chemically compatible with the host rock and with the materials already in the repository.

4.0 Modeling Approach for PCS-2012 PA

A new PA baseline was established by the PABC-2009 (Clayton et al., 2010). The differences between the PABC-2009 and the PCS-2012 PA will be a direct consequence of the revised design of the PCS. More specifically, the PCS-2012 PA will use the BRAGFLO grid that was used for the PABC-2009, but with new properties for the materials that represent the ROM salt in the PCS and the disturbed rock zone directly around the PCS. Note that the Option D panel closure implemented in the PABC-2009 is 40 meters long (Figure 1) while the redesigned PCS modeled in the PCS-2012 is 100 feet (30.48 meters) long. The PABC-2009 BRAGFLO grid will be modified slightly to account for the reduction in length of the ROMPCS as compared to Option D.

The ROMPCS properties will be based on three time periods: from 0 to 100 years, from 100 years to 200 years, and from 200 years to 10,000 years. This is a refinement to the granularity of panel closure modeling undertaken in the 2006 PCS PA (Vugrin and Dunagan 2006) and the

2011 PC3R PA (Camphouse et al 2011). Three time periods are appropriate because the process to consolidate the ROM salt occurs over a primary time scale of approximately 100 years, while the process to heal fractures in the DRZ surrounding the PCS occurs over a longer time scale of approximately 200 years. The ROM salt will therefore be represented by three materials, denoted as PCS_T1 for the first 100 years, PCS_T2 for 100 to 200 years, and PCS_T3 for 200 to 10,000 years. Similarly, the DRZ directly above and below the ROM salt will be represented by materials DRZ_PCS_T1, DRZ_PCS_T2, and DRZ_PCS_T3.

The ventilation bulkheads are designed to provide isolation only during the operational period. These bulkheads are not expected to remain intact 100 years after repository closure because of creep closure of the panel entries. The explosion wall is also designed for the operational period. This wall is inspected on a regular basis, and the anticipated condition of the wall is also assessed through numerical modeling (e.g. RockSol, 2006). Figures 4 and 5 present photographs of the condition of the free face in Panel 1 during February 2012. The explosion wall shows surface spalling or slabbing of the concrete blocks as a result of the loading caused by inward creep of the salt. In contrast, the plastic properties on the ROMPCS will allow it to reconsolidate and heal under increasing load due to salt creep. The thickness of the slabs shown in Figure 4 is typically 1.2 to 1.5 inches and quite consistent. The rod in Figure 5 is anchored by a nut resting on a thin layer of bricks that have become detached and pushed out by the formation of a crack about an inch behind the free surface.

Figure 4. Surface spalling at the base of the explosion wall in the intake drift of Panel 1 during February 2012

Figure 5. Surface spalling at the top corner of the explosion wall in the intake drift of Panel 1 during February 2012.

Numerical stress analysis of the concrete explosion wall has demonstrated that the free faces and the rib contacts will be in a condition of plastic yield with an unyielded core by 7 years after emplacement (Rocksol, 2006, Figures 7 and 10). No long term stress analyses have been carried out; however, it is expected that the spalling and yield will be progressive, and that the walls will not be significant structures after the initial 100 year time period, due to the brittle, non-plastic behavior of concrete. The ventilation bulkheads and explosion walls will therefore have no significant impact on long-term performance of the panel closures and are not included in the analysis of material properties for the PCS and the DRZ surrounding the PCS. Additionally, during the initial 100 year period after repository closure, the primary potential flow path through the closure system will be through the DRZ so any influence from the bulkheads or explosion wall will be minimal.

5.0 PCS Parameters

As discussed in Section 2.0, the salt rock surrounding the panel entries is creeping closed, and this closure will cause consolidation of ROM salt emplaced in panel entries. Eventually the ROM salt will approach a condition equivalent to intact salt. During the consolidation process, as the ROM salt reaches higher fractional densities, a back stress will be imposed on the surrounding rock mass leading to healing of the DRZ and a reduction in DRZ porosity and permeability. These processes and their effect on porosity and permeability of the ROM salt and the surrounding DRZ are discussed in Section 2.0. This section of this memorandum provides values for a complete set of hydrologic parameters and the pore compressibility parameter for the ROM salt and for the DRZ directly above and below the PCS.

5.1 Hydrologic and Pore Compressibility Parameters for the ROM Salt

5.1.1 Porosity of ROM Salt

Estimates of the consolidation process have been made in a series of calculations (Herrick 2012) carried out using JAS3D (Blanford et al., 2001; DOE, 2012, Figures 4 through 7) with the Sjaardema and Krieg (1987) model for crushed salt, modified with a deviatoric creep compaction response (Stone, 1997). Separate calculations were performed for initial emplacement porosities of 20%, 25%, 30%, and 35%, which correspond to initial fractional densities of 80%, 75%, 70%, and 65%, respectively. These calculations show consolidation to a porosity of 5% in 65 years from an initial porosity of 20% and in 152 years from an initial porosity of 35%. The results from the JAS3D calculations during the first 150 years are summarized in Table 1 as a function of time and initial emplacement porosity.

Table 1. Porosity predicted by JAS3D for ROM salt in a panel entry as a function of time and initial emplacement porosity

Time After Emplacement (Years)	Porosity			
0	20%	25%	30%	35%
50	6.6%	10.3%	14.6%	18.7%
100	1.9%	4.2%	7.3%	10.7%
150	1.0%	1.2%	2.9%	5.2%

During the first time period, from 0 to 100 years, the data in Table 1 show that the porosity of the ROM salt decreases rapidly. In order to represent this time varying porosity in a way suitable for long-term performance assessment calculations, it is reasonable to define the range of porosity of the ROM salt at the midpoint of this time interval, 50 years. The porosity range for the first 100 years is then 6.6% to 18.7%, based on the second row of data in Table 1. This range explicitly accounts for the uncertainty in initial emplacement porosity for the ROM salt.

For the time period from 100 to 200 years, the porosity range is 2.5% to 7.5%, with an expected or mean porosity of 5%. The lower limit for the porosity range, 2.5%, is essentially the same as the lower limit of porosity from the JAS3D calculations at 100 years, 1.9% (see Table 1). The upper limit for the porosity range, 7.5%, is less than the maximum porosity from the JAS3D calculations at 100 years, which is 10.7% (see Table 1); however, the JAS3D calculation for ROM salt with an initial porosity of 35% predicts a porosity of 7.5% by 126 years after emplacement. The value of 7.5% as an upper limit is also consistent with the magnitude of the porosity range for intact halite. That is, the magnitude of the porosity range from 100 to 200 years is 7.5% - 2.5% = 5%, approximately equal to the magnitude of the observed porosity range for intact salt, which is 5.19% - 0.1% = 5.09% (DOE 2009, Appendix PA, Parameter 17; Ismail 2007). Finally, the mean porosity, 5%, is consistent with the JAS3D predictions at 100 years, which have a porosity range of 1.9% to 10.7% at 100 years after emplacement (see the 3rd row of data in Table 1).

A number of sources corroborate the use of a reduced upper limit, 7.5% rather than 10.7%, during the second time period. Hurtado et al. (1997) carried out a number of consolidation

estimates for the proposed crushed salt component of the shaft seals. The proposed crushed salt component of the shaft seals will consist of mined WIPP crushed salt, dynamically precompacted with added moisture to a porosity of 10%. Calculations of the consolidation of this component due to creep closure of the shaft indicate that the crushed salt will be at an essentially intact condition (a fractional density approaching 1) within 100 years at a depth of 515 m and within 60 years at a depth of 600 m (Hurtado et al. 1997, Figure 2-3). Additional calculations by Callahan (1999) show consolidation results for different crushed salt models at depths of 430 m, 515 m, and 600 m, indicating similar results to Hurtado et al. (1997). Callahan and DeVries (1991) conducted calculations on the closure of disposal rooms backfilled with crushed salt that show closure to essentially intact density in about 25 years. Collectively, these alternate calculations imply that a mean porosity of 5% and an upper limit of 7.5% by 100 years after emplacement are reasonable and conservative values.

The consolidation process will continue after 200 years, particularly for ROM salt that is emplaced dry with minimal compaction. This is accounted for by assigning a third time period, 200 to 10,000 years, during which consolidation of the ROM salt will continue and achieve a porosity similar to that of intact salt regardless of the emplacement strategy. *In situ* observations from the BAMBUS II project at the Sigmundshall mine in Germany indicate consolidation of a crushed salt slurry to essentially an intact condition within tens of years (Bechthold et al., 2004, Figure 2.57). Consolidation to an essentially intact condition is also confirmed by observations at the Rocanville mine, where a consolidated salt plug was emplaced after a water inflow, and has been effective in sealing off a hydrostatic groundwater pressure of about 1200 psi (8.3 MPa) (Van Sambeek et al., 1995). The state of the intact halite at WIPP therefore provides an analog for the long-term consolidated state of ROM salt in a panel entry. Table 2 summarizes the values for porosity of the ROM salt as a function of time.

The values in Table 2 indicate that there is a significant overlap between the porosity ranges for the 100 to 200 year and the 200 to 10,000 year time periods. More specifically, the 2.5% to 5.19% porosity range is included in both time periods, although this range represents the lower end of the porosity range from 100 to 200 years and the upper end of the porosity range from 200 to 10,000 years. This representation is very reasonable because the consolidation process will continue after 200 years, particularly for ROM salt that is emplaced with minimal compaction, and because the JAS3D predictions show that the rate of consolidation decreases significantly after 100 years, making an overlap in the porosity range likely to occur as porosity decreases to *in situ* values.

Table 2. Porosity of the ROM salt during three time periods

Parameter	Time Period	Assumed Porosity	Notes
PCS_T1:POROSITY	0 to 100 years	6.6% to 18.7%	Assumes ROM salt is emplaced with an initial porosity of 20% to 35%. An initial porosity of 35% represents no compaction during emplacement.
PCS_T2:POROSITY	100 to 200 yrs	2.5% to 7.5%	2.5% to 7.5% is consistent with the JAS3D calculations and is conservative relative to alternate computational predictions from several sources.
PCS_T3:POROSITY	200 to 10,000 yrs	0.1% to 5.19%	Assumes that the porosity of crushed salt after 200 years is equal to the porosity for intact halite.

5.1.2 Permeability of ROM Salt

Laboratory experiments on consolidated cores of crushed salt confirm that the intrinsic permeability of crushed salt decreases as the fractional density of the cores increases (Hurtado et al. 1997, Figure 2-1). This observation is corroborated by other experiments on the behavior of crushed salt under similar conditions to WIPP (Case et al., 1987; Zhang et al., 2007); although the cores tested by Zhang et al. (2007) are for salt from the Asse mine and some of the core tested by Case et al. (1987) is for salt from Avery Island, the overall behavior of the crushed material is expected to be similar. The general observations from testing of crushed salt cores are that: (1) intrinsic permeability decreases as the fractional density increases (or as the porosity decreases), (2) crushed salt cores with added moisture generally have lower values of intrinsic permeability than dry cores, and (3) cores of crushed salt with smaller grain sizes generally have lower values of intrinsic permeability than cores with larger grain sizes. The first and third observations are generally valid for all granular materials, while the second observation specifically relates to the microstructure of the salt cores and requires further explanation.

At equivalent fractional densities, dry consolidated salt cores are more permeable than wet consolidated salt cores because of the difference in the mechanism causing consolidation. Under dry conditions, the effective consolidation mechanism is crystal plasticity, while under wet conditions the effective consolidation mechanism is pressure solution/redeposition (Hurtado et al. 1997, page 2-7; Case et al., 1987, Section 4). Pressure solution/redeposition under wet conditions generally produces higher consolidation rates and more deformation than crystal plasticity under dry conditions, leading to lower measured permeability for wet consolidated salt than for dry consolidated salt at equivalent fractional densities (Hurtado et al. 1997, Figure 2-1; Case et al., 1987, data for Test 3 in Figure 1).

During the first time period, from 0 to 100 years, the porosity of the ROM salt varies from 6.6% to 18.7% (see Table 2). Table 3 summarizes permeability data for cores of crushed salt that are relevant to the maximum porosity of 18.7%. The data are from three sources: Hurtado et al. (1997), Case et al. (1987), and Zhang et al. (2007). Hurtado et al. (1997) summarizes data from (Brodsky 1994) and (Brodsky et al., 1996) for wet and dry cores, respectively. The permeability data from the three sources are remarkably consistent and provide a basis for defining the maximum permeability as approximately 10^{-12} m^2 at a porosity of 18.7%.

Table 3. Permeability data for cores of crushed salt at 18.7% porosity

Source	Porosity	Permeability (m^2)	Notes
(Brodsky et al., 1996), summarized in Table 2-1 of (Hurtado et al., 1997)	17.8%	4.11×10^{-13} m^2	For dry WIPP salt at fractional density of 0.822 (porosity of 17.8%). This core has the greatest porosity of the data in (Brodsky et al., 1996) and (Brodsky 1994).
Case et al., 1987, Figure 1	18.7%	1×10^{-13} m^2 to 2×10^{-12} m^2	For dry WIPP salt with 0.9 mm and 10 mm maximum grain sizes (Tests 1 and 2) and for moistened WIPP salt with 20 mm maximum grain size (Test 3).
Zhang et al., 2007, Figure 4	18.7%	2×10^{-13} m^2 to 1×10^{-12} m^2	For dry Asse salt cores with maximum grain size of 32 mm.

At the minimum porosity value of 6.6% during the first 100 years after facility closure, the measurements have a wide range of permeability because of the microstructure of the cores. Table 4 has the measured values that are relevant to a porosity of 6.6%. The gas permeability data for dry cores at 6.6% are relatively consistent from the three sources, falling within a permeability range of 10^{-15} m^2 to 10^{-14} m^2. The brine permeability from Case et al. (1987) is lower than the brine permeability from Hurtado (1994), which may be caused by the maximum grain size for the cores. Test 3 from Case et al. (1987, Table 1) has a maximum grain size of 20 mm, while the maximum grain size of ROM WIPP salt was measured at 1.5 inches (38 mm) (Pettigrew and Associates, 1993), or almost twice as large as the crushed salt for Test 3. Cores with finer grain sizes are expected to have lower permeability than cores with larger grain sizes, which may explain the observed difference in permeability from different sources.

Table 4. Permeability data* for cores of crushed salt at 18.7% porosity

Source	Porosity	Permeability (m^2)	Notes
(Brodsky et al., 1996) & (Brodsky, 1994), summarized in Table 2-1 of (Hurtado et al., 1997)	6.61%	4.95×10^{-15} m^2	For dry WIPP salt at a fractional density of 0.9339 (porosity of 6.61%)(Brodsky et al., 1996)
	6.67%	2.14×10^{-19} m^2	For wet WIPP salt at a fractional density of 0.9333 (porosity of 6.67%)(Brodsky 1994)
Case et al., 1987, Figure 1	6.6%	1×10^{-15} m^2 to 1×10^{-14} m^2	For dry WIPP salt with 0.9 mm and 10 mm maximum grain sizes (Test 1 and Test 2)
	6.6%	1×10^{-21} m^2 to 1×10^{-20} m^2	For wet WIPP salt with 20 mm maximum grain size (Test 3).
Zhang et al., 2007, Figure 4	18.7%	1×10^{-14} m^2	For dry Asse salt cores with maximum grain size of 8 mm.

*Data on fractional density and permeability from (Brodsky, 1994) and (Brodsky et al., 1996) are reproduced with the same number of digits in (Hurtado et al., 1997, Table 2-1) to facilitate identification of specific measurements in the data sets.

The range of permeability for performance assessment should encompass the range of laboratory measurements shown in Tables 3 and 4. At a porosity of 18.7%, the maximum permeability is approximately 10^{-12} m^2. At a porosity of 6.6%, the brine permeability from Hurtado et al. (1997) is about 2×10^{-19} m^2. The brine permeability data from Case et al. (1987) are not used here because the maximum grain size for Test 3, 20 mm, is somewhat smaller than the measured maximum grain size for WIPP salt, 38 mm. We therefore determine that the permeability of the ROM salt should be sampled from a log-uniform distribution, [2×10^{-19} m^2, 10^{-12} m^2], during the first time period, from 0 to 100 years.

During the second and third time periods, the permeability of consolidated ROM salt is based on the experimental measurements of consolidated WIPP salt cores summarized in Hurtado et al. (1997) and further documented in additional Sandia documents (Brodsky, 1994; Brodsky et al., 1996; Ahrens and Hansen, 1995). This analysis uses the brine permeability data from Brodsky (1994) for two reasons. First, the salt cores are based on ROM salt from the WIPP and provide a consistent data set for defining permeability as a function of porosity. Second, the fractional densities of the salt cores measured by Brodsky (1994) have a range of 0.8953 to 1.0051[1] (porosity of 10.47% to ~ 0%, resp.), which encompass the porosity range of interest during the second and third time periods (see Table 2). The alternate data sets are either sparsely populated

[1] A fractional density greater than 1 may imply uncertainty in the assumed density of intact salt.

at the porosities of interest during the second and third time periods or are based on crushed salt with finer grain sizes than ROM salt from the WIPP.

The permeability data from Brodsky (1994) are represented as a function of porosity through a two-step relationship: (1) a least squares fit to the permeability data as a function of fractional density, and (2) a normal distribution that represents the residuals of the data about the least squares fit. This approach captures the mean variability of permeability with porosity and represents the uncertainty in the data set. Figure 6 shows the least squares fit to the data from (Brodsky, 1994). Figure 7 is a quantile-quantile plot showing that a normal distribution provides a good representation of the residuals of the individual data points about the least squares fit. (The closeness of the individual points to the straight line in Figure 7 indicates the goodness of fit by a normal distribution.) This normal distribution has a mean of 0.0 and a standard deviation of 0.86. The parameters for the normal distribution are determined by the data, without adjustment or expert judgment. Given the limited number of data points from Brodsky (1994), the normal distribution will be truncated at plus or minus two standard deviations.

The relationship between porosity and permeability can be mathematically written as:

$$\log(k_e) = -21.187(1-\phi) + 1.5353, \tag{1}$$

$$k = 10^{\log(k_e)+\alpha} = k_e 10^{\alpha}, \tag{2}$$

where k_e is the expected value of permeability from the least squares fit,
ϕ is the sampled value of porosity,
k is the final value of permeability, and
α is the sampled value of a normal distribution with a mean of 0, a standard deviation of 0.86, and truncated at ±2 standard deviations.

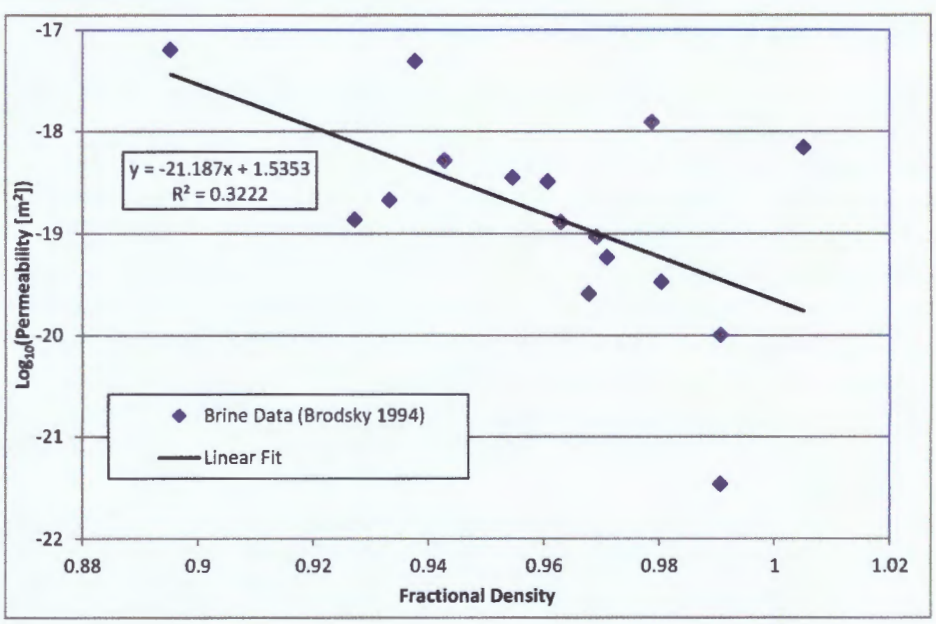

Figure 6. Least squares fit to brine permeability measurements for WIPP crushed salt

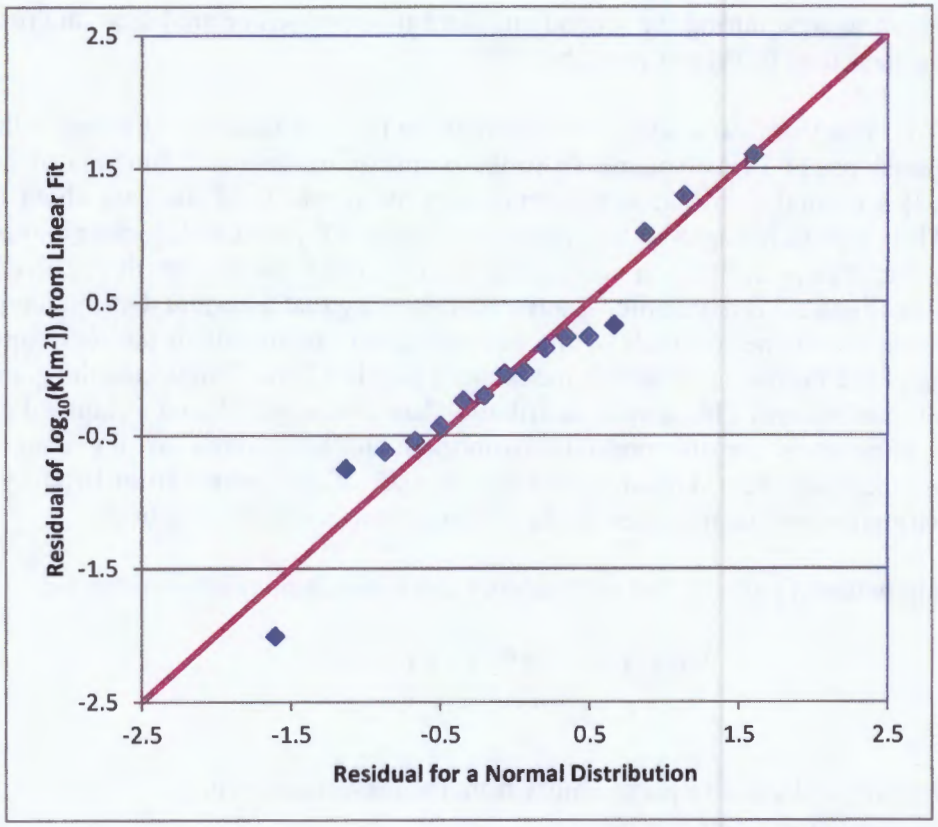

Figure 7. Quantile-quantile plot of the data residuals relative to the linear fit and of the predicted residuals for a normal distribution with mean of 0.0 and standard deviation of 0.86

The following algorithm for representing the values of PCS_T1:PRMX_LOG, PCS_T2:PRMX_LOG and PCS_T3:PRMX_LOG in PA should be used:

1. The value of PCS_T1:POROSITY is sampled from a uniform distribution, [6.6%, 18.7%], in each realization.
2. The permeability [m^2] of ROM salt from 0 to 100 years, PCS_T1:PRMX, is sampled from a log-uniform distribution, [2×10^{-19} m^2, 10^{-12} m^2], in each realization. The values of PCS_T1:PRMY and PCS_T1:PRMZ are set equal to PCS_T1:PRMX.
3. For each realization, the value for PCS_T2:POROSITY between 100 and 200 years is sampled from a uniform distribution with a minimum of 0.025 and a maximum of 0.075. The value for PCS_T3:POROSITY between 200 and 10,000 years is sampled from a uniform distribution with a minimum of 0.001 and a maximum of 0.0519.
4. Calculate the expected values of the $\log_{10}(k_e)$, the logarithm of the expected permeability, using Equation (1) with the sampled values of PCS_T2:POROSITY and PCS_T3:POROSITY.
5. Sample a normal distribution (mean of zero, standard deviation of 0.86) that is truncated at ±2 standard deviations and calculate the final value of the permeability, k, using Equation (2). This calculation is performed twice, once for 100 to 200 years, and a second time for 200 to 10,000 years. This sampling is performed once per realization.

6. The values of PCS_T2:PRMX, PCS_T2:PRMY, and PCS_T2:PRMZ are set equal to the value of k for the second time period. The values of PCS_T3:PRMX, PCS_T3:PRMY, and PCS_T3:PRMZ are set equal to the value of k for the 200 to 10,000 year time period.

Figure 8 shows the range of permeability as a function of fractional density for this algorithm. Table 5 presents numerical values of the minimum, and maximum permeability from 0 to 100 years, from 100 to 200 years, and from 200 to 10,000 years based on this approach. For the latter two time periods, the mean permeability is based on the sampled value of porosity (between 0.025 and 0.075 for 100 to 200 years, and between 0.001 and 0.0519 for 200 to 10,000 years), as defined by the least squares fit (Equation (1)). The minimum and maximum permeability values correspond to -2 and +2 standard deviations on the normal distribution, respectively (Equation (2)).

The 2.5% to 5.19% porosity range is included in both the 100 to 200 year and the 200 to 10,000 year time periods (see discussion in Section 5.1.1), and represents the lower end of the porosity range from 100 to 200 years and the upper end of the porosity range from 200 to 10,000 years. This provides an overlap in the permeability ranges for these two time periods, although the effect is mitigated by sampling the uncertainty in the data about the least squares fit in Figure 8.

With this algorithm, the calculated permeability value for 200 to 10,000 years may be greater than the calculated permeability value for 100 to 200 years. This is not a reasonable outcome, so the permeability value for 200 to 10,000 years should be sampled so that it is never greater than the permeability value for 100 to 200 years.

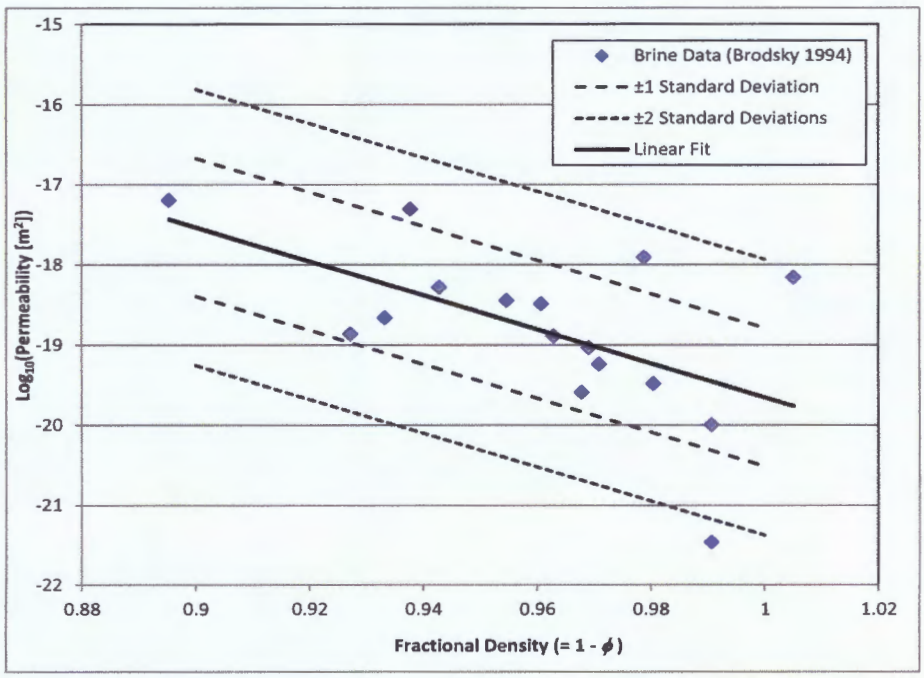

Figure 8. Variation of permeability with fractional density, based on the least squares fit and a normal distribution with a mean of 0.0 and a standard deviation of 0.86

Table 5. Permeability of the ROM salt during three time periods

Parameter(s)	Porosity	Fractional Density	Minimum[a,b] Permeability	Maximum[a,b] Permeability
PCS_T1: PRMX_LOG, PRMY_LOG, PRMZ_LOG	6.6% to 18.7%	0.825 to 0.933	-18.7 (2×10^{-19} m^2)	-12 (1×10^{-12} m^2)
PCS_T2: PRMX_LOG, PRMY_LOG, PRMZ_LOG	0.025	0.975	-20.8 (1.44×10^{-21})	-17.4 (3.96×10^{-18})
	0.075	0.925	-19.8 (1.65×10^{-20})	-16.3 (4.55×10^{-17})
PCS_T3: PRMX_LOG, PRMY_LOG, PRMZ_LOG	0.001	0.999	-21.4 (4.46×10^{-22})	-17.9 (1.23×10^{-18})
	0.0519	0.9481	-20.3 (5.34×10^{-21})	-16.8 (1.47×10^{-17})

[a] Each cell has the log(k[m^2]) and the corresponding value of k in parentheses.
[b] Minimum corresponds to -2 standard deviations below the least squares fit; maximum corresponds to +2 standard deviations above the least squares fit.

The permeability values in Table 5 and Figure 8 are reasonable and appropriate and are supported from several viewpoints:

- From 0 to 100 years, the crushed salt is assigned a permeability range of 2×10^{-19} m^2 to 10^{-12} m^2, representative of the combined test results from Hurtado et al. (1997), Case et al. (1987), and Zhang et al. (2007) for loosely consolidated ROM salt.

- From 100 to 200 years, the permeability range in Table 5 encompasses a wide range of possible outcomes, from a minimum permeability of 1.44×10^{-21} m^2 to a maximum permeability of 4.55×10^{-17} m^2. This range will produce a range of hydrologic responses for the ROM salt, from very "tight" to much "looser" in terms of brine and gas flows across the closure. This wide range has been chosen because of the uncertainties in emplacement of the ROM salt.

- From 200 to 10,000 years, the permeability range in Table 5 represents the response of fully compacted salt, with a minimum permeability of 4.46×10^{-22} m^2 and a maximum permeability of 1.47×10^{-17} m^2. This range of values is purposefully greater than the range for intact halite in PA, which is 10^{-24} m^2 to 10^{-21} m^2. The consolidation mechanisms for moistened versus dry crushed salt are different and can lead to different degrees of interconnected porosity and permeability for a given effective porosity. In this situation, the very low permeability of intact salt may not be attained for thousands of years by the ROM salt.

- After 100 years, the range of permeability in Table 5 is similar to the permeability range for material DRZ_PCS in the PABC-2009, which is 2×10^{-21} m^2 to 1×10^{-17} m^2 (Clayton et al. 2010), as discussed in Section 5.2 of this memorandum. The ranges of permeability after 100 years are therefore consistent with the expected response for a healed DRZ above and below a panel closure, as represented in PABC-2009.

5.1.3 Residual Brine Saturation and Residual Gas Saturation of ROM Salt

The residual gas saturation is the degree of gas saturation necessary to create an incipient interconnected pathway for a porous material to be permeable to gas. The residual gas saturation for all materials in the original shaft seal model, including crushed salt, was defined for the CCA (DOE, 1996, Appendix PAR, Parameter 14). The residual gas saturation was based on a literature review for consolidated geologic materials, concrete, and asphalt, and on professional judgment. Similarly the residual brine saturation for all shaft seal materials, including crushed salt, was defined for the CCA based on a literature review and on professional judgment (DOE, 1996, Appendix PAR, Parameter 15). The residual brine saturation and residual gas saturation of the ROM salt in the PCS will use the same distributions as the corresponding parameters for the crushed salt component of the shaft seals. These distributions are summarized in Table 6.

Table 6. Residual brine saturation and residual gas saturation of the ROM salt

Parameter	Distribution
PCS_T1:SAT_RBRN PCS_T2:SAT_RBRN PCS_T3:SAT_RBRN	Cumulative distribution: **Probability Value** 0.0 0.0 0.5 0.2 1.0 0.6
PCS_T1:SAT_RGAS PCS_T2:SAT_RGAS PCS_T3:SAT_RGAS	Uniform distribution: Minimum value: 0.0 Maximum value: 0.4

5.1.4 Relative Permeability Model and Capillary Pressure Model for ROM Salt

Several two phase flow models have been implemented in the BRAGFLO code, and the values of the parameters RELP_MOD and CAP_MOD define the relative permeability model and the capillary pressure model for a material, respectively. Most materials mapped to the BRAGFLO grid use a modified Brooks-Corey model for relative permeability, with the exception of the anhydrite Marker Beds and Anhydrite Layers a and b (DOE, 2009, Table PA-4), which switch between the Brooks-Corey and Van Genuchten models for relative permeability. The two phase flow model for the ROM salt will also use the modified Brooks-Corey model, which corresponds to relative permeability model number 4 (i.e., RELP_MOD = 4) (DOE, 2009, footnote to Table PA-4) and use capillary pressure model number 2 (i.e., CAP_MOD = 2), which has a fixed maximum capillary pressure. The choice of these models is independent of the timing of the consolidation process. Table 7 summarizes these values.

Table 7. Relative permeability model and capillary pressure model for the ROM salt

Parameters	Value
PCS_T1:RELP_MOD PCS_T2:RELP_MOD PCS_T3:RELP_MOD	4 (a modified Brooks –Corey model)
PCS_T1:CAP_MOD PCS_T2:CAP_MOD PCS_T3:CAP_MOD	2 (fixed maximum capillary pressure)

5.1.5 Other Two Phase Flow Parameters

Table 8 identifies seven parameters for the relative permeability and capillary pressure models for the ROM salt. All WIPP PA materials use the same values for KPT, PC_MAX, and PO_MIN. The crushed salt materials and concrete-related materials for the original shaft seal model use the same values and distributions for the COMP_RCK, PCT_A, PCT_EXP, and PORE_DIS parameters shown in Table 8. The values or distribution in Table 8 will be used for the ROM salt, independent of the time period.

Table 8. Two phase flow parameters for the ROM salt

Parameter	Description	Type	Value
COMP_RCK	Bulk Compressibility	Constant	8.0×10^{-11} Pa^{-1}
KPT	Flag for permeability determined threshold	Constant	0.0 (dimensionless)
PO_MIN	Minimum brine pressure for capillary model KPC=3	Constant	1.01325×10^{5} Pa
PC_MAX	Maximum allowable capillary pressure	Constant	1×10^{8} Pa
PCT_A	Threshold pressure linear parameter	Constant	0.56 Pa
PCT_EXP	Threshold pressure exponential parameter	Constant	-0.346 (dimensionless)
PORE_DIS	Brooks-Corey pore distribution parameter	Cumulative distribution	Probability Value 0.0 0.11 0.5 0.94 1.0 8.1

5.2 Hydrologic and Pore Compressibility Parameters of the DRZ Surrounding the ROMPCS

5.2.1 Porosity and Permeability of the DRZ

Initially it is expected that the DRZ around the PCS will be no different from that around the disposal rooms, since there will be only very small back stress from the consolidating ROM salt. Calculations for closure of panel entries and consolidation of the ROM salt have been performed for two bounding cases: (1) ROM salt that is emplaced and compacted to 20% porosity (80% fractional density), and (2) ROM salt that is emplaced without compaction to 35% porosity (65% fractional density) (Herrick 2012). The results of these calculations demonstrate that the time dependent backstress does not become appreciable until approximately 200 years after emplacement. While the back stress is low, the state of the DRZ surrounding the PCS will be similar to the state of the DRZ surrounding the disposal rooms, and it is appropriate to maintain the same ranges of DRZ porosity and DRZ permeability above and below the PCS as those around the disposal rooms during the first 200 years. Thus, the porosity of DRZ surrounding the PCS lies between 0.0039 and 0.0548 for the first 200 years (i.e. the same porosity range prescribed for material DRZ_1 in the PABC-2009). The permeability of the DRZ surrounding the PCS has a range of $10^{-12.5}$ m^2 to $10^{-19.4}$ m^2 for the first 200 years.

After 200 years, back pressures will have built up to values of the order of 6 to 10 MPa, as shown in Figures 9 and 10. It has been shown by several authors that fractures in salt will heal rapidly under these levels of stress (e.g., IT Corporation, 1987 and Costin and Wawersik, 1980). For example, Costin and Wawersik state:

- Tensile fractures in salt will heal when subjected to nominal overburden pressures (10-35 MPa), to the extent that the resistance to crack propagation along the pre-existing fracture plane is approximately 70-80% of that through virgin material.
- The healing process takes place rapidly compared to the time scale over which mining or storage in salt occurs.
- The principal mechanism in healing appears to be creep of contact asperities along the fracture surface.

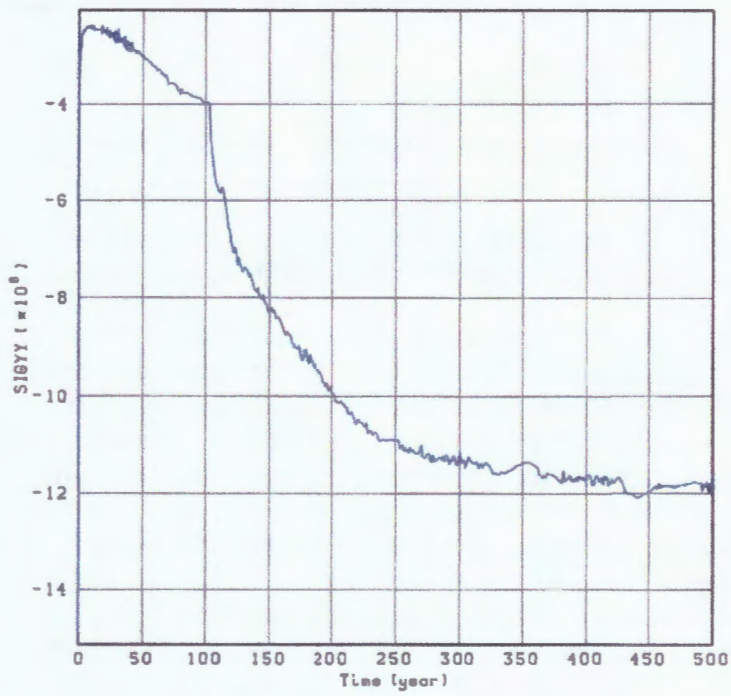

Figure 9. Vertical back stress on the roof of the panel entry for ROM salt with an initial emplacement porosity of 20% (fractional density of 80%) (Herrick 2012)

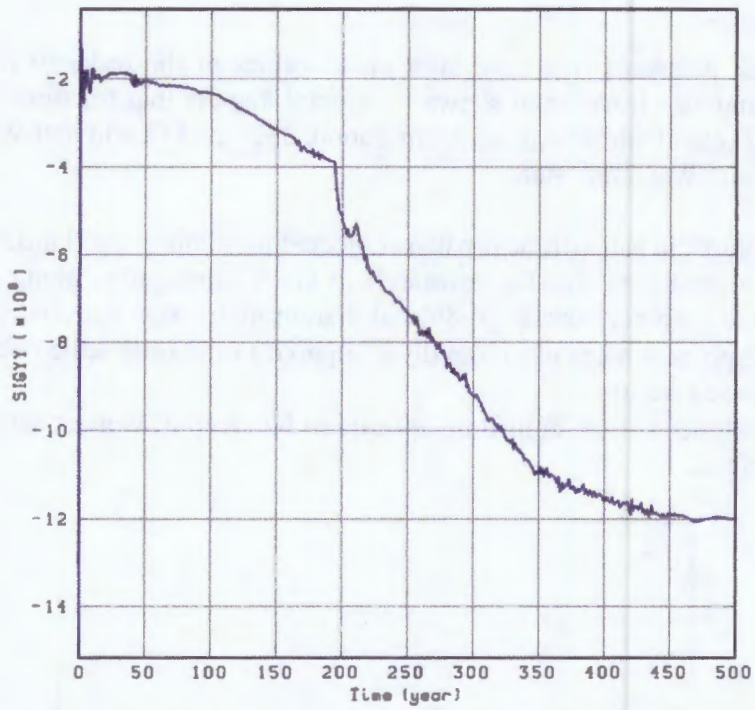

Figure 10. Vertical back stress on the roof of the panel entry for ROM salt with an initial emplacement porosity of 35% (fractional density of 65%) (Herrick 2012)

Given the values of back stress calculated for closures with some degree of emplaced compaction, and the rapid increase of stress even for the most extreme case of salt that is emplaced without compaction (see Figure 10), the back stress is expected to heal the DRZ directly above and below the ROMPCS, reducing its porosity and its permeability. It is then appropriate to assume that the porosity and permeability of the DRZ after 200 years will be equivalent to the state of the DRZ surrounding the Option D panel closure in the PA for CRA-2009 (DOE, 2009, Appendix PA) and in the PABC-2009. The porosity of the DRZ directly above and below the Option D panel closure in the PA for CRA-2009 and in the PABC-2009 has a minimum value of 0.0039 and a maximum value of 0.0548 at all times. The permeability of the DRZ directly above and below the Option D panel closure has a minimum value of 2×10^{-21} m^2 and a maximum value of 1×10^{-17} m^2 (DOE, 2009, Appendix PA, Sections PA-4.2.8.2 and PA-4.2.8.3). We have chosen that these ranges be used for the DRZ surrounding the ROMPCS after 200 years. Table 9 summarizes the ranges for porosity and permeability for the DRZ directly above and below the ROMPCS.

The selected porosity for the DRZ directly above and below the PCS is constant at all times. After 200 years, it is reasonable to expect that the healing of the DRZ caused by increasing back stress will reduce the DRZ porosity. A reduction in DRZ porosity should have minimal impact on the PCS-2012 PA because sensitivity calculations have demonstrated that PA results are insensitive to the porosity of a panel closure, and by extension to the porosity of the DRZ directly above and below the ROMPCS (DOE 2012, Response to EPA Question 1.2b).

Table 9. Porosity and permeability of the DRZ surrounding the PCS

Parameter	Value	Notes
DRZ_PCS_T1:POROSITY DRZ_PCS_T2:POROSITY DRZ_PCS_T3:POROSITY	0.0039 to 0.0548	Same range in the PA for CRA-2009 and the PABC-2009 as for the DRZ (material DRZ_1) around disposal rooms at all times.
DRZ_PCS_T1:PERMEABILITY DRZ_PCS_T2:PERMEABILITY	$10^{-19.4}$ m^2 to $10^{-12.5}$ m^2	Same permeability range in the PA for CRA-2009 and PABC-2009 for the DRZ (material DRZ_1) surrounding disposal rooms from 0 to 200 years.
DRZ_PCS_T3:PERMEABILITY	2×10^{-21} m^2 to 1×10^{-17} m^2	Same permeability range in the PA for CRA-2009 and PABC-2009 for the DRZ_PCS above and below the Option D panel closures after healing of the DRZ.

5.2.2 Two Phase Flow Parameters for Materials DRZ_PCS_T1 and DRZ_PCS_T2

During the first 200 years, while the back stress is low, the state of the DRZ surrounding the PCS will be similar to the state of the DRZ surrounding the disposal rooms, and it is appropriate to maintain the same values for two phase flow parameters for the DRZ directly above and below the ROMPCS as those for the DRZ around the disposal rooms. Table 10 identifies the values for the two phase flow parameters and their sources during the first 200 years.

5.2.3 Two Phase Flow Parameters for DRZ_PCS_T3 After 200 Years

After 200 years, the back pressure from the consolidated ROM salt is expected to heal the fractures in the DRZ directly above and below the PCS. In this state, the DRZ above and below the consolidated ROM salt is expected to have similar properties to the DRZ above and below the Option D monolith in the PA for the CRA-2009 and the PABC-2009. Therefore, the two phase flow parameters for the DRZ directly above and below the ROM salt shall be assigned the same values and distribution as the DRZ_PCS in the PA for CRA-2009 or the PABC-2009. Table 11 identifies the values for the two phase flow parameters and their sources after 200 years.

Table 10. Two phase flow parameters for the DRZ directly above and below the ROMPCS during the first 200 years

Parameter	Description	Value	Source
DRZ_PCS_T1:SAT_RBRN DRZ_PCS_T2:SAT_RBRN	Residual brine saturation	0.0	DOE, 2009, Table PA-3 for material DRZ_1
DRZ_PCS_T1:SAT_RGAS DRZ_PCS_T2:SAT_RGAS	Residual gas saturation	0.0	DOE, 2009, Table PA-3 for material DRZ_1
DRZ_PCS_T1:RELP_MOD DRZ_PCS_T2:RELP_MOD	Relative permeability model number	4 (modified Brooks-Corey model)	DOE, 2009, Table PA-4 for material DRZ_1
DRZ_PCS_T1:CAP_MOD DRZ_PCS_T2:CAP_MOD	Capillary pressure model number	1 (capillary pressure is unbounded)	DOE, 2009, Table PA-4 for material DRZ_1
DRZ_PCS_T1:KPT DRZ_PCS_T2:KPT	Flag for permeability determined threshold	0.0	Stein, SNL, ERMS 520524, Table 2
DRZ_PCS_T1:PO_MIN DRZ_PCS_T2:PO_MIN	Minimum brine pressure for capillary model KPC=3	1.01325×10^5 (Pa)	Stein, SNL, ERMS 520524, Table 2
DRZ_PCS_T1:PC_MAX DRZ_PCS_T2:PC_MAX	Maximum allowable capillary pressure	1.0×10^8 (Pa)	Stein, SNL, ERMS 520524, Table 2
DRZ_PCS_T1:PCT_A DRZ_PCS_T2:PCT_A	Threshold pressure linear parameter	0.0	DOE, 2009, Table PA-3 for material DRZ_1
DRZ_PCS_T1:PCT_EXP DRZ_PCS_T2:PCT_EXP	Threshold pressure exponential parameter	0.0	DOE, 2009, Table PA-3 for material DRZ_1
DRZ_PCS_T1:PORE_DIS DRZ_PCS_T2:PORE_DIS	Brooks-Corey pore distribution parameter	0.7	DOE, 2009, Table PA-3 for material DRZ_1

Table 11. Two phase flow parameters for the DRZ directly above and below the ROMPCS after 200 years

Parameter	Description	Value	Source
DRZ_PCS_T3:SAT_RBRN	Residual brine saturation	0.0	DOE, 2009, Table PA-3 for material DRZ_PCS
DRZ_PCS_T3:SAT_RGAS	Residual gas saturation	0.0	DOE, 2009, Table PA-3 for material DRZ_PCS
DRZ_PCS_T3:RELP_MOD	Relative permeability model number	4 (modified Brooks-Corey model)	DOE, 2009, Table PA-4 for material DRZ_PCS
DRZ_PCS_T3:CAP_MOD	Capillary pressure model number	1 (capillary pressure is unbounded)	DOE, 2009, Table PA-4 for material DRZ_PCS
DRZ_PCS_T3:KPT	Flag for permeability determined threshold	0.0	Stein, SNL, ERMS 520524, Table 2
DRZ_PCS_T3:PO_MIN	Minimum brine pressure for capillary model KPC=3	1.01325×10^5 (Pa)	Stein, SNL, ERMS 520524, Table 2
DRZ_PCS_T3:PC_MAX	Maximum allowable capillary pressure	1.0×10^8 (Pa)	Stein, SNL, ERMS 520524, Table 2
DRZ_PCS_T3:PCT_A	Threshold pressure linear parameter	0.0	DOE, 2009, Table PA-3 for material DRZ_PCS
DRZ_PCS_T3:PCT_EXP	Threshold pressure exponential parameter	0.0	DOE, 2009, Table PA-3 for material DRZ_PCS
DRZ_PCS_T3:PORE_DIS	Brooks-Corey pore distribution parameter	0.7	DOE, 2009, Table PA-3 for material DRZ_PCS

6.0 Summary

The DOE has submitted a planned change request to the EPA proposing that a revised panel closure design be approved for use in all WIPP waste panels. Panel closures are emplaced in the WIPP to protect workers during the operational phase of the facility. They are represented in PA because they are a significant physical feature of the repository. Long-term repository performance has been repeatedly shown to be insensitive to panel closure material properties. The revised panel closure design proposed by the DOE is comprised of 100 feet of run-of-mine salt with barriers at each end. A performance assessment named the PCS-2012 PA is planned to quantify regulatory compliance impacts resulting from the incorporation of the new closure design in the repository. PA materials, properties, and timings are developed to allow for modeling of the revised panel closure system in the PCS-2012. These parameter choices are reasonable values that will adequately represent the PCS within PA, and are based on sound science, modeling, and external data sources where available.

7.0 References

Ahrens, E.H., and F.D. Hansen. 1995. Large-Scale Dynamic Compaction Demonstration Using WIPP Salt: Fielding and Preliminary Results. Sandia National Laboratories. Albuquerque, NM. SAND95-1941.

Bechthold, W., E. Smailos, S. Heusermann ,T. Bollingerfehr, B Bazargan Sabet, T. Rothfuchs, P. Kamlot, J Grupa, S. Olivella, and F. D. Hansen. 2004. *Backfilling and Sealing of Underground Repositories for Radioactive Waste in Salt (BAMBUS II Project)*: final report. European Commission, Directorate General for Research, Office for Official Publications of the European Communities. Call No: EUR 20621 EN. Showcased in Research for Europe: Successful EU-funded projects by the Directorate General for Research.

Blanford, M.L., M.W. Heinstein, and S.W. Key. 2001. JAS3D: A Multi-Strategy Iterative Code for Solid Mechanics Analysis User's Instructions, Release 2.0. Sandia National Laboratories. ERMS 552358.

Brodsky, N.S., 1994. Hydrostatic and Shear Consolidation Tests With Permeability Measurements on Waste Isolation Pilot Plant Crushed Salt. Sandia National Laboratories. Albuquerque, NM. SAND93-7058.

Brodsky, N.S., F.D. Hansen, and T. Pfeifle. 1996. "Properties of Dynamically Compacted WIPP Salt." *Proceedings of the 4th International Conference on the Mechanical Behavior of Salt, Montreal, Quebec, Canada, June 17-18, 1996.* Sandia National Laboratories. Albuquerque, NM. SAND96-0838C.

Callahan G.D. and K.L. DeVries. 1991. Analyses of Backfilled Transuranic Wastes Disposal Rooms. Sandia National Laboratories. SAND91-7052.

Callahan, G.D., M .C. Loken, L.L. Van Sambeek, R. Chen, T.W. Pfeifle, J.D. Nieland, and F.D. Hansen. 1995. Evaluation of Potential Crushed-Salt Constitutive Models. Sandia National Laboratories. Albuquerque, NM. SAND95-2143.

Callahan, G.D. 1999. Crushed Salt Constitutive Model. Sandia National Laboratories, SAND98-2680.

Camphouse, R.C., Clayton, D.J., Kicker, D.C., and Pasch, J.J. 2011. Summary Report for the AP-151 (PC3R) Performance Assessment, Revision 1. Sandia National Laboratories, Carlsbad, NM. ERMS 555489.

Case, John B., Peter C. Kelsall, and James L. Withiam. 1987. *Laboratory Investigation of Crushed Salt Consolidation.* 28th US Symposium on Rock Mechanics, Tucson, Arizona, 29 June – 1 July 1987.

Clayton, D.C., Camphouse, R. C., Garner, J. W., Ismail, A. E., Kirchner, T. B., Kuhlman, K. L., and Nemer, M. B.. 2010. Summary Report of the CRA-2009 Performance Assessment Baseline Calculation, Revision 1. Sandia National Laboratories. Carlsbad, New Mexico, ERMS 553039.

Costin, L.S. and W. R. Wawersik. 1980. Creep Healing of Fractures in Rock Salt. Sandia National Laboratories. SAND80-0392.

DOE (U.S. Department of Energy). 1996. Title 40 CFR Part 191 Compliance Certification Application for the Waste Isolation Pilot Plant. DOE/CAO-1996-2184. U.S. Department of Energy, Waste Isolation Pilot Plant, Carlsbad Area Office. Carlsbad, NM.

DOE (U.S. Department of Energy). 2004. Title 40 CFR Part 191 Compliance Recertification Application for the Waste Isolation Pilot Plant. DOE/WIPP 2004-3231, 10 vols. U.S. Department of Energy, Carlsbad Field Office. Carlsbad, NM.

DOE (U.S. Department of Energy). 2009. Title 40 CFR 191 Parts B and C Compliance Recertification Application. DOE/WIPP-09-3424. Carlsbad Field Office. Carlsbad, New Mexico.

DOE (U.S. Department of Energy), 2011. Panel Closure System Design, Planned Change Request to the EPA 40 CFR Part 194 Certification of the Waste Isolation Pilot Plant. U.S. Department of Energy, Carlsbad Field Office. Carlsbad, New Mexico.

DOE (U.S. Department of Energy), 2012. Response to First Set of EPA Questions to DOE, December 22, 2011. Letter from Mr. Juan Franco, Manager, Carlsbad Area Field Office, U.S. Department of Energy, to Mr. Jonathan Edwards, Director, Radiation Protection Division, U.S. Environmental Protection Agency, dated April 17, 2012.

Dunagan, S. C. 2003. Complementary Cumulative Distribution Functions (CCDFs) for the Technical Baseline Migration (TBM), Revision 0. Sandia National Laboratories, Carlsbad, NM. ERMS 525707.

EPA (U.S. Environmental Protection Agency). 1998. Criteria for the Certification and Re-Certification of the Waste Isolation Pilot Plants Compliance with the 40 CFR Part 191 Disposal Regulations: Certification Decision; Final Rule, *Federal Register*, Vol. 63, No. 95, pp. 27353-27406. U.S. Environmental Protection Agency, Office of Air and Radiation, Washington, D.C.

Hansen, C. W. 2002. Analysis Report for the Panel Closure Impact Assessment. Sandia National Laboratories, Carlsbad, NM. ERMS 523935.

Hansen, F.D. 2003. The Disturbed Rock Zone at the Waste Isolation Pilot Plant. Sandia National Laboratories. Albuquerque, NM. SAND2003-3407.

Herrick, C.G. 2012. JAS3D Calculations Performed in Support of the PCS-2012 PA Parameter Selections. Sandia National Laboratories, Carlsbad, NM.

Hurtado, L.D., Knowles, M.K., Kelly, V.A., Jones, T.L., Ogintz, J.B., and T.W. Pfeifle. 1997. WIPP Shaft Seal System Parameters Recommended to Support Compliance Calculations. Sandia National Laboratories. Albuquerque, New Mexico. SAND97-1287.

IT Corporation. 1987. Laboratory Investigation of Crushed Salt Consolidation and Fracture Healing. Prepared for Office of Nuclear Waste Isolation. BMI/ONWI-631.

MacKinnon R. and G. Freeze, 1997. Supplemental Summary of EPA-Mandated Performance Assessment Verification Test (All Replicates) and Comparison with the Compliance Certification Application Calculations, Sandia National Laboratories, Carlsbad, NM. ERMS 414880. (EPA Docket A-93-02, II-G-28.)

Pettigrew and Associates. 1993. *Sieve Analysis on Salt Backfill Sample #1* and *Sieve Analysis on Salt Backfill Sample #2*. Carlsbad, New Mexico.

RockSol Consulting Group, Inc. 2006. Further Assessment of the Short-term Stability of the 12 Foot Explosion Isolation Wall. Report prepared for Washington TRU Solutions, LLC.

Rothfuchs, Tilmann, and Klaus Wieczorek. 2010. *Backfill Compaction and EDZ Recovery.* US-German Workshop on Salt Repository Research, May 25-28, 2010, Jackson, Mississippi.

Sjaardema, G.D., and R.D. Krieg. 1987. A Constitutive Model for the Consolidation of WIPP Crushed Salt and It's Use in Analyses of Backfilled Shaft and Drift Configurations. Sandia National Laboratories. Albuquerque, NM. SAND87-1977.

Spiers, C.J., J.L. Urai, and G.S. Lister. 1988. "The Effect of Brine (Inherent or Added) on Rheology and Deformation Mechanisms in Salt Rock," *The Mechanical Behavior of Salt, Proceedings of the Second Conference, Federal Institute for Geosciences and Natural Resources, Hanover, Federal Republic of Germany, September 24-28, 1984*, 89 to 102. H.R. Hardy, Jr. and M. Langer (eds.). Clausthall-Zellerfeld, Germany: Trans Tech Publications.

Van Sambeek, L.L., T. J. Eyerman, and F. D. Hansen. 1995. Case Studies of Sealing Methods and Materials Used in the Salt and Potash Mining Industries. Sandia National Laboratories. Albuquerque, NM. SAND95-1120.

Vugrin, E.D. and S.C. Dunagan. 2006. Analysis Package for the Impact Assessment of the Redesigned Panel Closure System, Rev. 0. Sandia National Laboratories. Carlsbad, NM. ERMS 543865.

Vugrin, E., and S. Wagner. 2006. Panel Closure Summary Report. Sandia National Laboratories. Carlsbad, NM. ERMS 544802.

Weatherby, J. R. 1989. Finite Element Analysis of TRU Storage Rooms Filled With Waste and Crushed Salt. Sandia National Laboratories Internal Memorandum to B. M. Butcher, Division 6332, Albuquerque, NM.

Zhang, Chun-Liang, Tilman Rothfuchs, and Johannes Droste, 2007. *Post-tests on thermo-mechanically compacted salt backfill.* The Mechanical Behavior of Salt – Understanding of THMC Processes in Salt, Wallner, Lux, Minkley and Hardy, Jr., Editors.

Date: June 7, 2012

Sandia National Laboratories

Operated for the U.S. Department of Energy by the
Sandia Corporation
Defense Waste Management Programs
4100 National Parks Highway
Carlsbad, New Mexico 88220

To: Paul Shoemaker

From: R. Chris Camphouse (6211)

Technical Review: Dan Clayton

QA Review: Shelly Nielsen

Management Review: Janis Trone

Subject: An overview of the BRAGFLO two-phase flow parameters used to model the run-of-mine salt panel closures implemented in the PCS-2012 PA

Introduction

BRAGFLO Version 6.0 is the WIPP PA code used in the PABC-2009 to calculate brine and gas flows in and around the repository. Version 6.0 is the most recent qualified version of BRAGFLO, and is the code version that will be used for the PCS-2012 PA. BRAGFLO assumes an immiscible water/gas system (Nemer 2007). Immiscible fluids are not capable of mixing and have interfaces across which pressure discontinuities exist. This interfacial tension produces a capillary pressure between the water and gas phases. Capillary pressure modeling is a component of the overall flow modeling implemented in BRAGFLO.

This memo describes the two-phase flow model and the parameters associated with the run-of-mine (ROM) salt panel closures to be implemented in the PCS-2012 (Camphouse et al 2012). Generally, the two-phase flow flags used in BRAGFLO specify the relative permeability model and whether the capillary pressure model is to be used or not for a given material. Capillary pressure, which is a function of saturation and threshold pressure, is used to constrain the brine and gas pressures. Parameters associated with these models must be chosen carefully as they can cause BRAGFLO numerical difficulties. In particular, capillary pressure modeling in BRAGFLO typically causes numerical difficulties when materials undergo instantaneous changes in permeability. Capillary pressure modeling in BRAGFLO is often disabled for these kinds of materials.

BRAGFLO Capillary Pressure Modeling

Several PA parameters are used as part of the capillary pressure modeling implemented in BRAGFLO. The threshold capillary pressure, P_T, characterizes the point at which gas, the non wetting phase, can start to flow in the porous media saturated with brine, and thus defines the capillary pressure at 100%

brine saturation. The capillary pressure must exceed the threshold capillary pressure before the gas phase can start to drain the porous medium and flow.

There are two BRAGFLO material parameters that are used to calculate the threshold capillary pressure for a given material. These two parameters are named PCT_A and PCT_EXP. In BRAGFLO, the practice has been to correlate the threshold capillary pressure to permeability according to (Vaughn 1996)

$$P_T = PCT_A * k^{PCT_EXP}, \quad \text{(Equation 1)}$$

where k is the brine permeability (m^2) in the x direction. A capability was included in BRAGFLO during the preparation of the CCA that provided a dependence of threshold capillary pressure on dynamic changes in permeability. The database parameter KPT is used as a flag that provides an instruction to BRAGFLO to dynamically update the threshold capillary pressure as k changes temporally. Setting KPT = 1 allows threshold capillary pressure to be updated if permeability changes in the material. The quantity P_T is not updated when KPT is set to 0. KPT has been set to 0 for all BRAGFLO materials in the CCA and every PA performed since, so threshold capillary pressure has never been dynamically updated in WIPP PA.

BRAGFLO solves a system of two mass balance equations for brine pressure and gas saturation as well as two constraint equations for saturation and capillary pressure in the calculation of two-phase flow (Nemer 2007). Instantaneous changes in permeability, due to material changes in a grid region, cause difficulty in numerically satisfying the convergence criterion for the capillary pressure constraint equation. When the convergence criterion cannot be satisfied, the capillary pressure model is disabled for the responsible materials so that a convergent solution can be obtained from BRAGFLO. The flag for this is to set PCT_A = 0, which results in the capillary pressure component being disabled. When this occurs, the convention is to also set PCT_EXP = 0.

BRAGFLO grid regions used to represent the ROM salt panel closures in the PCS-2012 will undergo instantaneous changes in permeability. Specifically, the permeability prescribed to these BRAGFLO grid regions will change instantaneously at 100 and 200 years as closure materials change from PCS_T1 to PCS_T2 and from PCS_T2 to PCS_T3 (Camphouse et al 2012). It is currently planned that capillary pressure modeling will be enabled for these materials. However if numerical convergence difficulties are encountered in BRAGFLO, then capillary pressure modeling will be disabled for them.

In addition to properties PCT_A and PCT_EXP, each material in BRAGFLO has a flag named CAP_MOD associated with it. A value of 1 or 2 is prescribed to CAP_MOD in WIPP PA for all BRAGFLO materials. As illustrated in the BRAGFLO Version 6.0 User's Manual (see e.g. Figure 18 and Figure 19), capillary pressure can be unbounded as a function of brine saturation, depending on the relative permeability model employed. A value of CAP_MOD = 2 results in the capillary pressure being bounded above by a maximum value which is assigned to material property PC_MAX. PC_MAX is 1×10^8 Pa by default for all materials in BRAGFLO. The convention used in WIPP PA is to set CAP_MOD = 1 for materials that have capillary pressure disabled, and to set CAP_MOD = 2 otherwise. That is, CAP_MOD = 1 for materials that also have PCT_A = 0. Thus, all BRAGFLO materials in which capillary pressure is used have a default value of 1×10^8 Pa specified for PC_MAX (and have since the CCA).

Property CAP_MOD is denoted as KPC inside the actual BRAGFLO Fortran code. There is a capillary pressure model number 3 (KPC = 3) included in the BRAGFLO Fortran code in which a minimum brine pressure is defined, denoted by P0_MIN. However, while the capillary pressure model 3 (CAP_MOD = 3) was developed and coded in BRAGFLO in preparation for the original certification of WIPP, it has never actually been used in any PA, including the original certification PA. Even though CAP_MOD = 3 has never been used in PA, BRAGFLO still expects a value to be specified for P0_MIN for all materials, so all BRAGFLO materials have a prescribed value of 1.01325×10^5 Pa for property PO_MIN,

A summary of the parameters used in BRAGFLO capillary pressure modeling is provided in the following bulleted list and Table 1:

- In WIPP PA, threshold capillary pressure is defined by Equation (1). The threshold capillary pressure is constant, based on the initial permeability of each material, and has never been dynamically updated as a function of temporal permeability changes. Material property flag KPT has been set to 0 for all BRAGFLO materials since the CCA.
- Capillary pressure modeling is disabled by setting PCT_A = 0. The convention used in PA is to set PCT_EXP = 0 when PCT_A = 0.
- The convention used in PA is to set CAP_MOD = 1 for materials that have the capillary pressure model disabled. CAP_MOD = 2 corresponds to capillary pressure being bounded above by PC_MAX. All BRAGFLO materials have a value of PC_MAX = 1×10^8 Pa prescribed to them.
- CAP_MOD = 3 corresponds to a capillary pressure model that depends on the minimum brine pressure P0_MIN. This model has never been used in any PA, including the original certification PA. BRAGFLO still expects a value to be specified for P0_MIN for all materials, however. The value used for P0_MIN is 1.01325×10^5 Pa.

Table 1: Parameters Used for BRAGFLO Capillary Pressure Modeling

Property	**Description**	**Value** Capillary Pressure Model Enabled	**Value** Capillary Pressure Model Disabled
PCT_A	Threshold Capillary Pressure Linear Parameter	Material Dependent Nonzero Value	0
PCT_EXP	Threshold Capillary Pressure Exponential Parameter	Material Dependent Nonzero Value	0
CAP_MOD	Capillary Pressure Model Number	2	1
PC_MAX (Pa)	Maximum Allowable Capillary Pressure	1×10^8	1×10^8
KPT	Flag for Permeability Determined Threshold Capillary Pressure	0	0
P0_MIN (Pa)	Minimum Brine Pressure for Capillary Pressure Model 3 (CAP_MOD = 3 has never been used in PA)	1.01325×10^5	1.01325×10^5

BRAGFLO Relative Permeability Modeling

The relative permeability model associated with a given material in BRAGFLO is specified by property RELP_MOD. BRAGFLO panel closure materials have been given a value of RELP_MOD = 4 in WIPP PA. RELP_MOD = 4 corresponds to the Second Modified Brooks-Corey Model illustrated in Figure 20 of the BRAGFLO Version 6.0 User's Manual (Nemer 2007) and the discussion pertaining to that figure. In this model, capillary pressure is a function of the effective saturation which depends on the current brine saturation and both the residual brine and gas saturations. The model also depends on a pore size distribution parameter, denoted as property PORE_DIS in WIPP PA. The run-of-mine (ROM) salt panel closures implemented in the PCS-2012 PA, specifically materials PCS_T1, PCS_T2, and PCS_T3, will be assigned a value of RELP_MOD = 4.

The DRZ has two components for the PCS-2012 PA: DRZ_1 and DRZ_PCS. The DRZ region overall (i.e. material DRZ_1) used a value of RELP_MOD = 4 in the PABC-2009. DRZ_PCS models the healed DRZ above and below panel closures, and also uses RELP_MOD = 4. The material properties assigned to material DRZ_PCS are exactly the same as those used for material DRZ_1, with the exception of permeability. The permeabilities are defined by their logarithm in the x, y, and z directions, and denoted by PRMX_LOG, PRMY_LOG, and PRMZ_LOG, respectively (Stein 2002). Materials DRZ_1 and DRZ_PCS will also be used in the PCS-2012 PA, and will use the same relative permeability model (RELP_MOD = 4) and permeability parameters as used in the PABC-2009.

References

Camphouse, R., Gross, M., Herrick, C., Kicker, D., and Thompson, B. 2012. Recommendations and Justifications of Parameter Values for the Run-of-Mine Salt Panel Closure System Design Modeled in the PCS-2012 PA. Memo to WIPP Records Center dated May 3, 2012. Sandia National Laboratories. Carlsbad, NM. ERMS 557396.

Nemer, M. 2007. WIPP PA User's Manual for BRAGFLO, Version 6.0. Sandia National Laboratories. Carlsbad, NM. ERMS 545016.

Stein, J. 2002. Parameter Values for new materials CONC_PCS and DRZ_PCS. Memo to Kathryn Knowles dated February 13, 2002. Sandia National Laboratories. Carlsbad, NM. ERMS 520524.

Vaughn, P. 1996. KPT Modeling Feature. Memo to Martin Tierney dated February 19, 1996. Sandia National Laboratories. Carlsbad, NM. ERMS 235271.

6/14/2012

RESPONSE TO EPA COMMENT DATED JUNE 7, 2012:
Review of Alternate Data Sets for Defining Permeability of Crushed Salt

EPA Comment Dated June 7, 2012:
Please provide an explanation why DOE believes that the current approach of using only the Brodsky 1994 porosity (density) – permeability correlation is appropriate, even though there appears to be additional applicable and relevant data (e.g., Spiers et al 1988) on the salt permeability and density relationship.

EPA-Provided Background
DOE has elected to use the Brodsky 1994 (SAND93-7058) permeability versus density data set to establish permeability ranges for the T2 and T3 times for the ROM salt panel closure.

In addition to the Brodsky 1994 data, our review identified that there are laboratory and in situ permeability test results that may be applicable to the panel closure permeability issue. For example, Hansen et al., 1993 (Figure 4, SAND-93-1348C) and Case et al. 1987 provide additional relevant data. In addition Spiers et al. 1988 reports laboratory results on the constitutive properties of ROM salt which include permeability, porosity/density correlations (pages 82-93) with several correlations dependant on the moisture content and porosity type of the consolidated salt. IT (IT Corporation, 1987) conducted laboratory tests on crushed salt producing permeability with respect to density. The data are given in Table 1 and plotted in Figure 1 below. Figure 2 provides a slightly different perspective.

DOE RESPONSE

1.0 Introduction

The U.S. Department of Energy (DOE) has prepared recommendations for defining the hydrologic parameters for run-of-mine (ROM) salt in a panel entry (Camphouse et al., 2012). The ROM salt will be generated by ongoing mining operations at WIPP. The grain size of the ROM salt is generally less than 1.5 inches, but includes some large pieces of salt between 2 and 6 inches on a side. The ROM salt has a moisture content of 0.5% to 2% by weight, based on recent measurements in the underground (personal communication from Ty Zimmerly of Washington TRU Solutions, 2012). After emplacement in a panel entry, creep closure of the entry is expected to consolidate the ROM salt to a state approaching that of the intact salt in the Salado formation. Given the dynamic nature of this process, DOE has defined the porosity-permeability relationship for ROM salt during three time periods: 0 to 100 years, 100 to 200 years, and 200 to 10,000 years. These time periods are denoted as T1, T2, and T3, respectively.

The DOE's proposed porosity-permeability relationship during the T2 and T3 time periods is based on brine permeability measurements performed by Brodsky (1994). Other investigators have also performed permeability measurements on partly consolidated salt cores from various sites, including Brodsky et al. (1996), Hansen and Ahrens (1996), and Case et al. (1987) using WIPP salt, Spiers et al. (1988) using an engineered salt backfill, Zhang et al. (1987) using salt from the Asse mine in Germany, and Case et al. (1987) using salt from the Avery Island mine in

Kansas. (IT Corporation, 1987) provides additional details on the experiments by Case et al. (1987).

This response provides a critical review of these alternate data sources and explains the DOE's rationale for selecting specific data sets and excluding other data sets in defining the porosity-permeability relationship during T2 and T3. This response also summarizes the DOE's basis for assigning the permeability range of ROM salt during the T1 time period.

2.0 Observations on Long-Term Consolidation of ROM Salt

The studies of Spiers et al. (1988) and Hurtado et al. (1997) demonstrate that permeability measurements of dry salt core in the laboratory are biased toward permeability values that are much greater than would be observed *in situ* for ROM salt in a panel entry during the T2 and T3 time periods. This is an important observation because it implies that laboratory testing with moistened or wet salt core is more relevant to the T2 and T3 time periods than testing with dry core. The technical basis for these statements is summarized here, with additional details provided in Appendix A of this response.

The consolidation of ROM salt in a panel entry occurs in a quasi-static, low strain rate environment over a time scale of 100 years to as much as 300 years. Spiers et al. (1988) carried out a series of experiments to investigate the influence of the quasi-static consolidation process on the microstructure, permeability, and cohesion properties of salt backfill under long-term repository conditions (Spiers et al., 1988, Section 6.3). Based on the results of these "annealing" experiments, they concluded that: (1) the laboratory measurements for the permeability of moistened core versus total porosity gives an upper bound estimate for long-term permeability (Spiers et al., 1988, Section 6.3.4, Item (1)), and (2) the long-term microstructure and physical properties of the salt backfill can be expected to approach those of intact halite (Spiers et al., 1988, Section 6.3.4, Item (2))

The conclusions from the work of Spiers et al. (1988) are confirmed by a number of independent observations:

- *In situ* observations from the BAMBUS II project at the Sigmundshall mine in Germany (Bechthold et al., 2004, Figure 2.57) and at the Rocanville mine (Van Sambeek et al., 1995) indicate consolidation of crushed salt to essentially an intact condition within tens of years. These results confirm that crushed salt can be expected to consolidate to a state approaching that of intact halite, as Spiers et al. (1988) concluded.

- The data from Brodsky (1994) ignore the reduction in permeability that is observed during individual tests (Brodsky, 1994, Tables 5-10 and 5-11). This reduction, which occurred over a typical time scale of 60 days, indicates the potential for slow consolidation to cause pore occlusion that further reduces the long-term permeability of consolidating salt, similar to the effect of the quasi-static annealing mechanism discussed by Spiers et al. (1988).

- Laboratory measurements of permeability with moistened salt core are generally greater than the permeability of intact salt. Measurements by Brodsky (1994) and by Case et al. (1987, Test 3) are generally greater than 10^{-21} m^2, while the permeability of intact salt is represented as less than 10^{-21} m^2 in WIPP performance assessment. This confirms that laboratory measurements provide an upper bound on the permeability of intact halite, as Spiers et al. (1988) concluded.

- The permeability of cores of WIPP crushed salt has been observed to be sensitive to the microstructure of the cores. At equivalent fractional densities, the pressure solution/redeposition observed for moistened core produces more deformation and lower permeability than crystal plasticity, which is observed for dry salt core (Hurtado et al. 1997, Figure 2-1; Case et al., 1987, data for Test 3 in Figure 1). Spiers et al. (1988, Section 3.4 (ii) and (iii)) also observe similar differences in the microstructure of wet- versus dry-compacted material.

DOE's conclusion from the studies of Spiers et al. (1988) and Hurtado et al. (1997) is that laboratory measurements of the permeability of dry salt core are biased toward permeability values that are much greater than would be observed *in situ* for ROM salt in a panel entry during the T2 and T3 time periods. Testing with moistened or wet salt core is more relevant to the T2 and T3 time periods because the long-term annealing caused by quasi-static consolidation of ROM salt in a panel entry results in significant pore occlusion, similar to that found in the microstructure of a wet or moistened core. Note that the long-term mechanism driving annealing, identified as fluid assisted diffusional transfer by Spiers et al. (1988), should occur in ROM salt from the WIPP as well as in salt from other sources.

3.0 Criteria for Selection of Data Sets

In evaluating the various sources of permeability data for crushed salt, the DOE has used the following criteria to define the data sets that are most relevant to ROM salt in a panel entry:

- **Porosity or Fractional Density.** Crushed salt cores are precompacted to a specific porosity or fractional density prior to testing. Cores with porosity or fractional density that falls within the predicted ranges for ROM salt during the T1, T2, or T3 time periods are most relevant for defining permeability. Table 1 defines the predicted porosity ranges of ROM salt as a function of time (Camphouse et al., 2012, Section 5.1.1 and Table 2). Table 1 also defines the corresponding values of fractional density, defined as the ratio of core density to the density of intact salt. In terms of porosity, fractional density equals 1 minus the (total) porosity of the core.

Table 1. Predicted porosities and fractional densities of ROM salt during three time periods

Time Period	Porosity*	Fractional Density**
T1, from 0 to 100 years	6.6% to 18.7%	0.813 to 0.934
T2, from 100 to 200 years	2.5% to 7.5%	0.925 to 0.975
T3, from 200 to 10,000 years	0.1% to 5.19%	0.948 to 0.999

* The range of porosity during T1 is based on the midpoint of the time interval, 50 years.
** Fractional density is defined as 1 minus the (total) porosity.

- **Dry versus Wet Salt.** The measured permeability of dry cores of crushed salt is often significantly greater than the measured permeability for moistened core. DOE believes that the primary cause of this difference is the variation in the microstructure of dry core versus wet core. A secondary cause of this difference is the Klinkenberg effect for "gas slippage" (Bear, 1988, Section 5.3.3). In practice, the Klinkenberg effect is relatively modest and the orders of magnitude difference between wet and dry permeability measurements for salt cores is caused primarily by differences in microstructure.

- **Grain Size.** The grain size of ROM salt from the WIPP site is generally less than 1.5 inches (38 mm), and has a maximum size of 6 inches (150 mm) (personal communication from Ty Zimmerly, Washington TRU Solutions, 2012). However, most cores for laboratory testing use smaller grain sizes. For example, Brodsky used crushed WIPP salt with a maximum grain size of 9.5 mm (Brodsky, 1994, Section 2.2.2). The testing by Spiers et al. (1988) used a backfill with 75-80% mass fraction composed of sieved analytic grade NaCl powder with a grain size of 275±25 μm (0.275±0.025 mm) (Spiers et al., 1988, pp. 81 and 83).

  For porosities above 20%, the permeability of wet or dry core is a function of both porosity and grain size (Case et al., 1987, Section 4). On the other hand, Spiers et al. found that permeability of wet backfill is largely independent of grain size (Spiers et al., 1988, Section 6.2.5). The impact of grain size on permeability measurements for moistened cores of crushed salt is ambiguous at this time.

- **Origin.** Cores based on mined salt from the WIPP site are more relevant that salt cores from other sites, such as the Asse mine in Germany. It is unclear whether or not origin and the presence of impurities is a major factor in permeability measurements.

4.0 Sources of Permeability Data

DOE has considered permeability data for crushed salt from six sources, listed below. The key features of each data set relative to the selection criteria are also summarized.

- Brodsky, 1994. Brine permeability testing with wet cores of WIPP salt (data presented in Figure 1). Porosity range of 0% to 10.5% for the cores is relevant to the T2 and T3 time periods, which have a porosity range from 0.1% to 7.5%. These brine permeability data are directly relevant to the T2 and T3 time periods.

- Brodsky et al., 1996 and Hansen and Ahrens, 1996. Brodsky et al. performed gas permeability testing with dry cores of WIPP salt, and Hansen and Ahrens performed *in situ* testing using a gas permeant (data presented in Figure 1). The porosity range of 6.6% to 17.8% for the cores and *in situ* tests is directly relevant to the T1 time period, which has a porosity range of 6.6% to 18.7%. These data were also considered for the T2 and T3 time periods, although most data points are outside the porosity range for T2 and T3.

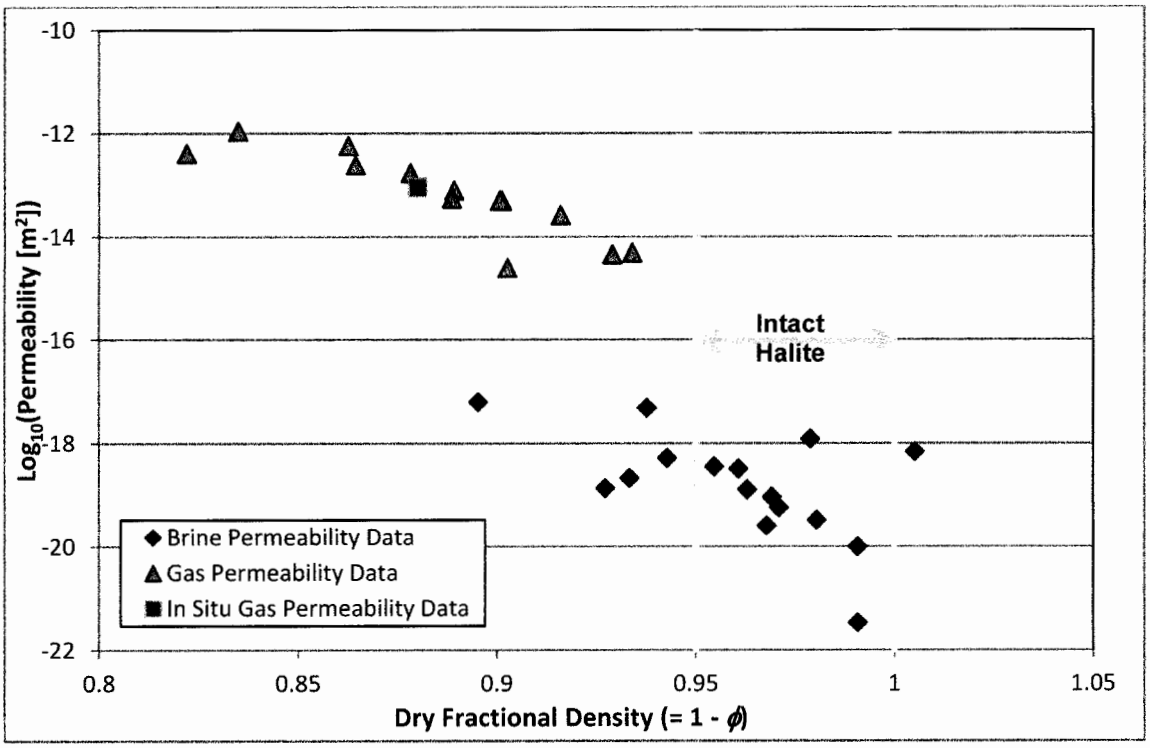

Figure 1. Permeability data from (Brodsky, 1994), (Brodsky et al., 1996), and (Hansen and Ahrens, 1996)

- Case et al., 1987. Gas permeability testing with dry and moistened cores of WIPP salt and with salt from the Avery Island Mine (data presented in Figure 2). The results from Consolidation Test 3 are directly relevant to the T2 and T3 time periods. Test 3 consisted of WIPP salt with a moisture content of 2.3% and a maximum particle size of 20 mm. Test 3 achieved a final porosity of about 5% and a final permeability of about 10^{-6} millidarcy (10^{-21} m^2). The data from Tests 1, 2, and 4 are not relevant to time periods T2 and T3 because these tests used dry cores, but are considered for the T1 time period. The detailed test data are documented in (IT Corporation, 1987).

- Zhang et al., 2007. Crushed salt with maximum grain size of 32-mm was used to create cores with porosity between 7% and 30% (data presented in Figure 3). These results are relevant to the T1 time period, which has a porosity range of 6.6% to 18.7%. Crushed salt with a maximum grain size of 8-mm was used to create dry cores with porosity between 1.5% and 10%. This porosity range is relevant to the T2 and T3 time periods, although the use of salt from the Asse mine and the use of dry core for testing make these data less relevant than the (Brodsky, 1994) data set.

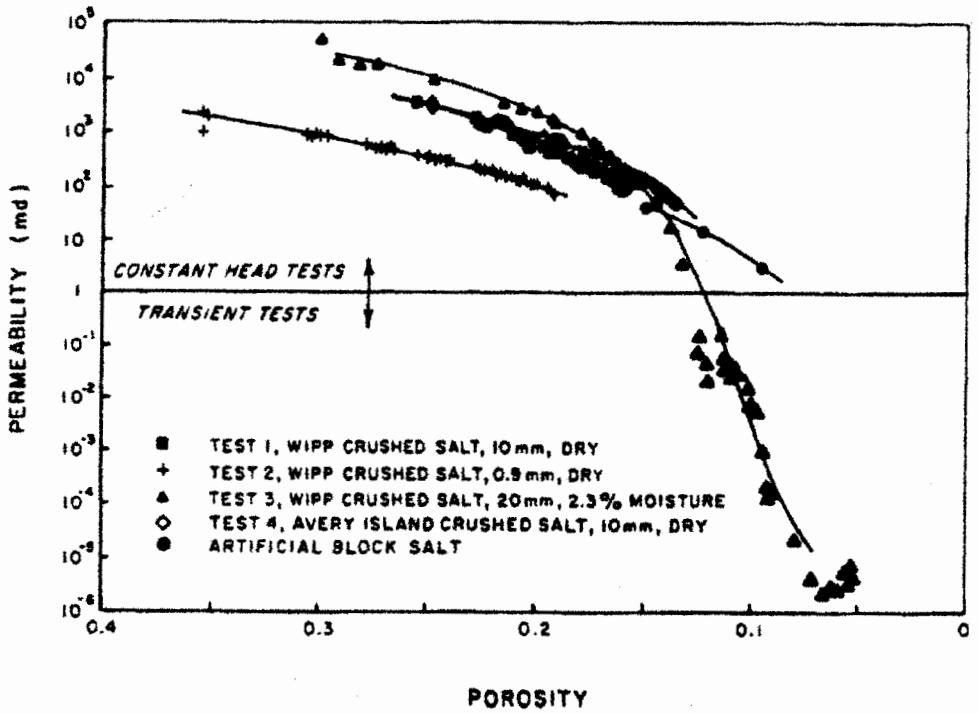

Figure 2. Permeability data from (Case et al., 1987) and (IT Corporation, 1987)

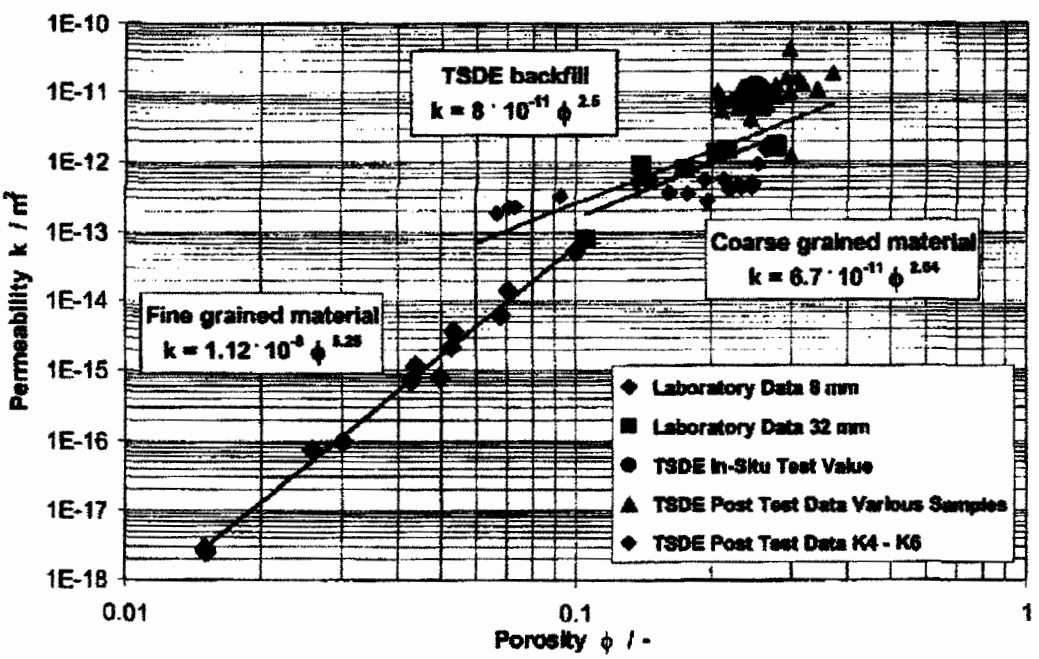

Figure 3. Permeability data from (Zhang et al., 2007)

- Spiers et al., 1988. Spiers et al. conducted a series of experiments on engineered backfill under dry and wet conditions. The engineered backfill had the following composition:

    - Dry backfill: ~ 80% fine salt (275 μm ± 25 μm), ~ 17% coarse salt filler (1 to 5 cm), 2-3% plus Fe_2O_3 (Spiers et al., 1988, Section 6.1)
    - Wet backfill: 75.5% ± 0.5% fine salt (275 μm ± 25 μm), ≈ 14.3% ± 0.5% coarse salt filler (1 cm), 2.5% ± 0.5% anhydrite plus Fe_2O_3, 4.75% ± 0.1 weight percent brine (Spiers et al., 1988, Section 6.2.2).

  Samples were compacted dry to a starting porosity of 38.8% ± 0.5% or 24.8% ± 1% and the prescribed amount of brine was subsequently added. The final value of total porosity for the "Bazooka" experiment with wet backfill is above 6% (Spiers et al., 1988, Figure 6.7) and not directly applicable to the T2 and T3 time periods. The "Bazooka" experiment with dry backfill has four points below 10% porosity (Spiers et al., 1988, Figure 6.2), although the use of dry core for testing make these data less relevant than the (Brodsky, 1994) data set. In addition, the relevance of permeability data for a very fine grained (275 μm ± 25 μm) salt powder relative to the ROM salt from WIPP is unknown at this time.

5.0 Porosity-Permeability Relationship During Time Period T1

The permeability range during T1 is based on data for dry and wet cores from Brodsky (1994), Brodsky et al. (1996), Hansen and Ahrens (1996), Case et al. (1987) and Zhang (2007). The rationale for this approach is that the ROM salt may have undergone minimal compaction or substantial compaction during this initial time period, so test results for dry and wet core have been considered in defining the permeability range during T1.

A porosity-permeability relationship is not defined during the T1 time period. Instead, the limits of the porosity range are used to define the minimum and maximum permeability during T1. More specifically, the minimum porosity of 6.6% during T1 (see Table 1) is the basis for defining the minimum permeability during T1 and the maximum porosity of 18.7% is the basis for defining the maximum permeability during T1. This approach propagates the variability in permeability during the T1 time period into the performance assessment.

Table 2 summarizes the permeability data for cores of crushed salt that are relevant to the maximum porosity of 18.7%. The data are from three sources: Brodsky et al. (1996), Case et al. (1987), and Zhang et al. (2007). The data from Brodsky et al. (1996) provide an upper bound for the data from Brodsky (1994) and from Hansen and Ahrens (1996), so these latter sources are implicitly included in Table 2.

The permeability data in Table 2 are remarkably consistent and provide a basis for defining the maximum permeability during T1 as 10^{-12} m^2. The data from Spiers et al. (1988) for dry or wet core are also consistent with this choice. The permeability of the dry and wet cores is between 10^{-13} and 10^{-12} m^2 at 18.7% porosity (Spiers et al., 1988, Figures 6.2 and 6.7). However, the relevance of testing an engineered backfill with very fine grained (275 μm ± 25 μm) salt powder to WIPP's ROM salt is unclear at this time, so these data are not included in Table 2.

Table 2. Permeability data for cores of crushed salt at 18.7% porosity

Source	Porosity	Permeability (m^2)	Notes
(Brodsky et al., 1996), summarized in Table 2-1 of (Hurtado et al., 1997)	16.5%	1.1×10^{-12} m^2	For dry WIPP salt at fractional density of 0.835 (porosity of 16.5%). This core has the greatest permeability of the data in (Brodsky et al., 1996) and (Brodsky 1994).
Case et al., 1987, Figure 1	18.7%	1×10^{-13} m^2 to 2×10^{-12} m^2	For dry WIPP salt with 0.9 mm and 10 mm maximum grain sizes (Tests 1 and 2) and for moistened WIPP salt with 20 mm maximum grain size (Test 3).
Zhang et al., 2007, Figure 4	18.7%	2×10^{-13} m^2 to 1×10^{-12} m^2	For dry Asse salt cores with maximum grain size of 32 mm.

At the minimum porosity of 6.6%, there is a wide range of permeability because of the microstructure of dry versus wet core. Table 3 summarizes the measured values that are relevant to a porosity of 6.6%. The permeability data in Table 3 for dry cores are relatively consistent, falling within a permeability range of 10^{-15} m^2 to 10^{-13} m^2. The permeability data in Table 3 for wet cores are significantly lower, with a minimum value of 2.26×10^{-21} m^2 from Test 3 of Case et al. (1987). (Numerical values for Test 3 are documented in (IT Corporation, 1987, Appendix D.1).)

Table 3. Permeability data for cores of crushed salt at 6.6% porosity

Source	Porosity	Permeability (m^2)	Notes
(Brodsky et al., 1996) & (Brodsky, 1994), summarized in Table 2-1 of (Hurtado et al., 1997)	6.61% 6.67%	4.95×10^{-15} m^2 2.14×10^{-19} m^2	For dry WIPP salt at a fractional density of 0.9339 (porosity of 6.61%)(Brodsky et al., 1996) For wet WIPP salt at a fractional density of 0.9333 (porosity of 6.67%)(Brodsky 1994)
Case et al., 1987, Figure 1	6.7%	1×10^{-15} m^2 to 1×10^{-14} m^2	For dry WIPP salt with 0.9 mm and 10 mm maximum grain sizes (Test 1 and Test 2)
IT Corporation*, 1987, Appendix D.1, Consolidation Test 3 – Test Data	6.5%	2.26×10^{-21} m^2	Minimum permeability between 5% and 7% porosity for moistened WIPP salt with 20 mm maximum grain size (Test 3).
Zhang et al., 2007, Figure 4	6.6%	7×10^{-15} m^2 9×10^{-14} m^2	For dry Asse salt cores, maximum grain size of 8 mm. For dry Asse salt cores, maximum grain size of 32 mm

*(IT Corporation, 1987) provides numerical data for the results presented in (Case et al., 1987).

The data from Spiers et al. (1988) for dry or wet core lie between 10^{-13} and 10^{-15} m^2 at a porosity of about 6% (Spiers et al., 1988, Figures 6.2 and 6.7). These data have not been included in Table 3 because the relevance of testing an engineered backfill with very fine grained (275 μm ± 25 μm) salt powder to WIPP's ROM salt is unclear at this time.

The minimum value from Test 3 of (Case et al., 1987), 2.26×10^{-21} m^2, has been corrected for the Klinkenberg effect, based on the formulation in the BRAGFLO code (Nemer, 2007, Section 4.12, Equation (139)). The corrected value is 1.07×10^{-21} m^2, based on an average flowing pressure of 500 psi (3.45×10^{6} Pa) (IT Corporation, 1987, Section 3.1.5). The minimum permeability during the T1 time period is based on this value and approximated as 10^{-21} m^2.

In summary, the recommended porosity range during T1 is 10^{-21} m^2 to 10^{-12} m^2. The upper bound is the same value that is recommended in (Camphouse et al., 2012, Section 4.1.2), while the lower bound is reduced by approximately two orders of magnitude from the value in (Camphouse et al., 2012, Section 4.1.2). DOE also recommends that the permeability of the ROM salt during T1 should be sampled from a log-uniform distribution to provide robust representation of the full range of permeability in performance assessment. The sampled value for the permeability of ROM salt is independent of the sampled value for the porosity of ROM salt during the T1 time period.

6.0 Assessment of Data for the Porosity-Permeability Relationship During Time Periods T2 and T3

During the second and third time periods, the permeability of consolidated ROM salt is based on the experimental measurements of Brodsky (1994) because the salt cores are based on ROM salt from the WIPP, because the salt cores are wetted with a brine permeant, resulting in a microstructure that is more similar to quasi-static compaction during T2 and T3 than dry core, and because the initial porosity of the core has a range of 0% to 10.5%, which spans the porosity range of interest during the T2 and T3 time periods, which is 0.1% to 7.5%. The porosity-permeability relationship based on (Brodsky, 1994) is defined in (Camphouse et al., 2012, Section 4.1.2, particularly Figures 5 and 7), and not repeated here.

The alternate data sets identified in Section 4 are less suitable for WIPP performance assessment than the data in (Brodsky, 1994):

- (Brodsky et al., 1996) and (Hansen and Ahrens, 1996) have gas permeability data for WIPP salt in the porosity range of 6.6% to 17.8%. However, only 2 out of 14 data points are within the T2 and T3 porosity range, which is 0.1% to 7.5%. Figure 1 (on page 5) presents the permeability measurements for these two sources and for (Brodsky, 1994).

  DOE's position is that (1) the dry cores do not represent the long-term pore structure of the ROM salt during the T2 and T3 time periods, (2) the porosity range for the dry cores is not applicable to the porosity range of ROM salt during the T2 and T3 time periods, and (3) these gas permeability data represent a distinct data set that should not be combined with the brine permeability data of (Brodsky, 1994). This final point is illustrated in Figure 4, which includes: (1) a fit to the brine permeability data (Brodsky, 1994), shown in purple, (2) a fit to the gas permeability data (Brodsky et al., 1996; Hansen and Ahrens, 1996), shown in green, and (3) a fit to the combined data, shown as a black dashed line.

  The fits to the individual data sets, for brine data only or for gas data only, provide good representations of the mean permeability of these data sets as a function of fractional density. A least squares fit to all the data provides a poor representation of the mean permeability of the individual data sets, in spite of its R^2 value of 0.77, as shown in Figure 4. This poor representation is attributed to the difference in the microstructure of the dry cores for gas permeability testing versus the microstructure of the wet cores for brine permeability testing. DOE believes the gas permeability data represent a separate

and distinct data set that should not be combined with the brine permeability data from (Brodsky, 1994).

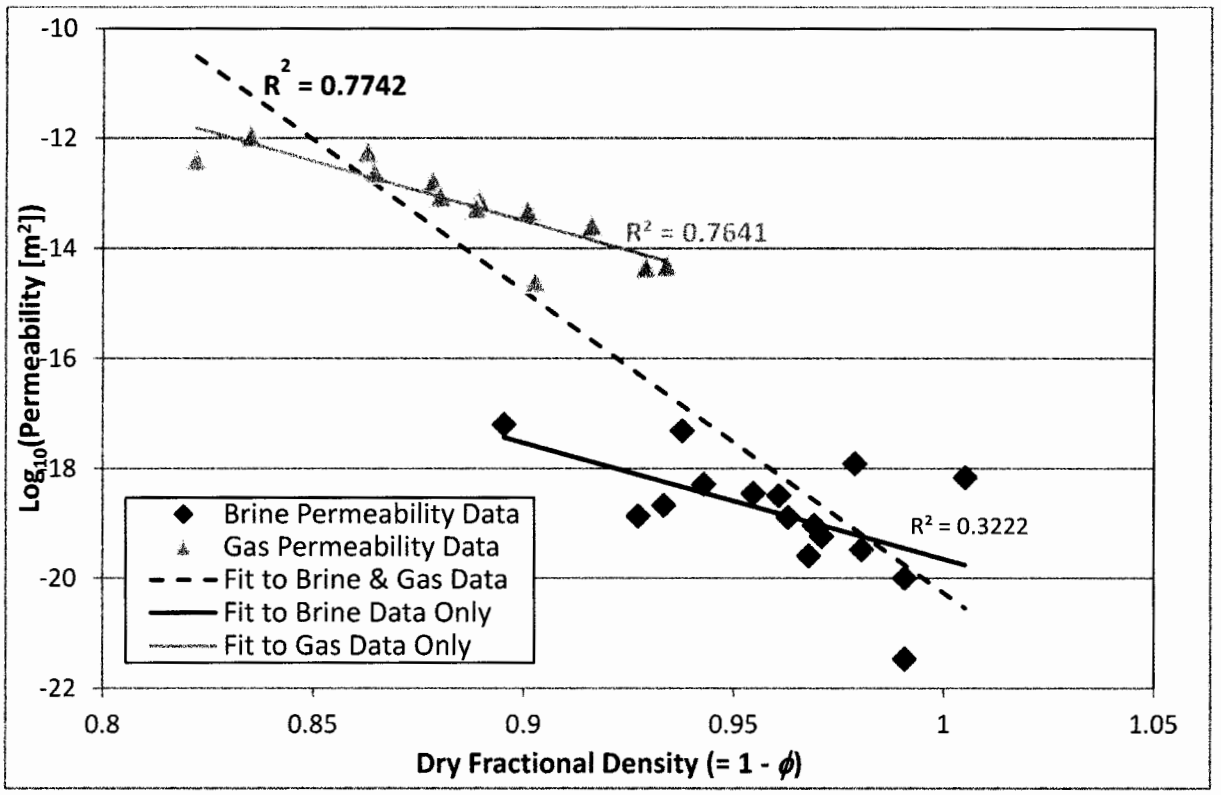

Figure 4. Comparison of least squares fits to the brine permeability data (only), to the gas permeability data (only), and to the combined data sets

- (Case et al., 1987, Table 1) has gas permeability data for two dry cores of WIPP salt with maximum particle sizes of 0.9 mm and 10 mm (Tests 1 and 2), for one core of moistened WIPP salt with maximum particle size of 20 mm (Test 3), and for one dry core of Avery Island Mine salt with maximum particle size of 10 mm (Test 4). Figure 2 (on page 5) presents the permeability measurements for Tests 1 through 4.

  The final porosity of the dry cores is greater than 13.5% (IT Corporation, 1987, Appendix D.1). The DOE position is that the dry cores do not represent the long-term pore structure of the ROM salt during the T2 and T3 time periods and that the porosity range for the dry cores is not applicable to the porosity range of ROM salt during the T2 and T3 time periods. DOE recommends that the data from Tests 1, 2, and 4 of (Case et al., 1987) not be included in the porosity-permeability relationship for ROM salt during the T2 and T3 time periods.

  Figure 5 presents the combined data from Test 3 of (Case et al., 1987) and from (Brodsky, 1994). Figure 5 includes the data from Test 3 with porosity less than or equal to 10.5%, which is the maximum porosity for brine permeability testing in (Brodsky, 1994). Numerical values for Test 3 are available in (IT Corporation, 1987, Appendix D.1,

tabular listing for Consolidation Test 3 – Test Data). These values were corrected for the Klinkenberg effect, using the formulation in the BRAGFLO code (Nemer, 2007, Section 4.12, Equation (139)). Figure 5 also includes least squares fits to the (Brodsky, 1994) data (alone), shown as the purple line, and to the combined data sets from (Brodsky, 1994) and (Case et al., 1987, Test 3), shown as the red line.

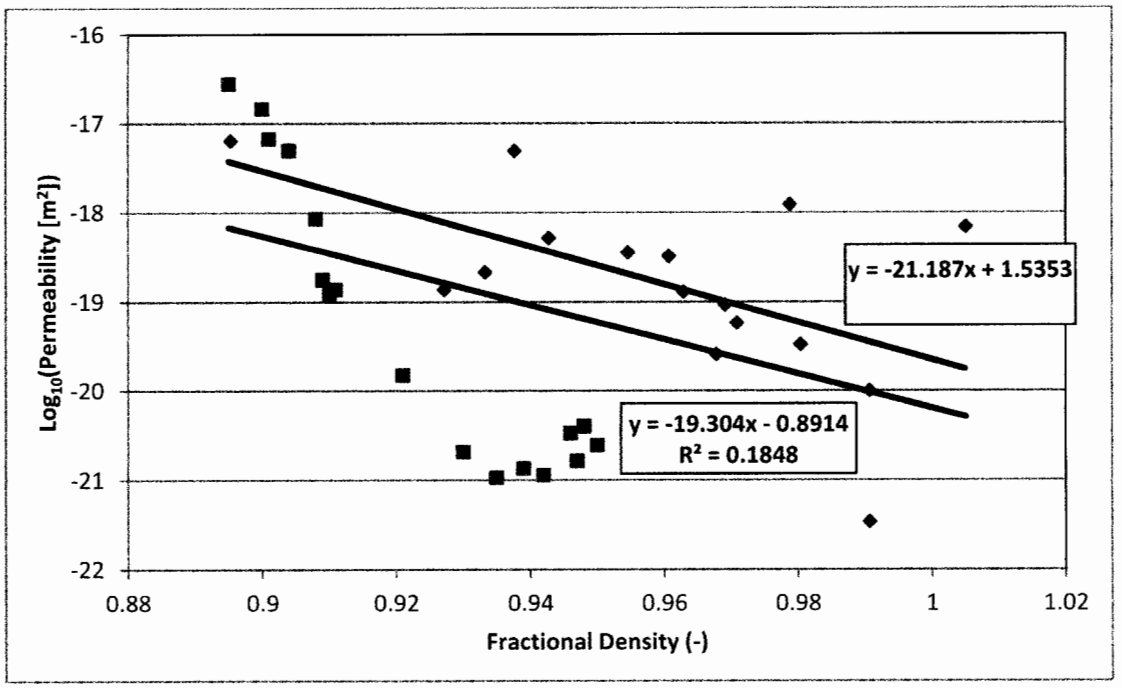

Figure 5. Permeability data from (Case et al., 1987). Data from (Brodsky, 1994) are shown as purple diamonds and data from Test 3 of (Case et al., 1987) are shown as red squares. Purple line is linear fit to (Brodsky, 1994), and red line is linear fit to the combined data sets.

The least squares fits in Figure 5 are rather similar, although the scatter in the combined data set reduces the R^2 value from 0.3222 to 0.1848, implying that there is a weak correlation of porosity and permeability for the combined data set. This is caused, in part, by the fact that the data from Test 3 are skewed to very low values - there are a cluster of 8 points with permeability less than 10^{-20} m^2 from Test 3. The clustering of these points is an artifact of the test procedure, wherein the single core for Test 3 was progressively compressed to lower porosity in a stepwise fashion, and permeability was measured at each of the individual steps. The number of points with permeability less than 10^{-20} m^2 is then a reflection of the test procedure, not an indication of the relative frequency of randomly compacted core samples.

Given the bias toward low permeability in the data from Test 3 and the fact that the data from Test 3 do not represent a random sampling of tests with multiple cores (as is true for the data from (Brodsky, 1994)),, DOE recommends that the Test 3 data should not be combined with the data from (Brodsky, 1994) in defining the porosity-permeability relationship for the ROM salt during the T2 and T3 time periods.

- (Zhang et al., 2007) provide a range of permeability data for Asse salt, including laboratory testing of dry crushed salt cores with maximum grain sizes of 32 mm and 8 mm (see Figure 3 on page 6). The test data for the coarse-grained cores span a porosity range from about 7% to almost 40%, and the fine-grained cores span a porosity range from 1.5% to 10%. DOE's position is that (1) the dry cores do not represent the long-term pore structure of the ROM salt during the T2 and T3 time periods, (2) the porosity range for the dry coarse-grained cores is not applicable to the porosity range of ROM salt during the T2 and T3 time periods, and (3) the cores are based on salt from the Asse mine rather than WIPP salt, although the impact of this difference is unknown. DOE recommends that the data from (Zhang et al., 2007) not be included in the porosity-permeability relationship for ROM salt during the T2 and T3 time periods.

- (Spiers et al., 1988, Figures 6.2 and 6.7) provide permeability testing on cores with an engineered backfill that is composed primarily of very fine grained (275 μm ± 25 μm) salt powder. The total porosity of the moistened cores is greater than 10% and is not relevant to the porosity range for the T2 and T3 time periods. The porosity of the dry cores is as low as 0.4%. DOE recommends that the data from (Spiers et al., 1988) not be included in the porosity-permeability relationship for ROM salt during the T2 and T3 time periods because the relevance of testing an engineered backfill versus the ROM salt at WIPP is unclear and because the pore structure of dry core is not relevant to the long-term pore structure of ROM salt during the T2 and T3 time periods.

DOE recommends that, for the T2 and T3 time periods, the PCS-2012 performance assessment should retain the original porosity-permeability model defined in (Camphouse et al., 2012) using the data from (Brodsky, 1994) alone, without the other data sources discussed in this section.

7.0 Conclusions

DOE has performed a critical review of the permeability measurements from 6 alternate sources: Brodsky (1994), Brodsky et al. (1996), Hansen and Ahrens (1996), and Case et al. (1987) using WIPP salt, Zhang et al. (1987) using salt from the Asse mine in Germany, Spiers et al. (1988) using an engineered salt backfill, and Case et al. (1987) using salt from the Avery Island mine in Kansas.

The review considered the short-term and long-term processes driving changes in the microstructure of the cores. DOE's conclusion from the studies of Spiers et al. (1988) and Hurtado et al. (1997) is that laboratory measurements of the permeability of dry salt core are biased toward permeability values that are much greater than would be observed *in situ* for ROM salt in a panel entry during the T2 and T3 time periods. Testing with moistened or wet salt core is more relevant to the T2 and T3 time periods because the long-term annealing caused by quasi-static consolidation of ROM salt in a panel entry results in significant pore occlusion, similar to that found in the microstructure of a wet or moistened core. Note that the long-term mechanism driving annealing, identified as fluid assisted diffusional transfer by Spiers et al. (1988), should occur in ROM salt from the WIPP as well as in salt from other sources.

During the T1 time period, the permeability range is based on data for dry and wet cores from Brodsky (1994), Brodsky et al. (1996), Hansen and Ahrens (1996), Case et al. (1987) and Zhang (2007). The rationale for this approach is that the ROM salt may have undergone minimal compaction or substantial compaction during this initial time period, so test results for dry and wet core have been considered in defining the permeability range during T1.

A porosity-permeability relationship is not defined during the T1 time period. Instead, the limits of the porosity range are used to define the minimum and maximum permeability during T1. The recommended porosity range during T1 is 10^{-21} m^2 to 10^{-12} m^2. The lower bound of this range, 10^{-21} m^2, is two orders of magnitude less than the lower bound defined in (Camphouse et al., 2012). DOE also recommends that the permeability of the ROM salt during T1 should be sampled from a log-uniform distribution to provide robust representation of the full range of permeability in performance assessment.

During the T2 and T3 time periods, the PCS-2012 performance assessment should retain the original porosity-permeability model defined in (Camphouse et al., 2012) using the data from (Brodsky, 1994) alone. The rationale for this approach is that (1) the linear fit to the (Brodsky, 1994) data has a higher R^2 value, 0.32, than the corresponding value of R^2 for the combined (Brodsky, 1994/Case et al., 1987, Test3) data set, providing a stronger relationship between porosity and permeability; (2) the linear fit to the combined (Brodsky, 1994/Brodsky et al., 1996) data set provides a poor fit to the mean response of the wet core from (Brodsky, 1994), as illustrated in Figure 4. Again, the use of (Brodsky, 1994) data alone provide a stronger relationship between porosity and permeability; and (3) the alternate data sources are less suitable for WIPP performance assessment, as outlined in Section 6 of this document.

8.0 References

Ahrens, E.H., and F.D. Hansen, 1995. Large-Scale Dynamic Compaction Demonstration Using WIPP Salt: Fielding and Preliminary Results. SAND95-1941. Albuquerque, NM: Sandia National Laboratories.

Bear, Jacob, 1988. Dynamics of Fluids in Porous Media. Dover Publications, Inc., New York, New York.

Bechthold, W., E. Smailos, S. Heusermann ,T. Bollingerfehr, B Bazargan Sabet, T. Rothfuchs, P. Kamlot, J Grupa, S. Olivella, and F. D. Hansen. 2004. *Backfilling and Sealing of Underground Repositories for Radioactive Waste in Salt (BAMBUS II Project)*: final report. European Commission, Directorate General for Research, Office for Official Publications of the European Communities. Call No: EUR 20621 EN. Showcased in Research for Europe: Successful EU-funded projects by the Directorate General for Research.

Brodsky, N.S., 1994. Hydrostatic and Shear Consolidation Tests With Permeability Measurements on Waste Isolation Pilot Plant Crushed Salt. SAND93-7058. Albuquerque, NM: Sandia National Laboratories.

Brodsky, N.S., F.D. Hansen, and T. Pfeifle, 1996. "Properties of Dynamically Compacted WIPP Salt," *Proceedings of the 4th International Conference on the Mechanical Behavior of Salt, Montreal, Quebec, Canada, June 17-18, 1996.* SAND96-0838C. Albuquerque, NM: Sandia National Laboratories.

Camphouse, R.C., Gross, M., Herrick, C.G., Kicker, D.C., and B. Thompson. 2012. Recommendations and Justifications of Parameter Values for the Run-of-Mine Salt Panel Closure System Design Modeled in the PCS-2012 PA, Sandia National Laboratories, Carlsbad, New Mexico. May 3, 2012.

Case, John B., Peter C. Kelsall, and James L. Withiam, 1987. *Laboratory Investigation of Crushed Salt Consolidation.* 28th US Symposium on Rock Mechanics, Tucson, Arizona, 29 June – 1 July 1987.

Clayton, D.C., R. C. Camphouse, J. W. Garner, A. E. Ismail, T. B. Kirchner, K. L. Kuhlman, and M. B. Nemer, 2010. *Summary Report of the CRA-2009 Performance Assessment Baseline Calculation,* Revision 1, Sandia National Laboratories, Carlsbad, New Mexico, ERMS 553039.

DOE (U.S. Department of Energy), 2009. Title 40 CFR 191 Parts B and C Compliance Recertification Application. DOE/WIPP-09-3424. Carlsbad Field Office, Carlsbad, New Mexico.

Hurtado, L.D., Knowles, M.K., Kelly, V.A., Jones, T.L., Ogintz, J.B., and T.W. Pfeifle, 1997. WIPP Shaft Seal System Parameters Recommended to Support Compliance Calculations. SAND97-1287. Sandia National Laboratories, Albuquerque, New Mexico.
IT Corporation, 1987.

IT Corporation, 1987. Laboratory Investigation of Crushed Salt Consolidation and Fracture Healing. BMI/ONWI-631. Office of Nuclear Waste Isolation, Battelle Memorial Institute, Columbus, Ohio. January, 1987.

Nemer, M.B. 2007. User's Manual for BRAGFLO, Version 6.0. ERMS 545016. Carlsbad, NM: Sandia National Laboratories.

RockSol Consulting Group, Inc., 2006. "Further Assessment of the Short-term Stability of the 12 Foot Explosion Isolation Wall," Report prepared for Washington TRU Solutions, LLC, June 30, 2006.

Spiers, C.J., Peach, C.J., Brzesowski, R.H., Schutjens, P.M.T.M., Liezenberg, J.J., and H.J. Zwart. 1988. Long-term rheological and transport properties of dry and wet salt rocks. EUR 11848 EN. Final Report. Commission of the European Communities, Directorate-General Science, Research and Development.

Van Sambeek, L.L., T. J. Eyerman, and F. D. Hansen, 1995. *Case Studies of Sealing Methods and Materials Used in the Salt and Potash Mining Industries.* Sandia National Laboratories, Albuquerque, NM. Call No:SAND95-1120.

Zhang, Chun-Liang, Tilman Rothfuchs, and Johannes Droste, 2007. *Post-tests on thermo-mechanically compacted salt backfill.* The Mechanical Behavior of Salt – Understanding of THMC Processes in Salt, Wallner, Lux, Minkley and Hardy, Jr., Editors.

APPENDIX A

Observations on the Long-Term Consolidation of ROM Salt

The consolidation of crushed salt core for laboratory experiments occurs over a much shorter time scale than the consolidation process for run-of-mine (ROM) salt in a panel entry. Individual salt cores may be prepared and consolidated over a day or two, although this is not always the case[1]. The subsequent permeability measurements typically occur over a limited time frame, typically a week to a month. The consolidation of ROM salt, on the other hand, is anticipated to occur over 100 years to as much as 300 years.

Consolidation of ROM salt in a panel entry therefore occurs in a quasi-static, low strain rate environment. Spiers et al. (1988) carried out a series of annealing experiments to investigate the influence of static annealing processes on the micro-structure and permeability of consolidated salt. The rationale for the annealing experiments was:

> *"Examination of the theory of compaction creep by FADT[2] shows that conditions of decreasing strain rate, decreasing effective pressure, and/or decreasing porosity are accompanied by a decrease in the grain-scale free energy gradients driving FADT. Under these conditions, surface energy driving forces will eventually become dominant, giving rise to "static annealing" processes such as static pore occlusion and fluid-assisted grain growth (Coble, 1961). These effects can be expected to have a substantial influence on the micro-structure, permeability and cohesion properties of salt backfill and cement under long term repository conditions...."* (Spiers et al., 1988, Section 6.3)

To investigate this effect, they carried out annealing experiments at elevated temperature (to accelerate the kinetics of mass transfer, and to allow these effects to be seen at laboratory time scales). Typical results quoted show a reduction in permeability of 1.21×10^{-15} m^2 to 9.96×10^{-17} m^2, or about 1 order of magnitude. This was accompanied by a reduction in connected porosity from 5.49% to 3.83%, but no change in total porosity. Spiers et al. conclude that:

> *"Under repository-relevant, pseudo-static conditions .. surface energy driving forces do lead to pore occlusion and grain growth in wet salt backfill and cement. These processes produce substantial permeability reduction, but their kinetics and influence on permeability cannot presently be quantified in a manner appropriate for long term numerical predictions. Nonetheless, the results obtained provide a firm basis for concluding that the κ vs φ_t relation given in equation 6.3[3] gives an upper bound estimate for the long term permeability of the proposed backfill recipe."* (Spiers et al., 1988, Section 6.3.4, Item (1))

---

[1] (Case et al., 1987) performed a stepwise compaction of a single core over approximately 30 days.

[2] Fluid Assisted Diffusional Transfer

[3] Equation 6.3 is the relationship between permeability, κ, and total porosity, ϕ_t.

They also conclude that:

> *"... the long term microstructure and physical properties of these materials can be expected to approach those of natural salt rock ..."* (Spiers et al., 1988, Section 6.3.4, Item (2))

The conclusions from the experimental and theoretical work of Spiers et al. (1988) on annealing processes are corroborated by a number of independent observations:

- *In situ* observations from the BAMBUS II project at the Sigmundshall mine in Germany indicate consolidation of a crushed salt slurry to essentially an intact condition within tens of years (Bechthold et al., 2004, Figure 2.57). Consolidation to an essentially intact condition is also confirmed by observations at the Rocanville mine, where a consolidated salt plug was emplaced after a water inflow, and has been effective in sealing off a hydrostatic groundwater pressure of about 1200 psi (8.3 MPa) (Van Sambeek et al., 1995). These results indicate that crushed salt can be expected to consolidate to a state approaching that of intact halite, as Spiers et al. (1988) concluded.

- The data from Brodsky (1994) ignore the reduction in permeability that is observed during individual tests (Brodsky, 1994, Tables 5-10 and 5-11). This reduction, which typically occurred over a typical time scale of 60 days, indicates the potential for processes causing pore occlusion to further reduce the long-term permeability of consolidating salt, similar to the annealing mechanism discussed by Spiers et al. (1988).

- Laboratory measurements of permeability are generally greater than the permeability of intact salt with moistened salt cores. Brodsky (1994) measured the brine permeability of 16 salt cores with porosities between ~0% and 10.5%. Fifteen of these cores had permeability greater than 10^{-21} m^2, which is the upper limit for the permeability of intact halite in WIPP performance assessment. Similarly, the measured permeability for a crushed salt core with 2.3% moisture content was greater than 10^{-21} m^2 for porosity between 5 and 10% (Case et al., 1987, Test 3). These results demonstrate that the permeability in the laboratory for moistened or wet salt cores provides an upper bound on the permeability of intact halite, as Spiers et al. (1988) concluded.

The permeability of cores of WIPP crushed salt has been observed to be sensitive to the microstructure of the cores. At equivalent fractional densities, dry consolidated salt cores are more permeable than wet consolidated salt cores because of the difference in the mechanism causing consolidation. Under dry conditions, the effective consolidation mechanism is crystal plasticity, while under wet conditions the effective consolidation mechanism is pressure solution/redeposition (Hurtado et al. 1997, page 2-7; Case et al., 1987, Section 4). Pressure solution/redeposition generally produces more deformation than crystal plasticity, leading to occlusion of pores and lower permeability for wet consolidated salt than for dry consolidated salt at equivalent fractional densities (Hurtado et al. 1997, Figure 2-1; Case et al., 1987, data for Test 3 in Figure 1).

Spiers et al. (1988, Section 3.4 (ii) and (iii)) also observe significant differences in the microstructure of wet- versus dry-compacted material. Dry compacted material had a highly porous aggregate structure consisting of a more or less randomly packed array of cubes with relatively few contact points and little evidence for plastic deformation or indentation/truncation structures at grain contact points (Spiers et al., 1988, Section 3.4 (ii)). Wet compacted material had a very different microstructure and was observed to have grain-to-grain indentation, contact truncation, grain shape changes, and overgrowth changes on pore walls that provide evidence of fluid assisted diffusional transfer (Spiers et al., 1988, Section 3.4 (iii)).

DOE's conclusion from the studies of Spiers et al. (1988) and Hurtado et al. (1997) is that laboratory measurements of the permeability of dry salt core are biased toward permeability values that are much greater than would be observed *in situ* for ROM salt in a panel entry during the T2 and T3 time periods. Testing with moistened or wet salt core is more relevant to the T2 and T3 time periods because the microstructure of the wet or moistened core has more deformation and more pore occlusion, similar to the effects of long-term annealing caused by quasi-static consolidation of ROM salt in a panel entry. Note that the long-term mechanism driving annealing, identified as fluid assisted diffusional transfer by Spiers et al. (1988), should occur in ROM salt from the WIPP as well as in salt from other sources.

6/15/2012

Text (Partial) of E-Mail to Tom Peake Regarding Capillary Pressure Models

Capillary pressure is a measure of the pressure difference between the non-wetting phase (gas in this case) and the wetting phase (brine), which varies with the saturations of the two phases. The capillary pressure model in BRAGFLO, Version 6.0, may be turned "on" or "off" for various materials in a BRAGFLO grid. The status of the key parameters for the BRAGFLO capillary pressure model in the "on" or "off" condition is summarized in the following table:

Table 1. Key parameters for BRAGFLO capillary pressure model

Capillary Pressure Model is Turned Off	The threshold capillary pressure[1], P_t, is 0, with PCT_A = 0, defined by input, and PCT_EXP = 0, defined by input CAP_MOD = 1, defined by input. PC_MAX is defined by input[2] but not used, and P0_MIN is defined by input[2] but not used.
Capillary Pressure Model is Turned On	The threshold capillary pressure, P_t, is nonzero; PCT_A and PCT_EXP are nonzero values, defined by input. A nonzero value for P_t results in a positive capillary pressure[3], P_c, which is a function of the time-dependent brine saturation. CAP_MOD = 2, defined by input. PC_MAX is defined by input[2] and is an upper bound on the capillary pressure; P0_MIN is defined by input[2] but not used.

Footnotes:

[1] The threshold capillary pressure, P_t, is defined by $P_t = (\text{PCT_A})k^{\text{PCT_EXP}}$, where k is permeability and PCT_A and PCT_EXP are input parameters for each material. The values of PCT_A and PCT_EXP for the PA for the Compliance Recertification Application of 2009 (CRA-2009) and for the PABC-2009 (Clayton et al., 2010) are documented in Table PA-3 of Appendix PA of CRA-2009 (DOE, 2009).

[2] PC_MAX is equal to 10^8 Pascals for all materials but is only used when CAP_MOD = 2. P0_MIN is equal to 1.01325×10^5 Pascals for all materials but has never been used in a performance assessment.

[3] The equation for capillary pressure, P_c, depends on the model for relative permeability for a given material. The models and equations for relative permeability and capillary pressure are documented in Section PA-4.2.1 of Appendix PA of CRA-2009 (DOE, 2009). The relative permeability model is defined by the BRAGFLO input parameter RELP_MOD, whose values are documented in Table PA-4 of Appendix PA of CRA-2009 (DOE, 2009).

References

Clayton, D.J., Camphouse, R.C., Garner, J.W., Ismail, A.E., Kirchner, T.B., Kuhlman, K.L., and M.B. Nemer. 2010. Summary Report of the CRA-2009 Performance Assessment Baseline Calculation. Sandia National Laboratories, Carlsbad, New Mexico. ERMS 553039.

DOE (U.S. Department of Energy), 2009. Title 40 CFR 191 Parts B and C Compliance Recertification Application. DOE/WIPP-09-3424. Carlsbad Field Office, Carlsbad, New Mexico.

Go ahead with the panel closure calculations when ready

Tom Peake to: russ.patterson 06/19/2012 05:08 PM

Cc: "Shoemaker, Paul E", "Leigh, Christi - SNL", "Gross, Mike", Kathleen Economy, Jonathan Walsh, Shankar Ghose, Jonathan Edwards, Alan Perrin, Daniel Schultheisz, Lee.Raymond, Alton.Harris,

From: Tom Peake/DC/USEPA/US

To: russ.patterson@wipp.ws

Cc: "Shoemaker, Paul E" <peshoem@sandia.gov>, "Leigh, Christi - SNL" <CDLEIGH@sandia.gov>, "Gross, Mike" <mike_gross@earthlink.net>, Kathleen Economy/DC/USEPA/US@EPA, Jonathan Walsh/DC/USEPA/US@EPA, Shankar

Russ,
We have reviewed the June 15 information on the permeability (etc.) of the panel closures and we agree with the proposed data values and ranges that you have provided. We also agree that the multi-phase flow flags in BRAGFLO should remain as they have in past performance assessments for this PA (but we will be looking at them for the 2014 PA).

We will be following up with some clarifying questions in the next few weeks related to the information that you have provided, but they won't affect the actual values used.

So, go ahead with the calculations for the PA to support the panel closure rulemaking when you have the analysis plan, etc, ready.

Tom Peake
Director
Center for Waste Management and Regulations
US EPA (6608J)
1200 Pennsylvania Ave, NW
Washington, DC 20460
phone: 202-343-9765

Physical Location and for deliveries:
Room 529
1310 L St, NW
Washington, DC 20005

IMPORTANT NOTICE: The current official version of this document is available via the Sandia National Laboratories WIPP Online Documents web site. A printed copy of this document may not be the version currently in effect.

SANDIA NATIONAL LABORATORIES
WASTE ISOLATION PILOT PLANT

AP-161

Analysis Plan for the 2012 WIPP Panel Closure System Performance Assessment

Task 1.4.1.2

Effective Date: July 2, 2012

Authored by:	Chris Camphouse	*Original signed by Chris Camphouse*	*7/2/12*
	Print Name	Signature	Date
Reviewed by:	Bwalya Malama	*Original signed by Bwalya Malama*	*07/02/12*
	Print Name Technical Reviewer	Signature	Date
Reviewed by:	Shelly Nielsen	*Original signed by Shelly R. Nielsen*	*7-2-12*
	Print Name Quality Assurance Reviewer	Signature	Date
Approved by:	Janis Trone	*Original signed by Janis Trone*	*7/2/12*
	Print Name Department Manager	Signature	Date

© 2012 Sandia Corporation

Table of Contents

1 Introduction and Objectives 4
2 Approach 7
2.1 ROMPCS Model 8
2.2 Calculation Methodology 10
2.3 Reports and Documentation 13
3 Tasks 14
4 Software 15
5 Special Considerations 15
6 Applicable Procedures 16
7 References 16

List of Figures and Tables

Figure 1: A Schematic of the "Option D" Panel Closure 5
Figure 2. Schematic diagram of the revised panel closure design..... 6

Table 1: PCS_T1, PCS_T2, and PCS_T3 Properties to be used in the PCS-2012 PA 9
Table 2: WIPP PA BRAGFLO Scenarios 11
Table 3: PA Intrusion Scenarios Used in Calculating Direct Brine Releases 12
Table 4: Task List and Estimated Schedule for the PCS-2012 PA. 14
Table 5: Codes to be used for the PCS-2012 PA. 15
Table 6: WIPP PA Alpha Cluster 15

1 Introduction and Objectives

The Waste Isolation Pilot Plant (WIPP), located in southeastern New Mexico, has been developed by the U.S. Department of Energy (DOE) for the geologic (deep underground) disposal of transuranic (TRU) waste. Containment of TRU waste at the WIPP is regulated by the U.S. Environmental Protection Agency (EPA) according to the regulations set forth in Title 40 of the Code of Federal Regulations (CFR), Part 191. The DOE demonstrates compliance with the containment requirements according to the Certification Criteria in Title 40 CFR Part 194 by means of performance assessment (PA) calculations performed by Sandia National Laboratories (SNL). WIPP PA calculations estimate the probability and consequence of potential radionuclide releases from the repository to the accessible environment for a regulatory period of 10,000 years after facility closure. The models used in PA are maintained and updated with new information as part of an ongoing process. Improved information regarding important WIPP features, events, and processes typically results in refinements and modifications to PA models and the parameters used in them. Planned changes to the repository and/or the components therein also result in updates to WIPP PA models. WIPP PA models are used to support the repository recertification process that occurs at five-year intervals following the receipt of the first waste shipment at the site in 1999.

WIPP waste panel closures comprise a feature of the repository that has been represented in WIPP PA regulatory compliance demonstration since the Compliance Certification Application (CCA) of 1996. Panel closures are included in the repository as a safety measure during the operational period. In particular, their presence in the repository is a means to protect workers from exposure to two potential hazards: 1) volatile organic compounds that may be present in emplaced waste materials and 2) an explosion which has been hypothesized to occur from gas generation causing methane concentration in the waste panels to reach a sufficiently high level. Panel closures were not developed to isolate radionuclides in the repository after closure. The DOE stated in the CCA (DOE 1996) that *"The panel closure system was not designed or intended to support long-term repository performance."* Panel closures are included in WIPP PA models principally because they are part of the disposal system, not because they play a substantive role in inhibiting the release of radionuclides to the outside environment.

The WIPP was certified to receive TRU waste in 1998. The 1998 rulemaking had several conditions. Condition 1 involved the design of the panel closure system (PCS) implemented in the repository. The DOE presented four design options in the CCA, and

> "The EPA based its certification decision on the condition that DOE implement the most robust design [referred to in the CCA as "Option D"]. The Agency found the Option D design to be adequate, but also determined that the use of a Salado Mass Concrete - using brine rather than fresh water - would produce concrete seal permeabilities in the repository more consistent with the values used in DOE's performance assessment. Therefore, Condition 1 of the EPA's certification requires DOE to implement the Option D PCS at the WIPP, with Salado Mass Concrete" (EPA 1998).

The Option D panel closure system consists of three primary components: 1) a concrete block wall (the explosion wall), 2) open drift, and 3) a concrete monolith. The arrangement and dimensions of these components are illustrated in Figure 1.

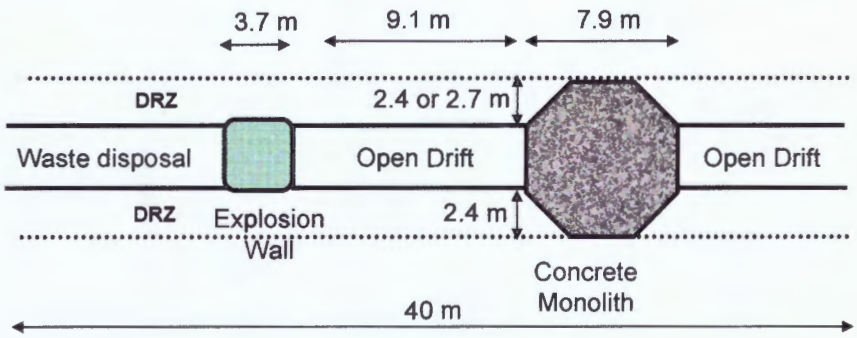

Figure 1: A Schematic of the "Option D" Panel Closure

Extensive refinement to WIPP panel closure modeling in PA has occurred since the implementation used in the CCA (Vugrin and Wagner 2006). In the CCA and the PAVT (MacKinnon and Freeze 1997) that followed, regulatory compliance was demonstrated with a generic panel closure that was not Option D. Following certification of the WIPP in 1998, and the mandate that Option D be implemented as the panel closure in WIPP, a PA was conducted in 2002 (Hansen 2002) with the aim of implementing an Option D panel closure into the repository models used in WIPP PA, and to assess the impacts of panel closure design on long-term repository performance. Two panel closure cases were considered. The first was modeled upon the mandated Option D panel closure design. The second was the generic panel closure design implemented in the CCA and PAVT. Upon completion of the analysis, it was found that total normalized releases resulting from the two panel closure cases were nearly identical. Moreover, nearly identical distributions for each release component were calculated in the two panel closure cases. A more granular representation of the Option D panel closure was developed during the 2002 – 2003 Technical Baseline Migration (TBM) PA. Upon completion of the TBM PA, it was again found that the TBM and PAVT produced releases that are nearly identical, indicating that repository performance is not significantly affected by changes in the panel closure properties (Dunagan 2003). The Option D panel closure representation developed during the TBM was used for the panel closure representation in the 2004 and 2009 Compliance Recertification Applications (CRA-2004 and CRA-2009, respectively).

The DOE has submitted a planned change request (PCR) to the EPA requesting that EPA modify Condition 1 of the Final Certification Rulemaking for 40 CFR Part 194 (EPA, 1998) for the WIPP. Following the selection of the Option D panel closure design in 1998, the DOE has reassessed the engineering of the panel closure and established a revised design which is simpler, easier to construct and equally effective at performing its operational-period isolating function. Accordingly, the PCR submitted to EPA requested that Condition 1 be changed, and that a revised design for the panel closures be approved for use in all panels (DOE, 2011). The revised design of the PCS, known as the Run-of-Mine Panel Closure System (ROMPCS), comprises 100 feet of run-of-mine (ROM) salt with barriers at each end (Figure 2). The ROM salt is generated from ongoing mining operations at the WIPP and may be compacted and/or moistened as it is emplaced in a panel entry. The ROM salt will be emplaced to all salt surfaces (back, walls, etc.)

as completely as practicable. After emplacement, creep closure of the panel entries will cause the ROM salt to consolidate to a condition approaching intact salt, with low porosity and low permeability.

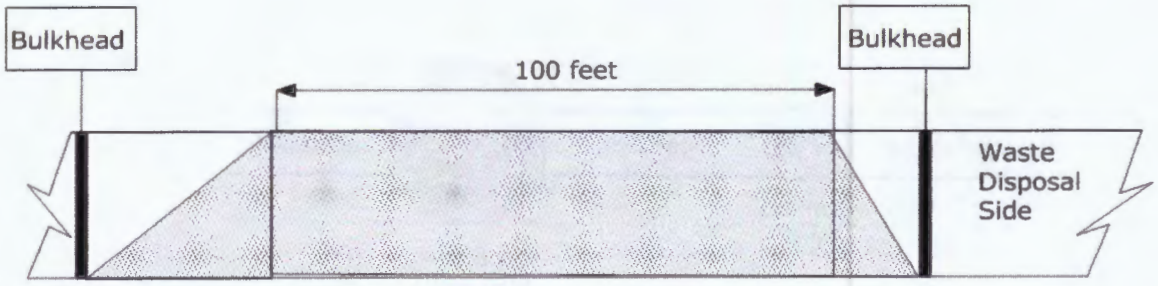

(a) Panel closure with 100 feet of ROM salt between two ventilation bulkheads

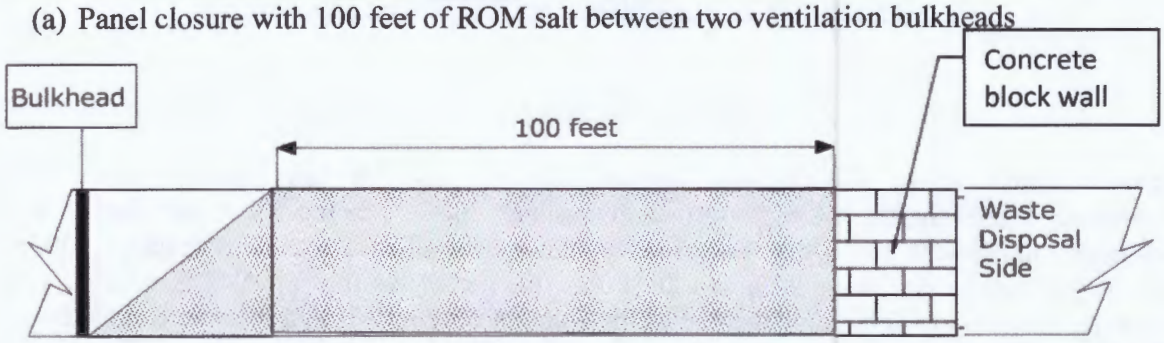

(b) Panel closure with 100 feet of ROM salt between a ventilation bulkhead & explosion wall

Figure 2. Schematic diagram of the revised panel closure design

The barriers will consist of ventilation bulkheads, similar to those currently used in the panels as room closures. The ventilation bulkheads are designed to restrict air flows and prevent personnel access into waste-filled areas during the operational phase. In Panels 1, 2, and 5, where explosion walls fabricated from concrete blocks have already been emplaced in the panel entries, an explosion wall is the inner barrier and a ventilation bulkhead will be the outer barrier, as shown in Figure 2b.

Panel closures are represented in PA by way of their material properties and spatial extent. Due to the regulatory time scale of 10,000 years for which regulatory compliance must be demonstrated, there are uncertainties associated with panel closure material properties. These uncertainties in material properties are incorporated in PA. A material property with an associated uncertainty is assigned a distribution, and this distribution is randomly sampled. This sampling process allows for repository performance to be quantified over a range of material conditions, as well as an analysis of performance sensitivity to changes in material properties. As briefly described above, numerous studies have been conducted to date, often by way of full PA analyses, to quantify the impact of changes in panel closure material properties on regulatory compliance. In addition, several PA analyses have been performed (Hansen 2002, Vugrin & Dunagan 2006, Camphouse et al 2011) with the aim of determining the impact of panel closure redesigns on repository performance. Regulatory compliance has been met in all PA analyses performed to date, including those that incorporated changes to panel closure modeling. Regulatory compliance has been repeatedly shown to be primarily insensitive to panel closure material properties. An additional PA is to be executed that incorporates the ROMPC design

into the current PA baseline established by the 2009 Performance Assessment Baseline Calculation (PABC-2009) (Clayton et al., 2010). The name given to this new panel closure PA is PCS-2012.

The PCS-2012 PA will quantify impacts of the ROMPCS design by comparing total normalized releases to those found in the PABC-2009 where Option D was implemented as the panel closure. The PCS-2012 PA will incorporate material parameters and timings to account for the following physical processes and rock mechanics principles:

1. Creep closure of the salt rock surrounding panel entries will cause consolidation of ROM salt emplaced in panel entries.
2. Eventually, the ROM salt comprising the closures will approach a condition similar to intact salt.
3. As ROM salt reaches higher fractional densities during consolidation, back stress will be imposed on the surrounding rock mass leading to eventual healing of the disturbed rock zone (DRZ).
4. DRZ healing above and below the ROM salt panel closures will reduce DRZ porosity and permeability in those areas.

Calculations and analyses have been performed to develop material properties to be used in the PCS-2012 PA, and are documented in Camphouse (2012), DOE (2012), and Herrick (2012). Potential regulatory compliance impacts resulting from the use of the ROMPCS design in WIPP will be determined by way of a comparison of release probabilities to those calculated in the PABC-2009. Differences seen between the PABC-2009 and the PCS-2012 PA will be a direct consequence of the revised design of the PCS. This document details how SNL will conduct the compliance decision analysis for the PCS-2012 PA.

2 Approach

The PCS-2012 PA analysis will be used to demonstrate compliance of the WIPP repository with the containment requirements according to the Certification Criteria in Title 40 CFR Part 194. A focused set of PA calculations will be executed to determine the impact of the panel closure changes being proposed. The results of PCS-2012 PA calculations will be compared to those obtained in the PABC-2009. The PCS-2012 PA will examine all aspects of repository performance that are potentially impacted by the panel closure design.

The approach used for the PCS-2012 PA will be very similar to that used for PABC-2009 (Clayton 2009). The PCS-2012 PA begins with an assessment that identifies and evaluates the features, events, and processes (FEPs) that are related to the changes introduced by the proposed panel closure design. The purpose of the FEPs evaluation is to determine if the current FEPs baseline (currently the PABC-2009 FEPs baseline) is suitable to evaluate the new closure design, or if changes to FEPs descriptions, screening arguments, or decisions are necessary. The results of this assessment concluded that no changes are needed to the FEPs baseline (Kirkes 2011) [1]. It should be pointed out that the FEPs analysis only determines that the WIPP design features are

[1] Note that Kirkes (2011) also evaluated changes associated with a proposed reconfiguration of the repository layout; the PCS changes are a subset of this FEP evaluation. Only the elements (and FEPs) relating to the PCS redesign are germane to this Analysis Plan and resulting analyses.

appropriately identified, described, and screened according to established FEPs screening methods. WIPP FEPs W109 *Panel Closure Geometry* and W110, *Panel Closure Properties*, are directly related to the changes proposed by the new PCS design and were the focus of the FEPs assessment. These two FEPs have been screened in (represented) as part of previous performance assessments in all scenarios, and continue to be so in the PCS-2012 PA. Any differences in the representation of these FEPs within the WIPP repository model is described in this analysis plan, and proper parameterization of the PCS elements that represent these FEPs is described in Camphouse et al. (2012).

The impacts of the ROMPCS design on regulatory compliance will be determined by a direct comparison of PCS-2012 PA results to those obtained in the PABC-2009. The FEPs baseline utilized in the PABC-2009 will also be applied to the PCS-2012 PA, as no changes were recommended in Kirkes (2011). As such, this will enable a "like for like" comparison between the two analyses, with any compliance impacts seen in the PCS-2012 being solely attributable to the ROMPCS closure design and its material parameters.

The following sections detail the implementation of the PCS-2012 PA with particular attention being given to the way panel closure design changes will be captured in individual PA codes and parameters.

2.1 ROMPCS Model

The PCS-2012 PA will replace the PABC-2009 representation of the Option D panel closure with a representation of the ROMPCS within the WIPP repository model. As discussed in relation to Figure 2, concrete block explosion walls have already been emplaced in waste panels 1, 2, and 5. The ventilation bulkheads used in the ROMPCS are designed to provide isolation only during the operational period. These bulkheads are not expected to remain intact 100 years after repository closure because of creep closure of the panel entries. The explosion wall is also designed for the operational period. These walls are inspected on a regular basis, and their anticipated condition is also assessed through numerical modeling (e.g. RockSol, 2006). Installed explosion walls show surface spalling or slabbing of the concrete blocks as a result of the loading caused by inward creep of the salt. Numerical stress analysis of the concrete explosion wall has demonstrated that the free faces and the rib contacts will be in a condition of plastic yield with an unyielded core by 7 years after emplacement (Rocksol, 2006, Figures 7 and 10). No long term stress analyses have been carried out; however, it is expected that the spalling and yield will be progressive, and that the walls will not be significant structures after the initial 100 year time period, due to the brittle, non-plastic behavior of concrete. The ventilation bulkheads and explosion walls will therefore have no significant impact on long-term performance of the panel closures and are therefore not included in the PCS-2012 PA representation of the ROMPCS. Consequently, the ROMPCS will be modeled as consisting of 100 feet of ROM salt.

The ROMPCS properties will be based on three time periods: from 0 to 100 years, from 100 years to 200 years, and from 200 years to 10,000 years. This is a refinement to the granularity of panel closure modeling undertaken in the 2006 PCS PA (Vugrin and Dunagan 2006) and the 2011 PC3R PA (Camphouse et al 2011). Three time periods are appropriate because the process to consolidate the ROM salt occurs over a primary time scale of approximately 100 years, while the process to heal fractures in the DRZ surrounding the PCS occurs over a longer time scale of

approximately 200 years. The ROM salt will therefore be represented by three materials, denoted as PCS_T1 for the first 100 years, PCS_T2 for 100 to 200 years, and PCS_T3 for 200 to 10,000 years. Analyses and calculations have shown (Camphouse et al 2012) that the time-dependent back stress imposed on the DRZ by the re-consolidated ROM salt panel closure does not become appreciable until roughly 200 years after emplacement of the ROM salt in the drift. As a result, it is reasonable and appropriate to maintain the same properties for the DRZ above and below the ROMPCS for the first 200 years after closure as are specified to the DRZ surrounding the disposal rooms. After 200 years, the DRZ above and below the ROMPCS will be modeled as having healed, and this sub-region of the DRZ will be represented by material DRZ_PCS. Material DRZ_PCS was developed during the TBM PA to represent healed DRZ above Option D panel closures (Stein 2002). Material DRZ_PCS has been used since the TBM PA to represent healed DRZ regions above and below panel closures, and will be used in the PCS-2012 to maintain consistency in material names with prior analyses.

The effective permeability and porosity of the ROMPCS are the two parameters expected to have the greatest impact on calculations of pressure and brine saturation in repository waste areas. Consequently, materials PCS_T1, PCS_T2, and PCS_T3 will be assigned porosities and permeabilities appropriate for representation of the ROMPCS. Properties specified for material DRZ_PCS will be identical to those used in the PABC-2009 PA. BRAGFLO calculations require that two-phase flow properties be specified for all materials. A brief discussion of the two-phase flow parameters used for PCS_T1, PCS_T2, and PCS_T3, particularly their implementation in regard to BRAGFLO capillary pressure modeling, is given in Camphouse (2012). A full list of properties to be established for materials PCS_T1, PCS_T2, and PCS_T3 is given in Table 1. In addition to the properties listed in Table 1, the initial brine saturation of the ROMPCS will be specified. This parameter corresponds to property SAT_IBRN for material PCS_T1. With the exception of these parameters, the PCS-2012 PA will use the same parameters and parameter values that were used for the PABC-2009 (Clayton 2009).

Table 1: PCS_T1, PCS_T2, and PCS_T3 Properties to be used in the PCS-2012 PA

Property	Description
CAP_MOD	Capillary Pressure Model Number (CAP_MOD = 1 or 2 has been used in every PA to date for all materials in BRAGFLO)
COMP_RCK	Bulk Compressibility
KPT	Flag to Enable Dynamic Updating of Threshold Capillary Pressure as a Function of Permeability (KPT = 0 has been used in every PA to date for all materials in BRAGFLO)
PC_MAX	Maximum Allowable Capillary Pressure (PC_MAX = 1 x 10^8 Pa has been used for all BRAGFLO materials since the CCA)
PCT_A	Threshold Capillary Pressure Linear Parameter
PCT_EXP	Threshold Capillary Pressure Exponential Parameter
PO_MIN	Minimum Brine Pressure for Capillary Model 3 (CAP_MOD = 3 has never been used in PA)

Property	Description
PORE_DIS	Brooks-Corey Pore Distribution Parameter
POROSITY	Effective Porosity
PRMX_LOG	Log of Intrinsic Permeability, X-Direction
PRMY_LOG	Log of Intrinsic Permeability, Y-Direction
PRMZ_LOG	Log of Intrinsic Permeability, Z-Direction
RELP_MOD	Relative Permeability Model Number
SAT_RBRN	Residual Brine Saturation
SAT_RGAS	Residual Gas Saturation

2.2 Calculation Methodology

2.2.1 Rationale

The aim of the PCS-2012 PA is to quantify regulatory compliance impacts associated with the ROMPCS design. Impacts will be determined by direct comparison of PCS-2012 PA results to the current compliance baseline established by the PABC-2009. To enable the direct comparison of results obtained in the two analyses, the PCS-2012 PA is constructed so that the structure of calculations performed are as similar as possible to that used in the PABC-2009. To that end, the PCS-2012 PA will utilize the same waste inventory information, intrusion scenarios, drilling rate and plugging pattern parameters, radionuclide solubility parameters, and hydrologic transmissivity fields as were used in the PABC-2009. The PCS-2012 PA will consist of a full set of PA compliance calculations. That is, three replicates of PA calculations, each replicate consisting of 100 vectors, will be performed. The random seeds from the PABC-2009 will be preserved so that results from the PCS-2012 PA analysis can be compared to those from the PABC-2009 on a vector-by-vector basis.

The design of the ROMPCS potentially alters pressure profiles in repository waste regions as compared to Option D design implemented in the PABC-2009. Pressure changes in the waste panels translate directly to changes in spallings releases as pressure changes yield changes in spallings volumes. Moreover, pressure changes in waste areas potentially alter the influx of brine into these regions, corresponding to changes in brine saturation. Direct brine releases are a function of pressure and brine saturation at the time of intrusion. Two conditions must be met for a DBR to occur. First, the brine saturation in the intruded panel must exceed the residual brine saturation of the waste, a sampled parameter in PA. Second, the repository pressure near the drilling location must exceed the hydrostatic pressure of the drilling fluid, which is specified in PA to be 8 MPa. The combined impact of pressure and brine saturation changes resulting from implementation of the ROMPCS potentially alters the released brine volume associated with a particular intrusion event as compared to the PABC-2009. The potential for changes to released brine volumes translates directly to changes in DBRs. For these reasons, spallings and DBRs are the primary release mechanisms of interest in the PCS-2012 PA. Changes to the panel closure design have no impact on releases due to cuttings and cavings. Transport releases through the Culebra had virtually no impact on total normalized releases in the PABC-2009 (Clayton et al 2010). Implementation of the ROMPCS will not change this result. In addition, hydrologic transmissivity fields are not being updated as part of the PCS-2012 PA. Consequently, Culebra transport results obtained in the PABC-2009 will also be used in the PCS-2012 PA.

The calculations to be conducted for the PCS-2012 PA are listed below. Results generated from the PABC-2009 will be used for codes not discussed below.

2.2.2 Parameter Sampling: LHS

Three replicates of 100 vectors will be created using the computer code LHS. LHS version 2.42 will be used for the PCS-2012 PA, which is the same code used for the PABC-2009. The random seed and parameter ordering from the PABC-2009 will be used for the PCS-2012 PA. Use of the PABC-2009 random seeds and ordering will result in identical sampled parameter values for parameters that are common to both the PCS-2012 PA and the PABC-2009. This approach enables comparison of the PCS-2012 PA and the PABC-2009 on a vector-by-vector basis.

PA material CONC_PCS was used in the PABC-2009 to represent the concrete monolith component of the Option D panel closure. In the PCS-2012 PA, material CONC_PCS will be replaced by materials PCS_T1, PCS_T2, and PCS_T3 and their corresponding properties. Distributions prescribed to these three materials are listed in Camphouse et al (2012).

2.2.3 Salado Flow: BRAGFLO

The two-phase flow code BRAGFLO simulates the brine and gas flow in and around the WIPP repository and incorporates the effects of disposal room closure, gas generation, brine consumption, and inter-bed fracturing in response to gas pressure. The results of BRAGFLO scenarios S1-BF to S5-BF are used as input for the subsequent calculation of Salado radionuclide transport, DBRs, and spallings releases. BRAGFLO scenario S6-BF is used in the calculation of radionuclide transport to the Culebra. The scenarios modeled in BRAGFLO are listed in Table 2.

Table 2: WIPP PA BRAGFLO Scenarios

Scenario	# of Drilling Intrusions	Time of Intrusion (Years)	Castile Brine Pocket encountered
S1-BF	0 (Undisturbed)	NA	NA
S2-BF	1	350	Yes
S3-BF	1	1,000	Yes
S4-BF	1	350	No
S5-BF	1	1,000	No
S6-BF	2	1,000 and 2,000	Only at 2,000

Implementation of the ROMPCS will slightly alter the BRAGFLO computational grid and material map that were used in the PABC-2009. In particular, Option D panel closures represented in the PABC-2009 BRAGFLO grid will be replaced by panel closures consisting of ROM salt for the PCS-2012 PA. Healing of the DRZ directly above and below redesigned panel closures as discussed in Section 1 will also be captured in PCS-2012 PA calculations. Finally, the Option D panel closure implemented in the PABC-2009 is 40 meters long (Figure 1) while the ROMPCS modeled in the PCS-2012 is 100 feet (30.48 meters) long. The PABC-2009

BRAGFLO grid will be modified slightly to account for the reduction in length of the ROMPCS as compared to Option D.

A complete suite of BRAGFLO calculations will be executed for the PCS-2012 PA. These calculations will consist of 3 replicates, 100 vectors per replicate, and 6 scenarios (see Table 2) per vector. The codes PREBRAG version 8.0, BRAGFLO version 6.0 and POSTBRAG version 4.00A will be used for the PCS-2012 PA, which are the same codes used for PABC-2009.

2.2.4 Spallings: DRSPALL and CUTTINGS_S

Repository pressures may be affected by the implementation of the ROMPCS design. Changes in repository pressures have the potential to impact spallings results. Consequently, spallings releases for the PCS-2012 PA may differ from those found in the PABC-2009 due to differences in repository pressures calculated by BRAGFLO. Spallings volumes from a single borehole intrusion are calculated by code DRSPALL at initial repository pressures of 10, 12, 14, and 14.8 MPa. DRSPALL calculations that were utilized to generate spallings volumes at these pressures in the PABC-2009 will also be used in the PCS-2012 PA. The PCS-2012 PA will use the same procedure as was used for the PABC-2009 to interpolate between these DRSPALL volumes to calculate spallings volumes corresponding to a particular drilling intrusion. The initial repository pressure for a given scenario, time, location, and vector will be retrieved from the BRAGFLO results, and CUTTINGS_S will use this initial pressure to calculate a spallings volume for each scenario, time, location, and vector combination by interpolating between DRSPALL results. The code CUTTINGS_S version 6.02 will be used for the PCS-2012 PA, which is the same code used for the PABC-2009.

2.2.5 Direct Brine Releases: BRAGFLO

In addition to its role as a tool used to simulate brine and gas flow in and around the WIPP repository, BRAGFLO is also used in PA to calculate DBR volumes. As the implementation of the ROMPCS design potentially impacts pressures and brine saturations in waste-containing repository regions, DBR calculations will be performed as part of the PCS-2012 PA. The numerical grid and material map used to calculate DBRs will be updated to reflect the ROMPCS design. Conditions required for the initiation of a DBR release will remain unchanged from the PABC-2009, and the DBR volumes will be calculated for the same scenarios and times (Table 3) used in that analysis. The codes PREBRAG version 8.0, BRAGFLO version 6.0 and POSTBRAG version 4.00A will be used for the PCS-2012 PA, which are the same codes used for the PABC-2009.

Table 3: PA Intrusion Scenarios Used in Calculating Direct Brine Releases

Scenario	Conditioning (or 1st) Intrusion Time (year) and Type	Intrusion Times – Subsequent (year)
S1-DBR	None	100, 350, 1000, 3000, 5000, 10000
S2-DBR	350, E1	550, 750, 2000, 4000, 10000
S3-DBR	1000, E1	1200, 1400, 3000, 5000, 10000
S4-DBR	350, E2	550, 750, 2000, 4000, 10000
S5-DBR	1000, E2	1200, 1400, 3000, 5000, 10000

2.2.6 CCDF Construction: CCDFGF

Implementation of the ROMPCS design will have a negligible impact on potential releases from the Culebra. As a result, the PCS-2012 PA will calculate CCDFs of individual vectors for total normalized releases using Culebra release results calculated in the PABC-2009. The PCS-2012 PA will calculate CCDFs of individual vectors for total normalized releases, cuttings and cavings releases, spallings releases, and DBRs. (The use of the ROMPCS design will have no impact on cuttings and cavings releases. Nonetheless, new cuttings and cavings release volumes will be calculated in the PCS-2012 PA as a by-product of the spallings calculation.) Mean CCDFs for each release pathway will be calculated by replicate and across all replicates. The 95% confidence limit on the mean across all replicates will also be calculated. The codes PRECCDFGF version 1.01 and CCDFGF version 5.02 will be used for the PCS-2012 PA, which are the same codes used for the PABC-2009.

2.2.7 Sensitivity Analysis: STEPWISE

The PCS-2012 PA will implement sensitivity analyses for results from the major codes in a manner consistent with those employed for the PABC-2009. Specifically, global sensitivity analyses will be conducted on the results from CCDFGF using the linear regression code STEPWISE version 2.21. Since the Salado flow results from the BRAGFLO calculations are used as input to many other codes, additional sensitivity analyses may be performed using BRAGFLO results. WIPP PA codes such as PCCSRC, as well as Commercial Off-The Shelf (COTS) statistical software, may be used to assess the sensitivity of BRAGFLO results to input parameters.

2.3 Reports and Documentation

Several reports will be generated as a result of this analysis plan. Each set of calculations discussed in Section 2.2 and its subsections will be documented in an analysis report. These reports will include:

1) discussion of any implementation changes (parameters, modeling assumptions, etc.) relative to the corresponding PABC-2009 calculations; and
2) analysis of results relevant to the long term performance of the repository. The analysis will include comparisons of PCS-2012 PA results with PABC-2009 results.

A summary report describing the major results of the PA will also be written. The summary report will include the run control record as an appendix. This appendix will contain:

1. A description of the hardware platform and operating system used to perform the calculations.
2. A listing of the codes and versions used to perform the calculations.
3. A listing of the scripts used to run each calculation.
4. A listing of the input and output files for each calculation.
5. A listing of the library and class where each file is stored.
6. File naming conventions.

The analyses performed under this analysis plan are in support of a rulemaking decision to replace the current WIPP Option D panel closure design with the ROMPCS design. As such, it

is likely that additional analyses and calculations will be performed as part of the regulatory review and approval process. These additional tasks and documentation, if they become necessary, will also fall under AP-161.

3 Tasks

The tasks, responsible personnel and estimated task schedule are summarized below in Table 4.

Table 4: Task List and Estimated Schedule for the PCS-2012 PA.

Task	Description	Guiding Document	Approximate Completion Date	Responsible Individual(s)
1	Parameters			
1a	Development of ROMPCS parameters	SP 9-5	7/11/12	Camphouse Gross Herrick Kicker Thompson
1b	Entry of ROMPCS parameters into PAPDB	SP 9-5	7/12/12	Long
2	Preparation Tasks			
2a	Input files prepared	AP-161	7/25/12	Camphouse Clayton Kicker Kirchner Malama
2b	Input file review	AP-161	8/1/12	Camphouse
3	Code Run Environment Preparation			
3a	Libraries Update	AP-161	8/1/12	Long
3b	Run Control Script Update	AP-161	9/14/12	Long
4	Calculations			
4a	Parameter Sampling: LHS	AP-161	8/2/12	Long
4b	BRAGFLO Testing with new parameters and por/perm relationship	AP-161	8/10/12	Camphouse Malama
4c	Salado Flow: BRAGFLO	AP-161	8/17/12	Long
4d	Cuttings & Cavings, Spallings: CUTTINGS_S	AP-161	8/24/12	Long
4e	Direct Brine Releases: BRAGFLO	AP-161	8/31/12	Long
4f	CCDF Construction: CCDFGF	AP-161	9/7/12	Long
4g	Sensitivity Analysis: STEPWISE	AP-161	9/14/12	Kirchner
5	Analysis & Documentation			
5a	Parameter Sampling: LHS	AP-161	9/6/12	Kirchner
5b	Salado Flow: BRAGFLO	AP-161	9/21/12	Camphouse Malama
5d	Spallings: CUTTINGS_S	AP-161	9/28/12	Kicker
5c	Direct Brine Releases: BRAGFLO	AP-161	10/5/12	Malama Camphouse
5d	CCDF Construction: CCDFGF	AP-161	10/12/12	Kicker
5e	Sensitivity Analysis: STEPWISE	AP-161	10/19/12	Kirchner
5f	Summary Report with Run Control as Appendix	AP-161	11/9/12	Camphouse Long

4 Software

The major WIPP PA codes to be used for this analysis are listed in Table 5. These codes will be executed on the WIPP PA Alpha Cluster, which is listed in Table 6. Additionally, COTS software, such as MATHEMATICA®, MATLAB®, MATHCAD®, Excel®, Access®, Grapher®, or Kaleidagraph® may be utilized. The use of any COTS application will be verified per NP 9-1 Appendix C as appropriate.

Table 5: Codes to be used for the PCS-2012 PA.

Code	Version	Build Date	Executable
ALGEBRACDB	2.35	31-JAN-1996	ALGEBRACDB_PA96.EXE
BRAGFLO	6.0	12-FEB-2007	BRAGFLO_QB0600.EXE
CCDFGF	5.02	13-DEC-2004	CCDFGF_QB0502.EXE
CUTTINGS_S	6.02	9-JUN-2005	CUTTINGS_S_QA0602.EXE
GENMESH	6.08	31-JAN-1996	GM_PA96.EXE
ICSET	2.22	1-FEB-1996	ICSET_PA96.EXE
LHS	2.42	18-JAN-2005	LHS_QA0242.EXE
MATSET	9.10	29-NOV-2001	MATSET_QA0910.EXE
PCCSRC	2.21	23-MAY-1996	PCCSRC_PA96.EXE
POSTBRAG	4.00A	28-MAR-2007	POSTBRAG_QA0400A.EXE
POSTLHS	4.07A	25-APR-2005	POSTLHS_QA0407A.EXE
PREBRAG	8.00	8-MAR-2007	PREBRAG_QA0800.EXE
PRECCDFGF	1.01	7-JUL-2005	PRECCDFGF_QA0101.EXE
PRELHS	2.30	27-NOV-2001	PRELHS_QA0230.EXE
RELATE	1.43	6-MAR-1996	RELATE_PA96.EXE
STEPWISE	2.21	2-DEC-1996	STEPWISE_PA96_2.EXE
SUMMARIZE	3.01	21-DEC-2005	SUMMARIZE_QB0301.EXE

Table 6: WIPP PA Alpha Cluster

Node	Hardware Type	CPU	Operating System
CCR	HP AlphaServer ES45	Alpha EV68	Open VMS 8.2
TDN	HP AlphaServer ES45	Alpha EV68	Open VMS 8.2
BTO	HP AlphaServer ES45	Alpha EV68	Open VMS 8.2
CSN	HP AlphaServer ES45	Alpha EV68	Open VMS 8.2
GNR	HP AlphaServer ES47	Alpha EV7	Open VMS 8.2
MC5	HP AlphaServer ES47	Alpha EV7	Open VMS 8.2
TRS	HP AlphaServer ES47	Alpha EV7	Open VMS 8.2
TBB	HP AlphaServer ES47	Alpha EV7	Open VMS 8.2

5 Special Considerations

None

6 Applicable Procedures

All applicable WIPP QA procedures will be followed when conducting these analyses.

- Training of personnel will be conducted in accordance with the requirements of NP 2-1, *Qualification and Training*.
- Analyses will be conducted and documented in accordance with the requirements of NP 9-1, *Analyses*.
- All software used will meet the requirements laid out in NP 19-1, *Software Requirements* and NP 9-1, as applicable.
- The analyses will be reviewed following NP 6-1, *Document Review Process*.
- All required records will be submitted to the WIPP Records Center in accordance with NP 17-1, *Records*.
- New and revised parameters will be created as discussed in NP 9-2, *Parameters*.

7 References

Camphouse, R.C. 2012. An overview of the BRAGFLO two-phase flow parameters used to model the run-of-mine salt panel closures implemented in the PCS-2012 PA. Memo to Paul Shoemaker dated June 7, 2012. Sandia National Laboratories, Carlsbad, NM. ERMS 557653.

Camphouse, R.C., Gross, M., Herrick, C.G., Kicker, D.C., and Thompson, B. 2012. Recommendations and Justifications of Parameter Values for the Run-of-Mine Salt Panel Closure System Design Modeled in the PCS-2012 PA. Memo to WIPP Records Center dated May 3, 2012. Sandia National Laboratories, Carlsbad, NM. ERMS 557396.

Camphouse, R.C., Clayton, D.J., Kicker, D.C., and Pasch, J.J. 2011. Summary Report for the AP-151 (PC3R) Performance Assessment, Revision 1. Sandia National Laboratories, Carlsbad, NM. ERMS 555489.

Clayton, D.C., Camphouse, R. C., Garner, J. W., Ismail, A. E., Kirchner, T. B., Kuhlman, K. L., and Nemer, M. B.. 2010. Summary Report of the CRA-2009 Performance Assessment Baseline Calculation, Revision 1. Sandia National Laboratories. Carlsbad, New Mexico, ERMS 553039.

DOE (U.S. Department of Energy). 1996. Title 40 CFR Part 191 Compliance Certification Application for the Waste Isolation Pilot Plant. DOE/CAO-1996-2184. U.S. Department of Energy, Waste Isolation Pilot Plant, Carlsbad Area Office. Carlsbad, NM.

DOE (U.S. Department of Energy), 2011. Panel Closure System Design, Planned Change Request to the EPA 40 CFR Part 194 Certification of the Waste Isolation Pilot Plant. U.S. Department of Energy, Carlsbad Field Office. Carlsbad, New Mexico.

DOE (U.S. Department of Energy), 2012. Response to First Set of EPA Questions to DOE, December 22, 2011. Letter from Mr. Juan Franco, Manager, Carlsbad Area Field Office, U.S. Department of Energy, to Mr. Jonathan Edwards, Director, Radiation Protection Division, U.S. Environmental Protection Agency, dated April 17, 2012.

Dunagan, S. C. 2003. Complementary Cumulative Distribution Functions (CCDFs) for the Technical Baseline Migration (TBM), Revision 0. Sandia National Laboratories, Carlsbad, NM. ERMS 525707.

EPA (U.S. Environmental Protection Agency). 1998. Criteria for the Certification and Re-Certification of the Waste Isolation Pilot Plants Compliance with the 40 CFR Part 191 Disposal Regulations: Certification Decision; Final Rule, *Federal Register*, Vol. 63, No. 95, pp. 27353-27406. U.S. Environmental Protection Agency, Office of Air and Radiation, Washington, D.C.

Hansen, C. W. 2002. Analysis Report for the Panel Closure Impact Assessment. Sandia National Laboratories, Carlsbad, NM. ERMS 523935.

Herrick, C.G. 2012. JAS3D Calculations Performed in Support of the PCS-2012 PA Parameter Selections. Sandia National Laboratories, Carlsbad, NM.

Kirkes, G. R. 2011. Features, Events, and Processes Assesssment for Changes Described in Analysis Plan – 151, Revision 0. March 2011. Sandia National Laboratories, Carlsbad, NM. ERMS 555237.

MacKinnon R. and G. Freeze, 1997. Supplemental Summary of EPA-Mandated Performance Assessment Verification Test (All Replicates) and Comparison with the Compliance Certification Application Calculations, Sandia National Laboratories, Carlsbad, NM. ERMS 414880. (EPA Docket A-93-02, II-G-28.)

RockSol Consulting Group, Inc. 2006. Further Assessment of the Short-term Stability of the 12 Foot Explosion Isolation Wall. Report prepared for Washington TRU Solutions, LLC.

Stein, J.S. 2002. Parameter values for new materials CONC_PCS and DRZ_PCS. Memo to Kathryn Knowles dated February 13, 2002. Sandia National Laboratories, Carlsbad, NM. ERMS 520524.

Vugrin, E.D. and S.C. Dunagan. 2006. Analysis Package for the Impact Assessment of the Redesigned Panel Closure System, Rev. 0. Sandia National Laboratories. Carlsbad, NM. ERMS 543865.

Vugrin, E., and S. Wagner. 2006. Panel Closure Summary Report. Sandia National Laboratories. Carlsbad, NM. ERMS 544802.

This work of authorship was prepared as an account of work sponsored by an agency of the United States Government. Accordingly, the United States Government retains a nonexclusive, royalty-free license to publish or reproduce the published form of this contribution, or allow others to do so for United States Government purposes. Neither Sandia Corporation, the United States Government, nor any agency thereof, nor any of their employees makes any warranty, express or implied, or assumes any legal liability or responsibility for the accuracy, completeness, or usefulness of any information, apparatus, product, or process disclosed, or represents that its use would not infringe privately-owned rights. Reference herein to any specific commercial product, process, or service by trade name, trademark, manufacturer, or otherwise does not necessarily constitute or imply its endorsement, recommendation, or favoring by Sandia Corporation, the United States Government, or any agency thereof. The views and opinions expressed herein do not necessarily state or reflect those of Sandia Corporation, the United States Government or any agency thereof.

Sandia National Laboratories is a multi-program laboratory operated by Sandia Corporation, a wholly owned subsidiary of Lockheed Martin Corporation, for the U.S. Department of Energy's National Nuclear Security Administration under contract DE-AC04-94AL85000.

Parties are allowed to download copies at no cost for internal use within your organization only provided that any copies made are true and accurate. Copies must include a statement acknowledging Sandia Corporation's authorship of the subject matter.

558129

Generation of the LHS Samples for the AP-161 (PCS-2012) Revision 0 PA Calculations

Author:	Thomas Kirchner	Thomas Kirchner	9/5/12
	Print	Signature	Date
Technical Review:	Janis Trone		9/5/12
	Print	Signature	Date
Management Review:	Sean Dunagan		9/5/12
	Print	Signature	Date
QA Review:	Shelly Nielsen	Shelly R. Nielsen	9-6-12
	Print	Signature	Date

WIPP:1.4.1.2:PA:QA-L:557313

Information Only

Table of Contents

Table of Contents 2
Table of Figures 3
I. Introduction 11
II. Run Control 13
III. PRELHS Input Files 13
IV. LHS Output files 13
V. Imposing Additional Limits on Some Variables 14
VI. Summary and Conclusions 15
VII. References 16
Appendix I. Input file to PRELHS for Replicate 1 108
Appendix II. Input file to PRELHS for Replicate 2 113
Appendix III. Input file to PRELHS for Replicate 3 119
Appendix IV. PRELHS Output (Transfer) File for Replicate 1 124
Appendix V. PRELHS Output (Transfer) File for Replicate 2 131
Appendix VI. PRELHS Output (Transfer) File for Replicate 3 138
Appendix VII. Comparison of Sampled Data to Expected Range 145
Appendix VIII. LHS_EDIT 163
1.1. Description and Requirements 163
1.2. Platform and Source Code Description 163
1.3. Usage 164
Files 164
Execution 164
1.4. Testing of LHS_EDIT 164
Test Procedure 164
Acceptance Criteria 168
Evaluation 168
1.5. Source Code 168

Information Only

Table of Figures

Figure 1. Observed and Expected CDFs for AM+3:MKD_AM (Loguniform Distribution) Replicate 1. 17
Figure 2. Observed and Expected CDFs for BH_SAND:PRMX_LOG (Uniform Distribution) Replicate 1. 17
Figure 3. Observed and Expected CDFs for BOREHOLE:DOMEGA (User Continuous Distribution) Replicate 1. 18
Figure 4. Observed and Expected CDFs for BOREHOLE:TAUFAIL (Loguniform Distribution) Replicate 1. 18
Figure 5. Observed and Expected CDFs for CASTILER:COMP_RCK (Triangular Distribution) Replicate 1. 19
Figure 6. Observed and Expected CDFs for CASTILER:PRESSURE (Triangular Distribution) Replicate 1. 19
Figure 7. Observed and Expected CDFs for CASTILER:PRMX_LOG (Triangular Distribution) Replicate 1. 20
Figure 8. Observed and Expected CDFs for CONC_PLG:PRMX_LOG (Uniform Distribution) Replicate 1. 20
Figure 9. Observed and Expected CDFs for CULEBRA:APOROS (Loguniform Distribution) Replicate 1. 21
Figure 10. Observed and Expected CDFs for CULEBRA:DPOROS (User Continuous Distribution) Replicate 1. 21
Figure 11. Observed and Expected CDFs for CULEBRA:HMBLKLT (Uniform Distribution) Replicate 1. 22
Figure 12. Observed and Expected CDFs for CULEBRA:MINP_FAC (Uniform Distribution) Replicate 1. 22
Figure 13. Observed and Expected CDFs for DRZ_1:PRMX_LOG (Uniform Distribution) Replicate 1. 23
Figure 14. Observed and Expected CDFs for DRZ_PCS:PRMX_LOG (Triangular Distribution) Replicate 1. 23
Figure 15. Observed and Expected CDFs for GLOBAL:CLIMTIDX (User Continuous Distribution) Replicate 1. 24
Figure 16. Observed and Expected CDFs for GLOBAL:OXSTAT (Uniform Distribution) Replicate 1. 24
Figure 17. Observed and Expected CDFs for GLOBAL:PBRINE (Uniform Distribution) Replicate 1. 25
Figure 18. Observed and Expected CDFs for GLOBAL:TRANSIDX (Uniform Distribution) Replicate 1. 25
Figure 19. Observed and Expected CDFs for PCS_T1:PORE_DIS (User Continuous Distribution) Replicate 1. 26
Figure 20. Observed and Expected CDFs for PCS_T1:POROSITY (Uniform Distribution) Replicate 1. 26
Figure 21. Observed and Expected CDFs for PCS_T1:PRMX_LOG (Uniform Distribution) Replicate 1. 27
Figure 22. Observed and Expected CDFs for PCS_T1:SAT_IBRN (Uniform Distribution) Replicate 1. 27

Information Only

Figure 23. Observed and Expected CDFs for PCS_T1:SAT_RBRN (User Continuous Distribution) Replicate 1. 28
Figure 24. Observed and Expected CDFs for PCS_T1:SAT_RGAS (Uniform Distribution) Replicate 1. 28
Figure 25. Observed and Expected CDFs for PCS_T2:POR2PERM (Normal Distribution) Replicate 1. 29
Figure 26. Observed and Expected CDFs for PCS_T2:POROSITY (Uniform Distribution) Replicate 1. 29
Figure 27. Observed and Expected CDFs for PCS_T3:POROSITY (Uniform Distribution) Replicate 1. 30
Figure 28. Observed and Expected CDFs for PHUMOX3:PHUMCIM (User Continuous Distribution) Replicate 1. 30
Figure 29. Observed and Expected CDFs for PU+3:MKD_PU (Loguniform Distribution) Replicate 1. 31
Figure 30. Observed and Expected CDFs for PU+4:MKD_PU (Loguniform Distribution) Replicate 1. 31
Figure 31. Observed and Expected CDFs for S_HALITE:COMP_RCK (Uniform Distribution) Replicate 1. 32
Figure 32. Observed and Expected CDFs for S_HALITE:POROSITY (User Continuous Distribution) Replicate 1. 32
Figure 33. Observed and Expected CDFs for S_HALITE:PRESSURE (Uniform Distribution) Replicate 1. 33
Figure 34. Observed and Expected CDFs for S_HALITE:PRMX_LOG (Uniform Distribution) Replicate 1. 33
Figure 35. Observed and Expected CDFs for S_MB139:PORE_DIS (Student Distribution) Replicate 1. 34
Figure 36. Observed and Expected CDFs for S_MB139:PRMX_LOG (Student Distribution) Replicate 1. 34
Figure 37. Observed and Expected CDFs for S_MB139:RELP_MOD (User Discrete (Delta) Distribution) Replicate 1. 35
Figure 38. Observed and Expected CDFs for S_MB139:SAT_RBRN (Student Distribution) Replicate 1. 35
Figure 39. Observed and Expected CDFs for SHFTL_T1:PRMX_LOG (User Continuous Distribution) Replicate 1. 36
Figure 40. Observed and Expected CDFs for SHFTL_T2:PRMX_LOG (User Continuous Distribution) Replicate 1. 36
Figure 41. Observed and Expected CDFs for SHFTU:PRMX_LOG (User Continuous Distribution) Replicate 1. 37
Figure 42. Observed and Expected CDFs for SHFTU:SAT_RBRN (User Continuous Distribution) Replicate 1. 37
Figure 43. Observed and Expected CDFs for SHFTU:SAT_RGAS (Uniform Distribution) Replicate 1. 38
Figure 44. Observed and Expected CDFs for SOLMOD3:SOLVAR (User Continuous Distribution) Replicate 1. 38
Figure 45. Observed and Expected CDFs for SOLMOD4:SOLVAR (User Continuous Distribution) Replicate 1. 39

Information Only

Figure 46. Observed and Expected CDFs for SPALLMOD:PARTDIAM (Loguniform Distribution) Replicate 1. 39
Figure 47. Observed and Expected CDFs for SPALLMOD:REPIPERM (Loguniform Distribution) Replicate 1. 40
Figure 48. Observed and Expected CDFs for SPALLMOD:REPIPOR (Uniform Distribution) Replicate 1. 40
Figure 49. Observed and Expected CDFs for SPALLMOD:TENSLSTR (Uniform Distribution) Replicate 1. 41
Figure 50. Observed and Expected CDFs for STEEL:CORRMCO2 (Uniform Distribution) Replicate 1. 41
Figure 51. Observed and Expected CDFs for TH+4:MKD_TH (Loguniform Distribution) Replicate 1. 42
Figure 52. Observed and Expected CDFs for U+4:MKD_U (Loguniform Distribution) Replicate 1. 42
Figure 53. Observed and Expected CDFs for U+6:MKD_U (Loguniform Distribution) Replicate 1. 43
Figure 54. Observed and Expected CDFs for WAS_AREA:BIOGENFC (Uniform Distribution) Replicate 1. 43
Figure 55. Observed and Expected CDFs for WAS_AREA:GRATMICH (Uniform Distribution) Replicate 1. 44
Figure 56. Observed and Expected CDFs for WAS_AREA:GRATMICI (Uniform Distribution) Replicate 1. 44
Figure 57. Observed and Expected CDFs for WAS_AREA:PROBDEG (User Discrete (Delta) Distribution) Replicate 1. 45
Figure 58. Observed and Expected CDFs for WAS_AREA:SAT_RBRN (Uniform Distribution) Replicate 1. 45
Figure 59. Observed and Expected CDFs for WAS_AREA:SAT_RGAS (Uniform Distribution) Replicate 1. 46
Figure 60. Observed and Expected CDFs for WAS_AREA:SAT_WICK (Uniform Distribution) Replicate 1. 46
Figure 61. Observed and Expected CDFs for AM+3:MKD_AM (Loguniform Distribution) Replicate 2. 47
Figure 62. Observed and Expected CDFs for BH_SAND:PRMX_LOG (Uniform Distribution) Replicate 2. 47
Figure 63. Observed and Expected CDFs for BOREHOLE:DOMEGA (User Continuous Distribution) Replicate 2. 48
Figure 64. Observed and Expected CDFs for BOREHOLE:TAUFAIL (Loguniform Distribution) Replicate 2. 48
Figure 65. Observed and Expected CDFs for CASTILER:COMP_RCK (Triangular Distribution) Replicate 2. 49
Figure 66. Observed and Expected CDFs for CASTILER:PRESSURE (Triangular Distribution) Replicate 2. 49
Figure 67. Observed and Expected CDFs for CASTILER:PRMX_LOG (Triangular Distribution) Replicate 2. 50
Figure 68. Observed and Expected CDFs for CONC_PLG:PRMX_LOG (Uniform Distribution) Replicate 2. 50

Information Only

Figure 69. Observed and Expected CDFs for CULEBRA:APOROS (Loguniform Distribution) Replicate 2. 51
Figure 70. Observed and Expected CDFs for CULEBRA:DPOROS (User Continuous Distribution) Replicate 2. 51
Figure 71. Observed and Expected CDFs for CULEBRA:HMBLKLT (Uniform Distribution) Replicate 2. 52
Figure 72. Observed and Expected CDFs for CULEBRA:MINP_FAC (Uniform Distribution) Replicate 2. 52
Figure 73. Observed and Expected CDFs for DRZ_1:PRMX_LOG (Uniform Distribution) Replicate 2. 53
Figure 74. Observed and Expected CDFs for DRZ_PCS:PRMX_LOG (Triangular Distribution) Replicate 2. 53
Figure 75. Observed and Expected CDFs for GLOBAL:CLIMTIDX (User Continuous Distribution) Replicate 2. 54
Figure 76. Observed and Expected CDFs for GLOBAL:OXSTAT (Uniform Distribution) Replicate 2. 54
Figure 77. Observed and Expected CDFs for GLOBAL:PBRINE (Uniform Distribution) Replicate 2. 55
Figure 78. Observed and Expected CDFs for GLOBAL:TRANSIDX (Uniform Distribution) Replicate 2. 55
Figure 79. Observed and Expected CDFs for PCS_T1:PORE_DIS (User Continuous Distribution) Replicate 2. 56
Figure 80. Observed and Expected CDFs for PCS_T1:POROSITY (Uniform Distribution) Replicate 2. 56
Figure 81. Observed and Expected CDFs for PCS_T1:PRMX_LOG (Uniform Distribution) Replicate 2. 57
Figure 82. Observed and Expected CDFs for PCS_T1:SAT_IBRN (Uniform Distribution) Replicate 2. 57
Figure 83. Observed and Expected CDFs for PCS_T1:SAT_RBRN (User Continuous Distribution) Replicate 2. 58
Figure 84. Observed and Expected CDFs for PCS_T1:SAT_RGAS (Uniform Distribution) Replicate 2. 58
Figure 85. Observed and Expected CDFs for PCS_T2:POR2PERM (Normal Distribution) Replicate 2. 59
Figure 86. Observed and Expected CDFs for PCS_T2:POROSITY (Uniform Distribution) Replicate 2. 59
Figure 87. Observed and Expected CDFs for PCS_T3:POROSITY (Uniform Distribution) Replicate 2. 60
Figure 88. Observed and Expected CDFs for PHUMOX3:PHUMCIM (User Continuous Distribution) Replicate 2. 60
Figure 89. Observed and Expected CDFs for PU+3:MKD_PU (Loguniform Distribution) Replicate 2. 61
Figure 90. Observed and Expected CDFs for PU+4:MKD_PU (Loguniform Distribution) Replicate 2. 61
Figure 91. Observed and Expected CDFs for S_HALITE:COMP_RCK (Uniform Distribution) Replicate 2. 62

Information Only

Figure 92. Observed and Expected CDFs for S_HALITE:POROSITY (User Continuous Distribution) Replicate 2. 62
Figure 93. Observed and Expected CDFs for S_HALITE:PRESSURE (Uniform Distribution) Replicate 2. 63
Figure 94. Observed and Expected CDFs for S_HALITE:PRMX_LOG (Uniform Distribution) Replicate 2. 63
Figure 95. Observed and Expected CDFs for S_MB139:PORE_DIS (Student Distribution) Replicate 2. 64
Figure 96. Observed and Expected CDFs for S_MB139:PRMX_LOG (Student Distribution) Replicate 2. 64
Figure 97. Observed and Expected CDFs for S_MB139:RELP_MOD (User Discrete (Delta) Distribution) Replicate 2. 65
Figure 98. Observed and Expected CDFs for S_MB139:SAT_RBRN (Student Distribution) Replicate 2. 65
Figure 99. Observed and Expected CDFs for SHFTL_T1:PRMX_LOG (User Continuous Distribution) Replicate 2. 66
Figure 100. Observed and Expected CDFs for SHFTL_T2:PRMX_LOG (User Continuous Distribution) Replicate 2. 66
Figure 101. Observed and Expected CDFs for SHFTU:PRMX_LOG (User Continuous Distribution) Replicate 2. 67
Figure 102. Observed and Expected CDFs for SHFTU:SAT_RBRN (User Continuous Distribution) Replicate 2. 67
Figure 103. Observed and Expected CDFs for SHFTU:SAT_RGAS (Uniform Distribution) Replicate 2. 68
Figure 104. Observed and Expected CDFs for SOLMOD3:SOLVAR (User Continuous Distribution) Replicate 2. 68
Figure 105. Observed and Expected CDFs for SOLMOD4:SOLVAR (User Continuous Distribution) Replicate 2. 69
Figure 106. Observed and Expected CDFs for SPALLMOD:PARTDIAM (Loguniform Distribution) Replicate 2. 69
Figure 107. Observed and Expected CDFs for SPALLMOD:REPIPERM (Loguniform Distribution) Replicate 2. 70
Figure 108. Observed and Expected CDFs for SPALLMOD:REPIPOR (Uniform Distribution) Replicate 2. 70
Figure 109. Observed and Expected CDFs for SPALLMOD:TENSLSTR (Uniform Distribution) Replicate 2. 71
Figure 110. Observed and Expected CDFs for STEEL:CORRMCO2 (Uniform Distribution) Replicate 2. 71
Figure 111. Observed and Expected CDFs for TH+4:MKD_TH (Loguniform Distribution) Replicate 2. 72
Figure 112. Observed and Expected CDFs for U+4:MKD_U (Loguniform Distribution) Replicate 2. 72
Figure 113. Observed and Expected CDFs for U+6:MKD_U (Loguniform Distribution) Replicate 2. 73
Figure 114. Observed and Expected CDFs for WAS_AREA:BIOGENFC (Uniform Distribution) Replicate 2. 73

Information Only

Figure 115. Observed and Expected CDFs for WAS_AREA:GRATMICH (Uniform Distribution) Replicate 2. 74
Figure 116. Observed and Expected CDFs for WAS_AREA:GRATMICI (Uniform Distribution) Replicate 2. 74
Figure 117. Observed and Expected CDFs for WAS_AREA:PROBDEG (User Discrete (Delta) Distribution) Replicate 2. 75
Figure 118. Observed and Expected CDFs for WAS_AREA:SAT_RBRN (Uniform Distribution) Replicate 2. 75
Figure 119. Observed and Expected CDFs for WAS_AREA:SAT_RGAS (Uniform Distribution) Replicate 2. 76
Figure 120. Observed and Expected CDFs for WAS_AREA:SAT_WICK (Uniform Distribution) Replicate 2. 76
Figure 121. Observed and Expected CDFs for AM+3:MKD_AM (Loguniform Distribution) Replicate 3. 77
Figure 122. Observed and Expected CDFs for BH_SAND:PRMX_LOG (Uniform Distribution) Replicate 3. 77
Figure 123. Observed and Expected CDFs for BOREHOLE:DOMEGA (User Continuous Distribution) Replicate 3. 78
Figure 124. Observed and Expected CDFs for BOREHOLE:TAUFAIL (Loguniform Distribution) Replicate 3. 78
Figure 125. Observed and Expected CDFs for CASTILER:COMP_RCK (Triangular Distribution) Replicate 3. 79
Figure 126. Observed and Expected CDFs for CASTILER:PRESSURE (Triangular Distribution) Replicate 3. 79
Figure 127. Observed and Expected CDFs for CASTILER:PRMX_LOG (Triangular Distribution) Replicate 3. 80
Figure 128. Observed and Expected CDFs for CONC_PLG:PRMX_LOG (Uniform Distribution) Replicate 3. 80
Figure 129. Observed and Expected CDFs for CULEBRA:APOROS (Loguniform Distribution) Replicate 3. 81
Figure 130. Observed and Expected CDFs for CULEBRA:DPOROS (User Continuous Distribution) Replicate 3. 81
Figure 131. Observed and Expected CDFs for CULEBRA:HMBLKLT (Uniform Distribution) Replicate 3. 82
Figure 132. Observed and Expected CDFs for CULEBRA:MINP_FAC (Uniform Distribution) Replicate 3. 82
Figure 133. Observed and Expected CDFs for DRZ_1:PRMX_LOG (Uniform Distribution) Replicate 3. 83
Figure 134. Observed and Expected CDFs for DRZ_PCS:PRMX_LOG (Triangular Distribution) Replicate 3. 83
Figure 135. Observed and Expected CDFs for GLOBAL:CLIMTIDX (User Continuous Distribution) Replicate 3. 84
Figure 136. Observed and Expected CDFs for GLOBAL:OXSTAT (Uniform Distribution) Replicate 3. 84
Figure 137. Observed and Expected CDFs for GLOBAL:PBRINE (Uniform Distribution) Replicate 3. 85

Information Only

Figure 138. Observed and Expected CDFs for GLOBAL:TRANSIDX (Uniform Distribution) Replicate 3. 85
Figure 139. Observed and Expected CDFs for PCS_T1:PORE_DIS (User Continuous Distribution) Replicate 3. 86
Figure 140. Observed and Expected CDFs for PCS_T1:POROSITY (Uniform Distribution) Replicate 3. 86
Figure 141. Observed and Expected CDFs for PCS_T1:PRMX_LOG (Uniform Distribution) Replicate 3. 87
Figure 142. Observed and Expected CDFs for PCS_T1:SAT_IBRN (Uniform Distribution) Replicate 3. 87
Figure 143. Observed and Expected CDFs for PCS_T1:SAT_RBRN (User Continuous Distribution) Replicate 3. 88
Figure 144. Observed and Expected CDFs for PCS_T1:SAT_RGAS (Uniform Distribution) Replicate 3. 88
Figure 145. Observed and Expected CDFs for PCS_T2:POR2PERM (Normal Distribution) Replicate 3. 89
Figure 146. Observed and Expected CDFs for PCS_T2:POROSITY (Uniform Distribution) Replicate 3. 89
Figure 147. Observed and Expected CDFs for PCS_T3:POROSITY (Uniform Distribution) Replicate 3. 90
Figure 148. Observed and Expected CDFs for PHUMOX3:PHUMCIM (User Continuous Distribution) Replicate 3. 90
Figure 149. Observed and Expected CDFs for PU+3:MKD_PU (Loguniform Distribution) Replicate 3. 91
Figure 150. Observed and Expected CDFs for PU+4:MKD_PU (Loguniform Distribution) Replicate 3. 91
Figure 151. Observed and Expected CDFs for S_HALITE:COMP_RCK (Uniform Distribution) Replicate 3. 92
Figure 152. Observed and Expected CDFs for S_HALITE:POROSITY (User Continuous Distribution) Replicate 3. 92
Figure 153. Observed and Expected CDFs for S_HALITE:PRESSURE (Uniform Distribution) Replicate 3. 93
Figure 154. Observed and Expected CDFs for S_HALITE:PRMX_LOG (Uniform Distribution) Replicate 3. 93
Figure 155. Observed and Expected CDFs for S_MB139:PORE_DIS (Student Distribution) Replicate 3. 94
Figure 156. Observed and Expected CDFs for S_MB139:PRMX_LOG (Student Distribution) Replicate 3. 94
Figure 157. Observed and Expected CDFs for S_MB139:RELP_MOD (User Discrete (Delta) Distribution) Replicate 3. 95
Figure 158. Observed and Expected CDFs for S_MB139:SAT_RBRN (Student Distribution) Replicate 3. 95
Figure 159. Observed and Expected CDFs for SHFTL_T1:PRMX_LOG (User Continuous Distribution) Replicate 3. 96
Figure 160. Observed and Expected CDFs for SHFTL_T2:PRMX_LOG (User Continuous Distribution) Replicate 3. 96

Information Only

Figure 161. Observed and Expected CDFs for SHFTU:PRMX_LOG (User Continuous Distribution) Replicate 3. 97
Figure 162. Observed and Expected CDFs for SHFTU:SAT_RBRN (User Continuous Distribution) Replicate 3. 97
Figure 163. Observed and Expected CDFs for SHFTU:SAT_RGAS (Uniform Distribution) Replicate 3. 98
Figure 164. Observed and Expected CDFs for SOLMOD3:SOLVAR (User Continuous Distribution) Replicate 3. 98
Figure 165. Observed and Expected CDFs for SOLMOD4:SOLVAR (User Continuous Distribution) Replicate 3. 99
Figure 166. Observed and Expected CDFs for SPALLMOD:PARTDIAM (Loguniform Distribution) Replicate 3. 99
Figure 167. Observed and Expected CDFs for SPALLMOD:REPIPERM (Loguniform Distribution) Replicate 3. 100
Figure 168. Observed and Expected CDFs for SPALLMOD:REPIPOR (Uniform Distribution) Replicate 3. 100
Figure 169. Observed and Expected CDFs for SPALLMOD:TENSLSTR (Uniform Distribution) Replicate 3. 101
Figure 170. Observed and Expected CDFs for STEEL:CORRMCO2 (Uniform Distribution) Replicate 3. 101
Figure 171. Observed and Expected CDFs for TH+4:MKD_TH (Loguniform Distribution) Replicate 3. 102
Figure 172. Observed and Expected CDFs for U+4:MKD_U (Loguniform Distribution) Replicate 3. 102
Figure 173. Observed and Expected CDFs for U+6:MKD_U (Loguniform Distribution) Replicate 3. 103
Figure 174. Observed and Expected CDFs for WAS_AREA:BIOGENFC (Uniform Distribution) Replicate 3. 103
Figure 175. Observed and Expected CDFs for WAS_AREA:GRATMICH (Uniform Distribution) Replicate 3. 104
Figure 176. Observed and Expected CDFs for WAS_AREA:GRATMICI (Uniform Distribution) Replicate 3. 104
Figure 177. Observed and Expected CDFs for WAS_AREA:PROBDEG (User Discrete (Delta) Distribution) Replicate 3. 105
Figure 178. Observed and Expected CDFs for WAS_AREA:SAT_RBRN (Uniform Distribution) Replicate 3. 105
Figure 179. Observed and Expected CDFs for WAS_AREA:SAT_RGAS (Uniform Distribution) Replicate 3. 106
Figure 180. Observed and Expected CDFs for WAS_AREA:SAT_WICK (Uniform Distribution) Replicate 3. 106
Figure 181. The conditional relationship introduced between WAS_AREA:GRATMICI and WAS_AREA:GRATMICH also produces a correlation between the variables. 107

Information Only

I. Introduction

The Waste Isolation Pilot Plant (WIPP), located in southeastern New Mexico, has been developed by the U.S. Department of Energy (DOE) for the geologic (deep underground) disposal of transuranic (TRU) waste. Containment of TRU waste at the WIPP is regulated by the U.S. Environmental Protection Agency (EPA) according to the regulations set forth in Title 40 of the Code of Federal Regulations (CFR), Part 191. The DOE demonstrates compliance with the containment requirements according to the Certification Criteria in Title 40 CFR Part 194 by means of performance assessment (PA) calculations performed by Sandia National Laboratories (SNL). WIPP PA calculations estimate the probability and consequence of potential radionuclide releases from the repository to the accessible environment for a regulatory period of 10,000 years after facility closure. The models used in PA are maintained and updated with new information as part of an ongoing process. Improved information regarding important WIPP features, events, and processes typically results in refinements and modifications to PA models and the parameters used in them. Planned changes to the repository and/or the components therein also result in updates to WIPP PA models. WIPP PA models are used to support the repository recertification process that occurs at five-year intervals following the receipt of the first waste shipment at the site in 1999.

Waste panel closures comprise a repository feature that has been represented in WIPP PA since the original Compliance Certification Application (CCA) of 1996. Panel closures are included in WIPP PA models principally because they are a part of the disposal system, not because they play a substantive role in inhibiting the release of radionuclides to the outside environment. The DOE stated in the CCA (DOE 1996) that *"The panel closure system was not designed or intended to support long-term repository performance."* The 1998 rulemaking that certified WIPP to receive transuranic waste placed conditions on the panel closure design to be implemented in the repository. The mandated design consists of a concrete block wall, an open drift section, and a concrete monolith, and was termed the "Option D" panel closure. Following the selection of the Option D design in 1998, the engineering of the panel closure has been re-assessed, and a revised design has been established that is simpler, cheaper, and easier to construct. The revised panel closure design, termed the Run-of-Mine Panel Closure System (ROMPCS), is comprised of 100 feet of ROM salt with barriers at each end. The ROM salt is generated from ongoing mining operations at the WIPP and may be compacted and/or moistened as it is emplaced in a panel entry. The barriers consist of ventilation bulkheads, similar to those currently used in the panels as room closures.

The DOE has submitted a planned change request (PCR) to the EPA requesting that EPA modify Condition 1 of the Final Certification Rulemaking for 40 CFR Part 194 (EPA, 1998) for the WIPP. The PCR submitted to EPA requests that Condition 1 be changed, and that the ROMPCS design be approved for use in all panels (DOE, 2011). In support of this rulemaking change, a performance assessment has been completed that incorporates the ROMPCS design into the current PA baseline established by the 2009 Performance Assessment Baseline Calculation

Information Only

(PABC-2009) (Clayton et al., 2010). The name given to this new panel closure PA is PCS-2012, and the plan for its execution is detailed in AP-161 (Camphouse 2012).

The program LHS is used to sample the distributions of parameters having epistemic uncertainty using a Latin Hypercube sampling design. PRELHS is run prior to LHS and is used to obtain from the WIPP Parameter Database the data describing the distributions and to create an input file to LHS based on that data. PRELHS Version 2.40 was used in this analysis, which is a deviation from the analysis plan (Camphouse 2012). The analysis plan specified the wrong version number for PRELHS. The user creates an input file for PRELHS that specifies which parameters are to be sampled using their "material" and "property" identifiers. PRELHS performs limited error checking on the data extracted from the database. LHS can reorder sampled data to induce or restrict correlations among the parameters. However, other conditional relationships were specified by the code analysts for three parameters. These conditional relationships restricted the value for one parameter to be less than the sampled value of another parameter. This conditional relationship was enforced using the utility LHS_EDIT Version 1.0 (Appendix VIII) to modify the output file generated by LHS. This report documents the use of PRELHS Version 2.40, LHS Version 2.42 and LHS_EDIT to provide three sets of sampled data for use in the 2012 PCS-2012 PA (Camphouse 2012). These three sets represent three replicates of one hundred samples for each of 75 variables. Sixty of these variables are associated with model parameters. However, there are also 15 "placeholder" variables sampled. These placeholders are included to enable users to add additional parameters and run LHS while preserving the ability to regenerate the values previously sampled for the model parameters.

The execution of LHS was verified by:

1. Checking the LHS input files to ensure that the headers properly document the analysis and that the random number seeds are correct.
2. Verifying that the proper set of parameters is being sampled. This was done by comparing the set to the specifications of the analysis plan (AP) for the analysis (AP161).
3. Checking the EVAL script input files to ensure that any conditional relationships imposed using LHS_EDIT.EXE are properly specified.
4. Examining the LHS log files for any obvious errors or failures.
5. Examining the PRELHS transfer (output) file to verify that the data were properly extracted from the database.
6. Examining the correlation matrices for "significant" values and to verify that non-zero correlations specified in the input file were properly generated.
7. Checking the values generated to ensure that they do not exceed the specified range.
8. Checking that the distributions match those specified in the parameter database.
9. Plotting the empirical Cumulative Distribution Function (CDF) against the expected CDF and looking for anomalies.

Information Only

II. Run Control

The script EVAL_LHS.COM was used to execute PRELHS, LHS and LHS_EDIT. This script processes an input file which lists the specific information required to run these codes. The details of run control are documented in Camphouse et al. (2012). The script and its input files are stored in LIBAP161_EVAL (PACMS2:[CMS_AP161.AP161_EVAL]).

III. PRELHS Input Files

The three input files for PRELHS are listed in appendices I to III. These files are named LHS1_AP161_R1.INP, LHS1_AP161_R2.INP and LHS1_AP161_R3.INP, respectively for replicates 1 to 3.Except for the title and random seed these three files are identical. Different random seeds are assigned in each input file to cause LHS to generate three unique sets of values. The random seeds used were those used in the PABC09, as specified in AP-161. This sampling design eliminates from comparisons of the results to the PABC09 results the impact of sampling of the distributions of the parameters having epistemic uncertainty. The corresponding output (transfer) files from PRELHS for the three replicates are listed in appendices IV to VI. These files are named LHS1_AP161_R1.TRN, LHS1_AP161_R2.TRN and LHS1_AP161_R3.TRN, respectively for replicates 1 to 3. The three transfer files are also identical except for titles and the random seed values. These files were inspected to verify that the data used to construct the distributions were properly extracted from the library.

IV. LHS Output files

The LHS output files were examined for errors. The ranges of the sampled variables were compared to the range specified as input for the distribution (Appendix VII). No values were found to exceed the specified ranges of the distributions although a few were found to cover less than 90% of the specified range, e.g. 77.4 % of the range was covered by the samples for S_MB139:PRMX_LOG (*material:property*) in replicate 3 (Fig. 156). These low coverage values are undoubtedly due to the shape of the distribution; the tails of the CDF curves are nearly horizontal, so that the width of 1 % and 99 % quantiles sampled by LHS are relatively wide. The width of the intervals (covering 1 % of the probability) is set by the number of LHS samples in the replicate (100).

The LHS output file lists the correlation coefficients between the sampled variables. The sampled data for those variables for which a correlation matrix was entered showed correlations that were close to those specified (Table 1). No significant ($\alpha = 0.01$) spurious correlations were observed among the uncorrelated variables, although in replicate 2 the correlation between the ranks of the variables CASTILER:PRESSURE and WAS_AREA:PROBDEG was -0.234 which is significant at $\alpha = 0.05$. However, WAS_AREA:PROBDEG is a discrete user-specified distribution (Delta distribution) having only 2 possible values (Figure 57). This restriction undoubtedly limits the ability of LHS to shuffle the values to enforce a correlation near zero. In addition, the significance test on the correlation coefficient is questionable in any case because the data fails to even come close to meeting the assumptions of normality of the data.

Information Only

To evaluate the frequency with which high correlation coefficients would be expected in such variables, a test was conducted (Kirchner 2009). In the test, 1000 LHS samples were generated and the correlation coefficients greater than 0.197 (the test statistic for the correlation coefficient for n=100) were tabulated. To generate these values, the LHS2_LHS.FOR code was modified to 1) run 1000 iterations of LHS sampling and 2) to output the data that exceeded 0.197. The modified code was named LHS2_LHS_TEST.FOR and stored with the executable and input files in library LIBCRA09_LHSCORR (PACMS2:[CMS_CRA09.CRA09_LHSCORR). For this informal test, all correlations were specified to be zero. Out of the 1000 samples, 502 ($\alpha = 0.05$) and 2 ($\alpha = 0.01$) "significant" correlations were generated. All of these correlations involved either WAS_AREA:PROBDEG or S_MB139:RELP_MOD, both of which have discrete distributions having only two possible values. These results suggest that the number of values exceeding the standard test statistics for correlation coefficients may be relatively high when LHS samples discrete distributions having few possible values.

□a□□□□□i□nifi□ant □orr□lation□□□t□□□n □aram□t□r□□

Replicate	Between		Expected Correlation	Observed Correlation	Significance[2]
1	CASTILER:COMP_RCK	CASTILER:PRMX_LOG	-0.75	-0.7281	**
	S_HALITE:COMP_RCK	S_HALITE:PRMX_LOG	-0.99	-0.9869	**
2	CASTILER:COMP_RCK	CASTILER:PRMX_LOG	-0.75	-0.7242	**
	CASTILER:PRESSURE[1]	WAS_AREA:PROBDEG	0.00	-0.234	*
	S_HALITE:COMP_RCK	S_HALITE:PRMX_LOG	-0.99	-0.9907	**
3	CASTILER:COMP_RCK	CASTILER:PRMX_LOG	-0.75	-0.7252	**
	S_HALITE:COMP_RCK	S_HALITE:PRMX_LOG	-0.99	-0.9834	**

1 This correlation is spurious.

2 * = Significant at $p<0.05$, ** = Significant at $p<0.01$

The sampled distributions were compared to the expected distributions. Cumulative distribution functions for the sampled data were constructed by ordering the data from smallest to largest value and assigning the probability $i/100-0.005$ to the ith ordered value, i.e. the midpoint of the interval containing the value based on order statistics (Figures 1 through 180). With the exception of the variables modified using LHS_EDIT (Figures 26, 27 and 55 for replicate 1, Figures 86, 87 and 115 for replicate 2 and Figures 146,147 and 175 for replicate 3), the differences between the CDFs of the sampled values and the CDFs of the expected distributions are due to the differences between the estimated probability assigned to the values and the true probability associated with the data.

V. Imposing Additional Limits on Some Variables

LHS_EDIT was used to enforce a conditional relationship between three pairs of variables. The relationships were WAS_AREA:GRATMICH ≤ WAS_AREA:GRATMICI (Clayton 2008, Nemer and Stein 2005) and PCS_T3: POROSITY ≤ PCS_T2: POROSITY ≤

Information Only

PCS_T1:POROSITY (Camphouse 2012). The relationships were enforced by modifying values in the LHS transfer file, thus making the conditioned values available for use in the sensitivity analysis. For each pair of variables LHS_EDIT rescales the sampled value of the parameter to the left of the $\leq$ symbol to the new "controlled" value using the equation

$$v_i' = \frac{v_i - U_{V,lower}}{U_{V,upper} - U_{V,lower}} \times \left(Min(x_i, U_{V,upper}) - U_{V,lower} \right) + U_{V,lower}$$

Where v_i' is the conditioned value of left hand variable, v_i is the sampled value of that variable, x_i is the sampled value of the right hand variable, and $U_{V,lower}$ and $U_{V,upper}$ are the bounds of the distribution assigned to the left hand variable. This method preserves the probability associated with the value of the left hand variable. The CDFs for the original sampled values and the conditioned values are shown in Figures 27, 28 and 56 for replicate 1, Figures 88, 89 and 117 for replicate 2 and Figures 149,150 and 178 for replicate 3. This conditional relationship results in a positive correlation between the pairs of variables. For example, the correlation between WAS_AREA:GRATMICH and WAS_AREA:GRATMICI was computed for Replicate 1 using Excel and found to be 0.74 (Figure 181). The nature of these correlations is fundamentally different than that which LHS could induce between the variables. LHS achieves correlations between variables by reordering the sampled data whereas LHS_EDIT changes the range of the left hand sampled variable. If instead of limiting the value of the left hand variable an equivalent correlation had been specified between the variables in the input file to LHS then LHS would have generated values for the left hand variable that could have exceeded the corresponding value for the right hand variable.

VI. Summary and Conclusions

LHS was used to generate one hundred vectors of sampled parameter values for each of three replicates. A unique random number seed was assigned to each of the three replicates. These seed values were identical to those used in the PABC09 analysis. The resulting sampled data had the expected correlation structure and the values fell within the expected ranges. The LHS results were subsequently modified to enforce a conditional relationship between WAS_AREA:GRATMICH and WAS_AREA:GRATMICI, PCS_T3: POROSITY and PCS_T2: POROSITY, and PCS_T2: POROSITY and PCS_T1:POROSITY.

Information Only

VII. References

Camphouse, C. 2012. Analysis Plan for the 2012 WIPP Panel Closure System Performance Assessment, Revision 0. July 2, 2012. Carlsbad, NM: Sandia National Laboratories. ERMS #557726

Camphouse, R.C., Kicker, D.C., Kirchner, T.B., Long, J.J., Malama, B., and Zeitler, T.R. 2012. Summary Report and Run Control for the 2012 WIPP Panel Closure System Performance Assessment. Sandia National Laboratories, Carlsbad, NM.

Clayton, D. J. 2008. Analysis Plan for the Performance Assessment for the 2009 Compliance Recertification Application. Sandia National Laboratories, Carlsbad, N.M. ERMS #547515.

Clayton, D.J., Camphouse, R. C., Garner, J. W., Ismail, A. E., Kirchner, T. B., Kuhlman, K. L., and Nemer, M. B.. 2010. Summary Report of the CRA-2009 Performance Assessment Baseline Calculation, Revision 1. Sandia National Laboratories. Carlsbad, New Mexico, ERMS 553039.

DOE (U.S. Department of Energy). 1996. Title 40 CFR Part 191 Compliance Certification Application for the Waste Isolation Pilot Plant. DOE/CAO-1996-2184. U.S. Department of Energy, Waste Isolation Pilot Plant, Carlsbad Area Office. Carlsbad, NM.

DOE (U.S. Department of Energy), 2011. Panel Closure System Design, Planned Change Request to the EPA 40 CFR Part 194 Certification of the Waste Isolation Pilot Plant. U.S. Department of Energy, Carlsbad Field Office. Carlsbad, New Mexico.

EPA (U.S. Environmental Protection Agency). 1998. Criteria for the Certification and Re-Certification of the Waste Isolation Pilot Plants Compliance with the 40 CFR Part 191 Disposal Regulations: Certification Decision; Final Rule, Federal Register, Vol. 63, No. 95, pp. 27353-27406. U.S. Environmental Protection Agency, Office of Air and Radiation, Washington, D.C.

Kirchner, T. 2009. Generation of the LHS Samples for the AP-137 Revision 0 (CRA09) PA Calculations. Carlsbad, NM: Sandia National Laboratories. ERMS #547971

Nemer, M. B. and J. S. Stein. 2005. "Analysis Package for BRAGFLO: 2004 Compliance Recertification Application Performance Assessment Baseline Calculation." Analysis Report, June 28, 2005. Carlsbad, NM: Sandia National Laboratories. ERMS 540527.

Information Only

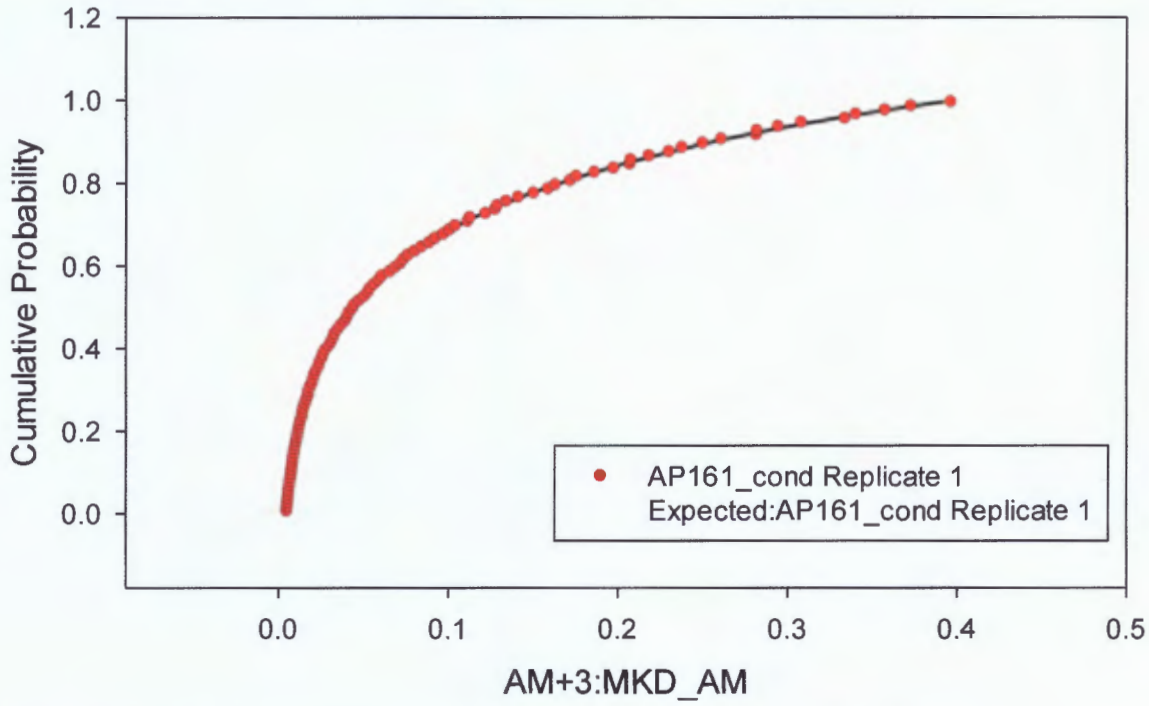

□i□r□□O□□r□□an□□□□□t□□□□□for □□ □□□□ □□□□ □□o□□niform □i□ri□□tion□□□□li□at□□

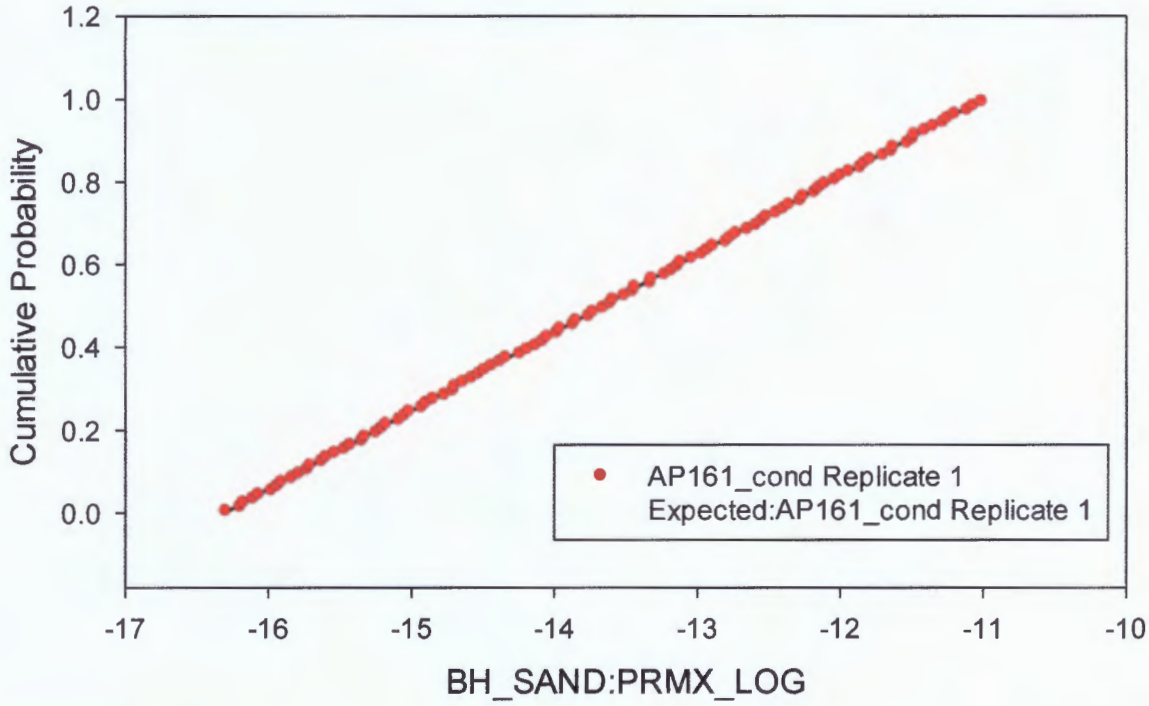

□i□r□□O□□r□□an□□□□□t□□□□□for □□□□□□□□□ □□O□ □□niform □i□ri□□tion□□□□li□at□□

Information Only

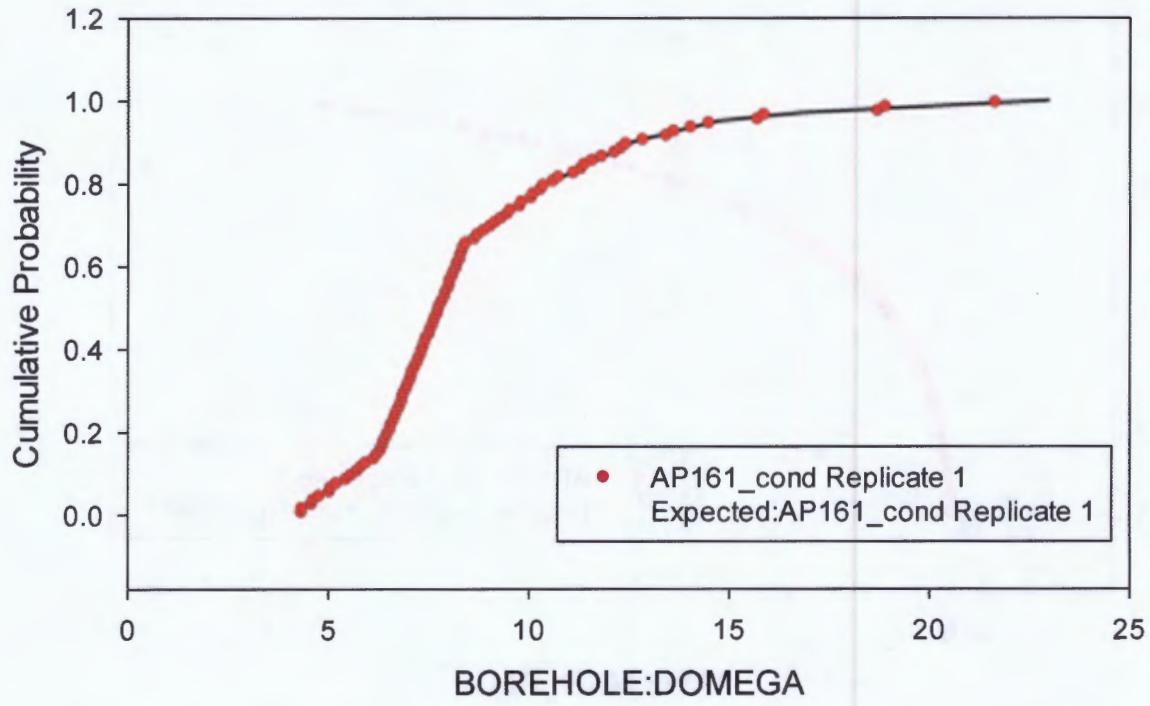

□i□r□□O□□r□□an□□□□□t□□□□□for □O□□□O□□□□O□ □□□ □□□r □ontin□o□□□i□ri□□tion□□□□li□at□□

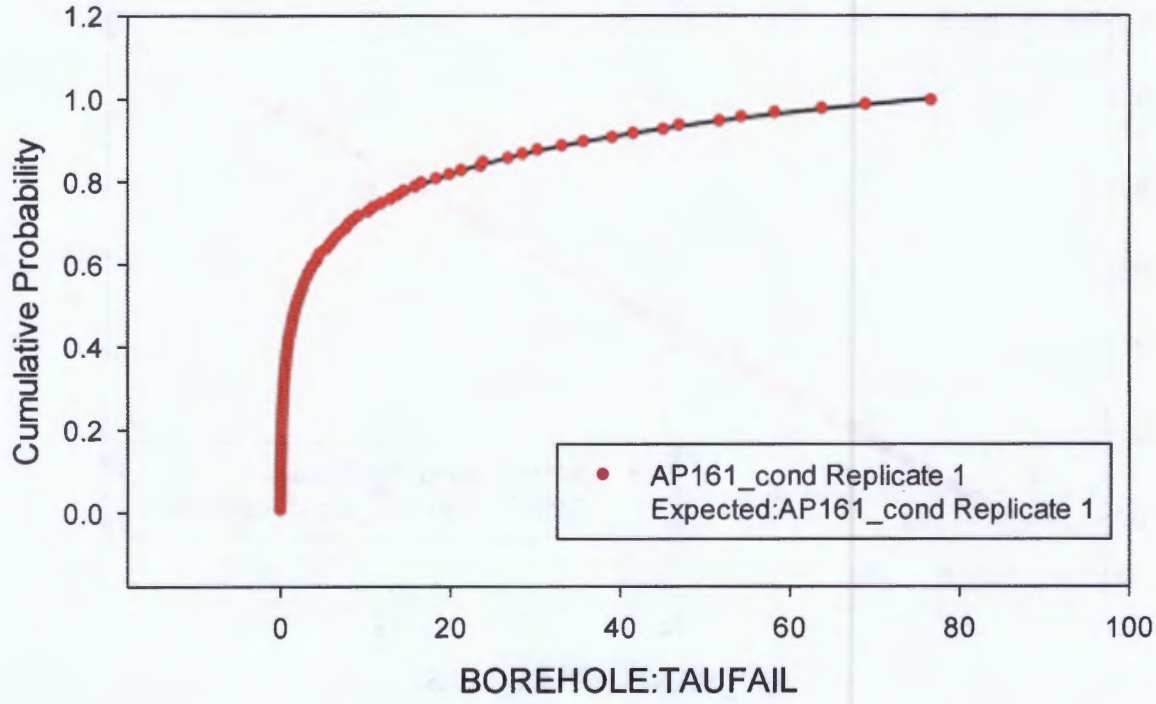

□i□r□□O□□r□□an□□□□□t□□□□□for □O□□□O□□□□□□□I□ □□o□□niform □i□ri□□tion□□□□li□at□□

Information Only

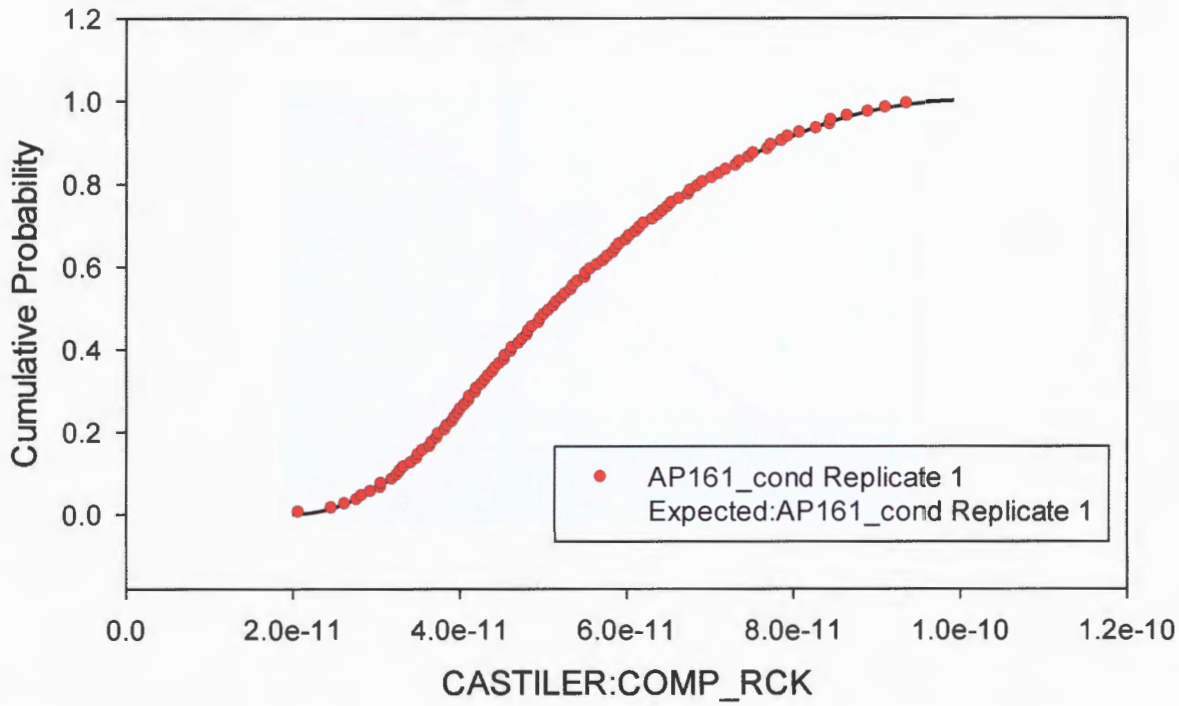

□i□□r□□□O□□□r□□□an□□□□□□t□□□□□□for □□□□□□□□□□□O□ □□□□□ □□rian□□lar □i□tri□□tion□□□□i□at□□□

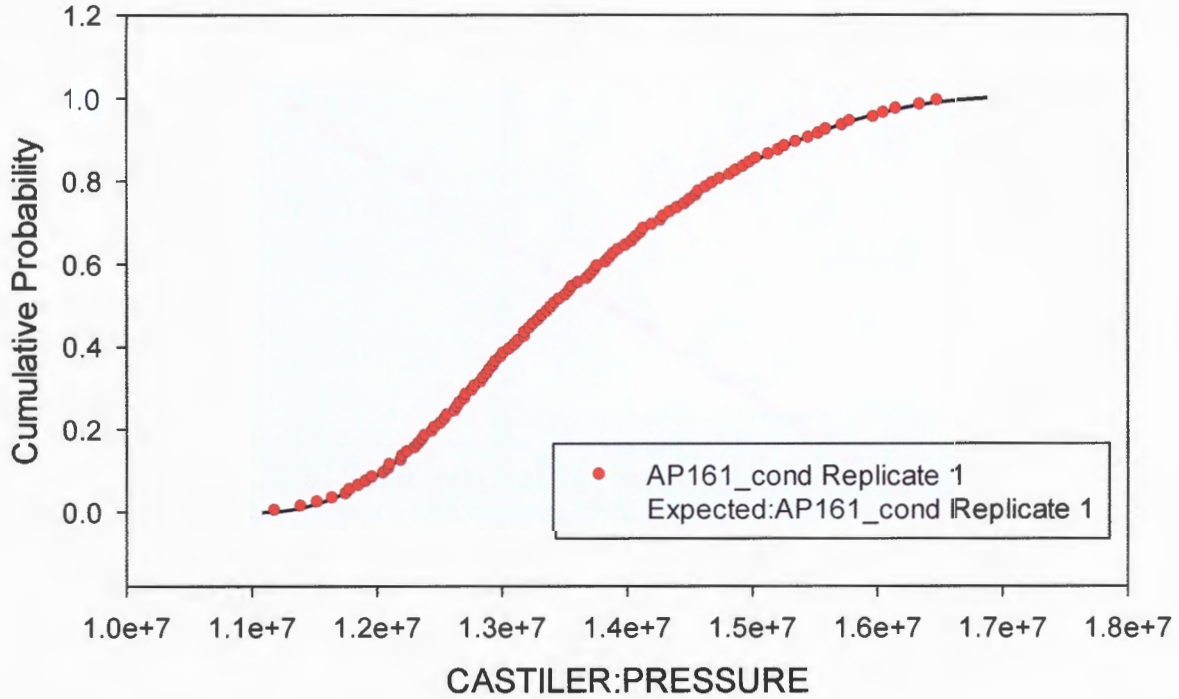

□i□□r□□□O□□□r□□□an□□□□□□t□□□□□□for □□□□□□□□□□□□□□□□□□ □□rian□□lar □i□tri□□tion□□□□i□at□□□

Information Only

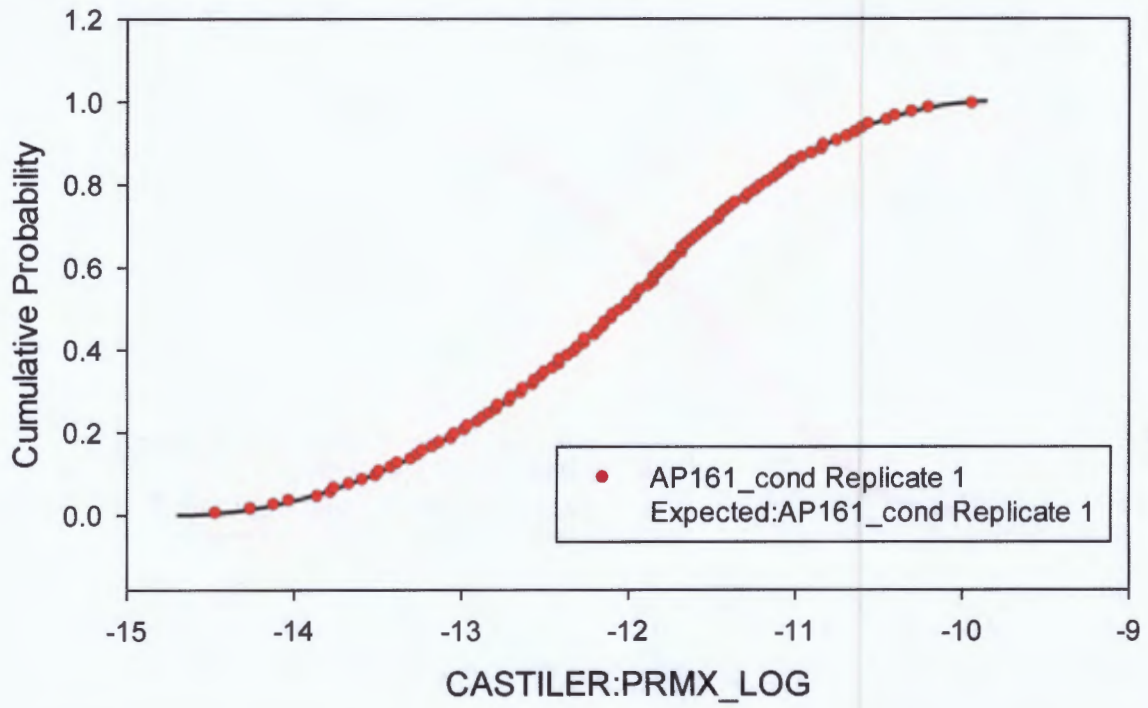

□i□r□□O□□r□□an□□□□t□□□□for □□□□l□□□□□□ □□O□ □□rian□□ar □i□ri□□tion□□□li□at□□

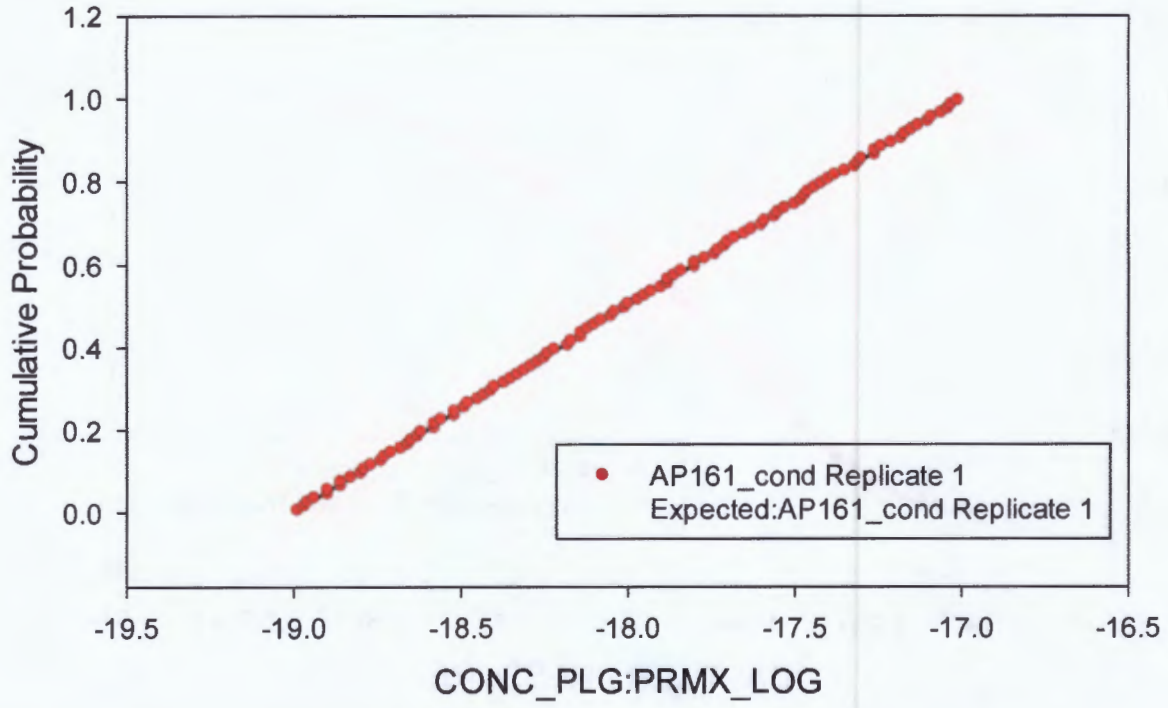

□i□r□□O□□r□□an□□□□t□□□□for □O□□□□□□□□ □□O□ □□niform □i□ri□□tion□□□li□at□□

Information Only

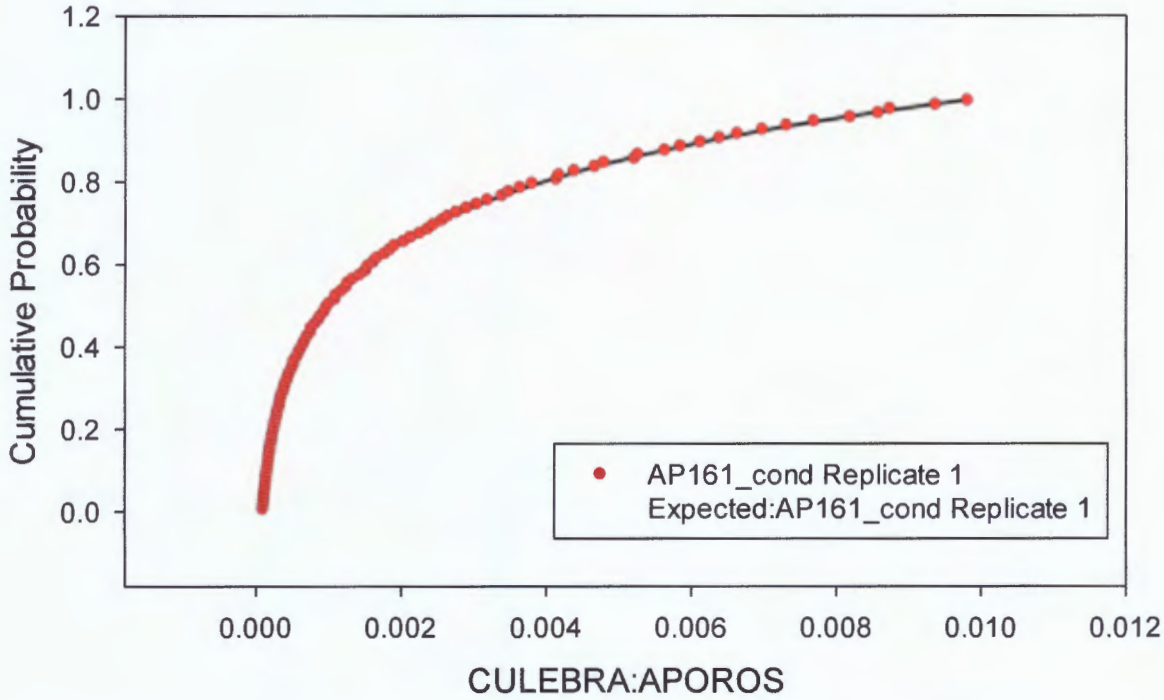

□i□□r□□□O□□□r□□□an□□□□□□t□□□□□□for □□□□□□□□□□□O□O□□□o□□niform □i□tri□□tion□□□□li□at□□□

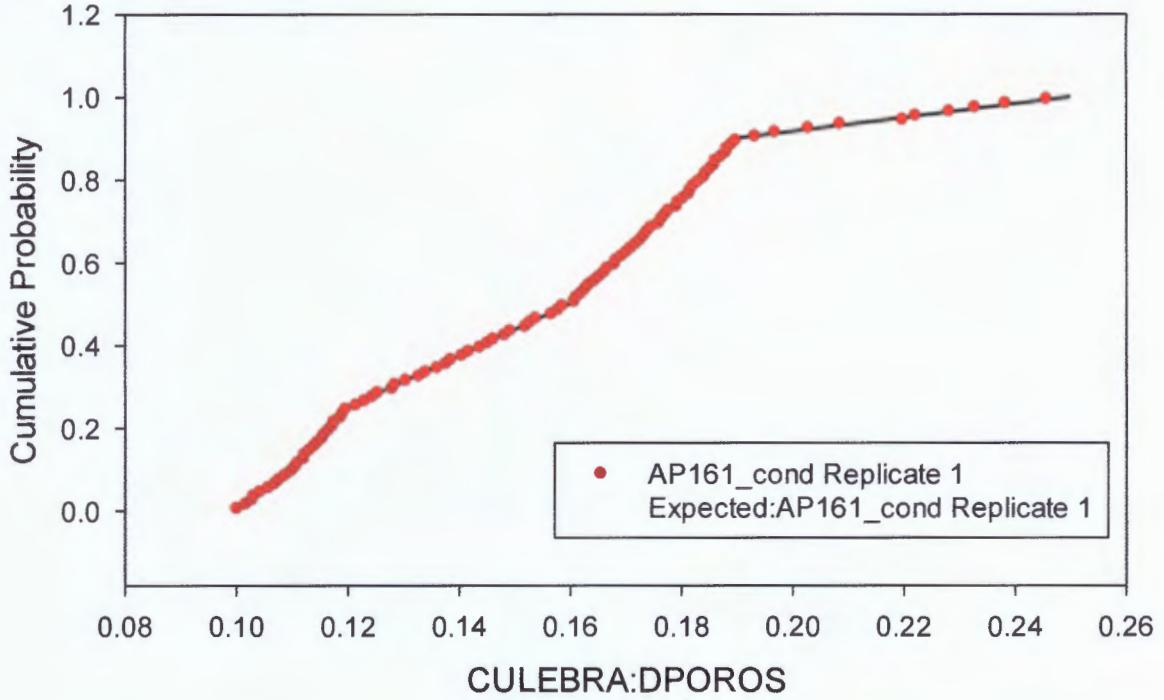

□i□□r□□□O□□□r□□□an□□□□□□t□□□□□□for □□□□□□□□□□□O□O□□□□r □ontin□o□□□i□tri□□tion□□□□li□at□□□

Information Only

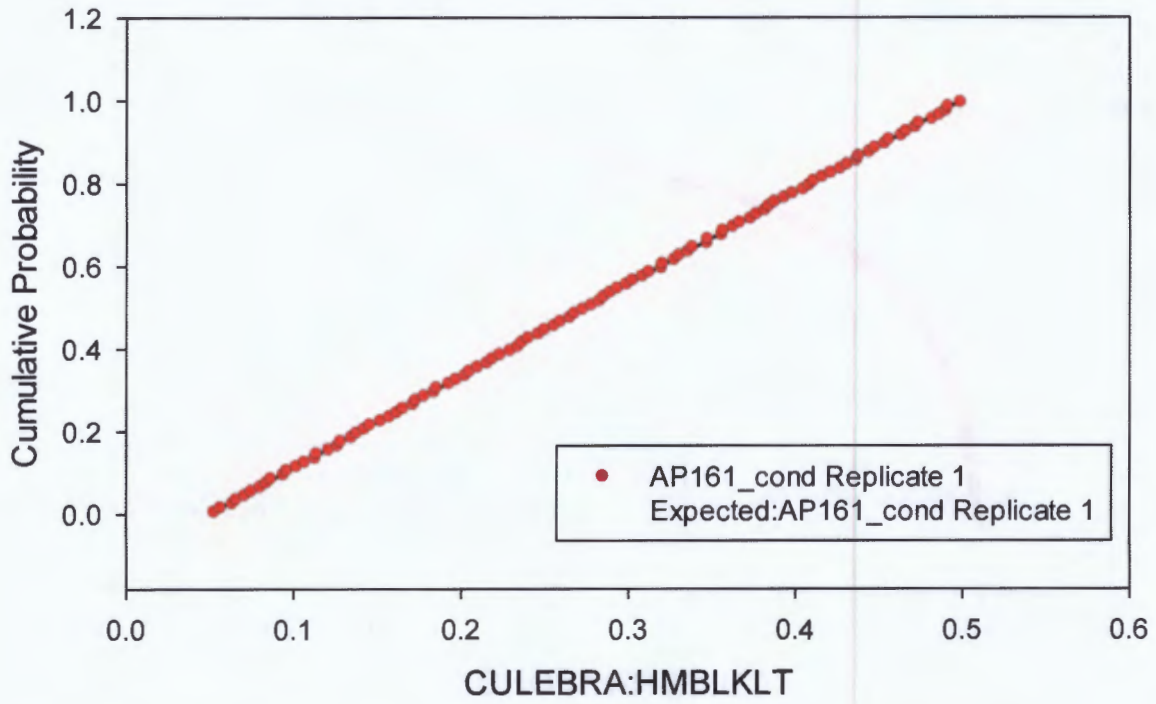

□i□r□□□O□□r□□an□ □□□□t□□ □□□□for □□□□□□□□□□ □□□□□ □□niform □i□ri□□tion□□□□li□at□□

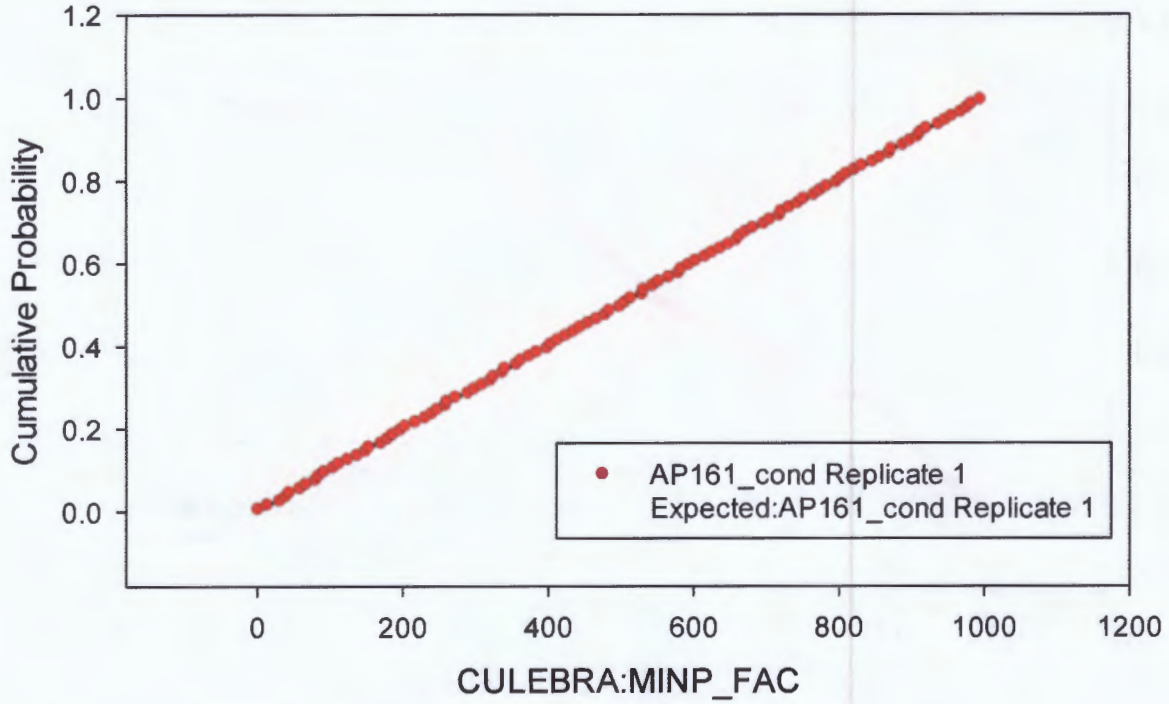

□i□r□□□O□□r□□an□ □□□□t□□ □□□□for □□□□□□□□□ I□□□□□ □□niform □i□ri□□tion□□□□li□at□□

Information Only

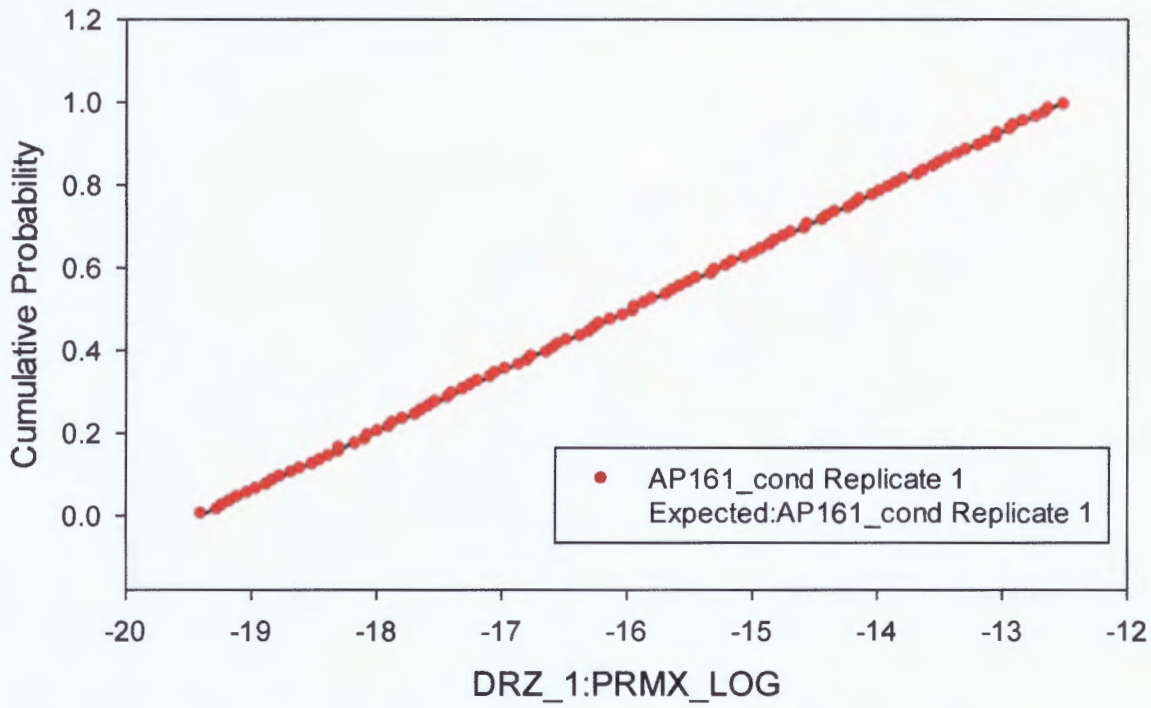

□i□□r□□□□O□□□r□□□an□□□□□□t□□ □□□□for □□□□□□□□□□ □□□O□ □□niform □i□tri□□tion□□□□li□at□□□

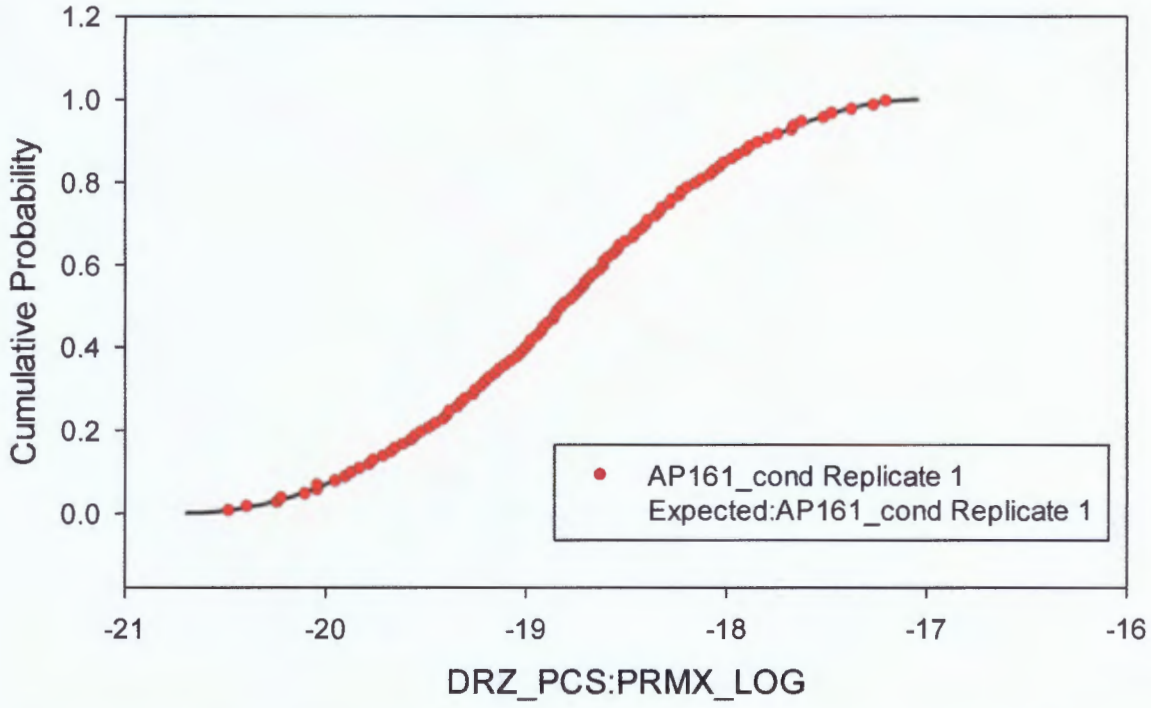

□i□□r□□□□O□□□r□□□an□□□□□□t□□ □□□□for □□□□□□□□□□□□ □□□O□ □□rian□□lar □i□tri□□tion□□□□li□at□□□

Information Only

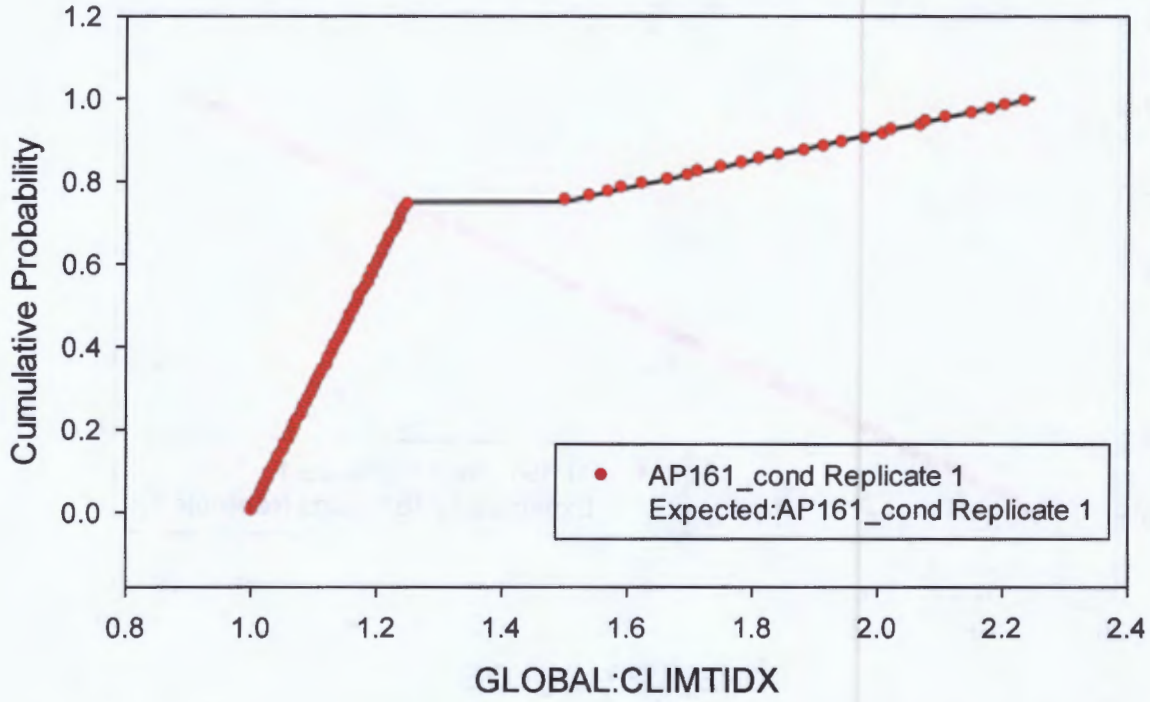

□i□□r□□□□O□□□r□□□an□ □□□□□□t□□ □□□□for □ □O□□□□□□I□ □I□□ □□□□r □ontin□b□□□i□ri□□tion□□□□i□at□□

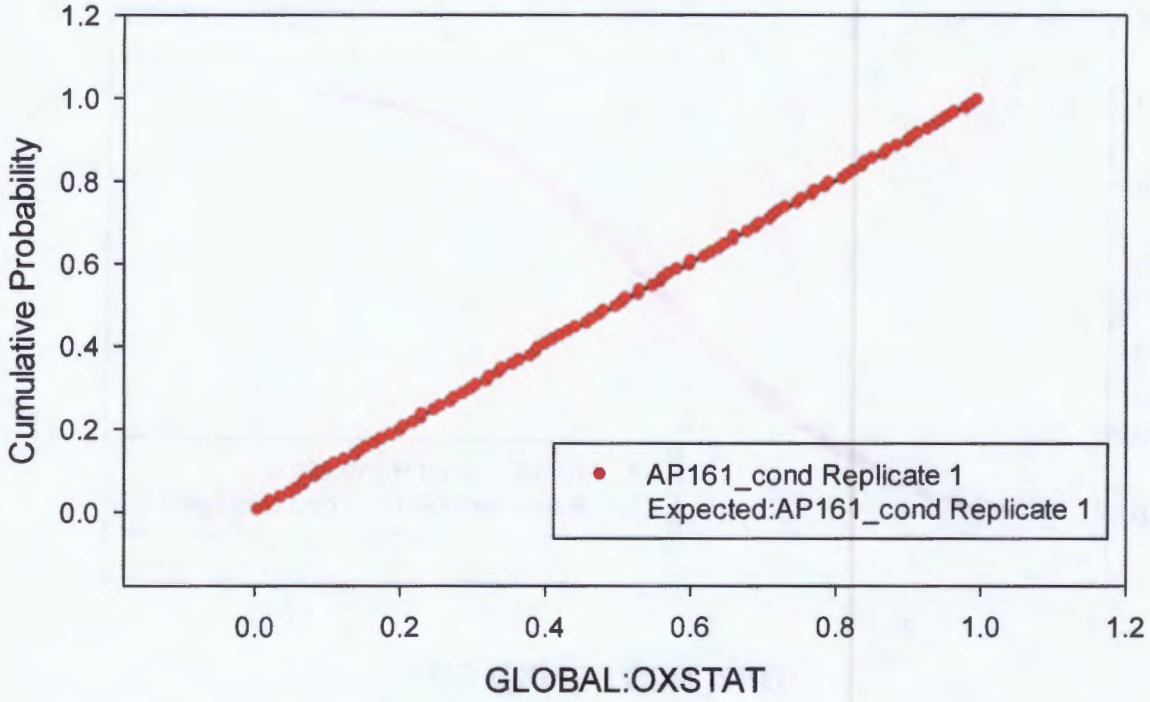

□i□□r□□□□O□□□r□□□an□ □□□□□□t□□ □□□□for □ □O□□□□□O□□□□□ □□niform □i□ri□□tion□□□□i□at□□□

Information Only

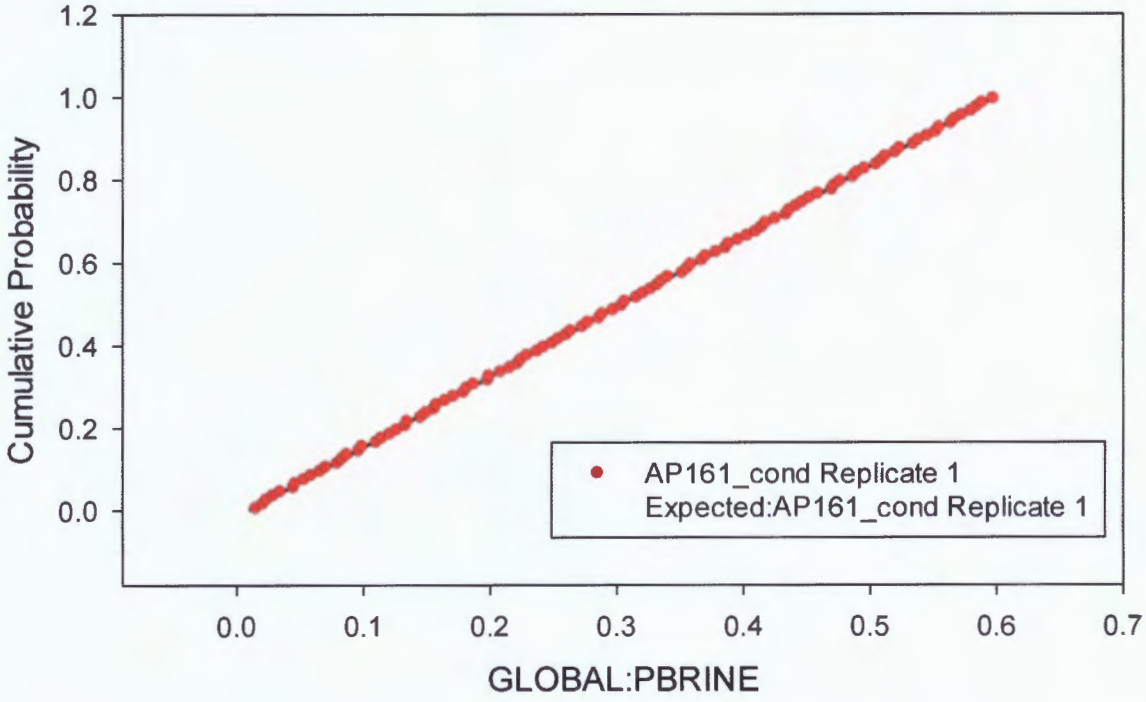

□i□□r□□□□O□□□r□□□an□□□□□□□t□□□□□□for□□□O□□□□□□□□□I□□□□niform□i□ri□□tion□□□□li□at□□□

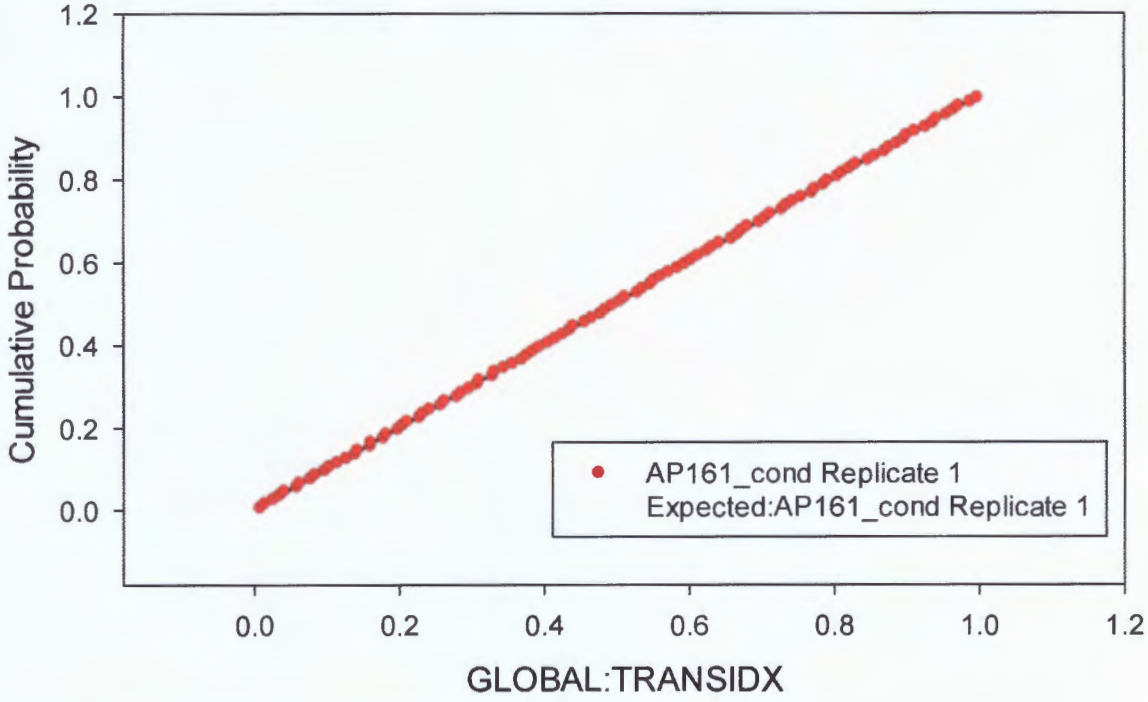

□i□□r□□□□O□□□r□□□an□□□□□□□t□□□□□□for□□□O□□□□□□□□□□I□□□□niform□i□ri□□tion□□□□li□at□□□

Information Only

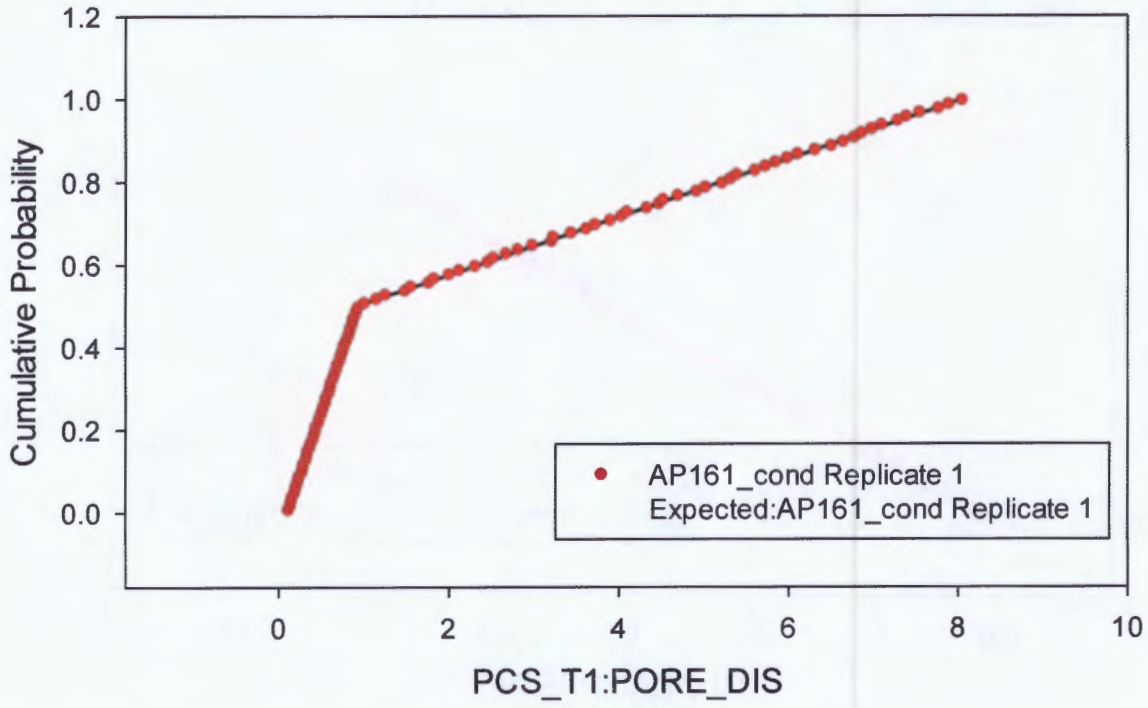

□i□r□□□O□□r□□an□ □□□□t□□ □□□□for □□□□□□O□□□□I□ □□□r □ontin□o□□□i□ri□□tion□□□□li□at□□

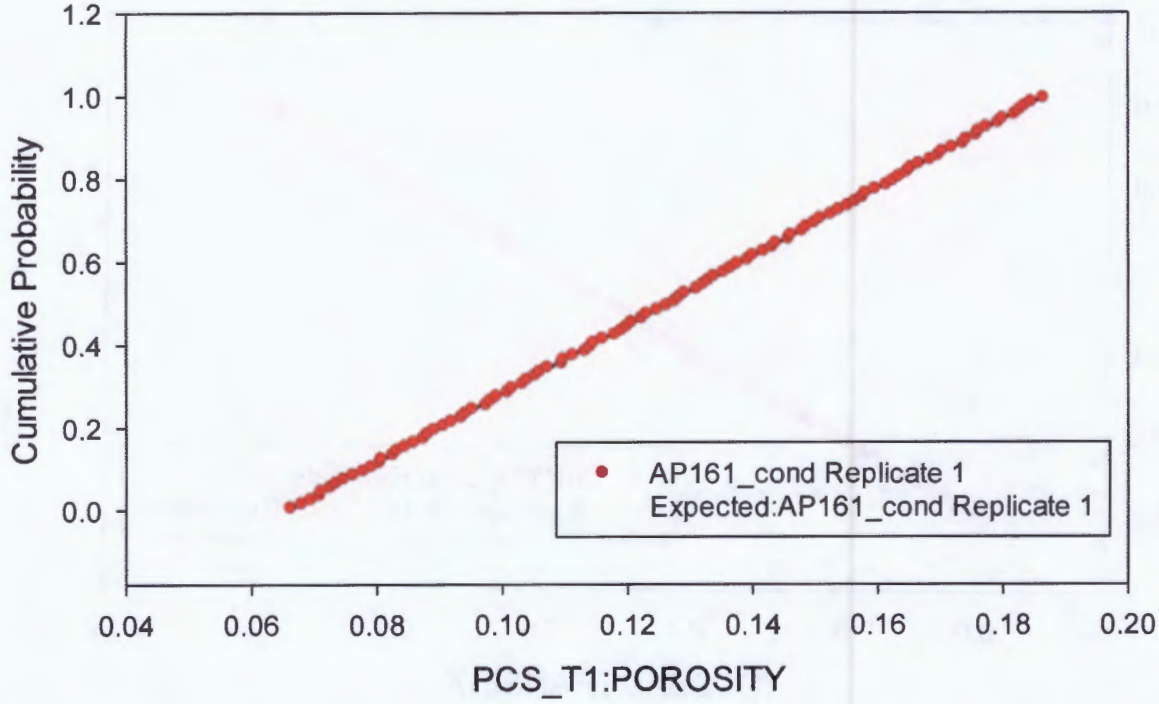

□i□r□□□O□□r□□an□ □□□□t□□ □□□□for □□□□□□O□O□I□□ □□niform □i□ri□□tion□□□li□at□□

Information Only

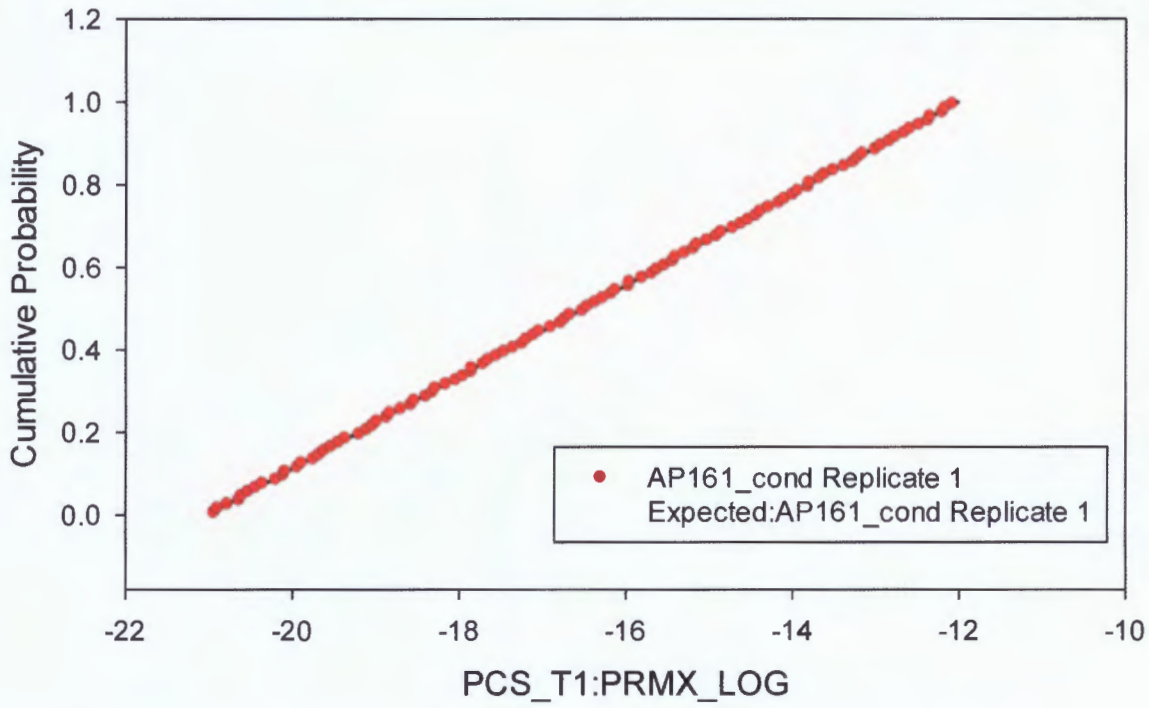

□i□r□□□O□□r□□an□ □□□□t□□ □□□□for □□□□□□□□□ □□□O□ □□niform □i□ri□□tion□□□□li□at□□

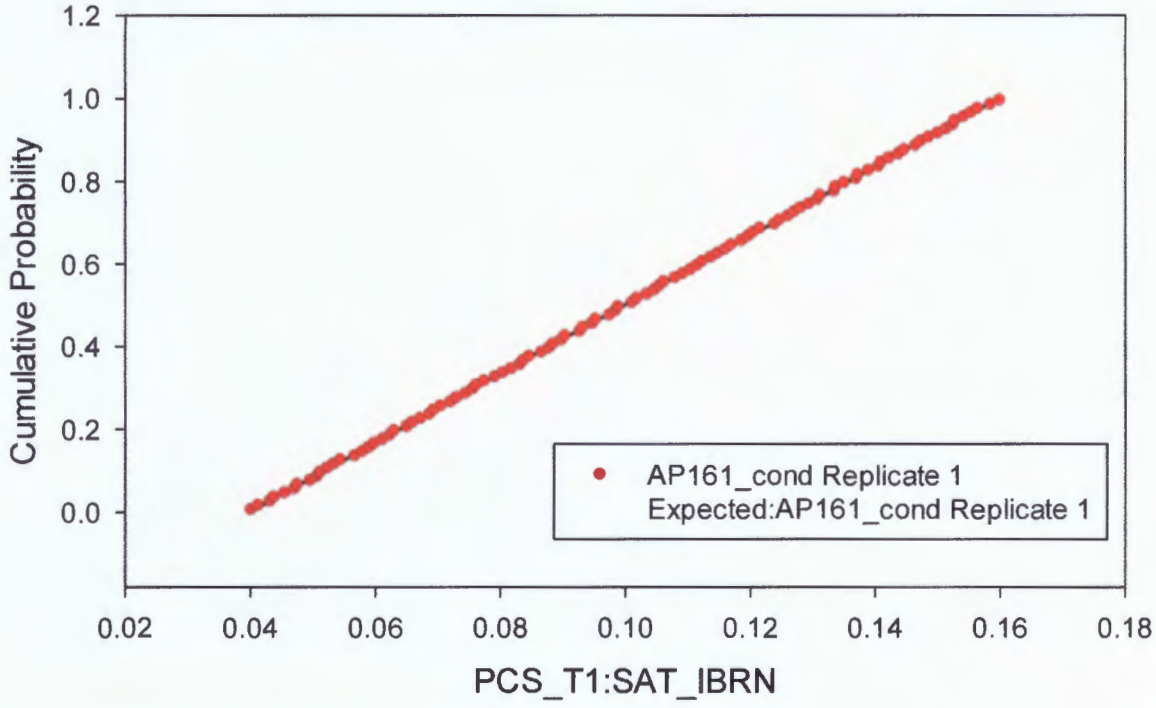

□i□r□□□O□□r□□an□ □□□□t□□ □□□□for □□□□□□□□□□□□ □□niform □i□ri□□tion□□□□li□at□□

Information Only

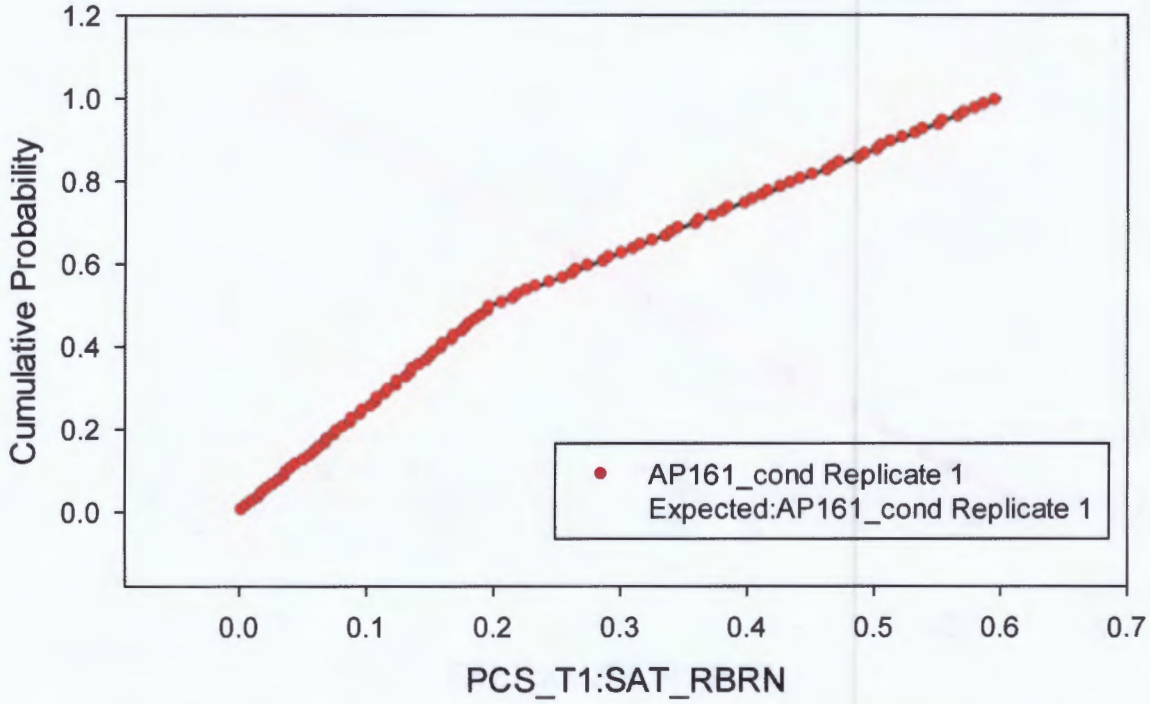

□i□r□□□O□□r□□an□ □□□□t□□ □□□□for □□□□□□□□□□□□□ □□□r □ontin□o□□□i□ri□□tion□□□□li□at□□

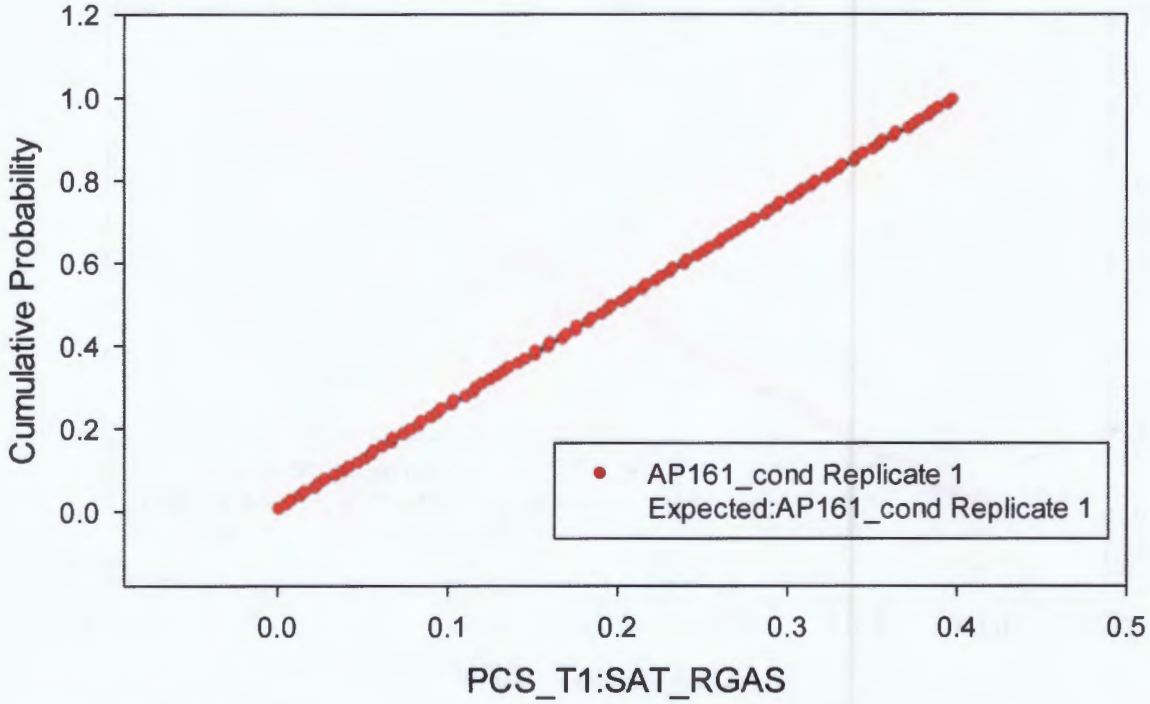

□i□r□□□O□□r□□an□ □□□□t□□ □□□□for □□□□□□□□□□□□□ □□niform □i□ri□□tion□□□□li□at□□

Information Only

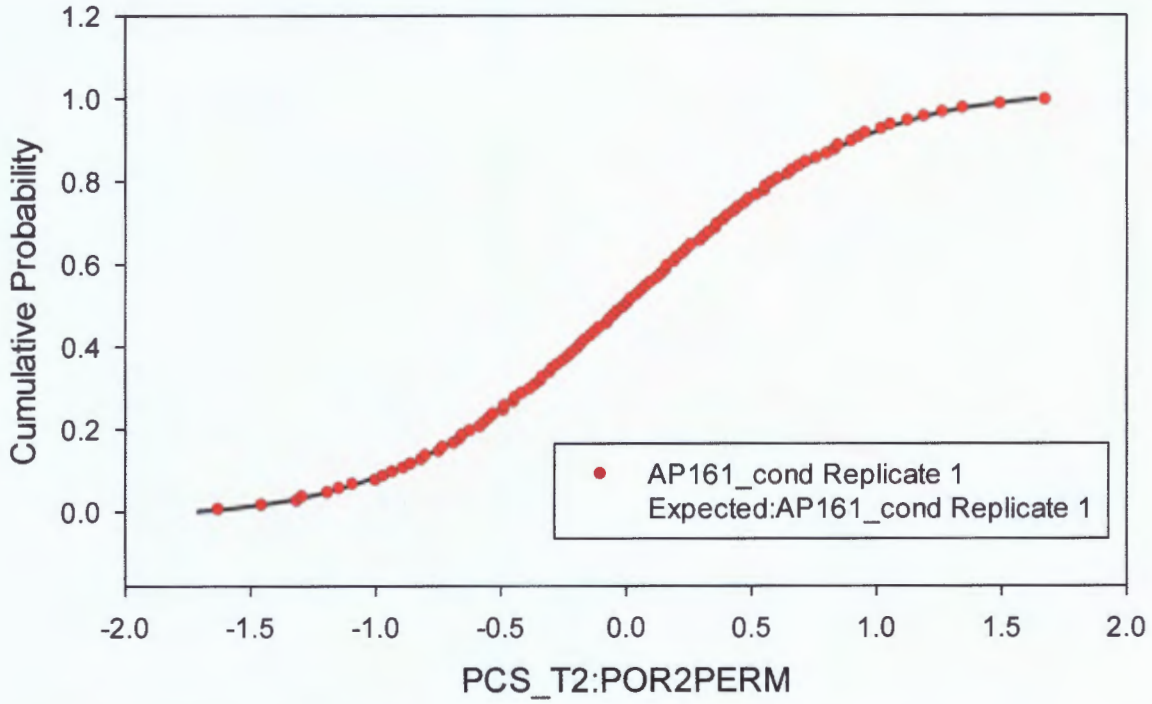

□i□r□□□O□□r□□□an□ □□□□□t□□ □□□□for □□□□□□□O□□□□□ □□ormal □i□ri□□tion□□□□li□at□□

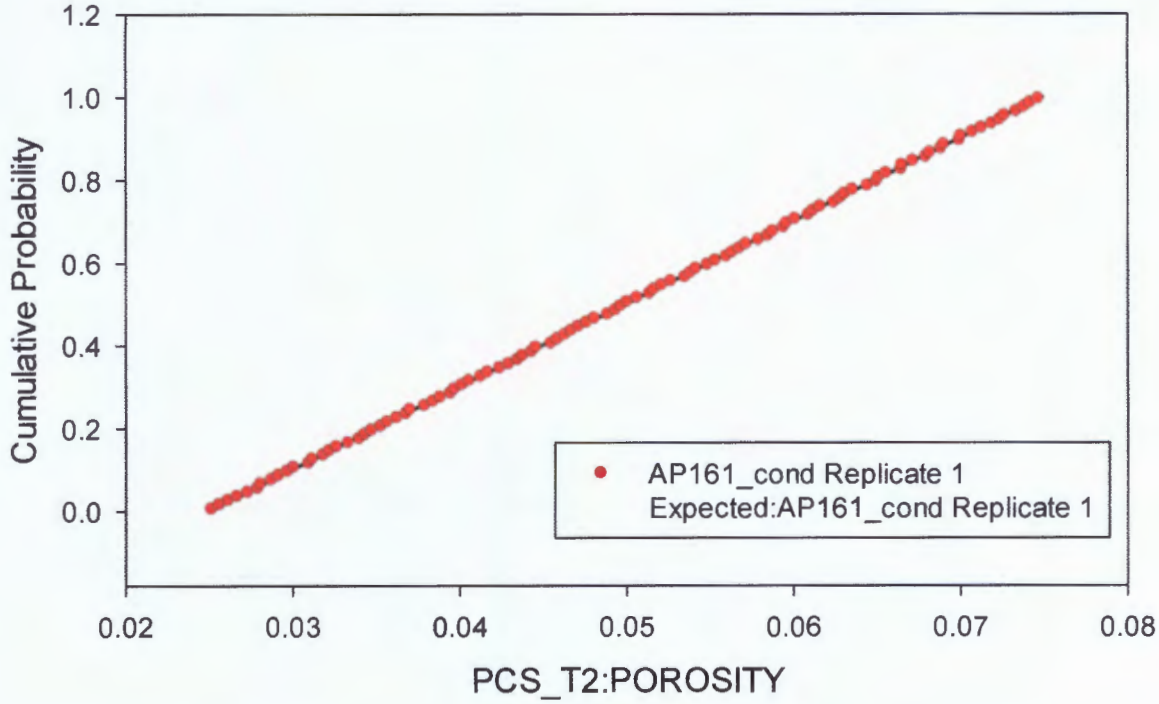

□i□r□□□O□□r□□□an□ □□□□□t□□ □□□□for □□□□□□□O□O□I□□ □□niform □i□ri□□tion□□□□li□at□□

Information Only

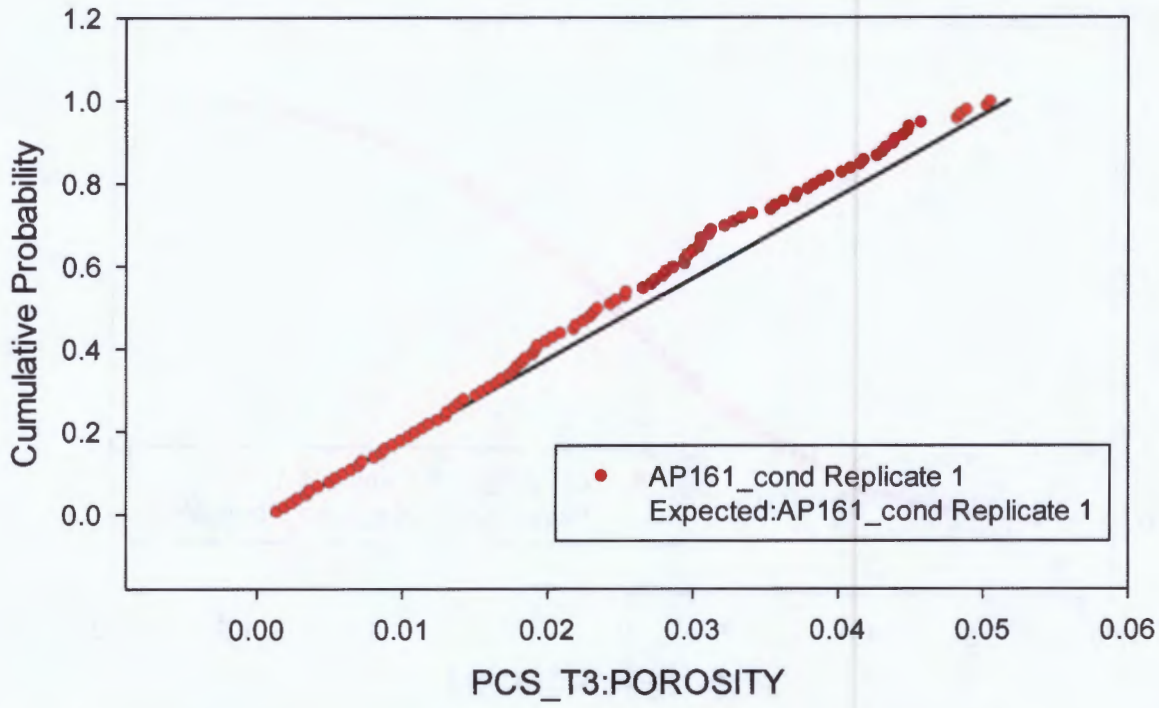

□i□□r□□□□O□□□r□□□an□□□□□□t□□□□□□for □□□□□□□O□O□I□□ □□niform □i□ri□□tion□□□□li□at□□

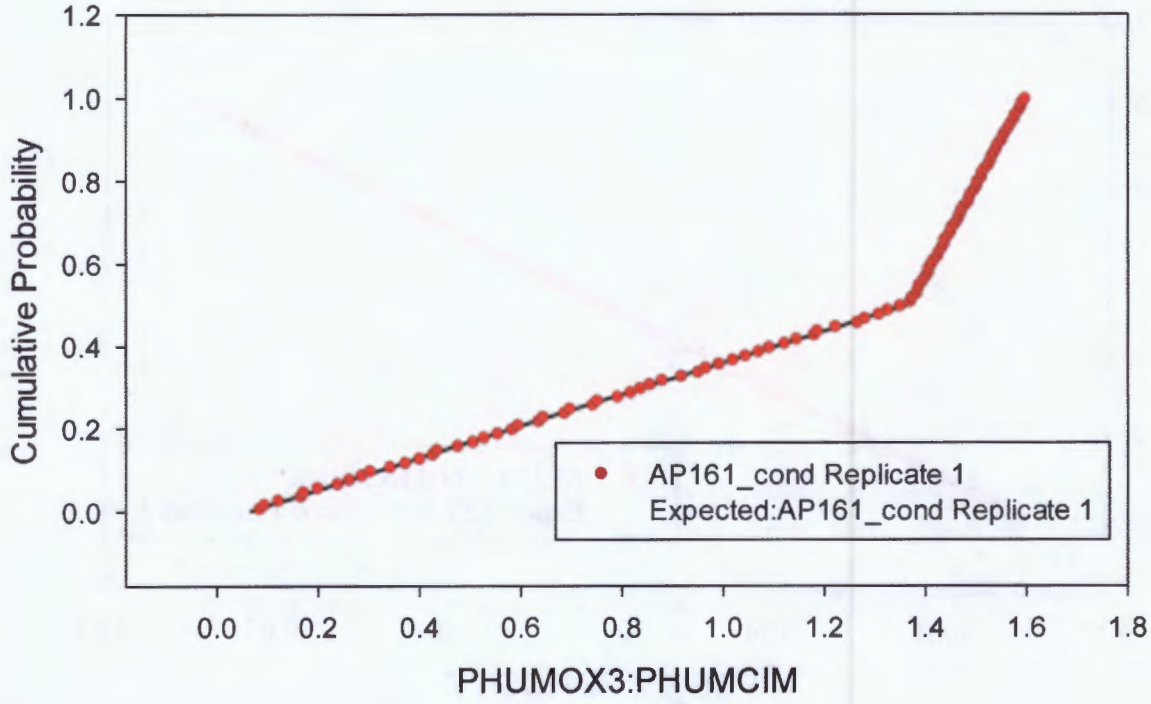

□i□□r□□□□O□□□r□□□an□□□□□□t□□□□□□for □□□□ O□□□□□□□ □I□ □□□r □ontin□o□□□i□ri□□tion□□□□li□at□□

Information Only

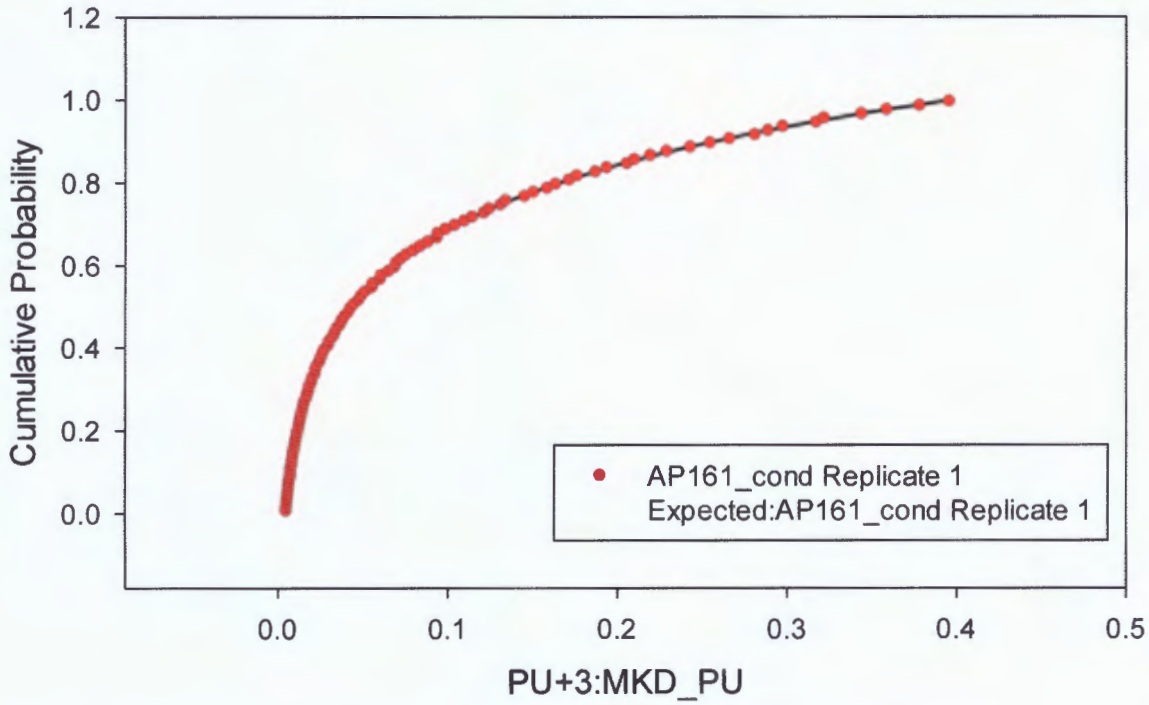

□i□□r□□□□O□□□r□□□an□□□□□□t□□□□□□for □□□□□□ □□□□□ □□o□□niform □i□tri□□tion□□□□i□at□□

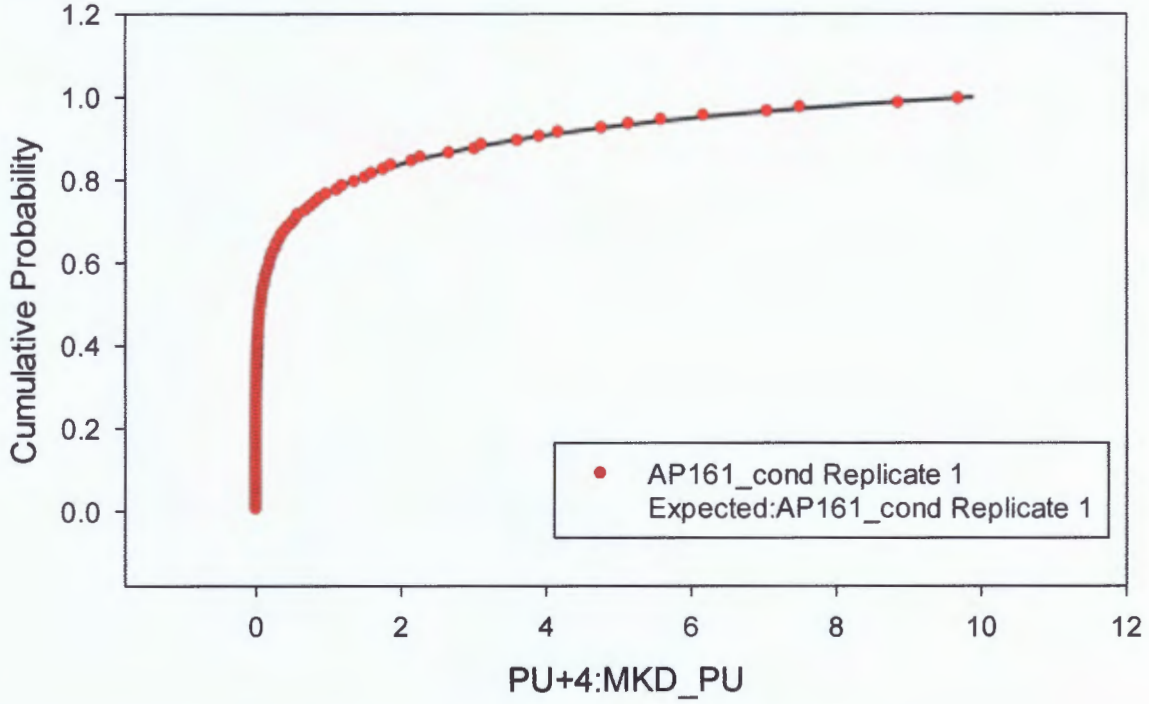

□i□□r□□□□O□□□r□□□an□□□□□□t□□□□□□for □□□□□□ □□□□□ □□o□□niform □i□tri□□tion□□□□i□at□□

Information Only

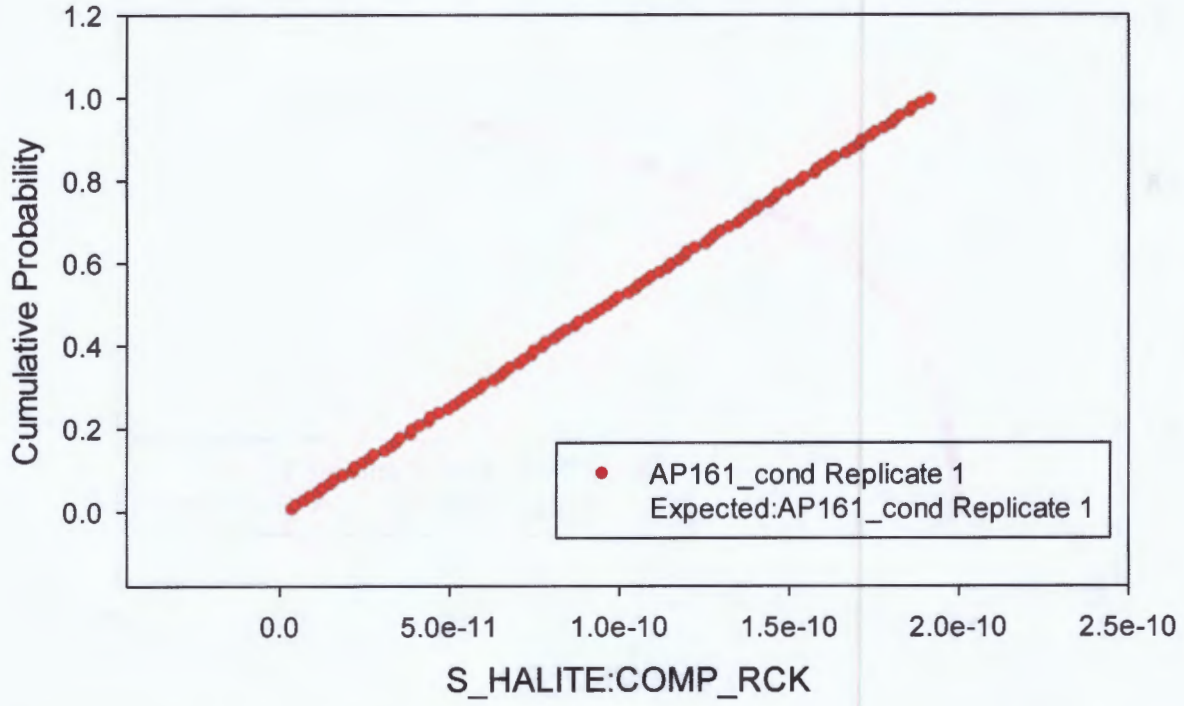

□i□r□□□O□□r□□an□ □□□□□t□□ □□□□for □□□ □□I□□□□O□ □□□□□ □□niform □i□tri□□tion□□□□li□at□□

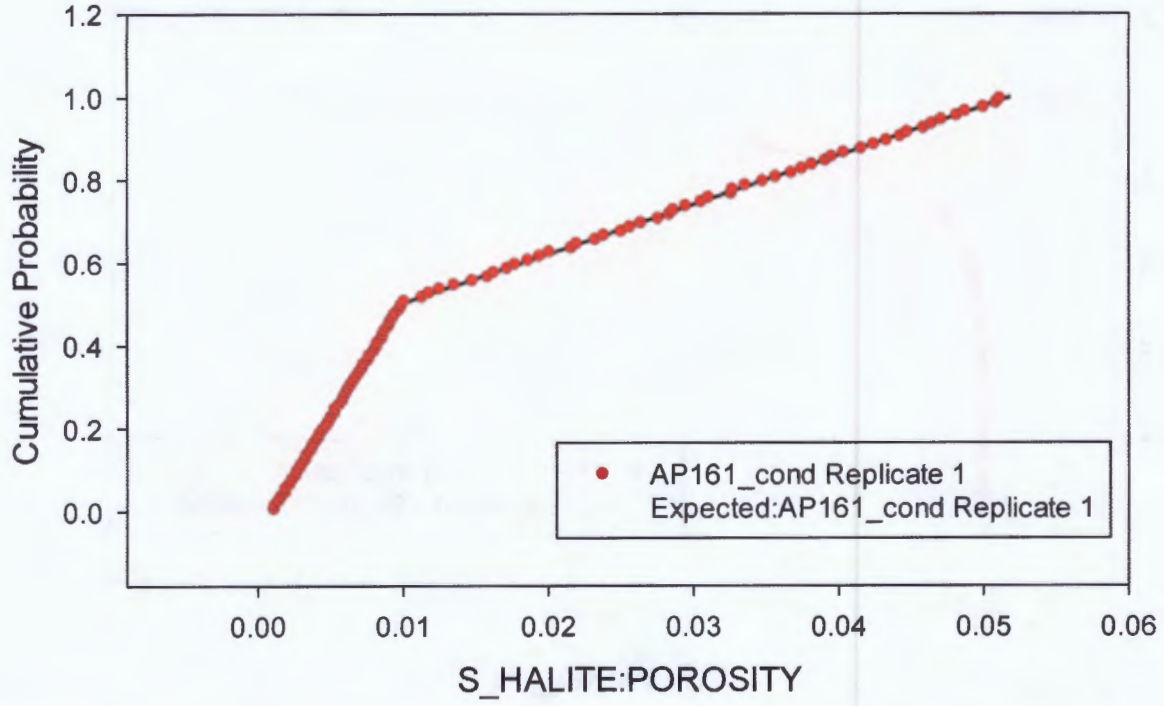

□i□r□□□O□□r□□an□ □□□□□t□□ □□□□for □□□ □□I□□□□O□O□I□□ □□□r □ontin□o□□□i□tri□□tion□□□□li□at□□

Information Only

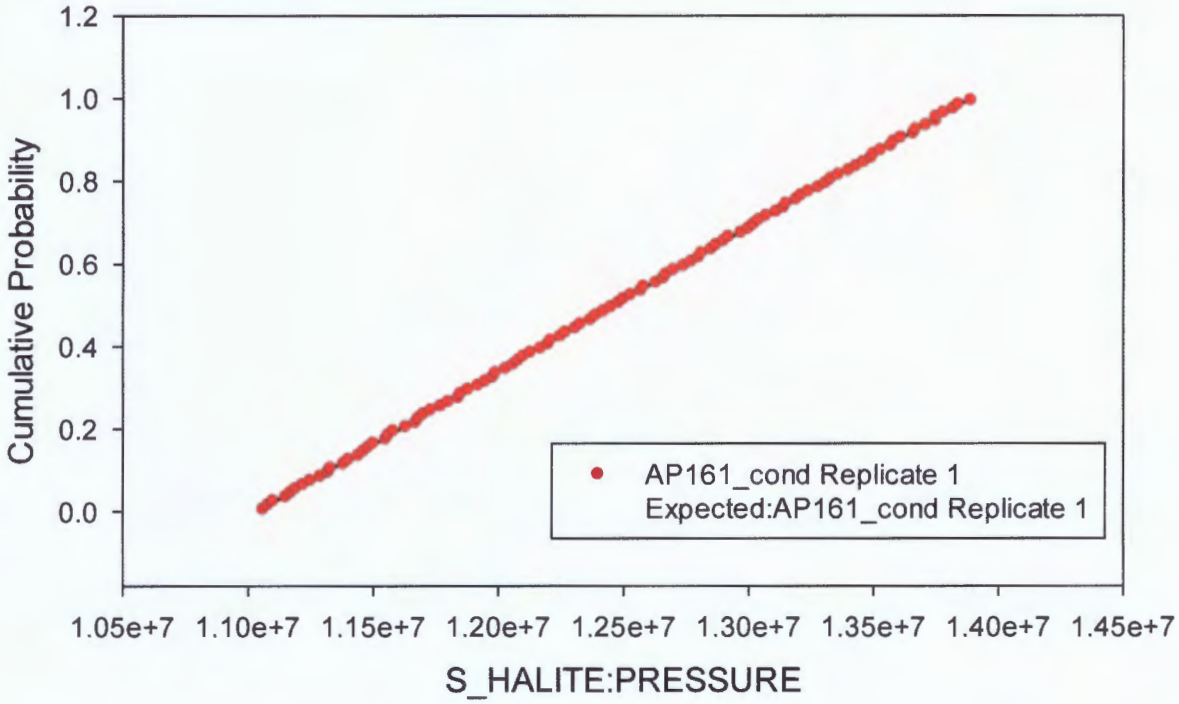

□i□□r□□□□O□□□r□□□an□ □□□□□t□□ □□□□for □□□ □□l□□□□□□□□□□ □□□niform □i□tri□□tion□□□□li□at□□□

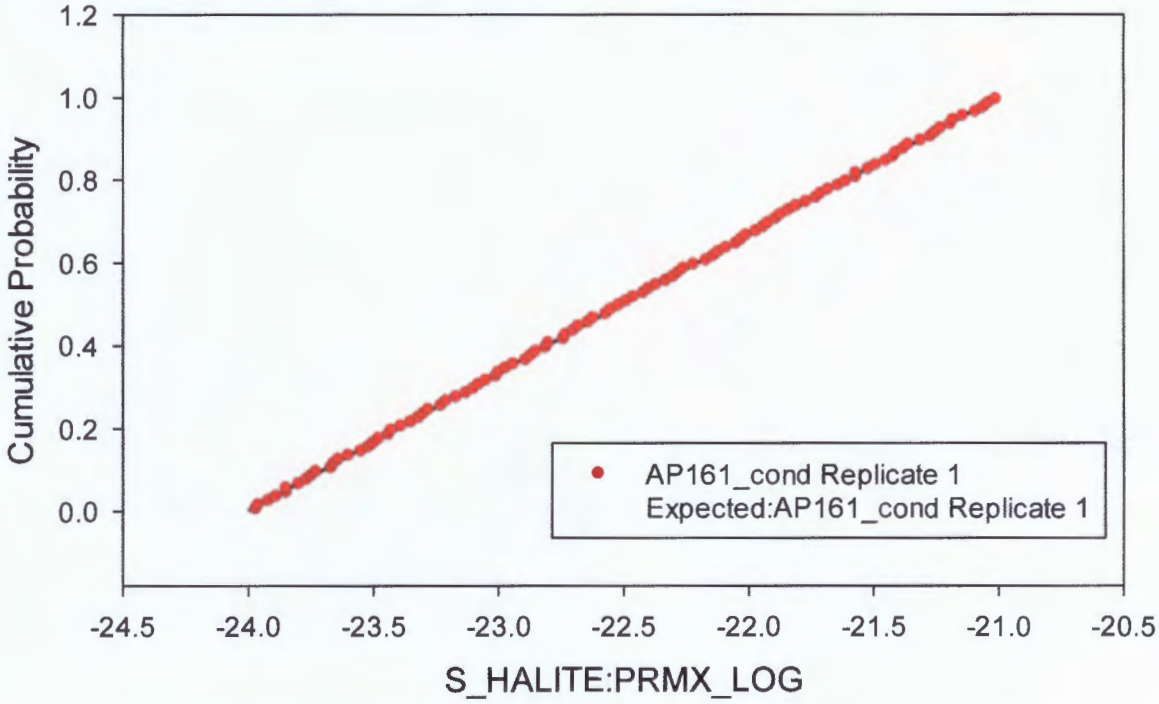

□i□□r□□□□O□□□r□□□an□ □□□□□t□□ □□□□for □□□ □□l□□□□□ □□□O□ □□niform □i□tri□□tion□□□□li□at□□□

Information Only

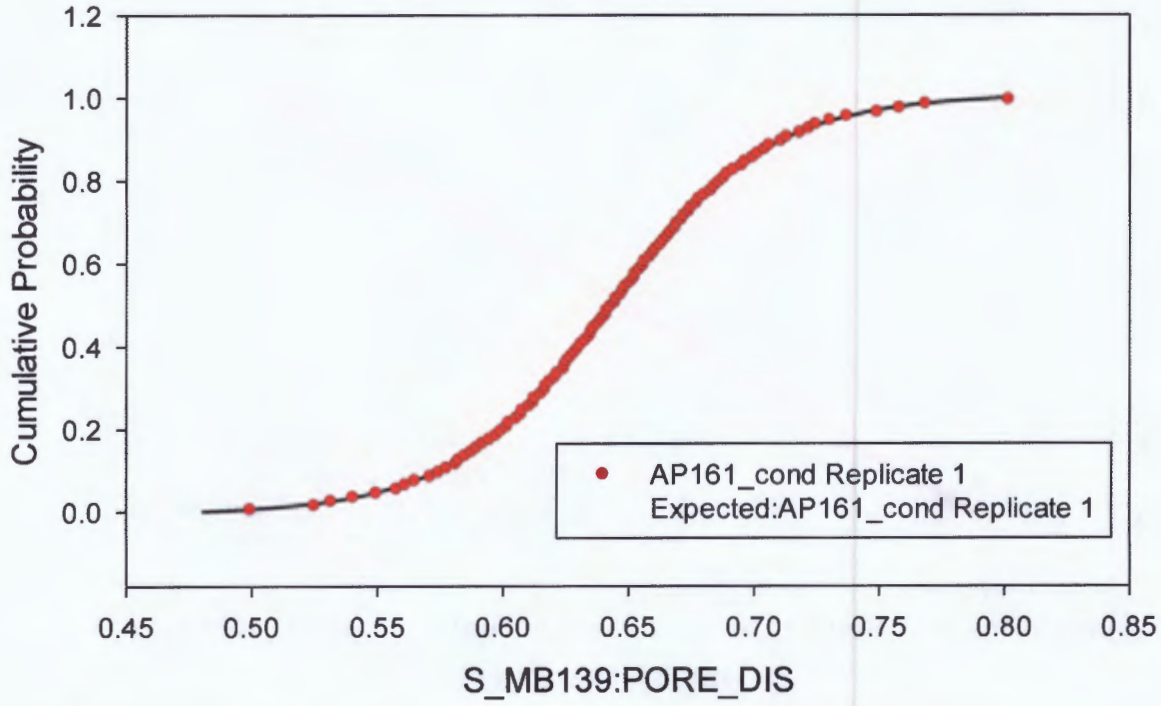

□i□r□□□O□□r□□an□ □□□□t□□ □□□□for □□□ □□□□□□O□□□□I□ □□t□□□nt □i□ri□□tion□□□□li□at□□

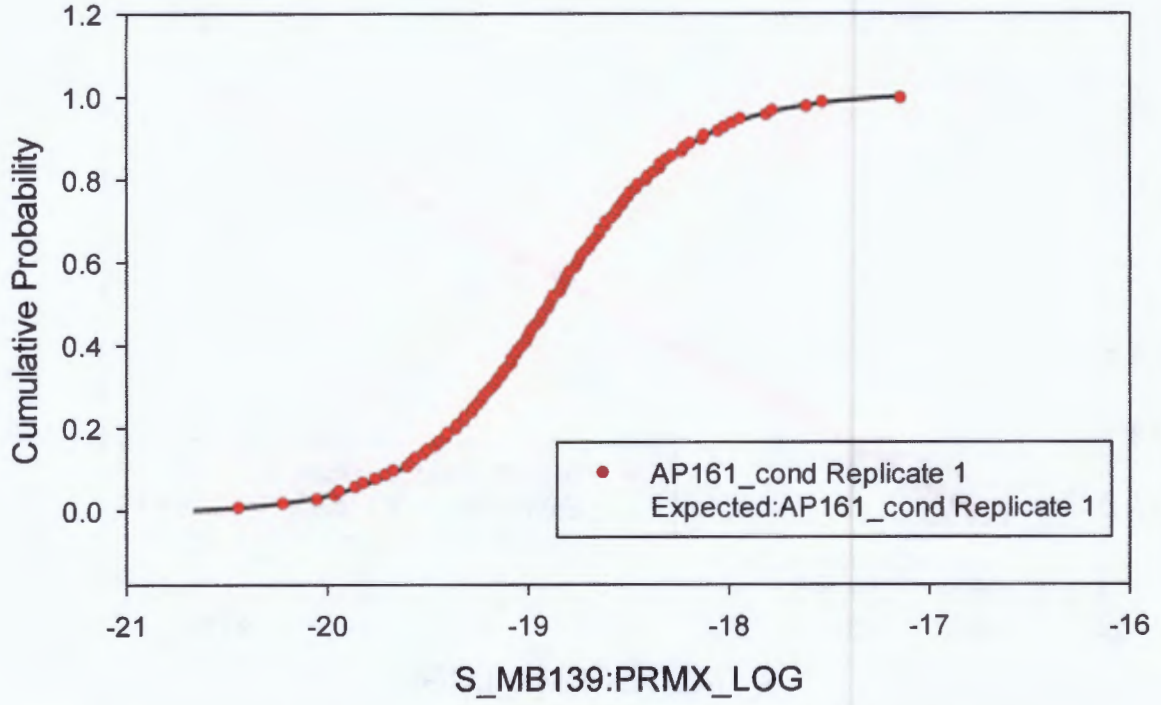

□i□r□□□O□□r□□an□ □□□□t□□ □□□□for □□□ □□□□□□□□ □□□O□ □□t□□□nt □i□ri□□tion□□□□li□at□□

Information Only

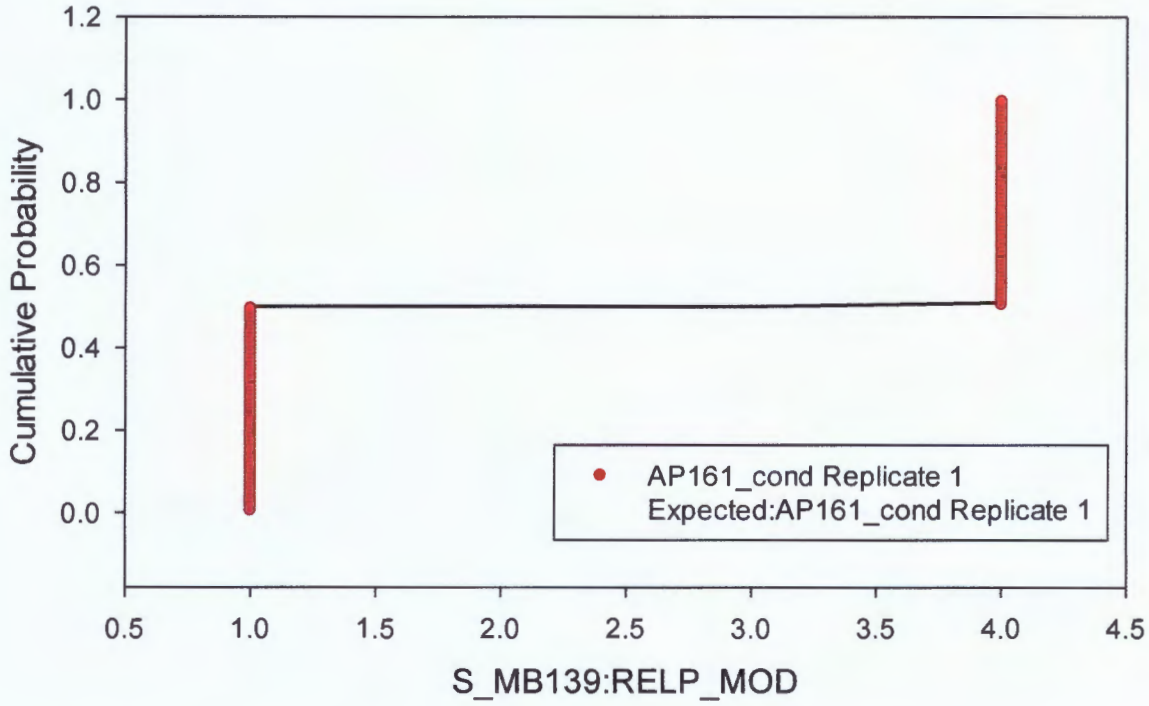

□i□r□□□O□□r□□an□□□□□t□□□□□for □□□ □□□□□□□□□□ O□ □□□r □i□r□t□□□□ta□□i□ri□□tion□□□□li□at□□

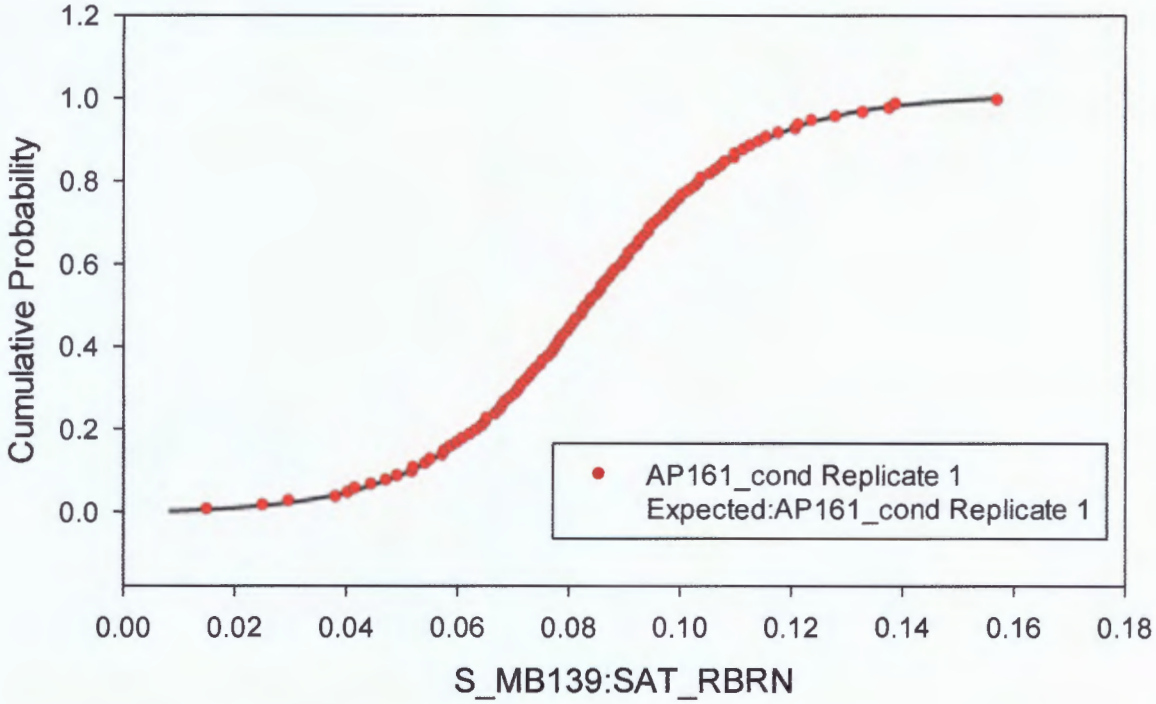

□i□r□□□O□□r□□an□□□□□t□□□□□for □□□ □□□□□□□□□□□□ □□t□□□nt □i□ri□□tion□□□□li□at□□

Information Only

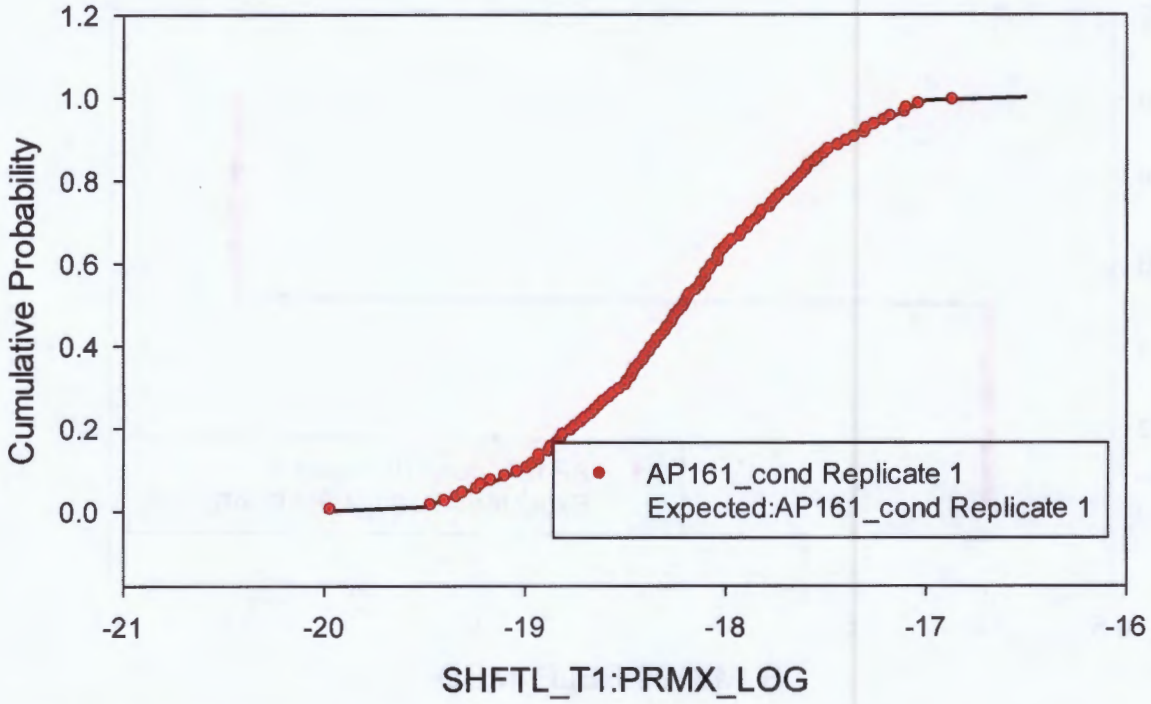

□i□r□□□O□□r□□an□ □□□□t□□ □□□□for □□□□□□□□□□ □□□O□ □□□r □ontin□o□□□i□ri□□tion□□□□i□at□□

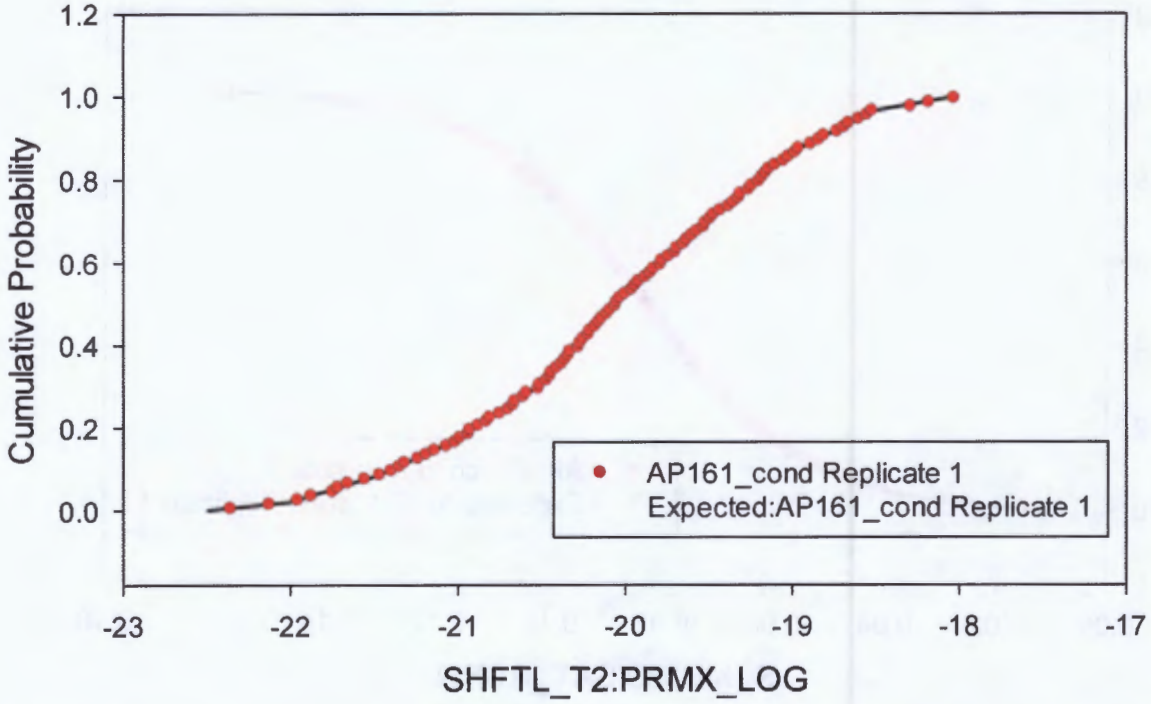

□i□r□□□O□□r□□an□ □□□□t□□ □□□□for □□□□□□□□□□ □□□O□ □□□r □ontin□o□□□i□ri□□tion□□□□i□at□□

Information Only

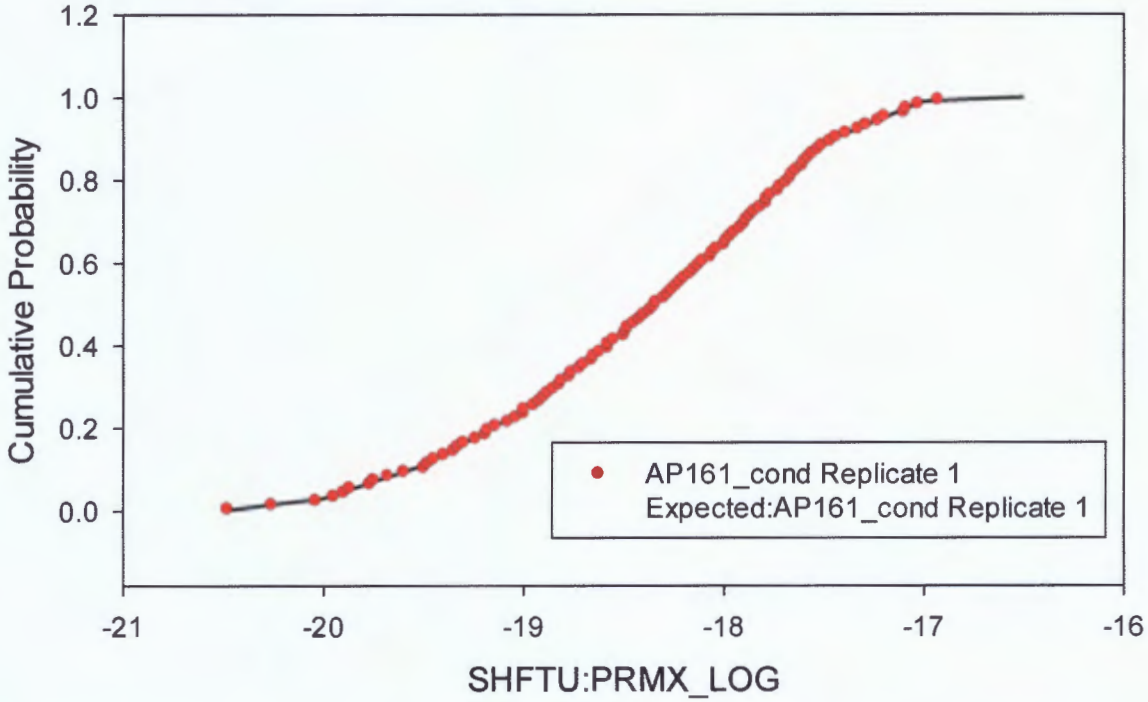

□i□r□□□O□□r□□□an□□□□□t□□□□□for □□□□□□□□□ □□□O□ □□□r □ontin□o□□□i□ri□□tion□□□li□at□□□

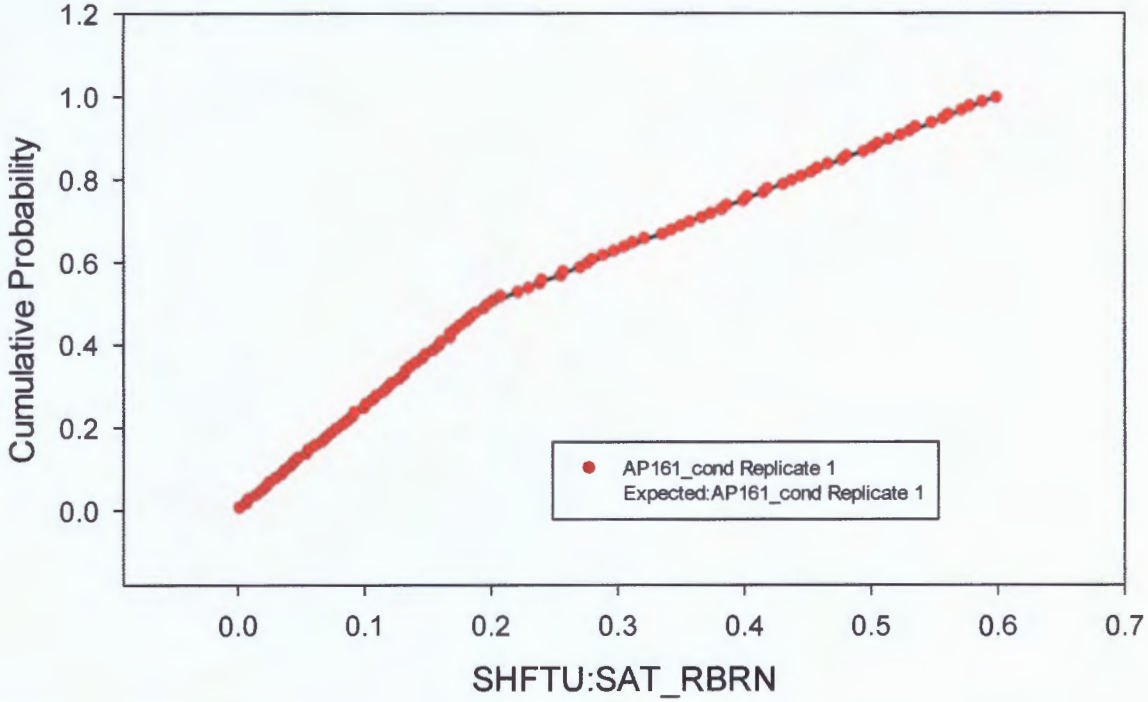

□i□r□□□O□□r□□□an□□□□□t□□□□□for □□□□□□□□□□□□□ □□□r □ontin□o□□□i□ri□□tion□□□li□at□□□

Information Only

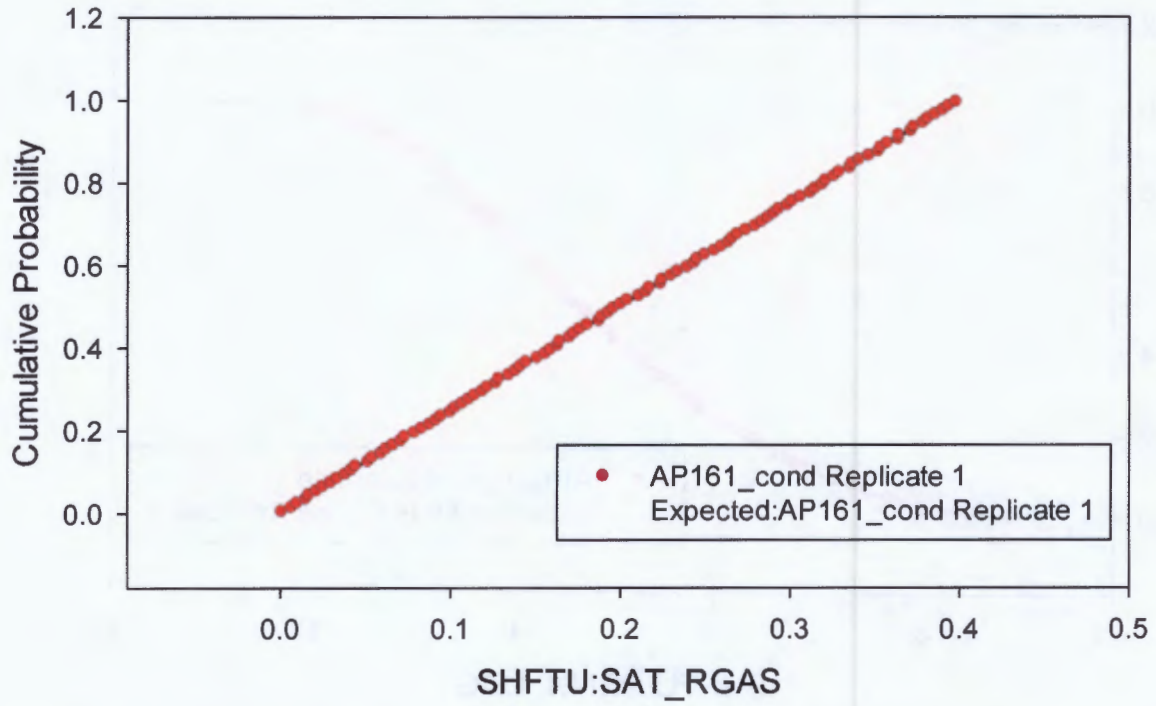

□i□r□□□O□□r□□an□□□□□t□□□□□for □□□□□□□□□□□□□ □□niform □i□ri□□tion□□□li□at□□

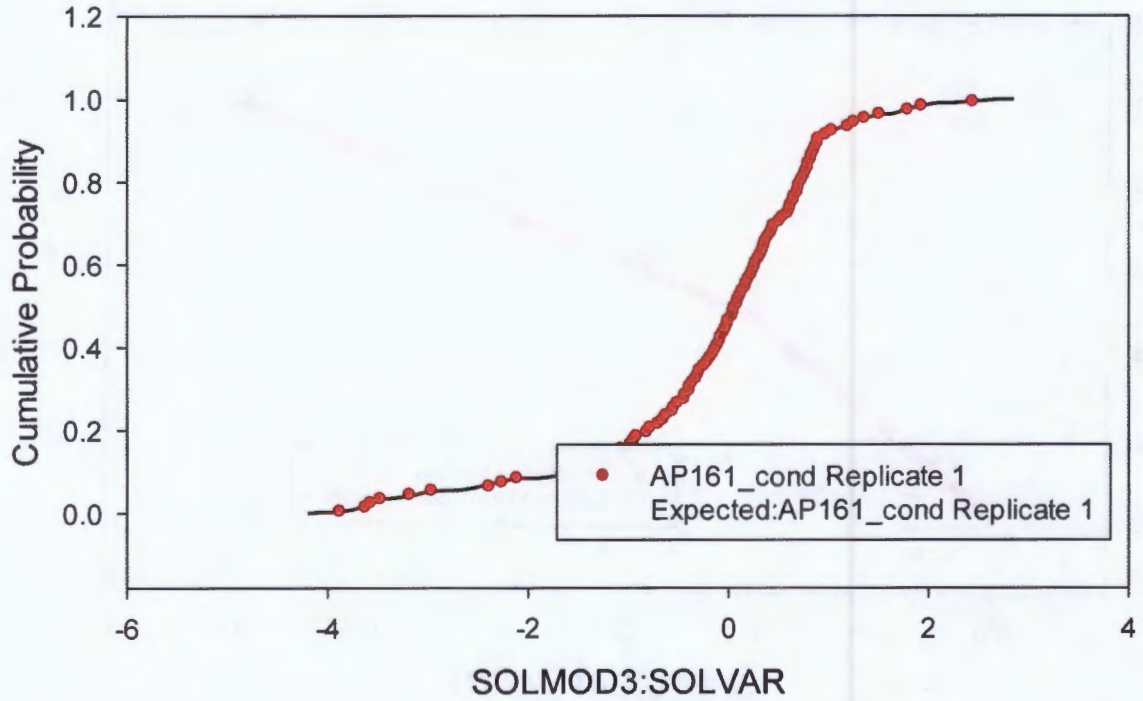

□i□r□□□O□□r□□an□□□□□t□□□□□for □O□□ O□□□O□□□□ □□□r □ontin□o□□□i□ri□□tion□□□li□at□□

Information Only

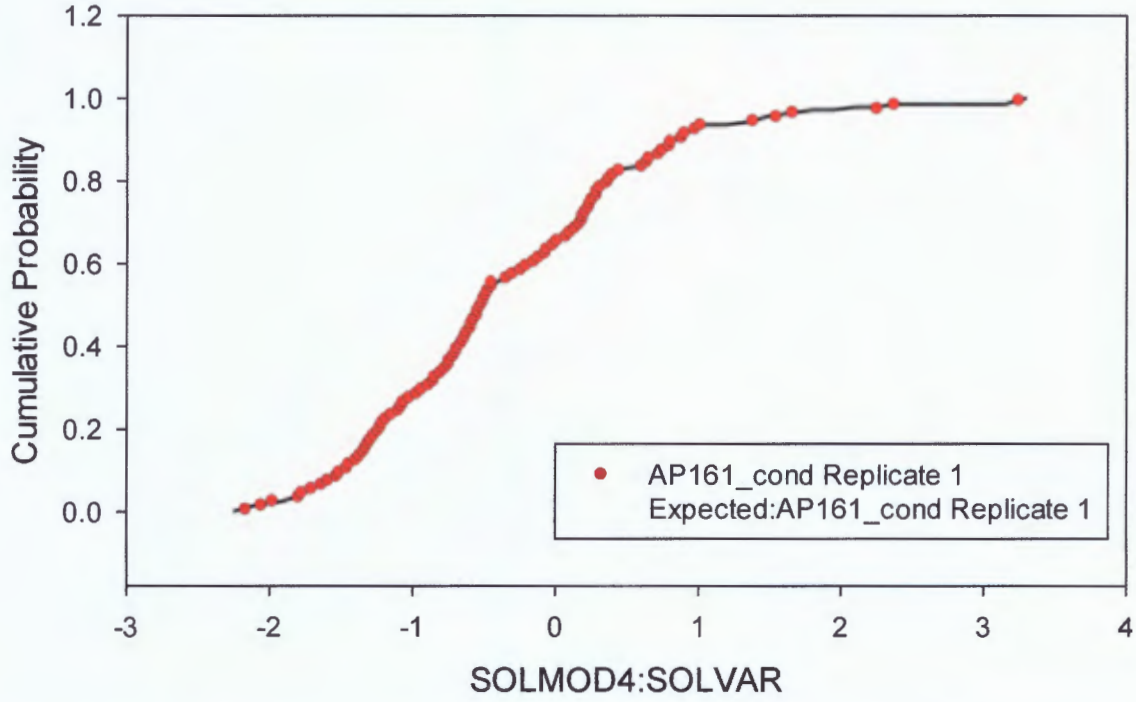

□i□□r□□□□O□□□r□□□an□□□□□□t□□□□□□for □O□□ O□□□□O□□□□ □□□□r □ontin□b□□□i□ri□□tion□□□□li□at□□□

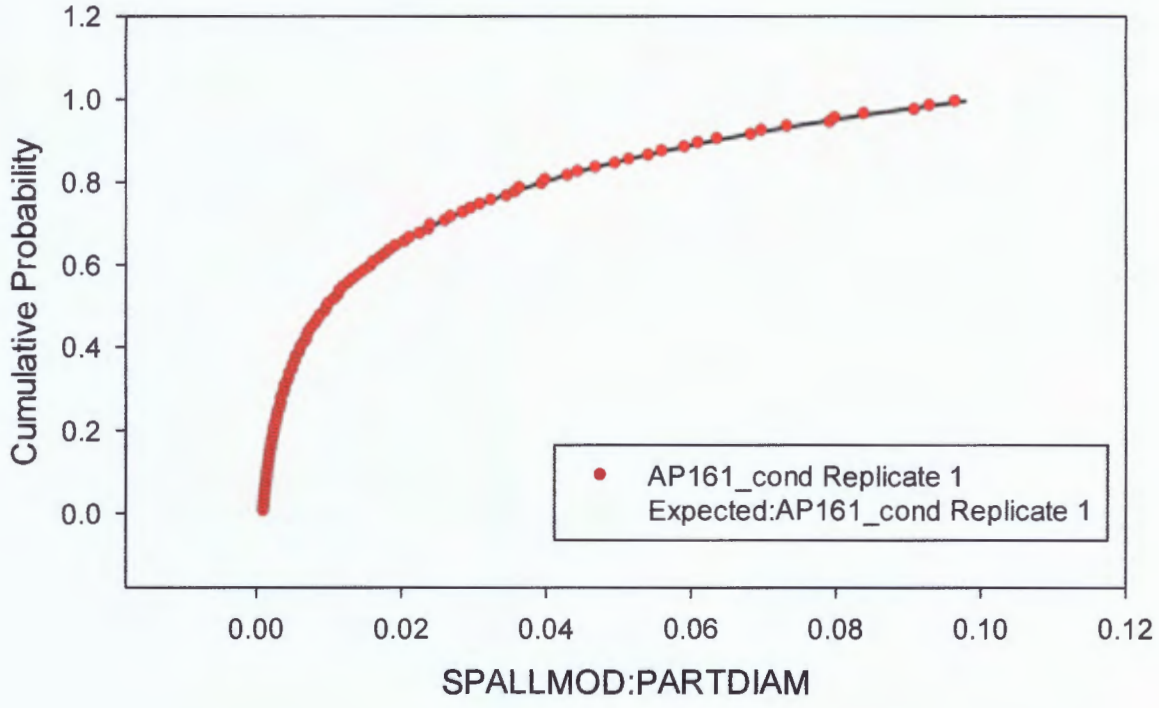

□i□□r□□□□O□□□r□□□an□□□□□□t□□□□□□for □□□□□□ O□□□□□□□I□□ □□o□□niform □i□ri□□tion□□□□li□at□□□

Information Only

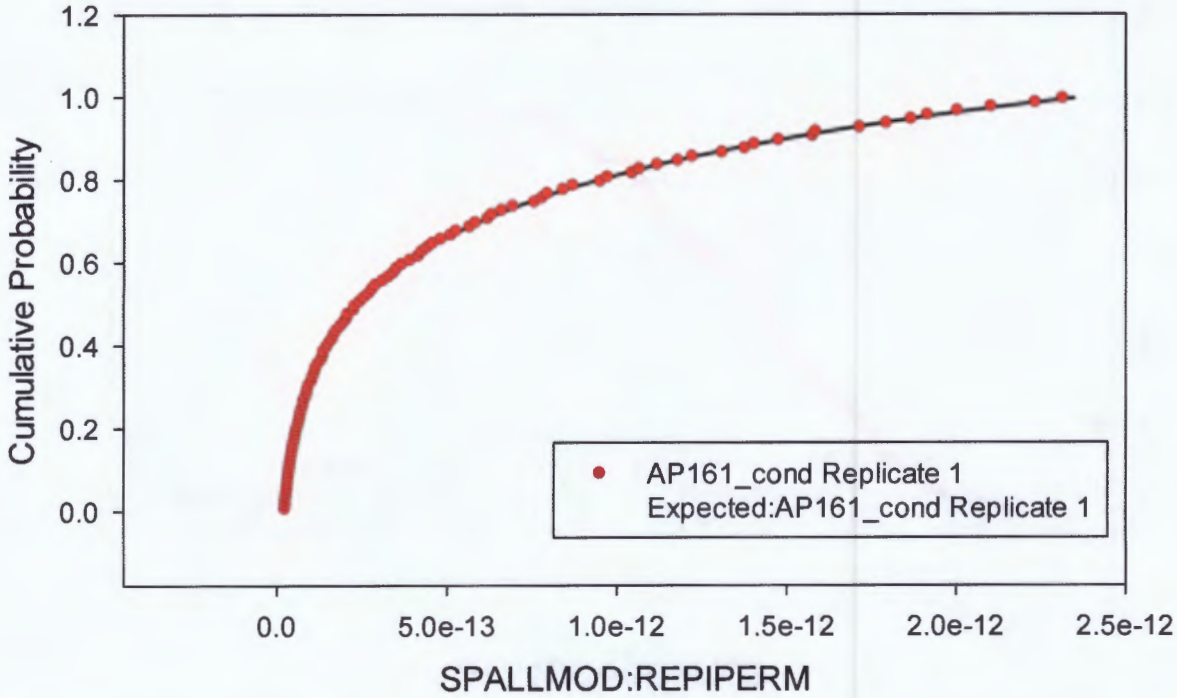

□i□□r□□□□O□□□r□□□an□ □□□□□t□□ □□□□for □□□□□□ O□□□□□□□□□□ □□o□□niform □i□ri□□tion□□□□li□at□□□

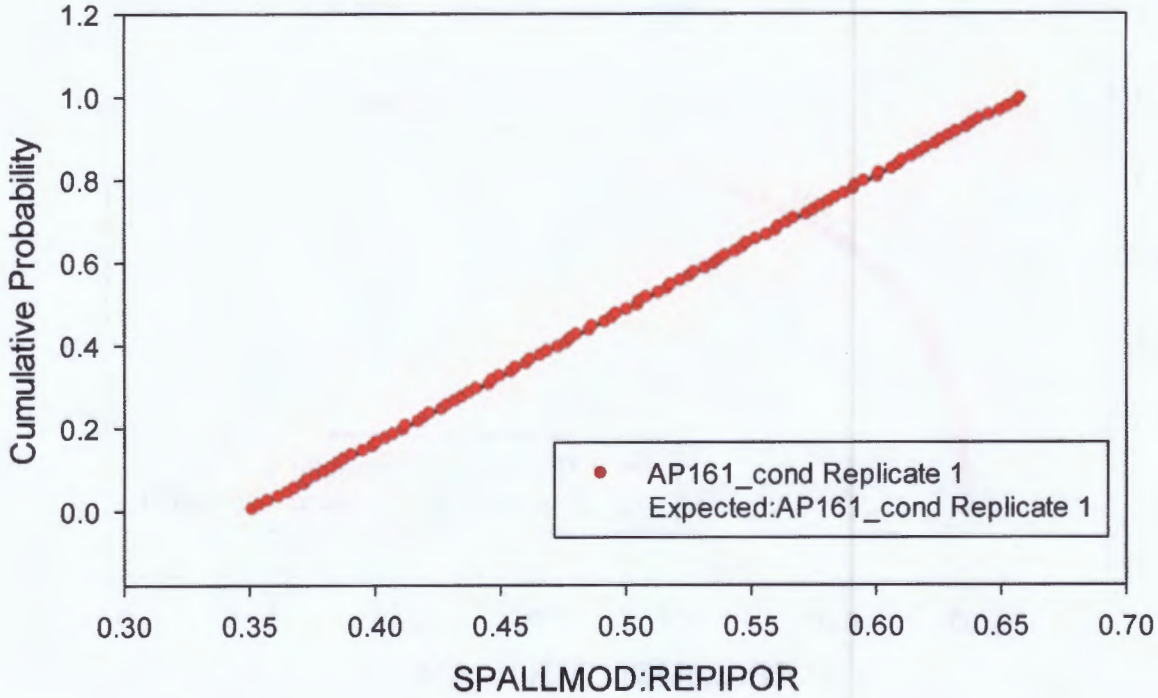

□i□□r□□□□O□□□r□□□an□ □□□□□t□□ □□□□for □□□□□□ O□□□□□□□O□ □□niform □i□ri□□tion□□□□li□at□□□

Information Only

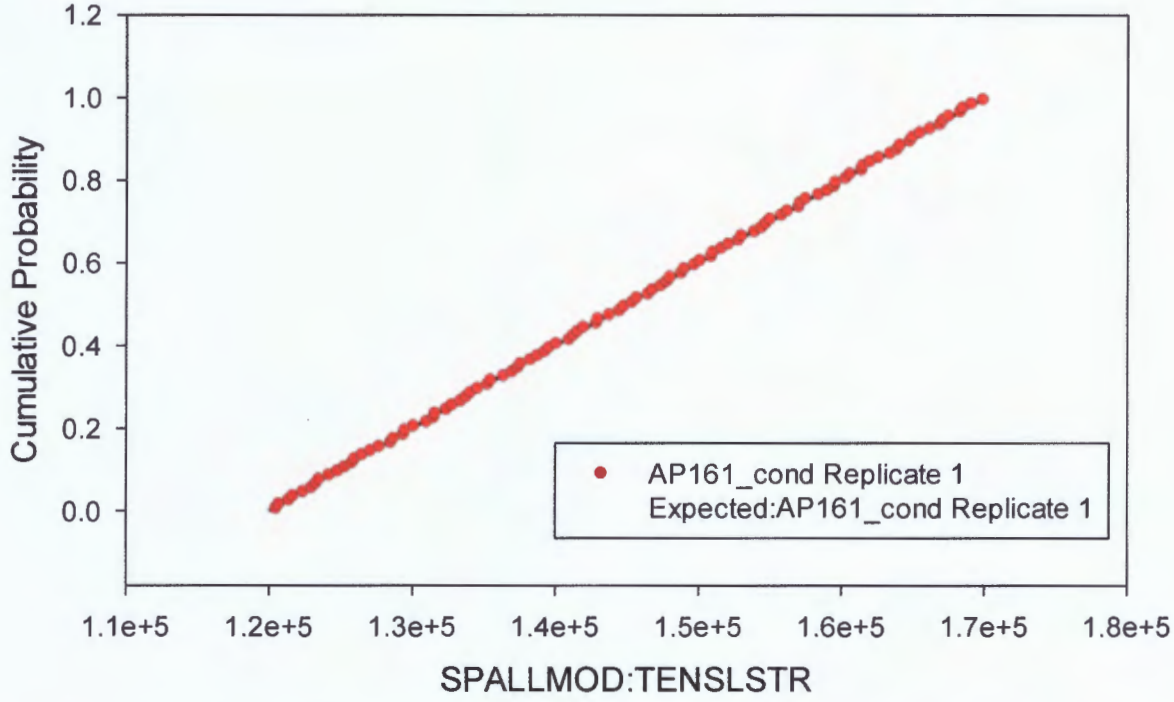

□i□□r□□□□O□□□r□□□an□ □□□□□t□□ □□□□for □□□□□□ O□□□□□□□□□ □□niform □i□tri□□tion□□□□li□at□□□

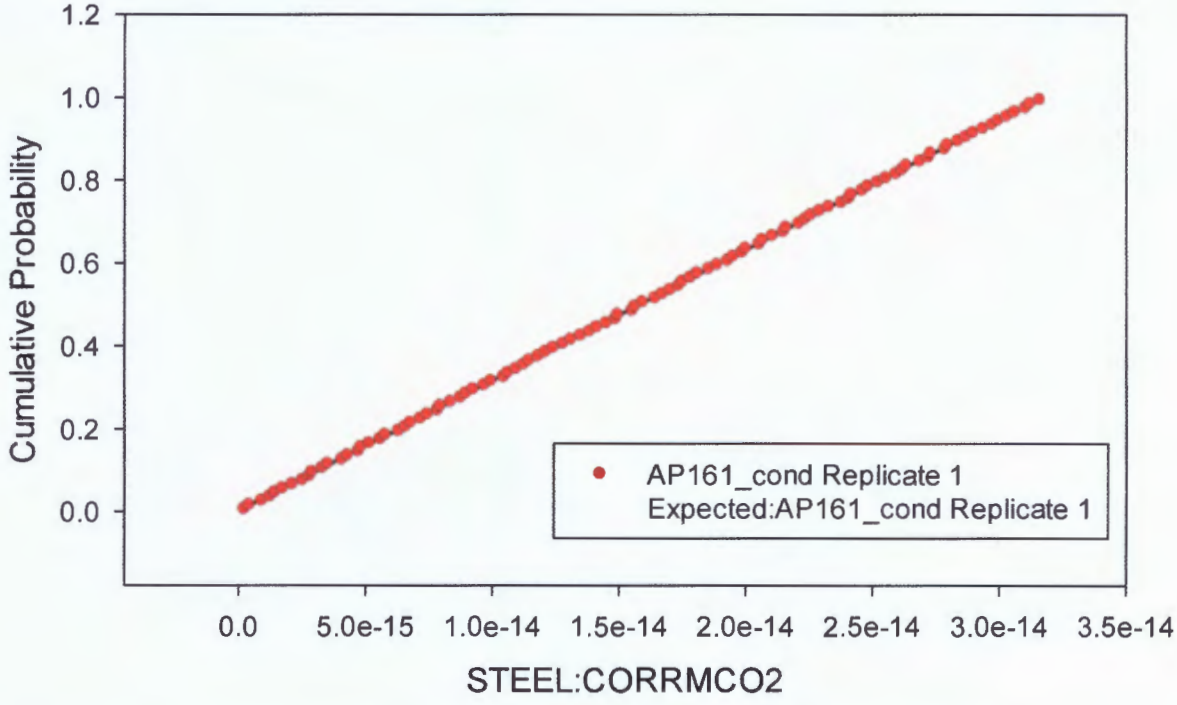

□i□□r□□□□O□□□r□□□an□ □□□□□t□□ □□□□for □□□□□□□O□□□ □O□□□niform □i□tri□□tion□□□□li□at□□□

Information Only

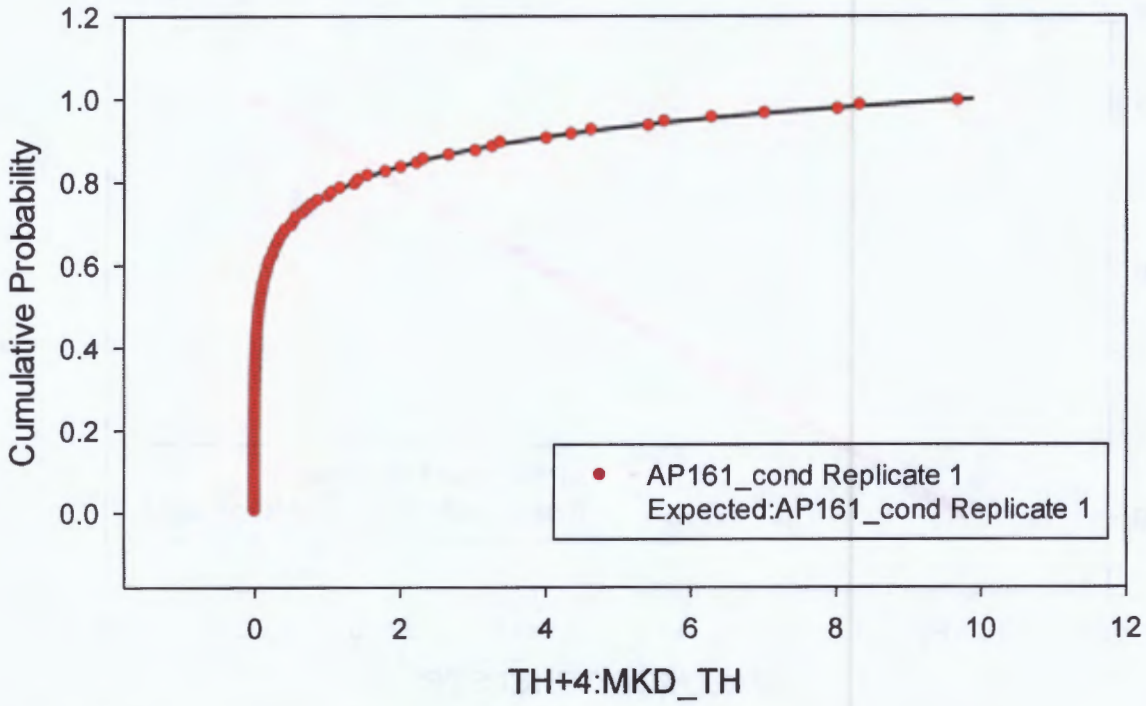

□i□r□□□O□□r□□an□□□□□t□□□□□for □□□□□ □□□□ □□o□niform □i□ri□□tion□□□li□at□□

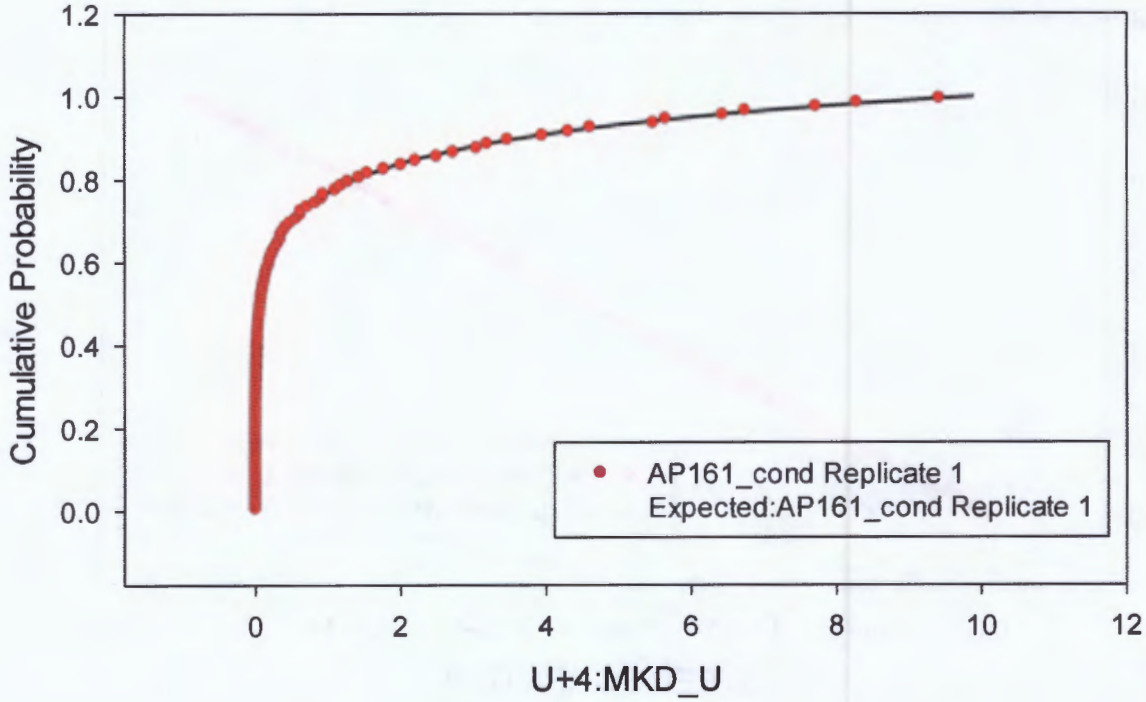

□i□r□□□O□□r□□an□□□□□t□□□□□for □□□□□ □□□□ □□o□niform □i□ri□□tion□□□li□at□□

Information Only

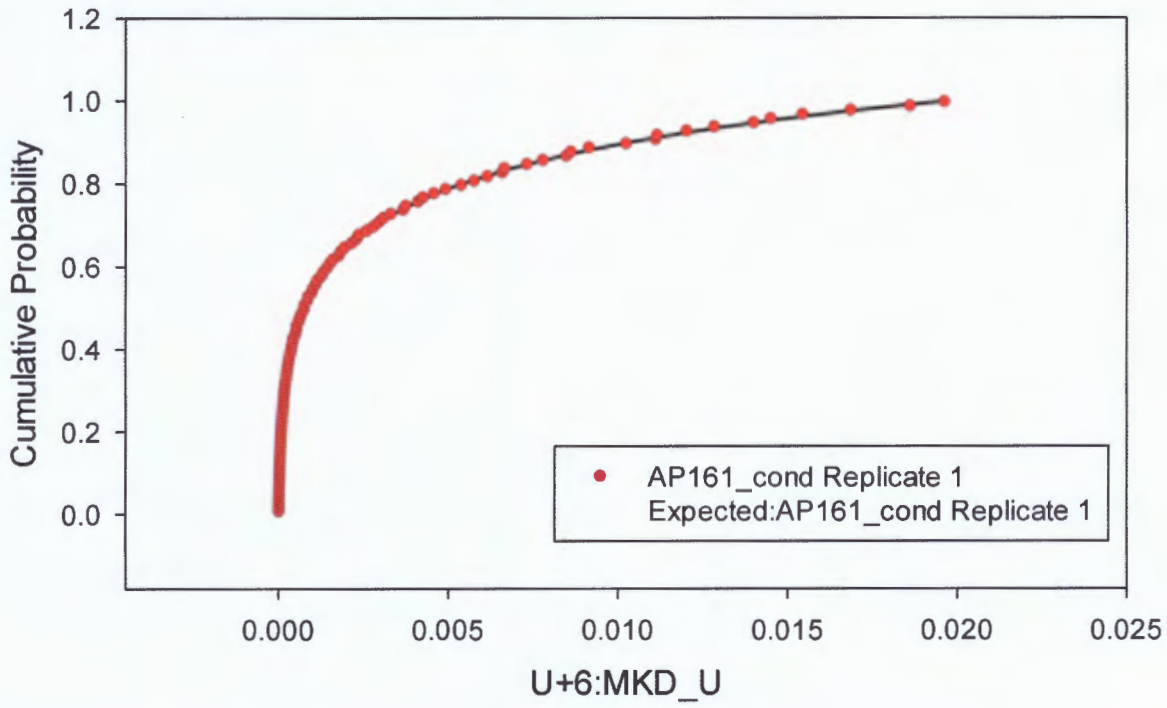

□i□□r□□□□O□□□r□□□an□ □□□□□t□□ □□□□for □□□□□ □ □□□ □□o□□niform □i□tri□□tion□□□□li□at□□□

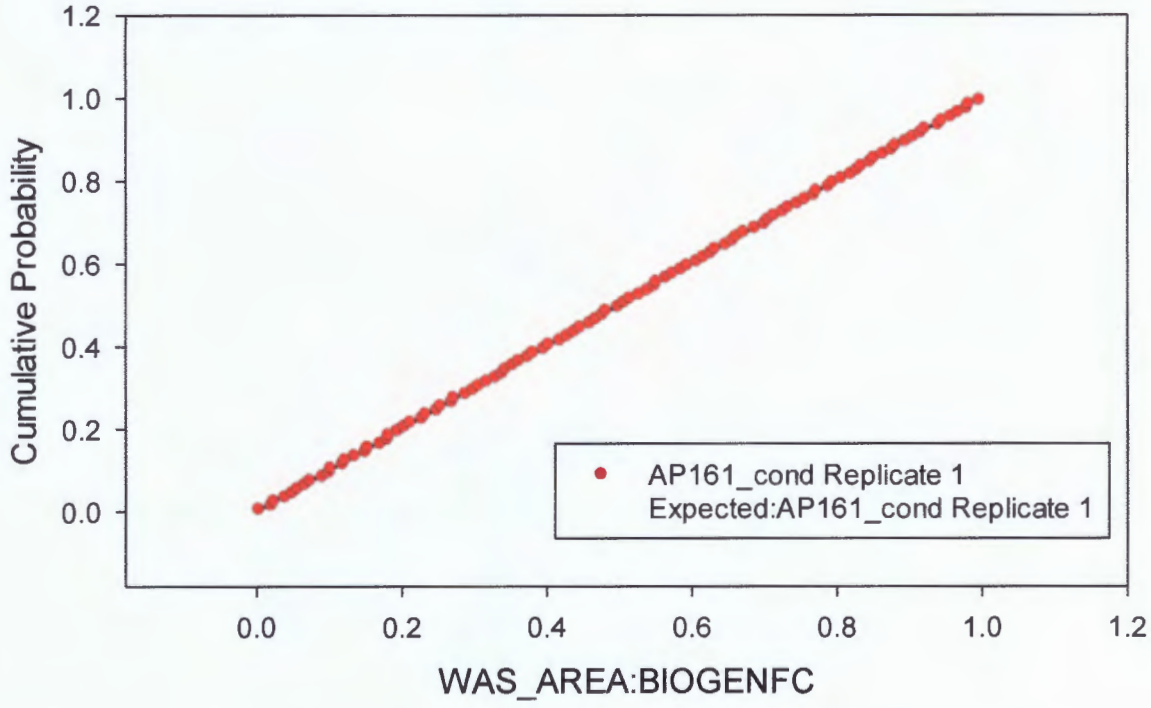

□i□□r□□□□O□□□r□□□an□ □□□□□t□□ □□□□for □ □□□□□□□□□IO□□□□□ □□niform □i□tri□□tion□□□□li□at□□□

Information Only

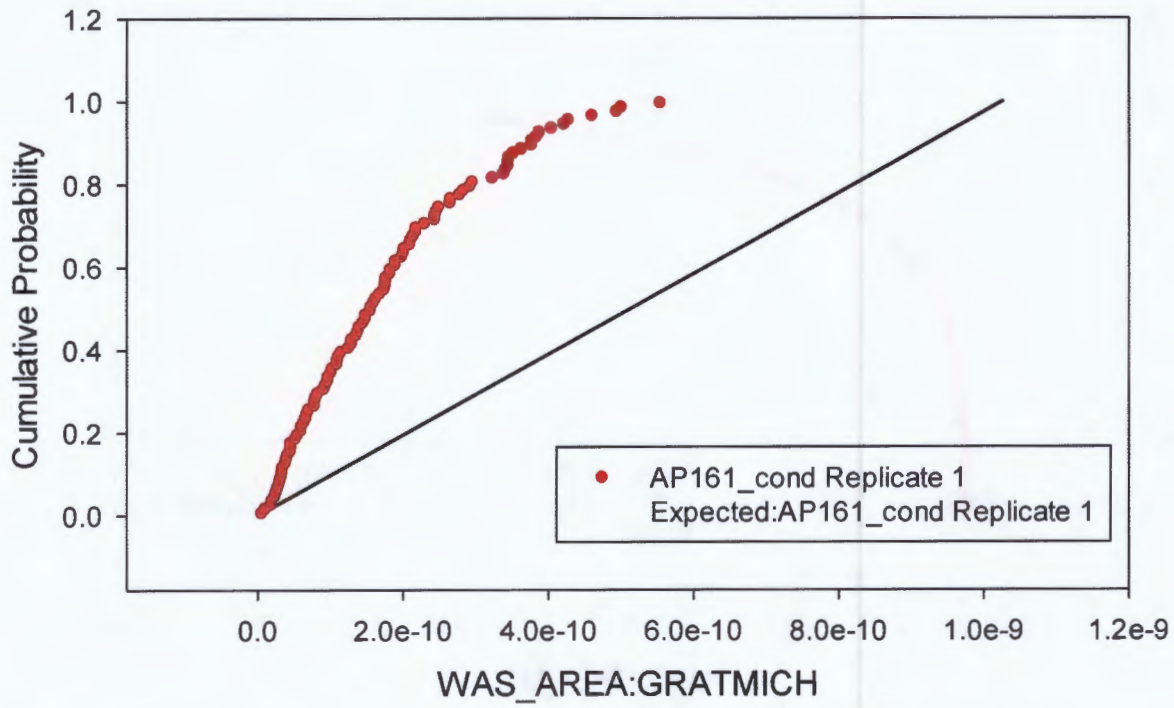

□i□r□□□O□□r□□an□□□□□t□□□□□for □ □□□□□□□□□□□□ I□□ □□niform □i□ri□□tion□□□li□at□□

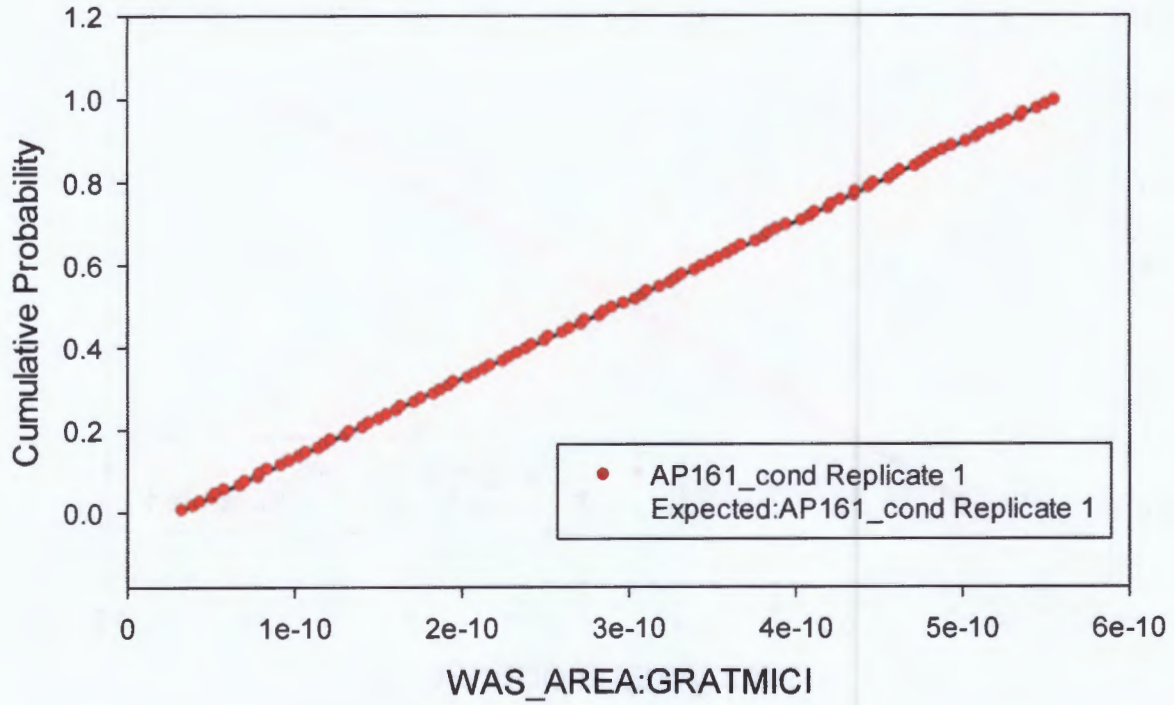

□i□r□□□O□□r□□an□□□□□t□□□□□for □ □□□□□□□□□□□□ I□I □□niform □i□ri□□tion□□□li□at□□

Information Only

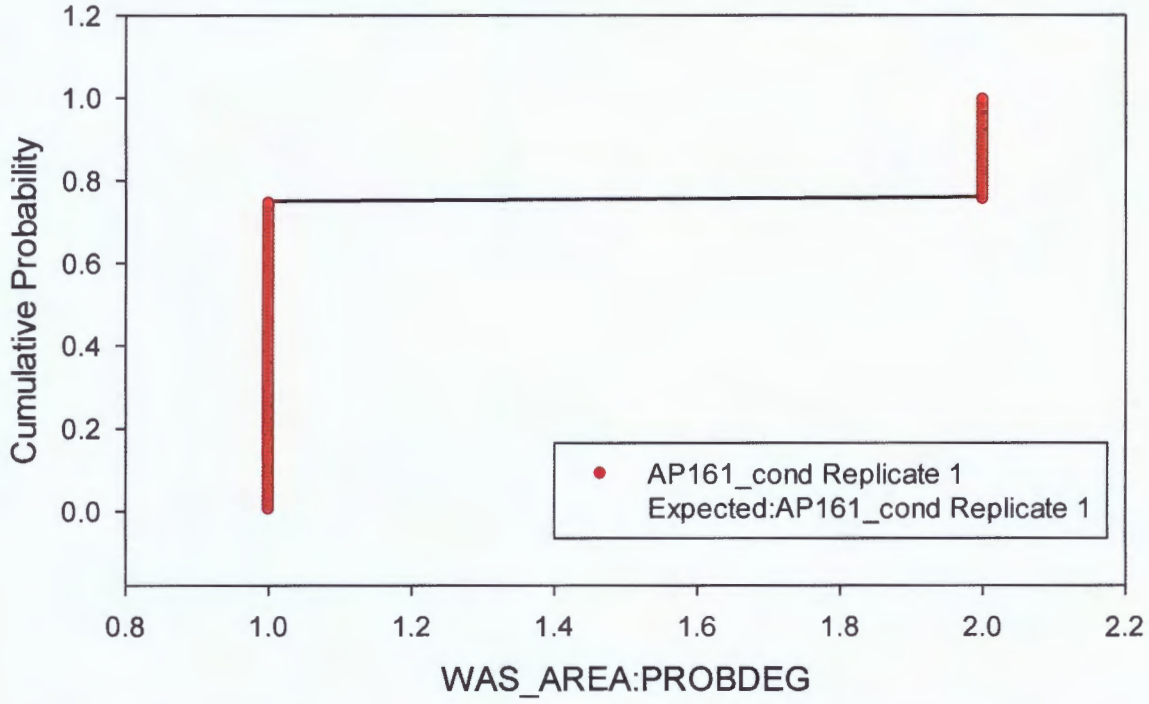

□i□r□□□O□□r□□□an□□□□□t□□□□□for □ □□□□□□□□□O□□□□ □□□r □i□r□t□□□□ta□□i□ri□□tion□□□□i□at□□□

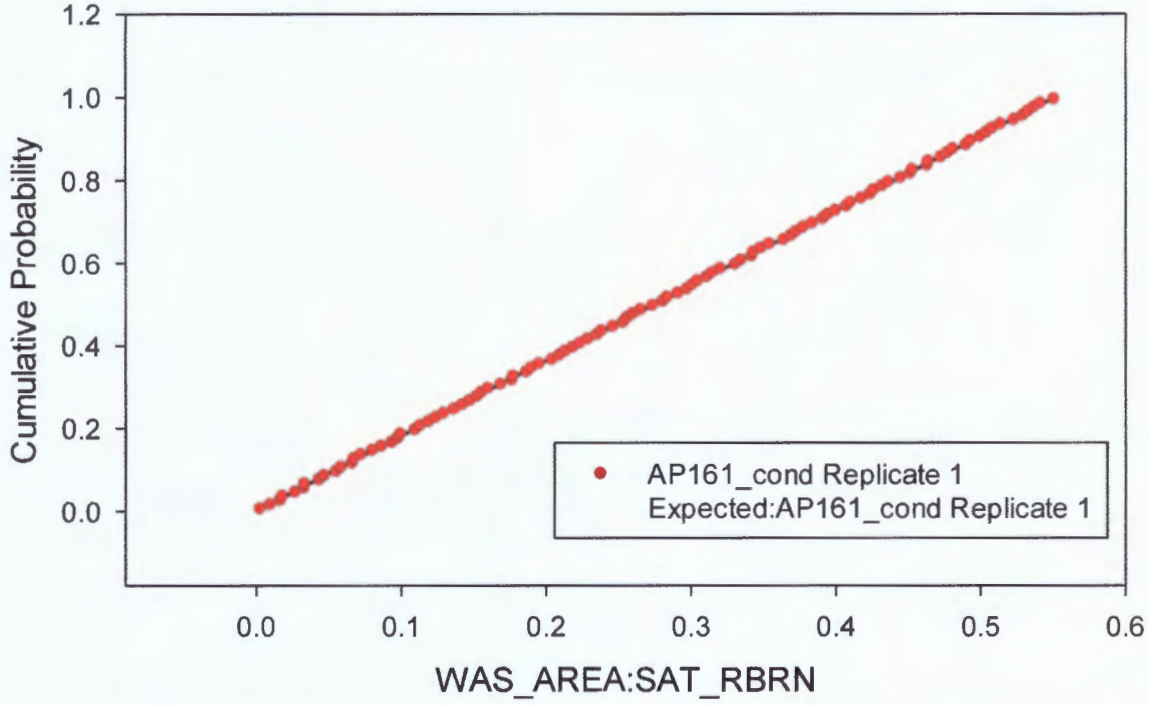

□i□r□□□O□□r□□□an□□□□□t□□□□□for □ □□□□□□□□□□□□□□□□ □□niform □i□ri□□tion□□□□i□at□□□

Information Only

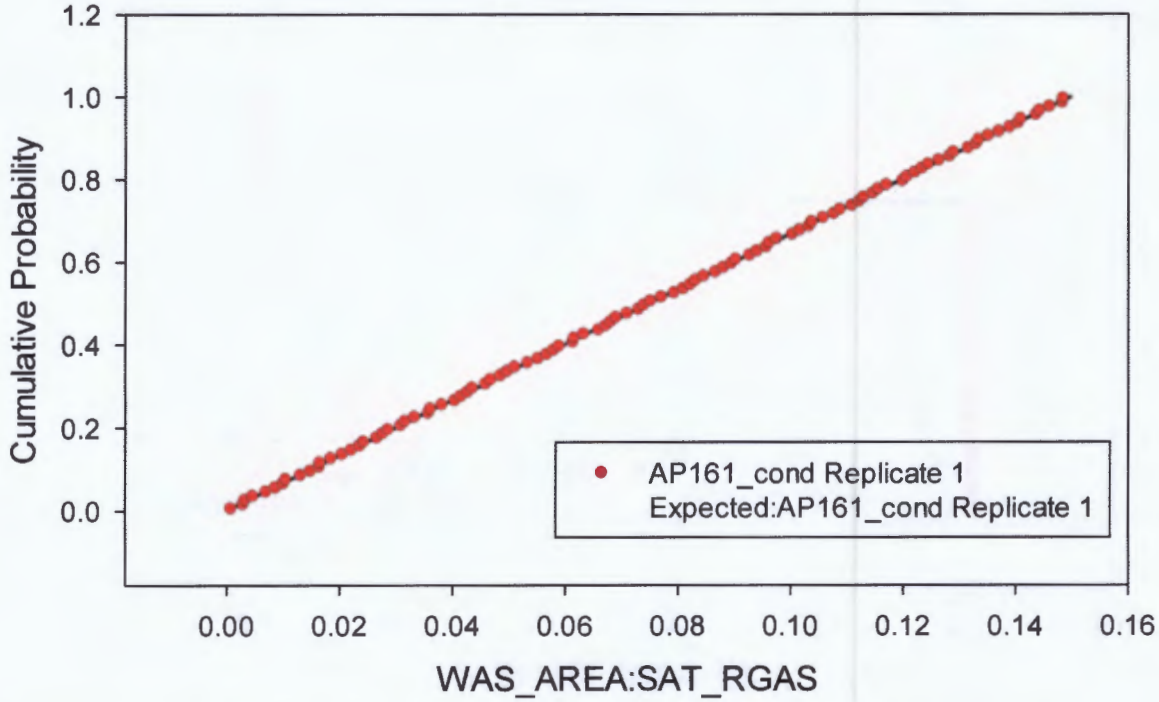

□i□□r□□□□O□□□r□□□an□□□□□□t□□□□□□for □ □□□□□□□□□□□□□□□□□□□niform □i□ri□□tion□□□□li□at□□□

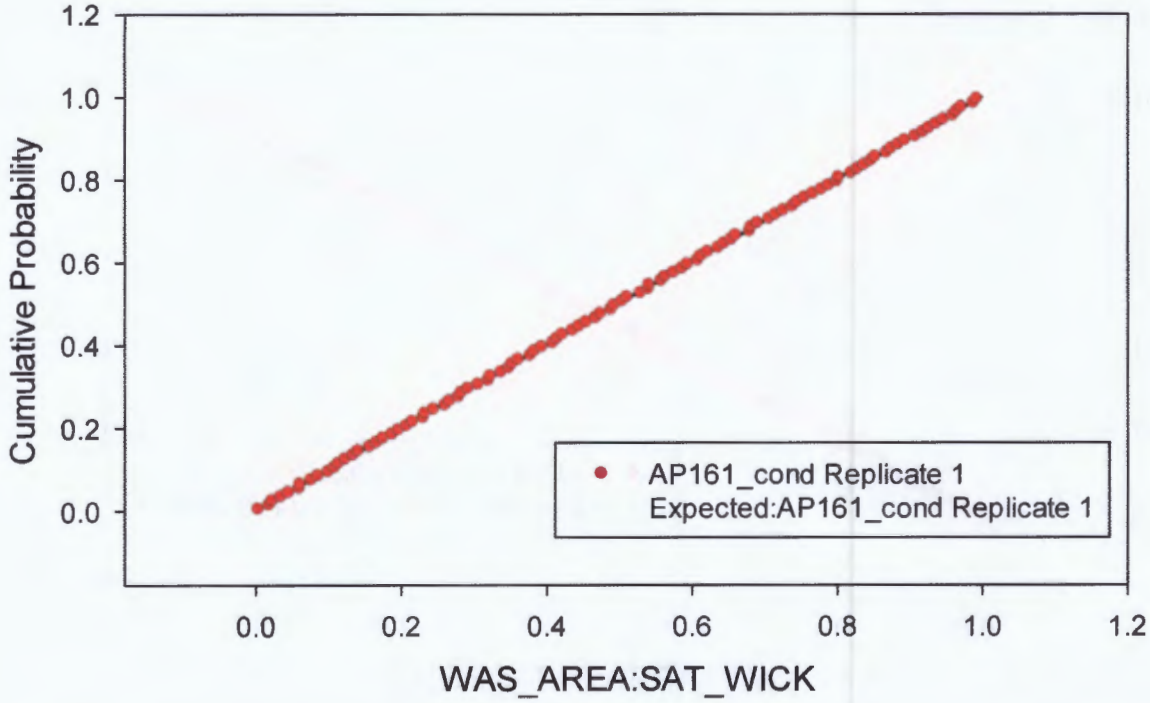

□i□□r□□□□O□□□r□□□an□□□□□□t□□□□□□for □ □□□□□□□□□□□□□□□□□ I□□ □□niform □i□ri□□tion□□□□li□at□□□

Information Only

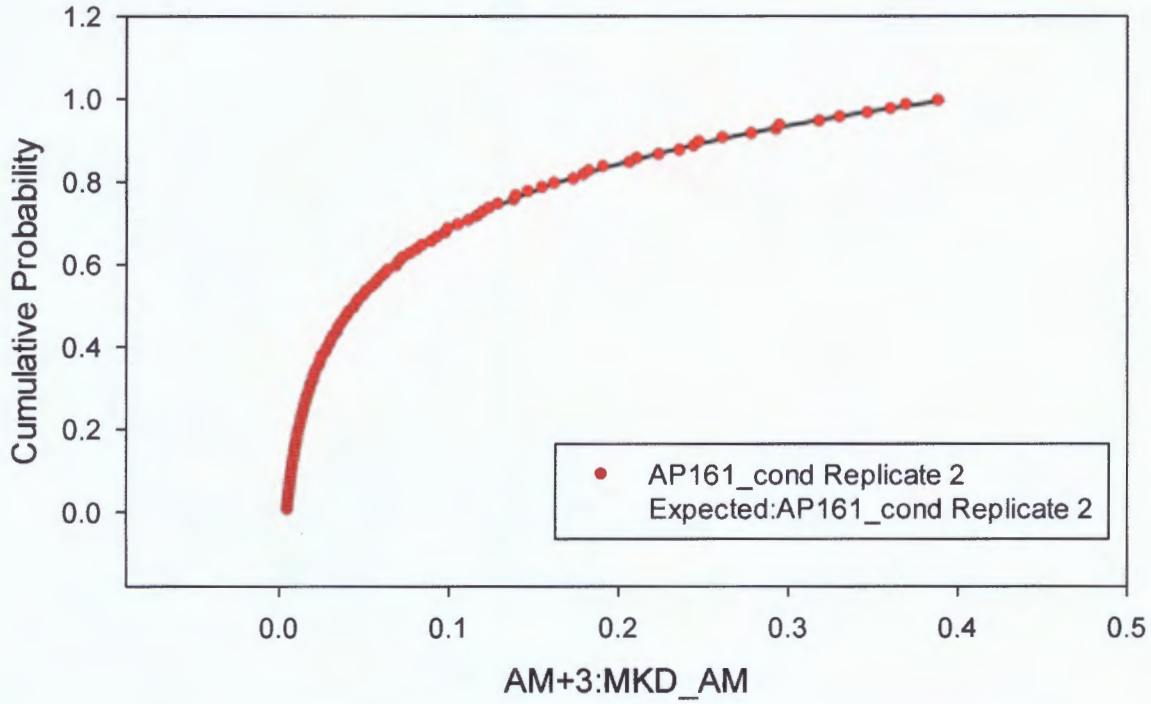

□i□r□□□O□□r□□an□ □□□□t□□ □□□□for □□ □□□□ □□□□ □□o□□niform □i□tri□□tion□□□□li□at□□

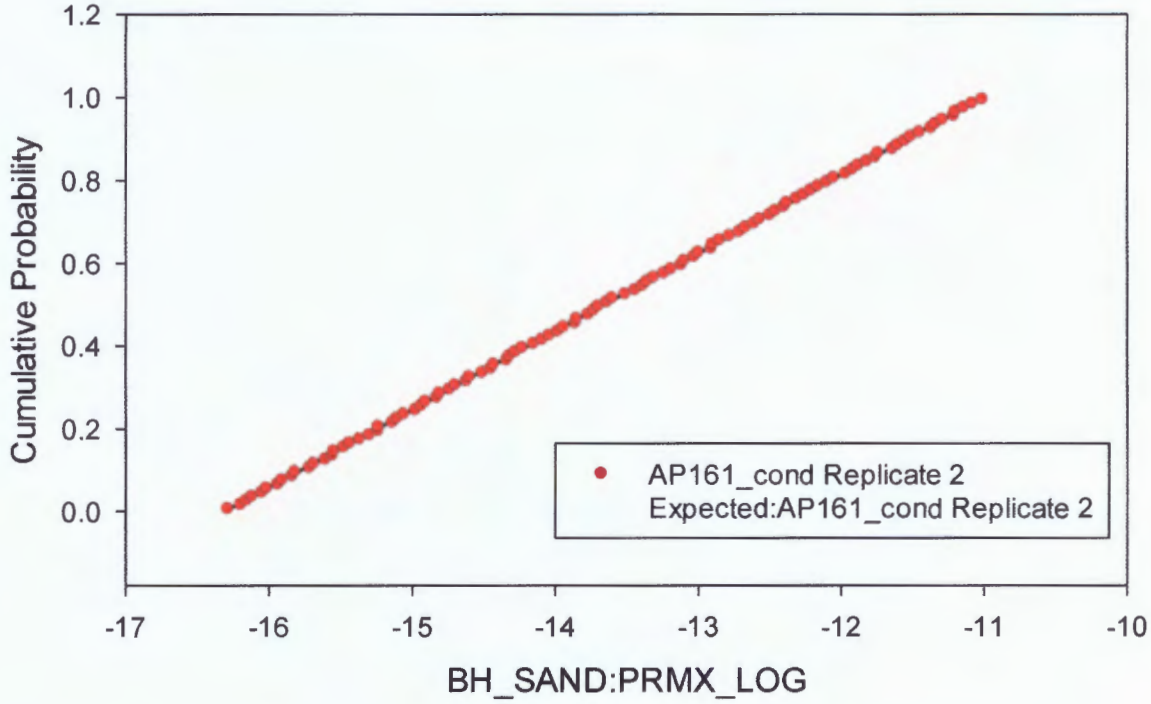

□i□r□□□O□□r□□an□ □□□□t□□ □□□□for □□□□□□□□□ □□□O□ □□niform □i□tri□□tion□□□□li□at□□

Information Only

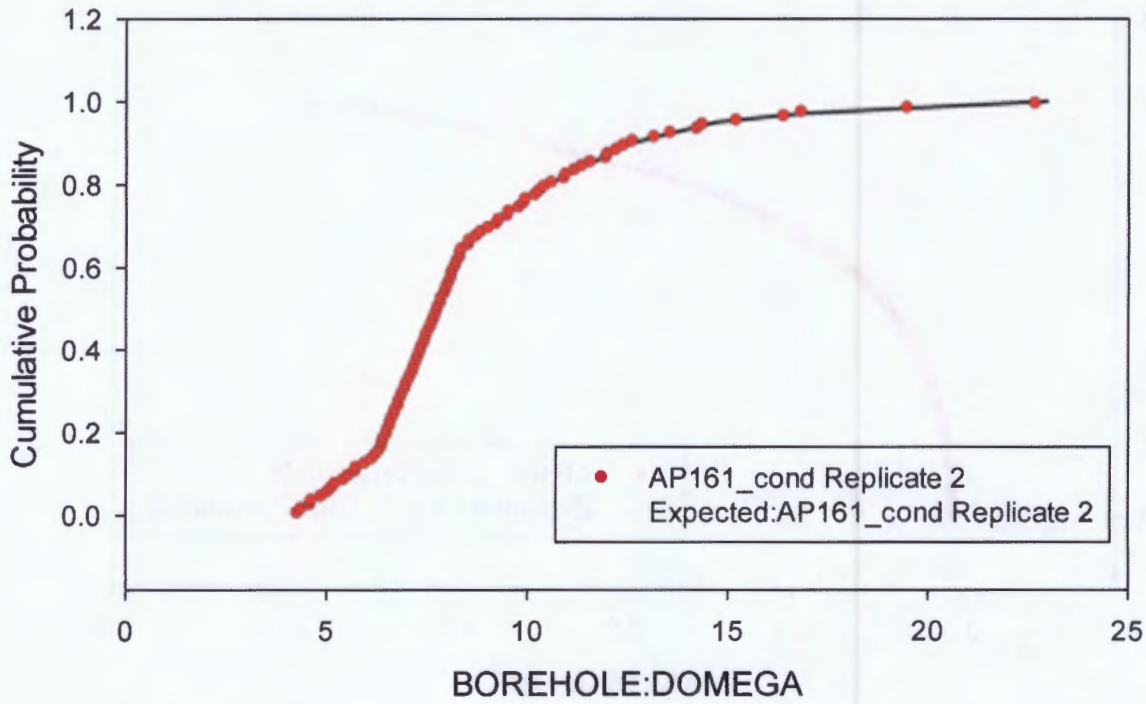

□i□r□□□O□□r□□□an□□□□□t□□□□□for □O□□□O□□□□O□ □□□ □□□r □ontin□b□□□i□ri□□tion□□□li□at□□

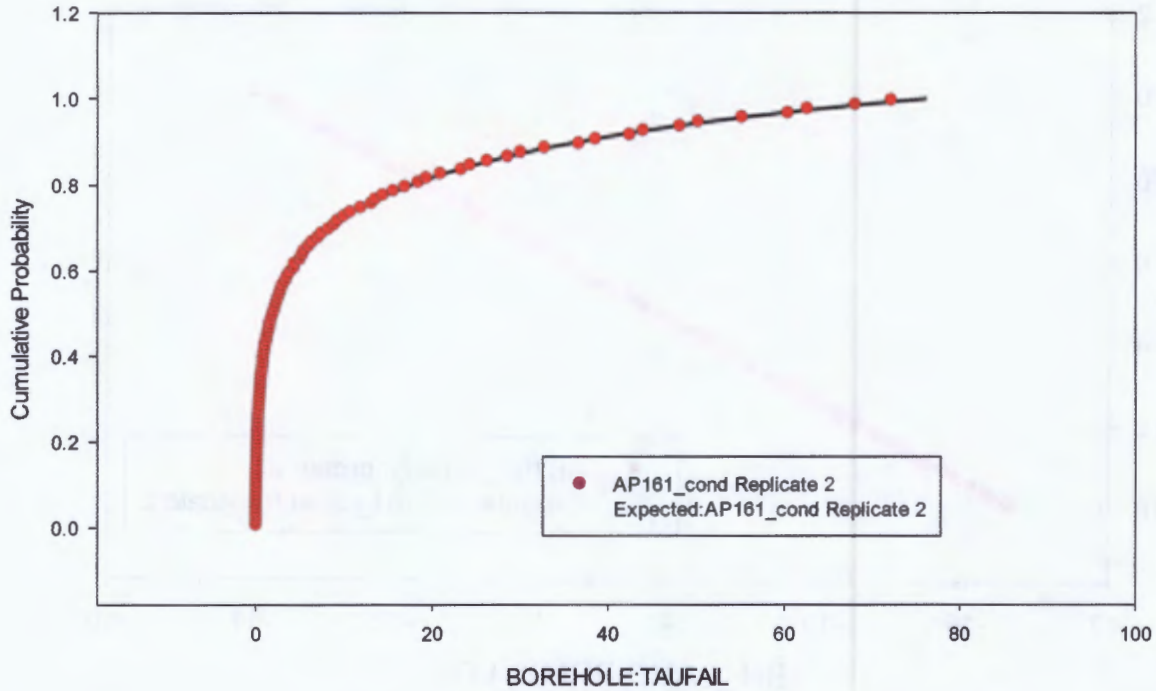

□i□r□□□O□□r□□□an□□□□□t□□□□□for □O□□□O□□□□□□□□I□ □□o□□niform □i□ri□□tion□□□li□at□□

Information Only

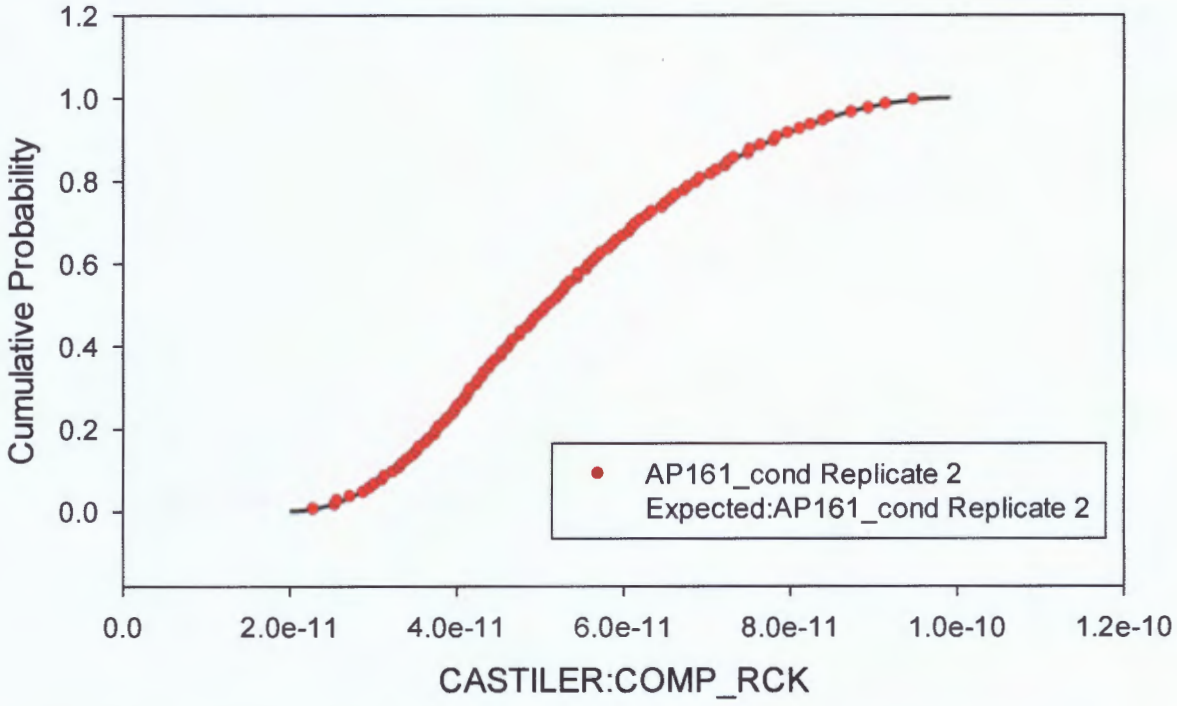

□i□□r□□□□O□□□r□□□an□□□□□□□□□□□□□for □□□□□I□□□□□□□O□ □□□□□ □□rian□□lar □i□ri□□tion□□□□li□at□□

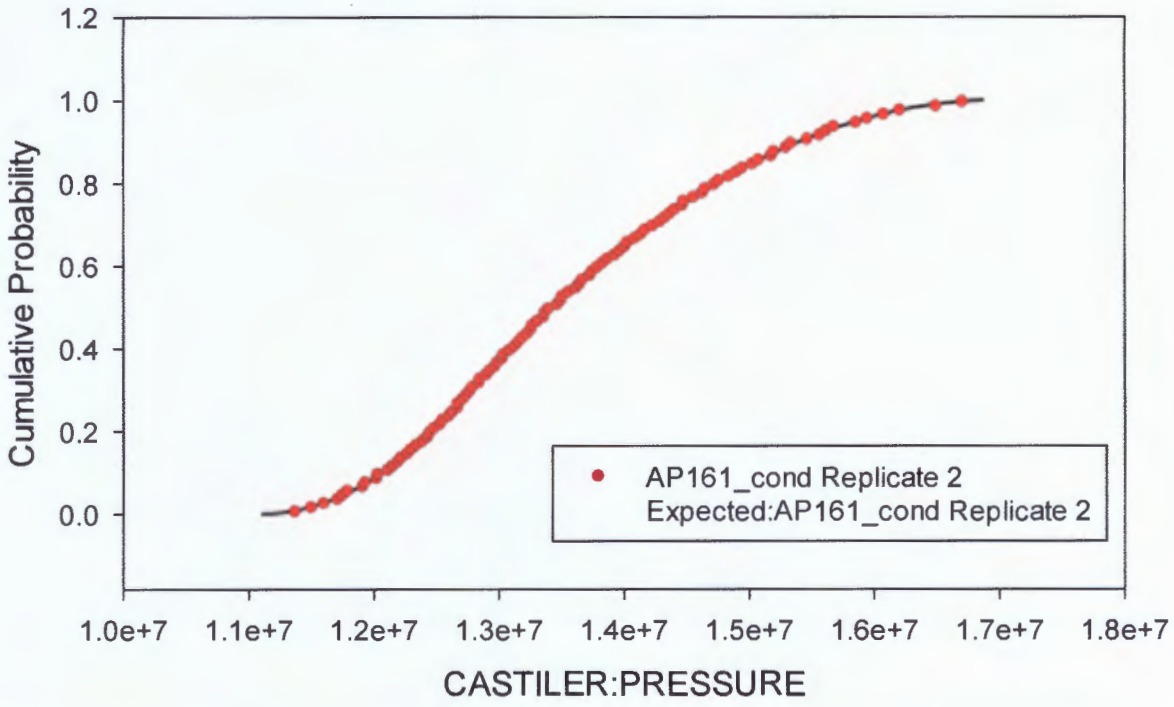

□i□□r□□□□O□□□r□□□an□□□□□□□□□□□□□

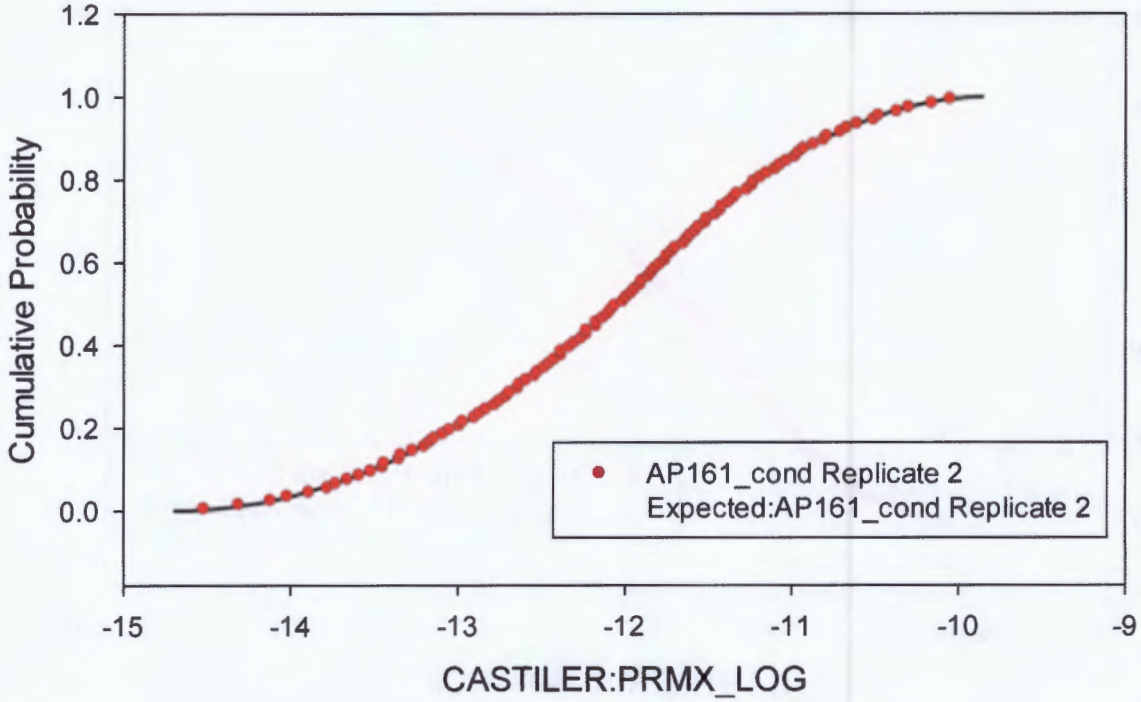

□i□□r□□□□O□□□r□□□an□□□□□□t□□□□□□for □□□□I□□□□□□□□ □□□O□ □□rian□□lar □i□ri□□tion□□□□i□at□□

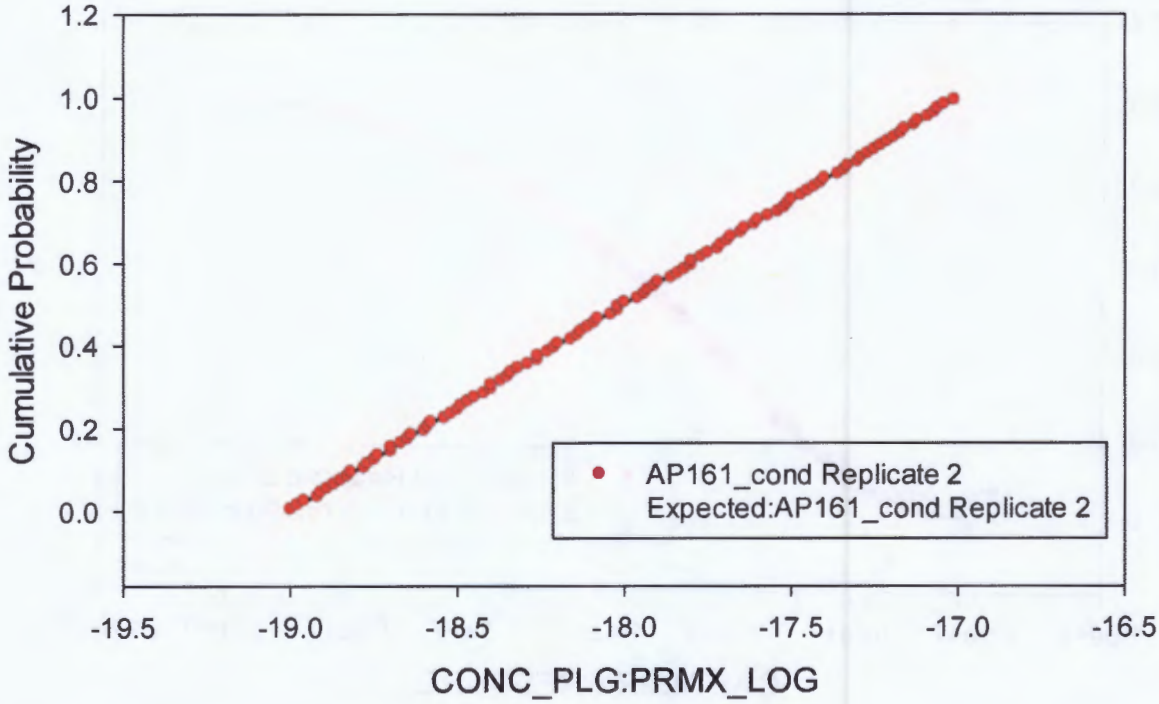

□i□□r□□□□O□□□r□□□an□□□□□□t□□□□□□for □O□□□□□□□□□□ □□□O□ □□niform □i□ri□□tion□□□□i□at□□

Information Only

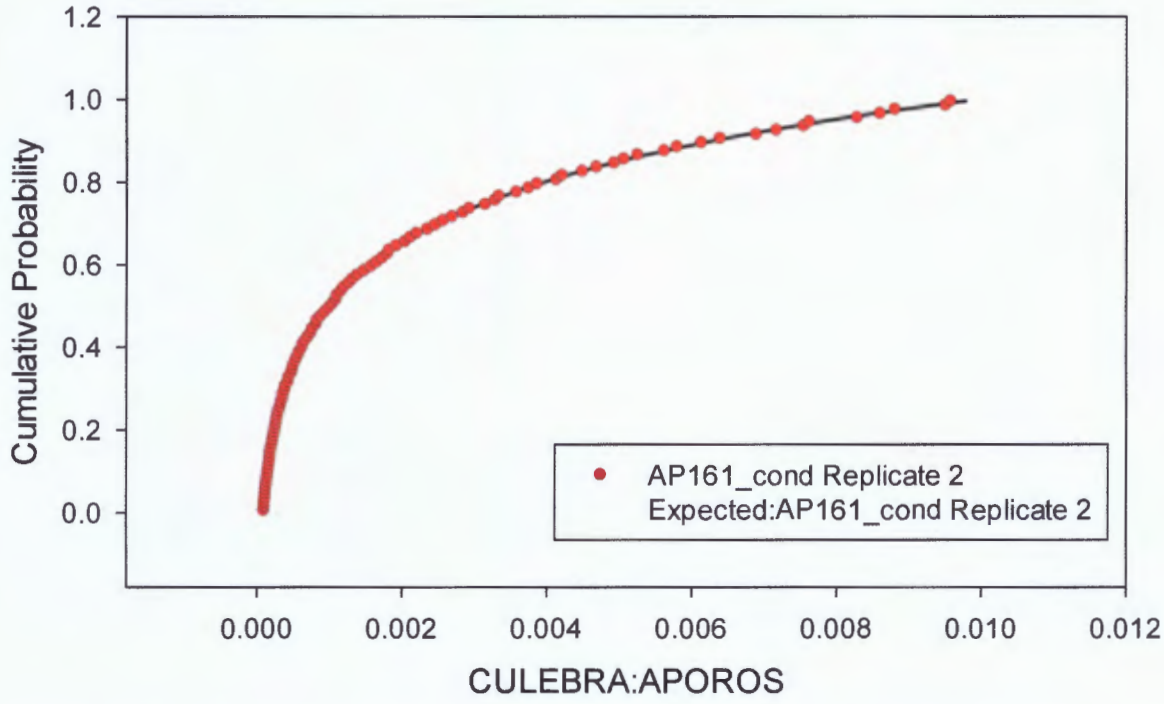

□i□□r□□□□O□□□r□□□an□ □□□□□t□□ □□□□for □□□□□□□□□□□O□O□ □□o□□niform □i□tri□□tion□□□□li□at□□

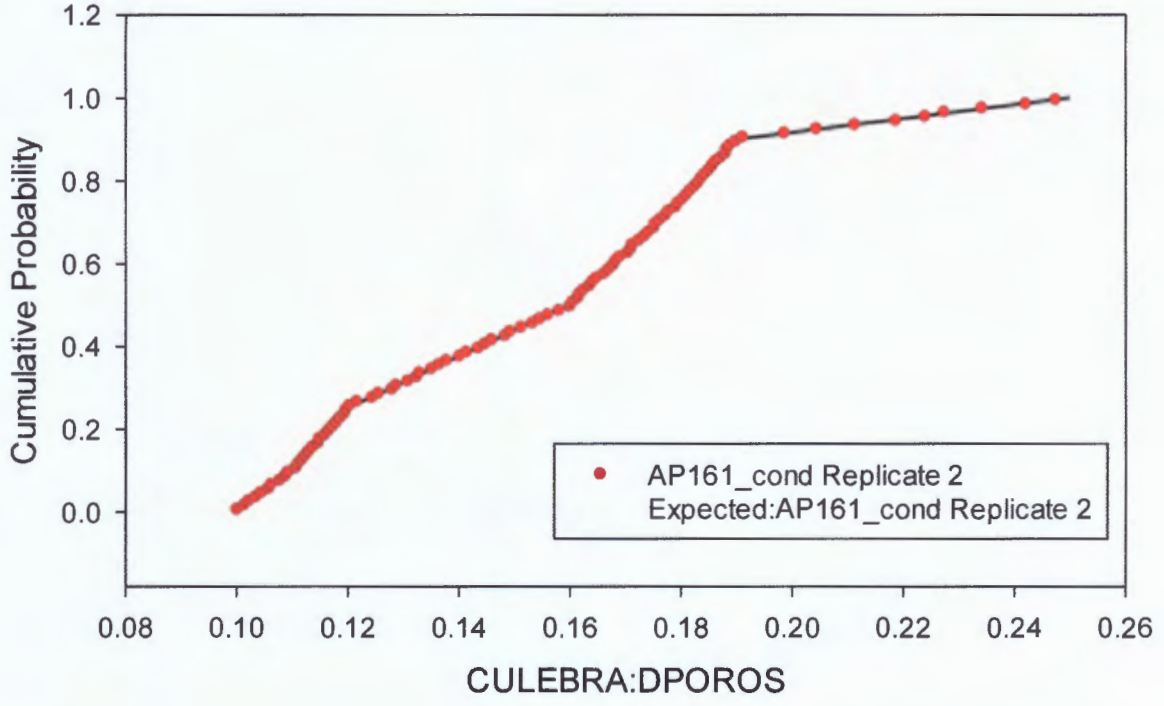

□i□□r□□□□O□□□r□□□an□ □□□□□t□□ □□□□for □□□□□□□□□□□O□O□ □□□□r □ontin□o□□□i□tri□□tion□□□□li□at□□

Information Only

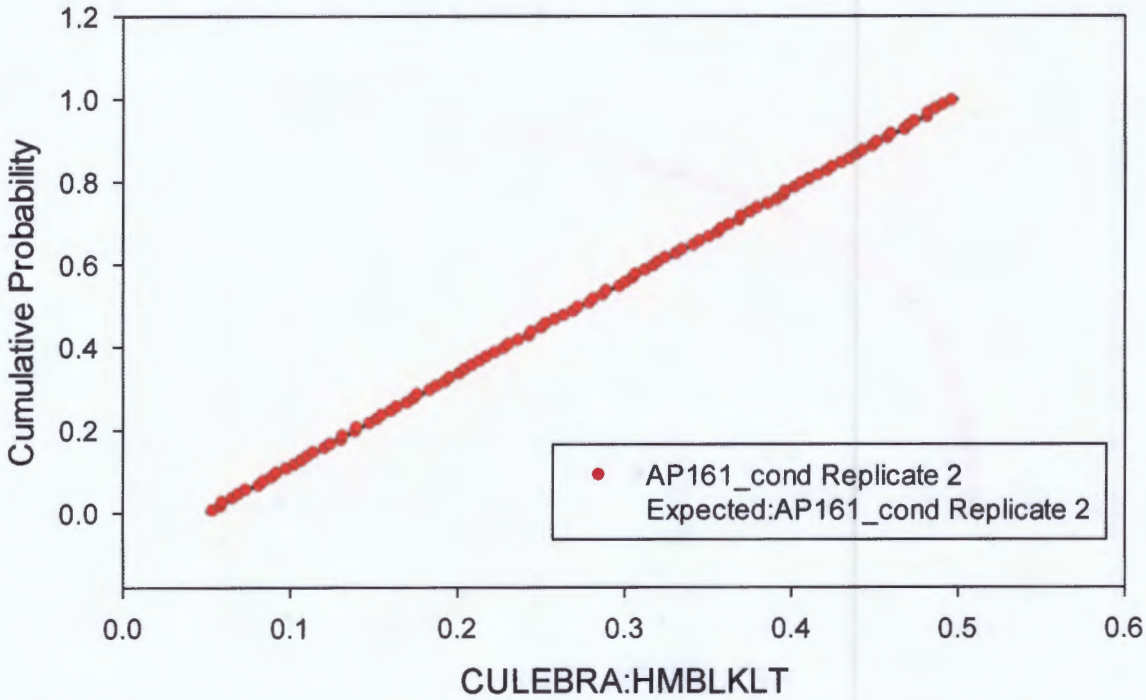

□i□r□□□O□□r□□an□□□□□t□□□□□for □□□□□□□□□□ □□□□□ □□niform □i□ri□□tion□□□li□at□□

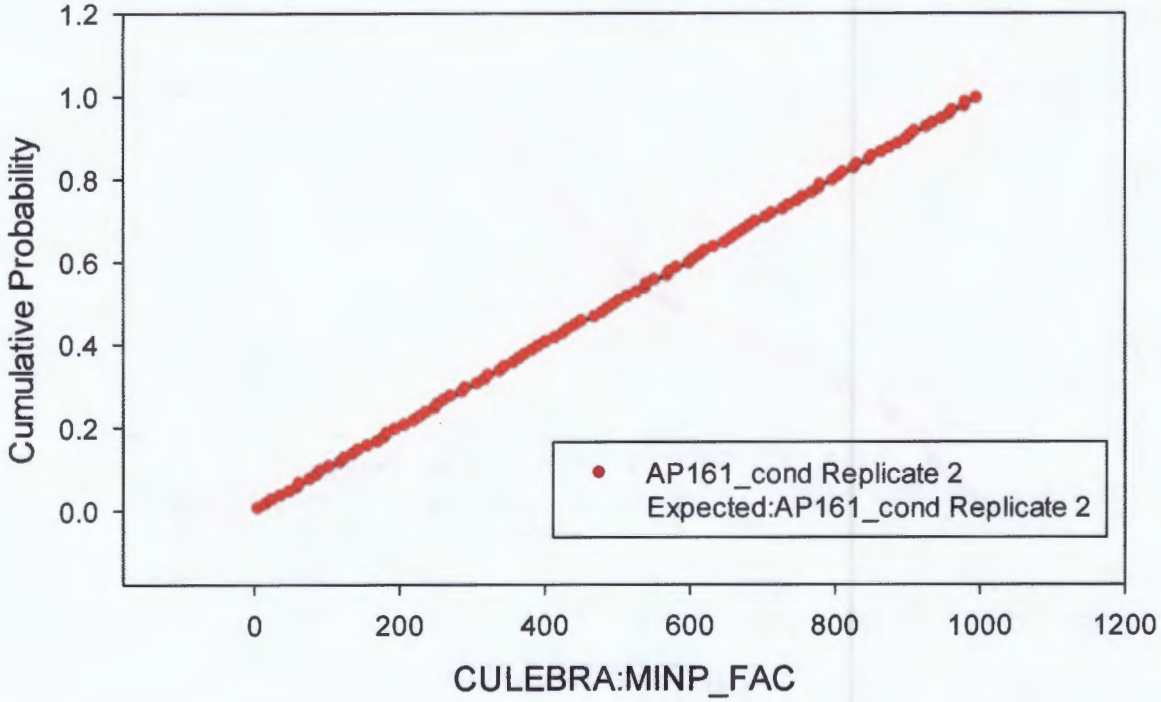

□i□r□□□O□□r□□an□□□□□t□□□□□for □□□□□□□□□ I□□□□□ □□niform □i□ri□□tion□□□li□at□□

Information Only

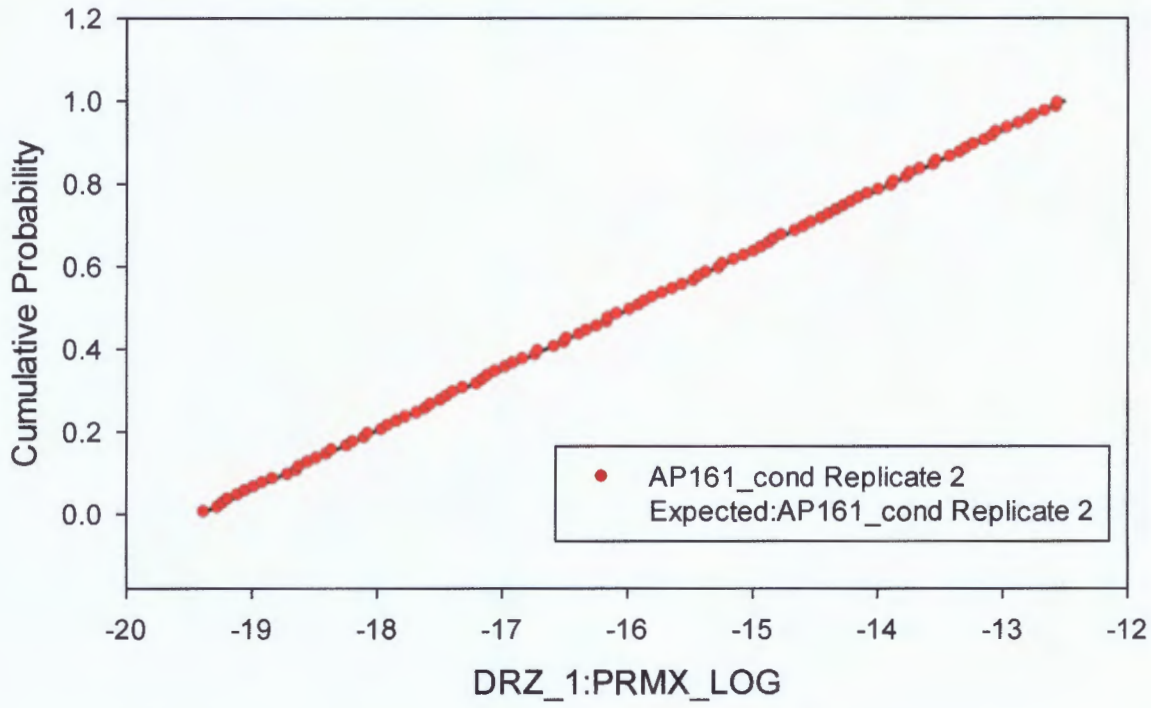

□i□r□□□O□□r□□an□□□□□t□□□□□for □□□□□□□□□ □□O□ □□niform □i□tri□□tion□□□□i□at□□

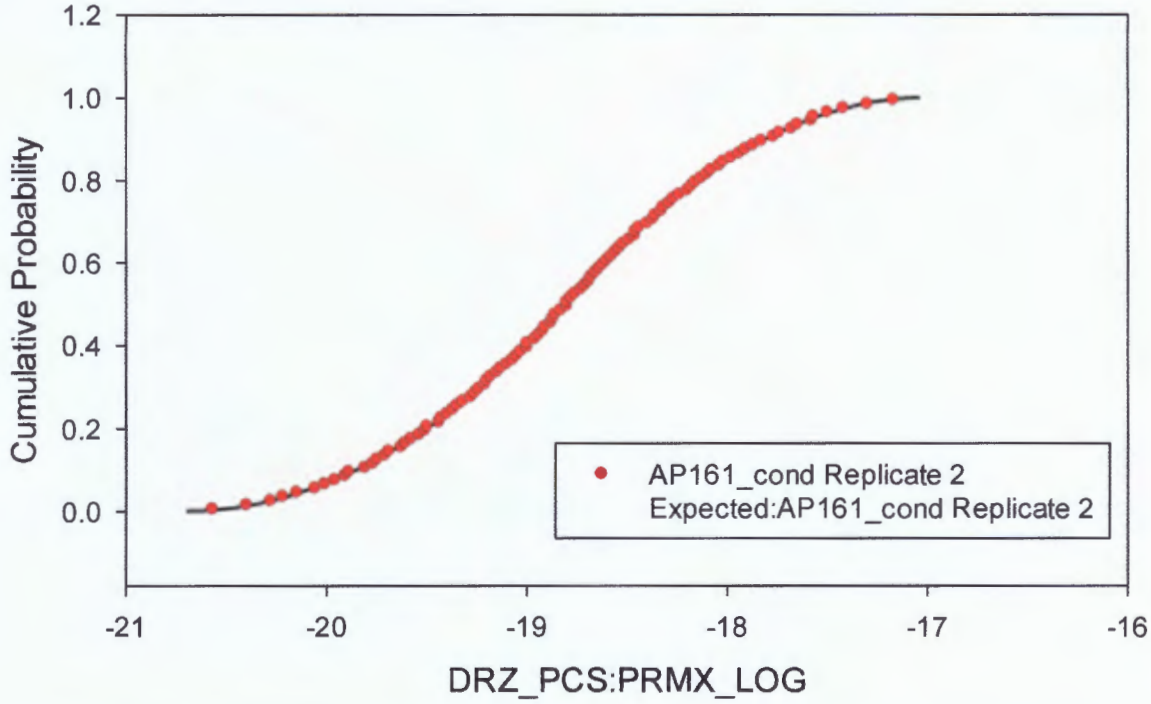

□i□r□□□O□□r□□an□□□□□t□□□□□for □□□□□□□□□□ □□O□ □□rian□□lar □i□tri□□tion□□□□i□at□□

Information Only

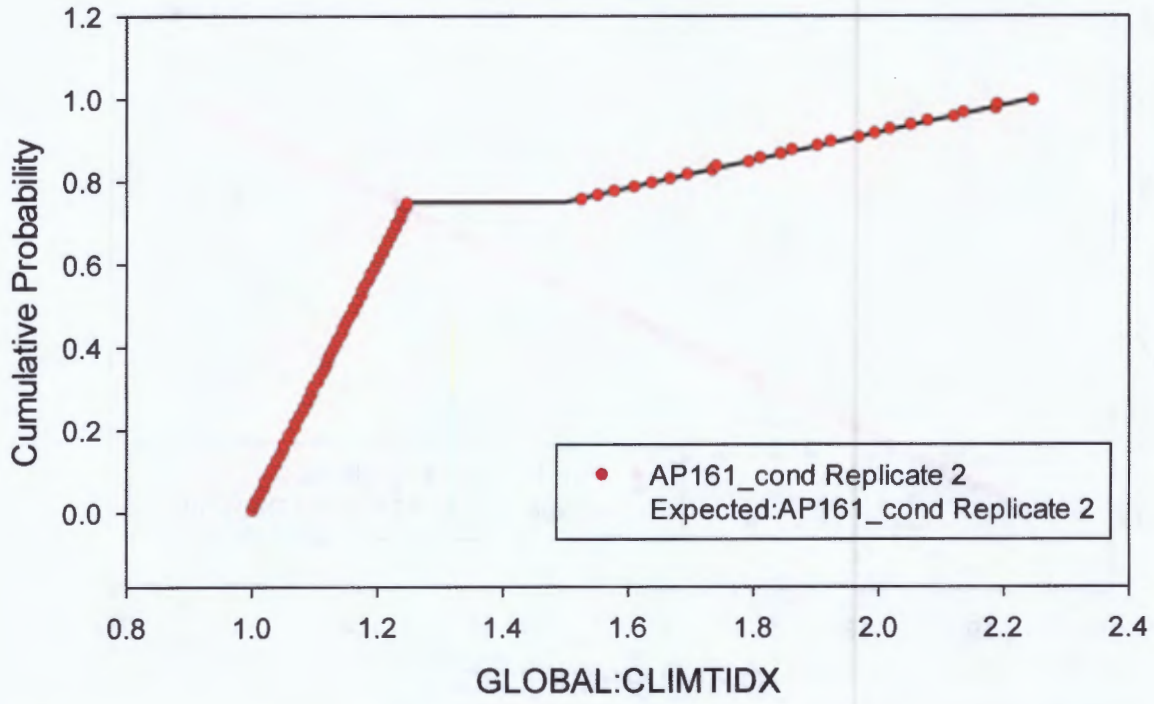

□i□□r□□□□O□□□r□□□an□ □□□□□t□□ □□□□for □□O□□□□□□□I□ □□□□ □□□□r □ontin□o□□□i□tri□□tion□□□□li□at□□

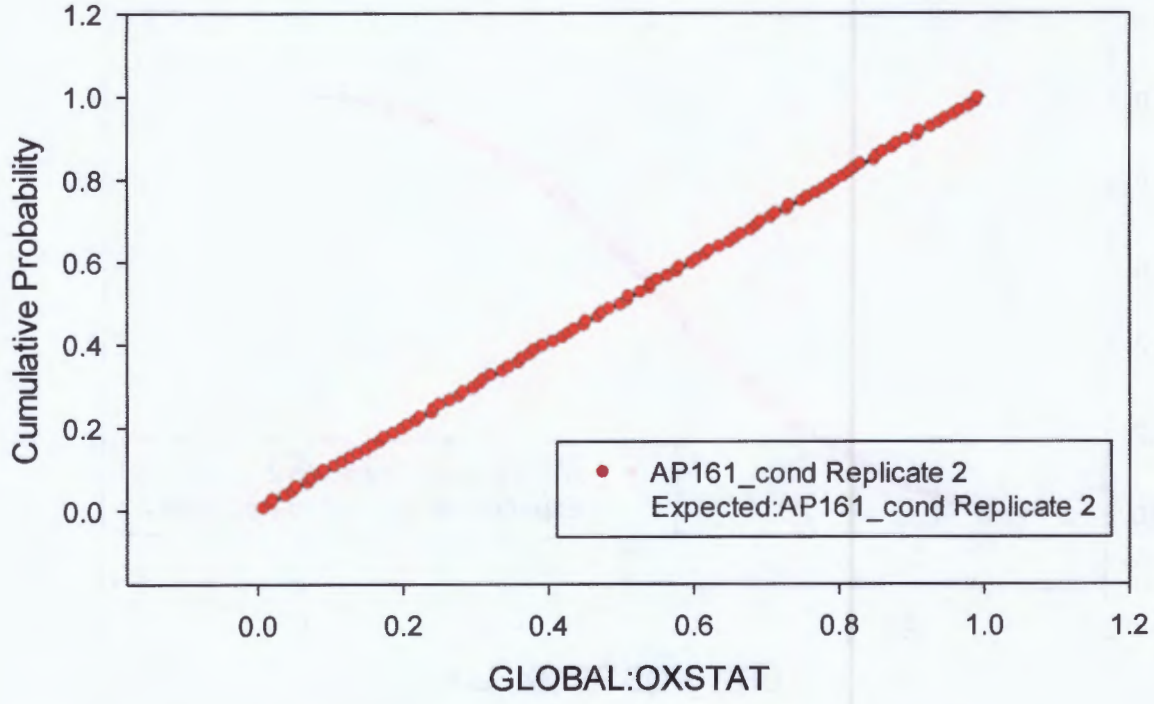

□i□□r□□□□O□□□r□□□an□ □□□□□t□□ □□□□for □□O□□□□O□□□□□ □□niform □i□tri□□tion□□□□li□at□□

Information Only

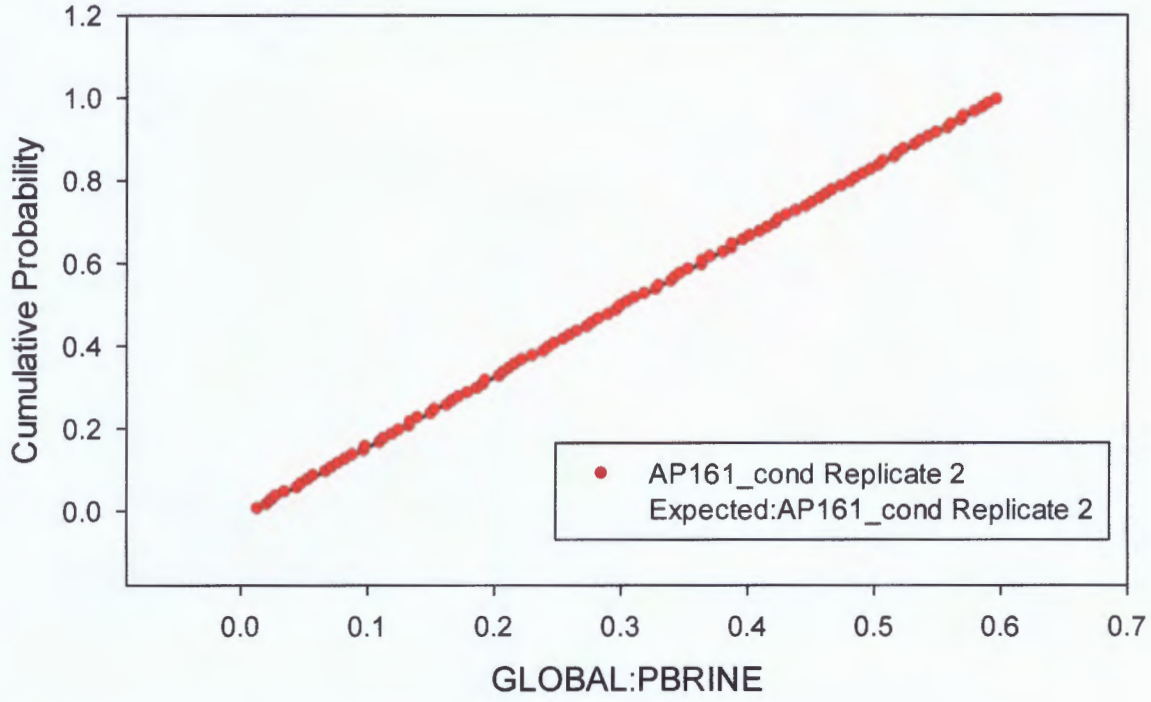

□i□□r□□□□O□□□r□□□an□□□□□□t□□□□□□for□□O□□□□□□□□□I□□□□niform□i□tri□□tion□□□□li□at□□□

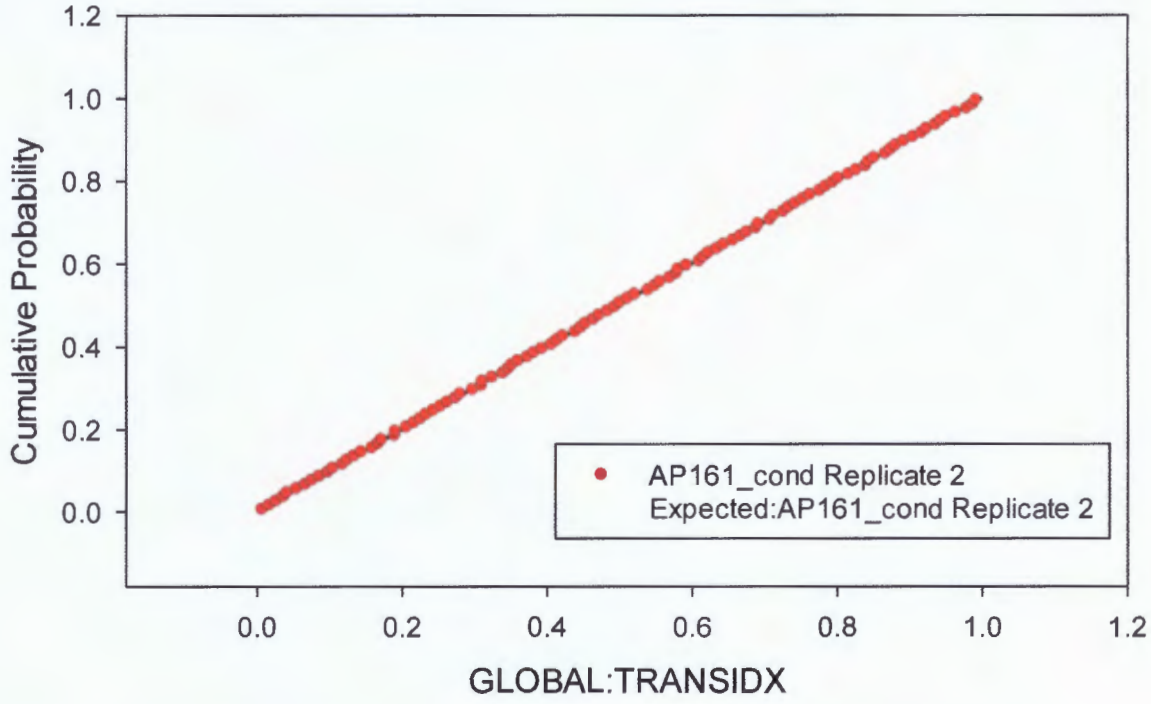

□i□□r□□□□O□□□r□□□an□□□□□□t□□□□□□for□□O□□□□□□□□□□I□□□□niform□i□tri□□tion□□□□li□at□□□

Information Only

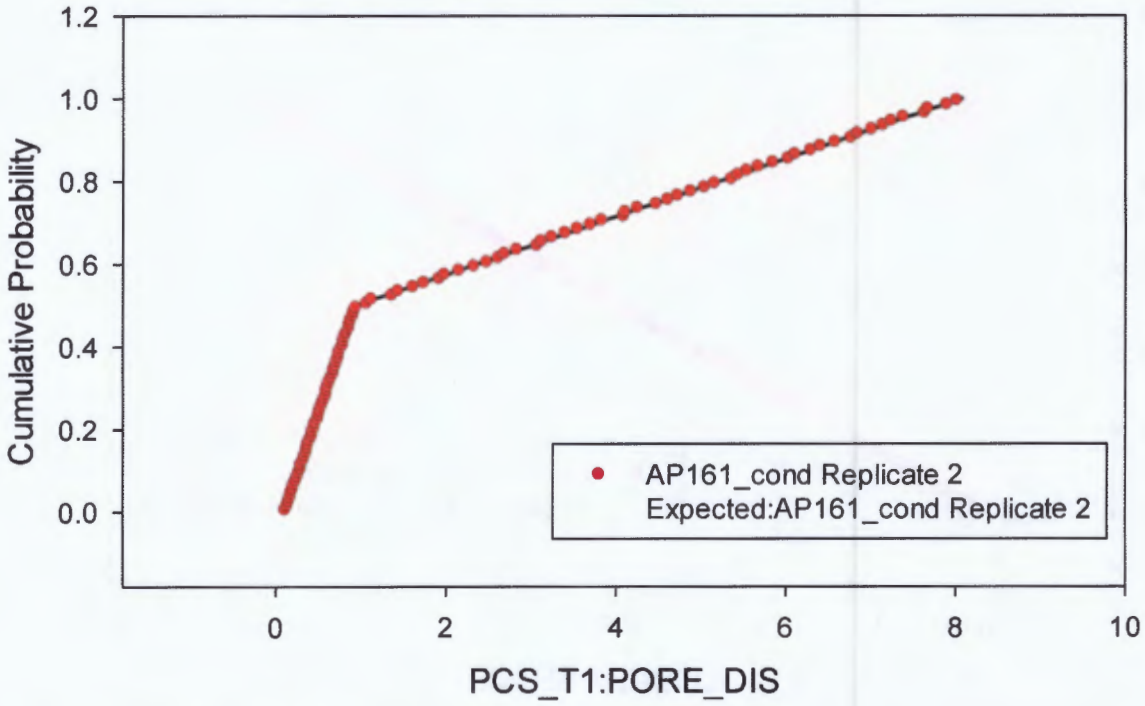

□i□r□□□O□□r□□□an□□□□□t□□□□□for □□□□□□O□□□□I□□□□r □ontin□b□□□i□ri□□tion□□□□i□at□□

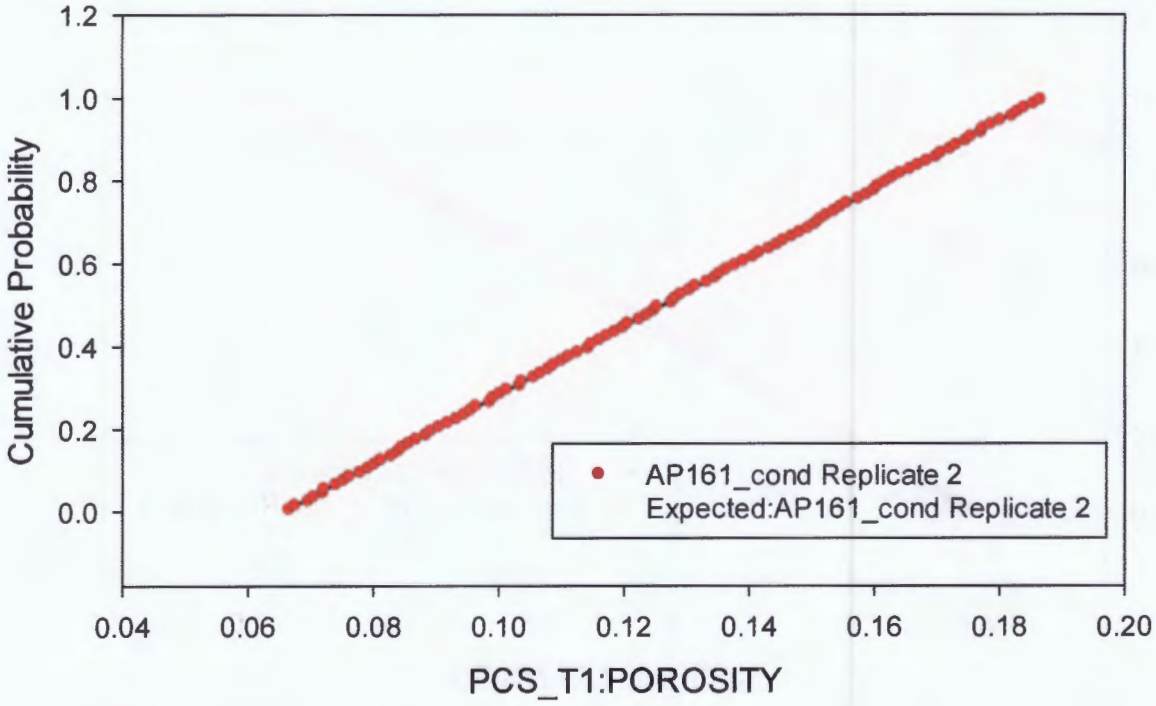

□i□r□□□O□□r□□□an□□□□□t□□□□□for □□□□□□O□O□I□□ □□niform □i□ri□□tion□□□□i□at□□

Information Only

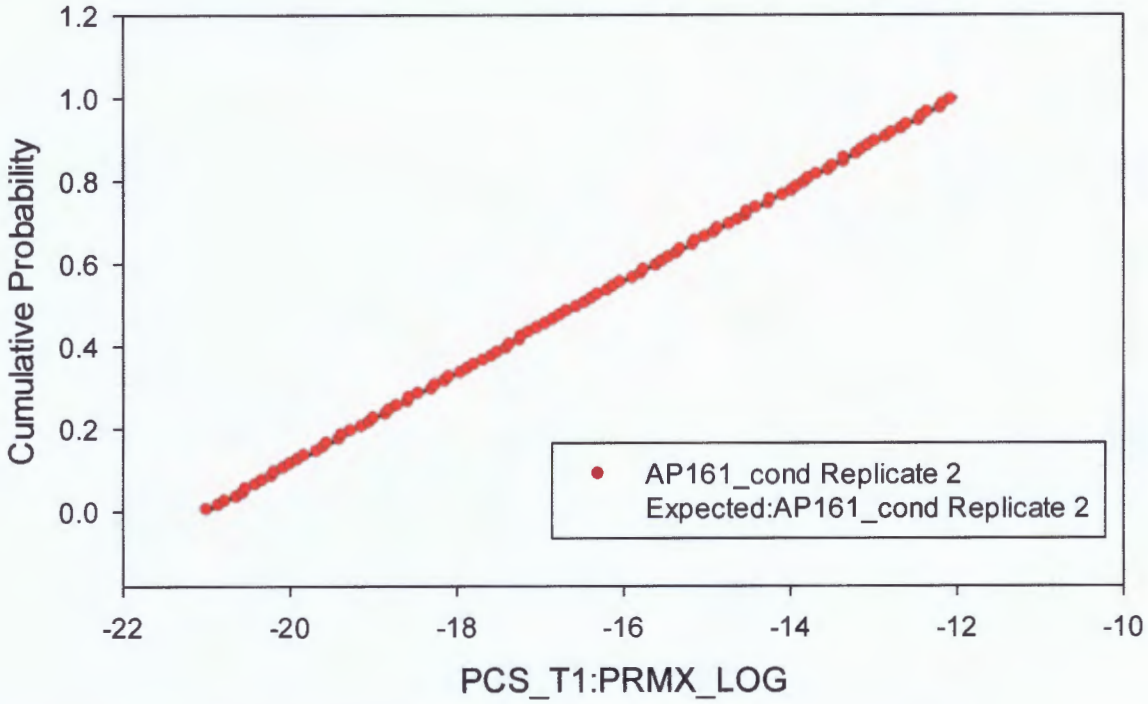

□i□r□□□O□□r□□□an□□□□□t□□□□□for □□□□□□□□□ □□□O□ □□niform □i□ri□□tion□□□□li□at□□

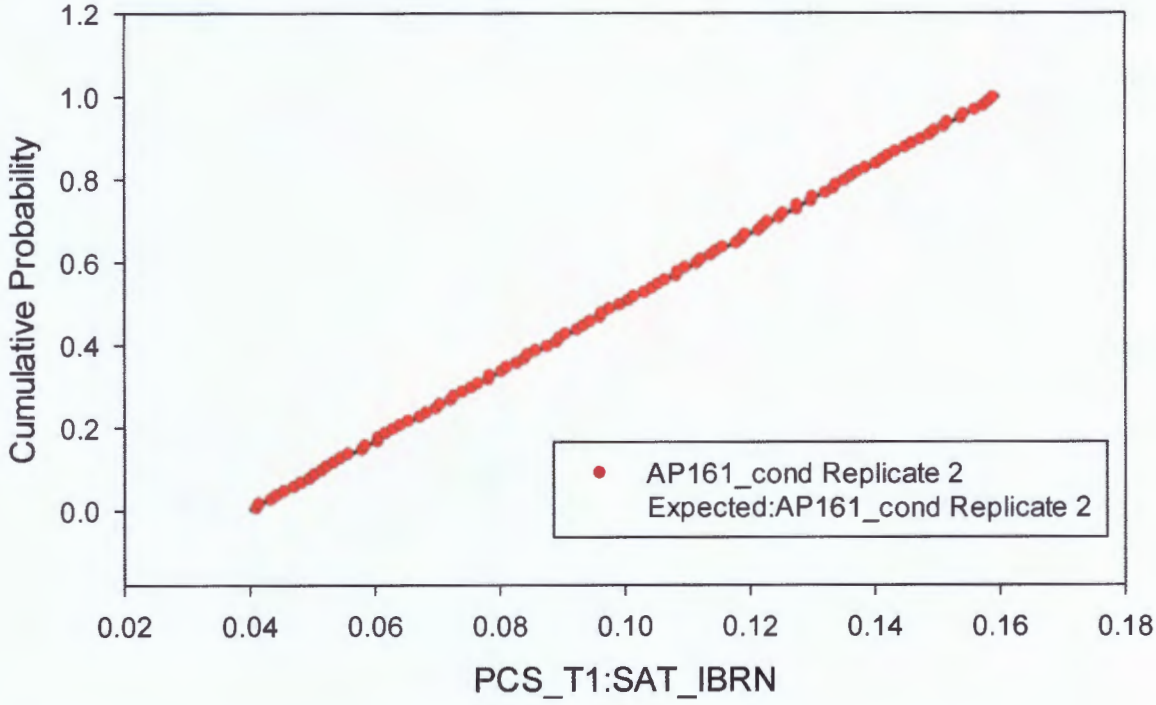

□i□r□□□O□□r□□□an□□□□□t□□□□□for □□□□□□□□□□□□□ □□niform □i□ri□□tion□□□□li□at□□

Information Only

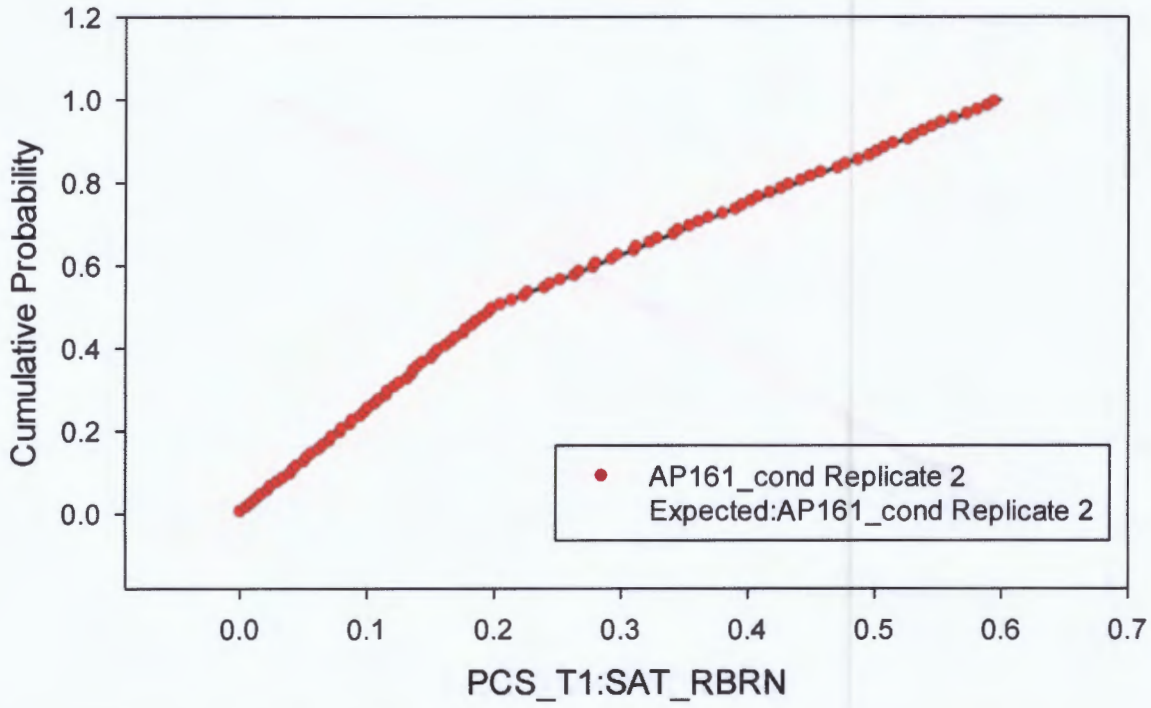

□i□□r□□□□O□□□r□□□an□ □□□□□t□□ □□□□for □□□□□□□□□□□□□□□□ □□□□r □ontin□o□□□□i□ri□□tion□□□□li□at□□

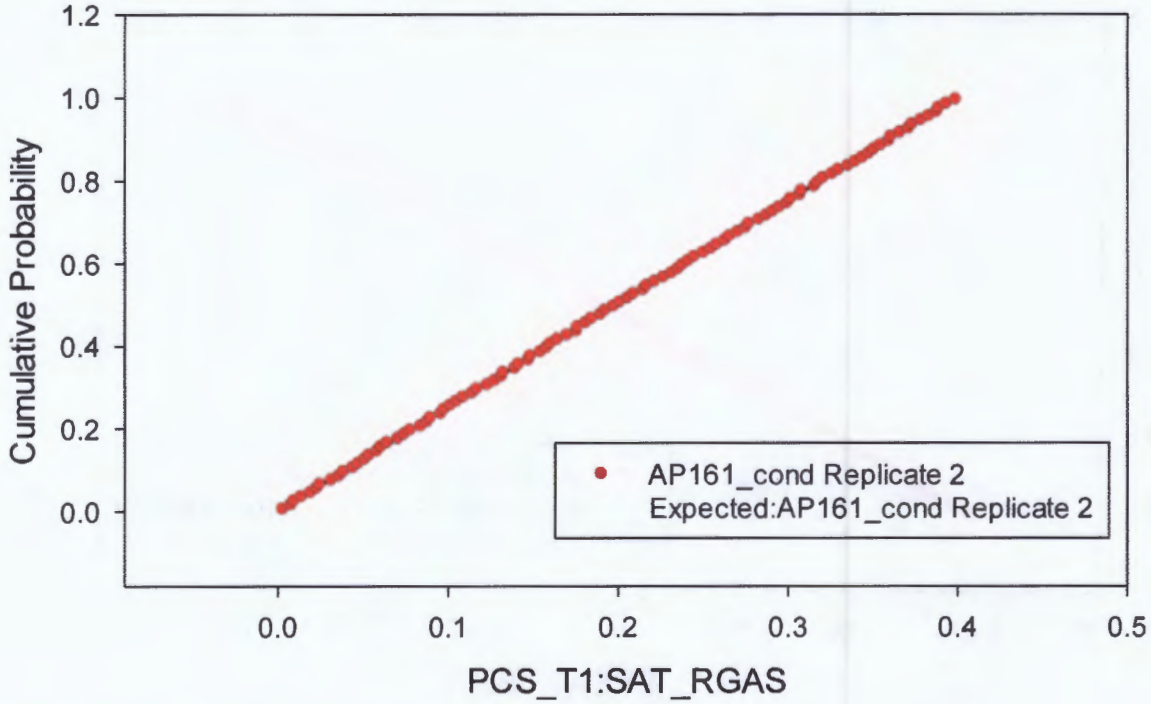

□i□□r□□□□O□□□r□□□an□ □□□□□t□□ □□□□for □□□□□□□□□□□□□□□□□□niform □i□ri□□tion□□□□li□at□□

Information Only

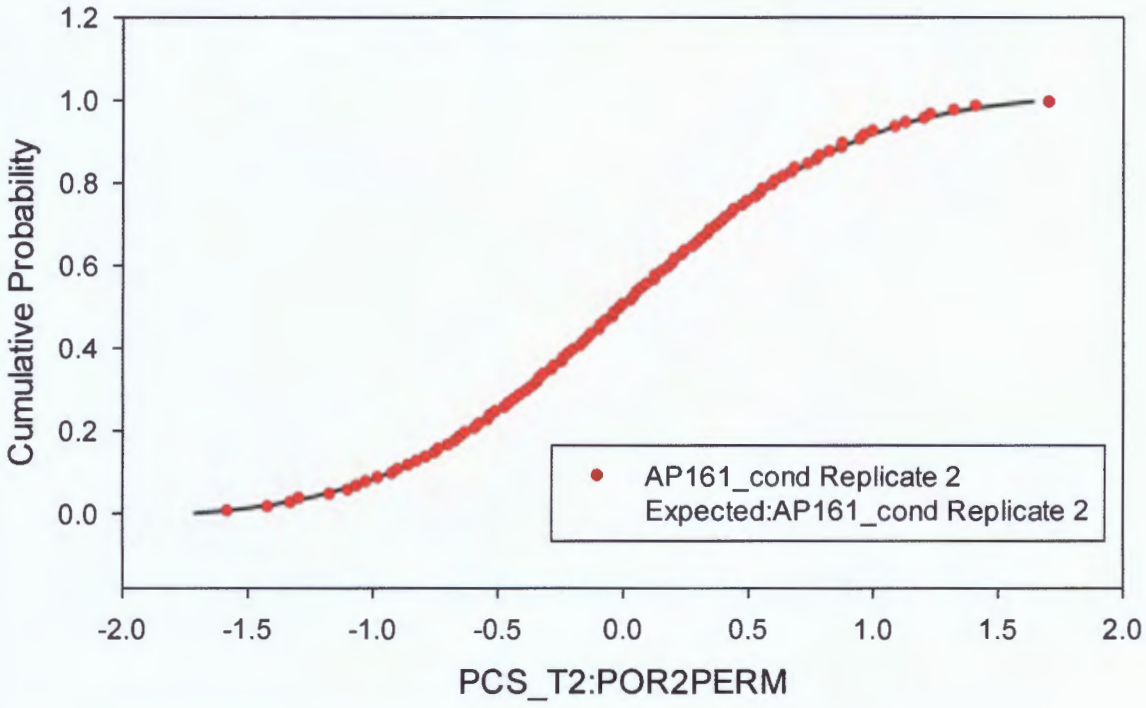

□i□□r□□□□O□□□r□□□an□ □□□□□t□□ □□□□for □□□□□□□□O□□□□□□ □□ormal □i□tri□□tion□□□□i□at□□

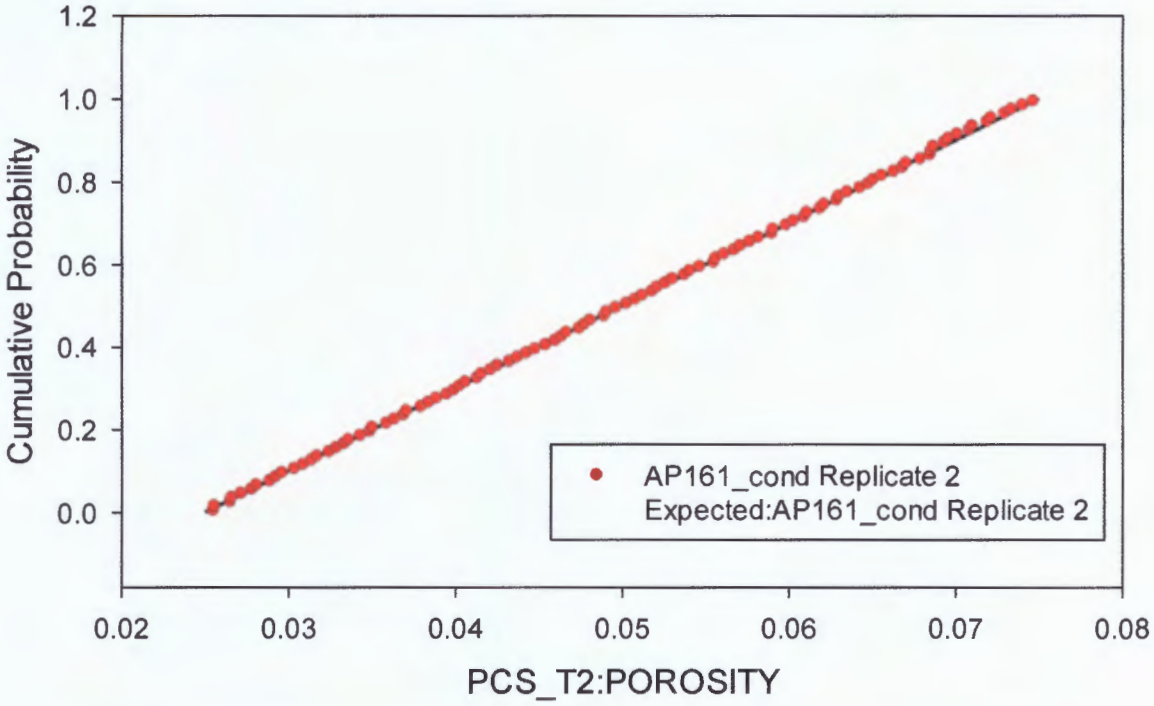

□i□□r□□□□O□□□r□□□an□ □□□□□t□□ □□□□for □□□□□□□□O□O□I□□ □□niform □i□tri□□tion□□□□i□at□□

Information Only

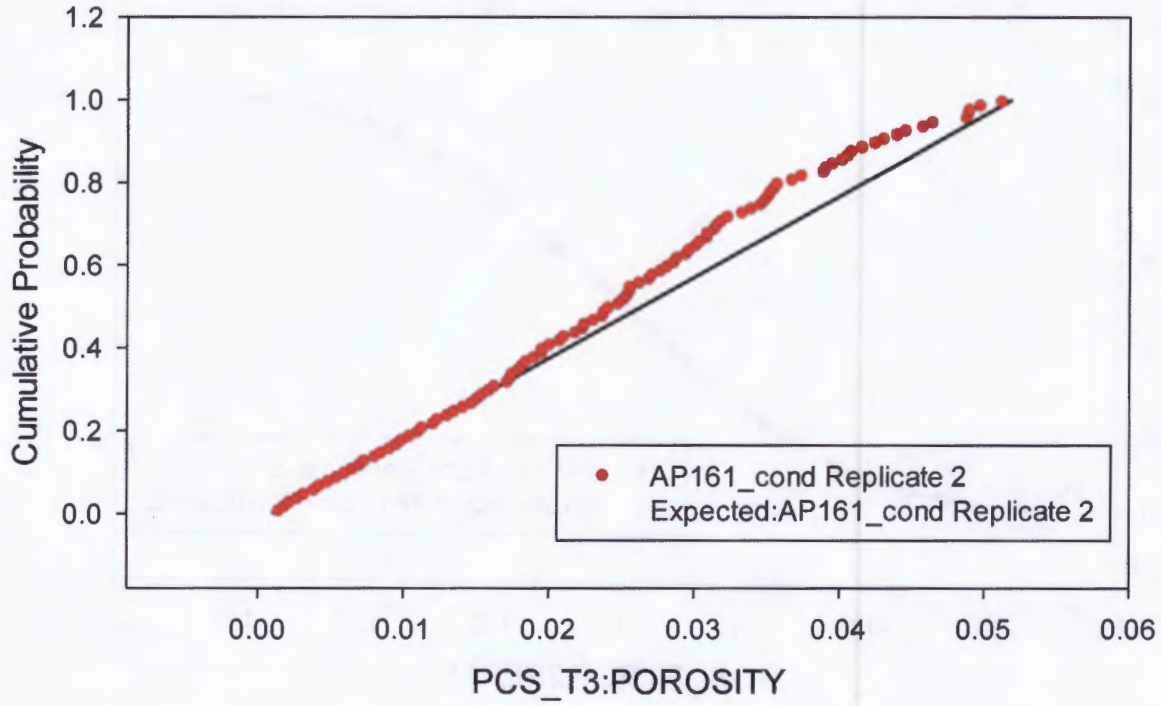

□i□□r□□□□O□□□r□□□an□ □□□□□t□□ □□□□for □□□□□□□O□O□I□□ □□niform □i□ri□□tion□□□□i□at□□

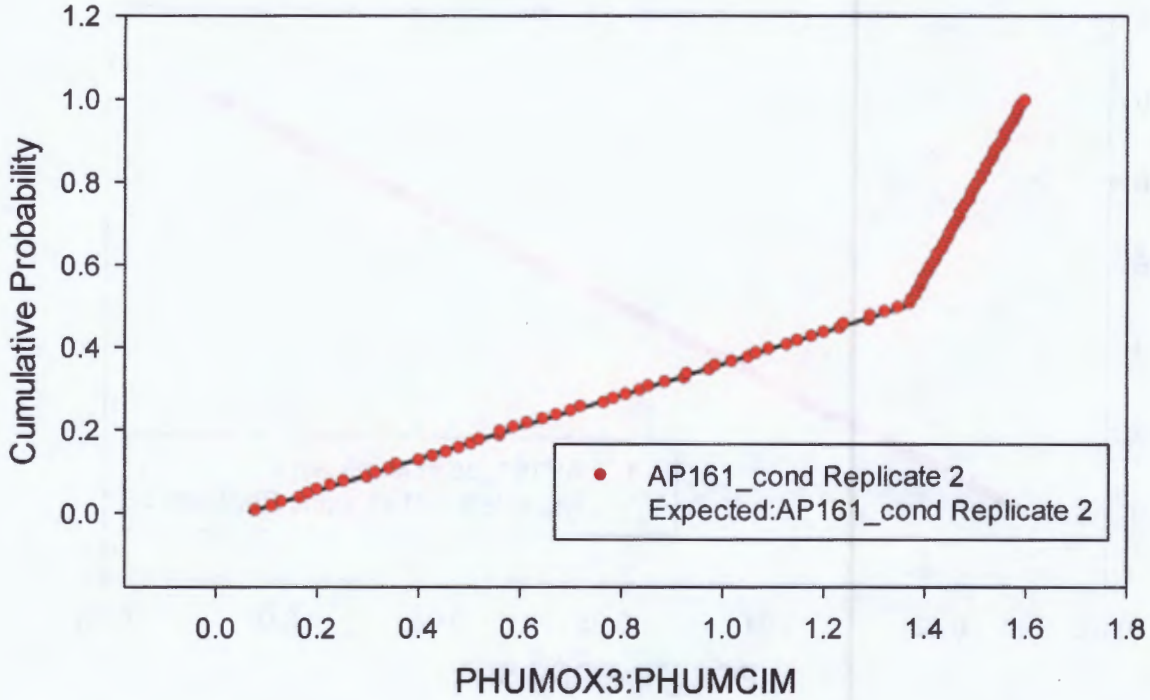

□i□□r□□□□O□□□r□□□an□ □□□□□t□□ □□□□for □□□□ O□□□□□□ □I□ □□□r □ontin□b□□□i□ri□□tion□□□□i□at□□

Information Only

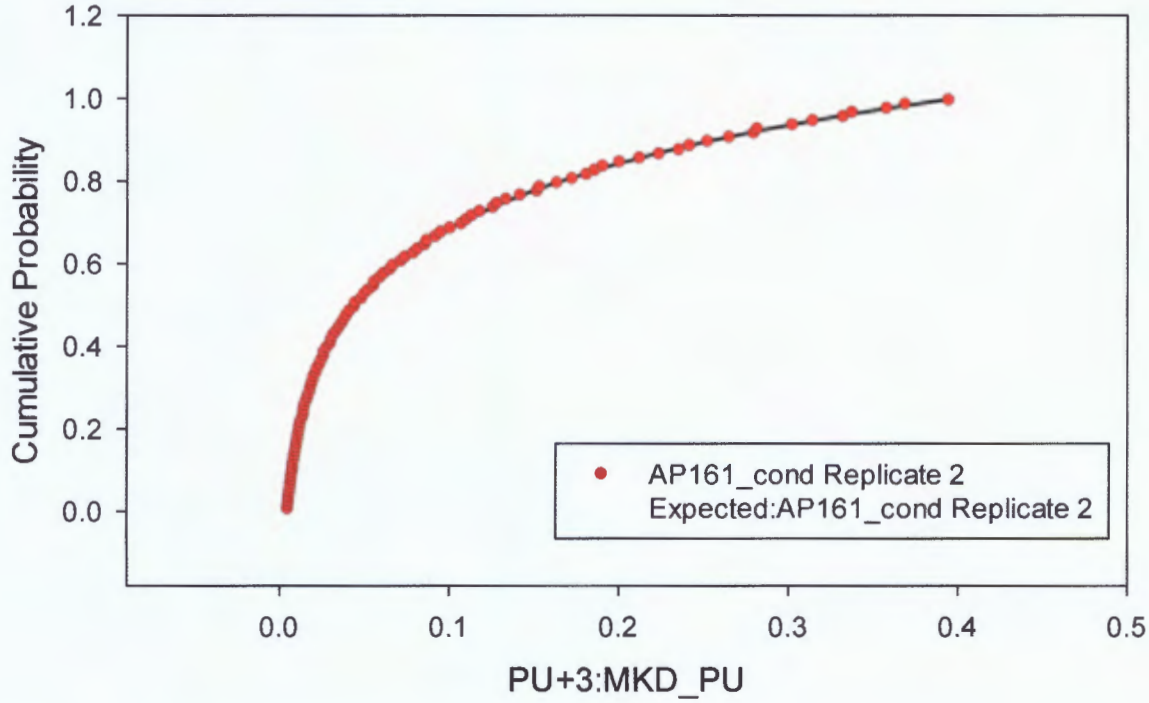

□i□r□□□O□□r□□an□□□□□t□□□□□for □□□□□ □□□□ □□o□niform □i□ri□□tion□□□li□at□□

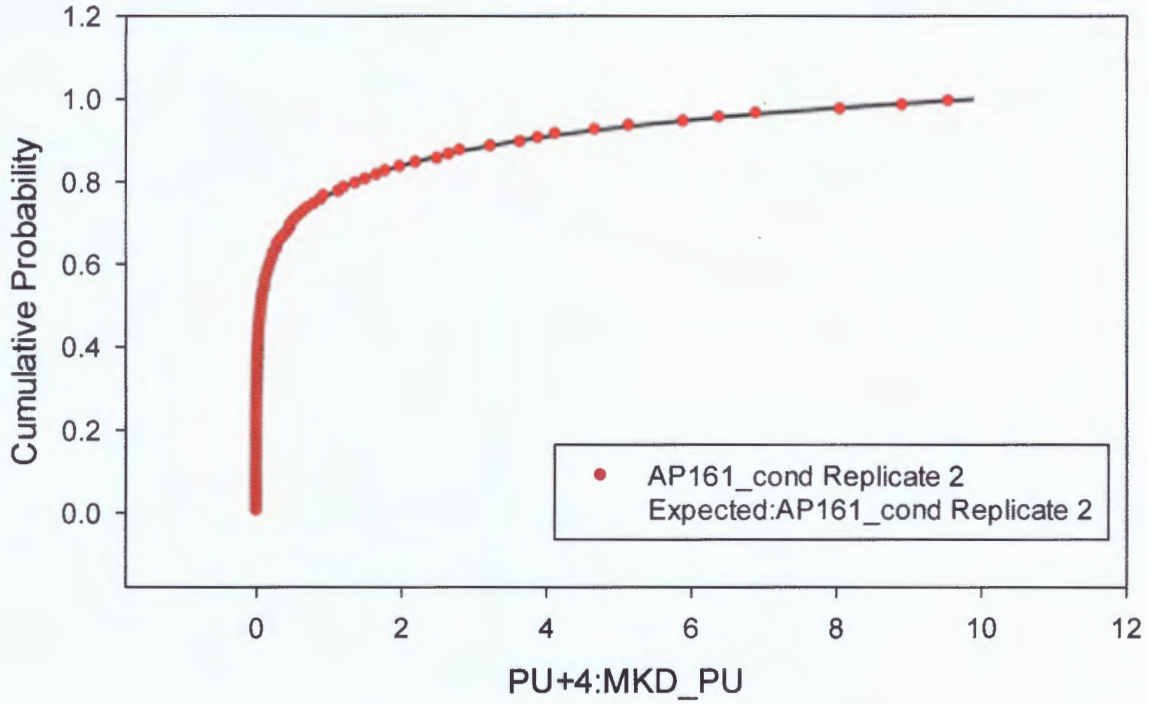

□i□r□□□O□□r□□an□□□□□t□□□□□for □□□□□ □□□□ □□o□niform □i□ri□□tion□□□li□at□□

Information Only

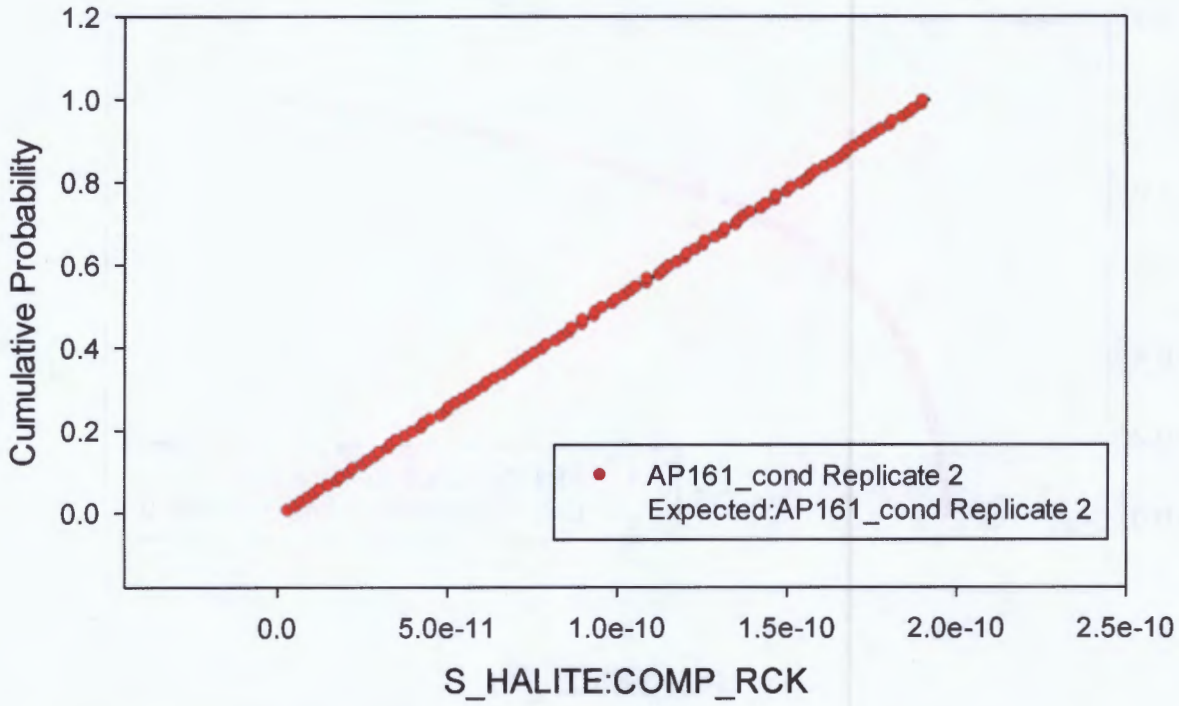

□i□r□□□O□□r□□□an□□□□□t□□□□□for □□□□□I□□□□O□ □□□□□ □□niform □i□tri□□tion□□□li□at□□

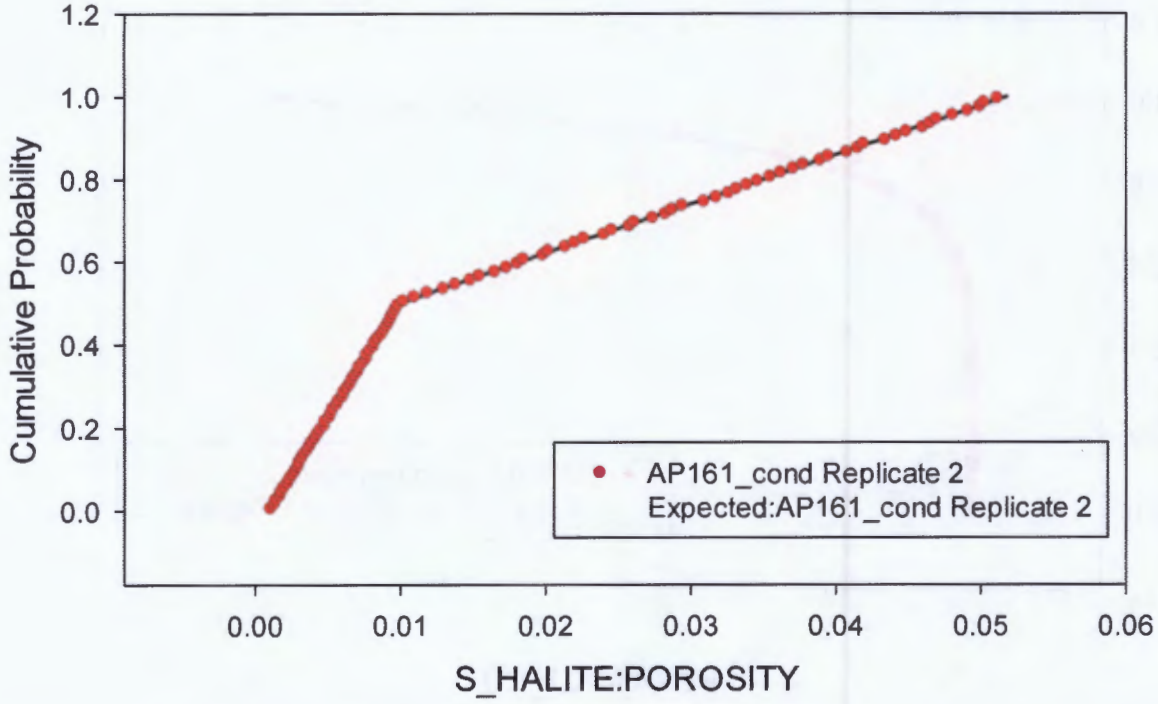

□i□r□□□O□□r□□□an□□□□□t□□□□□for □□□□□I□□□□O□O□I□□ □□□r □ontin□b□□□i□tri□□tion□□□li□at□□

Information Only

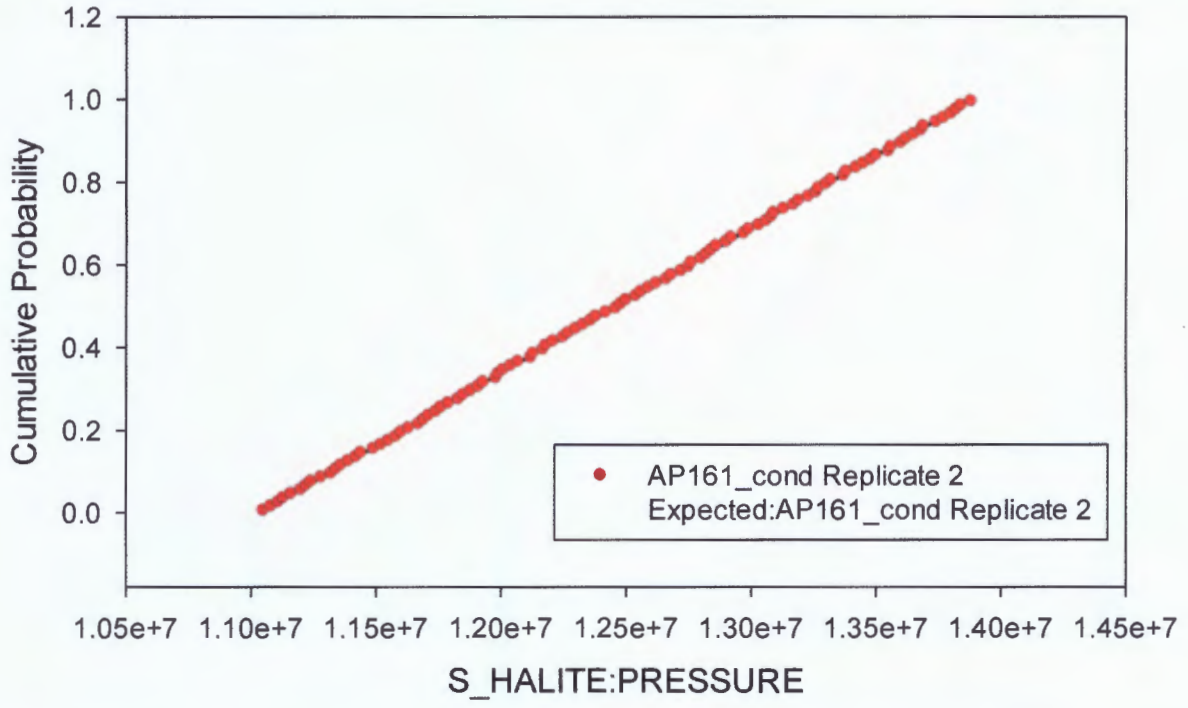

□i□r□□□O□□r□□□an□□□□□t□□□□□for □□□□□l□□□□□□□□□□ □□niform □i□ri□□tion□□□□i□at□□

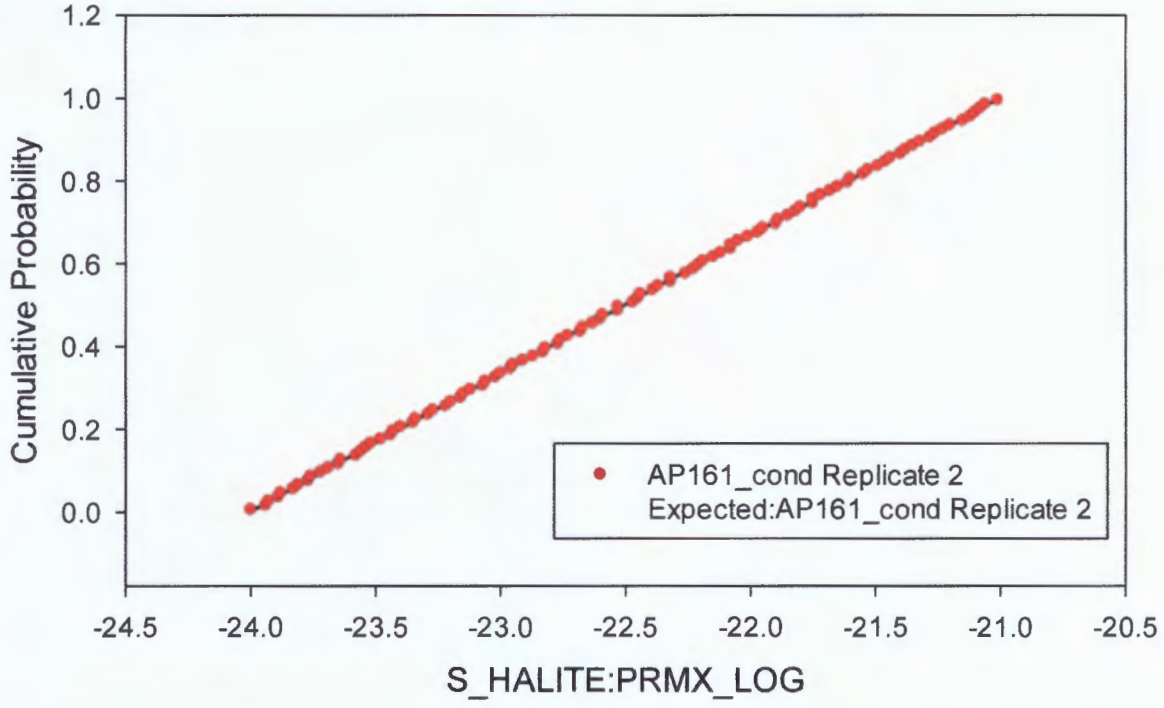

□i□r□□□O□□r□□□an□□□□□t□□□□□for □□□□□l□□□□□□ □□□O□ □□niform □i□ri□□tion□□□□i□at□□

Information Only

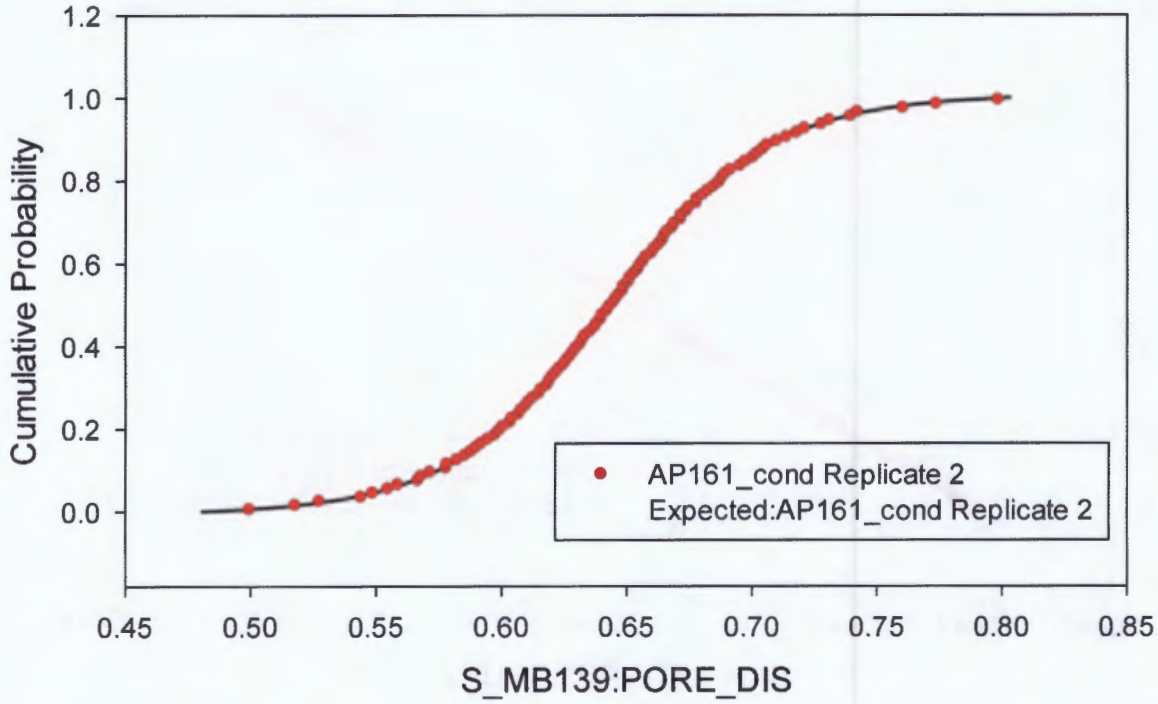

□i□r□□□O□□r□□an□ □□□□t□□ □□□□for □□□ □□□□□O□□□□I□ □□t□□□nt □i□tri□□tion□□□□li□at□□□

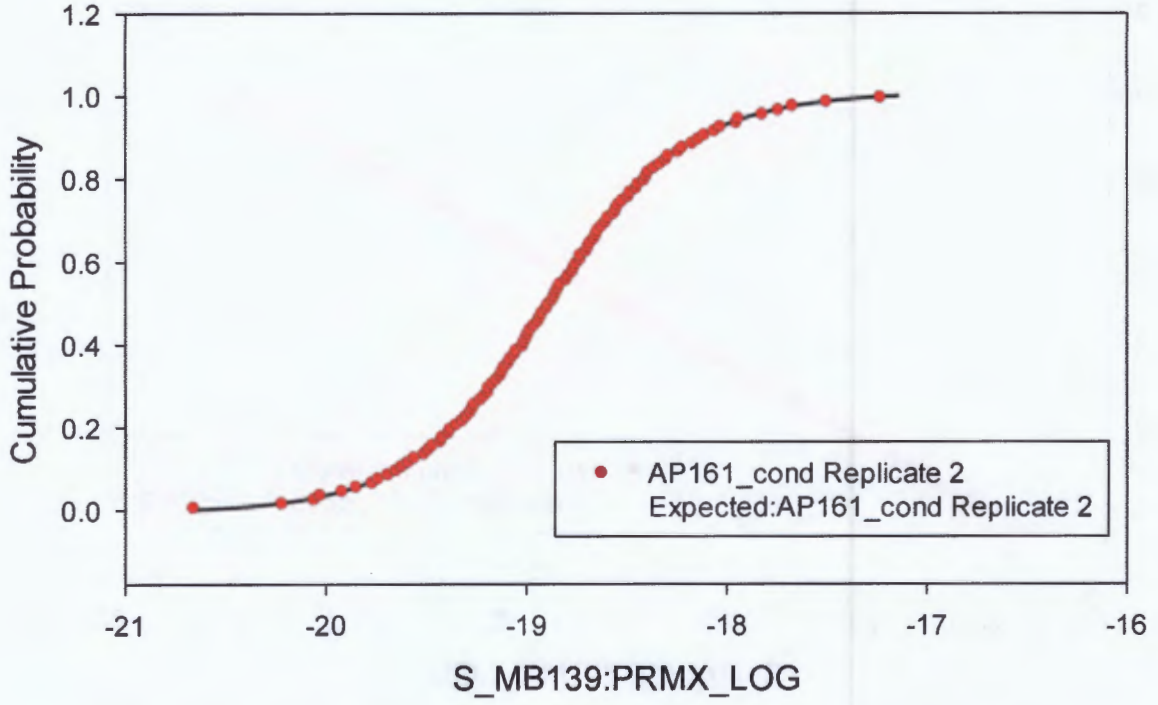

□i□r□□□O□□r□□an□ □□□□t□□ □□□□for □□□ □□□□□□□□ □□□O□ □□t□□□nt □i□tri□□tion□□□□li□at□□□

Information Only

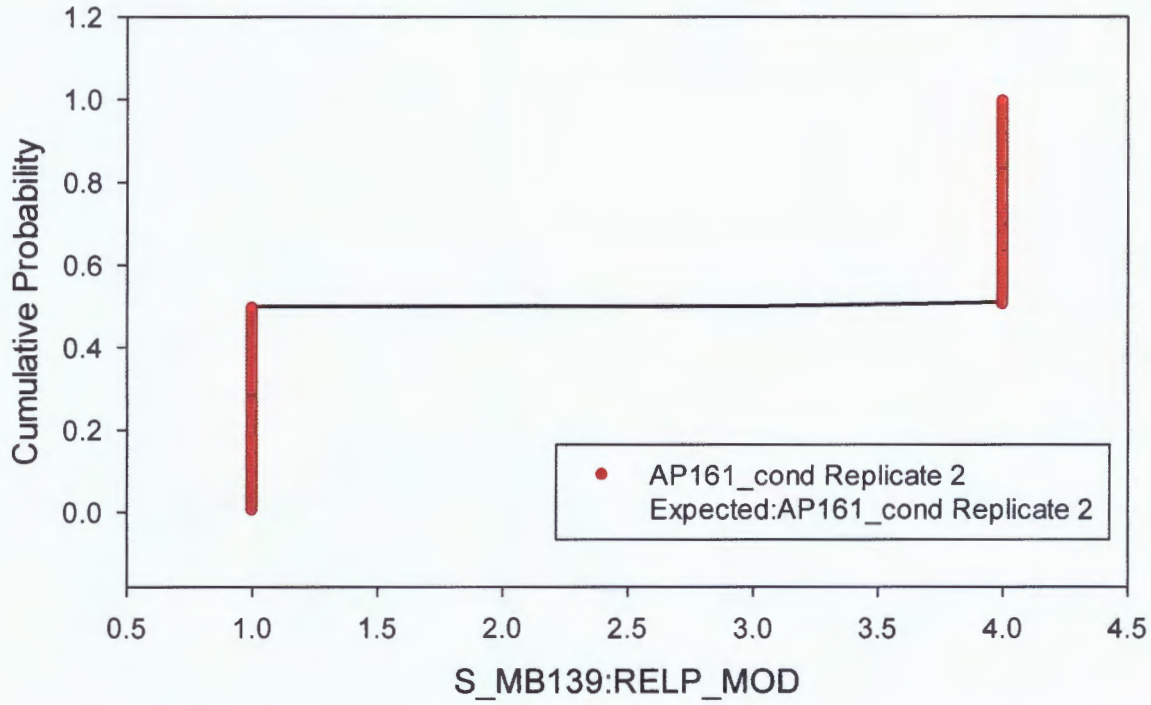

□i□□r□□□□O□□□r□□□an□ □□□□□t□□ □□□□for □□□ □□□□□□□□□□□ O□ □□□r □i□□r□t□□□□□ta□□i□ri□□tion□□ □□i□at□□□

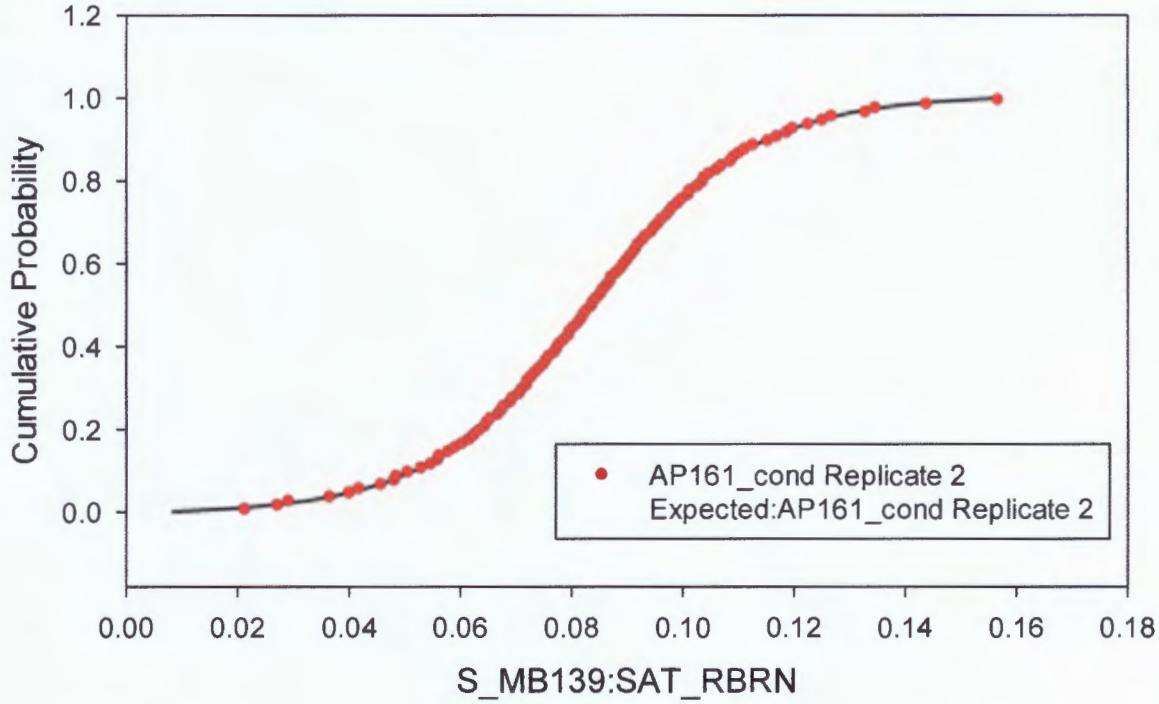

□i□□r□□□□O□□□r□□□an□ □□□□□t□□ □□□□for □□□ □□□□□□□□□□□□□□ □□t□□□nt □i□ri□□tion□□ □□i□at□□□

Information Only

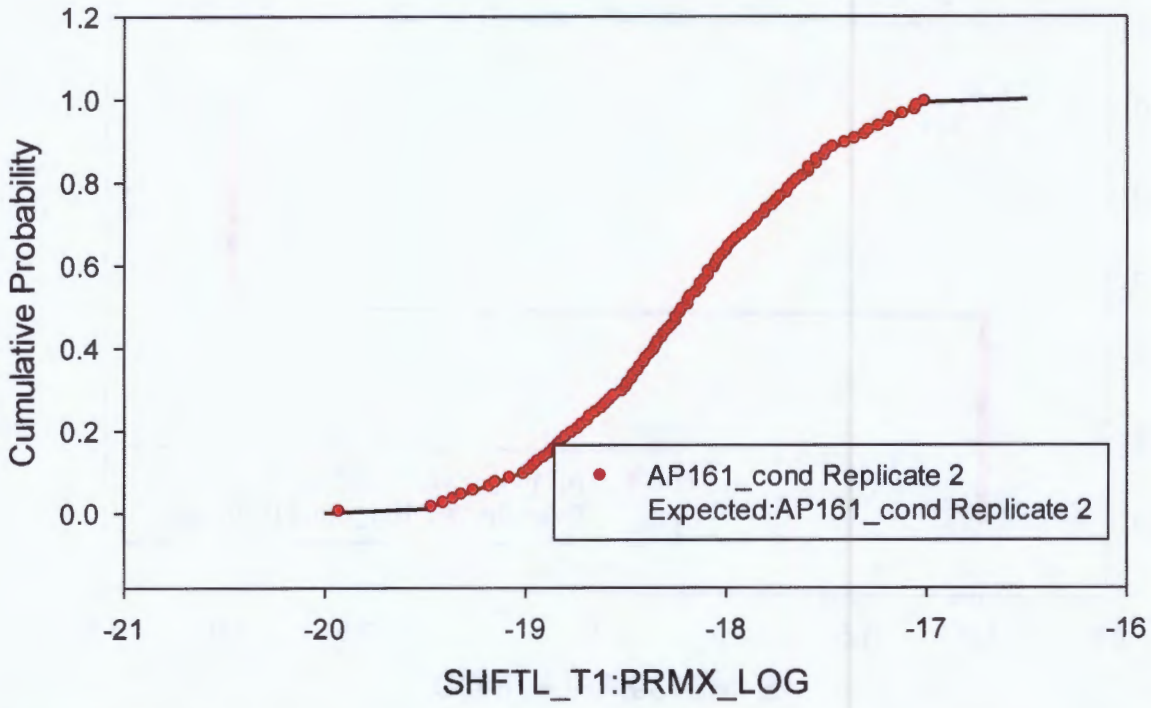

□i□r□□□O□□r□□an□□□□□t□□□□for □□□□□□□□□□□ □□O□ □□□r □ontin□o□□□i□ri□□tion□□□li□at□□

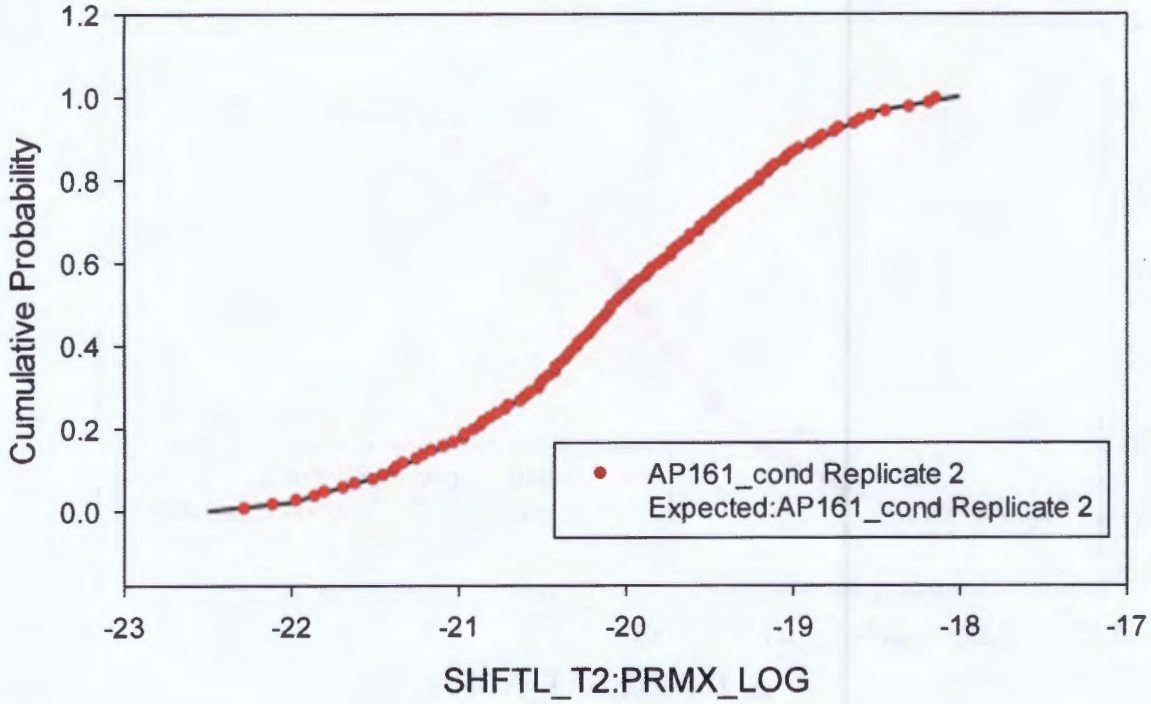

□i□r□□□O□□r□□an□□□□□t□□□□for □□□□□□□□□□□ □□O□ □□□r □ontin□o□□□i□ri□□tion□□□li□at□□

Information Only

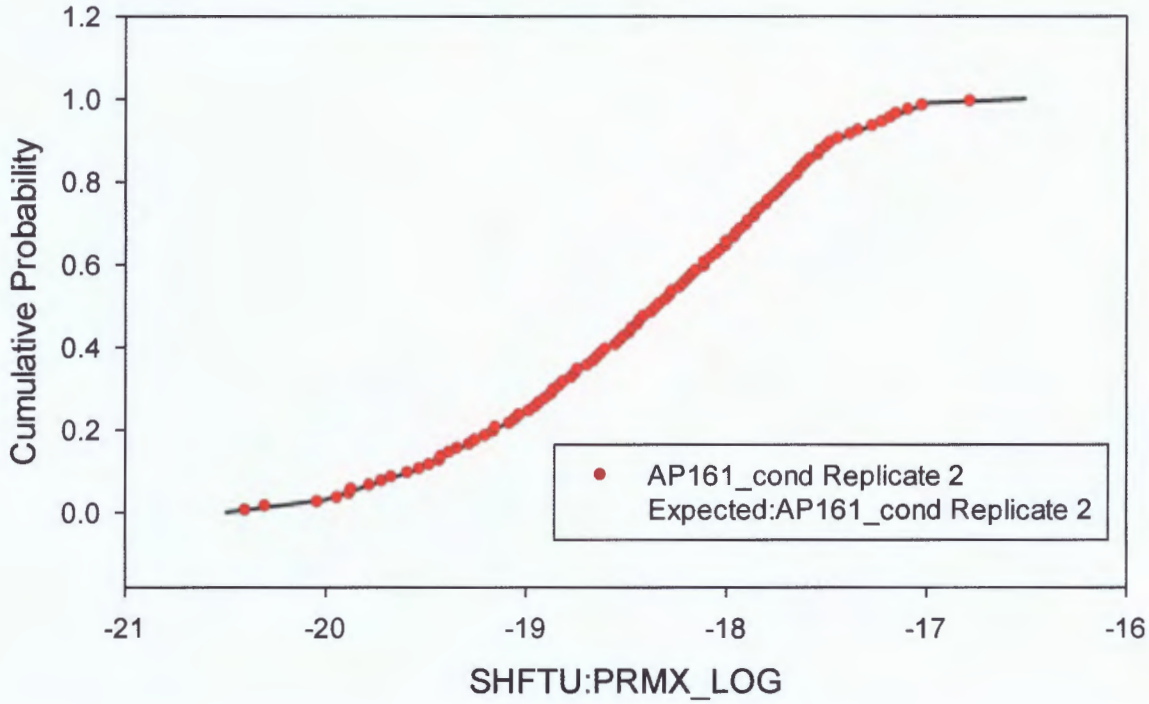

□i□r□□□□O□□r□□an□□□□□t□□□□□for □□□□□□□□ □□O□ □□□r □ontin□o□□□i□ri□□tion□□□li□at□□

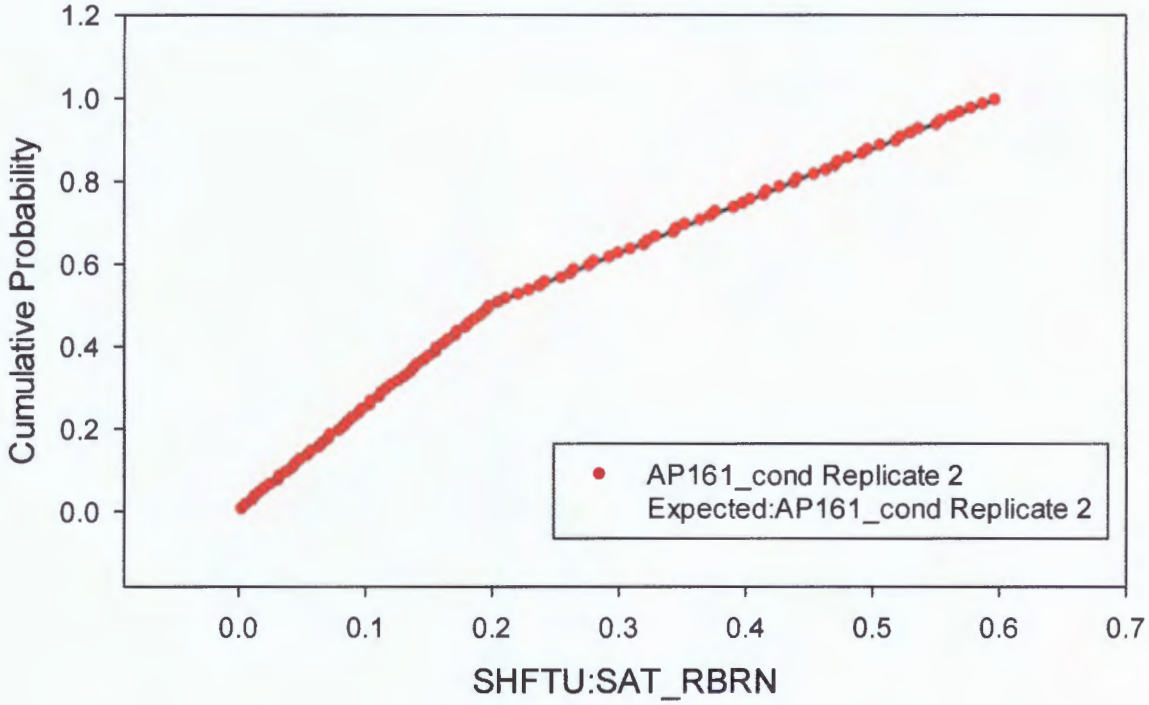

□i□r□□□□O□□r□□an□□□□□t□□□□□for □□□□□□□□□□□□ □□□r □ontin□o□□□i□ri□□tion□□□li□at□□

Information Only

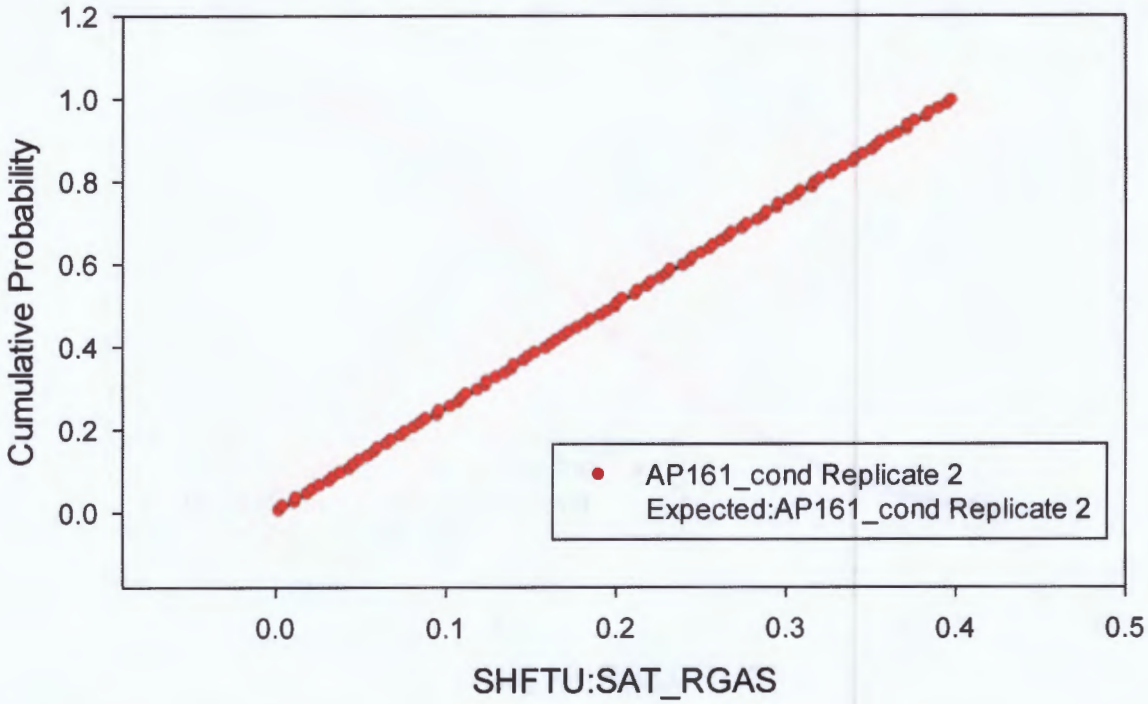

□i□r□□□□O□□r□□□an□□□□□□□□□□□□for □□□□□□□□□□□□□□□niform □i□ri□□tion□□□li□at□□

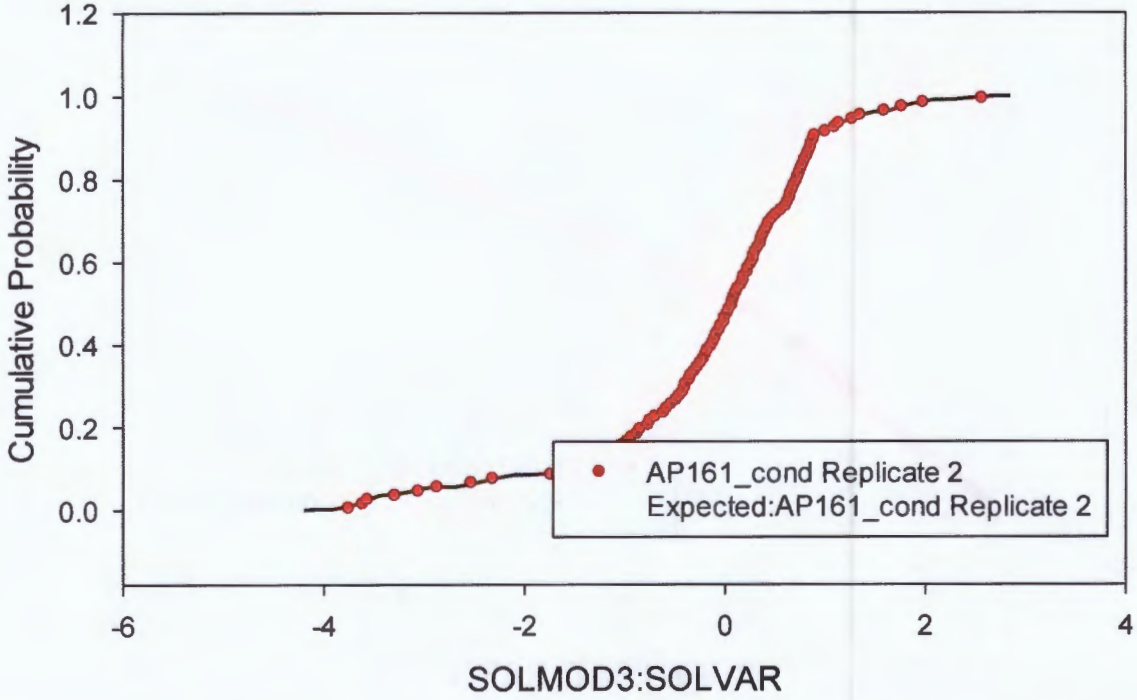

□i□r□□□□O□□r□□□an□□□□□□□□□□□□for □O□□ O□□□O□□□□ □□□r □ontin□o□□□i□ri□□tion□□□li□at□□

Information Only

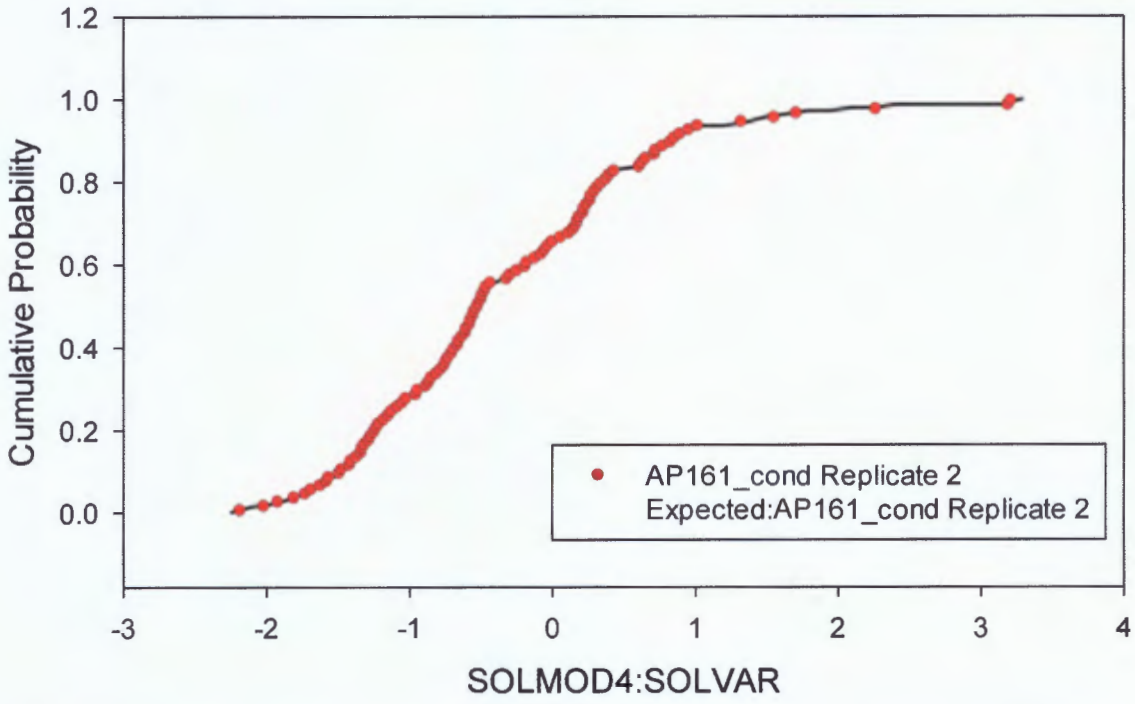

□i□□r□□□□□O□□□r□□□an□□□□□□t□□□□□□for □O□□ O□□□□O□□□□ □□□r □ontin□b□□□i□ri□□tion□□□□li□at□□□

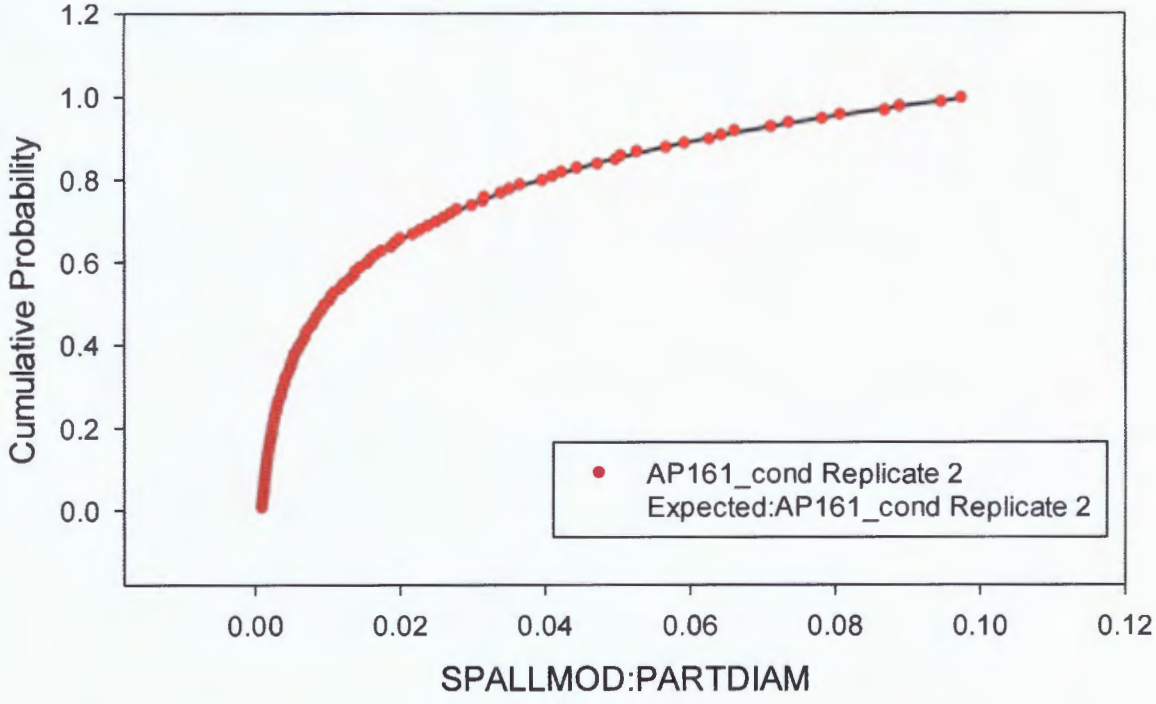

□i□□r□□□□□O□□□r□□□an□□□□□□t□□□□□□for □□□□□□ O□□□□□□□□I□□ □□o□□niform □i□ri□□tion□□□□li□at□□□

Information Only

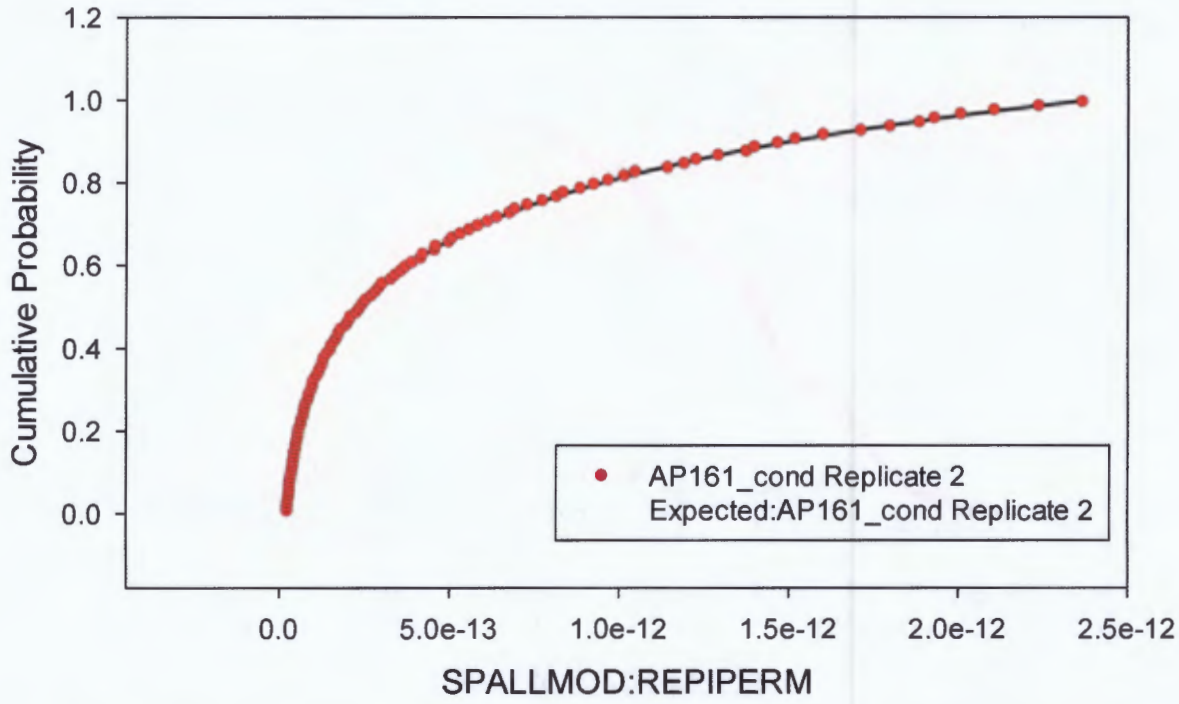

□i□r□□□□O□□r□□an□□□□□t□□ □□□□for □□□□□ O□□□□□□□□□ □□o□□niform □i□tri□□tion□□□□li□at□□

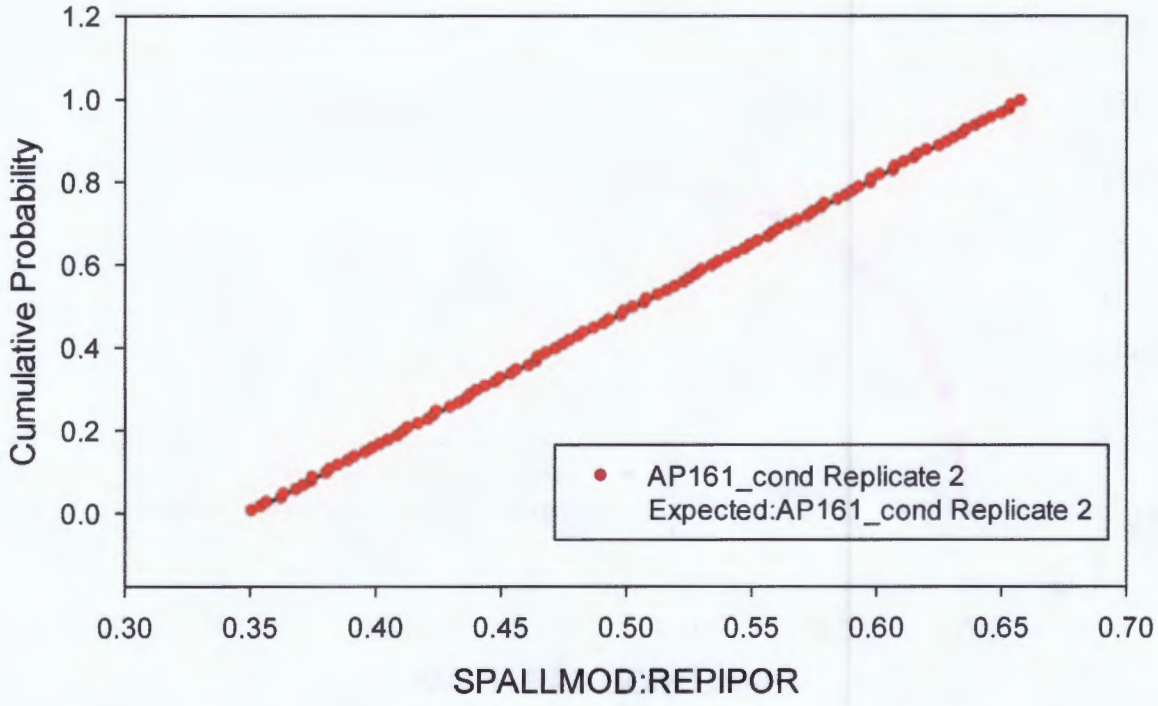

□i□r□□□□O□□r□□an□□□□□t□□ □□□□for □□□□□ O□□□□□□□O□ □□niform □i□tri□□tion□□□□li□at□□

Information Only

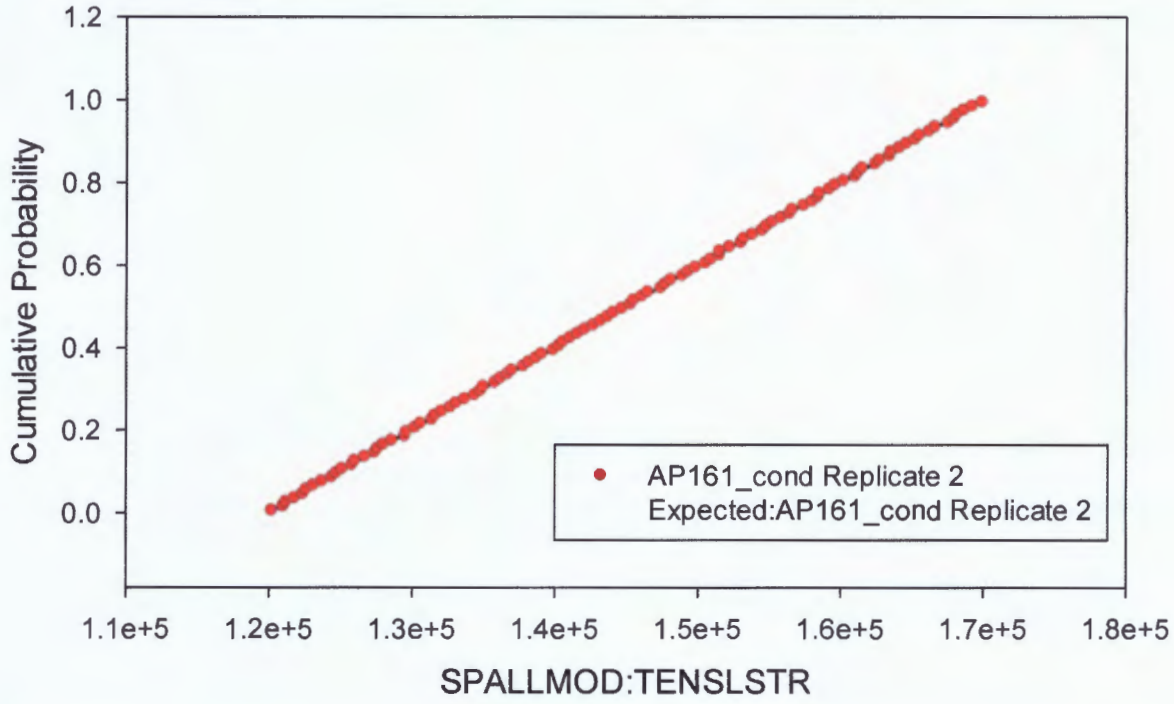

□i□□r□□□□O□□□r□□□an□□□□□□t□□ □□□□for □□□□□□ O□□□□□□□□□□ □□niform □i□ri□□tion□□□□li□at□□□

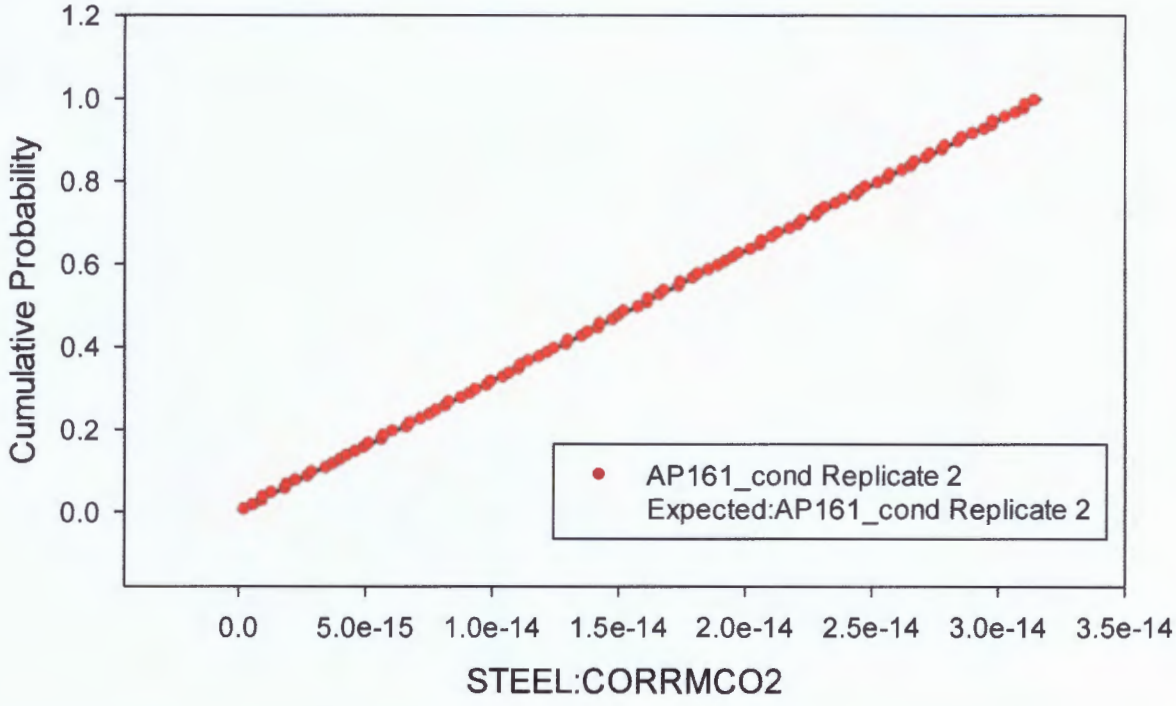

□i□□r□□□□O□□□r□□□an□□□□□□t□□ □□□□for □□□□□□□O□□□ □O□□□niform □i□ri□□tion□□□□li□at□□□

Information Only

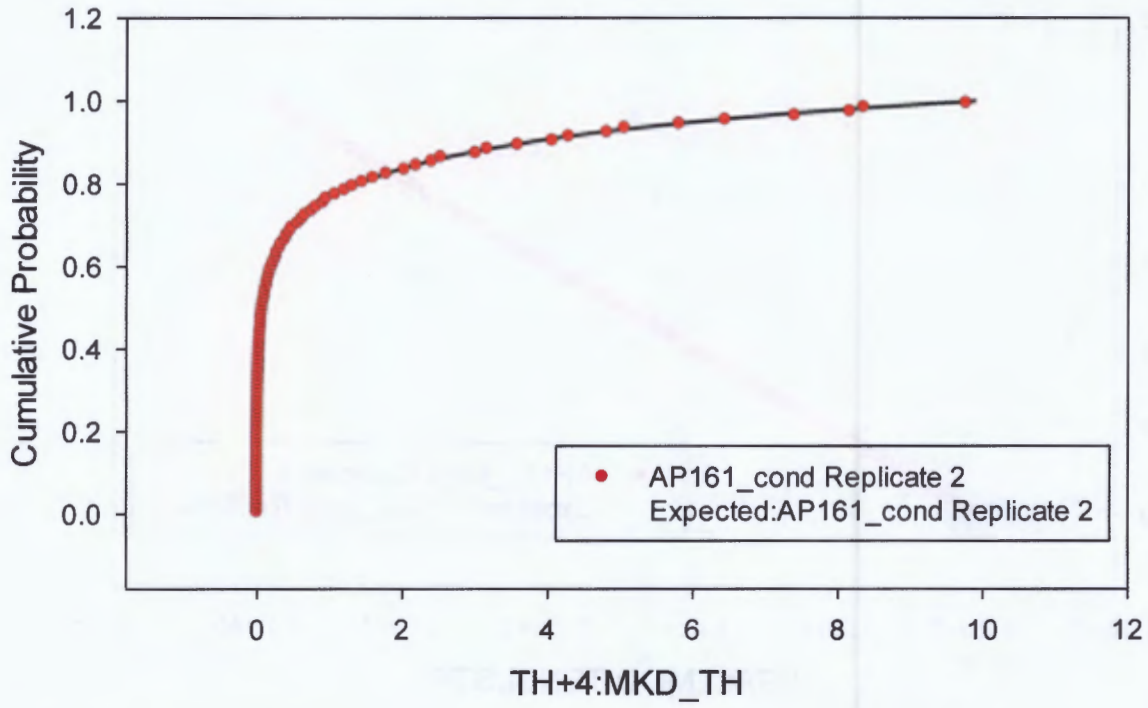

□i□r□□□□O□□r□□an□□□□□t□□□□□for □□□□□ □□□□ □□o□niform □i□ri□□tion□□□□li□at□□

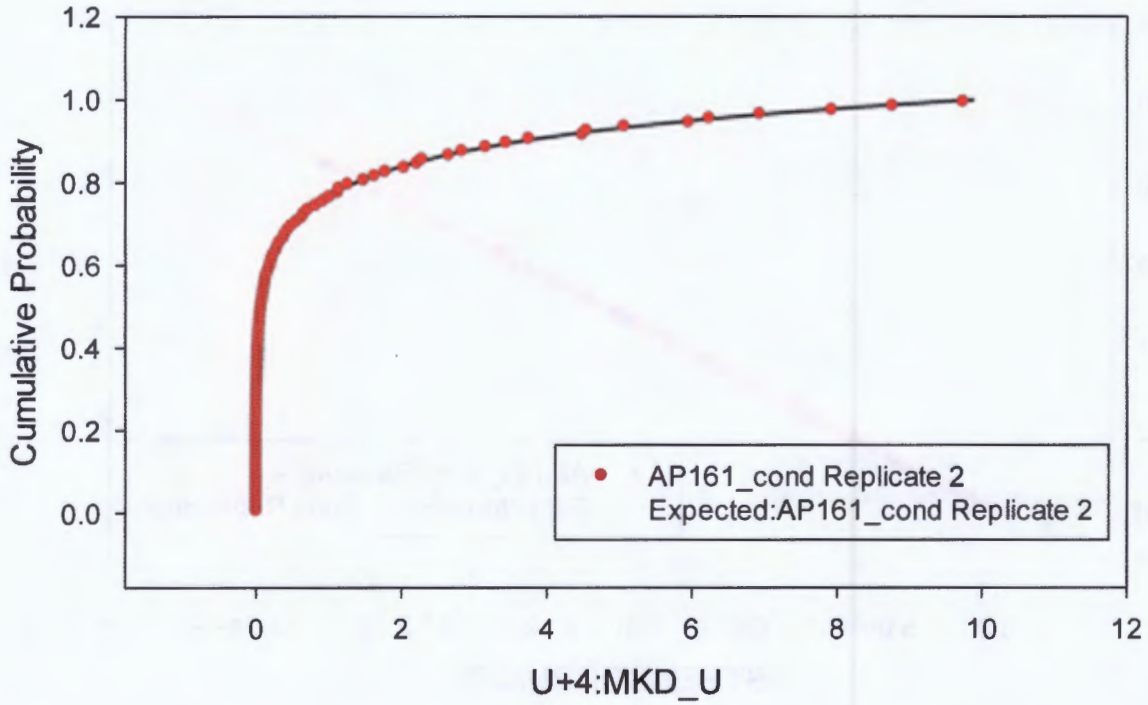

□i□r□□□□O□□r□□an□□□□□t□□□□□for □□□□ □□□□ □□o□niform □i□ri□□tion□□□□li□at□□

Information Only

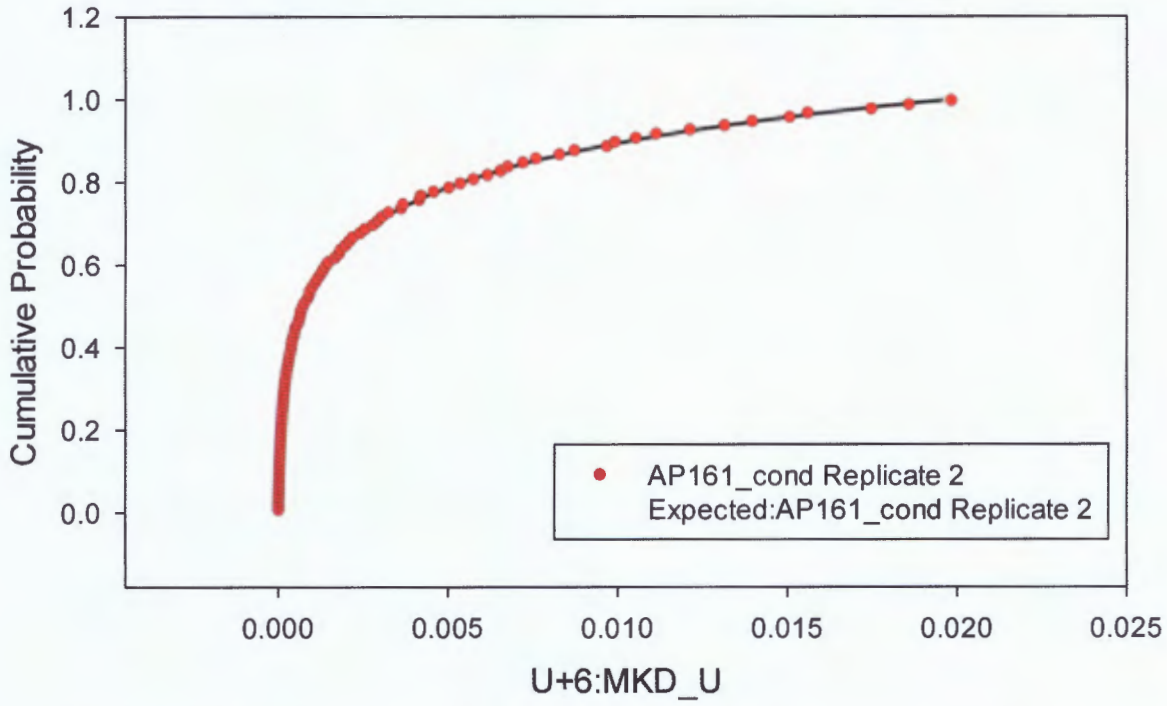

□i□□r□□□□O□□r□□an□□□□□t□□□□□for □□□□ □□□□ □□o□□niform □i□ri□□tion□□□li□at□□

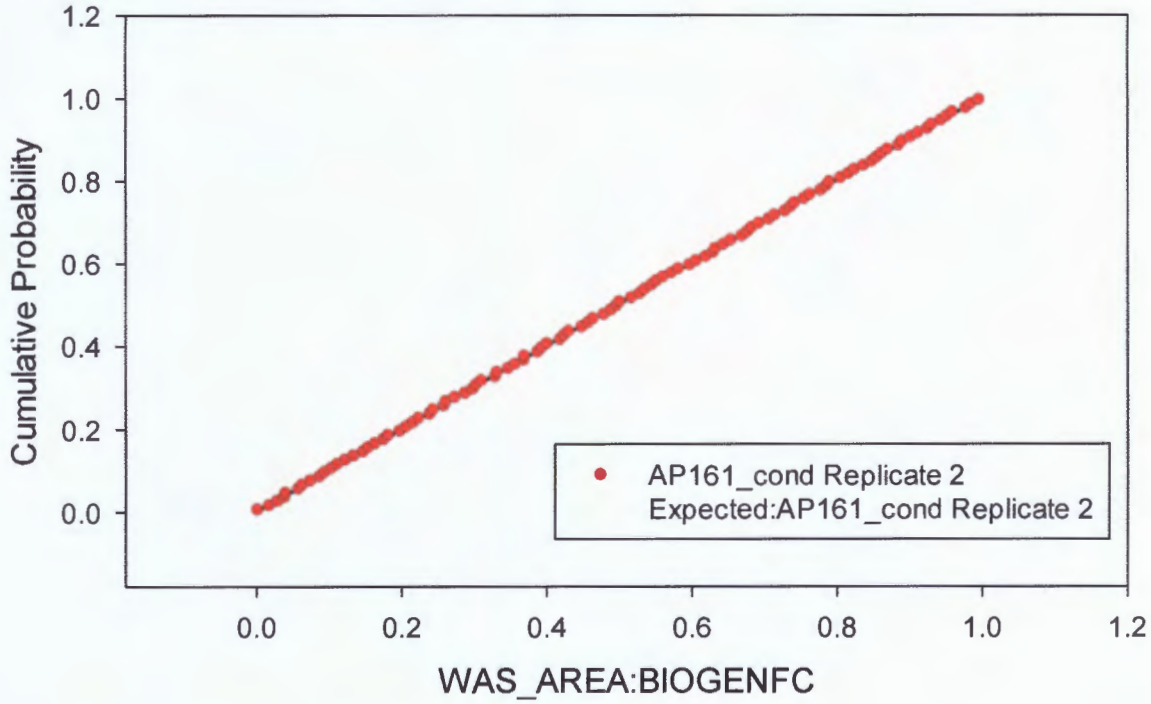

□i□□r□□□□O□□r□□an□□□□□t□□□□□for □ □□□□□□□□IO□□□□□ □□niform □i□ri□□tion□□□li□at□□

Information Only

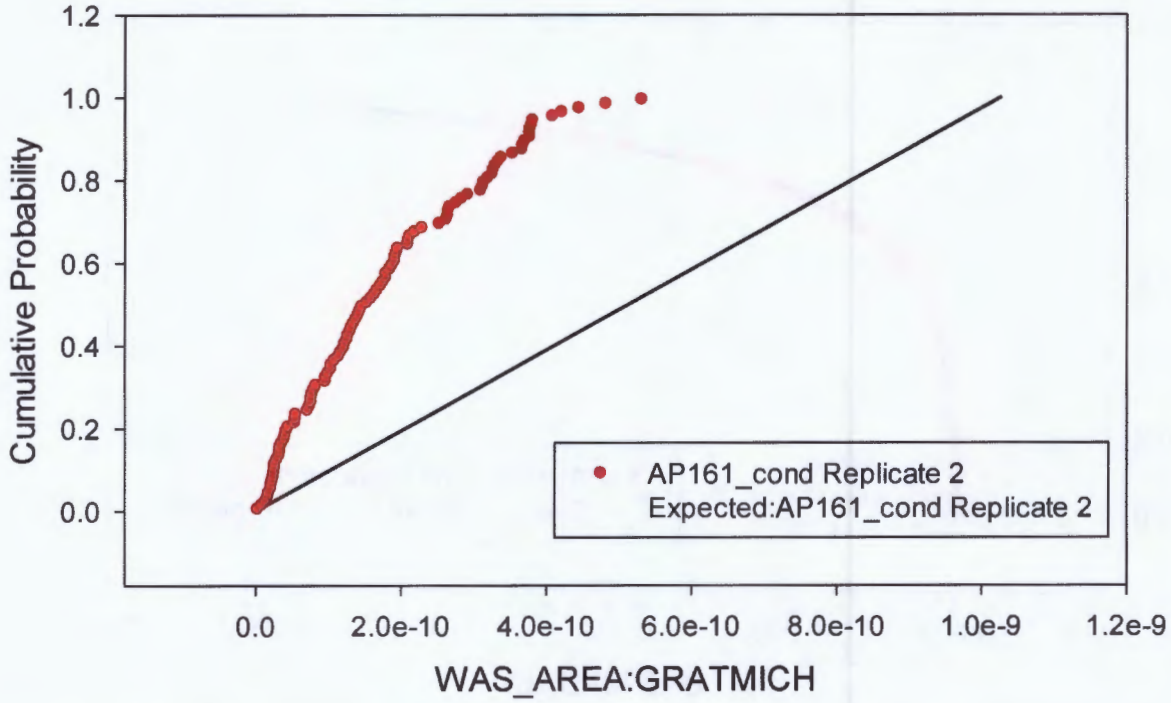

□i□r□□□□O□□r□□an□□□□□t□□□□□for □ □□□□□□□□□□□□ I□□ □□niform □i□ri□□tion□□□□i□at□□

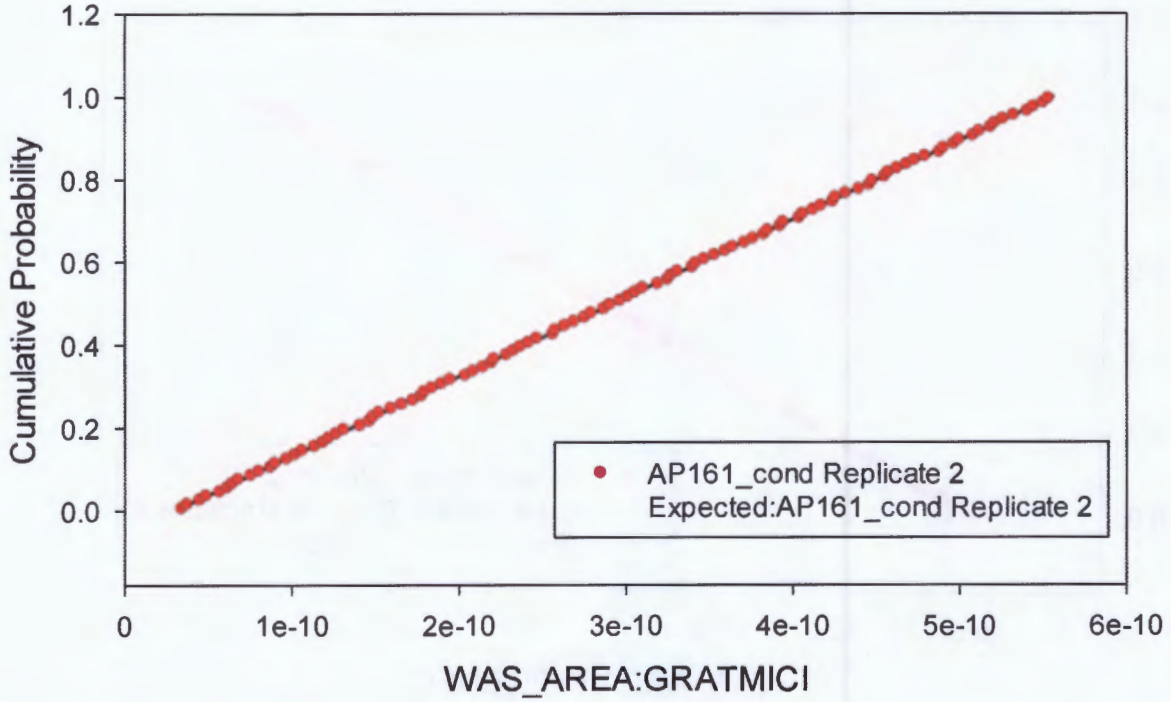

□i□r□□□□O□□r□□an□□□□□t□□□□□for □ □□□□□□□□□□□□ I□I □□niform □i□ri□□tion□□□□i□at□□

Information Only

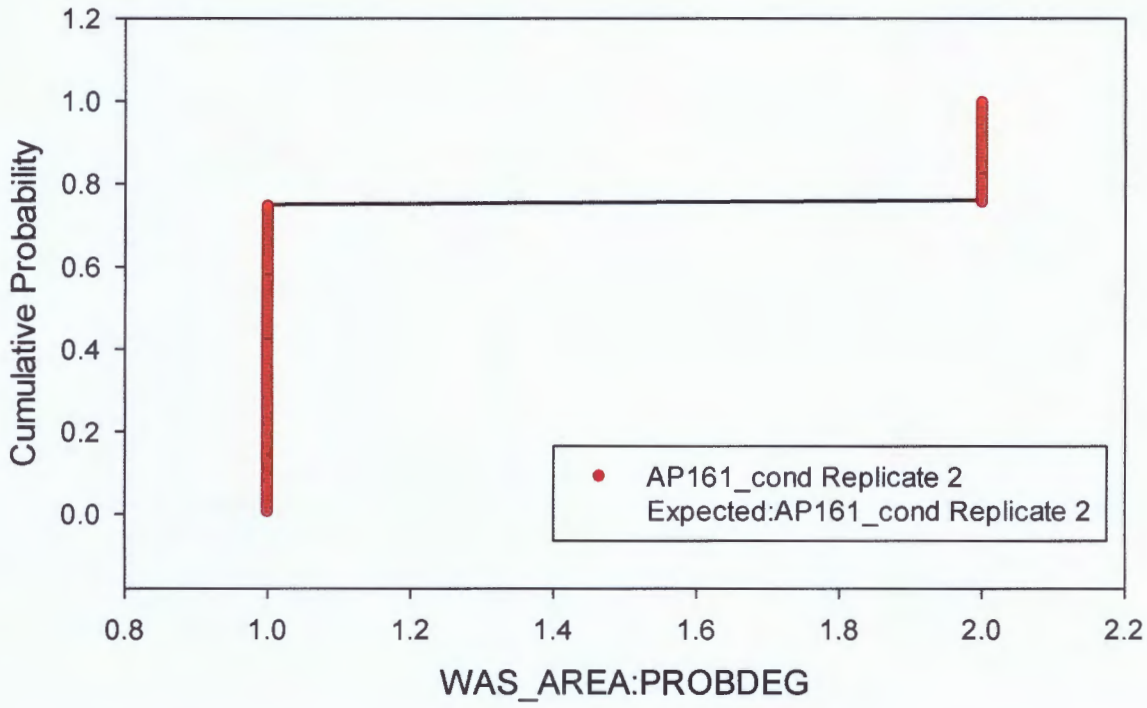

□i□□r□□□□□O□□□r□□□an□□□□□□t□□□□□□for □ □□□□□□□□□□□O□□□□□ □□□□r □i□□r□t□□□□□□ta□□i□ri□□tion□□□□□i□at□□□

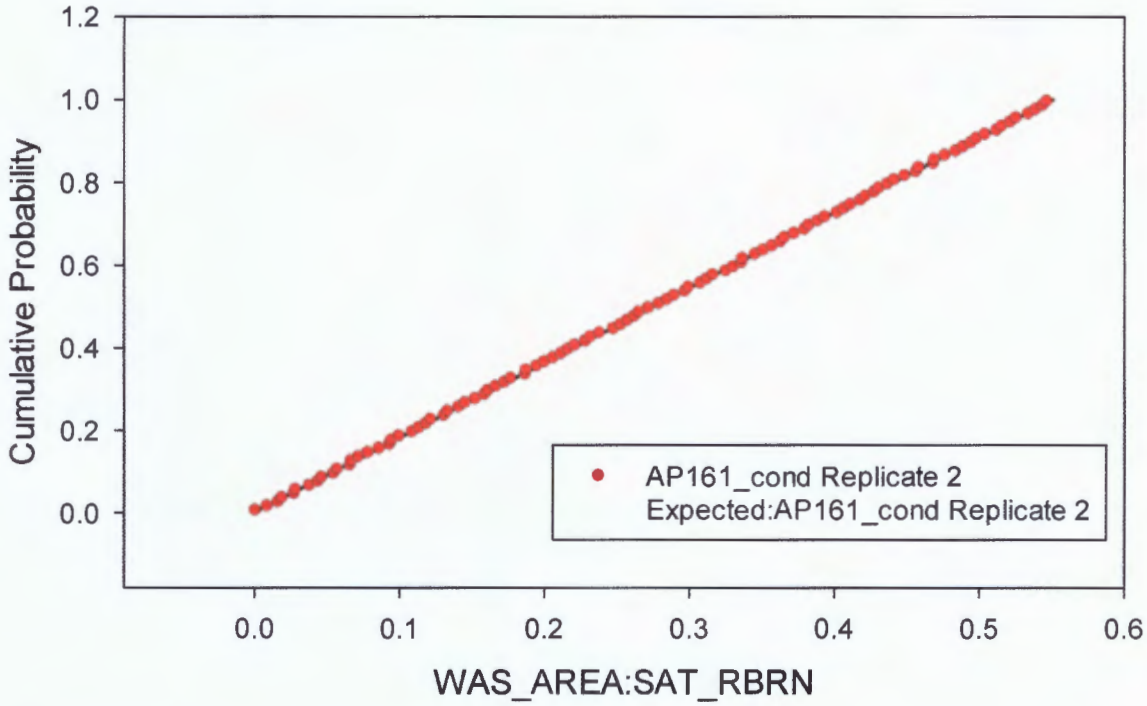

□i□□r□□□□□O□□□r□□□an□□□□□□t□□□□□□for □ □□□□□□□□□□□□□□□□□ □□niform □i□ri□□tion□□□□i□at□□□

Information Only

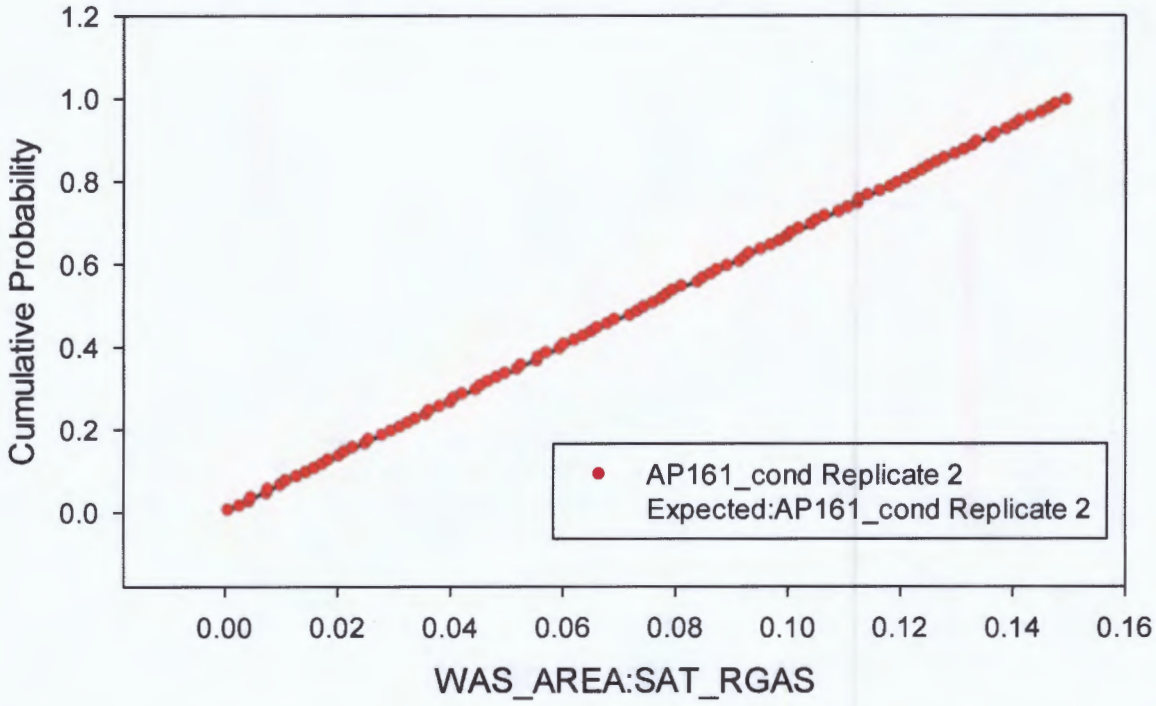

□i□r□□□□O□□r□□an□□□□□t□□ □□□□for □ □□□□□□□□□□□□□□□□niform □i□ri□□tion□□□□li□at□□

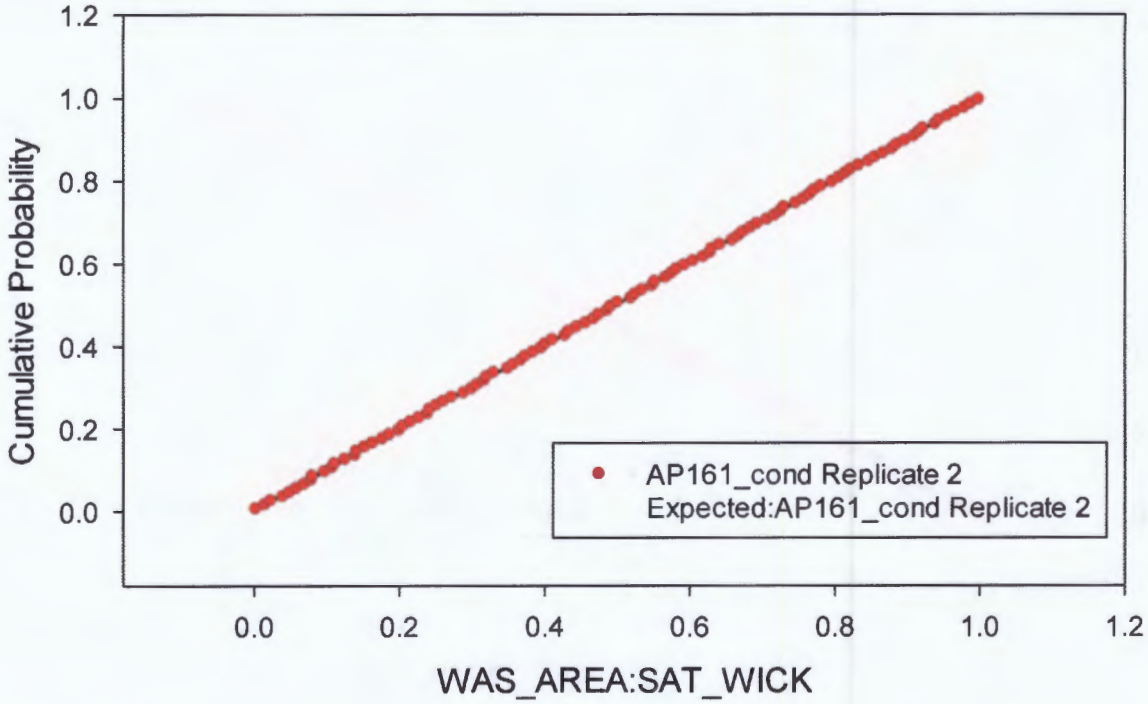

□i□r□□□□O□□r□□an□□□□□t□□ □□□□for □ □□□□□□□□□□□□ I□□ □□niform □i□ri□□tion□□□□li□at□□

Information Only

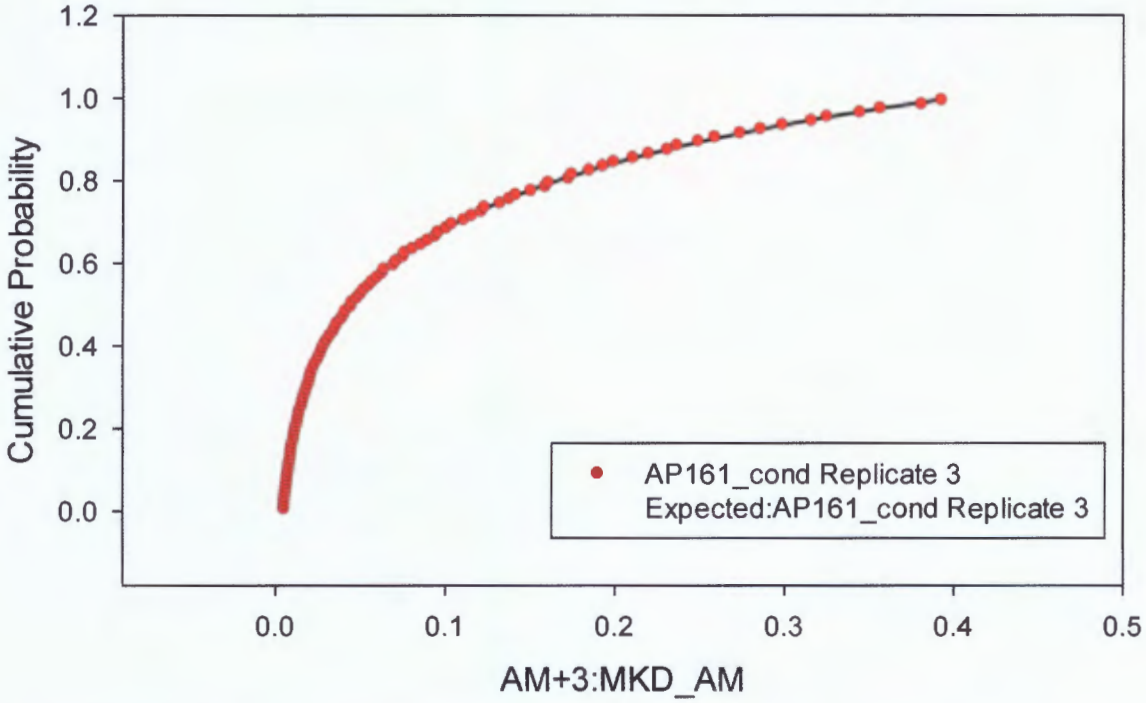

□i□□r□□□□O□□r□□an□□□□□t□□ □□□□for □□ □□□□ □□□□ □□o□□niform □i□ri□□tion□□□□li□at□□

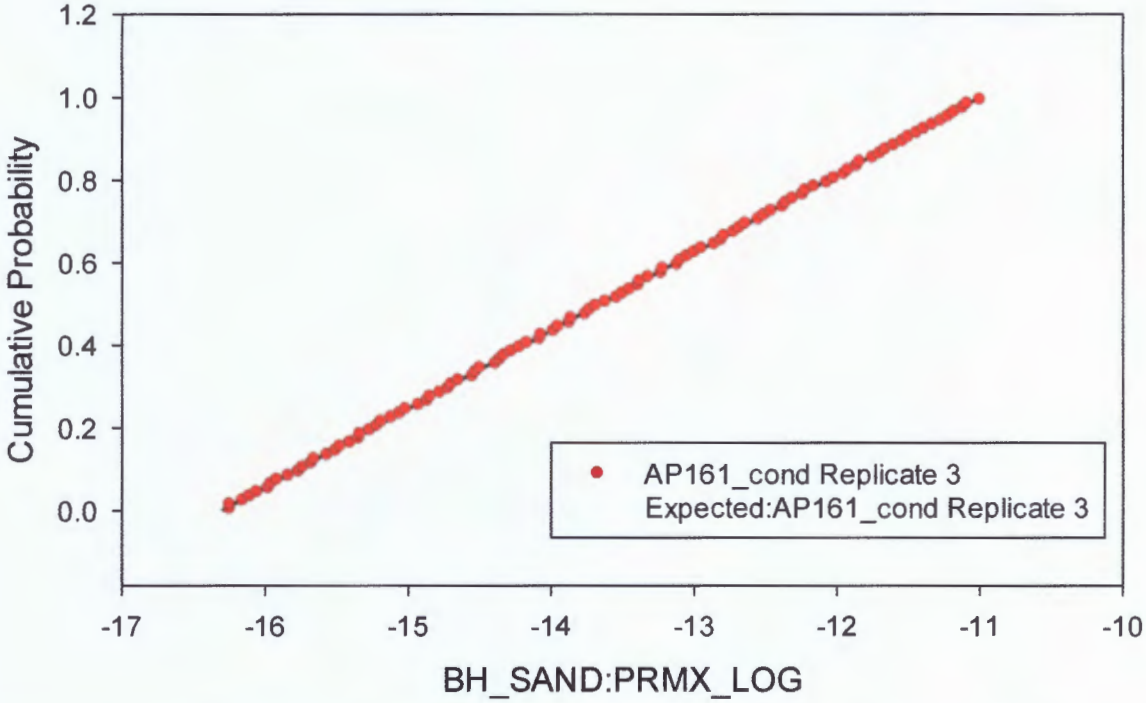

□i□□r□□□□O□□r□□an□□□□□t□□ □□□□for □□□□□□□□□ □□□O□ □□niform □i□ri□□tion□□□□li□at□□

Information Only

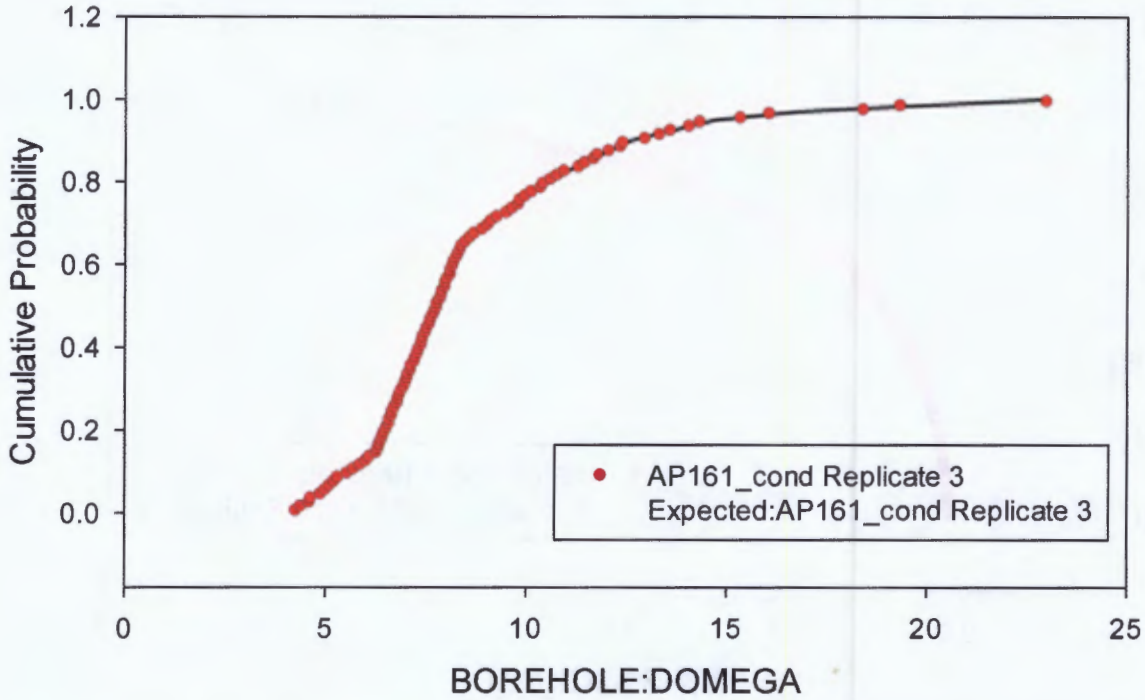

□i□r□□□□O□□r□□□an□□□□□t□□ □□□□for □O□□□O□□□□O□ □□□ □□□r □ontin□o□□□i□ri□□tion□□□□li□at□□

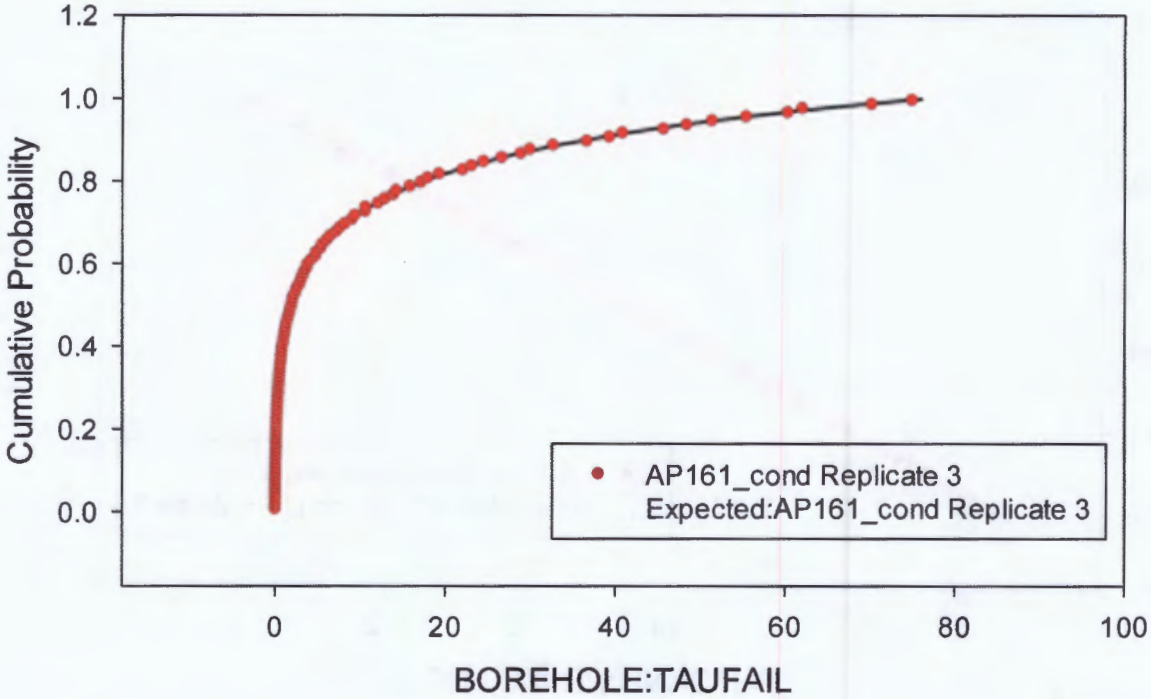

□i□r□□□□O□□r□□□an□□□□□t□□ □□□□for □O□□□O□□□□□□□I□ □□o□□niform □i□ri□□tion□□□□li□at□□

Information Only

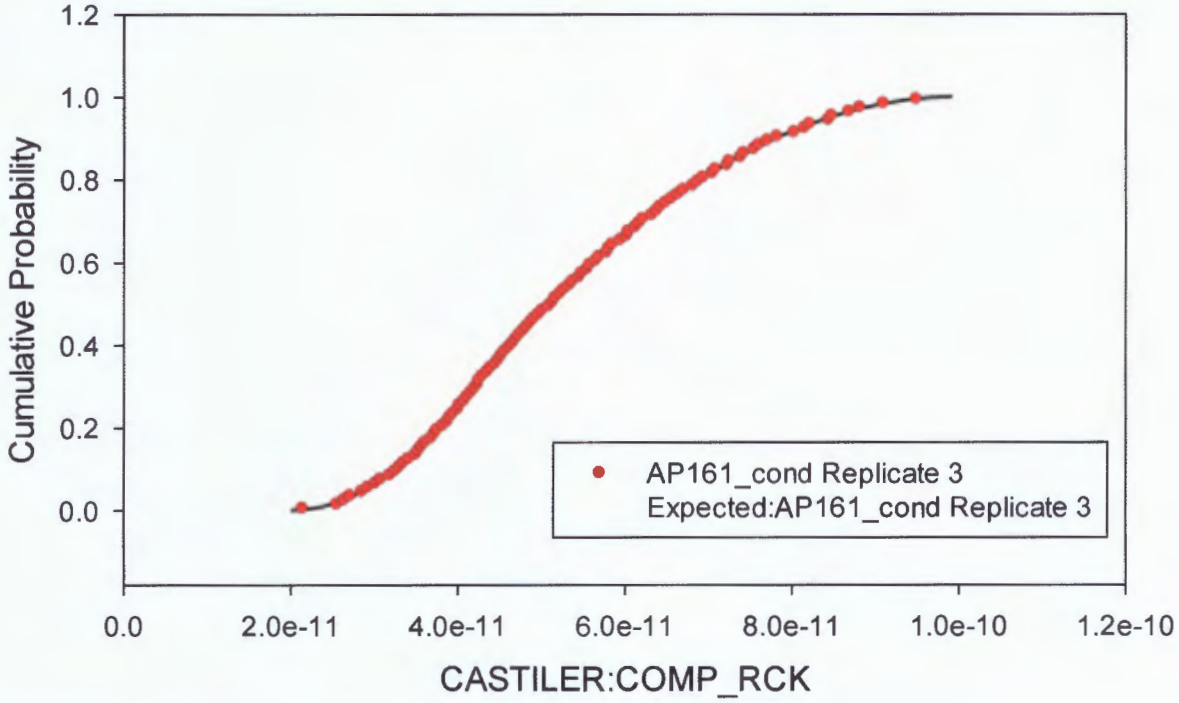

□i□□r□□□□□O□□□r□□□an□□□□□□t□□ □□□□for □□□□I□□□□□□O□ □□□□□ □□rian□□lar □i□tri□□tion□□□□li□at□□

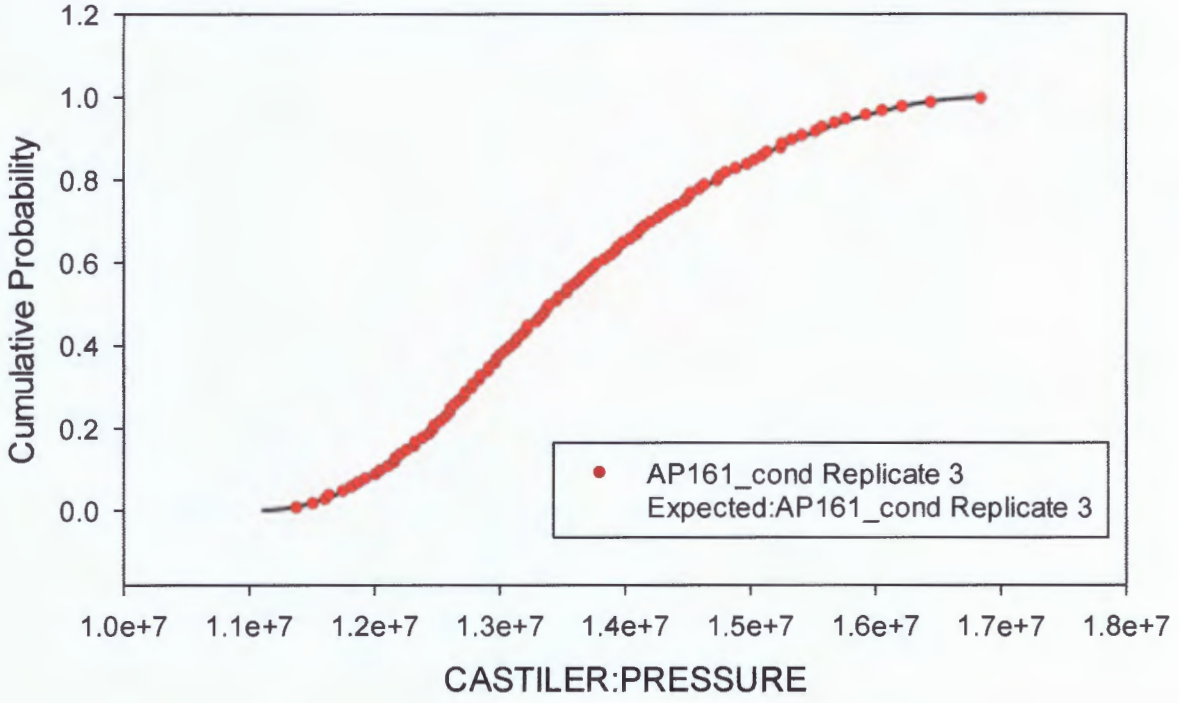

□i□□r□□□□□O□□□r□□□an□□□□□□t□□ □□□□for □□□□I□□□□□□□□□□□□ □□rian□□lar □i□tri□□tion□□□□li□at□□

Information Only

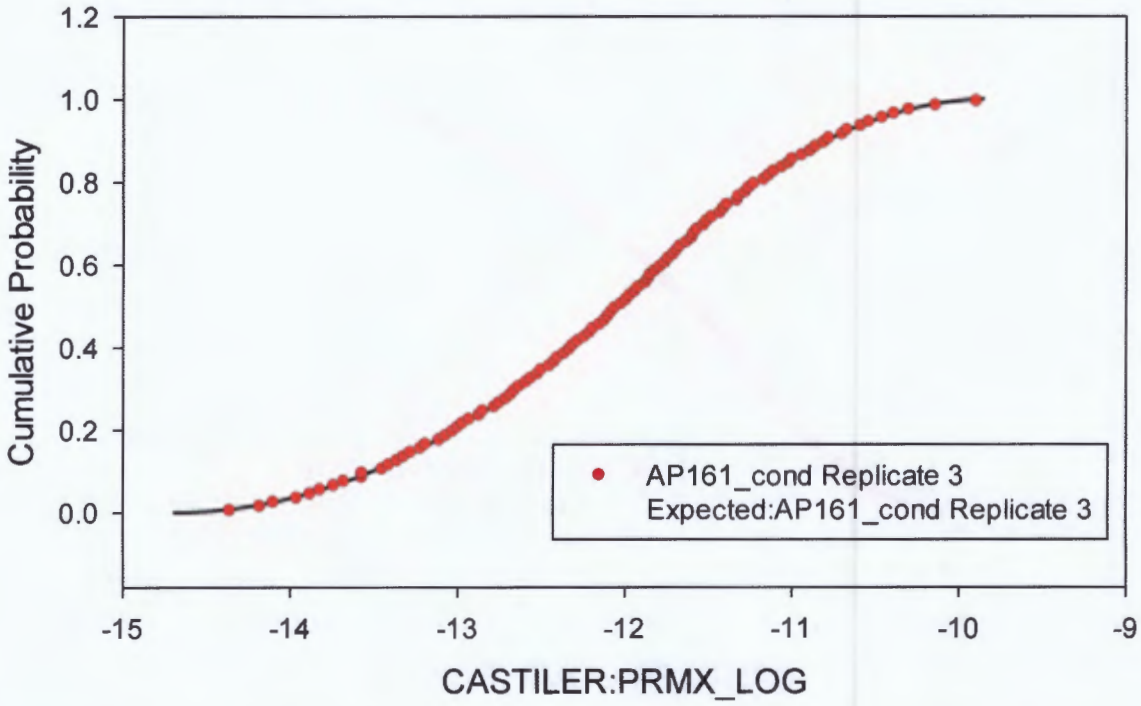

□i□r□□□□O□□r□□an□□□□□t□□ □□□□for □□□□I□□□□□□ □□□O□ □□rian□□lar □i□ri□□tion□□□□li□at□□

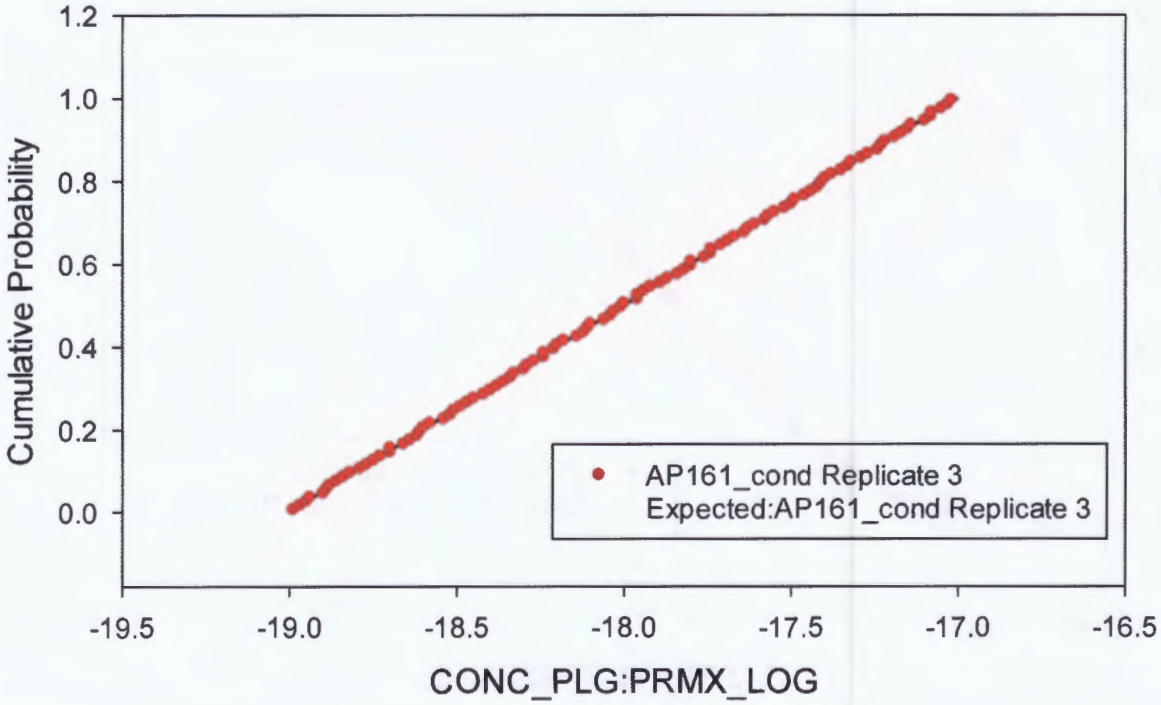

□i□r□□□□O□□r□□an□□□□□t□□ □□□□for □O□□□□□□□□□ □□□O□ □□niform □i□ri□□tion□□□□li□at□□

Information Only

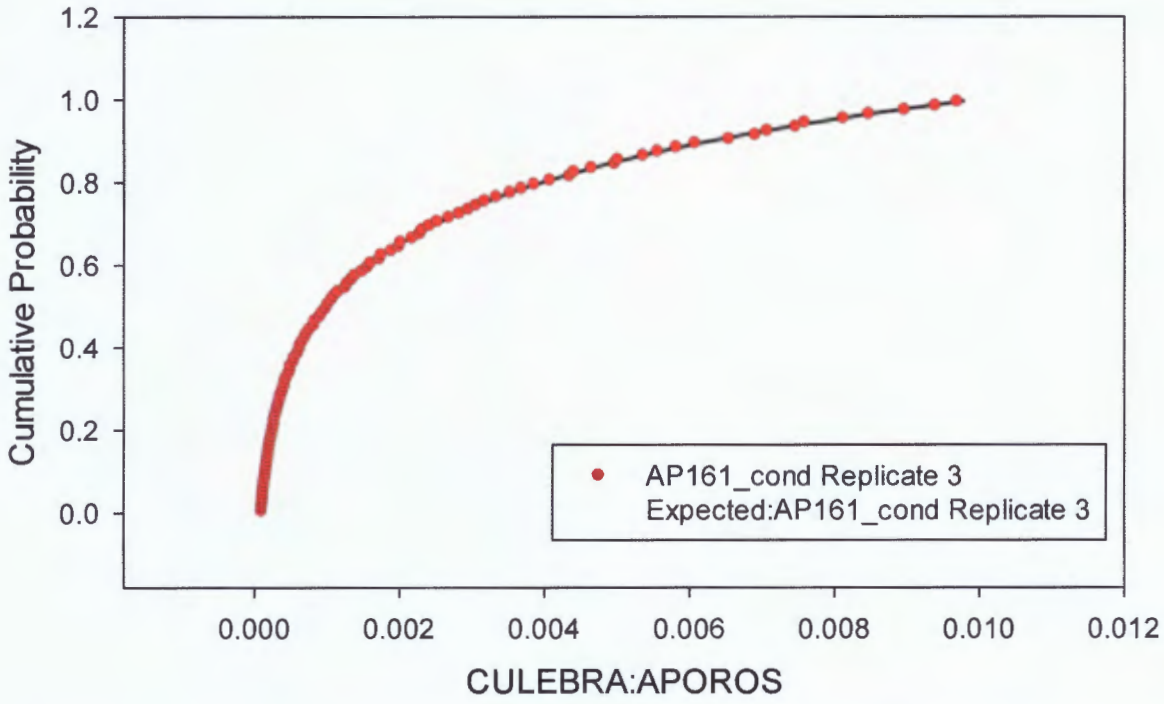

□i□□r□□□□□O□□□r□□□an□□□□□□t□□□□□□for □□□□□□□□□□□O□O□□□□o□□niform □i□tri□□tion□□□□li□at□□□

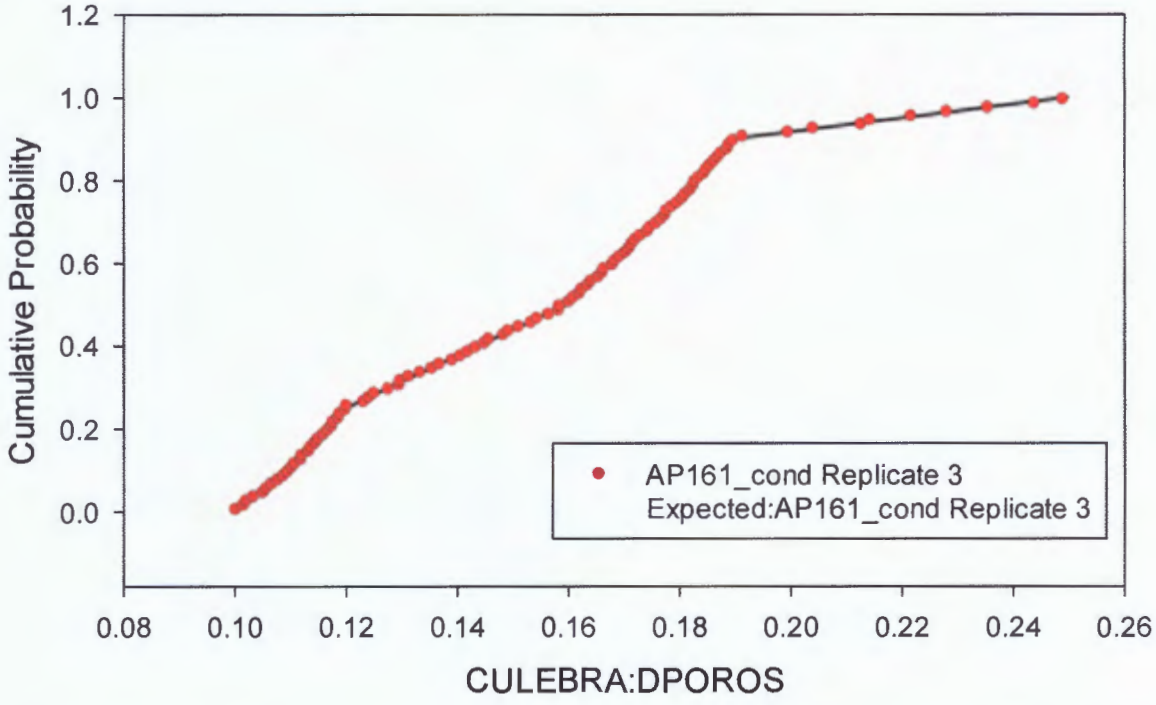

□i□□r□□□□□O□□□r□□□an□□□□□□t□□□□□□for □□□□□□□□□□□O□O□□□□□r □ontin□o□□□i□tri□□tion□□□□li□at□□□

Information Only

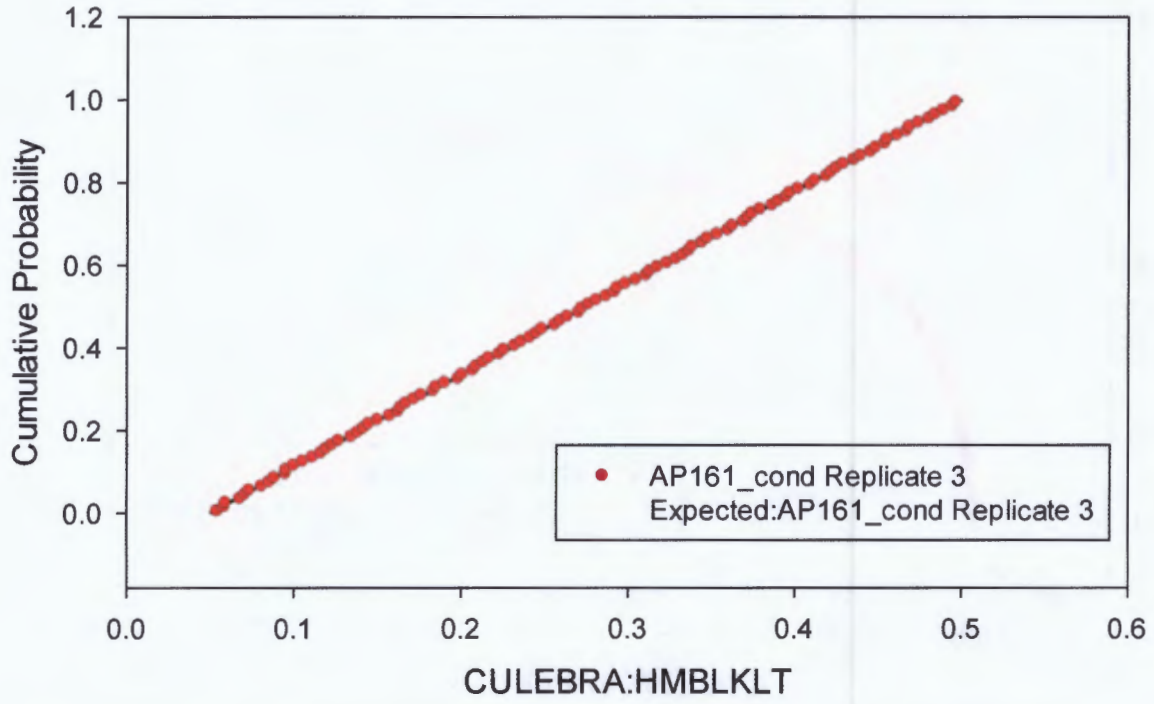

□i□r□□□□O□□r□□□an□□□□□t□□ □□□□for □□□□□□□□□□ □ □□□□□ □□niform □i□tri□□tion□□□□i□at□□

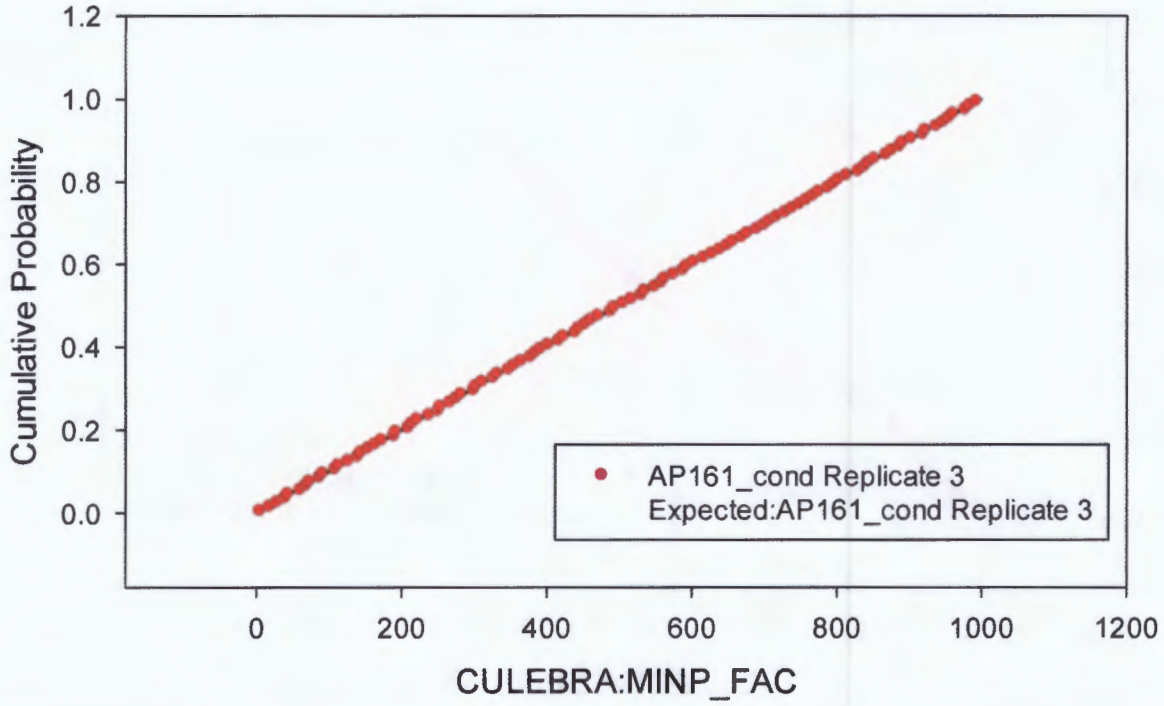

□i□r□□□□O□□r□□□an□□□□□t□□ □□□□for □□□□□□□□□ I□□□□□□ □□niform □i□tri□□tion□□□□i□at□□

Information Only

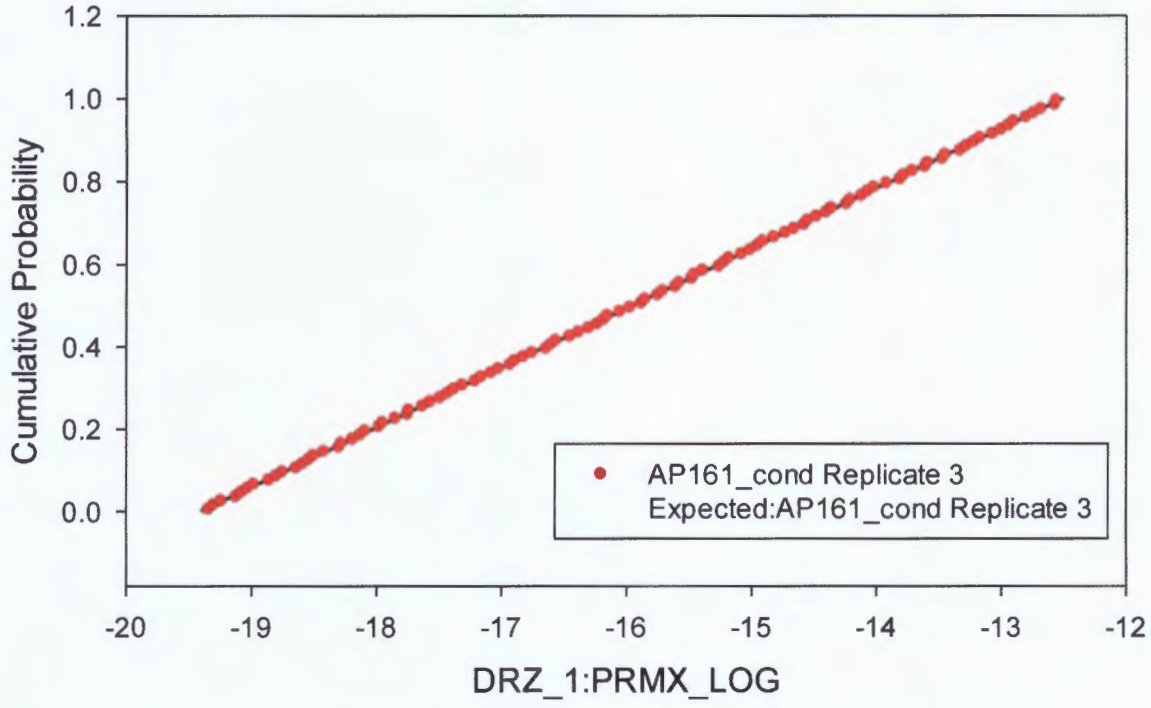

□i□r□□□□O□□r□□an□□□□□t□□ □□□□for □□□□□□□□□ □□□O□ □□niform □i□ri□□tion□□□□i□at□□

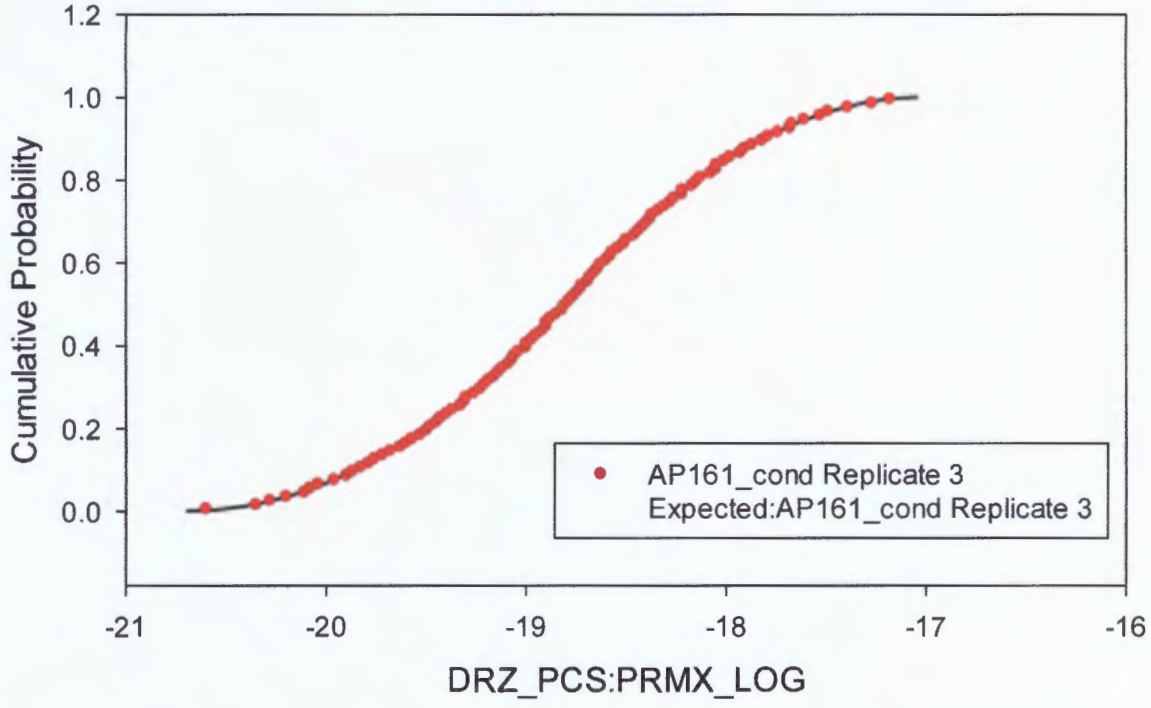

□i□r□□□□O□□r□□an□□□□□t□□ □□□□for □□□□□□□□□□ □□□O□ □□rian□□lar □i□ri□□tion□□□□i□at□□

Information Only

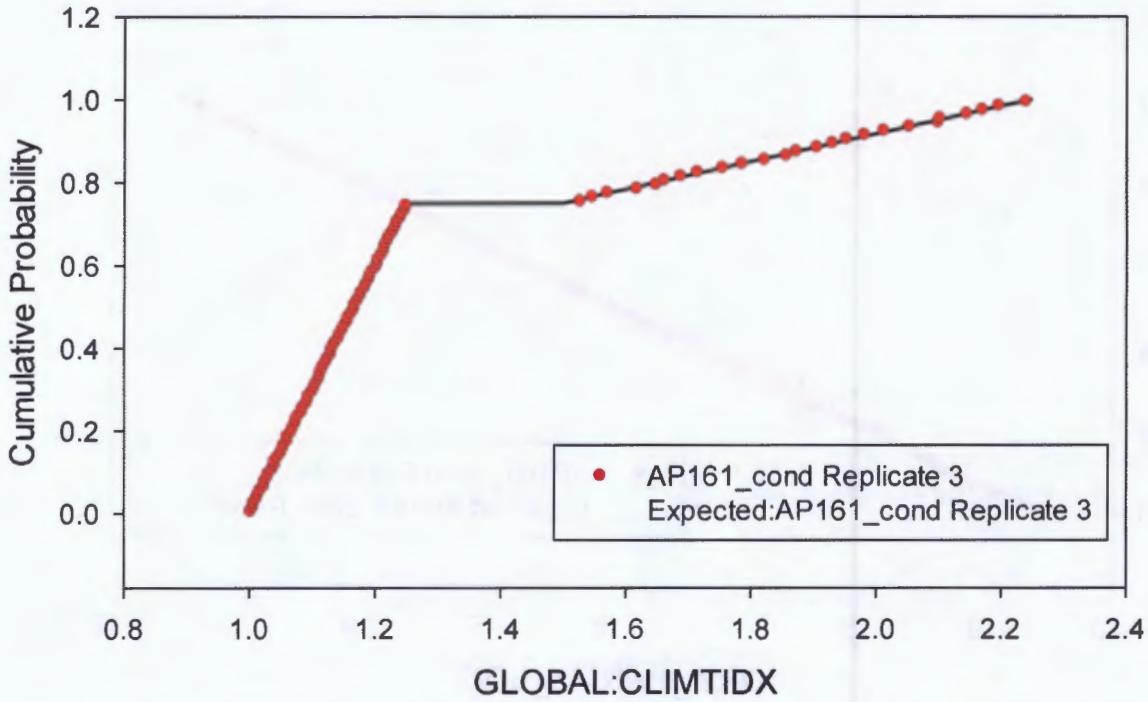

□i□r□□□□O□□r□□an□□□□□t□□□□□for □□O□□□□□□I□ □I□□ □□□r □ontin□o□□□i□ri□□tion□□□li□at□□

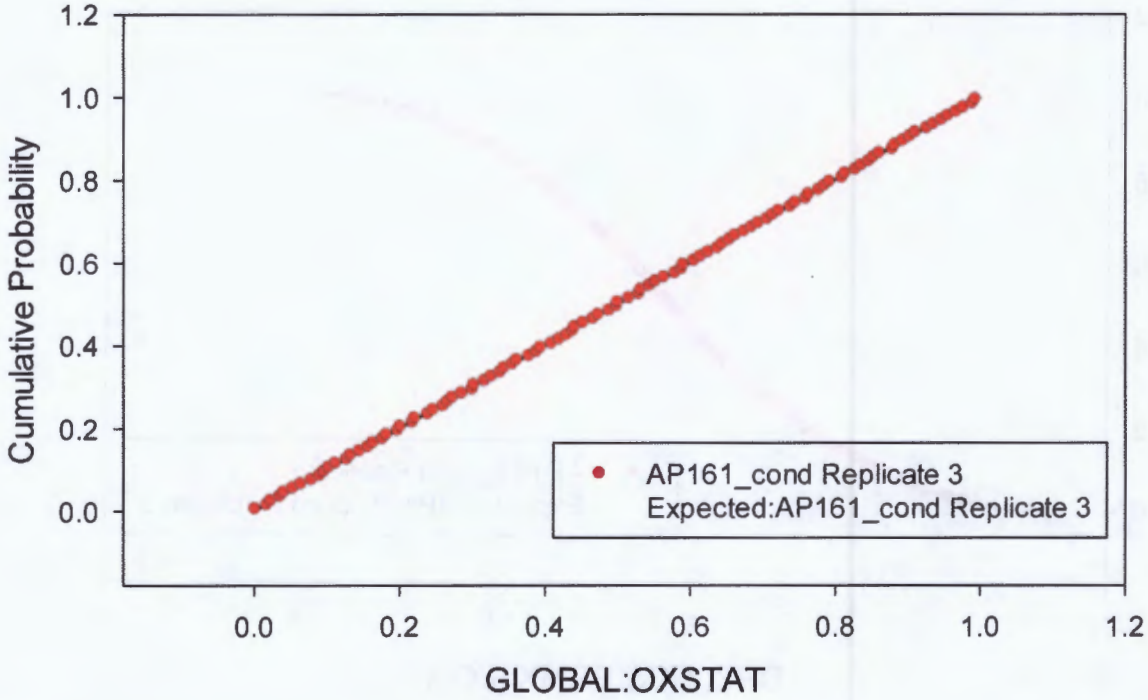

□i□r□□□□O□□r□□an□□□□□t□□□□□for □□O□□□□O□□□□□ □□niform □i□ri□□tion□□□li□at□□

Information Only

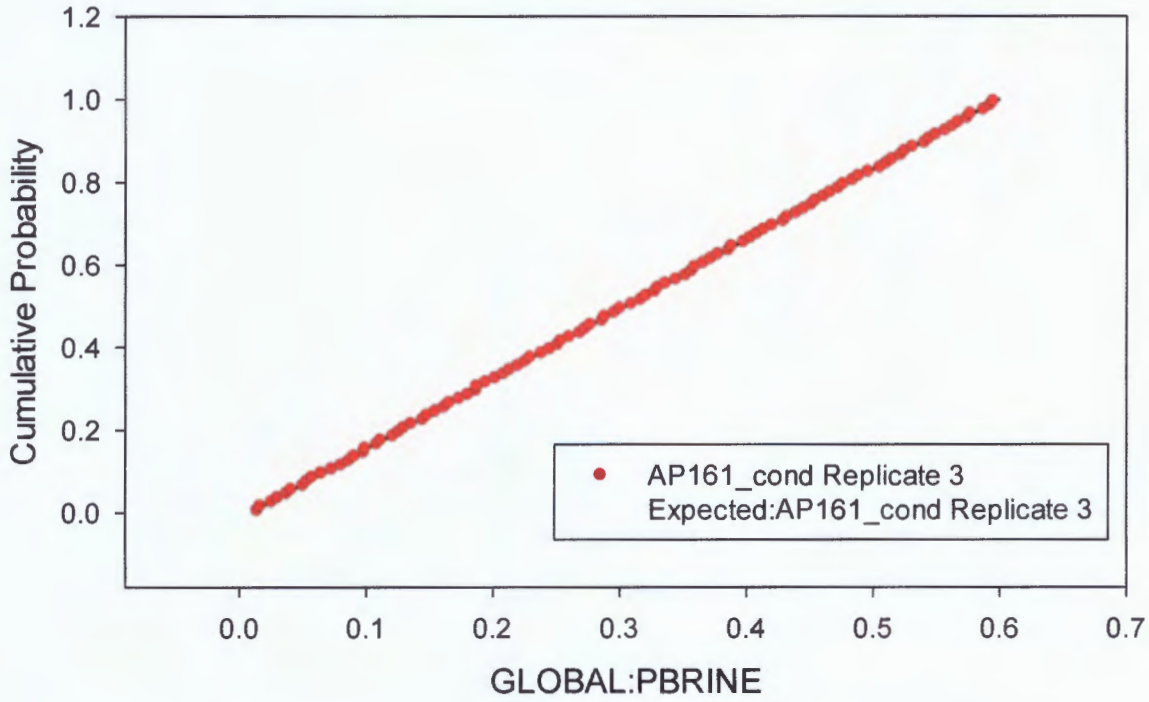

□i□□r□□□□□O□□□r□□□an□□□□□□□□□□□□□□for □□O□□□□□□□□□□□□□□□niform □i□ri□□tion□□□□li□at□□□

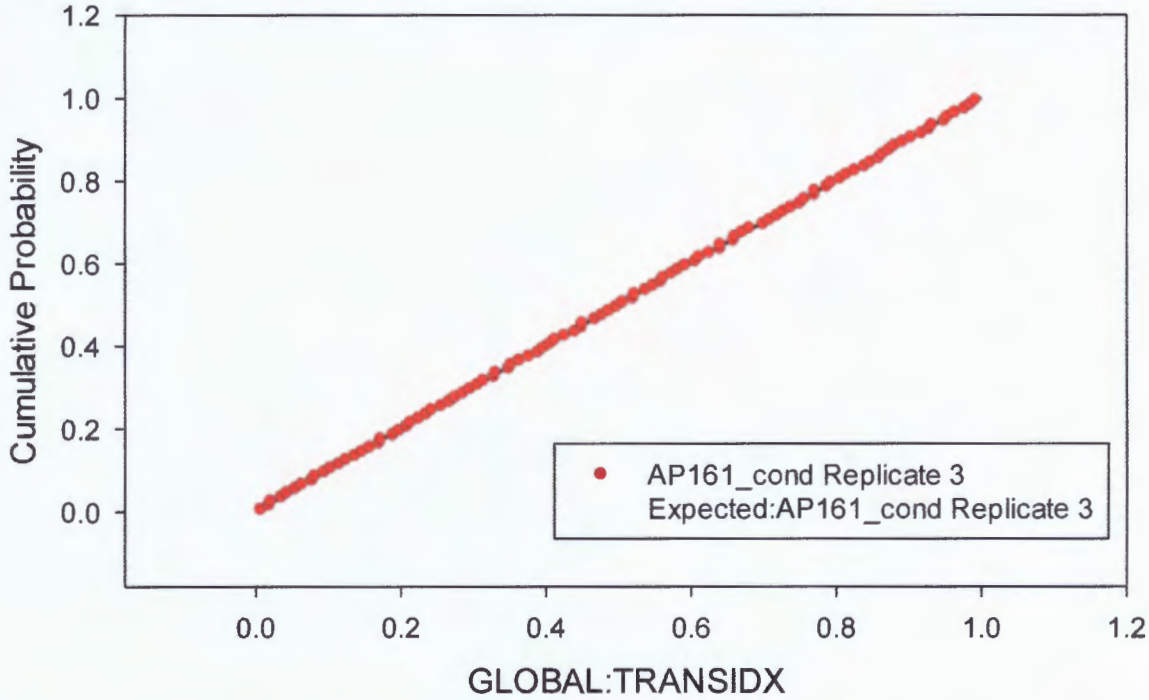

□i□□r□□□□□O□□□r□□□an□□□□□□□□□□□□□□for □□O□□□□□□□□□□□□□□□niform □i□ri□□tion□□□□li□at□□□

Information Only

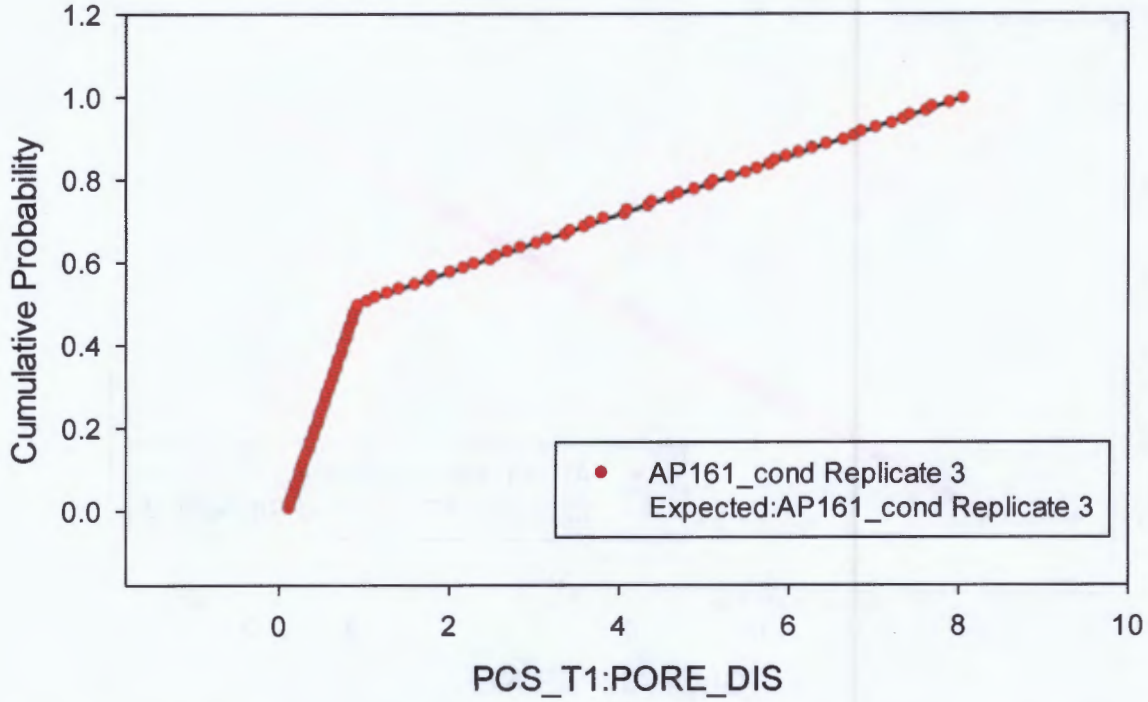

□i□r□□□□O□□r□□an□□□□□t□□□□□for □□□□□□O□□□□I□□□r □ontin□o□□□i□ri□□tion□□□li□at□□

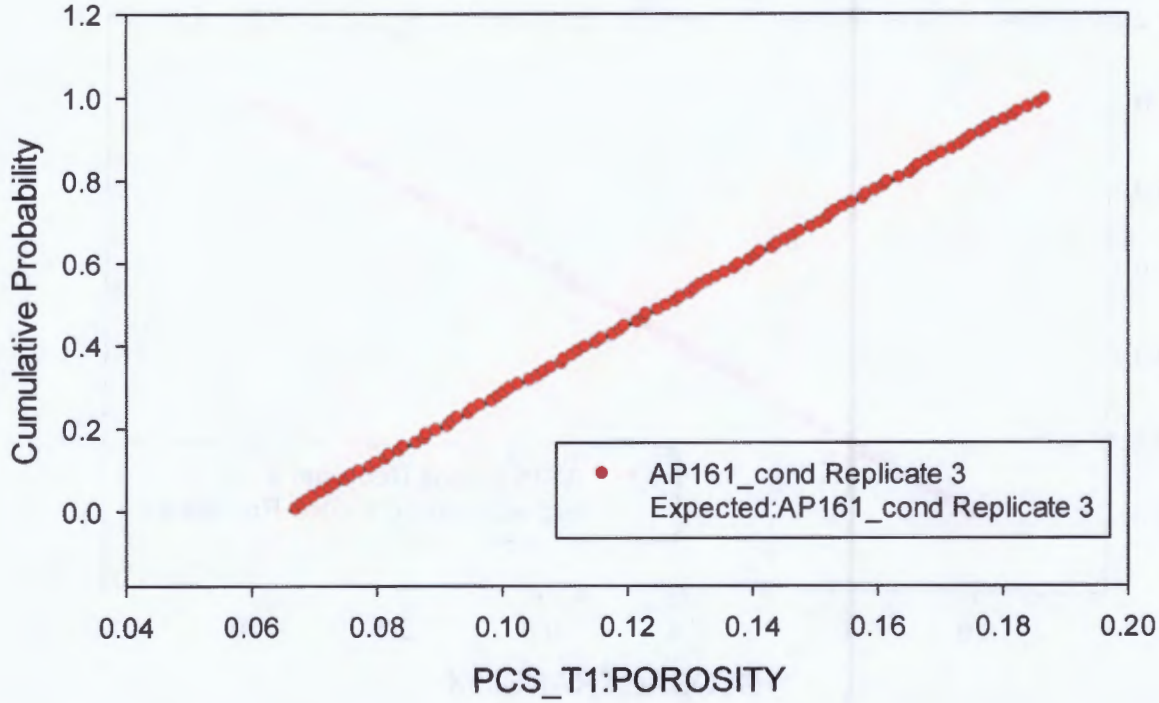

□i□r□□□□O□□r□□an□□□□□t□□□□□for □□□□□□O□O□I□□ □□niform □i□ri□□tion□□□li□at□□

Information Only

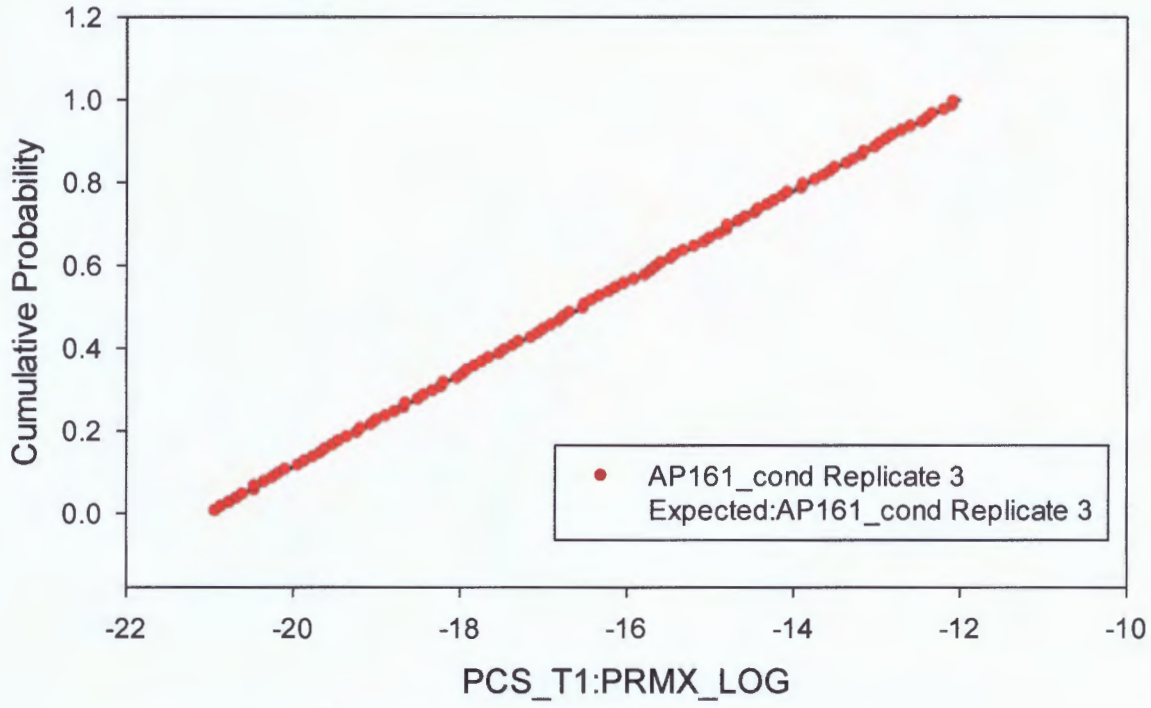

□i□r□□□□O□□r□□an□□□□□t□□ □□□□for □□□□□□□□ □□□O□ □□niform □i□ri□□tion□□□□li□at□□

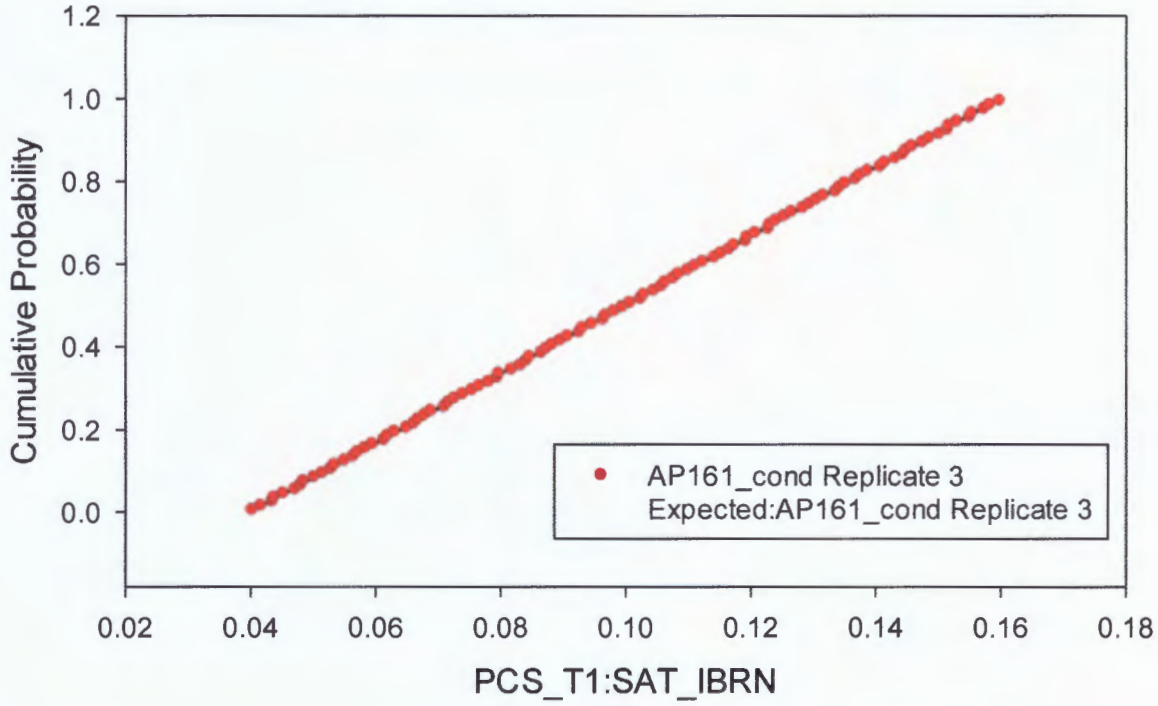

□i□r□□□□O□□r□□an□□□□□t□□ □□□□for □□□□□□□□□□□□ □□niform □i□ri□□tion□□□□li□at□□

Information Only

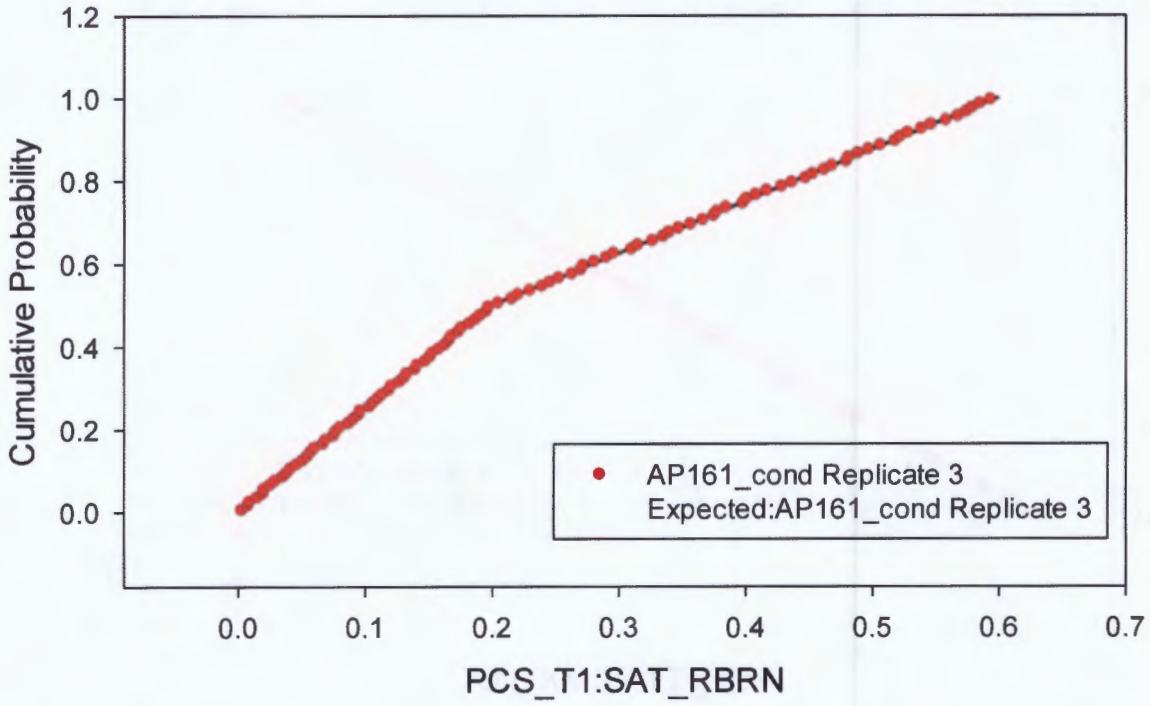

□i□r□□□□O□□r□□an□□□□□□□□□for □□□□□□□□□□□□□□□□ □□□r □ontin□b□□□i□ri□□tion□□□□li□at□□

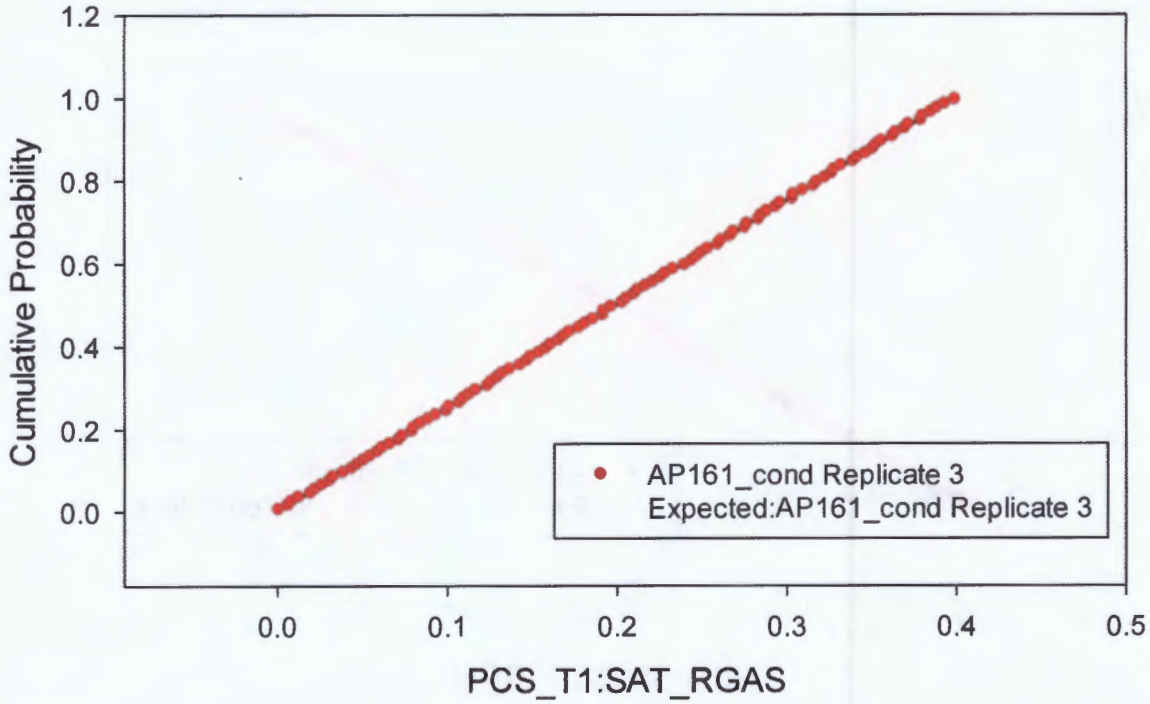

□i□r□□□□O□□r□□an□□□□□□□□□for □□□□□□□□□□□□□□□□□niform □i□ri□□tion□□□□li□at□□

Information Only

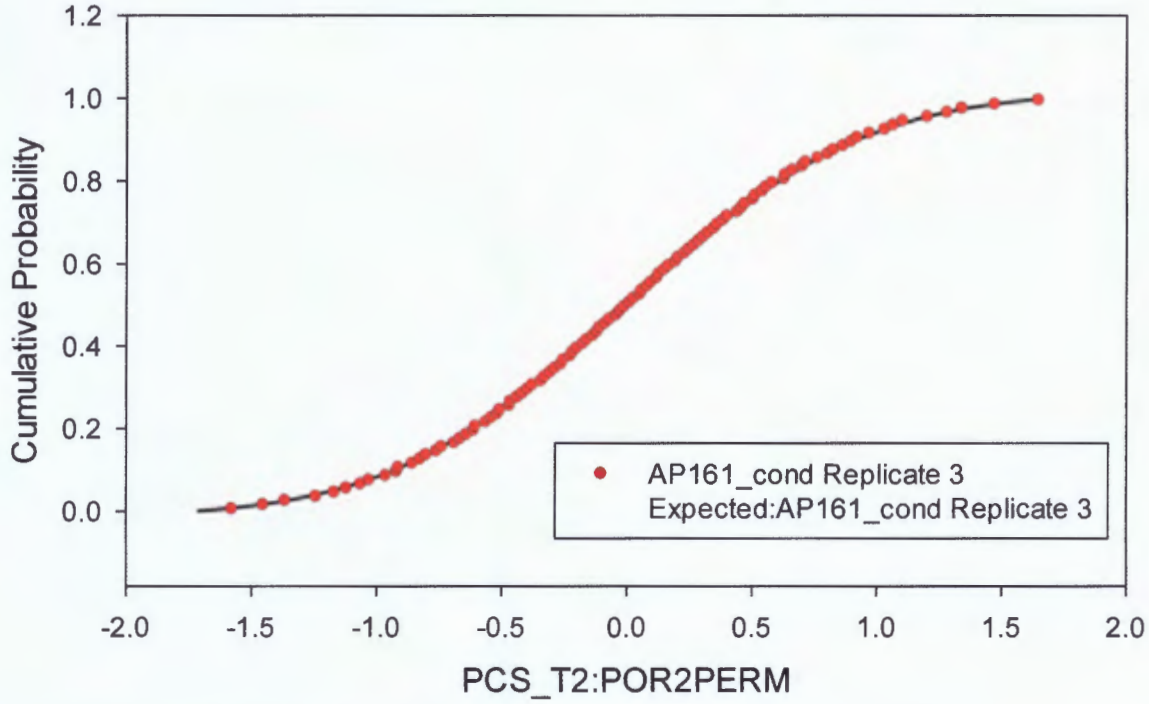

□i□□r□□□□□O□□□r□□□an□□□□□□t□□□□□□for □□□□□□□□O□□□□□□ □□ormal □i□ri□□tion□□□□li□at□□

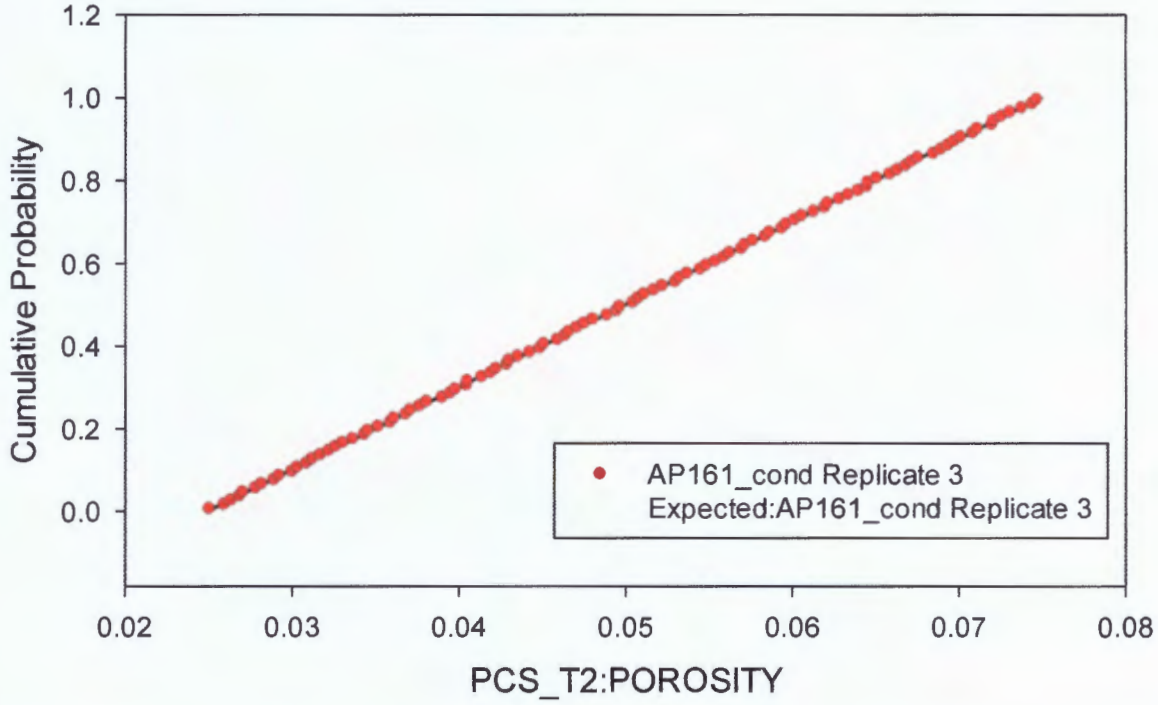

□i□□r□□□□□O□□□r□□□an□□□□□□t□□□□□□for □□□□□□□□O□O□□□ □□niform □i□ri□□tion□□□□li□at□□

Information Only

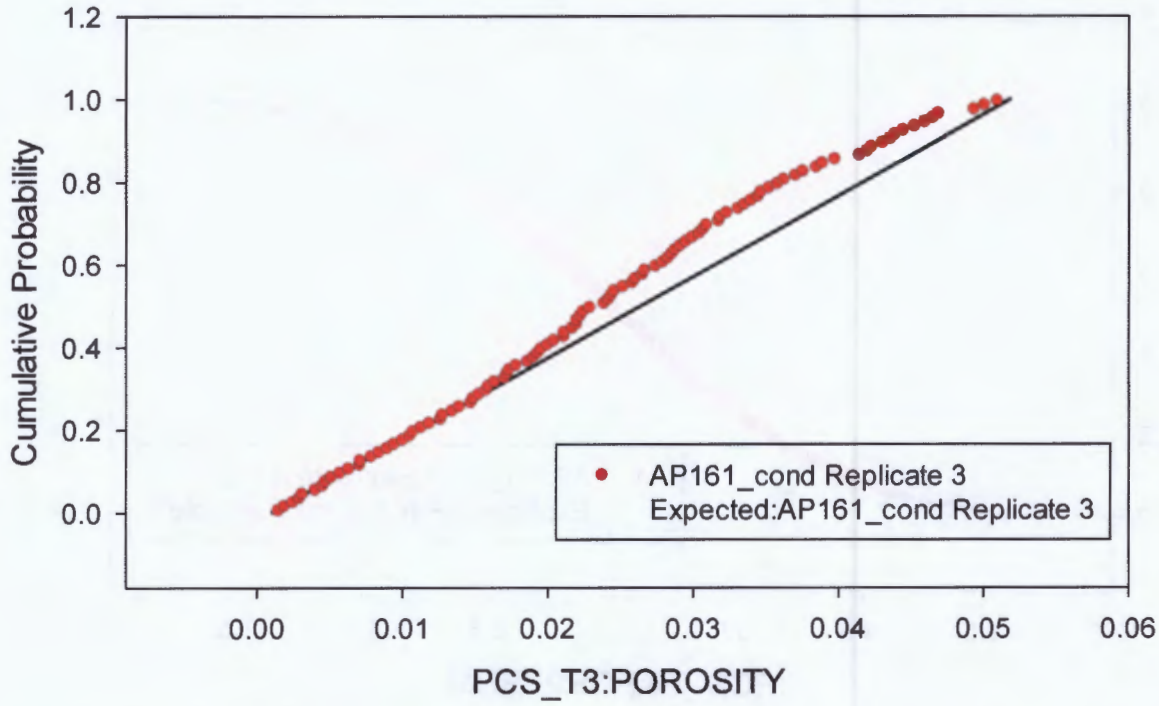

□i□□r□□□□□O□□□r□□□an□□□□□□t□□ □□□□for □□□□□□□□O□O□□□ □□niform □i□ri□□tion□□□□i□at□□

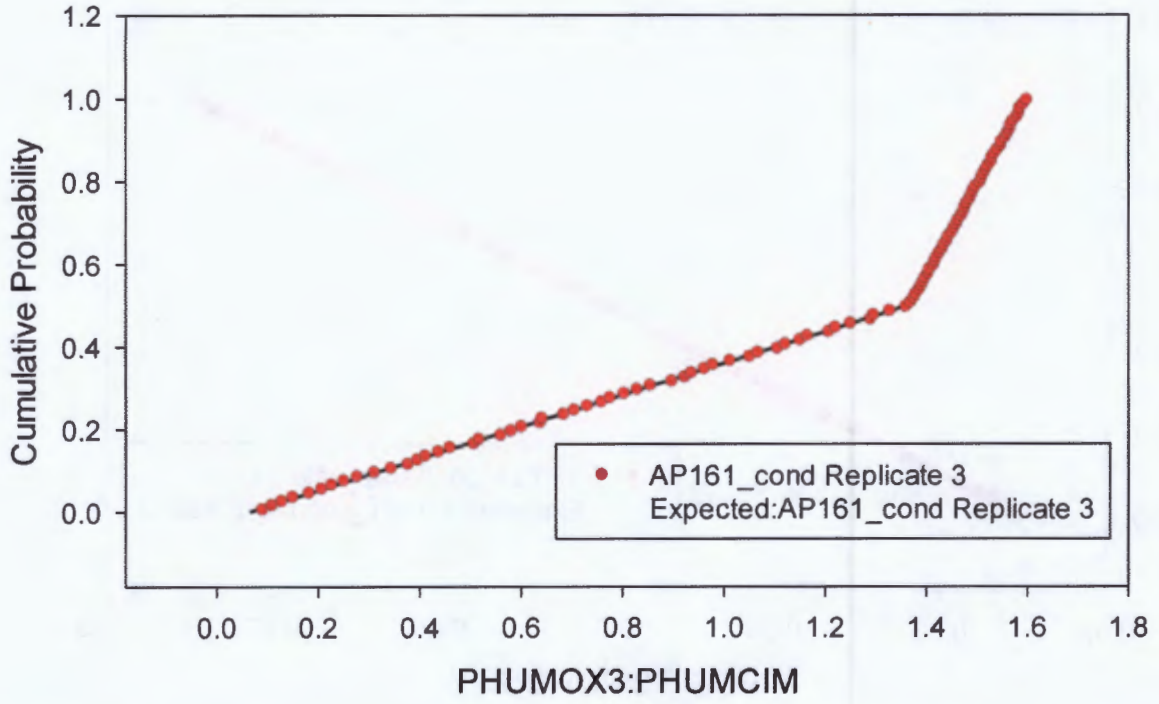

□i□□r□□□□□O□□□r□□□an□□□□□□t□□ □□□□for □□□□ O□□□□□□□ □I□ □□□r □ontin□o□□□i□ri□□tion□□□□i□at□□

Information Only

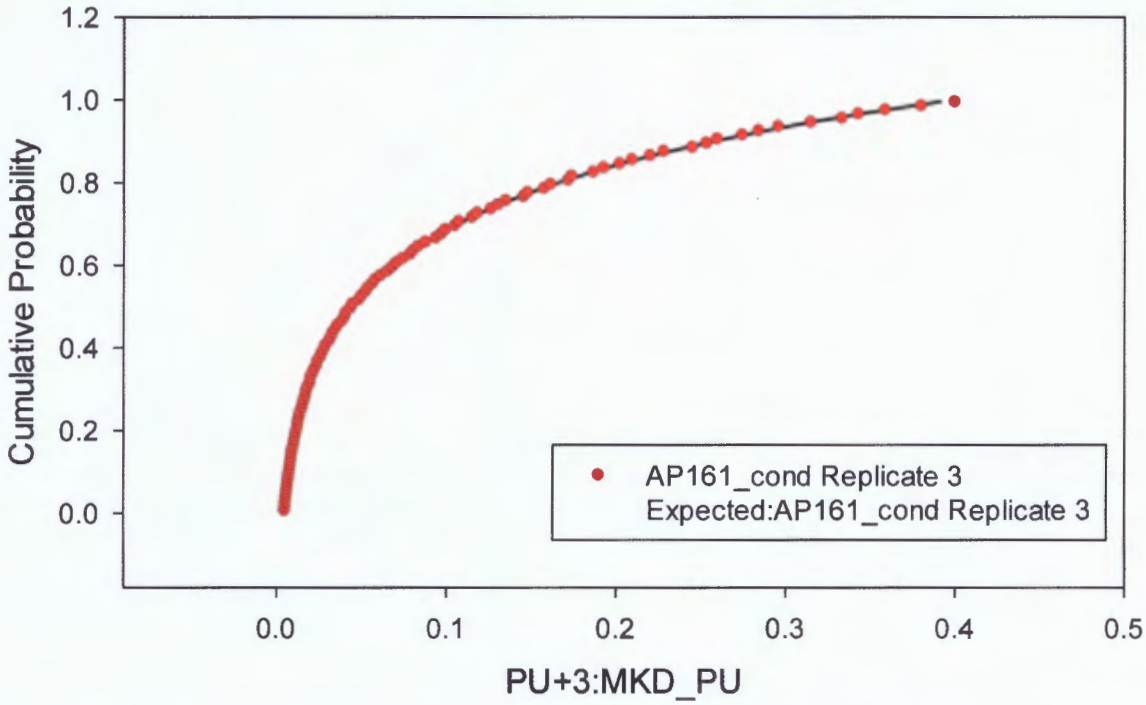

□i□r□□□□O□□r□□an□□□□□t□□□□□for □□□□□ □□□□ □□o□niform □i□ri□□tion□□□□i□at□□

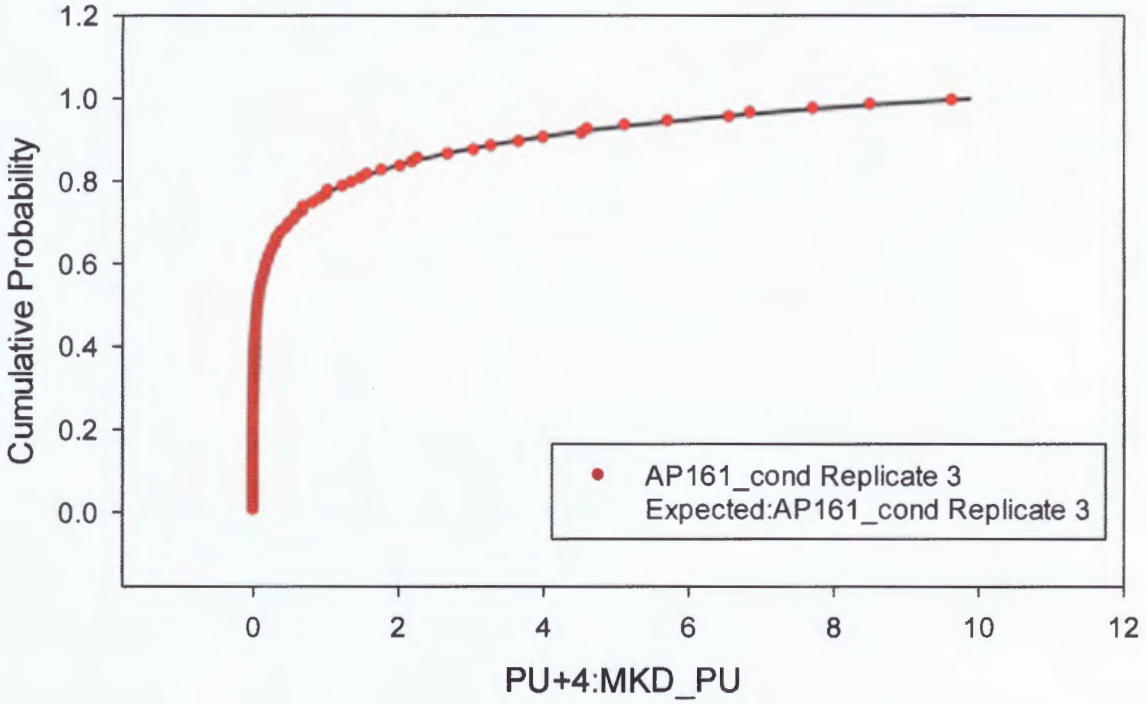

□i□r□□□□O□□r□□an□□□□□t□□□□□for □□□□□ □□□□ □□o□niform □i□ri□□tion□□□□i□at□□

Information Only

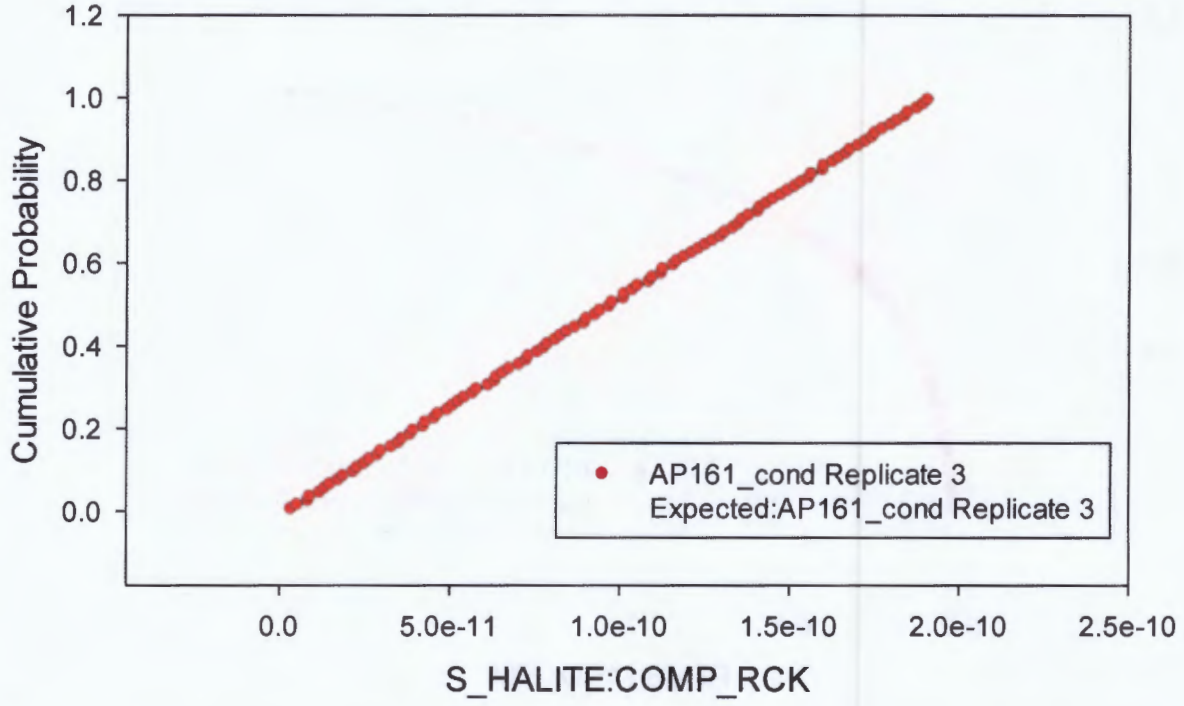

□i□□r□□□□O□□r□□□an□□□□□t□□□□□for □□□□□I□□□□O□ □□□□□ □□niform □i□ri□□tion□□□□li□at□□□

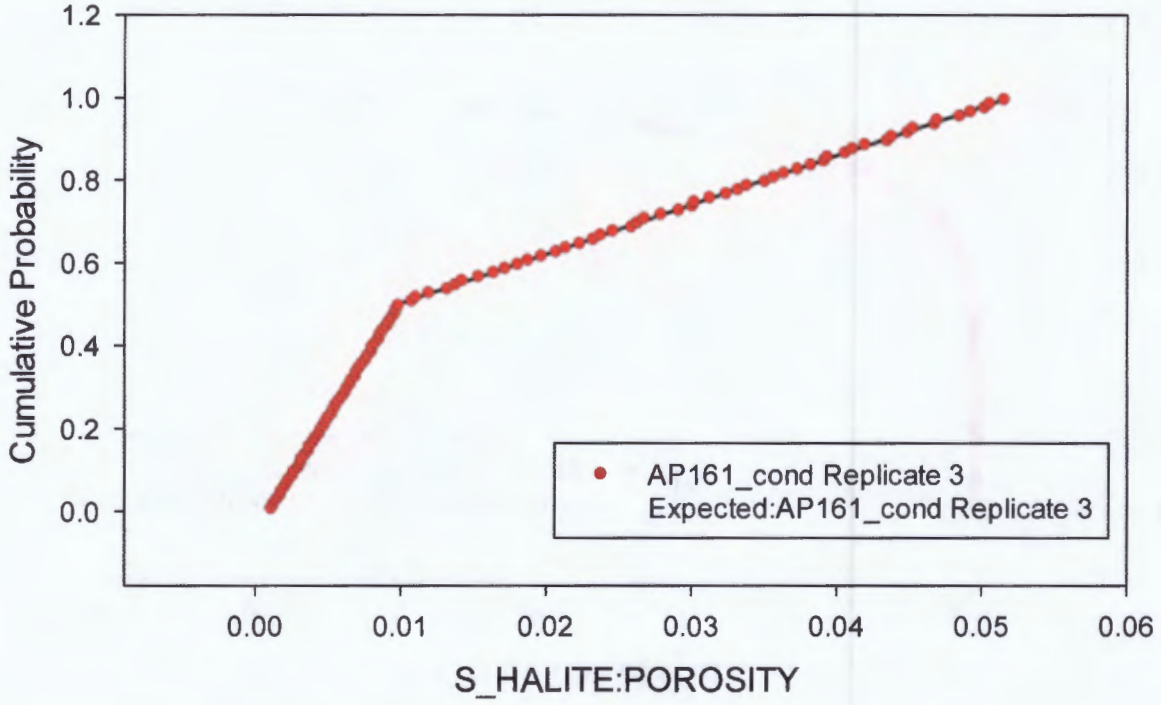

□i□□r□□□□O□□r□□□an□□□□□t□□□□□for □□□□□I□□□□O□O□I□□ □□□r □ontin□o□□□i□ri□□tion□□□□li□at□□□

Information Only

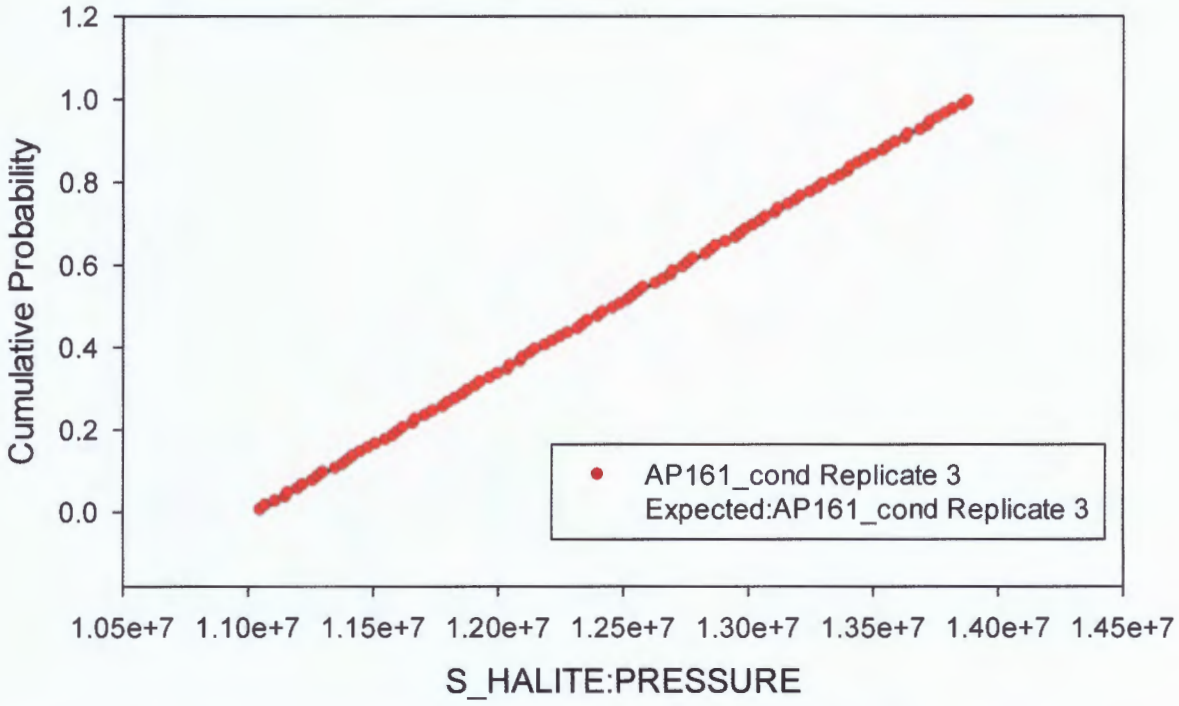

□i□□r□□□□O□□r□□an□□□□□t□□ □□□□for □□□ □□I□□□□□□□□□ □□niform □i□tri□□tion□□□□li□at□□

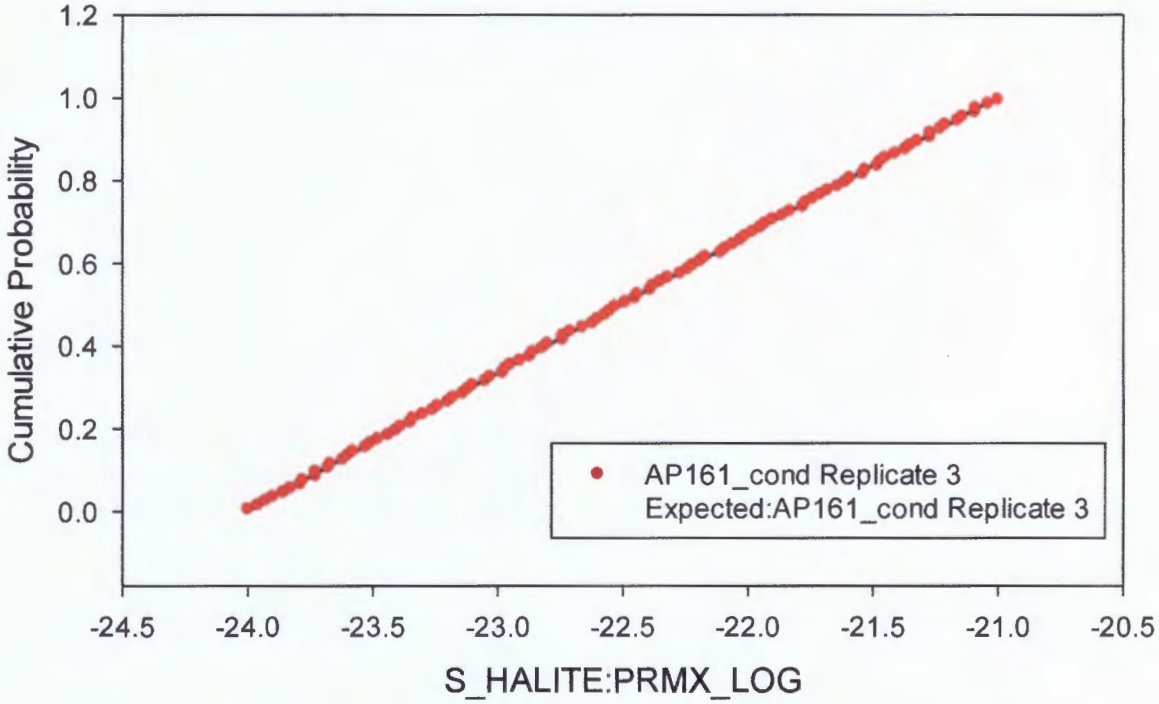

□i□□r□□□□O□□r□□an□□□□□t□□ □□□□for □□□ □□I□□□□□ □□□O□ □□niform □i□tri□□tion□□□□li□at□□

Information Only

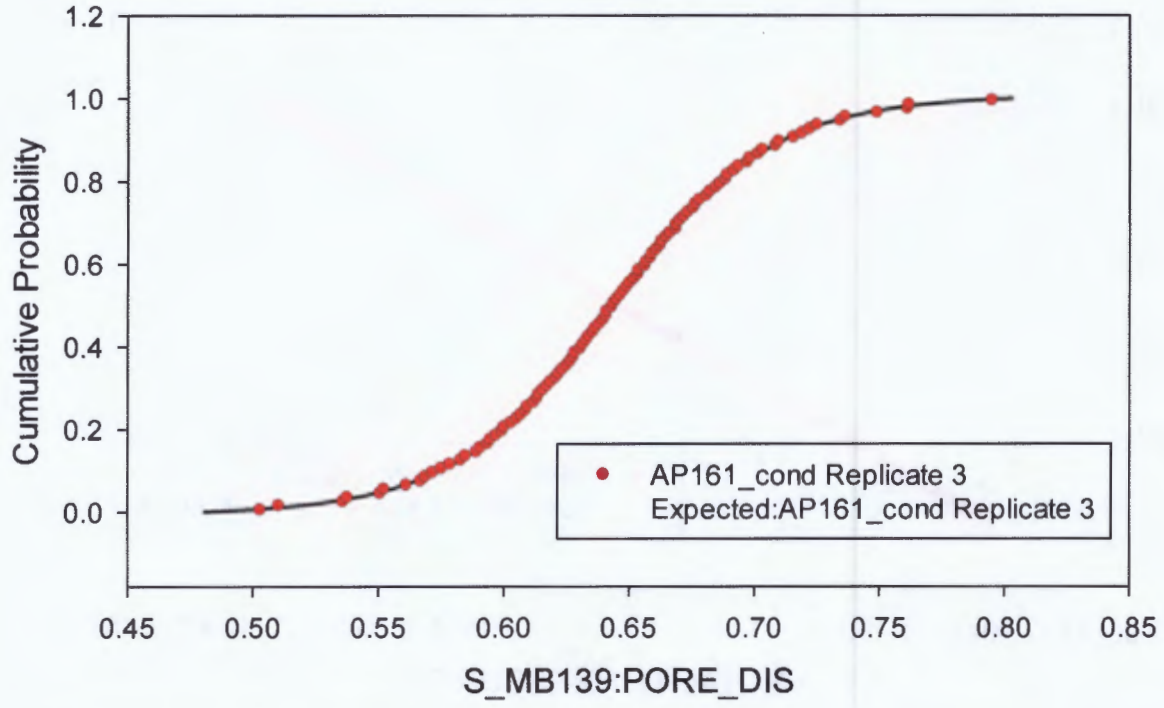

□i□□r□□□□□O□□□r□□□an□□□□□□t□□ □□□□for □□□ □□□□□□O□□□□I□□□t□□□nt □i□tri□□tion□□□□li□at□□

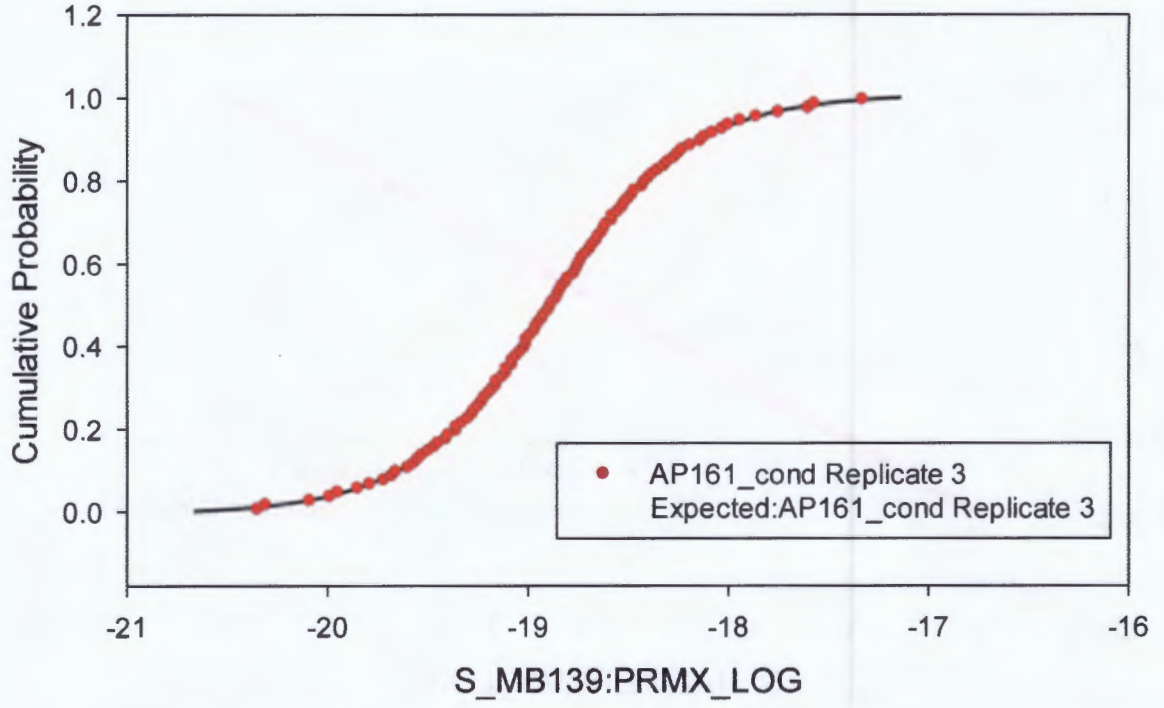

□i□□r□□□□□O□□□r□□□an□□□□□□t□□ □□□□for □□□ □□□□□□□□□ □□□O□ □□t□□□nt □i□tri□□tion□□□□li□at□□

Information Only

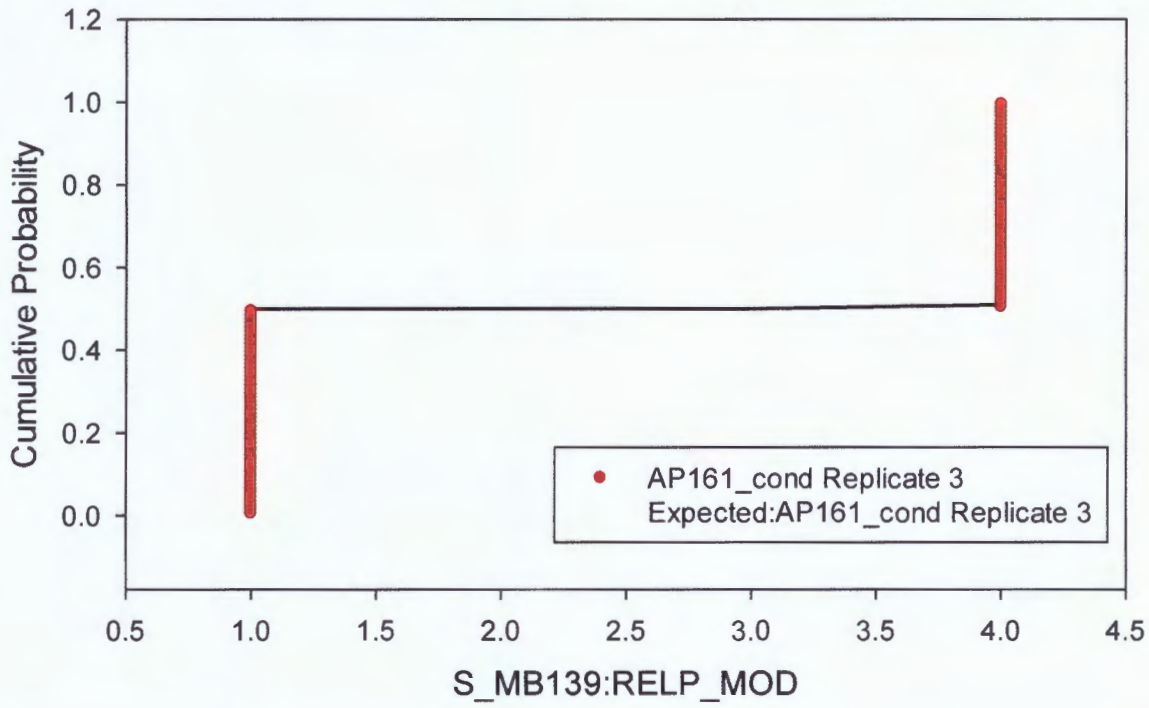

□i□r□□□□O□□r□□an□□□□□t□□□□□for □□□ □□□□□□□□□□ O□ □□□r □i□r□t□□□□ta□□i□ri□□tion□□□li□at□□

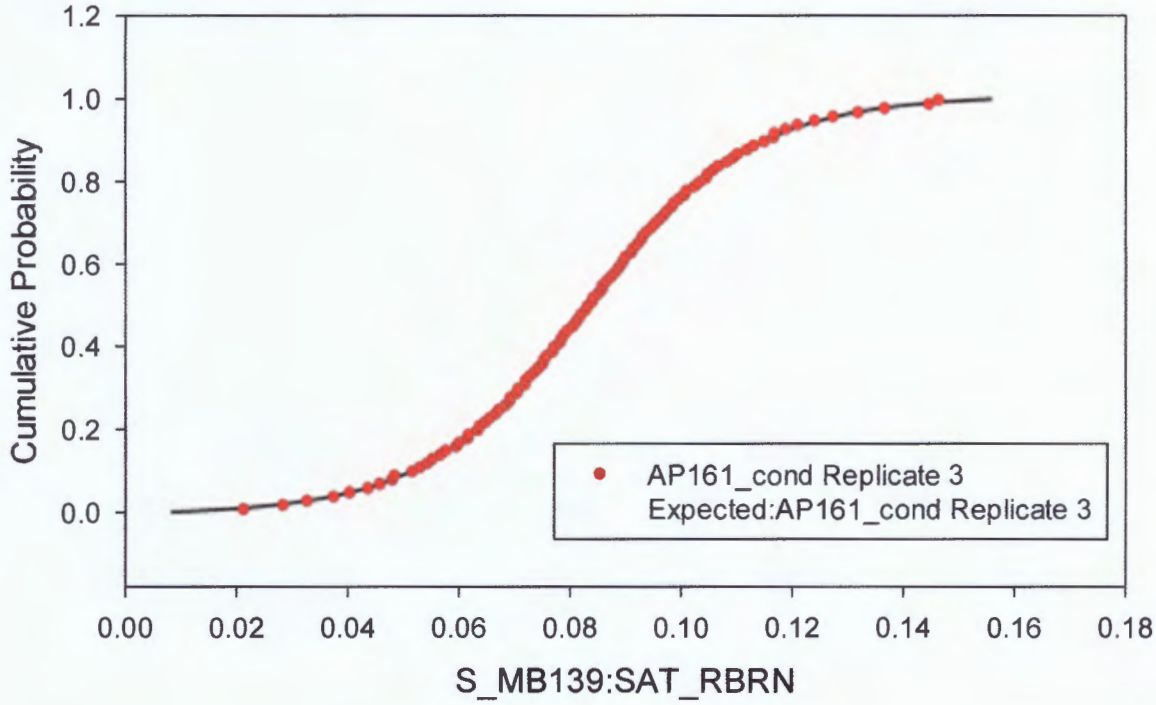

□i□r□□□□O□□r□□an□□□□□t□□□□□for □□□ □□□□□□□□□□□□ □□t□□□ht □i□ri□□tion□□□li□at□□

Information Only

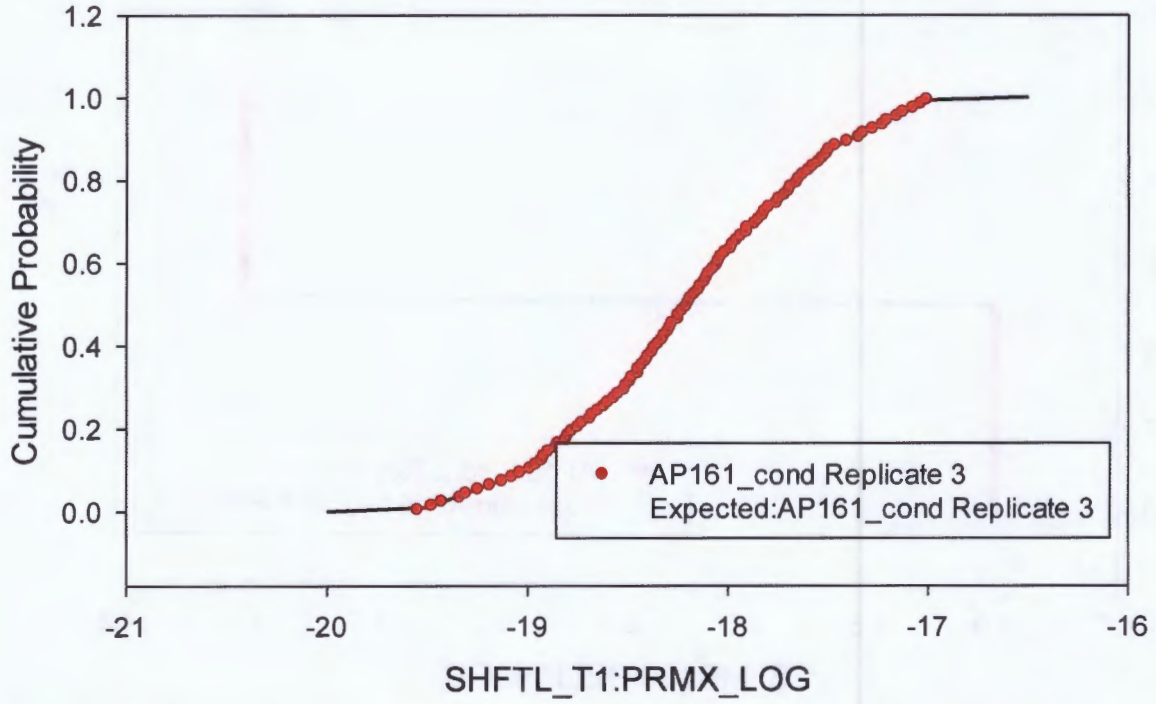

□i□r□□□□O□□r□□□an□□□□□t□□□□□for □□□□□□□□□□□ □□□O□ □□□r □ontin□o□□□i□ri□□tion□□□li□at□□

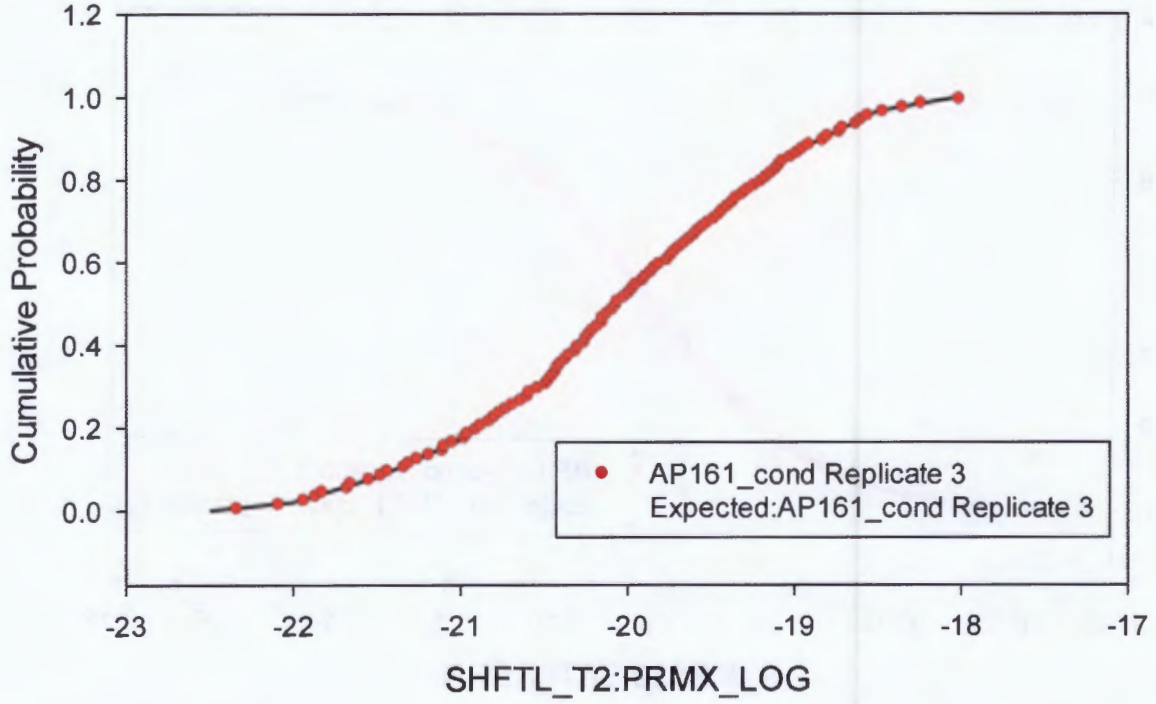

□i□r□□□□O□□r□□□an□□□□□t□□□□□for □□□□□□□□□□□ □□□O□ □□□r □ontin□o□□□i□ri□□tion□□□li□at□□

Information Only

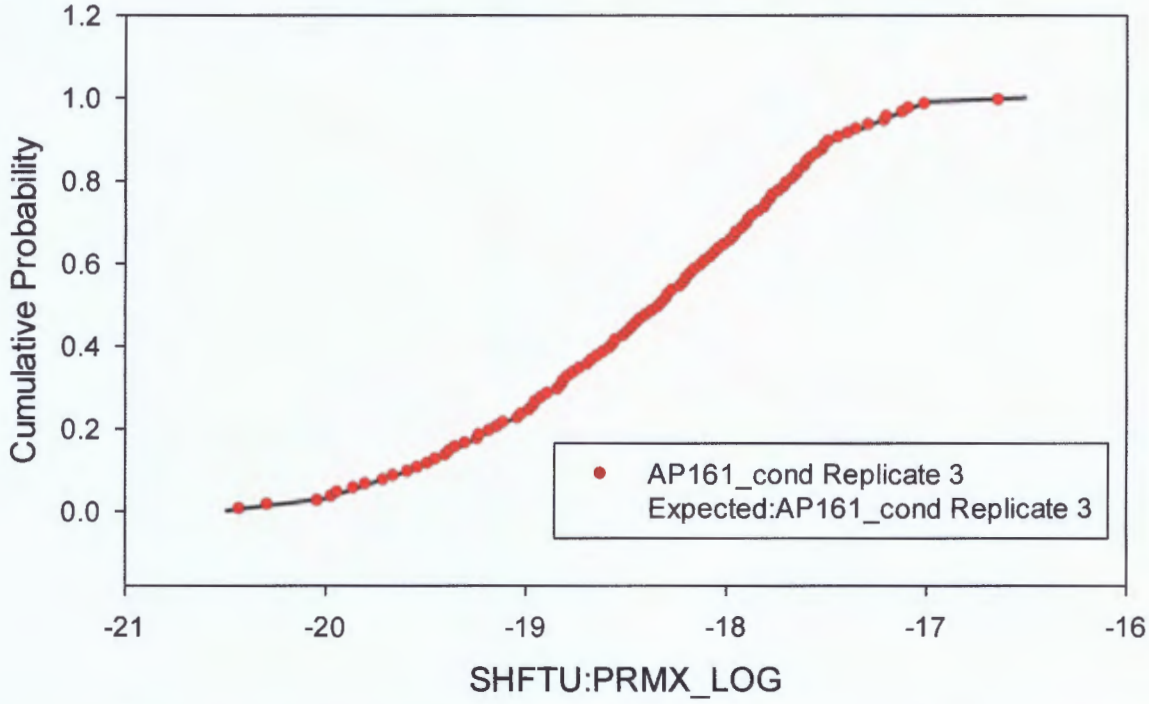

□i□□r□□□□□O□□□r□□□an□□□□□□t□□□□□□for □□□□□□□□□□ □□□O□ □□□□r □ontin□o□□□i□ri□□tion□□□□li□at□□□

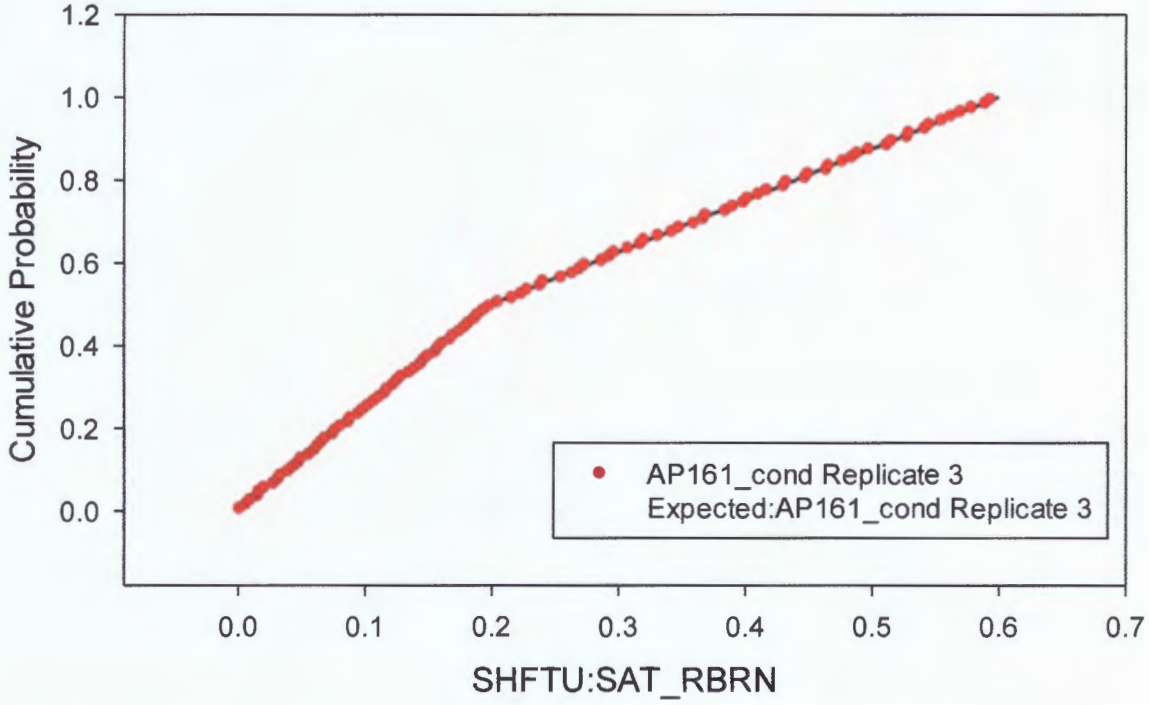

□i□□r□□□□□O□□□r□□□an□□□□□□t□□□□□□for □□□□□□□□□□□□□□□ □□□□r □ontin□o□□□i□ri□□tion□□□□li□at□□□

Information Only

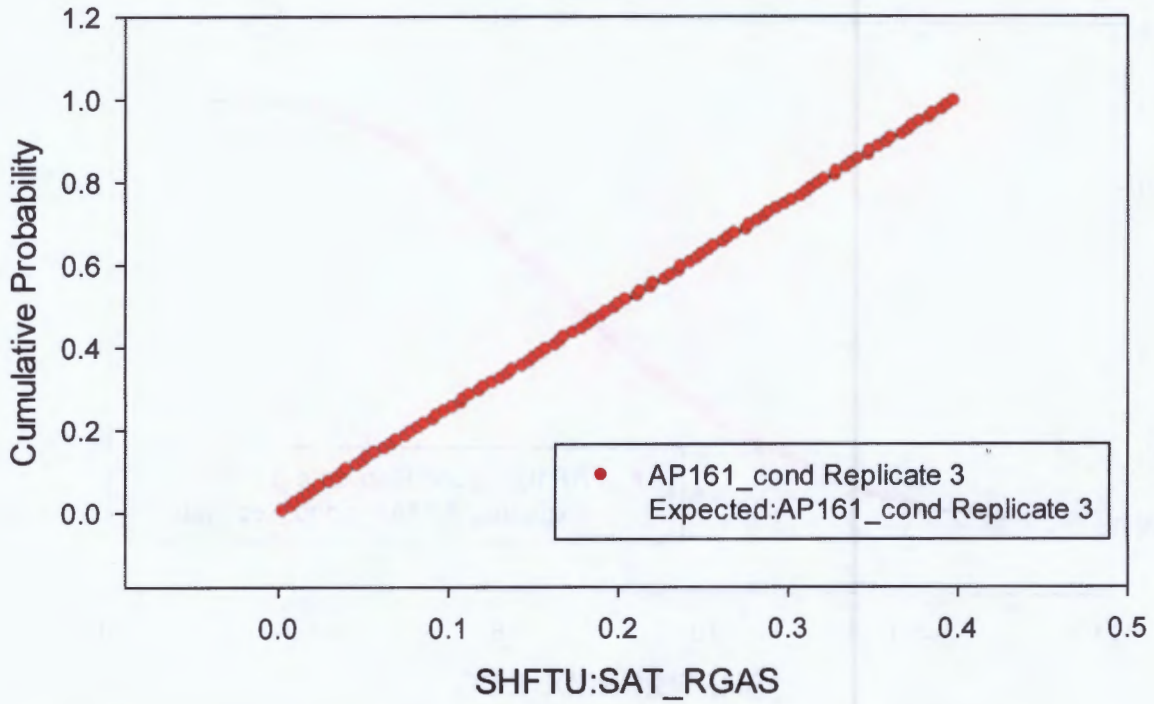

□i□□r□□□□□O□□□r□□□an□□□□□□t□□ □□□□for □□□□□□□□□□□□□□□□niform □i□ri□□tion□□□□li□at□□□

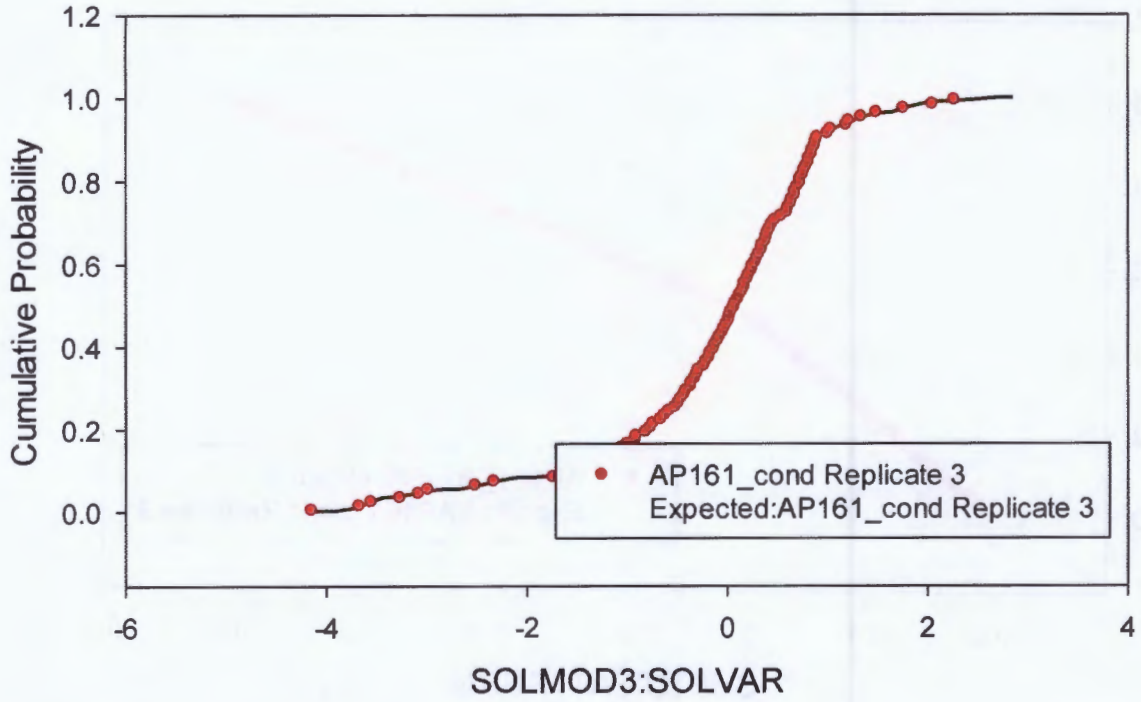

□i□□r□□□□□O□□□r□□□an□□□□□□t□□ □□□□for □O□□ O□□□□O□□□□ □□□r □ontin□b□□□i□ri□□tion□□□□li□at□□□

Information Only

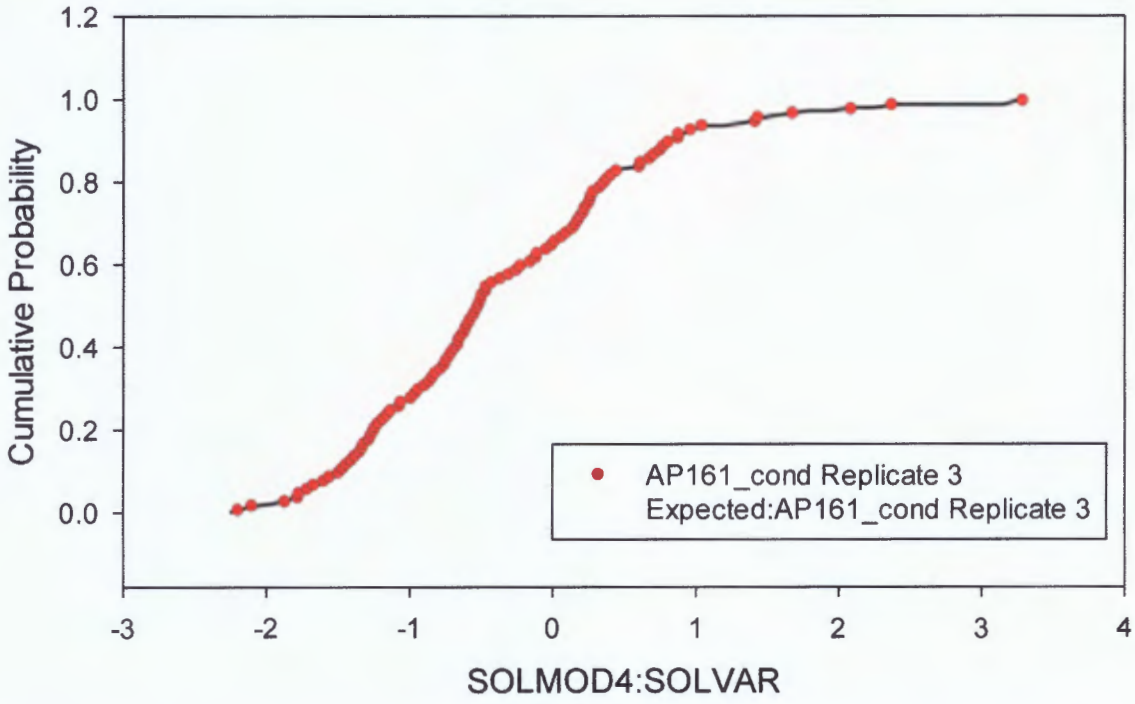

□i□r□□□□O□□r□□an□□□□□t□□□□□for □O□□ O□□□O□□□□ □□□r □ontin□o□□□i□tri□□tion□□□□li□at□□

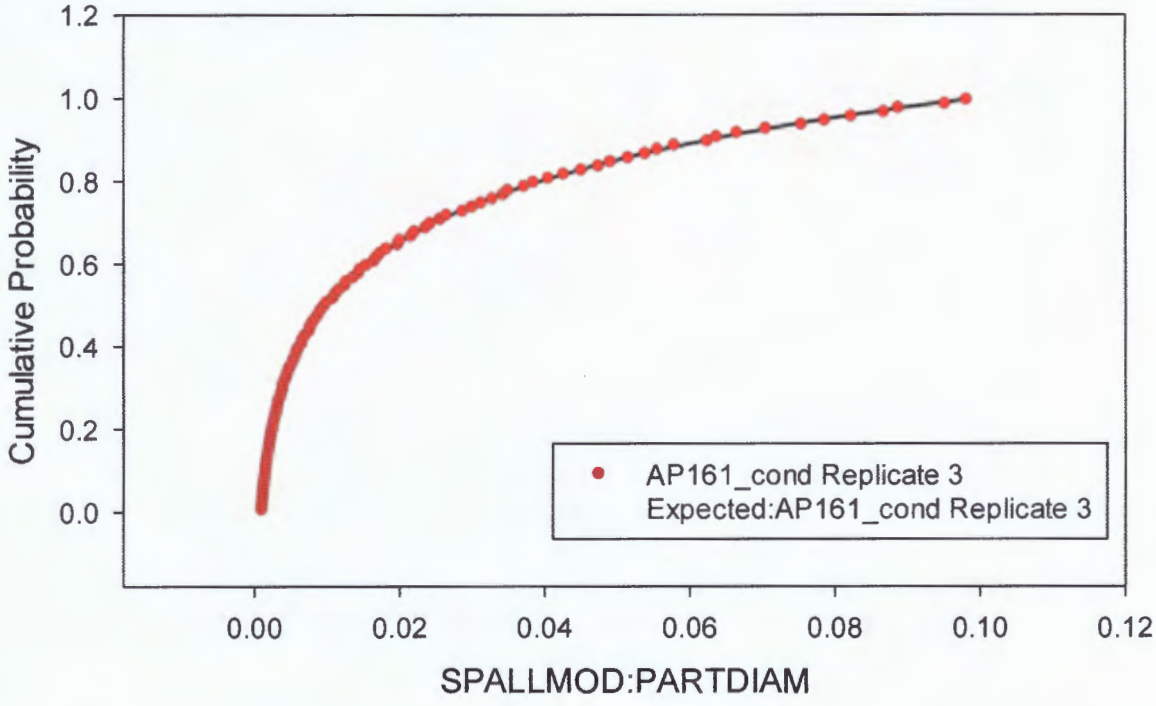

□i□r□□□□O□□r□□an□□□□□t□□□□□for □□□□□□ O□□□□□□□I□□ □□o□□niform □i□tri□□tion□□□□li□at□□

Information Only

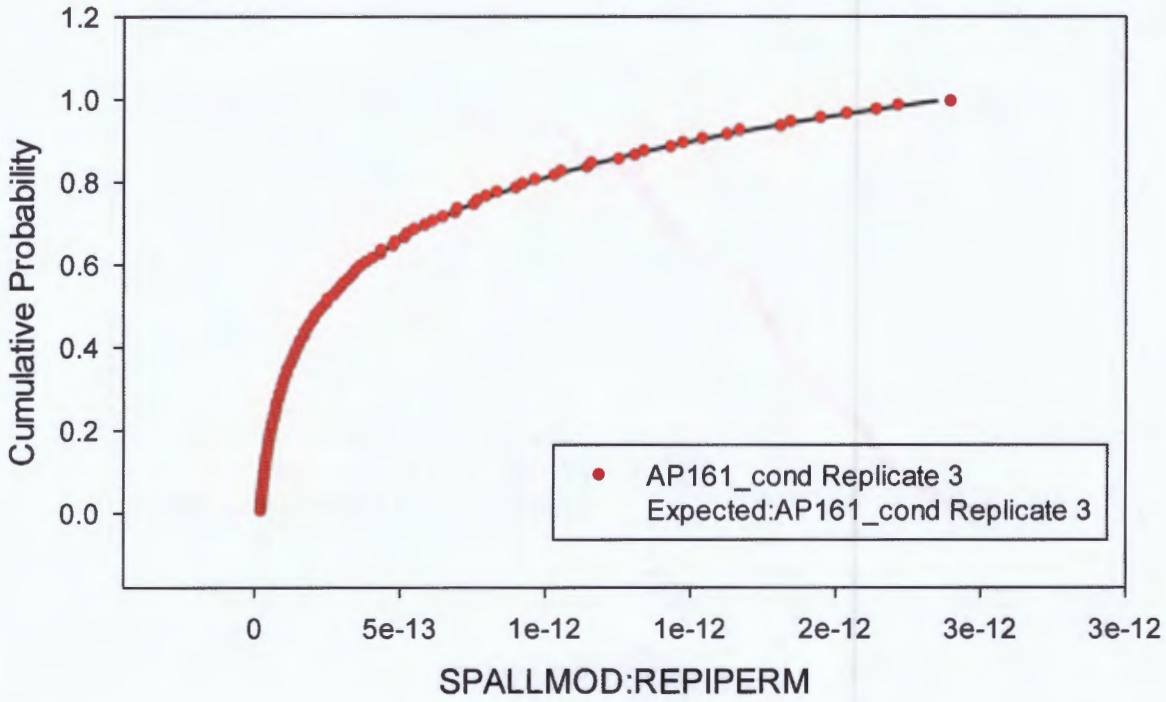

□i□r□□□□O□□r□□an□□□□□t□□□□□for □□□□□ O□□□□□I□□□□ □□o□□niform □i□ri□□tion□□□□i□at□□

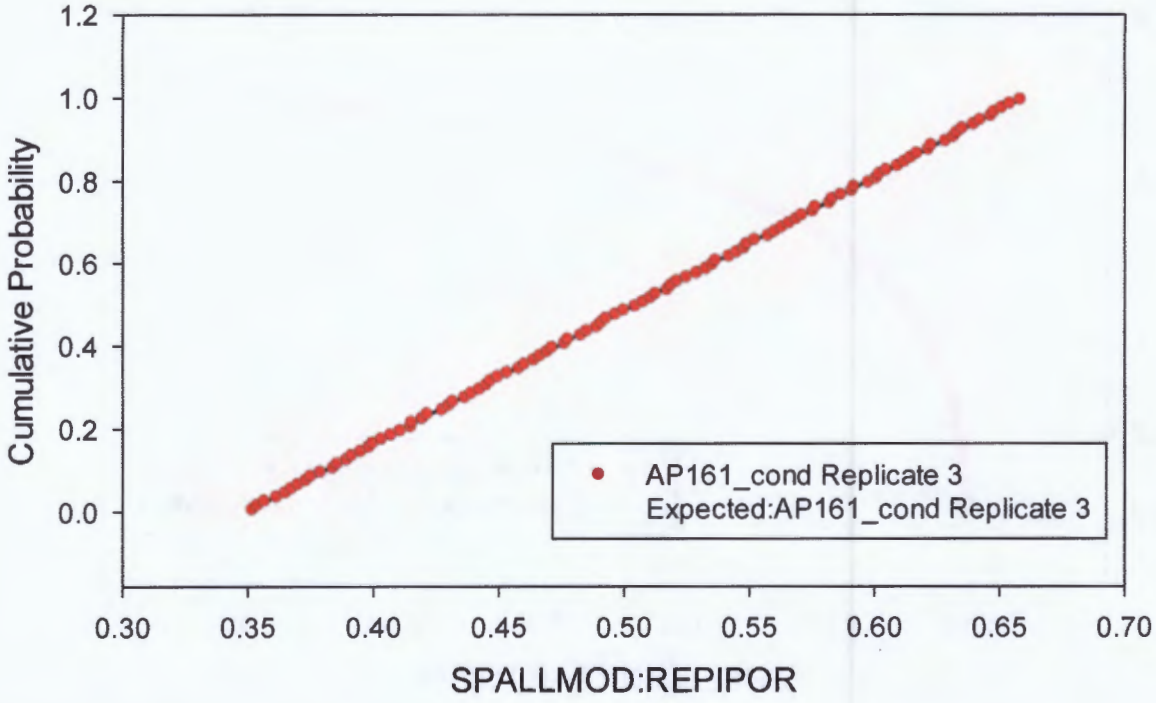

□i□r□□□□O□□r□□an□□□□□t□□□□□for □□□□□ O□□□□□I□O□ □□niform □i□ri□□tion□□□□i□at□□

Information Only

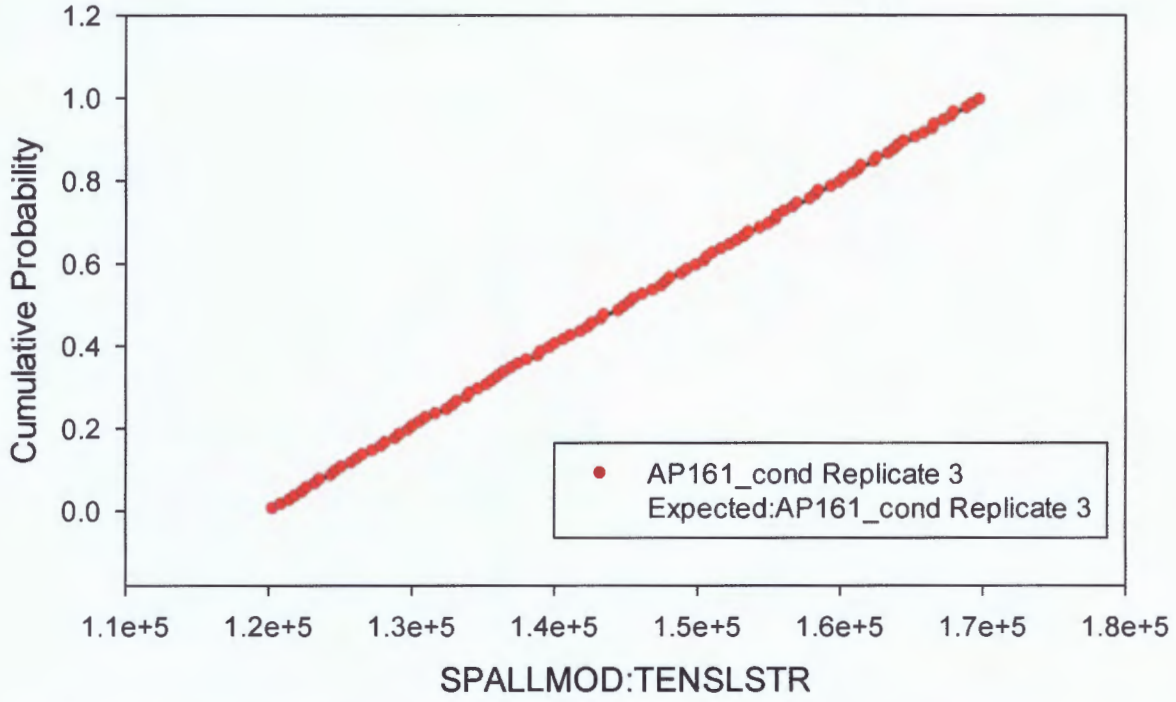

□i□□r□□□□O□□□r□□□an□□□□□□t□□ □□□□for □□□□□□ O□□□□□□□□□□ □□niform □i□tri□□tion□□□□li□at□□□

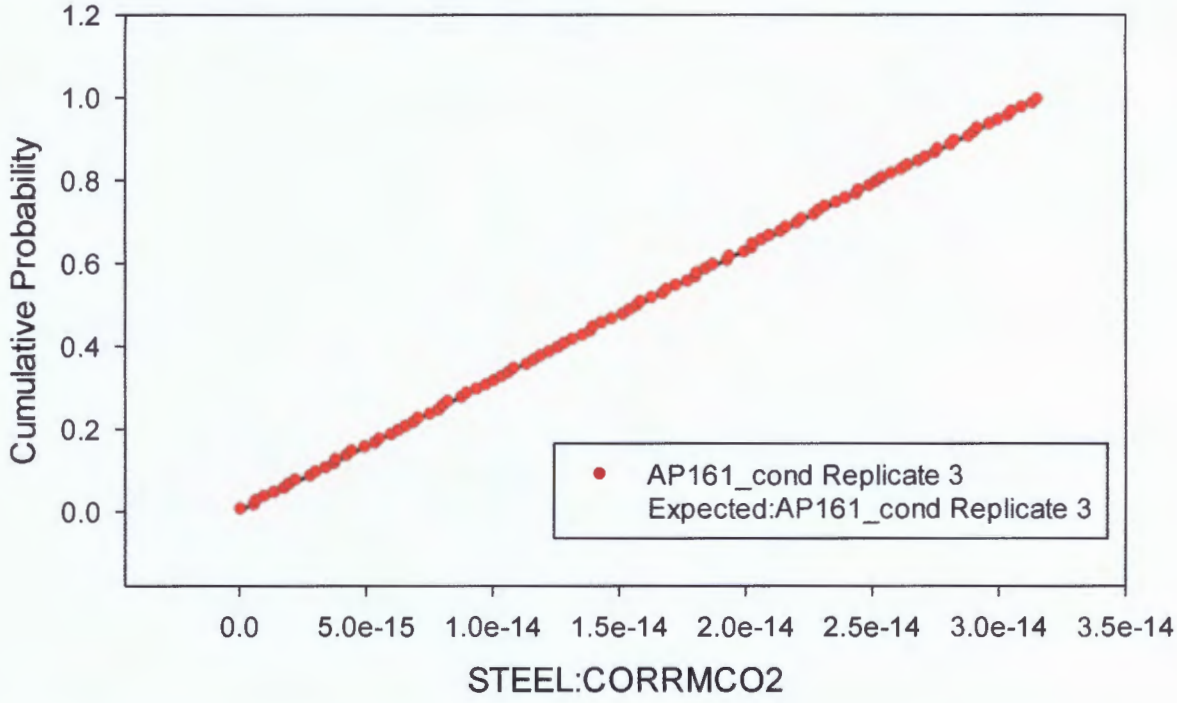

□i□□r□□□□O□□□r□□□an□□□□□□t□□ □□□□for □□□□□□□O□□□ □O□□□niform □i□tri□□tion□□□□li□at□□□

Information Only

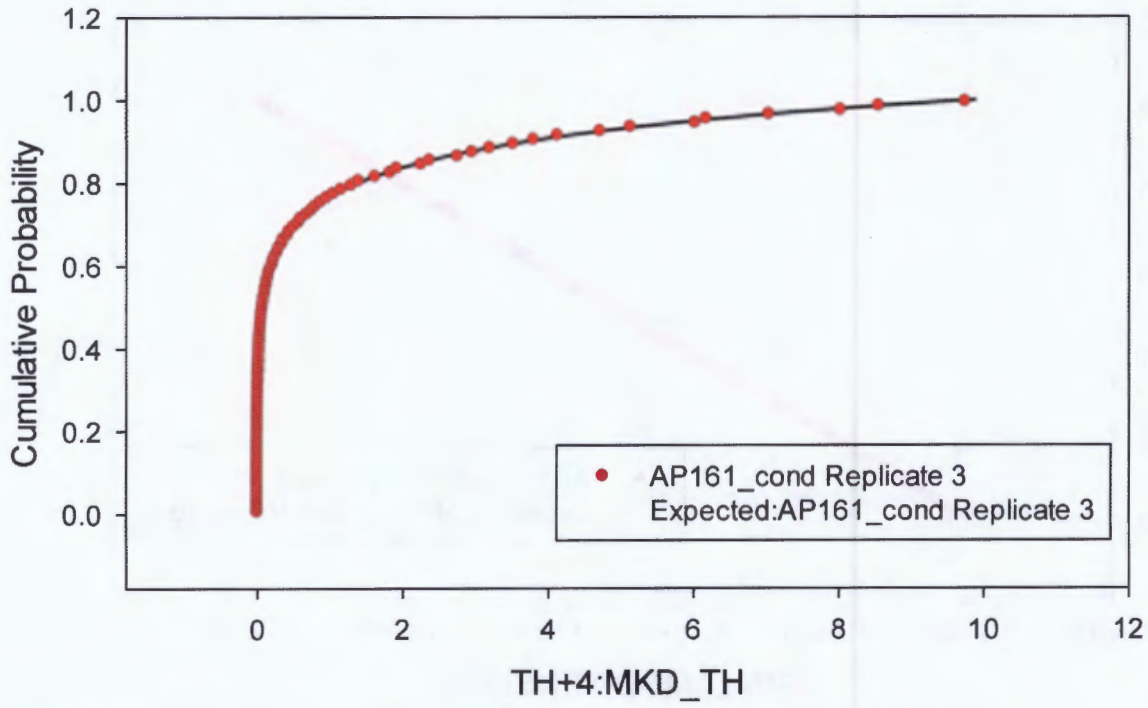

□i□r□□□□O□□r□□an□□□□□t□□□□□for □□□□□ □□□□ □□o□□niform □i□ri□□tion□□□□i□at□□

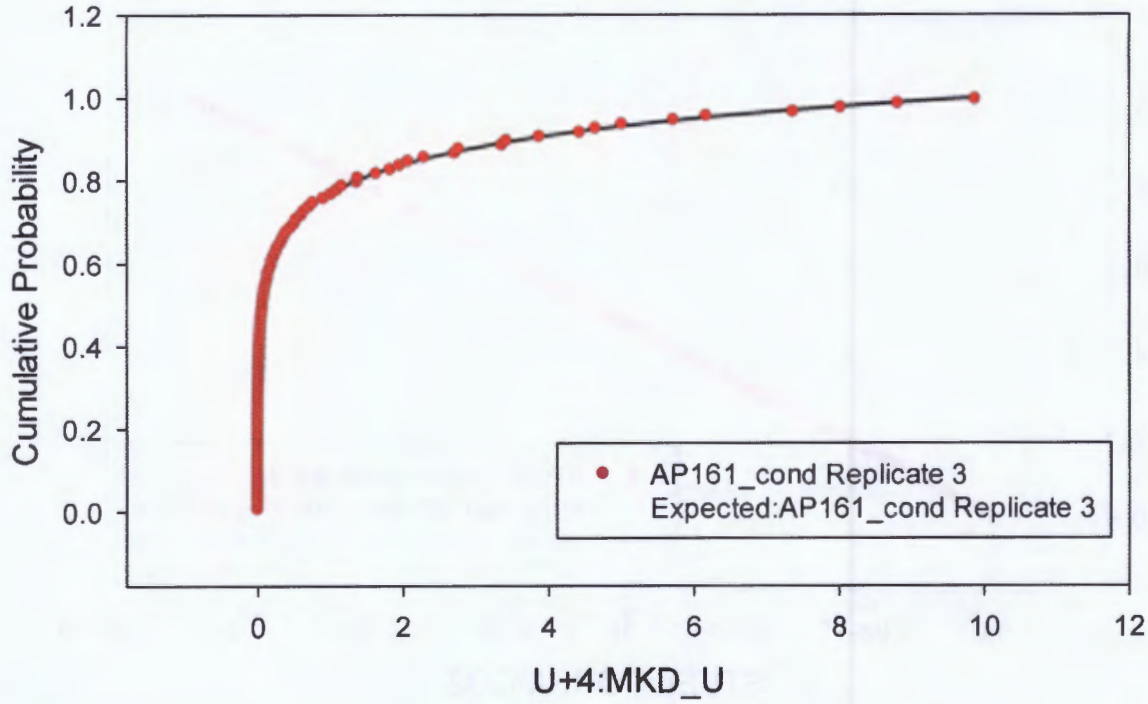

□i□r□□□□O□□r□□an□□□□□t□□□□□for □□□□□ □□□□ □□o□□niform □i□ri□□tion□□□□i□at□□

Information Only

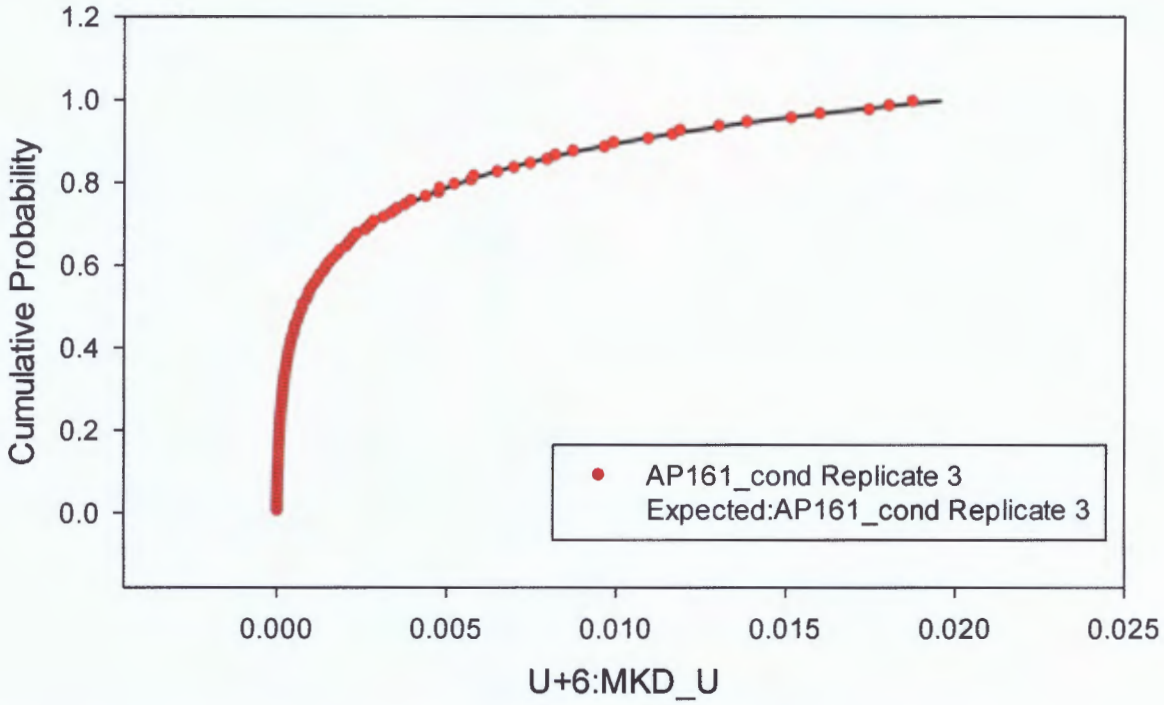

□i□r□□□□O□□r□□□an□□□□□t□□□□□for □□□□ □□□□ □□o□□niform □i□tri□□tion□□□li□at□□

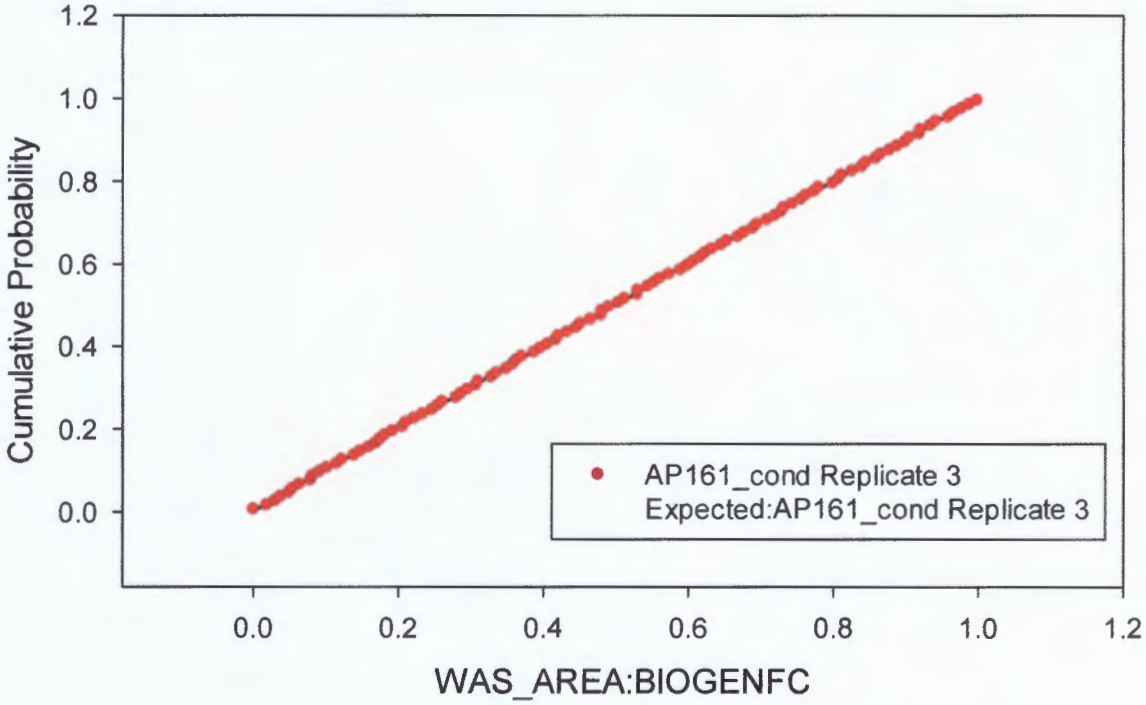

□i□r□□□□O□□r□□□an□□□□□t□□□□□for □ □□□□□□□□□IO□□□□□ □□niform □i□tri□□tion□□□li□at□□

Information Only

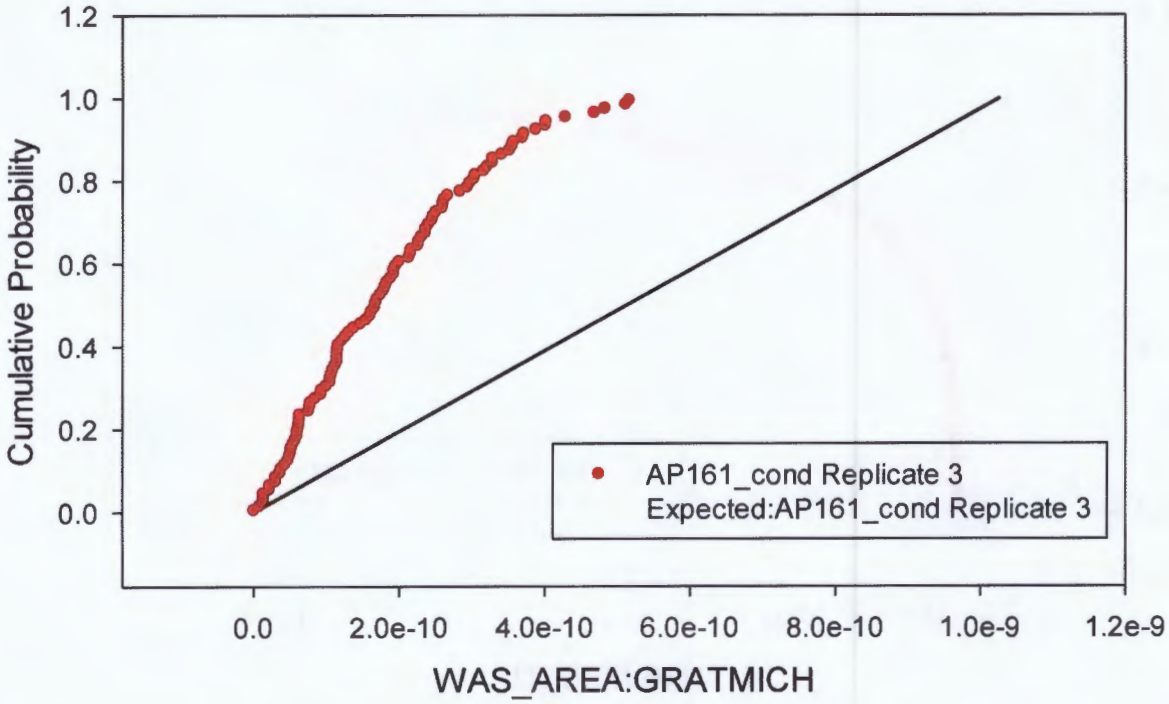

□i□r□□□□O□□r□□an□□□□□t□□□□□for □ □□□□□□□□□□□□ I□□ □□niform □i□ri□□tion□□□□li□at□□

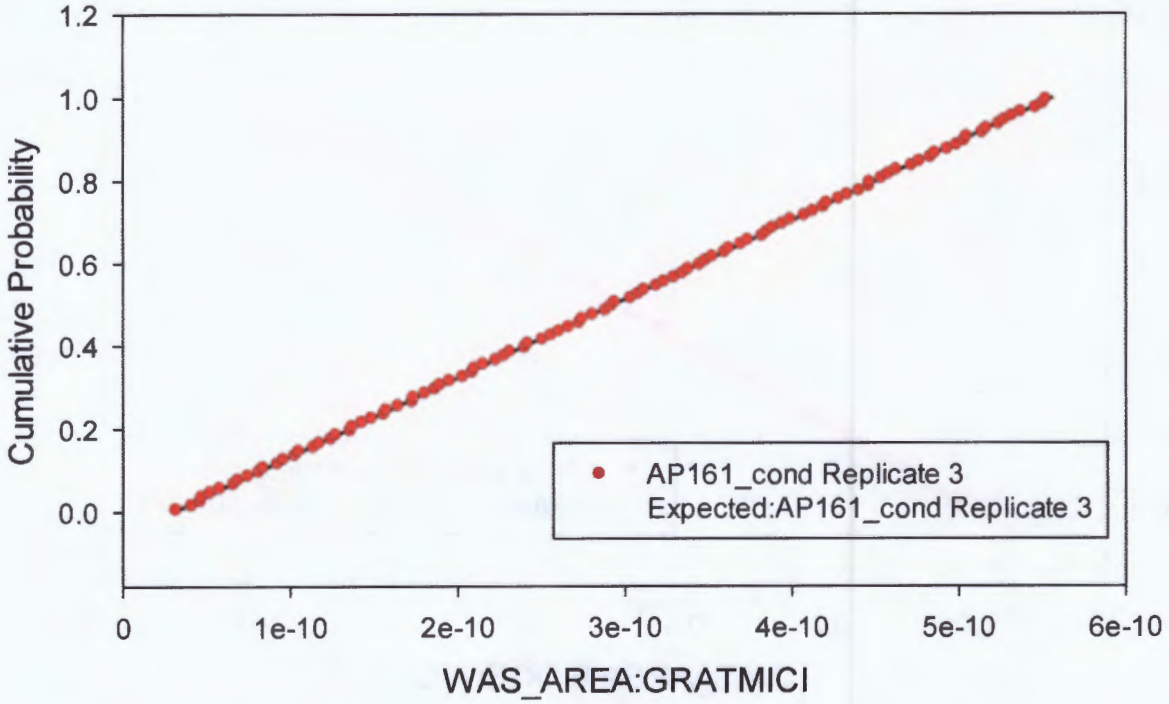

□i□r□□□□O□□r□□an□□□□□t□□□□□for □ □□□□□□□□□□□□ I□I □□niform □i□ri□□tion□□□□li□at□□

Information Only

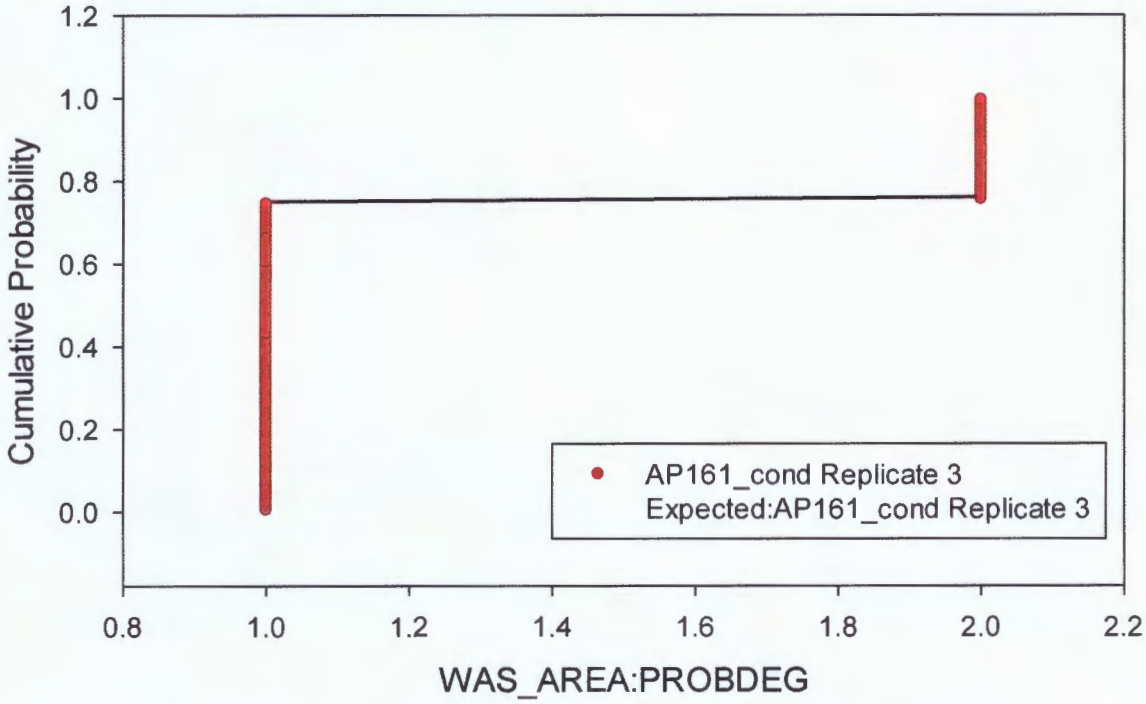

□i□r□□□□O□□r□□an□□□□□t□□□□□for □ □□□□□□□□□O□□□□ □□□r □i□r□t□□□□ta□□i□ri□□tion□□□□li□at□□

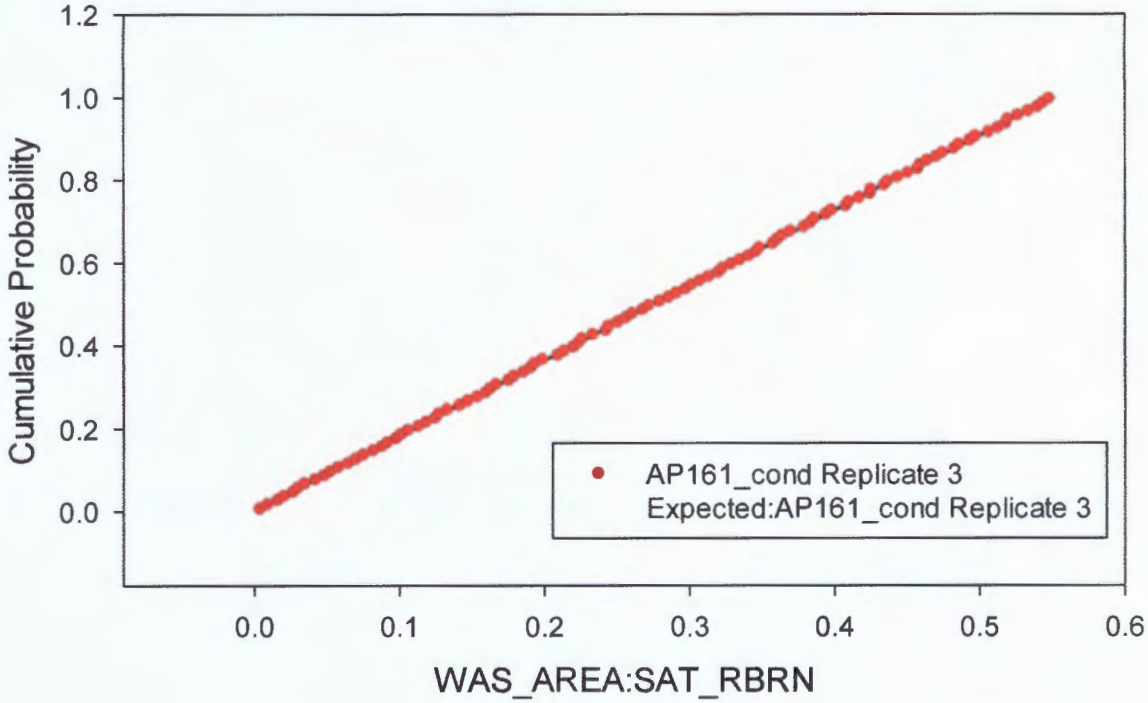

□i□r□□□□O□□r□□an□□□□□t□□□□□for □ □□□□□□□□□□□□□□□□ □□niform □i□ri□□tion□□□□li□at□□

Information Only

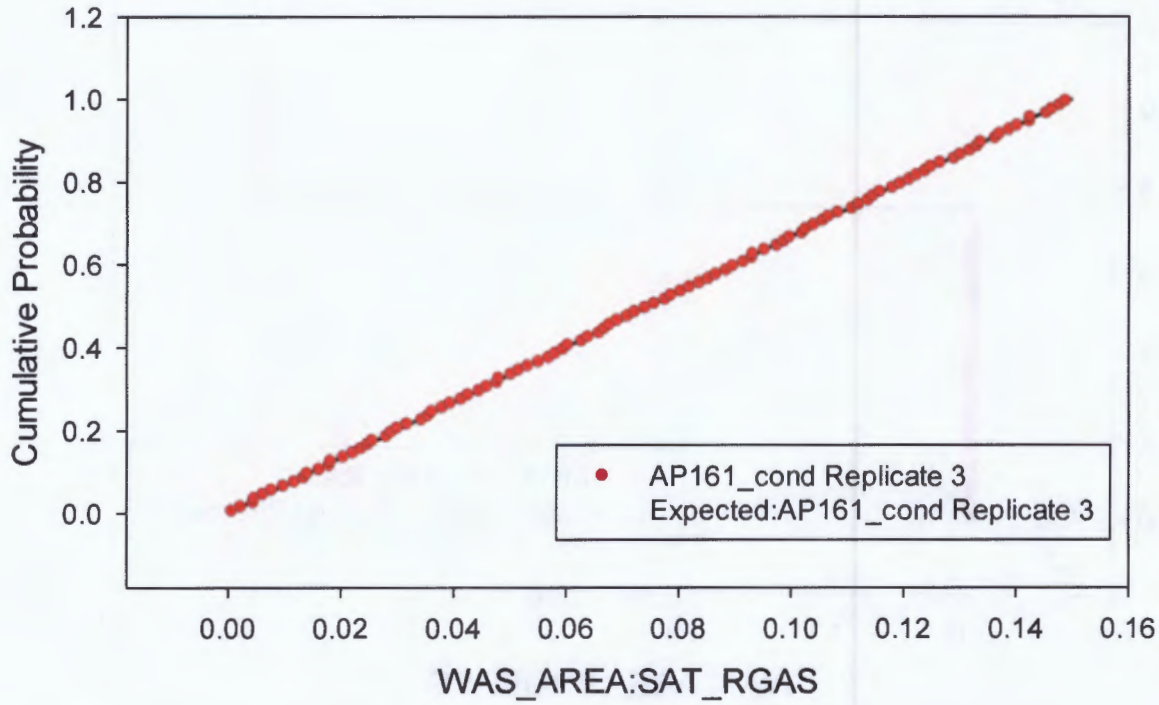

□i□□r□□□□□O□□□r□□□an□□□□□□t□□ □□□□for □ □□□□□□□□□□□□□□□□□□niform □i□tri□□tion□□□□i□at□□□

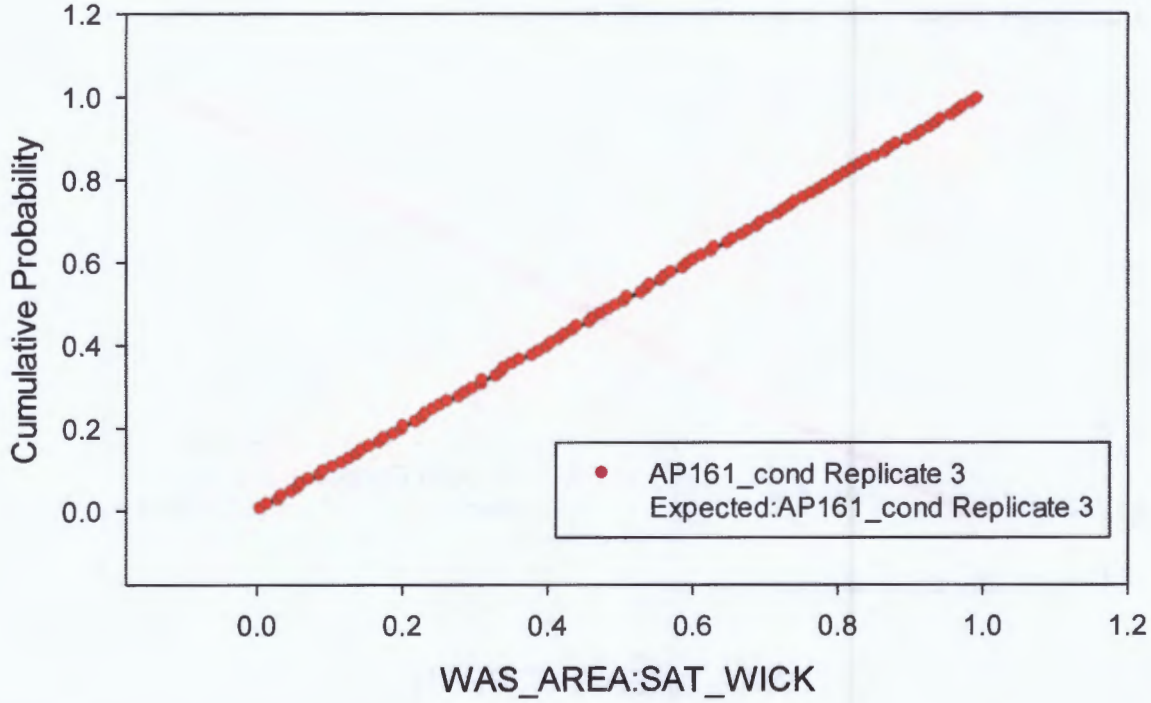

□i□□r□□□□□O□□□r□□□an□□□□□□t□□ □□□□for □ □□□□□□□□□□□□□ I□□ □□niform □i□tri□□tion□□□□i□at□□□

Information Only

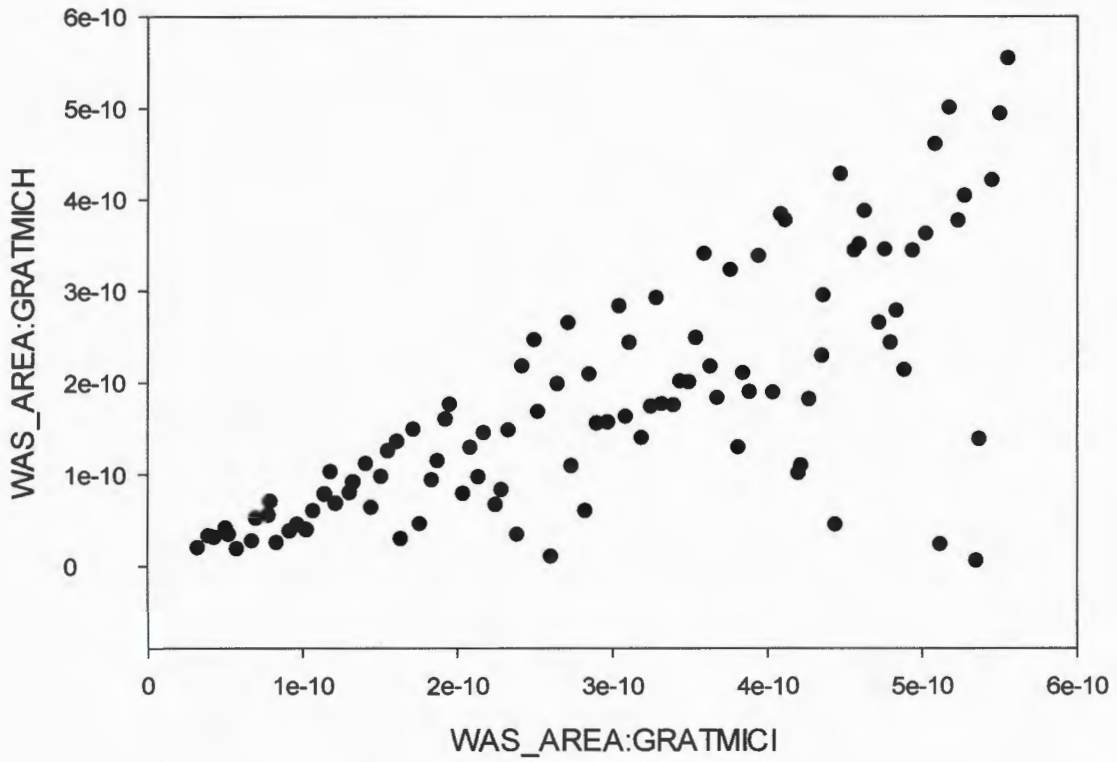
6e-10
5e-10
4e-10
3e-10
2e-10
1e-10
0
WAS_AREA:GRATMICH
0
1e-10
2e-10
3e-10
4e-10
5e-10
6e-10
WAS_AREA:GRATMICI

**□i□□r□□□

Appendix I. Input file to PRELHS for Replicate 1

```
! TITLE:          PCS-2012 PRELHS (LHS1) Input File
! ANALYSIS PLAN: AP-161
! ANALYST:        Tom Kirchner
! CREATED:        July 2012
!
!  LHSCALC = PCS-2012 REALIZATION 1
!==========================================================================
!
!  DESCRIPTION:
!
!  WIPP PCS-2012 Performance Assessment Baseline Calculation,
!  aka  (AP161)
!
!  This input file to PRELHS is used to generate, as an output file, an
LHS
!  input file containing all distribution information and execution
options
!  required to create a sample for Replicate R1 for the WIPP PCS-2012 PA
!
!  Changes from PABC09 analyses: CELLULS:FBETA removed
!                                Material CONC_PCS replaced by PCS_T1 for
4 properties
!                                      (PRMX_LOG, SAT_RBRN, SAT_RGAS, and
POR_DIS)
!                                PCS_T1:POROSITY added
!                                PCS_T2:POROSITY added
!                                PCS_T3:POROSITY added
!                                PCS_T2:POR2PERM added
!                                PCS_T1:SAT_IBRN added
!
!Also, LHS_EDIT should control 41<42, and 74<73<72 (WAS_AREA:GRATMICI <
WAS_AREA:GRATMICH and
!    PCS_T3:POROSITY < PCS_T2:POROSITY < PCS_T1:POROSITY)
!
!========= No Comments Allowed between *ECHOLHS and *ENDECHO
================
!
*ECHOLHS
TITLE PABC09, AP161, Replicate R1 Input File for the LHS Code
NOBS           100
RANDOM SEED    582592385
CORRELATION MATRIX
    2
    53  54 -0.99
    61  62 -0.75
OUTPUT CORR HIST DATA
*ENDECHO
!
!== PROPERTIES TO BE RETRIEVED FROM WIPP PA CALCULATION DATABASE ==
!
*RETRIEVE
!1    CCDFGF
```


Information Only

```
     MATERIALS,  GLOBAL
     PROPERTIES, PBRINE
!2
     MATERIALS,  REFCON
     PROPERTIES, LHSBLANK
!3
     MATERIALS,  REFCON
     PROPERTIES, LHSBLANK
!4   CUTTINGS_S
     MATERIALS,  BOREHOLE
     PROPERTIES, DOMEGA
!5   CUTTINGS_S
     MATERIALS,  BOREHOLE
     PROPERTIES, TAUFAIL
!6
     MATERIALS,  REFCON
     PROPERTIES, LHSBLANK
!7
     MATERIALS,  REFCON
     PROPERTIES, LHSBLANK
!8   DRSPALL
     MATERIALS,  SPALLMOD
     PROPERTIES, REPIPERM
!9   DRSPALL
     MATERIALS,  SPALLMOD
     PROPERTIES, TENSLSTR
!10  DRSPALL
     MATERIALS,  SPALLMOD
     PROPERTIES, PARTDIAM
!11  DRSPALL
     MATERIALS,  SPALLMOD
     PROPERTIES, REPIPOR
!12
     MATERIALS,  REFCON
     PROPERTIES, LHSBLANK
!13
     MATERIALS,  REFCON
     PROPERTIES, LHSBLANK
!14
     MATERIALS,  REFCON
     PROPERTIES, LHSBLANK
!15  PANEL
       MATERIALS,      SOLMOD3
       PROPERTIES,     SOLVAR
!16  PANEL
       MATERIALS,      SOLMOD4
       PROPERTIES,     SOLVAR
!17  PANEL
     MATERIALS,  PHUMOX3
     PROPERTIES, PHUMCIM
!18  PANEL/SECOTP2D
     MATERIALS,  GLOBAL
     PROPERTIES, OXSTAT
!19
```


Information Only

```
     MATERIALS,  REFCON
     PROPERTIES, LHSBLANK
!20
     MATERIALS,  REFCON
     PROPERTIES, LHSBLANK
!21
     MATERIALS,  REFCON
     PROPERTIES, LHSBLANK
!22
     MATERIALS,  REFCON
     PROPERTIES, LHSBLANK
!23  SECOTP2D
     MATERIALS,  CULEBRA
     PROPERTIES, MINP_FAC
!24  SECOTP2D
     MATERIALS,  GLOBAL
     PROPERTIES, TRANSIDX
!25  SECOTP2D
     MATERIALS,  GLOBAL
     PROPERTIES, CLIMTIDX
!26  SECOTP2D
     MATERIALS,  CULEBRA
     PROPERTIES, HMBLKLT
!27  SECOTP2D
     MATERIALS,  CULEBRA
     PROPERTIES, APOROS
!28  SECOTP2D
     MATERIALS,  CULEBRA
     PROPERTIES, DPOROS
!29  SECOTP2D
     MATERIALS,  U+6
     PROPERTIES, MKD_U
!30  SECOTP2D
     MATERIALS,  U+4
     PROPERTIES, MKD_U
!31  SECOTP2D
     MATERIALS,  PU+3
     PROPERTIES, MKD_PU
!32  SECOTP2D
     MATERIALS,  PU+4
     PROPERTIES, MKD_PU
!33  SECOTP2D
     MATERIALS,  TH+4
     PROPERTIES, MKD_TH
!34  SECOTP2D
     MATERIALS,  AM+3
     PROPERTIES, MKD_AM
!35
     MATERIALS,  REFCON
     PROPERTIES, LHSBLANK
!36
     MATERIALS,  REFCON
     PROPERTIES, LHSBLANK
!37
```


Information Only

```
      MATERIALS,  REFCON
      PROPERTIES, LHSBLANK
!38
      MATERIALS,  REFCON
      PROPERTIES, LHSBLANK
!39   BRAGFLO
      MATERIALS,  STEEL
      PROPERTIES, CORRMCO2
!40   BRAGFLO/PANEL
      MATERIALS,  WAS_AREA
      PROPERTIES, PROBDEG
!41   BRAGFLO
      MATERIALS,  WAS_AREA
      PROPERTIES, GRATMICI
!42   BRAGFLO
      MATERIALS,  WAS_AREA
      PROPERTIES, GRATMICH
!43   BRAGFLO
      MATERIALS,  PCS_T1
      PROPERTIES, SAT_IBRN
!44   BRAGFLO
      MATERIALS,  WAS_AREA
      PROPERTIES, SAT_RGAS
!45   BRAGFLO
      MATERIALS,  WAS_AREA
      PROPERTIES, SAT_RBRN
!46   BRAGFLO
      MATERIALS,  WAS_AREA
      PROPERTIES, SAT_WICK
!47   BRAGFLO
      MATERIALS,  DRZ_PCS
      PROPERTIES, PRMX_LOG
!48   BRAGFLO
      MATERIALS,  PCS_T1
      PROPERTIES, PRMX_LOG
!49   BRAGFLO
      MATERIALS,  PCS_T1
      PROPERTIES, SAT_RGAS
!50   BRAGFLO
      MATERIALS,  PCS_T1
      PROPERTIES, SAT_RBRN
!51   BRAGFLO
      MATERIALS,  PCS_T1
      PROPERTIES, PORE_DIS
!52   BRAGFLO
      MATERIALS,  S_HALITE
      PROPERTIES, POROSITY
!53   BRAGFLO
      MATERIALS,  S_HALITE
      PROPERTIES, PRMX_LOG
!54   BRAGFLO
      MATERIALS,  S_HALITE
      PROPERTIES, COMP_RCK
!55   BRAGFLO
```


Information Only

```
     MATERIALS,  S_MB139
     PROPERTIES, PRMX_LOG
!56  BRAGFLO
     MATERIALS,  S_MB139
     PROPERTIES, RELP_MOD
!57  BRAGFLO
     MATERIALS,  S_MB139
     PROPERTIES, SAT_RBRN
!58  BRAGFLO
     MATERIALS,  S_MB139
     PROPERTIES, PORE_DIS
!59  BRAGFLO
     MATERIALS,  S_HALITE
     PROPERTIES, PRESSURE
!60  BRAGFLO
     MATERIALS,  CASTILER
     PROPERTIES, PRESSURE
!61  BRAGFLO
     MATERIALS,  CASTILER
     PROPERTIES, PRMX_LOG
!62  BRAGFLO
     MATERIALS,  CASTILER
     PROPERTIES, COMP_RCK
!63  BRAGFLO
     MATERIALS,  BH_SAND
     PROPERTIES, PRMX_LOG
!64  BRAGFLO
     MATERIALS,  DRZ_1
     PROPERTIES, PRMX_LOG
!65  BRAGFLO
     MATERIALS,  CONC_PLG
     PROPERTIES, PRMX_LOG
!66  BRAGFLO
     MATERIALS,  SHFTU
     PROPERTIES, SAT_RBRN
!67  BRAGFLO
     MATERIALS,  SHFTU
     PROPERTIES, SAT_RGAS
!68  BRAGFLO
     MATERIALS,  SHFTU
     PROPERTIES, PRMX_LOG
!69  BRAGFLO
     MATERIALS,  SHFTL_T1
     PROPERTIES, PRMX_LOG
!70  BRAGFLO
     MATERIALS,  SHFTL_T2
     PROPERTIES, PRMX_LOG
!71  BRAGFLO
     MATERIALS,  WAS_AREA
     PROPERTIES, BIOGENFC
!72
     MATERIALS,  PCS_T1
     PROPERTIES, POROSITY
!73
```


Information Only

```
     MATERIALS,  PCS_T2
     PROPERTIES, POROSITY
!74
     MATERIALS,  PCS_T3
     PROPERTIES, POROSITY
!75
     MATERIALS,  PCS_T2
     PROPERTIES, POR2PERM
!
!==========================================================================
!
*END
```

Appendix II. Input file to PRELHS for Replicate 2

```
! TITLE:          PCS-2012 PRELHS (LHS1) Input File
! ANALYSIS PLAN: AP-161
! ANALYST:        Tom Kirchner
! CREATED:        July 2012
!
!  LHSCALC = PCS-2012 REALIZATION 2
!==========================================================================
!
!  DESCRIPTION:
!
!  WIPP PCS-2012 Performance Assessment Baseline Calculation,
!  aka  (AP161)
!
!  This input file to PRELHS is used to generate, as an output file, an
LHS
!  input file containing all distribution information and execution
options
!  required to create a sample for Replicate R2 for the WIPP PCS-2012 PA
!
!  Changes from PABC09 analyses: CELLULS:FBETA removed
!                                Material CONC_PCS replaced by PCS_T1 for
4 properties
!                                     (PRMX_LOG, SAT_RBRN, SAT_RGAS, and
POR_DIS)
!                                     PCS_T1:POROSITY added
!                                     PCS_T2:POROSITY added
!                                     PCS_T3:POROSITY added
!                                     PCS_T2:POR2PERM added
!                                     PCS_T1:SAT_IBRN added
!
!Also, LHS_EDIT should control 41<42, and 74<73<72 (WAS_AREA:GRATMICI <
WAS_AREA:GRATMICH and
!    PCS_T3:POROSITY < PCS_T2:POROSITY < PCS_T1:POROSITY)
!
!========= No Comments Allowed between *ECHOLHS and *ENDECHO
================
!
*ECHOLHS
```


Information Only

```
TITLE PABC09, AP161 Replicate R2 Input File for the LHS Code
NOBS            100
RANDOM SEED     168866235
CORRELATION MATRIX
    2
    53  54 -0.99
    61  62 -0.75
OUTPUT CORR HIST DATA
*ENDECHO
!
!== PROPERTIES TO BE RETRIEVED FROM WIPP PA CALCULATION DATABASE ==
!
*RETRIEVE
!1    CCDFGF
      MATERIALS,  GLOBAL
      PROPERTIES, PBRINE
!2
      MATERIALS,  REFCON
      PROPERTIES, LHSBLANK
!3
      MATERIALS,  REFCON
      PROPERTIES, LHSBLANK
!4    CUTTINGS_S
      MATERIALS,  BOREHOLE
      PROPERTIES, DOMEGA
!5    CUTTINGS_S
      MATERIALS,  BOREHOLE
      PROPERTIES, TAUFAIL
!6
      MATERIALS,  REFCON
      PROPERTIES, LHSBLANK
!7
      MATERIALS,  REFCON
      PROPERTIES, LHSBLANK
!8    DRSPALL
      MATERIALS,  SPALLMOD
      PROPERTIES, REPIPERM
!9    DRSPALL
      MATERIALS,  SPALLMOD
      PROPERTIES, TENSLSTR
!10   DRSPALL
      MATERIALS,  SPALLMOD
      PROPERTIES, PARTDIAM
!11   DRSPALL
      MATERIALS,  SPALLMOD
      PROPERTIES, REPIPOR
!12
      MATERIALS,  REFCON
      PROPERTIES, LHSBLANK
!13
      MATERIALS,  REFCON
      PROPERTIES, LHSBLANK
!14
      MATERIALS,  REFCON
```


Information Only

```
     PROPERTIES, LHSBLANK
!15  PANEL
       MATERIALS,      SOLMOD3
       PROPERTIES,     SOLVAR
!16  PANEL
       MATERIALS,      SOLMOD4
       PROPERTIES,     SOLVAR
!17  PANEL
     MATERIALS,  PHUMOX3
     PROPERTIES, PHUMCIM
!18  PANEL/SECOTP2D
     MATERIALS,  GLOBAL
     PROPERTIES, OXSTAT
!19
     MATERIALS,  REFCON
     PROPERTIES, LHSBLANK
!20
     MATERIALS,  REFCON
     PROPERTIES, LHSBLANK
!21
     MATERIALS,  REFCON
     PROPERTIES, LHSBLANK
!22
     MATERIALS,  REFCON
     PROPERTIES, LHSBLANK
!23  SECOTP2D
     MATERIALS,  CULEBRA
     PROPERTIES, MINP_FAC
!24  SECOTP2D
     MATERIALS,  GLOBAL
     PROPERTIES, TRANSIDX
!25  SECOTP2D
     MATERIALS,  GLOBAL
     PROPERTIES, CLIMTIDX
!26  SECOTP2D
     MATERIALS,  CULEBRA
     PROPERTIES, HMBLKLT
!27  SECOTP2D
     MATERIALS,  CULEBRA
     PROPERTIES, APOROS
!28  SECOTP2D
     MATERIALS,  CULEBRA
     PROPERTIES, DPOROS
!29  SECOTP2D
     MATERIALS,  U+6
     PROPERTIES, MKD_U
!30  SECOTP2D
     MATERIALS,  U+4
     PROPERTIES, MKD_U
!31  SECOTP2D
     MATERIALS,  PU+3
     PROPERTIES, MKD_PU
!32  SECOTP2D
     MATERIALS,  PU+4
```


Information Only

```
     PROPERTIES, MKD_PU
!33  SECOTP2D
     MATERIALS,  TH+4
     PROPERTIES, MKD_TH
!34  SECOTP2D
     MATERIALS,  AM+3
     PROPERTIES, MKD_AM
!35
     MATERIALS,  REFCON
     PROPERTIES, LHSBLANK
!36
     MATERIALS,  REFCON
     PROPERTIES, LHSBLANK
!37
     MATERIALS,  REFCON
     PROPERTIES, LHSBLANK
!38
     MATERIALS,  REFCON
     PROPERTIES, LHSBLANK
!39  BRAGFLO
     MATERIALS,  STEEL
     PROPERTIES, CORRMCO2
!40  BRAGFLO/PANEL
     MATERIALS,  WAS_AREA
     PROPERTIES, PROBDEG
!41  BRAGFLO
     MATERIALS,  WAS_AREA
     PROPERTIES, GRATMICI
!42  BRAGFLO
     MATERIALS,  WAS_AREA
     PROPERTIES, GRATMICH
!43  BRAGFLO
     MATERIALS,  PCS_T1
     PROPERTIES, SAT_IBRN
!44  BRAGFLO
     MATERIALS,  WAS_AREA
     PROPERTIES, SAT_RGAS
!45  BRAGFLO
     MATERIALS,  WAS_AREA
     PROPERTIES, SAT_RBRN
!46  BRAGFLO
     MATERIALS,  WAS_AREA
     PROPERTIES, SAT_WICK
!47  BRAGFLO
     MATERIALS,  DRZ_PCS
     PROPERTIES, PRMX_LOG
!48  BRAGFLO
     MATERIALS,  PCS_T1
     PROPERTIES, PRMX_LOG
!49  BRAGFLO
     MATERIALS,  PCS_T1
     PROPERTIES, SAT_RGAS
!50  BRAGFLO
     MATERIALS,  PCS_T1
```


Information Only

```
     PROPERTIES, SAT_RBRN
!51  BRAGFLO
     MATERIALS,  PCS_T1
     PROPERTIES, PORE_DIS
!52  BRAGFLO
     MATERIALS,  S_HALITE
     PROPERTIES, POROSITY
!53  BRAGFLO
     MATERIALS,  S_HALITE
     PROPERTIES, PRMX_LOG
!54  BRAGFLO
     MATERIALS,  S_HALITE
     PROPERTIES, COMP_RCK
!55  BRAGFLO
     MATERIALS,  S_MB139
     PROPERTIES, PRMX_LOG
!56  BRAGFLO
     MATERIALS,  S_MB139
     PROPERTIES, RELP_MOD
!57  BRAGFLO
     MATERIALS,  S_MB139
     PROPERTIES, SAT_RBRN
!58  BRAGFLO
     MATERIALS,  S_MB139
     PROPERTIES, PORE_DIS
!59  BRAGFLO
     MATERIALS,  S_HALITE
     PROPERTIES, PRESSURE
!60  BRAGFLO
     MATERIALS,  CASTILER
     PROPERTIES, PRESSURE
!61  BRAGFLO
     MATERIALS,  CASTILER
     PROPERTIES, PRMX_LOG
!62  BRAGFLO
     MATERIALS,  CASTILER
     PROPERTIES, COMP_RCK
!63  BRAGFLO
     MATERIALS,  BH_SAND
     PROPERTIES, PRMX_LOG
!64  BRAGFLO
     MATERIALS,  DRZ_1
     PROPERTIES, PRMX_LOG
!65  BRAGFLO
     MATERIALS,  CONC_PLG
     PROPERTIES, PRMX_LOG
!66  BRAGFLO
     MATERIALS,  SHFTU
     PROPERTIES, SAT_RBRN
!67  BRAGFLO
     MATERIALS,  SHFTU
     PROPERTIES, SAT_RGAS
!68  BRAGFLO
     MATERIALS,  SHFTU
```


Information Only

```
     PROPERTIES, PRMX_LOG
!69  BRAGFLO
     MATERIALS,  SHFTL_T1
     PROPERTIES, PRMX_LOG
!70  BRAGFLO
     MATERIALS,  SHFTL_T2
     PROPERTIES, PRMX_LOG
!71  BRAGFLO
     MATERIALS,  WAS_AREA
     PROPERTIES, BIOGENFC
!72
     MATERIALS,  PCS_T1
     PROPERTIES, POROSITY
!73
     MATERIALS,  PCS_T2
     PROPERTIES, POROSITY
!74
     MATERIALS,  PCS_T3
     PROPERTIES, POROSITY
!75
     MATERIALS,  PCS_T2
     PROPERTIES, POR2PERM
!
!==============================================================================
!
*END
```


Information Only

Appendix III. Input file to PRELHS for Replicate 3

```
! TITLE:          PCS-2012 PRELHS (LHS1) Input File
! ANALYSIS PLAN: AP-161
! ANALYST:        Tom Kirchner
! CREATED:        July 2012
!
!  LHSCALC = PCS-2012 REALIZATION 3
!==========================================================================
!
!  DESCRIPTION:
!
!  WIPP PCS-2012 Performance Assessment Baseline Calculation,
!  aka  (AP161)
!
!  This input file to PRELHS is used to generate, as an output file, an
LHS
!  input file containing all distribution information and execution
options
!  required to create a sample for Replicate R3 for the WIPP PCS-2012 PA
!
!  Changes from PABC09 analyses: CELLULS:FBETA removed
!                                Material CONC_PCS replaced by PCS_T1 for
4 properties
!                                     (PRMX_LOG, SAT_RBRN, SAT_RGAS, and
POR_DIS)
!                                PCS_T1:POROSITY added
!                                PCS_T2:POROSITY added
!                                PCS_T3:POROSITY added
!                                PCS_T2:POR2PERM added
!                                PCS_T1:SAT_IBRN added
!
!Also, LHS_EDIT should control 41<42, and 74<73<72 (WAS_AREA:GRATMICI <
WAS_AREA:GRATMICH and
!    PCS_T3:POROSITY < PCS_T2:POROSITY < PCS_T1:POROSITY)
!
!========= No Comments Allowed between *ECHOLHS and *ENDECHO
================
!
*ECHOLHS
TITLE PABC09, AP161 Replicate R3 Input File for the LHS Code
NOBS           100
RANDOM SEED    292058223
CORRELATION MATRIX
    2
    53  54 -0.99
    61  62 -0.75
OUTPUT CORR HIST DATA
*ENDECHO
!
!== PROPERTIES TO BE RETRIEVED FROM WIPP PA CALCULATION DATABASE ==
!
*RETRIEVE
!1    CCDFGF
```


Information Only

```
     MATERIALS,  GLOBAL
     PROPERTIES, PBRINE
!2
     MATERIALS,  REFCON
     PROPERTIES, LHSBLANK
!3
     MATERIALS,  REFCON
     PROPERTIES, LHSBLANK
!4   CUTTINGS_S
     MATERIALS,  BOREHOLE
     PROPERTIES, DOMEGA
!5   CUTTINGS_S
     MATERIALS,  BOREHOLE
     PROPERTIES, TAUFAIL
!6
     MATERIALS,  REFCON
     PROPERTIES, LHSBLANK
!7
     MATERIALS,  REFCON
     PROPERTIES, LHSBLANK
!8   DRSPALL
     MATERIALS,  SPALLMOD
     PROPERTIES, REPIPERM
!9   DRSPALL
     MATERIALS,  SPALLMOD
     PROPERTIES, TENSLSTR
!10  DRSPALL
     MATERIALS,  SPALLMOD
     PROPERTIES, PARTDIAM
!11  DRSPALL
     MATERIALS,  SPALLMOD
     PROPERTIES, REPIPOR
!12
     MATERIALS,  REFCON
     PROPERTIES, LHSBLANK
!13
     MATERIALS,  REFCON
     PROPERTIES, LHSBLANK
!14
     MATERIALS,  REFCON
     PROPERTIES, LHSBLANK
!15  PANEL
       MATERIALS,      SOLMOD3
       PROPERTIES,     SOLVAR
!16  PANEL
       MATERIALS,      SOLMOD4
       PROPERTIES,     SOLVAR
!17  PANEL
     MATERIALS,  PHUMOX3
     PROPERTIES, PHUMCIM
!18  PANEL/SECOTP2D
     MATERIALS,  GLOBAL
     PROPERTIES, OXSTAT
!19
```


Information Only

```
     MATERIALS,  REFCON
     PROPERTIES, LHSBLANK
!20
     MATERIALS,  REFCON
     PROPERTIES, LHSBLANK
!21
     MATERIALS,  REFCON
     PROPERTIES, LHSBLANK
!22
     MATERIALS,  REFCON
     PROPERTIES, LHSBLANK
!23  SECOTP2D
     MATERIALS,  CULEBRA
     PROPERTIES, MINP_FAC
!24  SECOTP2D
     MATERIALS,  GLOBAL
     PROPERTIES, TRANSIDX
!25  SECOTP2D
     MATERIALS,  GLOBAL
     PROPERTIES, CLIMTIDX
!26  SECOTP2D
     MATERIALS,  CULEBRA
     PROPERTIES, HMBLKLT
!27  SECOTP2D
     MATERIALS,  CULEBRA
     PROPERTIES, APOROS
!28  SECOTP2D
     MATERIALS,  CULEBRA
     PROPERTIES, DPOROS
!29  SECOTP2D
     MATERIALS,  U+6
     PROPERTIES, MKD_U
!30  SECOTP2D
     MATERIALS,  U+4
     PROPERTIES, MKD_U
!31  SECOTP2D
     MATERIALS,  PU+3
     PROPERTIES, MKD_PU
!32  SECOTP2D
     MATERIALS,  PU+4
     PROPERTIES, MKD_PU
!33  SECOTP2D
     MATERIALS,  TH+4
     PROPERTIES, MKD_TH
!34  SECOTP2D
     MATERIALS,  AM+3
     PROPERTIES, MKD_AM
!35
     MATERIALS,  REFCON
     PROPERTIES, LHSBLANK
!36
     MATERIALS,  REFCON
     PROPERTIES, LHSBLANK
!37
```


Information Only

```
     MATERIALS,  REFCON
     PROPERTIES, LHSBLANK
!38
     MATERIALS,  REFCON
     PROPERTIES, LHSBLANK
!39  BRAGFLO
     MATERIALS,  STEEL
     PROPERTIES, CORRMCO2
!40  BRAGFLO/PANEL
     MATERIALS,  WAS_AREA
     PROPERTIES, PROBDEG
!41  BRAGFLO
     MATERIALS,  WAS_AREA
     PROPERTIES, GRATMICI
!42  BRAGFLO
     MATERIALS,  WAS_AREA
     PROPERTIES, GRATMICH
!43  BRAGFLO
     MATERIALS,  PCS_T1
     PROPERTIES, SAT_IBRN
!44  BRAGFLO
     MATERIALS,  WAS_AREA
     PROPERTIES, SAT_RGAS
!45  BRAGFLO
     MATERIALS,  WAS_AREA
     PROPERTIES, SAT_RBRN
!46  BRAGFLO
     MATERIALS,  WAS_AREA
     PROPERTIES, SAT_WICK
!47  BRAGFLO
     MATERIALS,  DRZ_PCS
     PROPERTIES, PRMX_LOG
!48  BRAGFLO
     MATERIALS,  PCS_T1
     PROPERTIES, PRMX_LOG
!49  BRAGFLO
     MATERIALS,  PCS_T1
     PROPERTIES, SAT_RGAS
!50  BRAGFLO
     MATERIALS,  PCS_T1
     PROPERTIES, SAT_RBRN
!51  BRAGFLO
     MATERIALS,  PCS_T1
     PROPERTIES, PORE_DIS
!52  BRAGFLO
     MATERIALS,  S_HALITE
     PROPERTIES, POROSITY
!53  BRAGFLO
     MATERIALS,  S_HALITE
     PROPERTIES, PRMX_LOG
!54  BRAGFLO
     MATERIALS,  S_HALITE
     PROPERTIES, COMP_RCK
!55  BRAGFLO
```


Information Only

```
     MATERIALS,  S_MB139
     PROPERTIES, PRMX_LOG
!56  BRAGFLO
     MATERIALS,  S_MB139
     PROPERTIES, RELP_MOD
!57  BRAGFLO
     MATERIALS,  S_MB139
     PROPERTIES, SAT_RBRN
!58  BRAGFLO
     MATERIALS,  S_MB139
     PROPERTIES, PORE_DIS
!59  BRAGFLO
     MATERIALS,  S_HALITE
     PROPERTIES, PRESSURE
!60  BRAGFLO
     MATERIALS,  CASTILER
     PROPERTIES, PRESSURE
!61  BRAGFLO
     MATERIALS,  CASTILER
     PROPERTIES, PRMX_LOG
!62  BRAGFLO
     MATERIALS,  CASTILER
     PROPERTIES, COMP_RCK
!63  BRAGFLO
     MATERIALS,  BH_SAND
     PROPERTIES, PRMX_LOG
!64  BRAGFLO
     MATERIALS,  DRZ_1
     PROPERTIES, PRMX_LOG
!65  BRAGFLO
     MATERIALS,  CONC_PLG
     PROPERTIES, PRMX_LOG
!66  BRAGFLO
     MATERIALS,  SHFTU
     PROPERTIES, SAT_RBRN
!67  BRAGFLO
     MATERIALS,  SHFTU
     PROPERTIES, SAT_RGAS
!68  BRAGFLO
     MATERIALS,  SHFTU
     PROPERTIES, PRMX_LOG
!69  BRAGFLO
     MATERIALS,  SHFTL_T1
     PROPERTIES, PRMX_LOG
!70  BRAGFLO
     MATERIALS,  SHFTL_T2
     PROPERTIES, PRMX_LOG
!71  BRAGFLO
     MATERIALS,  WAS_AREA
     PROPERTIES, BIOGENFC
!72
     MATERIALS,  PCS_T1
     PROPERTIES, POROSITY
!73
```


Information Only

```
     MATERIALS,  PCS_T2
     PROPERTIES, POROSITY
!74
     MATERIALS,  PCS_T3
     PROPERTIES, POROSITY
!75
     MATERIALS,  PCS_T2
     PROPERTIES, POR2PERM
!
!==========================================================================
!
*END
```

Appendix IV. PRELHS Output (Transfer) File for Replicate 1

```
TITLE SDB: ParamDB            Calc: AP161        Ver: 2.00     07/27/12
16:17:03
TITLE PABC09, AP161, Replicate R1 Input File for the LHS Code
NOBS           100
RANDOM SEED    582592385
UNIFORM                 GLOBAL    PBRINE
    1.00000E-02    6.00000E-01
UNIFORM                 REFCON    LHSBLANK
    0.00000E+00    1.00000E+00
UNIFORM                 REFCON    LHSBLANK
    0.00000E+00    1.00000E+00
USER DISTRIBUTION  (CUMULATIVE)       BOREHOLE  DOMEGA
        10          SPECIFIED    CONTINUOUS
    4.20000E+00   0.15000
    6.30000E+00   0.50000
    8.40000E+00   0.15000
    1.05000E+01   0.10000
    1.26000E+01   0.05000
    1.47000E+01   0.02000
    1.68000E+01   0.01000
    1.88000E+01   0.01000
    2.09000E+01   0.01000
    2.30000E+01   0.00000
LOGUNIFORM              BOREHOLE  TAUFAIL
    5.00000E-02    7.70000E+01
UNIFORM                 REFCON    LHSBLANK
    0.00000E+00    1.00000E+00
UNIFORM                 REFCON    LHSBLANK
    0.00000E+00    1.00000E+00
LOGUNIFORM              SPALLMOD  REPIPERM
    2.40000E-14    2.40000E-12
UNIFORM                 SPALLMOD  TENSLSTR
    1.20000E+05    1.70000E+05
LOGUNIFORM              SPALLMOD  PARTDIAM
    1.00000E-03    1.00000E-01
UNIFORM                 SPALLMOD  REPIPOR
    3.50000E-01    6.60000E-01
UNIFORM                 REFCON    LHSBLANK
```


Information Only

```
    0.00000E+00    1.00000E+00
UNIFORM                 REFCON    LHSBLANK
    0.00000E+00    1.00000E+00
UNIFORM                 REFCON    LHSBLANK
    0.00000E+00    1.00000E+00
USER DISTRIBUTION  (CUMULATIVE)       SOLMOD3   SOLVAR
        48          SPECIFIED    CONTINUOUS
   -4.20000E+00   0.00290
   -4.05000E+00   0.00000
   -3.90000E+00   0.00580
   -3.75000E+00   0.01150
   -3.60000E+00   0.01450
   -3.45000E+00   0.00290
   -3.30000E+00   0.00580
   -3.15000E+00   0.00860
   -3.00000E+00   0.00290
   -2.85000E+00   0.00000
   -2.70000E+00   0.00580
   -2.55000E+00   0.00870
   -2.40000E+00   0.00860
   -2.25000E+00   0.00580
   -2.10000E+00   0.00000
   -1.95000E+00   0.00290
   -1.80000E+00   0.00580
   -1.65000E+00   0.00580
   -1.50000E+00   0.00570
   -1.35000E+00   0.02610
   -1.20000E+00   0.02600
   -1.05000E+00   0.02890
   -9.00000E-01   0.02600
   -7.50000E-01   0.02890
   -6.00000E-01   0.03760
   -4.50000E-01   0.06070
   -3.00000E-01   0.05200
   -1.50000E-01   0.07220
    0.00000E+00   0.07810
    1.50000E-01   0.07800
    3.00000E-01   0.07800
    4.50000E-01   0.03470
    6.00000E-01   0.08380
    7.50000E-01   0.08960
    9.00000E-01   0.02030
    1.05000E+00   0.01440
    1.20000E+00   0.01450
    1.35000E+00   0.00860
    1.50000E+00   0.00290
    1.65000E+00   0.01160
    1.80000E+00   0.00860
    1.95000E+00   0.00580
    2.10000E+00   0.00000
    2.25000E+00   0.00290
    2.40000E+00   0.00290
    2.55000E+00   0.00290
    2.70000E+00   0.00000
```


Information Only

```
    2.85000E+00   0.00000
USER DISTRIBUTION  (CUMULATIVE)        SOLMOD4    SOLVAR
        38          SPECIFIED     CONTINUOUS
   -2.25000E+00   0.01430
   -2.10000E+00   0.00710
   -1.95000E+00   0.01430
   -1.80000E+00   0.02860
   -1.65000E+00   0.02860
   -1.50000E+00   0.05000
   -1.35000E+00   0.07850
   -1.20000E+00   0.04290
   -1.05000E+00   0.03570
   -9.00000E-01   0.05710
   -7.50000E-01   0.08580
   -6.00000E-01   0.10710
   -4.50000E-01   0.02140
   -3.00000E-01   0.03570
   -1.50000E-01   0.04290
    0.00000E+00   0.03570
    1.50000E-01   0.09290
    3.00000E-01   0.05000
    4.50000E-01   0.00710
    6.00000E-01   0.04290
    7.50000E-01   0.03570
    9.00000E-01   0.02140
    1.05000E+00   0.00000
    1.20000E+00   0.00720
    1.35000E+00   0.01420
    1.50000E+00   0.00720
    1.65000E+00   0.00710
    1.80000E+00   0.00000
    1.95000E+00   0.00720
    2.10000E+00   0.00000
    2.25000E+00   0.00710
    2.40000E+00   0.00000
    2.55000E+00   0.00000
    2.70000E+00   0.00000
    2.85000E+00   0.00000
    3.00000E+00   0.00000
    3.15000E+00   0.01430
    3.30000E+00   0.00000
USER DISTRIBUTION  (CUMULATIVE)        PHUMOX3    PHUMCIM
         3          SPECIFIED     CONTINUOUS
    6.50000E-02   0.50000
    1.37000E+00   0.50000
    1.60000E+00   0.00000
UNIFORM                 GLOBAL     OXSTAT
    0.00000E+00    1.00000E+00
UNIFORM                 REFCON     LHSBLANK
    0.00000E+00    1.00000E+00
UNIFORM                 REFCON     LHSBLANK
    0.00000E+00    1.00000E+00
UNIFORM                 REFCON     LHSBLANK
    0.00000E+00    1.00000E+00
```


Information Only

```
UNIFORM                 REFCON    LHSBLANK
    0.00000E+00    1.00000E+00
UNIFORM                 CULEBRA   MINP_FAC
    1.00000E+00    1.00000E+03
UNIFORM                 GLOBAL    TRANSIDX
    0.00000E+00    1.00000E+00
USER DISTRIBUTION  (CUMULATIVE)       GLOBAL    CLIMTIDX
         4          SPECIFIED    CONTINUOUS
    1.00000E+00   0.75000
    1.25000E+00   0.00000
    1.50000E+00   0.25000
    2.25000E+00   0.00000
UNIFORM                 CULEBRA   HMBLKLT
    5.00000E-02    5.00000E-01
LOGUNIFORM              CULEBRA   APOROS
    1.00000E-04    1.00000E-02
USER DISTRIBUTION  (CUMULATIVE)       CULEBRA   DPOROS
         7          SPECIFIED    CONTINUOUS
    1.00000E-01   0.10000
    1.10000E-01   0.15000
    1.20000E-01   0.25000
    1.60000E-01   0.25000
    1.80000E-01   0.15000
    1.90000E-01   0.10000
    2.50000E-01   0.00000
LOGUNIFORM              U+6       MKD_U
    3.00000E-05    2.00000E-02
LOGUNIFORM              U+4       MKD_U
    5.00000E-04    1.00000E+01
LOGUNIFORM              PU+3      MKD_PU
    5.00000E-03    4.00000E-01
LOGUNIFORM              PU+4      MKD_PU
    5.00000E-04    1.00000E+01
LOGUNIFORM              TH+4      MKD_TH
    5.00000E-04    1.00000E+01
LOGUNIFORM              AM+3      MKD_AM
    5.00000E-03    4.00000E-01
UNIFORM                 REFCON    LHSBLANK
    0.00000E+00    1.00000E+00
UNIFORM                 REFCON    LHSBLANK
    0.00000E+00    1.00000E+00
UNIFORM                 REFCON    LHSBLANK
    0.00000E+00    1.00000E+00
UNIFORM                 REFCON    LHSBLANK
    0.00000E+00    1.00000E+00
UNIFORM                 STEEL     CORRMCO2
    0.00000E+00    3.17000E-14
USER DISTRIBUTION  (DELTA)           WAS_AREA  PROBDEG
         2          SPECIFIED    DISCRETE
    1.00000E+00   0.75000
    2.00000E+00   0.25000
UNIFORM                 WAS_AREA  GRATMICI
    3.08269E-11    5.56921E-10
UNIFORM                 WAS_AREA  GRATMICH
```


Information Only

```
    0.00000E+00    1.02717E-09
UNIFORM                 PCS_T1    SAT_IBRN
    4.00000E-02    1.60000E-01
UNIFORM                 WAS_AREA  SAT_RGAS
    0.00000E+00    1.50000E-01
UNIFORM                 WAS_AREA  SAT_RBRN
    0.00000E+00    5.52000E-01
UNIFORM                 WAS_AREA  SAT_WICK
    0.00000E+00    1.00000E+00
TRIANGULAR              DRZ_PCS   PRMX_LOG
   -2.06990E+01   -1.87496E+01   -1.70000E+01
UNIFORM                 PCS_T1    PRMX_LOG
   -2.10000E+01   -1.20000E+01
UNIFORM                 PCS_T1    SAT_RGAS
    0.00000E+00    4.00000E-01
USER DISTRIBUTION  (CUMULATIVE)       PCS_T1    SAT_RBRN
         3          SPECIFIED    CONTINUOUS
    0.00000E+00   0.50000
    2.00000E-01   0.50000
    6.00000E-01   0.00000
USER DISTRIBUTION  (CUMULATIVE)       PCS_T1    PORE_DIS
         3          SPECIFIED    CONTINUOUS
    1.10000E-01   0.50000
    9.40000E-01   0.50000
    8.10000E+00   0.00000
USER DISTRIBUTION  (CUMULATIVE)       S_HALITE  POROSITY
         3          SPECIFIED    CONTINUOUS
    1.00000E-03   0.50000
    1.00000E-02   0.50000
    5.19000E-02   0.00000
UNIFORM                 S_HALITE  PRMX_LOG
   -2.40000E+01   -2.10000E+01
UNIFORM                 S_HALITE  COMP_RCK
    2.94000E-12    1.92000E-10
STUDENT                 S_MB139   PRMX_LOG
         6
 -2.10000E+01 -1.92000E+01 -1.91000E+01 -1.88000E+01 -1.81000E+01 -
1.71000E+01
USER DISTRIBUTION  (DELTA)           S_MB139   RELP_MOD
         4          SPECIFIED    DISCRETE
    1.00000E+00   0.50000
    2.00000E+00   0.00000
    3.00000E+00   0.00000
    4.00000E+00   0.50000
STUDENT                 S_MB139   SAT_RBRN
         6
  7.78460E-03  6.88420E-02  6.98600E-02  7.26200E-02  1.08610E-01
1.74010E-01
STUDENT                 S_MB139   PORE_DIS
         6
  4.90530E-01  5.57750E-01  6.52000E-01  6.55000E-01  6.64520E-01
8.41780E-01
UNIFORM                 S_HALITE  PRESSURE
    1.10400E+07    1.38900E+07
```


Information Only

```
TRIANGULAR                CASTILER  PRESSURE
    1.11000E+07    1.27000E+07    1.70000E+07
TRIANGULAR                CASTILER  PRMX_LOG
   -1.47000E+01   -1.18000E+01   -9.80000E+00
TRIANGULAR                CASTILER  COMP_RCK
    2.00000E-11    4.00000E-11    1.00000E-10
UNIFORM                   BH_SAND   PRMX_LOG
   -1.63000E+01   -1.10000E+01
UNIFORM                   DRZ_1     PRMX_LOG
   -1.94000E+01   -1.25000E+01
UNIFORM                   CONC_PLG  PRMX_LOG
   -1.90000E+01   -1.70000E+01
USER DISTRIBUTION  (CUMULATIVE)        SHFTU     SAT_RBRN
         3          SPECIFIED    CONTINUOUS
    0.00000E+00   0.50000
    2.00000E-01   0.50000
    6.00000E-01   0.00000
UNIFORM                   SHFTU     SAT_RGAS
    0.00000E+00    4.00000E-01
USER DISTRIBUTION  (CUMULATIVE)        SHFTU     PRMX_LOG
         9          SPECIFIED    CONTINUOUS
   -2.05000E+01   0.03000
   -2.00000E+01   0.08000
   -1.95000E+01   0.13000
   -1.90000E+01   0.19000
   -1.85000E+01   0.22000
   -1.80000E+01   0.24000
   -1.75000E+01   0.10000
   -1.70000E+01   0.01000
   -1.65000E+01   0.00000
USER DISTRIBUTION  (CUMULATIVE)        SHFTL_T1  PRMX_LOG
         8          SPECIFIED    CONTINUOUS
   -2.00000E+01   0.01000
   -1.95000E+01   0.09000
   -1.90000E+01   0.20700
   -1.85000E+01   0.33000
   -1.80000E+01   0.23600
   -1.75000E+01   0.12000
   -1.70000E+01   0.00700
   -1.65000E+01   0.00000
USER DISTRIBUTION  (CUMULATIVE)        SHFTL_T2  PRMX_LOG
        10          SPECIFIED    CONTINUOUS
   -2.25000E+01   0.02000
   -2.20000E+01   0.06000
   -2.15000E+01   0.09000
   -2.10000E+01   0.13500
   -2.05000E+01   0.22000
   -2.00000E+01   0.17500
   -1.95000E+01   0.16500
   -1.90000E+01   0.10000
   -1.85000E+01   0.03500
   -1.80000E+01   0.00000
UNIFORM                   WAS_AREA  BIOGENFC
    0.00000E+00    1.00000E+00
```


Information Only

```
UNIFORM                    PCS_T1     POROSITY
    6.60000E-02     1.87000E-01
UNIFORM                    PCS_T2     POROSITY
    2.50000E-02     7.50000E-02
UNIFORM                    PCS_T3     POROSITY
    1.00000E-03     5.19000E-02
NORMAL                     PCS_T2     POR2PERM
   -1.72000E+00     1.72000E+00
CORRELATION MATRIX
    2
    53  54 -0.99
    61  62 -0.75
OUTPUT CORR HIST DATA
TITLE SDB: ParamDB            Calc: AP161        Ver: 2.00     07/27/12
16:17:03
```


Information Only

Appendix V. PRELHS Output (Transfer) File for Replicate 2

```
TITLE SDB: ParamDB            Calc: AP161        Ver: 2.00     07/27/12
16:17:28
TITLE PABC09, AP161 Replicate R2 Input File for the LHS Code
NOBS           100
RANDOM SEED    168866235
UNIFORM                 GLOBAL    PBRINE
    1.00000E-02    6.00000E-01
UNIFORM                 REFCON    LHSBLANK
    0.00000E+00    1.00000E+00
UNIFORM                 REFCON    LHSBLANK
    0.00000E+00    1.00000E+00
USER DISTRIBUTION  (CUMULATIVE)       BOREHOLE  DOMEGA
        10          SPECIFIED    CONTINUOUS
    4.20000E+00   0.15000
    6.30000E+00   0.50000
    8.40000E+00   0.15000
    1.05000E+01   0.10000
    1.26000E+01   0.05000
    1.47000E+01   0.02000
    1.68000E+01   0.01000
    1.88000E+01   0.01000
    2.09000E+01   0.01000
    2.30000E+01   0.00000
LOGUNIFORM              BOREHOLE  TAUFAIL
    5.00000E-02    7.70000E+01
UNIFORM                 REFCON    LHSBLANK
    0.00000E+00    1.00000E+00
UNIFORM                 REFCON    LHSBLANK
    0.00000E+00    1.00000E+00
LOGUNIFORM              SPALLMOD  REPIPERM
    2.40000E-14    2.40000E-12
UNIFORM                 SPALLMOD  TENSLSTR
    1.20000E+05    1.70000E+05
LOGUNIFORM              SPALLMOD  PARTDIAM
    1.00000E-03    1.00000E-01
UNIFORM                 SPALLMOD  REPIPOR
    3.50000E-01    6.60000E-01
UNIFORM                 REFCON    LHSBLANK
    0.00000E+00    1.00000E+00
UNIFORM                 REFCON    LHSBLANK
    0.00000E+00    1.00000E+00
UNIFORM                 REFCON    LHSBLANK
    0.00000E+00    1.00000E+00
USER DISTRIBUTION  (CUMULATIVE)       SOLMOD3   SOLVAR
        48          SPECIFIED    CONTINUOUS
   -4.20000E+00   0.00290
   -4.05000E+00   0.00000
   -3.90000E+00   0.00580
   -3.75000E+00   0.01150
   -3.60000E+00   0.01450
   -3.45000E+00   0.00290
   -3.30000E+00   0.00580
```


Information Only

```
   -3.15000E+00   0.00860
   -3.00000E+00   0.00290
   -2.85000E+00   0.00000
   -2.70000E+00   0.00580
   -2.55000E+00   0.00870
   -2.40000E+00   0.00860
   -2.25000E+00   0.00580
   -2.10000E+00   0.00000
   -1.95000E+00   0.00290
   -1.80000E+00   0.00580
   -1.65000E+00   0.00580
   -1.50000E+00   0.00570
   -1.35000E+00   0.02610
   -1.20000E+00   0.02600
   -1.05000E+00   0.02890
   -9.00000E-01   0.02600
   -7.50000E-01   0.02890
   -6.00000E-01   0.03760
   -4.50000E-01   0.06070
   -3.00000E-01   0.05200
   -1.50000E-01   0.07220
    0.00000E+00   0.07810
    1.50000E-01   0.07800
    3.00000E-01   0.07800
    4.50000E-01   0.03470
    6.00000E-01   0.08380
    7.50000E-01   0.08960
    9.00000E-01   0.02030
    1.05000E+00   0.01440
    1.20000E+00   0.01450
    1.35000E+00   0.00860
    1.50000E+00   0.00290
    1.65000E+00   0.01160
    1.80000E+00   0.00860
    1.95000E+00   0.00580
    2.10000E+00   0.00000
    2.25000E+00   0.00290
    2.40000E+00   0.00290
    2.55000E+00   0.00290
    2.70000E+00   0.00000
    2.85000E+00   0.00000
USER DISTRIBUTION  (CUMULATIVE)      SOLMOD4   SOLVAR
        38          SPECIFIED    CONTINUOUS
   -2.25000E+00   0.01430
   -2.10000E+00   0.00710
   -1.95000E+00   0.01430
   -1.80000E+00   0.02860
   -1.65000E+00   0.02860
   -1.50000E+00   0.05000
   -1.35000E+00   0.07850
   -1.20000E+00   0.04290
   -1.05000E+00   0.03570
   -9.00000E-01   0.05710
   -7.50000E-01   0.08580
```


Information Only

```
   -6.00000E-01   0.10710
   -4.50000E-01   0.02140
   -3.00000E-01   0.03570
   -1.50000E-01   0.04290
    0.00000E+00   0.03570
    1.50000E-01   0.09290
    3.00000E-01   0.05000
    4.50000E-01   0.00710
    6.00000E-01   0.04290
    7.50000E-01   0.03570
    9.00000E-01   0.02140
    1.05000E+00   0.00000
    1.20000E+00   0.00720
    1.35000E+00   0.01420
    1.50000E+00   0.00720
    1.65000E+00   0.00710
    1.80000E+00   0.00000
    1.95000E+00   0.00720
    2.10000E+00   0.00000
    2.25000E+00   0.00710
    2.40000E+00   0.00000
    2.55000E+00   0.00000
    2.70000E+00   0.00000
    2.85000E+00   0.00000
    3.00000E+00   0.00000
    3.15000E+00   0.01430
    3.30000E+00   0.00000
USER DISTRIBUTION  (CUMULATIVE)       PHUMOX3   PHUMCIM
         3          SPECIFIED    CONTINUOUS
    6.50000E-02   0.50000
    1.37000E+00   0.50000
    1.60000E+00   0.00000
UNIFORM                 GLOBAL    OXSTAT
    0.00000E+00    1.00000E+00
UNIFORM                 REFCON    LHSBLANK
    0.00000E+00    1.00000E+00
UNIFORM                 REFCON    LHSBLANK
    0.00000E+00    1.00000E+00
UNIFORM                 REFCON    LHSBLANK
    0.00000E+00    1.00000E+00
UNIFORM                 REFCON    LHSBLANK
    0.00000E+00    1.00000E+00
UNIFORM                 CULEBRA   MINP_FAC
    1.00000E+00    1.00000E+03
UNIFORM                 GLOBAL    TRANSIDX
    0.00000E+00    1.00000E+00
USER DISTRIBUTION  (CUMULATIVE)       GLOBAL    CLIMTIDX
         4          SPECIFIED    CONTINUOUS
    1.00000E+00   0.75000
    1.25000E+00   0.00000
    1.50000E+00   0.25000
    2.25000E+00   0.00000
UNIFORM                 CULEBRA   HMBLKLT
    5.00000E-02    5.00000E-01
```


Information Only

```
LOGUNIFORM              CULEBRA   APOROS
    1.00000E-04    1.00000E-02
USER DISTRIBUTION  (CUMULATIVE)       CULEBRA   DPOROS
         7          SPECIFIED    CONTINUOUS
    1.00000E-01   0.10000
    1.10000E-01   0.15000
    1.20000E-01   0.25000
    1.60000E-01   0.25000
    1.80000E-01   0.15000
    1.90000E-01   0.10000
    2.50000E-01   0.00000
LOGUNIFORM              U+6       MKD_U
    3.00000E-05    2.00000E-02
LOGUNIFORM              U+4       MKD_U
    5.00000E-04    1.00000E+01
LOGUNIFORM              PU+3      MKD_PU
    5.00000E-03    4.00000E-01
LOGUNIFORM              PU+4      MKD_PU
    5.00000E-04    1.00000E+01
LOGUNIFORM              TH+4      MKD_TH
    5.00000E-04    1.00000E+01
LOGUNIFORM              AM+3      MKD_AM
    5.00000E-03    4.00000E-01
UNIFORM                 REFCON    LHSBLANK
    0.00000E+00    1.00000E+00
UNIFORM                 REFCON    LHSBLANK
    0.00000E+00    1.00000E+00
UNIFORM                 REFCON    LHSBLANK
    0.00000E+00    1.00000E+00
UNIFORM                 REFCON    LHSBLANK
    0.00000E+00    1.00000E+00
UNIFORM                 STEEL     CORRMCO2
    0.00000E+00    3.17000E-14
USER DISTRIBUTION  (DELTA)           WAS_AREA  PROBDEG
         2          SPECIFIED    DISCRETE
    1.00000E+00   0.75000
    2.00000E+00   0.25000
UNIFORM                 WAS_AREA  GRATMICI
    3.08269E-11    5.56921E-10
UNIFORM                 WAS_AREA  GRATMICH
    0.00000E+00    1.02717E-09
UNIFORM                 PCS_T1    SAT_IBRN
    4.00000E-02    1.60000E-01
UNIFORM                 WAS_AREA  SAT_RGAS
    0.00000E+00    1.50000E-01
UNIFORM                 WAS_AREA  SAT_RBRN
    0.00000E+00    5.52000E-01
UNIFORM                 WAS_AREA  SAT_WICK
    0.00000E+00    1.00000E+00
TRIANGULAR              DRZ_PCS   PRMX_LOG
   -2.06990E+01   -1.87496E+01   -1.70000E+01
UNIFORM                 PCS_T1    PRMX_LOG
   -2.10000E+01   -1.20000E+01
UNIFORM                 PCS_T1    SAT_RGAS
```


Information Only

```
    0.00000E+00    4.00000E-01
USER DISTRIBUTION  (CUMULATIVE)       PCS_T1    SAT_RBRN
         3          SPECIFIED    CONTINUOUS
    0.00000E+00   0.50000
    2.00000E-01   0.50000
    6.00000E-01   0.00000
USER DISTRIBUTION  (CUMULATIVE)       PCS_T1    PORE_DIS
         3          SPECIFIED    CONTINUOUS
    1.10000E-01   0.50000
    9.40000E-01   0.50000
    8.10000E+00   0.00000
USER DISTRIBUTION  (CUMULATIVE)       S_HALITE  POROSITY
         3          SPECIFIED    CONTINUOUS
    1.00000E-03   0.50000
    1.00000E-02   0.50000
    5.19000E-02   0.00000
UNIFORM                 S_HALITE  PRMX_LOG
   -2.40000E+01   -2.10000E+01
UNIFORM                 S_HALITE  COMP_RCK
    2.94000E-12    1.92000E-10
STUDENT                 S_MB139   PRMX_LOG
         6
 -2.10000E+01 -1.92000E+01 -1.91000E+01 -1.88000E+01 -1.81000E+01 -
1.71000E+01
USER DISTRIBUTION  (DELTA)           S_MB139   RELP_MOD
         4          SPECIFIED    DISCRETE
    1.00000E+00   0.50000
    2.00000E+00   0.00000
    3.00000E+00   0.00000
    4.00000E+00   0.50000
STUDENT                 S_MB139   SAT_RBRN
         6
  7.78460E-03  6.88420E-02  6.98600E-02  7.26200E-02  1.08610E-01
1.74010E-01
STUDENT                 S_MB139   PORE_DIS
         6
  4.90530E-01  5.57750E-01  6.52000E-01  6.55000E-01  6.64520E-01
8.41780E-01
UNIFORM                 S_HALITE  PRESSURE
    1.10400E+07    1.38900E+07
TRIANGULAR              CASTILER  PRESSURE
    1.11000E+07    1.27000E+07    1.70000E+07
TRIANGULAR              CASTILER  PRMX_LOG
   -1.47000E+01   -1.18000E+01   -9.80000E+00
TRIANGULAR              CASTILER  COMP_RCK
    2.00000E-11    4.00000E-11    1.00000E-10
UNIFORM                 BH_SAND   PRMX_LOG
   -1.63000E+01   -1.10000E+01
UNIFORM                 DRZ_1     PRMX_LOG
   -1.94000E+01   -1.25000E+01
UNIFORM                 CONC_PLG  PRMX_LOG
   -1.90000E+01   -1.70000E+01
USER DISTRIBUTION  (CUMULATIVE)       SHFTU     SAT_RBRN
         3          SPECIFIED    CONTINUOUS
```


Information Only

```
    0.00000E+00   0.50000
    2.00000E-01   0.50000
    6.00000E-01   0.00000
UNIFORM                 SHFTU     SAT_RGAS
    0.00000E+00    4.00000E-01
USER DISTRIBUTION  (CUMULATIVE)       SHFTU     PRMX_LOG
         9          SPECIFIED    CONTINUOUS
   -2.05000E+01   0.03000
   -2.00000E+01   0.08000
   -1.95000E+01   0.13000
   -1.90000E+01   0.19000
   -1.85000E+01   0.22000
   -1.80000E+01   0.24000
   -1.75000E+01   0.10000
   -1.70000E+01   0.01000
   -1.65000E+01   0.00000
USER DISTRIBUTION  (CUMULATIVE)       SHFTL_T1  PRMX_LOG
         8          SPECIFIED    CONTINUOUS
   -2.00000E+01   0.01000
   -1.95000E+01   0.09000
   -1.90000E+01   0.20700
   -1.85000E+01   0.33000
   -1.80000E+01   0.23600
   -1.75000E+01   0.12000
   -1.70000E+01   0.00700
   -1.65000E+01   0.00000
USER DISTRIBUTION  (CUMULATIVE)       SHFTL_T2  PRMX_LOG
        10          SPECIFIED    CONTINUOUS
   -2.25000E+01   0.02000
   -2.20000E+01   0.06000
   -2.15000E+01   0.09000
   -2.10000E+01   0.13500
   -2.05000E+01   0.22000
   -2.00000E+01   0.17500
   -1.95000E+01   0.16500
   -1.90000E+01   0.10000
   -1.85000E+01   0.03500
   -1.80000E+01   0.00000
UNIFORM                 WAS_AREA  BIOGENFC
    0.00000E+00    1.00000E+00
UNIFORM                 PCS_T1    POROSITY
    6.60000E-02    1.87000E-01
UNIFORM                 PCS_T2    POROSITY
    2.50000E-02    7.50000E-02
UNIFORM                 PCS_T3    POROSITY
    1.00000E-03    5.19000E-02
NORMAL                  PCS_T2    POR2PERM
   -1.72000E+00    1.72000E+00
CORRELATION MATRIX
    2
    53  54 -0.99
    61  62 -0.75
OUTPUT CORR HIST DATA
```


Information Only

Information Only

Appendix VI. PRELHS Output (Transfer) File for Replicate 3

```
TITLE SDB: ParamDB            Calc: AP161        Ver: 2.00     07/27/12
16:17:47
TITLE PABC09, AP161 Replicate R3 Input File for the LHS Code
NOBS            100
RANDOM SEED     292058223
UNIFORM                 GLOBAL    PBRINE
    1.00000E-02    6.00000E-01
UNIFORM                 REFCON    LHSBLANK
    0.00000E+00    1.00000E+00
UNIFORM                 REFCON    LHSBLANK
    0.00000E+00    1.00000E+00
USER DISTRIBUTION  (CUMULATIVE)       BOREHOLE  DOMEGA
        10          SPECIFIED    CONTINUOUS
    4.20000E+00   0.15000
    6.30000E+00   0.50000
    8.40000E+00   0.15000
    1.05000E+01   0.10000
    1.26000E+01   0.05000
    1.47000E+01   0.02000
    1.68000E+01   0.01000
    1.88000E+01   0.01000
    2.09000E+01   0.01000
    2.30000E+01   0.00000
LOGUNIFORM              BOREHOLE  TAUFAIL
    5.00000E-02    7.70000E+01
UNIFORM                 REFCON    LHSBLANK
    0.00000E+00    1.00000E+00
UNIFORM                 REFCON    LHSBLANK
    0.00000E+00    1.00000E+00
LOGUNIFORM              SPALLMOD  REPIPERM
    2.40000E-14    2.40000E-12
UNIFORM                 SPALLMOD  TENSLSTR
    1.20000E+05    1.70000E+05
LOGUNIFORM              SPALLMOD  PARTDIAM
    1.00000E-03    1.00000E-01
UNIFORM                 SPALLMOD  REPIPOR
    3.50000E-01    6.60000E-01
UNIFORM                 REFCON    LHSBLANK
    0.00000E+00    1.00000E+00
UNIFORM                 REFCON    LHSBLANK
    0.00000E+00    1.00000E+00
UNIFORM                 REFCON    LHSBLANK
    0.00000E+00    1.00000E+00
USER DISTRIBUTION  (CUMULATIVE)       SOLMOD3   SOLVAR
        48          SPECIFIED    CONTINUOUS
   -4.20000E+00   0.00290
   -4.05000E+00   0.00000
   -3.90000E+00   0.00580
   -3.75000E+00   0.01150
   -3.60000E+00   0.01450
   -3.45000E+00   0.00290
   -3.30000E+00   0.00580
```


Information Only

```
   -3.15000E+00   0.00860
   -3.00000E+00   0.00290
   -2.85000E+00   0.00000
   -2.70000E+00   0.00580
   -2.55000E+00   0.00870
   -2.40000E+00   0.00860
   -2.25000E+00   0.00580
   -2.10000E+00   0.00000
   -1.95000E+00   0.00290
   -1.80000E+00   0.00580
   -1.65000E+00   0.00580
   -1.50000E+00   0.00570
   -1.35000E+00   0.02610
   -1.20000E+00   0.02600
   -1.05000E+00   0.02890
   -9.00000E-01   0.02600
   -7.50000E-01   0.02890
   -6.00000E-01   0.03760
   -4.50000E-01   0.06070
   -3.00000E-01   0.05200
   -1.50000E-01   0.07220
    0.00000E+00   0.07810
    1.50000E-01   0.07800
    3.00000E-01   0.07800
    4.50000E-01   0.03470
    6.00000E-01   0.08380
    7.50000E-01   0.08960
    9.00000E-01   0.02030
    1.05000E+00   0.01440
    1.20000E+00   0.01450
    1.35000E+00   0.00860
    1.50000E+00   0.00290
    1.65000E+00   0.01160
    1.80000E+00   0.00860
    1.95000E+00   0.00580
    2.10000E+00   0.00000
    2.25000E+00   0.00290
    2.40000E+00   0.00290
    2.55000E+00   0.00290
    2.70000E+00   0.00000
    2.85000E+00   0.00000
USER DISTRIBUTION  (CUMULATIVE)       SOLMOD4   SOLVAR
        38          SPECIFIED    CONTINUOUS
   -2.25000E+00   0.01430
   -2.10000E+00   0.00710
   -1.95000E+00   0.01430
   -1.80000E+00   0.02860
   -1.65000E+00   0.02860
   -1.50000E+00   0.05000
   -1.35000E+00   0.07850
   -1.20000E+00   0.04290
   -1.05000E+00   0.03570
   -9.00000E-01   0.05710
   -7.50000E-01   0.08580
```


Information Only

```
   -6.00000E-01   0.10710
   -4.50000E-01   0.02140
   -3.00000E-01   0.03570
   -1.50000E-01   0.04290
    0.00000E+00   0.03570
    1.50000E-01   0.09290
    3.00000E-01   0.05000
    4.50000E-01   0.00710
    6.00000E-01   0.04290
    7.50000E-01   0.03570
    9.00000E-01   0.02140
    1.05000E+00   0.00000
    1.20000E+00   0.00720
    1.35000E+00   0.01420
    1.50000E+00   0.00720
    1.65000E+00   0.00710
    1.80000E+00   0.00000
    1.95000E+00   0.00720
    2.10000E+00   0.00000
    2.25000E+00   0.00710
    2.40000E+00   0.00000
    2.55000E+00   0.00000
    2.70000E+00   0.00000
    2.85000E+00   0.00000
    3.00000E+00   0.00000
    3.15000E+00   0.01430
    3.30000E+00   0.00000
USER DISTRIBUTION  (CUMULATIVE)       PHUMOX3   PHUMCIM
         3          SPECIFIED    CONTINUOUS
    6.50000E-02   0.50000
    1.37000E+00   0.50000
    1.60000E+00   0.00000
UNIFORM                 GLOBAL    OXSTAT
    0.00000E+00    1.00000E+00
UNIFORM                 REFCON    LHSBLANK
    0.00000E+00    1.00000E+00
UNIFORM                 REFCON    LHSBLANK
    0.00000E+00    1.00000E+00
UNIFORM                 REFCON    LHSBLANK
    0.00000E+00    1.00000E+00
UNIFORM                 REFCON    LHSBLANK
    0.00000E+00    1.00000E+00
UNIFORM                 CULEBRA   MINP_FAC
    1.00000E+00    1.00000E+03
UNIFORM                 GLOBAL    TRANSIDX
    0.00000E+00    1.00000E+00
USER DISTRIBUTION  (CUMULATIVE)       GLOBAL    CLIMTIDX
         4          SPECIFIED    CONTINUOUS
    1.00000E+00   0.75000
    1.25000E+00   0.00000
    1.50000E+00   0.25000
    2.25000E+00   0.00000
UNIFORM                 CULEBRA   HMBLKLT
    5.00000E-02    5.00000E-01
```


Information Only

```
LOGUNIFORM              CULEBRA   APOROS
    1.00000E-04    1.00000E-02
USER DISTRIBUTION  (CUMULATIVE)       CULEBRA   DPOROS
         7          SPECIFIED    CONTINUOUS
    1.00000E-01   0.10000
    1.10000E-01   0.15000
    1.20000E-01   0.25000
    1.60000E-01   0.25000
    1.80000E-01   0.15000
    1.90000E-01   0.10000
    2.50000E-01   0.00000
LOGUNIFORM              U+6       MKD_U
    3.00000E-05    2.00000E-02
LOGUNIFORM              U+4       MKD_U
    5.00000E-04    1.00000E+01
LOGUNIFORM              PU+3      MKD_PU
    5.00000E-03    4.00000E-01
LOGUNIFORM              PU+4      MKD_PU
    5.00000E-04    1.00000E+01
LOGUNIFORM              TH+4      MKD_TH
    5.00000E-04    1.00000E+01
LOGUNIFORM              AM+3      MKD_AM
    5.00000E-03    4.00000E-01
UNIFORM                 REFCON    LHSBLANK
    0.00000E+00    1.00000E+00
UNIFORM                 REFCON    LHSBLANK
    0.00000E+00    1.00000E+00
UNIFORM                 REFCON    LHSBLANK
    0.00000E+00    1.00000E+00
UNIFORM                 REFCON    LHSBLANK
    0.00000E+00    1.00000E+00
UNIFORM                 STEEL     CORRMCO2
    0.00000E+00    3.17000E-14
USER DISTRIBUTION  (DELTA)           WAS_AREA  PROBDEG
         2          SPECIFIED    DISCRETE
    1.00000E+00   0.75000
    2.00000E+00   0.25000
UNIFORM                 WAS_AREA  GRATMICI
    3.08269E-11    5.56921E-10
UNIFORM                 WAS_AREA  GRATMICH
    0.00000E+00    1.02717E-09
UNIFORM                 PCS_T1    SAT_IBRN
    4.00000E-02    1.60000E-01
UNIFORM                 WAS_AREA  SAT_RGAS
    0.00000E+00    1.50000E-01
UNIFORM                 WAS_AREA  SAT_RBRN
    0.00000E+00    5.52000E-01
UNIFORM                 WAS_AREA  SAT_WICK
    0.00000E+00    1.00000E+00
TRIANGULAR              DRZ_PCS   PRMX_LOG
   -2.06990E+01   -1.87496E+01   -1.70000E+01
UNIFORM                 PCS_T1    PRMX_LOG
   -2.10000E+01   -1.20000E+01
UNIFORM                 PCS_T1    SAT_RGAS
```


Information Only

```
    0.00000E+00    4.00000E-01
USER DISTRIBUTION  (CUMULATIVE)       PCS_T1    SAT_RBRN
         3          SPECIFIED    CONTINUOUS
    0.00000E+00   0.50000
    2.00000E-01   0.50000
    6.00000E-01   0.00000
USER DISTRIBUTION  (CUMULATIVE)       PCS_T1    PORE_DIS
         3          SPECIFIED    CONTINUOUS
    1.10000E-01   0.50000
    9.40000E-01   0.50000
    8.10000E+00   0.00000
USER DISTRIBUTION  (CUMULATIVE)       S_HALITE  POROSITY
         3          SPECIFIED    CONTINUOUS
    1.00000E-03   0.50000
    1.00000E-02   0.50000
    5.19000E-02   0.00000
UNIFORM                 S_HALITE  PRMX_LOG
   -2.40000E+01   -2.10000E+01
UNIFORM                 S_HALITE  COMP_RCK
    2.94000E-12    1.92000E-10
STUDENT                 S_MB139   PRMX_LOG
         6
 -2.10000E+01 -1.92000E+01 -1.91000E+01 -1.88000E+01 -1.81000E+01 -
1.71000E+01
USER DISTRIBUTION  (DELTA)           S_MB139   RELP_MOD
         4          SPECIFIED    DISCRETE
    1.00000E+00   0.50000
    2.00000E+00   0.00000
    3.00000E+00   0.00000
    4.00000E+00   0.50000
STUDENT                 S_MB139   SAT_RBRN
         6
  7.78460E-03  6.88420E-02  6.98600E-02  7.26200E-02  1.08610E-01
1.74010E-01
STUDENT                 S_MB139   PORE_DIS
         6
  4.90530E-01  5.57750E-01  6.52000E-01  6.55000E-01  6.64520E-01
8.41780E-01
UNIFORM                 S_HALITE  PRESSURE
    1.10400E+07    1.38900E+07
TRIANGULAR              CASTILER  PRESSURE
    1.11000E+07    1.27000E+07    1.70000E+07
TRIANGULAR              CASTILER  PRMX_LOG
   -1.47000E+01   -1.18000E+01   -9.80000E+00
TRIANGULAR              CASTILER  COMP_RCK
    2.00000E-11    4.00000E-11    1.00000E-10
UNIFORM                 BH_SAND   PRMX_LOG
   -1.63000E+01   -1.10000E+01
UNIFORM                 DRZ_1     PRMX_LOG
   -1.94000E+01   -1.25000E+01
UNIFORM                 CONC_PLG  PRMX_LOG
   -1.90000E+01   -1.70000E+01
USER DISTRIBUTION  (CUMULATIVE)       SHFTU     SAT_RBRN
         3          SPECIFIED    CONTINUOUS
```


Information Only

```
    0.00000E+00   0.50000
    2.00000E-01   0.50000
    6.00000E-01   0.00000
UNIFORM                 SHFTU     SAT_RGAS
    0.00000E+00    4.00000E-01
USER DISTRIBUTION  (CUMULATIVE)       SHFTU     PRMX_LOG
         9          SPECIFIED    CONTINUOUS
   -2.05000E+01   0.03000
   -2.00000E+01   0.08000
   -1.95000E+01   0.13000
   -1.90000E+01   0.19000
   -1.85000E+01   0.22000
   -1.80000E+01   0.24000
   -1.75000E+01   0.10000
   -1.70000E+01   0.01000
   -1.65000E+01   0.00000
USER DISTRIBUTION  (CUMULATIVE)       SHFTL_T1  PRMX_LOG
         8          SPECIFIED    CONTINUOUS
   -2.00000E+01   0.01000
   -1.95000E+01   0.09000
   -1.90000E+01   0.20700
   -1.85000E+01   0.33000
   -1.80000E+01   0.23600
   -1.75000E+01   0.12000
   -1.70000E+01   0.00700
   -1.65000E+01   0.00000
USER DISTRIBUTION  (CUMULATIVE)       SHFTL_T2  PRMX_LOG
        10          SPECIFIED    CONTINUOUS
   -2.25000E+01   0.02000
   -2.20000E+01   0.06000
   -2.15000E+01   0.09000
   -2.10000E+01   0.13500
   -2.05000E+01   0.22000
   -2.00000E+01   0.17500
   -1.95000E+01   0.16500
   -1.90000E+01   0.10000
   -1.85000E+01   0.03500
   -1.80000E+01   0.00000
UNIFORM                 WAS_AREA  BIOGENFC
    0.00000E+00    1.00000E+00
UNIFORM                 PCS_T1    POROSITY
    6.60000E-02    1.87000E-01
UNIFORM                 PCS_T2    POROSITY
    2.50000E-02    7.50000E-02
UNIFORM                 PCS_T3    POROSITY
    1.00000E-03    5.19000E-02
NORMAL                  PCS_T2    POR2PERM
   -1.72000E+00    1.72000E+00
CORRELATION MATRIX
    2
    53  54 -0.99
    61  62 -0.75
OUTPUT CORR HIST DATA
```


Information Only

Information Only

Appendix VII. Comparison of Sampled Data to Expected Range

				Observed			Parameter Database				
Analysis	Material	Property	Rep	Minimum	Maximum	Mean	Minimum	Maximum	Mean	RPD of Means	% Range Covered
AP161	AM+3	MKD_AM	1	5.0220E-03	3.9660E-01	9.0040E-02	5.0000E-03	4.0000E-01	9.0000E-02	0.04%	99.1%
AP161	AM+3	MKD_AM	2	5.1740E-03	3.8880E-01	9.0275E-02	5.0000E-03	4.0000E-01	9.0000E-02	0.31%	97.1%
AP161	AM+3	MKD_AM	3	5.2060E-03	3.9280E-01	8.9972E-02	5.0000E-03	4.0000E-01	9.0000E-02	0.03%	98.1%
AP161	BH_SAND	PRMX_LOG	1	-1.6300E+01	-1.1010E+01	-1.3648E+01	-1.6300E+01	-1.1000E+01	-1.3650E+01	0.01%	99.8%
AP161	BH_SAND	PRMX_LOG	2	-1.6290E+01	-1.1010E+01	-1.3649E+01	-1.6300E+01	-1.1000E+01	-1.3650E+01	0.01%	99.6%
AP161	BH_SAND	PRMX_LOG	3	-1.6250E+01	-1.1000E+01	-1.3647E+01	-1.6300E+01	-1.1000E+01	-1.3650E+01	0.02%	99.1%
AP161	BOREHOLE	DOMEGA	1	4.3370E+00	2.1650E+01	8.6254E+00	4.2000E+00	2.3000E+01	8.6300E+00	0.05%	92.1%
AP161	BOREHOLE	DOMEGA	2	4.2740E+00	2.2680E+01	8.6183E+00	4.2000E+00	2.3000E+01	8.6300E+00	0.14%	97.9%
AP161	BOREHOLE	DOMEGA	3	4.2740E+00	2.2990E+01	8.6407E+00	4.2000E+00	2.3000E+01	8.6300E+00	0.12%	99.6%
AP161	BOREHOLE	TAUFAIL	1	5.0040E-02	7.6740E+01	1.0500E+01	5.0000E-02	7.7000E+01	1.0500E+01	0.00%	99.7%
AP161	BOREHOLE	TAUFAIL	2	5.1040E-02	7.2230E+01	1.0427E+01	5.0000E-02	7.7000E+01	1.0500E+01	0.70%	93.8%
AP161	BOREHOLE	TAUFAIL	3	5.1200E-02	7.4990E+01	1.0521E+01	5.0000E-02	7.7000E+01	1.0500E+01	0.20%	97.4%
AP161	CASTILER	COMP_RCK	1	2.0740E-11	9.3580E-11	5.3286E-11	2.0000E-11	1.0000E-10	5.3000E-11	0.54%	91.1%
AP161	CASTILER	COMP_RCK	2	2.2830E-11	9.4830E-11	5.3349E-11	2.0000E-11	1.0000E-10	5.3000E-11	0.66%	90.0%

Information Only

AP161	CASTILER	COMP_RCK	3	2.1390E-11	9.4920E-11	5.3273E-11	2.0000E-11	1.0000E-10	5.3000E-11	0.51%	91.9%

Information Only

				Observed			Parameter Database				
Analysis	Material	Property	Rep	Minimum	Maximum	Mean	Minimum	Maximum	Mean	RPD of Means	% Range Covered
AP161	CASTILER	PRESSURE	1	1.1200E+07	1.6500E+07	1.3595E+07	1.1100E+07	1.7000E+07	1.3600E+07	0.03%	89.8%
AP161	CASTILER	PRESSURE	2	1.1370E+07	1.6710E+07	1.3606E+07	1.1100E+07	1.7000E+07	1.3600E+07	0.04%	90.5%
AP161	CASTILER	PRESSURE	3	1.1380E+07	1.6850E+07	1.3602E+07	1.1100E+07	1.7000E+07	1.3600E+07	0.02%	92.7%
AP161	CASTILER	PRMX_LOG	1	-1.4470E+01	-9.9370E+00	-1.2099E+01	-1.4700E+01	-9.8000E+00	-1.2100E+01	0.01%	92.5%
AP161	CASTILER	PRMX_LOG	2	-1.4520E+01	-1.0050E+01	-1.2101E+01	-1.4700E+01	-9.8000E+00	-1.2100E+01	0.01%	91.2%
AP161	CASTILER	PRMX_LOG	3	-1.4360E+01	-9.8950E+00	-1.2096E+01	-1.4700E+01	-9.8000E+00	-1.2100E+01	0.03%	91.1%
AP161	CONC_PLG	PRMX_LOG	1	-1.8990E+01	-1.7010E+01	-1.8001E+01	-1.9000E+01	-1.7000E+01	-1.8000E+01	0.00%	99.0%
AP161	CONC_PLG	PRMX_LOG	2	-1.9000E+01	-1.7010E+01	-1.8000E+01	-1.9000E+01	-1.7000E+01	-1.8000E+01	0.00%	99.5%
AP161	CONC_PLG	PRMX_LOG	3	-1.8990E+01	-1.7020E+01	-1.7999E+01	-1.9000E+01	-1.7000E+01	-1.8000E+01	0.01%	98.5%
AP161	CULEBRA	APOROS	1	1.0140E-04	9.8170E-03	2.1380E-03	1.0000E-04	1.0000E-02	2.1000E-03	1.79%	98.1%
AP161	CULEBRA	APOROS	2	1.0220E-04	9.5810E-03	2.1522E-03	1.0000E-04	1.0000E-02	2.1000E-03	2.46%	95.7%
AP161	CULEBRA	APOROS	3	1.0140E-04	9.6960E-03	2.1448E-03	1.0000E-04	1.0000E-02	2.1000E-03	2.11%	96.9%
AP161	CULEBRA	DPOROS	1	1.0000E-01	2.4570E-01	1.5495E-01	1.0000E-01	2.5000E-01	1.6000E-01	3.21%	97.1%
AP161	CULEBRA	DPOROS	2	1.0000E-01	2.4750E-01	1.5499E-01	1.0000E-01	2.5000E-01	1.6000E-01	3.18%	98.3%
AP161	CULEBRA	DPOROS	3	1.0010E-01	2.4900E-01	1.5498E-01	1.0000E-01	2.5000E-01	1.6000E-01	3.19%	99.3%
AP161	CULEBRA	HMBLKLT	1	5.2590E-02	4.9880E-01	2.7524E-01	5.0000E-02	5.0000E-01	2.7500E-01	0.09%	99.2%
AP161	CULEBRA	HMBLKLT	2	5.3870E-02	4.9640E-01	2.7502E-01	5.0000E-02	5.0000E-01	2.7500E-01	0.01%	98.3%
AP161	CULEBRA	HMBLKLT	3	5.4100E-02	4.9640E-01	2.7484E-01	5.0000E-02	5.0000E-01	2.7500E-01	0.06%	98.3%
AP161	CULEBRA	MINP_FAC	1	1.0190E+00	9.9530E+02	5.0069E+02	1.0000E+00	1.0000E+03	5.0050E+02	0.04%	99.5%
AP161	CULEBRA	MINP_FAC	2	5.5620E+00	9.9620E+02	5.0051E+02	1.0000E+00	1.0000E+03	5.0050E+02	0.00%	99.2%

Information Only

AP161	CULEBRA	MINP_FAC	3	4.3420E+00	9.9240E+02	5.0036E+02	1.0000E+00	1.0000E+03	5.0050E+02	0.03%	98.9%

Information Only

				Observed			Parameter Database				
Analysis	Material	Property	Rep	Minimum	Maximum	Mean	Minimum	Maximum	Mean	RPD of Means	% Range Covered
AP161	DRZ_1	PRMX_LOG	1	-1.9400E+01	-1.2510E+01	-1.5949E+01	-1.9400E+01	-1.2500E+01	-1.6000E+01	0.32%	99.9%
AP161	DRZ_1	PRMX_LOG	2	-1.9380E+01	-1.2560E+01	-1.5951E+01	-1.9400E+01	-1.2500E+01	-1.6000E+01	0.31%	98.8%
AP161	DRZ_1	PRMX_LOG	3	-1.9340E+01	-1.2560E+01	-1.5948E+01	-1.9400E+01	-1.2500E+01	-1.6000E+01	0.33%	98.3%
AP161	DRZ_PCS	PRMX_LOG	1	-2.0480E+01	-1.7200E+01	-1.8815E+01	-2.0699E+01	-1.7000E+01	-1.8816E+01	0.01%	88.7%
AP161	DRZ_PCS	PRMX_LOG	2	-2.0570E+01	-1.7170E+01	-1.8819E+01	-2.0699E+01	-1.7000E+01	-1.8816E+01	0.01%	91.9%
AP161	DRZ_PCS	PRMX_LOG	3	-2.0600E+01	-1.7180E+01	-1.8816E+01	-2.0699E+01	-1.7000E+01	-1.8816E+01	0.00%	92.5%
AP161	GLOBAL	CLIMTIDX	1	1.0010E+00	2.2350E+00	1.3121E+00	1.0000E+00	2.2500E+00	1.3100E+00	0.16%	98.7%
AP161	GLOBAL	CLIMTIDX	2	1.0020E+00	2.2480E+00	1.3128E+00	1.0000E+00	2.2500E+00	1.3100E+00	0.21%	99.7%
AP161	GLOBAL	CLIMTIDX	3	1.0020E+00	2.2400E+00	1.3121E+00	1.0000E+00	2.2500E+00	1.3100E+00	0.16%	99.0%
AP161	GLOBAL	OXSTAT	1	4.3770E-03	9.9540E-01	5.0010E-01	0.0000E+00	1.0000E+00	5.0000E-01	0.02%	99.1%
AP161	GLOBAL	OXSTAT	2	7.8880E-03	9.9170E-01	5.0070E-01	0.0000E+00	1.0000E+00	5.0000E-01	0.14%	98.4%
AP161	GLOBAL	OXSTAT	3	8.1050E-04	9.9350E-01	5.0016E-01	0.0000E+00	1.0000E+00	5.0000E-01	0.03%	99.3%
AP161	GLOBAL	PBRINE	1	1.5250E-02	5.9770E-01	3.0496E-01	1.0000E-02	6.0000E-01	3.0500E-01	0.01%	98.7%
AP161	GLOBAL	PBRINE	2	1.3550E-02	5.9710E-01	3.0508E-01	1.0000E-02	6.0000E-01	3.0500E-01	0.03%	98.9%
AP161	GLOBAL	PBRINE	3	1.4130E-02	5.9490E-01	3.0522E-01	1.0000E-02	6.0000E-01	3.0500E-01	0.07%	98.4%
AP161	GLOBAL	TRANSIDX	1	7.9510E-03	9.9810E-01	4.9977E-01	0.0000E+00	1.0000E+00	5.0000E-01	0.05%	99.0%
AP161	GLOBAL	TRANSIDX	2	6.8330E-03	9.9180E-01	4.9963E-01	0.0000E+00	1.0000E+00	5.0000E-01	0.07%	98.5%
AP161	GLOBAL	TRANSIDX	3	6.6100E-03	9.9240E-01	5.0027E-01	0.0000E+00	1.0000E+00	5.0000E-01	0.05%	98.6%
AP161	PCS_T1	PORE_DIS	1	1.1970E-01	8.0570E+00	2.5202E+00	1.1000E-01	8.1000E+00	2.5200E+00	0.01%	99.3%
AP161	PCS_T1	PORE_DIS	2	1.1040E-01	8.0170E+00	2.5170E+00	1.1000E-01	8.1000E+00	2.5200E+00	0.12%	99.0%

Information Only

AP161	PCS_T1	PORE_DIS	3	1.2600E-01	8.0650E+00	2.5231E+00	1.1000E-01	8.1000E+00	2.5200E+00	0.12%	99.4%

Information Only

				Observed			Parameter Database				
Analysis	Material	Property	Rep	Minimum	Maximum	Mean	Minimum	Maximum	Mean	RPD of Means	% Range Covered
AP161	PCS_T1	POROSITY	1	6.6190E-02	1.8650E-01	1.2643E-01	6.6000E-02	1.8700E-01	1.2650E-01	0.05%	99.4%
AP161	PCS_T1	POROSITY	2	6.6540E-02	1.8660E-01	1.2651E-01	6.6000E-02	1.8700E-01	1.2650E-01	0.01%	99.2%
AP161	PCS_T1	POROSITY	3	6.7130E-02	1.8680E-01	1.2647E-01	6.6000E-02	1.8700E-01	1.2650E-01	0.03%	98.9%
AP161	PCS_T1	PRMX_LOG	1	-2.0940E+01	-1.2080E+01	-1.6499E+01	-2.1000E+01	-1.2000E+01	-1.6500E+01	0.01%	98.4%
AP161	PCS_T1	PRMX_LOG	2	-2.1000E+01	-1.2070E+01	-1.6503E+01	-2.1000E+01	-1.2000E+01	-1.6500E+01	0.02%	99.2%
AP161	PCS_T1	PRMX_LOG	3	-2.0930E+01	-1.2080E+01	-1.6502E+01	-2.1000E+01	-1.2000E+01	-1.6500E+01	0.01%	98.3%
AP161	PCS_T1	SAT_IBRN	1	4.0120E-02	1.6000E-01	1.0003E-01	4.0000E-02	1.6000E-01	1.0000E-01	0.03%	99.9%
AP161	PCS_T1	SAT_IBRN	2	4.1100E-02	1.5900E-01	9.9965E-02	4.0000E-02	1.6000E-01	1.0000E-01	0.04%	98.3%
AP161	PCS_T1	SAT_IBRN	3	4.0200E-02	1.5980E-01	9.9965E-02	4.0000E-02	1.6000E-01	1.0000E-01	0.03%	99.7%
AP161	PCS_T1	SAT_RBRN	1	1.9560E-03	5.9540E-01	2.5009E-01	0.0000E+00	6.0000E-01	2.5000E-01	0.04%	98.9%
AP161	PCS_T1	SAT_RBRN	2	6.9290E-04	5.9460E-01	2.4978E-01	0.0000E+00	6.0000E-01	2.5000E-01	0.09%	99.0%
AP161	PCS_T1	SAT_RBRN	3	2.9130E-03	5.9380E-01	2.5013E-01	0.0000E+00	6.0000E-01	2.5000E-01	0.05%	98.5%
AP161	PCS_T1	SAT_RGAS	1	9.6070E-04	3.9780E-01	2.0010E-01	0.0000E+00	4.0000E-01	2.0000E-01	0.05%	99.2%
AP161	PCS_T1	SAT_RGAS	2	2.7790E-03	3.9900E-01	2.0019E-01	0.0000E+00	4.0000E-01	2.0000E-01	0.09%	99.1%
AP161	PCS_T1	SAT_RGAS	3	5.9480E-04	3.9940E-01	1.9982E-01	0.0000E+00	4.0000E-01	2.0000E-01	0.09%	99.7%
AP161	PCS_T2	POR2PERM	1	-1.6280E+00	1.6770E+00	5.6467E-04	-1.7200E+00	1.7200E+00	0.0000E+00	200.00%	96.1%
AP161	PCS_T2	POR2PERM	2	-1.5800E+00	1.7040E+00	1.1361E-03	-1.7200E+00	1.7200E+00	0.0000E+00	200.00%	95.5%
AP161	PCS_T2	POR2PERM	3	-1.5770E+00	1.6490E+00	1.1791E-03	-1.7200E+00	1.7200E+00	0.0000E+00	200.00%	93.8%
AP161	PCS_T2	POROSITY	1	2.5110E-02	7.4680E-02	4.9999E-02	2.5000E-02	7.5000E-02	5.0000E-02	0.00%	99.1%
AP161	PCS_T2	POROSITY	2	2.5480E-02	7.4660E-02	4.9990E-02	2.5000E-02	7.5000E-02	5.0000E-02	0.02%	98.4%

Information Only

AP161	PCS_T2	POROSITY	3	2.5030E-02	7.4690E-02	5.0003E-02	2.5000E-02	7.5000E-02	5.0000E-02	0.01%	99.3%

Information Only

				Observed			Parameter Database				
Analysis	Material	Property	Rep	Minimum	Maximum	Mean	Minimum	Maximum	Mean	RPD of Means	% Range Covered
AP161	PCS_T3	POROSITY	1	1.4370E-03	5.1710E-02	2.6468E-02	1.0000E-03	5.1900E-02	5.0000E-02	61.55%	98.8%
AP161	PCS_T3	POROSITY	2	1.4620E-03	5.1820E-02	2.6493E-02	1.0000E-03	5.1900E-02	5.0000E-02	61.46%	98.9%
AP161	PCS_T3	POROSITY	3	1.4910E-03	5.1620E-02	2.6441E-02	1.0000E-03	5.1900E-02	5.0000E-02	61.64%	98.5%
AP161	PHUMOX3	PHUMCIM	1	8.4750E-02	1.5980E+00	1.1019E+00	6.5000E-02	1.6000E+00	1.1000E+00	0.17%	98.6%
AP161	PHUMOX3	PHUMCIM	2	7.8790E-02	1.5990E+00	1.1012E+00	6.5000E-02	1.6000E+00	1.1000E+00	0.11%	99.0%
AP161	PHUMOX3	PHUMCIM	3	9.0390E-02	1.6000E+00	1.1012E+00	6.5000E-02	1.6000E+00	1.1000E+00	0.11%	98.3%
AP161	PU+3	MKD_PU	1	5.0200E-03	3.9600E-01	9.0271E-02	5.0000E-03	4.0000E-01	9.0000E-02	0.30%	99.0%
AP161	PU+3	MKD_PU	2	5.0610E-03	3.9480E-01	9.0160E-02	5.0000E-03	4.0000E-01	9.0000E-02	0.18%	98.7%
AP161	PU+3	MKD_PU	3	5.0360E-03	3.9980E-01	9.0145E-02	5.0000E-03	4.0000E-01	9.0000E-02	0.16%	99.9%
AP161	PU+4	MKD_PU	1	5.1950E-04	9.6900E+00	1.0052E+00	5.0000E-04	1.0000E+01	1.0000E+00	0.51%	96.9%
AP161	PU+4	MKD_PU	2	5.2120E-04	9.5510E+00	1.0141E+00	5.0000E-04	1.0000E+01	1.0000E+00	1.40%	95.5%
AP161	PU+4	MKD_PU	3	5.3760E-04	9.6400E+00	1.0128E+00	5.0000E-04	1.0000E+01	1.0000E+00	1.28%	96.4%
AP161	S_HALITE	COMP_RCK	1	3.7690E-12	1.9170E-10	9.7462E-11	2.9400E-12	1.9200E-10	9.7500E-11	0.04%	99.4%
AP161	S_HALITE	COMP_RCK	2	3.2040E-12	1.9010E-10	9.7516E-11	2.9400E-12	1.9200E-10	9.7500E-11	0.02%	98.9%
AP161	S_HALITE	COMP_RCK	3	3.4650E-12	1.9060E-10	9.7436E-11	2.9400E-12	1.9200E-10	9.7500E-11	0.07%	99.0%
AP161	S_HALITE	POROSITY	1	1.1270E-03	5.1150E-02	1.8230E-02	1.0000E-03	5.1900E-02	1.8200E-02	0.17%	98.3%
AP161	S_HALITE	POROSITY	2	1.0540E-03	5.1150E-02	1.8224E-02	1.0000E-03	5.1900E-02	1.8200E-02	0.13%	98.4%
AP161	S_HALITE	POROSITY	3	1.1080E-03	5.1560E-02	1.8243E-02	1.0000E-03	5.1900E-02	1.8200E-02	0.24%	99.1%
AP161	S_HALITE	PRESSURE	1	1.1060E+07	1.3890E+07	1.2465E+07	1.1040E+07	1.3890E+07	1.2470E+07	0.04%	99.3%
AP161	S_HALITE	PRESSURE	2	1.1050E+07	1.3880E+07	1.2464E+07	1.1040E+07	1.3890E+07	1.2470E+07	0.05%	99.3%
AP161	S_HALITE	PRESSURE	3	1.1050E+07	1.3880E+07	1.2466E+07	1.1040E+07	1.3890E+07	1.2470E+07	0.03%	99.3%
AP161	S_HALITE	PRMX_LOG	1	-2.3970E+01	-2.1010E+01	-2.2499E+01	-2.4000E+01	-2.1000E+01	-2.2500E+01	0.00%	98.7%

Information Only

				Observed			Parameter Database				
Analysis	Material	Property	Rep	Minimum	Maximum	Mean	Minimum	Maximum	Mean	RPD of Means	% Range Covered
AP161	S_HALITE	PRMX_LOG	2	-2.4000E+01	-2.1010E+01	-2.2500E+01	-2.4000E+01	-2.1000E+01	-2.2500E+01	0.00%	99.7%
AP161	S_HALITE	PRMX_LOG	3	-2.4000E+01	-2.1000E+01	-2.2502E+01	-2.4000E+01	-2.1000E+01	-2.2500E+01	0.01%	100.0%
AP161	S_MB139	PORE_DIS	1	4.9930E-01	8.0180E-01	6.4383E-01	4.9053E-01	8.4178E-01	6.4360E-01	0.04%	86.1%
AP161	S_MB139	PORE_DIS	2	4.9960E-01	7.9860E-01	6.4367E-01	4.9053E-01	8.4178E-01	6.4360E-01	0.01%	85.1%
AP161	S_MB139	PORE_DIS	3	5.0300E-01	7.9520E-01	6.4362E-01	4.9053E-01	8.4178E-01	6.4360E-01	0.00%	83.2%
AP161	S_MB139	PRMX_LOG	1	-2.0440E+01	-1.7140E+01	-1.8880E+01	-2.1000E+01	-1.7100E+01	-1.8890E+01	0.05%	84.6%
AP161	S_MB139	PRMX_LOG	2	-2.0660E+01	-1.7230E+01	-1.8883E+01	-2.1000E+01	-1.7100E+01	-1.8890E+01	0.04%	87.9%
AP161	S_MB139	PRMX_LOG	3	-2.0350E+01	-1.7330E+01	-1.8884E+01	-2.1000E+01	-1.7100E+01	-1.8890E+01	0.03%	77.4%
AP161	S_MB139	RELP_MOD	1	1.0000E+00	4.0000E+00	2.5000E+00	1.0000E+00	4.0000E+00	4.0000E+00	46.15%	100.0%
AP161	S_MB139	RELP_MOD	2	1.0000E+00	4.0000E+00	2.5000E+00	1.0000E+00	4.0000E+00	4.0000E+00	46.15%	100.0%
AP161	S_MB139	RELP_MOD	3	1.0000E+00	4.0000E+00	2.5000E+00	1.0000E+00	4.0000E+00	4.0000E+00	46.15%	100.0%
AP161	S_MB139	SAT_RBRN	1	1.5000E-02	1.5710E-01	8.3627E-02	7.7846E-03	1.7401E-01	8.3620E-02	0.01%	85.5%
AP161	S_MB139	SAT_RBRN	2	2.1280E-02	1.5680E-01	8.3789E-02	7.7846E-03	1.7401E-01	8.3620E-02	0.20%	81.5%
AP161	S_MB139	SAT_RBRN	3	2.1350E-02	1.4650E-01	8.3763E-02	7.7846E-03	1.7401E-01	8.3620E-02	0.17%	75.3%
AP161	SHFTL_T1	PRMX_LOG	1	-1.9970E+01	-1.6870E+01	-1.8214E+01	-2.0000E+01	-1.6500E+01	-1.8000E+01	1.18%	88.6%
AP161	SHFTL_T1	PRMX_LOG	2	-1.9930E+01	-1.7010E+01	-1.8214E+01	-2.0000E+01	-1.6500E+01	-1.8000E+01	1.18%	83.4%
AP161	SHFTL_T1	PRMX_LOG	3	-1.9550E+01	-1.7010E+01	-1.8210E+01	-2.0000E+01	-1.6500E+01	-1.8000E+01	1.16%	72.6%
AP161	SHFTL_T2	PRMX_LOG	1	-2.2360E+01	-1.8030E+01	-2.0063E+01	-2.2500E+01	-1.8000E+01	-1.9800E+01	1.32%	96.2%

Information Only

AP161	SHFTL_T2	PRMX_LOG	2	-2.2280E+01	-1.8140E+01	-2.0064E+01	-2.2500E+01	-1.8000E+01	-1.9800E+01	1.32%	92.0%

Information Only

				Observed			Parameter Database				
Analysis	Material	Property	Rep	Minimum	Maximum	Mean	Minimum	Maximum	Mean	RPD of Means	% Range Covered
AP161	SHFTL_T2	PRMX_LOG	3	-2.2340E+01	-1.8010E+01	-2.0065E+01	-2.2500E+01	-1.8000E+01	-1.9800E+01	1.33%	96.2%
AP161	SHFTU	PRMX_LOG	1	-2.0480E+01	-1.6930E+01	-1.8422E+01	-2.0500E+01	-1.6500E+01	-1.8200E+01	1.21%	88.8%
AP161	SHFTU	PRMX_LOG	2	-2.0400E+01	-1.6780E+01	-1.8420E+01	-2.0500E+01	-1.6500E+01	-1.8200E+01	1.20%	90.5%
AP161	SHFTU	PRMX_LOG	3	-2.0430E+01	-1.6640E+01	-1.8421E+01	-2.0500E+01	-1.6500E+01	-1.8200E+01	1.21%	94.8%
AP161	SHFTU	SAT_RBRN	1	1.7920E-03	5.9980E-01	2.5011E-01	0.0000E+00	6.0000E-01	2.5000E-01	0.04%	99.7%
AP161	SHFTU	SAT_RBRN	2	2.7560E-03	5.9740E-01	2.5008E-01	0.0000E+00	6.0000E-01	2.5000E-01	0.03%	99.1%
AP161	SHFTU	SAT_RBRN	3	9.6720E-04	5.9340E-01	2.5007E-01	0.0000E+00	6.0000E-01	2.5000E-01	0.03%	98.7%
AP161	SHFTU	SAT_RGAS	1	9.0910E-04	3.9790E-01	2.0013E-01	0.0000E+00	4.0000E-01	2.0000E-01	0.07%	99.2%
AP161	SHFTU	SAT_RGAS	2	2.0540E-03	3.9780E-01	1.9999E-01	0.0000E+00	4.0000E-01	2.0000E-01	0.00%	98.9%
AP161	SHFTU	SAT_RGAS	3	2.6970E-03	3.9760E-01	1.9997E-01	0.0000E+00	4.0000E-01	2.0000E-01	0.01%	98.7%
AP161	SOLMOD3	SOLVAR	1	-3.8830E+00	2.4390E+00	-1.4695E-01	-4.2000E+00	2.7000E+00	-1.4200E-01	3.42%	91.6%
AP161	SOLMOD3	SOLVAR	2	-3.7570E+00	2.5670E+00	-1.3553E-01	-4.2000E+00	2.7000E+00	-1.4200E-01	4.66%	91.7%
AP161	SOLMOD3	SOLVAR	3	-4.1540E+00	2.2650E+00	-1.4769E-01	-4.2000E+00	2.7000E+00	-1.4200E-01	3.93%	93.0%
AP161	SOLMOD4	SOLVAR	1	-2.1670E+00	3.2440E+00	-3.4862E-01	-2.2500E+00	3.3000E+00	-3.4600E-01	0.75%	97.5%
AP161	SOLMOD4	SOLVAR	2	-2.1840E+00	3.2140E+00	-3.3934E-01	-2.2500E+00	3.3000E+00	-3.4600E-01	1.94%	97.3%
AP161	SOLMOD4	SOLVAR	3	-2.1960E+00	3.2910E+00	-3.4969E-01	-2.2500E+00	3.3000E+00	-3.4600E-01	1.06%	98.9%
AP161	SPALLMOD	PARTDIAM	1	1.0090E-03	9.6550E-02	2.1478E-02	1.0000E-03	1.0000E-01	2.1500E-02	0.10%	96.5%
AP161	SPALLMOD	PARTDIAM	2	1.0010E-03	9.7620E-02	2.1560E-02	1.0000E-03	1.0000E-01	2.1500E-02	0.28%	97.6%
AP161	SPALLMOD	PARTDIAM	3	1.0420E-03	9.8220E-02	2.1569E-02	1.0000E-03	1.0000E-01	2.1500E-02	0.32%	98.2%

Information Only

AP161	SPALLMOD	REPIPERM	1	2.4240E-14	2.3160E-12	5.1466E-13	2.4000E-14	2.4000E-12	5.1600E-13	0.26%	96.5%

Information Only

				Observed			Parameter Database				
Analysis	Material	Property	Rep	Minimum	Maximum	Mean	Minimum	Maximum	Mean	RPD of Means	% Range Covered
AP161	SPALLMOD	REPIPERM	2	2.4940E-14	2.3680E-12	5.1489E-13	2.4000E-14	2.4000E-12	5.1600E-13	0.22%	98.6%
AP161	SPALLMOD	REPIPERM	3	2.4470E-14	2.3970E-12	5.1606E-13	2.4000E-14	2.4000E-12	5.1600E-13	0.01%	99.9%
AP161	SPALLMOD	REPIPOR	1	3.5090E-01	6.5790E-01	5.0482E-01	3.5000E-01	6.6000E-01	5.0500E-01	0.04%	99.0%
AP161	SPALLMOD	REPIPOR	2	3.5070E-01	6.5790E-01	5.0501E-01	3.5000E-01	6.6000E-01	5.0500E-01	0.00%	99.1%
AP161	SPALLMOD	REPIPOR	3	3.5170E-01	6.5850E-01	5.0508E-01	3.5000E-01	6.6000E-01	5.0500E-01	0.02%	99.0%
AP161	SPALLMOD	TENSLSTR	1	1.2050E+05	1.6990E+05	1.4499E+05	1.2000E+05	1.7000E+05	1.4500E+05	0.01%	98.8%
AP161	SPALLMOD	TENSLSTR	2	1.2020E+05	1.6990E+05	1.4497E+05	1.2000E+05	1.7000E+05	1.4500E+05	0.02%	99.4%
AP161	SPALLMOD	TENSLSTR	3	1.2030E+05	1.6980E+05	1.4501E+05	1.2000E+05	1.7000E+05	1.4500E+05	0.00%	99.0%
AP161	STEEL	CORRMCO2	1	2.1650E-16	3.1590E-14	1.5849E-14	0.0000E+00	3.1700E-14	1.5850E-14	0.01%	99.0%
AP161	STEEL	CORRMCO2	2	2.3720E-16	3.1440E-14	1.5860E-14	0.0000E+00	3.1700E-14	1.5850E-14	0.06%	98.4%
AP161	STEEL	CORRMCO2	3	5.5960E-17	3.1540E-14	1.5855E-14	0.0000E+00	3.1700E-14	1.5850E-14	0.03%	99.3%
AP161	TH+4	MKD_TH	1	5.2030E-04	9.6890E+00	1.0108E+00	5.0000E-04	1.0000E+01	1.0000E+00	1.07%	96.9%
AP161	TH+4	MKD_TH	2	5.2540E-04	9.7620E+00	1.0153E+00	5.0000E-04	1.0000E+01	1.0000E+00	1.52%	97.6%
AP161	TH+4	MKD_TH	3	5.2410E-04	9.7480E+00	1.0098E+00	5.0000E-04	1.0000E+01	1.0000E+00	0.97%	97.5%
AP161	U+4	MKD_U	1	5.4480E-04	9.4190E+00	1.0034E+00	5.0000E-04	1.0000E+01	1.0000E+00	0.34%	94.2%
AP161	U+4	MKD_U	2	5.2020E-04	9.7440E+00	1.0082E+00	5.0000E-04	1.0000E+01	1.0000E+00	0.81%	97.4%

Information Only

AP161	U+4	MKD_U	3	5.0740E-04	9.8830E+00	1.0138E+00	5.0000E-04	1.0000E+01	1.0000E+00	1.38%	98.8%
AP161	U+6	MKD_U	1	3.1430E-05	1.9660E-02	3.0715E-03	3.0000E-05	2.0000E-02	3.1000E-03	0.92%	98.3%

Information Only

				Observed			Parameter Database				
Analysis	Material	Property	Rep	Minimum	Maximum	Mean	Minimum	Maximum	Mean	RPD of Means	% Range Covered
AP161	U+6	MKD_U	2	3.1100E-05	1.9860E-02	3.0796E-03	3.0000E-05	2.0000E-02	3.1000E-03	0.66%	99.3%
AP161	U+6	MKD_U	3	3.0650E-05	1.8760E-02	3.0749E-03	3.0000E-05	2.0000E-02	3.1000E-03	0.81%	93.8%
AP161	WAS_AREA	BIOGENFC	1	2.8190E-03	9.9660E-01	5.0055E-01	0.0000E+00	1.0000E+00	5.0000E-01	0.11%	99.4%
AP161	WAS_AREA	BIOGENFC	2	1.8050E-03	9.9670E-01	5.0033E-01	0.0000E+00	1.0000E+00	5.0000E-01	0.07%	99.5%
AP161	WAS_AREA	BIOGENFC	3	2.6460E-04	9.9900E-01	5.0033E-01	0.0000E+00	1.0000E+00	5.0000E-01	0.07%	99.9%
AP161	WAS_AREA	GRATMICH	1	5.5740E-12	1.0240E-09	5.1335E-10	0.0000E+00	1.0272E-09	5.1359E-10	0.05%	99.1%
AP161	WAS_AREA	GRATMICH	2	2.6550E-12	1.0170E-09	5.1354E-10	0.0000E+00	1.0272E-09	5.1359E-10	0.01%	98.8%
AP161	WAS_AREA	GRATMICH	3	6.7330E-13	1.0260E-09	5.1376E-10	0.0000E+00	1.0272E-09	5.1359E-10	0.03%	99.8%
AP161	WAS_AREA	GRATMICI	1	3.2590E-11	5.5550E-10	2.9402E-10	3.0827E-11	5.5692E-10	2.9387E-10	0.05%	99.4%
AP161	WAS_AREA	GRATMICI	2	3.4030E-11	5.5340E-10	2.9363E-10	3.0827E-11	5.5692E-10	2.9387E-10	0.08%	98.7%
AP161	WAS_AREA	GRATMICI	3	3.1480E-11	5.5230E-10	2.9375E-10	3.0827E-11	5.5692E-10	2.9387E-10	0.04%	99.0%
AP161	WAS_AREA	PROBDEG	1	1.0000E+00	2.0000E+00	1.2500E+00	1.0000E+00	2.0000E+00	1.2500E+00	0.00%	100.0%
AP161	WAS_AREA	PROBDEG	2	1.0000E+00	2.0000E+00	1.2500E+00	1.0000E+00	2.0000E+00	1.2500E+00	0.00%	100.0%
AP161	WAS_AREA	PROBDEG	3	1.0000E+00	2.0000E+00	1.2500E+00	1.0000E+00	2.0000E+00	1.2500E+00	0.00%	100.0%
AP161	WAS_AREA	SAT_RBRN	1	2.7080E-03	5.5090E-01	2.7620E-01	0.0000E+00	5.5200E-01	2.7600E-01	0.07%	99.3%

Information Only

AP1.51	WAS_AREA	SAT_RBRN	2	6.6340E-04	5.4700E-01	2.7587E-01	0.0000E+00	5.5200E-01	2.7600E-01	0.05%	99.0%

Information Only

				Observed			Parameter Database				
Analysis	Material	Property	Rep	Minimum	Maximum	Mean	Minimum	Maximum	Mean	RPD of Means	% Range Covered
AP161	WAS_AREA	SAT_RBRN	3	3.9740E-03	5.4820E-01	2.7631E-01	0.0000E+00	5.5200E-01	2.7600E-01	0.11%	98.6%
AP161	WAS_AREA	SAT_RGAS	1	7.7230E-04	1.4850E-01	7.4990E-02	0.0000E+00	1.5000E-01	7.5000E-02	0.01%	98.5%
AP161	WAS_AREA	SAT_RGAS	2	6.3450E-04	1.4960E-01	7.4972E-02	0.0000E+00	1.5000E-01	7.5000E-02	0.04%	99.3%
AP161	WAS_AREA	SAT_RGAS	3	7.0690E-04	1.4880E-01	7.5076E-02	0.0000E+00	1.5000E-01	7.5000E-02	0.10%	98.7%
AP161	WAS_AREA	SAT_WICK	1	3.0550E-03	9.9240E-01	5.0024E-01	0.0000E+00	1.0000E+00	5.0000E-01	0.05%	98.9%
AP161	WAS_AREA	SAT_WICK	2	2.3240E-03	9.9930E-01	5.0047E-01	0.0000E+00	1.0000E+00	5.0000E-01	0.09%	99.7%
AP161	WAS_AREA	SAT_WICK	3	4.4040E-03	9.9270E-01	4.9988E-01	0.0000E+00	1.0000E+00	5.0000E-01	0.02%	98.8%

Information Only

Appendix VIII. LHS_EDIT

1.1. Description and Requirements

LHS_EDIT was created to impose conditional relationships between pairs of variables for the case where 1) one variable was restricted to having values less than or equal to the other "controlling" variable and 2) the restricted, or conditioned, variable has a uniform distribution. LHS_EDIT is designed to read the LHS output (transfer) file and:

1) Extract the upper and lower bounds for the uniform distribution of the variable to be restricted,
2) Extract the sampled values for each pair of variables,
3) Compare the value of the variable to be restricted to the value of the controlling variable,
4) Rescale the restricted value if it exceeds the value of the controlling variable, and
5) Write a new transfer file containing the modified data.

The restricted value is rescaled by assuming that the distribution of the restricted value is a uniform distribution with an upper bound that is the minimum of the upper bound assigned to the parameter in the parameter data base and the sampled value of the controlling variable. The conditioned value of the restricted variable is computed using:

$$v_i' = \frac{v_i - U_{V,lower}}{U_{V,upper} - U_{V,lower}} \times \left(Min(x_i, U_{V,upper}) - U_{V,lower} \right) + U_{V,lower}$$

where v_i' is the conditioned value of the restricted variable, v_i is the sampled value of the restricted variable, x_i is the sampled value of the controlling variable, and $U_{V,lower}$ and $U_{V,upper}$ are the bounds of the distribution assigned to the restricted variable. This method preserves the probability associated with the value of the restricted variable but will affect the rank-order correlations with the other variables.

The format of the numbers in the listing of the distribution parameters in the LHS transfer file is limited to four digits after the decimal point, whereas the database can store more significant digits. The variables that were modified by LHS_EDIT have 1 more digit stored in the Parameter Database than can be represented by the LHS format, thus introducing a small error in the rescaling calculation. However, the error is insignificant because the rounding occurs in the fourth digit after the decimal point, i.e. the fifth significant digit.

1.2. Platform and Source Code Description

The LHS_EDIT source code was written in FORTRAN 90 and executed on OpenVMS Version 7.3-1 operating system.

Information Only

1.3. Usage

Files

LHS_EDIT requires as input the LHS output (transfer) file and a control file listing the pairs of variables to be related. The control file contains a record for each pair of variables and the variables are identified by a number corresponding to the numeric sequence of the variables in the PRELHS input file. The format for the record is (I2,1x,I2). The output files for LHS_EDIT are a new transfer file having the conditioned data and a file called CHECK.TXT. CHECK.TXT lists the values of the controlling, restricted and conditioned variables in a comma-delimited format. CHECK.TXT can be used to easily check whether LHS_EDIT is functioning properly.

Execution

File names are passed to LHS_EDIT using VMS logical variables. These variables are assigned values using the define command. The logical variables are LHS_CONTROL, LHS2_TRN, and LHS_EDIT_OUT for the control, LHS transfer file and the new transfer file, respectively. For example:

```
$  define LHS_CONTROL lhs_control_R1.inp
$  define LHS2_TRN lhs2_AP132_R1.trn
$  define LHS_EDIT_OUT lhs2_AP132_R1_CON.trn
$  run LHS_EDIT
```

For the PCS-2012 PA LHS_EDIT was executed using the EVAL_LHS.COM script and the file names were passed to EVAL_LHS.COM through its input file (EVAL_LHS_AP161_R*n*.INP, where *n* is 1, 2 or 3 for the three replicates). The script and input files are stored in the SCMS library PACMS2:[CMS_AP161.AP161_EVAL]

1.4. Testing of LHS_EDIT

Test Procedure

The test of the performance of LHS_EDIT was conducted by examining the data for Replicate 1 of the LHS transfer file and the LHS_EDIT output file. There have been no changes to LHS_EDIT since the test documented in Kirchner (2009). The data for WAS_AREA:GRATMICI and WAS_AREA:GRATMICH were extracted from these files and put into tables using the "Load LHS File" function of the Access database CCDFGF_Analysis. The maximum and minimum for the distribution of WAS_AREA:GRATMICH were obtained from the PA Parameter Database (PAPDB) table ParamAttributes. The query TestLHS_EDIT was used to compare the values produced by LHS_Edit to independently computed values.

Information Only

```
SELECT LHS_ParamValues.Vector, LHS_ParamValues.Value AS GRATMICI, LHS_ParamValues_1.Value AS GRATMICH,
ParamAttributes.value AS [Min], ParamAttributes_1.value AS [Max], IIf([GRATMICH]>[GRATMICI],([GRATMICH]-[Min])/([Max]-
[Min])*([GRATMICI]-[Min])+[Min],[GRATMICH]) AS TestValue, LHS_ParamValues_2.Value AS ConditionedValue,
IIf((Abs([ConditionedValue]-[TestValue])/[ConditionedValue]>0.001) Or [ConditionedValue]>[GRATMICI],"error",""") AS
ErrorFlag

FROM LHS_FileNames AS LHS_FileNames_1 INNER JOIN ((((LHS_ParamValues INNER JOIN LHS_FileNames ON
LHS_ParamValues.FileID = LHS_FileNames.FileID) INNER JOIN LHS_ParamValues AS LHS_ParamValues_1 ON
(LHS_ParamValues.Vector = LHS_ParamValues_1.Vector) AND (LHS_FileNames.FileID = LHS_ParamValues_1.FileID)) INNER
JOIN ((AnalysisToVersion INNER JOIN ParamAttributes ON AnalysisToVersion.VersionNumber =
ParamAttributes.VersionNumber) INNER JOIN ParamAttributes AS ParamAttributes_1 ON AnalysisToVersion.VersionNumber =
ParamAttributes_1.VersionNumber) ON (LHS_ParamValues_1.Property = AnalysisToVersion.Property) AND
(LHS_ParamValues_1.Material = AnalysisToVersion.Material) AND (LHS_ParamValues_1.Property =
ParamAttributes_1.Property) AND (LHS_ParamValues_1.Material = ParamAttributes_1.Material) AND
(LHS_ParamValues_1.Property = ParamAttributes.Property) AND (LHS_ParamValues_1.Material = ParamAttributes.Material))
INNER JOIN LHS_ParamValues AS LHS_ParamValues_2 ON (LHS_ParamValues_1.Vector = LHS_ParamValues_2.Vector) AND
(LHS_ParamValues_1.Property = LHS_ParamValues_2.Property) AND (LHS_ParamValues_1.Material =
LHS_ParamValues_2.Material)) ON LHS_FileNames_1.FileID = LHS_ParamValues_2.FileID

WHERE (((LHS_ParamValues.Material)="WAS_AREA") AND ((LHS_ParamValues.Property)="GRATMICI") AND
((LHS_ParamValues_1.Material)="WAS_AREA") AND ((LHS_ParamValues_1.Property)="GRATMICH") AND
((LHS_FileNames.Analysis)="ap161") AND ((LHS_FileNames.Replicate)=1) AND ((ParamAttributes.Attribute)="Minimum") AND
((AnalysisToVersion.Analysis)="ap161") AND ((AnalysisToVersion.Code)="BRAGFLO") AND
((ParamAttributes_1.Attribute)="Maximum") AND ((LHS_FileNames_1.Analysis)="ap161_cond") AND
((LHS_FileNames_1.Replicate)=1))

ORDER BY LHS_ParamValues.Vector;
```

□□□□□ □ **for t□□□□t□□□□□□l□ □□□ry□**

The "Test Value" was computed using the formula "IIf([GRATMICH] > [GRATMICI],([GRATMICH]-[Min])/([Max]-[Min])*([GRATMICI]-[Min])+[Min],[GRATMICH])", where Min is the minimum and Max is the maximum for the distribution of WAS_AREA:GRATMICH. This formula is equivalent to Eq. 2. The Error Flag field was set to "Error" if the conditioned value did not equal the Test Value to within 0.1 % or if the conditioned value exceeded the value of WAS_AREA:GRATMICI. No such errors were observed. The CCDFGF_Analysis.mdb and the associated CCDFGF_Data.mdb files are contained in the CCDFGF_Analysis.zip file and stored in the library LIBAP161_LHS.

□a□□□□□r□a□□□□t r□□□t□□□b□in□in□□□□n□□ntly □om□□t□□ □al□□□□□□t □al□□□for WAS_AREA:
□□□□□ I□□□

Vector	GRATMICI	GRATMICH	Test Value	Conditioned GRATMICH	Error Flag
1	2.386E-10	3.388E-11	3.388E-11	3.388E-11	

Information Only

2	7.815E-11	7.244E-10	5.511E-11	5.511E-11	
3	3.285E-10	2.922E-10	2.922E-10	2.922E-10	
4	7.927E-11	9.082E-10	7.009E-11	7.009E-11	
5	5.275E-10	7.871E-10	4.042E-10	4.042E-10	
6	4.086E-10	9.649E-10	3.838E-10	3.838E-10	
7	5.085E-10	4.603E-10	4.603E-10	4.603E-10	
8	3.044E-10	9.548E-10	2.830E-10	2.829E-10	
9	5.452E-10	7.937E-10	4.213E-10	4.213E-10	
10	3.320E-10	1.764E-10	1.764E-10	1.764E-10	
11	5.351E-10	5.574E-12	5.574E-12	5.574E-12	
12	1.215E-10	5.749E-10	6.800E-11	6.800E-11	
13	3.190E-10	4.495E-10	1.396E-10	1.396E-10	
14	1.305E-10	6.290E-10	7.991E-11	7.991E-11	
15	1.833E-10	5.237E-10	9.346E-11	9.345E-11	
16	1.717E-10	8.889E-10	1.486E-10	1.486E-10	
17	2.606E-10	1.032E-11	1.032E-11	1.032E-11	
18	3.259E-11	6.244E-10	1.981E-11	1.981E-11	
19	1.924E-10	8.524E-10	1.597E-10	1.597E-10	
20	2.853E-10	7.522E-10	2.089E-10	2.089E-10	
21	4.886E-10	2.134E-10	2.134E-10	2.134E-10	
22	2.248E-10	3.043E-10	6.660E-11	6.660E-11	
23	2.082E-10	6.378E-10	1.293E-10	1.293E-10	
24	3.950E-11	8.538E-10	3.283E-11	3.283E-11	
25	4.442E-10	4.511E-11	4.511E-11	4.511E-11	
26	1.143E-10	7.013E-10	7.804E-11	7.804E-11	
27	2.332E-10	6.518E-10	1.480E-10	1.480E-10	
28	4.361E-10	6.953E-10	2.952E-10	2.952E-10	
29	4.324E-11	7.338E-10	3.089E-11	3.089E-11	
30	3.814E-10	1.294E-10	1.294E-10	1.294E-10	
31	9.191E-11	4.245E-10	3.798E-11	3.798E-11	
32	2.648E-10	1.980E-10	1.980E-10	1.980E-10	
33	4.720E-10	2.652E-10	2.652E-10	2.652E-10	
34	4.038E-10	4.806E-10	1.889E-10	1.889E-10	
35	2.497E-10	1.012E-09	2.460E-10	2.460E-10	
36	1.507E-10	6.626E-10	9.721E-11	9.721E-11	
37	4.595E-10	3.513E-10	3.513E-10	3.513E-10	
38	3.887E-10	5.004E-10	1.894E-10	1.894E-10	
39	3.592E-10	9.742E-10	3.407E-10	3.407E-10	
40	3.539E-10	2.486E-10	2.486E-10	2.486E-10	

Information Only

41	4.200E-10	1.010E-10	1.010E-10	1.010E-10	
42	1.611E-10	8.643E-10	1.356E-10	1.356E-10	
43	4.470E-10	9.822E-10	4.274E-10	4.274E-10	
44	5.175E-10	9.931E-10	5.003E-10	5.003E-10	
45	8.357E-11	3.108E-10	2.529E-11	2.529E-11	
46	2.521E-10	6.831E-10	1.677E-10	1.676E-10	
47	1.027E-10	3.940E-10	3.939E-11	3.939E-11	
48	2.285E-10	3.723E-10	8.282E-11	8.282E-11	
49	3.250E-10	1.735E-10	1.735E-10	1.735E-10	
50	5.025E-10	3.628E-10	3.628E-10	3.628E-10	
51	2.718E-10	9.993E-10	2.644E-10	2.644E-10	
52	5.368E-10	1.380E-10	1.380E-10	1.380E-10	
53	3.494E-10	5.884E-10	2.001E-10	2.001E-10	
54	2.902E-10	5.489E-10	1.551E-10	1.551E-10	
55	4.835E-10	2.779E-10	2.779E-10	2.779E-10	
56	5.058E-11	8.385E-10	4.129E-11	4.129E-11	
57	4.563E-10	7.754E-10	3.445E-10	3.444E-10	
58	3.086E-10	5.417E-10	1.627E-10	1.627E-10	
59	4.218E-10	1.097E-10	1.097E-10	1.097E-10	
60	5.232E-10	7.400E-10	3.769E-10	3.769E-10	
61	1.067E-10	5.755E-10	5.978E-11	5.978E-11	
62	3.634E-10	6.134E-10	2.170E-10	2.170E-10	
63	1.409E-10	8.140E-10	1.117E-10	1.117E-10	
64	6.744E-11	4.164E-10	2.734E-11	2.734E-11	
65	5.117E-10	2.362E-11	2.362E-11	2.362E-11	
66	9.678E-11	4.838E-10	4.558E-11	4.558E-11	
67	1.952E-10	9.249E-10	1.758E-10	1.758E-10	
68	2.828E-10	6.035E-11	6.035E-11	6.035E-11	
69	3.945E-10	8.815E-10	3.386E-10	3.385E-10	
70	1.636E-10	1.862E-10	2.966E-11	2.966E-11	
71	5.503E-10	9.219E-10	4.939E-10	4.939E-10	
72	2.421E-10	2.177E-10	2.177E-10	2.177E-10	
73	4.759E-10	3.455E-10	3.455E-10	3.455E-10	
74	3.438E-10	6.009E-10	2.011E-10	2.011E-10	
75	2.973E-10	1.563E-10	1.563E-10	1.563E-10	
76	5.555E-10	1.024E-09	5.538E-10	5.538E-10	
77	1.757E-10	2.672E-10	4.571E-11	4.570E-11	
78	1.444E-10	6.379E-11	6.379E-11	6.379E-11	
79	1.327E-10	9.124E-11	9.124E-11	9.124E-11	

Information Only

80	7.024E-11	7.611E-10	5.205E-11	5.204E-11
81	3.677E-10	5.104E-10	1.827E-10	1.827E-10
82	1.180E-10	8.947E-10	1.028E-10	1.028E-10
83	2.038E-10	7.849E-11	7.849E-11	7.849E-11
84	5.259E-11	6.730E-10	3.446E-11	3.446E-11
85	4.794E-10	2.433E-10	2.433E-10	2.433E-10
86	5.762E-11	3.288E-10	1.844E-11	1.844E-11
87	4.940E-10	7.164E-10	3.445E-10	3.445E-10
88	2.739E-10	4.093E-10	1.091E-10	1.091E-10
89	4.272E-10	4.368E-10	1.817E-10	1.817E-10
90	1.873E-10	1.148E-10	1.148E-10	1.148E-10
91	3.111E-10	8.042E-10	2.436E-10	2.436E-10
92	1.552E-10	8.290E-10	1.253E-10	1.253E-10
93	4.354E-10	2.292E-10	2.292E-10	2.292E-10
94	4.629E-10	3.874E-10	3.874E-10	3.874E-10
95	3.842E-10	5.618E-10	2.101E-10	2.101E-10
96	3.763E-10	3.229E-10	3.229E-10	3.229E-10
97	3.397E-10	5.294E-10	1.751E-10	1.751E-10
98	4.116E-10	9.420E-10	3.775E-10	3.775E-10
99	2.171E-10	1.445E-10	1.445E-10	1.445E-10
100	2.134E-10	4.645E-10	9.650E-11	9.650E-11

Acceptance Criteria

The acceptance criteria for the test is that an independent calculation of the conditioned value for WAS_AREA:GRATMICH match with the reported precision the value computed by LHS_EDIT.

Evaluation

The Test Values matched the values computed by LHS_EDIT in every case where WAS_AREA:GRATMICH exceeded WAS_AREA:GRATMICI.

1.5. Source Code

The source code for LHS_EDIT Version 1.0 can be found in the file LHS_EDIT.FOR in the SCMS library PACMS2:[CMS_AP132.AP132_LHS] (LIBAP132_LHS) in the LHS_EDIT_V1.0 class. The executable LHS_EDIT.EXE is found in the same library and class. The source code is reproduced below.

Information Only

```
      Program LHSedit
!.....Purpose: Edit a LHS output file by restricting the value in column col2
to
!              to never exceed the value in col1
!     Author: Tom Kirchner
!     Version: 1.0

!.....Edit a LHS output file by restricting the value in column col2 to
!     never exceed the value in col1
      Character*160 line
      Double precision a,b    !Endpoints of the first (rightmost)
distribution
      Double precision c,d    !Endpoints of the second (leftmost)
distribution
      Integer col1, col2      !The primary and conditional variables
      Double precision current(100,75)
      Character*160 spacer(4,7)
      Common/NewData/current,spacer

!.....Load the data into value()
      Call ReadFloats(current,spacer)

!.....Open the "control" file
      OPEN(2,file='LHS_CONTROL')
      Open(3,FILE="check.txt")
    5 Read(2,'(i2,1x,i2)',END=50) col1, col2
!.........Read the distribution definition section
          Call ReadDistInfo(col1, a, b, col2, c, d)
          write(*,*) "Column 1: ", col1," Range: ",a,b
          write(*,*) "Column 2: ", col2," Range: ",c,d
          write(*,'(a,i2,2a,i2)') " Data in column ",col2," to be ",
     &             "conditioned on column ",col1

!.........Now mofify the file
          Call MakeConditional(col1,col2,a,b,c,d)
      GoTo 5
   50 Close(2)
      Close(3)

!.....Now write the new file
      Call WriteFile

      Stop
  100 Format(a160)
  110 Format(a160)
      End

      Subroutine ReadFloats(fpvalue,spacer)
!.....Read the sampled values into the fpvalue array, preserving the
!     headers between "pages" in the spacer array
      Double precision fpvalue(100,75)
      Character*160 spacer(4,7)
      Character*160 line
      Integer LineNum
```


Information Only

```
      Open(1,FILE='LHS2_TRN',ERR=75)
      Do While (.not.eof(1))
          Read(1,210) line
        If (line(1:14).eq." RUN NO.  X(1)") then
              Do k=1,7
                  Do i=1,100
                      Read(1,200) LineNum,(fpvalue(i,(k-1)*10+j),j=1,10)
                End Do
                Do i=1,4
                      Read(1,210) spacer(i,k)
                End Do
               End Do

              Do i=1,100
                Read(1,200) LineNum,(fpvalue(i,70+j),j=1,5)
              End Do
              Close(1)
              Return
           End If
      End Do
      Close (1)
      Return
   75 Write(*,*) "Error opening file"
  200 Format(3x,i3,10(1x,f10.3))
  210 Format(a160)
      End

      Subroutine MakeConditional(col1,col2,a,b,c,d)
!.....Modify values in column col2
!     by 1) reading values from columns col1 and col2 of LHS2_TRN
!        2) rescaling the value in col2 so that it is alway greater than
!           that in col1
!     A new file is written which leaves all the data in LHS2_TRN above and
!     below the sampled values unchanged.
      Integer col1, col2
      Character*160 line
      Double precision current(100,75)
      Character*160 spacer(4,7)
      Common/NewData/current,spacer
      Double precision Rescale, v, a, b, c, d, upper

!...... Now replace the data
        Write(3,*) "Column 1, Column 2, Conditioned Column 2"
      Do i=1,100
          v=Rescale(i,current,col1,col2, a,b,c,d)
          Write(3,*) current(i,col1),",",current(i,col2),',',v
          current(i,col2)=v
      End Do
      Return
      End

      Subroutine WriteFile
!.......Write out the file with the modify values
```


Information Only

```
!     A new file is written which leaves all the data in LHS2_TRN above and
!     below the sampled values unchanged.
      character*160 line
      Double precision current(100,75)
      character*160 spacer(4,7)
      Common/NewData/current,spacer
      Character*3 fmt

      fmt="0  "

      Open(1,FILE='LHS2_TRN')
      Open(2,FILE='LHS_EDIT_OUT',recl=160)
        Write(2,'(a)') "1"
      Do While (.not.eof(1))
          Read(1,410) line
          If (line(1:14).eq." RUN NO.  X(1)") then
              Write(2,'(a)') trim(line)
!           and write the new values out
            Do k=1,7
                Do i=1,100
                    Write(2,400)fmt,i,(current(i,(k-1)*10+j),
     &                          j=1,10)
                End Do
                Do i=1,4
                      Write(2,'(a)') trim(spacer(i,k))
                End Do
            End Do
            Do i=1,100
                Write(2,400) fmt,i,(current(i,70+j),j=1,5)
            End Do

          Else
              Write(2,'(a)') trim(line)
          End If
      End Do
      Return
  400   Format(a3,i3,10(1x,1pE10.3))
  410   Format(a160)
      End

      Double Precision Function Rescale(i,current,col1, col2, a, b, c, d)
!.....Adjust col2 so that it never exceeds col1
!     The distribution of col2 ranges from [c-d]
!     The distribution of col1 ranges from [a-b]
      Double precision current(100,75), a, b, c, d, upper
      Integer i, col1, col2
      Double precision v

      v=current(i,col2)
      If (current(i,col2).GT.current(i,col1)) then
          upper=current(i,col1)
          v=(current(i,col2)-c)/(d-c)*(upper-c)+c
      End If
```


Information Only

```
      Rescale = v

      Return
      End

      Subroutine ReadDistInfo(col1, a, b, col2, c, d)
!.....Read the distribution information and save the range limits
!     for the uniform distribution for the col1 variable
      Integer col2, col1
      Integer VarNum
      Double Precision a, b, c, d
      Character*160 line
!     Open the file
      Open(1,FILE='LHS2_TRN')
!     Skip the first page of the header
      Do While (line(1:26).ne."    VARIABLE  DISTRIBUTION")
         Read(1,800) line
      End Do
!.....Now process the definitions
      Do While (line(1:1).ne."1")          !marks the end of the data
        Read(1,800) line
        If (line(11:21).eq."    UNIFORM") Then
!             Get the variable number
              Read(line,'(7x,i2)') VarNum
            If (VarNum.eq.col2) Then
!             Get the minimum and maximum
                  Read(line,'(33x,e10.4)') c
                  Read(line,'(49x,e10.4)') d
            Else if (VarNum.eq.col1) Then
!             Get the minimum and maximum
                  Read(line,'(33x,e10.4)') a
                  Read(line,'(49x,e10.4)') b
            End if
        End If
      End Do
      Close (1)
      return
  800 Format(a160)
      End
```


Information Only

558204

Sandia National Laboratories
Waste Isolation Pilot Plant

Analysis Package for Salado Flow Modeling Done in the AP-161 (PCS-2012) Performance Assessment

Revision 0

Author:	Chris Camphouse		9/17/2012
	Print	Signature	Date
Technical Review:	Bwalya Malama		09/17/2012
	Print	Signature	Date
QA Review:	Shelly Nielsen	Shelly R. Nielsen	9-17-12
	Print	Signature	Date
Management Review:	Sean Dunagan		9/17/2012
	Print	Signature	Date

WIPP:1.4.1.2:PA:QA-L:557393

Information Only

Table of Contents

1 Executive Summary 5
2 Introduction 6
3 Conceptual Approach for PCS-2012 PA 7
3.1 Repository Representation in BRAGFLO 7
3.2 Panel Closure Parameterization 17
3.2.1 Capillary Pressure Parameters 19
4 Salado Flow Modeling Methodology 21
4.1 Initial Conditions 22
4.2 Boundary Conditions 23
5 Run Control 24
6 Results 24
6.1.1 Results for an Undisturbed Repository (Scenario S1-BF) 27
6.1.2 Results for an E1 Intrusion at 350 Years (Scenario S2-BF) 43
6.1.3 Results for an E2 Intrusion at 350 Years (Scenario S4-BF) 53
6.1.4 Results for an E2 Intrusion at 1000 Years Followed by a E1 Intrusion at 2000 Years (Scenario S6-BF) 66
7 Summary 69
8 References 70

Information Only

List of Figures

Figure 3-1: A Schematic of the "Option D" Panel Closure 7
Figure 3-2: PABC-2009 BRAGFLO Grid and Material Map (Δx, Δy, and Δz dimensions in meters). 8
Figure 3-3: Schematic Diagram of the ROMPCS 10
Figure 3-4: PCS-2012 BRAGFLO Grid and Material Map, Years 0 to 100 12
Figure 3-5: PCS-2012 BRAGFLO Grid and Material Map, Years 100 to 200 13
Figure 3-6: PCS-2012 BRAGFLO Grid and Material Map, Years 200 to Time of Intrusion 14
Figure 3-7: PCS-2012 BRAGFLO Grid and Material Map for an E1 Intrusion 15
Figure 3-8: PCS-2012 BRAGFLO Grid and Material Map for an E2 Intrusion 16
Figure 6-1: PCS-2012 PA Definition of Cumulative Flow toward the Waste Panel, across the Southernmost Panel Closure Plane 28
Figure 6-2: PABC-2009 Definition of Cumulative Flow toward the Waste Panel, across the Southernmost Panel Closure Plane 28
Figure 6-3: Horsetail Plot of Cumulative Brine Inflow to the Waste Panel, Scenario S1-BF 32
Figure 6-4: Means of Cumulative Brine Inflow to the Waste Panel, Scenario S1-BF 32
Figure 6-5: Overall Means of Cumulative Brine Inflow to the Waste Panel, Scenario S1-BF. 33
Figure 6-6: Overall Means of Cumulative Brine Inflow to the Waste Panel, Scenario S1-BF and Years 0 to 1,000 33
Figure 6-7: Overall Means of Cumulative Brine Flow Southward from the Panel Closure Plane and toward the Waste Panel, Scenario S1-BF 34
Figure 6-8: Overall Means of Cumulative Brine Flow Southward from the Panel Closure Plane and toward the Waste Panel, Scenario S1-BF and Years 0 to 1,000. 34
Figure 6-9: Horsetail Plot of Waste Panel Brine Saturation, Scenario S1-BF. 35
Figure 6-10: Means of Waste Panel Brine Saturation, Scenario S1-BF. 35
Figure 6-11: Overall Means of Waste Panel Brine Saturation, Scenario S1-BF. 36
Figure 6-12: Overall Means of Waste Panel Brine Saturation, Scenario S1-BF and Years 0 to 1,000. 36
Figure 6-13: Horsetail Plot of Waste Panel Gas Generation (in moles), Scenario S1-BF. 37
Figure 6-14: Means of Waste Panel Gas Generation (in moles), Scenario S1-BF. 37
Figure 6-15: Overall Means of Waste Panel Gas Generation (in moles), Scenario S1-BF. 38
Figure 6-16: Horsetail Plot of Waste Panel Pressure, Scenario S1-BF 38
Figure 6-17: Means of Waste Panel Pressure, Scenario S1-BF 39
Figure 6-18: Overall Means of Waste Panel Pressure, Scenario S1-BF 39
Figure 6-19: Overall Means of Waste Panel Pressure, Scenario S1-BF and Years 0 to 1,000 40
Figure 6-20: Overall Means of Pressure in the Operations Region, Scenario S1-BF. 40
Figure 6-21: Overall Means of Pressure in the Experimental Region, Scenario S1-BF. 41
Figure 6-22: Horsetail Plot of Brine Flow up the Shaft, Scenario S1-BF. 41
Figure 6-23: Means of Brine Flow up the Shaft, Scenario S1-BF. 42
Figure 6-24: Overall Means of Brine Flow up the Shaft, Scenario S1-BF. 42
Figure 6-25: Horsetail Plot of Waste Panel Pressure, Scenario S2-BF 45
Figure 6-26: Means of Waste Panel Pressure, Scenario S2-BF 45
Figure 6-27: Overall Means of Waste Panel Pressure, Scenario S2-BF 46
Figure 6-28: Horsetail Plot of Cumulative Brine Inflow to the Waste Panel, Scenario S2-BF 46
Figure 6-29: Means of Cumulative Brine Inflow to the Waste Panel, Scenario S2-BF 47
Figure 6-30: Overall Means of Cumulative Brine Inflow to the Waste Panel, Scenario S2-BF 47
Figure 6-31: Horsetail Plot of Waste Panel Brine Saturation, Scenario S2-BF. 48
Figure 6-32: Means of Waste Panel Brine Saturation, Scenario S2-BF. 48
Figure 6-33: Overall Means of Waste Panel Brine Saturation, Scenario S2-BF. 49
Figure 6-34: Horsetail Plot of Waste Panel Gas Generation (in moles), Scenario S2-BF. 49
Figure 6-35: Means of Waste Panel Gas Generation (in moles), Scenario S2-BF. 50
Figure 6-36: Overall Means of Waste Panel Gas Generation (in moles), Scenario S2-BF. 50
Figure 6-37: Horsetail Plot of Brine Flow up the Borehole, Scenario S2-BF. 51
Figure 6-38: Means of Brine Flow up the Borehole, Scenario S2-BF. 51
Figure 6-39: Means of Brine Flow up the Borehole, Scenario S2-BF for the PABC-2009. 52
Figure 6-40: Overall Means of Brine Flow up the Borehole, Scenario S2-BF. 52

Information Only

Figure 6-41: Horsetail Plot of Waste Panel Pressure, Scenario S4-BF. 56
Figure 6-42: Means of Waste Panel Pressure, Scenario S4-BF. 56
Figure 6-43: Overall Means of Waste Panel Pressure, Scenarios S1-BF and S4-BF for Years 0 to 1,000. 57
Figure 6-44: Overall Means of Waste Panel Pressure, Scenario S4-BF. 57
Figure 6-45: Horsetail Plot of Cumulative Brine Inflow to the Waste Panel, Scenario S4-BF. 58
Figure 6-46: Means of Cumulative Brine Inflow to the Waste Panel, Scenario S4-BF. 58
Figure 6-47: Overall Means of Cumulative Brine Inflow to the Waste Panel, Scenarios S1-BF and S4-BF for Years 0 to 1,000. 59
Figure 6-48: Overall Means of Cumulative Brine Inflow to the Waste Panel, Scenario S4-BF. 59
Figure 6-49: Horsetail Plot of Waste Panel Brine Saturation, Scenario S4-BF. 60
Figure 6-50: Means of Waste Panel Brine Saturation, Scenario S4-BF. 60
Figure 6-51: Overall Means of Waste Panel Brine Saturation, Scenarios S1-BF and S4-BF for Years 0 to 1,000. 61
Figure 6-52: Overall Means of Waste Panel Brine Saturation, Scenario S4-BF. 61
Figure 6-53: Horsetail Plot of Waste Panel Gas Generation (in moles), Scenario S4-BF. 62
Figure 6-54: Means of Waste Panel Gas Generation (in moles), Scenario S4-BF. 62
Figure 6-55: Overall Means of Waste Panel Gas Generation (in moles), Scenarios S1-BF and S4-BF for Years 0 to 1,000. 63
Figure 6-56: Overall Means of Waste Panel Gas Generation (in moles), Scenario S4-BF. 63
Figure 6-57: Horsetail Plot of Brine Flow up the Borehole, Scenario S4-BF. 64
Figure 6-58: Means of Brine Flow up the Borehole, Scenario S4-BF. 64
Figure 6-59: Means of Brine Flow up the Borehole, Scenario S4-BF for the PABC-2009. 65
Figure 6-60: Overall Means of Brine Flow up the Borehole, Scenario S4-BF. 65
Figure 6-61: PCS-2012 PA Horsetail Plot of Brine Flow up the Borehole, Scenario S6-BF. 67
Figure 6-62: PABC-2009 Horsetail Plot of Brine Flow up the Borehole, Scenario S6-BF. 67
Figure 6-63: PCS-2012 PA Means of Brine Flow up the Borehole, Scenario S6-BF. 68
Figure 6-64: PABC-2009 Means of Brine Flow up the Borehole, Scenario S6-BF. 68
Figure 6-65: Overall Means of Brine Flow up the Borehole, Scenario S6-BF. 69

List of Tables

Table 1: Option D Panel Closure Parameters Used in the PABC-2009 17
Table 2: ROMPCS Parameters Used in the PCS-2012 PA 18
Table 3: BRAGFLO Modeling Scenarios 22
Table 4: Summary Statistics for Scenario S1-BF 31
Table 5: Summary Statistics for Scenario S2-BF 44
Table 6: Summary Statistics for Scenario S4-BF 55
Table 7: Summary Statistics for Scenario S6-BF 66

Information Only

1 EXECUTIVE SUMMARY

Waste panel closures comprise a repository feature that has been represented in WIPP PA since the original Compliance Certification Application (CCA) of 1996. The 1998 rulemaking that certified WIPP to receive transuranic waste placed conditions on the panel closure design to be implemented in the repository. The mandated design consists of a concrete block wall, an open drift section, and a concrete monolith, and was termed the "Option D" panel closure. Following the selection of the Option D design in 1998, the engineering of the panel closure has been re-assessed, and a revised design has been established that is simpler, cheaper, and easier to construct. The revised panel closure design, termed the Run-of-Mine Panel Closure System (ROMPCS), is comprised of 100 feet of ROM salt with barriers at each end. The PCS-2012 PA quantifies WIPP repository performance impacts associated with the replacement of the currently approved Option D panel closure design with the ROMPCS. Impacts are assessed via a direct comparison of results obtained in the PABC-2009 (where Option D was used) to those calculated in the PCS-2012 PA with the ROMPCS.

For undisturbed conditions, implementation of the ROMPCS yields higher long-term waste panel pressure (on average) than was seen in the PABC-2009. The increase in mean waste panel pressure is accompanied by an increase in the average waste panel brine saturation for the ROMPCS results. The ROMPCS design allows more brine inflow to the waste panel during the first 200 years when compared to Option D results. This increased brine inflow, combined with the tightness of the ROMPCS after 200 years, results in increased waste panel gas generation (on average) and a subsequent increase to waste panel mean pressure.

The lower long-term permeability range of the ROMPCS as compared to Option D yields a period of increased waste panel pressurization following an E1 intrusion. The increased waste panel mean pressure slightly inhibits brine flow into the panel after the intrusion, with a corresponding slight decrease to the mean waste panel brine saturation as compared to PABC-2009 E1 intrusion results.

For E2 intrusion scenarios, the PCS-2012 PA mean waste panel pressure is higher than that seen in the PABC-2009 at the time of intrusion, and it remains higher for the duration of the 10,000 year regulatory period. Similarly, the mean waste panel brine saturation is higher at the time of intrusion in the PCS-2012 PA, resulting in higher long-term waste panel brine saturations for E2 intrusion scenarios.

Brine flows up the borehole that are used to calculate the radionuclide source term in WIPP PA are negligibly impacted by the replacement of Option D with the ROMPCS.

Information Only

2 INTRODUCTION

The Waste Isolation Pilot Plant (WIPP), located in southeastern New Mexico, has been developed by the U.S. Department of Energy (DOE) for the geologic (deep underground) disposal of transuranic (TRU) waste. Containment of TRU waste at the WIPP is regulated by the U.S. Environmental Protection Agency (EPA) according to the regulations set forth in Title 40 of the Code of Federal Regulations (CFR), Part 191. The DOE demonstrates compliance with the containment requirements according to the Certification Criteria in Title 40 CFR Part 194 by means of performance assessment (PA) calculations performed by Sandia National Laboratories (SNL). WIPP PA calculations estimate the probability and consequence of potential radionuclide releases from the repository to the accessible environment for a regulatory period of 10,000 years after facility closure. The models used in PA are maintained and updated with new information as part of an ongoing process. Improved information regarding important WIPP features, events, and processes typically results in refinements and modifications to PA models and the parameters used in them. Planned changes to the repository and/or the components therein also result in updates to WIPP PA models. WIPP PA models are used to support the repository recertification process that occurs at five-year intervals following the receipt of the first waste shipment at the site in 1999.

Waste panel closures comprise a repository feature that has been represented in WIPP PA since the original Compliance Certification Application (CCA) of 1996. Panel closures are included in WIPP PA models principally because they are a part of the disposal system, not because they play a substantive role in inhibiting the release of radionuclides to the outside environment. The DOE stated in the CCA (DOE 1996) that *"The panel closure system was not designed or intended to support long-term repository performance."* The 1998 rulemaking that certified WIPP to receive transuranic waste placed conditions on the panel closure design to be implemented in the repository. The mandated design consists of a concrete block wall, an open drift section, and a concrete monolith, and was termed the "Option D" panel closure. Following the selection of the Option D design in 1998, the engineering of the panel closure has been re-assessed, and a revised design has been established that is simpler, cheaper, and easier to construct. The revised panel closure design, termed the Run-of-Mine Panel Closure System (ROMPCS), is comprised of 100 feet of ROM salt with barriers at each end. The ROM salt is generated from ongoing mining operations at the WIPP and may be compacted and/or moistened as it is emplaced in a panel entry. The barriers consist of ventilation bulkheads, similar to those currently used in the panels as room closures.

The DOE has submitted a planned change request (PCR) to the EPA requesting that the EPA modify Condition 1 of the Final Certification Rulemaking for 40 CFR Part 194 (EPA, 1998) for the WIPP. The PCR submitted to EPA requests that Condition 1 be changed, and that the ROMPCS design be approved for use in all panels (DOE, 2011). In support of this rulemaking change, a performance assessment has been completed that incorporates the ROMPCS design into the current PA baseline established by the 2009 Performance Assessment Baseline Calculation (PABC-2009) (Clayton et al., 2010). The name given to this new panel closure PA is PCS-2012, and the plan for its execution is detailed in AP-161 (Camphouse 2012a). PCS-2012 PA results are compared to those obtained in the PABC-2009 as a means to quantify

Information Only

potential impacts due to the panel closure redesign. This analysis package consists of the Salado flow modeling component of the PCS-2012 PA.

3 CONCEPTUAL APPROACH FOR PCS-2012 PA

The conceptual models implemented in the BRAGFLO simulations for the PCS-2012 PA are unchanged from those used in the PABC-2009. The computational grid, particularly the material map used by BRAGFLO, is changed for the PCS-2012 PA in order to incorporate the ROMPCS into the calculations. These changes are discussed below. Gas generation rates and the creep closure model have not changed from the PABC-2009 to the PCS-2012 PA. Consequently, the same porosity surface is used in this calculation as was used in the PABC-2009.

3.1 Repository Representation in BRAGFLO

The goal of the PCS-2012 PA is to quantify regulatory compliance impacts resulting from the replacement of the Option D panel closure with the ROMPCS. For the sake of reference, a schematic of the Option D panel closure is given in Figure 3-1. As seen in that figure, the Option D panel closure is 40 meters long and consists of three components, namely a concrete explosion wall, an open drift section, and a concrete monolith. This panel closure has been implemented in PA analyses done in support of WIPP re-certification since the CRA-2004 PA (Stein & Zelinski 2003). The PABC-2009 is the current regulatory baseline. The BRAGFLO grid and material map used in the PABC-2009 also represented the Option D closure, and is shown in Figure 3-2. Note that a minor error has been corrected in the material map schematic shown in Figure 3-2. That figure depicts an E1 intrusion into the repository. The BRAGFLO schematic included with the PABC-2009 Salado flow analysis package (Nemer 2010) depicts the lower borehole extending only to the bottom horizon of the lower DRZ. In actuality, the lower borehole extends to the floor of the intruded waste panel. The PABC-2009 BRAGFLO grid and material map shown in Figure 3-2 has been modified so that it represents the correct extent of the lower borehole in an E1 intrusion.

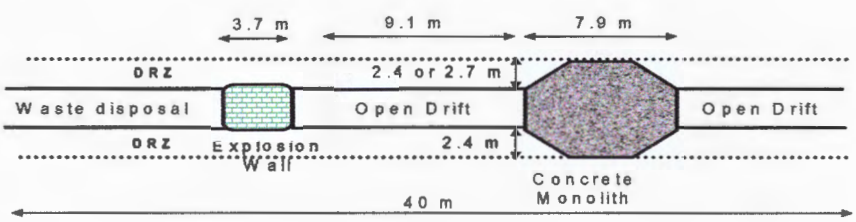

Figure 3-1: A Schematic of the "Option D" Panel Closure

Information Only

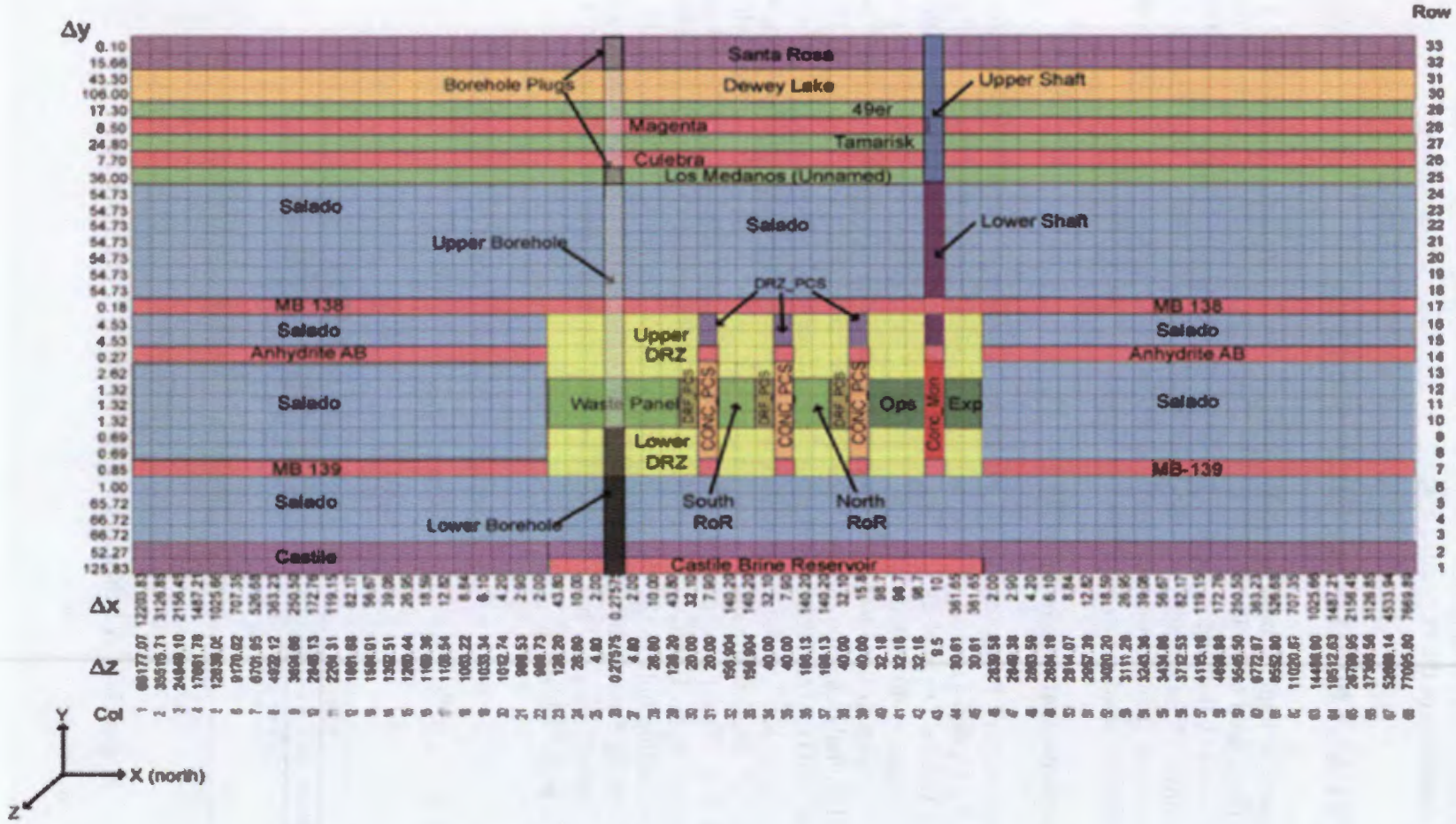

Figure 3-2: PABC-2009 BRAGFLO Grid and Material Map (Δx, Δy, and Δz dimensions in meters).

Information Only

Several aspects of the Option D implementation in BRAGFLO are worth noting. First, the concrete monolith portion of the panel closure is "keyed in" to the lower and upper DRZ. The monolith portion of the panel closure is represented by material CONC_PCS, and this material extends above and below the upper and lower horizons of repository waste panels, extending into the surrounding DRZ.

The permeability in the x-direction prescribed for material CONC_PCS in the PABC-2009 varies between a minimum value of 2.0×10^{-21} m^2 and a maximum of 1.0×10^{-17} m^2. The value assigned for each particular vector is obtained through parameter sampling over this range. The impact of the Option D panel closure on the overlaying DRZ in the PABC-2009 is also of note. The Option D panel closure was modeled as having an immediate healing effect on the DRZ above it in the PABC-2009. This healed portion of DRZ is represented by material DRZ_PCS, and its spatial extent can be seen in Figure 3-2. The permeability range assigned to material DRZ_PCS is equal to that prescribed to material CONC_PCS in the x-direction.

Segments of interbed material were included in the PABC-2009 representation of the Option D panel closure. As seen in Figure 3-2, segments of the Anhydrite AB layer are located between materials CONC_PCS and DRZ_PCS. Likewise, segments of the MB-139 layer can be found between material CONC_PCS and the underlaying Salado halite. The reasoning for including these interbed segments is provided in the BRAGFLO analysis performed in support of CRA-2004 (Stein & Zelinski 2003). Essentially, they are included to capture the impacts of brine and gas effectively bypassing the panel closure by flowing through the interbed layers.

Now that the most salient features of the Option D implementation in BRAGFLO have been discussed, attention is given to the implementation of the ROMPCS in the PCS-2012 PA. The ROMPCS is comprised of 100 feet of run-of-mine (ROM) salt with barriers at each end, and is illustrated in Figure 3-3. The ROM salt is generated from ongoing mining operations at the WIPP and may be compacted and/or moistened as it is emplaced in a panel entry. The barriers consist of ventilation bulkheads, similar to those currently used in the panels as room closures. The ventilation bulkheads are designed to restrict air flows and prevent personnel access into waste-filled areas during the operational phase. In Panels 1, 2, and 5, where explosion walls fabricated from concrete blocks have already been emplaced in the panel entries, an explosion wall is the inner barrier and a ventilation bulkhead will be the outer barrier, as shown in Figure 3-3(b). Explosion walls are inspected on a regular basis, and their anticipated condition is also assessed through numerical modeling (e.g. RockSol, 2006). Installed explosion walls show surface spalling or slabbing of the concrete blocks as a result of the loading caused by inward creep of the salt. Numerical stress analysis of the concrete explosion wall has demonstrated that the free faces and the rib contacts will be in a condition of plastic yield with an unyielded core by 7 years after emplacement (Rocksol, 2006, Figures 7 and 10). No long term stress analyses have been carried out; however, it is expected that the spalling and yield will be progressive, and that the walls will not be significant structures after the initial 100 year time period, due to the brittle, non-plastic behavior of concrete. The ventilation bulkheads and explosion walls are therefore expected to have no significant impact on long-term performance of the panel closures and are therefore not included in the PCS-2012 PA representation of the ROMPCS. Consequently, the ROMPCS is modeled as consisting of 100 feet of ROM salt in the PCS-2012 PA.

Information Only

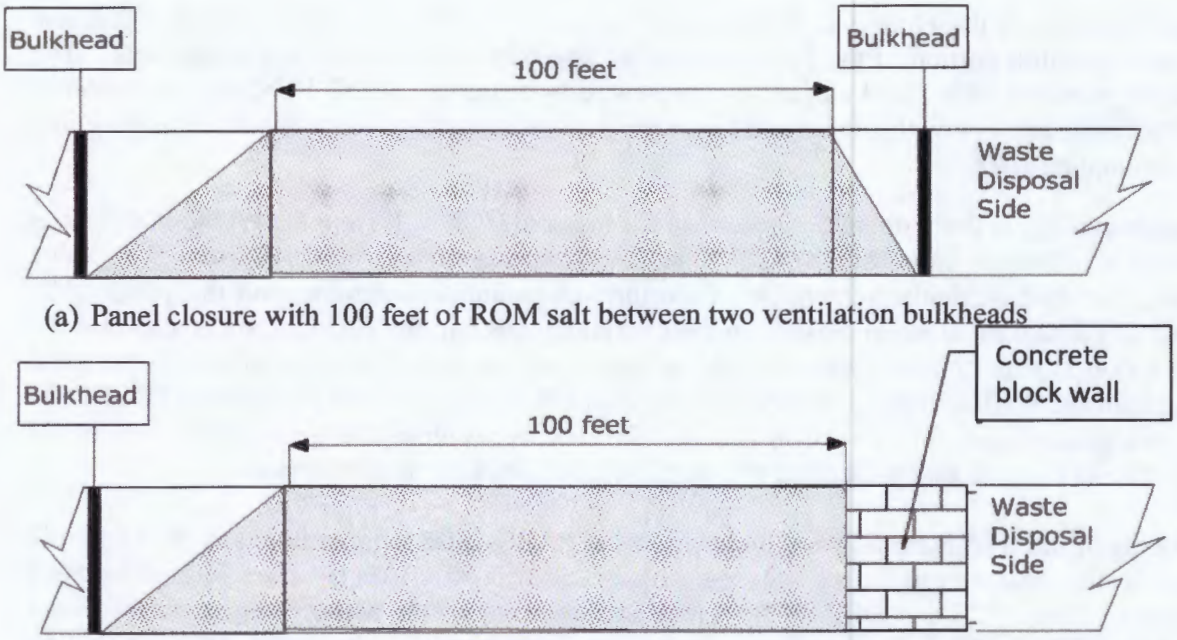

(a) Panel closure with 100 feet of ROM salt between two ventilation bulkheads

(b) Panel closure with 100 feet of ROM salt between a ventilation bulkhead & explosion wall

Figure 3-3: Schematic Diagram of the ROMPCS

The ROMPCS properties are based on three time periods: from 0 to 100 years, from 100 years to 200 years, and from 200 years to 10,000 years. Three time periods are appropriate because the process to consolidate the ROM salt occurs over a primary time scale of approximately 100 years, while the process to heal fractures in the DRZ surrounding the PCS occurs over a longer time scale of approximately 200 years. The ROM salt is therefore represented by three materials, denoted as PCS_T1 for the first 100 years, PCS_T2 from 100 to 200 years, and PCS_T3 for 200 to 10,000 years. Analyses and calculations have shown (Camphouse et al 2012a) that the time-dependent back stress imposed on the DRZ by the re-consolidated ROM salt panel closure does not become appreciable until roughly 200 years after emplacement of the ROM salt in the drift. As a result, it is reasonable and appropriate to maintain the same properties for the DRZ above and below the ROMPCS for the first 200 years after closure as are specified to the DRZ surrounding the disposal rooms. After 200 years, the DRZ above and below the ROMPCS is modeled as having healed, and this sub-region of the DRZ is represented by material DRZ_PCS. Material DRZ_PCS has the same property values in the PCS-2012 PA as were assigned to it in the PABC-2009.

The 200-year delay of DRZ healing in the PCS-2012 PA is an important distinction between the panel closure representations used in the PABC-2009 and the PCS-2012 PA. As noted above, the Option D panel closure was modeled in the PABC-2009 (and prior analyses) as having an immediate healing effect on the DRZ above it, with material DRZ_PCS being in place at t = 0. In contrast, the ROMPCS in the PCS-2012 PA is modeled as having no healing effect on the DRZ until 200 years after panel closure emplacement. For the first 200 years, the DRZ above and below the ROMPCS is indistinguishable from the DRZ above and below the waste panels.

Information Only

The DRZ overall (PA parameter DRZ_1) has a permeability range varying from a minimum value of 3.98 x 10^{-20} m^2 to a maximum of 3.16 x 10^{-13} m^2 in the x, y, and z directions. As a result, there is a path of increased permeability (on average) above and below panel closures in the PCS-2012 PA for the first 200 years as compared to the PABC-2009. An expected consequence of this increased permeability is an increase in brine and gas flow through the DRZ and around the panel closure for the first 200 years. In effect, the panel closures in the PCS-2012 PA are "looser" than those implemented in the PABC-2009 for the first 200 years due to the higher permeability (on average) of the DRZ material above and below them.

The temporal evolution of the ROMPCS in BRAGFLO for the PCS-2012 PA is illustrated in Figure 3-4 to Figure 3-6. As seen in Figure 3-4 and Figure 3-5, the only change in the BRAGFLO grid and material map for time periods 0 to 100 years and 100 to 200 years is the material used to represent the panel closure. Material PCS_T1 is used to represent the ROMPCS for years 0 to 100 while material PCS_T2 represents the panel closure for years 100 to 200. As discussed above, the ROMPCS is modeled as having no impact on the DRZ above and below the closure for the first 200 years after emplacement. For the first 200 years, the DRZ material above and below the closure in the BRAGFLO material map is the same as the material above and below other repository regions. After 200 years, the material used to represent the ROMPCS changes to PCS_T3, and the regions of healed DRZ above and below the closure is modeled by material DRZ_PCS, as shown in Figure 3-6. The repository representation shown in Figure 3-6 is used for times between 200 years and the time of intrusion. The BRAGFLO grid and element maps corresponding to particular intrusion types are shown in Figure 3-7 and Figure 3-8.

The Option D panel closure implemented in the PABC-2009 is 40 meters long, while the ROMPCS implemented in the PCS-2012 PA is 100 feet (30.48 meters) long. Consequently, the panel closure length is reduced to a value of 30.48 meters in the PCS-2012 PA, with panel closures represented by two elements in the x-direction, each 15.24 meters long.

Information Only

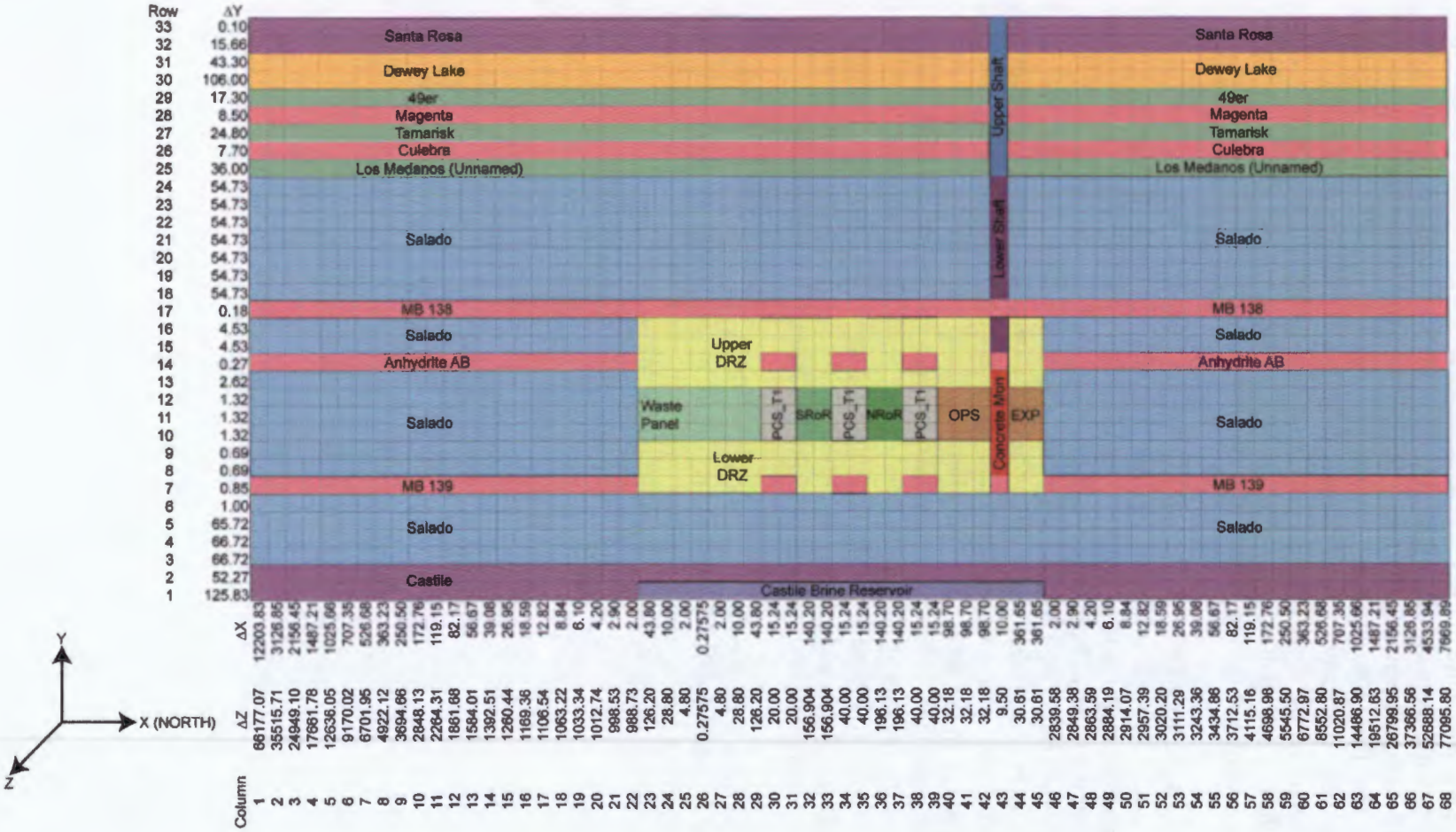

Figure 3-4: PCS-2012 BRAGFLO Grid and Material Map, Years 0 to 100

Information Only

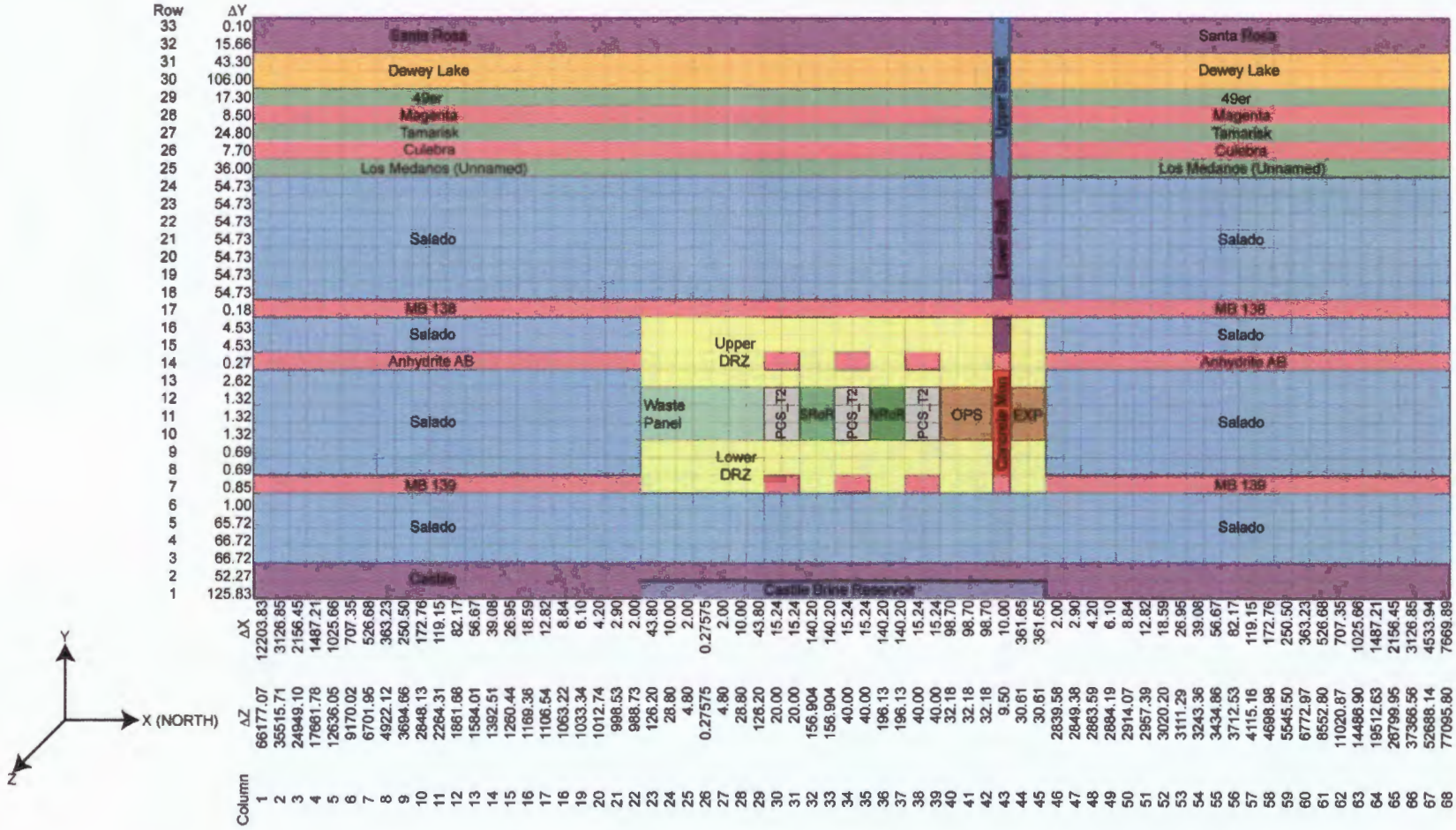

Figure 3-5: PCS-2012 BRAGFLO Grid and Material Map, Years 100 to 200

Information Only

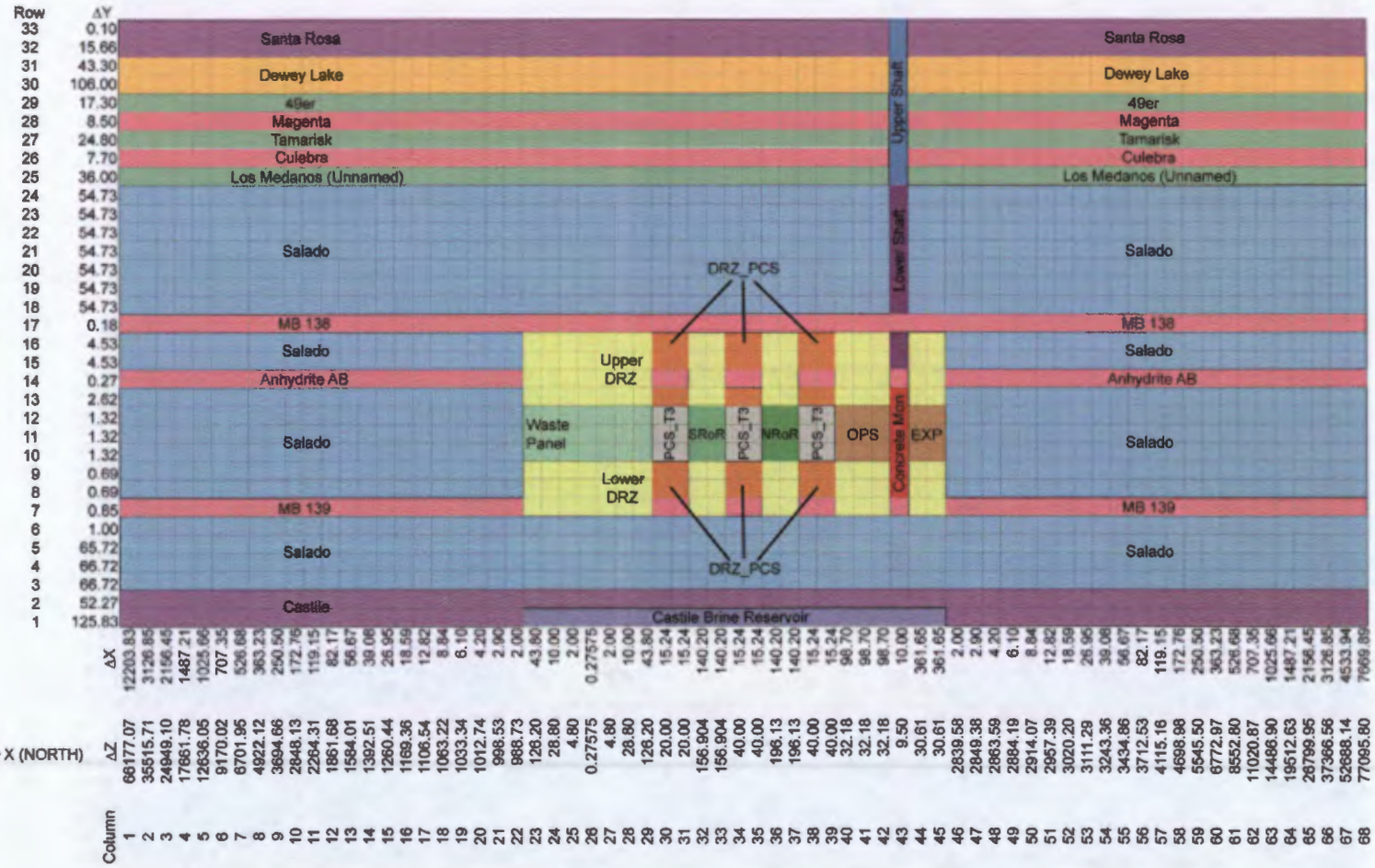

Figure 3-6: PCS-2012 BRAGFLO Grid and Material Map, Years 200 to Time of Intrusion

Information Only

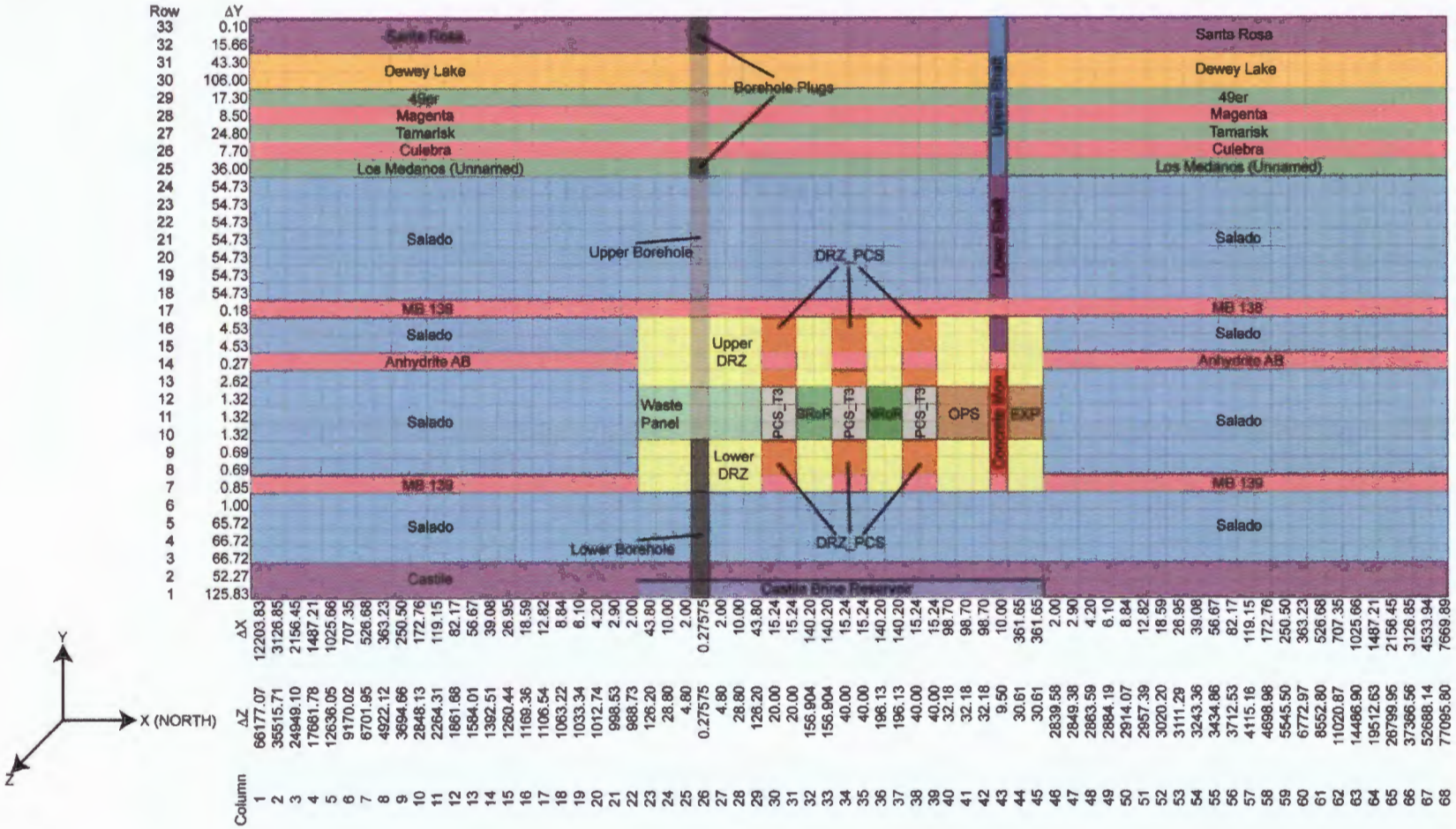

Figure 3-7: PCS-2012 BRAGFLO Grid and Material Map for an E1 Intrusion

Information Only

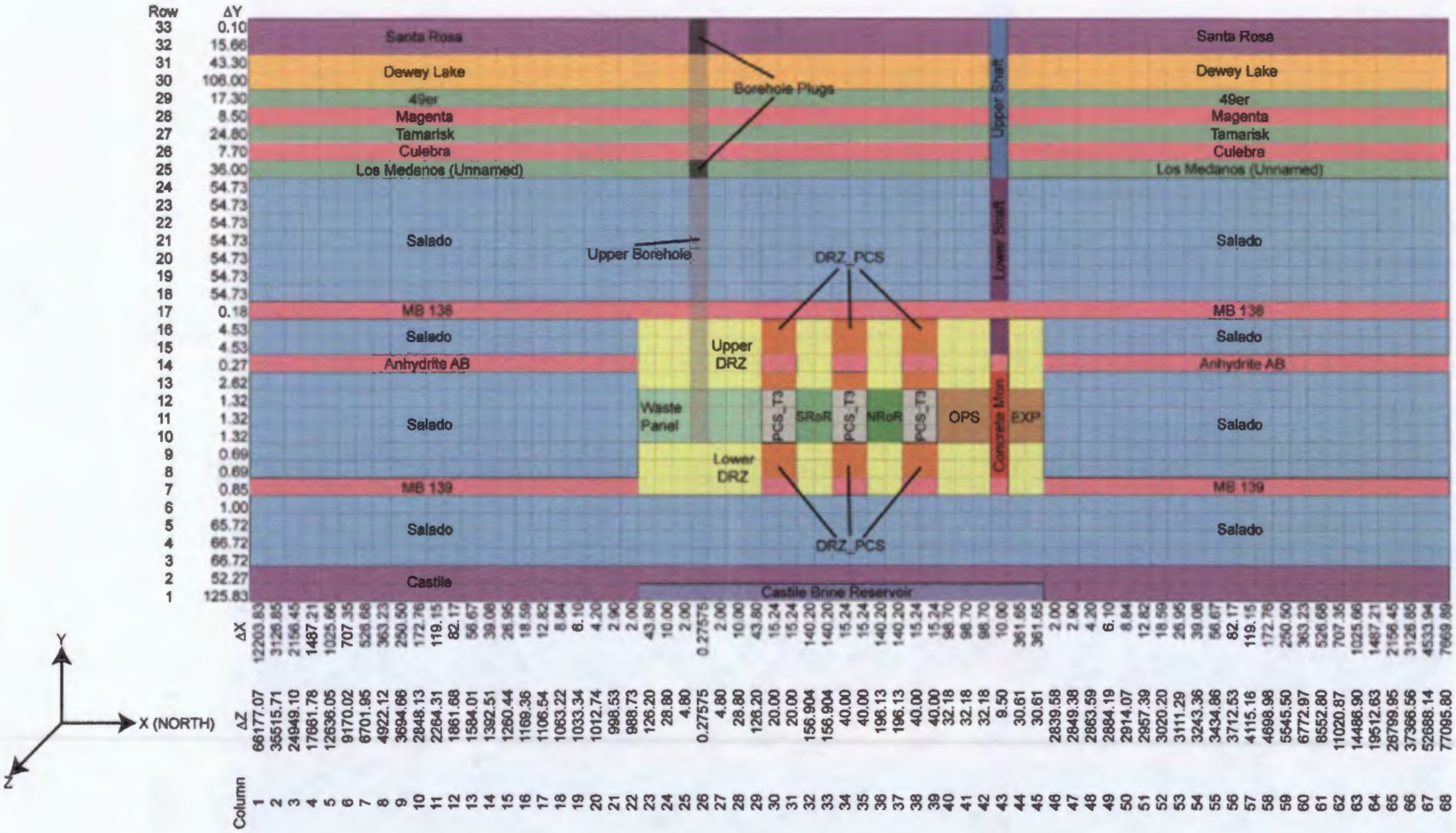

Figure 3-8: PCS-2012 BRAGFLO Grid and Material Map for an E2 Intrusion

Information Only

3.2 Panel Closure Parameterization

Numerous parameters were specified for the Option D panel closure in the PABC-2009. Of note are those prescribed for the porosity and permeability of the Option D concrete monolith (PA material CONC_PCS) as well as the DRZ overall (PA material DRZ_1) and the region of healed DRZ above the panel closure (PA material DRZ_PCS). These parameters are listed in Table 1.

Table 1: Option D Panel Closure Parameters Used in the PABC-2009

Material	Property	Distribution	Statistics
CONC_PCS	Porosity	Constant	0.05
	PRMX (m^2)	Triangular	Min = 2.0×10^{-21}
	PRMY (m^2)		Mean = 1.53×10^{-19}
	PRMZ (m^2)		Max = 1.0×10^{-17}
DRZ_1	Porosity	Cumulative	Min = 0.0039
			Mean = 0.0211
			Max = 0.0548
	PRMX (m^2)	Uniform	Min = 3.98×10^{-20}
	PRMY (m^2)		Mean = 1.0×10^{-16}
	PRMZ (m^2)		Max = 3.16×10^{-13}
DRZ_PCS	Porosity	Cumulative	Min = 0.0039
			Mean = 0.0211
			Max = 0.0548
	PRMX (m^2)	Triangular	Min = 2.0×10^{-21}
	PRMY (m^2)		Mean = 1.53×10^{-19}
	PRMZ (m^2)		Max = 1.0×10^{-17}

The full set of ROMPCS parameter values that are used in the PCS-2012 PA were developed in Camphouse et al (2012a), Patterson (2012), and Camphouse (2012b), with a discussion of BRAGFLO two-phase flow parameters given in Camphouse (2012c). As developed in Camphouse et al (2012a), permeability and porosity values are obtained through sampling for ROMPCS material PCS_T1. However, only porosity is sampled for materials PCS_T2 and PCS_T3. Sampled porosity values are then used to calculate permeability values for these materials according to the algorithm developed on page 15 of Camphouse et al (2012a). The algorithm used to calculate permeability from a sampled porosity value depends on an additional sampled parameter, quantity α in the algorithm developed in Camphouse et al (2012a). The name given to this additional parameter in the PCS-2012 PA is POR2PERM. Porosity and permeability ranges used for materials PCS_T1, PCS_T2, and PCS_T3 are shown in Table 2. As can be seen in that table, there is overlap in the porosity ranges specified for PCS_T1 and PCS_T2. This overlap could potentially result in an increase in panel closure porosity during the transition from PCS_T1 to PCS_T2 at 100 years, a non-physical result. To prevent this possibility, the porosity for PCS_T2 is conditionally sampled in the PCS-2012 PA such that PCS_T2:POROSITY $\leq$ PCS_T1:POROSITY (Camphouse 2012b). There is also overlap in the

Information Only

porosity ranges specified for PCS_T2 and PCS_T3. To prevent physically unrealistic increases in porosity during the transition from PCS_T2 to PCS_T3 at 200 years, the porosity for PCS_T3 is conditionally sampled so that PCS_T3:POROSITY ≤ PCS_T2:POROSITY. Similar constraints are placed on the calculated permeability values for PCS_T2 and PCS_T3. As can be seen in Table 2, a low sampled permeability value for PCS_T1 could be followed by a higher calculated permeability value for PCS_T2, dependent on the sampled PCS_T2 porosity and POR2PERM values. An instantaneous increase in panel closure permeability after 100 years of creep closure is an unrealistic occurrence. To prevent this non-physical result, the calculated permeability value for PCS_T2 is constrained in the PCS-2012 PA such that PCS_T2:PRMX ≤ PCS_T1:PRMX. The same is true for the calculated permeabilities in the y and z directions. A similar constraint is placed on the calculated permeability for PCS_T3 in order to prevent non-physical instantaneous increases in panel closure permeability at 200 years. The constraint placed on the calculated permeability for PCS_T3 is that PCS_T3:PRMX ≤ PCS_T2:PRMX, and likewise in the x and y directions.

Table 2: ROMPCS Parameters Used in the PCS-2012 PA

Material	Property	Distribution	Statistics
PCS_T1	Porosity	Uniform	Min = 0.066
			Mean = 0.1265
			Max = 0.187
	PRMX (m^2)	Uniform	Min = 1.0×10^{-21}
	PRMY (m^2)		Mean = 3.16×10^{-17}
	PRMZ (m^2)		Max = 1.0×10^{-12}
PCS_T2	Porosity	Uniform	Min = 0.025
			Mean = 0.05
			Max = 0.075
	POR2PERM	Normal	Min = -1.72
			Mean = 0.0
			Max = 1.72
	PRMX (m^2)	N/A – Permeability is calculated using the sampled Porosity and POR2PERM values	Min = 1.44×10^{-21}
	PRMY (m^2)		
	PRMZ (m^2)		Max = 4.55×10^{-17}
PCS_T3	Porosity	Uniform	Min = 0.001
			Mean = 0.05
			Max = 0.0519
	POR2PERM	Normal	Min = -1.72
			Mean = 0.0
			Max = 1.72
	PRMX (m^2)	N/A – Permeability is calculated using the sampled Porosity and POR2PERM values	Min = 4.46×10^{-22}
	PRMY (m^2)		
	PRMZ (m^2)		Max = 1.47×10^{-17}

Information Only

Distributions and statistics specified for materials DRZ_1 and DRZ_PCS are equal in the PABC-2009 and the PCS-2012 PA. Useful insight can be obtained by examining the Option D parameters in Table 1 and those developed for the ROMPCS in Table 2. For the first 100 years, the minimum permeability value allowed for ROMPCS material PCS_T1 is 1.0 x 10^{-21} m^2, comparable to the minimum value of 2.0 x 10^{-21} m^2 specified for the Option D concrete monolith. However, the maximum permeability value allowed for PCS_T1 is 1.0 x 10^{-12} m^2, which is significantly greater than the maximum value of 1.0 x 10^{-17} m^2 allowed for the Option D monolith. Moreover, the permeability range for material PCS_T1 is comparable to the permeability range specified to the DRZ overall (material DRZ_1 in Table 1). The DRZ above and below the ROMPCS does not heal until 200 years after emplacement, while the DRZ above the Option D panel closure is modeled as healing immediately by material DRZ_PCS. Consequently, one would expect the larger permeabilities associated with PCS_T1 and DRZ_1 to potentially result in increased brine and gas flow through the ROMPCS and the DRZ above and below it for the first 100 years when compared to the Option D panel closure.

At 100 years, the ROMPCS material transitions from PCS_T1 to PCS_T2. As seen in Table 1 and Table 2, the range of calculated permeabilities for PCS_T2 is quite comparable to the permeability range assigned to the Option D concrete monolith. However, the DRZ above and below the ROMPCS remains unhealed from 100 to 200 years, providing a pathway of increased permeability above and below the panel closure as compared to Option D. As a result, one would expect the larger permeabilities (on average) above and below material PCS_T2 to potentially result in brine and gas flows through the upper and lower DRZ, effectively bypassing the ROMPCS.

At 200 years, the ROMPCS material transitions from PCS_T2 to PCS_T3 with the DRZ region above and below PCS_T3 represented as healed by material DRZ_PCS. Under this configuration, the range of calculated permeabilities for PCS_T3 is comparable to the permeability range assigned to the Option D monolith, with the minimum value calculated for PCS_T3 being roughly an order of magnitude less than the minimum CONC_PCS permeability value. As material DRZ_PCS represents regions of healed DRZ for both the ROMPCS and the Option D closure, the final ROMPCS configuration comprises a panel closure that is slightly "tighter" (on average) than the Option D case.

3.2.1 Capillary Pressure Parameters

Two-phase flow parameters for PCS_T1, PCS_T2, and PCS_T3 are given in Camphouse et al (2012a). Tables 7 and 8 of that document assign values of CAP_MOD = 2, PCT_A = 0.56 Pa, and PCT_EXP = -0.346 for materials PCS_T1, PCS_T2, and PCS_T3. These particular material parameters are associated with capillary pressure modeling in BRAGFLO. The values listed in Camphouse et al (2012a) were obtained from the parameter developments undertaken in the 2006 PCS PA (Vugrin et al 2006), which also investigated regulatory compliance impacts of a panel closure redesign having a ROM salt component. Values of CAP_MOD = 2, PCT_A = 0.56 Pa, and PCT_EXP = -0.346 were initially planned in the 2006 PCS PA, but were subsequently changed to values of 1, 0.0 Pa, and 0.0, respectively. This change was made to maintain consistency with the corresponding properties of the salt materials used in the original

Information Only

shaft seal model (Vugrin and Dunagan 2006). These values (CAP_MOD = 1, PCT_A = 0.0 Pa, and PCT_EXP = 0.0) were also used for materials DRZ_1, DRZ_PCS, and the Option D material CONC_PCS in the PABC-2009. The PCS-2012 PA representation of the ROMPCS typically results in instantaneous changes in panel closure permeability at 100 and 200 years. Instantaneous changes in permeability, due to material changes in a grid region, cause difficulty in numerically satisfying the convergence criterion for the capillary pressure constraint equation used in BRAGFLO (Camphouse 2012c). Values of CAP_MOD = 2, PCT_A = 0.56 Pa, and PCT_EXP = -0.346 have not been used in BRAGFLO panel closure modeling since before 2002 as these values cause BRAGFLO numerical difficulties.

As discussed in Camphouse (2012c), values of CAP_MOD = 2, PCT_A = 0.56 Pa, and PCT_EXP = -0.346 for materials PCS_T1, PCS_T2, and PCS_T3 were expected to cause BRAGFLO numerical difficulties in the PCS-2012 PA. For the sake of brevity in what follows, denote these parameter values as Case 1. Denote values of CAP_MOD = 1, PCT_A = 0.0 Pa, and PCT_EXP = 0.0 for materials PCS_T1, PCS_T2, and PCS_T3 as Case 2. During the BRAGFLO testing phase of the PCS-2012 PA, sidebar calculations were performed to determine the computational feasibility of these two parameter cases. The results of these sidebar calculations are now briefly discussed.

Using the PCS-2012 PA BRAGFLO grid and material map, the first 20 vectors of replicate 1 were simulated using the parameter values of Case 1. The same was also done using the parameter values of Case 2. Every vector corresponding to Case 2 resulted in a 10,000-year BRAGFLO solution using default convergence criteria. On the other hand, 35% of vectors corresponding to Case 1 did not result in a 10,000-year BRAGFLO solution with default convergence criteria. Moreover, *every* vector corresponding to Case 1 required significantly more iterations in obtaining a BRAGFLO numerical solution. For most Case 1 vectors, several thousand additional iterations were required for vectors resulting in a 10,000-year BRAGFLO solution as compared to Case 2. For Case 1 vectors that did not yield 10,000-year solutions under default criteria, the maximum number of iterations allowed (20,000) were used with BRAGFLO exiting prior to the 10,000 year mark. The impact to computational time was substantial. For some Case 1 vectors, the time necessary to obtain a BRAGFLO solution increased by roughly a factor of 110 when compared to Case 2. For these reasons, it was determined that the parameters corresponding to Case 1 are not computationally feasible. As a result, values of CAP_MOD = 1, PCT_A = 0.0 Pa, and PCT_EXP = 0.0 are prescribed to materials PCS_T1, PCS_T2, and PCS_T3 in the PCS-2012 PA in order to have panel closure material consistency with the surrounding DRZ and salt properties of the original shaft seal model, as well as to prevent numerical difficulties in BRAGFLO. These values correspond to capillary pressure modeling being disabled for these materials (Camphouse 2012c).

Information Only

4 SALADO FLOW MODELING METHODOLOGY

The BRAGFLO software calculates the flow of brine and gas in the vicinity of the WIPP repository over a 10,000-year regulatory compliance period. The results of these calculations are used by other software to calculate potential radionuclide releases to the accessible environment. Some of the specific processes included in the BRAGFLO calculations include:

- Brine and gas flow.
- Pressure generation as a function of time and space.
- Creep closure of the waste filled regions within the repository.
- Physical changes (e.g. permeability and porosity) in the modeling domain over time.
- Cumulative brine flow into and out of the repository and its subregions.

There is significant uncertainty associated with characterizing the physical properties of geologic materials that influence these processes. WIPP PA addresses these uncertainties in two ways. Properties such as permeability and porosity are usually measured indirectly and vary significantly depending upon location. The uncertainty in particular physical property values is called subjective (epistemic) uncertainty. Subjective uncertainty can, in theory, be reduced by further study of the system. Subjective uncertainty is addressed within Salado flow modeling by the use of probability distributions for subjectively uncertain parameters. Multiple flow realizations are performed in which the values of uncertain parameters are sampled from their respective distributions. For subjectively uncertain, spatially distributed quantities, e.g. the permeability of the DRZ, one sampled value is used to specify a particular parameter value over its entire spatial extent in a single realization. To reduce the number of realizations required and to ensure that low probability (and possibly high consequence) combinations are represented, Latin Hypercube Sampling (LHS) is used to create the realizations. For the WIPP PA, the LHS software (Vugrin 2005) is used to create a "replicate" of 100 distinct parameter sets ("vectors") that are sampled from the full range of parameter uncertainty. To ensure that the Latin Hypercube replicates are representative, a total of three replicates are run for a total of 300 separate vectors.

Another type of uncertainty encountered in WIPP PA is that of stochastic (aleatory) uncertainty associated with incomplete knowledge of future events. Unlike subjective uncertainty, stochastic uncertainty cannot be reduced by further study. WIPP PA addresses stochastic uncertainty by employing a Monte Carlo sampling technique on random futures. In this context, a future is defined as one possible sequence of events. During BRAGFLO calculations, stochastic uncertainty is addressed by defining a set of six scenarios for which brine and gas flow is calculated for each of the vectors generated by the LHS software. The total number of BRAGFLO simulations that have to be run for a WIPP PA calculation is 300 vectors times 6 scenarios equaling 1,800 BRAGFLO simulations.

The six scenarios used in the PCS-2012 PA are unchanged from those used for the 1996 CCA and the PABC-2009. No changes to BRAGFLO scenarios are needed to address the differences in the ROMPCS and the Option D panel closure.

Information Only

Results obtained in the six scenarios from BRAGFLO are used to initialize flow and material properties in subsequent codes in the PA computational suite, e.g. in the calculation of direct brine releases. The intrusion types specified in PA code calculations subsequent to BRAGFLO are the same as those implemented in BRAGFLO. The intrusion times, however, are not always equal. To avoid confusion resulting from the use of identical scenario notation for scenarios with unequal intrusion times in the various PA codes, the scenarios in BRAGFLO are denoted as S1-BF to S6-BF. The scenarios include one undisturbed scenario (S1-BF), four scenarios that include a single inadvertent future drilling intrusion into the repository during the 10,000 year regulatory period (S2-BF to S5-BF), and one scenario investigating the effect of two intrusions into a single waste panel (S6-BF). Two types of intrusions, denoted as E1 and E2, are considered. An E1 intrusion assumes the borehole passes through a waste-filled panel and into a pressurized brine pocket that may exist under the repository in the Castile formation. An E2 intrusion assumes that the borehole passes through the repository but does not encounter a brine pocket. Scenarios S2-BF and S3-BF model the effect of an E1 intrusion occurring at 350 years and 1000 years, respectively, after the repository is closed. Scenarios S4-BF and S5-BF model the effect of an E2 intrusion at 350 and 1000 years. Scenario S6-BF models an E2 intrusion occurring at 1000 years, followed by an E1 intrusion into the same panel at 2000 years. BRAGFLO results obtained in Scenario S6-BF are used to calculate transport releases to the Culebra. Transport releases from the Culebra obtained in the PABC-2009 are also used in the PCS-2012 PA. Results from BRAGFLO scenario S6-BF are briefly discussed in this report to justify the appropriateness of PABC-2009 Culebra transport calculations for the PCS-2012 PA. Table 3 summarizes the six scenarios used in this analysis.

Table 3: BRAGFLO Modeling Scenarios

Scenario	Description
S1-BF	Undisturbed Repository
S2-BF	E1 intrusion at 350 years
S3-BF	E1 intrusion at 1,000 years
S4-BF	E2 intrusion at 350 years
S5-BF	E2 intrusion at 1,000 years
S6-BF	E2 intrusion at 1,000 years; E1 intrusion at 2,000 years.

4.1 Initial Conditions

BRAGFLO simulation of the six scenarios listed above requires the assignment of initial conditions including brine pressure, brine saturation, and concentrations of iron and biodegradable material. These initial conditions are provided to BRAGFLO through various pre-processing steps during which values are extracted or sampled from the WIPP PA Performance Assessment Parameter Database.

At the beginning of each BRAGFLO run (scenario-vector combination), the model simulates a short period of time representing disposal operations. This portion of the run is called the initialization period and lasts for 5 years (from t = -5 to 0 years), corresponding to the time a typical waste panel is expected to be open during disposal operations. All grid blocks require initial pressure and saturation at the beginning of the run (t = -5 years). At the beginning of the regulatory period (0 to 10,000 years), BRAGFLO resets initial conditions within the excavated regions and in the shaft.

Information Only

The initial conditions specified for BRAGFLO modeling are listed below:

- Brine pressure in all non-excavated regions is equal to lithostatic pressure. This pressure is sampled at a single location and assumed hydrostatic at all other locations.
- Pressure within excavated regions is set to one atmosphere (1.01325×10^5 Pa) at t = -5 years.
- At t = 0 years, pressure in the excavated waste regions is increased to 1.28039×10^5 Pa in order to account for the pressure increase (0.26714×10^5 Pa) associated with microbial gas produced at short times (see Subsection 4.2.1 of Nemer et al. 2005).
- Brine saturation within the non-excavated regions is set to 1.0.
- Brine saturation within the excavated regions is set to a value of 0 at t = -5 years.
- Brine saturation in the excavated regions at t = 0 is prescribed the following values:
    - 0.015 for the excavated waste regions, which was chosen to be conservative with respect to the WIPP Waste Acceptance Criteria which allows waste to come to WIPP with no more than 1 % liquids by volume (see Subsection 3.4.1 of DOE 2007).
    - 0.0 for the operations and experimental areas
    - 0.9999999 for the concrete portion of the shaft.
    - For each vector, the initial brine saturation of ROMPCS material PCS_T1 is assigned a sampled value obtained from a uniform distribution with a minimum of 0.04 and a maximum of 0.16 (Camphouse 2012b).

During the initialization period brine tends to flow into the excavated areas and the shaft, resulting in decreased pressure and saturation in the rock immediately adjacent to the excavations. At time t = 0 the pressure and saturation in all the excavations is reset to initial conditions for the materials used to represent these regions for the regulatory period. This practice is intended to capture the effect of evaporation of brine inflow during the operational period and the transport of this brine up the shaft ventilation system, as well as the depressurization of the surrounding rock formations due to excavation.

4.2 Boundary Conditions

The boundary conditions assigned for the BRAGFLO calculations in the PCS-2012 PA are the same as those for the PABC-2009.

- Constant pressure at the north and south ends of the Culebra and Magenta dolomites.
- Constant pressure (1.01325×10^5 Pa) and saturation (0.08363) conditions at the land surface boundary of the grid, except at the shaft cell on the land surface boundary (Vaughn 1996). The saturation in this cell is set along with the rest of the shaft to the initial saturation prescribed in the WIPP parameter database (SAT_IBRN) for each of the respective shaft materials.
- No-flow conditions at all other grid boundaries.

Information Only

5 RUN CONTROL

Run control, including code versions used and descriptions of code sequencing used to obtain BRAGFLO results in the PCS-2012 PA, is documented in Camphouse et al (2012b). PCS-2012 PA results obtained in the BRAGFLO post-processing step have file names ALG2_BF_AP161_Rr_Ss_Vvvv.CDB, where r (the replicate number) equals 1,2, or 3, s (the scenario number) equals 1,2,3,4,5, or 6, and vvv (the vector number) is between 001 and 100. These files are located in CMS library LIBAP161_BFRrSs under class AP161-0. PABC-2009 results obtained in the BRAGFLO post-processing step have file names ALG2_BF_PABC09_Rr_Ss_Vvvv.CDB, and are located in CMS library LIBPABC09_BFRrSs under class PABC09-0.

6 RESULTS

Computed results are now presented for the PCS-2012 PA and compared with those obtained in the PABC-2009. In the following sections, results are presented in terms of volume-averaged quantities such as volume-averaged pressure. Volume-averaged pressure is given by forming the product of grid block pressure and grid block volume for each grid block in the region of concern, summing this product up over all grid blocks in the region, and dividing by the bulk volume of the region. All other volume-averaged quantities are computed in the same manner. Cumulative flow volumes are also presented. Cumulative flow into a region is defined as the time-dependent flow into a region integrated over time. In the results that follow, the routine calculation of means and generation of plots were done with Matlab version R2008a, a Commercial off-the Shelf (COTS) software package. As discussed previously, Scenario S1-BF represents undisturbed repository conditions. Scenarios S2-BF through S6-BF capture consequences of drilling intrusions into the repository. The impact on repository performance following an intrusion through the repository and into a pressurized brine pocket in the Castile (an E1 event) are considered in Scenarios S2-BF and S3-BF. Drilling intrusions that do not encounter pressurized Castile brine (an E2 event) are considered in scenarios S4-BF and S5-BF. Transport releases to the Culebra are captured in Scenario S6-BF. Scenario S6-BF is used for determining the radionuclide source term to the Culebra in the PA code PANEL, and results of this BRAGFLO scenario are briefly discussed. The particular mechanics of each scenario are shown below. Note that the ROMPCS implemented in the PCS-2012 PA, as well as materials used to represent the shaft, attain their long-term permeability values at 200 years, well before the occurrence of any of the waste panel intrusions in scenarios S2-BF to S6-BF.

Scenario S1-BF (Undisturbed Conditions)

0 years: ROMPCS represented by material PCS_T1 with no healing of the DRZ above and below the panel closure.

100 years: ROMPCS material transitions from PCS_T1 to PCS_T2 with no healing of the DRZ above and below the panel closure.

200 years: ROMPCS material transitions from PCS_T2 to PCS_T3 with healed regions of DRZ above and below the panel closure represented by material DRZ_PCS. Lower shaft material properties are changed.

Information Only

Scenario S2-BF (E1 intrusion at 350 years)

0 years: ROMPCS represented by material PCS_T1 with no healing of the DRZ above and below the panel closure.

100 years: ROMPCS material transitions from PCS_T1 to PCS_T2 with no healing of the DRZ above and below the panel closure.

200 years: ROMPCS material transitions from PCS_T2 to PCS_T3 with healed regions of DRZ above and below the panel closure represented by material DRZ_PCS. Lower shaft material properties are changed.

350 years: Borehole intrusion through the Waste Panel and into a hypothetical pressurized brine reservoir in the underlying Castile Formation, with the borehole represented by material BH_OPEN. Concrete borehole plugs, represented by material CONC_PLG, immediately emplaced in the borehole below the Culebra and at the surface.

550 years: Borehole plugs fail, and the entire borehole is modeled as having properties equivalent to sand. The borehole, bottom to top, is represented by material BH_SAND.

1550 years: The permeability of the borehole between the repository and the Castile brine reservoir decreases due to creep closure of the salt. The lower borehole is represented by material BH_CREEP as a result.

Scenario S3-BF (E1 intrusion at 1000 years)

0 years: ROMPCS represented by material PCS_T1 with no healing of the DRZ above and below the panel closure.

100 years: ROMPCS material transitions from PCS_T1 to PCS_T2 with no healing of the DRZ above and below the panel closure.

200 years: ROMPCS material transitions from PCS_T2 to PCS_T3 with healed regions of DRZ above and below the panel closure represented by material DRZ_PCS. Lower shaft material properties are changed.

1000 years: Borehole intrusion through the Waste Panel and into a hypothetical pressurized brine reservoir in the underlying Castile Formation, with the borehole represented by material BH_OPEN. Concrete borehole plugs, represented by material CONC_PLG, immediately emplaced in the borehole below the Culebra and at the surface.

1200 years: Borehole plugs fail, and the entire borehole is modeled as having properties equivalent to sand. The borehole, bottom to top, is represented by material BH_SAND.

2200 years: The permeability of the borehole between the repository and the Castile brine reservoir decreases due to creep closure of the salt. The lower borehole is represented by material BH_CREEP as a result.

Scenario S4-BF (E2 intrusion at 350 years)

0 years: ROMPCS represented by material PCS_T1 with no healing of the DRZ above and below the panel closure.

100 years: ROMPCS material transitions from PCS_T1 to PCS_T2 with no healing of the DRZ above and below the panel closure.

200 years: ROMPCS material transitions from PCS_T2 to PCS_T3 with healed regions of DRZ above and below the panel closure represented by material DRZ_PCS. Lower shaft material properties are changed.

Information Only

350 years: Borehole intrusion terminating at the floor of the Waste Panel, with the borehole represented by material BH_OPEN. Concrete borehole plugs, represented by material CONC_PLG, immediately emplaced in the borehole below the Culebra and at the surface.

550 years: Borehole plugs fail, and the entire borehole is modeled as having properties equivalent to sand. The borehole, bottom to top, is represented by material BH_SAND.

Scenario S5-BF (E2 intrusion at 1000 years)

0 years: ROMPCS represented by material PCS_T1 with no healing of the DRZ above and below the panel closure.

100 years: ROMPCS material transitions from PCS_T1 to PCS_T2 with no healing of the DRZ above and below the panel closure.

200 years: ROMPCS material transitions from PCS_T2 to PCS_T3 with healed regions of DRZ above and below the panel closure represented by material DRZ_PCS. Lower shaft material properties are changed.

1000 years: Borehole intrusion terminating at the floor of the Waste Panel, with the borehole represented by material BH_OPEN. Concrete borehole plugs, represented by material CONC_PLG, immediately emplaced in the borehole below the Culebra and at the surface.

1200 years: Borehole plugs fail, and the entire borehole is modeled as having properties equivalent to sand. The borehole, bottom to top, is represented by material BH_SAND.

Scenario S6-BF (E2 intrusion at 1000 years, E1 intrusion at 2000 years)

0 years: ROMPCS represented by material PCS_T1 with no healing of the DRZ above and below the panel closure.

100 years: ROMPCS material transitions from PCS_T1 to PCS_T2 with no healing of the DRZ above and below the panel closure.

200 years: ROMPCS material transitions from PCS_T2 to PCS_T3 with healed regions of DRZ above and below the panel closure represented by material DRZ_PCS. Lower shaft material properties are changed.

1000 years: Borehole intrusion terminating at the floor of the Waste Panel, with the borehole represented by material BH_OPEN. Concrete borehole plugs, represented by material CONC_PLG, immediately emplaced in the borehole below the Culebra and at the surface.

1200 years: Borehole plugs fail, and the entire borehole is modeled as having properties equivalent to sand. The borehole, bottom to top, is represented by material BH_SAND.

2000 years: A second borehole intrusion connects the waste panel to a hypothetical pressurized brine reservoir in the underlying Castile Formation. The lower borehole is represented by material BH_OPEN.

2200 years: The lower borehole is modeled as having properties equivalent to sand, and is represented by material BH_SAND.

3200 years: The permeability of the borehole between the repository and the Castile brine reservoir decreases due to creep closure of the salt. The lower borehole is represented by material BH_CREEP as a result.

Information Only

6.1.1 Results for an Undisturbed Repository (Scenario S1-BF)

Results are now presented for undisturbed scenario S1-BF. For the sake of brevity in what follows, waste area results are discussed in terms of the waste panel. Trends discussed for the waste panel also apply to other repository waste areas.

A horsetail plot of cumulative brine flow into the waste panel, denoted by quantity BRNWASIC, is given in Figure 6-3. The horsetail plot shown in Figure 6-3 is assembled using all 300 scenario S1-BF vectors. Replicate means of BRNWASIC, as well as the overall BRNWASIC mean calculated over all 300 vectors, are shown in Figure 6-4. As seen in that figure, there is close agreement between the three replicate means, as well as the overall mean, of cumulative brine inflow to the waste panel.

The PCS-2012 PA overall mean of cumulative brine flow into the waste panel is compared to the PABC-2009 overall mean of the same quantity in Figure 6-5. As seen in that figure, there is an increase in the mean cumulative brine flow into the waste panel in the PCS-2012 PA as compared to the PABC-2009. As discussed in Section 3.2, the permeability range assigned to the ROMPCS during the first 100 years is comparable to the permeability range of the DRZ overall. The Option D concrete monolith, however, is much less permeable than the DRZ (on average). Moreover, the DRZ above the Option D panel closure heals immediately and is assigned the same permeability range prescribed to the concrete monolith. As the DRZ remains unhealed for the first 200 years in the ROMPCS model, there is a path of increased permeability through and around the ROMPCS for the first 100 years as compared to the Option D closure. The result is an increase in cumulative brine flow toward the waste panel during that time period. For 100 to 200 years, the permeability range prescribed to the ROMPCS is comparable to the range assigned to the Option D concrete monolith. The DRZ above and below the ROMPCS remains unhealed during this time period, however. The result is a path of increased permeability (on average) above and below the ROMPCS as compared to the Option D case, with a corresponding increase in cumulative brine flow into the waste panel. After 200 years, the DRZ above and below the ROMPCS is modeled as having healed by material DRZ_PCS, resulting in a final ROMPCS configuration that is slightly "tighter" on average than the Option D case. Consequently, the majority of the increase in quantity BRNWASIC for the PCS-2012 PA occurs during the first 200 years. The increase during the first 200 years is readily apparent in Figure 6-6, where the time scale used to plot BRNWASIC overall means is restricted to the first 1,000 years. As seen in that figure, the difference in the overall means obtained in the two analyses increases steadily until 200 years. At 200 years, the ROMPCS assumes its long-term properties with the DRZ healed above and below it. At 200 years in the PCS-2012 PA BRNWASIC overall mean in Figure 6-6, the rate of increase decreases sharply. At 200 years, the difference between the BRNWASIC overall means obtained in the two analyses is roughly 600 m^3, and this difference between the overall means remains fairly constant for the remainder of the regulatory period.

The impact of panel closure material and the DRZ around it is made more evident by examining the cumulative volume of brine flowing out of a panel closure plane and toward the waste panel. The name given for this quantity is BNWPSPCS (brine toward the waste panel, south from the panel closure system). The schematics shown in Figure 6-1 and Figure 6-2 illustrate how this

Information Only

quantity is calculated. In both of those figures, the southernmost panel closure plane is illustrated by a red vertical line. For both the PCS-2012 PA and the PABC-2009, this line intersects the waste panel/panel closure interface, and extends from the intact halite below the repository to the intact halite above it. Quantity BNWPSPCS is a cumulative tally of southward brine flow between the regions of intact halite below and above the repository and toward the region of intact halite immediately south of the repository. In the schematics shown in Figure 6-1 and Figure 6-2, brine flows used to calculate BNWPSPCS are right-to-left across the panel closure planes denoted by the red vertical lines. Note that Figure 6-1 shows the representation of the ROMPCS for the first 100 years. The ROMPCS southernmost panel closure plane is defined at the same location as in Figure 6-1 for years 100 to 200 and years 200 to 10,000.

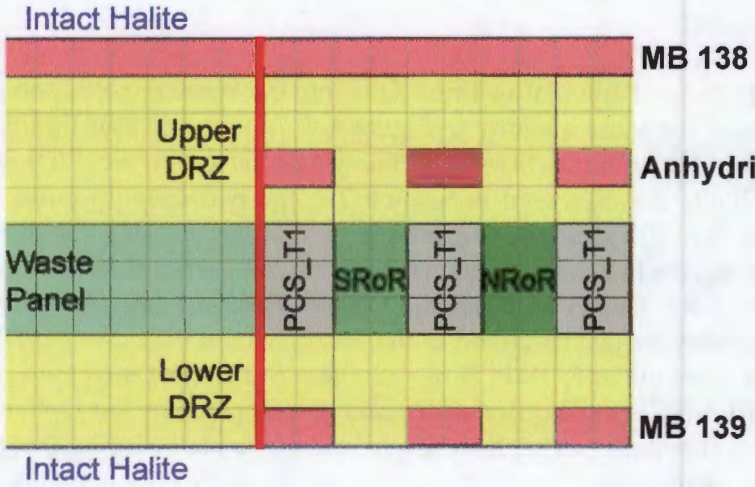

Figure 6-1: PCS-2012 PA Definition of Cumulative Flow toward the Waste Panel, across the Southernmost Panel Closure Plane

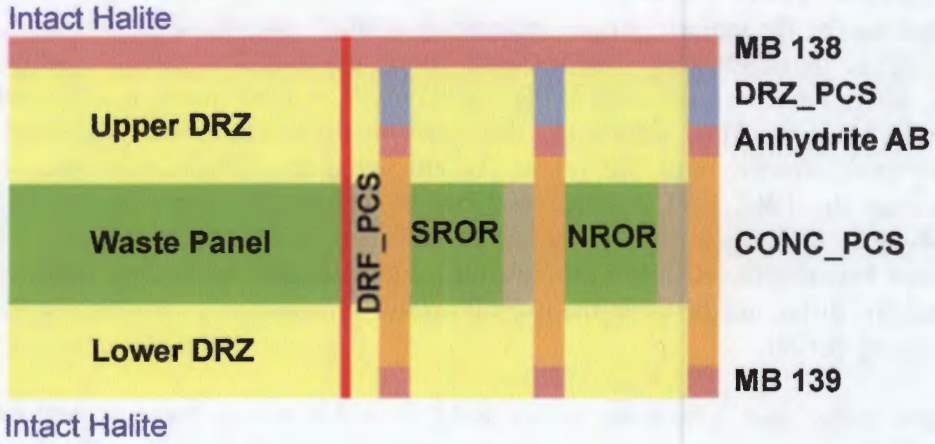

Figure 6-2: PABC-2009 Definition of Cumulative Flow toward the Waste Panel, across the Southernmost Panel Closure Plane

Information Only

Figure 6-7 shows the overall means of quantity BNWPSPCS for both the PCS-2012 PA and the PABC-2009. As seen in that figure, there is an increase in the BNWPSPCS overall mean in the PCS-2012 PA as compared to the PABC-2009. This increase is attributed to the increased permeability of the ROMPCS, and the DRZ above and below it, for the first 200 years as compared to Option D. Figure 6-8 shows overall means of quantity BNWPSPCS with the time scale restricted to the first 1,000 years. As seen in that figure, the rate of increase in the overall mean of BNWPSPCS for the PCS-2012 PA decreases slightly at 100 years. At 100 years, The ROMPCS model transitions from material PCS_T1 to PCS_T2. The reduction in the permeability range for material PCS_T2 has a slight reducing effect on the rate of increase of BNWPSPCS. At 200 years, the ROMPCS material transitions from PCS_T2 to PCS_T3 with the DRZ above and below the panel closure modeled as healed by material DRZ_PCS. In Figure 6-8, there is a sharp change in slope in the PCS-2012 PA BNWPSPCS overall mean at 200 years. Brine flow southward out of the southernmost panel closure plane is effectively stopped by the ROMPCS and healed DRZ, resulting in no increase to the BNWPSPCS overall mean for a period of time after 200 years. The difference between the BNWPSPCS overall means seen in the PCS-2012 PA and the PABC-2009 is roughly 550 m^3 after 200 years. This volume of brine corresponds very closely to the difference seen in the cumulative brine flow into the waste panel (Figure 6-6) after 200 years, indicating that the increase of cumulative brine flow into the waste panel is primarily due to the increase of brine flow through and around the ROMPCS for the first 200 years as compared to Option D.

The increase of brine flow into the waste panel results in a corresponding increase in the waste panel brine saturation, denoted by quantity WAS_SATB. A horsetail plot of waste panel brine saturation calculated in the PCS-2012 PA is shown Figure 6-9. The horsetail plot shown in that figure is assembled using all 300 realizations of waste panel brine saturation. The three individual replicate means, as well as the overall mean, of WAS_SATB are shown in Figure 6-10. As seen in that figure, there is very close agreement among the PCS-2012 PA replicate means as well as the overall mean.

The overall means for WAS_SATB obtained in the PCS-2012 PA and the PABC-2009 are plotted together in Figure 6-11. As seen in that figure, there is an increase in the mean for WAS_SATB in the PCS-2012 PA as compared to the PABC-2009. The increase in brine inflow to the waste panel during the first 200 years translates to an increase in the waste panel brine saturation. The impact of the ROMPCS temporal evolution on the waste panel brine saturation is more clearly seen in Figure 6-12. In that figure, overall means of WAS_SATB obtained in the two analyses are plotted together with the time scale restricted to the first 1,000 years. As seen in that figure, the overall mean for WAS_SATB obtained in the PCS-2012 PA increases at a higher rate than the mean calculated in the PABC-2009 for the first 200 years. At 200 years, the ROMPCS and the DRZ above and below it assume their long-term properties. At 200 years in Figure 6-12, the rate of increase in the WAS_SATB mean curve obtained in the PCS-2021 PA decreases sharply. Beyond 200 years, the WAS_SATB overall means obtained in the two analyses are qualitatively very similar with differences seen in the magnitude of the respective curves primarily due to increases seen in the PCS-2012 PA during the first 200 years.

Information Only

Increases in waste panel brine inflow and brine saturation potentially impact waste panel gas generation, denoted by quantity GASMOL_W. The horsetail plot of waste panel gas generation (in moles), assembled over all 300 vectors, for the PCS-2012 PA is shown in Figure 6-13. The three individual replicate means, as well as the overall mean, are shown in Figure 6-14. As seen in that figure, there is close agreement between the replicate and overall means for GASMOL_W. Overall means of waste panel gas generation obtained in the PCS-2012 PA and the PABC-2009 are plotted together in Figure 6-15. As seen in that figure, the overall mean for gas generated in the waste panel increased in the PCS-2012 PA. The increases seen in the mean waste panel brine inflow and mean waste panel brine saturation in the PCS-2012 PA result in a corresponding increase in waste panel gas generation.

The temporal evolution of the ROMPCS and the changes to waste panel gas generation seen in the PCS-2012 PA impact the waste panel pressure, denoted by quantity WAS_PRES. The horsetail plot for WAS_PRES, assembled over all 300 vectors, is shown in Figure 6-16. The three WAS_PRES replicate means, as well as the overall mean, are shown together in Figure 6-17. As seen in that figure, there is very close agreement between the replicate means and the overall mean of waste panel pressure.

Overall means of waste panel pressure obtained in the PCS-2012 PA and the PABC-2009 are shown together in Figure 6-18. As seen in that figure, there is a long-term increase in the mean waste panel pressure obtained in the PCS-2012 PA as compared to the PABC-2009. The increase in waste panel gas generation seen in the PCS-2012 PA results in a long-term increase in the waste panel mean pressure. The combined impacts of the ROMPCS temporal evolution and increased waste panel gas generation are more closely seen in Figure 6-19. In that figure, the overall means of waste panel pressure obtained in the PCS-2012 PA and the PABC-2009 are plotted together with the time scale restricted to the first 1,000 years. As seen in that figure, the PCS-2012 PA mean waste panel pressure is lower than that obtained in the PABC-2009 at early times. The higher permeability (on average) of the ROMPCS for the first 100 years, and the DRZ above and below it for the first 200 years, allows for increased release of pressure from the waste panel as compared to Option D. After the ROMPCS assumes its long-term properties at 200 years, with the DRZ modeled as healed above and below it, the PCS-2012 PA mean waste panel pressure curve steadily increases, eventually becoming greater than the PABC-2009 mean waste panel pressure curve. The combination of a "tighter" panel closure after 200 years and increased gas generation in the waste panel translates to an eventual increase in the PCS-2012 PA mean waste panel pressure.

The release of pressure from repository waste areas at early times to other repository regions can be clearly seen in Figure 6-20 and Figure 6-21. As seen in Figure 6-20, the mean pressure in the operations area, denoted by quantity OPS_PRES, is greater in the PCS-2012 PA at early times when compared to the PABC-2009. The same is also true for the mean pressure in the experimental area (Figure 6-21). After the ROMPCS and the DRZ above and below it assume their long-term properties at 200 years, the rate of pressure release from repository waste areas into the operations and experimental regions decreases. The "tighter" characteristics of the ROMPCS after 200 years results in less pressure being released to the experimental and operations regions as compared to Option D. The result is an eventual decrease in the mean pressure in these regions when compared to PABC-2009 results.

Information Only

As seen in the BRAGFLO schematics of Figure 3-2 and Figure 3-4 to Figure 3-8, the base of the repository shaft is modeled in WIPP PA as being directly between the operations and experimental regions. Consequently, the pressure in these two regions impacts the volume of brine moved up the shaft toward the ground surface. The horsetail plot of the volume of brine flowing up the shaft, denoted by quantity BNSHUDRZ, is shown in Figure 6-22. The three BNSHUDRZ replicate means obtained in the PCS-2012 PA, and the overall mean obtained for this quantity, are plotted together in Figure 6-23. As seen in that figure, there is good agreement between the means obtained for brine flow up the shaft in the PCS-2012 PA. The overall means of brine flow up the shaft obtained in the PCS-2012 PA and the PABC-2009 are shown together in Figure 6-24. As seen in that figure, the trends for brine flow up the shaft correspond closely to pressure trends in the operations and experimental areas. At early times, an increase is seen in the mean volume of brine flow up the shaft in the PCS-2012 PA. Eventually, however, the mean brine flow up the shaft is reduced in the PCS-2012 PA results, primarily due to the reductions in the mean pressure seen in the operations and experimental areas after the ROMPCS and surrounding DRZ assume their long-term properties.

Summary statistics for scenario S1-BF are shown in Table 4.

Table 4: Summary Statistics for Scenario S1-BF

Quantity (units)	Mean Value		Maximum Value	
	PABC-2009	PCS-2012 PA	PABC-2009	PCS-2012 PA
BRNWASIC ($x10^3$ m^3)	1.78	2.38	12.46	16.67
WAS_SATB (none)	0.16	0.20	0.99	0.99
GASMOL_W ($x10^6$ moles)	29.09	30.84	148.40	149.00
WAS_PRES (MPa)	6.52	6.77	16.19	16.29
BNSHUDRZ (m^3)	2.74	2.46	34.76	32.11

Information Only

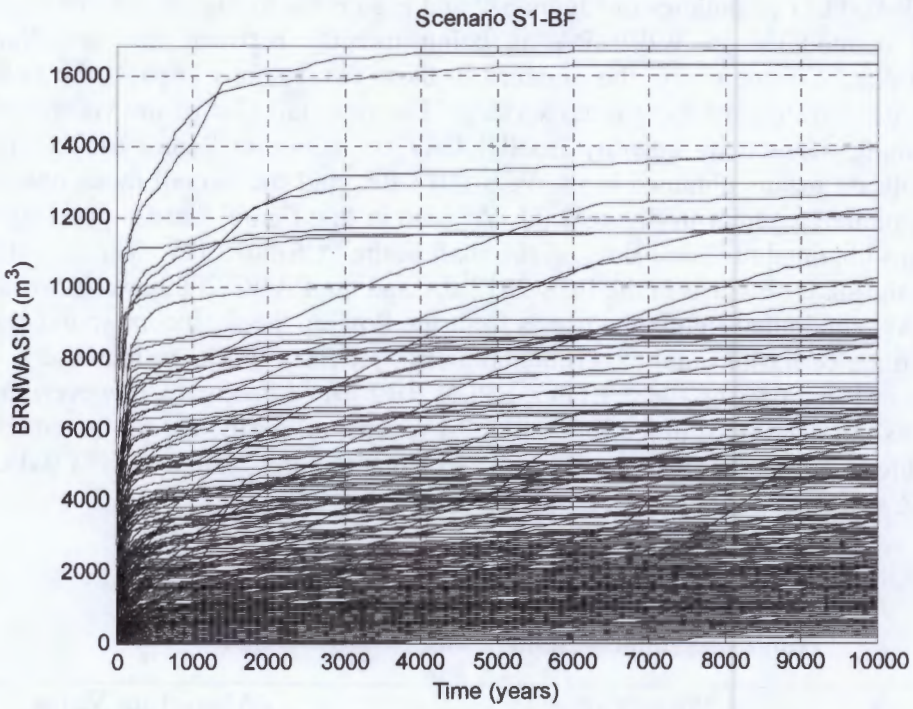

Figure 6-3: Horsetail Plot of Cumulative Brine Inflow to the Waste Panel, Scenario S1-BF.

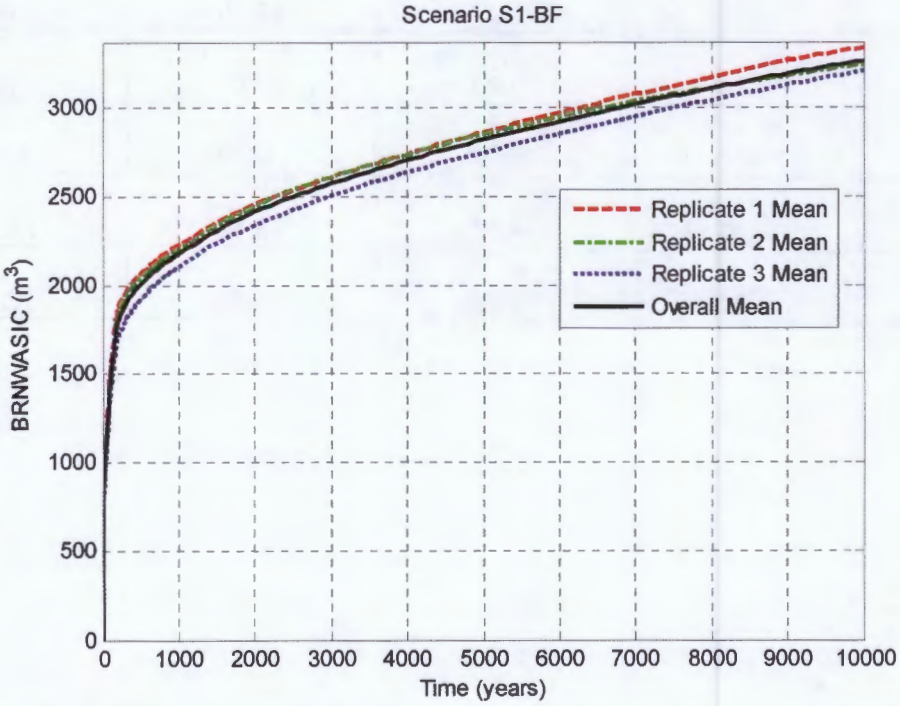

Figure 6-4: Means of Cumulative Brine Inflow to the Waste Panel, Scenario S1-BF.

Information Only

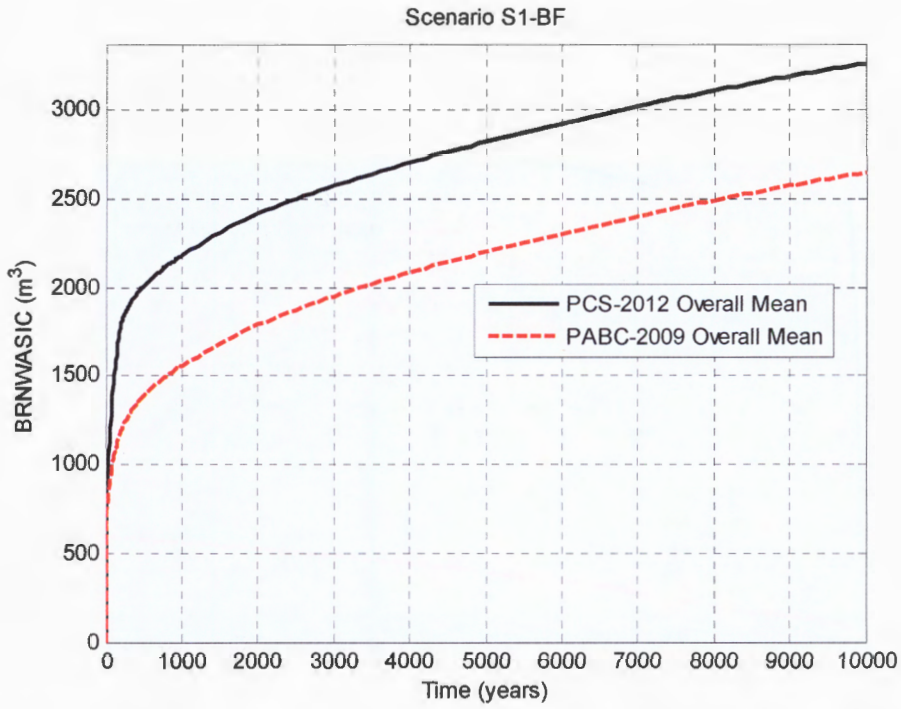

Figure 6-5: Overall Means of Cumulative Brine Inflow to the Waste Panel, Scenario S1-BF.

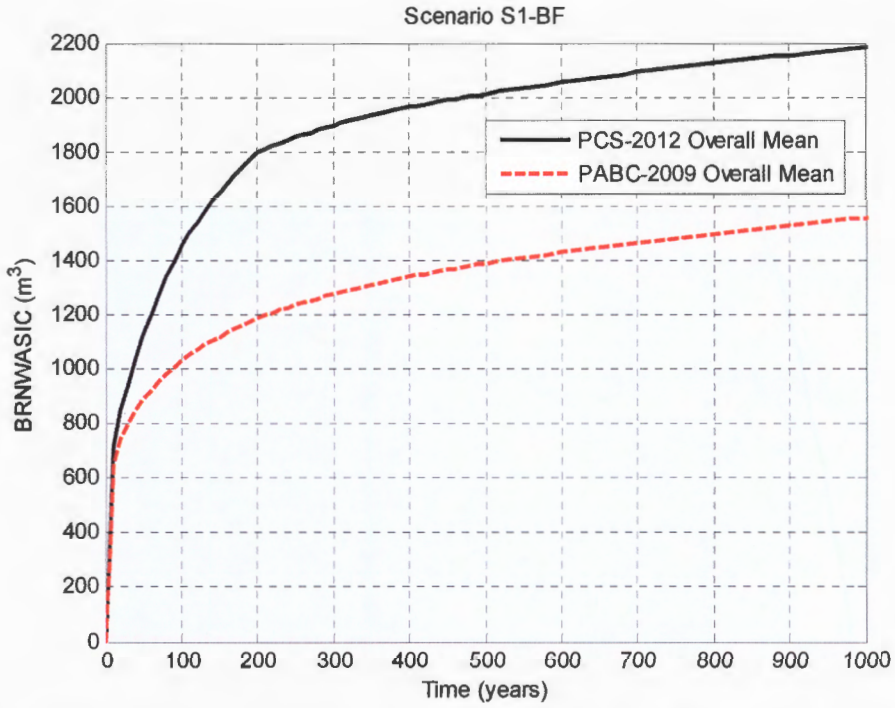

Figure 6-6: Overall Means of Cumulative Brine Inflow to the Waste Panel, Scenario S1-BF and Years 0 to 1,000.

Information Only

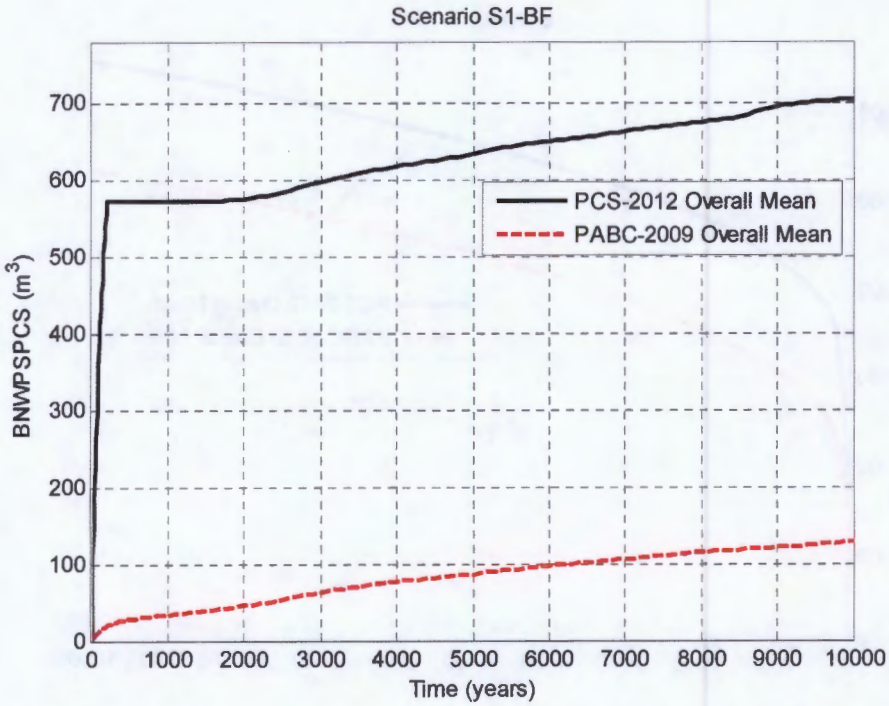

Figure 6-7: Overall Means of Cumulative Brine Flow Southward from the Panel Closure Plane and toward the Waste Panel, Scenario S1-BF

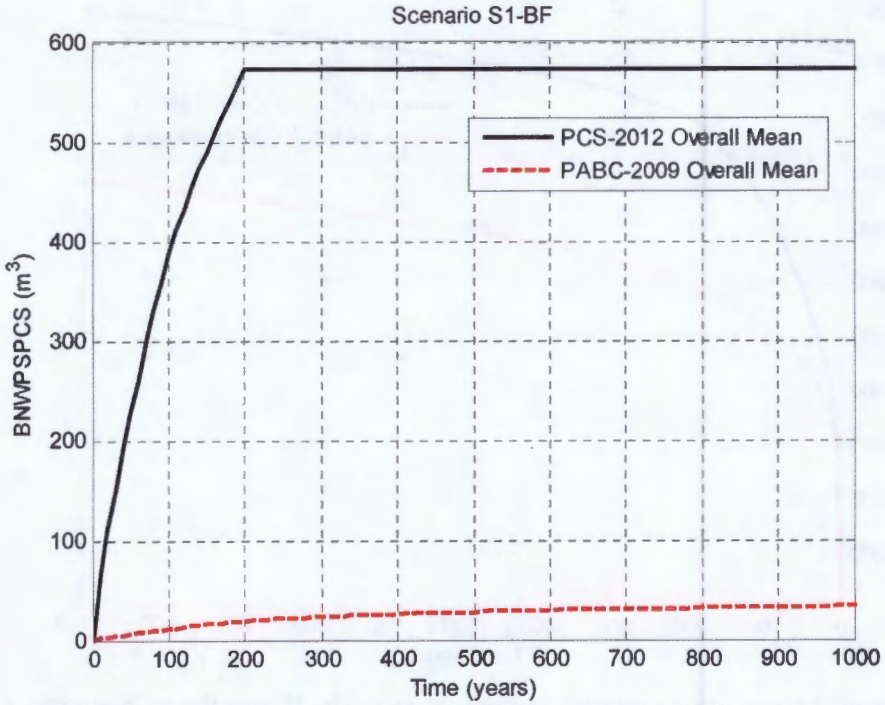

Figure 6-8: Overall Means of Cumulative Brine Flow Southward from the Panel Closure Plane and toward the Waste Panel, Scenario S1-BF and Years 0 to 1,000.

Information Only

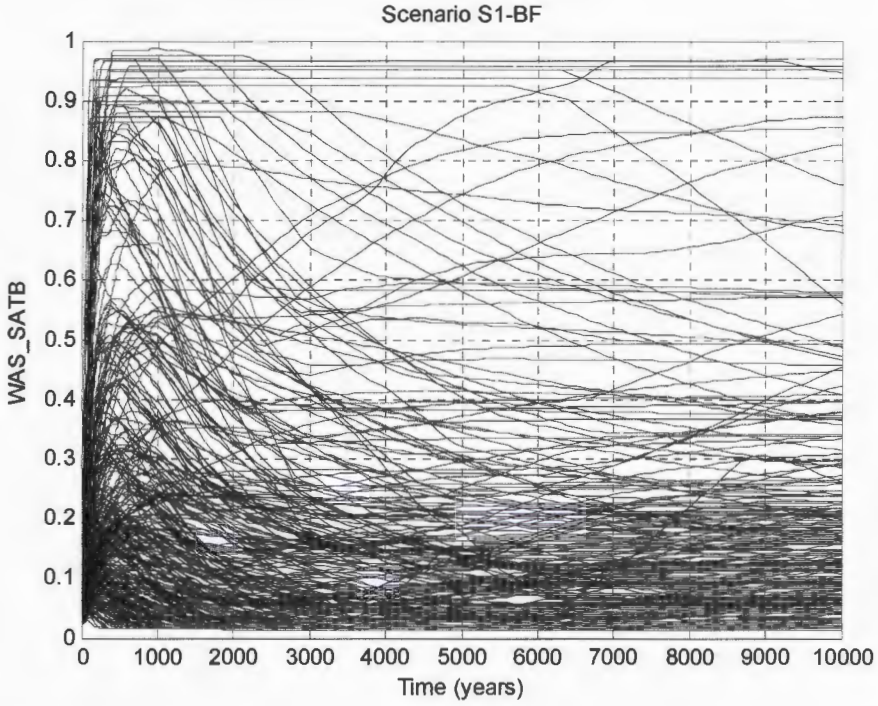

Figure 6-9: Horsetail Plot of Waste Panel Brine Saturation, Scenario S1-BF.

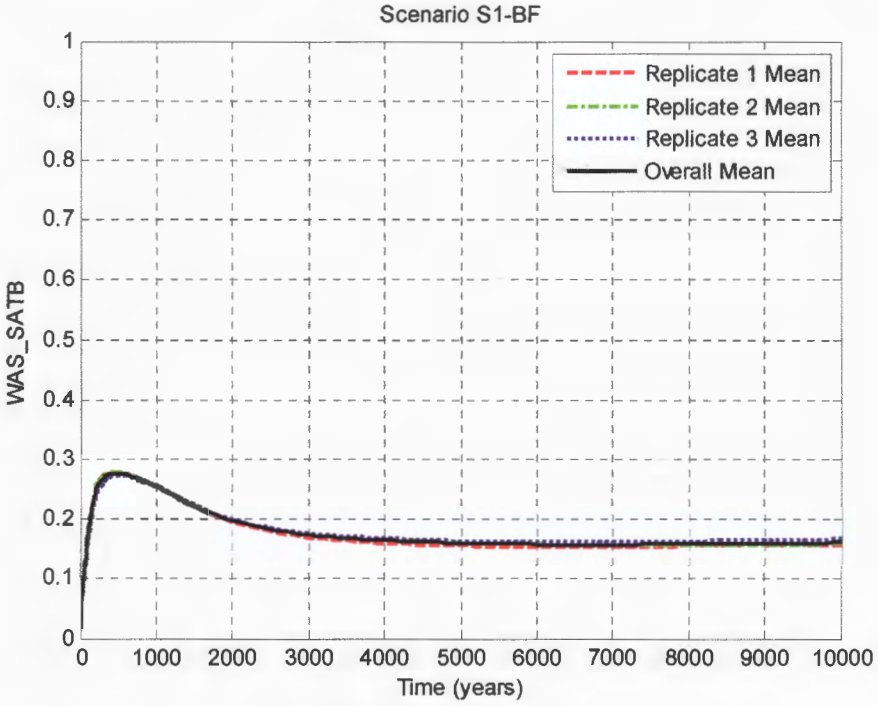

Figure 6-10: Means of Waste Panel Brine Saturation, Scenario S1-BF.

Information Only

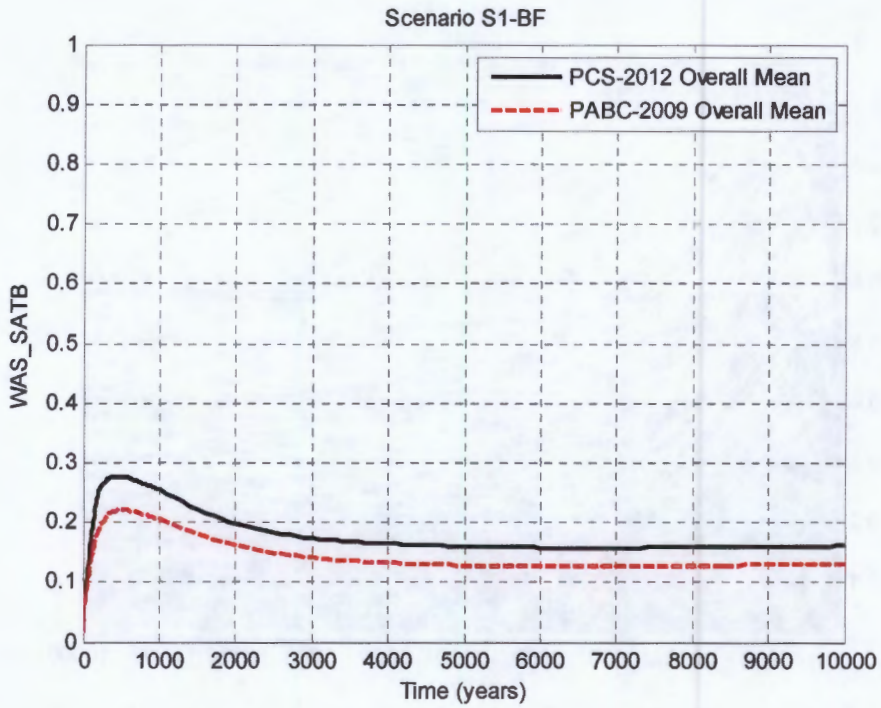

Figure 6-11: Overall Means of Waste Panel Brine Saturation, Scenario S1-BF.

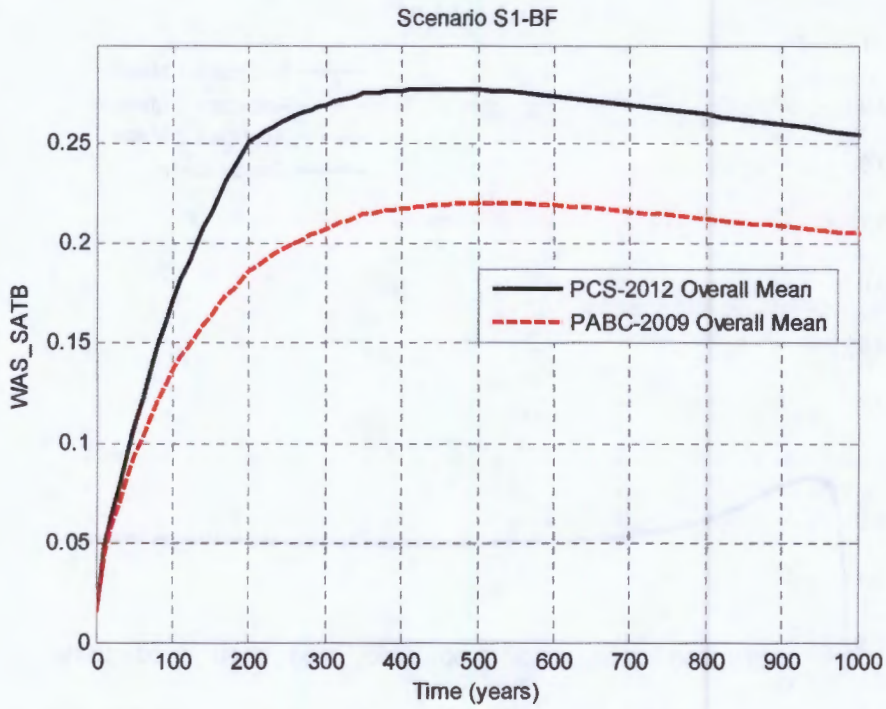

Figure 6-12: Overall Means of Waste Panel Brine Saturation, Scenario S1-BF and Years 0 to 1,000.

Information Only

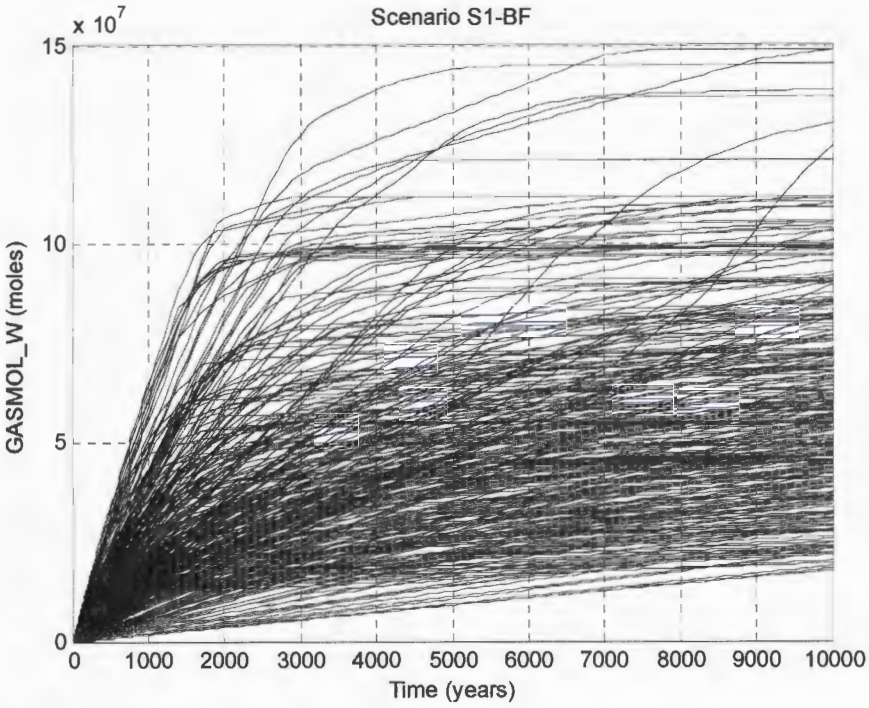

Figure 6-13: Horsetail Plot of Waste Panel Gas Generation (in moles), Scenario S1-BF.

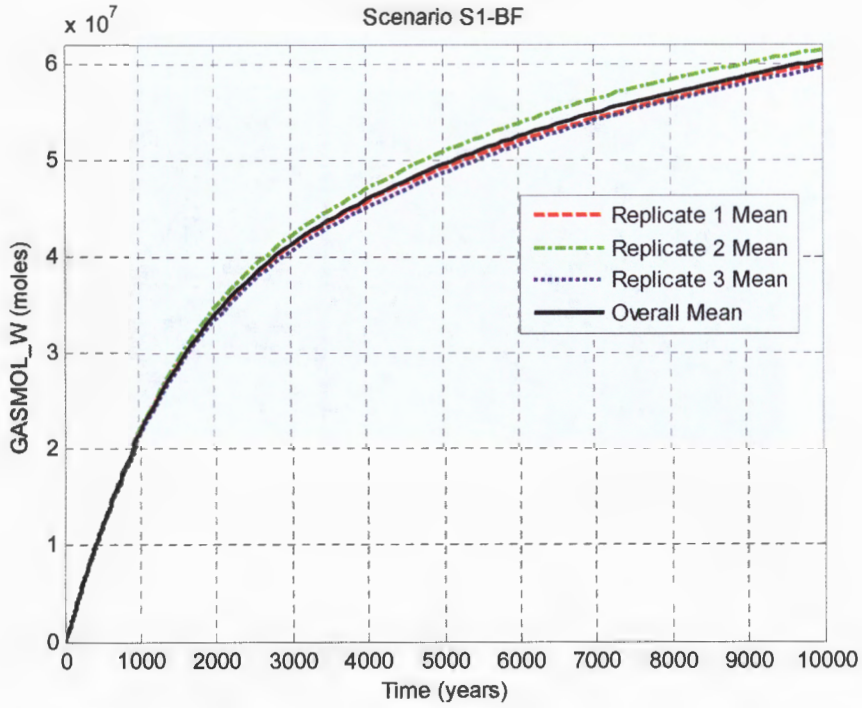

Figure 6-14: Means of Waste Panel Gas Generation (in moles), Scenario S1-BF.

Information Only

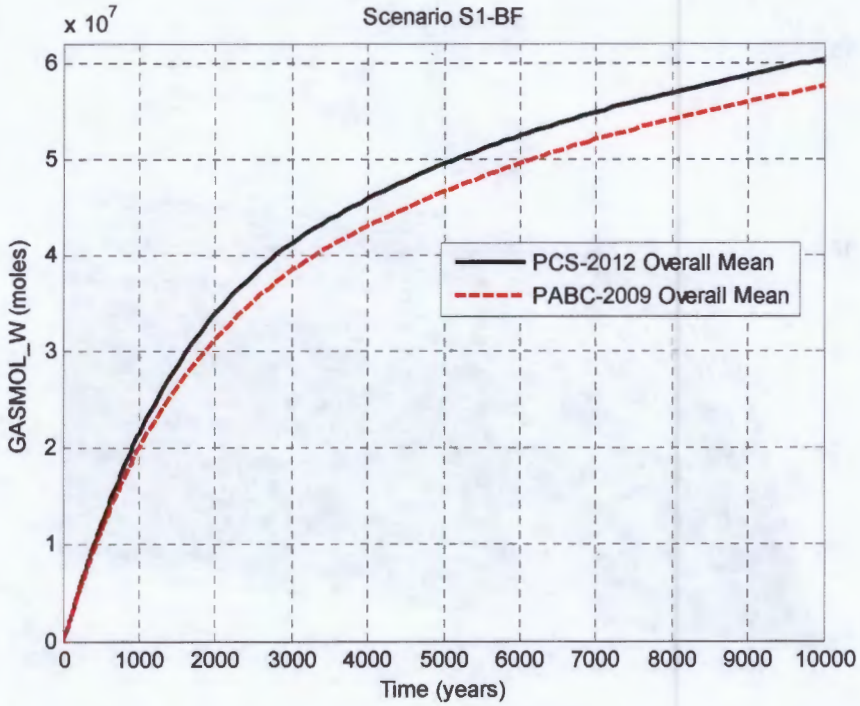

Figure 6-15: Overall Means of Waste Panel Gas Generation (in moles), Scenario S1-BF.

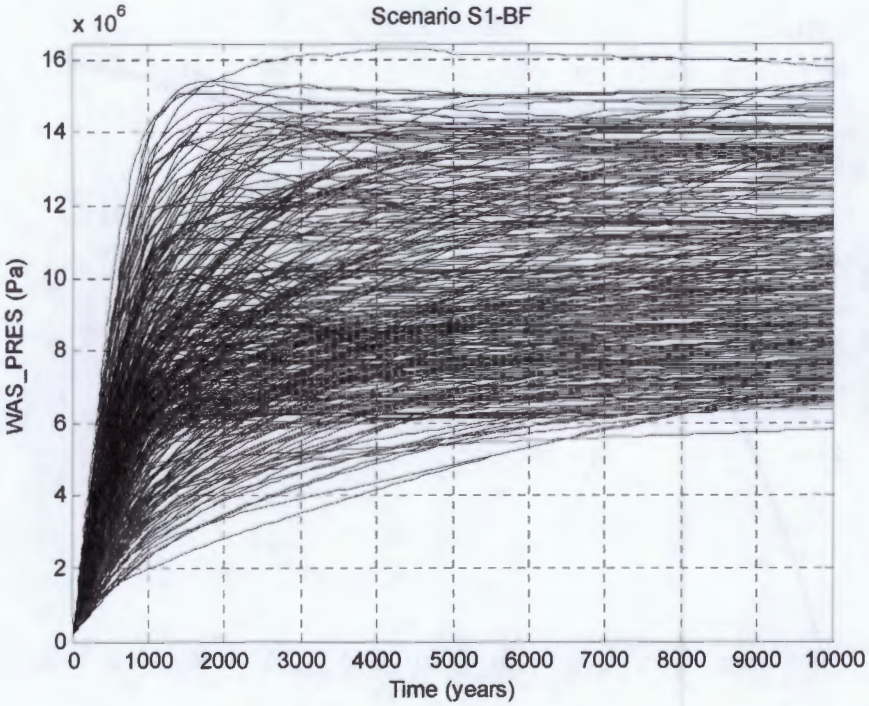

Figure 6-16: Horsetail Plot of Waste Panel Pressure, Scenario S1-BF.

Information Only

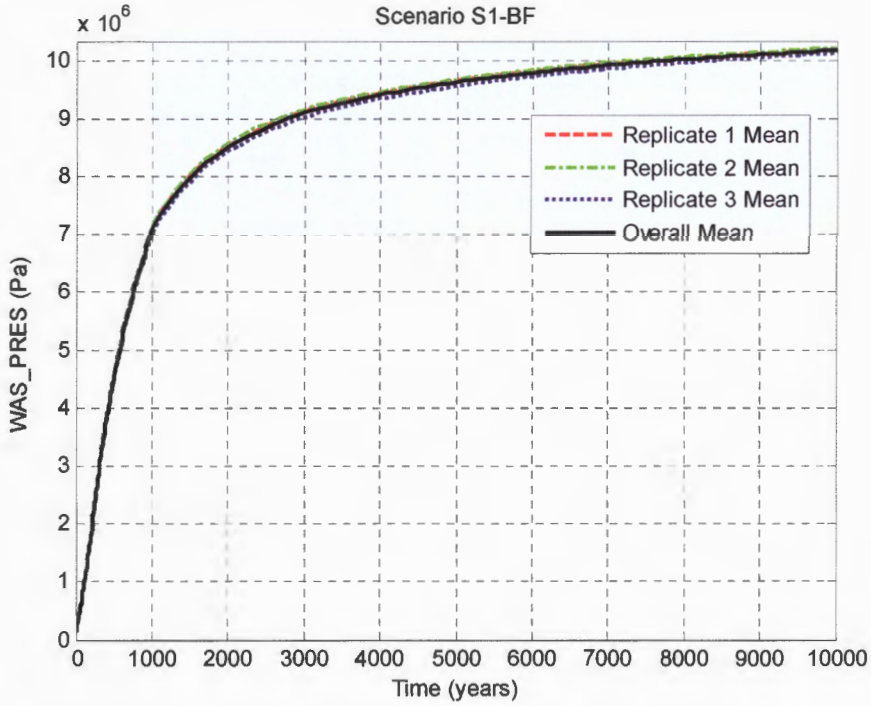

Figure 6-17: Means of Waste Panel Pressure, Scenario S1-BF.

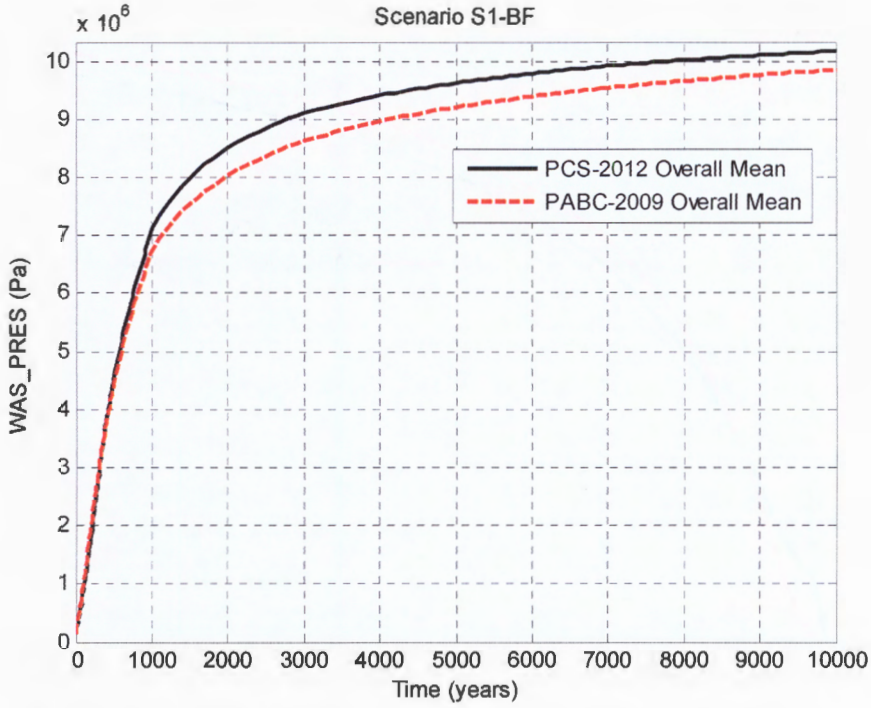

Figure 6-18: Overall Means of Waste Panel Pressure, Scenario S1-BF.

Information Only

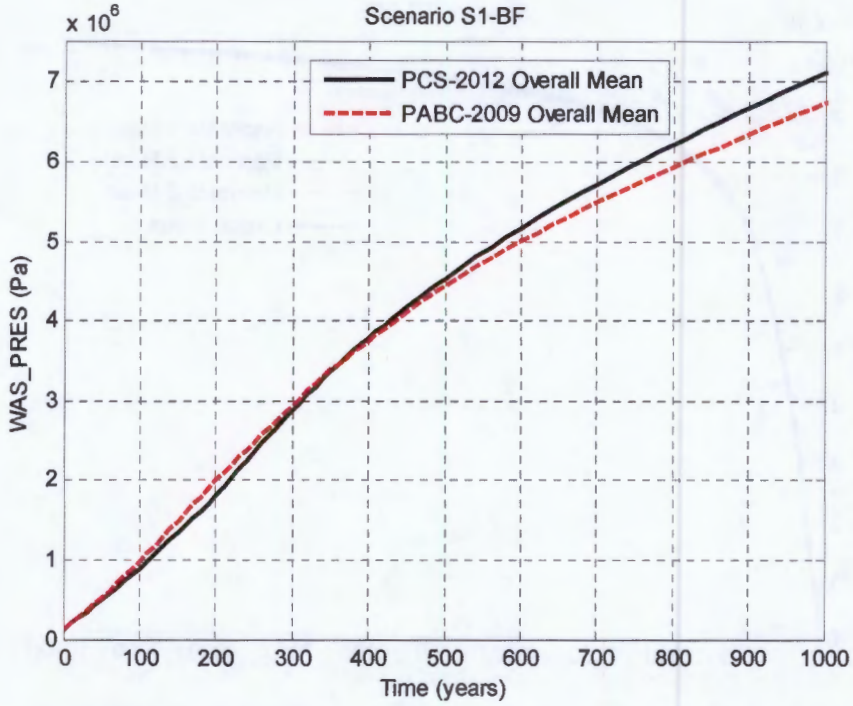

Figure 6-19: Overall Means of Waste Panel Pressure, Scenario S1-BF and Years 0 to 1,000.

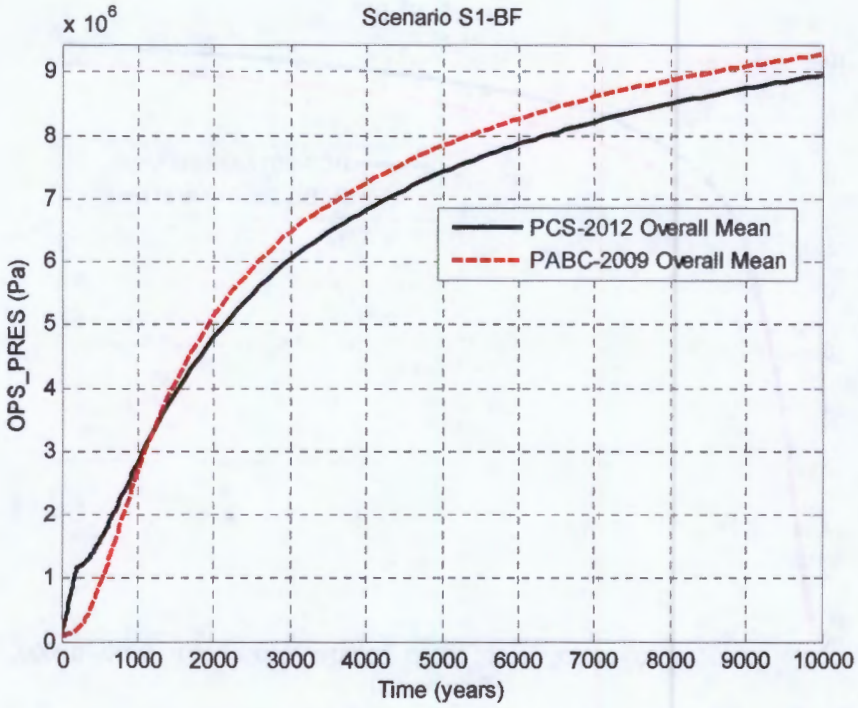

Figure 6-20: Overall Means of Pressure in the Operations Region, Scenario S1-BF.

Information Only

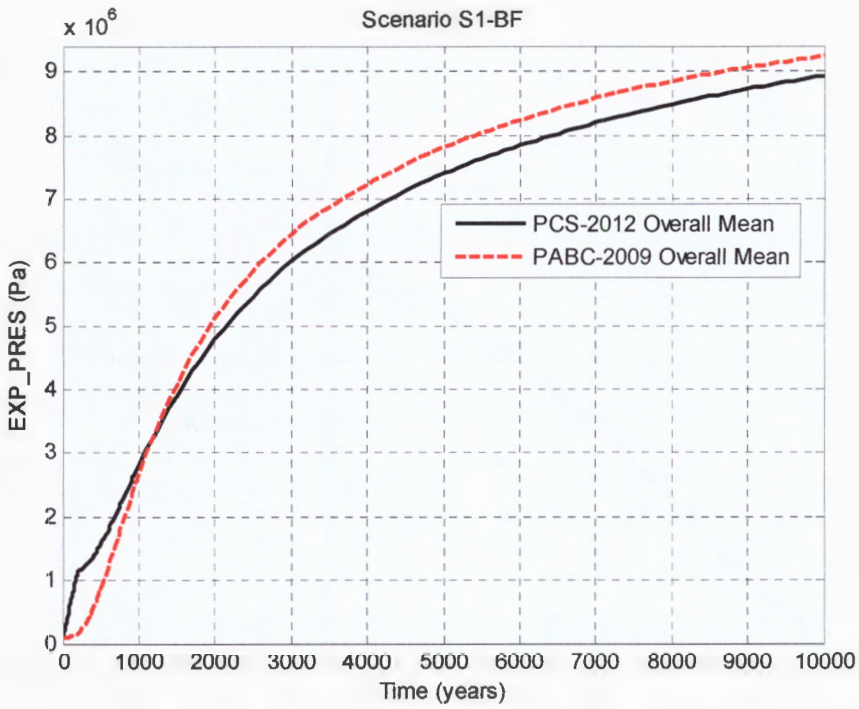

Figure 6-21: Overall Means of Pressure in the Experimental Region, Scenario S1-BF.

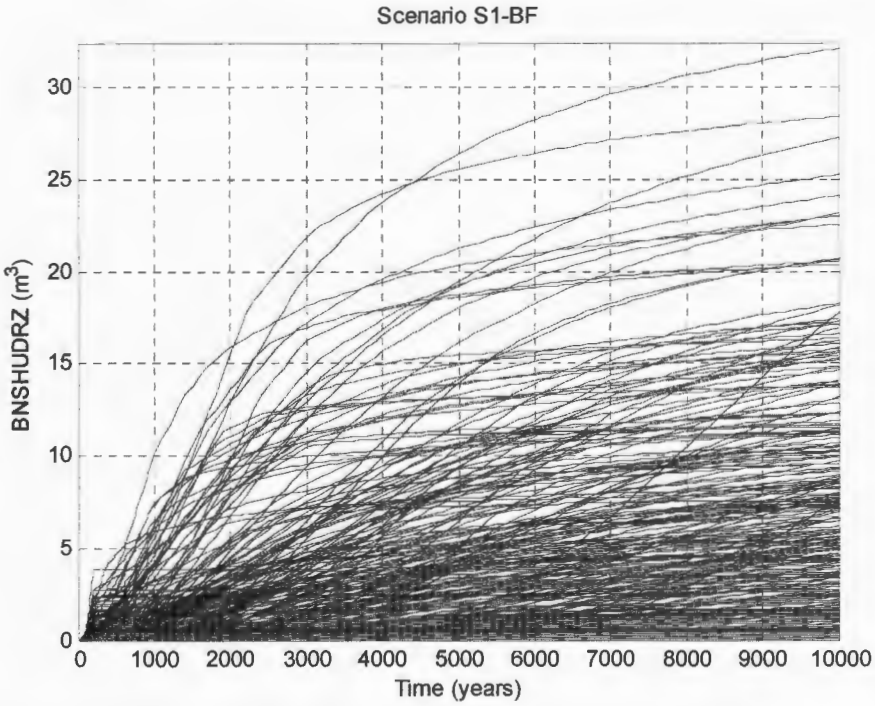

Figure 6-22: Horsetail Plot of Brine Flow up the Shaft, Scenario S1-BF.

Information Only

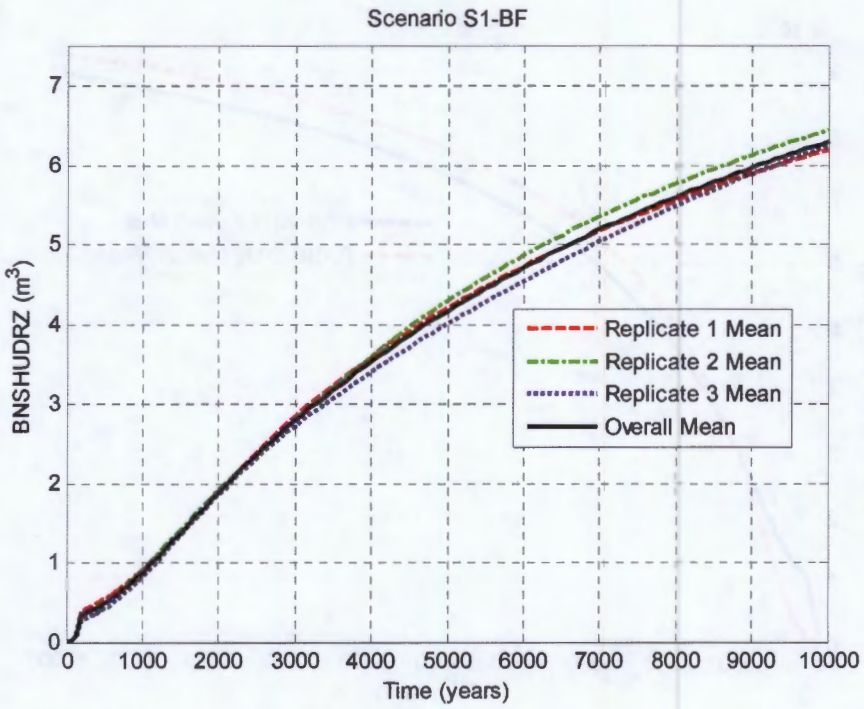

Figure 6-23: Means of Brine Flow up the Shaft, Scenario S1-BF.

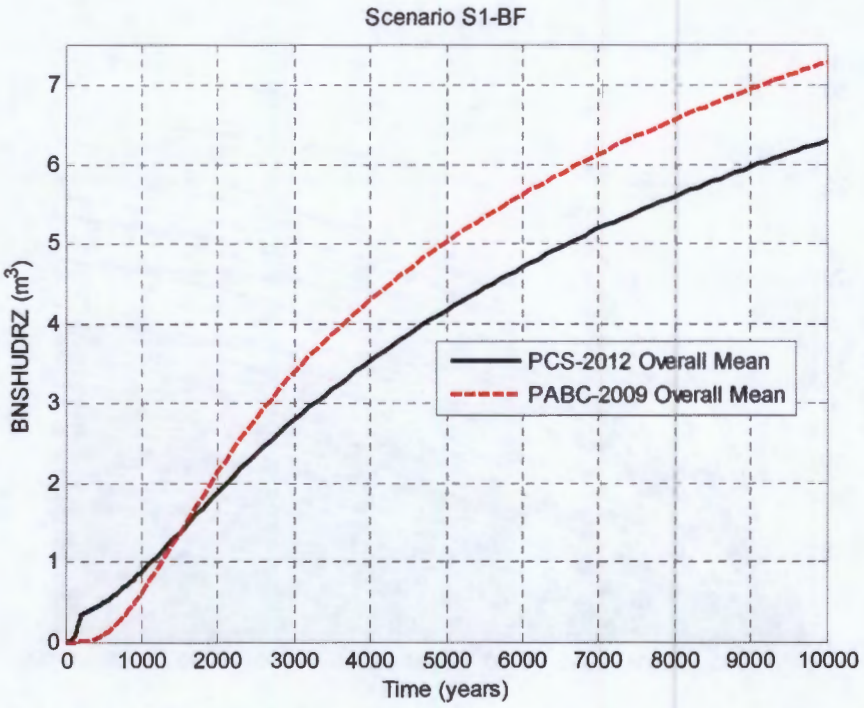

Figure 6-24: Overall Means of Brine Flow up the Shaft, Scenario S1-BF.

Information Only

6.1.2 Results for an E1 Intrusion at 350 Years (Scenario S2-BF)

Results are now presented for disturbance scenario S2-BF. Results presented for this scenario are representative of those calculated for E1 intrusion scenarios (scenarios S2-BF and S3-BF), with the only difference being the time of the intrusion. In the results that follow, PCS-2012 PA trends discussed for scenario S2-BF also apply to scenario S3-BF.

The fundamental characteristic of an E1 intrusion is the creation of a connected pathway between the repository waste panel and a region of pressurized brine in the Castile. Castile brine moves upward into the waste panel immediately after the intrusion, increasing waste panel pressure, brine saturation, and impacting other waste panel quantities.

A horsetail plot of waste panel pressure obtained for scenario S2-BF in the PCS-2012 PA is shown in Figure 6-25. The three replicate means, as well as the overall mean, of waste panel pressure for this scenario are shown in Figure 6-26. As seen in that figure, there is good agreement among the means of waste panel pressure obtained in the PCS-2012 PA.

The overall means of waste panel pressure obtained in the PCS-2012 PA and the PABC-2009 for scenario S2-BF are plotted together in Figure 6-27. As seen in that figure, the mean waste panel pressure calculated in the PCS-2012 PA is greater than that found in the PABC-2009 for a period of time after the intrusion. As discussed previously, the long-term permeability range of the ROMPCS is lower than that prescribed to the Option D design in the PABC-2009. This reduction results in less long-term brine and gas flow through the ROMPCS, away from the waste panel, as compared to Option D. Following the E1 intrusion at 350 years, the "tighter" ROMPCS design results in a period of increased waste panel pressurization as compared to the PABC-2009 results.

An increase in waste panel pressure potentially impacts the volume of cumulative brine inflow to the waste panel. The horsetail plot of quantity BRNWASIC for PCS-2012 PA scenario S2-BF is shown in Figure 6-28. The three replicate means, as well as the overall mean, are shown in Figure 6-29. As seen in that figure, there is fairly close agreement between the means obtained for cumulative waste panel brine inflow. The overall means of BRNWASIC obtained in the PCS-2012 PA and the PABC-2009 are shown together in Figure 6-30. As seen in that figure, the increased permeability range of the ROMPCS at early times results in greater brine inflow to the waste panel before the ROMPCS attains its long-term properties at 200 years. Following the intrusion time of 350 years, an increase in mean waste panel pressure occurs in the PCS-2012 PA results. This pressure increase slightly inhibits brine flow into the waste panel, resulting in a reduction in cumulative waste panel brine inflow as compared to the PABC-2009 results.

The reduction of brine flowing into the waste panel in the PCS-2012 PA impacts the waste panel brine saturation. The horsetail plot of waste panel brine saturation obtained in PCS-2012 PA scenario S2-BF is shown in Figure 6-31. The three replicate means, and the overall mean, of WAS_SATB are shown together in Figure 6-32. As seen in that figure, there is very close agreement between the replicate means and the overall mean of waste panel brine saturation. The overall means of quantity WAS_SATB obtained in the PCS-2012 PA and the PABC-2009 are shown together in Figure 6-33. As is evident in that figure, the mean waste panel brine

Information Only

saturation obtained in the PCS-2012 PA is reduced slightly from that calculated in the PABC-2009 after the intrusion at 350 years. The reduction of brine inflow to the waste panel translates to a reduction in waste panel brine saturation.

A horsetail plot of waste panel gas generation (in moles) is given in Figure 6-34. The three replicate means, and the overall mean, for quantity GASMOL_W are shown together in Figure 6-35. As seen in that figure, there is very good agreement among the scenario S2-BF means obtained for waste panel gas generation in the PCS-2012 PA. The overall means of waste panel gas generation obtained in the PCS-2012 PA and the PABC-2009 are shown together in Figure 6-36. The overall means obtained for quantity GASMOL_W obtained in the two analyses are nearly identical, with a very slight reduction seen in the PCS-2012 PA mean. This slight reduction in gas generation is most likely due to the reduction in waste panel brine inflow and brine saturation seen in the PCS-2012 PA results.

The volume of brine flow up the intrusion borehole is denoted by quantity BNBHUDRZ. The horsetail plot of quantity BNBHUDRZ is shown in Figure 6-37. The three replicate means, and the overall mean for quantity BNBHUDRZ, are shown together in Figure 6-38. As seen in that figure, there is variability among the PCS-2012 PA means obtained for quantity BNBHUDRZ. The means obtained in the PCS-2012 PA are almost identical to those obtained in the PABC-2009, however, as is evident by comparing Figure 6-38 and Figure 6-39. Overall means of BNBHUDRZ obtained in the PCS-2012 PA and the PABC-2009 are shown together in Figure 6-40. The overall means obtained in the two analyses are almost identical, with a very slight increase seen in the PCS-2012 PA result.

Summary statistics for scenario S2-BF are shown in Table 5.

Table 5: Summary Statistics for Scenario S2-BF

Quantity (units)	Mean Value		Maximum Value	
	PABC-2009	PCS-2012 PA	PABC-2009	PCS-2012 PA
BRNWASIC ($x10^3$ m^3)	14.03	13.68	182.15	182.08
WAS_SATB (none)	0.68	0.67	0.99	0.99
GASMOL_W ($x10^6$ moles)	54.75	54.57	149.00	149.00
WAS_PRES (MPa)	7.39	7.50	15.63	16.40
BNBHUDRZ ($x10^3$ m^3)	3.25	3.28	166.84	169.54

Information Only

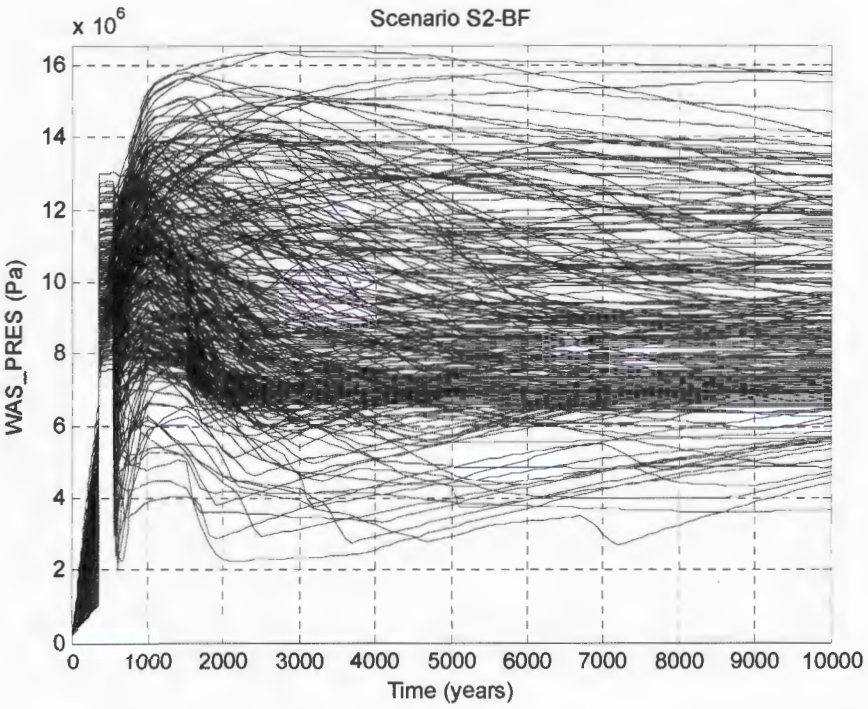

Figure 6-25: Horsetail Plot of Waste Panel Pressure, Scenario S2-BF.

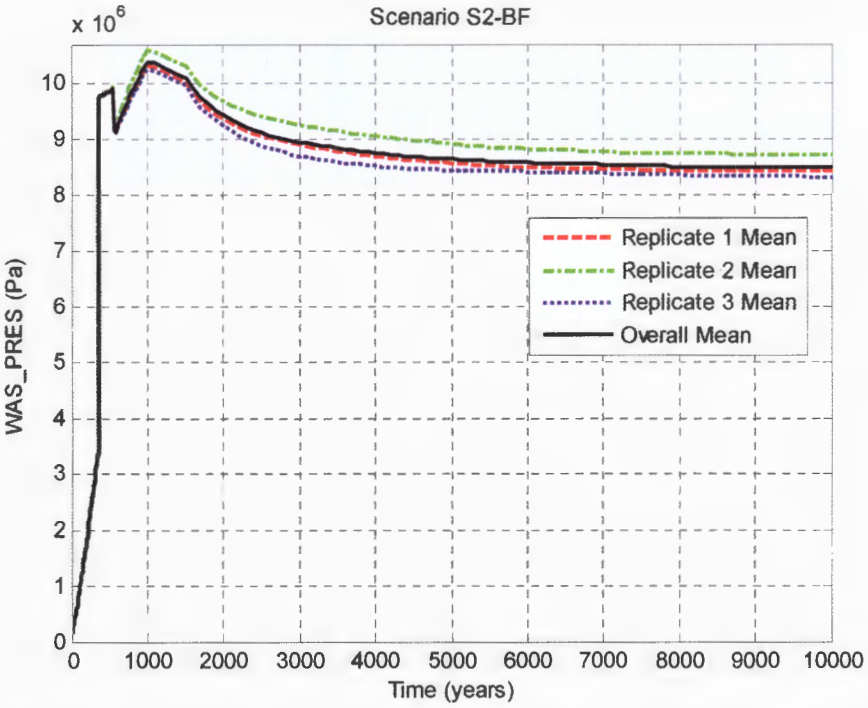

Figure 6-26: Means of Waste Panel Pressure, Scenario S2-BF.

Information Only

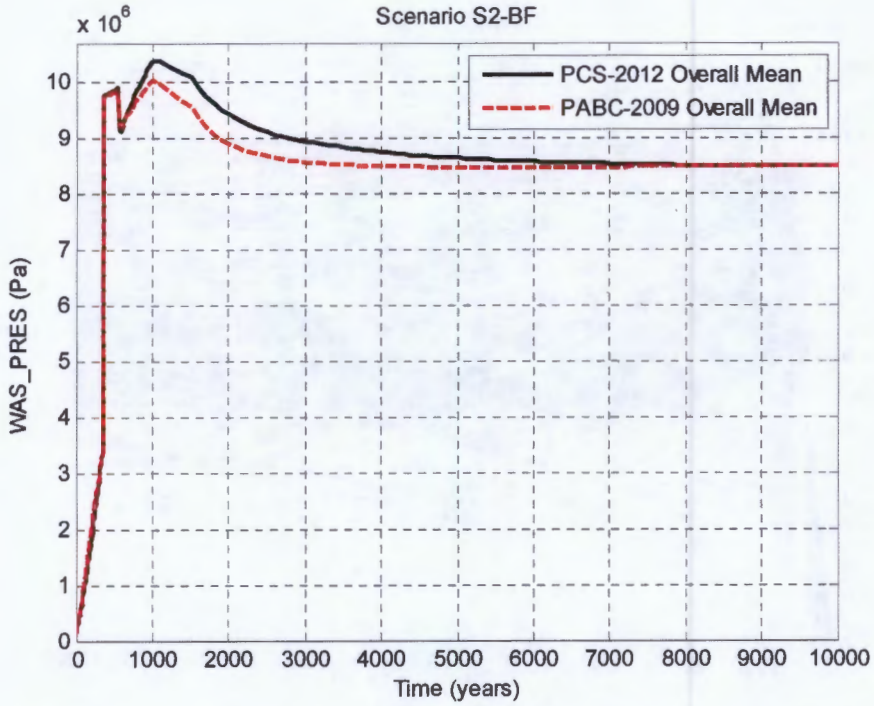

Figure 6-27: Overall Means of Waste Panel Pressure, Scenario S2-BF.

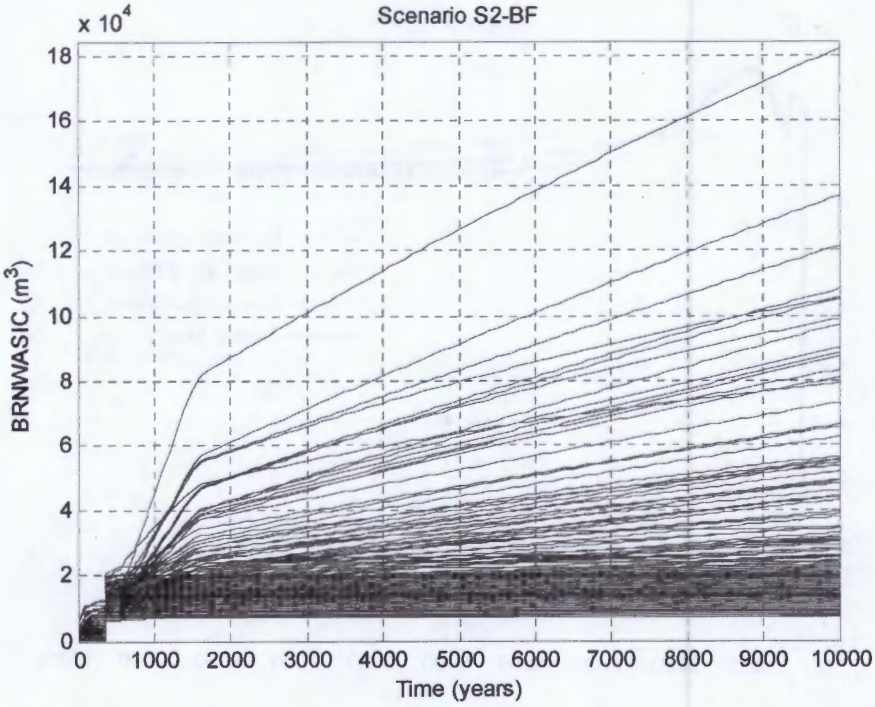

Figure 6-28: Horsetail Plot of Cumulative Brine Inflow to the Waste Panel, Scenario S2-BF.

Information Only

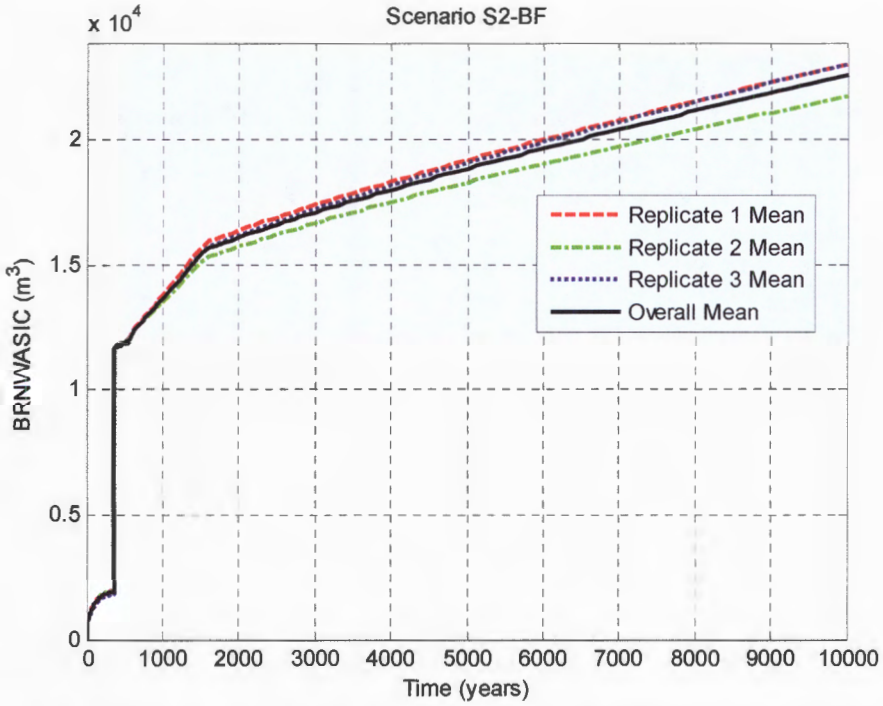

Figure 6-29: Means of Cumulative Brine Inflow to the Waste Panel, Scenario S2-BF.

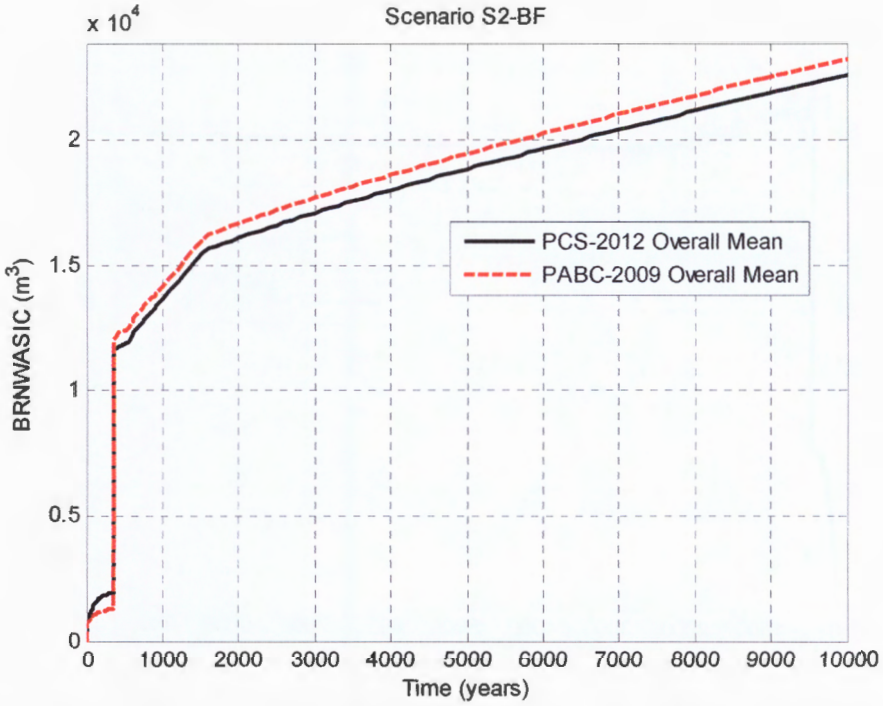

Figure 6-30: Overall Means of Cumulative Brine Inflow to the Waste Panel, Scenario S2-BF.

Information Only

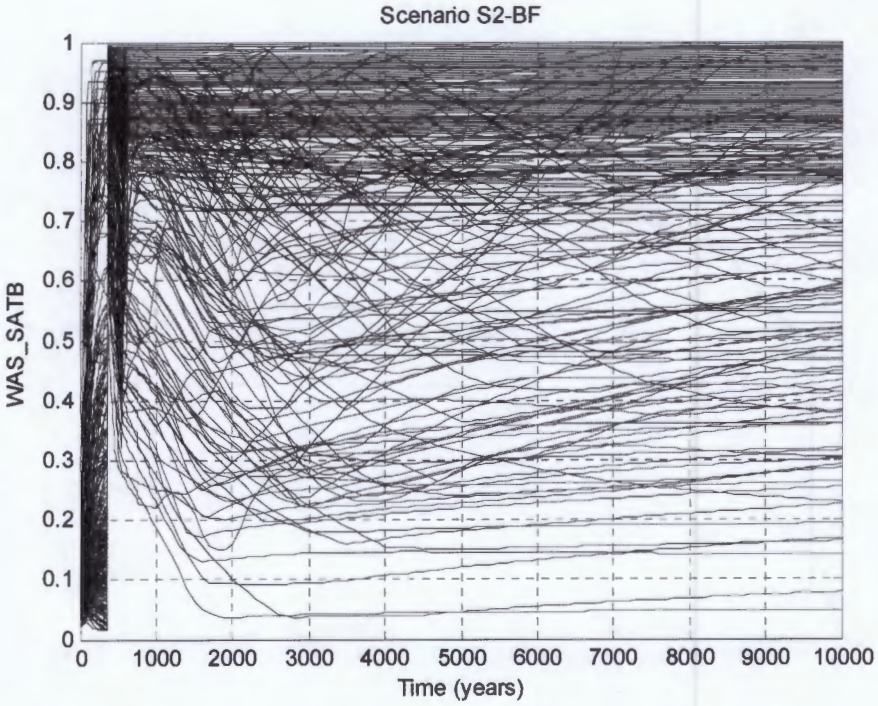

Figure 6-31: Horsetail Plot of Waste Panel Brine Saturation, Scenario S2-BF.

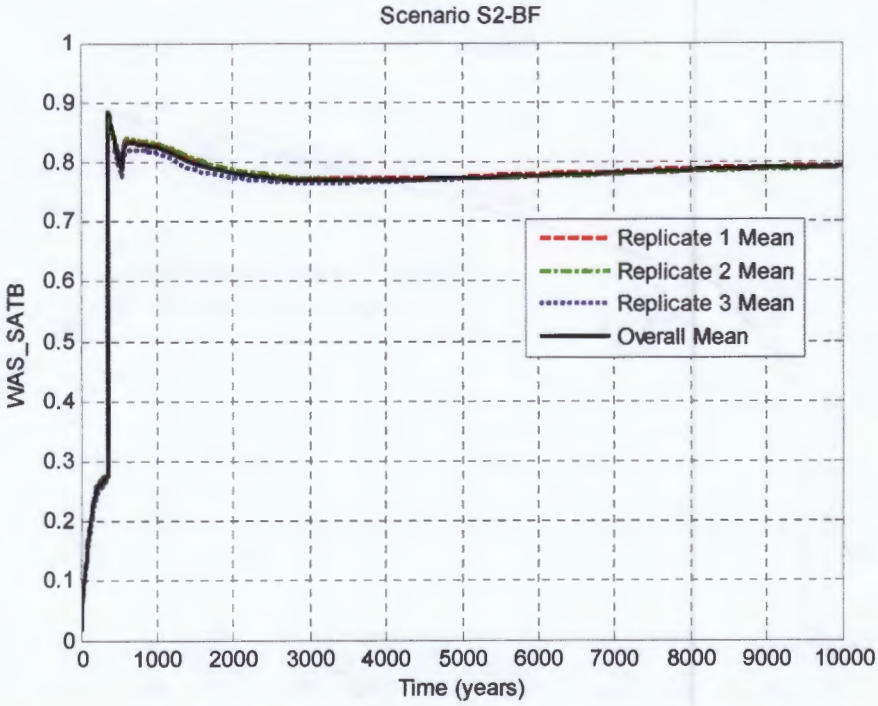

Figure 6-32: Means of Waste Panel Brine Saturation, Scenario S2-BF.

Information Only

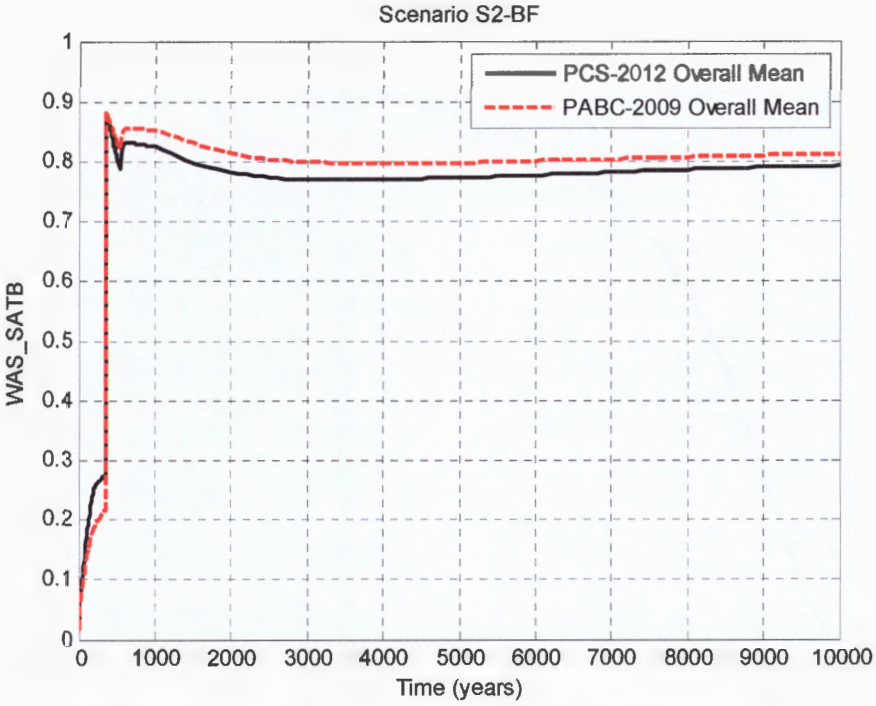

Figure 6-33: Overall Means of Waste Panel Brine Saturation, Scenario S2-BF.

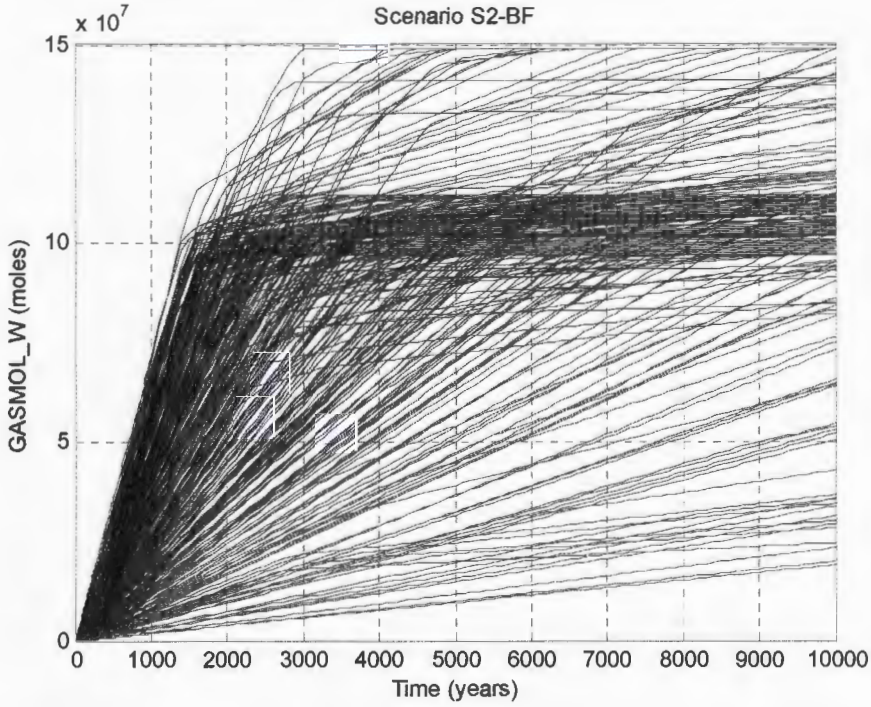

Figure 6-34: Horsetail Plot of Waste Panel Gas Generation (in moles), Scenario S2-BF.

Information Only

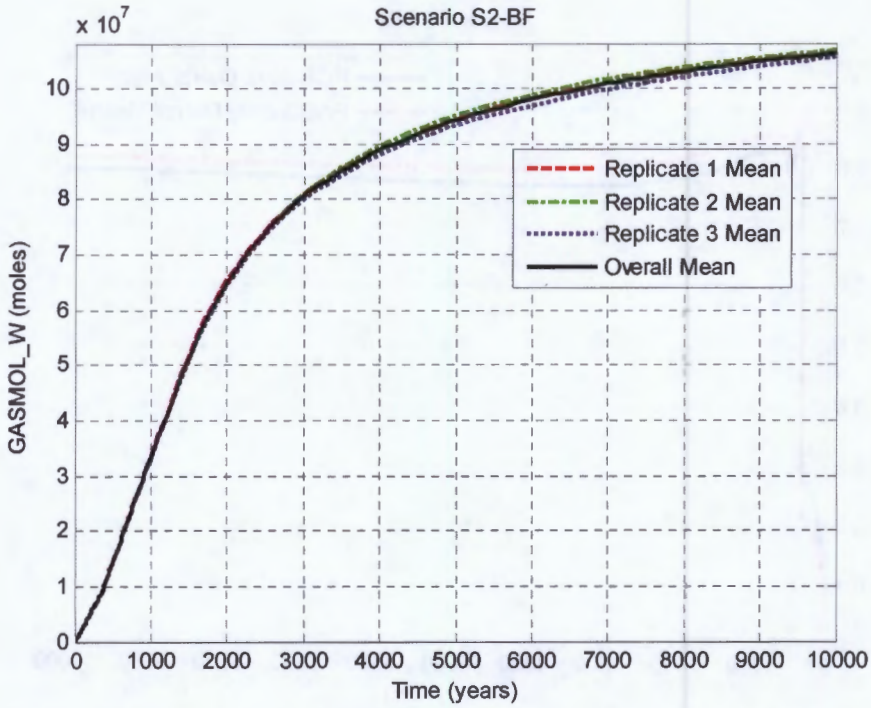

Figure 6-35: Means of Waste Panel Gas Generation (in moles), Scenario S2-BF.

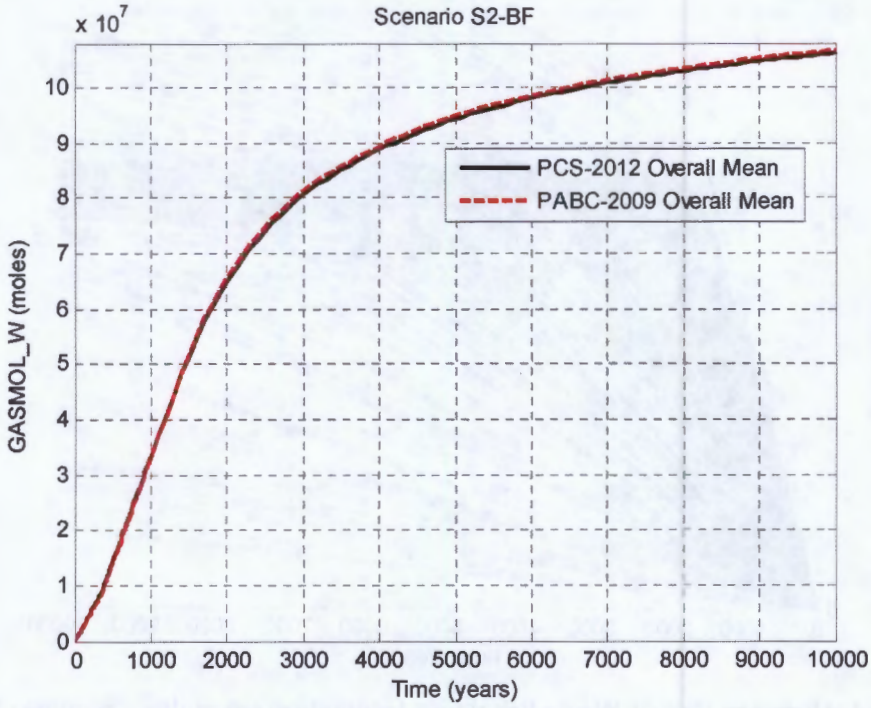

Figure 6-36: Overall Means of Waste Panel Gas Generation (in moles), Scenario S2-BF.

Information Only

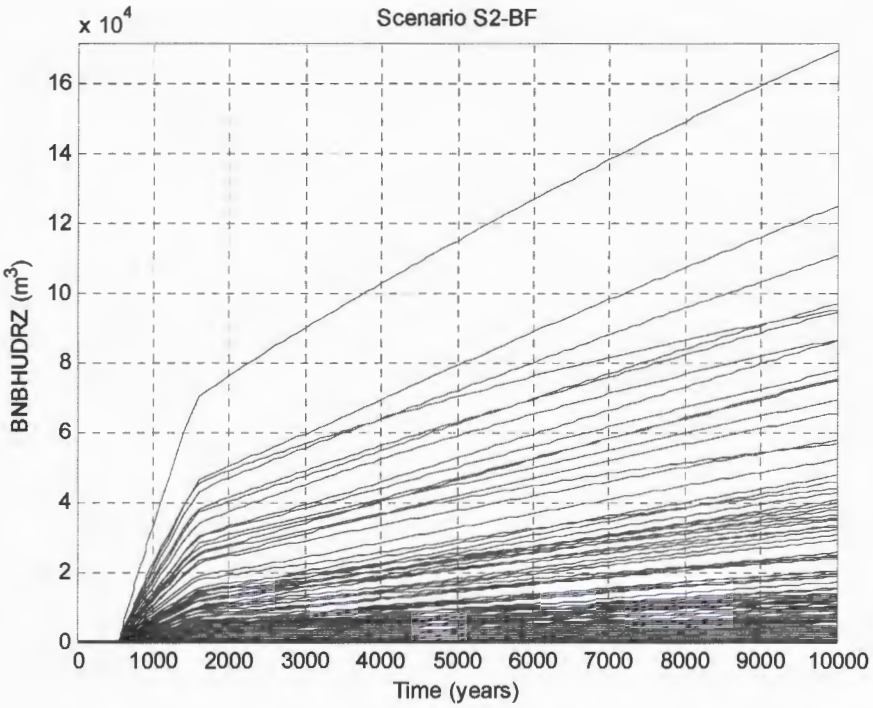

Figure 6-37: Horsetail Plot of Brine Flow up the Borehole, Scenario S2-BF.

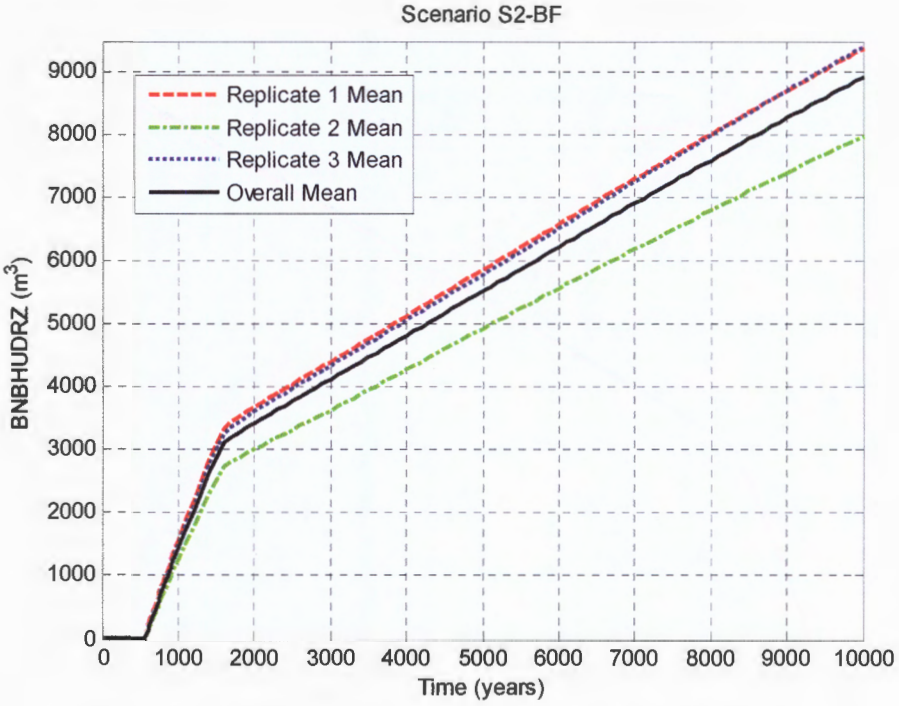

Figure 6-38: Means of Brine Flow up the Borehole, Scenario S2-BF.

Information Only

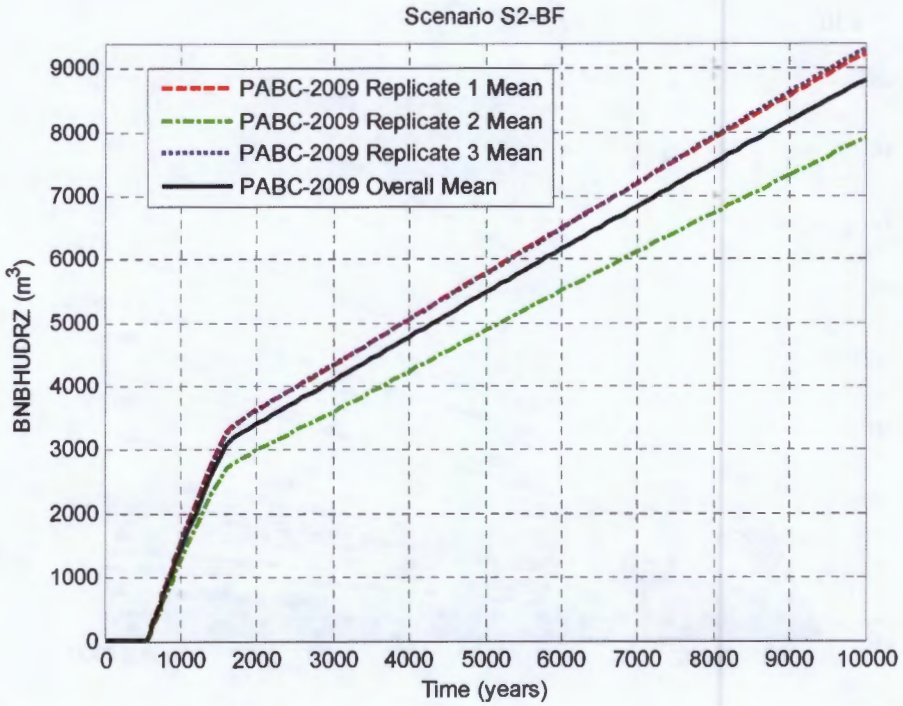

Figure 6-39: Means of Brine Flow up the Borehole, Scenario S2-BF for the PABC-2009.

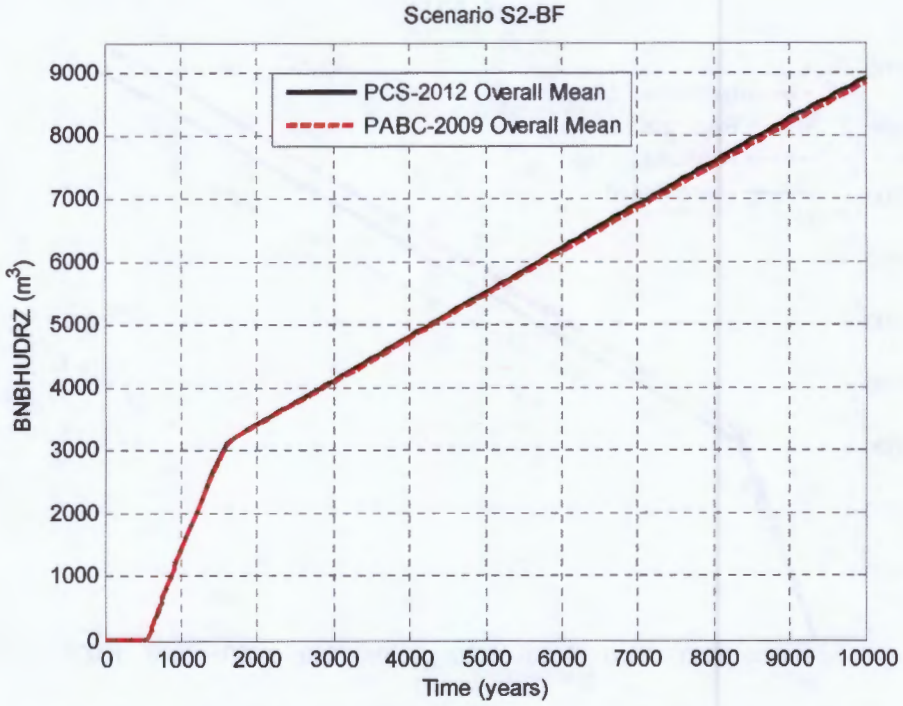

Figure 6-40: Overall Means of Brine Flow up the Borehole, Scenario S2-BF.

Information Only

6.1.3 Results for an E2 Intrusion at 350 Years (Scenario S4-BF)

Results are now presented for disturbance scenario S4-BF. Results presented for this scenario are representative of those calculated for E2 intrusion scenarios (scenarios S4-BF and S5-BF), with the only difference being the time of the intrusion. In the results that follow, PCS-2012 PA trends discussed for scenario S4-BF also apply to scenario S5-BF.

As seen in the previous section, an E1 intrusion scenario results in an immediate influx of pressurized Castile brine to the waste panel, resulting in an increase is waste panel pressure when compared to undisturbed conditions. An E2 intrusion typically has the opposite effect. For the E2 intrusion scenario, no connected pathway is created between pressurized Castile brine and the repository waste panel. Following the intrusion, concrete plugs are immediately emplaced in the borehole near the ground surface. Consequently, an E2 intrusion does not typically have a significant impact on waste panel quantities *at the time of intrusion*. 200 years after the time of intrusion, concrete plugs emplaced in the borehole are modeled as failing, with the entire borehole assuming properties equivalent to sand. The result is a depressurization of the waste panel, beginning 200 years after the intrusion. Whereas an E1 intrusion typically results in an immediate increase in waste panel pressure, an E2 intrusion typically results in a *reduction* in waste panel pressure 200 years after the intrusion as compared to undisturbed conditions.

A horsetail plot of waste panel pressure obtained in the PCS-2012 PA scenario S4-BF is shown in Figure 6-41. The three replicate means, and the overall mean, for quantity WAS_PRES are shown together in Figure 6-42. As seen in that figure, there is close agreement among the replicate means and the overall mean obtained for waste panel pressure in the PCS-2012 PA. The impact of the E2 intrusion on waste panel pressure is more closely seen in Figure 6-43. In that figure, PCS-2012 PA overall means of waste panel pressure obtained in scenarios S1-BF and S4-BF are plotted together with the time scale restricted to the first 1,000 years. As seen in that figure, no noticeable impact is seen in the mean waste panel pressure when the E2 intrusion occurs at 350 years. For the period of 350 years to 550 years, there is a slight increase in the mean pressure for scenario S4-BF as compared to undisturbed results. The borehole plugs fail at 550 years, creating a pathway for waste panel pressure release through the borehole and toward the ground surface. Consequently, the mean waste panel pressure for scenario S4-BF is reduced sharply at 550 years when compared to undisturbed results.

The overall means of waste panel pressure obtained for scenario S4-BF in the PCS-2012 PA and the PABC-2009 are shown together in Figure 6-44. As seen in that figure, the mean waste panel pressure obtained in the PCS-2012 PA is slightly greater than the PABC-2009 result. As already discussed, the PCS-2012 PA mean waste panel pressure is greater than that seen in the PABC-2009 for undisturbed conditions (Figure 6-18). Consequently, at the time of the E2 intrusion, the mean waste panel pressure is greater in the PCS-2012 PA, and is also greater 200 years later when the borehole plugs fail. The result is a slightly higher mean pressure in the PCS-2012 PA scenario S4-BF result when compared to the PABC-2009.

A horsetail plot of cumulative waste panel brine inflow for PCS-2012 PA scenario S4-BF is shown in Figure 6-45. The three replicate means, and the overall mean, for quantity

Information Only

BRNWASIC are shown together in Figure 6-46. As seen in that figure, there is close agreement among the PCS-2012 PA means for quantity BRNWASIC.

The impact of the E2 intrusion on cumulative waste panel brine inflow can be clearly seen in Figure 6-47. At the intrusion time of 350 years until the borehole plugs fail at 550 years, there is only a very slight increase in quantity BRNWASIC as compared to undisturbed conditions. After the borehole plugs fail, a decrease in the waste panel pressure occurs. This pressure reduction yields in an increase in brine flow into the waste panel at 550 years compared to the undisturbed case.

The overall mean for quantity BRNWASIC in the PCS-2012 PA and the PABC-2009 are plotted together in Figure 6-48. As evident in that figure, an increase to the mean waste panel cumulative brine inflow is seen in the PCS-2012 PA results. This increase is due to the increased waste panel brine inflow seen for undisturbed conditions (Figure 6-5). As discussed above, very little impact is seen in the mean curve for quantity BRNWASIC as compared to undisturbed conditions, until the borehole plugs fail at 550 years. The PCS-2012 PA mean waste panel brine inflow curve is already greater than that obtained in the PABC-2009 when the borehole plugs fail at 550 years. The increase in brine inflow seen after the borehole plugs fail results in a PCS-2012 PA mean waste panel brine inflow curve that remains greater than that seen in the PABC-2009.

The change to cumulative waste panel brine inflow seen in the PCS-2012 PA impacts the waste panel brine saturation. A horsetail plot of the PCS-2012 PA waste panel brine saturation is shown in Figure 6-49. The three replicate means, and the overall mean, obtained for quantity WAS_SATB are plotted together in Figure 6-50. As seen in that figure, there is good agreement between the means obtained in the PCS-2012 PA for the waste panel brine saturation. The impact of the E2 intrusion on quantity WAS_SATB is similar to that seen for cumulative brine flow into the waste panel. As seen in Figure 6-51, the mean waste panel brine saturation is changed very little as compared to undisturbed conditions for the time period of 350 to 550 years. After the borehole plugs fail at 550 years, an increase of brine inflow to the waste panel translates to a corresponding increase in brine saturation. The result is a PCS-2012 PA mean waste brine saturation curve that is greater than that seen in the PABC-2009 results (Figure 6-52). The increase in the mean cumulative brine inflow to the waste panel seen in the PCS-2012 PA translates to an increase in the mean waste panel brine saturation.

The increase in waste panel brine saturation impacts gas generation in the waste panel. A horsetail plot of PCS-2012 PA waste panel gas generation (in moles) is shown in Figure 6-53. The three replicate means, and the overall mean, for quantity GASMOL_W are plotted together in Figure 6-54. The impact of the E2 intrusion on waste panel gas generation can be seen in Figure 6-55. Between the intrusion time of 350 years to the time of borehole plug failure at 550 years, the mean waste panel gas generation curve is increased very slightly compared to undisturbed conditions. After the borehole plugs fail, the increase to waste panel brine saturation results in a corresponding increase to waste panel gas generation. More brine flows into the waste panel (on average) in PCS-2012 PA scenario S4-BF as compared to the PABC-2009, resulting in an overall mean for quantity GASMOL_W is the PCS-2012 PA that is greater than that seen in the PABC-2009 (Figure 6-56).

Information Only

The volume of brine flowing up the borehole toward the ground surface is denoted by quantity BNBHUDRZ. A horsetail plot of this quantity for the PCS-2012 PA scenario S4-BF is given in Figure 6-57. The three replicate means, and the overall mean, for BNBHUDRZ are plotted together in Figure 6-58. As seen in that figure, some variability exists among the means of brine flow up the borehole obtained in the PCS-2012 PA. This variability is not substantially different than that seen in the PABC-2009, as is evident by comparing Figure 6-58 and Figure 6-59. The increase in the mean waste panel pressure seen in the PCS-2012 PA yields a slight long-term increase in the means of quantity BNBHUDRZ. The overall mean of this quantity is greater in the PCS-2012 PA, as shown in Figure 6-60.

Summary statistics for scenario S4-BF are shown in Table 6.

Table 6: Summary Statistics for Scenario S4-BF

Quantity (units)	Mean Value		Maximum Value	
	PABC-2009	PCS-2012 PA	PABC-2009	PCS-2012 PA
BRNWASIC ($x10^3$ m^3)	2.73	3.29	23.81	19.39
WAS_SATB (none)	0.28	0.33	0.99	0.99
GASMOL_W ($x10^6$ moles)	36.40	38.35	149.00	149.00
WAS_PRES (MPa)	4.64	4.70	14.92	15.21
BNBHUDRZ (m^3)	34.76	43.76	4876.89	5287.28

Information Only

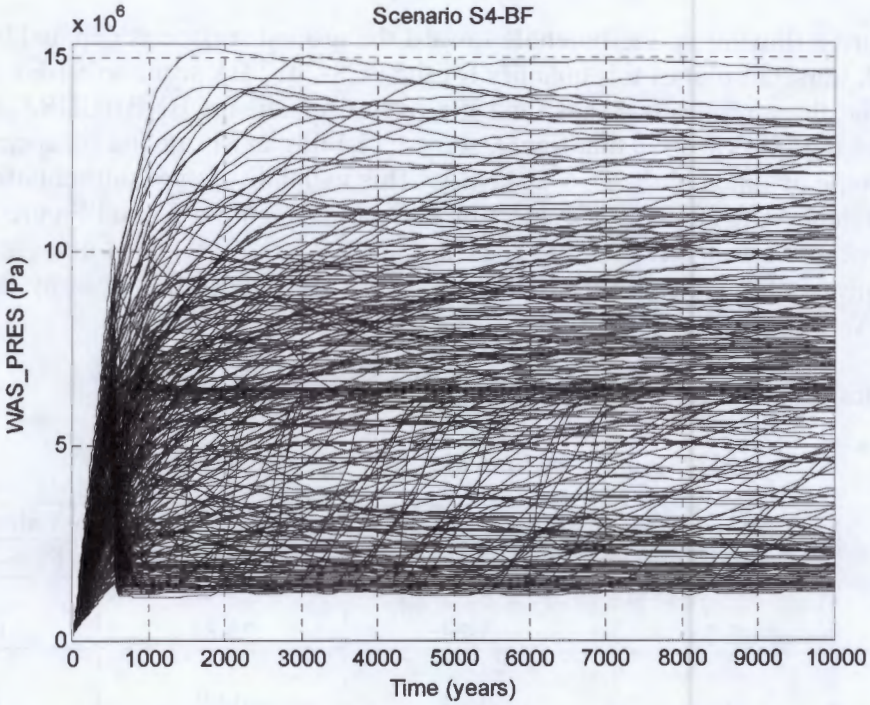

Figure 6-41: Horsetail Plot of Waste Panel Pressure, Scenario S4-BF.

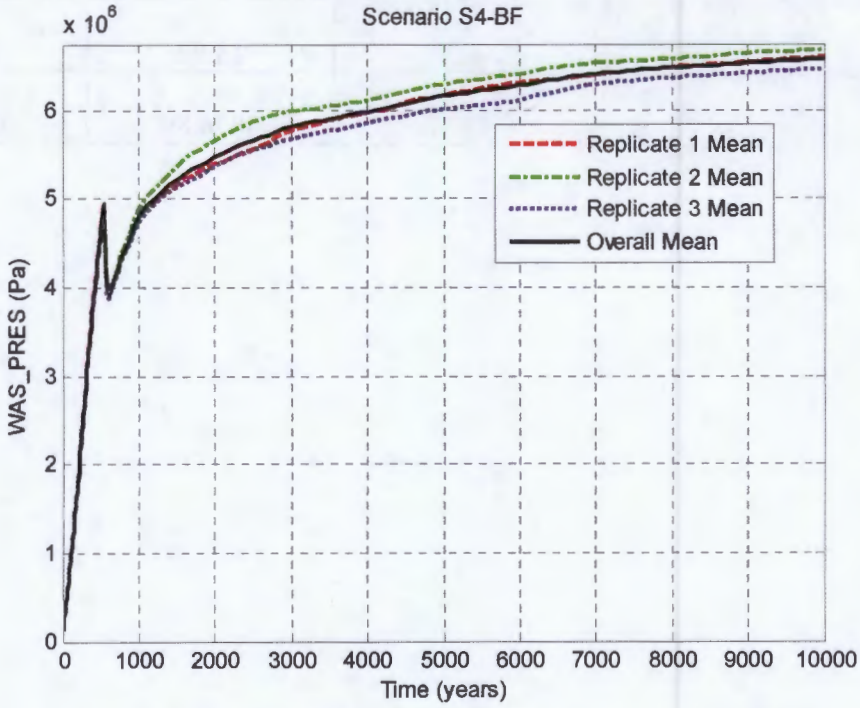

Figure 6-42: Means of Waste Panel Pressure, Scenario S4-BF.

Information Only

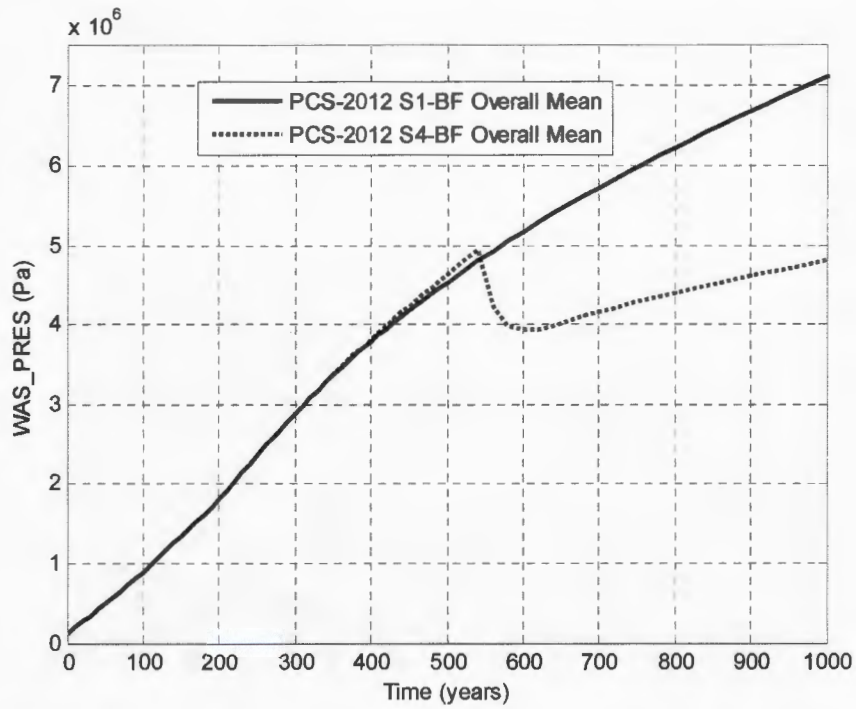

Figure 6-43: Overall Means of Waste Panel Pressure, Scenarios S1-BF and S4-BF for Years 0 to 1,000.

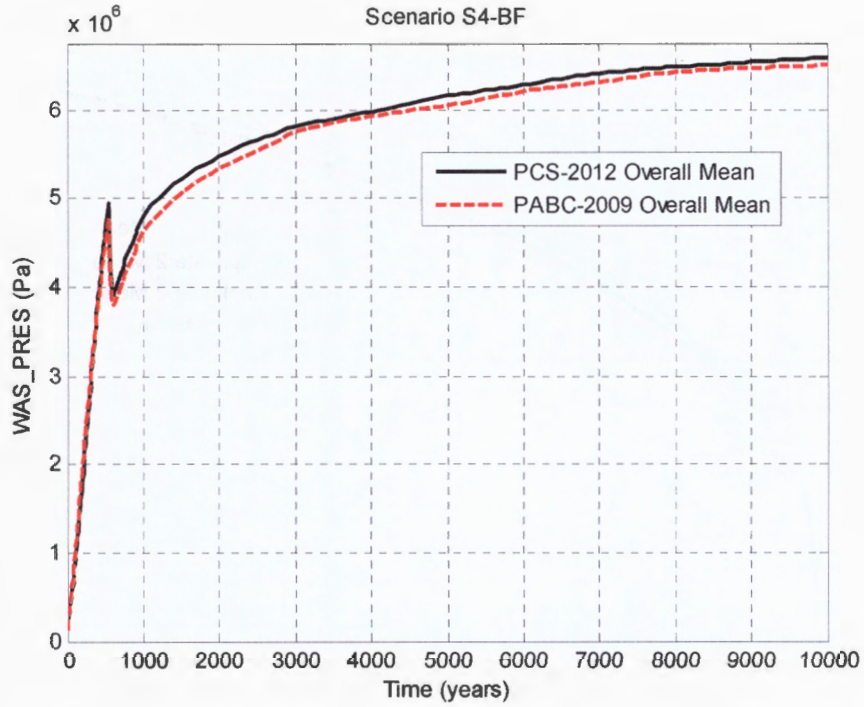

Figure 6-44: Overall Means of Waste Panel Pressure, Scenario S4-BF.

Information Only

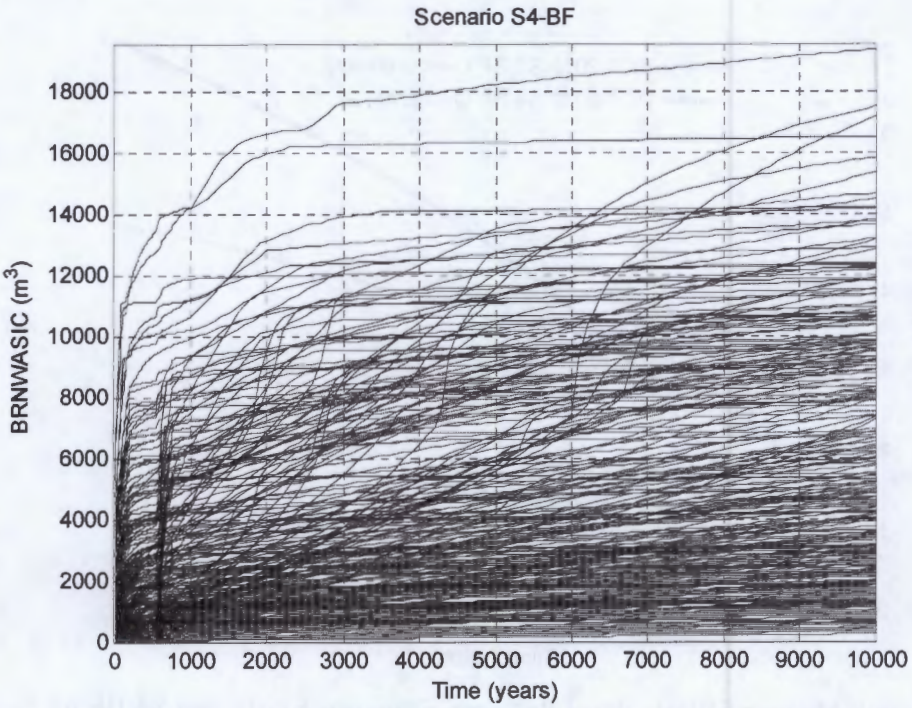

Figure 6-45: Horsetail Plot of Cumulative Brine Inflow to the Waste Panel, Scenario S4-BF.

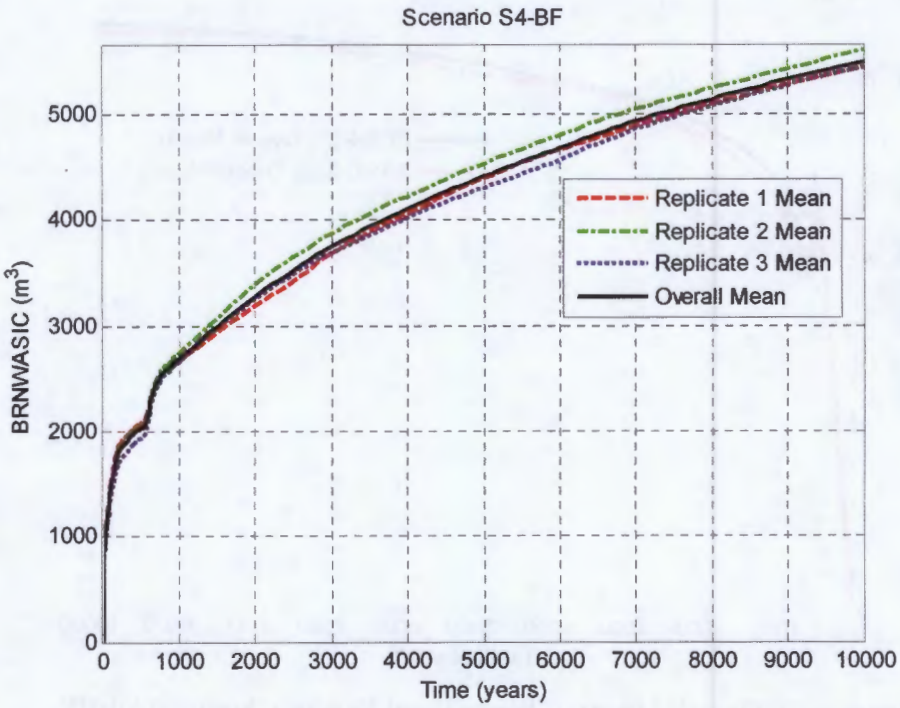

Figure 6-46: Means of Cumulative Brine Inflow to the Waste Panel, Scenario S4-BF.

Information Only

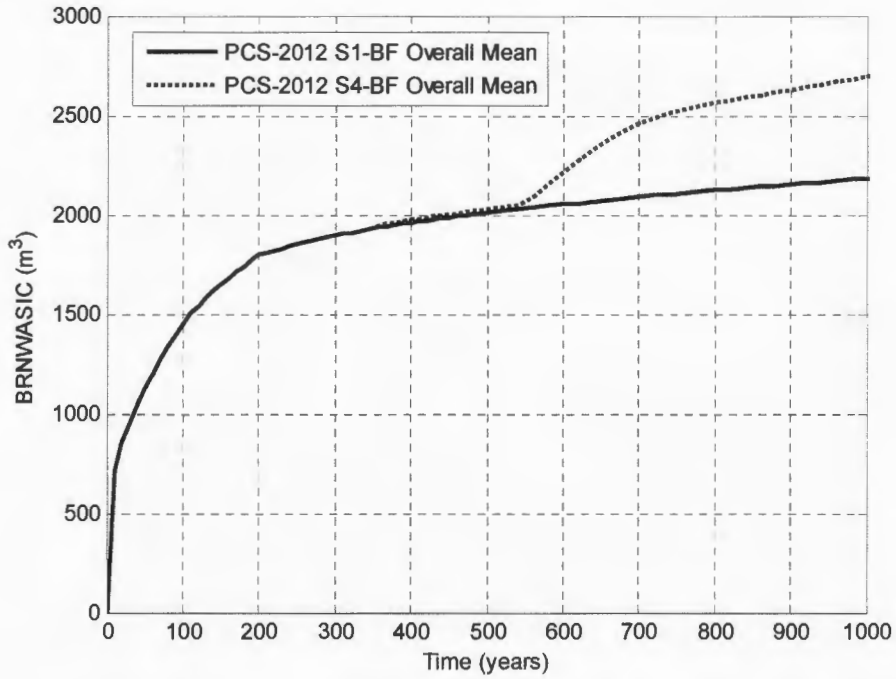

Figure 6-47: Overall Means of Cumulative Brine Inflow to the Waste Panel, Scenarios S1-BF and S4-BF for Years 0 to 1,000.

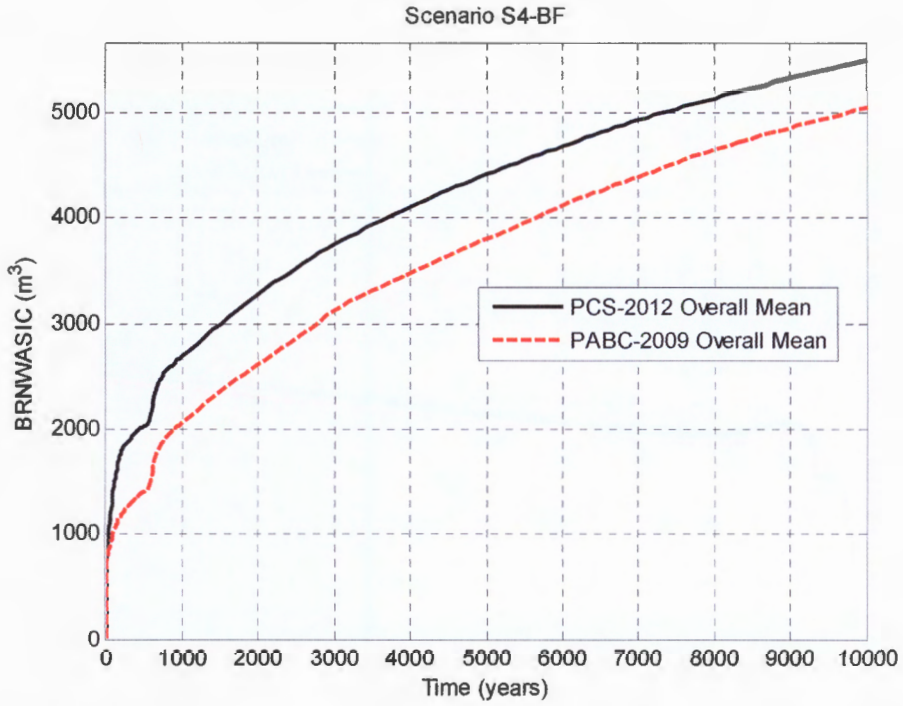

Figure 6-48: Overall Means of Cumulative Brine Inflow to the Waste Panel, Scenario S4-BF.

Information Only

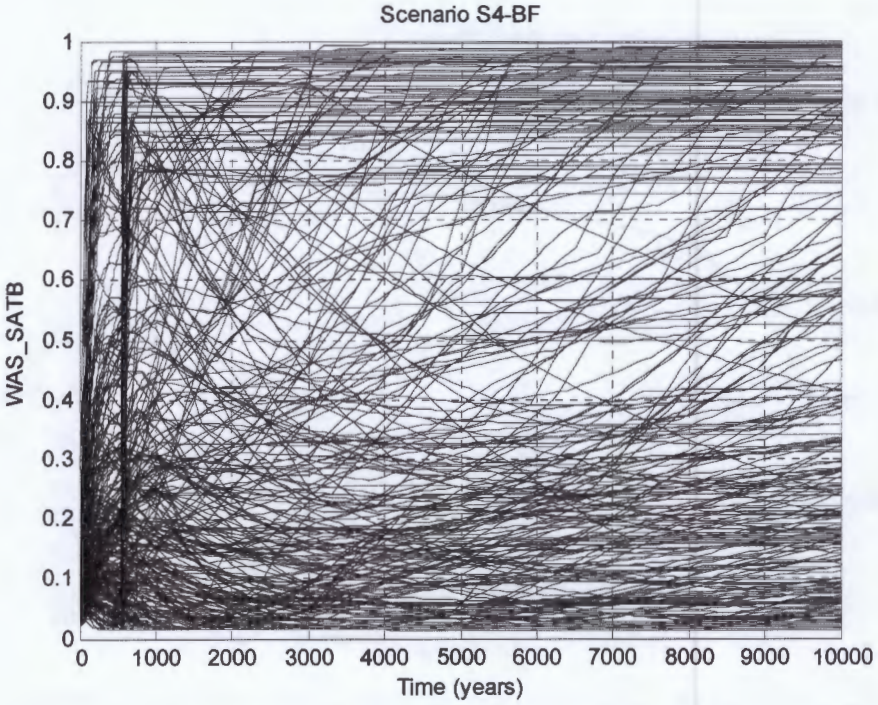

Figure 6-49: Horsetail Plot of Waste Panel Brine Saturation, Scenario S4-BF.

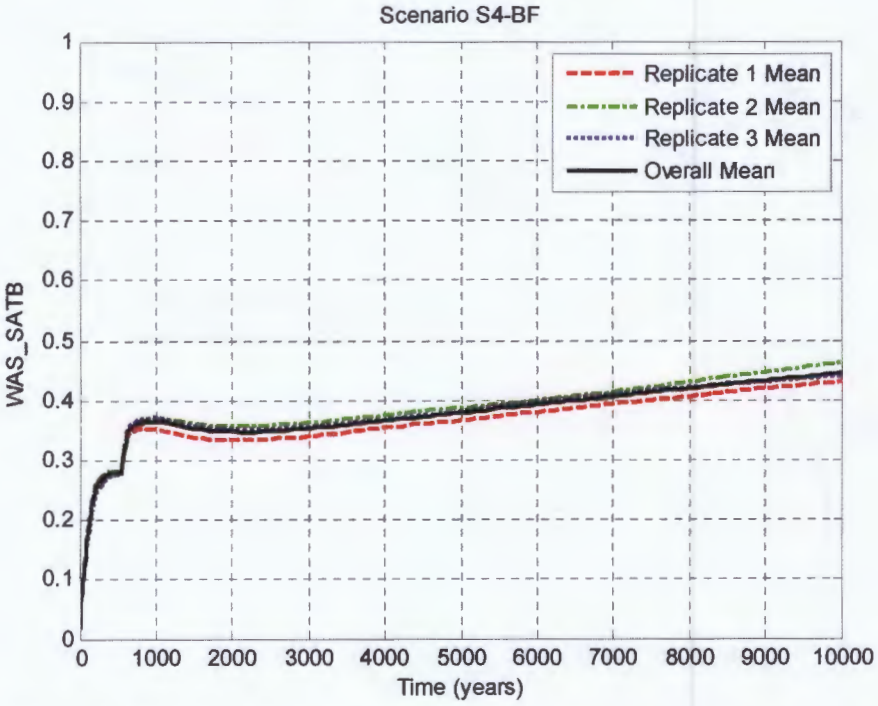

Figure 6-50: Means of Waste Panel Brine Saturation, Scenario S4-BF.

Information Only

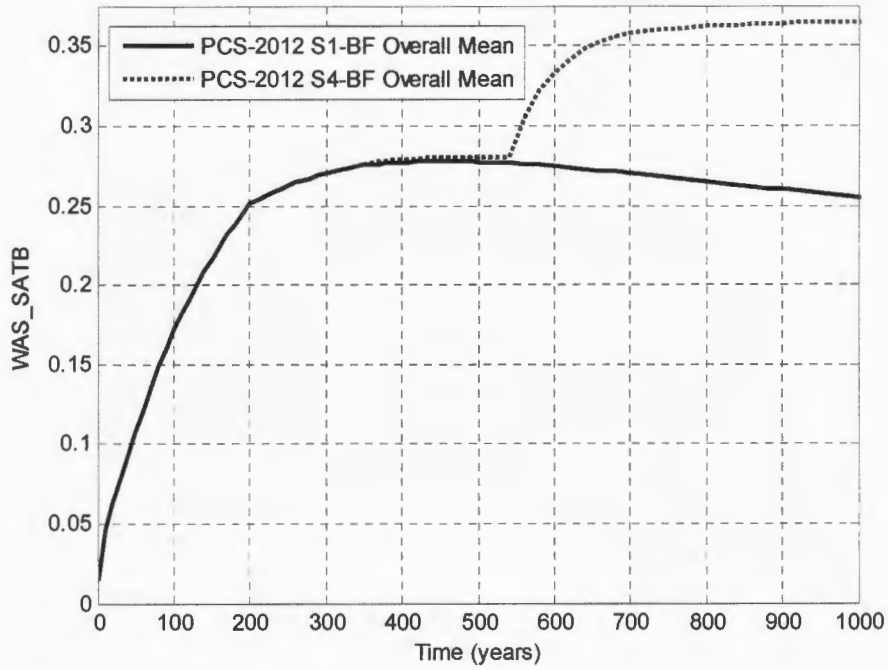

Figure 6-51: Overall Means of Waste Panel Brine Saturation, Scenarios S1-BF and S4-BF for Years 0 to 1,000.

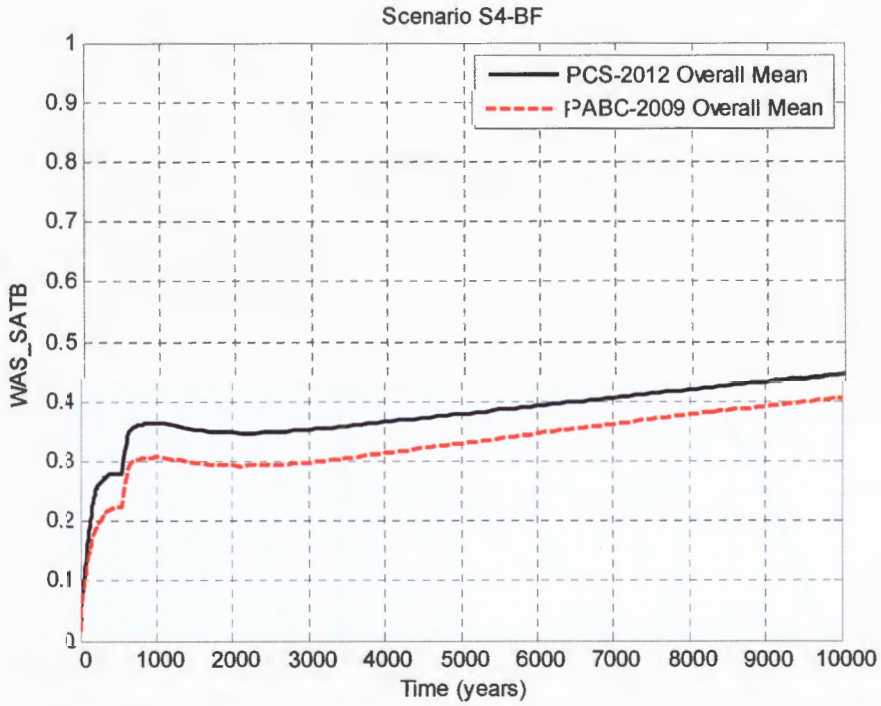

Figure 6-52: Overall Means of Waste Panel Brine Saturation, Scenario S4-BF.

Information Only

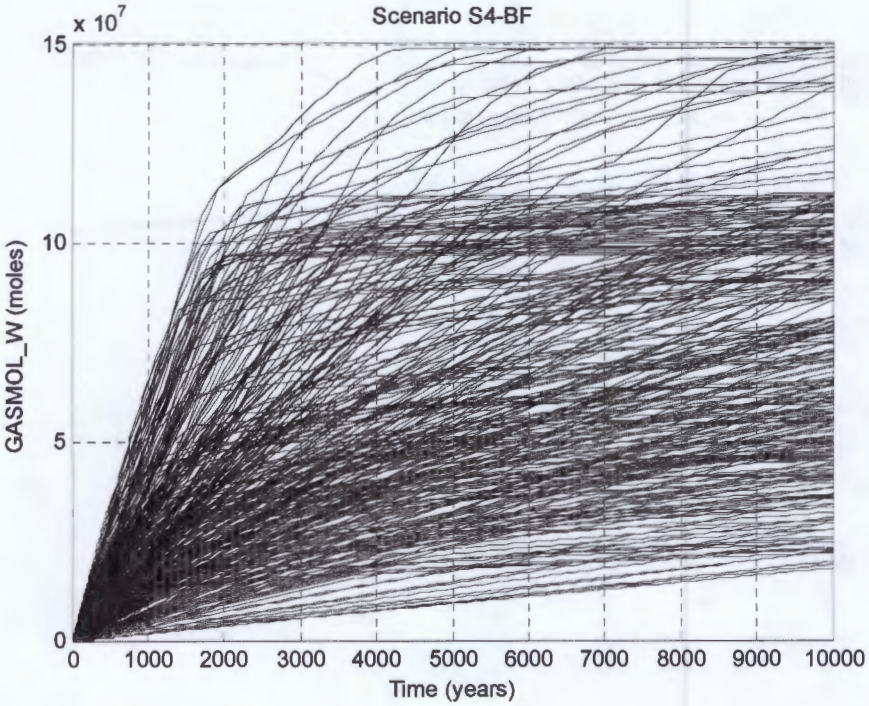

Figure 6-53: Horsetail Plot of Waste Panel Gas Generation (in moles), Scenario S4-BF.

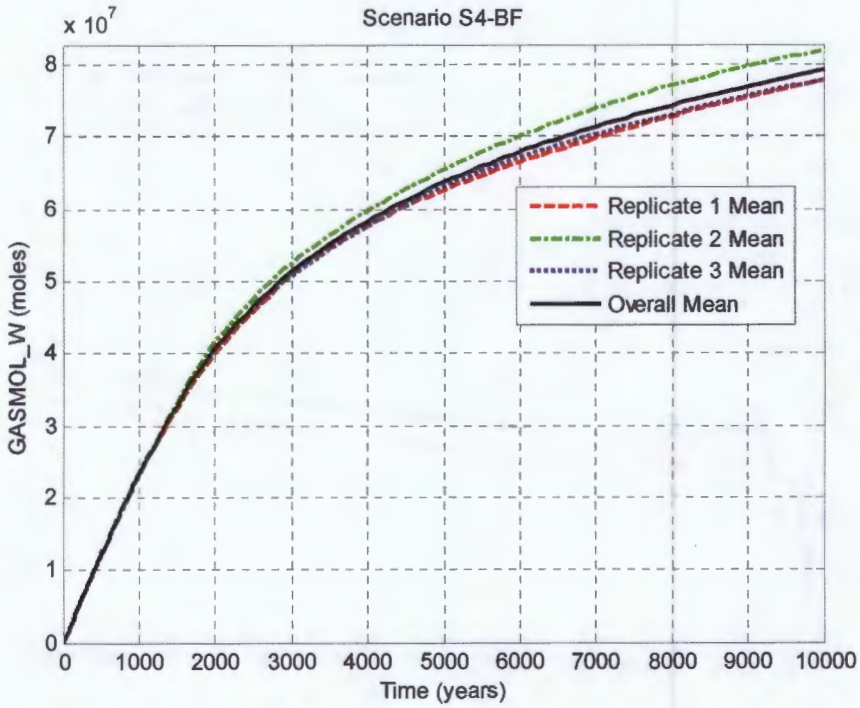

Figure 6-54: Means of Waste Panel Gas Generation (in moles), Scenario S4-BF.

Information Only

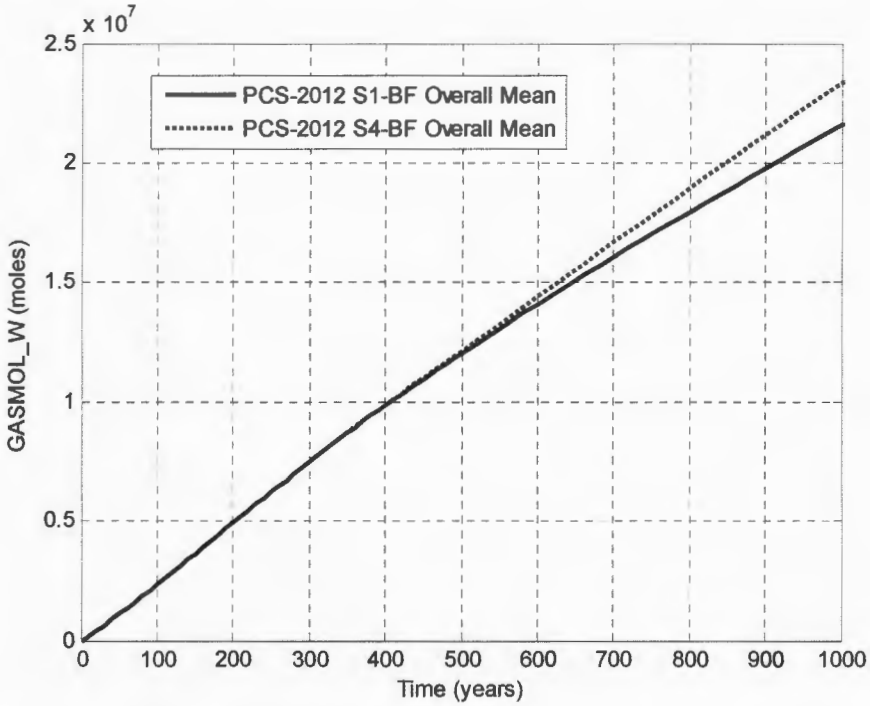

Figure 6-55: Overall Means of Waste Panel Gas Generation (in moles), Scenarios S1-BF and S4-BF for Years 0 to 1,000.

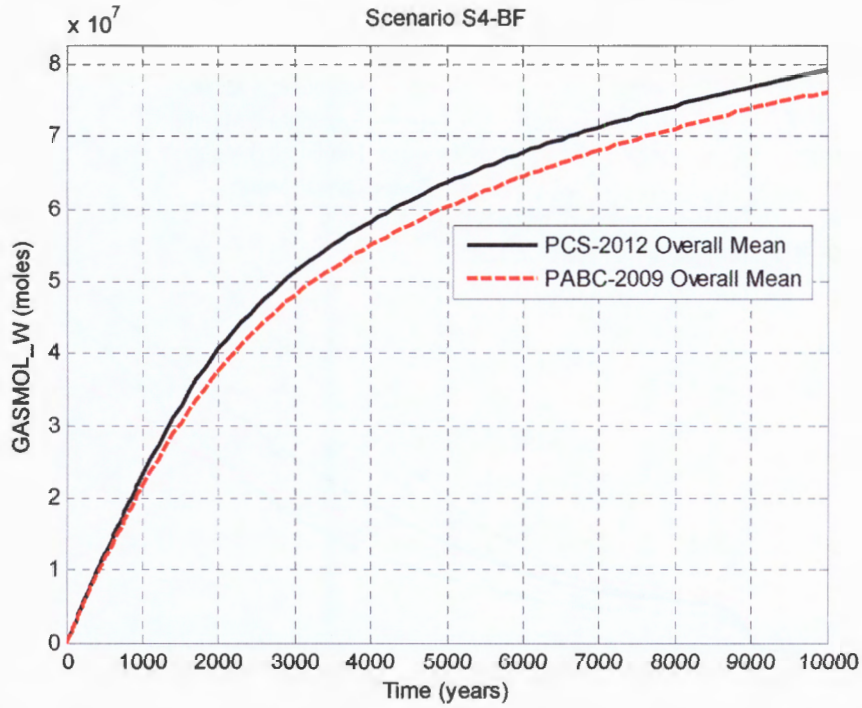

Figure 6-56: Overall Means of Waste Panel Gas Generation (in moles), Scenario S4-BF.

Information Only

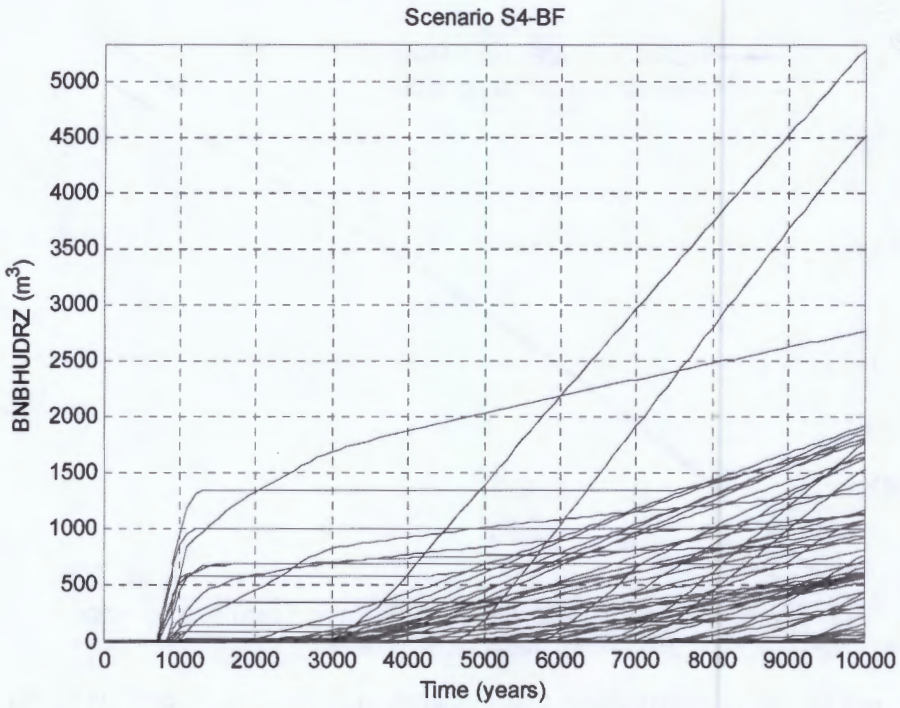

Figure 6-57: Horsetail Plot of Brine Flow up the Borehole, Scenario S4-BF.

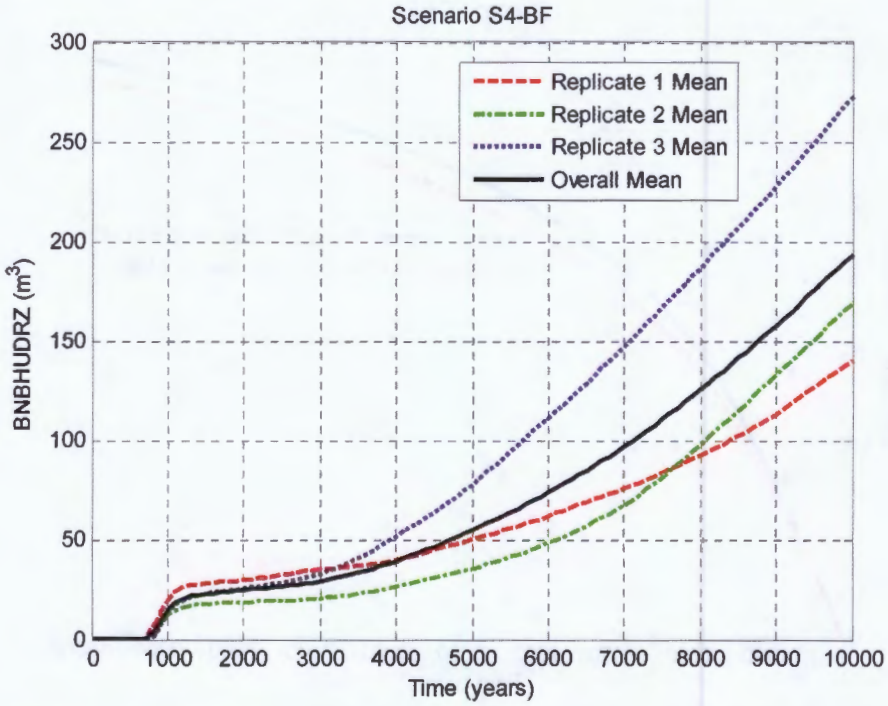

Figure 6-58: Means of Brine Flow up the Borehole, Scenario S4-BF.

Information Only

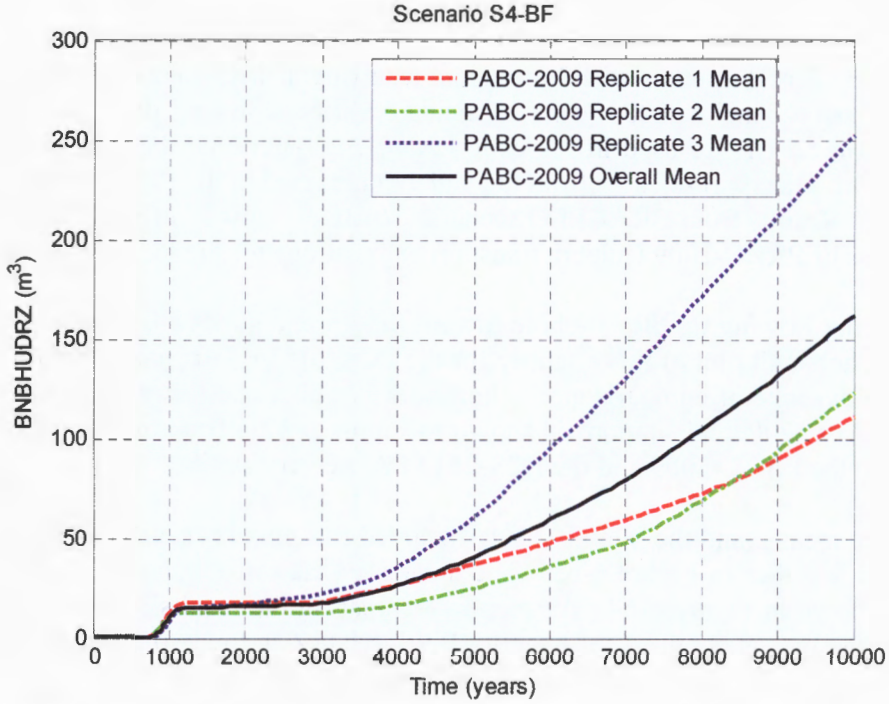

Figure 6-59: Means of Brine Flow up the Borehole, Scenario S4-BF for the PABC-2009.

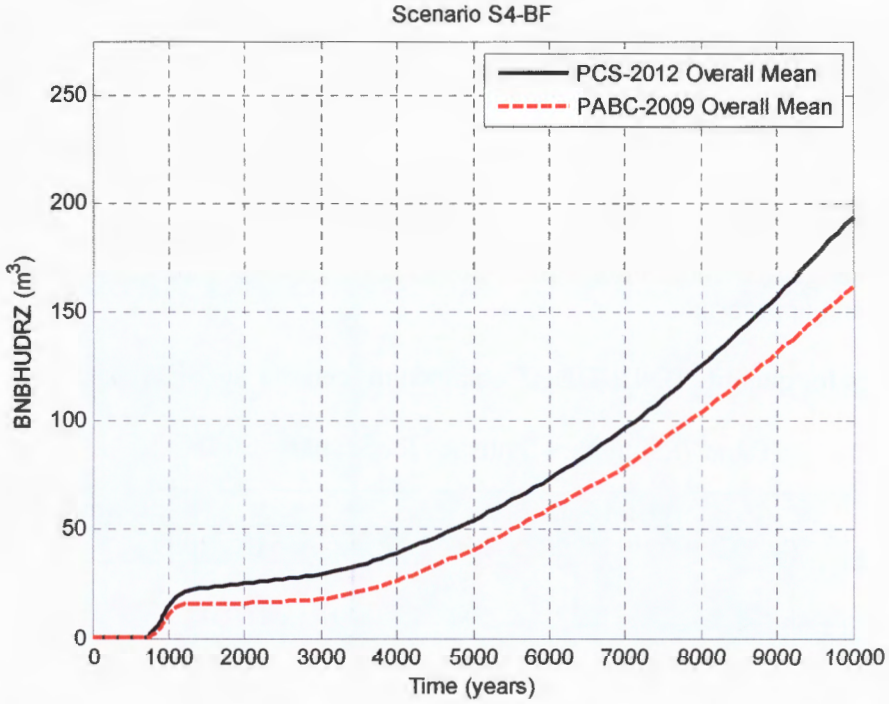

Figure 6-60: Overall Means of Brine Flow up the Borehole, Scenario S4-BF.

Information Only

6.1.4 Results for an E2 Intrusion at 1000 Years Followed by a E1 Intrusion at 2000 Years (Scenario S6-BF)

BRAGFLO scenario S6-BF models an E2 intrusion occurring at 1000 years, followed by an E1 intrusion into the same panel at 2000 years. Calculated brine flows up the intrusion borehole obtained in scenario S6-BF are used in PA code PANEL to determine the radionuclide source term to the Culebra. Transport releases from the Culebra obtained in the PABC-2009 are used in the PCS-2012 PA. Results from BRAGFLO scenario S6-BF are now briefly discussed to justify the appropriateness of PABC-2009 Culebra transport calculations for the PCS-2012 PA.

The volume of brine flowing up the borehole toward the ground surface is denoted by quantity BNBHUDRZ. A horsetail plot of this quantity for the PCS-2012 PA scenario S6-BF is given in Figure 6-61. For the sake of comparison, the horsetail plot obtained for quantity BNBHUDRZ obtained in the PABC-2009 calculations is shown in Figure 6-62. The horsetail plots obtained for this quantity in the PABC-2009 and the PCS-2012 PA are very similar.

The three replicate means, and the overall mean, obtained for quantity BNBHUDRZ in scenario S6-BF are plotted together in Figure 6-63. The analogous curves obtained in the PABC-2009 calculations are shown in Figure 6-64. As seen by comparing the results shown in Figure 6-63 and Figure 6-64, the means obtained for quantity BNBHUDRZ in the two analyses are virtually identical.

The overall means obtained for quantity BNBHUDRZ in the PCS-2012 PA and the PABC-2009 are shown together in Figure 6-65. As seen in that figure, there is very close agreement between the overall means obtained in the two analyses. The replacement of the Option D panel closure with the ROMPCS design has a negligible impact on brine flow up the intrusion borehole in BRAGFLO scenario S6-BF. Actinide solubilities, the repository waste inventory, and Culebra transmissivity fields are unchanged from the PABC-2009 to the PCS-2012 PA. As the brine flows up the intrusion borehole obtained in the two analyses are virtually identical in scenario S6-BF, the radionuclide source term to the Culebra is virtually unchanged by the ROMPCS design as compared to Option D results. Consequently, transport releases from the Culebra are also virtually unchanged. Incorporating PABC-2009 Culebra transport results into the PCS-2012 PA is reasonable and appropriate.

Summary statistics for quantity BNBHUDRZ obtained in scenario S6-BF are shown in Table 7.

Table 7: Summary Statistics for Scenario S6-BF

Quantity (units)	Mean Value		Maximum Value	
	PABC-2009	PCS-2012 PA	PABC-2009	PCS-2012 PA
BNBHUDRZ ($x10^3$ m^3)	2.92	2.94	169.03	169.30

Information Only

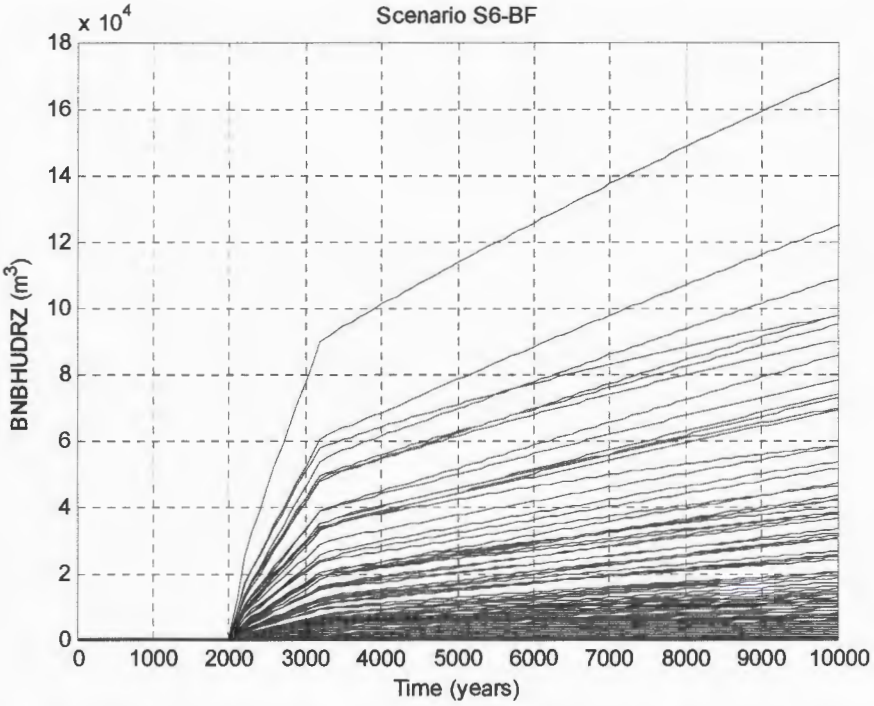

Figure 6-61: PCS-2012 PA Horsetail Plot of Brine Flow up the Borehole, Scenario S6-BF.

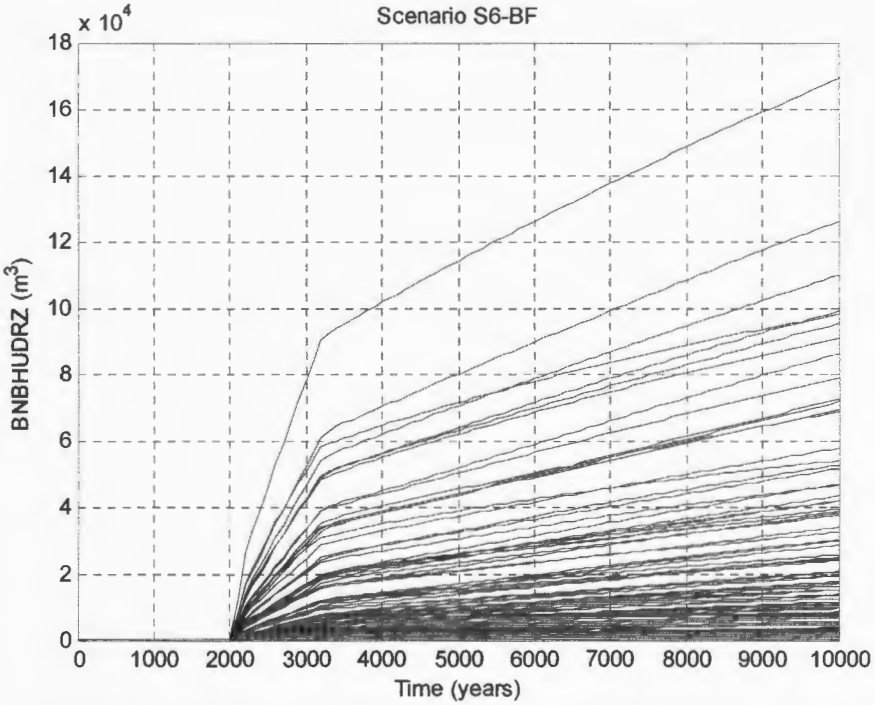

Figure 6-62: PABC-2009 Horsetail Plot of Brine Flow up the Borehole, Scenario S6-BF.

Information Only

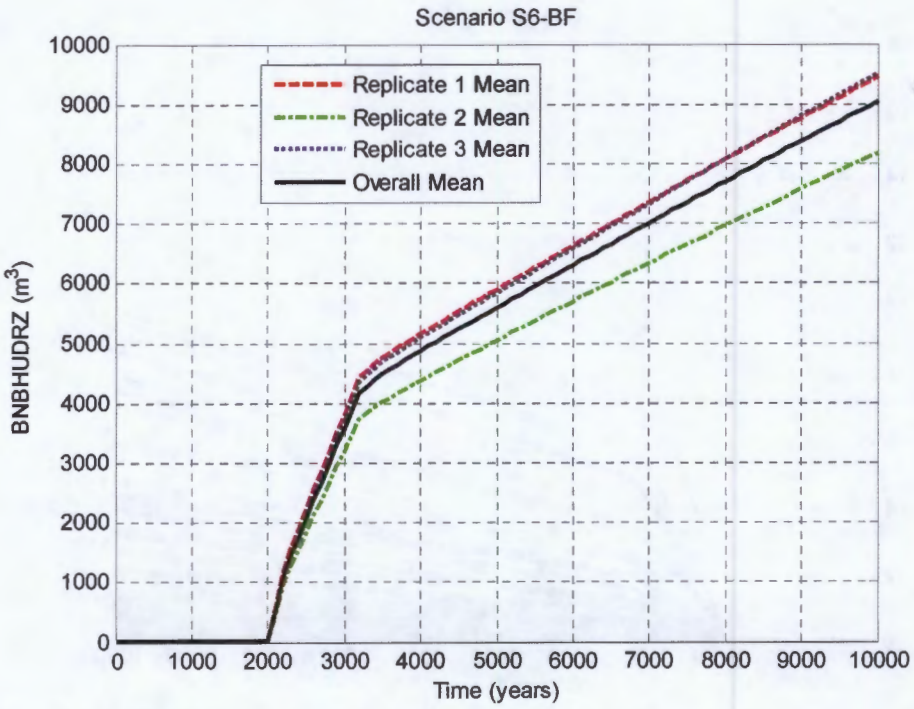

Figure 6-63: PCS-2012 PA Means of Brine Flow up the Borehole, Scenario S6-BF.

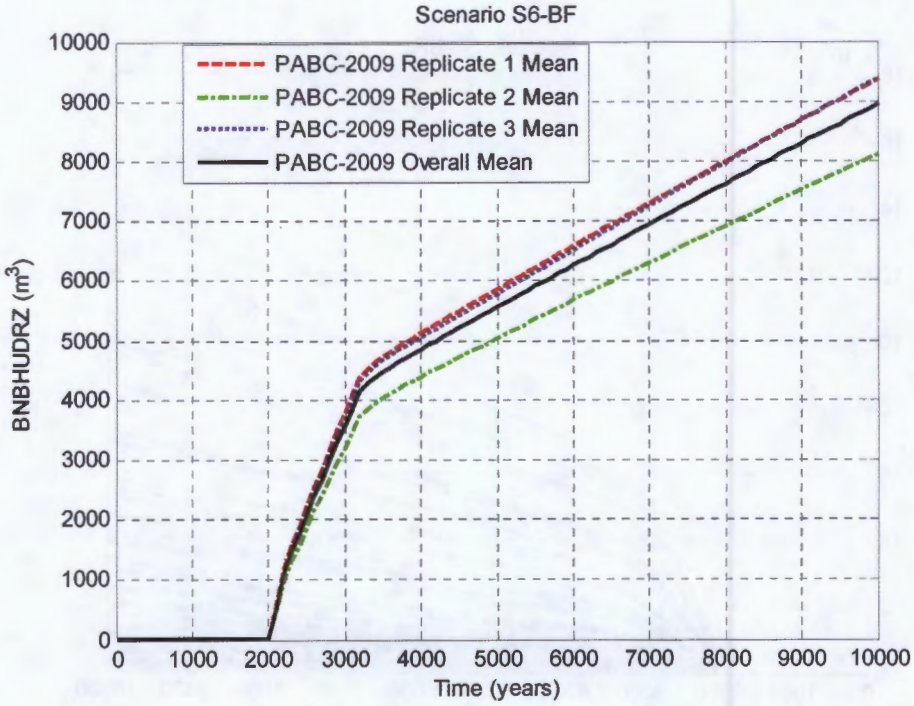

Figure 6-64: PABC-2009 Means of Brine Flow up the Borehole, Scenario S6-BF.

Information Only

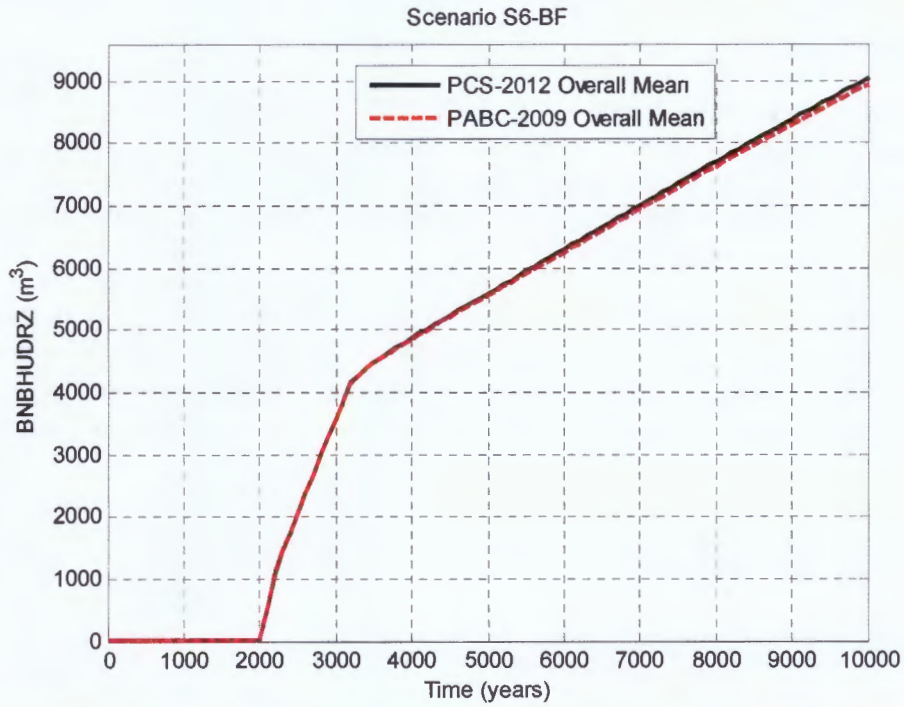

Figure 6-65: Overall Means of Brine Flow up the Borehole, Scenario S6-BF.

7 SUMMARY

Waste panel closures comprise a repository feature that has been represented in WIPP PA since the original Compliance Certification Application (CCA) of 1996. The 1998 rulemaking that certified WIPP to receive transuranic waste placed conditions on the panel closure design to be implemented in the repository. The mandated design consists of a concrete block wall, an open drift section, and a concrete monolith, and was termed the "Option D" panel closure. Following the selection of the Option D design in 1998, the engineering of the panel closure has been re-assessed, and a revised design has been established that is simpler, cheaper, and easier to construct. The revised panel closure design, termed the Run-of-Mine Panel Closure System (ROMPCS), is comprised of 100 feet of ROM salt with barriers at each end. The PCS-2012 PA quantifies WIPP repository performance impacts associated with the replacement of the currently approved Option D panel closure design with the ROMPCS. Impacts are assessed via a direct comparison of results obtained in the PABC-2009 (where Option D was used) to those calculated in the PCS-2012 PA with the ROMPCS.

For undisturbed conditions, implementation of the ROMPCS yields higher long-term waste panel pressure (on average) than was seen in the PABC-2009. The increase in mean waste panel pressure is accompanied by an increase in the average waste panel brine saturation for the ROMPCS results. The ROMPCS design allows more brine inflow to the waste panel during the first 200 years when compared to Option D results. This increased brine inflow, combined with

Information Only

the tightness of the ROMPCS after 200 years, results in increased waste panel gas generation (on average) and a subsequent increase to waste panel mean pressure.

The lower long-term permeability range of the ROMPCS as compared to Option D yields a period of increased waste panel pressurization following an E1 intrusion. The increased waste panel mean pressure slightly inhibits brine flow into the panel after the intrusion, with a corresponding slight decrease to the mean waste panel brine saturation as compared to PABC-2009 E1 intrusion results.

For E2 intrusion scenarios, the PCS-2012 PA mean waste panel pressure is higher than that seen in the PABC-2009 at the time of intrusion, and it remains higher for the duration of the 10,000 year regulatory period. Similarly, the mean waste panel brine saturation is higher at the time of intrusion in the PCS-2012 PA, resulting in higher long-term waste panel brine saturations for E2 intrusion scenarios.

Brine flows up the borehole that are used to calculate the radionuclide source term in WIPP PA are negligibly impacted by the replacement of Option D with the ROMPCS.

8 REFERENCES

Camphouse, R.C. 2012a. Analysis Plan for the 2012 WIPP Panel Closure System Performance Assessment. Sandia National Laboratories, Carlsbad, NM. ERMS 557726.

Camphouse, R.C. 2012b. A summary of parameters to be implemented in the PCS-2012 PA. Memo to Janis Trone dated July 10, 2012. Sandia National Laboratories, Carlsbad, NM. ERMS 557721.

Camphouse, R.C. 2012c. An overview of the BRAGFLO two-phase flow parameters used to model the run-of-mine salt panel closures implemented in the PCS-2012 PA. Memo to Paul Shoemaker dated June 7, 2012. Sandia National Laboratories, Carlsbad, NM. ERMS 557653.

Camphouse, R.C., Gross, M., Herrick, C.G., Kicker, D.C., and Thompson, B. 2012a. Recommendations and Justifications of Parameter Values for the Run-of-Mine Salt Panel Closure System Design Modeled in the PCS-2012 PA. Memo to WIPP Records Center dated May 3, 2012. Sandia National Laboratories, Carlsbad, NM. ERMS 557396.

Camphouse, R.C., Kicker, D.C., Kirchner, T.B., Long, J.J., Malama, B., and Zeitler, T.R. 2012b. Summary Report and Run Control for the 2012 WIPP Panel Closure System Performance Assessment. Sandia National Laboratories, Carlsbad, NM.

Clayton, D.J., Camphouse, R. C., Garner, J. W., Ismail, A. E., Kirchner, T. B., Kuhlman, K. L., and Nemer, M. B.. 2010. Summary Report of the CRA-2009 Performance Assessment Baseline Calculation, Revision 1. Sandia National Laboratories. Carlsbad, New Mexico, ERMS 553039.

Information Only

DOE (U.S. Department of Energy). 1996. Title 40 CFR Part 191 Compliance Certification Application for the Waste Isolation Pilot Plant. DOE/CAO-1996-2184. U.S. Department of Energy, Waste Isolation Pilot Plant, Carlsbad Area Office. Carlsbad, NM.

DOE (U.S. Department of Energy). 2007. "Transuranic Waste Acceptance Criteria for The Waste Isolation Pilot Plant, Revision 6.1." Carlsbad, NM: DOE/WIPP-02-3122.

DOE (U.S. Department of Energy), 2011. Panel Closure System Design, Planned Change Request to the EPA 40 CFR Part 194 Certification of the Waste Isolation Pilot Plant. U.S. Department of Energy, Carlsbad Field Office. Carlsbad, New Mexico.

EPA (U.S. Environmental Protection Agency). 1998. Criteria for the Certification and Re-Certification of the Waste Isolation Pilot Plants Compliance with the 40 CFR Part 191 Disposal Regulations: Certification Decision; Final Rule, *Federal Register*, Vol. 63, No. 95, pp. 27353-27406. U.S. Environmental Protection Agency, Office of Air and Radiation, Washington, D.C.

Nemer, M.B. 2010. Analysis Package for Salado Flow Modeling: CRA-2009 Performance Assessment Baseline Calculation. Sandia National Laboratories. Carlsbad, NM. ERMS 552956.

Nemer, M. B., J. S. Stein and W. Zelinski. 2005. Analysis Report for BRAGFLO Preliminary Modeling Results With New Gas Generation Rates Based Upon Recent Experimental Results. Sandia National Laboratories, Carlsbad, NM. ERMS 539437.

Patterson, Russell. 2012. Response to U.S. EPA Comment Dated June 7, 2012. U.S. Department of Energy, Waste Isolation Pilot Plant, Carlsbad Area Office. Carlsbad, NM.

RockSol Consulting Group, Inc. 2006. Further Assessment of the Short-term Stability of the 12 Foot Explosion Isolation Wall. Report prepared for Washington TRU Solutions, LLC.

Stein, J.S. and Zelinski, W. 2003. Analysis Package for BRAGFLO: Compliance Recertification Application. Sandia National Laboratories, Carlsbad, NM. ERMS 530163.

Vaughn, P. 1996. WIPP Parameter Entry Form for SANTAROS: SAT_IBRN. Sandia National Laboratories. Carlsbad, NM. WPO 33552.

Vugrin, E.D. 2005. User's Manual for LHS Version 2.42 Document Version 2.42. Sandia National Laboratories. Carlsbad, NM. ERMS 538374.

Vugrin, E.D. and S.C. Dunagan. 2006. Analysis Package for the Impact Assessment of the Redesigned Panel Closure System, Rev. 0. Sandia National Laboratories. Carlsbad, NM. ERMS 543865.

Vugrin, E.D., F. Hansen, and B. Thompson. 2006. Recommendation and Justification of Parameter Values Required for Representation of the Redesigned Panel Closure System. Memo to David Kessel dated March 23, 2006. Sandia National Laboratories, Carlsbad, NM. ERMS 542894.

Information Only

558226

Sandia National Laboratories
Waste Isolation Pilot Plant

Analysis Package for Direct Brine Releases: 2012 Panel Closure System Performance Assessment (PCS-2012 PA)

Author:	Bwalya Malama		09/28/12
	Print	Signature	Date
Technical Review:	Chris Camphouse		9/28/12
	Print	Signature	Date
QA Review:	Shelly R. Nielsen	Shelly R. Nielsen	10-1-12
	Print	Signature	Date
Management Review:	Sean Dunagan		9/28/12
	Print	Signature	Date

WIPP:1.4.1:PA:QA-L:557393

Information Only

Table of Contents

1 Introduction 5
2 Background 6
3 Approach 8
3.1 Model Geometry 8
3.2 Initial Conditions 10
4 Calculation Methodology 11
4.1 Modeled Scenarios 11
4.1.1 Scenario 1 (S1-DBR) 11
4.1.2 Scenario 2 (S2-DBR) 12
4.1.3 Scenario 3 (S3-DBR) 12
4.1.4 Scenario 4 (S4-DBR) 13
4.1.5 Scenario 5 (S5-DBR) 13
4.2 Run Control 13
5 Results 14
5.1 Summary 14
5.2 Direct Brine Releases from the Lower Drilling Location 15
5.3 Sensitivity of Direct Brine Releases to Input Parameters 27
6 Conclusions 31
7 References 31

Information Only

List of Tables

Table 4-1: Scenarios used in BRAGFLO Salado flow modeling. 11
Table 4-2: Intrusion times modeled by DBR for each scenario. 12
Table 5-1: Summary statistics for the PCS-2012 PA and PABC-2009 DBR calculations over all replicates and vectors. 15
Table 5-2: Summary table of number of vectors with non-zero, maximum and average DBR volumes over all three replicates for the S1-DBR calculations 17
Table 5-3: Summary table of number of vectors with non-zero, maximum and average DBR volumes over all three replicates for the S2-DBR calculations. 18
Table 5-4: Summary table of number of vectors with non-zero, maximum and average DBR volumes over all three replicates for the S3-DBR calculations. 19
Table 5-5: Summary table of number of vectors with non-zero, maximum and average DBR volumes over all three replicates for the S4-DBR calculations. 20
Table 5-6: Summary table of number of vectors with non-zero, maximum and average DBR volumes over all three replicates for the S5-DBR calculations. 21

List of Figures

Figure 3-1: PCS-2012 PA DBR material map (logical grid) with ROM salt PCS. 8
Figure 3-2: PABC-2009 DBR material map (logical grid) with Option D panel closure (after Clayton et al., 2010). 9
Figure 3-3. Regions to be used to transfer initial pressure and saturation between the 10,000 year BRAGFLO grid and the DBR grid for the PABC-2009. 10
Figure 5-1: PCS-2012 PA lower intrusion DBR volume percentile rankings for all replicates and vectors of the scenario S1-DBR. 22
Figure 5-2: PABC-2009 lower intrusion DBR volume percentile rankings for all replicates and vectors of scenario S1-DBR. 22
Figure 5-3: PCS-2012 PA lower intrusion DBR volume percentile rankings for all replicates and vectors of scenario S2-DBR. 23
Figure 5-4: PABC-2009 lower intrusion DBR volume percentile rankings for all replicates and vectors of scenario S2-DBR. 23
Figure 5-5: PCS-2012 PA lower intrusion DBR volume percentile rankings for all replicates and vectors of scenario S3-DBR. 24
Figure 5-6: PABC-2009 lower intrusion DBR volume percentile rankings for all replicates and vectors of scenario S3-DBR. 24
Figure 5-7: PCS-2012 PA lower intrusion DBR volume percentile rankings for all replicates and vectors of scenario S4-DBR. 25
Figure 5-8: PABC-2009 lower intrusion DBR volume percentile rankings for all replicates and vectors of scenario S4-DBR. 25
Figure 5-9: PCS-2012 PA lower intrusion DBR volume percentile rankings for all replicates and vectors of scenario S5-DBR. 26
Figure 5-10: PABC-2009 lower intrusion DBR volume percentile rankings for all replicates and vectors of scenario S5-DBR. 26

Information Only

Figure 5-11: Scatter plot of DBR volume versus pressure in the intruded panel for replicate 1, S2-DBR scenario, lower drilling intrusion, PCS-2012 PA. Symbols indicate intrusion times in years. 28
Figure 5-12: Scatter plot of DBR volume versus pressure in the intruded panel for replicate 1, S2-DBR scenario, lower drilling intrusion, PABC-2009. Symbols indicate intrusion times in years. 28
Figure 5-13: Scatter plot of DBR volume versus pressure in the intruded panel for replicate 1, S2-DBR scenario, lower drilling intrusion, PCS-2012 PA. Symbols indicate the range of mobile brine saturation (dimensionless). 29
Figure 5-14: Scatter plot of DBR volume versus pressure in the intruded panel for replicate 1, S2-DBR scenario, lower drilling intrusion, PABC-2009. Symbols indicate the range of mobile brine saturation (dimensionless). 29
Figure 5-15: Scatter plot of mobile brine saturation versus pressure for replicate 1, S2-DBR scenario, lower drilling intrusion, all intrusion times, PCS-2012 PA. Symbols indicate the range of DBR volumes in m^3. 30
Figure 5-16: Scatter plot of mobile brine saturation versus pressure for replicate 1, S2-DBR scenario, lower drilling intrusion, all intrusion times, PABC-2009. Symbols indicate the range of DBR volumes in m^3. 30

Information Only

1 INTRODUCTION

The Waste Isolation Pilot Plant (WIPP), located in southeastern New Mexico, has been developed by the U.S. Department of Energy (DOE) for geologic (deep underground) disposal of transuranic (TRU) waste. Containment of TRU waste at the WIPP is regulated by the U.S. Environmental Protection Agency (EPA) according to the regulations set forth in Title 40 of the Code of Federal Regulations (CFR), Part 191. The DOE demonstrates compliance with the containment requirements according to the Certification Criteria in Title 40 CFR Part 194 by means of performance assessment (PA) calculations performed by Sandia National Laboratories (SNL). WIPP PA calculations estimate the probability and consequence of potential radionuclide releases from the repository to the accessible environment for a regulatory period of 10,000 years after facility closure. The models used in PA are maintained and updated with new information as part of an ongoing process. Improved information regarding important WIPP features, events, and processes typically results in refinements and modifications to PA models and the parameters used in them. Planned changes to the repository and/or the components therein also result in updates to WIPP PA models. WIPP PA models are used to support the repository recertification process that occurs at five-year intervals following the receipt of the first waste shipment at the site in 1999.

Waste panel closures comprise a repository feature that has been represented in WIPP PA since the original Compliance Certification Application (CCA) of 1996. Panel closures are included in WIPP PA models principally because they are a part of the disposal system, not because they play a substantive role in inhibiting the release of radionuclides to the outside environment. The DOE stated in the CCA (DOE 1996) that *"The panel closure system was not designed or intended to support long-term repository performance."* The 1998 rulemaking that certified WIPP to receive transuranic waste placed conditions on the panel closure design to be implemented in the repository. The mandated design consists of a concrete block wall, an open drift section, and a concrete monolith, and was termed the "Option D" panel closure. Following the selection of the Option D design in 1998, the engineering of the panel closure has been re-assessed, and a revised design has been established that is simpler, cheaper, and easier to construct. The revised panel closure design, termed the Run-of-Mine Panel Closure System (ROMPCS), is comprised of 100 feet of ROM salt with barriers at each end. The ROM salt is generated from ongoing mining operations at the WIPP and may be compacted and/or moistened as it is emplaced in a panel entry. The barriers consist of ventilation bulkheads, similar to those currently used in the panels as room closures.

The DOE has submitted a planned change request (PCR) to the EPA requesting that the EPA modify Condition 1 of the Final Certification Rulemaking for 40 CFR Part 194 (EPA, 1998) for the WIPP. The PCR submitted to EPA requests that Condition 1 be changed, and that the ROMPCS design be approved for use in all panels (DOE, 2011). In support of this rulemaking change, a performance assessment has been completed that incorporates the ROMPCS design into the current PA baseline established by the 2009 Performance Assessment Baseline Calculation, referred to hereafter as PABC-2009 (Clayton et al., 2010). The name given to this new panel closure PA is PCS-2012, and the plan for its execution is detailed in AP-161 (Camphouse 2012a). PCS-2012 PA results are compared to those obtained in the PABC-2009 as

Information Only

a means to quantify potential impacts due to the panel closure redesign. This analysis package details the analysis of direct brine releases (DBRs) of the PCS-2012 PA.

2 BACKGROUND

DBRs are releases of contaminated brine originating in the repository and flowing up an intrusion borehole during the period of drilling. In order for DBR to occur, two criteria must be satisfied (Stoelzel and O'Brien 1996):

1. Volume averaged brine pressure in the vicinity of the repository encountered by drilling must exceed drilling fluid hydrostatic pressure (calculated to be 8 MPa).
2. Brine saturation in the repository must exceed the residual brine saturation of the waste material (sampled from a uniform distribution ranging from 0.0 to 0.552).

If both of these criteria are met, a DBR is calculated using the multi-phase flow code BRAGFLO with a two dimensional, semi-horizontally oriented grid, which represents the vicinity of the waste panels. If either of these conditions is not satisfied, no DBR is calculated.

DBRs are calculated from the following well deliverability equation in BRAGFLO (Mattax and Dalton 1990):

$$q_p(t) = J_p\left(P_p(t) - P_{wf}\right) \tag{1}$$

where $q_p(t)$ is the volumetric brine flux to the well as a function of time, J_p is the well productivity index, $P_p(t)$ is the volume averaged brine pressure of the repository in the vicinity of the intrusion as a function of time, and P_{wf} is the flowing bottom-hole pressure (assumed to be constant during each drilling intrusion). The flowing bottom-hole pressure is defined as the dynamic pressure at the inlet to the wellbore adjacent to the point of entry into the repository. It is less than the static pressure due to elevation, friction and acceleration effects (Stoelzel and O'Brien 1996).

The well productivity index, J_p, quantifies how readily brine can enter the well and flow to the surface. It is calculated from the following equation (Mattax and Dalton 1990; Chappelear and Williamson 1981):

$$J_p = \frac{2\pi k k_{rp} h}{\mu_p\left[\ln\left(\frac{r_e}{r_w}\right) + s - \frac{1}{2}\right]} \tag{2}$$

where

k Intrinsic permeability of the waste (constant: 2.4 x 10^{-13} m^2, WAS_AREA:PRMX_LOG)

k_{rp} Relative permeability of the waste assuming the modified Brooks-Corey relative permeability model: $k_{rp} = S_{el}^{(2+3\lambda)/\lambda}$, where λ is the pore distribution parameter (WAS_AREA:PORE_DIS), S_{el} is the effective brine saturation without correction for

Information Only

residual gas saturation $S_{el} = (S_b - S_{br})/(1 - S_{br})$, S_b is the brine saturation, and S_{br} is the residual brine saturation (WAS_AREA:SAT_RBRN)

h Crushed panel height, defined as $h = h_i(1-\phi_i)/(1-\phi)$, where h_i is initial panel height (3.96 m), ϕ_i is the initial room-scale porosity (0.848, WAS_AREA:POROSITY)), and ϕ is the room-scale porosity at the time of intrusion (calculated by BRAGFLO see Helton et al. 1998)

μ Brine dynamic viscosity (0.0021 Pa-s, BRINESAL:VISCO)

r_e Equivalent drainage radius of the grid block containing the well and is defined by $r_e = \sqrt{(\Delta x)(\Delta y)/\pi}$, where Δx and Δy are the grid cell dimensions of the grid cell containing the well.

r_w Well radius (0.1556 m, assuming a 12.25 in. drill bit diameter, BOREHOLE:DIAMMOD divided by two)

s Skin factor (enhanced well productivity due to the presence of a cavity at base of well)

The skin factor is calculated using (Lee 1982):

$$s = \left(\frac{k}{k_s} - 1\right)\ln\left(\frac{r_w}{r_s}\right), \tag{3}$$

where k_s is the permeability of an open channel as a result of cuttings, cavings and spallings releases, and r_s is the effective radius of the well bore with the cuttings, cavings and spallings volume (V_i) removed.

The effective radius r_s is obtained by converting the cuttings, cavings and spallings volume removed into a cylinder of equal volume with the initial height of the waste (h_i), and then computing the radius of the cylinder:

$$r_s = \sqrt{\frac{V_i}{h_i \pi}}. \tag{4}$$

For all WIPP PA calculations, k_s is assumed to be infinite, in which case Equation (3) simplifies to

$$s = \ln\left(\frac{r_w}{r_s}\right). \tag{5}$$

DBRs are calculated using the code BRAGFLO and a two-dimensional near-horizontal grid that dips 1° to the south. Five scenarios were simulated and are discussed in section 4.1.

Information Only

3 APPROACH

The conceptual models implemented in the PCS-2012 PA calculations are unchanged from those used in the PABC-2009 (Clayton et al., 2010). Changes incorporated in the PCS-2012 PA DBR calculations to model the ROMPCS are discussed below.

3.1 Model Geometry

The scenarios used for the PCS-2012 PA are the same as those used for the PABC-2009. The DBR numerical grid and material map used in the PCS-2012 PA calculations is shown in Figure 3-1. Note that the color scheme in Figure 3-1 has been chosen so as to correspond to the color scheme used in the PCS-2012 PA BRAGFLO grid and material map (Figure 3-4 to Figure 3-8 in Camphouse 2012b). The PABC-2009 DBR numerical grid and material map is shown in Figure 3-2.

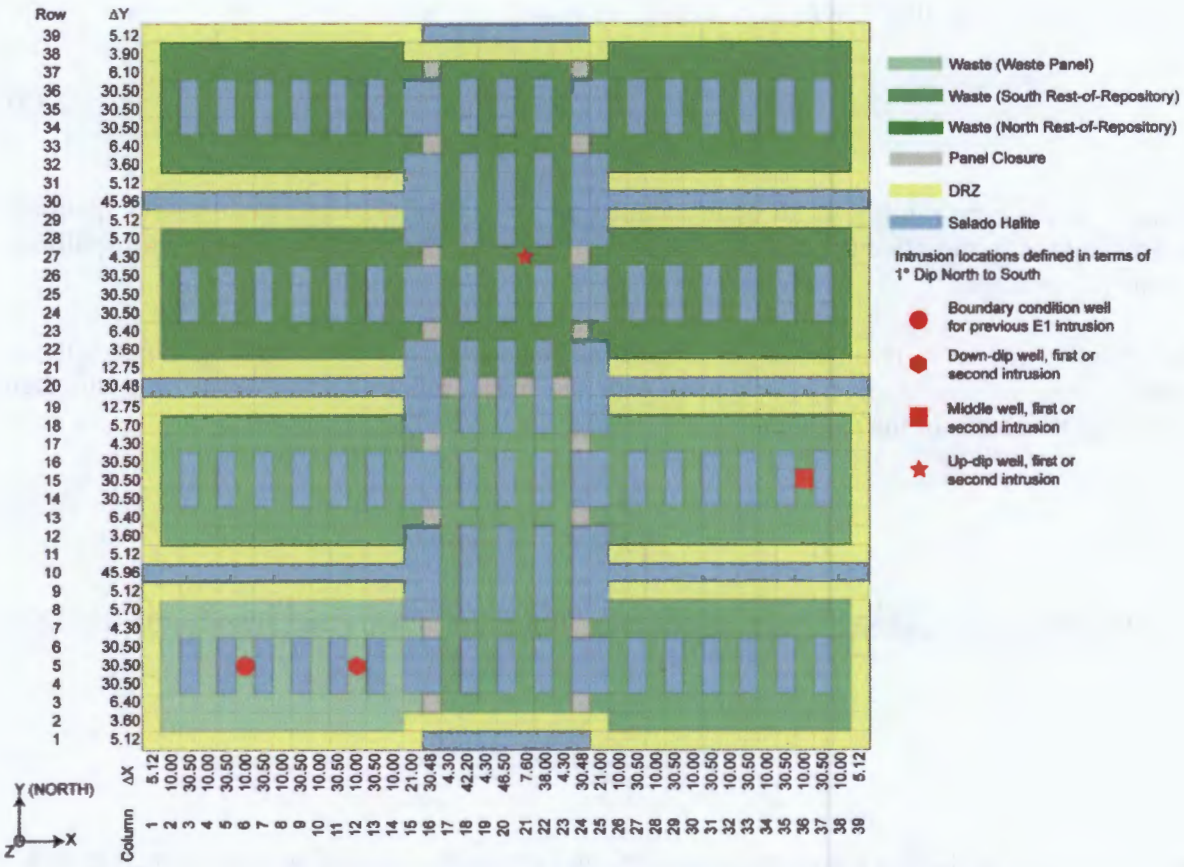

Figure 3-1: PCS-2012 PA DBR material map (logical grid) with ROM salt PCS.

The Option D panel closure modeled in the PABC-2009 is 40 meters long whereas the ROMPCS modeled in the PCS-2012 PA is 30.48 meters (100 feet) long. As a result, grid cell lengths corresponding to panel closures were reduced to 30.48 meters in the PCS-2012 PA. In addition,

Information Only

the ROMPCS, which is modeled as run-of-mine salt in the PCS-2012 PA, has no concrete component that is "keyed in" to the surrounding DRZ. As a result, material elements corresponding to equivalent DRZ/concrete in the PABC-2009 are replaced by DRZ in the PCS-2012 PA.

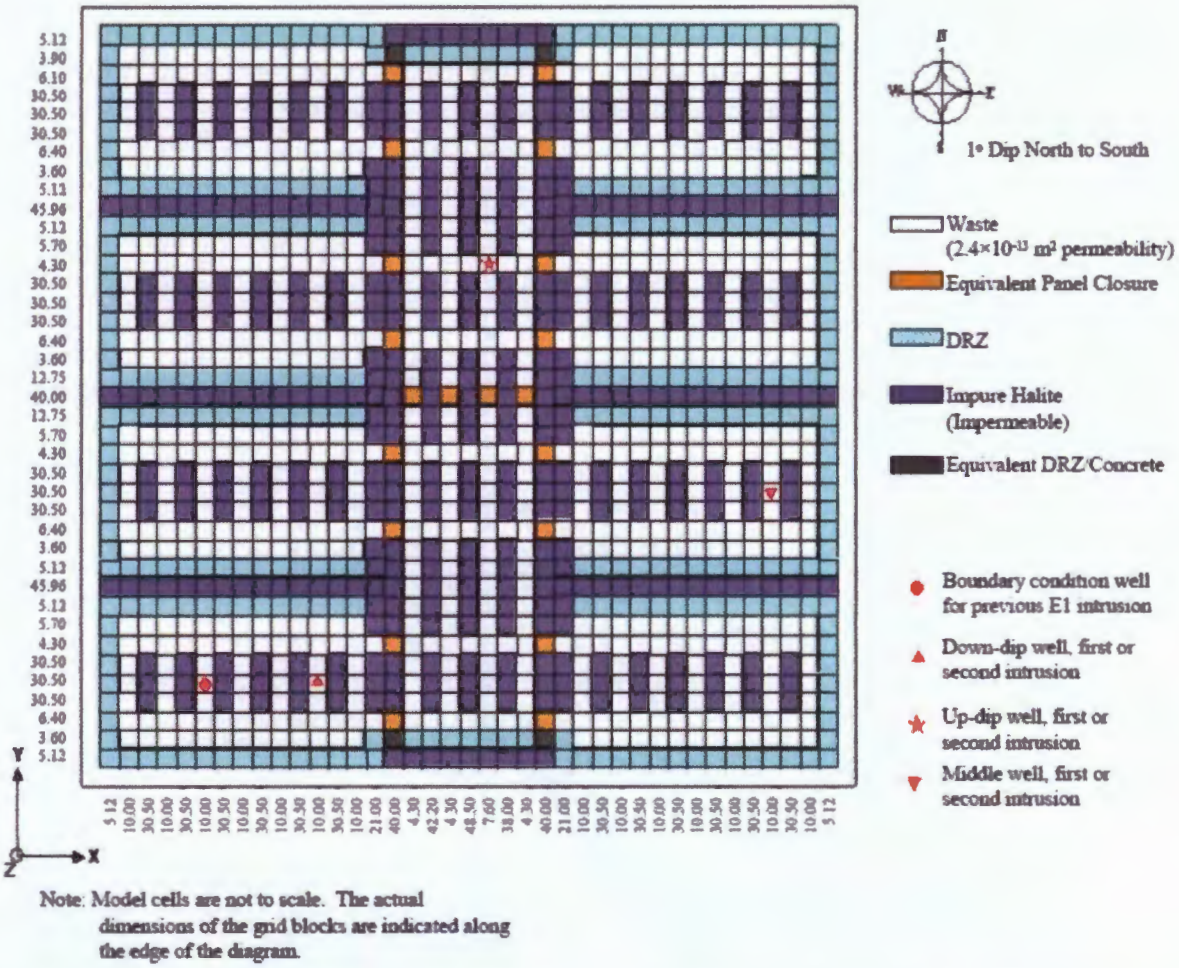

Figure 3-2: PABC-2009 DBR material map (logical grid) with Option D panel closure (after Clayton et al., 2010).

To calculate DBR volumes the same three drilling locations considered in PABC-2009 are considered in PCS-2012, namely: upper (up-dip), middle and lower (down-dip) locations. These are shown in Figure 3-1 (compare with Figure 3-2). Some of the calculations for DBR are for a drilling intrusion preceded by an earlier intrusion in either the same or different waste panel. The effects of these prior intrusions are incorporated into the calculations by specifying a boundary or initial condition well at their grid location, denoted by the red dot in Figure 3-1. The properties of the boundary condition well depend on the type of the prior intrusion and the time that has elapsed since its occurrence.

Information Only

3.2 Initial Conditions

Volume averaged brine pressures and brine saturations are calculated from the 10,000 year BRAGFLO simulations. The BRAGFLO results, corresponding to the time of intrusion, are used in the DBR simulations as initial conditions. The waste regions in the BRAGFLO grid and the DBR grid are each divided into three regions and volume-averaged brine pressure and saturations are transferred from corresponding regions in the BRAGFLO grid to the DBR grid. These regions corresponded to the single waste panel, south rest of repository (SRR), and north rest of repository (NRR). This method ensures that the relative volumes of these regions are equal between the 10,000 year BRAGFLO runs and the DBR runs. The definition of these repository regions can be seen in Figure 3-1.

Figure 3-3 illustrates the method used to transfer initial conditions in the waste for the PCS-2012 PA, which is unchanged from the PABC-2009 DBR runs. The volume averaged pressure and saturation from the three waste-filled regions in the BRAGFLO grid (WAS_AREA, SRR, NRR) at the time of the intrusion are used as the initial pressure and saturation for the three waste regions in the DBR grid (Lower, Middle, and Upper, respectively). The pressure and saturation can change during the DBR calculations.

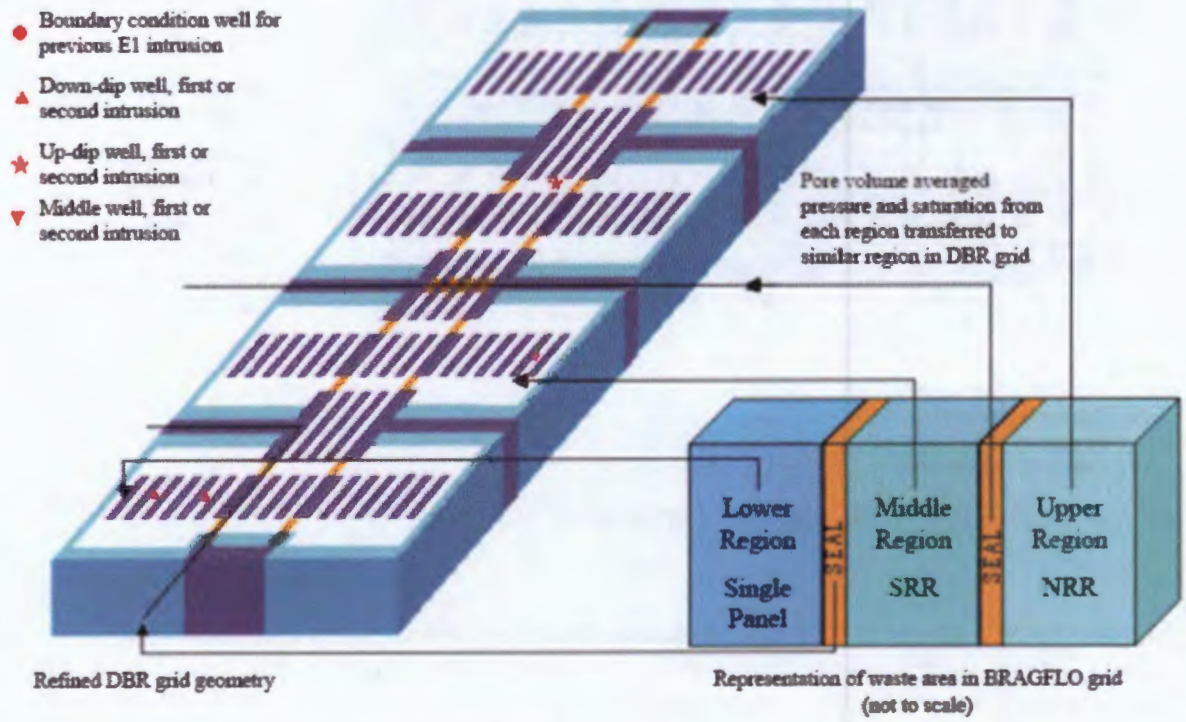

Figure 3-3. Regions to be used to transfer initial pressure and saturation between the 10,000 year BRAGFLO grid and the DBR grid for the PABC-2009.

Information Only

4 CALCULATION METHODOLOGY

DBR calculations are divided into five scenarios. Each DBR scenario represents an intrusion into the repository due to a drilling event. The initial conditions for the DBR simulations are obtained from the BRAGFLO Salado Flow simulations (Camphouse, 2012b) using an appropriate scenario and at an appropriate time for the particular drilling intrusion time. An E1 intrusion scenario is defined as an intrusion into the repository, which creates a pathway to a pressurized brine pocket below the repository. An E2 intrusion scenario is defined as an intrusion into the repository that terminates in the repository and does not create a pathway to a pressurized brine pocket below the repository. The results of the DBR calculations are the volumes of brine that leave the repository and reach the surface at the time of drilling and up to 4.5 days after. These results are used by the code CCDFGF to interpolate volumes of waste for the specific conditions that arise in a given future (location and timing of future drilling intrusions).

4.1 Modeled Scenarios

Below an overview is given of the DBR calculations performed for the PCS-2012 PA. In performing DBR calculations, the five BRAGLFO scenarios S1-BF to S5-BF used in Salado flow modeling are used to set volume-averaged brine pressure and brine saturation in the DBR calculations at the time of intrusion. These BRAGFLO Salado flow scenarios are listed in Table 4-1.

Table 4-1: Scenarios used in BRAGFLO Salado flow modeling.

Scenario	Description
S1-BF	Undisturbed Repository
S2-BF	E1 intrusion at 350 years
S3-BF	E1 intrusion at 1,000 years
S4-BF	E2 intrusion at 350 years
S5-BF	E2 intrusion at 1,000 years

With the brine pressure and brine saturation transferred from the Salado flow results, DBR calculations quantify impacts due to initial or subsequent intrusions into the repository. DBR simulations cover a range of intrusion scenarios, locations, and timing using five scenarios, S1-DBR to S5-DBR. A summary of intrusion times for each scenario is given in Table 4-2.

4.1.1 Scenario 1 (S1-DBR)

The BRAGFLO Salado modeling results from the S1-BF scenario are used as initial conditions to construct the first intrusion into the repository in which a DBR may occur. In the BRAGFLO Salado flow modeling (Camphouse, 2012b), this scenario represents an undisturbed repository. In the computation of DBRs for this scenario, upper, middle, and lower drilling intrusions are

Information Only

modeled at 100, 350, 1,000, 3,000, 5,000, and 10,000 years (3 locations × 6 intrusion times × 100 vectors = 1,800 calculations per replicate).

Table 4-2: Intrusion times modeled by DBR for each scenario.

Scenario	Intrusion times (years)
S1-DBR	100, 350, 1000, 3000, 5000, 10000
S2-DBR	550, 750, 2000, 4000, 10000
S3-DBR	1200, 1400, 3000, 5000, 10000
S4-DBR	550, 750, 2000, 4000, 10000
S5-DBR	1200, 1400, 3000, 5000, 10000

4.1.2 Scenario 2 (S2-DBR)

The BRAGFLO Salado flow modeling results from the S2-BF scenario are used as initial conditions to construct a second or subsequent intrusion into the repository in which a DBR may occur and in which the first intrusion had intersected a pressurized Castile brine reservoir at 350 years (Camphouse, 2012b). For the second or subsequent intrusion, upper, middle, and lower drilling intrusions were modeled at 550, 750, 2,000, 4,000 and 10,000 years (3 locations × 5 intrusion times × 100 vectors = 1,500 calculations per replicate). The effect of the prior E1 intrusion is incorporated in the calculations by the specification of a boundary condition well as denoted by the red dot in Figure 3-1. The properties of the boundary condition well correspond to the properties at the time of the second intrusion.

Runs for the lower drilling location assume that the second or subsequent intrusion occurs at the location labeled in Figure 3-1 as the "down-dip well". This represents an intrusion in the same panel that was intersected by a previous intrusion (assumed to be at the location labeled "boundary condition well") and therefore the abandoned borehole still connects the panel with the brine reservoir. Runs for the middle drilling location assume that the second or subsequent intrusion occurs at the location labeled in Figure 3-1 as the "middle well"; a previous intrusion is assumed to have occurred at the location labeled "boundary condition well," which is in an adjacent panel. Runs for the upper drilling location assume that the second or subsequent intrusion occurs at the location labeled "up-dip well" in Figure 3-1; a previous intrusion is assumed to have occurred at the location labeled "boundary condition well," which is in a panel that is not adjacent to the current intrusion.

4.1.3 Scenario 3 (S3-DBR)

The BRAGFLO Salado modeling results from the S3-BF scenario are used as initial conditions to construct a second or subsequent intrusion into the repository in which a DBR may occur and in which the first intrusion had intersected a pressurized Castile brine reservoir at 1,000 years (Camphouse, 2012b). Upper, middle, and lower second or subsequent intrusions are modeled at 1,200, 1,400, 3,000, 5,000 and 10,000 years (3 locations × 5 intrusion times × 100 vectors =

Information Only

1,500 calculations per replicate). The effect of the prior E1 intrusion and the lower, middle, and upper drilling locations are treated the same as for the S2-DBR scenario.

4.1.4 Scenario 4 (S4-DBR)

For this scenario, the BRAGFLO Salado flow modeling results from the S4-BF scenario are used as initial conditions to construct a second or subsequent intrusion into the repository in which a DBR may occur and in which the first intrusion occurs at 350 years without hitting a Castile brine reservoir (Camphouse, 2012b). Upper, middle, and lower second or subsequent intrusions are modeled at 550, 750, 2,000, 4,000 and 10,000 years (3 locations × 5 intrusion times × 100 vectors = 1,500 calculations per replicate). Runs for the lower drilling location assume the second or subsequent intrusion occurs at the location labeled in Figure 3-1 as the "down-dip well". This represents an intrusion into the same panel that was intersected by a previous E2 intrusion. The borehole from the previous intrusion is not represented explicitly in the model. Runs for the middle drilling location assume that the second or subsequent intrusion occurs at the location labeled in Figures 3-1 as the "middle well." Runs for the upper drilling location assume that the second or subsequent intrusion occurs at the location labeled "up-dip well" in Figure 3-1.

4.1.5 Scenario 5 (S5-DBR)

The BRAGFLO Salado flow modeling results from the S5-BF scenario are used as initial conditions to construct a second or subsequent intrusion into the repository in which a DBR may occur and in which the first intrusion occurs at 1,000 years without intersecting a Castile brine reservoir (Camphouse, 2012). Upper, middle, and lower second or subsequent intrusions are be modeled at 1,200, 1,400, 3,000, 5,000 and 10,000 years (3 locations × 5 intrusion times × 100 vectors = 1,500 calculations per replicate). The lower, middle, and upper drilling locations are treated the same as for the S4-DBR scenario.

4.2 Run Control

Run control, including code versions used and descriptions of code sequencing used to obtain DBR results in the PCS-2012 PA, are documented in Camphouse et al. (2012). PCS-2012 PA initial conditions and results obtained from BRAGFLO DBR pre- and post-processing, respectively, are contained in files with the names:

1. ALG2_DBR_AP161_Rr_Ss_Tttttt_Vvvv.CDB and
2. ALG3_DBR_AP161_Rr_Ss_Tttttt_ c_Vvvv.CDB,

where r (the replicate number) equals 1,2, or 3, s (the scenario number) equals 1,2,3,4,5, or 6, ttttt (time in years) equals 00550, 00750, 02000, 04000, or 10000, c (drilling location) is either L, M or U, and vvv (the vector number) is between 001 and 100. These files are located in CMS library LIBAP161_DBRRrSs under class AP161-0. PABC-2009 results used herein for purposes comparison have equivalent file names with 'AP161' replaced by 'PABC09', and are located in CMS library LIBPABC09_DBRRrSs under class PABC09-0.

Information Only

5 RESULTS

The DBR calculations over all three replicates of the PCS-2012 are presented in this section and compared to results from all three replicates of the PABC-2009. The analysis of the PABC-2009 results is described in Clayton (2008) and will only be summarized herein as appropriate. For consistency with previous analyses, non-zero volumes are defined as volumes that are greater than 10^{-7} m^3.

Each replicate of DBR calculations resulted in 7,800 (1,800 for first intrusion and 1,500×4= 6,000 for second intrusion) separate vector-scenario-drilling location-time combinations. These results are used as input to the code CCDFGF, which then calculates a release for any vector-intrusion time combination. This is done by first, linearly interpolating modeled volumes between the fixed intrusion times (Table 4-2) and second, multiplying the resulting intrusion-specific DBR volume with the radionuclide concentration calculated for that vector and intrusion time by the code PANEL (Garner 2010).

5.1 Summary

In this section, results from the PCS-2012 PA and the PABC-2009 are compared. Pertinent summary statistics for the calculations are listed in Table 5-1. The maximum DBR volumes shown in the table are over all three replicates, times, vectors and drilling locations. Overall there is a consistent increase in the maximum DBR volumes from PABC-2009 to PCS-2012 PA. The largest increases were observed in scenarios S4-DBR and S5-DBR which are associated with E2 intrusions. The BRAGFLO modeling results reported by Camphouse (2012b), show that E2 intrusion scenarios in the PCS-2012 PA yielded waste panel pressure that is higher, on average, than that seen in the PABC-2009 at the time of intrusion and it remains higher for the duration of the 10,000 year regulatory period. Similarly, the mean waste panel brine saturation is higher at the time of intrusion in the PCS-2012 PA, resulting in higher long-term waste panel brine saturations for E2 intrusion scenarios (Camphouse, 2012b). DBRs are strongly dependent on waste panel pressure and brine saturation at the time of intrusion. Hence, increases to these two quantities lead to the increased maximum DBR volumes observed in scenarios S4-DBR and S5-DBR, and to the higher overall number of non-zero brine volume vectors.

The moderate increases in maximum DBR volumes for scenarios S2-DBR and S3-DBR are due to the fact that the lower long-term permeability range of the ROMPCS as compared to Option D yields a period of increased waste panel pressurization following an E1 intrusion. The increased mean waste panel pressure slightly inhibits brine flow into the panel after the intrusion, resulting in only a slight decrease to the mean waste panel brine saturation as compared to PABC-2009 E1 intrusion results. The combination of increased pressure and a slight decrease to brine saturation yields an increase to the maximum DBR volume seen in the PCS-2012 PA E1 results.

For undisturbed conditions, implementation of the ROMPCS yields higher long-term waste panel pressure (on average) than was seen in the PABC-2009 (Camphouse, 2012b). The increase in mean waste panel pressure is accompanied by an increase in the average waste panel brine saturation for the ROMPCS results. The ROMPCS design allows more brine inflow to the waste panel during the first 200 years when compared to Option D results. This increased brine inflow,

Information Only

combined with the tightness of the ROMPCS after 200 years, results in increased waste panel gas generation (on average) and a subsequent increase to waste panel mean pressure. This explains the increase in the scenario S1-DBR maximum DBR volume for the PCS-2012 PA compared to the PABC-2009.

Table 5-1 shows a modest (~6%) increase in the number of non-zero DBR volumes for the PCS-2012 PA calculations compared with the PABC-2009, and modest increases in the average DBR volumes for all scenarios. These increases attributable to the increases in waste panel brine pressure and brine saturation discussed above and presented in more detail in Camphouse (2012b).

Table 5-1: Summary statistics for the PCS-2012 PA and PABC-2009 DBR calculations over all replicates and vectors.

	Number of Vectors		Maximum volume (m^3)		Average volume (m^3)	
Scenario	PABC-2009	PCS-2012 PA	PABC-2009	PCS-2012 PA	PABC-2009	PCS-2012 PA
S1-DBR	369	419	27.6	45.9	0.1	0.4
S2-DBR	1179	1174	48.2	52.9	2.8	2.9
S3-DBR	926	907	40.6	43.8	1.5	1.4
S4-DBR	211	281	20.4	42.5	0.1	0.2
S5-DBR	314	401	21.1	53.8	0.1	0.3
Overall	2999	3182	48.2	53.8	0.9	1.0

Note: The volume of direct brine released was obtained from the output variable BRIN_REL which is calculated in the ALGEBRACDB step 3 post-processing step, and contained in the ALG3 CDB files.

5.2 Direct Brine Releases from the Lower Drilling Location

Table 5-2 through Table 5-6 summarize the number of vectors for the PCS-2012 PA calculations with non-zero DBR volumes, and the maximum and average DBR volumes for the 300 vectors in each scenario-time-drilling location combination. The same summary statistics for the PABC-2009 are included in the tables for comparison.

One important result that is evident from Table 5-2 through Table 5-6 and has been reported consistently in previously analyses is that DBRs are less likely to occur in intrusions situated in the upper drilling location than in the lower drilling location. Of all the intrusions that had a non-zero DBR volume for the PCS-2012 PA, 63.4% occurred during a lower drilling intrusion, a modest decrease from the value of 66.5% for PABC-2009. Furthermore, of all the intrusions that had a non-zero DBR volume and occur during a lower drilling intrusion, 78.0% are found in scenarios S2-DBR and S3-DBR, a slight decrease from 82.9% for PABC-2009 (Clayton et al., 2010). Therefore, as has been observed previously (Clayton et al., 2010; Pasch and Camphouse, 2011), the majority of the non-zero DBR volumes occur when there is a previous E1 intrusion within the same panel. Not only are DBRs less likely to occur during upper drilling intrusions, but also the DBR volumes from such intrusions tend to be much smaller than those from lower drilling intrusions. For all three replicates of the PCS-2012 PA, the maximum DBR volume for the upper drilling location is 25.7 m^3 compared to 53.8 m^3 for the lower drilling location. These

Information Only

observations support the conclusion that lower drilling intrusions are the primary source for significant DBRs.

Figures 5-1 to 5-10 are probability plots of the DBR volumes for scenarios S1-DBR to S5-DBR for all three replicates. Results of the PCS-2012 PA are compared to those of the PABC-2009. The probability plots show the percentiles (x-axis) of the DBR volumes (y-axis). The plots of PCS-2012 PA results are generally similar to those of the PABC-2009. However, unlike the PABC-2009 where the largest DBR volume was observed in scenario S2-DBR, for the PCS-2012 PA the largest DBR volume occurs in scenario S5-DBR.

Information Only

Table 5-2: Summary table of number of vectors with non-zero, maximum and average DBR volumes over all three replicates for the S1-DBR calculations

Time (yrs)	Drilling Location	Number of Vectors		Maximum volume (m^3)		Average volume (m^3)	
		PABC-2009	PCS-2012 PA	PABC-2009	PCS-2012 PA	PABC-2009	PCS-2012 PA
100	L	0	0	0.00E+00	0.00E+00	0.00E+00	0.00E+00
350	L	0	0	0.00E+00	0.00E+00	0.00E+00	0.00E+00
1,000	L	26	40	1.51E+01	4.59E+01	1.80E-01	1.01E+00
3,000	L	37	52	5.92E+00	4.12E+01	1.16E-01	6.51E-01
5,000	L	46	55	2.19E+01	3.29E+01	2.92E-01	7.81E-01
10,000	L	46	56	2.03E+01	3.66E+01	4.26E-01	8.96E-01
100	M	0	0	0.00E+00	0.00E+00	0.00E+00	0.00E+00
350	M	0	0	0.00E+00	0.00E+00	0.00E+00	0.00E+00
1,000	M	19	23	6.33E+00	4.30E+01	5.14E-02	4.56E-01
3,000	M	32	33	2.27E+00	1.40E+01	3.95E-02	1.78E-01
5,000	M	29	32	2.25E+01	2.19E+01	1.24E-01	2.42E-01
10,000	M	31	30	2.76E+01	1.65E+01	1.32E-01	1.76E-01
100	U	0	0	0.00E+00	0.00E+00	0.00E+00	0.00E+00
350	U	0	0	0.00E+00	0.00E+00	0.00E+00	0.00E+00
1,000	U	16	17	6.15E+00	5.23E+00	4.75E-02	3.94E-02
3,000	U	29	27	1.73E+00	1.53E+00	3.13E-02	2.29E-02
5,000	U	28	26	2.02E+01	2.13E+01	7.82E-02	1.21E-01
10,000	U	30	28	1.91E+01	2.57E+01	9.37E-02	1.16E-01

Note: Volume releases less than 1×10^{-7} m^3 have been reduced to 0.0 for the purposes of this table. The maximum DBR volume is calculated as the maximum value of the 300 vectors for each replicate-scenario-time-drilling location combination. The average DBR volume is calculated by the total of the DBR volumes divided by the total number of vectors. The DBR volume was obtained from the output variable BRIN_REL which is calculated in the ALGEBRACDB step 3 post-processing step, and contained in the ALG3 CDB files.

Table 5-3: Summary table of number of vectors with non-zero, maximum and average DBR volumes over all three replicates for the S2-DBR calculations.

Time (yrs)	Drilling Location	Number of Vectors		Maximum volume (m^3)		Average volume (m^3)	
		PABC-2009	PCS-2012 PA	PABC-2009	PCS-2012 PA	PABC-2009	PCS-2012 PA
550	L	285	287	3.74E+01	4.01E+01	1.23E+01	1.19E+01
750	L	255	245	3.86E+01	3.80E+01	1.16E+01	1.10E+01
2,000	L	164	165	3.78E+01	4.43E+01	7.11E+00	7.93E+00
4,000	L	140	133	4.39E+01	4.43E+01	5.38E+00	5.82E+00
10,000	L	137	127	4.82E+01	5.29E+01	5.64E+00	5.10E+00
550	M	7	8	4.41E+00	1.33E+01	1.71E-02	5.40E-02
750	M	15	19	7.63E+00	2.98E+01	5.02E-02	3.45E-01
2,000	M	32	36	8.70E+00	3.38E+01	1.42E-01	3.27E-01
4,000	M	30	31	2.10E+01	1.04E+01	9.88E-02	1.39E-01
10,000	M	24	32	1.79E+01	1.37E+01	1.25E-01	1.77E-01
550	U	5	4	4.14E-01	4.38E-01	1.91E-03	1.67E-03
750	U	9	7	2.35E+00	1.16E-01	9.01E-03	6.33E-04
2,000	U	27	29	9.68E+00	7.25E+00	1.12E-01	9.15E-02
4,000	U	27	25	1.18E+00	8.23E-01	1.54E-02	1.02E-02
10,000	U	22	26	1.24E+01	2.46E+01	7.96E-02	1.14E-01

Note: Volume releases less than 1×10^{-7} m^3 have been reduced to 0.0 for the purposes of this table. The maximum DBR volume is calculated as the maximum value of the 300 vectors for each replicate-scenario-time-drilling location combination. The average DBR volume is calculated by the total of the DBR volumes divided by the total number of vectors. The DBR volume was obtained from the output variable BRIN_REL which is calculated in the ALGEBRACDB step 3 post-processing step, and contained in the ALG3 CDB files.

Table 5-4: Summary table of number of vectors with non-zero, maximum and average DBR volumes over all three replicates for the S3-DBR calculations.

Time (yrs)	Drilling Location	Number of Vectors		Maximum volume (m^3)		Average volume (m^3)	
		PABC-2009	PCS-2012 PA	PABC-2009	PCS-2012 PA	PABC-2009	PCS-2012 PA
1,200	L	231	221	3.68E+01	3.55E+01	8.76E+00	7.27E+00
1,400	L	166	159	3.25E+01	3.18E+01	5.41E+00	4.49E+00
3,000	L	96	85	2.68E+01	3.48E+01	2.47E+00	2.44E+00
5,000	L	90	74	3.76E+01	4.15E+01	2.70E+00	2.41E+00
10,000	L	90	77	4.06E+01	4.38E+01	2.76E+00	2.35E+00
1,200	M	27	32	1.81E+01	3.36E+01	1.58E-01	4.85E-01
1,400	M	32	35	1.98E+01	3.48E+01	2.13E-01	4.58E-01
3,000	M	29	34	3.59E+00	1.40E+01	4.48E-02	1.76E-01
5,000	M	26	30	2.17E+01	2.24E+01	1.21E-01	2.37E-01
10,000	M	21	32	1.34E+01	1.46E+01	6.40E-02	1.82E-01
1,200	U	23	22	4.39E+00	5.28E+00	4.45E-02	5.51E-02
1,400	U	23	24	2.64E+00	3.20E+00	3.60E-02	4.15E-02
3,000	U	29	31	1.95E+00	1.46E+00	3.39E-02	2.38E-02
5,000	U	24	25	1.96E+01	2.21E+01	7.33E-02	1.23E-01
10,000	U	19	26	1.22E+01	2.46E+01	7.35E-02	1.14E-01

Note: Volume releases less than 1×10^{-7} m^3 have been reduced to 0.0 for the purposes of this table. The maximum DBR volume is calculated as the maximum value of the 300 vectors for each replicate-scenario-time-drilling location combination. The average DBR volume is calculated by the total of the DBR volumes divided by the total number of vectors. The DBR volume was obtained from the output variable BRIN_REL which is calculated in the ALGEBRACDB step 3 post-processing step, and contained in the ALG3 CDB files.

Table 5-5: Summary table of number of vectors with non-zero, maximum and average DBR volumes over all three replicates for the S4-DBR calculations.

Time (yrs)	Drilling Location	Number of Vectors		Maximum volume (m^3)		Average volume (m^3)	
		PABC-2009	PCS-2012 PA	PABC-2009	PCS-2012 PA	PABC-2009	PCS-2012 PA
550	L	6	12	1.00E+00	3.17E+01	4.09E-03	2.33E-01
750	L	5	9	1.93E+01	1.62E+01	7.36E-02	2.19E-01
2,000	L	17	21	1.60E+01	4.25E+01	1.44E-01	6.19E-01
4,000	L	22	26	1.92E+01	3.52E+01	9.43E-02	4.04E-01
10,000	L	24	29	2.04E+01	3.91E+01	2.11E-01	6.97E-01
550	M	6	7	5.48E-01	1.17E+01	2.47E-03	4.94E-02
750	M	9	11	2.61E+00	2.57E+01	1.08E-02	1.82E-01
2,000	M	18	30	8.25E+00	3.30E+01	7.98E-02	3.25E-01
4,000	M	19	28	1.72E+00	1.02E+01	2.00E-02	1.29E-01
10,000	M	14	27	1.48E+00	1.49E+01	9.71E-03	1.75E-01
550	U	5	4	4.12E-01	4.35E-01	1.89E-03	1.63E-03
750	U	8	6	2.05E+00	1.12E-01	7.93E-03	6.00E-04
2,000	U	22	25	9.60E+00	6.89E+00	1.05E-01	8.01E-02
4,000	U	21	24	1.21E+00	9.62E-01	1.26E-02	1.14E-02
10,000	U	15	22	1.11E+01	2.44E+01	5.08E-02	1.15E-01

Note: Volume releases less than 1×10^{-7} m^3 have been reduced to 0.0 for the purposes of this table. The maximum DBR volume is calculated as the maximum value of the 300 vectors for each replicate-scenario-time-drilling location combination. The average DBR volume is calculated by the total of the DBR volumes divided by the total number of vectors. The DBR volume was obtained from the output variable BRIN_REL which is calculated in the ALGEBRACDB step 3 post-processing step, and contained in the ALG3 CDB files.

Table 5-6: Summary table of number of vectors with non-zero, maximum and average DBR volumes over all three replicates for the S5-DBR calculations.

Time (yrs)	Drilling Location	Number of Vectors		Maximum volume (m^3)		Average volume (m^3)	
		PABC-2009	PCS-2012 PA	PABC-2009	PCS-2012 PA	PABC-2009	PCS-2012 PA
1,200	L	31	50	1.97E+01	4.21E+01	3.17E-01	1.14E+00
1,400	L	15	18	2.11E+01	4.12E+01	2.05E-01	5.66E-01
3,000	L	18	21	6.01E+00	4.04E+01	6.79E-02	3.87E-01
5,000	L	23	25	9.25E+00	3.43E+01	6.25E-02	4.34E-01
10,000	L	24	29	2.03E+01	5.38E+01	2.10E-01	7.45E-01
1,200	M	25	29	1.81E+01	3.42E+01	1.53E-01	4.24E-01
1,400	M	26	33	1.98E+01	3.53E+01	2.11E-01	4.65E-01
3,000	M	21	31	4.17E+00	1.41E+01	4.01E-02	1.72E-01
5,000	M	19	26	1.58E+00	1.05E+01	1.28E-02	1.55E-01
10,000	M	14	27	1.48E+00	1.42E+01	1.02E-02	1.74E-01
1,200	U	21	20	4.32E+00	4.15E+00	3.56E-02	3.74E-02
1,400	U	20	22	2.67E+00	3.59E+00	3.81E-02	4.21E-02
3,000	U	23	25	2.03E+00	1.54E+00	3.13E-02	2.42E-02
5,000	U	19	23	1.15E+00	1.19E+01	7.91E-03	4.73E-02
10,000	U	15	22	1.11E+01	2.44E+01	5.03E-02	1.15E-01

Note: Volume releases less than 1×10^{-7} m^3 have been reduced to 0.0 for the purposes of this table. The maximum DBR volume is calculated as the maximum value of the 300 vectors for each replicate-scenario-time-drilling location combination. The average DBR volume is calculated by the total of the DBR volumes divided by the total number of vectors. The DBR volume was obtained from the output variable BRIN_REL which is calculated in the ALGEBRACDB step 3 post-processing step, and contained in the ALG3 CDB files.

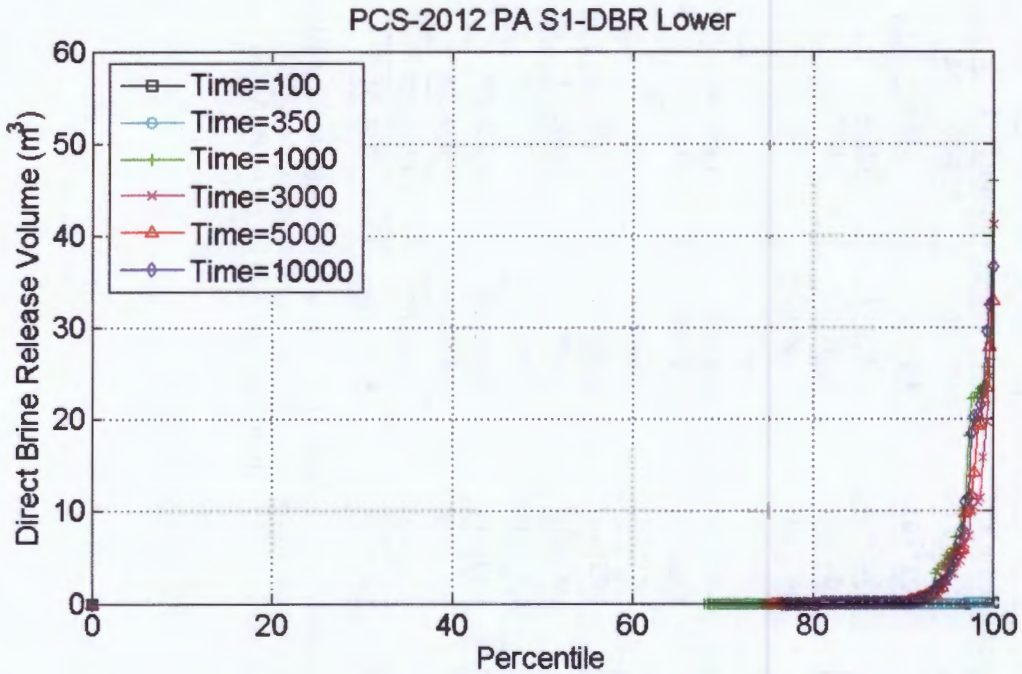

Figure 5-1: PCS-2012 PA lower intrusion DBR volume percentile rankings for all replicates and vectors of the scenario S1-DBR.

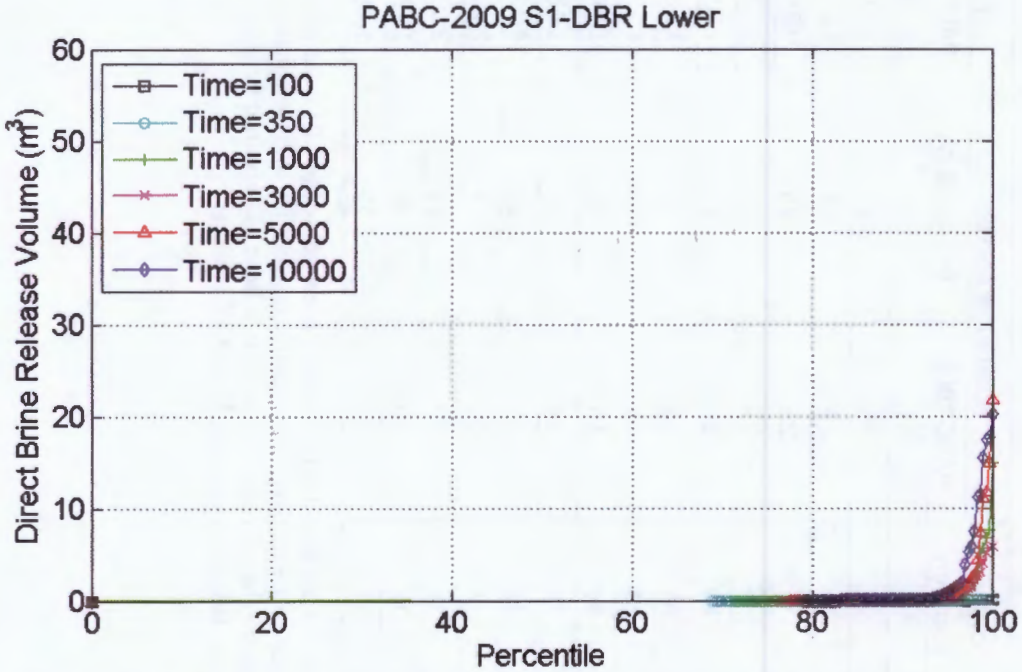

Figure 5-2: PABC-2009 lower intrusion DBR volume percentile rankings for all replicates and vectors of scenario S1-DBR.

Information Only

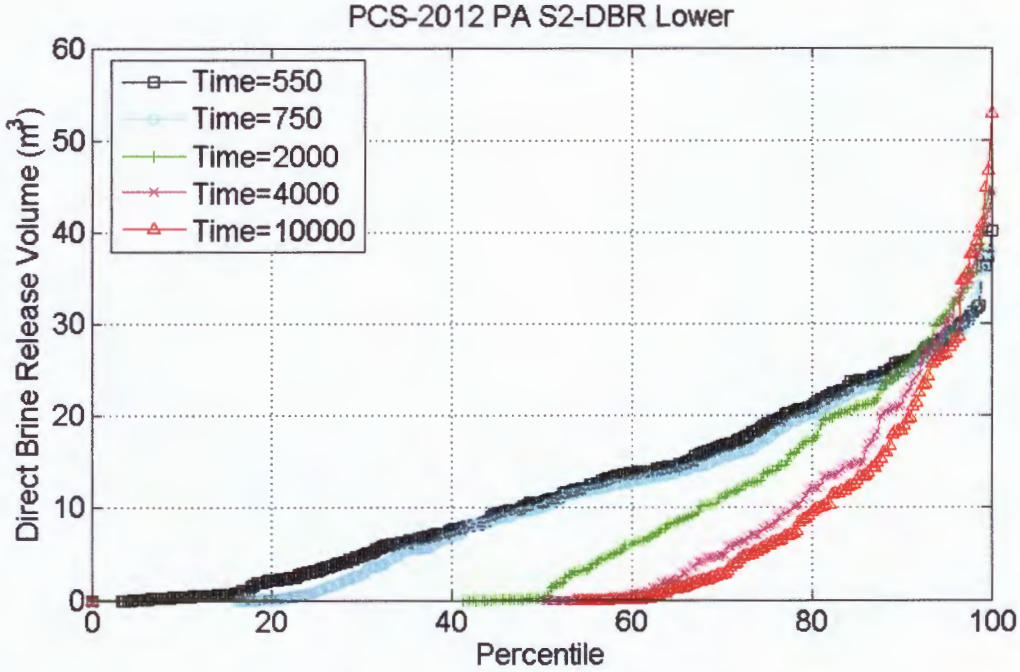

Figure 5-3: PCS-2012 PA lower intrusion DBR volume percentile rankings for all replicates and vectors of scenario S2-DBR.

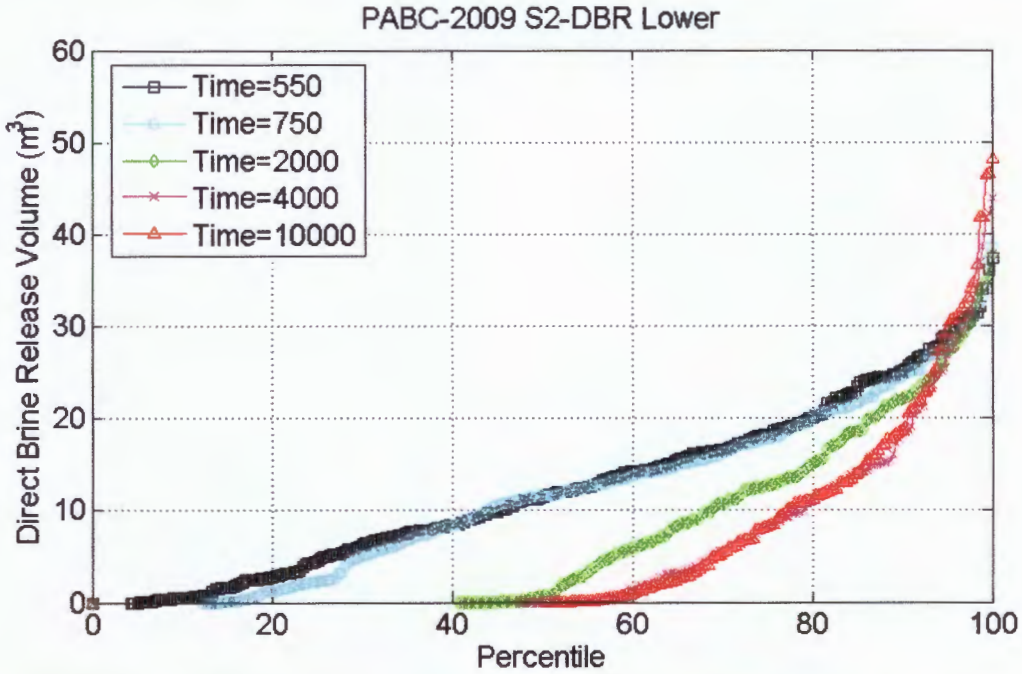

Figure 5-4: PABC-2009 lower intrusion DBR volume percentile rankings for all replicates and vectors of scenario S2-DBR.

Information Only

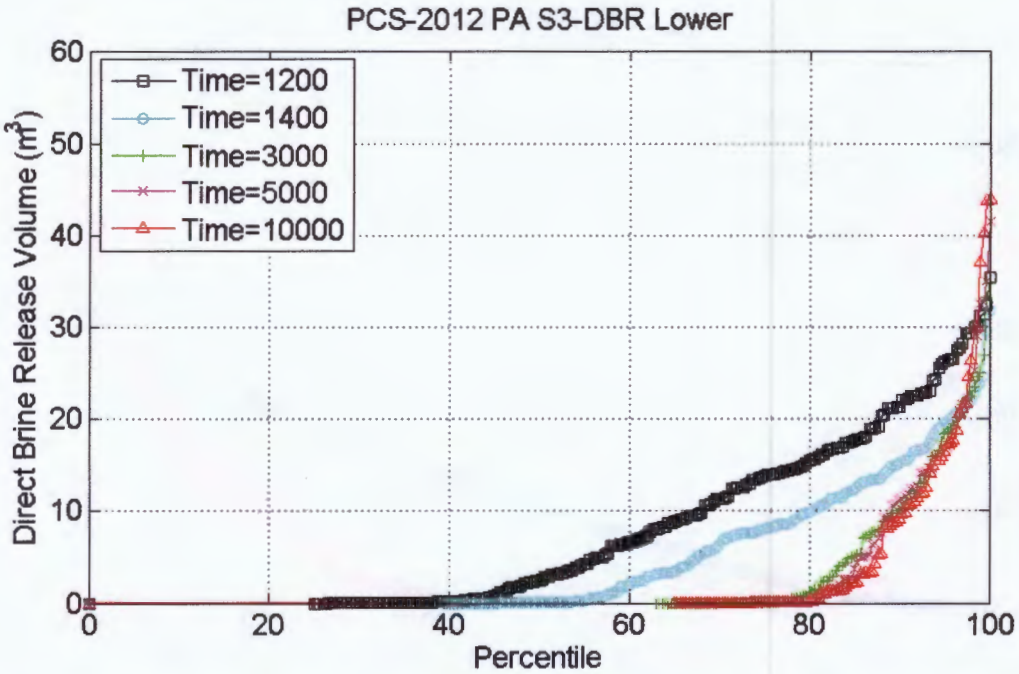

Figure 5-5: PCS-2012 PA lower intrusion DBR volume percentile rankings for all replicates and vectors of scenario S3-DBR.

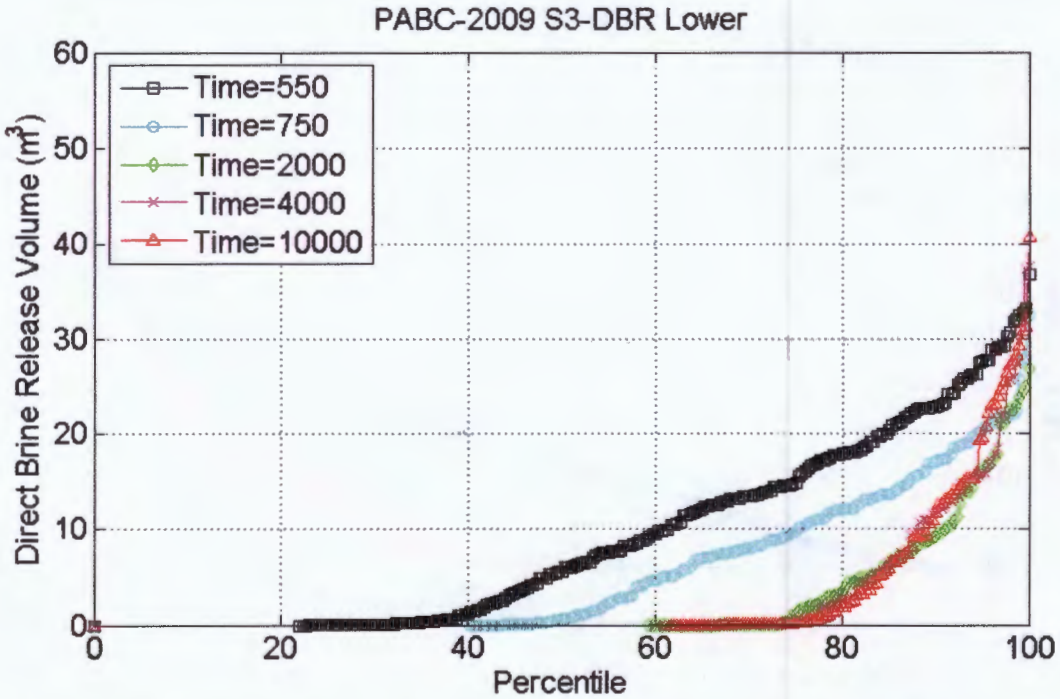

Figure 5-6: PABC-2009 lower intrusion DBR volume percentile rankings for all replicates and vectors of scenario S3-DBR.

Information Only

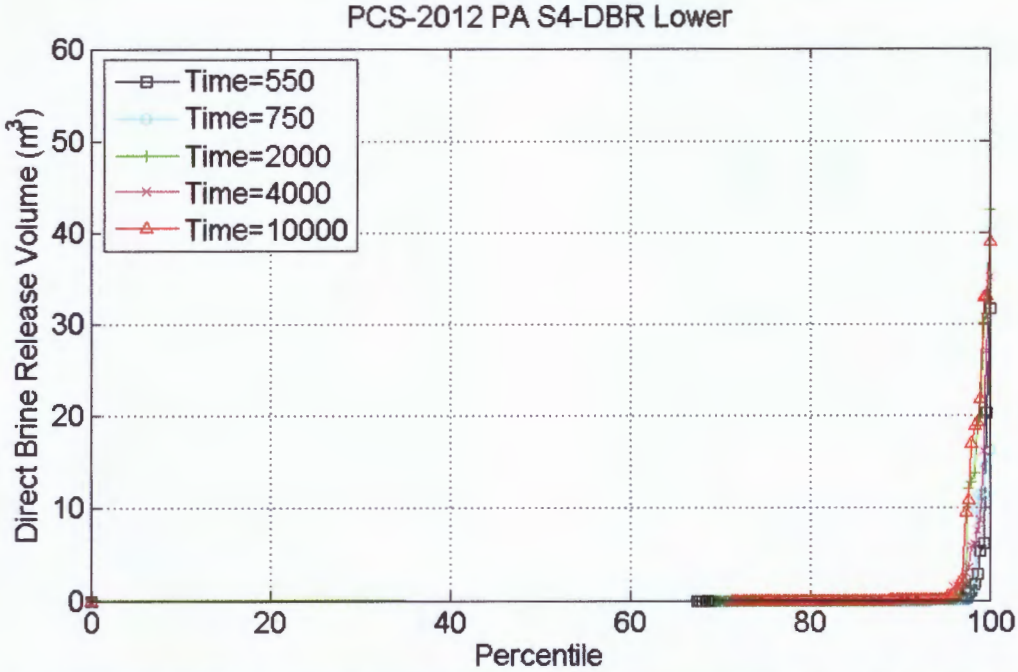

Figure 5-7: PCS-2012 PA lower intrusion DBR volume percentile rankings for all replicates and vectors of scenario S4-DBR.

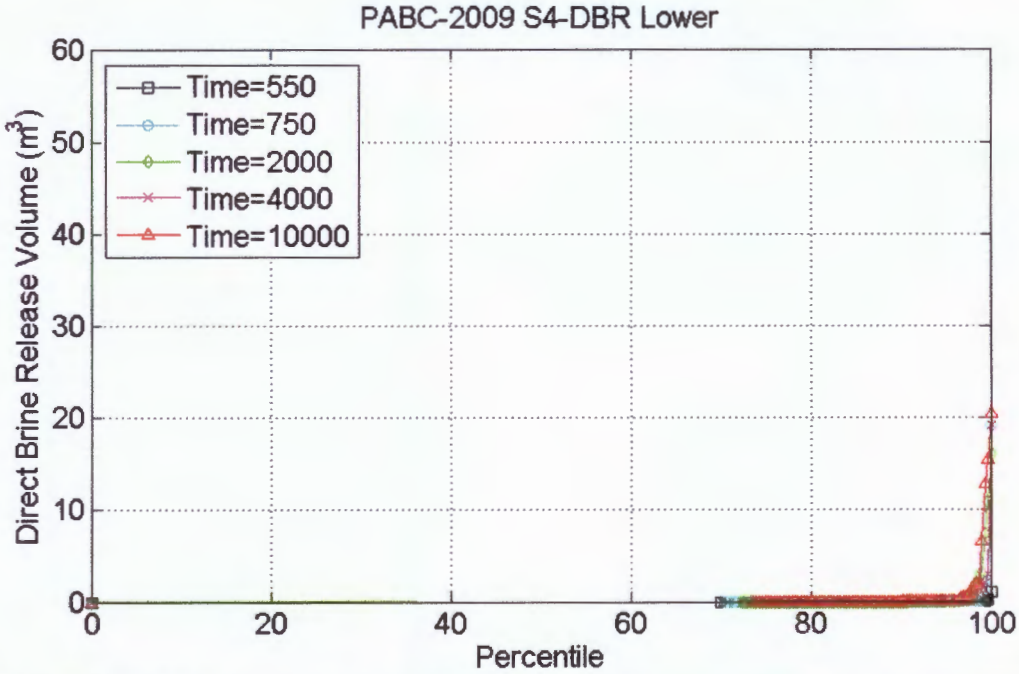

Figure 5-8: PABC-2009 lower intrusion DBR volume percentile rankings for all replicates and vectors of scenario S4-DBR.

Information Only

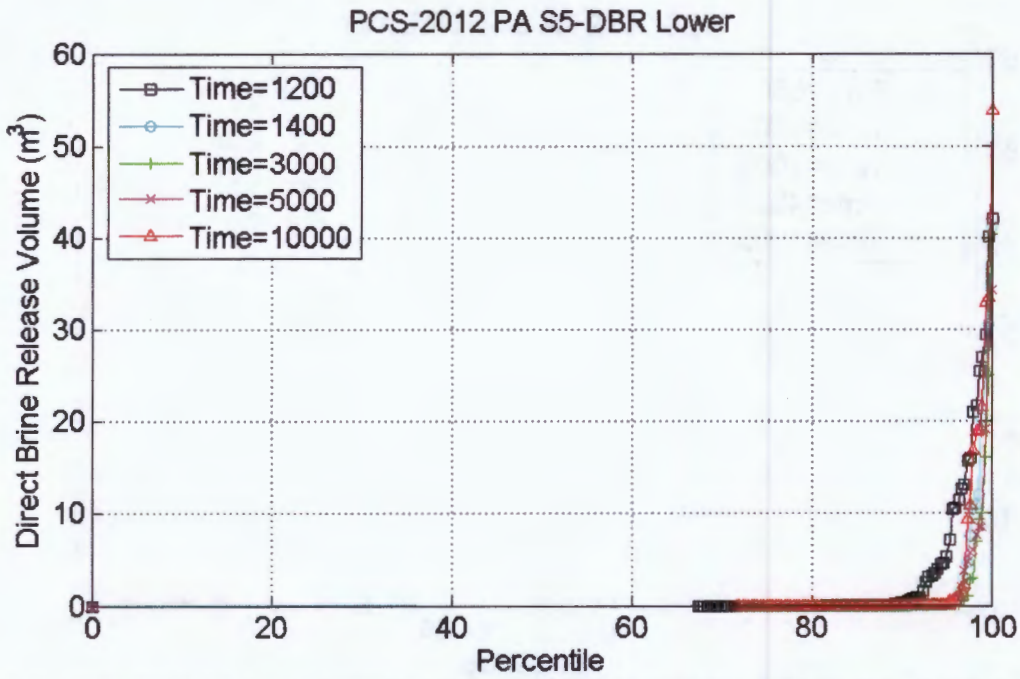

Figure 5-9: PCS-2012 PA lower intrusion DBR volume percentile rankings for all replicates and vectors of scenario S5-DBR.

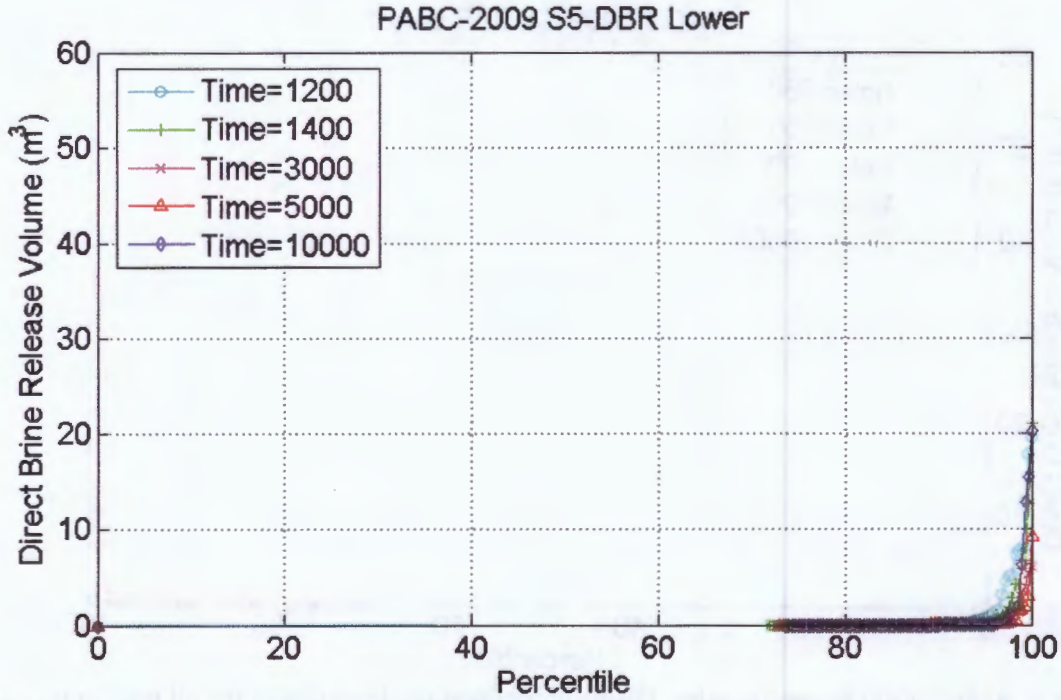

Figure 5-10: PABC-2009 lower intrusion DBR volume percentile rankings for all replicates and vectors of scenario S5-DBR.

Information Only

5.3 Sensitivity of Direct Brine Releases to Input Parameters

Volume averaged brine pressure and brine saturation in the intruded panel are the two most important variables that control DBR volumes (Clayton 2008). The sensitivity of the DBR volumes to these two variables is discussed qualitatively here. For the plots given below, the values of these parameters were extracted from the ALG2 files from the DBR calculations.

Scenarios S2-DBR and S3-DBR have significant DBR volumes because the presence of a previous borehole connecting the repository to the Castile brine reservoir has the general effect of simultaneously increasing the waste panel pressure and brine saturation. The sensitivity analysis presented here focuses on scenarios S2-DBR and S3-DBR because these scenarios have the greatest number of significant DBR volumes. As in previous DBR analyses performed hitherto, scenarios S1-DBR, S4-DBR, and S5-DBR have very few runs with non-zero DBR volumes and are thus excluded from the sensitivity analysis presented herein. Due to the close similarity between scenarios S2-DBR and S3-DBR, only scenario S2-DBR is discussed in the sensitivity analysis.

Volume averaged brine pressure in the intruded panel at the time of the intrusion is an important factor for many vectors. Figure 5-11 and Figure 5-12 show scenario S2-DBR scatter plots of DBR volume versus pressure in the intruded panel at different intrusion times for the case of a lower (down-dip) location of drilling intrusion for the PCS-2012 PA and the PABC-2009, respectively. As prescribed by the conceptual model, there are no DBRs until the brine pressure exceeds the hydrostatic threshold of 8 MPa, indicated in the figures by the vertical line. Above 8 MPa, there is still a significant number of vectors having zero DBR volumes; these vectors have associated mobile brine saturations that are less than zero and thus no brine is available in a mobile form to be released (Clayton et al., 2010). Figure 5-13 and Figure 5-14 show scatter plots of the same data as in Figures 5-11 and 5-12 but for different mobile brine saturation ranges. They show that DBR volumes tend to increase with increasing pressure and increasing mobile brine saturation, the variables to which DBR volumes are historically sensitive.

As the case was with the PABC-2009 results reported in Clayton et al. (2010) and reproduced here in Figures 5-12 and 5-14, the PCS-2012 PA results in Figures 5-11 and 5-13 show a clustering of the data about a linear trend (dashed line in the figures) with a slope of about 8 m^3/MPa and intersecting the pressure axis at 8 MPa. Comparing results in Figure 5-11 to those in Figure 5-13 reveals that the linearity of the clustering is more strongly dependent on mobile brine saturation than it is on intrusion time. The results further indicate that the linearity of the correlation between pressure and DBR volumes increases with increasing mobile brine saturation.

Figure 5-15 and Figure 5-16 are plots of mobile brine saturation versus pressure for the S2-DBR scenario for all intrusion times with symbols indicating the range of DBR volumes, for the PCS-2012 PA and the PABC-2009, respectively. Though these figures do not show any meaningful correlation between mobile brine saturation and brine pressure, they show the general increase in DBR volume with both brine saturation and pressure alluded to above, with only modest differences between the PCS-2012 PA and PABC-2009 results.

Information Only

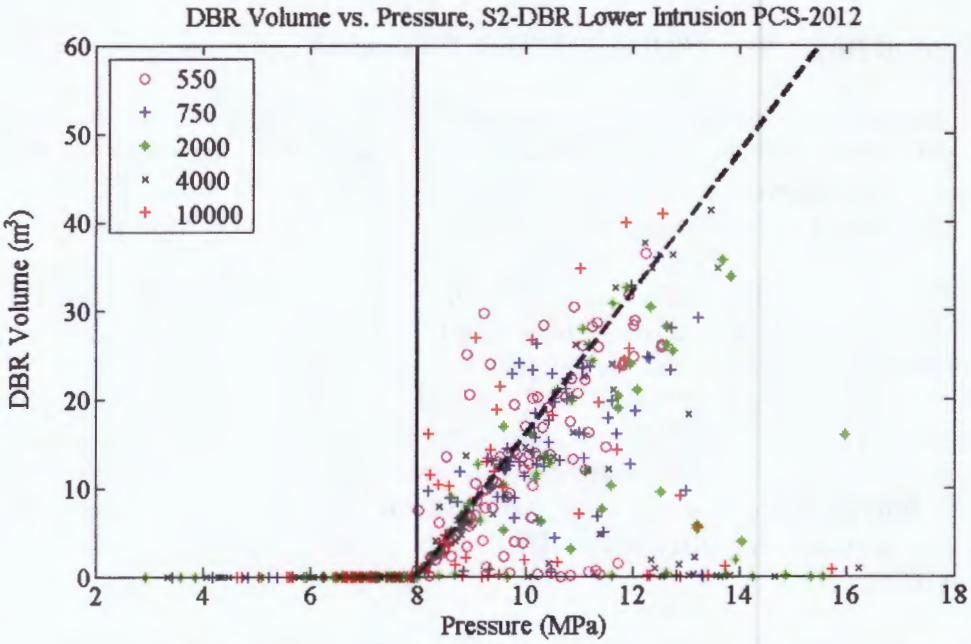

Figure 5-11: Scatter plot of DBR volume versus pressure in the intruded panel for replicate 1, S2-DBR scenario, lower drilling intrusion, PCS-2012 PA. Symbols indicate intrusion times in years.

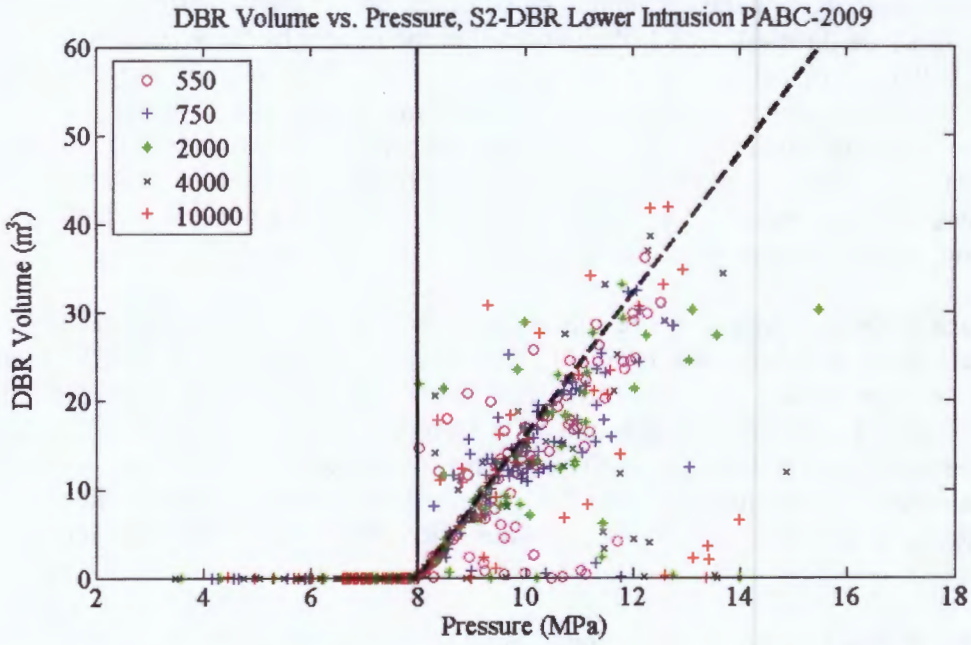

Figure 5-12: Scatter plot of DBR volume versus pressure in the intruded panel for replicate 1, S2-DBR scenario, lower drilling intrusion, PABC-2009. Symbols indicate intrusion times in years.

Information Only

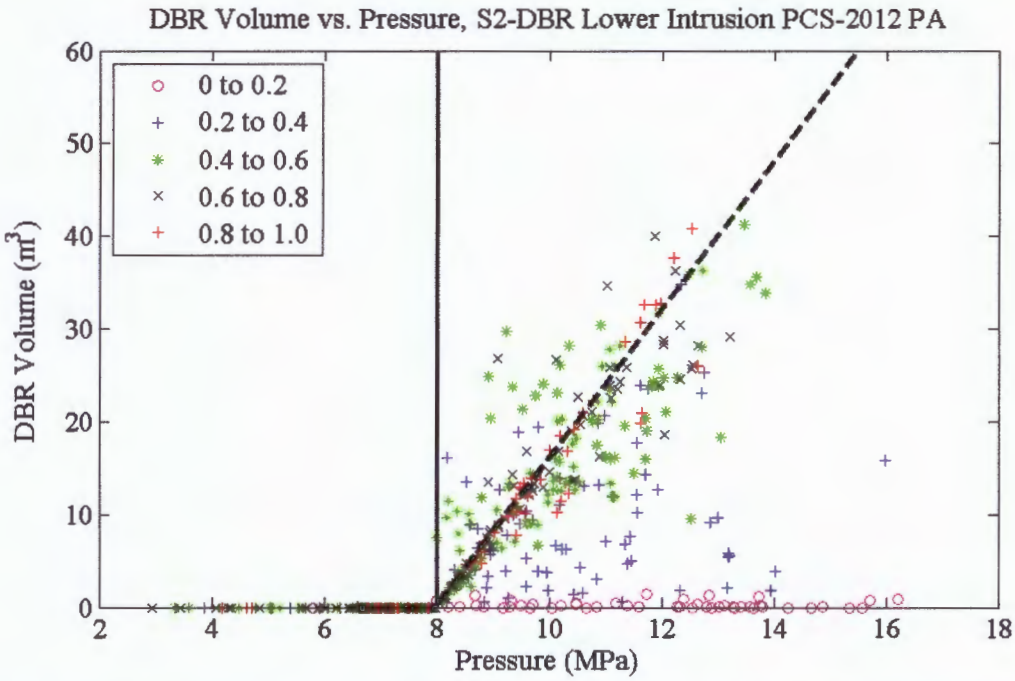

Figure 5-13: Scatter plot of DBR volume versus pressure in the intruded panel for replicate 1, S2-DBR scenario, lower drilling intrusion, PCS-2012 PA. Symbols indicate the range of mobile brine saturation (dimensionless).

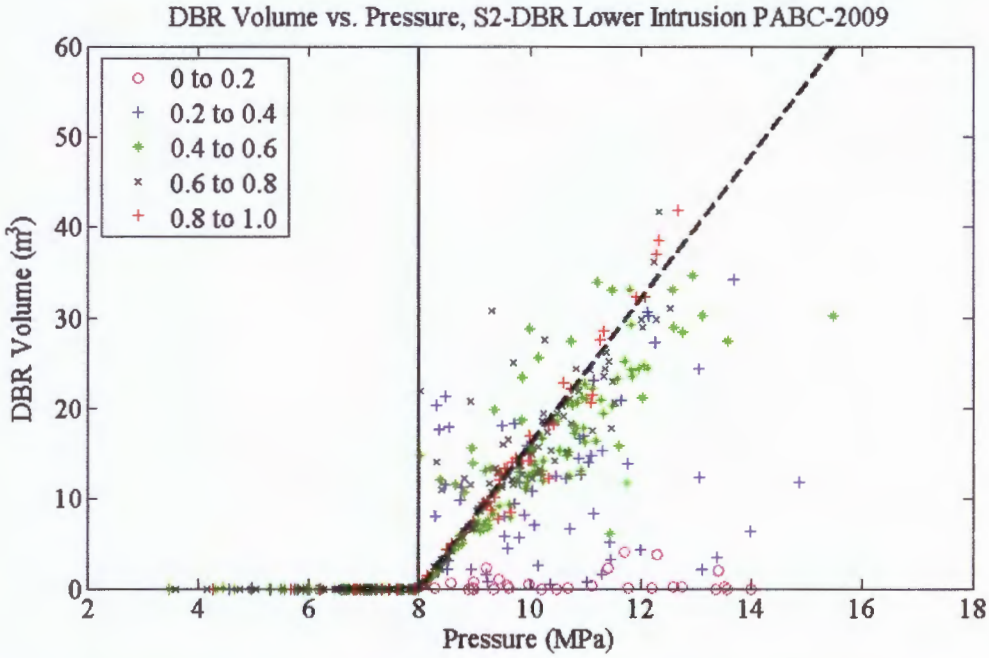

Figure 5-14: Scatter plot of DBR volume versus pressure in the intruded panel for replicate 1, S2-DBR scenario, lower drilling intrusion, PABC-2009. Symbols indicate the range of mobile brine saturation (dimensionless).

Information Only

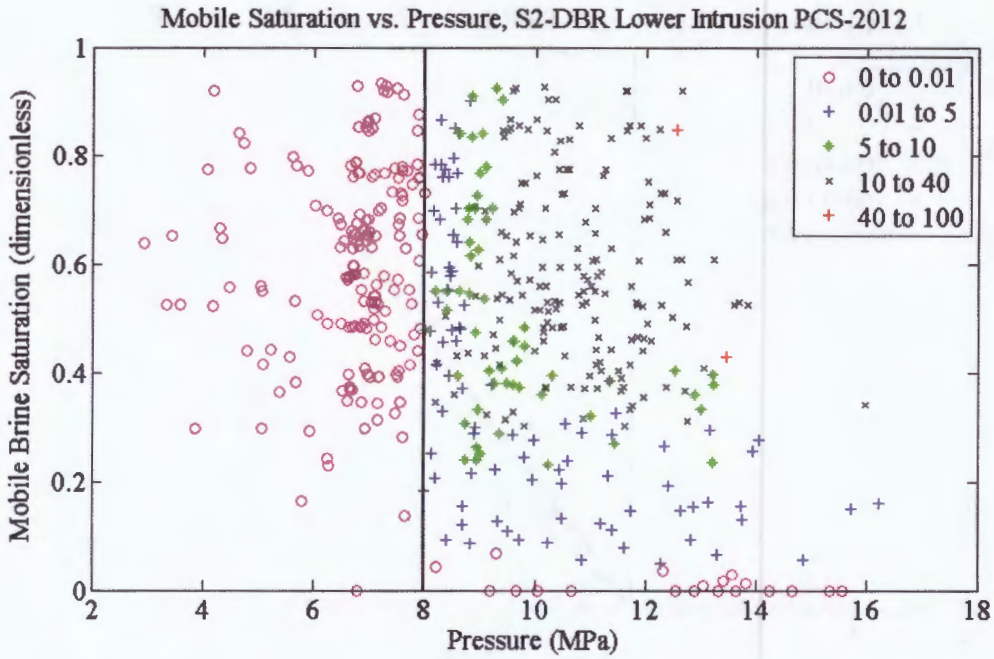

Figure 5-15: Scatter plot of mobile brine saturation versus pressure for replicate 1, S2-DBR scenario, lower drilling intrusion, all intrusion times, PCS-2012 PA. Symbols indicate the range of DBR volumes in m^3.

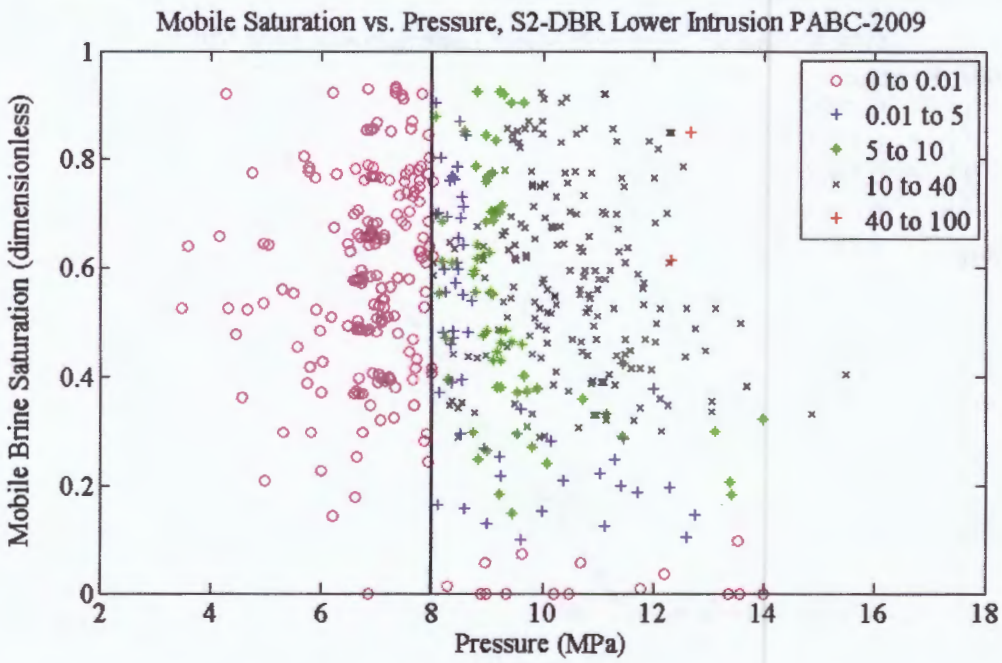

Figure 5-16: Scatter plot of mobile brine saturation versus pressure for replicate 1, S2-DBR scenario, lower drilling intrusion, all intrusion times, PABC-2009. Symbols indicate the range of DBR volumes in m^3.

Information Only

6 CONCLUSIONS

The DBR results from all three replicates of the PCS-2012 PA and PABC-2009 show that direct brine releases to the surface are very unlikely for most intrusions into the repository and in most cases such intrusions result in non-zero but inconsequential DBR volumes. The exception to this statement is for intrusions into a panel that had previously been intruded by an earlier bore hole that had also intruded an underlying pressurized Castile brine reservoir. Such intrusions are represented in PA by the lower drilling intrusions in the scenarios S2-DBR and S3-DBR. Based on a comparison of the results from the PCS-2012 PA to those from the PABC-2009, it is concluded that the PCS-2012 PA maximum DBR volumes are higher for each scenario, the frequency of DBR releases is slightly (almost imperceptibly) higher, and the variability in DBR volumes is higher. As in previous analyses, these results have been explained in terms of the parameters that affect DBR volumes.

7 REFERENCES

Camphouse, R.C. 2012a. Analysis Plan for the 2012 WIPP Panel Closure System Performance Assessment. AP-161, Revision 0. Sandia National Laboratories, Carlsbad, NM. ERMS 557726.

Camphouse, R.C. 2012b. Analysis Package for Salado Flow Modeling Done in the AP-161 (PCS-2012) Performance Assessment. Sandia National Laboratories, Carlsbad, NM. ERMS 558204.

Camphouse, R.C., D.C. Kicker, T.B. Kirchner, J.J. Long, B. Malama, and Zeitler, T.R. 2012. Summary Report and Run Control for the 2012 WIPP Panel Closure System Performance Assessment. Sandia National Laboratories, Carlsbad, NM. (in preparation)

Chappelear, J.E. and A.S. Williamson. 1981. Representing Wells in Numerical Reservoir Simulation. ERMS 249488.

Clayton, D.J. 2008. Analysis Package for Direct Brine Releases: Compliance Recertification Application – 2009. Sandia National Laboratories, Carlsbad, NM. ERMS 548571.

Clayton, D.J. 2010. Analysis Package for Direct Brine Releases: CRA-2009 Performance Assessment Baseline Calculation, Revision 0. Sandia National Laboratories. Carlsbad, NM. ERMS 552829.

Clayton, D.J., R.C. Camphouse, J.W. Garner, A.E. Ismail, T.B. Kirchner, K.L. Kuhlman, and M.B. Nemer. 2010. Summary Report of the CRA-2009 Performance Assessment Baseline Calculation. Sandia National Laboratories, Carlsbad, NM. ERMS 553039.

Hansen, C. W. 2002. Analysis Report for the Panel Closure Impact Assessment. Sandia National Laboratories, Carlsbad, NM. ERMS 523935.

Helton, J.C, J.E. Bean, F.W. Berglund, F.J. Davis, K. Economy, J.W. Garner, J.D. Johnson, R.J. MacKinnon, J. Miller, D.G. O'Brien, J.L. Ramsey, J.D. Schreiber, A. Shinta, L.N. Smith, D.M. Stoelzel, C. Stockman and P. Vaughn. 1998. Uncertainty and Sensitivity Analysis Results Obtained in the 1996 Performance Assessment for the Waste Isolation Pilot Plant. Sandia National Laboratories, Albuquerque, NM. SAND98-0365, ERMS 252619.

Information Only

Kirkes, G.R. 2011. Features, Events and Processes Assessment for Changes Described in Analysis Plan – 151, Revision 0. Sandia National Laboratories, Carlsbad, NM. ERMS 555237

Lee, J. 1982. Well Testing. SPE Textbook Series Vol. 1. New York, NY: Society of Petroleum Engineers of AIME.

Mattax, C.C. and R.L. Dalton. 1990. Reservoir Simulation. Henery L. Doherty Memorial Fund Society of Petroleum Engineers Inc., Richardson, TX.

Nemer, M.B. 2010. Analysis Package for Salado Flow Modeling: CRA-2009 Performance Assessment Baseline Calculation. Sandia National Laboratories. Carlsbad, NM. ERMS 552956

Pasch, J. and C. Camphouse, 2011. Analysis Package for Direct Brine Releases: Panel Closure Redesign and Repository Reconfiguration Performance Assessment (PC3R PA), Revision 0. Sandia National Laboratories. Carlsbad, NM. ERMS 555249.

Stoelzel, D.M. and D.G. O'Brien. 1996. Conceptual Model Description of BRAGFLO Direct Brine Release Calculations to Support the Compliance Certification Application (CCA MASS Attachment 16-2). U.S. Department of Energy, Carlsbad, NM. ERMS 239090.

U.S. Environmental Protection Agency (EPA). 1998. 40 CFR 194, Criteria for the Certification and Recertification of the Waste Isolation Pilot Plant's Compliance with the Disposal Regulations: Certification Decision: Final Rule. Federal Register, Vol. 63, 27354-27406. ERMS 251924.

U.S. Environmental Protection Agency (EPA). 2010. 40 CFR Part 194 Criteria for the Certification and Recertification of the Waste Isolation Pilot Plant's Compliance With the Disposal Regulations: Recertification Decision, Federal Register No. 222, Vol. 75, pp. 70584-70595, November 18, 2010.

Vugrin, E.D. and S.C. Dunagan. 2006. Analysis Package for the Impact Assessment of the Redesigned WIPP Panel Closure. Sandia National Laboratories, Carlsbad, NM. ERMS 543865.

Information Only

558337

Sandia National Laboratories

Waste Isolation Pilot Plant

CCDFGF Analysis Package for the AP-161 (PCS-2012) Performance Assessment

Revision 0

Author:	Todd R. Zeitler		10/11/2012
	Print	Signature	Date
Technical Review:	Thomas Kirchner		10/11/12
	Print	Signature	Date
QA Review:	Shelly Nielsen		10-15-12
	Print	Signature	Date
Management Review:	Sean Dunagan		10/11/12
	Print	Signature	Date

WIPP:1.4.1.2:PA:QA-L:557393

Information Only

Contents

1 INTRODUCTION 4

2 METHODOLOGY 5
2.1 Code Version 6
2.2 Random Seed in the CCDFGF Control Files 6
2.3 Run Control 6

3 ANALYSIS AND RESULTS 7
3.1 Cuttings and Cavings Normalized Releases 7
3.2 Spallings Normalized Releases 12
3.3 Normalized Direct Brine Releases 17
3.4 Normalized Transport Releases to the Culebra 22
3.5 Total Normalized Releases 24

4 SUMMARY 28

5 REFERENCES 29

Information Only

List of Figures

Figure 3-1: PC3R PA Replicate 1 Cuttings and Cavings Normalized Releases 8
Figure 3-2: PCS-2012 PA Replicate 2 Cuttings and Cavings Normalized Releases 8
Figure 3-3: PCS-2012 PA Replicate 3 Cuttings and Cavings Normalized Releases 9
Figure 3-4: PCS-2012 PA Mean and Quantile CCDFs for Cuttings and Cavings Normalized Releases, Replicates 1-3 9
Figure 3-5: PCS-2012 PA Confidence Limits on Overall Mean for Cuttings and Cavings Normalized Releases 10
Figure 3-6: PCS-2012 PA and PABC-2009 Overall Mean CCDFs for Normalized Cuttings and Cavings Releases 10
Figure 3-7: PCS-2012 PA and PABC-2009 Overall Mean CCDFs for Normalized Cuttings and Cavings Volumes 11
Figure 3-8: PCS-2012 PA Replicate 1 Spallings Normalized Releases 13
Figure 3-9: PCS-2012 PA Replicate 2 Spallings Normalized Releases 13
Figure 3-10: PCS-2012 PA Replicate 3 Spallings Normalized Releases 14
Figure 3-11: PCS-2012 PA Mean and Quantile CCDFs for Spallings Normalized Releases, Replicates 1-3 14
Figure 3-12: PCS-2012 PA Confidence Limits on Overall Mean for Spallings Normalized Releases 15
Figure 3-13: PCS-2012 PA and PABC-2009 Overall Mean CCDFs for Normalized Spallings Releases 15
Figure 3-14: PCS-2012 PA and PABC-2009 Overall Mean CCDFs for Spallings Volumes 16
Figure 3-15: PCS-2012 PA Replicate 1 Normalized Direct Brine Releases 18
Figure 3-16: PCS-2012 PA Replicate 2 Normalized Direct Brine Releases 18
Figure 3-17: PCS-2012 PA Replicate 3 Normalized Direct Brine Releases 19
Figure 3-18: PCS-2012 PA Mean and Quantile CCDFs for Normalized Direct Brine Releases, Replicates 1-3 19
Figure 3-19: PCS-2012 PA Confidence Limits on Overall Mean for Normalized Direct Brine Releases 20
Figure 3-20: PCS-2012 PA and PABC-2009 Overall Mean CCDFs for Normalized Direct Brine Releases 20
Figure 3-21: PCS-2012 PA and PABC-2009 Overall Mean CCDFs for Direct Brine Volumes 21
Figure 3-22: PCS-2012 PA and PABC-2009 Replicate Means for Normalized Transport Releases to the Culebra 23
Figure 3-23: PCS-2012 PA and PABC-2009 Overall Mean CCDFs for Transport Releases to the Culebra 23
Figure 3-24: PCS-2012 PA Replicate 1 Total Normalized Releases 25
Figure 3-25: PCS-2012 PA Replicate 2 Total Normalized Releases 25
Figure 3-26: PCS-2012 PA Replicate 3 Total Normalized Releases 26
Figure 3-27: PCS-2012 PA Mean and Quantile CCDFs for Total Normalized Releases, Replicates 1-3 26
Figure 3-28: PCS-2012 PA Confidence Limits on Overall Mean for Total Normalized Releases 27
Figure 3-29: PCS-2012 PA and PABC-2009 Overall Mean CCDFs for Total Normalized Releases 27
Figure 3-30: PCS-2012 PA Primary Components Contributing to Total Releases 28

List of Tables

Table 1: PCS-2012 PA and PABC-2009 Statistics on the Overall Mean for Total Normalized Releases in EPA Units at Probabilities of 0.1 and 0.001 24

Information Only

1 INTRODUCTION

The Waste Isolation Pilot Plant (WIPP), located in southeastern New Mexico, has been developed by the U.S. Department of Energy (DOE) for the geologic (deep underground) disposal of transuranic (TRU) waste. Containment of TRU waste at the WIPP is regulated by the U.S. Environmental Protection Agency (EPA) according to the regulations set forth in Title 40 of the Code of Federal Regulations (CFR), Part 191. The DOE demonstrates compliance with the containment requirements according to the Certification Criteria in Title 40 CFR Part 194 by means of performance assessment (PA) calculations performed by Sandia National Laboratories (SNL). WIPP PA calculations estimate the probability and consequence of potential radionuclide releases from the repository to the accessible environment for a regulatory period of 10,000 years after facility closure. The models used in PA are maintained and updated with new information as part of an ongoing process. Improved information regarding important WIPP features, events, and processes typically results in refinements and modifications to PA models and the parameters used in them. Planned changes to the repository and/or the components therein also result in updates to WIPP PA models. WIPP PA models are used to support the repository recertification process that occurs at five-year intervals following the receipt of the first waste shipment at the site in 1999.

Waste panel closures comprise a repository feature that has been represented in WIPP PA since the original Compliance Certification Application (CCA) of 1996. Panel closures are included in WIPP PA models principally because they are a part of the disposal system, not because they play a substantive role in inhibiting the release of radionuclides to the outside environment. The DOE stated in the CCA (DOE 1996) that *"The panel closure system was not designed or intended to support long-term repository performance."* The 1998 rulemaking that certified WIPP to receive transuranic waste placed conditions on the panel closure design to be implemented in the repository. The mandated design consists of a concrete block wall, an open drift section, and a concrete monolith, and was termed the "Option D" panel closure. Following the selection of the Option D design in 1998, the engineering of the panel closure has been re-assessed, and a revised design has been established that is simpler, cheaper, and easier to construct. The revised panel closure design, termed the Run-of-Mine Panel Closure System (ROMPCS), is comprised of 100 feet of ROM salt with barriers at each end. The ROM salt is generated from ongoing mining operations at the WIPP and may be compacted and/or moistened as it is emplaced in a panel entry. The barriers consist of ventilation bulkheads, similar to those currently used in the panels as room closures.

The DOE has submitted a planned change request (PCR) to the EPA requesting that EPA modify Condition 1 of the Final Certification Rulemaking for 40 CFR Part 194 (EPA, 1998) for the WIPP. The PCR submitted to EPA requests that Condition 1 be changed, and that the ROMPCS design be approved for use in all panels (DOE, 2011). In support of this rulemaking change, a performance assessment has been completed that incorporates the ROMPCS design into the current PA baseline established by the 2009 Performance Assessment Baseline Calculation (PABC-2009) (Clayton et al., 2010). The name given to this new panel closure PA is PCS-2012, and the plan for its execution is detailed in AP-161 (Camphouse 2012a). PCS-2012 PA results are compared to those obtained in the PABC-2009 as a means to quantify potential impacts due

Information Only

to the panel closure redesign. This analysis package consists of the CCDFGF component of the PCS-2012 PA.

2 METHODOLOGY

The performance assessment methodology accommodates both aleatory (i.e. stochastic) and epistemic (i.e. subjective) uncertainty in its constituent models. Aleatory uncertainty pertains to unknowable future events such as intrusion times and locations that may affect repository performance. It is accounted for by the generation of random sequences of future events. Epistemic uncertainty concerns parameter values that are assumed to be constants and the constants' true values are uncertain due to a lack of knowledge about the system. An example of a parameter with epistemic uncertainty is the permeability of a material. Epistemic uncertainty is accounted for by sampling of parameter values from assigned distributions. One set of sampled values required to run a WIPP PA calculation is termed a vector. The performance assessment models are executed for three replicates of 100 vectors, each vector being a realization resulting from a particular set of parameter values. A sample size of 10,000 possible sequences of future events is used in the calculations to estimate an exceedance probability of 0.001 (Helton et al. 1998). The releases for each of 10,000 possible sequences of future events are tabulated for each of the 300 vectors, totaling 3,000,000 possible sequences.

For a random variable, the complementary cumulative distribution function (CCDF) provides the probability of the variable being greater than a particular value. By regulation, performance assessment results are presented as a distribution of CCDFs of releases (U.S. EPA 1996). Each individual CCDF summarizes the likelihood of releases across all futures for one vector of parameter values. The uncertainty in parameter values results in a distribution of CCDFs.

Releases are quantified in terms of "EPA units". Releases in EPA units result from a normalization by radionuclide and the total inventory. For each radionuclide, the ratio of its 10,000 year cumulative release (in curies) to its release limit is calculated. The sum of these ratios is calculated across the set of radionuclides and normalized by the transuranic inventory (in curies) of α-emitters with half-lives greater than 20 years. Mathematically, the formula used to calculate releases in terms of EPA units is of the form

$$R = \frac{1 \times 10^6\, curies}{C} \sum_i \frac{Q_i}{L_i}$$

where R is the normalized release in EPA units. Quantity Q_i is the 10,000 year cumulative release (in curies) of radionuclide i. Quantity L_i is the release limit for radionuclide i, and C is the total transuranic inventory (in curies) of α-emitters with half-lives greater than 20 years.

Mean and quantile CCDFs are calculated to compare the distributions of CCDFs among replicates and to demonstrate sufficiency of sample size. At each value of normalized release R on the horizontal axis, the CCDFs for a single replicate define 100 values of probability. Forming the arithmetic mean of these 100 probabilities yields the mean probability that the release exceeds R. The curve defined by the mean probabilities for each value of R is the mean

Information Only

CCDF. The 10th and 90th quantile CCDFs for a particular replicate are determined from the sorted order of the 100 CCDFs found for that replicate.

The overall mean CCDF is computed as the arithmetic mean of the three mean CCDFs from each replicate. Confidence limits are computed about the overall mean CCDF using the Student's t-distribution, the mean CCDFs from each replicate, and the standard error based on the three replicate means. Confidence limits as they are implemented in PA are defined vertically about the mean, rather than horizontally. An artifact of this convention is that lower confidence limits can sometimes assume negative values, which cannot be plotted on a logarithmic scale. When this occurs, the resulting lower confidence curve appears incomplete.

CCDF curves and statistics are generated using the CCDFGF_Analysis database utility. A description of this utility can be found in Kirchner (2010). A DVD containing the data loaded into this utility resulting from PCS-2012 PA and PABC-2009 CCDFGF calculations, and subsequent SigmaPlot plots, are included as an attachment to this document.

2.1 Code Version

PRECCDFGF version 1.01 and CCDFGF version 5.02 were used for the PABC-2009 and the PCS-2012.

2.2 Random Seed in the CCDFGF Control Files

One of the features that the CCDFGF control file initializes is the random number generator in the code. Setting the random number seed in the control file determines the sequence of pseudo-random numbers used by CCDFGF. This sequence of numbers affects several stochastic parameters, such as the drilling location, depth, and type of plugging pattern, utilized when CCDFGF simulates the drilling of boreholes at the surface of the WIPP repository.

For the PCS-2012 PA, the same random seeds for CCDFGF were used as in the PABC-2009. This was done to allow a vector by vector comparison of the results of the PCS-2012 PA to those obtained in the PABC-2009. As the random seeds used to initialize the sampling of the epistemic parameters were unchanged in the PCS-2012 PA and the PABC-2009, any differences between the analyses can be attributed solely to the changes in parameters and geometry used in those calculations. Random seeds used in the PCS-2012 PA calculations are specified in the files CCGF_AP161_CONTROL_Rr.inp, where r = 1, 2, 3. These files are located in CMS library LIBAP161_CCGF.

2.3 Run Control

Run control, including code versions used and descriptions of code sequencing used to obtain CCDFGF results in the PCS-2012 PA, is documented in Camphouse et al. (2012c). PCS-2012 PA results generated by code CCDFGF have file names CCGF_AP161_Rr.OUT, where r (the replicate number) equals 1, 2, or 3. These files are located in CMS library LIBAP161_CCGF under class AP161-0. PABC-2009 results generated by CCDFGF have file names

Information Only

CCGF_PABC09_Rr.OUT, and are located in CMS library LIBPABC09_CCGF under class PABC09-0.

3 ANALYSIS AND RESULTS

Results obtained from PCS-2012 PA calculations are broken out in subsections for each component of release. At the conclusion of the subsection for each release component, results obtained for the PCS-2012 PA are compared to those found in the PABC-2009. Normalized releases for cuttings and cavings are discussed in Subsection 3.1. Spallings releases are presented in Subsection 3.2. Results found for direct brine releases are discussed in Subsection 3.3. New calculations for normalized transport releases through the Culebra were not performed as part of the PCS-2012 PA. BRAGFLO scenario S6-BF is used by PA code PANEL to determine the radionuclide source term to the Culebra. BRAGFLO scenario S6-BF results obtained in the PCS-2012 PA are virtually identical to those calculated in the PABC-2009 (Camphouse 2012b). Consequently, the radionuclide source term to the Culebra is unaffected by the change of the panel closure design from Option D to the ROMPCS. There have been no updates to the Culebra flow model, e.g. updated transmissivity fields, since the completion of the PABC-2009. As a result, it is reasonable and appropriate to incorporate Culebra transport results calculated in the PABC-2009 into the PCS-2012 PA.

Total normalized releases are shown in Subsection 3.5.

3.1 Cuttings and Cavings Normalized Releases

The change in panel closure design from Option D to the ROMPCS has no impact on cuttings and cavings releases. PA code CUTTINGS_S calculates cuttings and cavings release volumes, as well as spallings volumes. Spallings release volumes are potentially impacted by the panel closure redesign, and so are calculated as part of the PCS-2012 PA. As a result, cuttings and cavings releases are also calculated, even though they are identical to those obtained in the PABC-2009.

PCS-2012 PA cuttings and cavings releases are presented in this section and subsequently compared to results obtained in the PABC-2009. Figure 3-1, Figure 3-2, and Figure 3-3 contain PCS-2012 PA cuttings and cavings release CCDFs for replicates 1, 2, and 3, respectively. Mean and quantile CCDF distributions for the three replicates are shown together in Figure 3-4. As seen in that figure, the mean and quantile CCDFs obtained for the three replicates are nearly coincident. Figure 3-5 contains the 95 percent confidence limits about the overall cuttings and cavings mean. As is clear in that figure, the confidence limit is very tightly contained about the mean at all probabilities.

For the sake of reference, overall means of cuttings and cavings releases calculated in the PCS-2012 PA and the PABC-2009 are plotted simultaneously in Figure 3-6 and Figure 3-7. As seen in those figures, cuttings and cavings releases and volumes obtained for both analyses were identical as no changes were made to the underlying models or parameters used in their calculation for the PCS-2012 PA (Kicker 2012).

Information Only

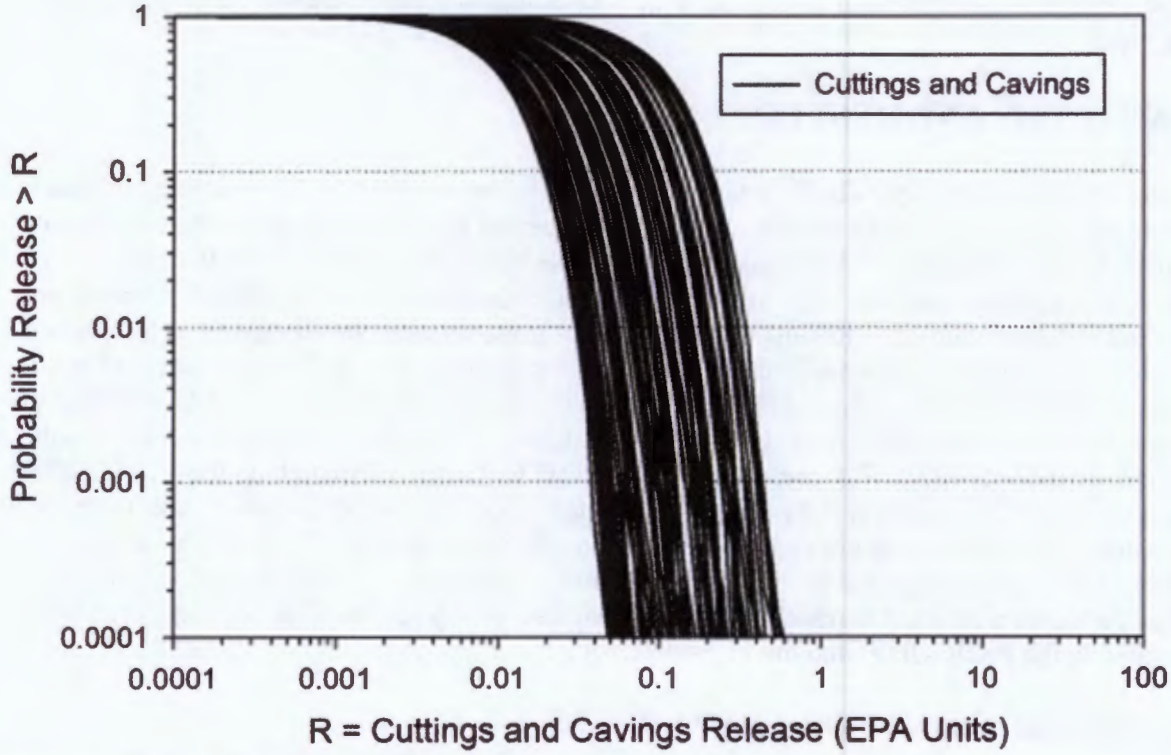

Figure 3-1: PCS-2012 PA Replicate 1 Cuttings and Cavings Normalized Releases

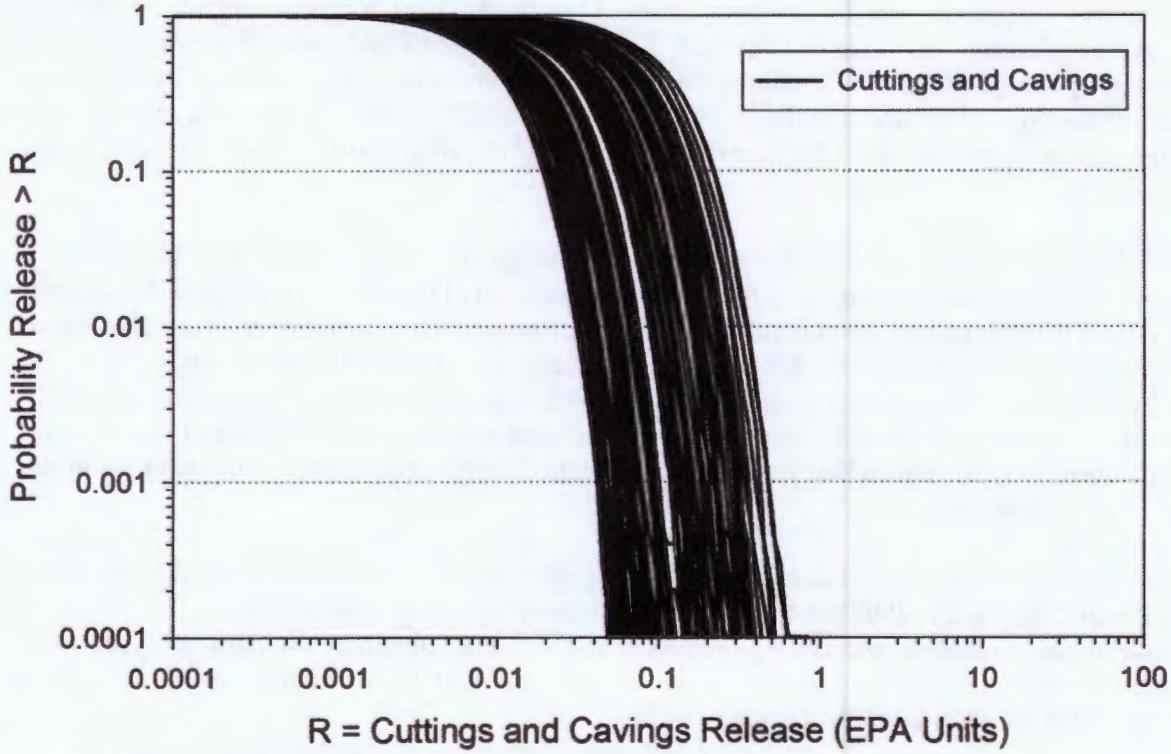

Figure 3-2: PCS-2012 PA Replicate 2 Cuttings and Cavings Normalized Releases

Information Only

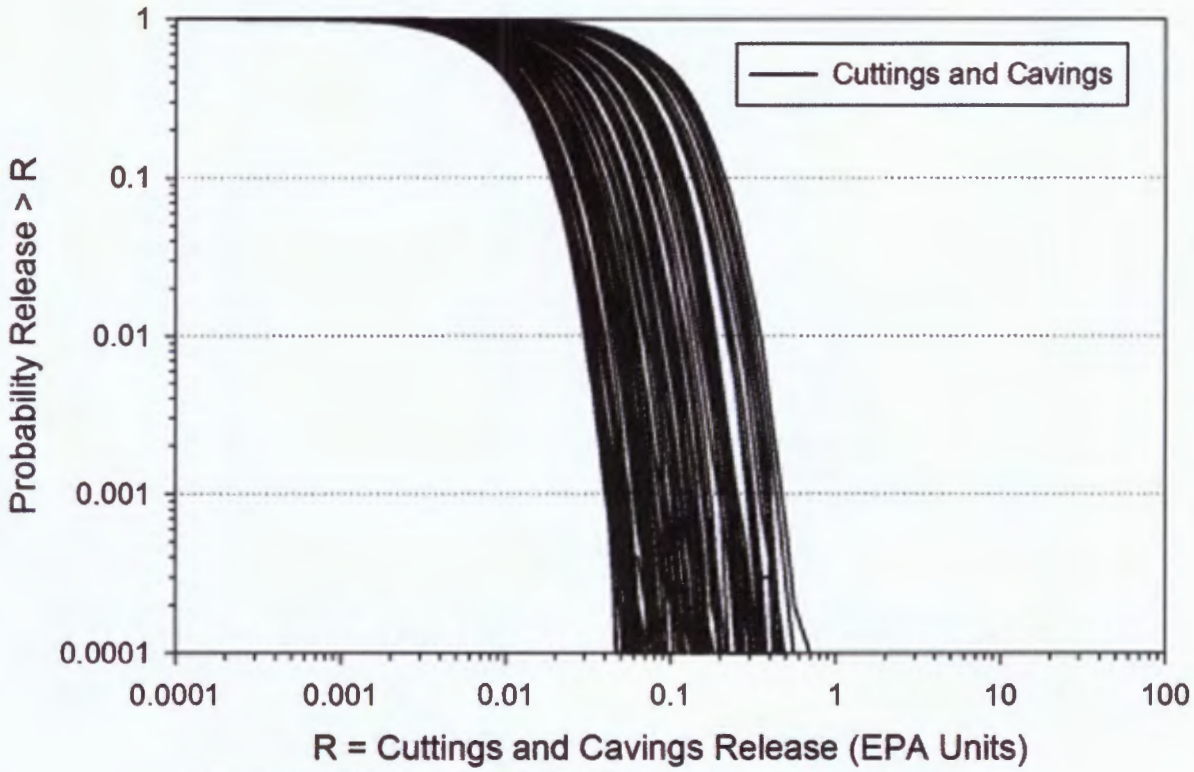

Figure 3-3: PCS-2012 PA Replicate 3 Cuttings and Cavings Normalized Releases

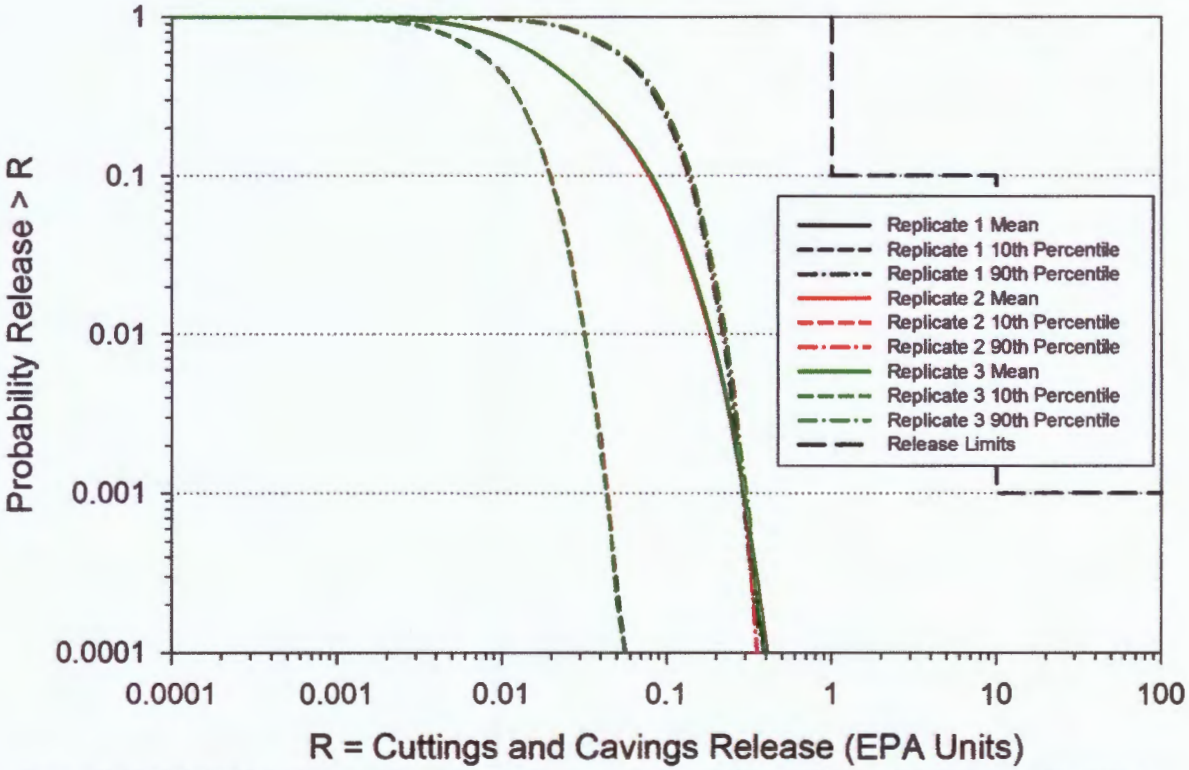

Figure 3-4: PCS-2012 PA Mean and Quantile CCDFs for Cuttings and Cavings Normalized Releases, Replicates 1-3

Information Only

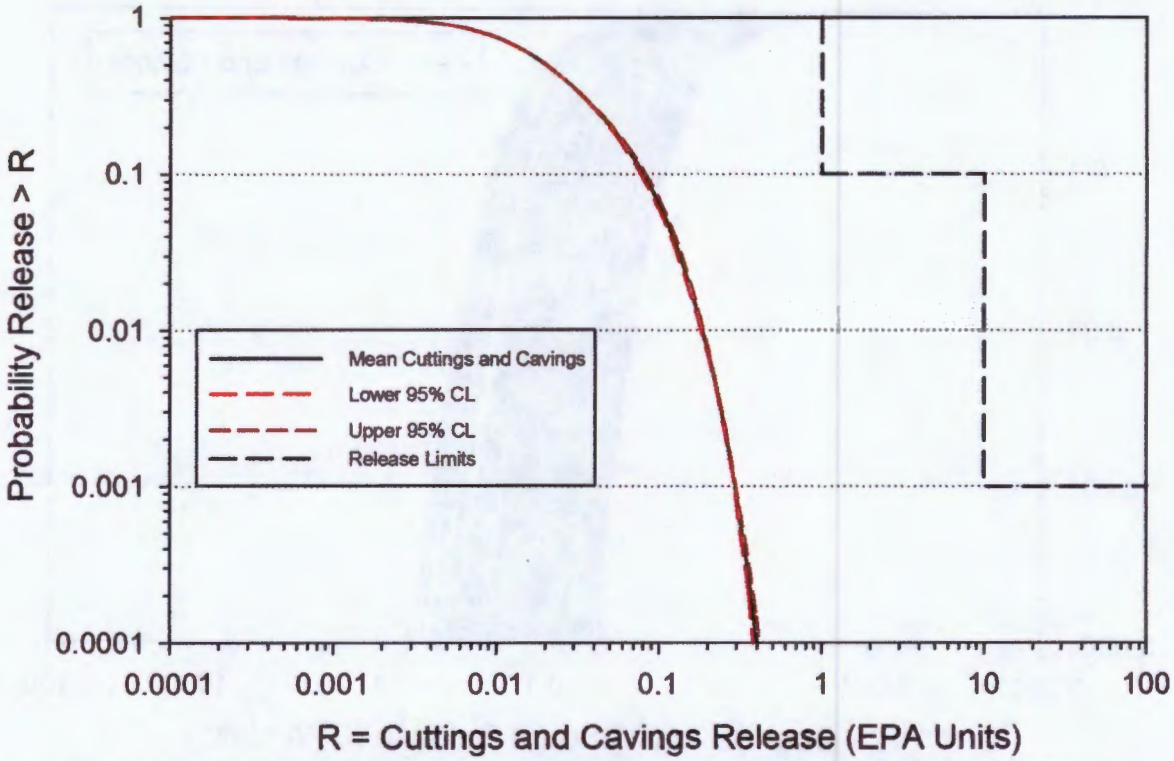

Figure 3-5: PCS-2012 PA Confidence Limits on Overall Mean for Cuttings and Cavings Normalized Releases

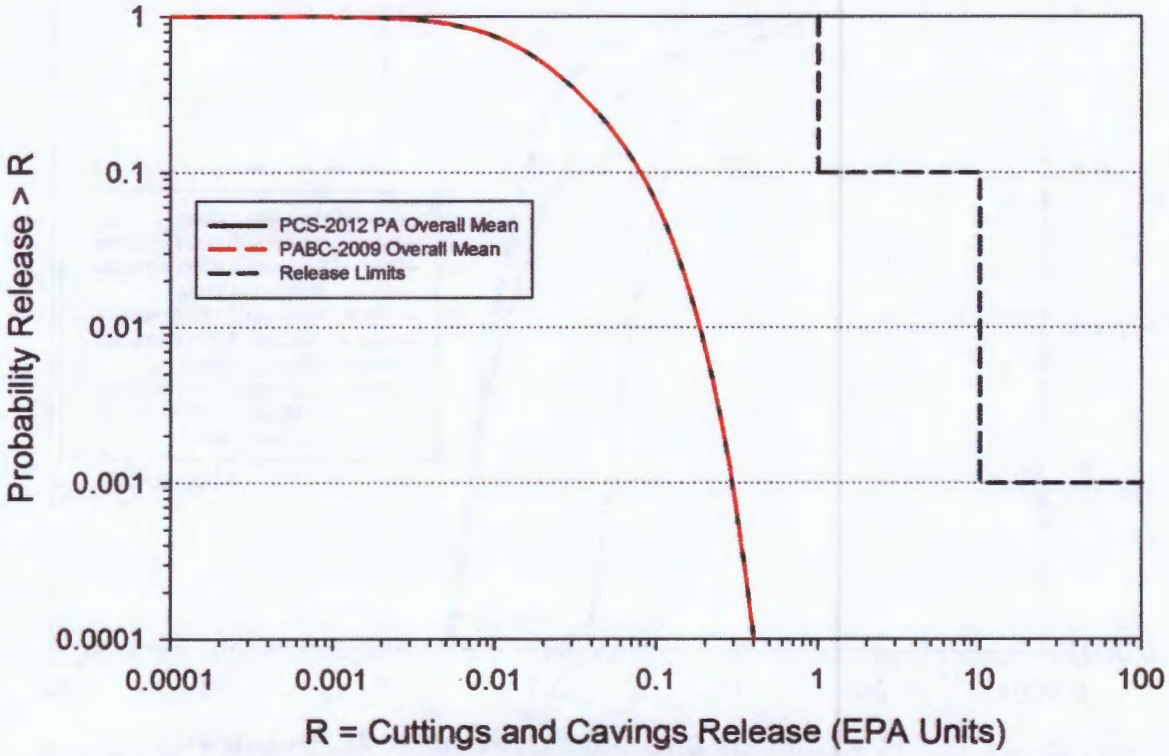

Figure 3-6: PCS-2012 PA and PABC-2009 Overall Mean CCDFs for Normalized Cuttings and Cavings Releases

Information Only

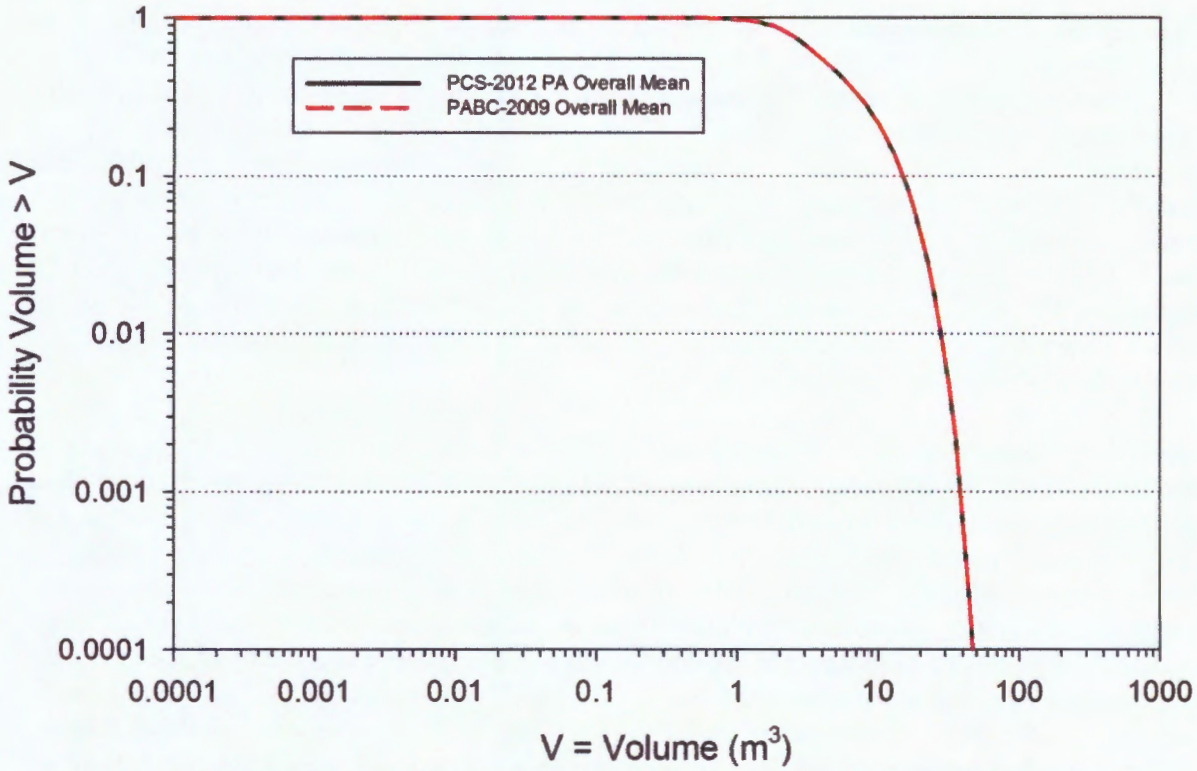

Figure 3-7: PCS-2012 PA and PABC-2009 Overall Mean CCDFs for Normalized Cuttings and Cavings Volumes

Information Only

3.2 Spallings Normalized Releases

PCS-2012 PA spallings releases are presented in this section and subsequently compared to results obtained in the PABC-2009. Figure 3-8, Figure 3-9, and Figure 3-10 contain PCS-2012 PA CCDFs for spallings releases. Mean and quantile CCDF distributions for the three replicates are shown together in Figure 3-11. As seen in that figure, the 10th percentiles for each replicate have releases sufficiently small as to not appear at all on the chosen axes. Moreover, the mean CCDF for each replicate becomes larger than the 90th percentile as releases increase. The large number of vectors with very small spallings releases causes the distribution to be heavily right-skewed. This results in a mean that exceeds the 90th percentile as releases increase. Figure 3-12 contains the 95 percent confidence limits about the spallings mean. In total, 38 % of the replicate 1 vector, 47 % of the replicate 2 vectors and 41 % of the replicate 3 vectors in the PCS-2012 PA showed non-zero spallings releases

To facilitate comparisons of spallings releases calculated in the PCS-2012 PA to those obtained in the PABC-2009, overall mean and volume CCDFs obtained in these two analyses are plotted simultaneously in Figure 3-13 and Figure 3-14. As seen in those figures, the PCS-2012 PA CCDF curves shown in Figure 3-13 and Figure 3-14 show increases in spallings releases and volumes when compared to PABC-2009 results. Spallings volumes, and their associated releases, are a function of repository pressure. A pressure increase in an intruded waste panel typically corresponds to an increase in spallings volumes. As nothing was changed regarding the waste inventory used in the PABC-2009 and the PCS-2012 PA, an increase in spallings volume results in an associated increase in spallings releases. The ROMPCS design implemented in the PCS-2012 PA has slightly lower long-term permeabilities (on average) than the Option D closures implemented in the PABC-2009. For intrusion scenarios that involve an encounter with a pressurized brine region below the repository, the reduction in closure permeability resulted in an increase in pressurization of the waste panel for a period of time following the intrusion. This increase in pressure translates directly to increases in PCS-2012 PA spallings volumes and releases as compared to the PABC-2009 results. For intrusion scenarios that do not involve an encounter with a region of pressurized brine below the repository, the mean average pressure in the intruded waste panel was higher in the PCS-2012 PA as compared to the PABC-2009. This increase in pressure also yields increases in spallings volumes and their associated releases. Increased pressure in repository waste areas is responsible for the increases seen in PCS-2012 PA spallings volumes and releases as compared to the PABC-2009 results (Kicker 2012).

Information Only

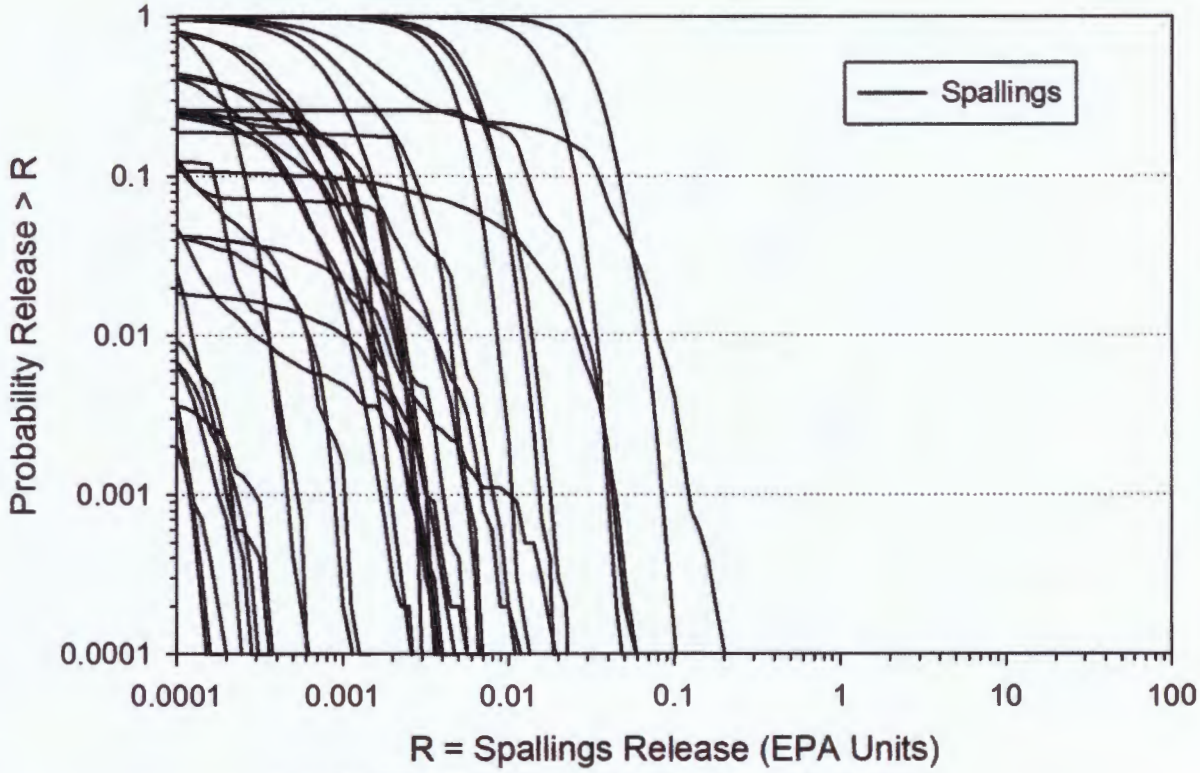

Figure 3-8: PCS-2012 PA Replicate 1 Spallings Normalized Releases

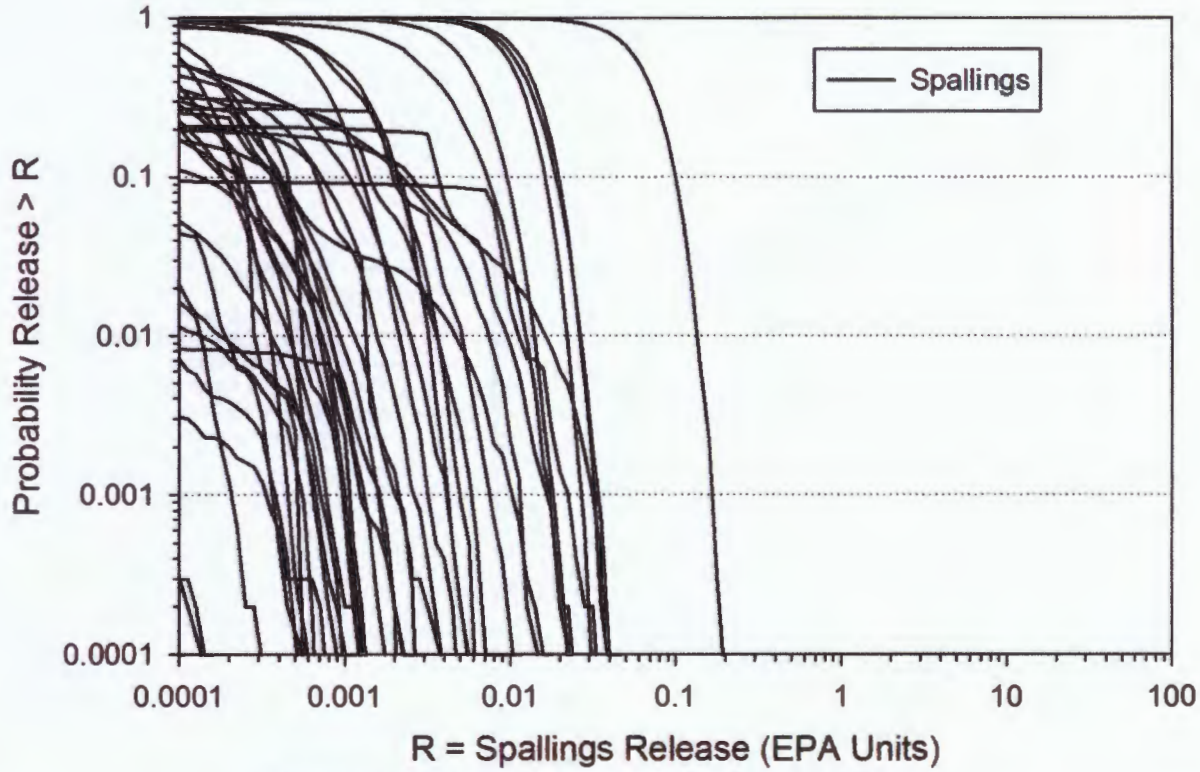

Figure 3-9: PCS-2012 PA Replicate 2 Spallings Normalized Releases

Information Only

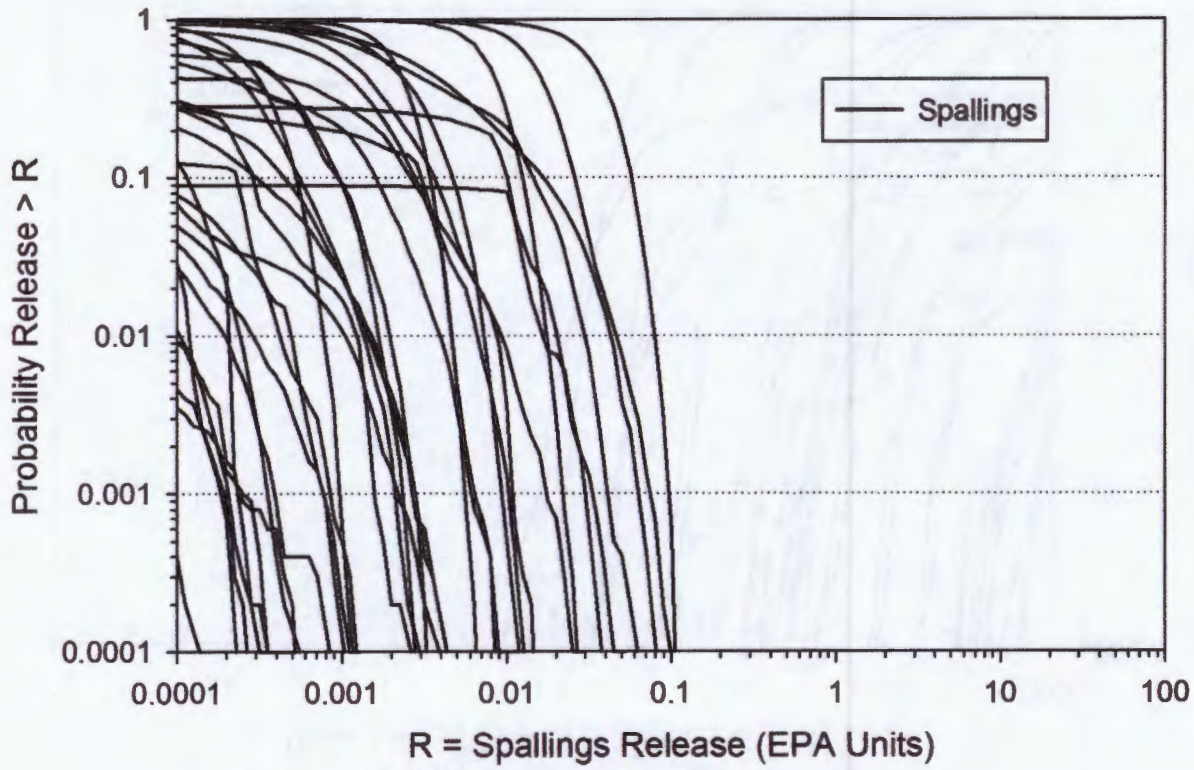

Figure 3-10: PCS-2012 PA Replicate 3 Spallings Normalized Releases

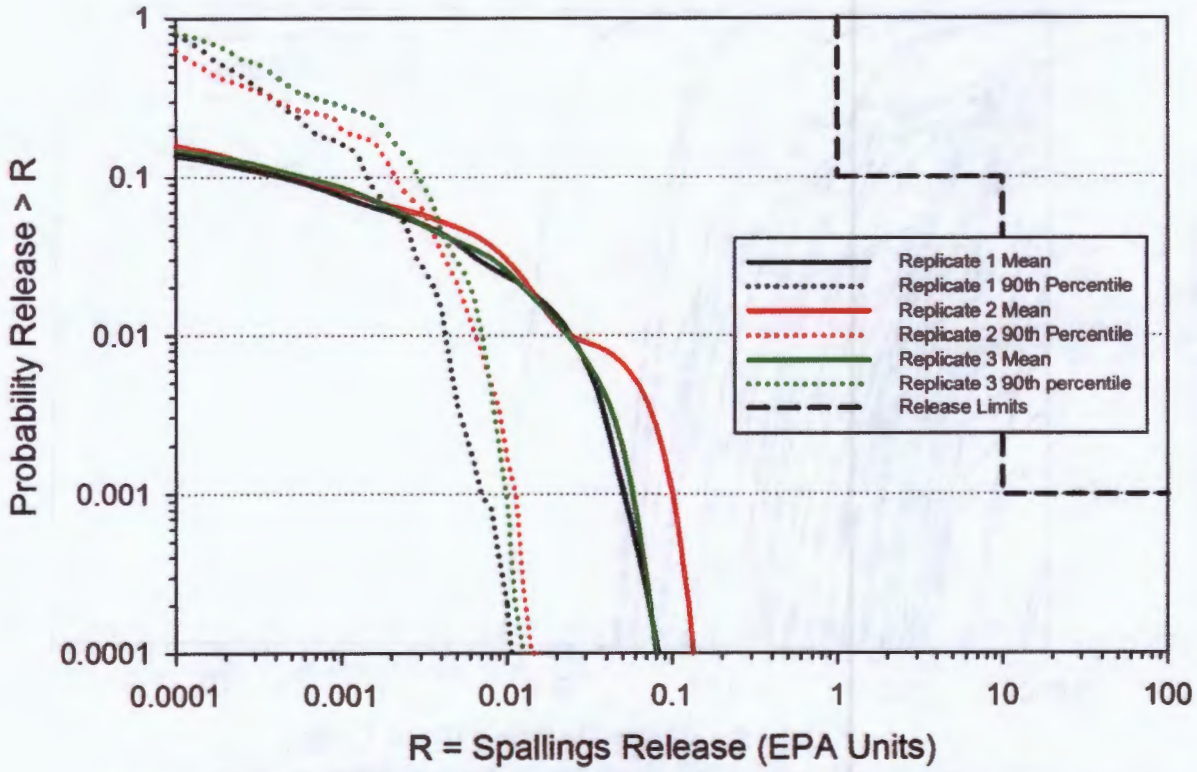

Figure 3-11: PCS-2012 PA Mean and Quantile CCDFs for Spallings Normalized Releases, Replicates 1-3

Information Only

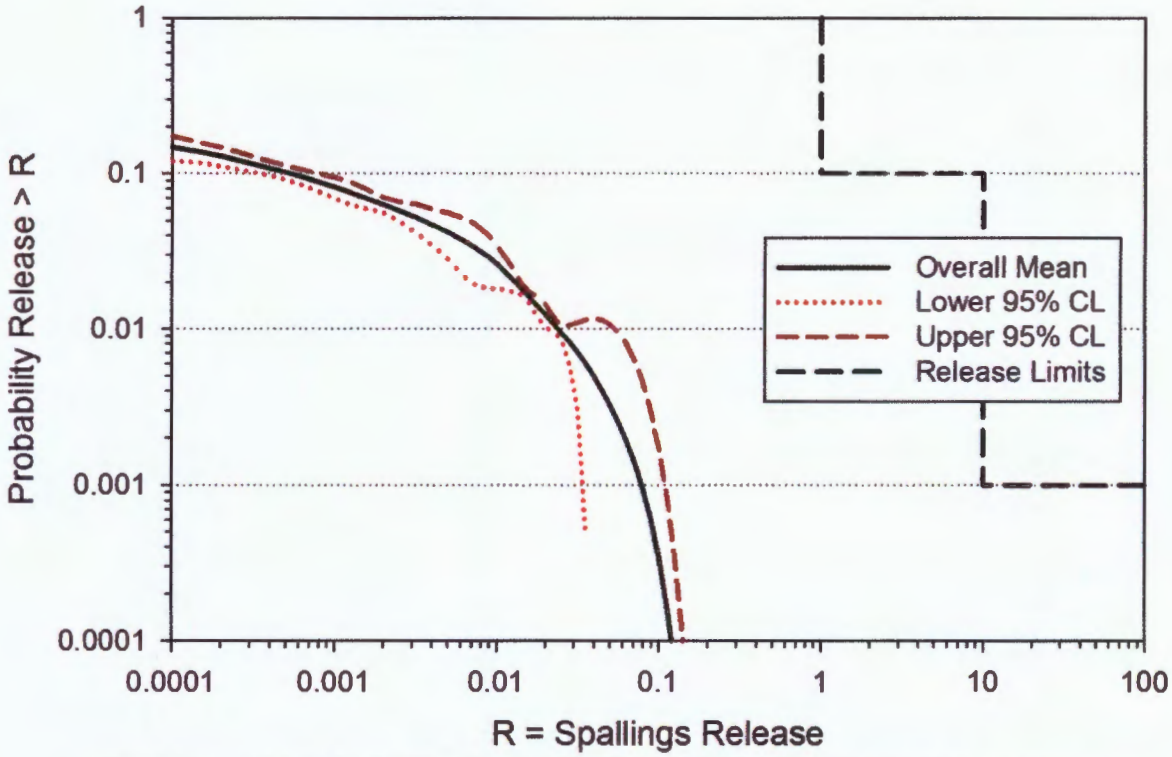

Figure 3-12: PCS-2012 PA Confidence Limits on Overall Mean for Spallings Normalized Releases

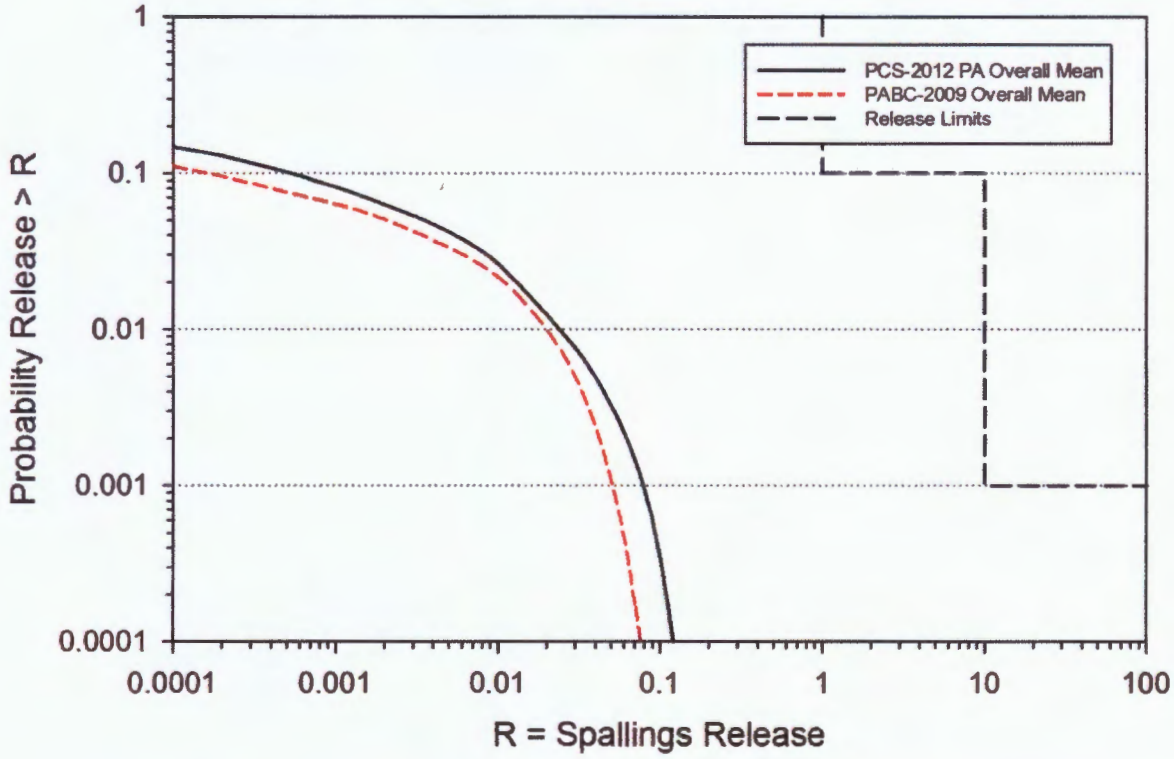

Figure 3-13: PCS-2012 PA and PABC-2009 Overall Mean CCDFs for Normalized Spallings Releases

Information Only

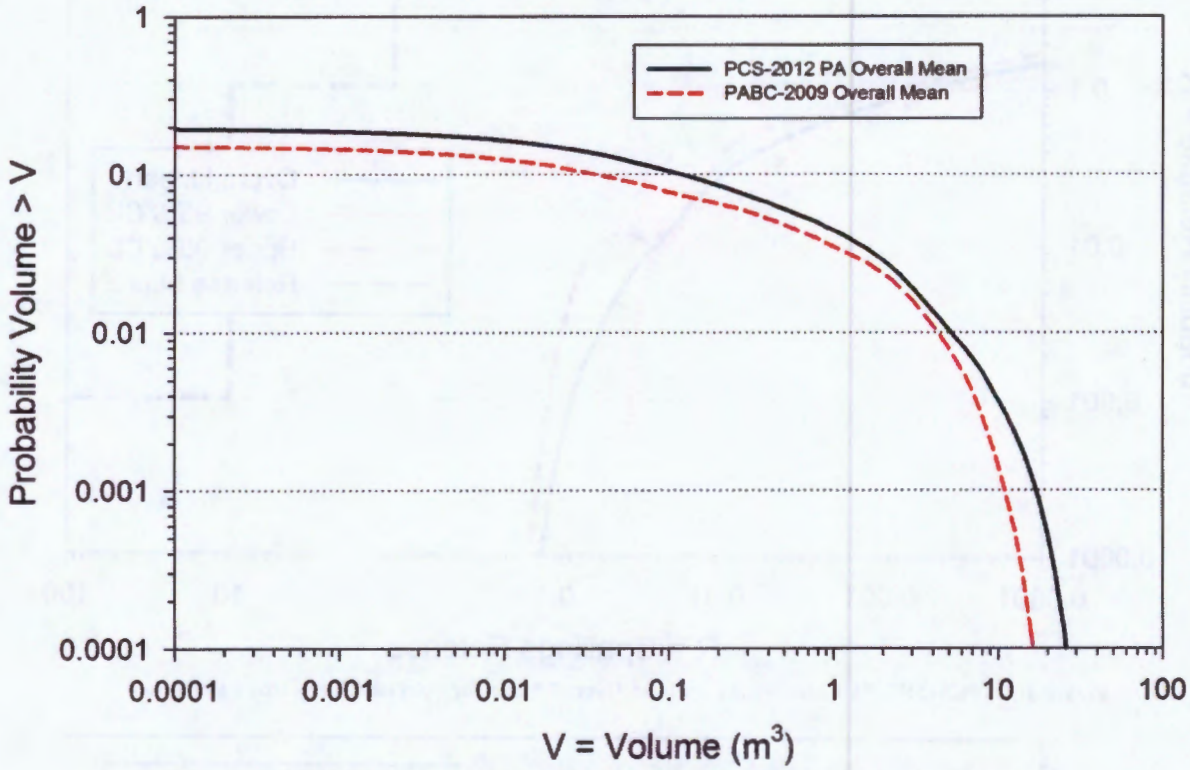

Figure 3-14: PCS-2012 PA and PABC-2009 Overall Mean CCDFs for Spallings Volumes

Information Only

3.3 Normalized Direct Brine Releases

PCS-2012 PA normalized direct brine releases are presented in this section and subsequently compared to results obtained in the PABC-2009. Figure 3-15, Figure 3-16, and Figure 3-17 contain PCS-2012 PA CCDFs for DBRs. Mean and quantile CCDF distributions for the three replicates are shown together in Figure 3-18. Figure 3-19 contains the 95 percent confidence limits about the DBR overall mean. As seen in Figure 3-19, the overall mean and its lower/upper 95% confidence limits are well below acceptable release limits.

To facilitate comparisons of DBRs calculated in the PCS-2012 PA to those obtained in the PABC-2009, overall mean and volume CCDFs obtained in these two analyses are plotted together in Figure 3-20 and Figure 3-21. As seen in Figure 3-20, the CCDF curve obtained for direct brine releases shows greater mean probabilities in the PCS-2012 PA for the majority of release values.

In the PCS-2012 PA, intrusion scenarios that involve drilling into a pressurized brine region underneath the repository exhibited an increase in the average pressure in the intruded waste panel when compared to the PABC-2009 results for a period of time following the intrusion (Malama 2012). Additionally, an increase in mean waste panel brine saturation was found for this type of intrusion (Malama 2012). The combination of an increase in waste panel pressure and brine saturation leads to an increase in DBR volumes, as well as a greater number of non-zero brine volume vectors for PCS-2012 PA compared to PABC-2009 (Camphouse 2012b). For intrusion scenarios that do not involve drilling into a pressurized brine region underneath the repository, there is an increase in mean waste panel pressure accompanied by a small decrease in brine saturation for the PCS-2012 PA compared to the PABC-2009 (Malama 2012). This results in an increase in maximum DBR volume for the PCS-2012 PA. This increase in pressure of the intruded panel as compared to the PABC-2009 impacted the number of DBR realizations used to calculate the DBR release tables (Malama 2012). The total number of nonzero DBR volumes increased from 2,999 in the PABC-2009 to 3,182 in the PCS-2012 PA, an increase of 183 realizations with a nonzero DBR volume (Malama 2012). For undisturbed conditions, the long-term mean waste panel pressure and brine pressure also increased from the PABC-2009 to the PCS-2012 PA. The is due to the implementation of the ROMPCS design, which allows greater brine flow into the waste panel than the Option D design, resulting in greater gas generation and thus mean waste panel pressure (Camphouse 2012b).

However, despite the greater number of nonzero DBR volumes found in the DBR analysis (Malama 2012), the number of nonzero DBR release vectors found in the CCDFGF analysis remains the same from the PABC-2009 to the PCS-2012 PA. The increase in mean DBR releases is due to increased releases in only a few vectors, and is not attributed to an overall increase in releases for a majority of vectors (Kirchner 2012). Additional evidence of the influence of a few vectors on the DBR volumes is found in Figures 5-1 to 5-10 of the PCS-2012 PA DBR report (Malama 2012), which show that the DBR volume distribution skews toward higher volumes only for the high end of the distribution. The final result is an increase in mean probabilities for the PCS-2012 PA compared to the PABC-2009 for the majority of DBR release values.

The overall mean CCDF curves for direct brine volumes obtained in the PCS-2012 PA and the PABC-2009 are shown together in Figure 3-21. For probabilities less than about 0.1, the mean

Information Only

DBR volume increased, most likely due to the increase in waste panel pressure observed in the Salado flow modeling results as compared to the PABC-2009. The increase in the number of realizations with a nonzero DBR volume combined with the increase in the maximum DBR volumes found in the Salado flow modeling results (Camphouse 2012b) explain the differences observed in the CCDF DBR volume curves obtained in the PABC-2009 and the PCS-2012 PA.

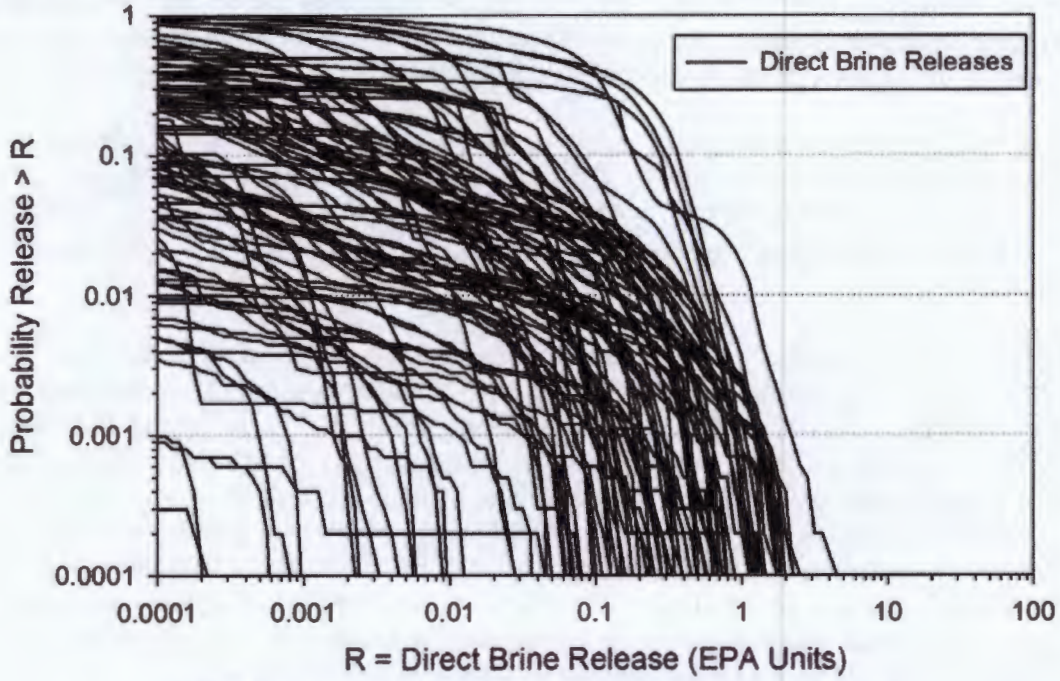

Figure 3-15: PCS-2012 PA Replicate 1 Normalized Direct Brine Releases

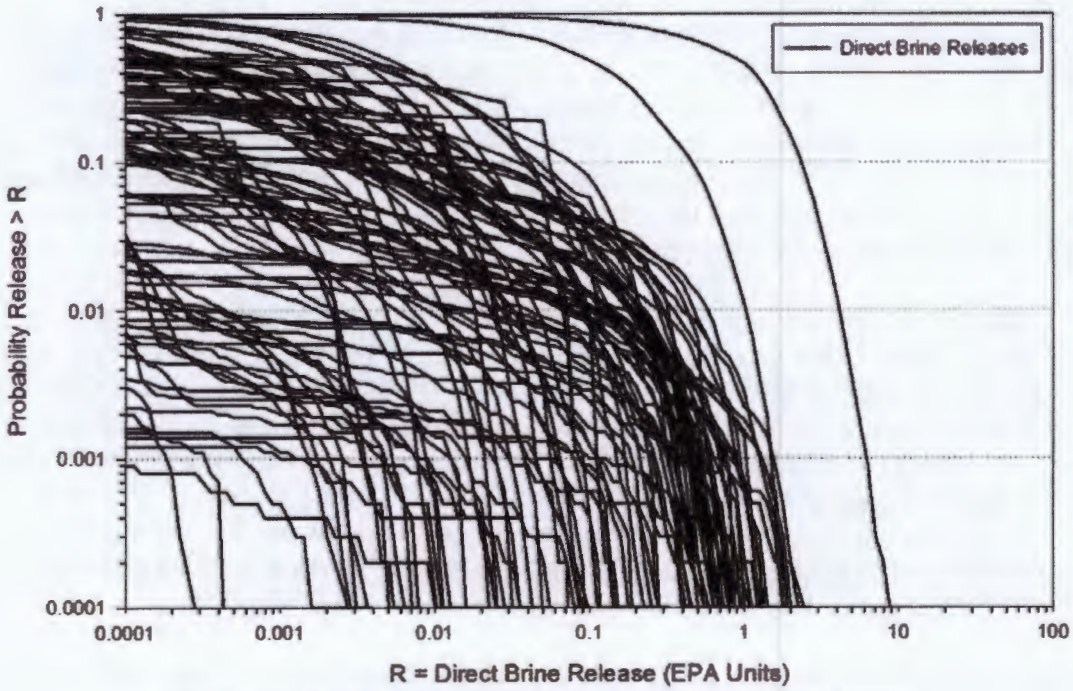

Figure 3-16: PCS-2012 PA Replicate 2 Normalized Direct Brine Releases

Information Only

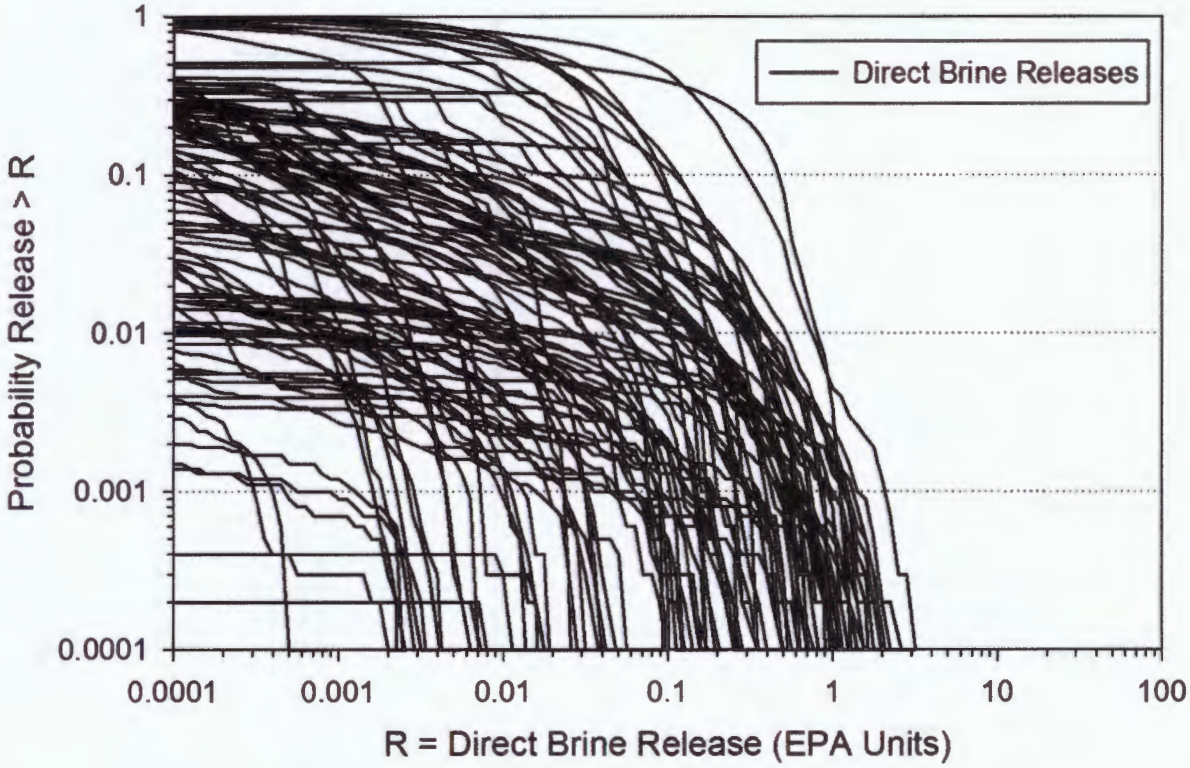

Figure 3-17: PCS-2012 PA Replicate 3 Normalized Direct Brine Releases

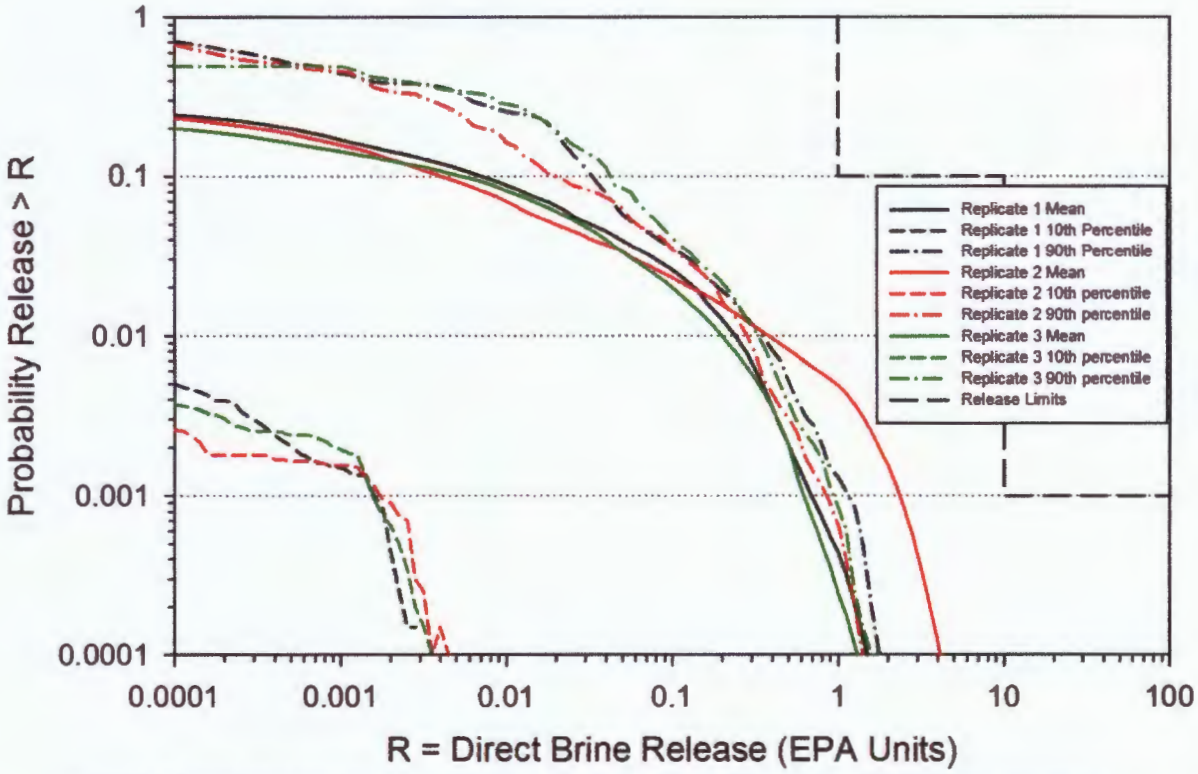

Figure 3-18: PCS-2012 PA Mean and Quantile CCDFs for Normalized Direct Brine Releases, Replicates 1-3

Information Only

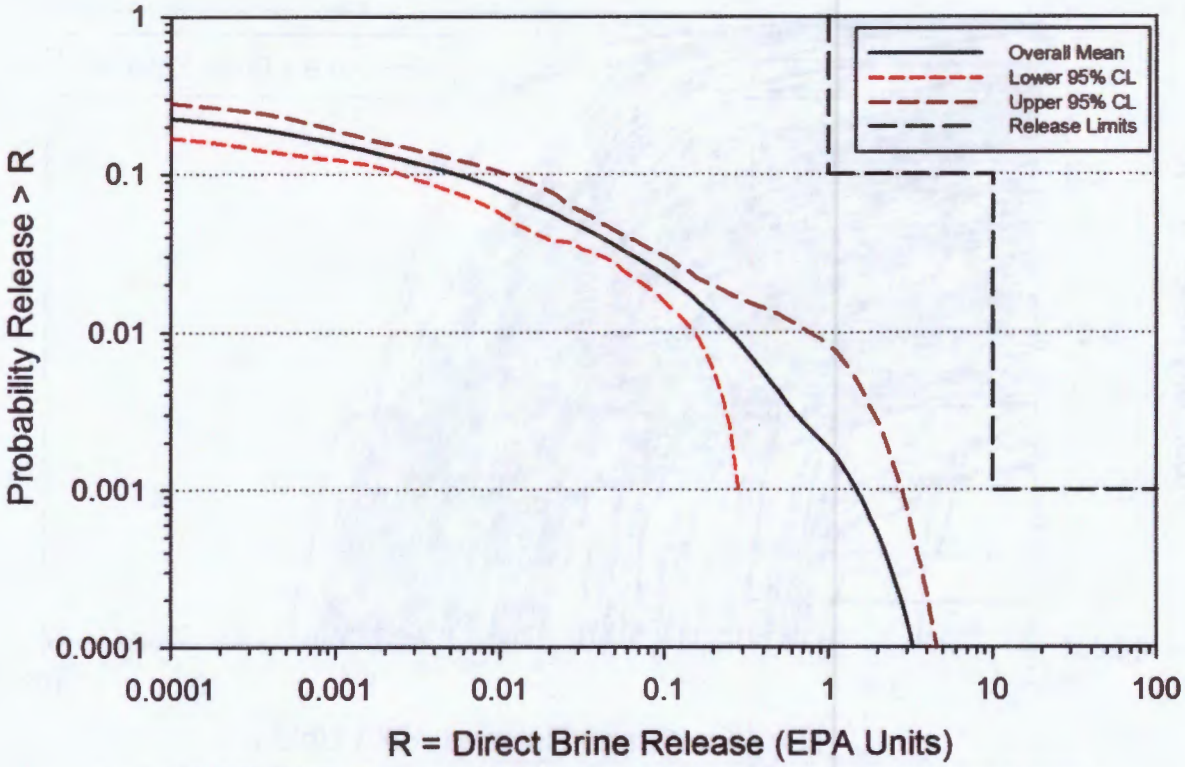

Figure 3-19: PCS-2012 PA Confidence Limits on Overall Mean for Normalized Direct Brine Releases

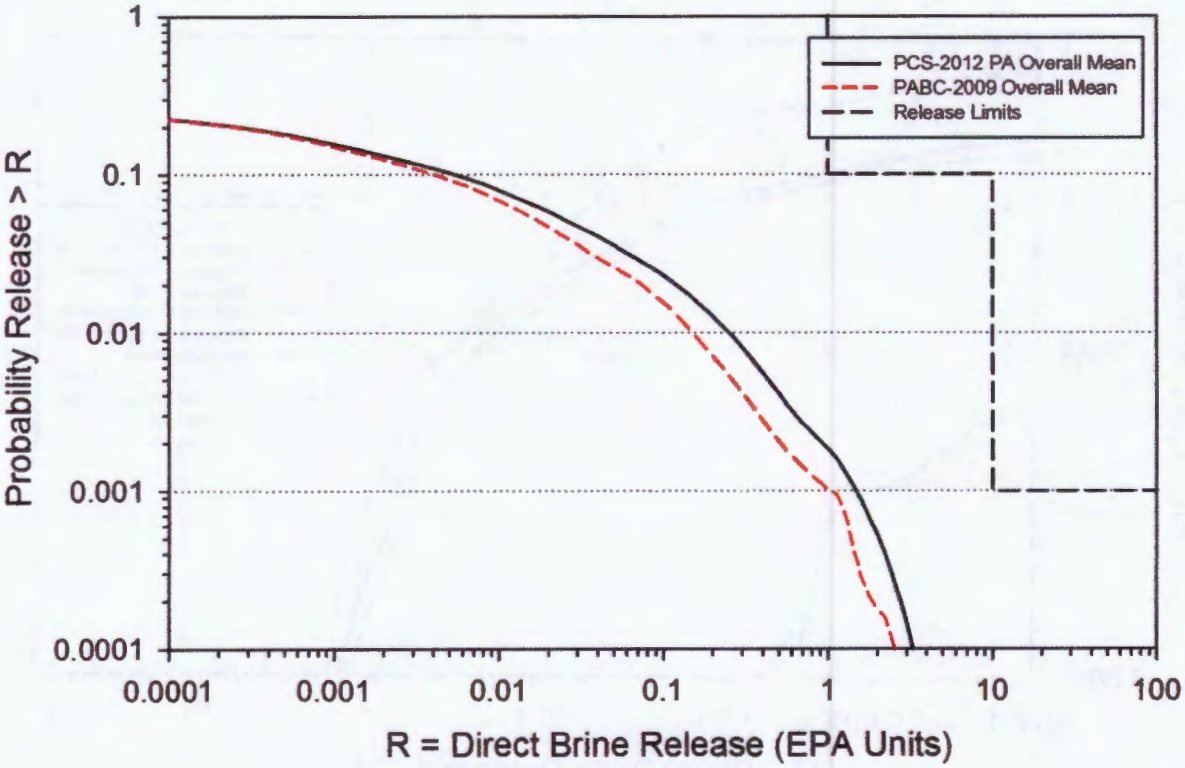

Figure 3-20: PCS-2012 PA and PABC-2009 Overall Mean CCDFs for Normalized Direct Brine Releases

Information Only

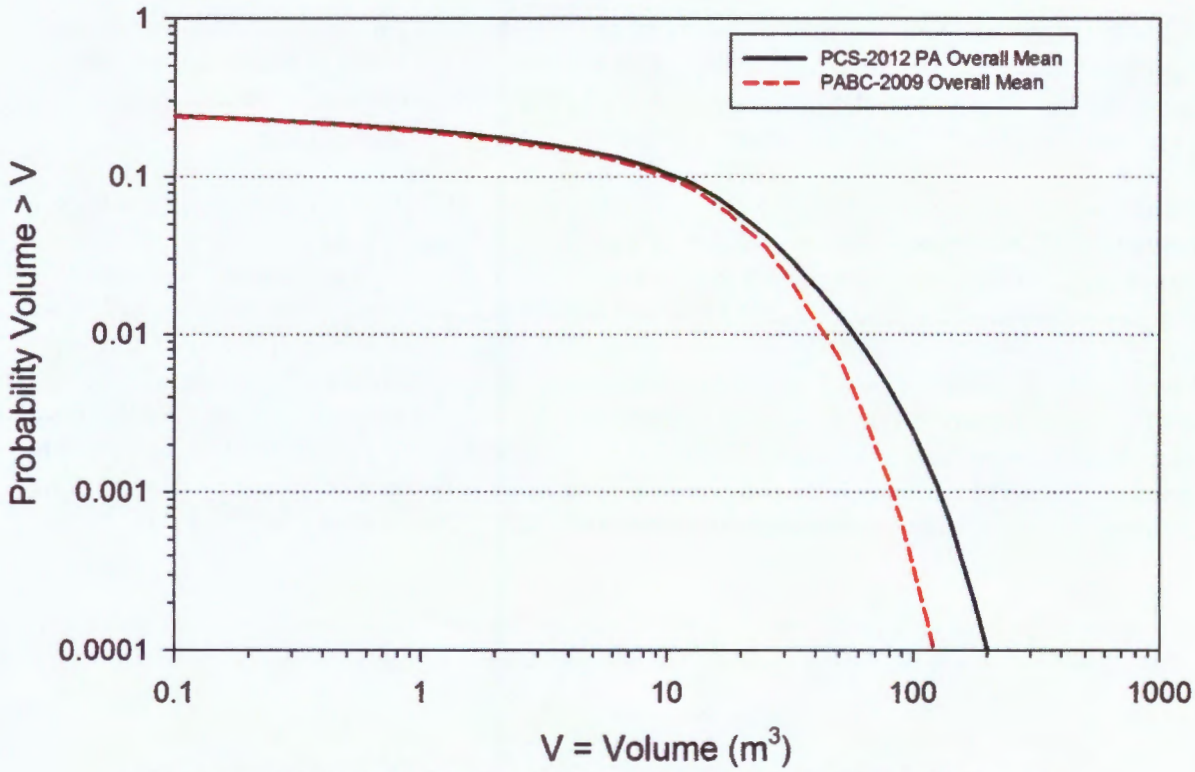

Figure 3-21: PCS-2012 PA and PABC-2009 Overall Mean CCDFs for Direct Brine Volumes

Information Only

3.4 Normalized Transport Releases to the Culebra

PCS-2012 PA normalized transport releases to the Culebra are discussed in this section and compared to those seen in the PABC-2009. These results are included primarily as a means to validate the expectation that the proposed changes to the PCS investigated in the PCS-2012 PA have minimal impact on Culebra transport releases.

Replicate means obtained in the PCS-2012 PA and the PABC-2009 for normalized transport releases to the Culebra are shown together in Figure 3-22. As seen in that figure, the means obtained in the two analyses for each replicate are identical. Overall means of transport releases to the Culebra obtained in the PCS-2012 PA and the PABC-2009 are shown together in Figure 3-23. As is evident from that figure, there is no difference in the overall mean of transport releases to the Culebra obtained in the two analyses. The individual replicate means and the overall mean of transport releases to the Culebra are primarily unaffected by the panel closure design changes implemented in the PCS-2012 PA. As a result, it is reasonable to conclude that normalized transport releases from the Culebra be primarily unchanged as well, since nothing was changed in the Culebra transport model from the PABC-2009 to the PCS-2012 PA.

Information Only

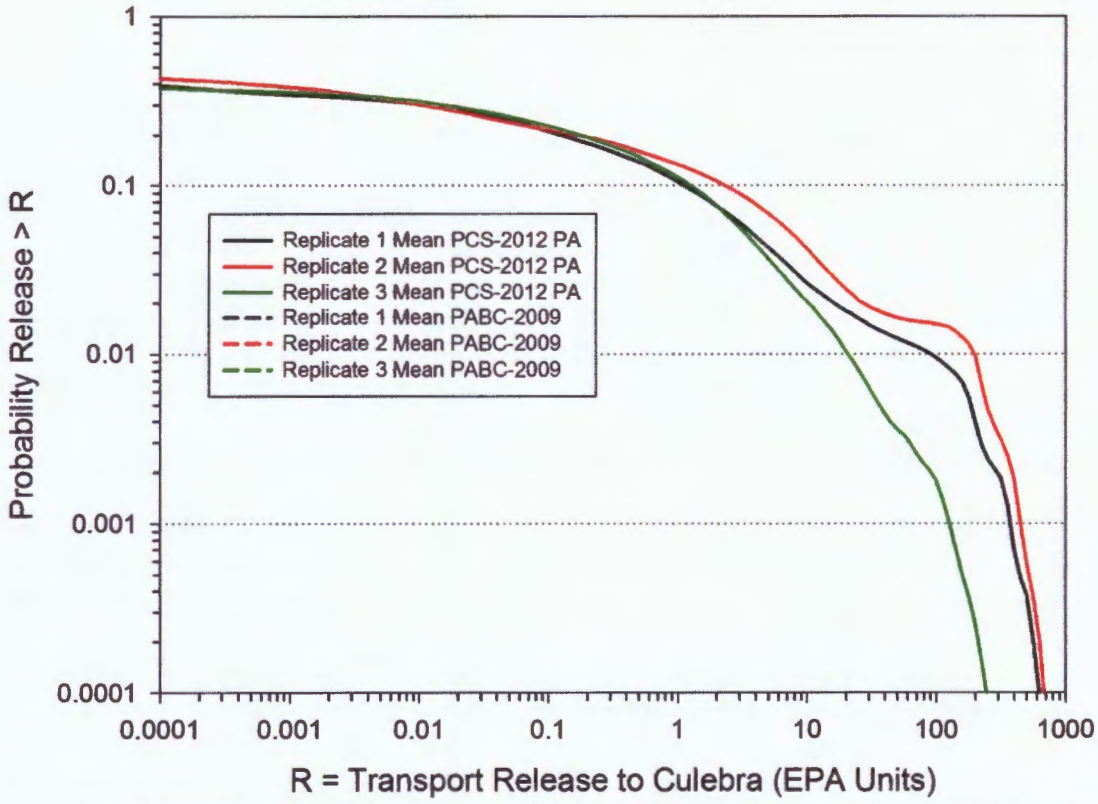

Figure 3-22: PCS-2012 PA and PABC-2009 Replicate Means for Normalized Transport Releases to the Culebra

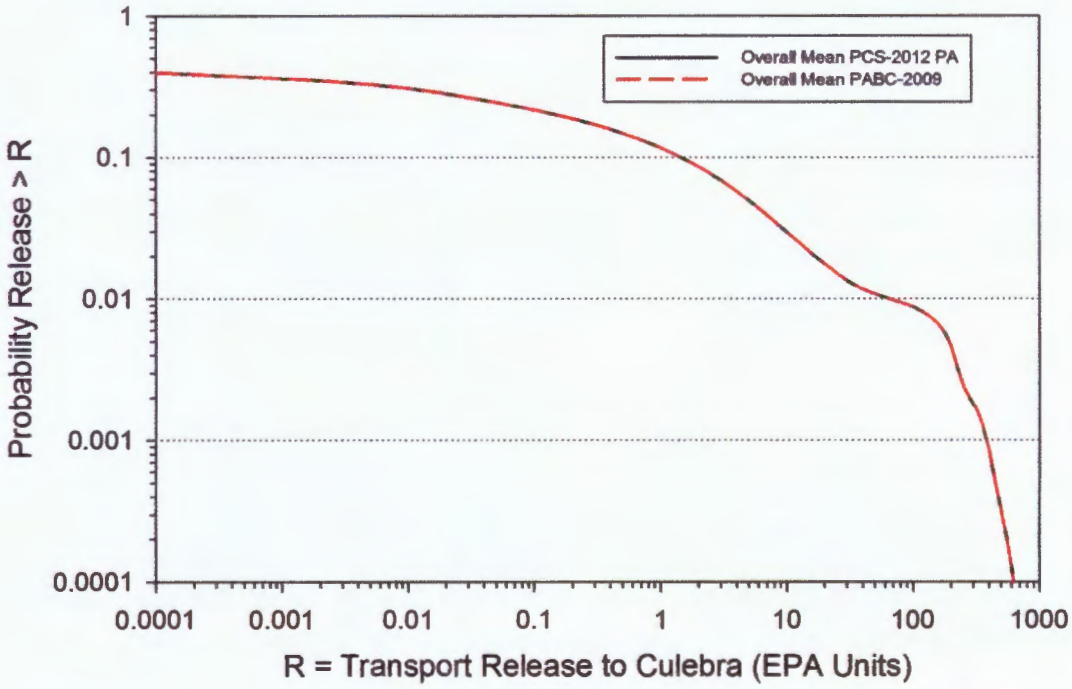

Figure 3-23: PCS-2012 PA and PABC-2009 Overall Mean CCDFs for Transport Releases to the Culebra

Information Only

3.5 Total Normalized Releases

Total normalized releases for PCS-2012 PA are presented in this section and subsequently compared to results obtained in the PABC-2009. Total releases are calculated by forming the summation of releases across each potential release pathway, namely cuttings and cavings releases, spallings releases, direct brine releases, and transport releases. PCS-2012 PA CCDFs for total releases are presented in Figure 3-24, Figure 3-25, and Figure 3-26 for replicates 1, 2, and 3, respectively. Mean and quantile CCDF distributions for the three replicates are shown together in Figure 3-27. Figure 3-28 contains the 95 percent confidence limits about the overall mean of total releases. As seen in Figure 3-28, the overall mean for normalized total releases and its lower/upper 95% confidence limits are well below acceptable release limits. As a result, the panel closure design and repository configuration changes investigated in the PCS-2012 PA do no result in WIPP non-compliance with the containment requirements of 40 CFR Part 191.

PCS-2012 PA and PABC-2009 overall mean CCDFs for total releases are shown together in Figure 3-29. As seen in that figure, the overall mean CCDFs obtained in the two analyses are nearly identical for release values less than approximately 0.1 EPA units. For releases greater than 0.1 EPA units, the CCDF curve obtained in the PCS-2012 PA is higher than that found in the PABC-2009. This increase corresponds primarily to the differences found for direct brine releases between the two analyses as discussed in Section 3.3 and illustrated in Figure 3-20. The differences found for spallings may slightly affect the total CCDF curve as well (Section 3.2, Figure 3-13). PCS-2012 PA cuttings and cavings results are unchanged from those found in the PABC-2009. The panel closure design change investigated in the PCS-2012 PA has an impact on the overall mean of total releases from the PABC-2009 to the PCS-2012 PA due to the changes in direct brine releases calculated in those analyses (Figure 3-30).

A comparison of the statistics on the overall mean for total normalized releases obtained in the PCS-2012 PA and the PABC-2009 can be seen in Table 1. At a probability of 0.1, values obtained for mean total releases has increased from 0.09 to 0.10 for the PCS-2012 PA. At a probability of 0.001, the increase in DBRs seen at that probability in the PCS-2012 PA results in an increase in the mean total release by approximately 0.41 EPA units. An increase is seen in the 95% confidence limit when compared to the PABC-2009 results, while the 90th percentile remains the same. An increase in the mean total release accompanied by no change to the 90th percentile value is additional evidence that only a few vectors have significantly increased releases.

Probability	Analysis	Mean Total Release	90th Percentile	Lower 95% CL	Upper 95% CL	Release Limit
0.1	PCS-2012 PA	0.10	0.17	0.10	0.10	1
	PABC-2009	0.09	0.16	0.09	0.10	1
0.001	PCS-2012 PA	1.51	1.00	0.33	2.81	10
	PABC-2009	1.10	1.00	0.37	1.77	10

Table 1: PCS-2012 PA and PABC-2009 Statistics on the Overall Mean for Total Normalized Releases in EPA Units at Probabilities of 0.1 and 0.001

Information Only

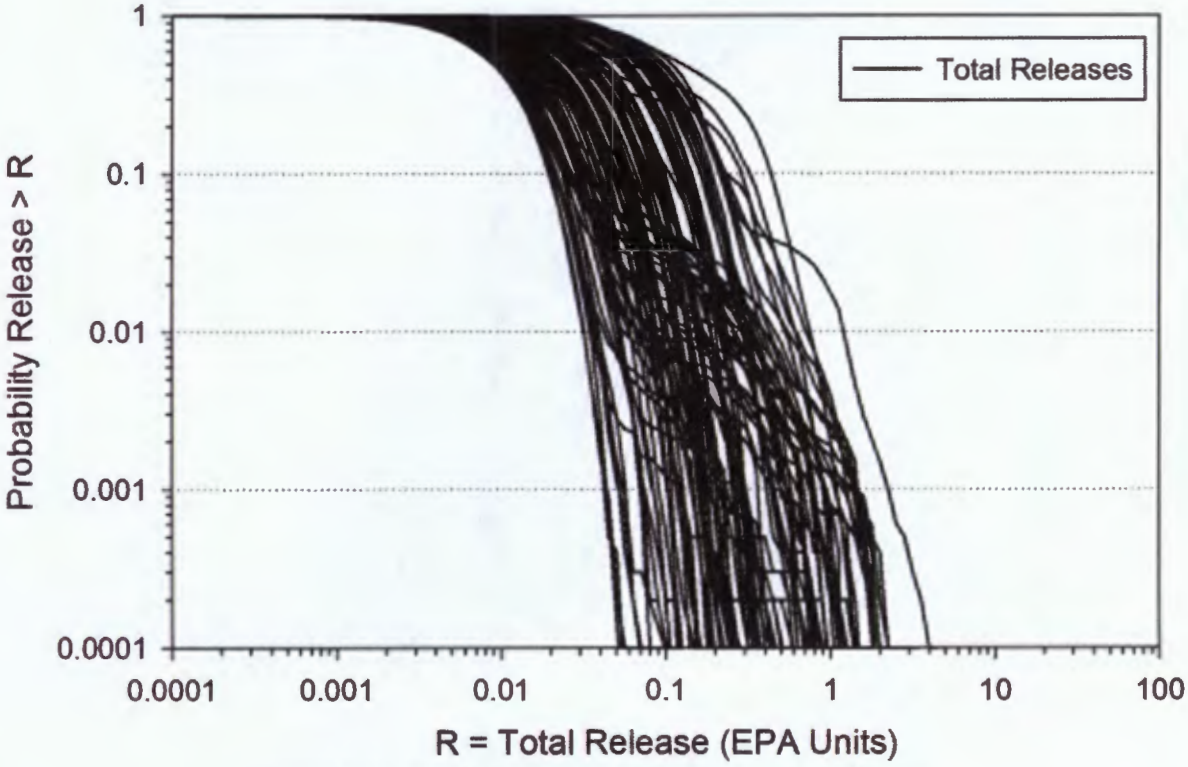

Figure 3-24: PCS-2012 PA Replicate 1 Total Normalized Releases

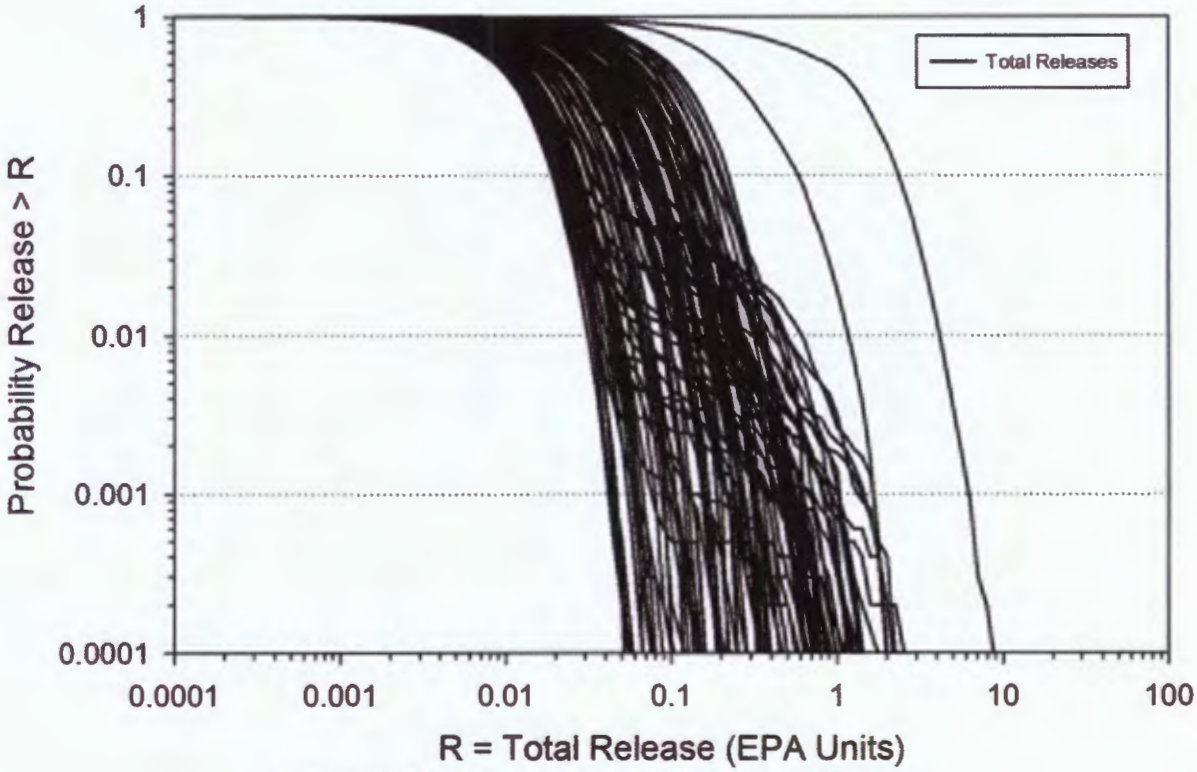

Figure 3-25: PCS-2012 PA Replicate 2 Total Normalized Releases

Information Only

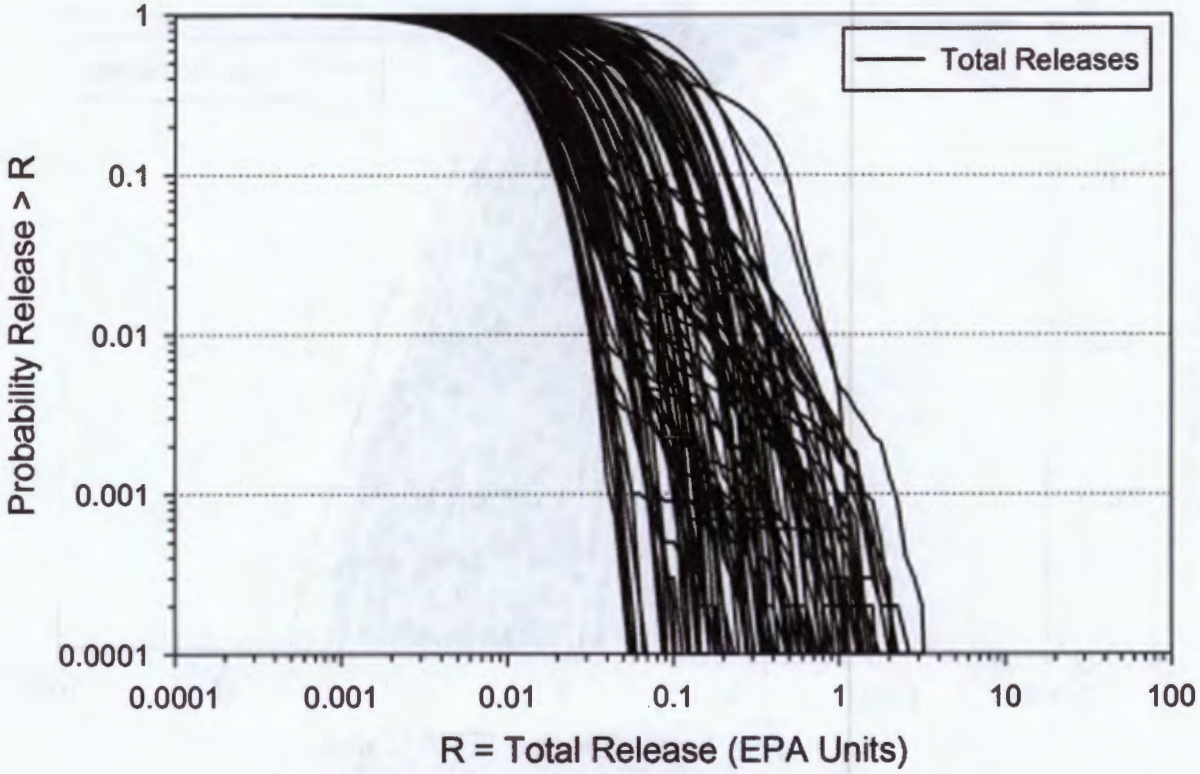

Figure 3-26: PCS-2012 PA Replicate 3 Total Normalized Releases

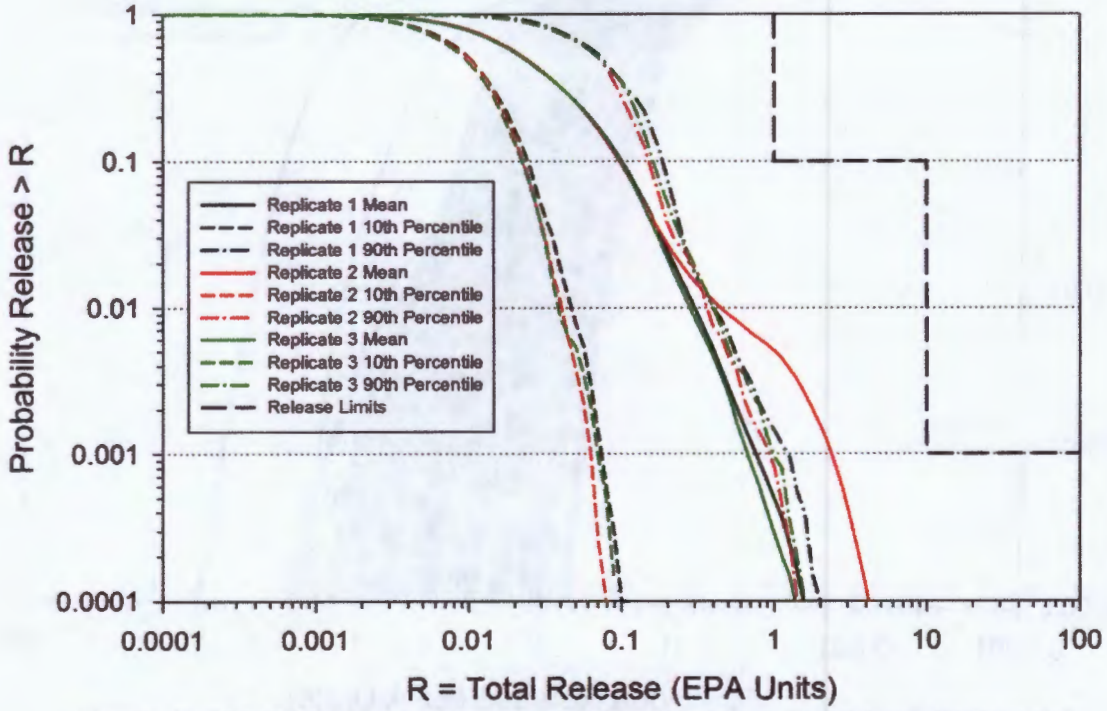

Figure 3-27: PCS-2012 PA Mean and Quantile CCDFs for Total Normalized Releases, Replicates 1-3

Information Only

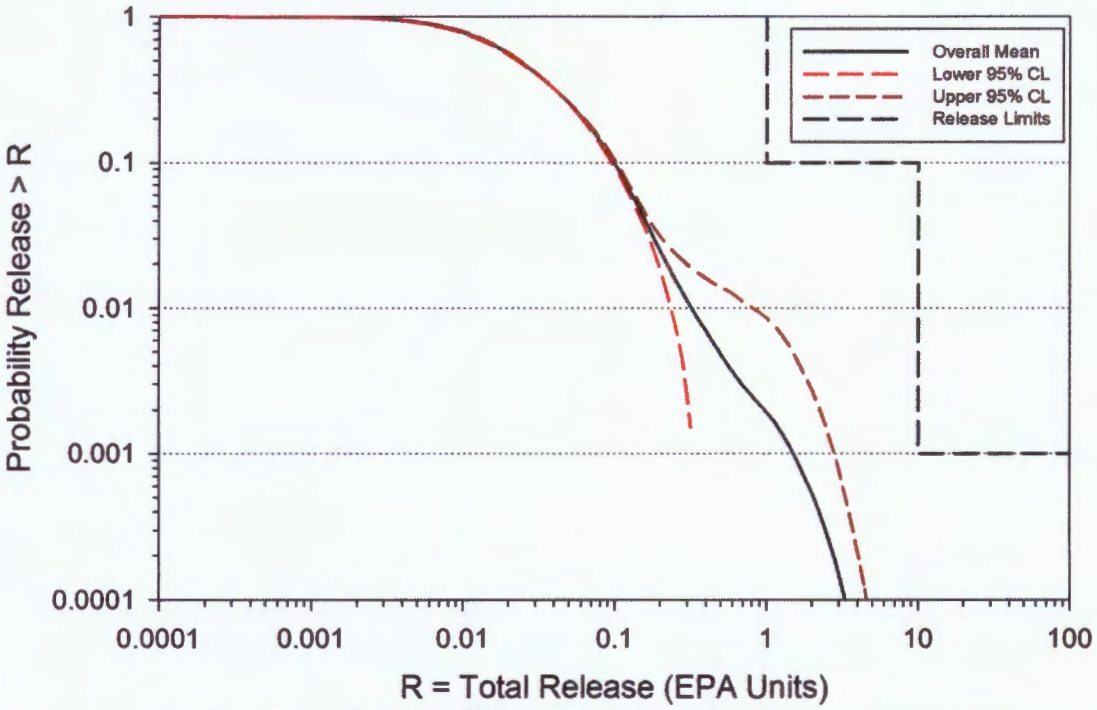

Figure 3-28: PCS-2012 PA Confidence Limits on Overall Mean for Total Normalized Releases

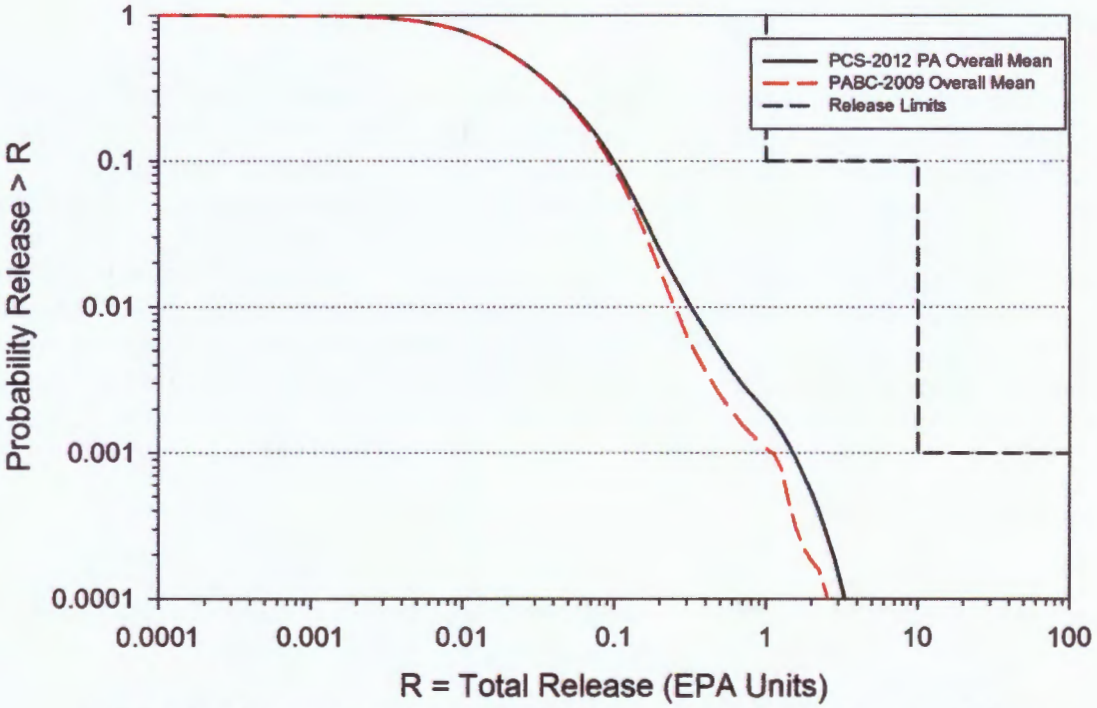

Figure 3-29: PCS-2012 PA and PABC-2009 Overall Mean CCDFs for Total Normalized Releases

Information Only

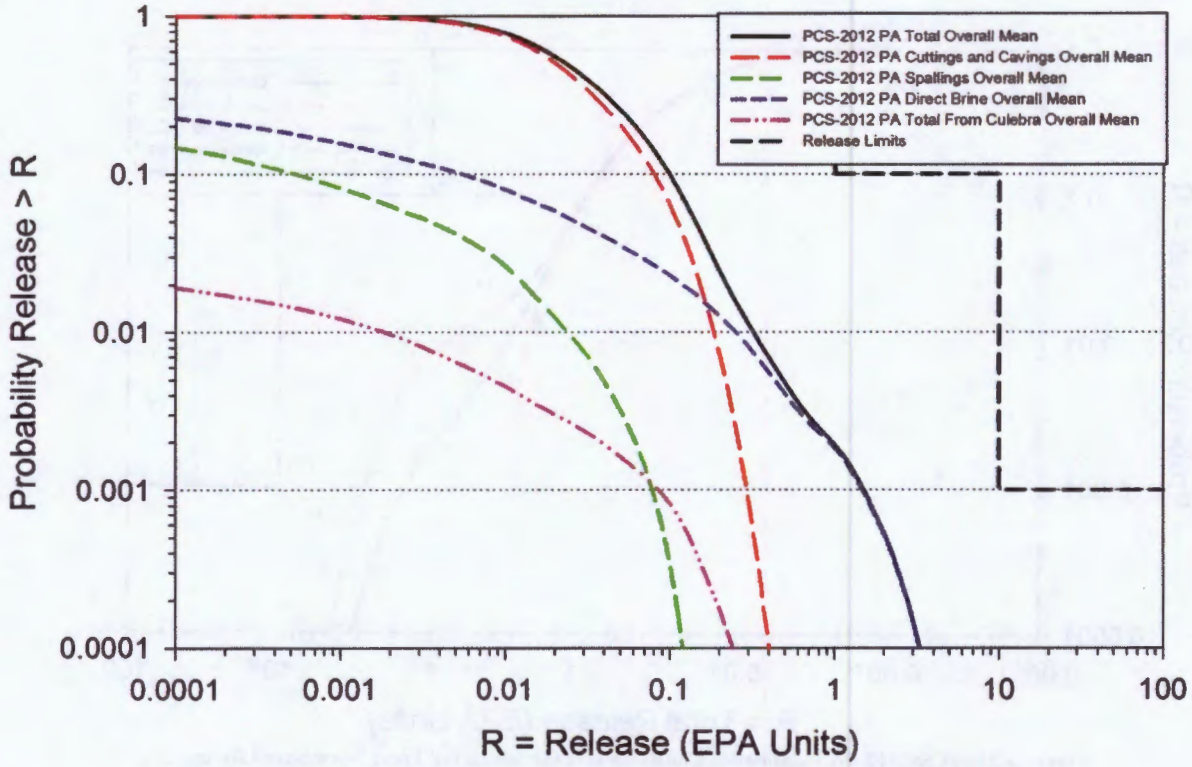

Figure 3-30: PCS-2012 PA Primary Components Contributing to Total Releases

4 SUMMARY

Total normalized releases calculated in the PCS-2012 PA remain below their regulatory limits. As a result, the panel closure design and repository configuration changes investigated in the PCS-2012 PA do not result in WIPP non-compliance with the containment requirements of 40 CFR Part 191. Cuttings and cavings releases and direct brine releases are the two primary release components contributing to total releases in the PCS-2012 PA. Cuttings and cavings releases are identical to those calculated in the PABC-2009. Changes in total releases are primarily attributed to changes calculated in direct brine releases from the PABC-2009 to the PCS-2012 PA. Increases are observed in PCS-2012 PA spallings releases as compared to the PABC-2009, but these differences are comparatively minor and do not have a significant impact on the overall total normalized releases found in the PCS-2012 PA.

Information Only

5 REFERENCES

Camphouse, R.C. 2012a. Analysis Plan for the 2012 WIPP Panel Closure System Performance Assessment A-161, Revision 0. Sandia National Laboratories, Carlsbad, NM. ERMS 557726.

Camphouse, R.C. 2012b. Analysis Package for Salado Flow Modeling Done in the AP-161 (PCS-2012) Performance Assessment. Carlsbad, NM, Sandia National Laboratories. ERMS 558204

Camphouse, R.C, D.C. Kicker, T.B. Kirchner, J.J. Long, B. Malama, and T.R. Zeitler. 2012c. *Summary Report and Run Control for the WIPP Panel Closure System Performance Assessment.* Carlsbad, NM: Sandia National Laboratories. ERMS 558226.

Clayton, D.C., Camphouse, R. C., Garner, J. W., Ismail, A. E., Kirchner, T. B., Kuhlman, K. L., and Nemer, M. B.. 2010. Summary Report of the CRA-2009 Performance Assessment Baseline Calculation. Sandia National Laboratories. Carlsbad, New Mexico, ERMS 553039.

DOE (U.S. Department of Energy). 1996. Title 40 CFR Part 191 Compliance Certification Application for the Waste Isolation Pilot Plant. DOE/CAO-1996-2184. U.S. Department of Energy, Waste Isolation Pilot Plant, Carlsbad Area Office. Carlsbad, NM.

DOE (U.S. Department of Energy), 2011. Panel Closure System Design, Planned Change Request to the EPA 40 CFR Part 194 Certification of the Waste Isolation Pilot Plant. U.S. Department of Energy, Carlsbad Field Office. Carlsbad, New Mexico.

EPA (U.S. Environmental Protection Agency). 1998. Criteria for the Certification and Re-Certification of the Waste Isolation Pilot Plants Compliance with the 40 CFR Part 191 Disposal Regulations: Certification Decision; Final Rule, *Federal Register*, Vol. 63, No. 95, pp. 27353-27406. U.S. Environmental Protection Agency, Office of Air and Radiation, Washington, D.C.

Helton, J. et al. 1998. Uncertainty and Sensitivity Analysis Results Obtained in the 1996 Performance Assessment for the Waste Isolation Pilot Plant. Sandia National Laboratories, Albuquerque, NM. SAND98-0365.

Kicker, D.C. 2012. Analysis Package for Cuttings, Cavings, and Spallings: Panel Closure System Performance Assessment (PCS-2012 PA). Sandia National Laboratories, Carlsbad, NM.

Kirchner, T. 2010. Sensitivity of the CRA-2009 Performance Assessment Baseline Calculation Releases to Parameters. Sandia National Laboratories, Carlsbad, NM. ERMS 552960.

Kirchner, T. 2012. Sensitivity of the AP-161 (PCS-2012) PA Releases to Parameters. Sandia National Laboratories, Carlsbad, NM.

Information Only

Malama, B. 2012. Analysis Package for Direct Brine Releases: 2012 Panel Closure System Performance Assessment (PCS-2012 PA). Sandia National Laboratories, Carlsbad, NM. ERMS 558226.

U.S. Environmental Protection Agency (EPA). 1996. 40 CFR Part 194: Criteria for the Certification and Recertification of the Waste Isolation Pilot Plant's Compliance with the 40 CFR Part 191 Disposal Regulations; Final Rule. Federal Register, Vol. 61, 5223-5245.

Information Only

558342

Sandia National Laboratories

Waste Isolation Pilot Plant

Sensitivity of the AP-161 (PCS-2012) PA Releases to Parameters

Revision 0

Author:	**Thomas Kirchner (6211)**	Thomas Kirchner	10/15/12
	Print	**Signature**	**Date**
Technical Review:	**Eric Vugrin (6921)**	Thomas Kirchner For Eric Vugrin	10/15/12
	Print	**Signature**	**Date**
Management Review:	**Sean Dunagan (6211)**	[illegible]	10/15/12
	Print	**Signature**	**Date**
QA Review:	**Shelly Nielsen (6210)**	Shelly R. Nielsen	10-15-12
	Print	**Signature**	**Date**

WIPP:1.4.1.2:PA:QA-L:557393

Information Only

Table of Contents

Introduction 3
The STEPWISE Procedure 4
Changes from the PABC-2009 PA 13
Total Releases 15
Cuttings and Cavings Releases 17
Spallings Releases 20
Direct Brine Release 23
Culebra Releases 27
Summary and Conclusions 30
References: 32

Information Only

Introduction

The Waste Isolation Pilot Plant (WIPP), located in southeastern New Mexico, has been developed by the U.S. Department of Energy (DOE) for the geologic (deep underground) disposal of transuranic (TRU) waste. Containment of TRU waste at the WIPP is regulated by the U.S. Environmental Protection Agency (EPA) according to the regulations set forth in Title 40 of the Code of Federal Regulations (CFR), Part 191. The DOE demonstrates compliance with the containment requirements according to the Certification Criteria in Title 40 CFR Part 194 by means of performance assessment (PA) calculations performed by Sandia National Laboratories (SNL). WIPP PA calculations estimate the probability and consequence of potential radionuclide releases from the repository to the accessible environment for a regulatory period of 10,000 years after facility closure. The models used in PA are maintained and updated with new information as part of an ongoing process. Improved information regarding important WIPP features, events, and processes typically results in refinements and modifications to PA models and the parameters used in them. Planned changes to the repository and/or the components therein also result in updates to WIPP PA models. WIPP PA models are used to support the repository recertification process that occurs at five-year intervals following the receipt of the first waste shipment at the site in 1999.

Waste panel closures comprise a repository feature that has been represented in WIPP PA since the original Compliance Certification Application (CCA) of 1996. Panel closures are included in WIPP PA models principally because they are a part of the disposal system, not because they play a substantive role in inhibiting the release of radionuclides to the outside environment (DOE 1996). The DOE stated in the CCA (DOE 1996) that *"The panel closure system was not designed or intended to support long-term repository performance."* The 1998 rulemaking that certified WIPP to receive transuranic waste placed conditions on the panel closure design to be implemented in the repository. The mandated design consists of a concrete block wall, an open drift section, and a concrete monolith, and was termed the "Option D" panel closure. Following the selection of the Option D design in 1998, the engineering of the panel closure has been re-assessed, and a revised design has been established that is simpler, cheaper, and easier to construct. The revised panel closure design, termed the Run-of-Mine Panel Closure System (ROMPCS), is comprised of 100 feet of ROM salt with barriers at each end. The ROM salt is generated from ongoing mining operations at the WIPP and may be compacted and/or moistened as it is emplaced in a panel entry. The barriers consist of ventilation bulkheads, similar to those currently used in the panels as room closures.

The DOE has submitted a planned change request (PCR) to the EPA requesting that EPA modify Condition 1 of the Final Certification Rulemaking for 40 CFR Part 194 (EPA 1998, DOE 2011) for the WIPP. The PCR submitted to EPA requests that Condition 1 be changed, and that the ROMPCS design be approved for use in all panels (DOE 2011). In support of this rulemaking change, a performance assessment has been completed that incorporates the ROMPCS design into the current PA baseline established by the 2009 Performance Assessment Baseline Calculation (PABC-2009) (Clayton et al. 2010). The name given to this new panel closure PA is PCS-2012, and the plan for its execution is detailed in AP-161 (Camphouse 2012a).

Information Only

Sensitivity of PCS-2012 PA Releases to Parameters

This report documents the analysis of the sensitivity of releases to parameters sampled using the code LHS for the PCS-2012 PA. Results are compared with those from the PABC-2009 PA. Variability in the releases computed using CCDFGF arises from two sources of uncertainty. First is systemic uncertainty in the values of certain parameters. This uncertainty represents a lack of knowledge about the values of parameters that are assumed to be constant and hence can be interpreted as the confidence one has that a parameter will have a particular value. Uncertainty in the results is also affected by the stochastic processes represented in CCDFGF, e.g. the occurrence of drilling intrusions. These stochastic processes are controlled by the aleatory parameters. The impact of the stochastic processes is assessed by running 10,000 possible futures for each vector of the sampled parameters. The sensitivity analysis performed using stepwise regression cannot be used to explain sensitivity of the results to the changes implemented in the models or constant (fixed) model parameters following the PABC-2009 PA. Likewise, variability due to the stochastic processes cannot be partitioned among the aleatory parameters because all aleatory parameters are independently sampled in all futures and because the mean releases computed across the 10,000 futures are regresses against the parameters and these means subsume the within-vector (aleatory) variability. The sensitivity analysis can only attempt to resolve the question of which *sampled* parameters contribute the most to the variability (uncertainty) observed in the mean releases across the 10,000 futures for each vector.

The STEPWISE Procedure

The code STEPWISE version 2.21 was used to determine the relative importance of the sampled parameters in the PCS-2012 analysis. STEPWISE receives sampled input parameter values and calculated release data that correspond to those input data. STEPWISE relates the sampled input parameter values to the calculated release data by performing a multiple regression analysis and reporting the results in tables. Additional analyses were performed on selected subsets of the data using Microsoft® Excel 2010. The spreadsheets are provided on the attached CD_ROM and are also stored in the CMS library LIBAP161_STPW in the compressed file AP161SimpleRegressionSpeadsheets.zip (Attachment 1).

WIPP PA employs stepwise linear multiple regression to evaluate the relative importance of the various sampled parameters on the estimates of potential releases. In the forward stepwise approach used by STEPWISE, a sequence of regression models is constructed, starting with the input parameter that has the strongest simple correlation with the output variable. Partial correlations between the output and the remaining variables are then computed. The partial correlations remove the linear effects of variables already included in the model. The variable having the largest significant partial correlation coefficient is added next, and the partial correlations for the remaining input variables are recomputed. Significance is determined using an F-test, and the significance level for adding an input variable to the model is $1-\alpha_{in}$, where α_{in} is the significance level for a Type I error that is set by the analyst. The F-test compares the variability contributed by the variable to the variability not accounted for by the regression, i.e. the variability of the residuals. By default STEPWISE sets $\alpha_{in} = 0.05$, so that one is 95% confident that there is a partial correlation between the input and output variables. This process is repeated until there are no variables remaining having significant correlations with the output

Information Only

variable. Variables excluded from the regression model contribute no statistically significant information in relation to the unexplained variability and hence the results are judged to be relatively insensitive to those parameters.

Input variables that are added to the regression model are not necessarily retained. For an input variable to be retained, its regression coefficient, i.e. the linear contribution of an input to the prediction of the output variable, must be statistically distinguishable from zero. A t-test is used to determine whether a regression coefficient is significantly different than zero. The t-test evaluates the null hypothesis that the regression coefficient is zero. The hypothesis is not rejected when random effects can give rise to the observed regression coefficient with probability α_{out}. The random effects are caused by the stochastic variability contributed by the input variables not in the regression model. In other words, the hypothesis is rejected, and the variable is included in the model when the $1-\alpha_{out}$ confidence interval of the regression coefficient does not encompass zero. By default the STEPWISE α_{out} -value for allowing a variable to enter the regression model is 0.05. Thus, in the default case, one is 95% confident that the input variables make a linear contribution to the response of the output variable. The user may specify different α-values in the input control file. However, the value allowing a variable to enter the model, $\alpha_{in,}$ must be less than or equal to the value by which a variable is allowed to leave the model, $\alpha_{out,}$ to avoid looping. In the following analyses, α_{in} was 0.05, and α_{out} was 0.05.

Setting α_{out} to α_{in} maximizes the number of variables in the model (as requested by EPA in C-23-18, U.S. Environmental Protection Agency 2004) but can increase the number of spurious correlations (Kirchner 2004a,b). A spurious correlation implies a linear relationship exists between two variables but in reality no such relationship exists. The predicted error sum of squares (PRESS) was computed to detect over-fitting of the regression model to the data. Over-fitting can occur when the regression methodology causes the fit to favor specific points rather than the general shape of the data curve. In such a case the minimum value of PRESS may occur earlier than the last step in the regression analysis. No such condition was observed in any of the rank correlation analyses reported herein.

The STEPWISE procedure constructs a multivariate linear regression model. One of the assumptions of this statistical model is that the dependent (output) variable shows a linear response to the independent (input) variables. In cases where the response is non-linear but monotonic, replacing the values of the data with their ranks tends to linearize the response curves and standardizes the variability in the outputs and parameters by mapping the data into identical ranges. The rank of a value is an integer representing its position in the sorted list of the values. Ranking also tends to de-emphasize the impact of "outliers," which are points having considerably larger or smaller values than the remainder of the sample population. Although the use of ranks precludes using the model to predict values of an output variable given an input variable, the results are usually well suited for ranking the importance of the contributions of the input variables to the response of the output variable. The STEPWISE procedure has the functionality to perform ranked regressions. For the cases described below, the ranked regressions showed stronger correlations than the regressions based on the unranked data. This result suggests that there are non-linear relationships between the dependent and independent variables, but it does not eliminate the possibility that there are also non-monotonic relationships.

Information Only

Sensitivity of PCS-2012 PA Releases to Parameters

Ranked regression was used to evaluate the sensitivity of the output variables to the sampled parameters. Analysts examined scatter plots of the dependent versus independent ranked variables to determine if there were any obvious non-monotonic relationships. Obvious non-monotonic relationships were not found although there are cases involving inputs that are categorized as discrete variables (e.g. GLOBAL:OXSTAT, which is sampled as a uniform distribution but is then mapped to one of two discrete values) and cases where there are large proportions of the vectors showing no release (e.g. releases from the Culebra in the CRA-2009 analysis). Application of linear regression to such cases is somewhat problematic in terms of the assumptions of normally-distributed residuals and homogeneous variance among the residuals. However, in terms of ranking the relative importance of the parameters these issues are probably not significant.

Most of the regression models produced by STEPWISE do not include all of the variables, even after ranking the data. This simply indicates that the uncertainties in many of the parameters have statistically insignificant effects on the output variable. Statistical insignificance can arise because the output variable has a low functional response to the input variable, because the magnitude of uncertainty in the input variable is small relative to the other inputs, or from a combination of both conditions. This is not to say that these non-significant variables have no influence on the releases. Their exclusion from the tables reflects the inability of this statistical technique to rank their importance with an acceptable degree of confidence. For example, if the response of the output variable to an input variable was non-monotonic then the regression analysis might fail to properly identify that variable's importance. This possibility is unlikely for total releases and cuttings and cavings releases because the R^2 value (coefficient of determination) indicates that more than 83% of the variability in the output variables has been accounted for by the listed input variables.

Several of the parameters that appear in the model often contribute very little to the R^2 value and, therefore, explain very little of the variability in the output variable. Parameters that have minor contributions can appear by chance, simply due to random correlations. Many of the parameters that account for only a few percent to the variability in an output from one replicate may show different rankings, or can even be absent, in another replicate. Thus, it is difficult to assess the importance of the parameters that improve the regression model very little and, in reality, they may have no importance at all. Therefore, only the parameters that appear to have significant impacts on the regression model will be explained in detail.

Analyses were performed using Microsoft Excel to supplement the STEPWISE results for spallings and Culebra releases because some of those releases were zero. These analyses illustrate the relationship between the non-zero releases and various parameters. Simple linear regression analyses were conducted on the ranks of the parameters and non-zero releases. Significance of the regressions is denoted by the probability that the correlation is due to random error, as in $p = 0.09$. A regression is considered significant only if $p \leq 0.05$, i.e. that there is less than a 5 % chance that the correlation is due to random error.

This report documents the results of the PCS-2012 PA sensitivity analysis and shows, for comparison, the results obtained for the PABC-2009 analysis (Kirchner 2009). The details of run control for the PRECCDFGF and CCDFGF results presented herein are documented in

Information Only

Camphouse et al. (2012). The files associated with the PCS-2012 PA STEPWISE analysis can be found in the CMS libraries LIBPAP161_EVAL, LIBPABC09_STPW, LIBAP161_LHS, LIBSTP and LIBAP161_CCGF (Table 1). These files include the run scripts (EVAL_STP.COM, EVAL_STP_AP161_RAW_R*r*.COM and EVAL_STP_AP161_RANK_R*r*.COM, the CCGFDF output files CCGF_AP161_R*r*.OUT, the input files containing the mean values of the model output variables (STP_AP161_MEANS_R*r*.TRN), the STEPWISE control files (STP_AP161_RANK_ALL_R*r*.INP and STP_AP161_RAW_ALL_R*r*.INP), the input file containing the sampled parameters (STP_AP161_LHS_R*r*.TRN) and the results of the regression analysis (STP_AP161_RANK_R*r*.TXT and STP_AP161_RAW_R*r*.TXT), where the *r* in the file names represents replicate number 1, 2 or 3.

The files of mean values of releases STP_AP161_MEANS_R*r*.TRN.TRN, were generated from the CCGF_AP161_R*r*.OUT files using the Microsoft® Access 2010 database CCDFGF_Analysis.mdb. The CCDFGF output files store the mean values and those mean values are extracted from those files along with the "binned" data. The "bins" are a series of equally spaced intervals on a logarithmic scale that encompass the data. Each datum is assigned to a bin and the frequency of values within the bin tabulated. The databases are provided on the attached CD in zipped format and the AP161_ANALYSISDATABASE.zip file is also stored in the CMS library LIBAP161_STPW (Attachment 1).

The EVAL_STP.COM script runs STEPWISE.EXE to perform the regression analysis for all three replicates on both the ranked and raw (un-ranked) data.

Table 1. Files used in the PCS-2012 PA sensitivity analysis.

File	Library
CCDFGF_Analysis.mdb[1]	LIBAP161_STPW
CCDFGF_Data.mdb[1]	LIBAP161_STPW
CCGF_AP161_R1.OUT	LIBAP161_CCGF
CCGF_AP161_R2.OUT	LIBAP161_CCGF
CCGF_AP161_R3.OUT	LIBAP161_CCGF
LHS1_AP161_R1.TRN	LIBAP161_LHS
LHS1_AP161_R2.TRN	LIBAP161_LHS
LHS1_AP161_R3.TRN	LIBAP161_LHS
LHS2_AP161_R1_CON.TRN	LIBAP161_LHS
LHS2_AP161_R2_CON.TRN	LIBAP161_LHS
LHS2_AP161_R3_CON.TRN	LIBAP161_LHS
EVAL_STP_AP161_RAW_R1.COM	LIBAP161_STPW
EVAL_STP_AP161_RAW_R2.COM	LIBAP161_STPW
EVAL_STP_AP161_RAW_R3.COM	LIBAP161_STPW
EVAL_STP_AP161_RANK_R*1*.COM	LIBAP161_STPW
EVAL_STP_AP161_RANK_R2.COM	LIBAP161_STPW

Information Only

File	Library
EVAL_STP_AP161_RANK_R3.COM	LIBAP161_STPW
STP_AP161_LHS_R*1*.TRN	LIBAP161_STPW
STP_AP161_LHS_R*2*.TRN	LIBAP161_STPW
STP_AP161_LHS_R*3*.TRN	LIBAP161_STPW
STP_AP161_MEANS_R1.TRN	LIBAP161_STPW
STP_AP161_MEANS_R*2*.TRN	LIBAP161_STPW
STP_AP161_MEANS_R*3*.TRN	LIBAP161_STPW
STP_AP161_RANK_ALL_R*1*.INP	LIBAP161_STPW
STP_AP161_RANK_ALL_R*2*.INP	LIBAP161_STPW
STP_AP161_RANK_ALL_R*3*.INP	LIBAP161_STPW
STP_AP161_RAW_ALL_R*1*.INP	LIBAP161_STPW
STP_AP161_RAW_ALL_R*2*.INP	LIBAP161_STPW
STP_AP161_RAW_ALL_R*3*.INP	LIBAP161_STPW
STP_AP161_RANK_R*1*.TXT	LIBAP161_STPW
STP_AP161_RANK_R*1*.SP	LIBAP161_STPW
STP_AP161_RANK_R*2*.TXT	LIBAP161_STPW
STP_AP161_RANK_R*2*.SP	LIBAP161_STPW
STP_AP161_RANK_R*3*.TXT	LIBAP161_STPW
STP_AP161_RANK_R3.SP	LIBAP161_STPW
STP_AP161_RAW_R*1*.TXT	LIBAP161_STPW
STP_AP161_RAW_R1*2.SP*	LIBAP161_STPW
STP_AP161_RAW_R*2*.TXT	LIBAP161_STPW
STP_AP161_RAW_R*2*.SP	LIBAP161_STPW
STP_AP161_RAW_R*3*.TXT	LIBAP161_STPW
STP_AP161_RAW_R*3*.SP	LIBAP161_STPW
STEPWISE_PA96_2.EXE	LIBSTP

[1] **Compressed and stored in AP161_ANALYSISDATABASE.ZIP**

The input files for STEPWISE use short names rather than material:property designations. These short names are required because of a limitation in the length of variable names in STEPWISE. Table 2 associates these names with the material and property names.

Information Only

Table 2. Material and property values associated with the variable names used in the PCS-2012 PA sensitivity analysis. References in this table refer to DOE(2004).

Variable Name	Material Name	Property Name	Description
CMKDAM3	AM+3	MKD_AM	Matrix distribution coefficient (m3/kg) for Am in +3 oxidation state. Defined in Equation (231).
BHPERM	BH_SAND	PRMX_LOG	Logarithm of intrinsic permeability (m2) of the silty sand-filled borehole (Table PA-5). Used in regions Upper Borehole and Lower Borehole in Figure PA-8.
DOMEGA	BOREHOLE	DOMEGA	Drill string angular velocity (rad/s). Defined in Equation (112b).
WTAUFAIL	BOREHOLE	TAUFAIL	Shear strength of waste (Pa). Defined in Equation (111).
BPCOMP	CASTILER	COMP_RCK	Bulk compressibility (Pa–1) of Castile brine reservoir. Defined fB in Equation (29) for region CASTILER of Figure PA-8
BPINTPRS	CASTILER	PRESSURE	Initial brine pore pressure in the Castile brine reservoir. Defined in Equation (50) for region CASTILER in Figure PA-8.
BPPRM	CASTILER	PRMX_LOG	Logarithm of intrinsic permeability (m2) of the Castile brine reservoir. Used in region CASTILER in Figure PA-8.
PLGPRM	CONC_PLG	PRMX_LOG	Logarithm of intrinsic permeability (m2) of the concrete borehole plugs (Table PA-5). Used in region Borehole Plugs in Figure PA-8.
CFRACPOR	CULEBRA	APOROS	Culebra fracture (i.e., advective) porosity (dimensionless). Defined in Equation (223).
CMTRXPOR	CULEBRA	DPOROS	Culebra matrix (i.e., diffusive) porosity (dimensionless). Defined in Equation (230).
CFRACSP	CULEBRA	HMBLKLT	Culebra fracture spacing (m). Equal to half the distance between fractures (i.e., the Culebra half matrix block length). Defined in Equation (236) and Figure PA-26.
CTRANSFM	CULEBRA	MINP_FAC	Multiplier (dimensionless) applied to transmissivity of the Culebra within the land withdrawal boundary after mining of potash reserves. MF defined in Equation (216) (see section PA-4.8.2).
DRZPRM	DRZ_1	PRMX_LOG	Logarithm of intrinsic permeability (m2) of the DRZ. Used in regions Upper DRZ and Lower DRZ in Figure PA-8.
DRZPCPRM	DRZ_PCS	PRMX_LOG	Logarithm of intrinsic permeability (m2) of the DRZ immediately above the panel closure concrete (Section PA-4.2.8.3). Used in region DRZ_PCS in Figure PA-8.
CCLIMSF	GLOBAL	CLIMTIDX	Climate scale factor (dimensionless) for Culebra flow field. SFC defined in

Information Only

Variable Name	Material Name	Property Name	Description
			Equation (221).
WOXSTAT	GLOBAL	OXSTAT	Indicator variable for elemental oxidation states (dim3ensionless). WOXSTAT ≤0.5 indicates use of CMKDPU3, CMKDU4, WSOLPU3C, WSOLPUS, , WSOLU4C, and WSOLU4S. WOXSTAT >0.5 implies use of CMKDPU4, CMKDU6, WSOLPU4C, WSOLPU4S, WSOLU6C, and WSOLU6S.
BPPROB	GLOBAL	PBRINE	Probability that a drilling intrusion penetrates pressurized brine in the Castile Formation. See Section PA-3.5 for definition.
CTRAN	GLOBAL	TRANSIDX	Indicator variable for selecting transmissivity field. See Section PA-4.8.2.
T1PDIS	PCS_T1	PORE_DIS	Panel Closure System for an initial time duration Brooks-Corey pore distribution parameter
T1POROS	PCS_T1	POROSITY	Panel Closure System for an initial time duration effective porosity
T1PRMX	PCS_T1	PRMX_LOG	Panel Closure System for an initial time duration log of intrinsic permeability, X-direction
T1SIBRN	PCS_T1	SAT_IBRN	Panel Closure System for an initial time duration initial brine saturation
T1SRBRN	PCS_T1	SAT_RBRN	Panel Closure System for an initial time duration Residual Brine Saturation
T1SRGAS	PCS_T1	SAT_RGAS	Panel Closure System for an initial time duration residual gas saturation
T2P2PERM	PCS_T2	POR2PERM	Panel Closure System for a secondary time duration, distribution used to calculate permeability from sampled porosity values
T2POROS	PCS_T2	POROSITY	Panel Closure System for a secondary time duration effective porosity
T3POROS	PCS_T3	POROSITY	Run-of-Mine Panel Closure System, tertiary time period effective porosity
WPHUMOX3	PHUMOX3	PHUMCIM	Ratio (dimensionless) of concentration of actinides attached to humic colloids to dissolved concentration of actinides for oxidation state +III in Castile brine. Defined SFHum(Castile, +3, Am) and SFHum(Castile, +3, Pu) for Equation (90).
CMKDPU3	PU+3	MKD_PU	Matrix distribution coefficient (m3/kg) for Pu in +3 oxidation state. Defined in Equation (231).
CMKDPU4	PU+4	MKD_PU	Matrix distribution coefficient (m3/kg) for Pu in +4 oxidation state. Defined in Equation (231).
HALCROCK	S_HALITE	COMP_RCK	Bulk compressibility of halite (Pa–1). Defined fB in Equation (31) for region

Information Only

Variable Name	Material Name	Property Name	Description
			Salado of Figure PA-8.
HALPOR	S_HALITE	POROSITY	Halite porosity (dimensionless). Defined in Equation (25g) for region Salado in Figure PA-8.
SALPRES	S_HALITE	PRESSURE	Initial brine pore pressure (Pa) in the Salado halite, applied at an elevation consistent with the intersection of MB 139. Defined in Equation (49) for region Salado. See Figure PA-8.
HALPRM	S_HALITE	PRMX_LOG	Logarithm of intrinsic halite permeability (m2). Used in region Salado in Figure PA-8.
ANHBCEXP	S_MB139	PORE_DIS	Brooks-Corey pore distribution parameter for anhydrite (dimensionless). Defined in Equation (32) for regions MB 138, Anhydrite AB, and MB 139 of Figure PA-8 for use with Brooks-Corey model; defined in Equations (36) for use with van Genuchten-Parker model in the same regions.
ANHPRM	S_MB139	PRMX_LOG	Logarithm of intrinsic anhydrite permeability (m2). Used in regions MB 138, Anhydrite AB, and MB 139 in Figure PA-8.
ANHBCVGP	S_MB139	RELP_MOD	Indicator for relative permeability model (dimensionless) for regions MB 138, Anhydrite AB and MB 139 in Figure PA-8. See Table PA-3.
ANRBRSAT	S_MB139	SAT_RBRN	Residual brine saturation in anhydrite (dimensionless). Sbr defined in Equation (35) for regions MB 138, Anhydrite AB, and MB 139 in Figure PA-8.
SHLPRM2	SHFTL_T1	PRMX_LOG	Logarithm of intrinsic permeability (m2) of lower shaft seal materials for the first 200 years after closure. Used in region Lower Shaft in Figure PA-8.
SHLPRM3	SHFTL_T2	PRMX_LOG	Logarithm of intrinsic permeability (m2) of lower shaft seal materials from 200 years to 10,000 years after closure. Used in region Lower Shaft in Figure PA-8.
SHUPRM	SHFTU	PRMX_LOG	Logarithm of intrinsic permeability (m2) of upper shaft seal materials. Used in region Upper Shaft in Figure PA-8.
SHURBRN	SHFTU	SAT_RBRN	Residual brine saturation in upper shaft seal materials (dimensionless). Sbr defined in Equation (35) for region Upper Shaft in Figure PA-8.
SHURGAS	SHFTU	SAT_RGAS	Residual gas saturation in upper shaft seal materials (dimensionless). Sgr defined in Equation (34) for region Upper Shaft in Figure PA-8.
WSOLVAR3	SOLMOD3	SOLVAR	Solubility multiplier for +III oxidation states

Information Only

Variable Name	Material Name	Property Name	Description
WSOLVAR4	SOLMOD4	SOLVAR	Solubility multiplier for +IV oxidation states
SPLPTDIA	SPALLMOD	PARTDIAM	Particle diameter of disaggregated waste.
REPIPERM	SPALLMOD	REPIPERM	Waste permeability of gas local to intrusion borehole.
SPLRPOR	SPALLMOD	REPIPOR	Waste porosity at time of drilling intrusion
TENSLSTR	SPALLMOD	TENSLSTR	Tensile strength of waste.
WGRCOR	STEEL	CORRMCO2	Rate of anoxic steel corrosion (m/s) under brine inundated conditions and with no CO2 present. Defined Rci in Equation (59) for areas Waste Panel, South RoR, and North RoR in Figure PA-8.
CMKDTH4	TH+4	MKD_TH	Matrix distribution coefficient (m3/kg) for Th in +4 oxidation state. Defined in Equation (231).
CMKDU4	U+4	MKD_U	Matrix distribution coefficient (m3/kg) for U in +4 oxidation state. Defined in Equation (231).
CMKDU6	U+6	MKD_U	Matrix distribution coefficient (m3/kg) for U in +6 oxidation state. Defined in Equation (231).
WBIOGENF	WAS_AREA	BIOGENFC	Probability of obtaining sampled microbial gas generation rates.
WGRMICH	WAS_AREA	GRATMICH	Rate of CPR biodegradation (mol C6H10O5 / kg C6H10O5 / s) under anaerobic, humid conditions. Defined Rmh in Equation (61) for areas Waste Panel, South RoR, and North RoR, in Figure PA-8.
WGRMICI	WAS_AREA	GRATMICI	Rate of CPR biodegradation (mol C6H10O5 / kg C6H10O5 / s) under anaerobic, brine-inundated conditions. Defined Rmi in Equation (61) for areas Waste Panel, South RoR, and North RoR, in Figure PA-8.
WMICDFLG	WAS_AREA	PROBDEG	Index for model of microbial degradation of CPR materials (dimensionless). Used in areas Waste Panel, South RoR, and North RoR in Figure PA-8.
WRBRNSAT	WAS_AREA	SAT_RBRN	Residual brine saturation in waste (dimensionless). Defined Sbr in Equation (34) for areas Waste Panel, South RoR, and North RoR, in Figure PA-8; also used in waste material in Figure PA-20 for calculation of DBR; see Section PA-4.7.
WRGSSAT	WAS_AREA	SAT_RGAS	Residual gas saturation in waste (dimensionless). Sgr defined in Equation (35) for areas Waste Panel, South RoR, and North RoR in Figure PA-8; also used in waste material in Figure PA-20 for

Information Only

Variable Name	Material Name	Property Name	Description
			calculation of DBR; see Section PA-4.7.
WASTWICK	WAS_AREA	SAT_WICK	Increase in brine saturation of waste due to capillary forces (dimensionless). Defined Swick in Equation (78) for areas Waste Panel, South RoR, and North RoR, in Figure PA-8.

In addition, three variables are created in STEPWISE through transformation of the variable GLOBAL:OXSTAT, the indicator variable for oxidation states of uranium and plutonium. GLOBAL:OXSTAT is sampled as a [0,1) uniform distribution but is treated in the code as a Bernoulli distribution (a distribution having only two discrete states). The computed variable OXSTAT is assigned 0 if GLOBAL:OXSTAT is less than 0.5 and is assigned 1 otherwise. The other two computed variables represent the K_ds for the +VI and +IV oxidation states of uranium and plutonium, respectively. A K_d value represents the matrix:water partitioning coefficient. If GLOBAL:OXSTAT is 0 then CMKDU is assigned U+6:MKD_U and CMKDPU is assigned PU+4:MKD_PU, i.e. the K_ds for the +VI and +IV oxidation states of uranium and plutonium, respectively. If GLOBAL:OXSTAT is 1 then CMKDU is assigned U+4:MKD_U and CMKDPU is assigned PU+3:MKD_PU, i.e. the K_ds for the +IV and +III oxidation states of uranium and plutonium, respectively. In the discussion below these variables are referenced as Composite:MKD_U and Composite:MKD_PU in order to denote their status as composites of pairs of sampled parameters.

Changes from the PABC-2009 PA

The changes implemented in the PCS-2012 analysis from the PABC-2009 PA analysis are documented in Camphouse (2012a).These changes focus on a revised design of the panel closure system (PCS), known as the Run-of-Mine Panel Closure System (ROMPCS). This design employs panel closures comprised of 100 feet of run-of-mine (ROM) salt with barriers at each end. The ROM salt is generated from ongoing mining operations at the WIPP and may be compacted and/or moistened as it is emplaced in a panel entry. The ROM salt will be emplaced to all salt surfaces (back, walls, etc.) as completely as practicable. After emplacement, creep closure of the panel entries will cause the ROM salt to consolidate to a condition approaching intact salt, with low porosity and low permeability.

The ROMPCS properties modeled in the PA were based on three time periods: from 0 to 100 years, from 100 years to 200 years, and from 200 years to 10,000 years. This was a refinement to the granularity of panel closure modeling undertaken in the 2006 PCS PA (Vugrin and Dunagan 2006) and the 2011 PC3R PA (Camphouse et al. 2011). Three time periods are appropriate because the process to consolidate the ROM salt occurs over a primary time scale of approximately 100 years, while the process to heal fractures in the DRZ surrounding the PCS occurs over a longer time scale of approximately 200 years. The ROM salt was therefore represented by three materials, denoted as PCS_T1 for the first 100 years, PCS_T2 for 100 to 200 years, and PCS_T3 for 200 to 10,000 years. The effective permeability and porosity of the ROMPCS are the two parameters expected to have the greatest impact on calculations of pressure and brine saturation in repository waste areas. A brief discussion of the two-phase flow parameters used for PCS_T1, PCS_T2, and PCS_T3, particularly their implementation in regard

Information Only

to BRAGFLO capillary pressure modeling, is given in Camphouse (2012b). In addition to the sampled parameters listed in Table 2, there were changes or additions of some non-sampled (constant) parameters (Table 3).

Table 3: Non-sampled PCS_T1, PCS_T2, and PCS_T3 Properties to be used in the PCS-2012 PA

Property	Description
CAP_MOD	Capillary Pressure Model Number (CAP_MOD = 1 or 2 has been used in every PA to date for all materials in BRAGFLO)
COMP_RCK	Bulk Compressibility
KPT	Flag to Enable Dynamic Updating of Threshold Capillary Pressure as a Function of Permeability (KPT = 0 has been used in every PA to date for all materials in BRAGFLO)
PC_MAX	Maximum Allowable Capillary Pressure (PC_MAX = 1×10^8 Pa has been used for all BRAGFLO materials since the CCA)
PCT_A	Threshold Capillary Pressure Linear Parameter
PCT_EXP	Threshold Capillary Pressure Exponential Parameter
PO_MIN	Minimum Brine Pressure for Capillary Model 3 (CAP_MOD = 3 has never been used in PA)
PRMY_LOG[1]	Log of Intrinsic Permeability, Y-Direction
PRMZ_LOG[1]	Log of Intrinsic Permeability, Z-Direction
RELP_MOD	Relative Permeability Model Number

[1] **Assigned the sampled values of PRMX_LOG (Camphouse 2012c).**

Information Only

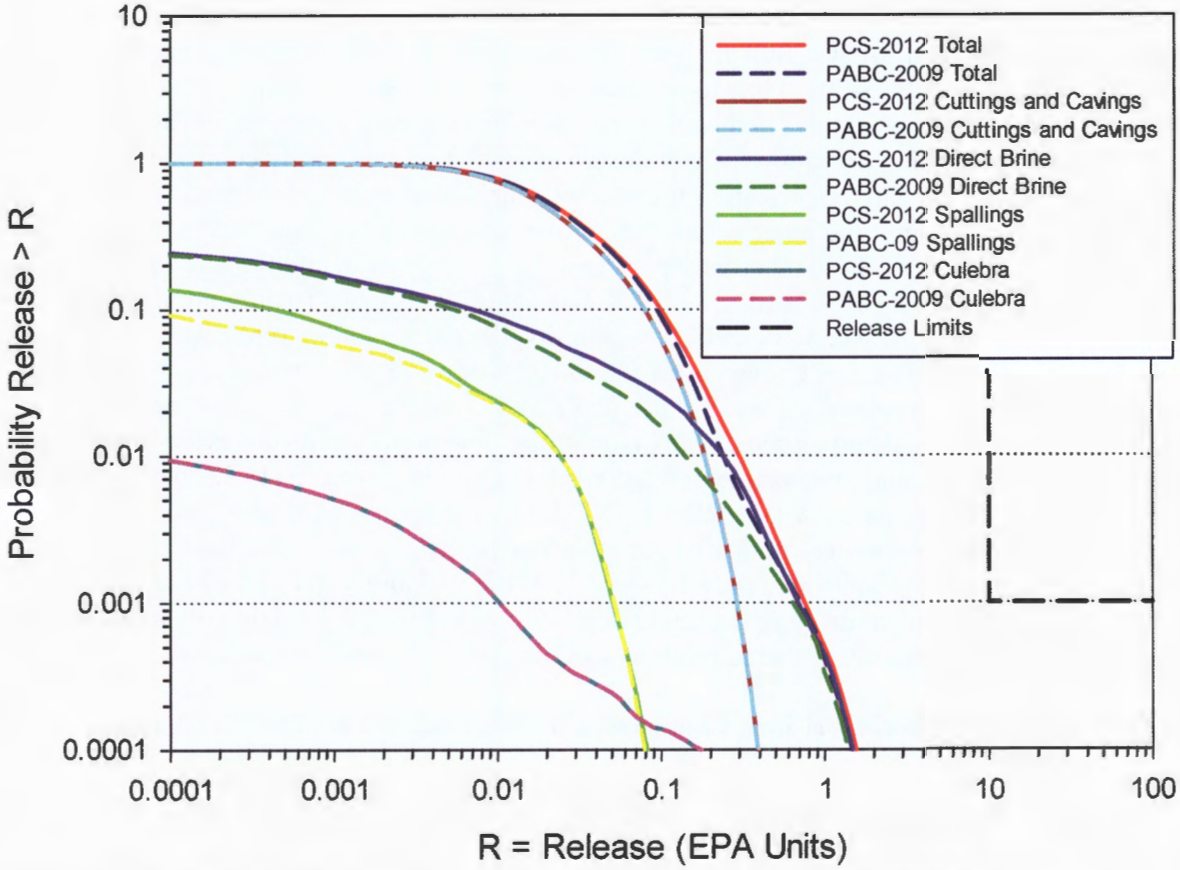

Figure 1. Mean CCDFs from Replicate 1 of the PCS-2012 analysis and the PABC-2009 PA analysis.

Most of the distributions used for the PCS-2012 analysis were identical to those used in the PABC-2009. The exceptions were those for material PCS_T1 (properties POR_DIS, POROSITY, PRMX_LOG, SAT_IBRN, SAT_RBRN, SAT_RGAS), PCS_T2 (properties POR2PERM and POROSITY) and PCS_T3:POROSITY which were not sampled in the PABC-2009. For material CONC_PCS, the following properties were sampled in PABC-2009 but not PCS-2012: PORE_DIS, PRMX_LOG, SAT_RBRN, and SAT_RGAS. The material:property CELLULS:FBETA was also sampled in the PABC-2009 but was not used in that analysis.

Total Releases

As in the PABC-2009 (Kirchner 2009), cuttings and cavings, direct brine and spallings releases account for the majority of the total releases estimated in the PABC-2009 (Figure 1). In the tables below the cumulative R^2 value represents the proportion of total variation explained by the fitted regression using the listed variables, starting with the greatest contributor to the variance. The number of variables used in the regression model is determined by the stepwise regression procedure, as discussed above. Across the three replicates of the PCS-2012 83 % to 86 % of the variability in total release is accounted for in the full regression model (Tables 4 and 5). The

Information Only

difference in the R^2 values for total releases between the first replicates of the PABC-2009 (87 %) and the PSC-2012 PA (83 %) is inconsequential (Table 4).

In both the PCS-2012 and PABC-2009 analyses the uncertainty in total normalized releases is largely (69 % to 74 % in PCS-2012) due to uncertainty in waste shear strength (BOREHOLE:TAUFAIL). Cuttings and cavings releases are normally combined because they are a direct result of drilling operations. The volumes of cavings are primarily controlled by shear strength, and the negative correlation found in the analysis is expected. There is little consistency in the ranking of the other variables identified as significant contributors to the variability in total releases. These other variables contribute less than an additional 14 % to the variability in total releases. CASTILER:PRESSURE is the initial brine pore pressure in the Castile and it contributes between 2% and 4% variability, depending on the replicate. S_HALITE:POROSITY is the effective porosity in intact halite and it contributes 3 % variability in replicate 3 and 2 % in replicates 1 and 2. DRZ_1:PRMXLOG, the log of intrinsic permeability in the X-direction for the disturbed rock zone in the initial time period, contributes 3% and 1% variability in replicates 1 and , respectively, but contributes nothing to replicate 2. The third-ranked parameter in replicate 2 is CULEBRA:MINP_FAC, the mining transmissivity multiplier. It is not included in the regression models of the other two replicates. The remaining variables in each of the three replicates contribute only 1 % to 2 % of the variability in total release, and hence are not important to controlling the total release. Correlations that explain only a few percent of the variation can occur due to random sampling and may well be spurious.

Table 4. Stepwise ranked regression analysis for mean total releases, replicate 1 of PCS-2012 PA and the ABC-2009.

	Expected Normalized Release					
	PCS-2012 Replicate 1			PABC-2009 Replicate 1		
Step[a]	Variable[b]	R^{2c}	SRRC[d]	Variable	R^2	SRRC
1	BOREHOLE:TAUFAIL	0.69	-0.83	BOREHOLE:TAUFAIL	0.76	-0.88
2	CASTILER:PRESSURE	0.71	0.16	SOLMOD3:SOLVAR	0.79	0.17
3	DRZ_1:PRMX_LOG	0.74	0.17	CELLULS:FBETA	0.81	-0.14
4	SOLMOD3:SOLVAR	0.76	0.14	CASTILER:PRESSURE	0.83	0.12
5	S_HALITE:POROSITY	0.78	0.13	GLOBAL:PBRINE	0.85	0.13
6	PCS_T1:SAT_IBRN	0.79	-0.12	SHFTU:SAT_RGAS	0.85	-0.10
7	GLOBAL:TRANSIDX	0.80	0.12	GLOBAL:TRANSIDX	0.86	0.09
8	CULEBRA:MINP_FAC	0.81	0.09	BOREHOLE:DOMEGA	0.87	0.08
9	S_MB139:RELP_MOD	0.82	-0.10			
10	S_MB139:SAT_RBRN	0.83	-0.09			

[a] Steps in stepwise regression analysis
[b] Variables listed in order of selection
[c] Cumulative R^2 value with entry of each variable into regression model
[d] Standardized Rank Regression Coefficient

Information Only

Table 5. Stepwise ranked regression analysis for mean total releases, replicates 2 and 3 of PCS-2012.

	Expected Normalized Release					
	PCS-2012 Replicate 2			PCS-2012 Replicate 3		
Step[a]	Variable[b]	R^{2c}	SRRC[d]	Variable	R^2	SRRC
1	BOREHOLE:TAUFAIL	0.71	-0.84	BOREHOLE:TAUFAIL	0.74	-0.85
2	CASTILER:PRESSURE	0.75	0.22	S_HALITE:POROSITY	0.77	0.18
3	CULEBRA:MINP_FAC	0.77	-0.14	CASTILER:PRESSURE	0.80	0.15
4	S_HALITE:POROSITY	0.79	0.12	SOLMOD3:SOLVAR	0.81	0.12
5	SOLMOD3:SOLVAR	0.80	0.12	BOREHOLE:DOMEGA	0.82	0.12
6	SPALLMOD:REPIPERM	0.81	-0.10	GLOBAL:PBRINE	0.83	0.10
7	PCS_T1:POROSITY	0.82	-0.10	CULEBRA:MINP_FAC	0.84	0.09
8	PCS_T1:PORE_DIS	0.83	-0.09	DRZ_1:PRMX_LOG	0.85	0.09
9	CASTILER:PRMX_LOG	0.84	0.09	GLOBAL:TRANSIDX	0.86	0.08
10				STEEL:CORRMCO2	0.86	-0.08

[a] Steps in stepwise regression analysis
[b] Variables listed in order of selection
[c] Cumulative R^2 value with entry of each variable into regression model
[d] Standardized Rank Regression Coefficient

Cuttings and Cavings Releases

CCDFGF only records the combined volume of cuttings and cavings, but only the cavings component is computed using sampled parameters. Tables 6 and 7 list the parameters that showed significant correlations to cuttings and cavings releases based on a stepwise regression using ranked data. The uncertainty in mean cuttings and cavings releases is primarily due to the uncertainty in the cavings volume. The other source of uncertainty is the stochastic selection of the waste streams intersected by the borehole. The results from the regression analyses of the PABC-2009 and PCS-2012 PA are identical for each of the three replicates (see Kirchner 2009). Waste shear strength (BOREHOLE:TAUFAIL) controls about 98 % of the variability in mean cuttings and cavings releases in all replicates. Cuttings and caving releases are primarily controlled by the volume of cuttings and cavings produced, which in turn is a highly non-linear function of BOREHOLE:TAUFAIL through its control on cavings volumes (Fig. 4). The drill string angular velocity (BOREHOLE:DOMEGA) has a very minor contribution as well, and is discussed in Dunagan (2004) and Ismail and Garner (2010). The remaining parameters in Tables 6 and 7 explain less than about 1 % of the variability in cuttings and cavings and are spurious because they have no influence on cuttings and cavings release volumes or on the selection of waste streams.

Table 6. Stepwise ranked regression analysis for mean Cuttings and Cavings releases.

	Expected Normalized Release					
	PCS-2012 Replicate 1			PABC-2009 Replicate 1		
Step[a]	Variable[b]	R^{2c}	SRRC[d]	Variable	R^2	SRRC
1	BOREHOLE:TAUFAIL	0.98	-0.99	BOREHOLE:TAUFAIL	0.98	-0.99
2	BOREHOLE:DOMEGA	1.00	0.11	BOREHOLE:DOMEGA	1.00	0.11
3	SHFTL_T1:PRMX_LOG	1.00	0.02	SHFTL_T1:PRMX_LOG	1.00	0.02
4	(Composite):OXSTAT	1.00	-0.02	(Composite):OXSTAT	1.00	-0.02
5	CULEBRA:HMBLKLT	1.00	0.02	CULEBRA:HMBLKLT	1.00	0.02
6	DRZ_PCS:PRMX_LOG	1.00	0.01	DRZ_PCS:PRMX_LOG	1.00	0.01

[a] Steps in stepwise regression analysis
[b] Variables listed in order of selection
[c] Cumulative R^2 value with entry of each variable into regression model
[d] Standardized Rank Regression Coefficient

Information Only

Table 7. Stepwise ranked regression analysis for mean Cuttings and Cavings releases, replicates 2 and 3 of PCS-2012.

	Expected Normalized Release					
	PCS-2012 Replicate 2			PCS-2012 Replicate 3		
Step[a]	Variable[b]	R^{2c}	SRRC[d]	Variable	R^2	SRRC
1	BOREHOLE:TAUFAIL	0.98	-0.99	BOREHOLE:TAUFAIL	0.98	-0.99
2	BOREHOLE:DOMEGA	0.99	0.11	BOREHOLE:DOMEGA	0.99	0.12
3	SHFTL_T1:PRMX_LOG	0.99	-0.02	(Composite):MKD_PU	0.99	0.02
4	PCS_T2:POR2PERM	0.99	0.02	SOLMOD3:SOLVAR	1.00	-0.02
5	STEEL:CORRMCO2	1.00	0.02			
6	GLOBAL:TRANSIDX	1.00	0.01			

[a] Steps in stepwise regression analysis

[b] Variables listed in order of selection

[c] Cumulative R^2 value with entry of each variable into regression model

[d] Standardized Rank Regression Coefficient

Information Only

A.

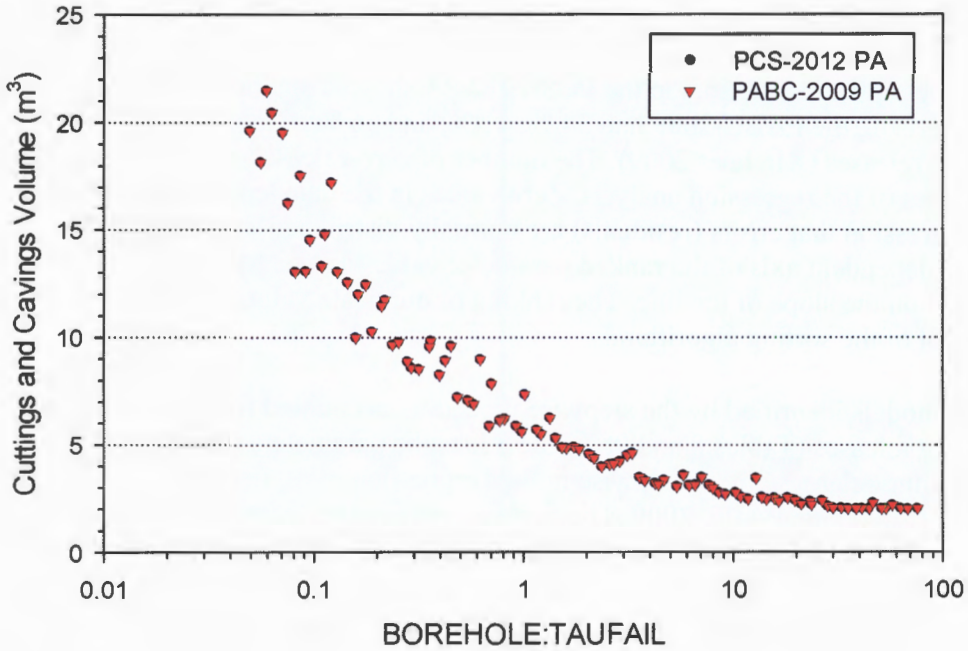

B.

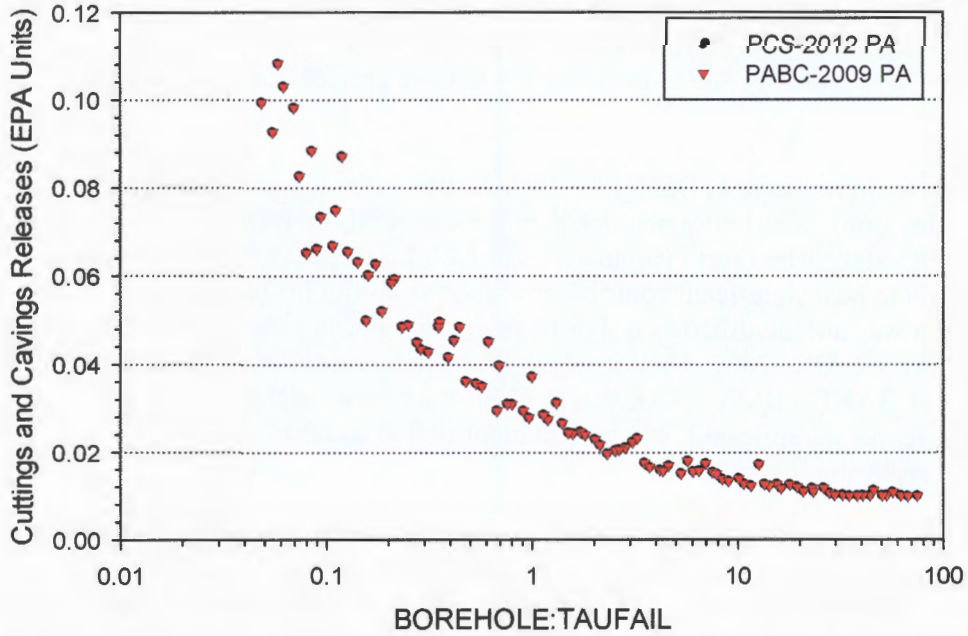

Figure 4. The volume of cuttings and cavings (A) and releases from cuttings and cavings (B) show significant nonlinear responses to WTAUFAIL. Note that the response is a curve even though BOREHOLE:TAUFAIL is plotted using a logarithmic axis.

Information Only

Spallings Releases

The probability of a spalling release volume less than two cubic meters was greater in the PCS-2012 PA as compared to the PABC-2009 (Fig. 5). The spallings releases were also higher in the PCS-2012 PA (Fig. 6). This increase was due in part to an increase in the number of vectors that produced spallings releases. Thirty-eight percent of the replicate 1 vectors, 47 % of the replicate 2 vectors and 41 % of the replicate 3 vectors in the PCS-2012 PA showed spallings releases (Zeitler 2012). In comparison, the PABC-2009 had 34 %, 41 %, and 36 % of the vectors in the three replicates showing releases (Kirchner 2009). The number of zero-releases was high enough to reduce the effectiveness of the regression analysis. Zero values in the data tend to negate the assumption of linear regression that errors (residuals) are normally distributed. In addition, the distribution along the independent axis of the ranked parameter values associated with the zeros can exert a lot of control on the slope of the line. The ranking of duplicate values (zeros in this case) is under the control of the sorting algorithm.

None of the regression models identified by the stepwise procedure accounted for even 50 % of the variability in spalling releases (Tables 8 and 9). Table 8 lists the parameters that showed correlation to mean spalling releases after a stepwise ranked regression using data from replicate 1 of both the PCS-2012 PA and the PABC-2009. The first two parameters from the analysis in both the PCS-2012 and the PABC-2009 PA analyses are the same and of similar magnitudes. The effective porosity of the Salado halite (S_HALITE:POROSITY) contributed the most to the variability in spalling releases across all the replicates, with the particle diameter of the disaggregated waste (SPALLMOD:PARTDIAM) being ranked second in two of the three replicates. The positive correlation shown by S_HALITE:POROSITY is likely to be due to having greater gas pressures under higher porosities due to greater brine flow into the repository. A negative correlation between SPALLMOD:PARTDIAM and spalling releases is observed in regressions whether releases of zero are included (Tables 8 and 9) or omitted ($p = 0.025$, Fig. 7; from spreadsheet SpalVsPartDiam.xlsx). The negative correlation with SPALLMOD:PARTDIAM is probably due to the tendency to have greater fluidization at smaller particle diameters.

The third-ranked parameter in replicate 1, DRZ_PCS:PRMX_LOG (the log of the intrinsic permeability in the X direction), contributes about 4 % of the variability in PCS-2012 compared to about 3 % in the PABC-2009. The fourth parameter, SPALLMOD:REPIPOR (initial waste porosity), was only found to be a significant contributor to the variability in spallings in replicate 1 of the PCS-2012 PA; it was not identified as a significant contributor in either of the other two replicates (Table 9) or in the PABC-2009. The log of the intrinsic permeability within a borehole filled with silty sand, BH_SAND:PRMX_LOG, was the last significant contributor to the variability in spalling releases in replicate 1. It was also identified as a contributor in the regression analyses for replicates 2 and 3.

There is little consistency among the replicates in the lists of the variables of step 3 or higher. These variables contribute only a few percent to the total variability and the ranking of their importance to determining spallings releases is thus questionable. CASTILER:PRESSURE is the far-field pore pressure in the Castile brine reserve. SHFTL_T1:PRMX_LOG is the logarithm of intrinsic permeability (m^2) of lower shaft seal materials from 0 years to 200 years after closure. WAS_AREA:GRATMICI is the rate of microbial degradation of CPR materials in inundates

Information Only

waste. WAS_AREA:SAT_RGAS is the residual gas saturation in the waste emplacement area. SPALLMOD:TENSLSTR is the tensile strength of waste and STEEL:CORRMCO2 is the inundated corrosion rate of steel when CO_2 is not present. While these parameters can perhaps influence pressures in the repository or the strength of the waste, and hence spallings releases, the lack of consistency across the replicates should be interpreted as evidence against their importance in controlling spallings.

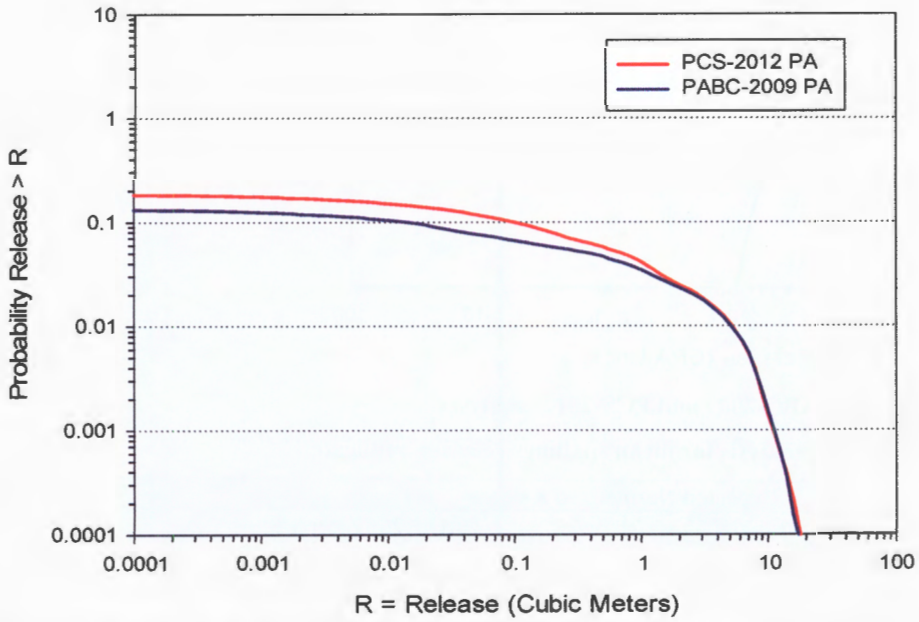

Figure 5. Spalling volume releases from the PABC-2009 and PCS-2012 analyses.

Information Only

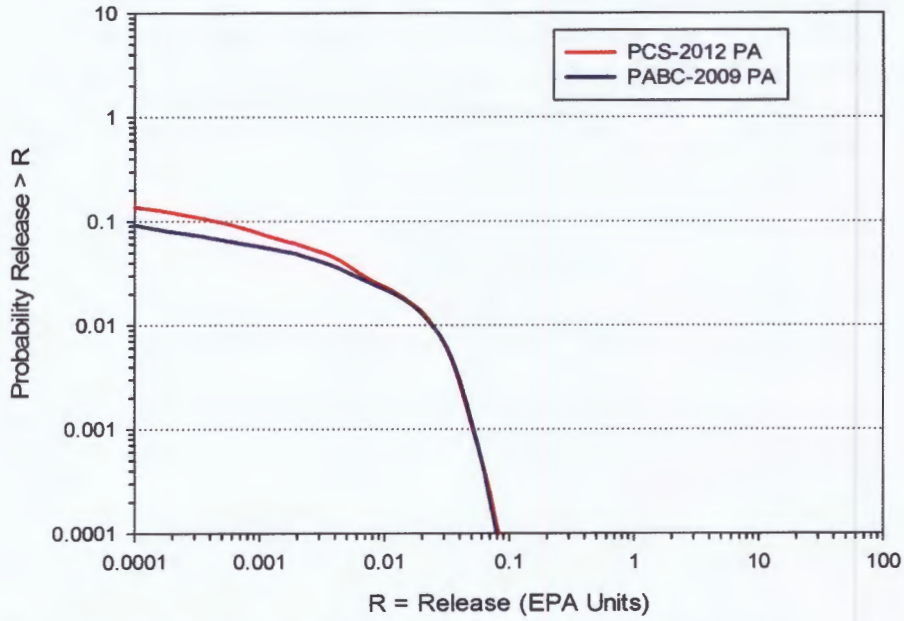

Figure 6. Spalling releases from the PABC-2009 and PCS-2012 analyses.

Table 8. Stepwise ranked regression analysis for mean spallings releases, replicate 1.

	Expected Normalized Release					
	PCS-2012 Replicate 1			PABC-2009 Replicate 1		
Step[a]	Variable[b]	R^{2c}	SRRC[d]	Variable	R^2	SRRC
1	S_HALITE:POROSITY	0.13	0.37	S_HALITE:POROSITY	0.14	0.34
2	SPALLMOD:PARTDIAM	0.21	-0.29	SPALLMOD:PARTDIAM	0.22	-0.28
3	DRZ_PCS:PRMX_LOG	0.25	-0.21	CULEBRA:DPOROS	0.26	-0.23
4	SPALLMOD:REPIPOR	0.29	-0.20	CASTILER:PRESSURE	0.30	0.19
5	BH_SAND:PRMX_LOG	0.32	-0.18	SHFTL_T2:PRMX_LOG	0.33	-0.18
6				WAS_AREA:PROBDEG	0.36	0.17
7				DRZ_PCS:PRMX_LOG	0.39	-0.18
8				S_MB139:PRMX_LOG	0.42	0.16

[a] Steps in stepwise regression analysis
[b] Variables listed in order of selection
[c] Cumulative R^2 value with entry of each variable into regression model
[d] Standardized Rank Regression Coefficient

Table 9. Stepwise ranked regression analysis for mean spallings releases, replicates 2 and 3 of PCS-2012.

	Expected Normalized Release					
	PCS-2012 Replicate 2			PCS-2012 Replicate 3		
Step[a]	Variable[b]	R^{2c}	SRRC[d]	Variable	R^2	SRRC
1	S_HALITE:POROSITY	0.15	0.37	S_HALITE:POROSITY	0.17	0.41
2	BH_SAND:PRMX_LOG	0.22	-0.28	SPALLMOD:PARTDIAM	0.27	-0.28
3	CASTILER:PRESSURE	0.29	0.27	DRZ_PCS:PRMX_LOG	0.34	-0.26
4	SPALLMOD:PARTDIAM	0.34	-0.23	WAS_AREA:SAT_RGAS	0.37	-0.18
5	WAS_AREA:GRATMICI	0.37	0.18	SPALLMOD:TENSLSTR	0.40	-0.18
6	SHFTL_T1:PRMX_LOG	0.40	0.16	STEEL:CORRMCO2	0.43	0.16
7	DRZ_PCS:PRMX_LOG	0.43	-0.16	BH_SAND:PRMX_LOG	0.46	-0.16

[a] Steps in stepwise regression analysis
[b] Variables listed in order of selection
[c] Cumulative R^2 value with entry of each variable into regression model
[d] Standardized Rank Regression Coefficient

Information Only

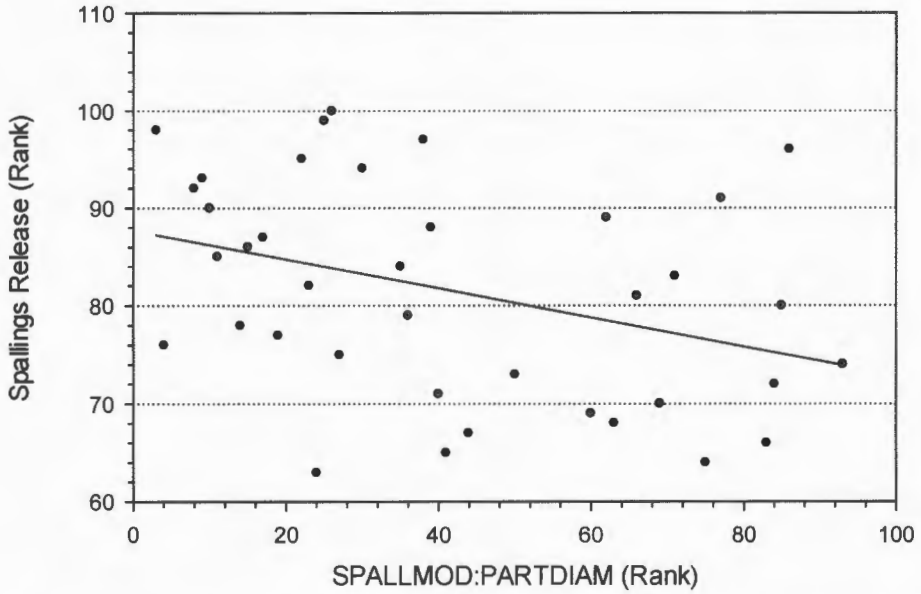

Figure 7. Non-zero spallings release shows a negative correlation (p = 0.025) with SPALLMOD:PARTDIAM.

Direct Brine Release

Direct brine releases (DBR) are releases of contaminated brine originating in the repository and flowing up an intrusion borehole during the period of drilling and before the hole is plugged. In order for DBR to occur volume-averaged pressure near the borehole must exceed 8 MPa and brine saturation in the repository must exceed the residual saturation of the waste material (Clayton 2008). Volume averaged brine pressure and brine saturation in the intruded panel strongly influence DBR volumes. The panel closure system defined by PCS-2012 impacted both of these factors (Camphouse et al. 2012). Overall, brine volumes increased in all of the PCS-2012 DBR scenarios modeled by BRAGFLO except one (Malama 2012).

Information Only

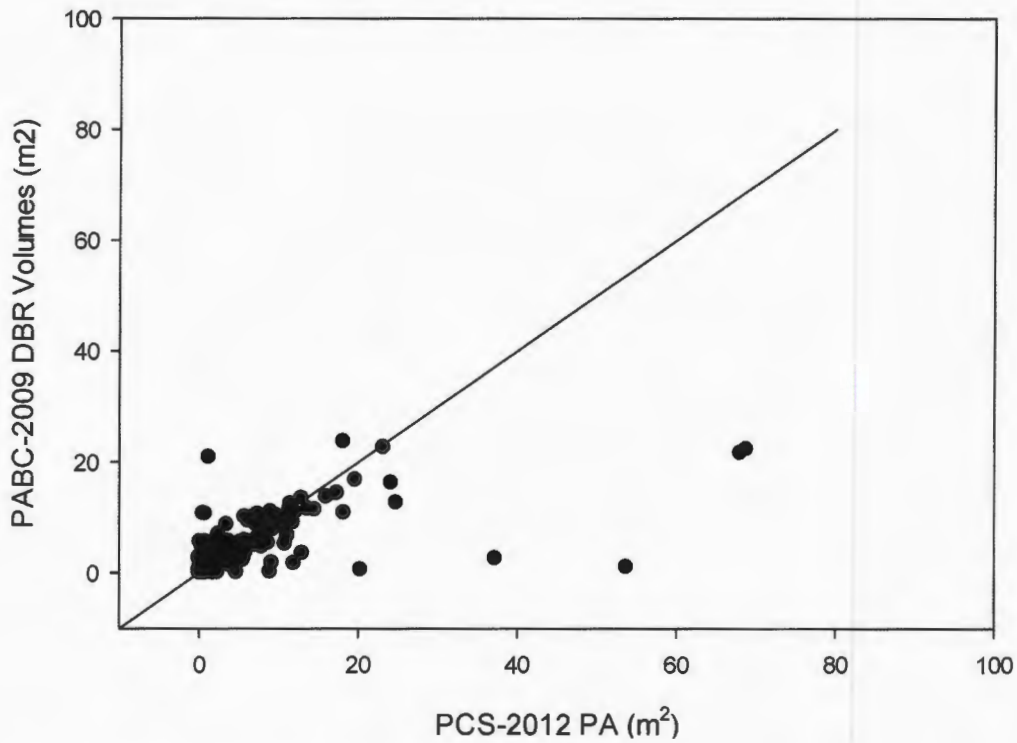

Figure 8. Mean DBR volumes for PABC-2009 and PCS-2012 paired by replicate and vector. The line represents equality in release volumes.

Of the pathways for release DBR showed the greatest increase over the PABC-2009 results (Fig. 1). However, the increase in the mean DBR release was controlled by very large increases in a few vectors, rather than an overall increase in most or all vectors, as shown in Fig. 8. PCS-2012 had eleven vectors across all three replicates that had negligible (<0.0001) release volumes while the PABC-2009 had nine such cases.

The PABC-2009 analysis shows that four variables (SOLMOD3:SOLVAR, CASTILER:PRESSURE, STEEL:CORRMCO2 and GLOBAL:PBRINE) account for more than 50 % of the uncertainty in DBR (Tables 10 and 11). These variables are also the four most important contributors to variability in DBR in all three replicates of the PCS-2012 PA analysis although variables are ranked differently from those of the PABC-2009 analysis. Somewhat surprisingly, only one of the new sampled parameters, PCS_T3:POROSITY, appeared in the analysis, and DBR was only weakly correlated with it in one replicate (replicate 3). SOLMOD3:SOLVAR is a "solubility multiplier" that represents uncertainty in solubilities for all actinides in the +III oxidation state (Xiong et al. 2009). STEEL:CORRMCO2 is the inundated corrosion rate for steel in the absence of CO_2. The corrosion of iron is expected to produce hydrogen but at the same time it consumes water. When the repository is flooded with brine from the intrusion of a brine pocket it is likely that the influence of STEEL:CORRMCO2 on DBR would be positive since the production of hydrogen would outweigh the minimal impact of the consumption of water. However, a negative correlation (p=0.001, spreadsheet

Information Only

DBRVsSteelCorr.xlsx) is observed between the ranked variables (Fig. 9 and Table 10), suggesting that the corrosion of steel is having its strongest influence when the repository is not saturated and DBR releases are expected to be small. CASTILER:PRESSURE is the initial brine pore pressure in the Castile. CASTILER:PRESSURE and GLOBAL:PBRINE control the frequency with which Castile brine intrudes the repository due to a drilling event and the initial pressure of that brine, thus their positive correlation with DBR is obvious.

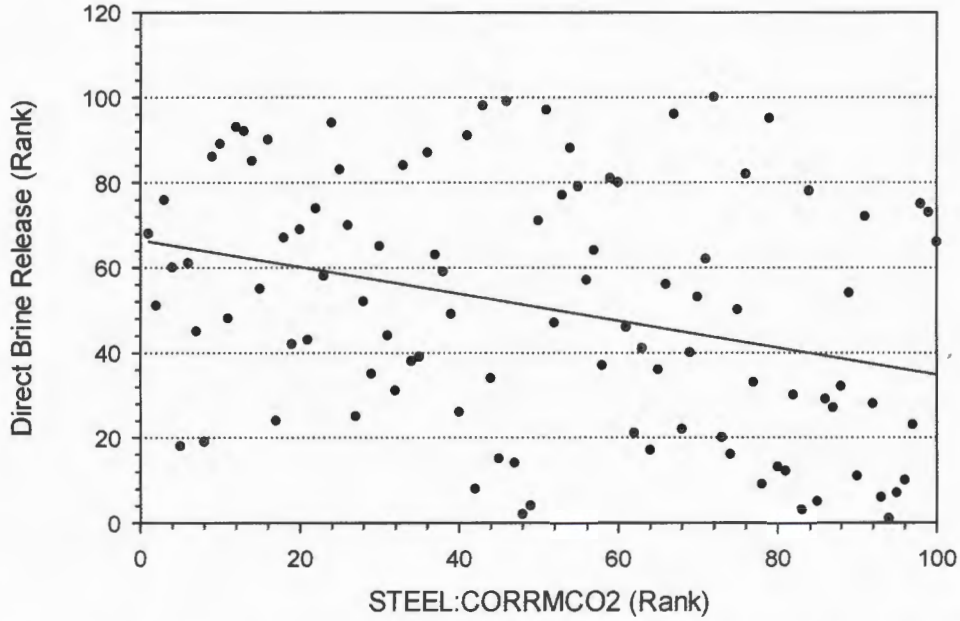

Figure 9. A significant (p = 0.001) negative correlation is observed between the ranks of Direct Brine Releases and the corrosion rate of steel (STEEL:CORRMCO2) in replicate 1 of the PCS-2012 PA.

There is no consistency in the names and orderings of the remaining parameters contributing to the uncertainty in DBR. These parameters each contribute about 1-5 % of the variability in DBR. Once the contribution of a parameter to the uncertainty drops to a few percent the correlation could arise from sampling rather than a mechanistic relationship. For example, BOREHOLE:DOMEGA, the drill string angular velocity, and the SPALLMOD (spallings model) properties should have no impact on DBR releases. That is not to say that all of these correlations are spurious. The remainder have the potential for impacting gas pressure, saturation levels or concentrations of radionuclides in the brine. For example, S_HALITE:POROSITY is the effective porosity in intact halite and it contributes from 1% to 3% to the variability in DBR. It influences the gas pressures in the repository, which in turn impacts the volume of direct brine releases. However, S_HALITE:POROSITY can have both positive and negative impacts on DBR. On the one hand, higher porosities could reduce gas pressures and potentially increase the inflow of brine with subsequent gas generation within the inundated panel, increasing brine saturation above the residual saturation levels and thus yielding higher direct brine releases. On the other hand, lower porosities could maintain higher gas pressures in the repository for longer periods and thus increase the release volumes. The overall impact is likely controlled by the timing of inundation and subsequent penetration of the repository, which is under the control of the aleatory parameters and hence not accounted for in the regression models. Another

Information Only

parameter, WAS_AREA:SAT_WICK, represents the increase in brine saturation due to capillary forces. The negative correlation is probably the result of an increase in iron consumption and thereby a reduction of brine as WAS_AREA:SAT_WICK increases. However, increased saturation could also lead to higher gas generation and thus greater direct brine releases, so again the impact of the parameter could be positive or negative depending on circumstances. WAS_AREA:SAT_WICK was ranked seventh, fifth and eleventh in in this analysis.

Table 10. Stepwise ranked regression analysis for mean Direct Brine releases.

	Expected Normalized Release					
	PCS-2012 Replicate 1			PABC-2009 Replicate 1		
Step[a]	Variable[b]	R^{2c}	SRRC[d]	Variable	R^2	SRRC
1	CASTILER:PRESSURE	0.15	0.40	SOLMOD3:SOLVAR	0.19	0.42
2	SOLMOD3:SOLVAR	0.28	0.36	CASTILER:PRESSURE	0.35	0.40
3	STEEL:CORRMCO2	0.40	-0.33	GLOBAL:PBRINE	0.45	0.33
4	GLOBAL:PBRINE	0.47	0.26	STEEL:CORRMCO2	0.55	-0.30
5	S_HALITE:POROSITY	0.50	0.17	S_MB139:RELP_MOD	0.58	-0.18
6	S_MB139:RELP_MOD	0 .53	-0.19	WAS_AREA:BIOGENFC	0.60	0.15
7	WAS_AREA:SAT_WICK	0.56	-0.15	S_HALITE:POROSITY	0.63	0.15
8	DRZ_1:PRMX_LOG	0.58	0.15	CONC_PCS:SAT_RGAS	0.65	-0.14
9	SOLMOD4:SOLVAR	0.60	0.16	S_MB139:PRMX_LOG	0.67	0.14
10	SHFTU:SAT_RBRN	0.62	0.14	WAS_AREA:SAT_WICK	0.69	-0.14
11	BOREHOLE:DOMEGA	0.64	-0.14			
12	WAS_AREA:BIOGENFC	0.66	0.13			
13	WAS_AREA:SAT_RBRN	0.67	-0.13			

[a] Steps in stepwise regression analysis
[b] Variables listed in order of selection
[c] Cumulative R^2 value with entry of each variable into regression model
[d] Standardized Rank Regression Coefficient

Table 11. Stepwise ranked regression analysis for mean Direct Brine releases, replicates 2 and 3 of PCS-2012.

	Expected Normalized Release					
	PCS-2012 Replicate 2			PCS-2012 Replicate 3		
Step[a]	Variable[b]	R^{2c}	SRRC[d]	Variable	R^2	SRRC
1	SOLMOD3:SOLVAR	0.16	0.43	CASTILER:PRESSURE	0.20	0.41
2	CASTILER:PRESSURE	0.31	0.31	SOLMOD3:SOLVAR	0.38	0.42
3	STEEL:CORRMCO2	0.44	-0.38	STEEL:CORRMCO2	0.48	-0.32
4	GLOBAL:PBRINE	0.52	0.29	GLOBAL:PBRINE	0.56	0.28
5	WAS_AREA:SAT_WICK	0.57	-0.22	CULEBRA:MINP_FAC	0.60	0.22
6	DRZ_PCS:PRMX_LOG	0.62	0.22	DRZ_PCS:PRMX_LOG	0.65	0.20
7	WAS_AREA:SAT_RBRN	0.65	-0.18	WAS_AREA:SAT_RBRN	0.68	-0.18
8	S_MB139:PRMX_LOG	0.67	0.17	DRZ_1:PRMX_LOG	0.70	0.17
9	WAS_AREA:PROBDEG	0.70	-0.17	CASTILER:COMP_RCK	0.72	-0.16
10	DRZ_1:PRMX_LOG	0.72	0.14	SPALLMOD:REPIPOR	0.74	0.13
11	SHFTU:PRMX_LOG	0.74	0.16	WAS_AREA:SAT_WICK	0.75	-0.12
12	BH_SAND:PRMX_LOG	0.76	-0.14	PCS_T3:POROSITY	0.76	0.11
13	S_HALITE:POROSITY	0.78	0.14	SPALLMOD:TENSLSTR	0.78	0.11
14	CULEBRA:APOROS	0.80	0.12	GLOBAL:CLIMTIDX	0.79	0.10
15	SPALLMOD:REPIPOR	0.81	0.11	S_HALITE:POROSITY	0.80	0.10

[a] Steps in stepwise regression analysis
[b] Variables listed in order of selection
[c] Cumulative R^2 value with entry of each variable into regression model
[d] Standardized Rank Regression Coefficient

Information Only

Culebra Releases

The regression results for releases both to and from the Culebra in the PCS-2012 analysis are very similar to those computed for the PABC-2009, with the regression models for releases from the Culebra for replicates 2 and 3, respectively, being identical (see Kirchner 2009). In the PABC-2009 and the PCS-2012 PA the percentages of vectors that had Culebra releases of zero were 9 %, 7 % and 6 %, respectively for replicates 1, 2 and 3. The releases of zero are due, for the most part, to transport rates frequently being too small to enable contaminants to reach the boundary within the simulation period, 10,000 years. The times of the intrusions giving rise to flows *to* the Culebra are also likely to influence whether or not such releases occur. These times are not represented in the "sampled" input parameters and thus cannot be associated with the releases in a sensitivity analysis.

The regression models show that 74 % to 82 % of the variability in Culebra releases is accounted for across the three replicates of the PCS-2012 PA (Tables 12 and 13). BH_SAND:PRMX_LOG and the K_ds for the radionuclides appear to be the most important factors controlling Culebra releases to the Culebra from the repository within the Culebra to the boundary of the WIPP site. The dominant parameter in the PCS-2012 analysis of releases both *to* the Culebra and *from* the Culebra is BH_SAND:PRMX_LOG, the logarithm of intrinsic permeability in the X-direction for a sand-filled borehole (Tables 12, 13, 14 and 15). Conceptually, the flow of brine up the borehole (and thus to the Culebra) should be positively influenced by increasing values for BH_SAND:PRMX_LOG (Stein and Zelinski 2003). This parameter accounts for 41 % to 55 % of the variability in releases *from* the Culebra and 80 % to 84 % of the releases *to* the Culebra across the three replicates of the PCS-2012 PA.

Table 12. Stepwise ranked regression analysis for mean Culebra releases.

	Expected Normalized Release					
	PCS-2012 Replicate 1			PABC-2009 Replicate 1		
Step[a]	Variable[b]	R^{2c}	SRRC[d]	Variable	R^2	SRRC
1	BH_SAND:PRMX_LOG	0.46	0.63	BH_SAND:PRMX_LOG	0.46	0.63
2	(Composite):MKD_U	0.58	-0.32	(Composite):MKD_U	0.58	-0.36
3	PCS_T2:POR2PERM	0.62	-0.20	DRZ_PCS:PRMX_LOG	0.61	0.17
4	DRZ_PCS:PRMX_LOG	0.65	0.17	SOLMOD4:SOLVAR	0.63	-0.17
5	CULEBRA:HMBLKLT	0.67	0.15	CULEBRA:HMBLKLT	0.65	0.16
6	SOLMOD4:SOLVAR	0.70	-0.16	CULEBRA:APOROS	0.67	-0.14
7	CULEBRA:APOROS	0.71	-0.13	(Composite):MKD_PU	0.69	-0.14
8	STEEL:CORRMCO2	0.73	-0.12	STEEL:CORRMCO2	0.71	-0.13
9	GLOBAL:TRANSIDX	0.74	0.11			

[a] Steps in stepwise regression analysis
[b] Variables listed in order of selection
[c] Cumulative R^2 value with entry of each variable into regression model
[d] Standardized Rank Regression Coefficient

Information Only

Table 13. Stepwise ranked regression analysis for mean Culebra releases, replicates 2 and 3 of PCS-2012.

	Expected Normalized Release					
	PCS-2012 Replicate 2			PCS-2012 Replicate 3		
Step[a]	Variable[b]	R^{2c}	SRRC[d]	Variable	R^2	SRRC
1	BH_SAND:PRMX_LOG	0.55	0.71	BH_SAND:PRMX_LOG	0.41	0.62
2	GLOBAL:OXSTAT	0.67	0.22	(Composite):MKD_U	0.55	-0.31
3	CULEBRA:MINP_FAC	0.70	-0.16	CULEBRA:APOROS	0.59	-0.21
4	(Composite):MKD_U	0.73	-0.21	WAS_AREA:SAT_WICK	0.62	-0.15
5	CONC_PLG:PRMX_LOG	0.74	-0.12	GLOBAL:CLIMTIDX	0.64	0.18
6	STEEL:CORRMCO2	0.75	-0.11	STEEL:CORRMCO2	0.67	-0.17
7	CULEBRA:HMBLKLT	0.77	0.11	CASTILER:PRESSURE	0.69	0.14
8	AM+3:MKD_AM	0.78	-0.12	PCS_T1:PORE_DIS	0.71	0.14
9	CASTILER:PRESSURE	0.79	0.11	DRZ_PCS:PRMX_LOG	0.73	0.12
10	PHUMOX3:PHUMCIM	0.80	0.11	PCS_T1:PRMX_LOG	0.74	0.12
11	WAS_AREA:SAT_RGAS	0.81	-0.10	S_HALITE:COMP_RCK	0.75	0.11
12	CULEBRA:APOROS	0.82	-0.10	CASTILER:PRMX_LOG	0.76	0.11
13				S_MB139:SAT_RBRN	0.77	-0.11

[a] Steps in stepwise regression analysis
[b] Variables listed in order of selection
[c] Cumulative R^2 value with entry of each variable into regression model
[d] Standardized Rank Regression Coefficient

There are three additional parameters found across all of the regression models for the three replicates of the PCS-2012 PA: Composite:MKD_U, CULEBRA:APOROS and STEEL:CORRMCO2. The parameter ranked second in two of the three analyses for releases *from* the Culebra is the matrix/water partition coefficient (K_d) for uranium, Composite:MKD_U. Composite:MKD_U is assigned U+6:MKD_U or U+4:MKD_U depending on the oxidation state for uranium. These are the K_ds for the +VI and +IV oxidation states of uranium, respectively. The negative correlation between Culebra releases and Composite:MKD_U was expected because high values of K_d suppress the transport of the radionuclide. In replicate 2, Composite:MKD_U is ranked fourth, preceded by two variables (GLOBAL:OXSTAT and CULEBRA:MINP_FAC) that do not appear in the regression models for the other two replicates. Composite:MKD_U contributes only to the regression model for releases *to* the Culebra in replicate 1, where it ranks sixth in importance (Table 14).

Culebra advective porosity (the fracture volume per unit volume of porous media, CULEBRA:APOROS), is ranked seventh, twelfth and third in the three replicates. Negative correlations are expected for this variable because it affects the velocity of transport. Low porosities increase the rate of transport as compared to high porosities and hence increase the likelihood of a release at the land withdrawl boundary within 10,000 years. Using the data from replicate 3, which ranked CULEBRA:APOROS third, a simple regression between Culebra releases and CULEBRA:APOROS (spreadsheet CulVsAporosRep3NZ.xlsx) shows a significance of $p = 0.01$ (releases of 0 excluded, Fig. 10) or $p = 0.06$ (spreadsheet CulVsAporosRep3.xlsx, releases of 0 included). CULEBRA:APOROS does not contribute to the variability of releases *to* the Culebra.

Information Only

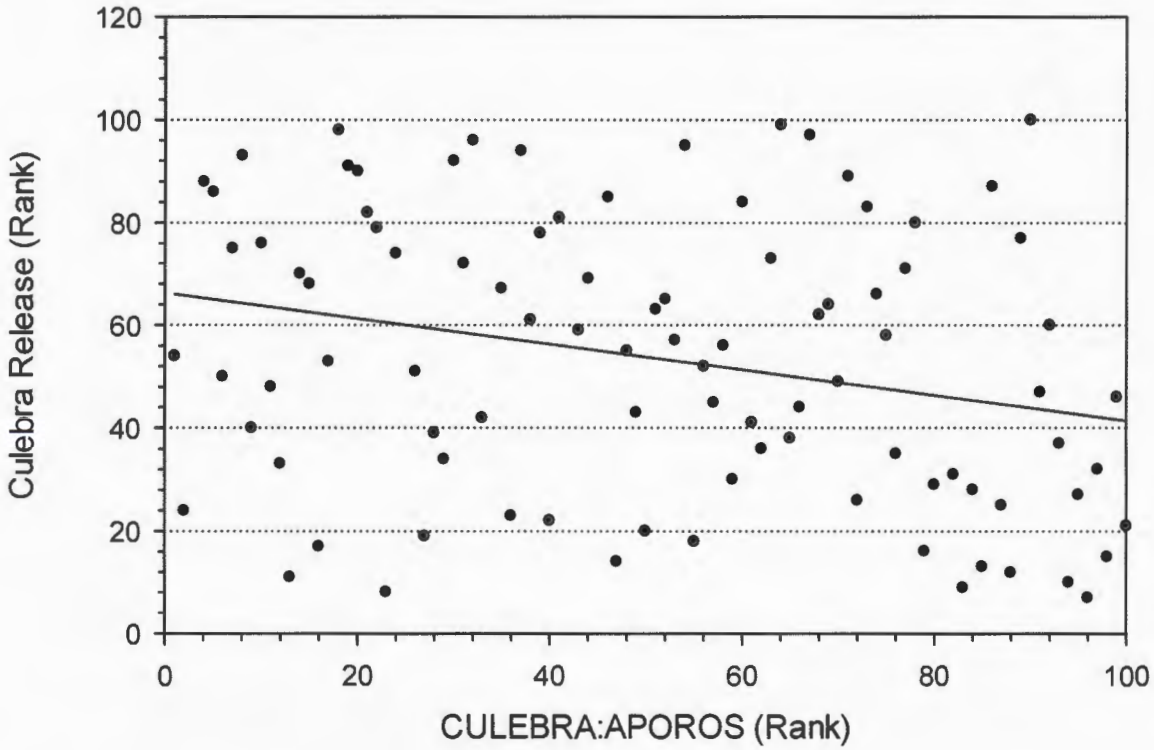

Figure 10. Correlation between the ranks of CULEBRA:APOROS (a unitless parameter) and Culebra Release (excluding zeros) in the PCS-2012 results for replicate 3.

STEEL:CORRMCO2 is the inundated corrosion rate for steel in the absence of CO_2. The corrosion of iron is expected to produce hydrogen but at the same time it consumes water. When the repository is flooded with brine from the intrusion of a brine pocket it is likely that the influence of STEEL:CORRMCO2 on Culebra releases would be positive since the production of hydrogen would outweigh the minimal impact of the consumption of water. However, a negative correlation is observed between the ranked variables (Tables 12 and 13), suggesting that the corrosion of steel is having its strongest influence when the repository is not saturated. STEEL:CORRMCO2 also contributes 1 % to 3 % of the variability in releases *to* the Culebra (Tables 14 and 15).

Information Only

Table 14. Stepwise ranked regression analysis for mean releases to Culebra, replicate 1.

	Expected Normalized Release					
	PCS-2012 Replicate 1			PABC-2009 Replicate 1		
Step[a]	Variable[b]	R^{2c}	SRRC[d]	Variable	R^2	SRRC
1	BH_SAND:PRMX_LOG	0.80	0.90	BH_SAND:PRMX_LOG	0.80	0.91
2	STEEL:CORRMCO2	0.82	-0.16	STEEL:CORRMCO2	0.82	-0.15
3	DRZ_PCS:PRMX_LOG	0.84	0.13	DRZ_PCS:PRMX_LOG	0.84	0.13
4	CASTILER:PRESSURE	0.84	0.08	CASTILER:PRESSURE	0.84	0.08
5	SOLMOD3:SOLVAR	0.85	0.11	SOLMOD3:SOLVAR	0.85	0.10
6	(Composite):MKD_U	0.86	0.09	(Composite):MKD_U	0.86	0.08
7	PCS_T2:POR2PERM	0.87	-0.09	SOLMOD4:SOLVAR	0.86	-0.08
8	WAS_AREA:PROBDEG	0.87	0.09	GLOBAL:TRANSIDX	0.87	0.08
9	GLOBAL:CLIMTIDX	0.88	-0.08			
10	SOLMOD4:SOLVAR	0.88	-0.08			
11	GLOBAL:TRANSIDX	0.89	0.08			

[a] Steps in stepwise regression analysis
[b] Variables listed in order of selection
[c] Cumulative R^2 value with entry of each variable into regression model
[d] Standardized Rank Regression Coefficient

Table 15. Stepwise ranked regression analysis for mean releases to Culebra, replicates 2 and 3 of the PCS-2012.

	Expected Normalized Release					
	PCS-2012 Replicate 2			PCS-2012 Replicate 3		
Step[a]	Variable[b]	R^{2c}	SRRC[d]	Variable	R^2	SRRC
1	BH_SAND:PRMX_LOG	0.83	0.92	BH_SAND:PRMX_LOG	0.84	0.90
2	SOLMOD3:SOLVAR	0.86	0.17	STEEL:CORRMCO2	0.86	-0.15
3	CASTILER:PRESSURE	0.88	0.12	CASTILER:PRESSURE	0.88	0.15
4	STEEL:CORRMCO2	0.89	-0.12	CASTILER:COMP_RCK	0.90	-0.12
5	PCS_T1:PORE_DIS	0.90	0.08	PCS_T2:POR2PERM	0.90	0.08
6	WAS_AREA:PROBDEG	0.90	-0.08			

[a] Steps in stepwise regression analysis
[b] Variables listed in order of selection
[c] Cumulative R^2 value with entry of each variable into regression model
[d] Standardized Rank Regression Coefficient

Summary and Conclusions

Of the four pathways of release, DBR and Spallings showed the greatest difference between the PABC-2009 and the PCS-2012 PA results. Releases from both of these pathways are controlled by pressures within the repository, although DBR is also controlled by brine saturation. In both cases it is the volume of the releases that account for the difference in activity releases between the PCS-2012 and PABC-2009 analyses since the other factors which impact these releases, such as inventory, solubilities, and drilling parameters were the same in both analyses. Surprisingly, correlations between these releases and the new PCS sampled parameters were nearly absent, with only a weak correlation found between PCS_T3:POROSITY and DBR in one replicate. The release tables generated by BRAGFLO for DBR showed increases in release volumes for all scenarios but one (Malama 2012), but the PCS-2012 DBR volumes were not consistently larger than those for the PABC-2009 analysis. It appears that the difference in mean DBR releases is due to just a few vectors having considerably larger releases in the PCS-2012 PA.

Information Only

Sensitivity of PCS-2012 PA Releases to Parameters

There were only small differences between the PCS-2012 and PABC-2009 sensitivity analyses for any of the release pathways (direct brine releases, spallings releases, releases from the Culebra , and cuttings and cavings releases). Cuttings and caving releases remain the primary contributor to total releases. BOREHOLE:TAUFAIL controls about 98 % of the variability in mean cuttings and cavings through its impact on cavings and shows a highly non-linear relationship with the volume of cuttings and cavings produced. The drill string angular velocity (BOREHOLE:DOMEGA) may also have a small effect on cuttings and cavings release volumes, again through its impact on cavings.

This analysis continues to show many weak correlations that are either undoubtedly (e.g. the correlation between BOREHOLE:DOMEGA and the SPALLMOD properties correlated with DBR releases) or probably spurious. To some extent these arise because of the request by EPA to see more variables listed in the analyses (EPA 2004), which is accomplished at the expense of having more parameters retained in the regression model than may be necessary and by setting the regression parameters to allow a moderate number of false-positive results.

Information Only

References:

Camphouse, R.C., Clayton, D.J., Kicker, D.C., and Pasch, J.J. 2011. Summary Report for the AP-151 (PC3R) Performance Assessment, Revision 1. Sandia National Laboratories, Carlsbad, NM. ERMS 555489.

Camphouse, C. 2012a. Analysis Plan for the 2012 WIPP Panel Closure System Performance Assessment, Revision 0. July 2, 2012. Carlsbad, NM: Sandia National Laboratories. ERMS #557726

Camphouse, R.C. 2012b. An overview of the BRAGFLO two-phase flow parameters used to model the run-of-mine salt panel closures implemented in the PCS-2012 PA. Memo to Paul Shoemaker dated June 7, 2012. C. ERMS 557653.

Camphouse, R. C. 2012c. A summary of parameters to be implemented in the PCS-2012 PA. Memo to Janis Trone dated July 12, 2012.

Camphouse, R.C., Kicker, D.C., Kirchner, T.B., Long, J.J., Malama, B., and Zeitler, T.R. 2012. Summary Report and Run Control for the 2012 WIPP Panel Closure System Performance Assessment. Sandia National Laboratories, Carlsbad, NM.

Clayton, D. J. 2008. Analysis Plan for the Performance Assessment for the 2009 Compliance Recertification Application. Sandia National Laboratories, Carlsbad, N.M. ERMS #547515.

Clayton, D.J., Camphouse, R. C., Garner, J. W., Ismail, A. E., Kirchner, T. B., Kuhlman, K. L., and Nemer, M. B.. 2010. Summary Report of the CRA-2009 Performance Assessment Baseline Calculation, Revision 1. Sandia National Laboratories. Carlsbad, New Mexico, ERMS 553039.

DOE (U.S. Department of Energy). 1996. Title 40 CFR Part 191 Compliance Certification Application for the Waste Isolation Pilot Plant. DOE/CAO-1996-2184. U.S. Department of Energy, Waste Isolation Pilot Plant, Carlsbad Area Office. Carlsbad, NM.

U.S. Department of Energy (DOE) 2004. Title 40 CFR Part 191 Compliance Recertification Application for the Waste Isolation Pilot Plant, , 10 vols., U.S. Department of Energy Waste Isolation Pilot Plant, Carlsbad Area Office, Carlsbad, NM. DOE/WIPP 2004-3231.

DOE (U.S. Department of Energy), 2011. Panel Closure System Design, Planned Change Request to the EPA 40 CFR Part 194 Certification of the Waste Isolation Pilot Plant. U.S. Department of Energy, Carlsbad Field Office. Carlsbad, New Mexico.

Dunagan, S. 2004. Analysis Package for Cuttings and Cavings: Compliance Recertification Application. Revision 1.0.Sandia National Laboratories. Carlsbad, NM. ERMS 533541.

Information Only

Ismail, A.E. and J.W. Garner. 2010. Analysis Package for Salado Transport Calculations: CRA-2009 Performance Assessment Baseline Calculation. Sandia National Laboratories. Carlsbad, NM.

Kirchner, T. 2004a. "Stepwise regression analysis of the final release for each release mechanism, in response to C-23-18, Revision 2." Memorandum to David Kessel dated December 6, 2004. Sandia National Laboratories. Carlsbad, NM. ERMS 537992.

Kirchner, T. 2004b. CRA Reponse Activity, Tracking Number 09/02/04Q, DOE Response to Comment C-23-18, Revision 1, ERMS 538114

Kirchner, T. 2009. Sensitivity of the CRA-2009 Performance Assessment Baseline Calculation Releases to Parameters. Sandia National Laboratories. Carlsbad, NM.

Malama, Bwalya. 2012. Analysis package for Direct Brine releases: 2012 Panel Closure System Performance Assessment (PCS_2012 PA). Sandia National Laboratories. Carlsbad, NM. ERMS 558226

Stein, J. S., and W. Zelinski. 2003. Analysis Package for BRAGFLO: Compliance Recertification Application. Analysis Report. Sandia National Laboratories, Carlsbad, NM. ERMS 530163.

U.S. Environmental Protection Agency (EPA). 1998. 40 CFR 194, Criteria for the Certification and Recertification of the Waste Isolation Pilot Plant's Compliance with the Disposal Regulations: Certification Decision: Final Rule, Federal Register. Vol. 63, 27354-27406. ERMS 251924.

U. S. Environmental Protection Agency (EPA). 2004. "EPA's Completeness Comments, 3rd Set." Letter from Elizabeth Cotsworth to Dr. R. Paul Detwiler. September 2, 2004. ERMS 536771.

Vugrin, E.D. and S.C. Dunagan. 2006. Analysis Package for the Impact Assessment of the Redesigned Panel Closure System, Rev. 0. Sandia National Laboratories. Carlsbad, NM. ERMS 543865.

Xiong, Y.L., L.H. Brush, A.E. Ismail, and J.J. Long. 2009. Uncertainty Analysis of Actinide Solubilities for the WIPP CRA-2009 PABC. Analysis report, December 1, 2009. Carlsbad, NM: Sandia National Laboratories. ERMS #552500.

Zeitler, T. 2012. CCDFGF Analysis Package for the AP-161 (PCS-2012) Performance Assessment. Sandia National Laboratories. Carlsbad, NM.

Information Only

Attachment 1. CD containing the CCDFGF_Analysis.mdb and CCDFGF_Data.mdb databases

The attached CD contains copies of the CCDFGF_Analysis.mdb and CCDFGF_Data.mdb databases within the WinZip file AP161_ANALYSISDATABASE.zip and the Excel spreadsheets in AP161SimpleRegressionSpreadsheets.zip. To utilize these databases or spreadsheets they must be extracted from the zip file and installed on a PC running Microsoft Windows XP or a compatible operating system. CCDFGF_Analysis.mdb contains the queries and code used in the analysis and contains links to some of the tables in CCDFGF_Data.mdb. CCDFGF_Data.mdb contains the data. These links can be updated using the Access menu item External Data/Linked Table Manager. The means are computed and the STEPWISE input file is generated by selecting the menu button in CCDFGF_Analysis labeled "Compute Vector Means for STEPWISE". This process also produces STEPWISE input files for the parameters. A copy of AP161_ANALYSISDATABASE.ZIP and AP161SimpleRegressionSpreadsheets.zip are also stored in the CMS library LIBAP161_STPW.

Information Only

558365

SANDIA NATIONAL LABORATORIES
WASTE ISOLATION PILOT PLANT

Summary Report and Run Control for the 2012 WIPP Panel Closure System Performance Assessment

Revision 0

Author:	R. Chris Camphouse		10/31/2012
	Print	Signature	Date
Author:	Dwayne C. Kicker		10/31/2012
	Print	Signature	Date
Author:	Thomas B. Kirchner		10/31/2012
	Print	Signature	Date
Author:	Jennifer J. Long		10/31/12
	Print	Signature	Date
Author:	Bwalya Malama		10/31/12
	Print	Signature	Date
Author:	Todd R. Zeitler		10/31/2012
	Print	Signature	Date

Technical Review:	Kristopher L. Kuhlman		10/31/2012
	Print	Signature	Date
QA Review	Shelly Nielsen		10-31-12
	Print	Signature	Date
Management Review:	Sean Dunagan		10/31/12
	Print	Signature	Date

WIPP:1.4.1.2:PA:QA-L:557393

Information Only

Table of Contents

Executive Summary 7
1 Introduction 8
2 Run-of-Mine Panel Closure System 9
2.1 ROMPCS Modeling and Parameterization 10
2.2 FEPs Assessment 18
3 Methodology 18
4 Run Control 19
5 Results 20
5.1 Salado Flow Results 20
5.1.1 Results for an Undisturbed Repository (Scenario S1-BF) 25
5.1.2 Results for an E1 Intrusion at 350 Years (Scenario S2-BF) 31
5.1.3 Results for an E2 Intrusion at 350 Years (Scenario S4-BF) 35
5.1.4 Results for an E2 Intrusion at 1000 Years Followed by a E1 Intrusion at 2000 Years (Scenario S6-BF) 42
5.2 Spallings 43
5.3 Direct Brine Releases 46
5.4 Total Normalized Releases 52
6 Summary 56
7 References 58
APPENDIX A PCS-2012 PA Code Execution 61
A.1 WIPP PA Codes 61
A.1.1 Deviation 61
A.2 Calculation Flow 62
A.2.1 Sampling of Uncertain Parameters (LHS) 62
A.2.2 Salado Flow Calculations (BRAGFLO) 63
A.2.2.1 Salado Flow Step 1 64
A.2.2.2 Salado Flow Step 2 65
A.2.2.3 Salado Flow Step 3 66
A.2.2.4 Salado Flow Step 4 66
A.2.2.5 Salado Flow Step 5 67
A.2.3 Single-Intrusion Solids Volume Calculations (CUTTINGS_S) 70
A.2.3.1 Solids Volume Step 1 71

Information Only

A.2.3.2 Solids Volume Step 2 72
A.2.3.3 Solids Volume Step 3 72
A.2.4 Single-Intrusion Direct Brine Release Calculations (BRAGFLO_DBR) 73
A.2.4.1 Direct Brine Release Step 1 74
A.2.4.2 Direct Brine Release Step 2 74
A.2.4.3 Direct Brine Release Step 3 76
A.2.5 CCDF Input Tabulation (SUMMARIZE) 77
A.2.5.1 CCDF Input Tabulation for Direct Brine Release 77
A.2.6 CCDF Construction (PRECCDFGF, CCDFGF) 78
A.2.6.1 CCDF Construction Step 1 79
A.2.6.2 CCDF Construction Step 2 79
A.2.6.3 CCDF Construction Step 3 80
A.2.7 Sensitivity Analysis (STEPWISE) 82
APPENDIX B Addendum 83

Information Only

List of Figures

Figure 2-1: A Schematic of the "Option D" Panel Closure 9
Figure 2-2: Schematic of the ROMPCS 10
Figure 5-1: PABC-2009 BRAGFLO Grid and Material Map for an E1 Intrusion (Δx, Δy, and Δz dimensions in meters). 23
Figure 5-2: PCS-2012 BRAGFLO Grid and Material Map for an E1 Intrusion (Δx, Δy, and Δz dimensions in meters). 24
Figure 5-3: Overall Means of Cumulative Brine Inflow to the Waste Panel, Scenario S1-BF 27
Figure 5-4: Overall Means of Cumulative Brine Inflow to the Waste Panel, Scenario S1-BF and Years 0 to 1,000. 27
Figure 5-5: Overall Means of Waste Panel Brine Saturation, Scenario S1-BF. 28
Figure 5-6: Overall Means of Waste Panel Gas Generation (in moles), Scenario S1-BF. 28
Figure 5-7: Overall Means of Waste Panel Pressure, Scenario S1-BF. 29
Figure 5-8: Overall Means of Pressure in the Operations Region, Scenario S1-BF. 29
Figure 5-9: Overall Means of Brine Flow up the Shaft, Scenario S1-BF. 30
Figure 5-10: Overall Means of Waste Panel Pressure, Scenario S2-BF. 33
Figure 5-11: Overall Means of Cumulative Brine Inflow to the Waste Panel, Scenario S2-BF 33
Figure 5-12: Overall Means of Waste Panel Brine Saturation, Scenario S2-BF. 34
Figure 5-13: Overall Means of Waste Panel Gas Generation (in moles), Scenario S2-BF. 34
Figure 5-14: Overall Means of Brine Flow up the Borehole, Scenario S2-BF. 35
Figure 5-15: Overall Means of Waste Panel Pressure, Scenarios S1-BF and S4-BF for Years 0 to 1,000. 38
Figure 5-16: Overall Means of Waste Panel Pressure, Scenario S4-BF. 38
Figure 5-17: Overall Means of Cumulative Brine Inflow to the Waste Panel, Scenarios S1-BF and S4-BF for Years 0 to 1,000. 39
Figure 5-18: Overall Means of Cumulative Brine Inflow to the Waste Panel, Scenario S4-BF 39
Figure 5-19: Overall Means of Waste Panel Brine Saturation, Scenarios S1-BF and S4-BF for Years 0 to 1,000. 40
Figure 5-20: Overall Means of Waste Panel Brine Saturation, Scenario S4-BF. 40
Figure 5-21: Overall Means of Waste Panel Gas Generation (in moles), Scenario S4-BF. 41
Figure 5-22: Overall Means of Brine Flow up the Borehole, Scenario S4-BF. 41
Figure 5-23: Overall Means of Brine Flow up the Borehole, Scenario S6-BF. 43
Figure 5-24: PCS-2012 PA and PABC-2009 Overall Mean CCDFs for Normalized Spallings Releases . 46
Figure 5-25: PCS-2012 PA DBR Computational Grid and Material Map (logical grid). 47
Figure 5-26: PABC-2009 DBR Computational Grid and Material Map (logical grid). 48
Figure 5-27: DBR Volume vs. Pressure, Scenario S2-DBR, Replicate 1, Lower Intrusion, PCS-2012 PA 51
Figure 5-28: PCS-2012 PA and PABC-2009 Overall Mean CCDFs for Normalized Direct Brine Releases 51
Figure 5-29: PCS-2012 PA Replicate 1 Total Normalized Releases 53
Figure 5-30: PCS-2012 PA Replicate 2 Total Normalized Releases 53
Figure 5-31: PCS-2012 PA Replicate 3 Total Normalized Releases 54
Figure 5-32: PCS-2012 PA Mean and Quantile CCDFs for Total Normalized Releases, Replicates 1-3 .. 54
Figure 5-33: PCS-2012 PA Confidence Limits on Overall Mean for Total Normalized Releases 55

Information Only

Figure 5-34: PCS-2012 PA and PABC-2009 Overall Mean CCDFs for Total Normalized Releases 55
Figure 5-35: PCS-2012 PA Primary Components Contributing to Total Releases 56
Figure B-1: Comparison of PCS-2012 PA Mean and Quantile CCDFs for Total Normalized Releases, Replicate 1 84

List of Tables

Table 2-1: Option D Panel Closure Parameters Used in the PABC-2009 11
Table 2-2: Sampled Panel Closure Parameters for the PCS-2012 PA 14
Table 2-3: Constant Panel Closure Parameters for the PCS-2012 PA 16
Table 5-1: BRAGFLO Modeling Scenarios 21
Table 5-2: Summary Statistics for Scenario S1-BF 26
Table 5-3: Summary Statistics for Scenario S2-BF 32
Table 5-4: Summary Statistics for Scenario S4-BF 37
Table 5-5: Summary Statistics for Scenario S6-BF 42
Table 5-6: PA Intrusion Scenarios Used in Calculating Direct Solids Releases 44
Table 5-7: Summary of Spallings Releases by Scenario 45
Table 5-8: DBR Summary Statistics for the PCS-2012 PA and PABC-2009 DBR Calculations 49
Table 5-9: PCS-2012 PA and PABC-2009 Statistics on the Overall Mean for Total Normalized Releases in EPA Units at Probabilities of 0.1 and 0.001 52
Table A-1: WIPP PA Alpha Cluster Nodes Used in PCS-2012 61
Table A-2: WIPP PA VMS Software Used for the AP161 Panel Closure PA 62
Table A-3: VMS Utility Codes Used in the PCS-2012 62
Table A-4: Parameter Sampling Run Control Script 63
Table A-5: Parameter Sampling Input and Output Files 63
Table A-6: BRAGFLO Scenarios 64
Table A-7: Salado Flow Run Control Scripts 64
Table A-8: Salado Flow Step 1 Input and Output Files 65
Table A-9: Salado Flow Step 2 Input and Output Files 65
Table A-10: Salado Flow Step 3 Input and Output Files 66
Table A-11: Salado Flow Step 4 Input and Output Files 67
Table A-12: Salado Flow Step 5 Input and Output Files (Generic Case) 68
Table A-13: Salado Flow Step 5 Modified Input Runs 69
Table A-14: Salado Flow Step 5 Modified Input Runs File Names 69
Table A-15: Solids Volume (CUTTINGS_S) Run Control Scripts 70
Table A-16: Solids Volume Step 1 Input and Output Files 71
Table A-17: Solids Volume Step 2 Input and Output Files 72
Table A-18: Solids Volume Step 3 Input and Output Files 73
Table A-19: Direct Brine Release Run Control Scripts 74
Table A-20: Direct Brine Release Step 1 Input and Output Files 74
Table A-21: Direct Brine Release Step 2 Input and Output Files 75
Table A-22: Direct Brine Release Step 3 Input and Output Files 76
Table A-23: CCDF Input Tabulation Run Control Scripts 77

Information Only

Table A-24: CCDF Input Tabulation Input and Output Files (Direct Brine Release) 78
Table A-25: CCDF Construction Run Control Scripts 78
Table A-26: CCDF Construction Step 1 Input and Output Files 79
Table A-27: CCDF Construction Step 2 Input and Output Files 80
Table A-28: CCDF Construction Step 3 Input and Output Files 81
Table A-29: Sensitivity Analysis Run Control Scripts 82
Table A-30: Sensitivity Analysis Input and Output Files 82

Information Only

EXECUTIVE SUMMARY

Waste panel closures comprise a repository feature that has been represented in WIPP PA since the original Compliance Certification Application of 1996. The 1998 rulemaking that certified WIPP to receive transuranic waste placed conditions on the panel closure design to be implemented in the repository. The mandated "Option D" design consists of a concrete block wall, an open drift section, and a concrete monolith. The engineering of the panel closure has been re-assessed, and a revised design is proposed that is simpler, cheaper, and easier to construct. The revised panel closure design, termed the Run-of-Mine Panel Closure System (ROMPCS), is comprised of 100 feet of run-of-mine (ROM) salt with barriers at each end. The PCS-2012 PA quantifies WIPP repository performance impacts associated with the replacement of the currently approved Option D panel closure design with the ROMPCS. Impacts are assessed via a direct comparison of results obtained in the 2009 Performance Assessment Baseline Calculation (PABC-2009) to those calculated in the PCS-2012 PA with the ROMPCS.

Total normalized releases calculated in the PCS-2012 PA are greater than those found in the PABC-2009, but continue to remain below their regulatory limits. As a result, replacement of the Option D panel closure with the ROMPCS design would not result in WIPP non-compliance with the containment requirements of 40 CFR Part 191. Cuttings and cavings releases and direct brine releases (DBRs) were the two primary release components contributing to total releases in the PABC-2009, and continue to be so in the PCS-2012 PA. Cuttings and cavings releases are not impacted by the change in panel closure design, and so remain unchanged from those calculated in the PABC-2009.

For both undisturbed and intruded repository conditions, implementation of the ROMPCS yields higher long-term waste panel pressure (on average) than was seen in the PABC-2009. Pressure increases translate to increases in spallings volumes and their frequency. As a result, increased spallings releases are seen in the PCS-2012 PA results when compared to the PABC-2009. These increases do not have a significant impact on total normalized releases found in the PCS-2012 PA.

Increased direct brine releases are also seen in the PCS-2012 PA results. DBRs depend on waste panel pressure and brine saturation at the time of intrusion. In addition to increases in waste panel pressure, implementation of the ROMPCS design results in increased mean waste panel brine saturation for undisturbed conditions as well as intrusion scenarios that do not intersect a Castile brine pocket. For intrusion scenarios that intersect a region of pressurized Castile brine, increases in pressure are accompanied by only slight reductions in the mean waste panel brine saturation in the PCS-2012 PA as compared to PABC-2009 results. The combined effect of these impacts is an increase to normalized direct brine releases in the PCS-2012 PA. The increase in total normalized releases seen in the PCS-2012 PA as compared to the PABC-2009 is primarily due to the increase in DBRs calculated in the PCS-2012 PA.

Information Only

1 INTRODUCTION

The Waste Isolation Pilot Plant (WIPP), located in southeastern New Mexico, has been developed by the U.S. Department of Energy (DOE) for the geologic (deep underground) disposal of transuranic (TRU) waste. Containment of TRU waste at the WIPP is regulated by the U.S. Environmental Protection Agency (EPA) according to the regulations set forth in Title 40 of the Code of Federal Regulations (CFR), Part 191. The DOE demonstrates compliance with the containment requirements according to the Certification Criteria in Title 40 CFR Part 194 by means of performance assessment (PA) calculations performed by Sandia National Laboratories. WIPP PA calculations estimate the probability and consequence of potential radionuclide releases from the repository to the accessible environment for a regulatory period of 10,000 years after facility closure. The models used in PA are maintained and updated with new information as part of an ongoing process. Improved information regarding important WIPP features, events, and processes typically results in refinements and modifications to PA models and the parameters used in them. Planned changes to the repository and the components therein also result in updates to WIPP PA models. WIPP PA models are used to support the repository recertification process that occurs at five-year intervals following the receipt of the first waste shipment at the site in 1999.

Waste panel closures comprise a repository feature that has been represented in WIPP PA since the original Compliance Certification Application (CCA) of 1996. Panel closures are included in WIPP PA models principally because they are a part of the disposal system, not because they play a substantive role in inhibiting the release of radionuclides to the outside environment. The DOE stated in the CCA (DOE 1996) that *"The panel closure system was not designed or intended to support long-term repository performance."* The 1998 rulemaking that certified WIPP to receive transuranic waste placed conditions on the panel closure design to be implemented in the repository. The mandated design consists of a concrete block wall, an open drift section, and a concrete monolith, and was termed the "Option D" panel closure. Following the selection of the Option D design in 1998, the engineering of the panel closure has been re-assessed, and a revised design has been established that is simpler, cheaper, and easier to construct. The revised panel closure design, termed the Run-of-Mine Panel Closure System (ROMPCS), is comprised of 100 feet of run-of-mine (ROM) salt with barriers at each end. The ROM salt is generated from ongoing mining operations at the WIPP and may be compacted and/or moistened as it is emplaced in a panel entry. The barriers consist of ventilation bulkheads, similar to those currently used in the panels as room closures.

The DOE has submitted a planned change request (PCR) to the EPA requesting that EPA modify Condition 1 of the Final Certification Rulemaking for 40 CFR Part 194 (EPA, 1998) for the WIPP. The PCR submitted to EPA requests that Condition 1 be changed, and that the ROMPCS design be approved for use in all panels (DOE, 2011). In support of this rulemaking change, a PA has been completed that incorporates the ROMPCS design into the current PA baseline

Information Only

established by the 2009 Performance Assessment Baseline Calculation (PABC-2009) (Clayton et al., 2010). The name given to this new panel closure PA is PCS-2012, and the plan for its execution is detailed in AP-161 (Camphouse 2012a). PCS-2012 PA results are compared to PABC-2009 results as a means to quantify potential panel closure redesign impacts. This document provides the summary report of the PCS-2012 PA analysis.

2 RUN-OF-MINE PANEL CLOSURE SYSTEM

The goal of the PCS-2012 PA is to quantify regulatory compliance impacts resulting from the replacement of the Option D panel closure with the ROMPCS. Figure 2-1 shows the Option D panel closure is 40 meters long and consists of three components, namely a concrete explosion wall, an open drift section, and a concrete monolith. This panel closure has been implemented in PA analyses done in support of WIPP re-certification since the CRA-2004 PA (Stein & Zelinski 2003).

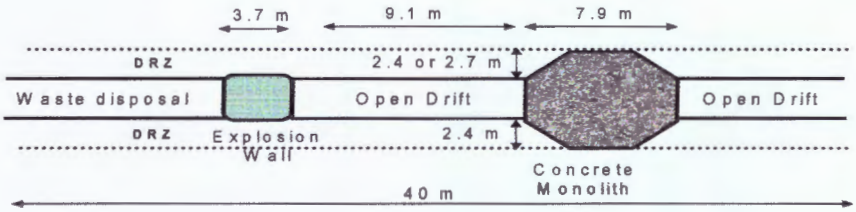

Figure 2-1: A Schematic of the "Option D" Panel Closure

The ROMPCS is comprised of 100 feet of run-of-mine salt with barriers at each end, and is illustrated in Figure 2-2. The ROM salt is generated from ongoing mining operations at the WIPP and may be compacted and/or moistened as it is emplaced in a panel entry. The barriers consist of ventilation bulkheads, similar to those currently used in the panels as room closures. The ventilation bulkheads are designed to restrict air flows and prevent personnel access into waste-filled areas during the WIPP operational phase. In Panels 1, 2, and 5, where explosion walls fabricated from concrete blocks have already been emplaced in the panel entries, an explosion wall is the inner barrier and a ventilation bulkhead will be the outer barrier, as shown in Figure 2-2(b). Explosion walls are inspected on a regular basis, and their anticipated condition is also assessed through numerical modeling (e.g. RockSol, 2006). Installed explosion walls show surface spalling or slabbing of the concrete blocks as a result of the loading caused by inward creep of the salt. Numerical stress analysis of the concrete explosion wall has demonstrated that the free faces and the rib contacts will be in a condition of plastic yield with an

Information Only

unyielded core by 7 years after emplacement (Rocksol, 2006, Figures 7 and 10). No long term stress analyses have been carried out; however, it is expected that the spalling and yield will be progressive, and that the walls will not be significant structures after the initial 100 year time period, due to the brittle, non-plastic behavior of concrete. The ventilation bulkheads and explosion walls are therefore expected to have no significant impact on long-term performance of the panel closures and are therefore not included in the PCS-2012 PA representation of the ROMPCS. Consequently, the ROMPCS is modeled as consisting of 100 feet of ROM salt in the PCS-2012 PA.

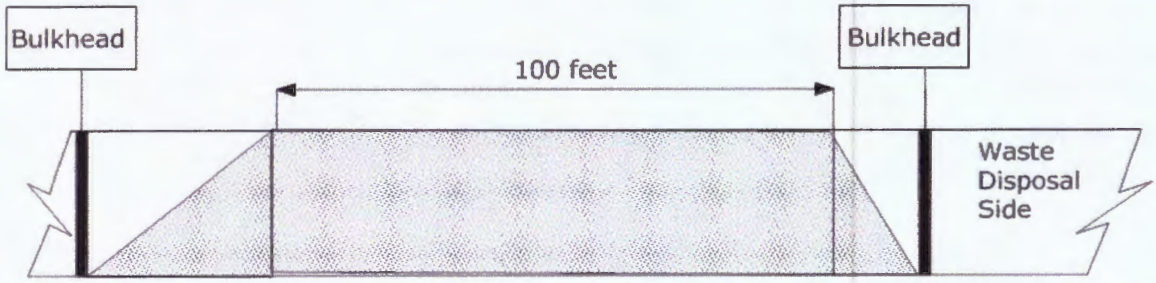

(a) Panel closure with 100 feet (30.5m) of ROM salt between two ventilation bulkheads

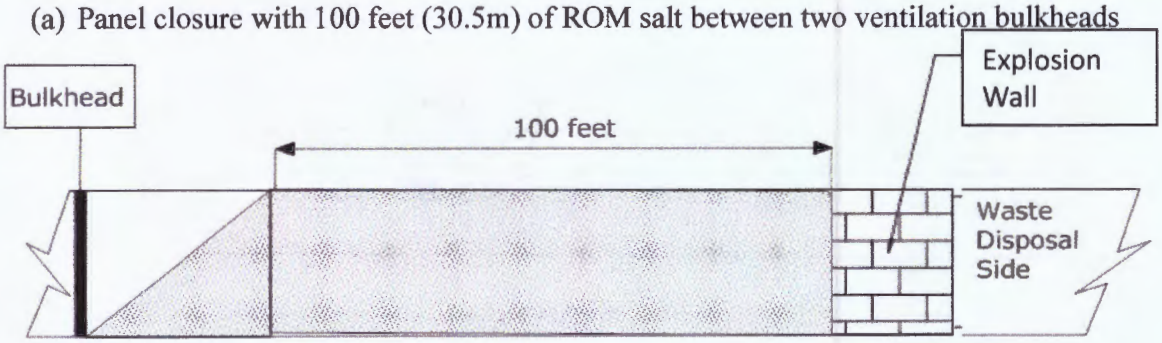

(b) Panel closure with 100 feet (30.5m) of ROM salt between a ventilation bulkhead & explosion wall

Figure 2-2: Schematic of the ROMPCS

2.1 ROMPCS Modeling and Parameterization

The modeling approach and parameter developments undertaken to represent the ROMPCS in the PCS-2012 PA are documented in Camphouse et al. (2012a), Patterson (2012), and Camphouse (2012b). These aspects of the PCS-2012 PA are now discussed. For the sake of clarity in the discussion that follows, select parameters used to model the Option D panel closure in the PABC-2009 are shown in Table 2-1.

Information Only

Table 2-1: Option D Panel Closure Parameters Used in the PABC-2009

Material	Property	Distribution	Statistics
CONC_PCS	Porosity	Constant	0.05
	PRMX (m^2)	Triangular	Min = 2.0×10^{-21}
	PRMY (m^2)		Mean = 1.53×10^{-19}
	PRMZ (m^2)		Max = 1.0×10^{-17}
DRZ_1	Porosity	Cumulative	Min = 0.0039
			Mean = 0.0211
			Max = 0.0548
	PRMX (m^2)	Uniform	Min = 3.98×10^{-20}
	PRMY (m^2)		Mean = 1.0×10^{-16}
	PRMZ (m^2)		Max = 3.16×10^{-13}
DRZ_PCS	Porosity	Cumulative	Min = 0.0039
			Mean = 0.0211
			Max = 0.0548
	PRMX (m^2)	Triangular	Min = 2.0×10^{-21}
	PRMY (m^2)		Mean = 1.53×10^{-19}
	PRMZ (m^2)		Max = 1.0×10^{-17}

ROMPCS properties in the PCS-2012 PA are based on three time periods: from 0 to 100 years, from 100 years to 200 years, and from 200 years to 10,000 years. Three time periods are appropriate because the process to consolidate the ROM salt occurs over a primary time scale of approximately 100 years, while the process to heal fractures in the DRZ surrounding the PCS occurs over a longer time scale of approximately 200 years. The ROM salt comprising the ROMPCS is therefore represented by three materials, denoted as PCS_T1 for the first 100 years, PCS_T2 from 100 to 200 years, and PCS_T3 for 200 to 10,000 years. Analyses and calculations have shown (Camphouse et al. 2012a) that the time-dependent back stress imposed on the DRZ by the re-consolidated ROM salt panel closure does not become appreciable until roughly 200 years after emplacement of the ROM salt in the drift. As a result, it is reasonable and appropriate to maintain the same properties for the DRZ above and below the ROMPCS for the first 200 years after closure as are specified to the DRZ surrounding the disposal rooms. After 200 years, the DRZ above and below the ROMPCS is modeled as having healed, and this sub-region of the DRZ is represented by material DRZ_PCS. Material DRZ_PCS has the same property values in the PCS-2012 PA as were assigned to it in the PABC-2009.

The 200-year delay of DRZ healing in the PCS-2012 PA is an important distinction between the Option D panel closure representation used in the PABC-2009 and the ROMPCS representation used in the PCS-2012 PA. The Option D panel closure was modeled in the PABC-2009 (and prior analyses) as having an immediate healing effect on the DRZ above it, with material DRZ_PCS being in place at t = 0. In contrast, the ROMPCS in the PCS-2012 PA is modeled as

Information Only

having no healing effect on the DRZ until 200 years after panel closure emplacement. For the first 200 years, the DRZ above and below the ROMPCS is indistinguishable from the DRZ above and below the waste panels. The DRZ overall (PA parameter DRZ_1 in Table 2-1) has a permeability range varying from a minimum value of 3.98×10^{-20} m^2 to a maximum value of 3.16×10^{-13} m^2 in the x, y, and z directions. Material DRZ_PCS has a permeability range varying from a minimum of 2.0×10^{-21} m^2 to a maximum of 1.0×10^{-17} m^2 in the x, y, and z directions. As a result, there is a path of increased permeability (on average) above and below panel closures in the PCS-2012 PA for the first 200 years as compared to the PABC-2009. An expected consequence of this increased permeability is an increase in brine and gas flow through the DRZ and around the panel closure for the first 200 years. In effect, the panel closures in the PCS-2012 PA are "looser" than those implemented in the PABC-2009 for the first 200 years due to the higher permeability (on average) of the DRZ material above and below them.

The complete set of parameters used to model the ROMPCS in the PCS-2012 PA is shown in Table 2-2 and Table 2-3. As developed in Camphouse et al. (2012a) and Patterson (2012), permeability and porosity values are obtained through sampling for ROMPCS material PCS_T1. However, only porosity is sampled for materials PCS_T2 and PCS_T3. Sampled porosity values are then used to calculate permeability values for these materials according to the algorithm developed on page 15 of Camphouse et al. (2012a). At 200 years, the ROMPCS material transitions from PCS_T2 to PCS_T3 with the DRZ region above and below PCS_T3 represented as healed by material DRZ_PCS. Under this configuration, the range of calculated permeabilities for PCS_T3 is comparable to the permeability range assigned to the Option D monolith (material CONC_PCS in Table 2-1), with the minimum value calculated for PCS_T3 being roughly an order of magnitude less than the minimum CONC_PCS permeability value. As material DRZ_PCS represents regions of healed DRZ for both the ROMPCS and the Option D closure (with equal DRZ_PCS property values prescribed for both panel closure cases), the final ROMPCS configuration comprises a panel closure that is slightly "tighter" (on average) than the Option D case.

The algorithm used to calculate permeability from a sampled porosity value depends on an additional sampled parameter, quantity α in the algorithm developed in Camphouse et al. (2012a). The name given to this additional parameter in the PCS-2012 PA is POR2PERM. Porosity and permeability ranges used for materials PCS_T1, PCS_T2, and PCS_T3 are shown in Table 2-2. As can be seen in that table, there is overlap in the porosity ranges specified for PCS_T1 and PCS_T2. This overlap could potentially result in an increase in panel closure porosity during the transition from PCS_T1 to PCS_T2 at 100 years, a non-physical result. To prevent this possibility, the porosity for PCS_T2 is conditionally sampled (Kirchner 2012a) in the PCS-2012 PA. Using the MATERIAL:PROPERTY parameter naming convention used in WIPP PA, the porosity for material PCS_T2 is conditionally sampled such that PCS_T2:POROSITY $\leq$ PCS_T1:POROSITY. There is also overlap in the porosity ranges specified for PCS_T2 and PCS_T3. To prevent physically unrealistic increases in porosity

Information Only

during the transition from PCS_T2 to PCS_T3 at 200 years, the porosity for PCS_T3 is conditionally sampled so that PCS_T3:POROSITY ≤ PCS_T2:POROSITY. Similar constraints are placed on the calculated permeability values for PCS_T2 and PCS_T3. As can be seen in Table 2-2, a low sampled permeability value for PCS_T1 could be followed by a higher calculated permeability value for PCS_T2, dependent on the sampled PCS_T2 porosity and POR2PERM values. An instantaneous increase in panel closure permeability after 100 years of creep closure is an unrealistic occurrence. To prevent this non-physical result, the calculated permeability value for PCS_T2 is constrained in the PCS-2012 PA such that PCS_T2:PRMX ≤ PCS_T1:PRMX. If a higher permeability value is calculated for material PCS_T2 than was sampled for material PCS_T1, then material PCS_T2 retains the permeability value for PCS_T1. The same is true for the calculated permeabilities in the y and z directions. A similar constraint is placed on the calculated permeability for PCS_T3 in order to prevent non-physical instantaneous increases in panel closure permeability at 200 years. The constraint placed on the calculated permeability for PCS_T3 is that PCS_T3:PRMX ≤ PCS_T2:PRMX, and likewise in the x and y directions. If the calculated permeability for PCS_T3 is greater than that obtained for PCS_T2, then PCS_T3 retains the permeabilities assigned to PCS_T2.

Information Only

Table 2-2: Sampled Panel Closure Parameters for the PCS-2012 PA

Parameter	Units	Description	Distribution Type	Distribution Parameters	Default Value	Source
PCS_T1:POROSITY	none	Porosity of run-of-mine panel closure, years 0 to 100	Uniform	Min = 0.066 Max = 0.187 Mean = 0.1265	0.1265	Camphouse et al. (2012a) Table 2 and page 15
PCS_T2:POROSITY[1]	none	Porosity of run-of-mine panel closure, years 100 to 200	Uniform	Min = 0.025 Max = 0.075 Mean = 0.05	0.05	Camphouse et al. (2012a) Table 2 and page 15
PCS_T3:POROSITY[2]	none	Porosity of run-of-mine panel closure, years 200 to 10,000	Uniform	Min = 0.001 Max = 0.0519 Mean = 0.0265	0.0265	Camphouse et al. (2012a) Table 2 and page 15
PCS_T1:PRMX_LOG[3] PCS_T1:PRMY_LOG PCS_T1:PRMZ_LOG	$\log(m^2)$	$\log_{10}$ of intrinsic permeability, X, Y, and Z directions.	Uniform	Min = -21.0 Max = -12.0 Mean = -16.5	-16.5	Patterson (2012) Page 13
PCS_T2:POR2PERM[4] PCS_T3:POR2PERM	none	Distribution used to calculate permeability from sampled porosity values	Normal	Min = -1.72 Max = 1.72 Mean = 0.0 SD = 0.86	0.0	Camphouse et al. (2012a) Page 15 (sampled α value)
PCS_T1:SAT_IBRN	none	Initial brine saturation of run-of-mine panel closure	Uniform	Min = 0.04 Max = 0.16 Mean = 0.1	0.1	Camphouse (2012b)

[1] PCS_T2:POROSITY is constrained such that PCS_T2:POROSITY ≤ PCS_T1:POROSITY for a given vector in order to avoid non-physical instantaneous increases in ROMPCS porosity at 100 years.
[2] PCS_T3:POROSITY is constrained such that PCS_T3:POROSITY ≤ PCS_T2:POROSITY for a given vector in order to avoid non-physical instantaneous increases in ROMPCS porosity at 200 years.
[3] Parameter values are sampled for PCS_T1:PRMX_LOG. PCS_T1:PRMY_LOG and PCS_T1:PRMZ_LOG inherit the sampled value obtained for PCS_T1:PRMX_LOG for each vector.
[4] Parameter values are sampled for PCS_T2:POR2PERM. PCS_T3:POR2PERM inherits the sampled value obtained for PCS_T2:POR2PERM for each vector.

Table 2 (cont): Sampled Panel Closure Parameters for the PCS-2012 PA						
PCS_T1:SAT_RBRN[5] PCS_T2:SAT_RBRN PCS_T3:SAT_RBRN	none	Residual Brine Saturation	Cumulative	(Prob,Value): (0,0) (0.5,0.2) (1.0,0.6)	0.2	Camphouse et al. (2012a) Table 6
PCS_T1:SAT_RGAS[6] PCS_T2:SAT_RGAS PCS_T3:SAT_RGAS	none	Residual Gas Saturation	Uniform	Min = 0.0 Max = 0.4 Mean = 0.2	0.2	Camphouse et al. (2012a) Table 6
PCS_T1:PORE_DIS[7] PCS_T2:PORE_DIS PCS_T3:PORE_DIS	none	Brooks-Corey pore distribution parameter	Cumulative	(Prob,Value): (0,0.11) (0.5,0.94) (1.0,8.1)	0.94	Camphouse et al. (2012a) Table 8

[5] Parameter values are sampled for PCS_T1:SAT_ RBRN. PCS_T2: SAT_ RBRN and PCS_T3: SAT_ RBRN inherit the sampled value obtained for PCS_T1:SAT_ RBRN for each vector.
[6] Parameter values are sampled for PCS_T1:SAT_ RGAS. PCS_T2: SAT_ RGAS and PCS_T3: SAT_ RGAS inherit the sampled value obtained for PCS_T1:SAT_ RGAS for each vector.
[7] Parameter values are sampled for PCS_T1:PORE_DIS. PCS_T2: PORE_DIS and PCS_T3: PORE_DIS inherit the sampled value obtained for PCS_T1: PORE_DIS for each vector.

Table 2-3: Constant Panel Closure Parameters for the PCS-2012 PA

Parameter	Units	Description	Value	Source
PCS_T2:PRMX_LOG[8] PCS_T2:PRMY_LOG PCS_T2:PRMZ_LOG	$\log(m^2)$	$\log_{10}$ of intrinsic permeability, X, Y, and Z directions.	-18.6	See Footnote
PCS_T3:PRMX_LOG[9] PCS_T3:PRMY_LOG PCS_T3:PRMZ_LOG	$\log(m^2)$	$\log_{10}$ of intrinsic permeability, X, Y, and Z directions.	-19.1	See Footnote
PCS_T1:RELP_MOD PCS_T2:RELP_MOD PCS_T3:RELP_MOD	none	Relative Permeability Model Number	4 (a modified Brooks-Corey Model)	Camphouse et al. (2012a) Table 7
PCS_T1:CAP_MOD PCS_T2:CAP_MOD PCS_T3:CAP_MOD	none	Capillary Pressure Model Number	1 (unbounded capillary pressure)	Camphouse (2012b) Camphouse (2012c)
PCS_T1:KPT PCS_T2:KPT PCS_T3:KPT	none	Flag to Enable Dynamic Updating of Threshold Capillary Pressure as a Function of Permeability	0.0	Camphouse et al. (2012a) Table 8
PCS_T1:PCT_A PCS_T2:PCT_A PCS_T3:PCT_A	Pa	Threshold Capillary Pressure Linear Parameter	0.0	Camphouse (2012b) Camphouse (2012c)
PCS_T1:PCT_EXP PCS_T2:PCT_EXP PCS_T3:PCT_EXP	none	Threshold Capillary Pressure Exponential Parameter	0.0	Camphouse (2012b) Camphouse (2012c)
PCS_T1:PC_MAX PCS_T2:PC_MAX PCS_T3:PC_MAX	Pa	Maximum Allowable Capillary Pressure	1×10^8	Camphouse et al. (2012a) Table 8

[8] Permeabilities of PCS_T2 in the X, Y, and Z directions are calculated from the sampled PCS_T2:POROSITY values as described in Camphouse et al. (2012a). A constant default log-permeability is specified, however, to allow for parameter traceability in PCS-2012 PA input files as compared to those used in the PABC-2009. The specified default value is the average of the minimum and maximum values listed in Table 5 of Camphouse et al. (2012a).

[9] Permeabilities of PCS_T3 in the X, Y, and Z directions are calculated from the sampled PCS_T3:POROSITY values as described in Camphouse et al. (2012a). The specified constant default value is the average of the minimum and maximum values listed in Table 5 of Camphouse et al. (2012a).

Table 3 (cont): Constant Panel Closure Parameters for the PCS-2012 PA				
PCS_T1:P0_MIN PCS_T2:P0_MIN PCS_T3:P0_MIN	Pa	Minimum Brine Pressure for Capillary Model 3 (CAP_MOD = 3 has never been used in PA)	1.01325×10^{5}	Camphouse et al. (2012a) Table 8
PCS_T1:COMP_RCK PCS_T2:COMP_RCK PCS_T3:COMP_RCK	Pa^{-1}	Bulk Compressibility	8.0×10^{-11}	Camphouse et al. (2012a) Table 8

2.2 FEPs Assessment

The PCS-2012 PA began with an assessment that identified and evaluated the features, events, and processes (FEPs) that are related to the changes introduced by the proposed panel closure design. The purpose of the FEPs evaluation was to determine if the current FEPs baseline (currently the PABC-2009 FEPs baseline) is suitable to evaluate the new closure design, or if changes to FEPs descriptions, screening arguments, or decisions are necessary. The results of this assessment concluded that no changes are needed to the FEPs baseline (Kirkes 2011) [10]. It should be pointed out that the FEPs analysis only determines that the WIPP design features are appropriately identified, described, and screened according to established FEPs screening methods. WIPP FEPs W109 *Panel Closure Geometry* and W110, *Panel Closure Properties*, are directly related to the changes proposed by the new PCS design and were the focus of the FEPs assessment. These two FEPs have been screened in (represented) as part of previous performance assessments in all scenarios, and continue to be so in the PCS-2012 PA.

3 METHODOLOGY

The PA methodology accommodates both aleatory (i.e. stochastic) and epistemic (i.e. subjective) uncertainty in its constituent models. Aleatory uncertainty pertains to unknowable future events such as intrusion times and locations that may affect repository performance. It is accounted for by the generation of random sequences of future events. Epistemic uncertainty concerns parameter values that are assumed to be constants and the constants' true values are uncertain due to a lack of knowledge about the system. An example of a parameter with epistemic uncertainty is the permeability of a material. Epistemic uncertainty is accounted for by sampling of parameter values from assigned distributions. One set of sampled values required to run a WIPP PA calculation is termed a vector. In the PCS-2012 PA, models were executed for three replicates of 100 vectors. Parameter sampling performed in the PCS-2012 PA is documented in Kirchner (2012a), and the sensitivities of variable output to sampled parameters are documented in Kirchner (2012b). A sample size of 10,000 possible sequences of future events is used in PA calculations to address aleatory uncertainty. The releases for each of 10,000 possible sequences of future events are tabulated for each of the 300 vectors, totaling 3,000,000 possible sequences.

For a random variable, the complementary cumulative distribution function (CCDF) provides the probability of the variable being greater than a particular value. By regulation, PA results are presented as a distribution of CCDFs of releases (EPA 1996). Each individual CCDF summarizes the likelihood of releases across all futures for one vector of parameter values. The uncertainty in parameter values results in a distribution of CCDFs.

[10] Kirkes (2011) also evaluated changes associated with a proposed reconfiguration of the repository layout; the PCS changes are a subset of this FEP evaluation. Only the elements (and FEPs) relating to the PCS redesign are germane to the PCS-2012 PA analyses.

Information Only

Releases are quantified in terms of "EPA units". Releases in EPA units result from a normalization by radionuclide and the total inventory. For each radionuclide, the ratio of its 10,000 year cumulative release (in curies) to its release limit is calculated. The sum of these ratios is calculated across the set of radionuclides and normalized by the transuranic inventory (in curies) of α-emitters with half-lives greater than 20 years. Mathematically, the formula used to calculate releases in terms of EPA units is of the form

$$R = \frac{1 \times 10^6 \text{ curies}}{C} \sum_i \frac{Q_i}{L_i}$$

where R is the normalized release in EPA units. Quantity Q_i is the 10,000 year cumulative release (in curies) of radionuclide i. Quantity L_i is the release limit for radionuclide i, and C is the total transuranic inventory (in curies) of α-emitters with half-lives greater than 20 years.

The PCS-2012 PA was developed so that the structure of calculations performed therein was as similar as possible to that used in the PABC-2009. PABC-2009 calculated results potentially impacted by the panel closure redesign were updated, while the results from previous PAs were used for individual numerical codes not affected by these changes. The PCS-2012 PA utilized the same waste inventory information, drilling rate and plugging pattern parameters, and radionuclide solubility parameters as were used in the PABC-2009. Separate documentation was prepared describing calculations performed and results obtained for each code executed in the PCS-2012 PA. Citations for this additional documentation are included in the references section of this summary report, and are indicated in the list below.

- Parameter Sampling (Kirchner 2012a)
- Sensitivity Analysis (Kirchner 2012b)
- Salado Flow (Camphouse 2012d)
- Cuttings, Cavings, and Spallings (Kicker 2012)
- Direct Brine Releases (Malama 2012)
- CCDF Normalized Releases (Zeitler 2012)

4 RUN CONTROL

Run control documentation of codes executed in the PCS-2012 PA is provided in APPENDIX Appendix A. This documentation contains:

1. A description of the hardware platform and operating system used to perform the calculations.
2. A listing of the codes and versions used to perform the calculations.
3. A listing of the scripts used to run each calculation.
4. A listing of the input and output files for each calculation.
5. A listing of the library and class where each file is stored.
6. File naming conventions.

Information Only

As described previously, PABC-2009 results were used for individual numerical codes primarily unaffected by the panel closure redesign. Documentation of run control for results calculated in the PABC-2009 is provided in Long (2010).

5 RESULTS

Replacement of the Option D panel closure with the ROMPCS design has no impact on cuttings and cavings releases resulting from drilling intrusions in repository waste areas. Cuttings and cavings results obtained in the PCS-2012 PA are identical to those found in the PABC-2009. In addition, Culebra transport results calculated in the PABC-2009 are also used in the PCS-202 PA calculations. Discussions of cuttings and cavings releases, as well as Culebra transport releases, calculated in the PABC-2009 can be found in Clayton et al. (2010) and the references therein. The primary focus of the PCS-2012 PA is a determination of pressure and brine saturation changes in waste-containing repository regions, and the impacts these changes have on spallings releases and DBRs. Spallings releases and DBRs are two of the release components used to calculate total normalized releases. As a result, the impact of pressure and brine saturation changes on total normalized releases is of interest as well.

Summary results obtained in the PCS-2012 PA are broken out in sections below, and are compared to PABC-2009 results. Salado flow modeling results are presented in Section 5.1. The use of PABC-2009 Culebra transport results for the PCS-2012 PA is justified in Section 5.1.4. Spallings results are presented in Section 5.2. Direct brine releases are presented in Section 5.3. The impact of the ROMPCS design on regulatory compliance is discussed in terms of total normalized releases in Section 5.4. As the CCDF is the regulatory metric used to demonstrate compliance, CCDFs obtained in the PCS-2012 PA and the PABC-2009 are compared for each component of release in the appropriate section.

Following the completion of the PCS-2012 PA calculations, but prior to the completion of the summary report, a transcription error was discovered in the ALG1 input file for BRAGFLO. This error has a negligible impact on results obtained in the PCS-2012 PA, and is discussed in Appendix B.

5.1 Salado Flow Results

PA code BRAGFLO calculates the flow of brine and gas in the vicinity of the WIPP repository over the 10,000-year regulatory compliance period. During BRAGFLO calculations, stochastic uncertainty is addressed by defining a set of six scenarios for which brine and gas flow is calculated for each of the vectors generated via parameter sampling. The total number of BRAGFLO simulations executed in the PCS-2012 PA is 1,800 (300 vectors times 6 scenarios).

The six scenarios used in the PCS-2012 PA are unchanged from those used for the PABC-2009. The scenarios include one undisturbed scenario (S1-BF), four scenarios that include a single

Information Only

inadvertent future drilling intrusion into the repository during the 10,000 year regulatory period (S2-BF to S5-BF), and one scenario investigating the effect of two intrusions into a single waste panel (S6-BF). Two types of intrusions, denoted as E1 and E2, are considered. An E1 intrusion assumes the borehole passes through a waste-filled panel and into a pressurized brine pocket that may exist under the repository in the Castile formation. An E2 intrusion assumes that the borehole passes through the repository but does not encounter a brine pocket. Scenarios S2-BF and S3-BF model the effect of an E1 intrusion occurring at 350 years and 1000 years, respectively, after the repository is closed. Scenarios S4-BF and S5-BF model the effect of an E2 intrusion at 350 and 1000 years. Scenario S6-BF models an E2 intrusion occurring at 1000 years, followed by an E1 intrusion into the same panel at 2000 years. Calculated brine flows up the intrusion borehole obtained in scenario S6-BF are used in PA code PANEL to determine the radionuclide source term to the Culebra. Transport releases from the Culebra obtained in the PABC-2009 are also used in the PCS-2012 PA. PCS-2012 PA results from BRAGFLO scenario S6-BF are briefly discussed to justify the appropriateness of PABC-2009 Culebra transport calculations for the PCS-2012 PA. Table 5-1 summarizes the six scenarios used in this analysis.

Table 5-1: BRAGFLO Modeling Scenarios

Scenario	Description
S1-BF	Undisturbed Repository
S2-BF	E1 intrusion at 350 years
S3-BF	E1 intrusion at 1000 years
S4-BF	E2 intrusion at 350 years
S5-BF	E2 intrusion at 1000 years
S6-BF	E2 intrusion at 1000 years; E1 intrusion at 2000 years.

Computed results are presented for the PCS-2012 PA and compared with those obtained in the PABC-2009. Results are discussed in terms of overall means. Overall means are obtained by forming the average of the 300 realizations calculated for a given quantity and scenario. Results are presented for undisturbed scenario S1-BF. Intruded results are presented for scenarios S2-BF and S4-BF, as these are representative of the intrusion types considered in scenarios S2-BF to S5-BF with the only differences being the timing of drilling intrusions. Results from scenario S6-BF are also briefly discussed.

Option D panel closures were implemented in the PABC-2009. The computational grid and material map used in the PABC-2009 Salado flow calculations are shown in Figure 5-1. A minor error has been corrected in the material map schematic shown in Figure 5-1. That figure depicts an E1 intrusion into the repository. The BRAGFLO schematic included with the PABC-2009 Salado flow analysis package (Nemer 2010) depicts the lower borehole extending only to the bottom horizon of the lower DRZ. In actuality, the lower borehole extends to the floor of the

Information Only

intruded waste panel. The PABC-2009 BRAGFLO grid and material map shown in Figure 5-1 has been modified so that it represents the correct extent of the lower borehole in an E1 intrusion. The analogous PCS-2012 PA BRAGFLO computational grid and material map are shown in Figure 5-2. As that figure also depicts an E1 intrusion scenario, with 350 years post-closure being the first time instance at which an intrusion occurs, materials DRZ_PCS and ROMPCS material PCS_T3 are in place at the time of all intrusions in the Salado flow calculations. The development of the PCS-2012 PA BRAGFLO grid, as well as the representation of the temporal evolution of the ROMPCS in the BRAGFLO material map, is fully discussed in Camphouse (2012d).

Information Only

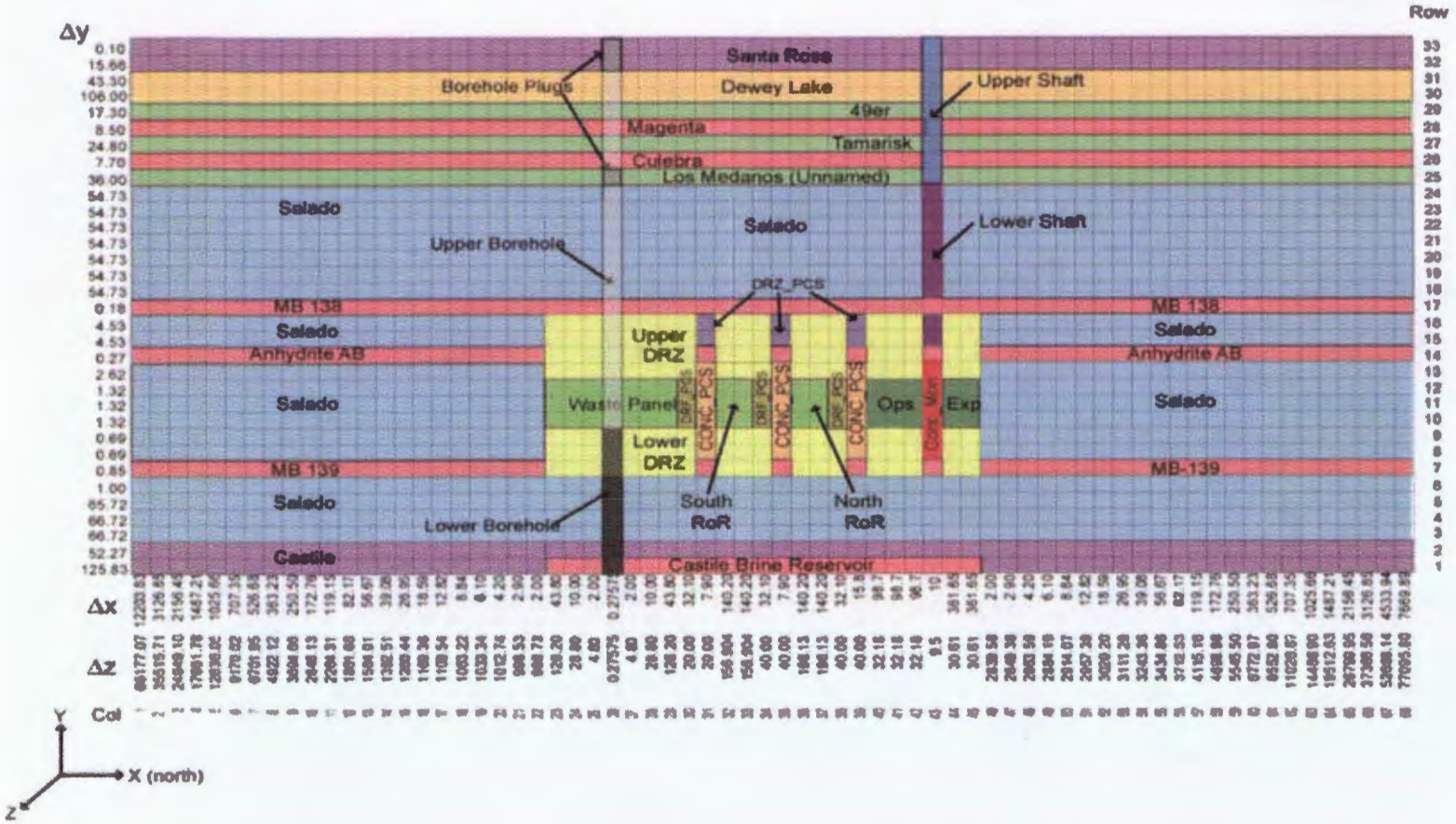

Figure 5-1: PABC-2009 BRAGFLO Grid and Material Map for an E1 Intrusion (Δx, Δy, and Δz dimensions in meters).

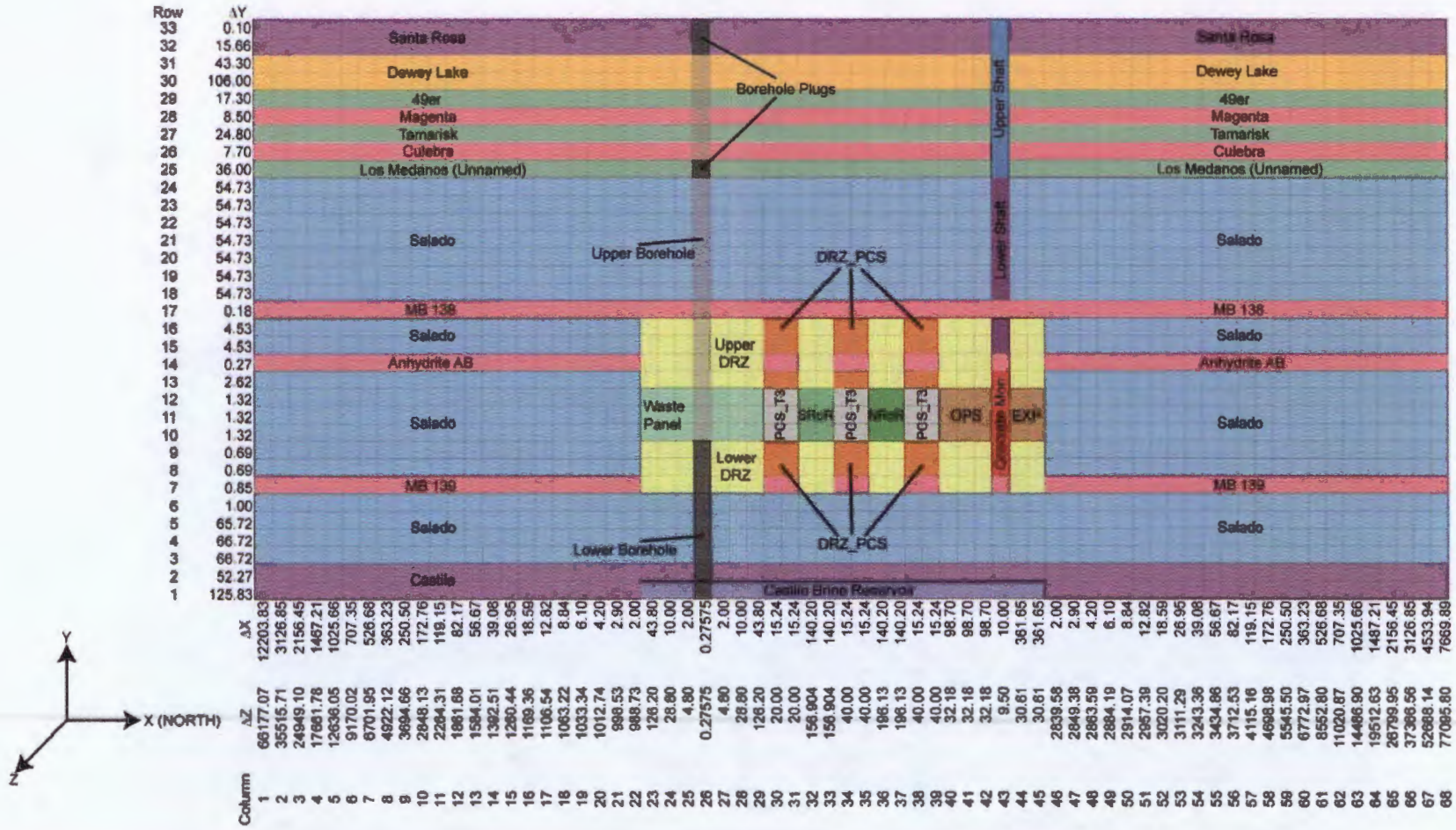

Figure 5-2: PCS-2012 BRAGFLO Grid and Material Map for an E1 Intrusion (Δx, Δy, and Δz dimensions in meters).

5.1.1 Results for an Undisturbed Repository (Scenario S1-BF)

Results are now presented for undisturbed scenario S1-BF. For the sake of brevity in what follows, waste area results are discussed in terms of the waste panel. Trends discussed for the waste panel also apply to other repository waste areas.

The PCS-2012 PA overall mean of cumulative brine flow into the waste panel, denoted by quantity BRNWASIC, is compared to the PABC-2009 overall mean of the same quantity in Figure 5-3. As seen in that figure, there is an increase in the mean cumulative brine flow into the waste panel in the PCS-2012 PA as compared to the PABC-2009. The majority of the increase in quantity BRNWASIC for the PCS-2012 PA occurs during the first 200 years. The increase during the first 200 years is readily apparent in Figure 5-4, where the time scale used to plot BRNWASIC overall means is restricted to the first 1,000 years. As seen in that figure, the difference in the overall means obtained in the two analyses increases steadily until 200 years. At 200 years, the ROMPCS assumes its long-term properties with the DRZ healed above and below it. At 200 years in the PCS-2012 PA BRNWASIC overall mean in Figure 5-4, the rate of increase decreases sharply. At 200 years, the difference between the BRNWASIC overall means obtained in the two analyses is roughly 600 m^3, and this difference between the overall means remains fairly constant for the remainder of the regulatory period.

The increase of brine flow into the waste panel results in a corresponding increase in the waste panel brine saturation, denoted by quantity WAS_SATB. The overall means for WAS_SATB obtained in the PCS-2012 PA and the PABC-2009 are plotted together in Figure 5-5. As seen in that figure, there is an increase in the mean for WAS_SATB in the PCS-2012 PA as compared to the PABC-2009. The increase in brine inflow to the waste panel during the first 200 years translates to an increase in the waste panel brine saturation. Beyond 200 years, the WAS_SATB overall means obtained in the two analyses are qualitatively very similar with differences seen in the magnitude of the respective curves primarily due to increases seen in the PCS-2012 PA during the first 200 years.

Increases in waste panel brine inflow and brine saturation potentially impact waste panel gas generation, denoted by quantity GASMOL_W. Overall means of waste panel gas generation obtained in the PCS-2012 PA and the PABC-2009 are plotted together in Figure 5-6. As seen in that figure, the overall mean for gas generated in the waste panel increased in the PCS-2012 PA. The increases seen in the mean waste panel brine inflow and mean waste panel brine saturation in the PCS-2012 PA result in a corresponding increase in waste panel gas generation.

Overall means of waste panel pressure obtained in the PCS-2012 PA and the PABC-2009 are shown together in Figure 5-7. As seen in that figure, there is a long-term increase in the mean waste panel pressure obtained in the PCS-2012 PA as compared to the PABC-2009. The increase in waste panel gas generation seen in the PCS-2012 PA translates to a long-term increase in the waste panel mean pressure.

Information Only

Pressure is released from repository waste areas to other repository regions before the ROMPCS and the surrounding DRZ assume their long-term properties at 200 years. The overall means of pressure in the operations area, denoted by quantity OPS_PRES, obtained in the PCS-2012 PA and the PABC-2009 are shown together in Figure 5-8. As seen in Figure 5-8, the mean pressure in the operations area is greater in the PCS-2012 PA at early times when compared to the PABC-2009. After the ROMPCS and the DRZ above and below it assume their long-term properties at 200 years, the rate of pressure release from repository waste areas into the operations area decreases. The "tighter" characteristics of the ROMPCS after 200 years results in less pressure being released to the operations region as compared to Option D. The result is an eventual decrease in the mean pressure in this region when compared to PABC-2009 results. Results obtained for the experimental region are virtually identical to those found for the operations area.

The base of the repository shaft is modeled in WIPP PA as being directly between the operations and experimental regions. Consequently, the pressure in these two regions impacts the volume of brine moved up the shaft toward the ground surface. The overall means of brine flow up the shaft, denoted by quantity BNSHUDRZ, obtained in the PCS-2012 PA and the PABC-2009 are shown together in Figure 5-9. As seen in that figure, the trends for brine flow up the shaft correspond closely to pressure trends in the operations and experimental areas. At early times, an increase is seen in the mean volume of brine flow up the shaft in the PCS-2012 PA. Eventually, however, the mean brine flow up the shaft is reduced in the PCS-2012 PA results, primarily due to the reductions in the mean pressure seen in the operations and experimental areas after the ROMPCS and surrounding DRZ assume their long-term properties.

Summary statistics for scenario S1-BF are shown in Table 5-2.

Table 5-2: Summary Statistics for Scenario S1-BF

Quantity (units)	Mean Value		Maximum Value	
	PABC-2009	PCS-2012 PA	PABC-2009	PCS-2012 PA
BRNWASIC ($x10^3$ m^3)	1.78	2.38	12.46	16.67
WAS_SATB (none)	0.16	0.20	0.99	0.99
GASMOL_W ($x10^6$ moles)	29.09	30.84	148.40	149.00
WAS_PRES (MPa)	6.52	6.77	16.19	16.29
BNSHUDRZ (m^3)	2.74	2.46	34.76	32.11

Information Only

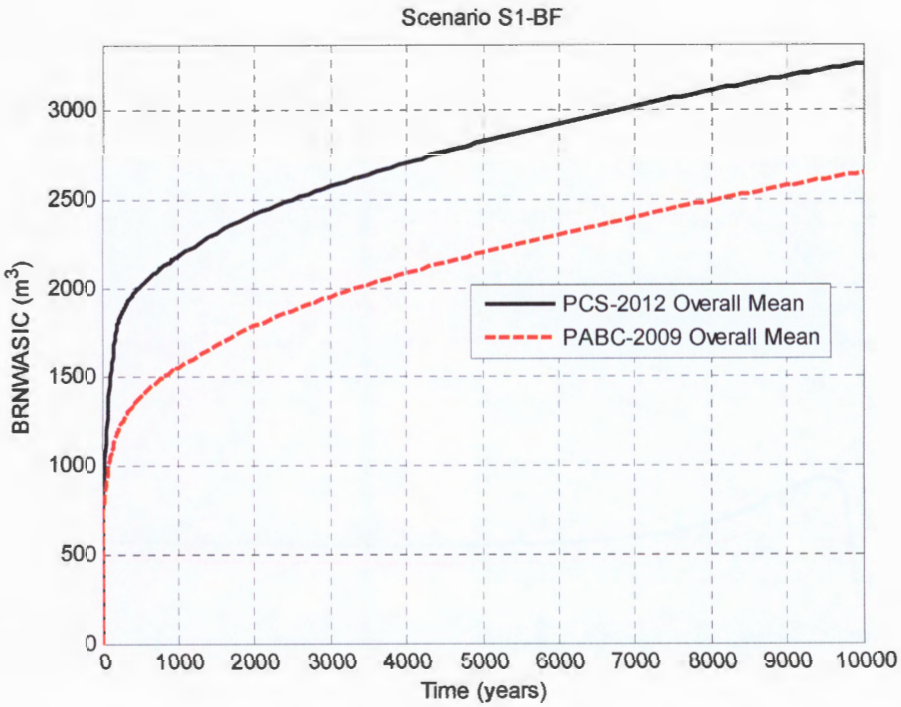

Figure 5-3: Overall Means of Cumulative Brine Inflow to the Waste Panel, Scenario S1-BF.

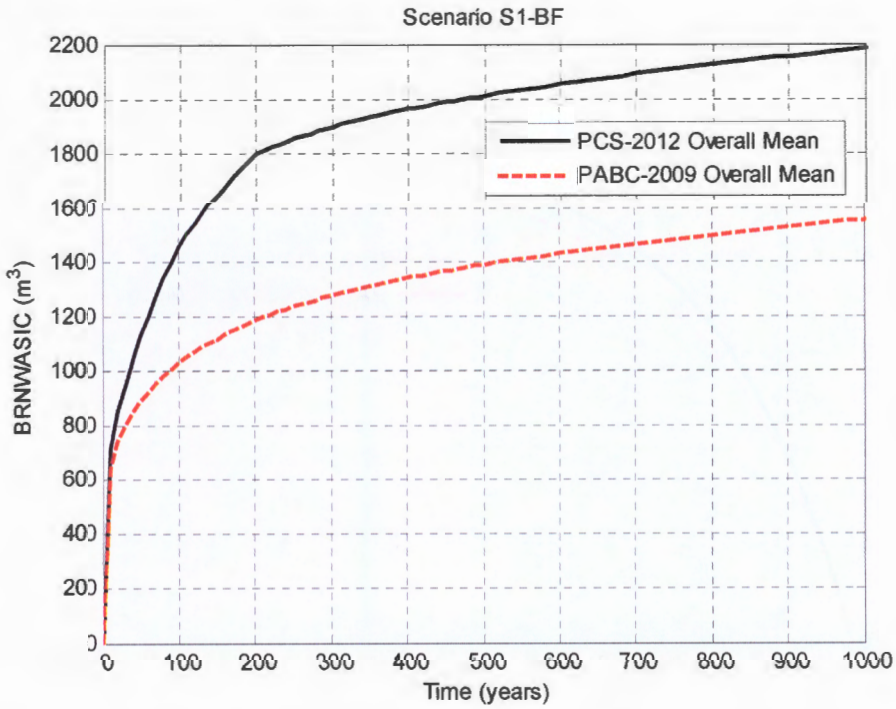

Figure 5-4: Overall Means of Cumulative Brine Inflow to the Waste Panel, Scenario S1-BF and Years 0 to 1,000.

Information Only

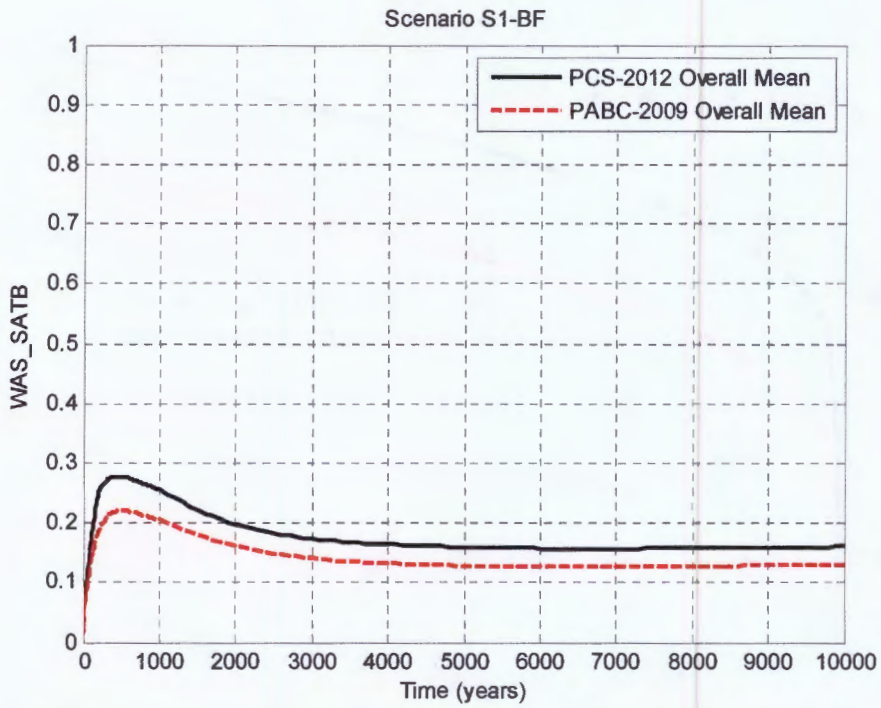

Figure 5-5: Overall Means of Waste Panel Brine Saturation, Scenario S1-BF.

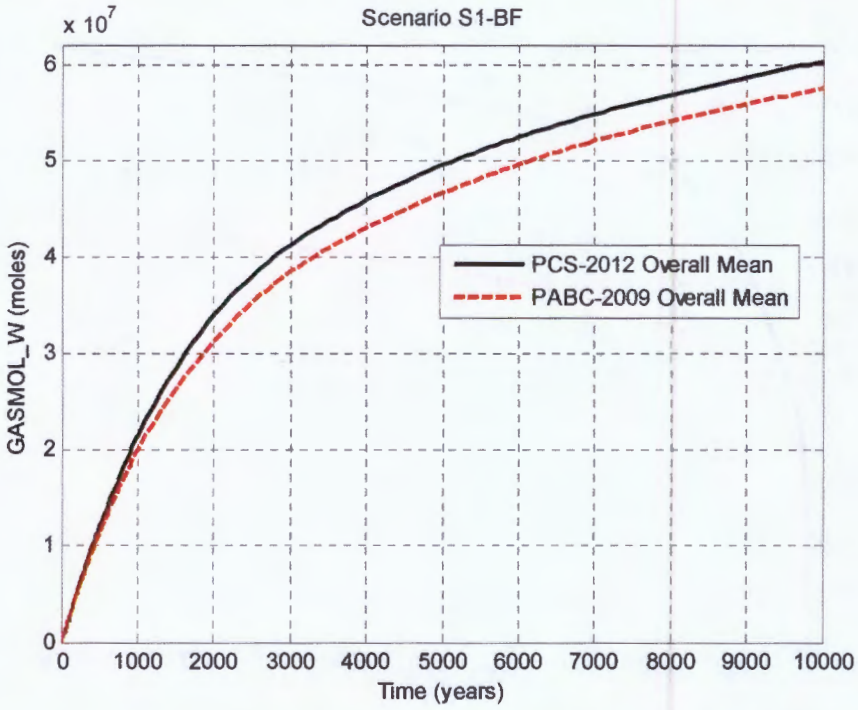

Figure 5-6: Overall Means of Waste Panel Gas Generation (in moles), Scenario S1-BF.

Information Only

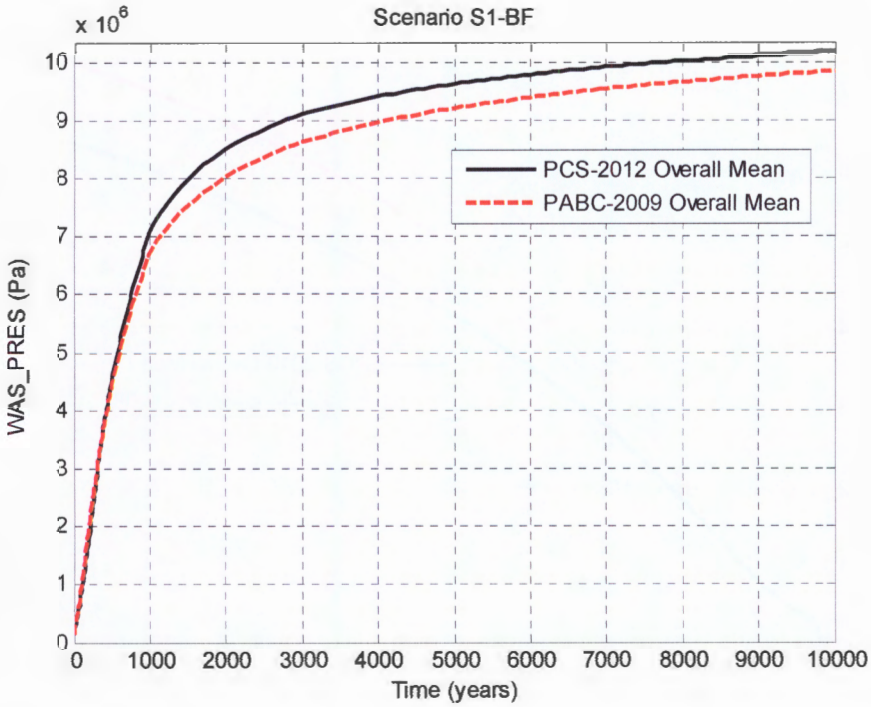

Figure 5-7: Overall Means of Waste Panel Pressure, Scenario S1-BF.

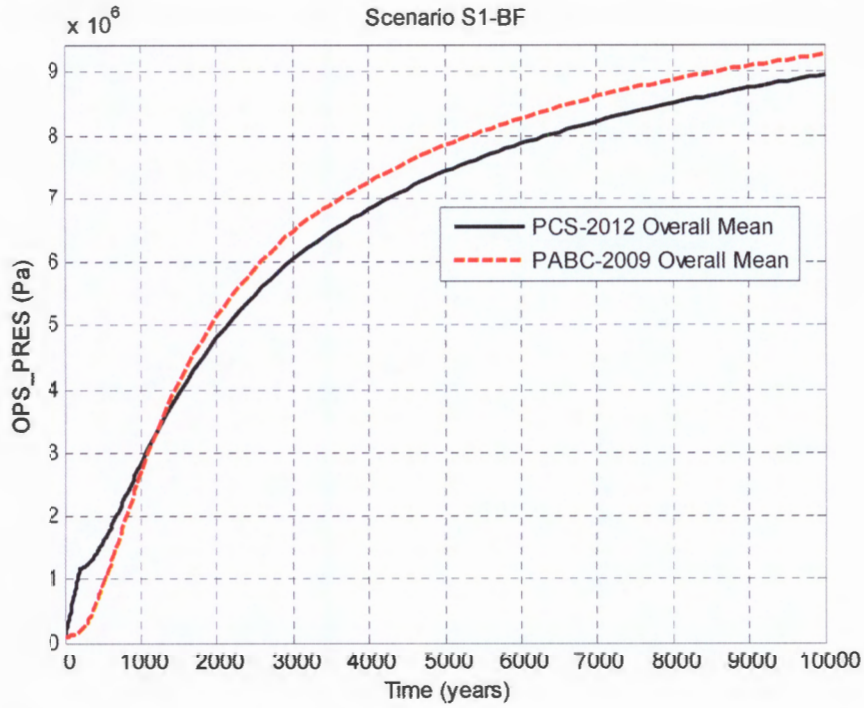

Figure 5-8: Overall Means of Pressure in the Operations Region, Scenario S1-BF.

Information Only

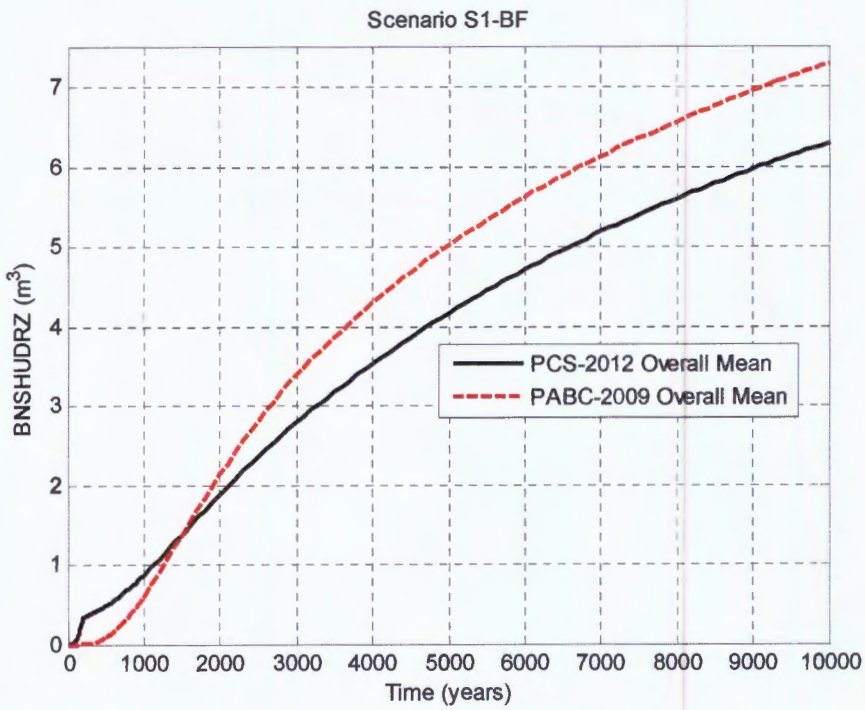

Figure 5-9: Overall Means of Brine Flow up the Shaft, Scenario S1-BF.

Information Only

5.1.2 Results for an E1 Intrusion at 350 Years (Scenario S2-BF)

Results are now presented for disturbance scenario S2-BF. Results presented for this scenario are representative of those calculated for E1 intrusion scenarios (scenarios S2-BF and S3-BF), with the only difference being the time of the intrusion. In the results that follow, PCS-2012 PA trends discussed for scenario S2-BF also apply to scenario S3-BF.

The fundamental characteristic of an E1 intrusion is the creation of a connected pathway between the repository waste panel and a region of pressurized brine in the Castile. Castile brine moves upward into the waste panel immediately after the intrusion, increasing waste panel pressure, brine saturation, and impacting other waste panel quantities.

The overall means of waste panel pressure obtained in the PCS-2012 PA and the PABC-2009 for scenario S2-BF are plotted together in Figure 5-10. As seen in that figure, the mean waste panel pressure calculated in the PCS-2012 PA is greater than that found in the PABC-2009 for a period of time after the intrusion. The long-term permeability range of the ROMPCS is lower than that prescribed to the Option D design in the PABC-2009. This reduction results in less long-term brine and gas flow through the ROMPCS, away from the waste panel, as compared to Option D. Following the E1 intrusion at 350 years, the "tighter" ROMPCS design results in a period of increased waste panel pressurization as compared to the PABC-2009 results.

An increase in waste panel pressure potentially impacts the volume of cumulative brine inflow to the waste panel, denoted by quantity BRNWASIC. The overall means of BRNWASIC obtained in the PCS-2012 PA and the PABC-2009 are shown together in Figure 5-11. As seen in that figure, the increased permeability range of the ROMPCS at early times results in greater brine inflow to the waste panel before the ROMPCS attains its long-term properties at 200 years. Following the intrusion time of 350 years, an increase in mean waste panel pressure occurs in the PCS-2012 PA results. This pressure increase slightly inhibits brine flow into the waste panel, resulting in a reduction in cumulative waste panel brine inflow as compared to the PABC-2009 results.

The reduction of brine flowing into the waste panel in the PCS-2012 PA impacts the waste panel brine saturation, denoted by quantity WAS_SATB. The overall means of quantity WAS_SATB obtained in the PCS-2012 PA and the PABC-2009 are shown together in Figure 5-12. As is evident in that figure, the mean waste panel brine saturation obtained in the PCS-2012 PA is reduced slightly from that calculated in the PABC-2009 after the intrusion at 350 years. The reduction of brine inflow to the waste panel translates to a reduction in waste panel brine saturation.

The overall means of waste panel gas generation (quantity GASMOL_W) obtained in the PCS-2012 PA and the PABC-2009 are shown together in Figure 5-13. The overall means obtained for quantity GASMOL_W obtained in the two analyses are nearly identical, with a very slight

Information Only

reduction seen in the PCS-2012 PA mean. This slight reduction in gas generation is most likely due to the reduction in waste panel brine inflow and brine saturation seen in the PCS-2012 PA results.

The volume of brine flow up the intrusion borehole is denoted by quantity BNBHUDRZ. Overall means of BNBHUDRZ obtained in the PCS-2012 PA and the PABC-2009 are shown together in Figure 5-14. The overall means obtained in the two analyses are almost identical, with a very slight increase seen in the PCS-2012 PA result.

Summary statistics for scenario S2-BF are shown in Table 5-3.

Table 5-3: Summary Statistics for Scenario S2-BF

Quantity (units)	Mean Value		Maximum Value	
	PABC-2009	PCS-2012 PA	PABC-2009	PCS-2012 PA
BRNWASIC ($x10^3$ m^3)	14.03	13.68	182.15	182.08
WAS_SATB (none)	0.68	0.67	0.99	0.99
GASMOL_W ($x10^6$ moles)	54.75	54.57	149.00	149.00
WAS_PRES (MPa)	7.39	7.50	15.63	16.40
BNBHUDRZ ($x10^3$ m^3)	3.25	3.28	166.84	169.54

Information Only

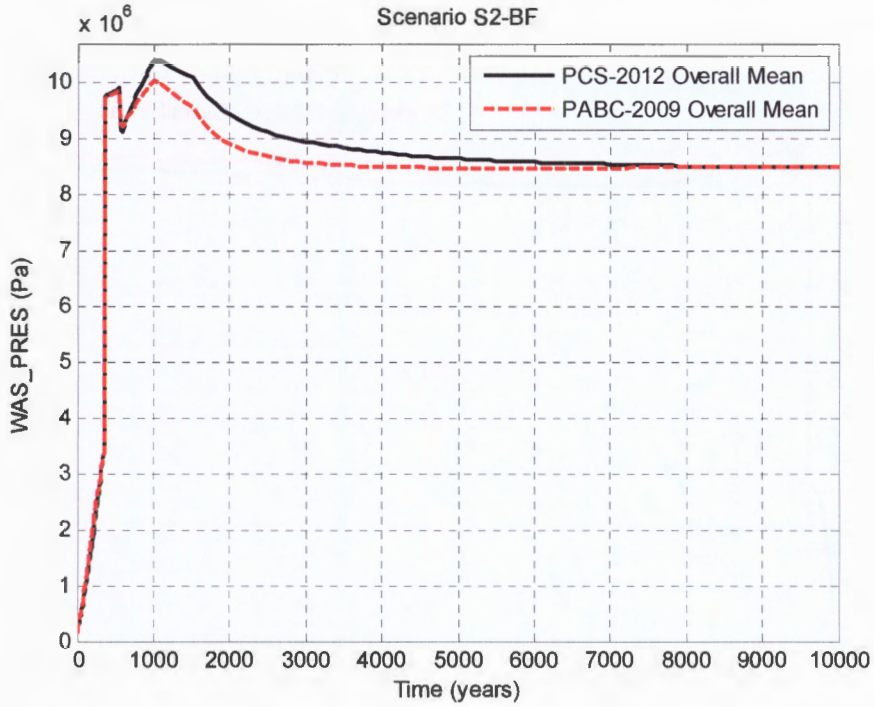

Figure 5-10: Overall Means of Waste Panel Pressure, Scenario S2-BF.

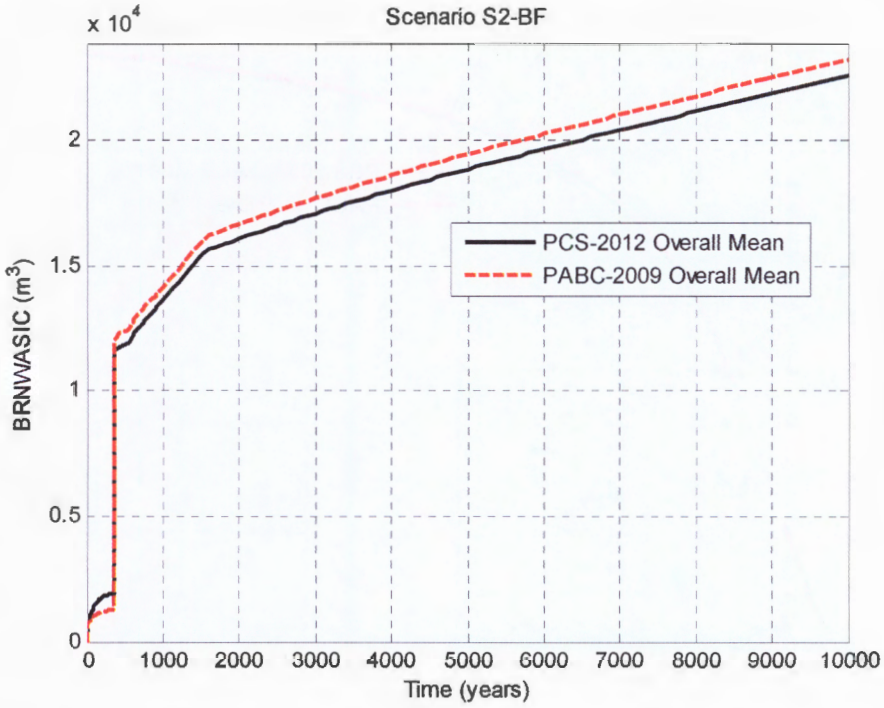

Figure 5-11: Overall Means of Cumulative Brine Inflow to the Waste Panel, Scenario S2-BF.

Information Only

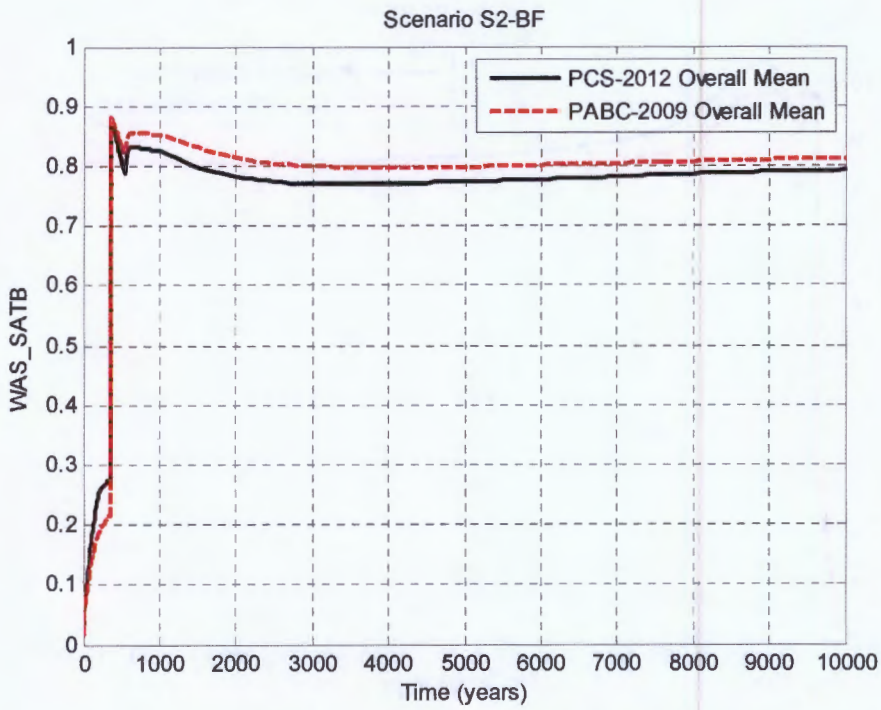

Figure 5-12: Overall Means of Waste Panel Brine Saturation, Scenario S2-BF.

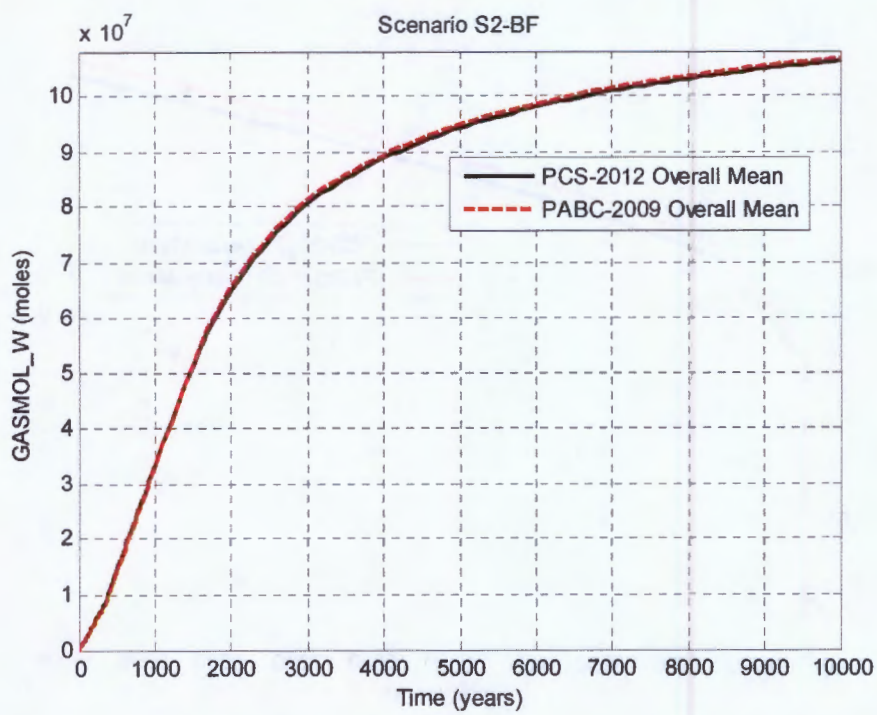

Figure 5-13: Overall Means of Waste Panel Gas Generation (in moles), Scenario S2-BF.

Information Only

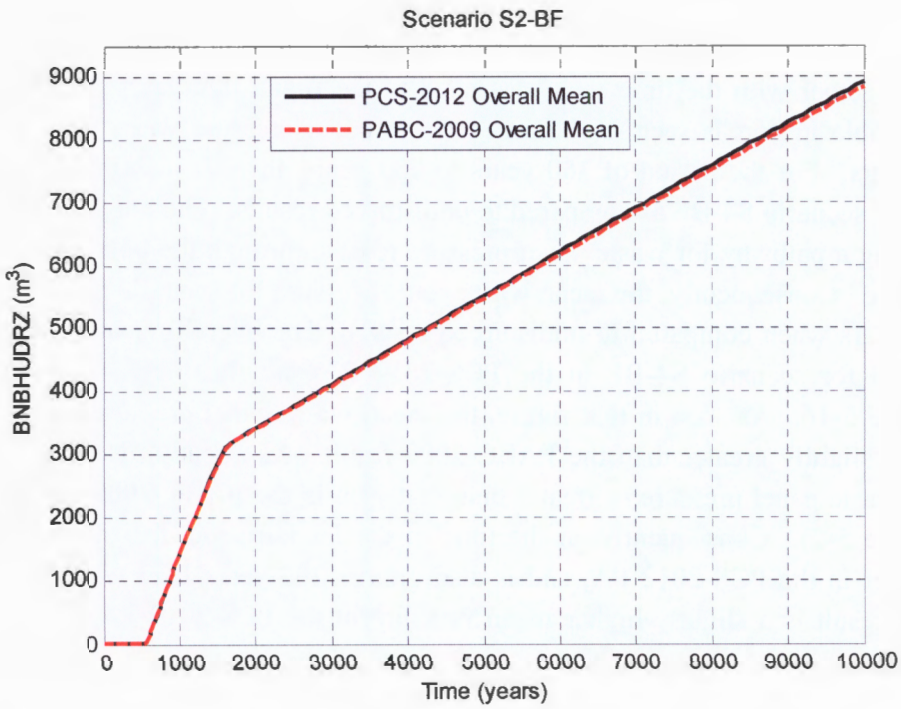

Figure 5-14: Overall Means of Brine Flow up the Borehole, Scenario S2-BF.

5.1.3 Results for an E2 Intrusion at 350 Years (Scenario S4-BF)

Results are now presented for disturbance scenario S4-BF. Results presented for this scenario are representative of those calculated for E2 intrusion scenarios (scenarios S4-BF and S5-BF), with the only difference being the time of the intrusion. In the results that follow, PCS-2012 PA trends discussed for scenario S4-BF also apply to scenario S5-BF.

As seen in the previous section, an E1 intrusion scenario results in an immediate influx of pressurized Castile brine to the waste panel, resulting in an increase is waste panel pressure when compared to undisturbed conditions. An E2 intrusion typically has the opposite effect. For the E2 intrusion scenario, no connected pathway is created between pressurized Castile brine and the repository waste panel. Following the intrusion, concrete plugs are immediately emplaced in the borehole near the ground surface. Consequently, an E2 intrusion does not typically have a significant impact on waste panel quantities *at the time of intrusion*. 200 years after the time of intrusion, concrete plugs emplaced in the borehole are modeled as failing, with the entire borehole assuming properties equivalent to sand. The result is a depressurization of the waste panel, beginning 200 years after the intrusion. Whereas an E1 intrusion typically results in an immediate increase in waste panel pressure, an E2 intrusion typically results in a *reduction* in waste panel pressure 200 years after the intrusion as compared to undisturbed conditions. The

Information Only

impact of the E2 intrusion on waste panel pressure is more closely seen in Figure 5-15. In that figure, PCS-2012 PA overall means of waste panel pressure obtained in scenarios S1-BF and S4-BF are plotted together with the time scale restricted to the first 1,000 years. As seen in that figure, no noticeable impact is seen in the mean waste panel pressure when the E2 intrusion occurs at 350 years. For the period of 350 years to 550 years, there is a slight increase in the mean pressure for scenario S4-BF as compared to undisturbed results. The borehole plugs fail at 550 years, creating a pathway for waste panel pressure release through the borehole and toward the ground surface. Consequently, the mean waste panel pressure for scenario S4-BF is reduced sharply at 550 years when compared to undisturbed results. The overall means of waste panel pressure obtained for scenario S4-BF in the PCS-2012 PA and the PABC-2009 are shown together in Figure 5-16. As seen in that figure, the mean waste panel pressure obtained in the PCS-2012 PA is slightly greater than the PABC-2009 result. As already discussed, the PCS-2012 PA mean waste panel pressure is greater than that seen in the PABC-2009 for undisturbed conditions (Figure 5-7). Consequently, at the time of the E2 intrusion, the mean waste panel pressure is greater in the PCS-2012 PA, and is also greater 200 years later when the borehole plugs fail. The result is a slightly higher mean pressure in the PCS-2012 PA scenario S4-BF result when compared to the PABC-2009.

The impact of the E2 intrusion on cumulative waste panel brine inflow can be clearly seen in Figure 5-17. At the intrusion time of 350 years until the borehole plugs fail at 550 years, there is only a very slight increase in quantity BRNWASIC as compared to undisturbed conditions. After the borehole plugs fail, a decrease in the waste panel pressure occurs. This pressure reduction yields in an increase in brine flow into the waste panel at 550 years compared to the undisturbed case. The overall means for quantity BRNWASIC in the PCS-2012 PA and the PABC-2009 are plotted together in Figure 5-18. As evident in that figure, an increase to the mean waste panel cumulative brine inflow is seen in the PCS-2012 PA results. This increase is due to the increased waste panel brine inflow seen for undisturbed conditions (Figure 5-4). Very little impact is seen in the mean curve for quantity BRNWASIC as compared to undisturbed conditions, until the borehole plugs fail at 550 years. The PCS-2012 PA mean waste panel brine inflow curve is already greater than that obtained in the PABC-2009 when the borehole plugs fail at 550 years. The increase in brine inflow seen after the borehole plugs fail results in a PCS-2012 PA mean waste panel brine inflow curve that remains greater than that seen in the PABC-2009.

The change to cumulative waste panel brine inflow seen in the PCS-2012 PA impacts the waste panel brine saturation. The impact of the E2 intrusion on quantity WAS_SATB is similar to that seen for cumulative brine flow into the waste panel. As seen in Figure 5-19, the mean waste panel brine saturation is changed very little as compared to undisturbed conditions for the time period of 350 to 550 years. After the borehole plugs fail at 550 years, an increase of brine inflow to the waste panel translates to a corresponding increase in brine saturation. The result is a PCS-2012 PA mean waste brine saturation curve that is greater than that seen in the PABC-2009

Information Only

results (Figure 5-20). The increase in the mean cumulative brine inflow to the waste panel seen in the PCS-2012 PA translates to an increase in the mean waste panel brine saturation.

The increase in waste panel brine saturation impacts gas generation in the waste panel. More brine flows into the waste panel (on average) in PCS-2012 PA scenario S4-BF as compared to the PABC-2009, resulting in an overall mean for quantity GASMOL_W in the PCS-2012 PA that is greater than that seen in the PABC-2009 (Figure 5-21).

The volume of brine flowing up the borehole toward the ground surface is denoted by quantity BNBHUDRZ. The increase in the mean waste panel pressure seen in the PCS-2012 PA yields a slight long-term increase in the means of quantity BNBHUDRZ. The overall mean of this quantity is greater in the PCS-2012 PA, as shown in Figure 5-22.

Summary statistics for scenario S4-BF are shown in Table 5-4.

Table 5-4: Summary Statistics for Scenario S4-BF

Quantity (units)	Mean Value		Maximum Value	
	PABC-2009	PCS-2012 PA	PABC-2009	PCS-2012 PA
BRNWASIC ($x10^3$ m^3)	2.73	3.29	23.81	19.39
WAS_SATB (none)	0.28	0.33	0.99	0.99
GASMOL_W ($x10^6$ moles)	36.40	38.35	149.00	149.00
WAS_PRES (MPa)	4.64	4.70	14.92	15.21
BNBHUDRZ (m^3)	34.76	43.76	4876.89	5287.28

Information Only

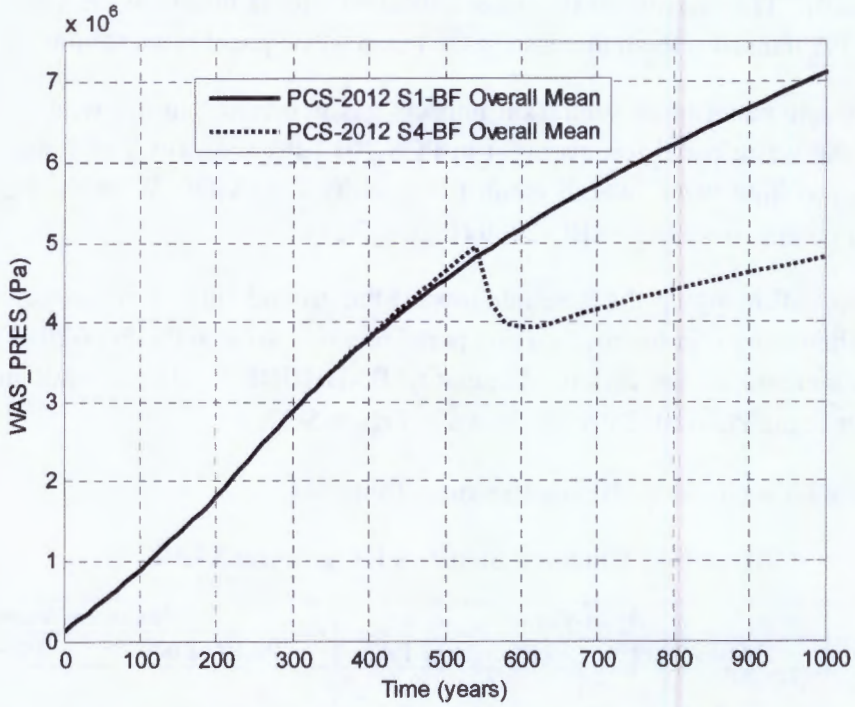

Figure 5-15: Overall Means of Waste Panel Pressure, Scenarios S1-BF and S4-BF for Years 0 to 1,000.

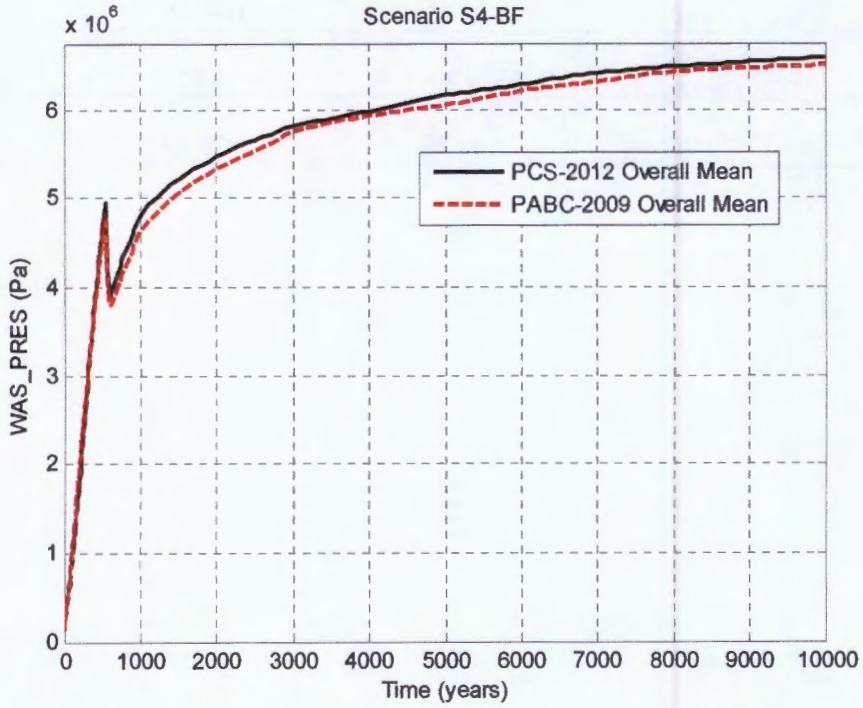

Figure 5-16: Overall Means of Waste Panel Pressure, Scenario S4-BF.

Information Only

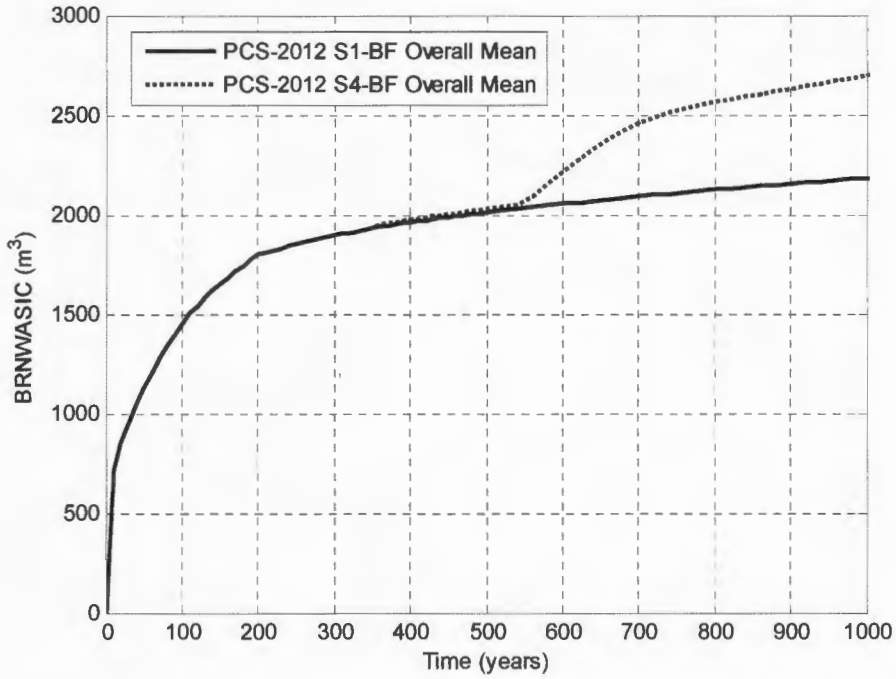

Figure 5-17: Overall Means of Cumulative Brine Inflow to the Waste Panel, Scenarios S1-BF and S4-BF for Years 0 to 1,000.

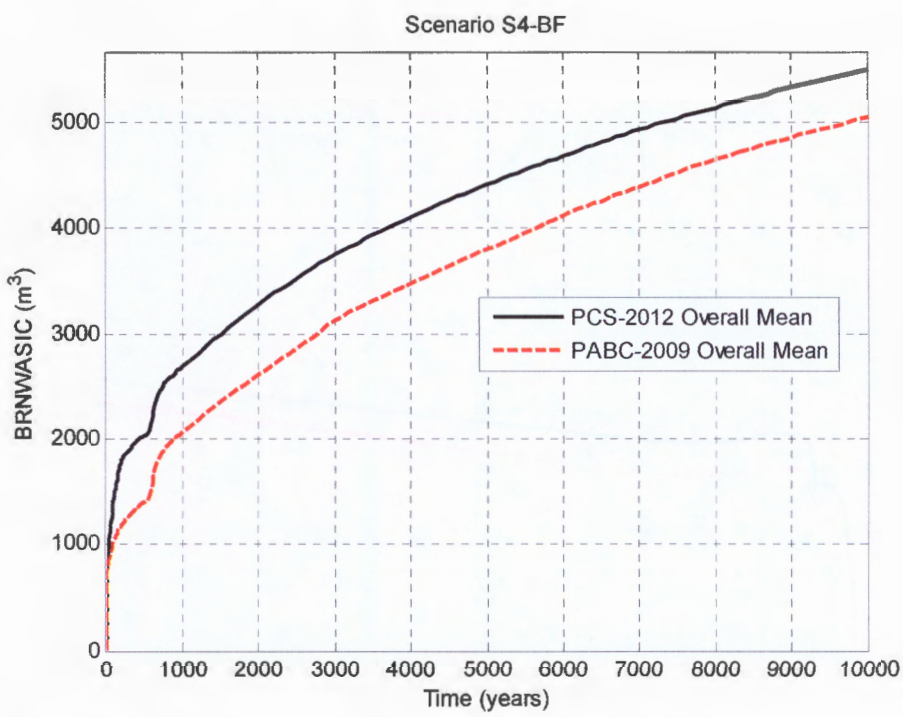

Figure 5-18: Overall Means of Cumulative Brine Inflow to the Waste Panel, Scenario S4-BF.

Information Only

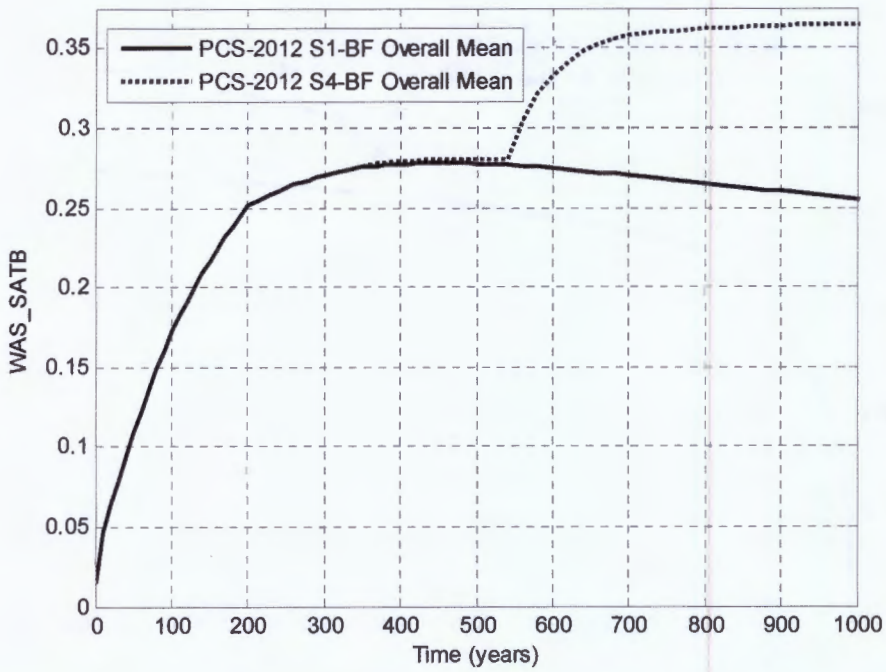

Figure 5-19: Overall Means of Waste Panel Brine Saturation, Scenarios S1-BF and S4-BF for Years 0 to 1,000.

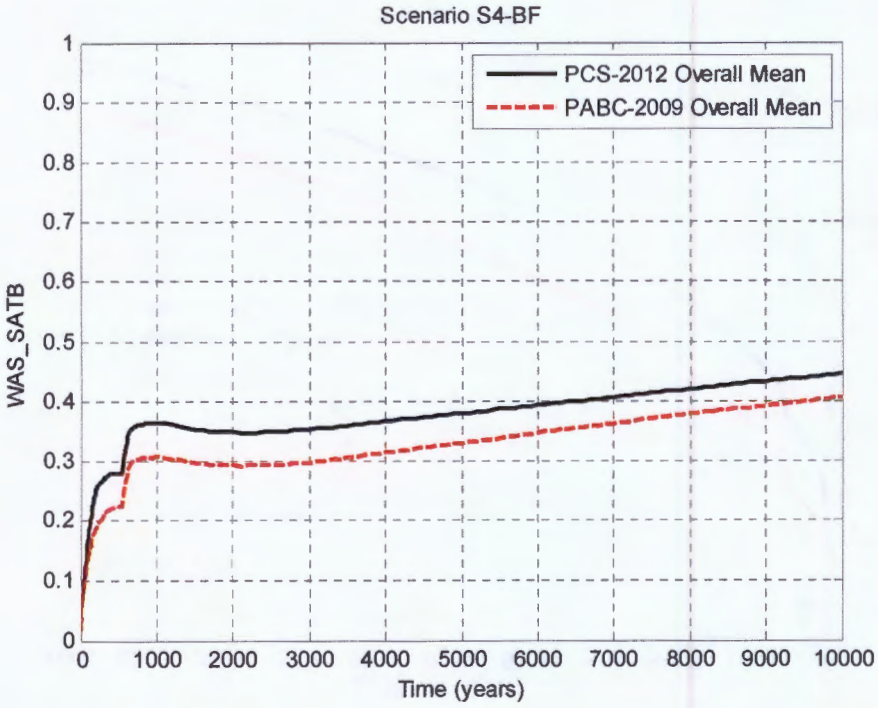

Figure 5-20: Overall Means of Waste Panel Brine Saturation, Scenario S4-BF.

Information Only

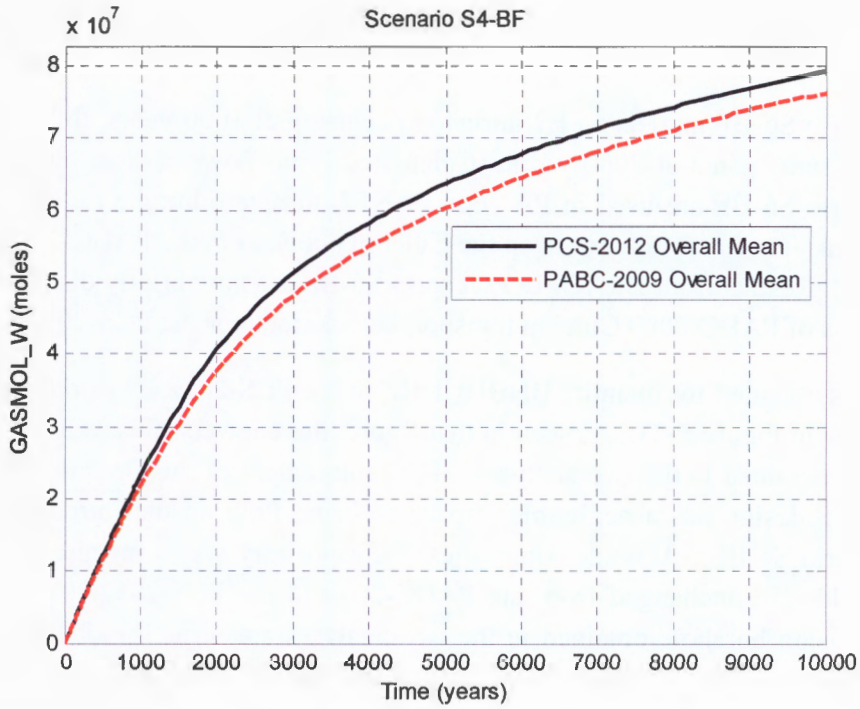

Figure 5-21: Overall Means of Waste Panel Gas Generation (in moles), Scenario S4-BF.

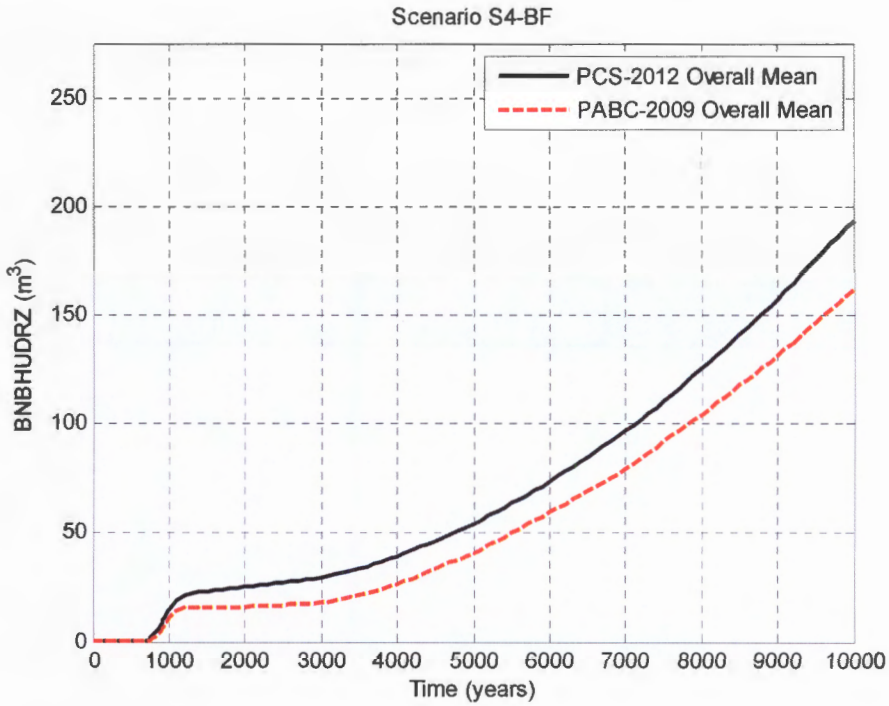

Figure 5-22: Overall Means of Brine Flow up the Borehole, Scenario S4-BF.

Information Only

5.1.4 Results for an E2 Intrusion at 1000 Years Followed by a E1 Intrusion at 2000 Years (Scenario S6-BF)

BRAGFLO scenario S6-BF models an E2 intrusion occurring at 1000 years, followed by an E1 intrusion into the same panel at 2000 years. Calculated brine flows up the intrusion borehole obtained in scenario S6-BF are used in PA code PANEL to determine the radionuclide source term to the Culebra. Transport releases from the Culebra obtained in the PABC-2009 are used in the PCS-2012 PA. Results from BRAGFLO scenario S6-BF are now briefly discussed to justify the appropriateness of PABC-2009 Culebra transport calculations for the PCS-2012 PA.

The overall means obtained for quantity BNBHUDRZ in the PCS-2012 PA and the PABC-2009 are shown together in Figure 5-23. As seen in that figure, there is very close agreement between the overall means obtained in the two analyses. The replacement of the Option D panel closure with the ROMPCS design has a negligible impact on brine flow up the intrusion borehole in BRAGFLO scenario S6-BF. Actinide solubilities, the repository waste inventory, and Culebra transmissivity fields are unchanged from the PABC-2009 to the PCS-2012 PA. As the brine flows up the intrusion borehole obtained in the two analyses are virtually identical in scenario S6-BF, the radionuclide source term to the Culebra is virtually unchanged by the ROMPCS design as compared to Option D results. Consequently, transport releases from the Culebra are also virtually unchanged. Incorporating PABC-2009 Culebra transport results into the PCS-2012 PA is reasonable and appropriate.

Summary statistics for quantity BNBHUDRZ obtained in scenario S6-BF are shown in Table 5-5.

Table 5-5: Summary Statistics for Scenario S6-BF

Quantity (units)	Mean Value		Maximum Value	
	PABC-2009	PCS-2012 PA	PABC-2009	PCS-2012 PA
BNBHUDRZ ($x10^3$ m^3)	2.92	2.94	169.03	169.30

Information Only

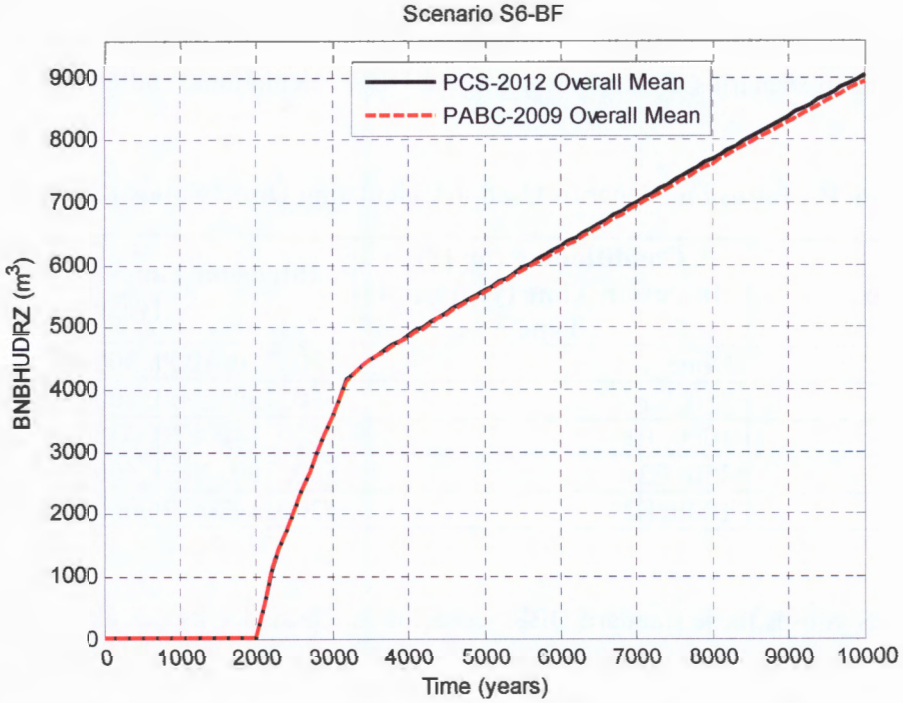

Figure 5-23: Overall Means of Brine Flow up the Borehole, Scenario S6-BF.

5.2 Spallings

The replacement of the Option D panel closure with the ROMPCS design has no impact on cuttings and cavings releases. Changes in repository pressures seen in the PCS-2012 PA BRAGFLO results potentially impact spallings releases, however. Calculation of the volume of solid waste material released to the surface from a single drilling intrusion into the repository due to spallings is a two-part procedure. First, PA code DRSPALL calculates the spallings volumes from a single drilling intrusion at four values of repository pressure (10, 12, 14, and 14.8 MPa). The second step in calculating spallings volumes from a single intrusion consists of using the code CUTTINGS_S to interpolate between DRSPALL volumes. The spallings volume for a given vector is determined in CUTTINGS_S by linearly interpolating between volumes calculated by DRSPALL based on the pressure calculated in each realization by BRAGFLO. DRSPALL volumes used in the PABC-2009 were also used in the PCS-2012 PA.

PA code CUTTINGS_S is also used as a transfer program between the BRAGFLO Salado flow calculation and the BRAGFLO DBR calculation. Results obtained by BRAGFLO for each realization in scenarios S1-BF to S5-BF are used to initialize the flow field properties necessary for the calculation of DBRs. This requires that results obtained on the BRAGFLO grid be mapped appropriately to the DBR grid. Code CUTTINGS_S is used to transfer the appropriate scenario results obtained with BRAGFLO to the DBR calculation. These transferred flow results

Information Only

are used as initial conditions in the calculation of DBRs. As a result, intrusion scenarios and times used in the calculation of spallings volumes correspond to those used in the calculation of DBRs. Five intrusion scenarios are considered in the DBR calculations, and are listed in Table 5-6.

Table 5-6: PA Intrusion Scenarios Used in Calculating Direct Solids Releases

Scenario	Conditioning (or 1st) Intrusion Time (year) and Type	Intrusion Times – Subsequent (year)
S1-DBR	None	100, 350, 1000, 3000, 5000, 10000
S2-DBR	350, E1	550, 750, 2000, 4000, 10000
S3-DBR	1000, E1	1200, 1400, 3000, 5000, 10000
S4-DBR	350, E2	550, 750, 2000, 4000, 10000
S5-DBR	1000, E2	1200, 1400, 3000, 5000, 10000

While CUTTINGS_S uses these standard DBR scenarios as a basis for its calculations, it does so to provide flow field results (generated with BRAGFLO) as initial conditions to the DBR calculation at each subsequent intrusion time. CUTTINGS_S does not model the intrusion scenario itself. Scenario S1-DBR corresponds to an initial intrusion into the repository, with repository flow conditions at the time of intrusion transferred from BRAGFLO scenario S1-BF results. Scenarios S2-DBR through S5-DBR are used to model an intrusion into a repository that has already been penetrated. The times at which intrusions are assumed to occur for each scenario are outlined in the last column of Table 5-6; six intrusion times are modeled for scenario S1-DBR, while five times are modeled for each of scenarios S2-DBR through S5-DBR.

Utilizing the spallings volumes calculated by DRSPALL and the PCS-2012 PA repository pressures calculated by BRAGFLO, the impact of the ROMPCS design on spallings volumes can be determined. Summary statistics of spallings volumes for the intrusion scenarios considered by CUTTINGS_S are shown in Table 5-7 for both the PCS-2012 PA and the PABC-2009. PABC-2009 results reported in that table (except for the percentage of nonzero volumes) are taken from Ismail (2010). While the results for the PABC-2009 and the PCS-2012 PA calculations are similar for some scenarios, some differences in the spallings volumes are noted. In general, the PCS-2012 results show increases in the maximum spallings volume across all three replicates. Replicate 1 showed very similar average nonzero spallings volumes in both PA calculations. In replicates 2 and 3, the average nonzero spallings volumes were higher for the PCS-2012 PA calculations compared to PABC-2009, with the most significant volume increases occurring in scenarios S2-DBR, S3-DBR, and S5-DBR. Overall, the general trend shows a slightly higher average nonzero spallings volume, a larger maximum volume, and a larger percentage of vectors with spallings considering the total from all scenarios across all three replicates (Kicker 2012).

Information Only

The change in spallings volumes between the PCS-2012 PA and the PABC-2009 is the result of changing repository pressures observed in BRAGFLO calculations for the PCS-2012 PA. Because spallings volumes directly depend on repository pressure, an increase in repository pressure translates into larger spallings volumes. Since there is a minimum threshold pressure required to create spallings, an increase in repository pressure also increases the percentage of vectors with spallings.

Table 5-7: Summary of Spallings Releases by Scenario

		Scenarios					Total
		S1-DBR	S2-DBR	S3-DBR	S4-DBR	S5-DBR	
PCS-2012 PA							
R1	Maximum [m^3]	2.34	9.35	8.69	1.67	1.67	9.35
	Average nonzero volume [m^3]	0.37	0.53	0.47	0.29	0.32	0.41
	Number of nonzero volumes	157	141	138	76	104	616
	Percent of nonzero volumes	8.7%	9.4%	9.2%	5.1%	6.9%	7.9%
R2	Maximum [m^3]	2.76	3.69	2.76	2.76	2.76	3.69
	Average nonzero volume [m^3]	0.37	0.42	0.44	0.52	0.55	0.44
	Number of nonzero volumes	184	165	151	79	107	686
	Percent of nonzero volumes	10.2%	11.0%	10.1%	5.3%	7.1%	8.8%
R3	Maximum [m^3]	6.09	7.32	3.31	2.70	3.29	7.32
	Average nonzero volume [m^3]	0.54	0.48	0.38	0.32	0.33	0.43
	Number of nonzero volumes	189	134	144	72	111	650
	Percent of nonzero volumes	10.5%	8.9%	9.6%	4.8%	7.4%	8.3%
PABC-2009							
R1	Maximum [m^3]	2.24	8.29	7.97	1.67	1.67	8.29
	Average nonzero volume [m^3]	0.37	0.54	0.50	0.30	0.37	0.43
	Number of nonzero volumes	142	117	111	59	77	506
	Percent of nonzero volumes	7.9%	7.8%	7.4%	3.9%	5.1%	6.5%
R2	Maximum [m^3]	2.36	2.76	1.86	2.26	1.93	2.76
	Average nonzero volume [m^3]	0.32	0.39	0.37	0.50	0.47	0.39
	Number of nonzero volumes	168	122	122	57	84	553
	Percent of nonzero volumes	9.3%	8.1%	8.1%	3.8%	5.6%	7.1%
R3	Maximum [m^3]	4.91	6.23	2.62	1.47	1.49	6.23
	Average nonzero volume [m^3]	0.53	0.39	0.28	0.30	0.28	0.38
	Number of nonzero volumes	156	113	118	45	72	504
	Percent of nonzero volumes	8.7%	7.5%	7.9%	3.0%	4.8%	6.5%

The impacts of the changes in spallings volumes on the overall mean CCDF for normalized spallings releases obtained in the PCS-2012 PA can be seen in Figure 5-24. As seen in that figure, the CCDF of spallings releases obtained in the PCS-2012 PA is consistently higher than that found in the PABC-2009. The increases in spallings volumes and in the number of vectors that result in a nonzero spallings volume translate to an increase in spallings releases as both analyses use the same waste inventory.

Information Only

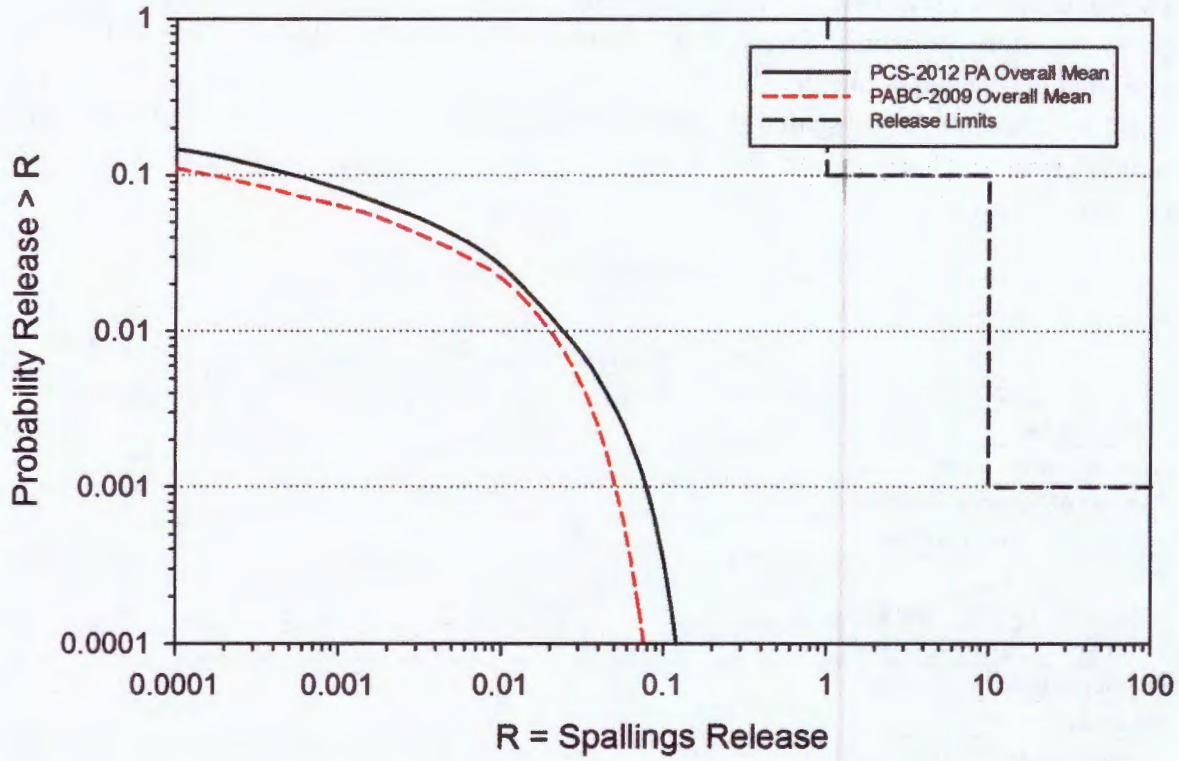

Figure 5-24: PCS-2012 PA and PABC-2009 Overall Mean CCDFs for Normalized Spallings Releases

5.3 Direct Brine Releases

PA code BRAGFLO is used in two ways in WIPP PA calculations. First, it is used to calculate the flow of brine and gas in and around the repository for undisturbed and disturbed conditions. PCS-2012 PA results from this application of BRAGFLO are shown in Section 5.1. Second, it is used for the calculation of direct brine releases. These two uses of BRAGFLO require different computational grids. Results obtained from the brine and gas flow calculation are used to initialize conditions in the DBR calculation. The representation of the waste area by three regions in the PCS-2012 PA and PABC-2009 BRAGFLO grids (see Figure 5-1 and Figure 5-2) yields initial conditions to waste regions comprising the Waste Panel (panel 5), the South Rest of Repository or SROR (panels 3,4,6, and 9), and the North Rest of Repository or NROR (panels 1,2,7,8, and 10) in the DBR calculation, with drilling intrusions considered in each of these regions. The types of intrusions considered in the DBR calculation and the times at which they occur are listed in Table 5-6. The scenarios, intrusion locations, and timings used for the PCS-2012 PA are the same as those used for the PABC-2009.

Information Only

The DBR numerical grid and material map used in the PCS-2012 PA calculations are shown in Figure 5-25, and are described in Malama (2012). The color scheme in Figure 5-25 has been chosen so as to correspond to the color scheme used in the PCS-2012 PA BRAGFLO grid and material map shown in Figure 5-2. The computational grid and material map used in the PABC-2009 DBR calculations are shown in Figure 5-26.

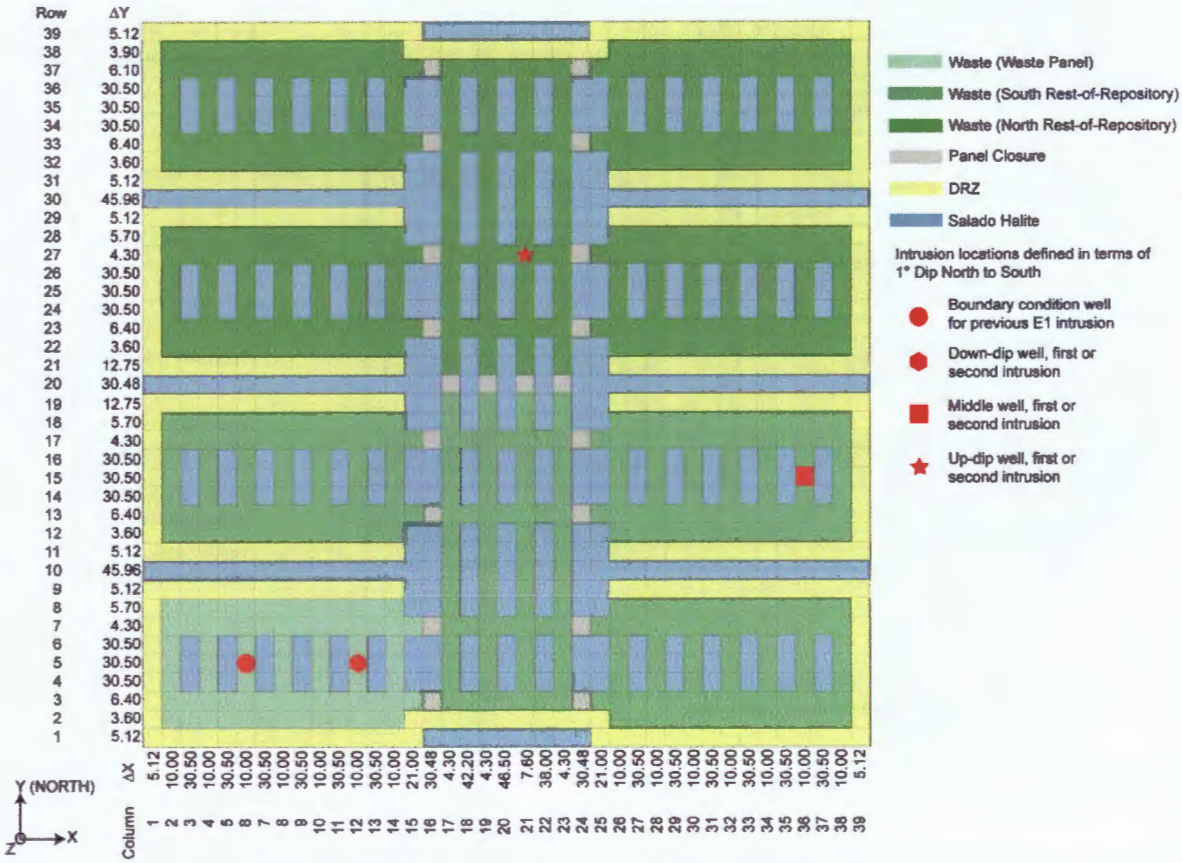

Figure 5-25: PCS-2012 PA DBR Computational Grid and Material Map (logical grid).

Information Only

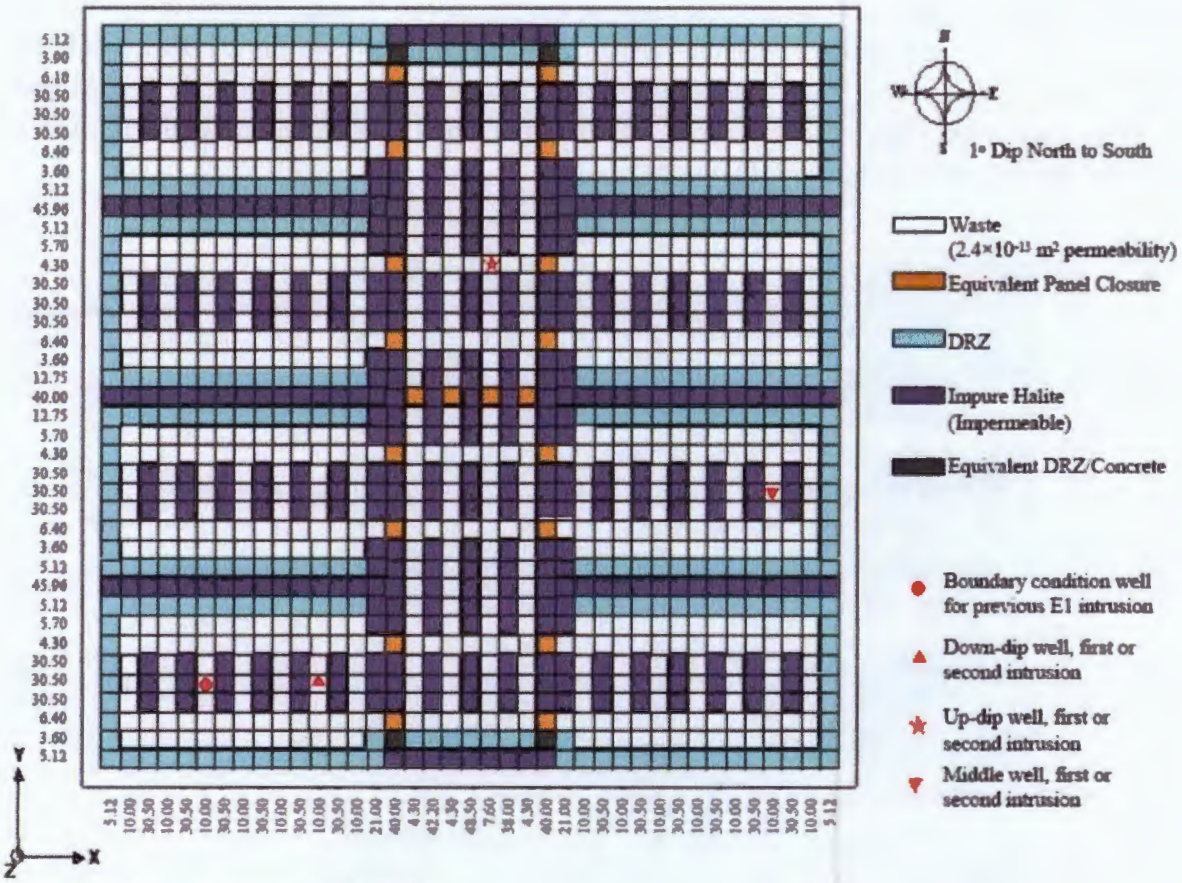

Note: Model cells are not to scale. The actual dimensions of the grid blocks are indicated along the edge of the diagram.

Figure 5-26: PABC-2009 DBR Computational Grid and Material Map (logical grid).

With the DBR computational grid and intrusion locations in hand, DBR results from the PCS-2012 PA and the PABC-2009 can now be compared. Summary statistics of the calculated DBR volumes for replicates 1-3 and scenarios S1-DBR to S5-DBR are provided in Table 5-8. The maximum DBR volumes shown in that table are assessed over all three replicates, times, vectors and drilling locations. As was also the case in the PABC-2009, release volumes that are less than $1x10^{-7}$ m^3 are considered to be inconsequential and are not included in the tally of vectors that result in DBR release volumes in the PCS-2012 PA calculations.

Overall there is a consistent increase in the maximum DBR volumes from PABC-2009 to PCS-2012 PA. The largest increases were observed in scenarios S4-DBR and S5-DBR which are associated with E2 intrusions. As previously discussed in the BRAGFLO results, E2 intrusion scenarios in the PCS-2012 PA yielded waste panel pressure that is higher, on average, than that seen in the PABC-2009 at the time of intrusion and it remains higher for the duration of the 10,000 year regulatory period. Similarly, the mean waste panel brine saturation is higher at the

Information Only

time of intrusion in the PCS-2012 PA, resulting in higher long-term waste panel brine saturations for E2 intrusion scenarios. DBR volumes are strongly dependent on waste panel pressure and brine saturation at the time of intrusion. Hence, increases to these two quantities lead to increased maximum DBR volumes observed in scenarios S4-DBR and S5-DBR, and to the higher overall number of non-zero brine volume vectors.

Table 5-8: DBR Summary Statistics for the PCS-2012 PA and PABC-2009 DBR Calculations

	Number of Vectors		Maximum volume (m^3)		Average volume (m^3)	
Scenario	PABC-2009	PCS-2012 PA	PABC-2009	PCS-2012 PA	PABC-2009	PCS-2012 PA
S1-DBR	369	419	27.6	45.9	0.1	0.4
S2-DBR	1179	1174	48.2	52.9	2.8	2.9
S3-DBR	926	907	40.6	43.8	1.5	1.4
S4-DBR	211	281	20.4	42.5	0.1	0.2
S5-DBR	314	401	21.1	53.8	0.1	0.3
Overall	2999	3182	48.2	53.8	0.9	1.0

The moderate increases in maximum DBR volumes for scenarios S2-DBR and S3-DBR are due to the fact that the lower long-term permeability range of the ROMPCS as compared to Option D yields a period of increased waste panel pressurization following an E1 intrusion. The increased mean waste panel pressure slightly inhibits brine flow into the panel after the intrusion, resulting in a slight decrease to the mean waste panel brine saturation as compared to PABC-2009 E1 intrusion results. The effects of increased pressure and decreased brine saturation effectively cancel, resulting in only a slight increase to the maximum DBR volume seen in the PCS-2012 PA E1 results.

For undisturbed conditions, implementation of the ROMPCS yields higher long-term waste panel pressure (on average) than was seen in the PABC-2009. The increase in mean waste panel pressure is accompanied by an increase in the average waste panel brine saturation for the ROMPCS results. The ROMPCS design allows more brine inflow to the waste panel during the first 200 years when compared to Option D results. This increased brine inflow, combined with the tightness of the ROMPCS after 200 years, results in increased waste panel gas generation (on average) and a subsequent increase to waste panel mean pressure. This explains the increase in the scenario S1-DBR maximum DBR volume for the PCS-2012 PA compared to the PABC-2009.

Table 5-8 shows a modest (~6%) increase in the number of non-zero DBR volumes for the PCS-2012 PA calculations compared with the PABC-2009, and modest increases in the average DBR volumes for all scenarios. These increases are attributable to the increases in waste panel brine pressure and brine saturation discussed above and presented in the BRAGFLO results in Section 5.1.

Information Only

DBR volume trends observed in the PCS-2012 PA are consistent with those found in prior analyses with regard to drilling location. DBRs are less likely to occur in intrusions situated in the upper drilling location than in the lower drilling location. Of all the intrusions that had a non-zero DBR volume for the PCS-2012 PA, 63.4% occurred during a lower drilling intrusion, a modest decrease from the value of 66.5% for PABC-2009. Furthermore, of all the intrusions that had a non-zero DBR volume and occur during a lower drilling intrusion, 78.0% are found in scenarios S2-DBR and S3-DBR, a slight decrease from 82.9% for PABC-2009 (Clayton et al. 2010). The majority of the non-zero DBR volumes occur when there is a previous E1 intrusion within the same panel. Not only are DBRs less likely to occur during upper drilling intrusions, but also the DBR volumes from such intrusions tend to be much smaller than those from lower drilling intrusions. For all three replicates of the PCS-2012 PA, the maximum DBR volume for the upper drilling location is 25.7 m^3 compared to 53.8 m^3 for the lower drilling location. These observations support the conclusion that lower drilling intrusions are the primary source for significant DBRs.

The combination of relatively high pressure and brine saturation in the intruded panel is required for direct brine release to the surface. Figure 5-27 shows a scatter plot of DBR volume versus pressure in the intruded panel at different intrusion times for scenario S2-DBR, replicate 1, lower drilling intrusion for the PCS-2012 PA. In that figure, symbols indicate the value of the mobile brine saturation, defined as brine saturation minus residual brine saturation in the waste. As prescribed by the conceptual model, there are no DBRs until pressures exceed the 8 MPa vertical line in that figure. Above 8 MPa, a significant number of vectors have zero volumes; these vectors have mobile brine saturations less than zero and thus no brine is available in a mobile form to be released. Figure 5-27 shows a high concentration of results that are near a line extending from (8 MPa, 0 m^3) to (12 MPa, 30 m^3). As mobile saturation increases, the correlation between pressure and DBR volumes also increases.

To further facilitate comparisons of DBRs calculated in the PCS-2012 PA to those obtained in the PABC-2009, the overall mean CCDFs obtained in these two analyses are plotted simultaneously in Figure 5-28. As seen in that figure, the CCDF curve obtained for direct brine releases shows greater mean probabilities in the PCS-2012 PA for the majority of release values.

Information Only

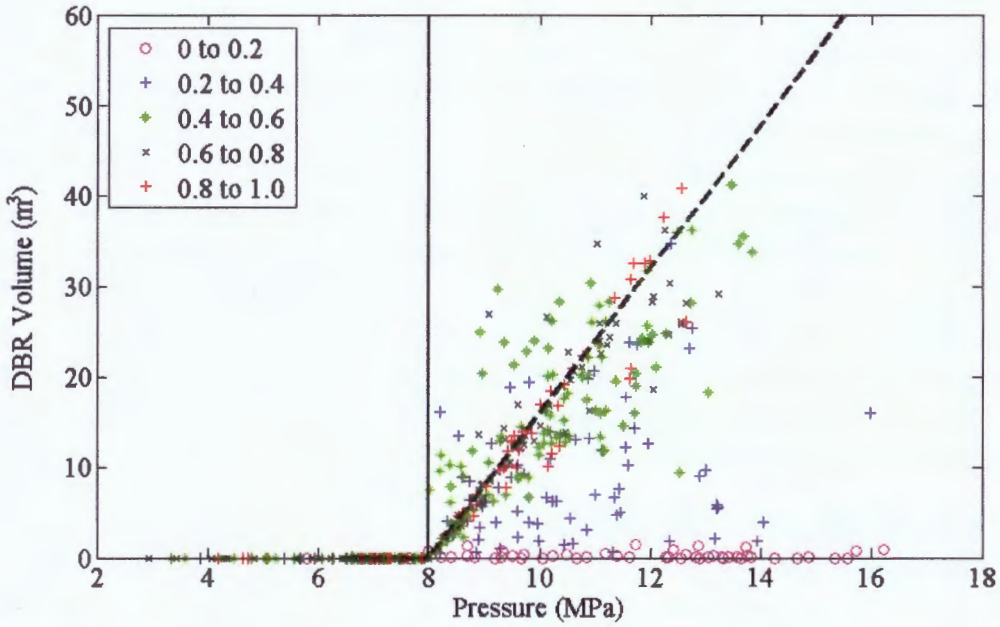

Figure 5-27: DBR Volume vs. Pressure, Scenario S2-DBR, Replicate 1, Lower Intrusion, PCS-2012 PA

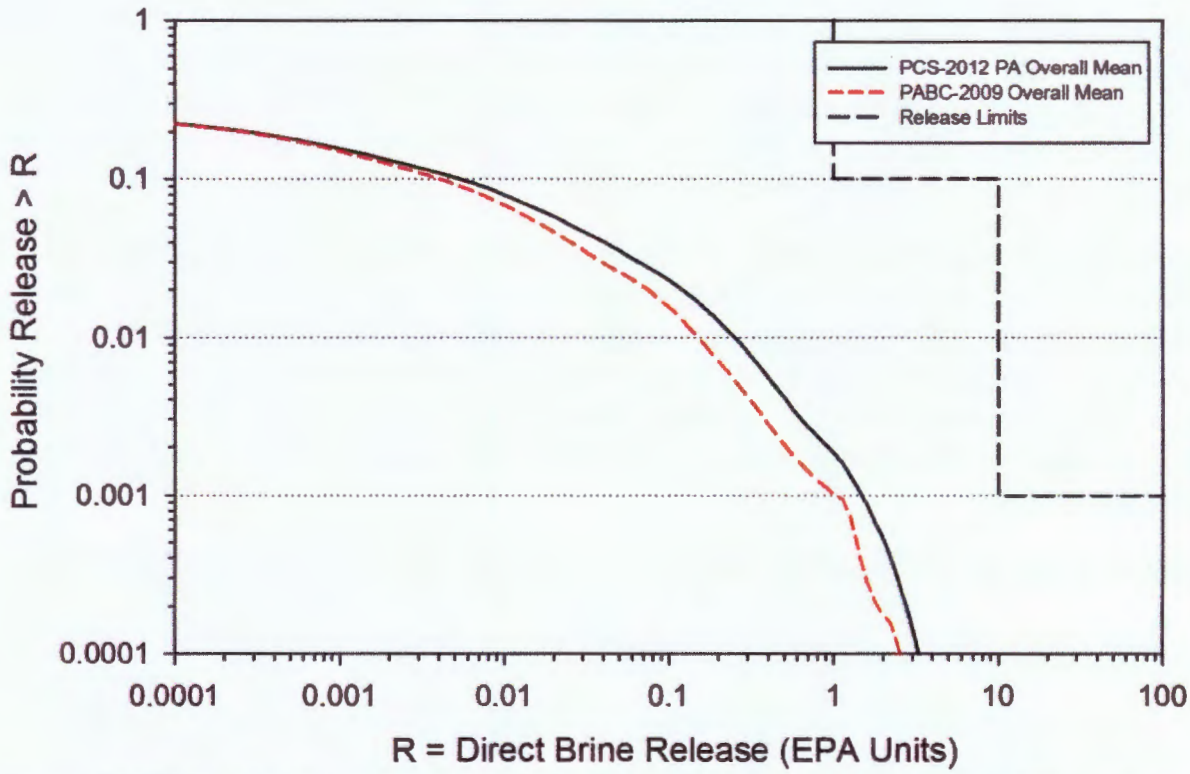

Figure 5-28: PCS-2012 PA and PABC-2009 Overall Mean CCDFs for Normalized Direct Brine Releases

Information Only

5.4 Total Normalized Releases

Total normalized releases for PCS-2012 PA are presented in this section and subsequently compared to results obtained in the PABC-2009. Total releases are calculated by forming the summation of releases across each potential release pathway, namely cuttings and cavings releases, spallings releases, direct brine releases, and transport releases. PCS-2012 PA CCDFs for total releases are presented in Figure 5-29, Figure 5-30, and Figure 5-31 for replicates 1, 2, and 3, respectively. Mean and quantile CCDF distributions for the three replicates are shown together in Figure 5-32. Figure 5-33 contains the 95 percent confidence limits about the overall mean of total releases. As seen in Figure 5-33, the overall mean for normalized total releases and its lower/upper 95% confidence limits are well below acceptable release limits. As a result, the ROMPCS design investigated in the PCS-2012 PA does not result in WIPP non-compliance with the containment requirements of 40 CFR Part 191.

PCS-2012 PA and PABC-2009 overall mean CCDFs for total releases are shown together in Figure 5-34. As seen in that figure, the overall mean CCDFs obtained in the two analyses are nearly identical for release values less than approximately 0.1 EPA units. For releases greater than 0.1 EPA units, the CCDF curve obtained in the PCS-2012 PA is higher than that found in the PABC-2009. This increase corresponds primarily to the differences found for direct brine releases between the two analyses as discussed in Section 5.3 and illustrated in Figure 5-28. The differences found for spallings may slightly affect the total CCDF curve as well (Section 5.2, Figure 5-24). PCS-2012 PA cuttings and cavings results are unchanged from those found in the PABC-2009. The ROMPCS design investigated in the PCS-2012 PA has an impact on the overall mean of total releases from the PABC-2009 to the PCS-2012 PA due to the changes in direct brine releases calculated in those analyses (Figure 5-35) (Zeitler 2012).

A comparison of the statistics on the overall mean for total normalized releases obtained in the PCS-2012 PA and the PABC-2009 can be seen in Table 5-9. At a probability of 0.1, values obtained for mean total releases has increased from 0.09 to 0.10 for the PCS-2012 PA. At a probability of 0.001, the increase in DBRs seen at that probability in the PCS-2012 PA results in an increase in the mean total release by approximately 0.41 EPA units. An increase is seen in the 95% confidence limit when compared to the PABC-2009 results, while the 90th percentile remains the same.

Table 5-9: PCS-2012 PA and PABC-2009 Statistics on the Overall Mean for Total Normalized Releases in EPA Units at Probabilities of 0.1 and 0.001

Probability	Analysis	Mean Total Release	90th Percentile	Lower 95% CL	Upper 95% CL	Release Limit
0.1	PCS-2012 PA	0.10	0.17	0.10	0.10	1
	PABC-2009	0.09	0.16	0.09	0.10	1
0.001	PCS-2012 PA	1.51	1.00	0.33	2.81	10
	PABC-2009	1.10	1.00	0.37	1.77	10

Information Only

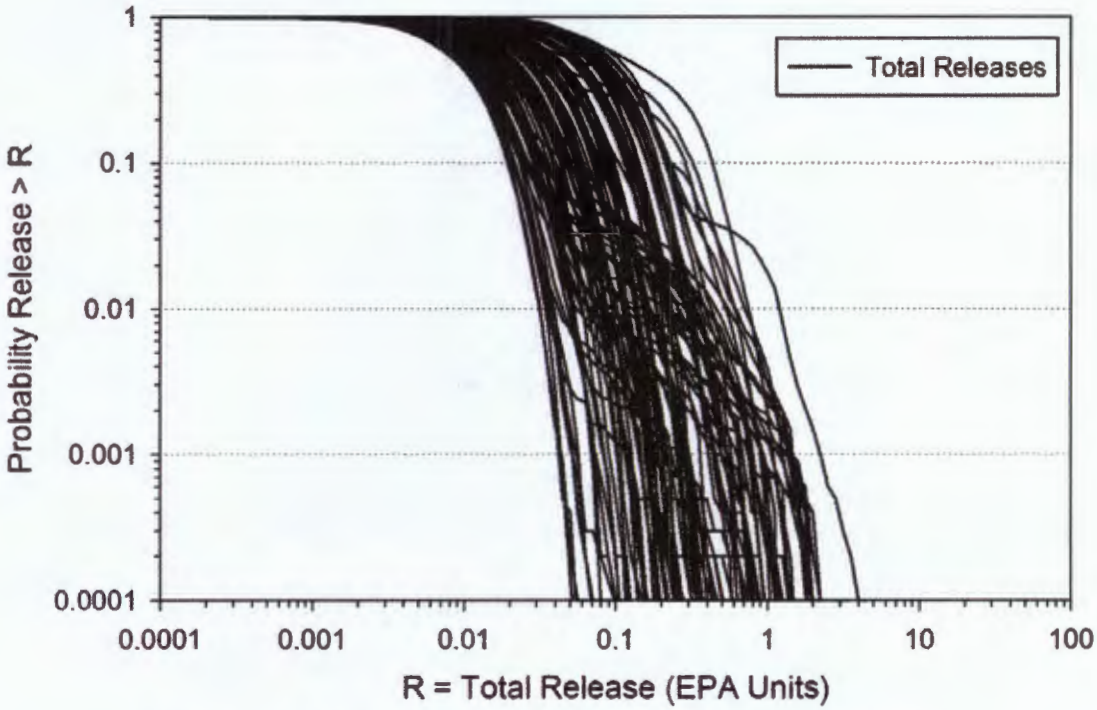

Figure 5-29: PCS-2012 PA Replicate 1 Total Normalized Releases

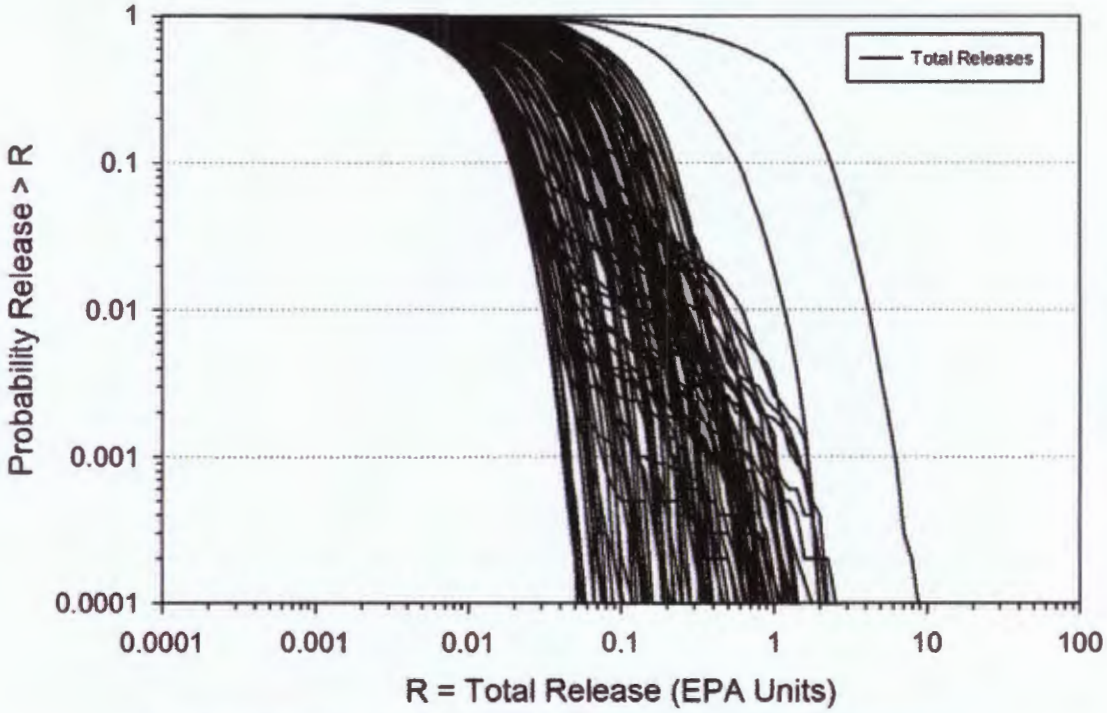

Figure 5-30: PCS-2012 PA Replicate 2 Total Normalized Releases

Information Only

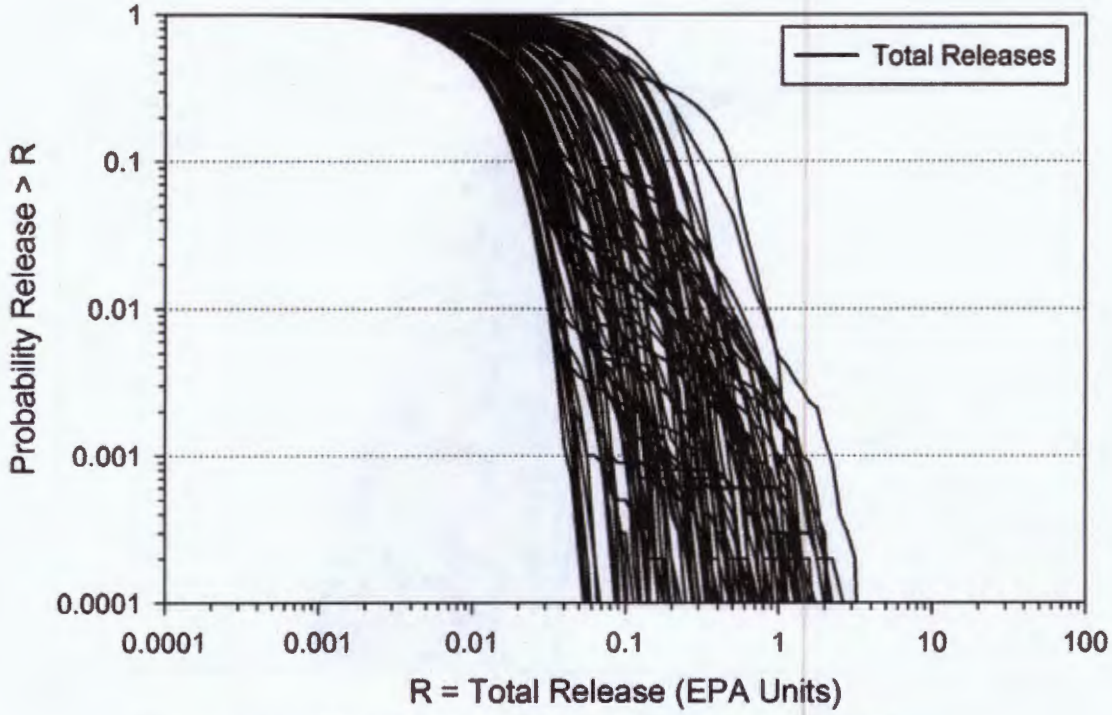

Figure 5-31: PCS-2012 PA Replicate 3 Total Normalized Releases

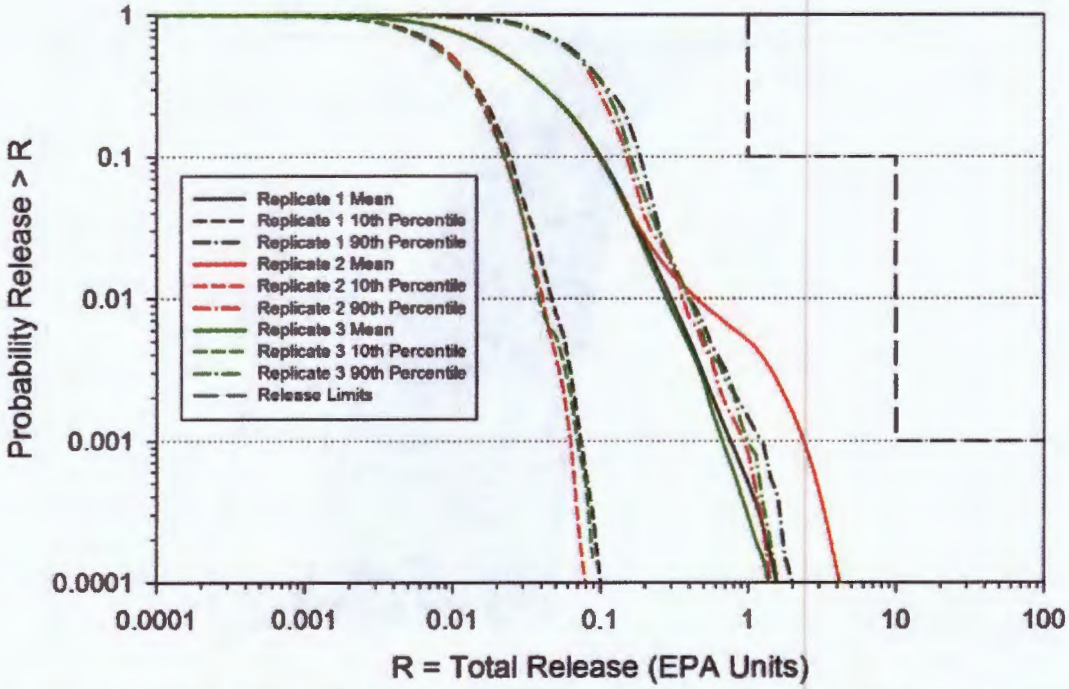

Figure 5-32: PCS-2012 PA Mean and Quantile CCDFs for Total Normalized Releases, Replicates 1-3

Information Only

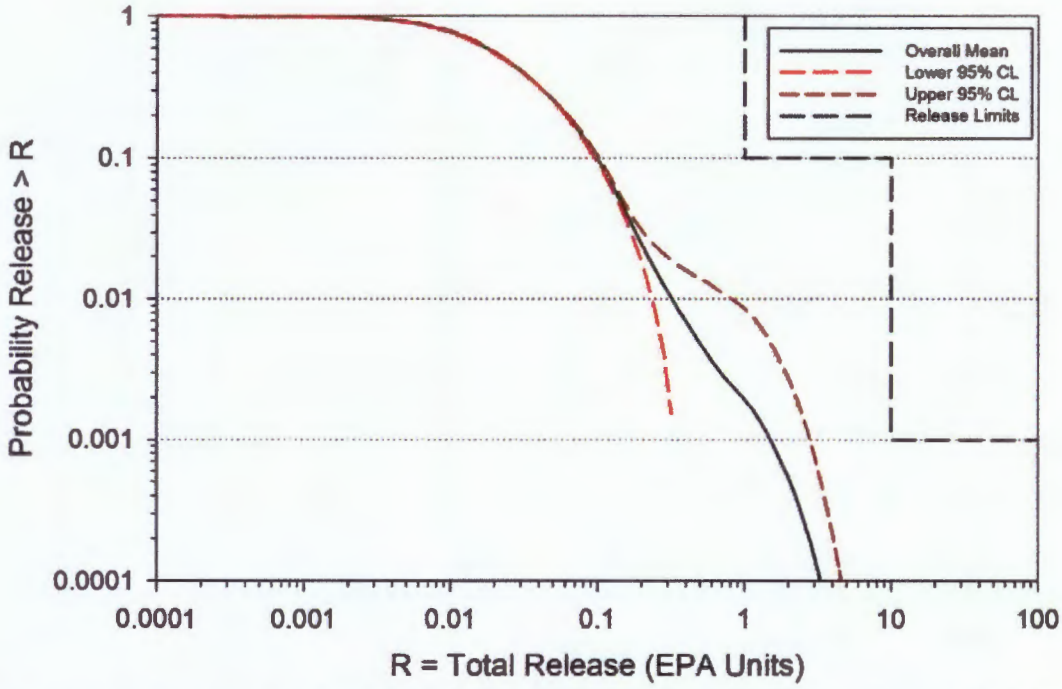

Figure 5-33: PCS-2012 PA Confidence Limits on Overall Mean for Total Normalized Releases

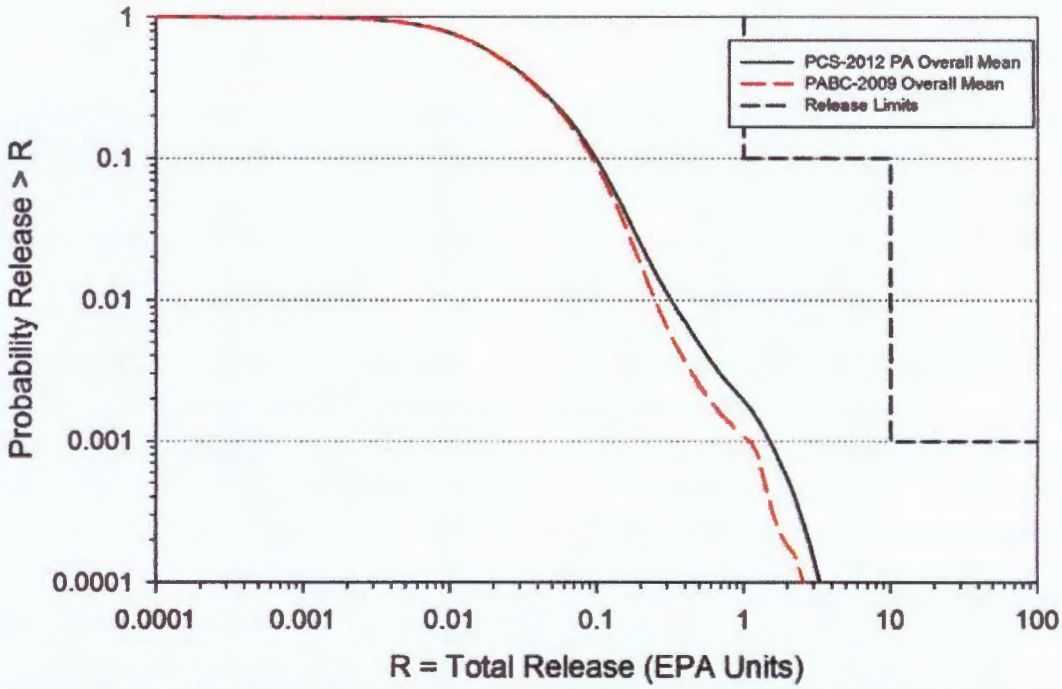

Figure 5-34: PCS-2012 PA and PABC-2009 Overall Mean CCDFs for Total Normalized Releases

Information Only

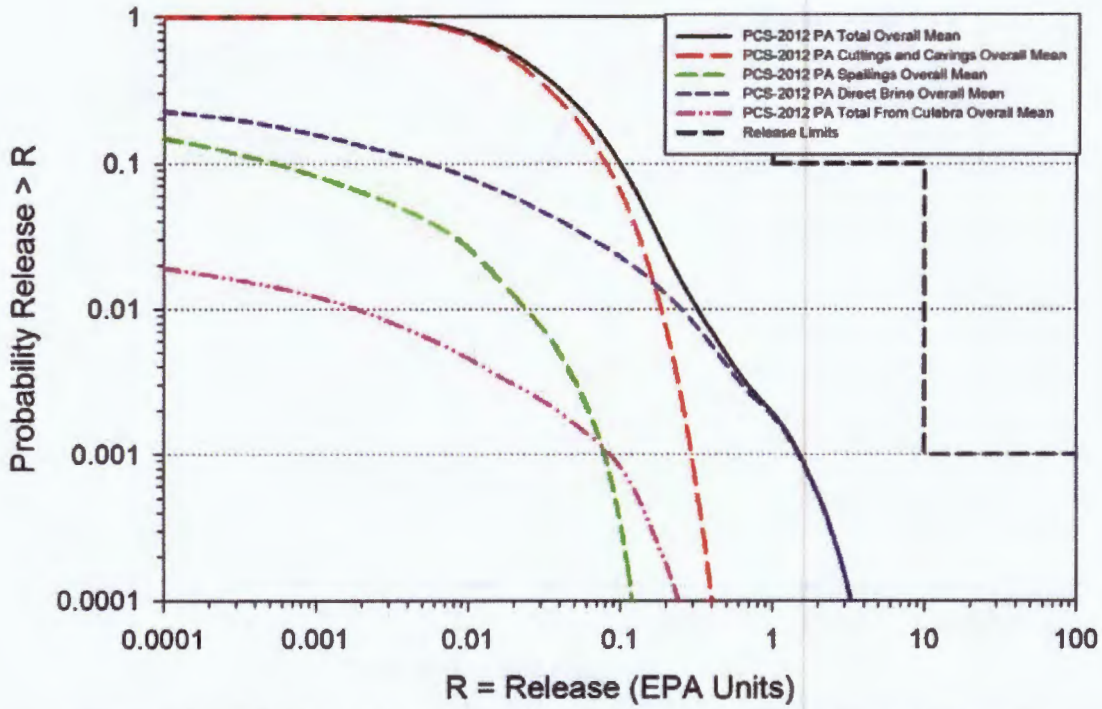

Figure 5-35: PCS-2012 PA Primary Components Contributing to Total Releases

6 SUMMARY

Waste panel closures comprise a repository feature that has been represented in WIPP PA since the original CCA of 1996. The 1998 rulemaking that certified WIPP to receive transuranic waste placed conditions on the panel closure design to be implemented in the repository. The mandated "Option D" design consists of a concrete block wall, an open drift section, and a concrete monolith. The engineering of the panel closure has been re-assessed, and a revised design is proposed that is simpler, cheaper, and easier to construct. The revised panel closure design, termed the ROMPCS, is comprised of 100 feet of ROM salt with barriers at each end. The PCS-2012 PA quantifies WIPP repository performance impacts associated with the replacement of the currently approved Option D panel closure design with the ROMPCS. Impacts are assessed via a direct comparison of results obtained in the PABC-2009 (where Option D was used) to those calculated in the PCS-2012 PA with the ROMPCS.

Total normalized releases calculated in the PCS-2012 PA are greater than those found in the PABC-2009, but continue to remain below their regulatory limits. As a result, replacement of the Option D panel closure with the ROMPCS design would not result in WIPP non-compliance with the containment requirements of 40 CFR Part 191. Cuttings and cavings releases and DBRs were the two primary release components contributing to total releases in the PABC-2009, and

Information Only

continue to be so in the PCS-2012 PA. Cuttings and cavings releases are not impacted by the change in panel closure design, and so remain unchanged from those calculated in the PABC-2009.

For both undisturbed and intruded repository conditions, implementation of the ROMPCS yields higher long-term waste panel pressure (on average) than was seen in the PABC-2009. Pressure increases translate to increases in spallings volumes and their frequency. As a result, increased spallings releases are seen in the PCS-2012 PA results when compared to the PABC-2009. These increases do not have a significant impact on total normalized releases found in the PCS-2012 PA.

Increased DBRs are also seen in the PCS-2012 PA results. DBRs depend on waste panel pressure and brine saturation at the time of intrusion. In addition to increases in waste panel pressure, implementation of the ROMPCS design results in increased mean waste panel brine saturation for undisturbed conditions as well as intrusion scenarios that do not intersect a Castile brine pocket. For intrusion scenarios that intersect a region of pressurized Castile brine, increases in pressure are accompanied by only slight reductions in the mean waste panel brine saturation in the PCS-2012 PA. The combined effect of these impacts is an increase to DBRs in the PCS-2012 PA. The increase in total normalized releases seen in the PCS-2012 PA as compared to the PABC-2009 is primarily due to the increase in DBRs calculated in the PCS-2012 PA.

Information Only

7 REFERENCES

Camphouse, R.C. 2012a. Analysis Plan for the 2012 WIPP Panel Closure System Performance Assessment. Sandia National Laboratories, Carlsbad, NM. ERMS 557726.

Camphouse, R.C. 2012b. A summary of parameters to be implemented in the PCS-2012 PA. Memo to Janis Trone dated July 10, 2012. Sandia National Laboratories, Carlsbad, NM. ERMS 557721.

Camphouse, R.C. 2012c. An overview of the BRAGFLO two-phase flow parameters used to model the run-of-mine salt panel closures implemented in the PCS-2012 PA. Memo to Paul Shoemaker dated June 7, 2012. Sandia National Laboratories, Carlsbad, NM. ERMS 557653.

Camphouse, R.C. 2012d. Analysis Package for Salado Flow Modeling Done in the AP-161 (PCS-2012) Performance Assessment. Sandia National Laboratories, Carlsbad, NM. ERMS 558204.

Camphouse, R.C., Gross, M., Herrick, C.G., Kicker, D.C., and Thompson, B. 2012. Recommendations and Justifications of Parameter Values for the Run-of-Mine Salt Panel Closure System Design Modeled in the PCS-2012 PA. Memo to WIPP Records Center dated May 3, 2012. Sandia National Laboratories, Carlsbad, NM. ERMS 557396.

Chavez, M. J. 2006. Nuclear Waste Management Procedure NP 9-1: Analyses, Revision 6. Sandia National Laboratories. Carlsbad, NM. ERMS 544236.

Clayton, D.C., Camphouse, R.C., Garner, J.W., Ismail, A.E., Kirchner, T.B., Kuhlman, K.L., and Nemer, M.B. 2010. Summary Report of the CRA-2009 Performance Assessment Baseline Calculation, Revision 1. Sandia National Laboratories. Carlsbad, New Mexico, ERMS 553039.

DOE (U.S. Department of Energy). 1996. Title 40 CFR Part 191 Compliance Certification Application for the Waste Isolation Pilot Plant. DOE/CAO-1996-2184. U.S. Department of Energy, Waste Isolation Pilot Plant, Carlsbad Area Office. Carlsbad, NM.

DOE (U.S. Department of Energy), 2011. Panel Closure System Design, Planned Change Request to the EPA 40 CFR Part 194 Certification of the Waste Isolation Pilot Plant. U.S. Department of Energy, Carlsbad Field Office. Carlsbad, New Mexico.

EPA (U.S. Environmental Protection Agency). 1996. 40 CFR Part 194: Criteria for the Certification and Recertification of the Waste Isolation Pilot Plant's Compliance with the 40 CFR Part 191 Disposal Regulations; Final Rule. Federal Register, Vol. 61, 5223-5245.

EPA (U.S. Environmental Protection Agency). 1998. Criteria for the Certification and Re-Certification of the Waste Isolation Pilot Plants Compliance with the 40 CFR Part 191 Disposal Regulations: Certification Decision; Final Rule, *Federal Register*, Vol. 63, No. 95,

Information Only

pp. 27353-27406. U.S. Environmental Protection Agency, Office of Air and Radiation, Washington, D.C.

Ismail, A.E. 2010. Analysis Package for Cuttings, Cavings, and Spallings: CRA-2009 Performance Assessment Baseline Calculation. Carlsbad, NM: Sandia National Laboratories. ERMS 552893.

Kanney, J. F., and Kirchner, T.B. 2005. Verification of the SUMMARIZE Interface in the CRA-2004 Performance Assessment Baseline Calculation. Sandia National Laboratories, Carlsbad, NM. ERMS 540977.

Kicker, D.C. 2012. Analysis Package for Cuttings, Cavings, and Spallings: Panel Closure System Performance Assessment (PCS-2012 PA). Sandia National Laboratories, Carlsbad, NM. ERMS 558300.

Kirchner, T.B. 2012a. Generation of the LHS Samples for the AP-161 (PCS-2012) Revision 0 PA Calculations. Sandia National Laboratories, Carlsbad, NM. ERMS 558129.

Kirchner, T.B. 2012b. Sensitivity of the AP-161 (PCS-2012) PA Releases to Parameters. Sandia National Laboratories, Carlsbad, NM. ERMS 558342.

Kirkes, G.R. 2011. 2011. Features, Events, and Processes Assesssment for Changes Described in Analysis Plan – 151, Revision 0. Sandia National Laboratories, Carlsbad, NM. ERMS 555237.

Long, J.J. 2010. Execution of Performance Assessment Codes for the CRA-2009 Performance Assessment Baseline Calculation, Revision 0. Sandia National Laboratories, Carlsbad, NM. ERMS 552947.

Long, J.J. 2012. Nuclear Waste Management Procedure NP 19-1: Software Requirements, Revision 13. Sandia National Laboratories, Carlsbad, NM. ERMS 557883.

Malama, B. 2012. Analysis Package for Direct Brine Releases: 2012 Panel Closure System Performance Assessment (PCS-2012 PA). Sandia National Laboratories, Carlsbad, NM. ERMS 558226.

Nemer, M.B. 2010. Analysis Package for Salado Flow Modeling: CRA-2009 Performance Assessment Baseline Calculation. Sandia National Laboratories. Carlsbad, NM. ERMS 552956.

Patterson, R. 2012. Response to U.S. EPA Comment Dated June 7, 2012. U.S. Department of Energy, Waste Isolation Pilot Plant, Carlsbad Area Office. Carlsbad, NM.

RockSol Consulting Group, Inc. 2006. Further Assessment of the Short-term Stability of the 12 Foot Explosion Isolation Wall. Report prepared for Washington TRU Solutions, LLC.

Information Only

Stein, J.S. and Zelinski, W. 2003. Analysis Package for BRAGFLO: Compliance Recertification Application. Sandia National Laboratories, Carlsbad, NM. ERMS 530163.

Stein, J. S., Nemer, M. and Trone, J. 2005. Analysis Package for Direct Brine Releases: AP132 PA. Sandia National Laboratories, Carlsbad, NM. ERMS 540633.

WIPP PA. 2005. Design Document for PRECCDFGF Version 1.01. Sandia National Laboratories, Carlsbad, NM. ERMS 539295

Zeitler, T.R. 2012. CCDFGF Analysis Package for the AP-161 (PCS-2012) Performance Assessment. Sandia National Laboratories, Carlsbad, NM. ERMS 558337.

Information Only

APPENDIX A PCS-2012 PA Code Execution

The WIPP PA Alpha Cluster consists of 8 Hewlett Packard (HP) AlphaServer nodes configured to share the same disk array (using Storage Area Network (SAN) technology for efficient disk utilization and data storage/management). This allows for highly distributed processing, while providing for integrated data access. The WIPP PA Alpha Cluster runs the OpenVMS operating system (Version 8.2). The node name and hardware description for the nodes used are provided in Table A-1.

Table A-1: WIPP PA Alpha Cluster Nodes Used in PCS-2012

Node	Hardware Type	# of CPUs	CPU	Operating System
TBB	HP AlphaServer ES47	4	Alpha EV7	Open VMS 8.2
TRS	HP AlphaServer ES47	4	Alpha EV7	Open VMS 8.2
GNR	HP AlphaServer ES47	4	Alpha EV7	Open VMS 8.2
MC5	HP AlphaServer ES47	4	Alpha EV7	Open VMS 8.2
CCR	HP AlphaServer ES45 Model 2	4	Alpha EV68	Open VMS 8.2
TDN	HP AlphaServer ES45 Model 2	4	Alpha EV68	Open VMS 8.2
BTO	HP AlphaServer ES45 Model 2	4	Alpha EV68	Open VMS 8.2
CSN	HP AlphaServer ES45 Model 2	4	Alpha EV68	Open VMS 8.2

A.1 WIPP PA Codes

The major WIPP PA codes used for the AP161 PCS-2012 PA on the Alpha Cluster are shown in Table A-2. The library and class associated with each code on the Content Management System (CMS) are also shown. These codes have been qualified under Nuclear Waste Management Procedure NP 19-1: Software Requirements (Long 2012).

A.1.1 Deviation

AP-161 (Camphouse 2012a) listed PRELHS Version 2.30 and Matset Version 9.10 as codes to be used in the PCS-2012 PA. The versions of these codes as listed in AP-161 are incorrect. PRELHS Version 2.40 and MATSET Version 9.20 were used in the PCS-2012 PA, and are correctly shown in Table A-2. This comprises a deviation from AP-161.

Information Only

Table A-2: WIPP PA VMS Software Used for the AP161 Panel Closure PA

Code	Version	Executable	Build Date	CMS Library	CMS Class
ALGEBRACDB	2.35	ALGEBRACDB_PA96.EXE	31-01-96	LIBALG	PA96
BRAGFLO	6.0	BRAGFLO_QB0600.EXE	12-02-07	LIBBF	QB0600
PREBRAG	8.00	PREBRAG_QA0800.EXE	08-03-07	LIBBF	QA0800
POSTBRAG	4.00A	POSTBRAG_QA0400A.EXE	28-03-07	LIBBF	QA0400A
CCDFGF	5.02	CCDFGF_QB0502.EXE	13-12-04	LIBCCGF	QB0502
PRECCDFGF	1.01	PRECCDFGF_QA0101.EXE	07-07-05	LIBCCGF	QA0101
CUTTINGS_S	6.02	CUTTINGS_S_QA0602.EXE	09-06-05	LIBCUSP	QA0602
GENMESH	6.08	GM_PA96.EXE	31-01-96	LIBGM	PA96
ICSET	2.22	ICSET_PA96.EXE	01-02-96	LIBIC	PA96
LHS	2.42	LHS_QA0242.EXE	18-01-05	LIBLHS	QA0242
PRELHS	2.40	PRELHS_QA0240.EXE	04-01-12	LIBLHS	QA0240
POSTLHS	4.07A	POSTLHS_QA0407A.EXE	25-04-05	LIBLHS	QA0407A
MATSET	9.20	MATSET_QA0920.EXE	04-01-12	LIBMS	QA0920
RELATE	1.43	RELATE_PA96.EXE	06-03-96	LIBREL	PA96
STEPWISE	2.21	STEPWISE_PA96_2.EXE	02-12-96	LIBSTP	PA96
SUMMARIZE	3.01	SUMMARIZE_QB0301.EXE	21-12-05	LIBSUM	QB0301

In addition to the major codes referenced in Table A-2, a utility code was qualified and used under Nuclear Waste Management Procedure NP 9-1: Analyses (Chavez 2006a). The VMS utility code used on the WIPP PA Alpha Cluster is listed in Table A-3, along with references to the storage location and to the appropriate section of this document.

Table A-3: VMS Utility Codes Used in the PCS-2012

Utility	Executable	CMS Library	CMS Class	Section
LHS_EDIT	LHS_EDIT.EXE	LIBCRA09_LHS	LHS_EDIT_V1.0	A.2.1

A.2 Calculation Flow

The following sections describe the calculation flow for the PCS-2012 PA. The code names, code input and output file names and storage locations, scripts used, and script input and output file names and storage locations are covered. The discussion is organized according to the main groups of calculations and the codes that are used to perform them.

A.2.1 Sampling of Uncertain Parameters (LHS)

Sampling of the uncertain parameters used by the various process model codes is performed with the PRELHS and LHS codes. PRELHS reads information about the ranges and distributions of the uncertain parameters from the PAPDB and formats this information for LHS. The LHS code implements the sampling algorithms. LHS is executed once per replicate (there are three replicates).

Information Only

PRELHS and LHS are executed in sequence by the DCL script EVAL_LHS.COM shown in Table A-4. The input and output files for PRELHS and LHS, as well as the input and log files for the script are shown in Table A-5.

Table A-4: Parameter Sampling Run Control Script

Codes	Script	CMS Library	CMS Class
PRELHS, LHS	EVAL_LHS.COM	LIBAP161_EVAL	AP161-0

Table A-5: Parameter Sampling Input and Output Files

	File Names[1]	CMS Library	CMS Class
SCRIPT			
Input	EVAL_LHS_AP161_R*r*.INP	LIBAP161_EVAL	AP161-0
Log	EVAL_LHS_AP161_R*r*.LOG	LIBAP161_LHS	AP161-0
PRELHS			
Input	LHS1_AP161_R*r*.INP	LIBAP161_LHS	AP161-0
Output	LHS1_AP161_R*r*.TRN	LIBAP161_LHS	AP161-0
Output	LHS1_AP161_R*r*.DBG	LIBAP161_LHS	AP161-0
LHS			
Input	LHS1_AP161_R*r*.TRN	LIBAP161_LHS	AP161-0
Output	LHS2_AP161_R*r*.TRN	LIBAP161_LHS	AP161-0
Output	LHS2_AP161_R*r*.DBG	LIBAP161_LHS	AP161-0
LHS Edit			
Input	LHS_CONTROL_R*r*.INP	NOT KEPT	NOT KEPT
Input	LHS2_AP161_R*r*.TRN	LIBAP161_LHS	AP161-0
Output	LHS2_AP161_R*r*_CON.TRN	LIBAP161_LHS	AP161-0

1. $r \in \{1,2,3\}$

A.2.2 Salado Flow Calculations (BRAGFLO)

Brine and gas flow in and around the repository and in overlying formations is calculated using the BRAGFLO suite of codes (PREBRAG, BRAGFLO, and POSTBRAG) in conjunction with several utility codes. The entire set of calculations is performed for three replicates. Each replicate includes six scenarios (S1-BF to S6-BF) designed to cover a range of drilling intrusion types and times, as shown in Table A-6. For each replicate/scenario combination, calculations are performed for 100 vectors of uncertain model input parameters.

Information Only

Table A-6: BRAGFLO Scenarios

BRAGFLO Scenario	Description[1,2]
S1-BF	Undisturbed
S2-BF	E1 intrusion at 350 years
S3-BF	E1 intrusion at 1000 years
S4-BF	E2 intrusion at 350 years
S5-BF	E2 intrusion at 1000 years
S6-BF	E2 intrusion at 1000 years, E1 intrusion at 2000 years

1. E1 intrusion penetrates the repository and intersects a brine pocket in the underlying Castile Formation.
2. E2 intrusion penetrates the repository but does not encounter a Castile brine pocket

The brine and gas flow calculations are divided into several steps. The steps, the codes run in each step, and the DCL script(s) used to perform the step are shown in Table A-7.

Table A-7: Salado Flow Run Control Scripts

Step	Codes in Step	Script(s)	CMS Library	CMS Class
1	GENMESH MATSET	EVAL_GENERIC_STEP1.COM	LIBAP161_EVAL	AP161-0
2	POSTLHS	EVAL_GENERIC_STEP2.COM	LIBAP161_EVAL	AP161-0
3	ICSET ALGEBRACDB	EVAL_BF_STEP3.COM	LIBAP161_EVAL	AP161-0
4	PREBRAG	EVAL_BF_STEP4.COM	LIBAP161_EVAL	AP161-0
5	BRAGFLO POSTBRAG ALGEBRACDB	EVAL_BF_STEP5_MASTER.COM EVAL_BF_STEP5_SLAVE.COM	LIBAP161_EVAL LIBAP161_EVAL	AP161-0 AP161-0

A.2.2.1 Salado Flow Step 1

Step 1 uses GENMESH and MATSET to generate the computational grid and assign material properties to element blocks. Step 1 is run once. The input and log files for the Step 1 script as well as the input and output files for GENMESH and MATSET are shown in Table A-8.

Information Only

Table A-8: Salado Flow Step 1 Input and Output Files

	File Names	CMS Library	CMS Class
SCRIPT			
Input	EVAL_BF_AP161_STEP1.INP	LIBAP161_EVAL	AP161-0
Log	EVAL_BF_AP161_STEP1.LOG	LIBAP161_BF	AP161-0
GENMESH			
Input	GM_BF_AP161.INP	LIBAP161_BF	AP161-0
Output	GM_BF_AP161.CDB	LIBAP161_BF	AP161-0
Output	GM_BF_AP161.DBG	NOT KEPT	NOT KEPT
MATSET			
Input	MS_BF_AP161.INP	LIBAP161_BF	AP161-0
Input	GM_BF_AP161.CDB	LIBAP161_BF	AP161-0
Output	MS_BF_AP161.CDB	LIBAP161_BF	AP161-0
Output	MS_BF_AP161.DBG	NOT KEPT	NOT KEPT

A.2.2.2 Salado Flow Step 2

Step 2 uses POSTLHS to assign the sampled parameter values used by BRAGFLO (generated by LHS) to the appropriate materials and element block properties. Step 2 is run once per replicate. POSTLHS loops over all 100 vectors in the replicate. The input and log files for the Step 2 script as well as the input and output files for POSTLHS are shown in Table A-9.

Table A-9: Salado Flow Step 2 Input and Output Files

	File Names[1,2]	CMS Library	CMS Class
SCRIPT			
Input	EVAL_BF_AP161_STEP2_R*r*.INP	LIBAP161_EVAL	AP161-0
Log	EVAL_BF_AP161_STEP2_R*r*.LOG	LIBAP161_BF	AP161-0
POSTLHS			
Input	LHS3_DUMMY.INP	LIBAP161_LHS	AP161-0
Input	LHS2_AP161_R*r*_CON.TRN	LIBAP161_LHS	AP161-0
Input	MS_BF_AP161.CDB	LIBAP161_BF	AP161-0
Output	LHS3_BF_AP161_R*r*_V*vvv*.CDB	LIBAP161_BF	AP161-0
Output	LHS3_BF_AP161_R*r*.DBG	LIBAP161_BF	AP161-0

1. $r \in \{1, 2, 3\}$
2. $vvv \in \{001, 002, ..., 100\}$ for each r

Information Only

A.2.2.3 Salado Flow Step 3

Step 3 assigns initial conditions with ICSET and performs some pre-processing of input data with ALGEBRACDB. Since ALGEBRACDB is used in multiple BRAGFLO steps, this use is referred to as ALG1. Step 3 is run once for each replicate. The script loops over all 100 vectors in the replicate. The input and log files for the Step 3 script as well as the input and output files for ICSET and ALGEBRACDB are shown in Table A-10.

Table A-10: Salado Flow Step 3 Input and Output Files

	File Names[1,2]	CMS Library	CMS Class
SCRIPT			
Input	EVAL_BF_AP161_STEP3_R*r*.INP	LIBAP161_EVAL	AP161-0
Log	EVAL_BF_AP161_STEP3_R*r*.LOG	LIBAP161_BF	AP161-0
ICSET			
Input	IC_BF_AP161.INP	LIBAP161_BF	AP161-0
Input	LHS3_BF_AP161_R*r*_V*vvv*.CDB	LIBAP161_BF	AP161-0
Output	IC_BF_AP161_R*r*_V*vvv*.CDB	LIBAP161_BF	AP161-0
Output	IC_BF_AP161_R*r*_V*vvv*.DBG	NOT KEPT	NOT KEPT
ALGEBRACDB			
Input	ALG1_BF_AP161.INP	LIBAP161_BF	AP161-0
Input	IC_BF_AP161_R*r*_V*vvv*.CDB	LIBAP161_BF	AP161-0
Output	ALG1_BF_AP161_R*r*_V*vvv*.CDB	LIBAP161_BF	AP161-0
Output	ALG1_BF_AP161_R*r*_V*vvv*.DBG	NOT KEPT	NOT KEPT

1. $r \in \{1, 2, 3\}$
2. $vvv \in \{001, 002, ..., 100\}$ for each r

A.2.2.4 Salado Flow Step 4

Step 4 consists of running the pre-processing code PREBRAG. Step 4 is repeated for each replicate/scenario combination. The script loops over all 100 vectors in the replicate/scenario combination. The input and log files for the Step 4 script as well as the input and output files for PREBRAG are shown in Table A-11.

Information Only

Table A-11: Salado Flow Step 4 Input and Output Files

	File Names[1,2,3]	CMS Library[1,2]	CMS Class
SCRIPT			
Script Input	EVAL_BF_AP161_STEP4_R*r*_S*s*.INP	LIBAP161_EVAL	AP161-0
Script Log	EVAL_BF_AP161_STEP4_R*r*_S*s*.LOG	LIBAP161_BFR*r*S*s*	AP161-0
PREBRAG			
Input	BF1_AP161_S*s*.INP	LIBAP161_BF	AP161-0
Input	ALG1_BF_AP161_R*r*_V*vvv*.CDB	LIBAP161_BF	AP161-0
Output	BF2_AP161_R*r*_S*s*_V*vvv*.INP	LIBAP161_BFR*r*S*s*	AP161-0
Output	BF1_AP161_R*r*_S*s*_V*vvv*.DBG	NOT KEPT	NOT KEPT

1. $r \in \{1, 2, 3\}$
2. $s \in \{1, 2, 3, 4, 5, 6\}$ for each r
3. $vvv \in \{001, 002, ..., 100\}$ for each s

A.2.2.5 Salado Flow Step 5

Step 5 runs BRAGFLO, POSTBRAG, and ALGEBRACDB (ALG2). This step has been separated from Step 4 to allow the analysts to edit/modify the BRAGFLO input file in cases where the generic numerical control parameters are not sufficient to obtain a converged solution.

In the paragraphs that follow, the procedure for the general case is described first and then the procedure followed to re-run certain replicate/scenario/vector combinations that were run with modified BRAGFLO input files due to convergence problems.

General Case

Two DCL run control scripts are used in Step 5. The master script is invoked once for each replicate/scenario combination. The master script loops over all 100 vectors in the replicate/scenario combination. For each vector, the master script writes an input file for the slave script, and then calls the slave script with that input file to run BRAGFLO, POSTBRAG, and ALGEBRACDB. The input and log files for the Step 5 script as well as the input and output files for BRAGFLO, POSTBRAG, and ALGEBRACDB are shown in Table A-12.

Information Only

Table A-12: Salado Flow Step 5 Input and Output Files (Generic Case)

	File Names[1,2,3,4]	CMS Library[1,2]	CMS Class
MASTER SCRIPT			
Input	EVAL_BF_AP161_STEP5_R*r*_S*s*.INP	LIBAP161_EVAL	AP161-0
Log	EVAL_BF_AP161_STEP5_R*r*_S*s*.LOG	LIBAP161_BFR*r*S*s*	AP161-0
SLAVE SCRIPT			
Log[4]	EVAL_BF_AP161_STEP5_R*r*_S*s*_V*vvv*.LOG	LIBAP161_BFR*r*S*s*	AP161-0
BRAGFLO			
Input	BF2_AP161_R*r*_S*s*_V*vvv*.INP	LIBAP161_BFR*r*S*s*	AP161-0
Input	BF2_PABC09_CLOSURE.DAT	LIBPABC09_BF	AP161-0
Output	BF2_AP161_R*r*_S*s*_V*vvv*.OUT	NOT KEPT	NOT KEPT
Output	BF2_AP161_R*r*_S*s*_V*vvv*.SUM	LIBAP161_BFR*r*S*s*	AP161-0
Output	BF2_AP161_R*r*_S*s*_V*vvv*.BIN	NOT KEPT	NOT KEPT
Output	BF2_AP161_R*r*_S*s*_V*vvv*.ROT	NOT KEPT	NOT KEPT
Output	BF2_AP161_R*r*_S*s*_V*vvv*.RIN	NOT KEPT	NOT KEPT
POSTBRAG			
Input	BF2_AP161_R*r*_S*s*_V*vvv*.BIN	NOT KEPT	NOT KEPT
Input	ALG1_BF_AP161_R*r*_V*vvv*.CDB	LIBAP161_BF	AP161-0
Output	BF3_AP161_R*r*_S*s*_V*vvv*.CDB	LIBAP161_BFR*r*S*s*	AP161-0
Output	BF3_AP161_R*r*_S*s*_V*vvv*.DBG	NOT KEPT	NOT KEPT
ALGEBRACDB			
Input	ALG2_BF_AP161.INP	LIBAP161_BF	AP161-0
Input	BF3_AP161_R*r*_S*s*_V*vvv*.CDB	LIBAP161_BFR*r*S*s*	AP161-0
Output	ALG2_BF_AP161_R*r*_S*s*_V*vvv*.CDB	LIBAP161_BFR*r*S*s*	AP161-0
Output	ALG2_BF_AP161_R*r*_S*s*_V*vvv*.DBG	NOT KEPT	NOT KEPT

1. $r \in \{1, 2, 3\}$
2. $s \in \{1, 2, 3, 4, 5, 6\}$ for each r
3. $vvv \in \{001, 002, ..., 100\}$ for each s
4. The script inputs are echoed into the log file, so the input file is not kept

Modified BRAGFLO Input Case

In the few instances when BRAGFLO failed to converge using the generic numerical control parameters, a new BRAGFLO input file was submitted by the analysts and the case was re-run in a manner similar to that described above. In order to track these cases a special tag ("MOD") was inserted into the BRAGFLO input file name, as well as the master script input file and log file names.

The replicate/scenario/vectors requiring modified BRAGFLO input files are shown in Table A-13. In that table, vector numbers with a (*) superscript correspond to vectors where quantity

Information Only

FTOL_SAT was changed from 1e-2 to 1e-1 in the BRAGFLO input file. Vector numbers with a (#) superscript correspond to vectors where quantity FTOL_SAT was changed from 1e-2 to 1e-1 and Convergence Test Flag was changed from 1 to 0 in the BRAGFLO input file. The modified file names are shown in Table A-14. All other files have the same names as for the generic case. Files in the libraries from the un-converged runs were replaced with files from the re-run.

Table A-13: Salado Flow Step 5 Modified Input Runs

Replicate	Scenario	Vectors
R1	S1	29*, 51#
	S2	51#
	S3	51#
	S4	29*, 51#
	S5	51#
	S6	51#
R2	S1	99*
	S4	99*
	S5	99*
R3	S1	35*
	S2	35*
	S3	35*
	S5	35*
	S6	35*

Table A-14: Salado Flow Step 5 Modified Input Runs File Names

	File Names[1,2,3]	CMS Library[1,2]	CMS Class
MASTER SCRIPT			
Input	EVAL_BF_AP161_STEP5_R*r*_S*s*_V*vvv*_MOD.INP	LIBAP161_EVAL	AP161-0
Log	EVAL_BF_AP161_STEP5_R*r*_S*s*_V*vvv*_MOD.LOG	LIBAP161_BFR*r*S*s*	AP161-0
BRAGFLO			
Input	BF2_AP161_R*r*_S*s*_V*vvv*_MOD.INP	LIBAP161_BFR*r*S*s*	AP161-0

1. $r \in \{1, 2, 3\}$ as shown in Table A-13
2. $s \in \{1, 2, 3, 4, 5, 6\}$ as shown in Table A-13
3. vectors as shown in Table A-13

Information Only

A.2.3 Single-Intrusion Solids Volume Calculations (CUTTINGS_S)

The total volume of radionuclide-contaminated solids that may reach the surface during a drilling intrusion event is calculated by the CUTTINGS_S code. The single intrusion solids volume calculations are divided into 3 steps. The codes run in each step, and the DCL script(s) used to perform the steps are shown in Table A-15. Step 3 also includes a small utility used to submit the script to a batch queue.

Table A-15: Solids Volume (CUTTINGS_S) Run Control Scripts

Step	Codes in Step	Scripts	Script CMS Library	Script CMS Class
1	GENMESH MATSET	EVAL_CUSP_STEP1.COM	LIBAP161_EVAL	AP161-0
2	POSTLHS	EVAL_CUSP_STEP2.COM	LIBAP161_EVAL	AP161-0
3	CUTTINGS_S	EVAL_CUSP_STEP3.COM SUB_CUSP_STEP3.COM	LIBAP161_EVAL	AP161-0

Three replicate calculations are performed. Five scenarios, S1-DBR to S5-DBR are included in each replicate. The cuttings calculation extracts volume-averaged brine pressure and brine saturation from Salado flow BRAGFLO results. These extracted quantities are then used downstream in the calculation of direct brine releases. As a result, the intrusion times and locations considered during the cuttings calculation are identical to those used in the DBR calculation. Cuttings scenarios indicate which BRAGFLO scenario provides the input conditions for the simulation (CUTTINGS_S scenario S1-DBR means that CUTTINGS_S uses BRAGFLO scenario S1-BF results as the inputs for the solids release calculations, CUTTINGS_S scenario S2-DBR means that CUTTINGS_S uses BRAGFLO scenario S2-BF results as the inputs for the solids release calculations, etc.). A number of intrusion times are considered for each scenario. For the CUTTINGS_S S1-DBR scenario, these are intrusions into an undisturbed repository. For other scenarios, these intrusions are considered subsequent to the intrusion contained in the BRAGFLO simulation. An intrusion time of 550 years in CUTTINGS_S scenario S2-DBR calculates the volume of solids released by an intrusion 200 years after the E1 intrusion at 350 years modeled in BRAGFLO scenario S2-BF. An intrusion time of 1200 years in CUTTINGS_S scenario S3-DBR calculates the volume of solids released by an intrusion 200 years after the E1 intrusion at 1000 years modeled in BRAGFLO scenario S3-BF.

Three drilling locations (upper, lower and middle) are considered for each replicate/scenario/intrusion time combination. See Stein et al. (2005) for an explanation of the drilling locations. Calculations are performed for a set of 100 uncertain input parameter vectors for each replicate/scenario/intrusion time/intrusion location combination.

Information Only

A.2.3.1 Solids Volume Step 1

Step 1 uses GENMESH and MATSET to generate the computational grid and assign material properties to element blocks. Step1 is run once. The input and log files for the script as well as the input and output files for GENMESH and MATSET are shown in Table A-16.

Table A-16: Solids Volume Step 1 Input and Output Files

	File Names	CMS Library	CMS Class
SCRIPT			
Input	EVAL_CUSP_AP161_STEP1.INP	LIBAP161_EVAL	AP161-0
Log	EVAL_CUSP_AP161_STEP1.LOG	LIBAP161_CUSP	AP161-0
GENMESH			
Input	GM_CUSP_AP161.INP	LIBAP161_CUSP	AP161-0
Output	GM_CUSP_AP161.CDB	LIBAP161_CUSP	AP161-0
Output	GM_CUSP_AP161.DBG	NOT KEPT	NOT KEPT
MATSET			
Input	MS_CUSP_AP161.INP	LIBAP161_CUSP	AP161-0
Input	GM_CUSP_AP161.CDB	LIBAP161_CUSP	AP161-0
Output	MS_CUSP_AP161.CDB	LIBAP161_CUSP	AP161-0
Output	MS_CUSP_AP161.DBG	NOT KEPT	NOT KEPT

Information Only

A.2.3.2 Solids Volume Step 2

Step 2 uses POSTLHS to assign the sampled parameter values (generated by LHS) used by CUTTINGS_S to the appropriate materials and element block properties. Step 2 is run once per replicate. POSTLHS loops over all 100 vectors in the replicate. The input and log files for the script as well as the input and output files for POSTLHS are shown in Table A-17.

Table A-17: Solids Volume Step 2 Input and Output Files

	File Names[1,2]	CMS Library	CMS Class
SCRIPT			
Script Input	EVAL_CUSP_AP161_STEP2_R*r*.INP	LIBAP161_EVAL	AP161-0
Script Log	EVAL_CUSP_AP161_STEP2_R*r*.LOG	LIBAP161_CUSP	AP161-0
POSTLHS			
Input	LHS3_DUMMY.INP	LIBAP161_LHS	AP161-0
Input	LHS2_AP161_R*r*_CON.TRN	LIBAP161_LHS	AP161-0
Input	MS_CUSP_AP161.CDB	LIBAP161_CUSP	AP161-0
Output	LHS3_CUSP_AP161_R*r*_V*vvv*.CDB	LIBAP161_CUSP	AP161-0
Output	LHS3_CUSP_AP161_R*r*.DBG	LIBAP161_CUSP	AP161-0

1. $r \in \{1, 2, 3\}$
2. $vvv \in \{001, 002, ..., 100\}$ for each r

A.2.3.3 Solids Volume Step 3

Step 3 runs the CUTTINGS_S code, and is invoked for each replicate. The script generates the CUTTINGS_S master input control file. The CUTTINGS_S code itself loops over scenarios, intrusion times, intrusion locations, and vectors. The input and log files for the Step 3 script as well as the input and output files for CUTTINGS_S are shown in Table A-18.

Information Only

Table A-18: Solids Volume Step 3 Input and Output Files

	File Names[1,2,3,4,5]	CMS Library[1,2]	CMS Class
SCRIPT			
Input	EVAL_CUSP_AP161_STEP3_R*r*.INP	LIBAP161_EVAL	AP161-0
Output	CUSP_AP161_MASTER_R*r*.INP	LIBAP161_CUSP	AP161-0
Log	EVAL_CUSP_AP161_STEP3_R*r*.LOG	LIBAP161_CUSP	AP161-0
CUTTINGS_S			
Input	CUSP_AP161_MASTER_R*r*.INP	LIBAP161_CUSP	AP161-0
Input	CUSP_AP161.INP	LIBAP161_CUSP	AP161-0
Input	LHS3_CUSP_AP161_R*r*_V*vvv*.CDB	LIBAP161_CUSP	AP161-0
Input	BF3_AP161_R*r*_S*s*_V*vvv*.CDB	LIBAP161_BFR*r*S*s*	AP161-0
Input	MSPALL_DRS_CRA1BC_R*r*.OUT	LIBCRA1BC_DRS	AP161-0
Output	CUSP_AP161_R*r*.TBL	LIBAP161_CUSP	AP161-0
Output	CUSP_AP161_R*r*_S*s*_T*ttttt*_*c*_V*vvv*.CDB	LIBAP161_CUSPR*r*S*s*	AP161-0
Output	CUSP_AP161_R*r*.DBG	LIBAP161_CUSP	AP161-0

1. $r \in \{1, 2, 3\}$
2. $s \in \{1, 2, 3, 4, 5\}$ for each r
3. $ttttt \in \begin{cases} \{100,350,1000,3000,5000,10000\} & \text{for S1} \\ \{550,750,2000,4000,10000\} & \text{for S2, S4} \\ \{1200,1400,3000,5000,10000\} & \text{for S3, S5} \end{cases}$
4. $c \in \{L, U, M\}$ for each intrusion time
5. $vvv \in \{001, 002, ..., 100\}$ for each c

A.2.4 Single-Intrusion Direct Brine Release Calculations (BRAGFLO_DBR)

Single-intrusion direct brine release volumes are calculated using the BRAGFLO suite of codes (PREBRAG, BRAGFLO, POSTBRAG), in conjunction with several utility codes. The steps, the codes run in each step, and the DCL script(s) used to perform the step are shown in Table A-19.

Three replicates are performed. Each replicate includes five scenarios (S1-DBR to S5-DBR). The scenario designations for the direct brine release calculations have the same meanings as those for the direct solids volume calculations. A number of intrusion times are considered for each scenario. For each intrusion time, intrusions into three locations (lower L, middle M and upper U) are modeled. See Stein et al. (2005) for a detailed discussion of the drilling locations. A set of 100 vectors is run for each replicate/scenario/intrusion time/intrusion location combination.

Information Only

Table A-19: Direct Brine Release Run Control Scripts

Step	Codes in Step	Script(s)	Script CMS Library	Script CMS Class
1	GENMESH MATSET	EVAL_DBR_STEP1.COM	LIBAP161_EVAL	AP161-0
2	ALGEBRACDB RELATE ICSET	EVAL_DBR_STEP2.COM SUB_DBR_STEP2.COM	LIBAP161_EVAL	AP161-0
3	PREBRAG BRAGFLO POSTBRAG ALGEBRACDB	EVAL_DBR_STEP3.COM SUB_DBR_STEP3.COM	LIBAP161_EVAL	AP161-0

A.2.4.1 Direct Brine Release Step 1

Step 1 uses GENMESH and MATSET to generate the computational grid and assign material properties to element blocks. Step 1 is run once. The input and log files for the script as well as the input and output files for GENMESH and MATSET are shown in Table A-20.

Table A-20: Direct Brine Release Step 1 Input and Output Files

	File Names	CMS Library	CMS Class
SCRIPT			
Input	EVAL_DBR_AP161_STEP1.INP	LIBAP161_EVAL	AP161-0
Log	EVAL_DBR_AP161_STEP1.LOG	LIBAP161_DBR	AP161-0
GENMESH			
Input	GM_DBR_AP161.INP	LIBAP161_DBR	AP161-0
Output	GM_DBR_AP161.CDB	LIBAP161_DBR	AP161-0
Output	GM_DBR_AP161.DBG	NOT KEPT	NOT KEPT
MATSET			
Input	MS_DBR_AP161.INP	LIBAP161_DBR	AP161-0
Input	GM_DBR_AP161.CDB	LIBAP161_DBR	AP161-0
Output	MS_DBR_AP161.CDB	LIBAP161_DBR	AP161-0
Output	MS_DBR_AP161.DBG	NOT KEPT	NOT KEPT

A.2.4.2 Direct Brine Release Step 2

Step 2 performs pre-processing of input data with ALGEBRACDB. ALGEBRACDB is run twice (ALG1 and ALG2). The RELATE code is used to assign material properties to element blocks. RELATE is run twice (RELATE_1 and RELATE_2). Finally, ICSET is used to assign initial conditions. The Step 2 script is run for each replicate/scenario combination. The script loops over the appropriate intrusion times for the scenario. For each intrusion time, the script loops over all 100 vectors. The input and log files for the Step 2 script as well as the input and output files for ALGEBRACDB, RELATE, and ICSET are shown in Table A-21.

Information Only

Table A-21: Direct Brine Release Step 2 Input and Output Files

	File Names[1,2,3,4]	CMS Library[1,2]	CMS Class
SCRIPT			
Input	EVAL_DBR_AP161_STEP2_R*r*_S*s*.INP	LIBAP161_EVAL	AP161-0
Log	EVAL_DBR_AP161_STEP2_R*r*_S*s*.LOG	LIBAP161_DBRR*r*S*s*	AP161-0
ALGEBRACDB			
Input	ALG1_DBR_AP161.INP	LIBAP161_DBR	AP161-0
Input	CUSP_AP161_R*r*_S*s*_T*ttttt*_L_V*vvv*.CDB[5]	LIBAP161_CUSPR*r*S*s*	AP161-0
Output	ALG1_DBR_AP161_R*r*_S*s*_T*ttttt*_V*vvv*.CDB	LIBAP161_DBRR*r*S*s*	AP161-0
Output	ALG1_DBR_AP161_R*r*_S*s*_T*ttttt*_V*vvv*.DBG	NOT KEPT	NOT KEPT
RELATE_1			
Input	REL1_DBR_AP161.INP	LIBAP161_DBR	AP161-0
Input	MS_DBR_AP161.CDB	LIBAP161_DBR	AP161-0
Input	ALG1_DBR_AP161_R*r*_S*s*_T*ttttt*_V*vvv*.CDB	LIBAP161_DBRR*r*S*s*	AP161-0
Output	REL1_DBR_AP161_R*r*_S*s*_T*ttttt*_V*vvv*.CDB	LIBAP161_DBRR*r*S*s*	AP161-0
Output	REL1_DBR_AP161_R*r*_S*s*_T*ttttt*_V*vvv*.DBG	NOT KEPT	NOT KEPT
RELATE_2			
Input	REL2_DBR_AP161_S*s*.INP	LIBAP161_DBR	AP161-0
Input	REL1_DBR_AP161_R*r*_S*s*_T*ttttt*_V*vvv*.CDB	LIBAP161_DBRR*r*S*s*	AP161-0
Input	BF3_AP161_R*r*_S*s*_V*vvv*.CDB	LIBAP161_BFR*r*S*s*	AP161-0
Output	REL2_DBR_AP161_R*r*_S*s*_T*ttttt*_V*vvv*.CDB	LIBAP161_DBRR*r*S*s*	AP161-0
Output	REL2_DBR_AP161_R*r*_S*s*_T*ttttt*_V*vvv*.DBG	NOT KEPT	NOT KEPT
ICSET			
Input	IC_DBR_AP161_S*s*.INP	LIBAP161_DBR	AP161-0
Input	REL2_DBR_AP161_R*r*_S*s*_T*ttttt*_V*vvv*.CDB	LIBAP161_DBRR*r*S*s*	AP161-0
Output	IC_DBR_AP161_R*r*_S*s*_T*ttttt*_V*vvv*.CDB	LIBAP161_DBRR*r*S*s*	AP161-0
Output	IC_DBR_AP161_R*r*_S*s*_T*ttttt*_V*vvv*.DBG	NOT KEPT	NOT KEPT
ALGEBRACDB			
Input	ALG2_DBR_AP161_S*s*.INP	LIBAP161_DBR	AP161-0
Input	IC_DBR_AP161_R*r*_S*s*_T*ttttt*_V*vvv*.CDB	LIBAP161_DBRR*r*S*s*	AP161-0
Output	ALG2_DBR_AP161_R*r*_S*s*_T*ttttt*_V*vvv*.CDB	LIBAP161_DBRR*r*S*s*	AP161-0
Output	ALG2_DBR_AP161_R*r*_S*s*_T*ttttt*_V*vvv*.DBG	NOT KEPT	NOT KEPT

1. $r \in \{1, 2, 3\}$
2. $s \in \{1, 2, 3, 4, 5\}$ for each r
3. $ttttt \in \begin{cases} \{00100, 00350, 01000, 03000, 05000, 10000\} & \text{for S1} \\ \{00550, 00750, 02000, 04000, 10000\} & \text{for S2, S4} \\ \{01200, 01400, 03000, 05000, 10000\} & \text{for S3, S5} \end{cases}$
4. $vvv \in \{001, 002, ..., 100\}$ for each intrusion
5. The files CUSP_AP161_R*r*_S*s*_T*ttttt*_L_V*vvv*.CDB do not have leading zeros in front of the intrusion time *ttttt*.

Information Only

A.2.4.3 Direct Brine Release Step 3

Step 3 runs PREBRAG, BRAGFLO, POSTBRAG, and ALGEBRACDB (ALG3). The Step 3 script is invoked for each replicate/scenario combination. The script loops over the appropriate intrusion times for the scenario. For each intrusion time, the script loops over all three intrusion locations. For each intrusion location, the script loops over all 100 vectors. The PREBRAG, BRAGFLO, POSTBRAG, ALGEBRACDB sequence is run for each replicate/scenario/intrusion time/intrusion location/vector combination. The input and log files for the Step 3 script as well as the input and output files for PREBRAG, BRAGFLO, POSTBRAG, ALGEBRACDB are shown in Table A-22.

Table A-22: Direct Brine Release Step 3 Input and Output Files

	File Names[1,2,3,4,5,6]	CMS Library[1,2]	CMS Class
SCRIPT			
Input	EVAL_DBR_AP161_STEP3_R*r*_S*s*.INP	LIBAP161_EVAL	AP161-0
Input	EVAL_DBR_AP161_STEP3_R1_S1_T100.INP[6]	LIBAP161_EVAL	AP161-0
Log	EVAL_DBR_AP161_STEP3_R*r*_S*s*.LOG	LIBAP161_DBRR*r*S*s*	AP161-0
PREBRAG			
Input	BF1_DBR_AP161_*c*.INP	LIBAP161_DBR	AP161-0
Input	BF1_DBR_AP161_S1_100_*c*.INP[6]	LIBAP161_DBR	AP161-0
Input	ALG2_DBR_AP161_R*r*_S*s*_T*ttttt*_V*vvv*.CDB	LIBAP161_DBRR*r*S*s*	AP161-0
Output	BF2_DBR_AP161_R*r*_S*s*_T*ttttt*_*c*_V*vvv*.INP	LIBAP161_DBRR*r*S*s*	AP161-0
Output	BF1_DBR_AP161_R*r*_S*s*_T*ttttt*_*c*_V*vvv*.DBG	NOT KEPT	NOT KEPT
BRAGFLO			
Input	BF2_DBR_AP161_R*r*_S*s*_T*ttttt*_*c*_V*vvv*.INP	LIBAP161_DBRR*r*S*s*	AP161-0
Output	BF2_DBR_AP161_R*r*_S*s*_T*ttttt*_*c*_V*vvv*.OUT	NOT KEPT	NOT KEPT
Output	BF2_DBR_AP161_R*r*_S*s*_T*ttttt*_*c*_V*vvv*.SUM	NOT KEPT	NOT KEPT
Output	BF2_DBR_AP161_R*r*_S*s*_T*ttttt*_*c*_V*vvv*.BIN	NOT KEPT	NOT KEPT
Output	BF2_DBR_AP161_R*r*_S*s*_T*ttttt*_*c*_V*vvv*.ROT	NOT KEPT	NOT KEPT
Output	BF2_DBR_AP161_R*r*_S*s*_T*ttttt*_*c*_V*vvv*.RIN	NOT KEPT	NOT KEPT
POSTBRAG			
Input	ALG2_DBR_AP161_R*r*_S*s*_T*ttttt*_V*vvv*.CDB	LIBAP161_DBRR*r*S*s*	AP161-0
Input	BF2_DBR_AP161_R*r*_S*s*_T*ttttt*_*c*_V*vvv*.BIN	NOT KEPT	NOT KEPT
Output	BF3_DBR_AP161_R*r*_S*s*_T*ttttt*_*c*_V*vvv*.CDB	LIBAP161_DBRR*r*S*s*	AP161-0
Output	BF3_DBR_AP161_R*r*_S*s*_T*ttttt*_*c*_V*vvv*.DBG	NOT KEPT	NOT KEPT
ALGEBRACDB			
Input	ALG3_DBR_AP161.INP	LIBAP161_DBR	AP161-0
Input	BF3_DBR_AP161_R*r*_S*s*_T*ttttt*_*c*_V*vvv*.CDB	LIBAP161_DBRR*r*S*s*	AP161-0
Output	ALG3_DBR_AP161_R*r*_S*s*_T*ttttt*_*c*_V*vvv*.CDB	LIBAP161_DBRR*r*S*s*	AP161-0
Output	ALG3_DBR_AP161_R*r*_S*s*_T*ttttt*_*c*_V*vvv*.DBG	NOT KEPT	NOT KEPT

Information Only

1. $r \in \{1, 2, 3\}$
2. $s \in \{1, 2, 3, 4, 5\}$ for each r
3. $ttttt \in \begin{cases} \{00100, 00350, 01000, 03000, 05000, 10000\} & \text{for S1} \\ \{00550, 00750, 02000, 04000, 10000\} & \text{for S2, S4} \\ \{01200, 01400, 03000, 05000, 10000\} & \text{for S3, S5} \end{cases}$
4. $c \in \{L, M, U\}$ for each intrusion
5. $vvv \in \{001, 002, ..., 100\}$ for each c
6. Files used for R1_S1_T00100 only.

A.2.5 CCDF Input Tabulation (SUMMARIZE)

The output CDB files from the various process model codes are combined into text tables by the SUMMARIZE code, for subsequent use in calculating releases to the accessible environment. The type of data extracted from each process model is described in the PRECCDFGF Design Document (WIPP PA 2005) and in Kanney and Kirchner (2005). The run control scripts used to process the CDB data for the various process models are shown in Table A-23. A single run control script is used to extract data from CDB files for all process model codes. The script performs the following steps:

- Fetch the required CDB files
- Write an input control file for SUMMARIZE by filling in items in an input control file template
- Run SUMMARIZE on the collection of CDB files

A small utility script is used to submit the main script to a batch queue.

Table A-23: CCDF Input Tabulation Run Control Scripts

Code	Script	Script CMS Library	Script CMS Class
SUMMARIZE	EVAL_SUM.COM SUB_SUM.COM	LIBAP161_EVAL	AP161-0

A.2.5.1 CCDF Input Tabulation for Direct Brine Release

SUMMARIZE is used to extract and tabulate brine release volume data from the appropriate post-BRAGFLO_DBR ALGEBRACDB output CDB files. The run control script is invoked for scenarios S1-DBR through S5-DBR for each replicate. The script loops over the appropriate intrusion times for each scenario. There is a single SUMMARIZE input control file template, which the script uses to generate a SUMMARIZE input control file for each replicate/scenario/intrusion time/intrusion location combination. The script input and log files along with the SUMMARIZE input and output files are shown in Table A-24.

Information Only

Table A-24: CCDF Input Tabulation Input and Output Files (Direct Brine Release)

	File Names[1,2,3,4,5]	CMS Library[1,2]	CMS Class
SCRIPT			
Input	EVAL_SUM_DBR_AP161_R*r*_S*s*.INP	LIBAP161_EVAL	AP161-0
Input	SUM_DBR_AP161.TMPL	LIBAP161_SUM	AP161-0
Output	SUM_DBR_AP161_R*r*_S*s*_T*ttttt*_*c*.INP	LIBAP161_SUM	AP161-0
Log	EVAL_SUM_DBR_AP161_R*r*_S*s*.LOG	LIBAP161_SUM	AP161-0
SUMMARIZE			
Input	SUM_DBR_AP161_R*r*_S*s*_T*ttttt*_*c*.INP	LIBAP161_SUM	AP161-0
Input	ALG3_DBR_AP161_R*r*_S*s*_T*ttttt*_*c*_V*vvv*.CDB	LIBAP161_DBRR*r*S*s*	AP161-0
Output	SUM_DBR_AP161_R*r*_S*s*_Tttttt_*c*.TBL	LIBAP161_SUM	AP161-0
Output	SUM_DBR_AP161_R*r*_S*s*_Tttttt_*c*.DBG	NOT KEPT	NOT KEPT

1. $r \in \{1, 2, 3\}$
2. $s \in \{1, 2, 3, 4, 5\}$ for each r
3. $ttttt \in \begin{cases} \{00100, 00350, 01000, 03000, 05000, 10000\} & \text{for S1} \\ \{00550, 00750, 02000, 04000, 10000\} & \text{for S2 and S4} \\ \{01200, 01400, 03000, 05000, 10000\} & \text{for S3 and S5} \end{cases}$
4. $c \in \{L, M, U\}$ for each intrusion time
5. $vvv \in \{001, 002, ..., 100\}$ for each c

A.2.6 CCDF Construction (PRECCDFGF, CCDFGF)

The complimentary cumulative distribution functions (CCDFs) for radionuclide releases to the accessible environment are constructed using the PRECCDFGF/CCDFGF code suite. The calculations are separated into several steps according to the number of times a particular code is run and to allow for timely inspection of intermediate results. The steps, the codes run in each step, and the DCL script(s) used to perform the steps are shown in Table A-25.

Table A-25: CCDF Construction Run Control Scripts

Step	Codes in Step	Scripts	CMS Library	CMS Class
1	GENMESH MATSET	EVAL_CCGF_STEP1.COM	LIBAP161_EVAL	AP161-0
2	POSTLHS	EVAL_CCGF_STEP2.COM	LIBAP161_EVAL	AP161-0
3	PRECCDFGF CCDFGF	EVAL_CCGF_STEP3.COM SUB_CCGF_STEP3.COM	LIBAP161_EVAL	AP161-0

Information Only

A.2.6.1 CCDF Construction Step 1

Step 1 uses GENMESH and MATSET to generate the computational grid and assign material properties to element blocks. Step 1 is run once. The input and log files for the script as well as the input and output files for GENMESH and MATSET and are shown in Table A-26.

Table A-26: CCDF Construction Step 1 Input and Output Files

	File Names	CMS Library	CMS Class
SCRIPT			
Script Input	EVAL_CCGF_AP161_STEP1.INP	LIBAP161_EVAL	AP161-0
Script Log	EVAL_CCGF_AP161_STEP1.LOG	LIBAP161_CCGF	AP161-0
GENMESH			
Input	GM_CCGF_AP161.INP	LIBAP161_CCGF	AP161-0
Output	GM_CCGF_AP161.CDB	LIBAP161_CCGF	AP161-0
Output	GM_CCGF_AP161.DBG	NOT KEPT	NOT KEPT
MATSET			
Input	MS_CCGF_AP161.INP	LIBAP161_CCGF	AP161-0
Input	GM_CCGF_AP161.CDB	LIBAP161_CCGF	AP161-0
Output	MS_CCGF_AP161.CDB	LIBAP161_CCGF	AP161-0
Output	MS_CCGF_AP161.DBG	NOT KEPT	NOT KEPT

A.2.6.2 CCDF Construction Step 2

Step 2 uses POSTLHS to assign the sampled parameter values (generated by LHS) used by CCDFGF to the appropriate materials and element block properties. Step 2 is run once per replicate. POSTLHS loops over all 100 vectors in the replicate. The input and log files for the script as well as the input and output files for POSTLHS are shown in Table A-27.

Information Only

Table A-27: CCDF Construction Step 2 Input and Output Files

	File Names[1,2]	CMS Library	CMS Class
STEP 2			
Script Input	EVAL_CCGF_AP161_STEP2_R*r*.INP	LIBAP161_EVAL	AP161-0
Script Log	EVAL_CCGF_AP161_STEP2_R*r*.LOG	LIBAP161_CCGF	AP161-0
POSTLHS			
Input	LHS3_DUMMY.INP	LIBAP161_LHS	AP161-0
Input	LHS2_AP161_R*r*_CON.TRN	LIBAP161_LHS	AP161-0
Input	MS_CCGF_AP161.CDB	LIBAP161_CCGF	AP161-0
Output	LHS3_CCGF_AP161_R*r*_V*vvv*.CDB	LIBAP161_CCGF	AP161-0
Output	LHS3_CCGF_AP161_R*r*.DBG	LIBAP161_CCGF	AP161-0

1. $r \in \{1, 2, 3\}$
2. $vvv \in \{001, 002, ..., 100\}$ for each r

A.2.6.3 CCDF Construction Step 3

Step 3 uses PRECCDFGF to organize and format output from all of the process model codes for use by CCDFGF (i.e. builds the release table file), then runs CCDFGF to compute the CCDFs. Step 3 is run once per replicate. The script loops over the appropriate scenarios and/or intrusions and/or waste types to fetch the large number of data files that are input to PRECCDFGF. The input and log files for the script as well as the input and output files for PRECCDFGF are shown in Table A-28.

Information Only

Table A-28: CCDF Construction Step 3 Input and Output Files

	File Names[1-7]	CMS Library	CMS Class
SCRIPT			
Script Input	EVAL_CCGF_STEP3_AP161_R*r*.INP	LIBAP161_EVAL	AP161-0
Script Log	EVAL_CCGF_STEP3_AP161_R*r*.LOG	LIBAP161_CCGF	AP161-0
PRECCDFGF			
Input	INTRUSIONTIMES.IN	LIBAP161_CCGF	AP161-0
Input	MS_CCGF_AP161.CDB	LIBAP161_CCGF	AP161-0
Input	LHS3_CCGF_AP161_R*r*_V*vvv*.CDB	LIBAP161_CCGF	AP161-0
Input	SUM_DBR_AP161_R*r*_S*s*_T*ttttt*_*c*.TBL	LIBAP161_SUM	AP161-0
Input	CUSP_AP161_R*r*.TBL	LIBAP161_CUSP	AP161-0
Input	SUM_NUT_PABC09_R*r*_S1.TBL	LIBPABC09_SUM	AP161-0
Input	SUM_NUT_PABC09_R*r*_S*s*_T*ttttt*.TBL	LIBPABC09_SUM	AP161-0
Input	SUM_PANEL_INT_PABC09_R*r*_S6_T*ttttt*.TBL	LIBPABC09_SUM	AP161-0
Input	SUM_ST2D_PABC09_R*r*_M*m*.TBL	LIBPABC09_SUM	AP161-0
Input	EPU_PABC09_*h*H.DAT	LIBPABC09_EPU	AP161-0
Input	SUM_PANEL_CON_PABC09_R*r*_S*s*.TBL	LIBPABC09_SUM	AP161-0
Input	SUM_PANEL_ST_PABC09_R*r*_S*s*.TBL	LIBPABC09_SUM	AP161-0
Output	CCGF_AP161_RELTAB_R*r*.DAT	LIBAP161_CCGF	AP161-0
CCDFGF			
Input	CCGF_AP161_CONTROL_R*r*.INP	LIBAP161_CCGF	AP161-0
Input	CCGF_AP161_RELTAB_R*r*.DAT	LIBAP161_CCGF	AP161-0
Output	CCGF_AP161_R*r*.OUT	LIBAP161_CCGF	AP161-0
Output	CCGF_AP161_R*r*.DBG	NOT KEPT	NOT KEPT

1. $r \in \{1, 2, 3\}$
2. $vvv \in \{001, 002, ..., 100\}$ for each r
3. $s \in \begin{cases} \{1, 2, 3, 4, 5\} \text{ for SUM_DBR} \\ \{2, 3, 4, 5\} \text{ for SUM_NUT} \\ \{1, 2\} \text{ for SUM_PANEL_CON and SUM_PANEL_ST} \end{cases}$
4. $ttttt \in \begin{cases} \{00100, 00350, 01000, 03000, 05000, 10000\} \text{ for S1 for each } r \text{ for SUM_DBR} \\ \{00550, 07500, 02000, 04000, 10000\} \text{ for S2, S4 for each } r \text{ for SUM_DBR} \\ \{01200, 01400, 03000, 05000, 10000\} \text{ for S3, S5 for each } r \text{ for SUM_DBR} \\ \{00100, 00350\} \text{ for S2, S4 for each } r \text{ for SUM_NUT} \\ \{01000, 03000, 05000, 07000, 09000\} \text{ for S3, S5 each } r \text{ for SUM_NUT} \\ \{00100, 00350, 01000, 02000, 04000, 06000, 09000\} \text{ for each } r \text{ for SUM_PANEL_INT} \end{cases}$
5. $c \in \{L, M, U\}$ for each intrusion for SUM_DBR
6. $m \in \{F, P\}$
7. $h \in \{C, H\}$

Information Only

A.2.7 Sensitivity Analysis (STEPWISE)

A global sensitivity analysis was conducted on the results from CCDFGF using the linear regression code STEPWISE. STEPWISE is executed twice per replicate once for ranked data (RANK) and once for raw data (RAW). The run control script is shown in Table A-29. The input and output files for STEPWISE, as well as the input and log files for the script are shown in Table A-30.

Table A-29: Sensitivity Analysis Run Control Scripts

Code	Script	Script CMS Library	Script CMS Class
STEPWISE	EVAL_STP.COM	LIBAP161_EVAL	AP161-0

Table A-30: Sensitivity Analysis Input and Output Files

	File Names[1,2]	CMS Library	CMS Class
SCRIPT			
Input	EVAL_STP_AP161_*_ALL_R*r*.INP	LIBAP161_EVAL	AP161-0
Log	EVAL_STP_AP161_*_ALL_R*r*.LOG	LIBAP161_STPW	AP161-0
STEPWISE			
Input	STP_AP161_*_ALL_R*r*.INP	LIBAP161_STPW	AP161-0
Input	STP_AP161_LHS_R*r*.TRN	LIBAP161_STPW	AP161-0
Input	STP_AP161_MEANS_R*r*.TRN	LIBAP161_STPW	AP161-0
Output	STP_AP161_*_R*r*.TXT	LIBAP161_STPW	AP161-0
Output	STP_AP161_*_R*r*.SP	LIBAP161_STPW	AP161-0

1. $r \in \{1,2,3\}$
2. $* \in \{RANK, RAW\}$ for each r

Information Only

APPENDIX B Addendum

Following the completion of the PCS-2012 PA calculations, but prior to the completion of the summary report, an error was discovered in the ALG1 input file for BRAGFLO. The error is associated with the calculation of permeability for ROMPCS materials PCS_T2 and PCS_T3. As seen in Camphouse et al. (2012), sampled porosity values for these materials are used to calculate their respective permeabilities according to

$$k = 10^{-21.187(1-\Phi) + 1.5353 + \alpha},$$

where k is the calculated permeability, Φ is the sampled porosity value, and α is the sampled value from a normal distribution with a mean of 0, a standard deviation of 0.86, and truncated at ±2 standard deviations. Upon closer inspection, the leading-term constant of -21.187 in the equation above was incorrectly transcribed to the ALG1 input file as -21.87 for both materials PCS_T2 and PCS_T3. This error leads to calculated permeabilities for materials PCS_T2 and PCS_T3 that are lower than the minimum listed in Camphouse et al. (2012) for some vectors.

This transcription error has a negligible impact on the PCS-2012 PA results presented and discussed in this report. Indeed, for the first 200 years post-closure, gas and brine flows toward or away from a waste panel in the PCS-2012 PA are through the upper and lower DRZ before the DRZ material about the ROMPCS is modeled as having healed (e.g., see Figure 6-8 in Camphouse 2012d). Slightly lower calculated permeabilites for the ROMPCS in some vectors will not appreciably impact these flow behaviors as the DRZ about the panel closure is more permeable (on average) than the ROMPCS before the DRZ heals at 200 years, with or without the transcription error. After 200 years, the DRZ above and below the ROMPCS is modeled as having healed, and is represented by material DRZ_PCS. Material DRZ_PCS is unchanged from the PABC-2009 to the PCS-2012 PA. After 200 years, the calculated ROMPCS permeability range presented in Camphouse et al. (2012) results in a panel closure that is "tighter" (on average) than the Option D closure. Permeabilities that are lower than intended for material PCS_T3, due to the transcription error, do not alter this comparison between the ROMPCS and Option D after 200 years.

To fully quantify the impact of the transcription error, the ALG1 input file to BRAGFLO was corrected, and replicate 1 of the PCS-2012 PA was re-run starting at the ALG1 BRAGFLO step through to CCDFGF. Files associated with this re-run are located in class CALC_MODS, and having the same library and naming conventions as listed in Appendix A. The results of the re-run are shown in Figure B-1, and are compared to the original PCS-2012 PA results with the transcription error. As is evident in that figure, the transcription error has essentially no impact on the replicate 1 mean for total normalized releases. The same is also true of the 10th and 90th percentiles obtained in the original and corrected cases. The transcription error in the ALG1

Information Only

input file to BRAGFLO has a negligible impact on the PCS-2012 PA results presented and discussed in this report.

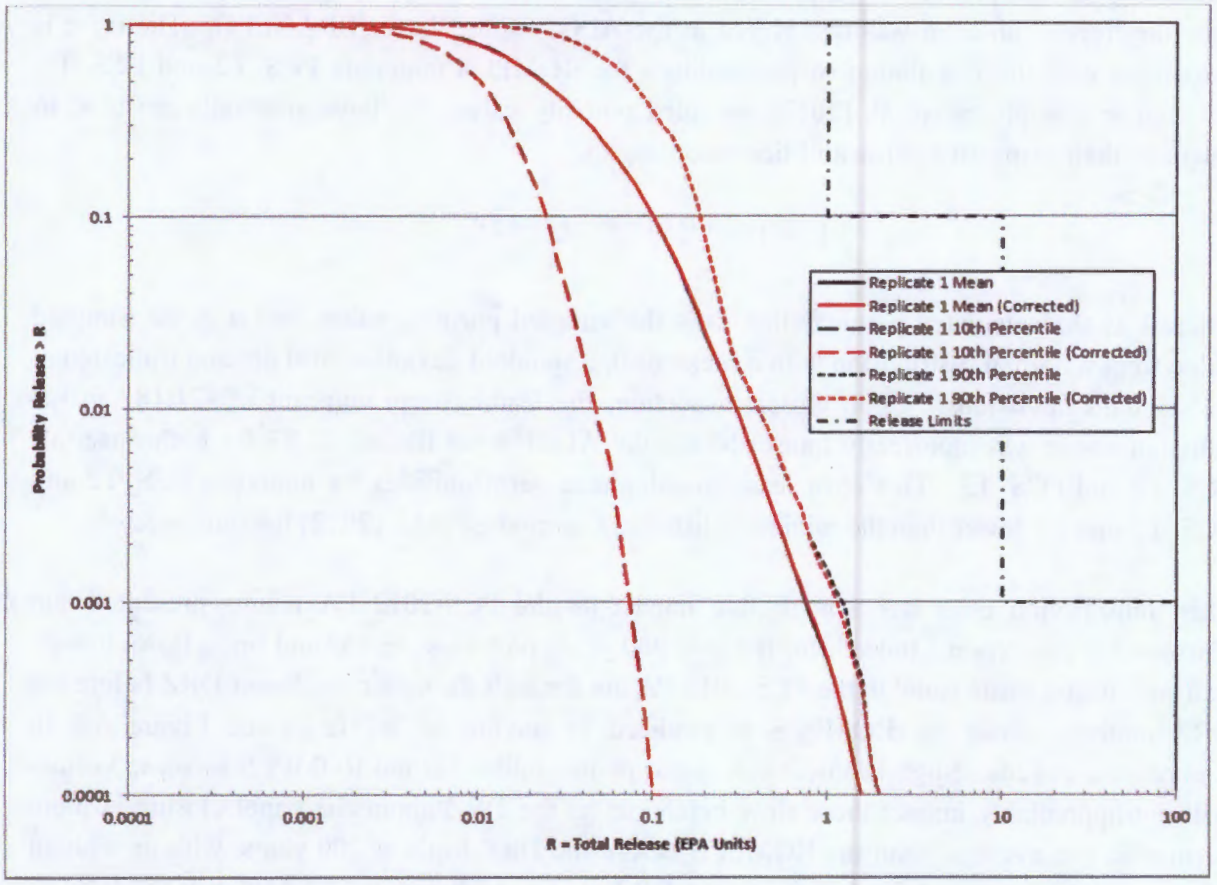

Figure B-1: Comparison of PCS-2012 PA Mean and Quantile CCDFs for Total Normalized Releases, Replicate 1

Information Only

November, 2012

Waste Isolation Pilot Plant

Fact Sheet

DOE Proposed Panel Closure Redesign Planned Change Request

Background

The Waste Isolation Pilot Plant (WIPP) is the nation's only repository for defense generated transuranic (TRU) waste. The WIPP underground facility is mined out 2,150 feet beneath the earth's surface in ancient salt beds that date back 250 million years. Both contact-handled and remote-handled TRU radioactive waste is disposed of in the WIPP underground facility.

The U.S. Department of Energy (DOE) has submitted a planned change request to the U.S. Environmental Protection Agency (EPA) to modify Condition 1 of EPA's Final WIPP Certification Decision (May 18, 1998) for 40 CFR Part 194. Condition 1 specifies that the panel closure system to be used at WIPP is the one designated as Option D. The Option D design consists of the installation of a concrete block explosion/isolation wall, removal of the majority of the disturbed rock zone (DRZ) in the area of the closure, and emplacement of a large Salado Mass Concrete (SMC) monolith. SMC is a salt-saturated concrete originally designed to seal the shafts on repository closure. The Option D panel closures would be installed in each panel of the repository after waste emplacement in that panel is complete.

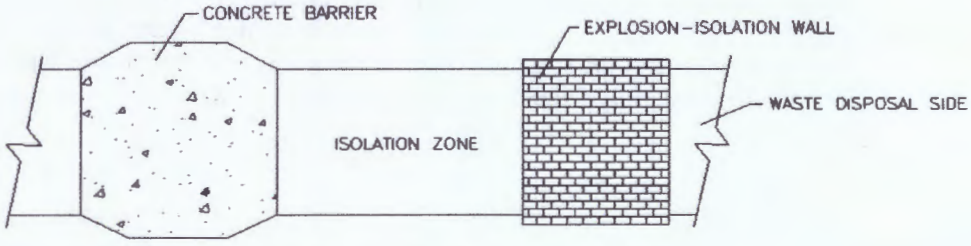

OPTION D. EXPLOSION ISOLATION WALL AND CONCRETE BARRIER WITH DRZ REMOVED

Figure 1. Option D Panel Closure

What is Proposed?

DOE is proposing to use a redesigned panel closure called the Run-Of-Mine Panel Closure (ROMPC). This closure system has two components: steel ventilation bulkheads and run-of-mine salt. In the base design, two ventilation bulkheads will be used at either end of the run-of-mine salt. In those panels where an explosion (block) wall has already been installed, this wall will form the inside end of the closure, with a steel ventilation bulkhead installed at the outer end after placement of the ROM salt. The ROM salt will be emplaced until the entire drift is filled over a minimum distance of 100 feet. The ROM salt will be placed in contact with the sides and roof of the drifts. A variety of techniques are available for emplacing the ROM salt. Over time, creep closure of the drifts will ensure that the salt consolidates to a condition approaching intact salt with a low permeability. The fabrication, installation, and maintenance of bulkheads, such as those proposed for the closure, are standard practices at the WIPP facility. The construction methods and materials to be used in the ROMPC design have been proven in mining and construction projects.

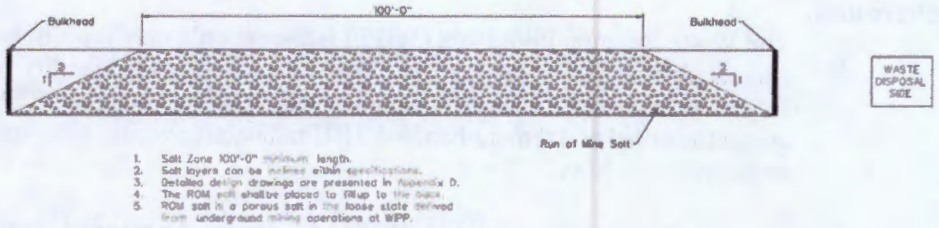

Figure 2. Conceptual Panel Closure Design

Impact on WIPP

The analyses provided with the planned change request (see electronic link below) demonstrate that the ROMPC design will contain Volatile Organic Compounds to below regulatory limits, and therefore perform its desired function of protecting workers, the public, and the environment before repository closure. After repository closure, analyses also confirm that while there might be a small difference in early performance, the long-term performance of the revised design will be very similar to that for Option D and that the impact of the proposed new closure design on long-term performance is within the EPA limits.

For More Information

This Planned Change Request is available for review on the EPA website at http://www.epa.gov/radiation/news/wipp-news.html#panelclosure

Panel Closure Redesign Planned Change Request

Review of Planned Change Request Submittal to the Environmental Protection Agency

December 2012

EM Environmental Management

safety ❖ performance ❖ cleanup ❖ closure

www.em.doe.gov

Topics

- Current Regulatory Status
- Option D and Concerns with Option D design
- Proposed new design: Run-of-Mine Panel Closure (ROMPC)
- Panel Closure System Planned Change Request History
- Conclusion

Current Regulatory Status

- *Condition 1: § 194.14(b), Disposal system design, panel closure system.*

The Department shall implement the panel seal design designated as Option D in Docket A-93-02, Item II-G-1 October 29, 1996, (Compliance Certification Application submitted to the Agency). The Option D design shall be implemented as described in Appendix PCS of Docket A-93-02, Item II-G-1, with the exception that the Department shall use Salado mass concrete (consistent with that proposed for the shaft seal system, and as described in Appendix SEAL of Docket A-93-02, Item II-G-1) instead of fresh water concrete.

Option D

•**Option D**: enlarged concrete barrier with Disturbed Rock Zone (DRZ) removed and a larger isolation wall. Concrete barrier fabricated from Salado Mass Concrete (SMC).

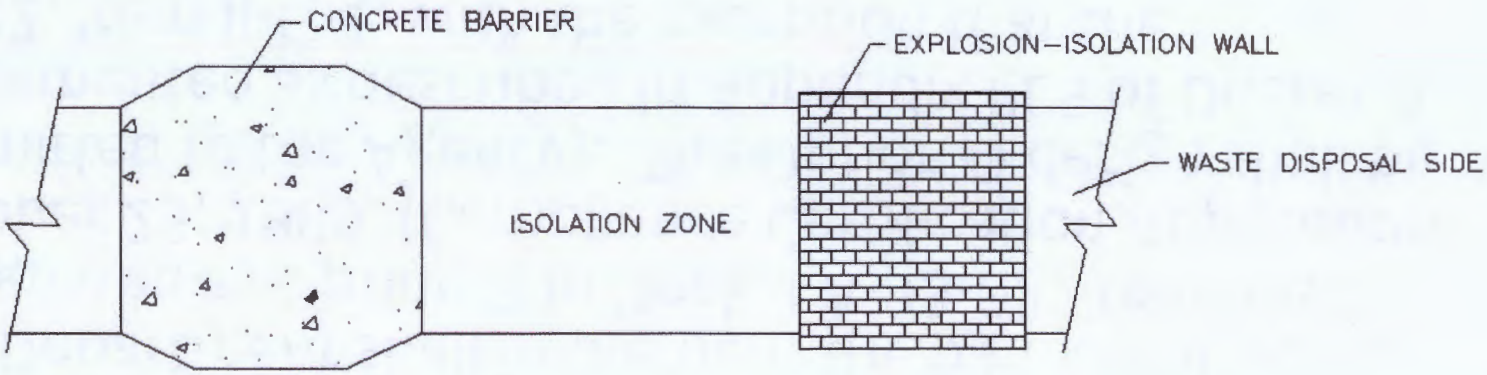

OPTION D. EXPLOSION ISOLATION WALL AND CONCRETE BARRIER WITH DRZ REMOVED

Concerns with Option D

- Cannot manufacture SMC to the specifications in the CCA while meeting the requirements of the Option D design
- Hydrogen and Methane monitoring data shows no need for explosion/isolation wall
- Option D design is very complex to construct
- Construction impacts disposal operations
- Option D design is significantly more expensive than the proposed design

Current Repository Status

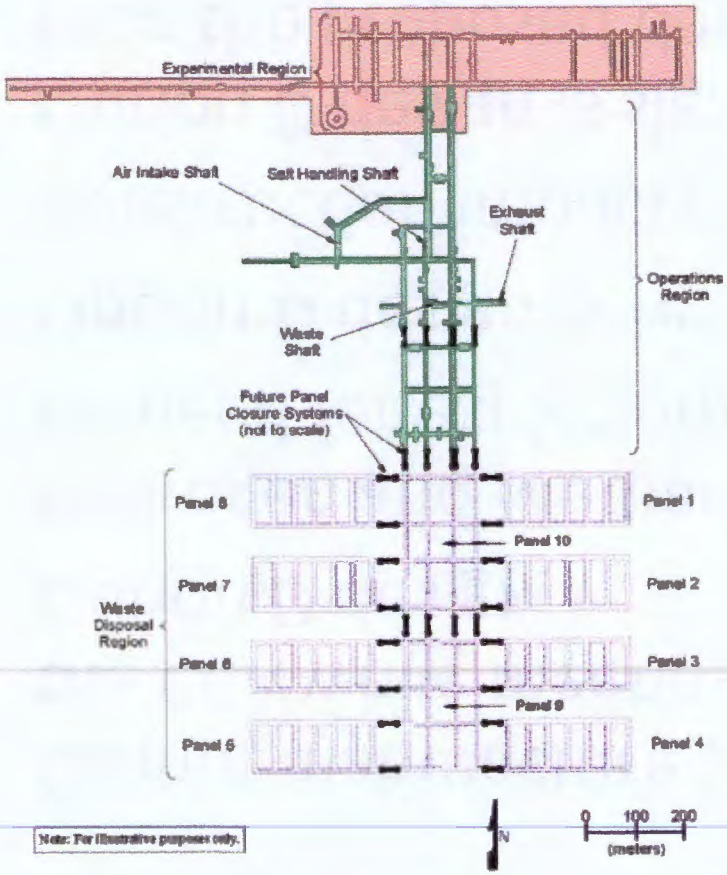

Current Status

- Panels 1, 2 & 5: Block Wall Already Installed
- Panels 3 & 4: Substantial Barriers and Bulkheads Installed
  - Hydrogen and Methane monitoring

EM Environmental Management
safety ❖ performance ❖ cleanup ❖ closure
www.em.doe.gov

Proposed New Design Run-of-Mine (ROM) Panel Closure

- One ventilation bulkhead at each end
  - Panels with existing block walls will have only one ventilation bulkhead at the entrance to the panel
- 100 foot backfill of Run-of-Mine (ROM) salt between bulkheads

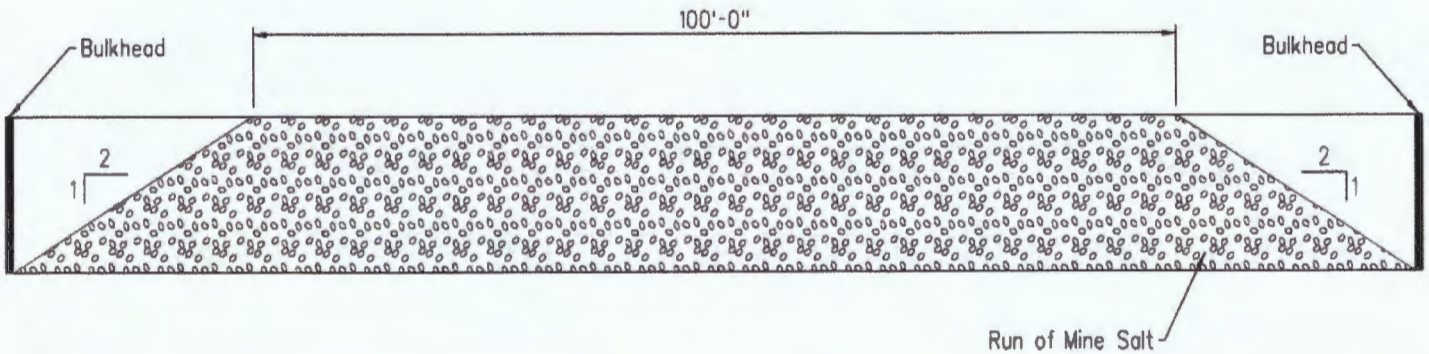

WASTE DISPOSAL SIDE

Panel Closure System PCR History

- September 28, 2011 DOE submitted Panel Closure PCR to EPA
- EPA submitted letter to DOE requesting additional information December 22, 2011.
- DOE provided response to the EPA letter on April 17, 2012.
- Five DOE/EPA technical meetings on PCS details held (October 2011, February, April, October, and November, 2012).
- Revised Panel Closure PA report submitted to EPA on November 5, 2012.

Conclusion

By moving to the new design:

- Enhance constructability due to simpler design and will meet operational performance requirements
- Increase worker safety during construction
- Reduce impact on disposal operations
- Similar long-term performance as Option D
- Less expensive to construct

Exceptional service in the national interest

Sandia National Laboratories

Performance Assessment of the WIPP Run-of-Mine Salt Panel Closure System

R. Chris Camphouse, PhD
Performance Assessment Department, 6211
Sandia National Laboratories

U.S. DEPARTMENT OF ENERGY NNSA

Sandia National Laboratories is a multi-program laboratory managed and operated by Sandia Corporation, a wholly owned subsidiary of Lockheed Martin Corporation, for the U.S. Department of Energy's National Nuclear Security Administration under contract DE-AC04-94AL85000. SAND NO. 2011-XXXXP

WIPP Performance Assessment

WIPP Regulatory Requirements

- Regulatory requirements guide the WIPP PA framework.
  - The WIPP must be designed to provide *reasonable expectation* that *cumulative releases* of radionuclides to the accessible environment for *10,000 years* after disposal from all *significant processes and events* shall be less than specified *releases limits*

WIPP Regulatory Requirements

- Reasonable expectation: regulations acknowledge substantial uncertainties
- 10,000 years: PA must predict behavior for entire regulatory time period
- Significant processes and events: PA must include all of these, including the possibility of human intrusion

Release Mechanisms

- Direct Releases (occur during or immediately after drilling)
  - Cuttings (Solids removed due to drilling)
  - Cavings (Solids from borehole wall)
  - Spallings (Solids from pressure release)
  - Direct Brine Release (Brine from pressure release)
- Long-term Releases
  - Groundwater Transport in Culebra

Direct Releases

Direct Releases Dominate Total Releases

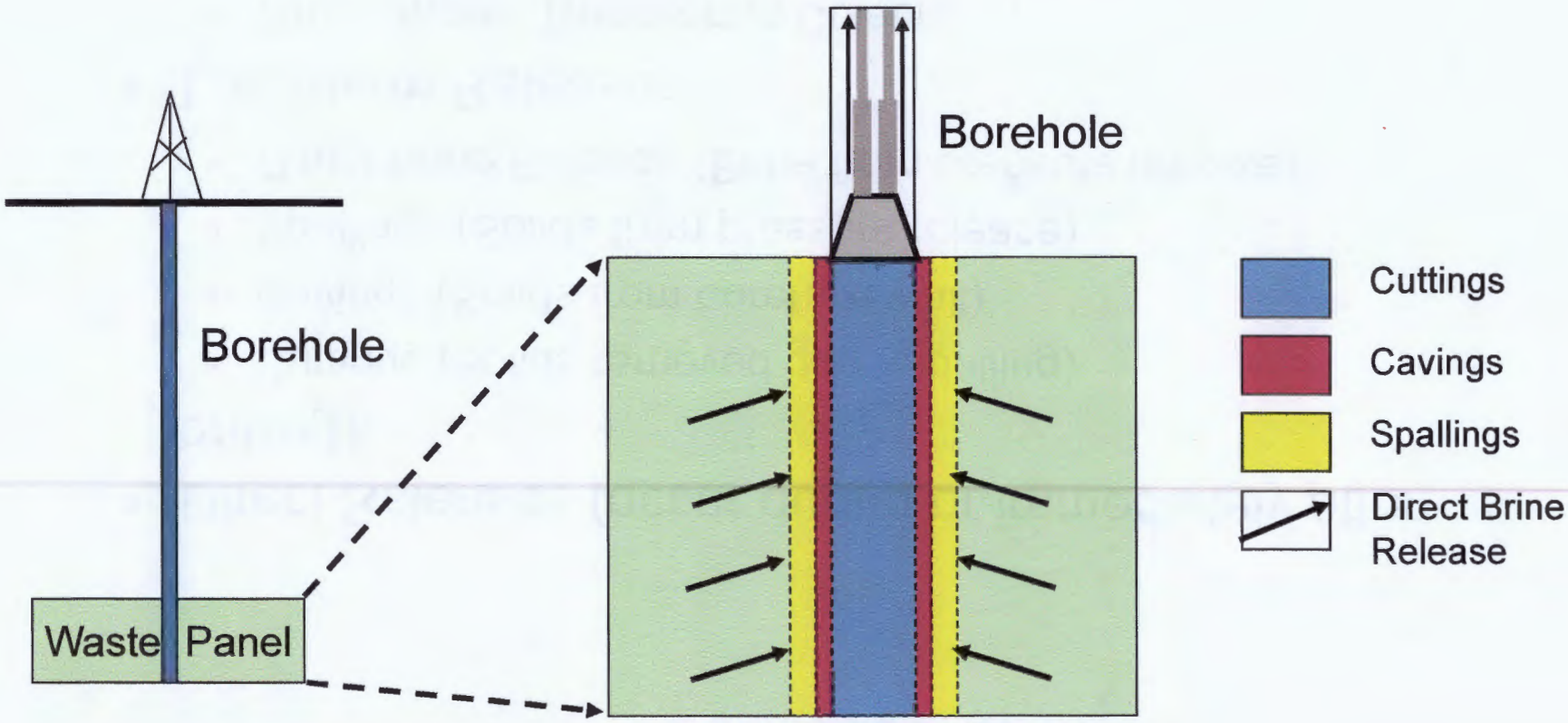

Release Pathways

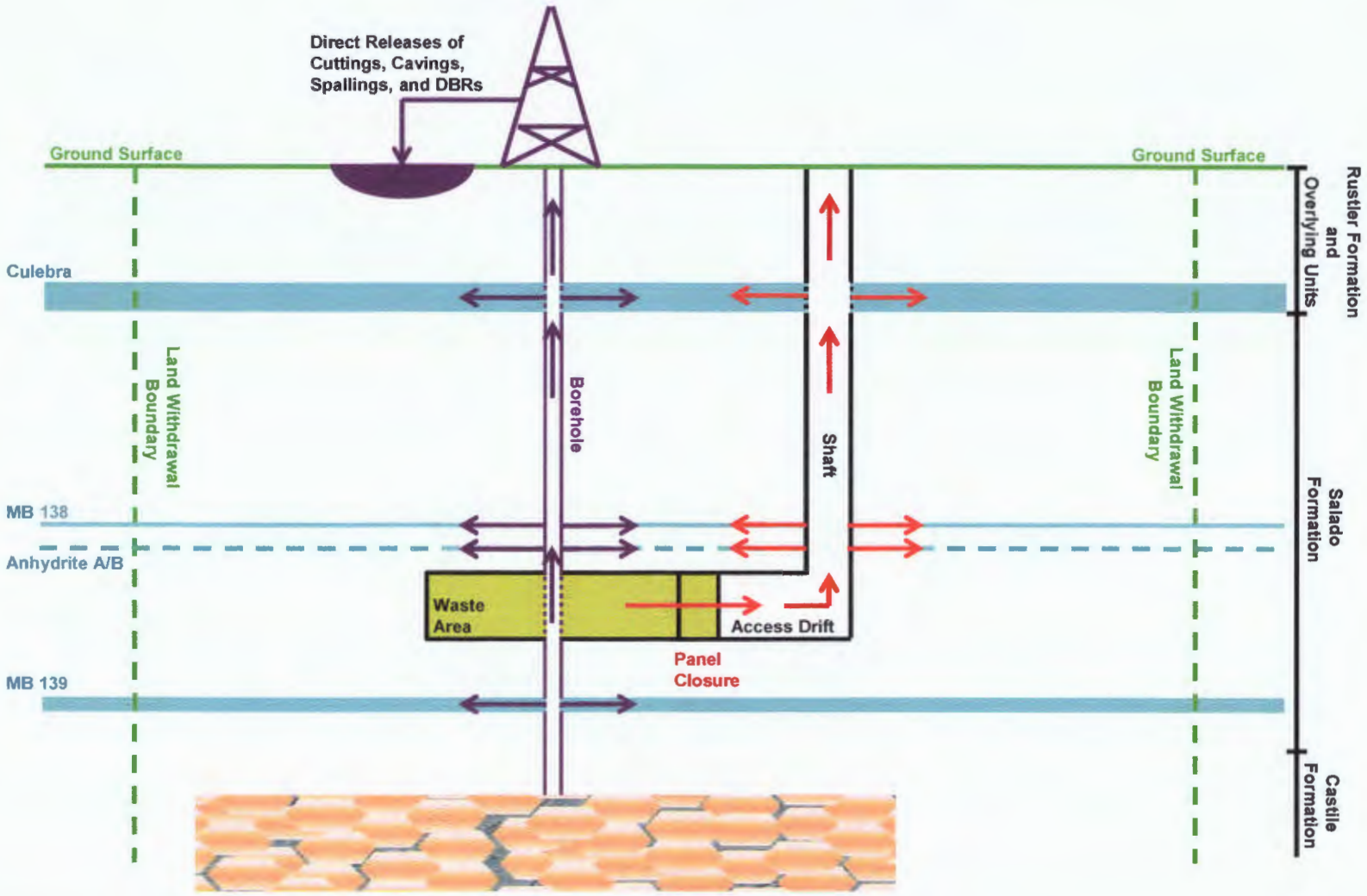

WIPP Panel Closures in PA

WIPP Panel Closures

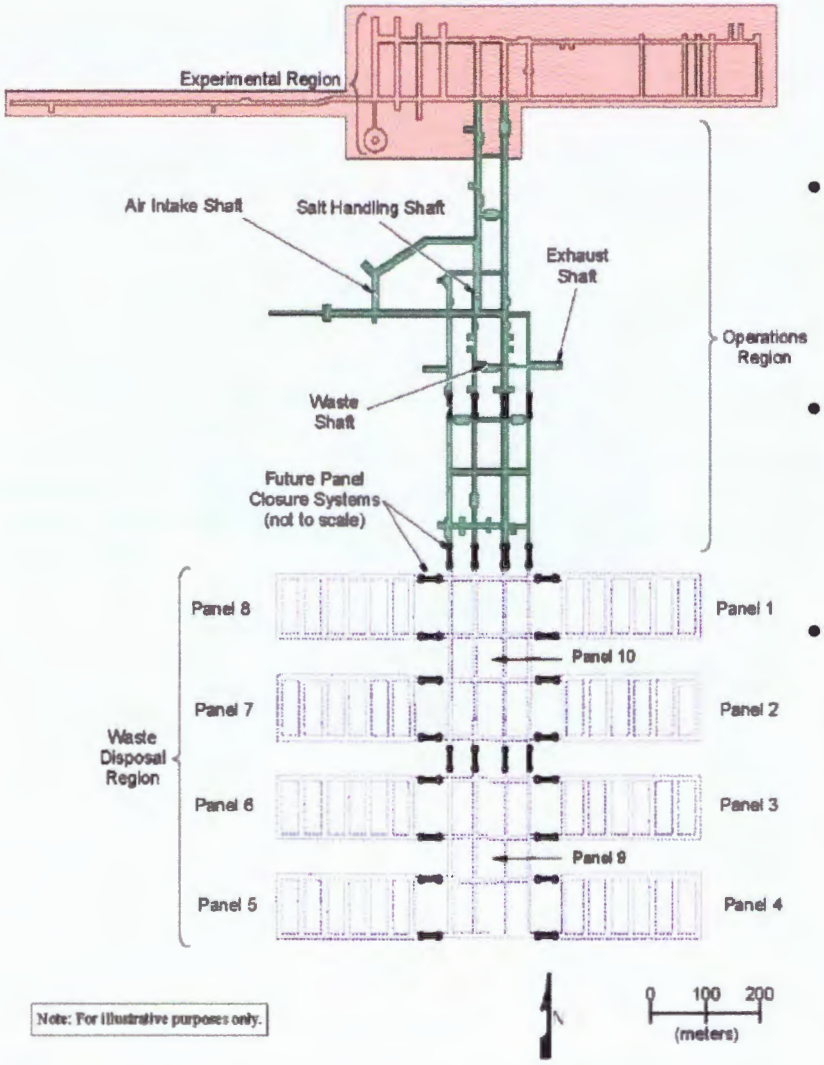

- WIPP panel closures have been represented in PA since the original 1996 Compliance Certification Application.
- The function of panel closures is to protect workers during the operational period of the repository.
- Panel closures are included in PA because they are part of the disposal system, not because they inhibit releases. *The panel closure system was not designed or intended to support long-term repository performance.*

Approved Design

The "Option D" Panel Closure

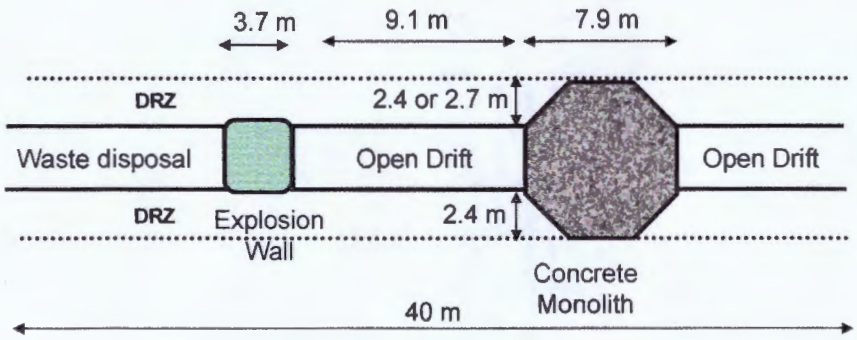

- The "Option D" design was designated as the approved panel closure in the 1998 rulemaking that certified the repository for waste disposal.
- The "Option D" design is exceedingly difficult to implement and is prohibitively expensive.
- A simpler panel closure design can meet operational requirements while being cost-effective and easier to implement.

Panel Closure Re-Design

The Run-of-Mine Panel Closure System
(ROMPCS)

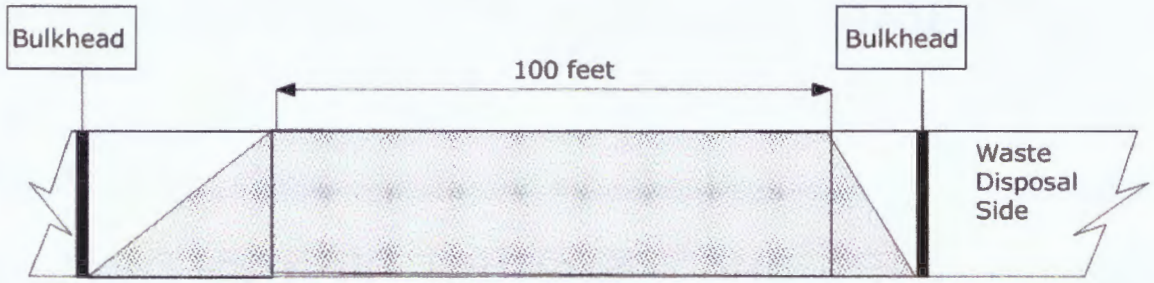

Panel closure with 100 feet of ROM salt between
two ventilation bulkheads

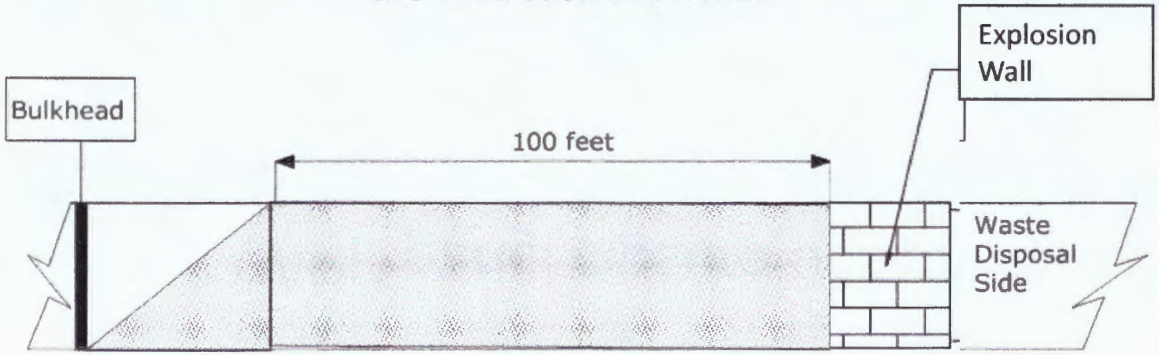

Panel closure with 100 feet of ROM salt between
a ventilation bulkhead & explosion wall

Changing the Approved WIPP Panel Closure Design

Sandia National Laboratories

- Changing the WIPP panel closure design from Option D to the ROMPCS invokes a federal rulemaking process.
- The DOE has submitted a Planned Change Request to the EPA to formally request a change to the approved design.
- A PA that demonstrates regulatory compliance impacts associated with the new design is included as part of the Planned Change Request. The PA is named PCS-2012.

PCS-2012 PA Approach and Results

Baseline Comparison

The current WIPP PA baseline was established by the 2009 Performance Assessment Baseline Calculation (PABC-2009)

- Option D panel closures were implemented in the PABC-2009
- The PCS-2012 PA incorporates the ROMPCS into the PABC-2009 baseline.
- ROMPCS compliance impacts are assessed via a direct comparison of PABC-2009 and PCS-2012 results.

ROMPCS Processes

The representation of the ROMPCS in the PCS-2012 PA accounts for several physical processes.

- Creep closure of the surrounding salt rock results in consolidation of ROM salt placed in panel entries.
- ROM salt comprising the closures will approach a condition similar to intact salt.
- Imposed back stress on the surrounding rock will result in eventual healing of the surrounding salt rock.

ROMPCS Parameters

Sandia National Laboratories

ROMPCS parameters and timings were developed over a period of 1 ½ years.

- ROMPCS represented as 100 feet of run-of-mine salt.
- Calculations and data analyses were performed to determine ROMPCS parameters and their temporal extent.
- Numerous technical exchanges were had with the EPA to discuss and refine ROMPCS parameters and timings prior to commencement of the PCS-2012 PA.

ROMPCS Evolution

The ROMPCS is modeled as having short-term and long-term characteristics in the PCS-2012 PA, with properties based on three time periods

- 0 to 100 years: Emplaced ROM salt undergoes some re-consolidation with no impact on surrounding salt rock.
- 100 to 200 years: ROMPCS continues to re-consolidate with no impact on surrounding salt rock.
- 200 to 10000 years: ROMPCS is re-consolidated and the surrounding salt rock is healed.

Results: Total Releases

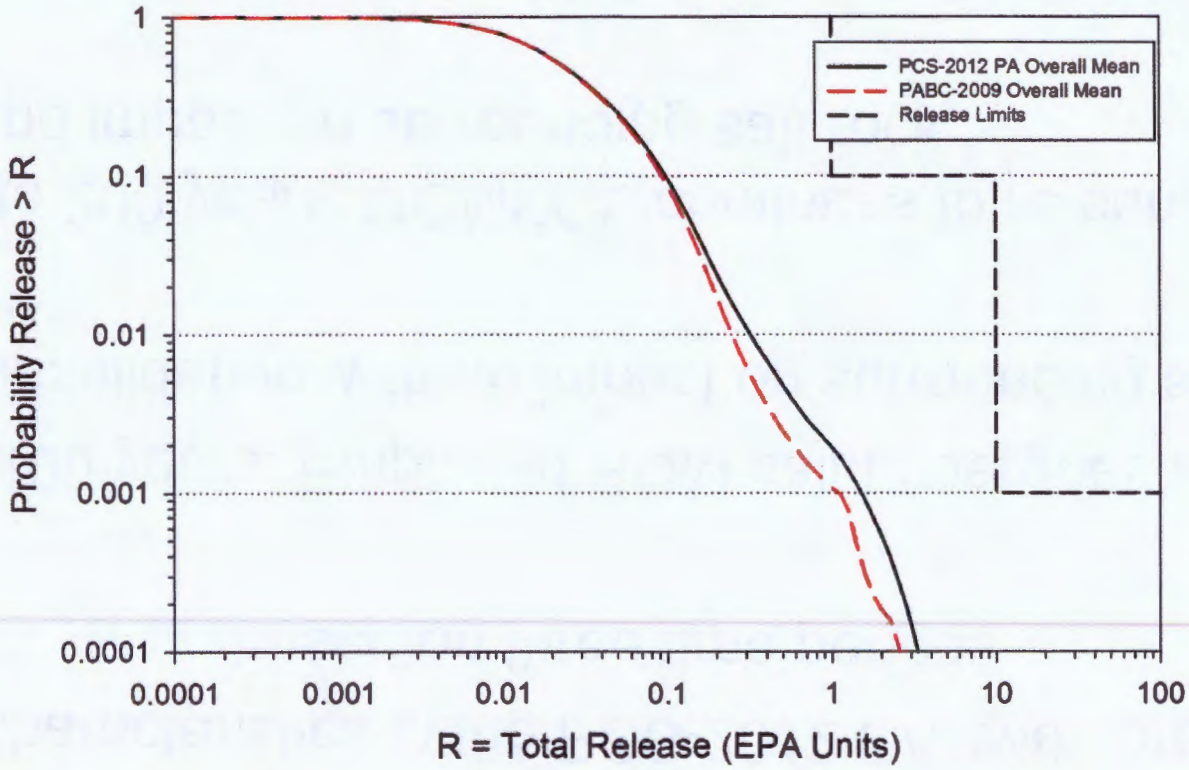

Results: Release Components

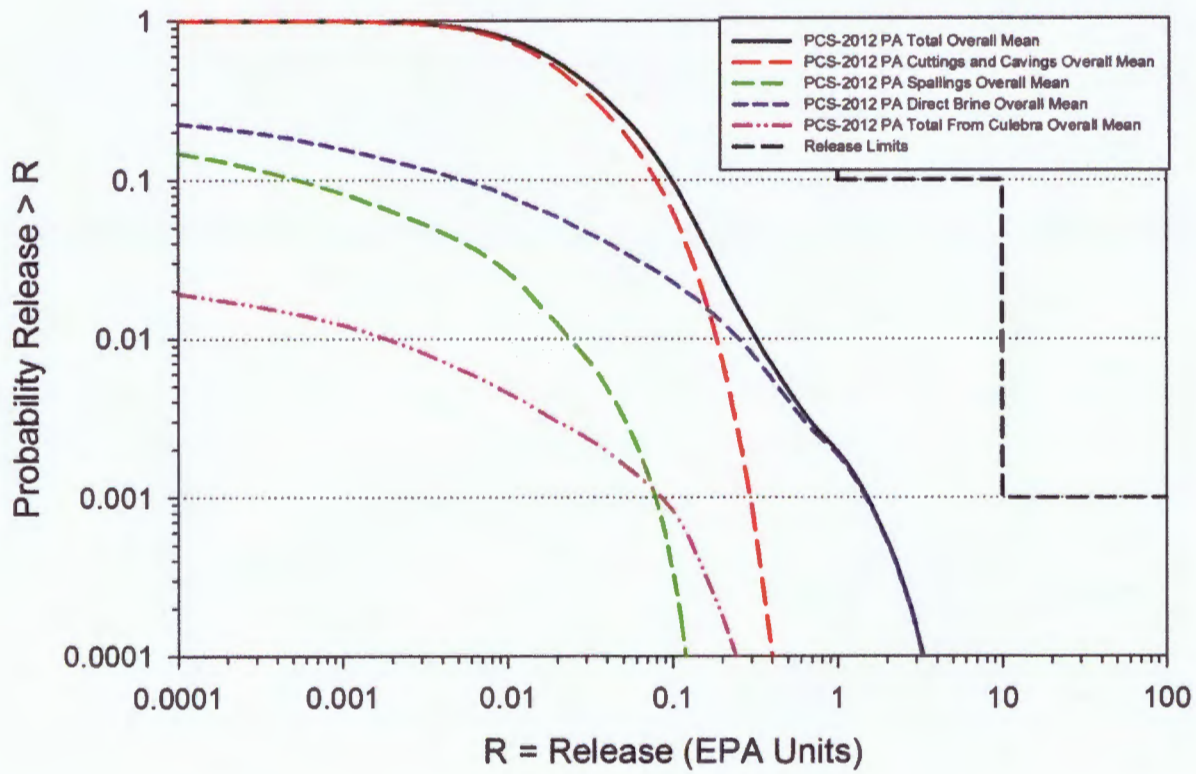

Results: Spallings Releases

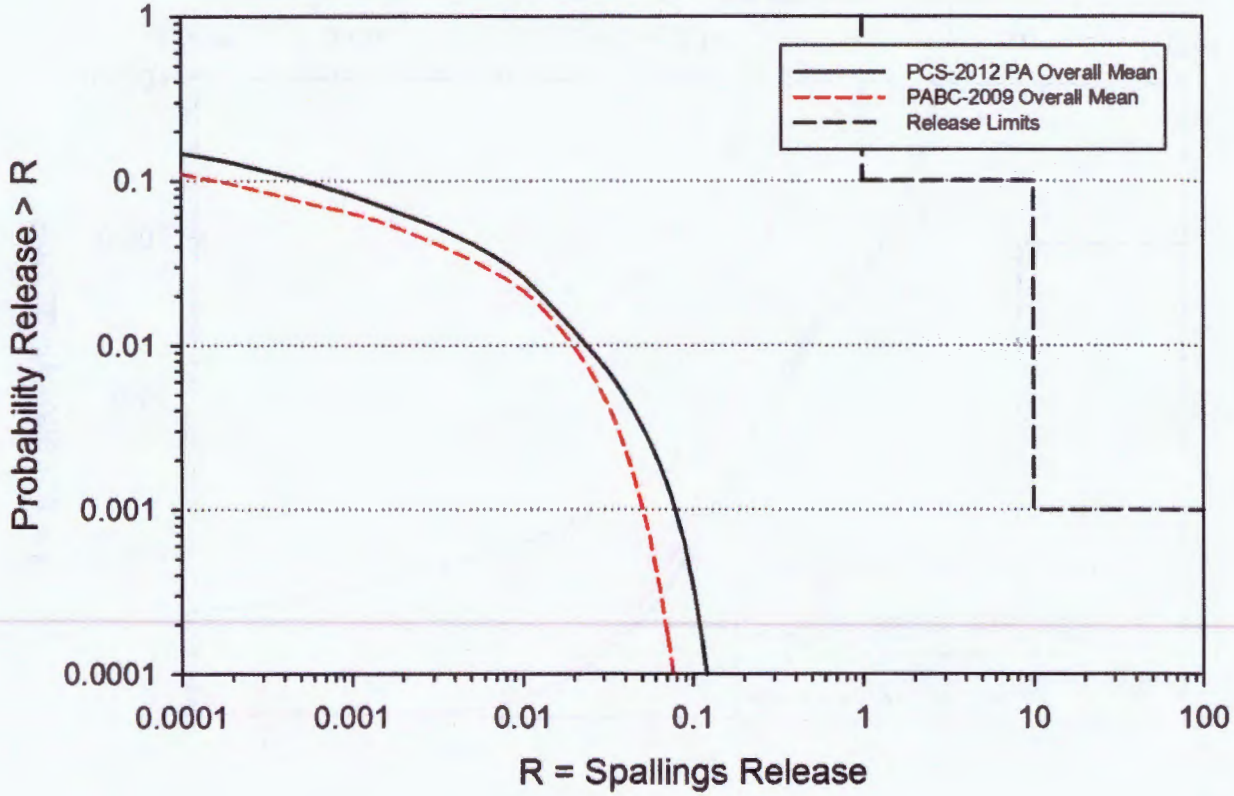

Results: Direct Brine Releases

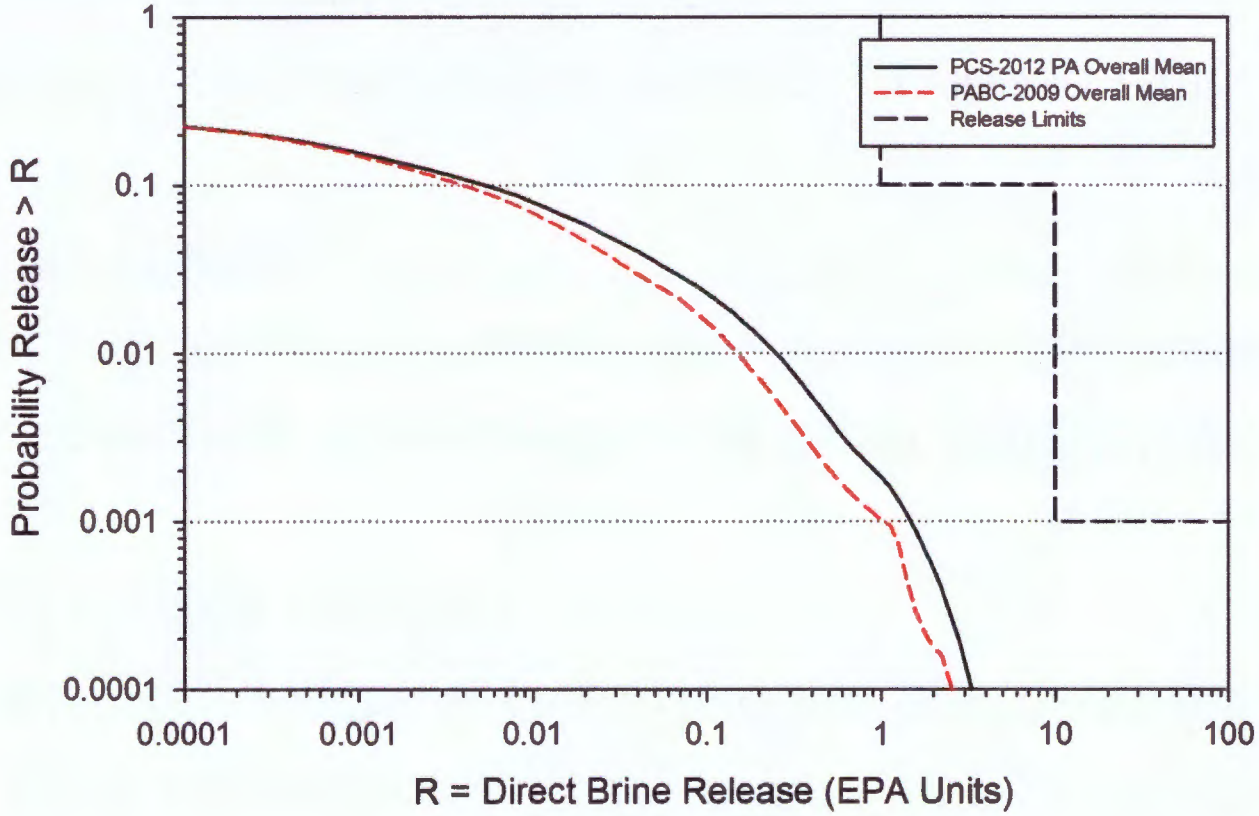

Summary

- The DOE has submitted a Planned Change Request to the EPA requesting a change to the approved WIPP panel closure system.
- A Performance Assessment has been completed that quantifies regulatory compliance impacts associated with the change.
- The WIPP remains below regulatory release limits with the revised panel closure system.

WIPP Panel Closure Redesign Rulemaking

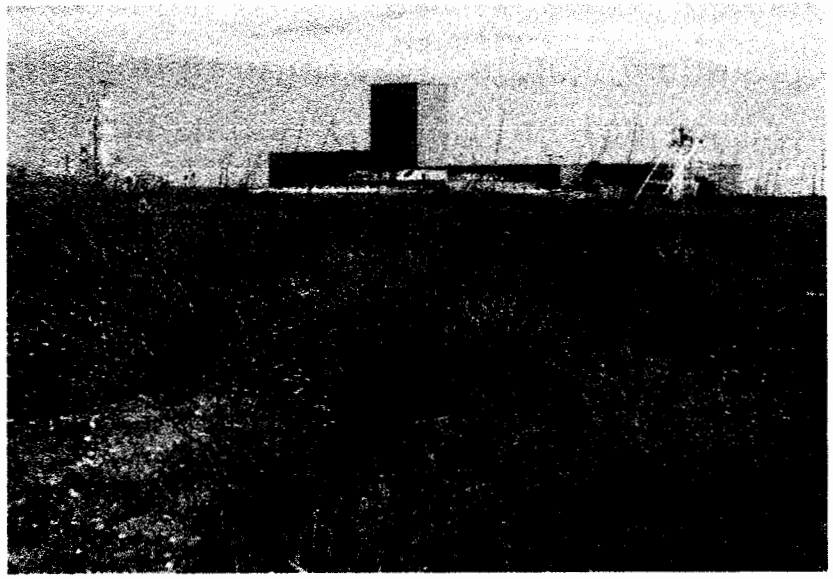

Fall 2012

EPA Radiation Protection Program

...protecting people & the environment

Overview

- Condition 1 of EPA's original certification of WIPP requires DOE to implement the Option D Panel Closure.
- The approval of any changes to the panel closure condition will be conducted via the Agency's rulemaking process.
- EPA's technical review of DOE's planned change began in 2011, and is ongoing.
- EPA's next step is to determine that DOE has provided adequate information to inform a complete technical review. Gathering input from the public is a significant part of this process.
- EPA anticipates proposing a rule modifying its panel closure condition in spring 2013, with a goal of finalizing the rule by the end of the calendar year.

Condition 1:

- In the 1996 CCA, DOE presented four options for the design of the panel closure system, but did not specify which one would be constructed at the WIPP.

- In the absence of data on waste contents and disposal system performance, EPA based its certification decision on DOE's use of the most physically robust design.

- 40 CFR Part 194, Appendix A, Condition 1 (*Federal Register*, Vol. 63 No.95, p.27355) requires DOE to implement the Option D panel closure system at WIPP, with Salado mass concrete replacing fresh water concrete.

- The Agency determined that the use of Salado mass concrete – using brine rather than fresh water – would produce concrete seal permeabilities in the repository more consistent with the values used in DOE's performance assessment.

Changes to Condition 1:

EPA's certification specifically addressed potential future changes to the panel closure design:

- "Nothing in this condition precludes DOE from reassessing the engineering of the panel seals at any time.

- "Should DOE determine at any time that improvements in materials or construction techniques warrant changes to the panel seal design, DOE must inform EPA.

- "If EPA concurs, and determines that such changes constitute a significant departure from the design on which certification is based, the Agency is authorized under §194.65 to initiate a rulemaking to appropriately modify the certification."

- *Federal Register*, Vol. 63 No.95, p.27362

Panel Closure Rulemaking Action Required by 40 CFR 194.65

- Action was commenced April 19, 2012 in anticipation of complete technical documentation from DOE.
- Designated as lowest level (Tier 3) regulatory action, not subject to White House OMB review.
- Regulatory process will include:
  - **Proposed regulatory modification to 40 CFR 194 panel closure requirement (Condition 1)**
  - **Public comment period with a public hearing if requested**
  - **A final regulation that modifies 40 CFR 194**
- Regulation is subject to judicial review.
  - U.S. Court of Appeals for the Tenth Circuit or for the District of Columbia
  - 60 days after final agency action (LWA, Sec. 18)

What has EPA done so far?

- The Panel Closure Redesign Planned Change Request (PCR) was received September 28, 2011.
- EPA initiated its technical review and correspondence with DOE.
- DOE agreed to conduct the Panel Closure System Performance Assessment (PCS-2012 PA), with the explicit goals of:
  - **Modeling the panel closure using parameters agreed upon by EPA and DOE (DOE memorandum, dated June 15, 2012)**
  - **Quantifying the predicted impacts of changing the panel closure on long-term repository performance**
  - **Allowing a direct comparison to the current baseline PA for certification (the PABC-09)**
- EPA received the PCS-2012 PA summary report on November 5, 2012.
- EPA's technical review is ongoing.

Rulemaking Milestones

- EPA technical staff will determine the completeness of DOE's request.
  - **Determine that DOE has provided EPA has sufficient information to review and support a decision**
  - **Incorporate public comments, correspondence with DOE**
- EPA staff will finish and document its technical review.
- Agency work group will develop proposed regulatory language.
- Draft Rule Revision to be proposed via publication in the Federal Register, Spring 2013.
- Proposal will open a 60-day public comment period.
- EPA's goal is to publish Final Rule and Response to Comments by the end of 2013.